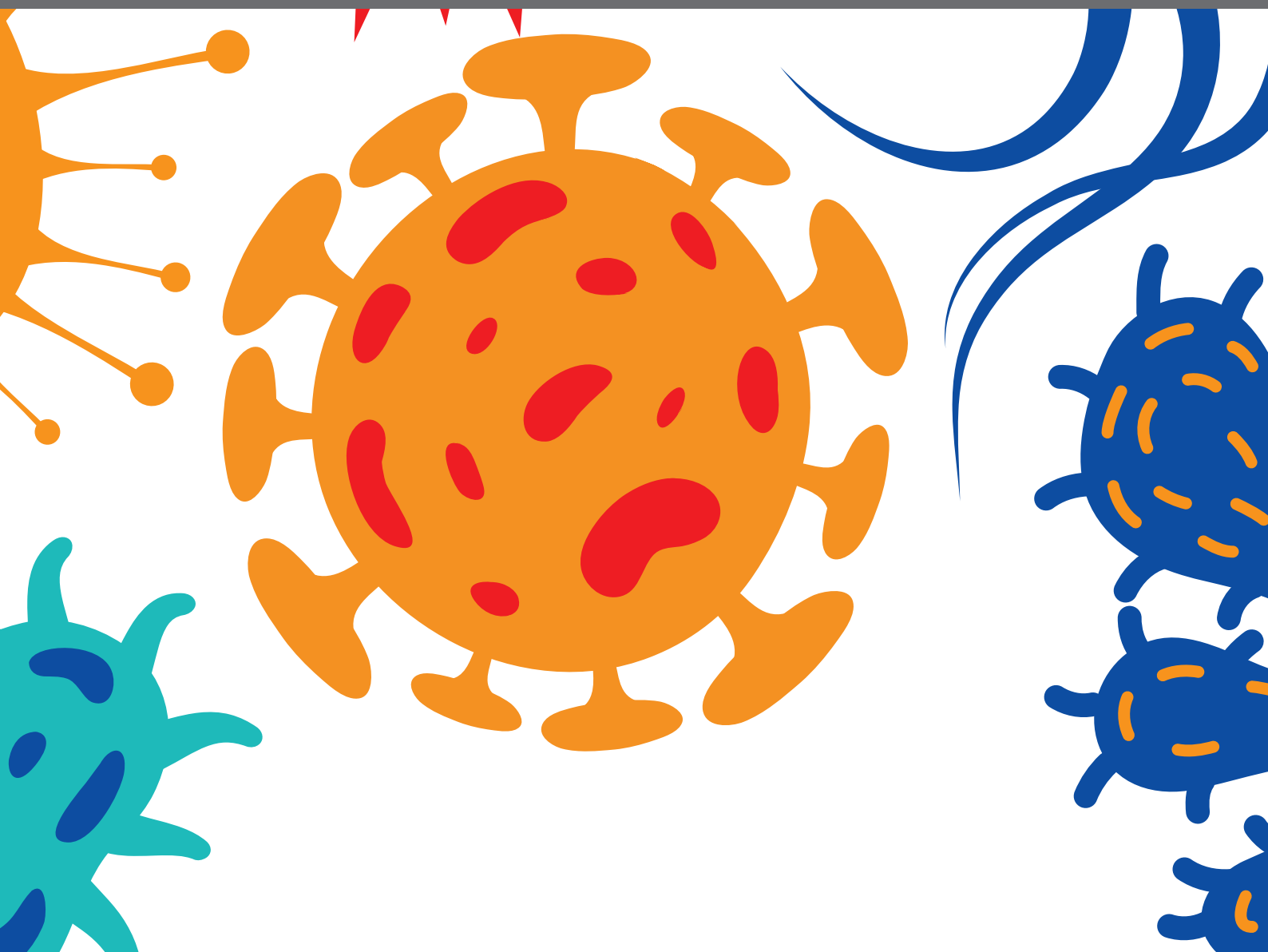


TULAREMIA: EPIDEMIOLOGY, ECOLOGY, GENOMICS, IMMUNITY AND PATHOGENESIS

EDITED BY: Marina Santic, Anders Sjöstedt, Thomas Henry, Jiri Stulik,
Max Maurin, Anders Johansson and Joseph Wayne Conlan
PUBLISHED IN: *Frontiers in Cellular and Infection Microbiology*





frontiers

Frontiers eBook Copyright Statement

The copyright in the text of individual articles in this eBook is the property of their respective authors or their respective institutions or funders. The copyright in graphics and images within each article may be subject to copyright of other parties. In both cases this is subject to a license granted to Frontiers.

The compilation of articles constituting this eBook is the property of Frontiers.

Each article within this eBook, and the eBook itself, are published under the most recent version of the Creative Commons CC-BY licence.

The version current at the date of publication of this eBook is CC-BY 4.0. If the CC-BY licence is updated, the licence granted by Frontiers is automatically updated to the new version.

When exercising any right under the CC-BY licence, Frontiers must be attributed as the original publisher of the article or eBook, as applicable.

Authors have the responsibility of ensuring that any graphics or other materials which are the property of others may be included in the CC-BY licence, but this should be checked before relying on the CC-BY licence to reproduce those materials. Any copyright notices relating to those materials must be complied with.

Copyright and source acknowledgement notices may not be removed and must be displayed in any copy, derivative work or partial copy which includes the elements in question.

All copyright, and all rights therein, are protected by national and international copyright laws. The above represents a summary only. For further information please read Frontiers' Conditions for Website Use and Copyright Statement, and the applicable CC-BY licence.

ISSN 1664-8714

ISBN 978-2-88963-363-0

DOI 10.3389/978-2-88963-363-0

About Frontiers

Frontiers is more than just an open-access publisher of scholarly articles: it is a pioneering approach to the world of academia, radically improving the way scholarly research is managed. The grand vision of Frontiers is a world where all people have an equal opportunity to seek, share and generate knowledge. Frontiers provides immediate and permanent online open access to all its publications, but this alone is not enough to realize our grand goals.

Frontiers Journal Series

The Frontiers Journal Series is a multi-tier and interdisciplinary set of open-access, online journals, promising a paradigm shift from the current review, selection and dissemination processes in academic publishing. All Frontiers journals are driven by researchers for researchers; therefore, they constitute a service to the scholarly community. At the same time, the Frontiers Journal Series operates on a revolutionary invention, the tiered publishing system, initially addressing specific communities of scholars, and gradually climbing up to broader public understanding, thus serving the interests of the lay society, too.

Dedication to Quality

Each Frontiers article is a landmark of the highest quality, thanks to genuinely collaborative interactions between authors and review editors, who include some of the world's best academicians. Research must be certified by peers before entering a stream of knowledge that may eventually reach the public - and shape society; therefore, Frontiers only applies the most rigorous and unbiased reviews. Frontiers revolutionizes research publishing by freely delivering the most outstanding research, evaluated with no bias from both the academic and social point of view. By applying the most advanced information technologies, Frontiers is catapulting scholarly publishing into a new generation.

What are Frontiers Research Topics?

Frontiers Research Topics are very popular trademarks of the Frontiers Journals Series: they are collections of at least ten articles, all centered on a particular subject. With their unique mix of varied contributions from Original Research to Review Articles, Frontiers Research Topics unify the most influential researchers, the latest key findings and historical advances in a hot research area! Find out more on how to host your own Frontiers Research Topic or contribute to one as an author by contacting the Frontiers Editorial Office: researchtopics@frontiersin.org

TULAREMIA: EPIDEMIOLOGY, ECOLOGY, GENOMICS, IMMUNITY AND PATHOGENESIS

Topic Editors:

Marina Santic, University of Rijeka, Croatia

Anders Sjöstedt, Umeå University, Sweden

Thomas Henry, UMR 5308 Centre International de Recherche en Infectiologie (CIRI), France

Jiri Stulik, University of Defence, Czechia

Max Maurin, Université Grenoble Alpes, France

Anders Johansson, Umeå University, Sweden

Joseph Wayne Conlan, National Research Council Canada (NRC-CNRC), Canada

Tularemia is a severe anthroponosis caused by *Francisella tularensis*. The genus *Francisella* contains five species: *F. tularensis*, *F. philomiragia*, *F. hispaniensis*, *F. noatunensis* and *F. novicida*. First described in 1911 in Tulare County, California, it has since been reported worldwide, capable of infecting more than 250 vertebrates and invertebrate species. Although it causes disease in various animal species, no animal has been identified as a main reservoir of this pathogen.

Humans acquire infection by several routes, including direct contact with infected animals, ingestion of water or food contaminated by infected animals, exposure to infected arthropod vectors or by inhalation of infective aerosols resulting in pneumonic, oropharyngeal, glandular, ulceroglandular or oculoglandular tularemia. The clinical presentation of human tularemia depends on route of the infection, the causative *Francisella* strain, and the immune response of the host. A live attenuated vaccine (LVS) has been available for more than 50 years, however, unlikely to become licensed in the future due to a lack of understanding of the genetic basis for its attenuation.

Due to the ease of its dissemination, its multiple routes of infection, its low dose of infection, severe morbidity, and high rate of mortality, *F. tularensis* subsp. *tularensis* has been classified as a category A bioterrorism agent by the CDC. Many virulence factors of *F. tularensis* have been discovered and investigated, but more in-depth host pathogen interaction analyses are needed to define mechanisms of pathogenicity and virulence of this unique pathogen.

Citation: Santic, M., Sjöstedt, A., Henry, T., Stulik, J., Maurin, M., Johansson, A., Conlan, J. W., eds. (2020). Tularemia: Epidemiology, Ecology, Genomics, Immunity and Pathogenesis. Lausanne: Frontiers Media SA.
doi: 10.3389/978-2-88963-363-0

Table of Contents

- 05** ***An In Vitro Co-culture Mouse Model Demonstrates Efficient Vaccine-Mediated Control of Francisella tularensis SCHU S4 and Identifies Nitric Oxide as a Predictor of Efficacy***
Igor Golovliov, Helena Lindgren, Kjell Eneslätt, Wayne Conlan, Amandine Mosnier, Thomas Henry and Anders Sjöstedt
- 19** ***Lack of OxyR and KatG Results in Extreme Susceptibility of Francisella tularensis LVS to Oxidative Stress and Marked Attenuation In vivo***
Marie Honn, Helena Lindgren, Gurram K. Bharath and Anders Sjöstedt
- 30** ***Role of Glycosylation/Deglycolysation Processes in Francisella tularensis Pathogenesis***
Monique Barel and Alain Charbit
- 36** ***Francisella tularensis Susceptibility to Antibiotics: A Comprehensive Review of the Data Obtained In vitro and in Animal Models***
Yvan Caspar and Max Maurin
- 54** ***Nramp1 and NrampB Contribute to Resistance Against Francisella in Dictyostelium***
Yannick Brenz, Denise Ohnezeit, Hanne C. Winther-Larsen and Monica Hagedorn
- 65** ***Isolation of F. novicida-Containing Phagosome From Infected Human Monocyte Derived Macrophages***
Valentina Marecic, Olga Shevchuk, Mateja Ozanic, Mirna Mihelcic, Michael Steinert, Antonija Jurak Begonja, Yousef Abu Kwaik and Marina Santic
- 76** ***Innate Immune Recognition: Implications for the Interaction of Francisella tularensis With the Host Immune System***
Zuzana Krocova, Ales Macela and Klara Kubelkova
- 90** ***The Multiple Localized Glyceraldehyde-3-Phosphate Dehydrogenase Contributes to the Attenuation of the Francisella tularensis dsbA Deletion Mutant***
Ivona Pavkova, Monika Kopeckova, Jana Klimentova, Monika Schmidt, Valeria Sheshko, Margarita Sobol, Jitka Zakova, Pavel Hozak and Jiri Stulik
- 109** ***Francisella tularensis Confronts the Complement System***
Susan R. Brock and Michael J. Parmely
- 121** ***Vaccine-Mediated Mechanisms Controlling Replication of Francisella tularensis in Human Peripheral Blood Mononuclear Cells Using a Co-culture System***
Kjell Eneslätt, Igor Golovliov, Patrik Rydén and Anders Sjöstedt
- 132** ***Tularemia in Germany—A Re-emerging Zoonosis***
Mirko Faber, Klaus Heuner, Daniela Jacob and Roland Grunow
- 142** ***Construction of a New Phage Integration Vector pFIV-Val for Use in Different Francisella Species***
Hana Tlapák, Kristin Köppen, Kerstin Rydzewski, Roland Grunow and Klaus Heuner

- 153** *Population Genomics of Francisella tularensis subsp. holarctica and its Implication on the Eco-Epidemiology of Tularemia in Switzerland*
Matthias Wittwer, Ekkehard Altpeter, Paola Pilo, Sebastian M. Gygli, Christian Beuret, Frederic Foucault, Rahel Ackermann-Gäumann, Urs Karrer, Daniela Jacob, Roland Grunow and Nadia Schürch
- 169** *The Cynomolgus Macaque Natural History Model of Pneumonic Tularemia for Predicting Clinical Efficacy Under the Animal Rule*
Tina Guina, Lynda L. Lanning, Kristian S. Omland, Mark S. Williams, Larry A. Wolfraim, Stephen P. Heyse, Christopher R. Houchens, Patrick Sanz and Judith A. Hewitt
- 187** *Adaptive Immunity to Francisella tularensis and Considerations for Vaccine Development*
Lydia M. Roberts, Daniel A. Powell and Jeffrey A. Frelinger
- 198** *Francisella tularensis D-Ala D-Ala Carboxypeptidase DacD is Involved in Intracellular Replication and it is Necessary for Bacterial Cell Wall Integrity*
Petra Spidlova, Pavla Stojkova, Vera Dankova, Iva Senitkova, Marina Santic, Dominik Pinkas, Vlada Philimonenko and Jiri Stulik
- 212** *The Francisella Type VI Secretion System*
Daniel L. Clemens, Bai-Yu Lee and Marcus A. Horwitz
- 232** *Environmental Surveillance of Zoonotic Francisella tularensis in the Netherlands*
Ingmar Janse, Rozemarijn Q. J. van der Plaats, Ana Maria de Roda Husman and Mark W. J. van Passel
- 243** *Live Attenuated Tularemia Vaccines for Protection Against Respiratory Challenge With Virulent F. tularensis subsp. tularensis*
Qingmei Jia and Marcus A. Horwitz
- 263** *Galleria mellonella Reveals Niche Differences Between Highly Pathogenic and Closely Related Strains of Francisella spp.*
Johanna Thelaus, Eva Lundmark, Petter Lindgren, Andreas Sjödin and Mats Forsman
- 273** *Further Characterization of the Capsule-Like Complex (CLC) Produced by Francisella tularensis Subspecies tularensis: Protective Efficacy and Similarity to Outer Membrane Vesicles*
Anna E. Champion, Aloka B. Bandara, Nrusingh Mohapatra, Kelly M. Fulton, Susan M. Twine and Thomas J. Inzana
- 294** *Molecular Survey of Tularemia and Plague in Small Mammals From Iran*
Ehsan Mostafavi, Ahmad Ghasemi, Mahdi Rohani, Leila Molaeipoor, Saber Esmaeili, Zeinolabedin Mohammadi, Ahmad Mahmoudi, Mansour Aliabadian and Anders Johansson
- 302** *Phylogenetic Lineages of Francisella tularensis in Animals*
Paola Pilo
- 313** *Cross Sectional Study and Risk Factors Analysis of Francisella tularensis in Soil Samples in Punjab Province of Pakistan*
Javed Muhammad, Masood Rabbani, Muhammad Zubair Shabbir, Khushi Muhammad, Muhammad Taslim Ghori, Haroon Rashid Chaudhry, Zia Ul Hassnain, Tariq Jamil, Tariq Abbas, Muhammad Hamid Chaudhry, Muhammad Haisem-ur-Rasool, Muhammad Asad Ali, Muhammad Nisar, Girish S. Kirimanjeswara and Bhushan M. Jayarao



An *In Vitro* Co-culture Mouse Model Demonstrates Efficient Vaccine-Mediated Control of *Francisella tularensis* SCHU S4 and Identifies Nitric Oxide as a Predictor of Efficacy

Igor Golovliov¹, Helena Lindgren¹, Kjell Eneslätt¹, Wayne Conlan², Amandine Mosnier³, Thomas Henry³ and Anders Sjöstedt^{1*}

¹ Laboratory for Molecular Infection Medicine Sweden, Department of Clinical Microbiology, Clinical Bacteriology, and Umeå University, Umeå, Sweden, ² National Research Council Canada, Institute for Biological Sciences, Ottawa, ON, Canada, ³ Centre International de Recherche en Infectiologie, Institut national de la santé et de la recherche médicale, U1111, Lyon, France

OPEN ACCESS

Edited by:

Alfredo G. Torres,
University of Texas Medical Branch,
USA

Reviewed by:

Tonyia Eaves-Pyles,
University of Texas Medical Branch,
USA

Cornelia Blume,

University of Southampton, UK

*Correspondence:

Anders Sjöstedt
anders.sjostedt@umu.se

Received: 10 September 2016

Accepted: 01 November 2016

Published: 25 November 2016

Citation:

Golovliov I, Lindgren H, Eneslätt K, Conlan W, Mosnier A, Henry T and Sjöstedt A (2016) An *In Vitro* Co-culture Mouse Model Demonstrates Efficient Vaccine-Mediated Control of *Francisella tularensis* SCHU S4 and Identifies Nitric Oxide as a Predictor of Efficacy. *Front. Cell. Infect. Microbiol.* 6:152. doi: 10.3389/fcimb.2016.00152

Francisella tularensis is a highly virulent intracellular bacterium and cell-mediated immunity is critical for protection, but mechanisms of protection against highly virulent variants, such as the prototypic strain *F. tularensis* strain SCHU S4, are poorly understood. To this end, we established a co-culture system, based on splenocytes from naïve, or immunized mice and *in vitro* infected bone marrow-derived macrophages that allowed assessment of mechanisms controlling infection with *F. tularensis*. We utilized the system to understand why the *clpB* gene deletion mutant, $\Delta clpB$, of SCHU S4 shows superior efficacy as a vaccine in the mouse model as compared to the existing human vaccine, the live vaccine strain (LVS). Compared to naïve splenocytes, $\Delta clpB$ -, or LVS-immune splenocytes conferred very significant control of a SCHU S4 infection and the $\Delta clpB$ -immune splenocytes were superior to the LVS-immune splenocytes. Cultures with the $\Delta clpB$ -immune splenocytes also contained higher levels of IFN- γ , IL-17, and GM-CSF and nitric oxide, and T cells expressing combinations of IFN- γ , TNF- α , and IL-17, than did cultures with LVS-immune splenocytes. There was strong inverse correlation between bacterial replication and levels of nitrite, an end product of nitric oxide, and essentially no control was observed when BMDM from iNOS^{-/-} mice were infected. Collectively, the co-culture model identified a critical role of nitric oxide for protection against a highly virulent strain of *F. tularensis*.

Keywords: *F. tularensis* SCHU S4, *in vitro* co-culture model, mouse immune response, correlates of protection

INTRODUCTION

Francisella tularensis is a highly virulent facultative intracellular bacterium causing the severe disease tularemia in many mammalian species (Sjöstedt, 2007). Two subspecies are common human pathogens, subspecies *tularensis* (type A), which causes disease with high mortality if untreated, and the less aggressive subspecies *holarctica* (type B), which despite its lower virulence

may cause serious illness in humans. Tularemia is widespread over the Northern hemisphere and a significant health problem, in particular in certain parts of Scandinavia, in parts of Eastern Europe, and in Turkey, but a rather uncommon disease in most other parts of the world. The live vaccine strain (LVS) is a human vaccine strain, which confers efficacious protection against laboratory-acquired infection, as demonstrated by the fact that the incidence of tularemia among the laboratory staff decreased by 95% after its introduction (Burke, 1977). Despite this success, studies on volunteers in the 1960s revealed that it did not confer efficacious protection against aerosol infection [reviewed by Conlan et al. (Conlan, 2011)]. Therefore, there is a need for development of more efficacious *Francisella* vaccines and previously, we analyzed if defined mutants of SCHU S4 (type A) could serve as such vaccine candidates and identified that the $\Delta clpB$ mutant conferred superior efficacy compared to LVS, despite that the former was more attenuated (Kadzhaev et al., 2009; Conlan et al., 2010; Ryden et al., 2012). It encodes an AAA+ chaperone, although the exact function in *F. tularensis* is still unknown.

Due to the essential role of CMI for host protection against tularemia, a thorough understanding of its characteristics will be necessary to identify how the infection is controlled. There is accumulating evidence that the protective mechanisms are effectuated via a complex interplay of multiple T cell subsets and other immune mechanisms, and not a single specific immune activity (Elkins et al., 2007; De Pascalis et al., 2008, 2012, 2014; Cowley and Elkins, 2011; Eneslätt et al., 2011, 2012; Mahawar et al., 2013; Griffin et al., 2015). Thus, the mechanisms cannot be delineated using simple proliferation assays but will require assays that closely mimic the *in vivo* situation. Therefore, new models are needed to better understand protective mechanisms and validate potential correlates of protective immunity. In this regard, a functional *in vitro* splenocyte-bone marrow-derived macrophage (BMDM) co-culture assay for measuring potential correlates of protection for tularemia vaccines was developed and substantial work has been performed with the aim to establish correlates of protection against *F. tularensis* (Cowley and Elkins, 2003; Cowley et al., 2005; Collazo et al., 2009; Elkins et al., 2011; De Pascalis et al., 2012, 2014; Mahawar et al., 2013; Griffin et al., 2015). Pascalis et al. showed that the greater efficacy of LVS vs. attenuated derivatives correlated with relative bactericidal activity in the co-culture system (De Pascalis et al., 2012). The relevance of such co-culture assays has to some extent been validated by the demonstration that the identified immune molecules play important roles *in vivo* (Kurtz et al., 2013; Melillo et al., 2013, 2014). A limitation of the published work using the splenocyte-BMDM co-culture model has been the extensive use of the attenuated LVS strain and there are very few studies, which have utilized fully virulent *F. tularensis* (Mahawar et al., 2013; Griffin et al., 2015).

The absence of any demonstrable correlate(s) of protection is an obstacle to the licensure of *F. tularensis* vaccines. Tularemia is in most countries an unusual disease and even in endemic areas, it appears with very irregular intervals (Sjöstedt, 2007). Therefore, efficacy in a vaccinated population will not be possible to evaluate. Moreover, although challenge studies of volunteers

were performed in the 1950s (Saslaw et al., 1961a,b), such studies, in view of the severity of respiratory tularemia, are very unlikely to be approved today. Therefore, a tularemia vaccine, as well as other vaccines against unusual, aggressive diseases, need to be evaluated according to the FDA Animal Rule (Snoy, 2010). The regulation stipulates that efficacy testing can be performed exclusively using animal models, provided that the mechanisms of action of the vaccine are sufficiently well characterized to permit extrapolation of efficacy to humans. Only one vaccine has so far been approved according to the Animal Rule (US. Food Drug Administration., 2015).

Efficacy of experimental tularemia vaccines has been demonstrated using mouse, rat, rabbit, and non-human primate models, but none of these have been approved by FDA. Thus, models to test tularemia vaccine efficacy will require further characterization before they can be approved, e.g., the identification of correlates of immunity and protection. This would also include models that would not necessitate lethal animal challenges. Therefore, we wanted to investigate if a co-culture assay based on infection of mouse bone marrow-derived macrophages could be utilized to assess vaccine efficacy against the highly virulent SCHU S4 strain. In view of the previously described superior vaccine-mediated protection conferred by the vaccine candidate $\Delta clpB$ compared to LVS (Kadzhaev et al., 2009; Conlan et al., 2010; Ryden et al., 2012), we asked if this superior trait also was reflected using the co-culture assay. Indeed, we observed that $\Delta clpB$ -immune splenocytes conferred superior control of the SCHU S4 strain compared to LVS-immune splenocytes and efficacy strongly correlated with levels of nitric oxide.

MATERIALS AND METHODS

Bacterial Strains

F. tularensis LVS was originally obtained from the American Type Culture Collection (ATCC 29684). *F. tularensis* strain SCHU S4 (*F. tularensis* subsp. *tularensis*) was obtained from the *Francisella* Strain Collection of the Swedish Defense Research Agency, Umeå, Sweden. The generation in our laboratory of the $\Delta clpB$ strain by allelic replacement of the *clpB* gene, a procedure that did not introduce any recombinant DNA in the strain, has been described previously (Conlan et al., 2010). All bacteriological work related to the SCHU S4 strain was carried out in a biosafety level 3 facility certified by the Swedish Work Environment Authority.

Animals

In the experiments, Balb/c or C57/BL6 mice obtained from Charles River, Germany were used. When required, mice were immunized with a dose of approximately 5×10^3 CFU of the LVS or the $\Delta clpB$ strain subcutaneously. The ensuing infection resulted in no or very mild objective symptoms between days 4 and 6 of the infection. Ethical approval for all of the described mouse experiments was obtained from the Ethical Committee on Animal Research, Umeå, Sweden, A99-11, and A67-14 and the University of Lyon, France (CECCAPP) under the protocol number #ENS_2012_061.

Generation of BMDM

Bone marrow was flushed from femurs of Balb/c or C57BL/6J mice with Dulbecco's Modified Eagle Medium (DMEM). Typically, femurs from two mice were used in each experiment. Cells were washed, a single-cell suspension was prepared by gentle pipetting in complete DMEM [DMEM supplemented with 10% of heat-inactivated fetal bovine serum, 0.2 of mM L-glutamine, (Life Technologies), 1 mM of HEPES buffer (Life Technologies), and 50 μ M of β -mercaptoethanol), and 10% of L-929 conditioned medium. After counting, 5×10^6 BMDM in 10 ml of DMEM were added to a 10 cm Petri dish and incubated at 37°C and 5% CO₂. After 3 days, 5 ml of complete DMEM containing L-929 conditioned medium were added. After 7 days of total incubation, medium was removed, 10 ml of cold PBS/10 mM EDTA was added and the dishes were incubated on ice for 30 min. The macrophages were carefully collected by pipetting, centrifuged, resuspended in complete DMEM and 5×10^5 cells per well were added to 24-well plates and incubated overnight at 37°C and 5% CO₂ and then used in the co-culture assay. The number of viable BMDM was determined after trypan blue staining using Vi-CELL XR cell viability analyzer (Beckman Coulter).

Splenocyte Preparation

Four to 5 weeks following immunization of Balb/c or C57/BL6 mice, spleens were aseptically removed from mice and cells were released by gently squeezing the organs with an L-shaped needle. Splenocytes from three mice were used for each group. Splenocytes were prepared essentially as described (Bosio and Elkins, 2001). A single-cell suspension was prepared, centrifuged and erythrocytes were lysed with ammonium chloride. Cells were washed by centrifugation with PBS + 2% FBS, and resuspended finally in complete DMEM. The number of viable splenocytes was determined after trypan blue staining using Vi-CELL XR cell viability analyzer (Beckman Coulter). The splenocytes were then used either in the co-culture assay or in the *in vitro* recall response assay.

Infection of the BMDM in the Co-culture Assay

Bacteria were grown overnight on Gc-agar plates, resuspended in PBS, and added to the BMDM monolayer at an MOI of 1:5 (bacteria:BMDM). After uptake for 2 h, medium was removed and the macrophage monolayer was washed twice using sterile PBS at RT. One ml of cDMEM containing 20 μ g/ml gentamicin was added to each well, plates were incubated for an additional 45 min and washed twice with PBS. Following the last wash, each BMDM monolayer was overlaid with 1 ml of complete DMEM with 2.5×10^6 of congenic splenocytes, giving a ratio BMDM:splenocytes of 1:5. Bacterial counts were determined by lysis of the cells and plating of serial dilutions (Golovliov et al., 2003). In indicated cultures, 1 mM of N^G-monomethyl-L-arginine (NMMLA) was added simultaneously with the splenocytes and maintained for the remainder of the experiment.

Optimization of the *in vitro* Splenocyte-BMDM Co-culture Model

The *in vitro* co-culture assay was previously established for the LVS strain (Bosio and Elkins, 2001; Cowley and Elkins, 2003). We now optimized the assay so it reproducibly could be used for the SCHU S4 strain as well. This involved the optimization of the ratio between T-cells with the antigen-presenting cells. It was found that a minimum of 4×10^5 BMDM per well and 5-fold more immune splenocytes, i.e., a ratio of 1:5, resulted in the best control of both intracellular LVS and SCHU S4. When the ratio was 1:1, the growth inhibition of LVS and SCHU S4 was on average 0.7 ± 0.1 and $1.3 \pm 0.4 \log_{10}$ CFU, respectively, less than the growth inhibition using the ratio of 1:5. A ratio of 1:10 led to results similar to those using the 1:5 ratio. Also, the role of the bacterial MOI was investigated and bacterial uptake was determined by lysis of the cultures after addition of bacteria for 120 min and it was determined that an MOI of 1:5 (bacteria/BMDM) resulted in optimal growth inhibition.

In vitro Recall Response and Lymphocyte Proliferation Assay

Splenocytes were prepared from naïve mice or from mice immunized with LVS or $\Delta clpB$ as described above and seeded at 2×10^5 in 200 μ L of complete DMEM supplemented with 50 μ M of β -mercaptoethanol per well in 96-well plates. Splenocytes were stimulated with a 1:1 mix of formalin-fixed LVS (fLVS) and formalin-fixed SCHU S4 (fSCHUS4) antigen at a final concentration of 0.5 bacteria/splenocyte or without antigen and incubated in a humidified atmosphere with 5% CO₂ at 37°C. After 3 days the proliferative response of the splenocytes was detected by measuring the [³H]-thymidine incorporation as previously described (Ericsson et al., 1994) or analyzed by FACS as described below.

Nitrite Measurement

The amount of NO₂⁻ in the culture supernatants after 72 h incubation was determined by use of the Griess reagent (Giovannoni et al., 1997). One hundred microliter of the culture supernatant was mixed with 100 μ l each of the Griess reagents, p-Aminobenzenesulfonamide (58 mM in 5% H₃PO₄), and 2,6,8-Trihydroxypurine (3.9 mM) (Sigma). After 10 min of incubation at RT, the absorbance at 540 nm was recorded. The concentration of NO₂⁻ was determined by preparing a standard curve of sodium nitrite. The lower limit of detection in the assay was 1.0 μ M, i.e., below that concentration, medium spiked with nitrite showed an absorbance indistinguishable from that of buffer alone.

Multiplex Cytokine Analysis

Cell culture supernatants, 50 μ L/well, were collected from the same cell cultures as used for assessment of intracellular bacterial replication and stored frozen at -80°C until analyzed using a commercial 23-plex kit (catalog #M60009RDPD) or a custom-made 9-plex kit according to the manufacturer's instructions with a Bio-Plex 200 system (BioRad Laboratories Inc, Hercules, CA, USA). The 9-plex kit contained following cytokines: IL-2, IL-6, IL-12p40, IL-17, IFN- γ , MIP-1 β , GM-CSF, RANTES, and TNF- α .

Flow Cytometry Analysis of Surface Markers and Intracellular Cytokine Staining

Cells were collected after 72 h of incubation from either the lymphocyte proliferation assay or from the co-culture assay. Non-adherent cells were transferred to a new plate and 5 $\mu\text{g}/\text{mL}$ of Brefeldin A was added. Four h later, plates were centrifuged for 3 min at $500 \times g$ and supernatants were removed. After blocking of the Fc γ receptors with CD16/CD32 mouse BD Fc block (clone 2.4G2, BD Biosciences), cells were labeled with cell surface marker monoclonal antibodies (mAb) and conjugated intracellular cytokine mAb as recommended by BD Biosciences. The following mAb conjugates were used: CD3-APCCy7 (clone 17A2, BD Biosciences), CD4-AF700 (clone RM4-5, BD Biosciences), CD8-PerCPCy5.5 (clone 53-6.7, BD Biosciences), IFN γ -PE-CF594 (clone XMG1.2, BD Biosciences), TNF- α -Brilliant violet 421 (clone MP6-XT22, BioLegend), IL17A-PE/Cy7 (clone TC11-18H10.1, BD Biosciences). Aqua Viability Dye (Molecular Probes/Invitrogen) was added to distinguish live and dead cells. Cells were acquired using an LSRII flow cytometer (BD Biosciences) with FACSDiva software (BD Biosciences). Results were analyzed using FlowJo software (Tree Star).

Data Analysis and Statistical Methods

Two sample 2-tailed *t*-test, Mann-Whitney U or for paired data, Wilcoxon's signed rank test, were used to identify significant differences ($P < 0.05$) between data sets. To analyze correlation between data sets, Spearman's rank correlation test was used. A correlation with a coefficient (RS) above 0.4 was considered to demonstrate significant correlation, and a coefficient above 0.7 was considered to indicate strong correlation. When multiple experiments formed the basis for the analysis, the cumulative data were presented as boxplots. In each boxplot, the line through each box shows the median, with quartile one, and three as the lower and upper limits of each box. The end of the vertical lines indicates maximum and minimum values, respectively.

RESULTS

Splenocyte Recall Response

Splenocytes from mice immunized with LVS or $\Delta clpB$ were stimulated with formalin-killed *F. tularensis* antigen *in vitro* to measure the recall response of the T-cells with regard to proliferation and expression of cytokines. To accommodate for the different backgrounds of the two strains, a mixture prepared of equal amounts from LVS and SCHU S4 was analyzed to assess the immune reactivity. Both LVS- and $\Delta clpB$ -immune Balb/c splenocytes responded with very prominent proliferative responses to the antigen and the responses were stronger, although not significantly stronger, of $\Delta clpB$ - compared to LVS-immune splenocytes ($P = 0.16$; **Figure 1A**). Intracellular staining for IFN γ and TNF- α showed that the percentages of CD4⁺ and CD8⁺ T-cells expressing the respective cytokine were significantly higher ($P < 0.05$) among $\Delta clpB$ - than LVS-immune splenocytes (**Figures 1B–E**).

Overall, the results show that $\Delta clpB$ -immune splenocytes demonstrated more prominent recall responses *in vitro* to the *F. tularensis* antigen than did LVS-immune splenocytes.

Growth Inhibition of *F. tularensis* LVS and Cytokine Production Conferred by LVS- or $\Delta clpB$ -Immune Splenocytes

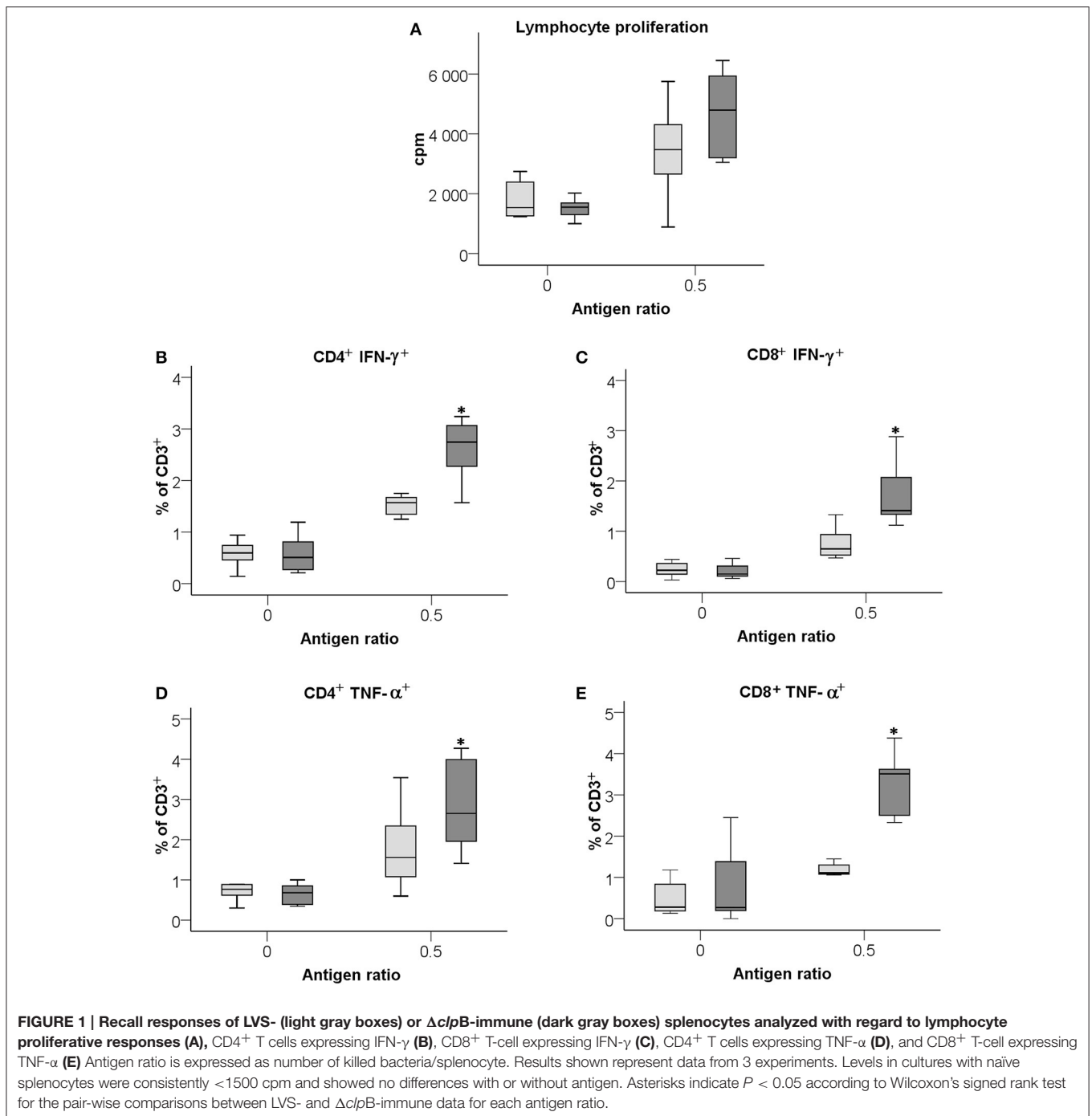
The capacity of splenocytes from LVS- or $\Delta clpB$ -immunized mice to inhibit the intracellular growth of LVS in splenocyte-BMDM co-cultures was assessed. Addition of either type of immune splenocyte to the cultures significantly inhibited growth of LVS better than did naïve splenocytes, the median growth and the interquartile (IQ) one and three for all experiments performed were 3.2 [2.4, 3.8] and 2.4 [1.7, 3.4] log₁₀ CFU for LVS-immune splenocytes and $\Delta clpB$ -immune splenocytes, respectively, vs. 5.2 [4.9, 5.6] log₁₀ CFU for naïve splenocytes ($P < 0.001$ for immune vs. naïve). The $\Delta clpB$ -immune splenocytes showed superior control compared to LVS-immune splenocytes, $P < 0.001$ (**Figure 2A**). Not only growth inhibition was more prominent in cultures with $\Delta clpB$ -immune than LVS-immune splenocytes, but also levels of IFN- γ , IL-17, and GM-CSF in the culture supernatants were higher ($P < 0.001$; $P < 0.05$ and $P < 0.001$, respectively; **Figures 2B–D**).

In total, levels of 23 cytokines were analyzed in the supernatants from the co-cultures and 17 of those were found to be upregulated more than 2-fold in cultures with either of the immune splenocytes vs. cultures with naïve splenocytes, whereas MIP-1 α was the sole cytokine being suppressed in cultures with immune splenocytes (Table S1). It was further analyzed how the cytokine levels of the supernatants correlated to the degree of protection, i.e., growth inhibition. Also, the correlations between the levels of the 23 cytokines and IFN- γ were analyzed. Growth inhibition was highly correlated ($P < 0.01$) to IFN- γ , GM-CSF, IL-10, IL-13, MIP-1 α , and RANTES and among these cytokines, GM-CSF, MIP-1 α , and RANTES were highly correlated ($P < 0.01$) to IFN- γ (**Table 1**). In addition, IFN- γ was highly correlated ($P < 0.01$) to IL-17, IL-6, IL-12p40, eotaxin, G-CSF, MCP-1, and MIP-1 β (**Table 1**). From the 23 cytokines, 9 cytokines were chosen for use in subsequent analyses, since they all discriminated between levels in cultures with LVS- vs. $\Delta clpB$ -immunized splenocytes.

In summary, several of the cytokines, including IFN- γ , strongly correlated to growth inhibition. Superior containment of LVS bacteria was observed in cultures with $\Delta clpB$ - vs. LVS-immune cells. The cytokine profile in the cultures with immune splenocytes reflected a Th1-type immune response.

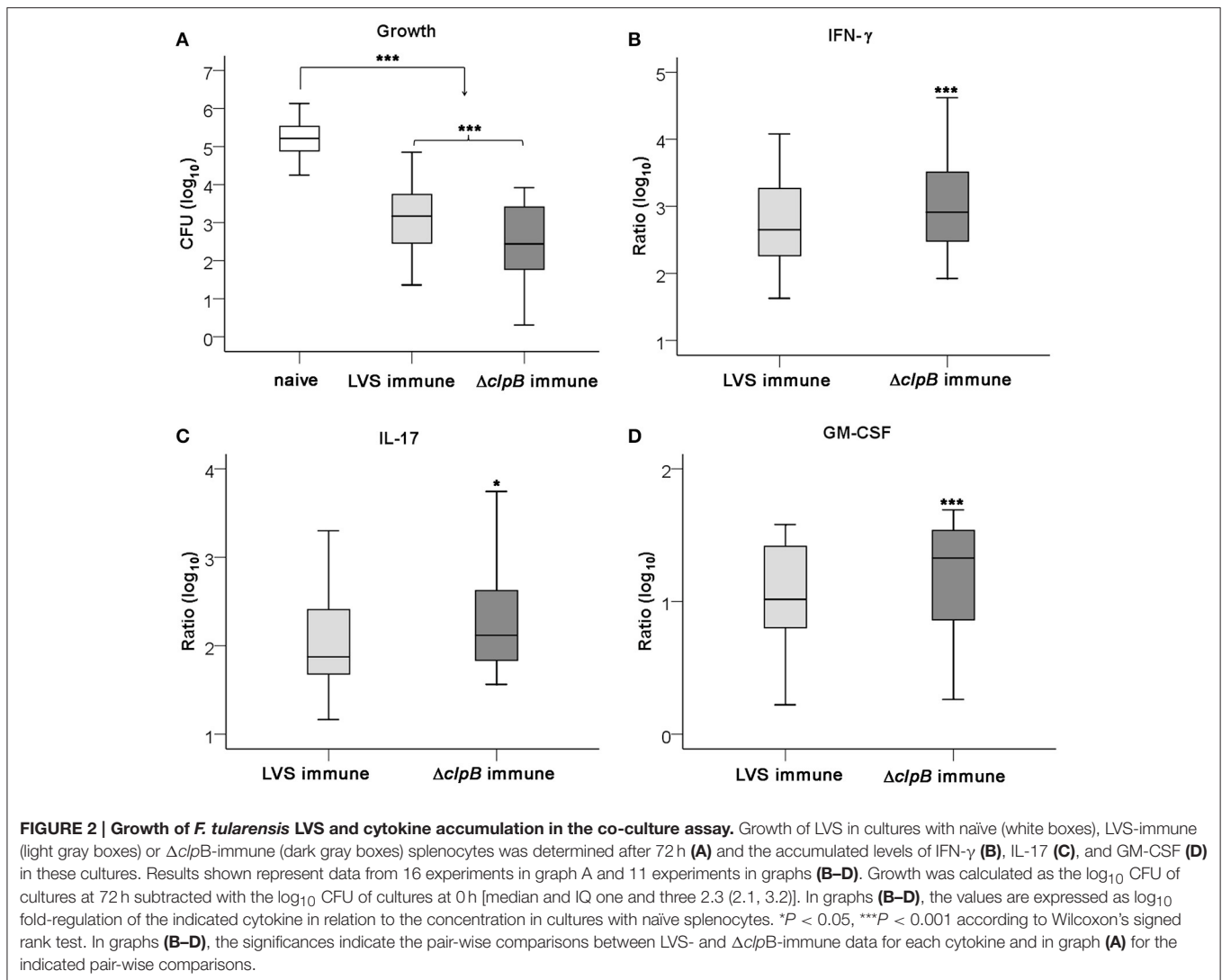
Characterization of Immune Splenocytes from the LVS-Infected Co-cultures

To better understand the enhanced ability of the $\Delta clpB$ -immune splenocytes to control the replication of *F. tularensis* LVS, the percentage of IFN- γ -, TNF- α -, and IL-17-producing T cells were quantified by FACS analysis. IL-17 has in several publications been found to correlate to protection against *F. tularensis* (Lin et al., 2009; Mahawar et al., 2013). Analysis was performed on non-adherent cells from the cultures after 72 h of incubation. There were higher percentages of CD4⁺ and CD8⁺ T cells expressing IFN- γ in cultures from the immunized groups vs. the naïve group ($P < 0.05$) and among the immunized groups, cultures with $\Delta clpB$ -immune splenocytes expressed higher percentages ($P < 0.05$) of IFN- γ -positive cells



among both the CD4⁺ and CD8⁺ subsets (Figure 3). Levels of cells expressing either IL-17 or TNF- α were similar between the immunized groups and the naïve group. Some studies have demonstrated that polyfunctional T cells demonstrate good correlation with host protection (Darrah et al., 2007; Derrick et al., 2011) and we identified such *F. tularensis*-specific T cells as part of the human immune response (Enesl tt et al., 2012). Also in the splenocyte-BMDM co-culture model, we observed the presence of polyfunctional *F. tularensis*-specific T cells, since in cultures with immune splenocytes, CD4⁺ and CD8⁺

T cells expressing IFN- γ and IL-17 or IFN- γ and TNF- α were significantly increased compared to cultures with naïve cells ($P < 0.05$). In all instances, the frequencies of the bifunctional T cells were significantly higher in cultures with $\Delta clpB$ -immune compared to LVS-immune splenocytes ($P < 0.05$) (Figure 3). Also, trifunctional CD4⁺ and CD8⁺ T cells were increased in cultures with immune splenocytes ($P < 0.05$) and, again, more frequent among $\Delta clpB$ -immune compared to LVS-immune splenocytes ($P < 0.05$; Figure 3). Median fluorescence intensity (MFI) of the immune splenocytes was analyzed for IFN- γ , IL-17,



and TNF- α . Whereas, there were no significant differences for the latter two cytokines, $\Delta clpB$ -immune splenocytes demonstrated significantly higher MFI of IFN- γ expression among the CD4⁺ T cell populations than did LVS-immune splenocytes, median levels were 2430 [1890, 7710] vs. 1210 [670, 3930] ($P < 0.05$).

Collectively, the data demonstrated that there were qualitative and quantitative differences between $\Delta clpB$ - and LVS-immune splenocytes with regard to cytokine expression, since the $\Delta clpB$ -immune population contained higher frequencies of polyfunctional CD4⁺ and CD8⁺ T cells expressing IFN- γ in combination with IL-17 and/or TNF- α and also higher MFI of the IFN- γ -expressing CD4⁺ T cells.

Growth Inhibition of *F. tularensis* SCHU S4 and Cytokine Production Conferred by LVS- or $\Delta clpB$ -Immune Splenocytes

In agreement with our present findings, the splenocyte-BMDM co-culture assay has previously been demonstrated to mediate

efficient control of LVS infection, but few studies have analyzed the requirements for the control of virulent *F. tularensis* strains (Mahawar et al., 2013; Griffin et al., 2015). Therefore, the same protocol as previously described for the LVS infection was used, but the highly virulent strain, SCHU S4, was instead used to infect the cultures. As was demonstrated for the LVS infection, $\Delta clpB$ -immune splenocytes conferred superior control of SCHU S4 compared to LVS-immune splenocytes ($P < 0.001$; Figure 4A). In fact, the LVS-immune cells did not restrict the growth of SCHU S4 to the same extent as of LVS, median growth was 4.2 [3.1, 4.4] vs. 3.2 [2.4, 3.8], respectively ($P < 0.001$; Figures 2A, 4A). In contrast, $\Delta clpB$ -immune Balb/c-derived splenocytes conferred as efficient growth inhibition of SCHU S4 as of LVS, median growth was 2.8 [1.9, 3.8] and 2.4 [1.7, 3.4] \log_{10} CFU, respectively ($P > 0.05$; Figures 2A, 4A). The cytokine profile of SCHU S4-infected cultures resembled that of LVS-infected cultures, but many of the cytokines were somewhat higher expressed in the cultures with SCHU S4 (Table S1). Thus, SCHU S4-infected cultures with $\Delta clpB$ -immune splenocytes contained higher levels

of IFN- γ , GM-CSF, and IL-17 than the cultures with LVS-immune splenocytes ($P < 0.01$ for IFN- γ and GM-CSF and $P < 0.05$ for IL-17: **Figures 4B–D**).

In summary, LVS-immune cells did not control SCHU S4 as well as it controlled LVS, whereas $\Delta clpB$ -immune cells showed superior control and controlled both strains to a similar extent. $\Delta clpB$ -immune cells induced higher levels of IFN- γ , IL-17, and GM-CSF than did LVS-immune cells.

Nitric Oxide Production in Splenocyte-BMDM Co-Cultures

Nitrite was measured in the supernatants of splenocyte-BMDM co-cultures infected with LVS and it was observed that the levels strongly correlated to growth inhibition (Spearman's rank correlation coefficient [ρ] = 0.679, $P < 0.01$; **Figure 5A**). Nitrite levels were also highly correlated ($P < 0.01$) to levels of IFN- γ , GM-CSF, IL-6, IL-10, IL-12(p40), and RANTES (**Table 1**). $\Delta clpB$ -immune Balb/c-derived splenocytes stimulated higher nitrite production than did LVS-immune splenocytes, medians were 21 μM [16, 26] vs. 16 μM [10, 23], respectively ($P < 0.05$; **Figure 6**). Also when SCHU S4 was the infecting agent, nitrite levels strongly correlated to growth inhibition ($\rho = 0.745$, $P < 0.001$; **Figure 5B**) and, again, cultures with $\Delta clpB$ -immune splenocytes displayed significantly higher levels of nitrite than did cultures with LVS-immune splenocytes, medians were 15 [9, 23] and 9 [5, 20] μM , respectively ($P < 0.01$; **Figure 6**).

In summary, these results demonstrate that $\Delta clpB$ -immune splenocytes showed superior capacity compared to LVS-immune

splenocytes to stimulate nitrite production in the splenocyte-BMDM co-cultures and identify nitrite as a correlate of growth inhibition of both LVS and the highly virulent strain SCHU S4.

Nitric Oxide-Dependent Growth Inhibition

Since nitrite levels correlated to the growth inhibition of *F. tularensis* effectuated by the immune splenocytes, it was further investigated if there was a direct correlation between the growth inhibition of *F. tularensis* and NO by use of the competitive inhibitor of iNOS, NMMLA. This treatment significantly reduced the growth inhibition of LVS or SCHU S4 conferred by the immune Balb/c-derived splenocytes (**Figures 7A,B**) and also reduced the nitrite production to about 1 μM compared to levels of at least 8.0 μM in its absence (**Figures 7C,D**). Levels in cultures with naïve splenocytes were consistently below 1 μM .

The role of NO was further investigated by use of BMDM derived from iNOS $^{-/-}$ C57BL/6 mice. It should be noted that also these mice, like Balb/c mice, generate robust immunity after vaccination, since a majority survived an intradermal challenge of 1900 CFU and all of 5 mice survived 190 CFU after intradermal immunization with $\Delta clpB$ (**Table 2**), whereas the lethal dose for naïve mice was one CFU. In contrast, all of LVS-immunized mice succumbed to a challenge of 19 CFU within 22 days and maximal survival was even shorter when the challenge dose was 190 or 1900 CFU (**Table 2**). Thus, as for Balb/c mice (Conlan et al., 2010), immunization with $\Delta clpB$ confers superior protection in C57BL/6 mice.

Similar to the splenocytes derived from Balb/c mice, C57BL/6-derived $\Delta clpB$ -immune splenocytes controlled growth of LVS and SCHU S4 better than did LVS-immune splenocytes, $P < 0.05$ and $P < 0.01$, respectively (**Figures 8A,B**), and induced higher nitrite production in the cultures, $P < 0.01$ and $P < 0.05$ for LVS- and SCHU S4-infected cultures, respectively

TABLE 1 | Correlations between growth inhibition, nitrite levels, IFN- γ levels and levels of other cytokines.

	Growth inhibition ^a	IFN- γ ^b	Nitrite ^c
Growth inhibition	1.000	0.481**	0.679**
IFN- γ	0.481 ^{d**}	1.000	0.525**
Nitrite	0.679**	0.525**	1.000
GM-CSF	0.356**	0.447**	0.435**
IL-10	0.499**	-0.007	0.560**
MIP-1 α	0.576**	0.727**	0.238
IL-13	0.672**	0.566**	0.440*
RANTES	0.380**	0.718**	0.643**
IL-17	0.145	0.697**	0.241
IL-6	0.281*	0.898**	0.416**
IL-12(p40)	0.252	0.607**	0.488**
Eotaxin	0.353*	0.441**	0.186
G-CSF	0.066	0.664**	-0.244
MCP-1	0.228	0.713**	-0.450*
MIP-1 β	0.307*	0.495**	0.342*

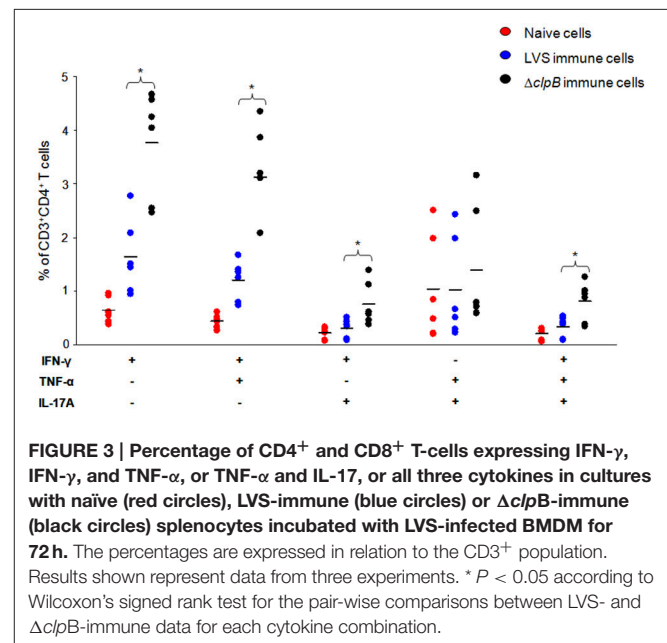
^a Growth inhibition of *F. tularensis* LVS in cultures with LVS-immune or $\Delta clpB$ -immune splenocytes vs. naïve splenocytes in the in vitro assay after 72 h.

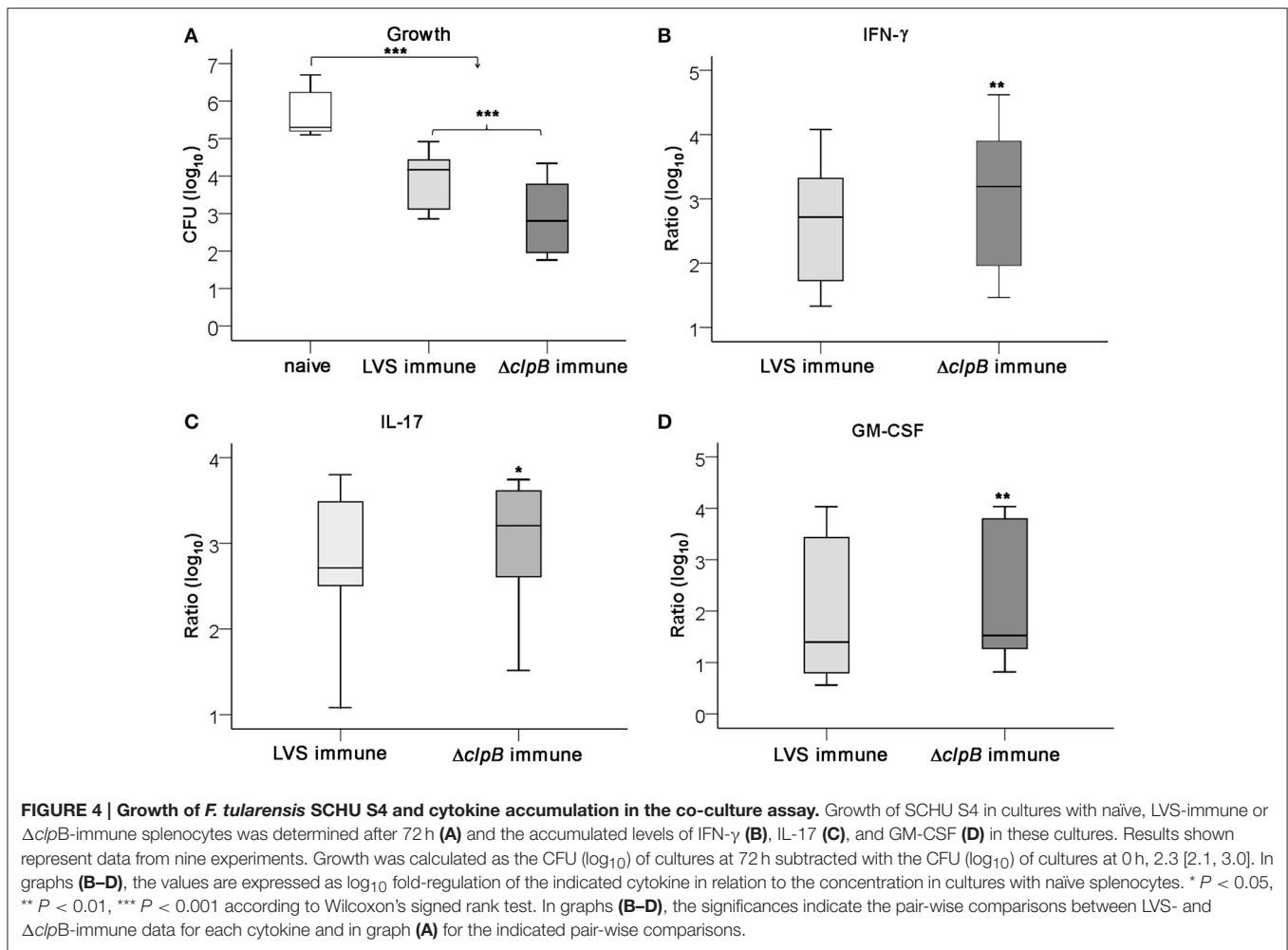
^b Levels of cytokines measured in the supernatants of the in vitro assay after 72 h.

^c Levels of nitrite measured in the supernatants of the in vitro assay after 72 h.

^d Spearman's rank correlation coefficient between indicated combination.

* $P < 0.05$; ** $P < 0.01$.





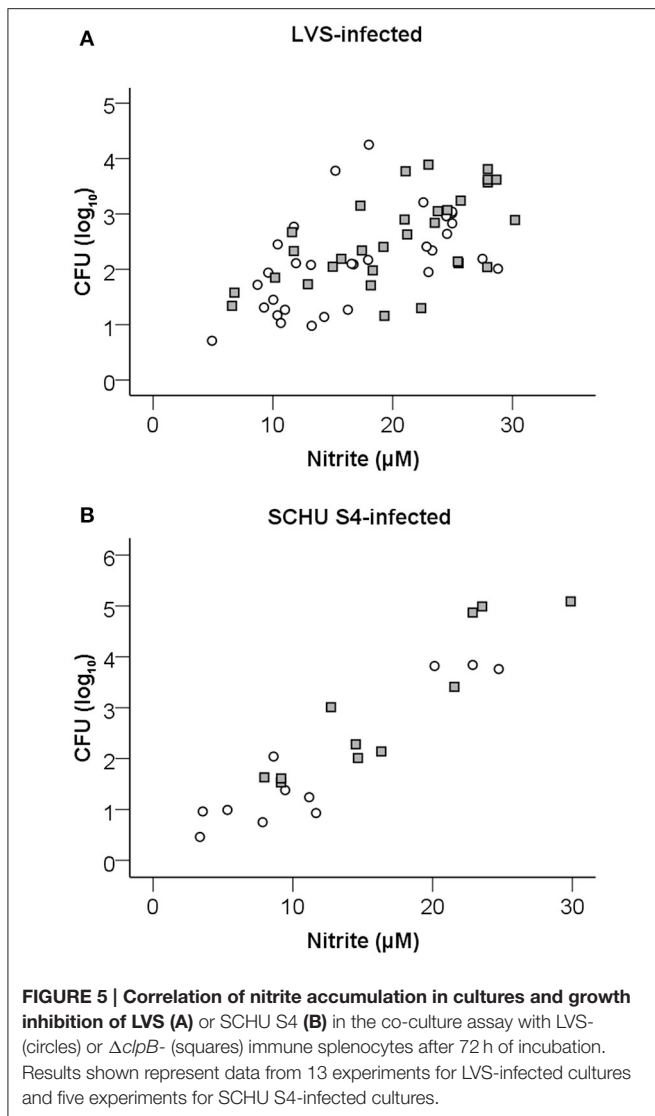
(Figures 8C,D). Also in cultures with C57BL/6 cells, as in cultures with Balb/cJ cells, the nitrite levels were highly correlated to the growth inhibition of both LVS and SCHU S4 ($\rho = 0.745$ and 0.771 , respectively, $P < 0.01$). Further corroborating the role of NO, the growth inhibition elicited by the immune splenocytes was significantly lower ($P < 0.001$) in cultures with $iNOS^{-/-}$ BMDM compared to C57BL/6 BMDM, whether or not the cultures were infected with LVS or SCHU S4 (Figures 8A,B). However, even in the absence of iNOS-derived NO, LVS- and $\Delta clpB$ -immune splenocytes still reduced the growth of LVS, median net growth were 4.3 [3.9, 4.7] and 3.5 [3.4, 3.7] \log_{10} CFU, respectively, vs. 5.1 [4.7, 5.1] for naïve splenocytes; $\Delta clpB$ -immune splenocytes being significantly superior to LVS-immune splenocytes ($P < 0.001$; Figure 8A). In contrast, growth inhibition of SCHU S4 in cultures with $iNOS^{-/-}$ BMDM was very minor or non-existent for both LVS- and $\Delta clpB$ -immune splenocytes (Figure 8B).

Collectively, the data obtained with C57BL/6-derived cells confirmed the results based on the Balb/c-derived cells, i.e., $\Delta clpB$ -immune splenocytes showed superior capacity compared to LVS-immune splenocytes to control the *F. tularensis* infection and the $\Delta clpB$ -immune splenocytes induced higher levels

of nitrite production, which strongly correlated to growth inhibition. In addition, iNOS was found to be critically required for the growth inhibition of SCHU S4 and contributed significantly to the control of LVS.

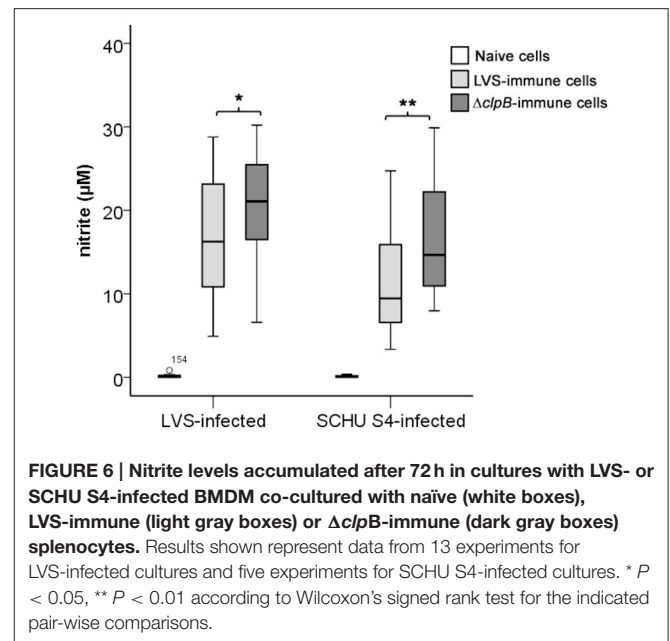
DISCUSSION

It is well-established that protection against many intracellular pathogens is critically dependent on cell-mediated immunity, however, there are no methods validated to identify correlates of protection to these pathogens. In addition, for diseases like tularemia, which is infrequent in most parts of the world, the power of human clinical trials is unlikely to be sufficient to provide unambiguous data regarding the efficacy of vaccine candidates. To this end, the Animal Rule is an option for licensing of future tularemia vaccines and this option is most likely applicable to biodefense agents and sporadically occurring diseases, both of which are relevant to tularemia. Critically required in this regard is the identification of correlates of protection, i.e., a measurement of a biologically relevant function for and correlated to the degree of protection conferred in



the animal model. For tularemia and other diseases caused by intracellular pathogens, e.g., tuberculosis, much focus has been on the role of IFN- γ as a correlate of protection. Although important for the protection *in vitro* to *Mycobacterium tuberculosis*, levels of the cytokine have not shown good correlation to protection in various clinical and experimental models (Goldsack and Kirman, 2007; Mittrücker et al., 2007; Jeevan et al., 2009). With regard to tularemia, IFN- γ appears to be necessary, although not sufficient for protection (Elkins et al., 2007; Conlan, 2011). Thus, there is a need to develop models to better define the correlates of protection against tularemia.

The use of the splenocyte-BMDM co-culture model demonstrates distinct advantages compared to commonly used animal models for tularemia, since the number of animals required will be far less and the mice that are immunized as a source of splenocytes receive a sublethal dose that results in few or no objective symptoms. Thus, the method leads to both distinct reduction of the number of animals required, as well as refinement, since the distress caused by the sublethal infection



will be minimal. In addition, the use of the co-culture model allows for direct comparisons of correlates with those identified in human models. In fact, a human co-culture model, based on the use of adherent and non-adherent peripheral blood mononuclear leukocytes from LVS-vaccinated individuals or former tularemia patients, shows promise in this regard (Eneslätt et al., unpublished). Since it is likely that human challenge studies never will be performed in the future, the use of a human co-culture model may be the only realistic way to identify correlates of immunity and protection. A limitation of co-culture models is there will be a selection of cell types included and the model may therefore not be representative for certain organ-specific immune responses *in vivo*. It should be noted that there are examples when organ-specific *F. tularensis* co-culture models have been utilized to overcome this limitation (De Pascalis et al., 2014).

Although previous studies based on splenocyte-BMDM co-culture models have revealed much about the vaccine-mediated protection; both the prerequisites for protection against LVS as well as putative correlates of protection, there have been very few studies with virulent *F. tularensis* strains based on a co-culture system (Mahawar et al., 2013; Griffin et al., 2015).

The present study used the LVS strain as benchmark for *F. tularensis* vaccine efficacy. Vaccination with LVS effectively prevents laboratory-acquired infection, but studies on volunteers have revealed that it affords only marginal protection against aerosol infection (Saslaw et al., 1961a,b; Burke, 1977). It was hypothesized that it would be possible to generate a superior *F. tularensis* vaccine and we and others have generated a number of targeted mutants of SCHU S4 and their efficacy has been evaluated using *in vivo* models with virulent *F. tularensis* strains (Kadzhaev et al., 2009; Conlan et al., 2010; Shen et al., 2010; Ryden et al., 2012; Santiago et al., 2015). In particular one mutant, $\Delta cIpB$, was found to confer superior efficacy to LVS, as

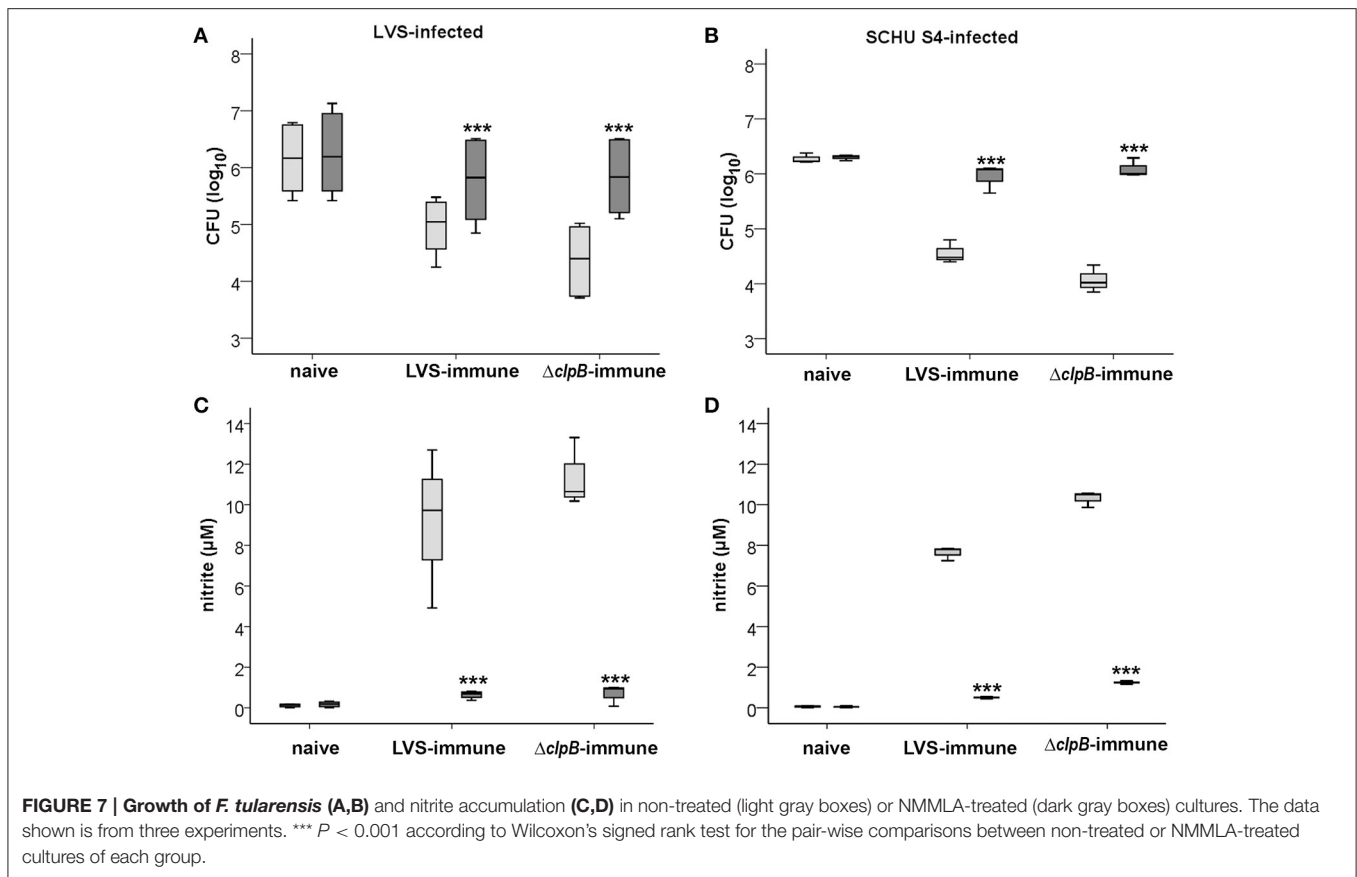


TABLE 2 | Protective effect of LVS or $\Delta clpB$ immunization of C57/BL6 mice against intradermal challenge with SCHU S4.

Immunization ^a	Challenge dose ^b	Time of survival (days)
LVS	19 CFU	7, 8, 9, 11, 22
$\Delta clpB$	19 CFU	24, >33, >33, >33, >33
LVS	190 CFU	7, 8, 12, 12
$\Delta clpB$	190 CFU	>33, >33, >33, >33, >33
LVS	1900 CFU	7, 8, 8, 9, 17
$\Delta clpB$	1900 CFU	17, 22, 33, 33, 33
None	19 CFU	6, 6, 6, 6, 6

^a Mice were intradermally immunized with 100,000 CFU of the LVS or the $\Delta clpB$ strain.

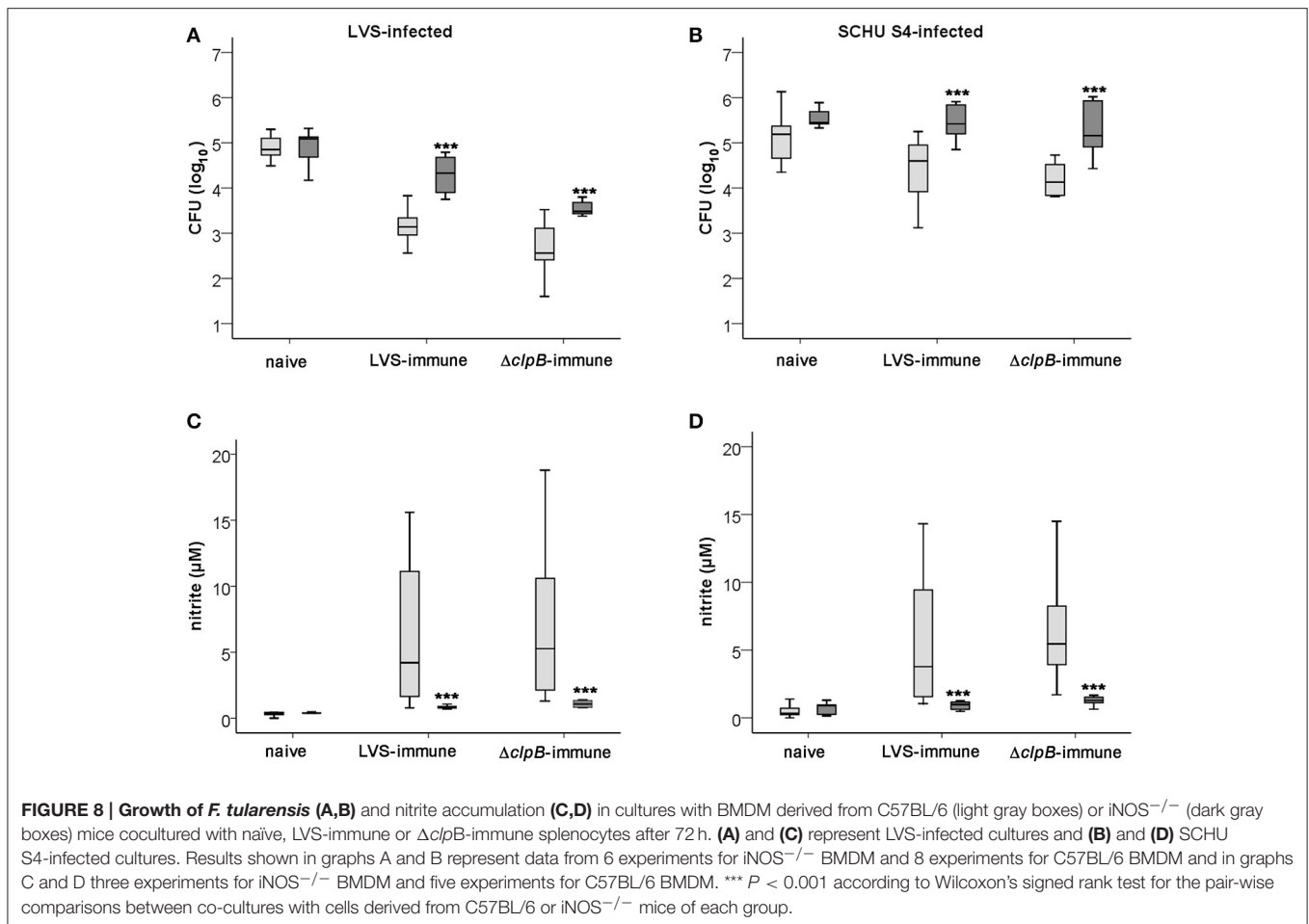
^b Mice were 6 weeks after immunization challenged intradermally with the indicated dose of SCHU S4.

demonstrated by survival after infection with SCHU S4 (Conlan et al., 2010). In agreement with the findings in both Balb/c and C57BL/6 mice, our findings using the splenocyte-BMDM co-culture method demonstrate that the $\Delta clpB$ -immune splenocytes were superior to LVS-immune splenocytes in several aspects, most notably that the $\Delta clpB$ -immune splenocytes conferred superior control of both LVS and SCHU S4 infection. In addition, LVS-immune splenocytes conferred significantly less control of SCHU S4 than LVS. Likewise, a previous study demonstrated

that LVS-immune splenocytes controlled SCHU S4 infection only when pre-stimulated *in vitro* (Griffin et al., 2015).

Although previous studies based on various splenocyte-BMDM co-culture models have revealed much about the vaccine-mediated protection; both the prerequisites for protection against LVS as well as putative correlates of protection, there have been very few studies with virulent *F. tularensis* strains based on a co-culture system (Mahawar et al., 2013; Griffin et al., 2015) and, therefore, the present study provides important information regarding the protective mechanisms operative against the highly virulent SCHU S4 strain. In agreement with the previous studies (Mahawar et al., 2013; Griffin et al., 2015), our findings demonstrate a strong correlation between the ability of the vaccine strains to confer protection to virulent strains *in vivo* and their capability to efficiently prime the protective efficacy of the immune cells as measured by the splenocyte-BMDM co-culture model. In addition, our study reveals that the quality of the immune responses elicited by LVS and $\Delta clpB$ are similar, although the response elicited by the $\Delta clpB$ vaccine is quantitatively more robust.

Multi-parameter flow cytometry has been used rather extensively to characterize memory T cells and the technique has enabled detailed descriptions of their phenotypic characteristics and functional abilities. In various experimental models, it has been argued that specific polyfunctional T cells demonstrate good correlation with host protection. While promising in the



context of mouse models of *Leishmania* and certain tuberculosis vaccines (Darrah et al., 2007; Derrick et al., 2011), polyfunctional T cells have in other cases failed to demonstrate correlation to protection (Connor et al., 2010; Kagina et al., 2010; Harari et al., 2011). Human responses to killed *F. tularensis* antigens from the LVS or SCHU S4 strains have been characterized using multi-parameter flow cytometry and it was found that IFN- γ and MIP-1 β strongly discriminated between immune and naïve individuals (Enesl tt et al., 2012). Also in the present study, we found evidence that the immune cell populations contained polyfunctional T cells, expressing combinations of IFN- γ , TNF- α , and IL-17. Interestingly, the relative frequencies of all variants of polyfunctional CD4⁺ and CD8⁺ T cells expressing IFN- γ was consistently higher among $\Delta clpB$ - than LVS-immune splenocytes.

Also in other important aspects, there were quantitative differences between the immune responses triggered by the $\Delta clpB$ - vs. the LVS-immune splenocytes, since the $\Delta clpB$ -immune splenocytes demonstrated stronger proliferative responses and higher production of NO, IFN- γ , GM-CSF, and IL-17, all of which correlated to growth inhibition. Altogether, all of these properties of the $\Delta clpB$ -immune splenocytes, together with their superior ability to confer growth inhibition of SCHU

S4, help to explain the efficaciousness of $\Delta clpB$. An interesting finding was that IFN- γ was the most strongly induced cytokine after addition of immune splenocytes, whether or not they were derived from $\Delta clpB$ - or LVS-immunized mice. Considering the critical role of IFN- γ for many aspects of immunity to *F. tularensis*, the finding shows that the splenocyte-BMDM co-culture system used herein mirrors relevant aspects of other models of tularemia.

The effect of adding splenocytes derived from either C57BL/6 or Balb/cJ was also analyzed. In both instances, $\Delta clpB$ -immune splenocytes showed superior capacity compared to LVS-immune splenocytes to control the *F. tularensis* infection and also to induce production of higher levels of NO. This demonstrates that the distinct differences between $\Delta clpB$ -immune and LVS-immune splenocytes were not affected by the genetic background of the splenocytes.

It has been shown that control of LVS in a macrophage-BMDM co-culture assay correlated with levels of nitrite (Bosio and Elkins, 2001; Elkins et al., 2009). Our results using the co-culture method provided strong evidence for the critical role of NO for control also of the SCHU S4 infection as supported both by experiments using an inhibitor of iNOS, as well as iNOS-deficient BMDM. Although this may appear somewhat

paradoxical, considering that NO plays a minor or insignificant role *in vitro* (Lindgren et al., 2005; Edwards et al., 2010), it is likely that NO production in the rather complex splenocyte-BMDM co-culture model used herein confers additional effects compared to the model based on monocytic cells only. In further support of the important role of NO, it exerts a critical function *in vivo*, since iNOS-deficient mice succumb even to the lowest inocula of an LVS infection (Lindgren et al., 2004).

The enhanced NO production in $\Delta clpB$ cultures was likely dependent on the higher secretion of IFN- γ and IL-17, and the higher frequency of polyfunctional T cells, expressing combinations of IFN-, TNF- α , and IL-17, since these cytokines regulate iNOS. Regulation of iNOS is in many aspects distinct among species, but the critical roles of IFN- γ , TNF- α , IL-1 β , and IL-17 to induce its expression appears to be conserved regardless of species (Pautz et al., 2010; Mühl et al., 2011). Many studies have demonstrated a critical role of NO in various murine infectious models, but there is also significant evidence supporting its role for control of human infectious diseases. One notable example is tuberculosis, the etiological agent of which is a facultative intracellular bacterium, as for tularemia. It has been observed that human *M. tuberculosis*-infected monocytes produce NO and this results in a bacteriostatic, and sometimes even bactericidal effect (Landes et al., 2015). Further corroborating an important role of NO, it has been observed that iNOS expression is increased in human granulomas (Mattila et al., 2013). Malaria is another important human disease where there is evidence for a critical role of NO, since endogenous production of asymmetrical dimethylarginine, an iNOS inhibitor, strongly correlated to mortality (Yeo et al., 2010). Collectively, such findings suggest that NO could have an important role in other human diseases, such as tularemia, and, therefore, that the findings regarding the

superior protection conferred by $\Delta clpB$ in the mouse model also will have relevance for the human situation.

Overall, our results provide new information as to why $\Delta clpB$ is superior to LVS as a vaccine for protection against highly virulent *F. tularensis*. The information is critical for the understanding of protective mechanisms and thereby for important for licensing of future vaccines against this potent pathogen.

AUTHOR CONTRIBUTIONS

Conceived and designed the experiments: IG, HL, KE, AS, Performed the experiments: IG, HL, KE, AM, WC, Analyzed the data: IG; HL, KE, WC, AS, Contributed reagents/materials/analysis tools: AM, TH. Wrote the paper: IG, HL, TH, AS.

FUNDING

Grant support was obtained from the Swedish Medical Research Council (K2012-3469 and K2013-8621), Västerbottens läns landsting (Spjutspetsmedel, VLL-582571, Centrala ALF medel, VLL-463691), the Medical Faculty, Umeå University, Umeå, Sweden, and from the ERC (ERC starting grant 311542 to TH). The work was performed in part at the Umeå Centre for Microbial Research (UCMR).

SUPPLEMENTARY MATERIAL

The Supplementary Material for this article can be found online at: <http://journal.frontiersin.org/article/10.3389/fcimb.2016.00152/full#supplementary-material>

REFERENCES

- Bosio, C. M., and Elkins, K. L. (2001). Susceptibility to secondary *Francisella tularensis* live vaccine strain infection in B-cell-deficient mice is associated with neutrophilia but not with defects in specific T-cell-mediated immunity. *Infect. Immun.* 69, 194–203. doi: 10.1128/IAI.69.1.194-203.2001
- Burke, D. S. (1977). Immunization against tularemia: analysis of the effectiveness of live *Francisella tularensis* vaccine in prevention of laboratory-acquired tularemia. *J. Infect. Dis.* 135, 55–60. doi: 10.1093/infdis/135.1.55
- Collazo, C. M., Meierovics, A. I., De Pascalis, R., Wu, T. H., Lyons, C. R., and Elkins, K. L. (2009). T cells from lungs and livers of *Francisella tularensis* - immune mice control the growth of intracellular bacteria. *Infect. Immun.* 77, 2010–2021. doi: 10.1128/IAI.01322-08
- Conlan, J. W. (2011). Tularemia vaccines: recent developments and remaining hurdles. *Future Microbiol.* 6, 391–405. doi: 10.2217/fmb.11.22
- Conlan, J. W., Shen, H., Golovliov, I., Zingmark, C., Oyston, P. C., Chen, W., et al. (2010). Differential ability of novel attenuated targeted deletion mutants of *Francisella tularensis* subspecies *tularensis* strain SCHU S4 to protect mice against aerosol challenge with virulent bacteria: effects of host background and route of immunization. *Vaccine* 28, 1824–1831. doi: 10.1016/j.vaccine.2009.12.001
- Connor, L. M., Harvie, M. C., Rich, F. J., Quinn, K. M., Brinkmann, V., Le Gros, G., et al. (2010). A key role for lung-resident memory lymphocytes in protective immune responses after BCG vaccination. *Eur. J. Immunol.* 40, 2482–2492. doi: 10.1002/eji.200940279
- Cowley, S. C., and Elkins, K. L. (2003). Multiple T cell subsets control *Francisella tularensis* LVS intracellular growth without stimulation through macrophage interferon gamma receptors. *J. Exp. Med.* 198, 379–389. doi: 10.1084/jem.20030687
- Cowley, S. C., and Elkins, K. L. (2011). Immunity to *Francisella*. *Front. Microbiol.* 2:26. doi: 10.3389/fmicb.2011.00026
- Cowley, S. C., Hamilton, E., Frelinger, J. A., Su, J., Forman, J., and Elkins, K. L. (2005). CD4-CD8- T cells control intracellular bacterial infections both *in vitro* and *in vivo*. *J. Exp. Med.* 202, 309–319. doi: 10.1084/jem.20050569
- Darrah, P. A., Patel, D. T., De Luca, P. M., Lindsay, R. W., Davey, D. F., Flynn, B. J., et al. (2007). Multifunctional TH1 cells define a correlate of vaccine-mediated protection against *Leishmania major*. *Nat. Med.* 13, 843–850. doi: 10.1038/nm1592
- De Pascalis, R., Chou, A. Y., Bosio, C. M., Huang, C. Y., Follmann, D. A., and Elkins, K. L. (2012). Development of functional and molecular correlates of vaccine-induced protection for a model intracellular pathogen, *Francisella tularensis* LVS. *PLoS Pathog.* 8:e1002494. doi: 10.1371/journal.ppat.1002494
- De Pascalis, R., Chou, A. Y., Ryden, P., Kennett, N. J., Sjöstedt, A., and Elkins, K. L. (2014). Models derived from *in vitro* analyses of spleen, liver, and lung leukocyte functions predict vaccine efficacy against the *Francisella tularensis* Live Vaccine Strain (LVS). *MBio* 5:e00936. doi: 10.1128/mbio.00936-13
- De Pascalis, R., Taylor, B. C., and Elkins, K. L. (2008). Diverse myeloid and lymphoid cell subpopulations produce gamma interferon during early innate immune responses to *Francisella tularensis* live vaccine strain. *Infect. Immun.* 76, 4311–4321. doi: 10.1128/IAI.00514-08

- Derrick, S. C., Yabe, I. M., Yang, A., and Morris, S. L. (2011). Vaccine-induced anti-tuberculosis protective immunity in mice correlates with the magnitude and quality of multifunctional CD4 T cells. *Vaccine* 29, 2902–2909. doi: 10.1016/j.vaccine.2011.02.010
- Edwards, J. A., Rockx-Brouwer, D., Nair, V., and Celli, J. (2010). Restricted cytosolic growth of *Francisella tularensis* subsp. *tularensis* by IFN-gamma activation of macrophages. *Microbiology* 156, 327–339. doi: 10.1099/mic.0.031716-0
- Elkins, K. L., Colombini, S. M., Krieg, A. M., and De Pascalis, R. (2009). NK cells activated *in vivo* by bacterial DNA control the intracellular growth of *Francisella tularensis* LVS. *Microbes Infect.* 11, 49–56. doi: 10.1016/j.micinf.2008.10.005
- Elkins, K. L., Cowley, S. C., and Bosio, C. M. (2007). Innate and adaptive immunity to *Francisella*. *Ann. N.Y. Acad. Sci.* 1105, 284–324. doi: 10.1196/annals.1409.014
- Elkins, K. L., Cowley, S. C., and Conlan, J. W. (2011). Measurement of macrophage-mediated killing of intracellular bacteria, including *Francisella* and mycobacteria. *Curr. Protoc. Immunol.* Chapter 14, Unit14 25. doi: 10.1002/0471142735.im1425s93
- Eneslätt, K., Normark, M., Björk, R., Rietz, C., Zingmark, C., Wolfraim, L. A., et al. (2012). Signatures of T cells as correlates of immunity to *Francisella tularensis*. *PLoS ONE* 7:e32367. doi: 10.1371/journal.pone.0032367
- Eneslätt, K., Rietz, C., Rydén, P., Stöven, S., House, R. V., Wolfraim, L. A., et al. (2011). Persistence of cell-mediated immunity three decades after vaccination with the live vaccine strain of *Francisella tularensis*. *Eur. J. Immunol.* 41, 974–980. doi: 10.1002/eji.201040923
- Ericsson, M., Sandström, G., Sjöstedt, A., and Tärnvik, A. (1994). Persistence of cell-mediated immunity and decline of humoral immunity to the intracellular bacterium *Francisella tularensis* 25 years after natural infection. *J. Infect. Dis.* 170, 110–114. doi: 10.1093/infdis/170.1.110
- Giovannoni, G., Land, J. M., Keir, G., Thompson, E. J., and Heales, S. J. (1997). Adaptation of the nitrate reductase and Griess reaction methods for the measurement of serum nitrate plus nitrite levels. *Ann. Clin. Biochem.* 34, 193–198. doi: 10.1177/000456329703400212
- Goldsack, L., and Kirman, J. R. (2007). Half-truths and selective memory: interferon gamma, CD4 T cells and protective memory against tuberculosis. *Tuberculosis (Edinb)* 87, 465–473. doi: 10.1016/j.tube.2007.07.001
- Golovliov, I., Baranov, V., Krocova, Z., Kovarova, H., and Sjöstedt, A. (2003). An attenuated strain of the facultative intracellular bacterium *Francisella tularensis* can escape the phagosome of monocytic cells. *Infect. Immun.* 71, 5940–5950. doi: 10.1128/IAI.71.10.5940-5950.2003
- Griffin, A. J., Crane, D. D., Wehrly, T. D., and Bosio, C. M. (2015). Successful protection against tularemia in C57BL/6 mice is correlated with expansion of *Francisella tularensis*-specific effector T cells. *Clin. Vaccine Immunol.* 22, 119–128. doi: 10.1128/CVI.00648-14
- Harari, A., Rozot, V., Bellutti Enders, F., Perreau, M., Stalder, J. M., Nicod, L. P., et al. (2011). Dominant TNF-alpha *Mycobacterium tuberculosis*-specific CD4 T cell responses discriminate between latent infection and active disease. *Nat. Med.* 17, 372–376. doi: 10.1038/nm.2299
- Jeevan, A., Bonilla, D. L., and McMurray, D. N. (2009). Expression of interferon-gamma and tumour necrosis factor-alpha messenger RNA does not correlate with protection in guinea pigs challenged with virulent *Mycobacterium tuberculosis* by the respiratory route. *Immunology* 128, e296–e305. doi: 10.1111/j.1365-2567.2008.02962.x
- Kadzaev, K., Zingmark, C., Golovliov, I., Bolanowski, M., Shen, H., Conlan, W., et al. (2009). Identification of genes contributing to the virulence of *Francisella tularensis* SCHU S4 in a mouse intradermal infection model. *PLoS ONE* 4:e5463. doi: 10.1371/journal.pone.0005463
- Kagina, B. M., Abel, B., Scriba, T. J., Hughes, E. J., Keyser, A., Soares, A., et al. (2010). Specific T cell frequency and cytokine expression profile do not correlate with protection against tuberculosis after bacillus Calmette-Guérin vaccination of newborns. *Am. J. Respir. Crit. Care Med.* 182, 1073–1079. doi: 10.1164/rccm.201003-0334OC
- Kurtz, S. L., Foreman, O., Bosio, C. M., Anver, M. R., and Elkins, K. L. (2013). Interleukin-6 is essential for primary resistance to *Francisella tularensis* live vaccine strain infection. *Infect. Immun.* 81, 585–597. doi: 10.1128/IAI.01249-12
- Landes, M. B., Rajaram, M. V., Nguyen, H., and Schlesinger, L. S. (2015). Role for NOD2 in *Mycobacterium tuberculosis*-induced iNOS expression and NO production in human macrophages. *J. Leukoc. Biol.* 97, 1111–1119. doi: 10.1189/jlb.3A1114-557R
- Lin, Y., Ritchea, S., Logar, A., Slight, S., Messmer, M., Rangel-Moreno, J., et al. (2009). Interleukin-17 is required for T helper 1 cell immunity and host resistance to the intracellular pathogen *Francisella tularensis*. *Immunity* 31, 799–810. doi: 10.1016/j.immuni.2009.08.025
- Lindgren, H., Stenman, L., Tärnvik, A., and Sjöstedt, A. (2005). The contribution of reactive nitrogen and oxygen species to the killing of *Francisella tularensis* LVS by murine macrophages. *Microbes Infect.* 7, 467–475. doi: 10.1016/j.micinf.2004.11.020
- Lindgren, H., Stenmark, S., Chen, W., Tärnvik, A., and Sjöstedt, A. (2004). Distinct roles of reactive nitrogen and oxygen species to control infection with the facultative intracellular bacterium *Francisella tularensis*. *Infect. Immun.* 72, 7172–7182. doi: 10.1128/IAI.72.12.7172-7182.2004
- Mahawar, M., Rabadi, S. M., Banik, S., Catlett, S. V., Metzger, D. W., Malik, M., et al. (2013). Identification of a live attenuated vaccine candidate for tularemia prophylaxis. *PLoS ONE* 8:e61539. doi: 10.1371/journal.pone.0061539
- Mattila, J. T., Ojo, O. O., Kepka-Lenhart, D., Marino, S., Kim, J. H., Eum, S. Y., et al. (2013). Microenvironments in tuberculous granulomas are delineated by distinct populations of macrophage subsets and expression of nitric oxide synthase and arginase isoforms. *J. Immunol.* 191, 773–784. doi: 10.4049/jimmunol.1300113
- Melillo, A. A., Foreman, O., Bosio, C. M., and Elkins, K. L. (2014). T-bet regulates immunity to *Francisella tularensis* live vaccine strain infection, particularly in lungs. *Infect. Immun.* 82, 1477–1490. doi: 10.1128/IAI.01545-13
- Melillo, A. A., Foreman, O., and Elkins, K. L. (2013). IL-12Rbeta2 is critical for survival of primary *Francisella tularensis* LVS infection. *J. Leukoc. Biol.* 93, 657–667. doi: 10.1189/jlb.1012485
- Mittrücker, H. W., Steinhoff, U., Köhler, A., Krause, M., Lazar, D., Mex, P., et al. (2007). Poor correlation between BCG vaccination-induced T cell responses and protection against tuberculosis. *Proc. Natl. Acad. Sci. U.S.A.* 104, 12434–12439. doi: 10.1073/pnas.0703510104
- Mühl, H., Bachmann, M., and Pfeilschifter, J. (2011). Inducible NO synthase and antibacterial host defence in times of Th17/Th22/T22 immunity. *Cell. Microbiol.* 13, 340–348. doi: 10.1111/j.1462-5822.2010.01559.x
- Pautz, A., Art, J., Hahn, S., Nowag, S., Voss, C., and Kleinert, H. (2010). Regulation of the expression of inducible nitric oxide synthase. *Nitric Oxide* 23, 75–93. doi: 10.1016/j.niox.2010.04.007
- Ryden, P., Twine, S., Shen, H., Harris, G., Chen, W., Sjöstedt, A., et al. (2012). Correlates of protection following vaccination of mice with gene deletion mutants of *Francisella tularensis* subspecies *tularensis* strain, SCHU S4 that elicit varying degrees of immunity to systemic and respiratory challenge with wild-type bacteria. *Mol. Immunol.* 54, 58–67. doi: 10.1016/j.molimm.2012.10.043
- Santiago, A. E., Mann, B. J., Qin, A., Cunningham, A. L., Cole, L. E., Grassel, C., et al. (2015). Characterization of *Francisella tularensis* Schu S4 defined mutants as live-attenuated vaccine candidates. *Pathog. Dis.* 73:ftv036. doi: 10.1093/femspd/ftv036
- Saslaw, S., Eigelsbach, H. T., Prior, J. A., Wilson, H. E., and Carhart, S. (1961a). Tularemia vaccine study. II. Respiratory challenge. *Arch. Intern. Med.* 107, 702–714. doi: 10.1001/archinte.1961.03620050068007
- Saslaw, S., Eigelsbach, H. T., Wilson, H. E., Prior, J. A., and Carhart, S. (1961b). Tularemia vaccine study. I. Intracutaneous challenge. *Arch. Intern. Med.* 107, 689–701. doi: 10.1001/archinte.1961.03620050055006
- Shen, H., Harris, G., Chen, W., Sjöstedt, A., Ryden, P., and Conlan, W. (2010). Molecular immune responses to aerosol challenge with *Francisella tularensis* in mice inoculated with live vaccine candidates of varying efficacy. *PLoS ONE* 5:e13349. doi: 10.1371/journal.pone.0013349
- Sjöstedt, A. (2007). Tularemia: history, epidemiology, pathogen physiology, and clinical manifestations. *Ann. N.Y. Acad. Sci.* 1105, 1–29. doi: 10.1196/annals.1409.009
- Snoy, P. (2010). Establishing efficacy of human products using animals: the US Food and Drug Administration's "animal rule." *Vet. Pathol.* 47, 774–778. doi: 10.1177/0300985810372506

US. Food and Drug Administration. (2015). *FDA Approves Vaccine for use After Known or Suspected Anthrax Exposure*. Available online at: <http://www.fda.gov/NewsEvents/Newsroom/PressAnnouncements/ucm474027.htm>

Yeo, T. W., Lampah, D. A., Tjitra, E., Gitawati, R., Darcy, C. J., Jones, C., et al. (2010). Increased asymmetric dimethylarginine in severe falciparum malaria: association with impaired nitric oxide bioavailability and fatal outcome. *PLoS Pathog.* 6:e1000868. doi: 10.1371/annotation/e49842d3-ea72-45a4-93d4-2f494baee962

Conflict of Interest Statement: The authors declare that the research was conducted in the absence of any commercial or financial relationships that could be construed as a potential conflict of interest.

The reviewer TEP and handling Editor declared their shared affiliation and the handling Editor states that the process nevertheless met the standards of a fair and objective review.

Copyright © 2016 Golovliov, Lindgren, Eneslätt, Conlan, Mosnier, Henry and Sjöstedt. This is an open-access article distributed under the terms of the Creative Commons Attribution License (CC BY). The use, distribution or reproduction in other forums is permitted, provided the original author(s) or licensor are credited and that the original publication in this journal is cited, in accordance with accepted academic practice. No use, distribution or reproduction is permitted which does not comply with these terms.



Lack of OxyR and KatG Results in Extreme Susceptibility of *Francisella tularensis* LVS to Oxidative Stress and Marked Attenuation *In vivo*

Marie Honn[†], Helena Lindgren[†], Gurram K. Bharath and Anders Sjöstedt*

Clinical Bacteriology, and Laboratory for Molecular Infection Medicine Sweden, Department of Clinical Microbiology, Umeå University, Umeå, Sweden

Francisella tularensis is an intracellular bacterium and as such is expected to encounter a continuous attack by reactive oxygen species (ROS) in its intracellular habitat and efficiently coping with oxidative stress is therefore essential for its survival. The oxidative stress response system of *F. tularensis* is complex and includes multiple antioxidant enzymes and pathways, including the transcriptional regulator OxyR and the H₂O₂-decomposing enzyme catalase, encoded by *katG*. The latter is regulated by OxyR. A deletion of either of these genes, however, does not severely compromise the virulence of *F. tularensis* and we hypothesized that if the bacterium would be deficient of both catalase and OxyR, then the oxidative defense and virulence of *F. tularensis* would become severely hampered. To test this hypothesis, we generated a double deletion mutant, $\Delta oxyR/\Delta katG$, of *F. tularensis* LVS and compared its phenotype to the parental LVS strain and the corresponding single deletion mutants. In accordance with the hypothesis, $\Delta oxyR/\Delta katG$ was distinctly more susceptible than $\Delta oxyR$ and $\Delta katG$ to H₂O₂, ONOO⁻, and O₂⁻, moreover, it hardly grew in mouse-derived BMDM or in mice, whereas $\Delta katG$ and $\Delta oxyR$ grew as well as *F. tularensis* LVS in BMDM and exhibited only slight attenuation in mice. Altogether, the results demonstrate the importance of catalase and OxyR for a robust oxidative stress defense system and that they act cooperatively. The lack of both functions render *F. tularensis* severely crippled to handle oxidative stress and also much attenuated for intracellular growth and virulence.

Keywords: *Francisella tularensis*, OxyR, KatG, oxidative stress, virulence

INTRODUCTION

Francisella tularensis, a Tier 1 select agent and the causative agent of tularemia, is a zoonotic, facultative intracellular bacterium with two clinically relevant subspecies, *tularensis* and *holarctica*, the former of which causes an aggressive disease with high mortality if left untreated (Oyston et al., 2004). Although there is no licensed vaccine against this potential bioterrorism agent, the subspecies *holarctica* live vaccine strain, LVS, is used to vaccinate laboratory workers, and is widely used in *Francisella* research as it is attenuated in humans, but retains its virulence in mice (Sjöstedt, 2006; Conlan, 2011).

OPEN ACCESS

Edited by:

Jing-Ren Zhang,
Tsinghua University, China

Reviewed by:

Roger Derek Pechous,
University of Arkansas for Medical
Sciences, USA
Girija Ramakrishnan,
University of Virginia, USA

*Correspondence:

Anders Sjöstedt
anders.sjostedt@umu.se

[†]These authors have contributed
equally to this work.

Received: 19 October 2016

Accepted: 10 January 2017

Published: 24 January 2017

Citation:

Honn M, Lindgren H, Bharath GK and
Sjöstedt A (2017) Lack of OxyR and
KatG Results in Extreme Susceptibility
of *Francisella tularensis* LVS to
Oxidative Stress and Marked
Attenuation *In vivo*.
Front. Cell. Infect. Microbiol. 7:14.
doi: 10.3389/fcimb.2017.00014

Francisella tularensis is capable of infecting numerous cell types, including professional phagocytes, like macrophages. Upon phagocytosis, it transiently resides within the phagosome before escaping into the cytosol to replicate (Bröms et al., 2010; Chong and Celli, 2010). Phagocytes constitute a hostile environment utilizing a wide array of anti-bacterial mechanisms, such as phagosome acidification, disruption of pathogen membrane integrity, removal or sequestration of nutrients, and the production of reactive oxygen species (ROS) (Flanagan et al., 2009) and since *F. tularensis* is an intracellular bacterium, it will encounter a continuous exposure to ROS. Vital macromolecules, such as proteins and DNA, will react with ROS, thereby disrupting their functions (Fridovich, 1998; Schaible and Kaufmann, 2004; Flanagan et al., 2009). There are several ROS with potent antibacterial effects, such as superoxide and H₂O₂. The former is produced at high levels by the phagocyte oxidase (phox) and it rapidly combines with nitric oxide (NO), which is produced at high levels by inducible nitric oxide synthase (iNOS), to form peroxynitrite, a highly reactive compound. H₂O₂ is toxic *per se*, but the damage it exerts can be exacerbated in combination with intracellular ferrous iron, resulting in the formation of hydroxyl radicals (HO•) and hydroxide anions (OH⁻) through the Fenton reaction.

Reactive oxygen species (ROS) are not only formed during host attack, but low levels are also formed as by-products of normal aerobic metabolism. Thus, pathogens, in particular intracellular pathogens, have a pressing need for defense mechanisms to combat the ever present levels of ROS, but even more so to combat the assault of ROS experienced within a host (Betteridge, 2000). The critical roles of ROS and NO for the host defense against tularemia are illustrated by the extreme susceptibility of phox-deficient and iNOS-deficient mice to an *F. tularensis* infection (Lindgren et al., 2004). Moreover, *ex vivo*, it has been demonstrated that the requirements for host protection vary depending on the cell type investigated, since killing of *F. tularensis* by mouse peritoneal cells is NO-dependent, but NO-independent by mouse pulmonary cells (Anthony et al., 1992; Polsinelli et al., 1994; Lindgren et al., 2005).

The oxidative stress defense system of *Escherichia coli* has been extensively studied and includes numerous detoxifying enzymes, such as catalase, superoxide dismutases (SODs), alkyl hydroperoxide reductase (Ahp), and the H₂O₂-activated transcriptional regulator OxyR. The latter combats the effect of H₂O₂ by dual mechanisms, since it regulates the expression of both catalase and the ferric uptake regulator (Fur) (Farr and Kogoma, 1991; Zheng et al., 1998, 1999; Pomposiello and Demple, 2001). Catalase renders H₂O₂ harmless by degrading it to oxygen and water, whilst Fur down-regulates the expression of genes involved in iron uptake, thus limiting the amount of iron with which H₂O₂ can combine in the Fenton reaction (Andrews et al., 2003; Troxell and Hassan, 2013). Catalase, SODs, AhpC and other detoxifying enzymes are employed as oxidative stress defense mechanisms also by *F. tularensis* (Bakshi et al., 2006; Lindgren et al., 2007; Melillo et al., 2009; Binesse et al., 2015). The *F. tularensis* catalase, encoded by *katG*, mediates H₂O₂ tolerance and is known to be important for the virulence of *F. tularensis* LVS (Lindgren et al., 2007). SodB, FeSOD, and SodC, CuZnSOD,

are both known to be important for the dismutation of O₂⁻ in *F. tularensis*, and SodB further acts in the defense against oxidative stress by harnessing iron (Bakshi et al., 2006; Melillo et al., 2009). The *F. tularensis* AhpC enzyme is important for the detoxification of O₂⁻ and peroxynitrite (ONOO⁻), but not of H₂O₂, in the highly virulent SCHU S4 strain (Binesse et al., 2015), but the importance in the LVS strain is yet unknown. *F. tularensis* also encodes an *oxyR* homolog, the role of which has been studied recently (Ma et al., 2016). It was found that the absence of OxyR rendered LVS defective for oxidative stress defense, growth in macrophages and epithelial cells, and virulence in mice. Moreover, it was demonstrated that OxyR regulates the expression of the *ahpC*, *katG*, and *sodB* genes, with the most pronounced regulatory effect exerted on *ahpC*.

A more thorough understanding of the *F. tularensis* antioxidant system will undoubtedly reveal virulence mechanisms of this bacterium, since ROS constitute such an essential threat to the pathogen. As aforementioned, antioxidant enzymes, such as catalase, AhpC, SodC, and SodB, all contribute to the virulence of *F. tularensis* in mice, although each appears to render the bacterium only moderately attenuated and this indicates that the antioxidant system of *F. tularensis* is complex and may in part possess overlapping functions (Lindgren et al., 2007; Ma et al., 2016). Indeed, a double deletion mutant of *katG* and *ahpC* has not been possible to generate in *F. tularensis* (Binesse et al., 2015) and this demonstrates that the cooperative functions of these enzymes are crucial, although either one is not essential. The aim of the present study was to better understand this interconnecting web of antioxidants in *F. tularensis*. To this end, a double deletion mutant, $\Delta oxyR/\Delta katG$, was generated since this mutant, besides lack of catalase activity, should have a repressed expression of OxyR-regulated antioxidant genes, one of which is AhpC (Ma et al., 2016). We hypothesized that the lack of both KatG and OxyR would lead to a severely impaired phenotype of *F. tularensis* LVS. We therefore characterized the phenotypes of single deletion mutants, $\Delta oxyR$ and $\Delta katG$, and a double deletion mutant, $\Delta oxyR/\Delta katG$, in comparison to the parental LVS strain.

MATERIALS AND METHODS

Bacterial Strains

The *F. tularensis* LVS strain was obtained from the *Francisella* strain collection (FSC) at FOI, Swedish Defense Research Agency. The *katG* deletion mutant ($\Delta katG$) has been described previously (Lindgren et al., 2007).

The $\Delta oxyR$ and $\Delta oxyR/\Delta katG$ mutants of the LVS strain were generated by allelic replacement as described previously (Golovliov et al., 2003). Briefly, sequences up- and down-stream of *oxyR* were amplified by PCR. The fragments contained complementary sequences, which were joined together by a second PCR. The resulting fragment was cloned into the pDM4 suicide-vector, which was transformed into *Escherichia coli* S17- λ pir and thereafter transferred to LVS by conjugation. Clones with a successful recombination event were selected on plates supplemented with Cm and polymyxin B. Correct integration was confirmed by PCR. Positive clones were subjected to sucrose

selection to select for a second recombination event and clones were screened by PCR to identify successful deletion mutants. The double deletion mutant $\Delta oxyR/\Delta katG$ was generated using the same procedure, apart from using the pDMK3 plasmid carrying kanamycin resistance. The deletions were verified by sequencing 1500 bp on each side of the deleted region.

Aerobic and Microaerobic Growth

Bacteria were cultivated overnight on plates based on modified GC-agar (MC plates) and then inoculated to an OD₆₀₀ of 0.1 in Chamberlain's chemically defined medium (CDM). All cultures were split into triplicates and were incubated at 37°C and 200 rpm in an aerobic (normal air) or a microaerobic (10% O₂ and 10% CO₂) milieu up to 48 h with monitoring of the OD₆₀₀.

H₂O₂ Susceptibility Assay

Bacteria were cultivated overnight on MC plates, inoculated to an OD₆₀₀ of 0.1 in CDM and H₂O₂ was added to the final concentration of 0.02, 0.1, or 0.5 mM, respectively. Controls were grown without the addition of H₂O₂. All cultures were split into triplicates and were incubated at 37°C and 200 rpm up to 24 h with monitoring of the OD₆₀₀.

Catalase Activity Assay

Catalase degrades H₂O₂ to O₂ and H₂O. H₂O₂ absorbs light at 240 nm and degradation of H₂O₂ can therefore be measured as a reduction of A₂₄₀ nm over time.

Strains were cultivated overnight after being diluted to an OD₆₀₀ of 0.1 in CDM. For each strain, one set of tubes were left untreated and another set of tubes were supplemented with H₂O₂ to a final concentration of 0.02, 0.1, or 0.2 mM. All cultures were split into triplicates and incubated at 37°C, 200 rpm for 2, 4, and 24 h before sampling for evaluation of catalase activity. Depending on the density and growth phase of the culture, a volume of 10–50 µl were withdrawn and diluted in PBS to reach a final volume of 120 µl in UV-clear 96-well plates (Greiner Bio-one, Frickenhausen, Germany). Then, 80 µl 100 mM H₂O₂ in PBS was added to each sample immediately before placing the plate in a Tecan Infinite 200 pro plate reader and measuring the reduction in absorption at 240 nm for 10 min. A molar extinction coefficient of H₂O₂ at 240 nm of 43.6 M⁻¹cm⁻¹ was used to calculate the concentration of H₂O₂ using the Beer-Lambert law, $A = \epsilon cl$. One unit of catalase is defined as the amount that decomposes 1 µmol of H₂O₂ per minute per OD₆₀₀ at 25°C. The catalase units were normalized against the OD of the culture.

Paraquat Susceptibility Assay

Susceptibility of *F. tularensis* strains to O₂⁻ was determined by use of the O₂⁻ generating compound paraquat dichloride hydrate (Sigma-Aldrich, St. Louis, USA) in a disc diffusion assay. Paraquat generates O₂⁻ through reacting with parts of the respiratory chain in bacteria, causing the reduction of O₂ to O₂⁻ (Hassan and Fridovich, 1979). Bacterial strains were cultivated on MC plates overnight, re-suspended in phosphate-buffered saline (PBS) and approximately 3 × 10⁵ CFU were plated onto MC plates. Sterile filter discs (Oxoid Blank Antimicrobial Susceptibility Discs, Thermo Scientific, MA, USA) were placed

in the center the plates once they had dried, and 10 µl of MQ-water, 1.25 mM, 5 mM or 20 mM paraquat solution was added to each disc. The plates were incubated for 4 days at 37°C, 5% CO₂ before the size of the growth inhibition zone surrounding each disc was determined.

Peroxynitrite Susceptibility Assay

3-morpholiniosydnonimine hydrochloride (SIN-1) (Molecular Probes, Oregon, USA) spontaneously releases (NO) and O₂⁻ under physiological conditions, thereby generating peroxynitrite (ONOO⁻). Under physiological conditions 1 mM SIN-1 generates 10 µM ONOO⁻/min (Lindgren et al., 2007).

Strains were cultivated in CDM to logarithmic growth phase and diluted to a density of approximately 2 × 10⁶ bacteria/ml in PBS. The bacterial suspensions were incubated with or without the addition of 0.48 mM SIN-1 with equal amounts of SIN-1 added at the start of the experiment and again after 1.5 h to ensure stable levels of ONOO⁻ (Lindgren et al., 2005). After 3 h samples were collected, diluted and plated on MC plates for determination of viable bacteria.

Analysis of Gene Expression by Real Time PCR

Bacteria were cultivated overnight on MC plates, inoculated to an OD₆₀₀ of 0.1 in CDM and incubated at 37°C, 5% CO₂ for 10 h before sampling. RNA extraction, cDNA synthesis and Real Time PCR (RT-PCR) were all performed as described previously (Honn et al., 2012).

Briefly, RNA was extracted using Trizol reagent (Invitrogen, CA, USA) from pelleted bacteria, 3 × 10⁹ CFU/sample. Contaminating DNA was removed using the DNA-free kit (Ambion, Inc, Austin, TX, USA) and RNA was quantified by Nanodrop (Thermo Fisher Scientific, Wilmington, DE, USA). cDNA was synthesized from 1 µg RNA/sample using iScript (BioRad, Hemel, Hempstead, UK), RT-PCR was performed using the Power SYBR green PCR Master Mix (Applied Biosystems, Foster City, CA, USA) and the ABI Prism 7900Ht Sequence Detection System (Applied Biosystems) as described (Honn et al., 2012). Trizol, DNA-free, iScript and Power SYBR green were all used in accordance with the instructions provided by the manufacturers. Forward and reverse primers were obtained from Invitrogen and have been published previously for *fslA* (FTL_1832), *fslB* (FTL_1833), *fslC* (FTL_1834), *fslD* (FTL_1835), *fslE* (FTL_1836), *fupA* (FTL_0439), *furA* (FTL_1831), (Lindgren et al., 2009), *tul4*, *iglC* (FTL_0113), (Bröms et al., 2009), *mglA* (FTL_0260), *feoB* (FTL_0133), and *katG* (FTL_1504) (Honn et al., 2012), sequences for, *grxA* (FTL_0985), *grxB* (FTL_1792), *gpx* (FTL_1383), *sspA* (FTL_1606), *ahpC1* (FTL_0542), *ahpC2* (FTL_1191), *sodB* (FTL_0380), *sodC* (FTL_1791), *clpB* (FTL_0094), *groES* (FTL_1715), *groEL* (FTL_1714), and *dnaK* (FTL_1191) are available upon request.

The Ct values of the selected genes were normalized to the Ct value of the house keeping gene *FTT0901* (*lpnA*) and relative copy numbers (RCN) were calculated according to the following equation: $RCN = 2^{-\Delta Ct} \times 100$, where ΔCt is Ct(target)–Ct(*FTT0901*) (Gavrilin et al., 2006). Thus, the copy

number of a given gene is related to the copy number of *FTT0901*. Normalized Ct values were used for statistical evaluation of the data by One way ANOVA followed by Tukey's honest significant difference (HSD).

Preparation and Infection of BMDM

The capacity of LVS and the mutants to proliferate intracellularly were assessed in bone marrow-derived macrophages (BMDMs). BMDMs were generated from C57BL/6 mice essentially as described previously (Bröms et al., 2011).

The day before infection, BMDM cells were seeded at a density of 4×10^5 cells/ml in 24-well tissue-culture plates and incubated at 37°C, 5% CO₂ with or without murine recombinant 1000 U/ml of IFN- γ (PeproTech, Rocky Hill, NJ, USA). The next day, the cells were washed and reconstituted with fresh, pre-warmed culture media. Bacteria were grown overnight on MC plates and re-suspended in PBS to a density of approximately 3×10^9 bacteria/ml. Bacteria were diluted in DMEM and added to each well at multiplicity of infection of 30 and bacterial uptake was allowed to occur for 90 min at 37°C, 5% CO₂. Remaining extracellular bacteria were removed by rinsing the monolayers three times with DMEM and incubating with gentamicin for 45 min followed by rinsing the monolayers three times. This time-point was defined as 0 h. After 0, 4 and 24 h incubation the macrophages were lysed in 0.1% deoxycholate in PBS. The lysate were serially diluted in PBS and plated on MC plates for determination of viable bacteria.

Mouse Experiments

Virulence of the mutant strains was determined by subcutaneous infection of female C57BL/6 mice with 4×10^3 CFU/mouse of LVS, $\Delta oxyR$, $\Delta katG$, and $\Delta oxyR/\Delta katG$. Mice were monitored for signs of illness and were euthanized by inhalation of isoflurane followed by CO₂ asphyxiation after 3 or 6 days, whereupon the number of viable bacteria in spleens and livers were determined by homogenizing the organs in PBS and plating dilutions on MC plates. All animal experiments were approved by the Local Ethical Committee on Laboratory Animals, Umeå, Sweden (no. A 1-09, A 99-11, and A 67-14).

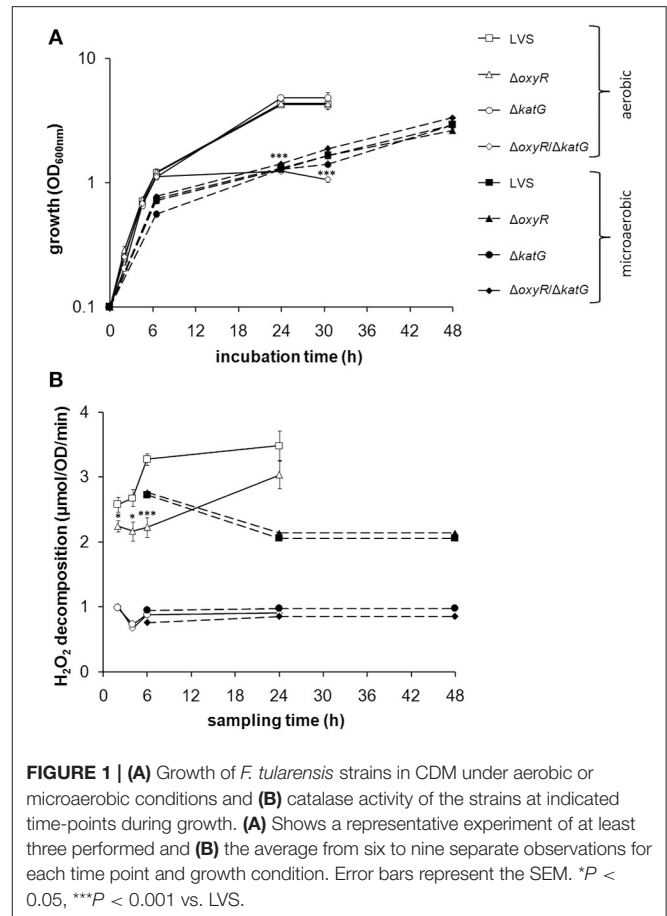
Statistical Analysis

One way ANOVA followed by Tukey's HSD test was used to determine statistical significant difference between groups.

RESULTS

Growth under Aerobic vs. Microaerobic Conditions

CDM effectively supports growth of LVS. We therefore compared growth of the bacterial strains, LVS, $\Delta oxyR$, $\Delta katG$, and $\Delta oxyR/\Delta katG$. The former three strains all replicated to the same extent, whereas $\Delta oxyR/\Delta katG$ showed intact growth to late log phase, but impaired growth thereafter. Therefore, it did not reach as high densities as LVS and the other strains at 24 h ($P < 0.001$; **Figure 1A**). To explore if a reduced oxygen tension could rescue the growth of $\Delta oxyR/\Delta katG$, the strains were cultivated under microaerobic conditions, i.e., 10% O₂ and



10% CO₂. Indeed, $\Delta oxyR/\Delta katG$ grew as well as the other strains and reached an optical density of > 2.0 within 48 h (**Figure 1A**). As noted before (Honn et al., 2012), the growth rate of LVS under microaerobic conditions was reduced compared to aerobic conditions (**Figure 1A**).

Catalase Activity under Aerobic vs. Microaerobic Conditions

The results so far suggested that LVS experienced oxidative stress during growth in an aerobic environment and to handle this stress, required either the function of catalase, or the expression of OxyR-regulated detoxifying mechanisms. OxyR is known to respond to oxidative stress by inducing antioxidant enzymes, such as catalase. As an indicator of oxidative stress and to investigate if catalase is under the regulation of *oxyR* in LVS, we measured the activity of the enzyme during growth of the bacteria in CDM. The catalase activity in LVS gradually increased during the two to 24 h period, whereas the catalase activity in $\Delta oxyR$ was sustained at a constant, but lower level compared to LVS from two to six h ($P < 0.05$ at 2 and 4 h and $P < 0.001$ at 6 h; **Figure 1B**). However, the catalase activity of the two strains was similar at 24 h (**Figure 1B**). In the microaerobic environment, the catalase activity of LVS and $\Delta oxyR$ was similar, but for both lower than in the aerobic environment (**Figure 1B**). The H₂O₂

decomposition in samples containing $\Delta katG$ or $\Delta oxyR/\Delta katG$ was below $1 \mu\text{mol}$, regardless of growth condition and time point, indicating the absence of catalase activity (**Figure 1B**).

In summary, $\Delta oxyR$ demonstrated a basal catalase activity, but did not induce this activity further during the aerobic logarithmic growth phase as LVS did. $\Delta oxyR/\Delta katG$, which lacks this basal catalase activity, failed to grow to high densities under the aerobic condition, but grew as well as LVS in the microaerobic milieu.

H₂O₂ Tolerance

$\Delta oxyR$ and $\Delta katG$ grew as well as LVS in CDM despite the reduced, or lack of catalase activity (**Figure 2A**). To investigate their adaptation to stress, H₂O₂, the substrate of catalase, was added to the cultures. Growth of LVS or $\Delta oxyR$ was not affected by 0.02 mM H₂O₂, whereas, initially, the growth rate of $\Delta katG$ was reduced ($P < 0.01$) and growth of $\Delta oxyR/\Delta katG$ almost completely inhibited ($P < 0.001$; **Figure 2B**). At 0.1 mM of H₂O₂, LVS and $\Delta oxyR$ still grew rapidly, in contrast to $\Delta katG$ and $\Delta oxyR/\Delta katG$ that did not grow at all ($P < 0.001$; **Figure 2C**). Growth of $\Delta oxyR$ was significantly reduced in the presence of 0.5 mM of H₂O₂ compared to LVS ($P < 0.001$; **Figure 2D**). Exposure

of the strains to H₂O₂ did not significantly change their catalase activity (data not shown).

In summary, the mutant strains displayed increased susceptibility to H₂O₂ as compared to LVS, with the effect being most pronounced for $\Delta oxyR/\Delta katG$, followed by $\Delta katG$, and the least affected strain being $\Delta oxyR$.

Susceptibility to Paraquat-Mediated Killing

O₂⁻ is continuously generated as a by-product of the respiratory chain during growth of bacteria. To investigate the capacity of the bacteria to defend against such ROS, LVS, $\Delta oxyR$, $\Delta katG$, and $\Delta oxyR/\Delta katG$ were exposed to paraquat in a disc diffusion assay (**Figure 3**). Paraquat dichloride hydrate generates O₂⁻ through a reaction with parts of the respiratory chain in bacteria, causing the reduction of O₂ to O₂⁻ (Hassan and Fridovich, 1979). $\Delta oxyR$ displayed a significantly larger zone of inhibition than did LVS in the presence of 1.25 and 5 mM paraquat ($P < 0.001$ and 0.01, respectively), but the zones were similar when exposed to 20 mM (**Figure 3**). The zone of inhibition for $\Delta katG$ was larger compared to LVS at 1.25 mM ($P < 0.05$), but similar at the two higher concentrations (**Figure 3**). A significantly larger zone of inhibition was observed for $\Delta oxyR/\Delta katG$ vs. LVS and $\Delta katG$ at

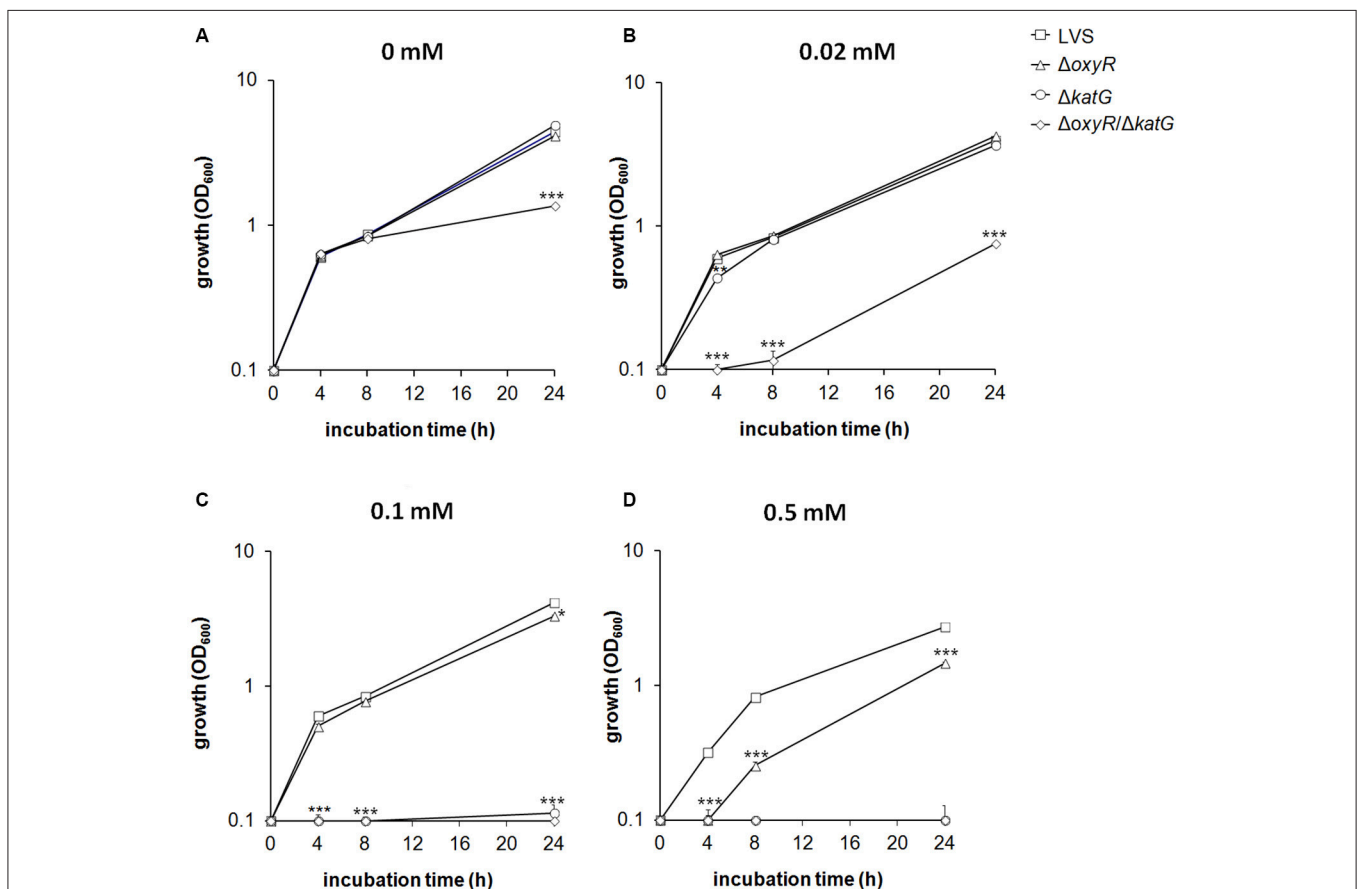


FIGURE 2 | Growth of *F. tularensis* strains in CDM during exposure to various concentrations of H₂O₂ (A) 0 mM, (B) 0.02 mM, (C) 0.1 mM, and (D) 0.5 mM. The results shown illustrate one representative experiment of at least three performed. Each value represents the average for triplicate samples and error bars represent the SEM. * $P < 0.05$, ** $P < 0.01$, *** $P < 0.001$ vs. LVS.

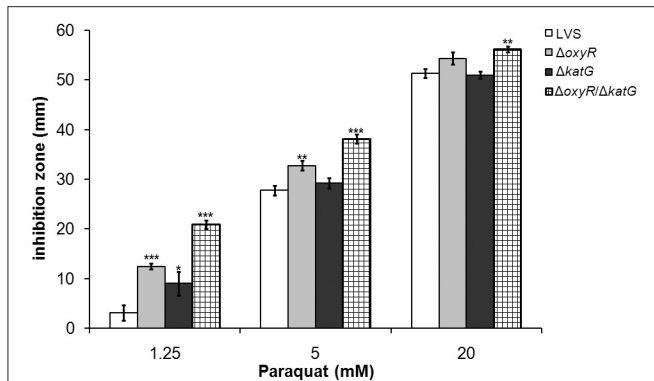


FIGURE 3 | *F. tularensis* strains were exposed to the O_2^- -generating compound paraquat in a disc diffusion assay. Each bar represents the average from three separate experiments with triplicate samples in each and error bars represent the SEM. * $P < 0.05$, ** $P < 0.01$, *** $P < 0.001$ vs. LVS for each concentration.

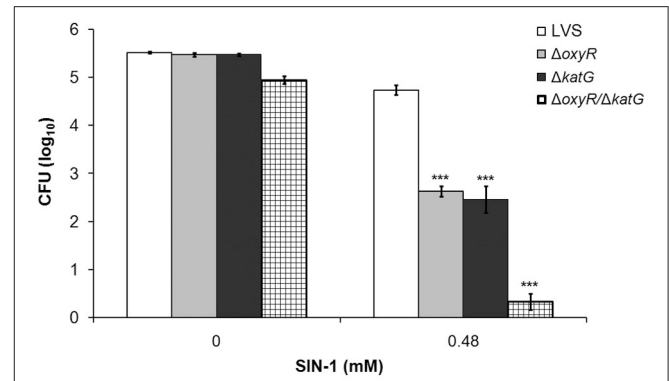


FIGURE 4 | *F. tularensis* strains were exposed to the peroxynitrite generating compound SIN-1 for 3 h. After 1.5 h of incubation, additional SIN-1 was added to the tubes to ensure a constant generation of peroxynitrite during the whole incubation period. Each bar represents the average from three separate experiments with triplicate samples in each and error bars represent the SEM. *** $P < 0.001$ vs. LVS.

all three concentrations of paraquat ($P < 0.001$ for 1.25 and 5 mM and $P < 0.01$ for 20 mM) and also larger compared to $\Delta oxyR$ at 1.25 and 5 mM ($P < 0.01$; **Figure 3**).

In summary, the results demonstrated that $\Delta oxyR$ and $\Delta oxyR/\Delta katG$ were more susceptible to paraquat-mediated killing compared to LVS, with $\Delta oxyR/\Delta katG$ being the most susceptible, whereas $\Delta katG$ was only slightly more susceptible than LVS.

Susceptibility to SIN-1-Mediated Killing

Peroxyntirite ($ONOO^-$) is a highly reactive and bactericidal ROS formed through the reaction between (NO) and O_2^- and it is active against *F. tularensis* in activated macrophages (Lindgren et al., 2005). Experimentally, SIN-1 can be used to mimic a continuous exposure to $ONOO^-$. SIN-1 slowly decomposes, thereby releasing both NO and O_2^- that combine to form $ONOO^-$, which quickly is internalized since it passes through lipid bilayers (Hogg et al., 1992; Murphy et al., 1998).

The exposure to 0.48 mM SIN-1 for 3 h reduced the viability of all strains in comparison to un-treated cultures ($P < 0.001$ for all strains), but affected the mutant strains to a greater extent compared to LVS ($P < 0.001$ vs. LVS for all; **Figure 4**). The viability of LVS decreased approximately 0.8 \log_{10} , of $\Delta oxyR$ 2.8 \log_{10} , of $\Delta katG$ 3.0 \log_{10} , and of $\Delta oxyR/\Delta katG$ 4.6 \log_{10} CFU. The latter was significantly more susceptible than any of the other strains ($P < 0.001$; **Figure 4**).

In summary, all mutant strains displayed increased susceptibility to $ONOO^-$ as compared to LVS, with the effect being similar for $\Delta oxyR$ and $\Delta katG$ and most pronounced for $\Delta oxyR/\Delta katG$.

Gene Expression

$\Delta oxyR/\Delta katG$ did not grow after the late logarithmic growth phase (**Figure 1A**), and we therefore found it of interest to explore the gene expression of the strains at 10 h, i.e., during the late logarithmic growth phase. The analysis was focused on genes expressing proteins influencing the oxidative stress response of

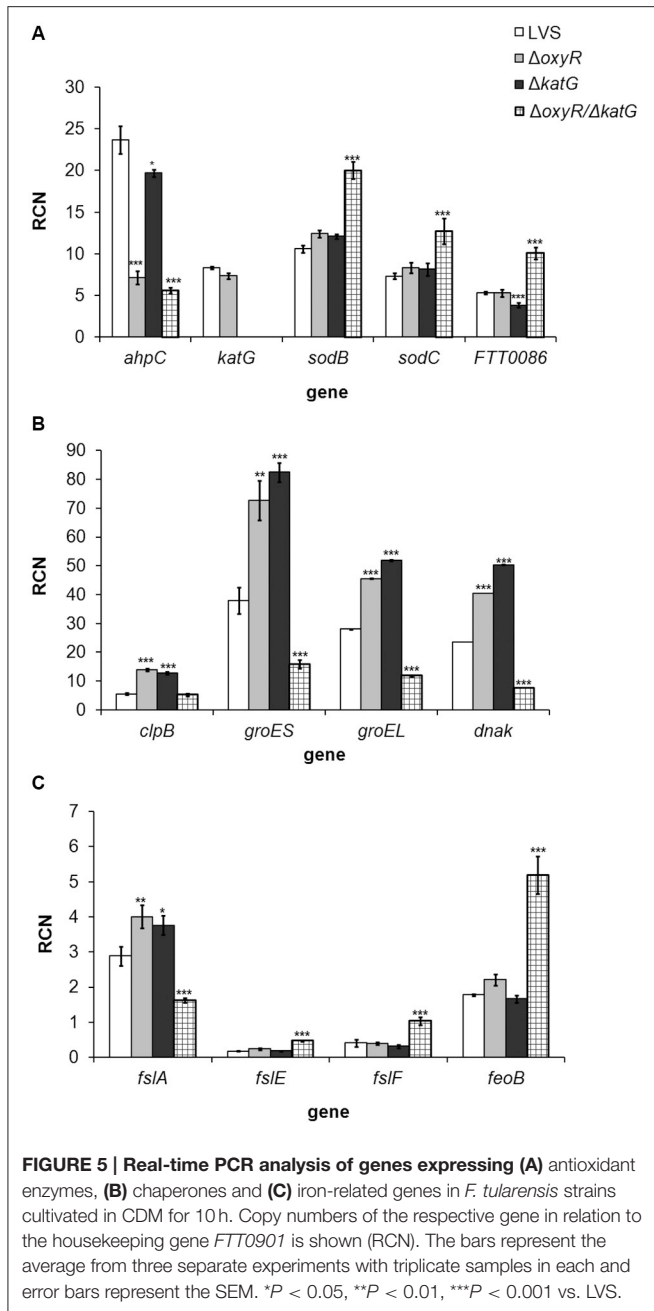
the bacterium, such as antioxidant enzymes, chaperones and iron-related proteins. Genes found to be differentially expressed vs. LVS are shown in **Figure 5**. Of all genes examined, *ahpC* was the sole gene significantly repressed in $\Delta oxyR$ ($P < 0.001$; **Figure 5A**). A similar degree of repression, about 3-fold, was observed in $\Delta oxyR/\Delta katG$, which in addition, had a 1.5 to 2-fold increased expression of *sodB*, *sodC* and *FTT0086* ($P < 0.001$ for all genes; **Figure 5A**). *ahpC* was not repressed in $\Delta katG$ and as expected, *katG* transcripts were not detected in either $\Delta katG$ or in $\Delta oxyR/\Delta katG$ (**Figure 5A**). All chaperone genes examined were upregulated 1.6 to 2.5-fold in $\Delta oxyR$ and $\Delta katG$ ($P < 0.001$ for all genes; **Figure 5B**). In contrast, these genes, except for *clpB*, were suppressed 2.4 to 3.1-fold in $\Delta oxyR/\Delta katG$ ($P < 0.001$ for all genes).

fslA, the first gene of the siderophore operon, was slightly up-regulated in $\Delta oxyR$ and $\Delta katG$, although only about 1.2-fold, whereas the other iron-related genes were expressed at similar levels as in LVS. In contrast, *fslA* was suppressed 1.8-fold in $\Delta oxyR/\Delta katG$ and *fslE*, *fslF* and *feoB* were upregulated 2.5 to 2.9-fold ($P < 0.001$; **Figure 5C**).

In summary, the absence of OxyR resulted in a suppressed expression of *ahpC* and an up-regulated expression of genes encoding chaperone proteins. Except for *ahpC*, the expression profile of $\Delta katG$ was similar to $\Delta oxyR$. In contrast, loss of both *oxyR* and *katG* changed the expression profile and low expression of chaperone-encoding genes was observed in $\Delta oxyR/\Delta katG$, together with high expression of antioxidant genes, except for *ahpC* and *katG*, and an altered expression of genes related to iron-uptake.

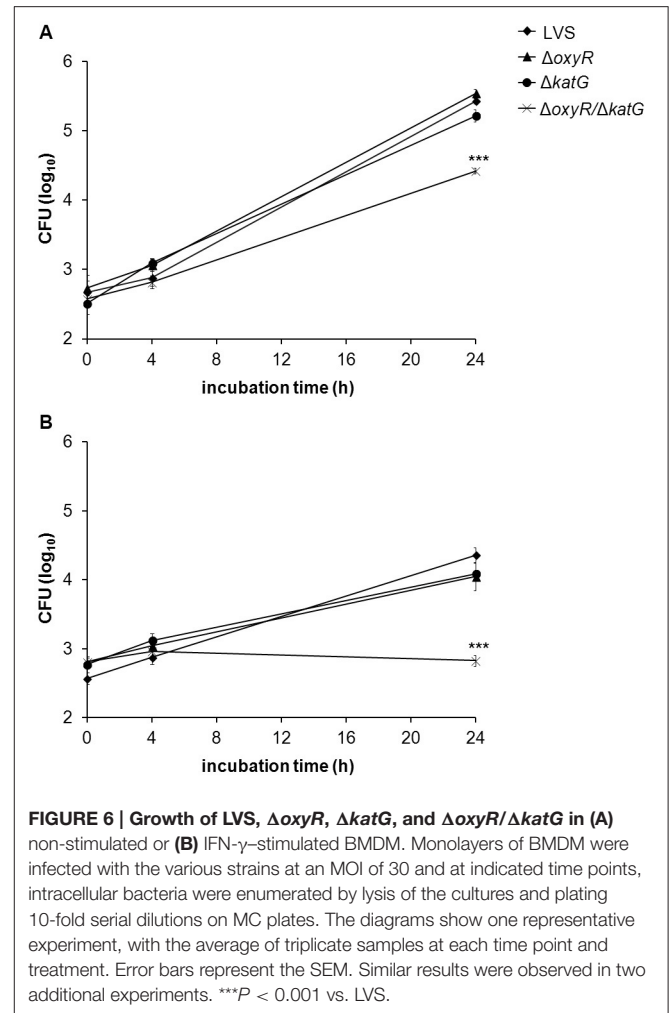
Intracellular Replication in BMDM

Based on the increased susceptibility to various ROS displayed by $\Delta oxyR$, $\Delta katG$, and $\Delta oxyR/\Delta katG$, it was of interest to test whether the strains were defective for replication in professional phagocytes. Non-stimulated or IFN- γ -stimulated BMDMs were infected with LVS, $\Delta oxyR$, $\Delta katG$, or $\Delta oxyR/\Delta katG$ at an MOI



of 30, and the viability of internalized bacteria was determined after 0 h, 4 h, and 24 h. In non-stimulated BMDM, LVS grew from approximately $2.5 \log_{10}$ CFU to more than $5.0 \log_{10}$ CFU within 24 h and also $\Delta oxyR$ and $\Delta katG$ grew to similar extent (Figure 6A). $\Delta oxyR/\Delta katG$ grew in non-stimulated cells, but reached approximately 10-fold lower numbers compared to the other strains after 24 h ($P < 0.001$; Figure 6A).

IFN- γ -stimulation of BMDM prior to infection reduced the numbers of LVS, $\Delta katG$, and $\Delta oxyR$ about 10-fold at 24 h vs. the numbers in non-stimulated cultures ($P < 0.001$; Figures 6A,B). There was no growth of $\Delta oxyR/\Delta katG$ in IFN- γ -stimulated cultures and, thus, significantly lower bacterial

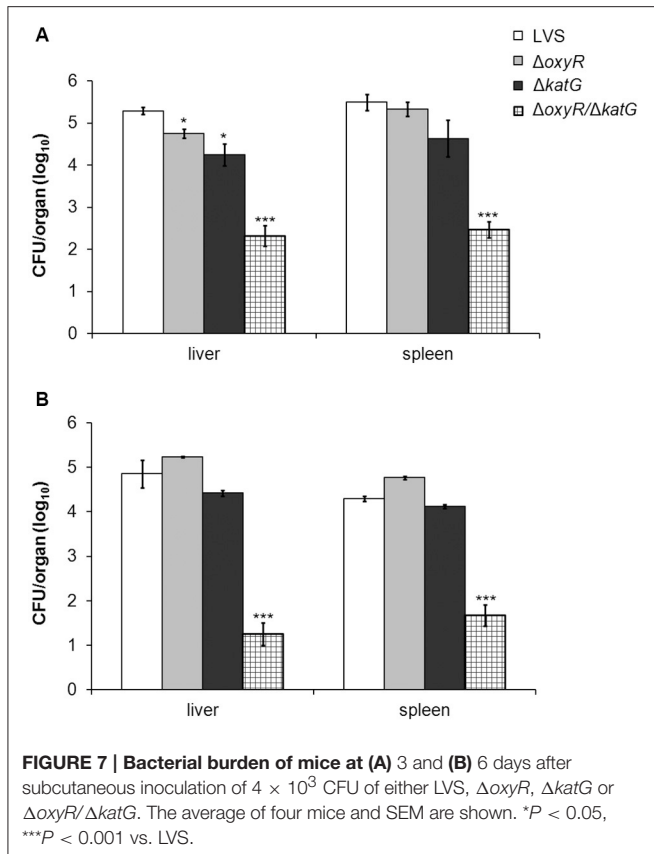


numbers compared to non-stimulated cultures at 24 h ($P < 0.001$; Figures 6A,B) and vs. all the other strains exposed to IFN- γ ($P < 0.001$; Figure 6B).

Thus, the $\Delta oxyR$ and $\Delta katG$ mutants showed intact capacity of intracellular replication, whereas the $\Delta oxyR/\Delta katG$ mutant showed impaired replication in BMDM, both in the presence and absence of IFN- γ .

Virulence in Mice

The virulence of LVS, $\Delta oxyR$, $\Delta katG$, and $\Delta oxyR/\Delta katG$ was determined by subcutaneous infection of C57BL/6 mice with 4×10^3 CFU/mouse, a non-lethal dose, and enumeration of viable bacteria in spleen and liver on day 3 and 6 of infection. Compared to LVS, there were lower numbers of both $\Delta oxyR$ and $\Delta katG$ on day 3 in the liver of the mice ($P < 0.05$; Figure 7A), whereas there were no differences between these strains in either the liver or spleen at the other time points (Figures 7A,B). Numbers of $\Delta oxyR/\Delta katG$ in both organs were at least 100-fold lower vs. all other strains at both time points ($P < 0.001$). Thus, both $\Delta oxyR$ and $\Delta katG$ showed slight attenuation in mice, whereas $\Delta oxyR/\Delta katG$ was highly attenuated.



DISCUSSION

Francisella tularensis is a versatile bacterium capable of surviving in many different hosts, vectors and in various cell types, including the normally bactericidal macrophages. Upon phagocytosis, *F. tularensis* is encased in a phagosome, a membrane-bound compartment designed for the annihilation of phagocytosed microbes, which is rich in antimicrobial molecules, such as reactive oxygen and nitrogen species. Although *F. tularensis* only transiently resides in this compartment, it must still muster defenses against highly reactive species in order to survive and escape to the cytosol, where it proceeds to replicate. By entering the cytosol, *F. tularensis* gains access to a nutrient-rich, protected niche in which it multiplies. As survival and replication in the intracellular niche is essential for the life cycle of *F. tularensis*, a thorough understanding of how the bacterium survives intracellularly is essential to fully grasp its defense mechanisms against oxidative stress. To this end, the study focused on understanding the interplay between catalase and OxyR, the latter being important for the expression of several antioxidant enzymes, in the defense against ROS and their impact on the survival of the bacterium in professional phagocytes.

To investigate if OxyR is involved in the oxidative stress response of LVS, we constructed an in-frame deletion of *oxyR*. A similar investigation has been performed recently by Ma et al. which studied the role of OxyR in LVS (Ma et al., 2016).

It was found that OxyR controlled transcription of *katG* and the findings agree with the reduced catalase activity of $\Delta oxyR$ observed in the present study. Nevertheless, our study revealed that even in the absence of OxyR, there was still prominent catalase activity. Overall, it appears that OxyR, as expected, regulates *katG* in the LVS strain, however, the regulation does not completely abolish its expression as is the case observed for various other bacterial species, e.g., *E. coli* (Michán et al., 1999), *Salmonella enterica* (Morgan et al., 1986), *Haemophilus influenza* (Whitby et al., 2012), or *Moraxella catarrhalis* (Hoopman et al., 2011). In both the present study, and in the previous study, it was observed that the lack of OxyR led to marked suppression of *ahpC2* (Ma et al., 2016). In addition Ma et al. demonstrated suppressed expression of both *katG* and *sodB* in $\Delta oxyR$ by real-time PCR and demonstrated that OxyR binds to the upstream promoter regions of each gene. In contrast, there was no down-regulation of *katG* or *sodB* observed in the present study. Likely, this is a consequence of the rapid on/off switch of the promoter binding capacity of OxyR in response to the oxidative levels in the bacteria leading to a limited window when elevated mRNA levels can be detected (Wei et al., 2012).

Besides antioxidant genes, our study revealed an aberrant expression of genes encoding chaperone proteins of the mutants. Such proteins are induced in response to various stresses, including oxidative stress (Hartl et al., 2011). Thus, the induced expression of these genes in $\Delta oxyR$ and in $\Delta katG$, also observed by Ma et al. (2016), likely is a reflection of oxidative stress encountered by the mutants. The chaperone network likely helps the bacterium to handle this stress through unfolding and/or degradation of mis-folded/damaged proteins. The reason behind the suppressed expression of multiple chaperone genes in $\Delta oxyR/\Delta katG$ is obscure, but should lead to an accumulation of damaged or mis-folded proteins and may explain why it was so impaired for growth in broth. The intact growth of $\Delta oxyR/\Delta katG$ under microaerobic conditions likely reflects that reduced levels of ROS are formed and therefore that antioxidant defenses are less important. The aberrant expression of genes related to iron-uptake did not result in a skewed iron content of $\Delta oxyR/\Delta katG$ (data not shown) and it is therefore not obvious that this would influence the susceptibility of the strain to various ROS.

The *F. tularensis* *ahpC2* gene is divergently transcribed from the *oxyR* promoter, a feature commonly seen for genes transcriptionally regulated by OxyR (Hahn et al., 2002; Maddocks and Oyston, 2008). AhpC belongs to the peroxiredoxin family, which is ubiquitously found in nature (Rhee et al., 2005) and is known to be involved in defenses against peroxides in *E. coli* (Storz et al., 1989), and both peroxides and peroxynitrite in, e.g., *Salmonella typhimurium* (Bryk et al., 2000), and in the defense against superoxide and peroxynitrite in the virulent SCHU S4 strain of *F. tularensis* subsp. *tularensis* (Binesse et al., 2015). In agreement with this, and in view of the reduced expression of AhpC in $\Delta oxyR$, this mutant was also highly susceptible to ONOO⁻. $\Delta katG$ was as susceptible as $\Delta oxyR$ to ONOO⁻ and in view of the substantial catalase activity remaining in $\Delta oxyR$, this result implies that the function of catalase overlaps with other OxyR-regulated detoxifying mechanisms, presumably AhpC, to

protect against ONOO⁻. Further corroborating the importance of AhpC and catalase was the failure to generate a *katG* and *ahpC* double deletion mutant and even an *ahpC* mutant in LVS. Hence, AhpC seems indispensable to LVS, which is in stark contrast to SCHU S4, where deletion of *ahpC* resulted in only slight attenuation (Binesse et al., 2015). This indicates that there is a disparity regarding the importance of the enzyme between the SCHU S4 and LVS strains, possibly a factor that to some extent explains the difference in virulence between the strains, since it implies that the detoxifying mechanisms of SCHU S4 are much more elaborate. Nevertheless, as for LVS, it has not been possible to generate a *katG* and *ahpC* double deletion mutant of SCHU S4 (Kadzhaev et al., 2009; Binesse et al., 2015). Collectively, this indicates that the mechanisms of protection conferred by these enzymes may be overlapping and the lack of both is detrimental to the survival of both LVS and highly virulent *F. tularensis* strains.

Based on the failure to generate a *katG* and *ahpC* double deletion mutant and the marked suppression of *ahpC* in the Δ *oxyR* mutant, we hypothesized that the absence of OxyR together with the absence of catalase would severely disarm the capability of the bacterium to handle ROS. Indeed, we observed that the Δ *oxyR*/ Δ *katG* mutant was hyper-susceptible to H₂O₂, ONOO⁻, and O₂⁻; much more so than either Δ *oxyR* or Δ *katG*. Collectively, the results demonstrate that the roles of OxyR-regulated antioxidant enzymes and catalase overlap to protect LVS against various ROS. We find it likely that the reduced activity of catalase and expression of *ahpC* observed in *oxyR* contributed to the increased susceptibility of the mutant to H₂O₂, O₂⁻, and ONOO⁻ through the increase of both Fenton-mediated toxicity and direct O₂⁻- and ONOO⁻-mediated damage. We further suggest that the reduced levels of AhpC together with the lack of catalase in the Δ *oxyR*/ Δ *katG* strain, despite an increased expression of *sodB*, *sodC* and *FTT0086*, resulted in enhanced Fenton-mediated toxicity and ONOO⁻-mediated damage, which likely account for the extreme susceptibility of the double mutant to O₂⁻, H₂O₂, and ONOO⁻. Our findings concur with those of Ma et al. (2016), and, in addition, demonstrate that the combined activity of catalase and OxyR-regulated detoxifying mechanisms are critical for ROS detoxification by *F. tularensis*.

Despite the enhanced susceptibility of both Δ *oxyR* and Δ *katG* to various ROS, the strains replicated as efficiently as LVS in mouse BMDM, but importantly, the capacity to replicate in professional phagocytes required either OxyR or catalase, since Δ *oxyR*/ Δ *katG* failed to replicate. IFN- γ -activation of BMDM restricted growth of LVS, Δ *katG*, and Δ *oxyR* to a similar degree and completely blocked the growth of Δ *oxyR*/ Δ *katG*. The majority of *F. tularensis* LVS escapes the phagosome of IFN- γ -activated macrophages (Lindgren et al., 2004), but the mechanism of growth inhibition appears to vary depending on the cell model used (Edwards et al., 2010). IFN- γ -mediated inhibition of intracellular growth of *F. novicida* is dependent on the expression of IRGB10 and various guanylate-binding proteins (Meunier et al., 2015; Man et al., 2016), however, the role of this pathway is unknown for other *F. tularensis* species.

Our results reveal elaborate interconnecting roles between OxyR-regulated ROS-detoxifying mechanisms and catalase and demonstrate that either needs to be intact for the bacterium to thrive in professional phagocytes. The roles of the anti-oxidative mechanisms could be to protect the bacterium from direct damage by various ROS, such as ONOO⁻, which has been demonstrated to be crucial for killing of *F. tularensis* in peritoneal cells (Lindgren et al., 2005). Alternatively, or additionally, the antioxidants may restrict macrophage activation through their ability to preserve phosphatase activity required for kinase signaling and proinflammatory cytokine production (Melillo et al., 2010).

Our finding that Δ *oxyR* replicated as efficiently as LVS in BMDM is in contrast to findings in a previous study, which reported that an *oxyR* mutant of LVS was markedly impaired with regard to escape from the phagosome, replication in professional phagocytes, and virulence in the mouse model (Ma et al., 2016). Notably, the LVS strain used by Ma et al. replicated less than 10-fold during 24 h in C57BL/6 BMDM, whereas the LVS strain used in the present study replicated about 500-fold. Isolates of LVS with different virulence are used in the research community (Griffin et al., 2015) and the distinct differences in the intracellular growth of these two LVS strains are additional examples of such distinct phenotypes. The phenotypic differences between the two LVS strains likely explain the discrepant findings of the two studies. The observation in the present study of the intact growth of the single mutants in BMDM was corroborated by findings *in vivo*, since the Δ *oxyR* and Δ *katG* mutants showed essentially intact growth in organs of mice, whereas Δ *oxyR*/ Δ *katG* hardly grew at all. Despite their effective growth in the organs, a previous study demonstrated a more distinct growth defect of the Δ *katG* mutant, most likely because a 100-fold higher dose was given (Lindgren et al., 2007). Moreover, by the intranasal route, Δ *oxyR* was demonstrated to be moderately attenuated (Ma et al.). Based on these collective findings, it can be concluded that both OxyR and KatG contribute to the virulence of *F. tularensis* LVS and that the concomitant loss is detrimental to the virulence of the bacterium.

Altogether, the results presented in this study clearly demonstrate the mutual importance of catalase and OxyR for a robust oxidative stress defense system and that either of these systems is vital for the intracellular replication of *F. tularensis* and for its virulence.

AUTHOR CONTRIBUTIONS

Conceived and designed the experiments: AS, MH, and HL. Performed the experiments: MH, HL, and GB. Analyzed the data: AS, MH, HL, and GB. Wrote the paper: HL, MH, and AS.

ACKNOWLEDGMENTS

Grant support was obtained from the Swedish Medical Research Council (K2010-9485, K2012-3469, and K2013-8621), and the Medical Faculty, Umeå University, Umeå, Sweden.

REFERENCES

- Andrews, S. C., Robinson, A. K., and Rodríguez-Quinones, F. (2003). Bacterial iron homeostasis. *FEMS Microbiol. Rev.* 27, 215–237. doi: 10.1016/S0168-6445(03)00055-X
- Anthony, L. S., Morrissey, P. J., and Nano, F. E. (1992). Growth inhibition of *Francisella tularensis* live vaccine strain by IFN-gamma-activated macrophages is mediated by reactive nitrogen intermediates derived from L-arginine metabolism. *J. Immunol.* 148, 1829–1834.
- Bakshi, C. S., Malik, M., Regan, K., Melendez, J. A., Metzger, D. W., Pavlov, V. M., et al. (2006). Superoxide dismutase B gene (sodB)-deficient mutants of *Francisella tularensis* demonstrate hypersensitivity to oxidative stress and attenuated virulence. *J. Bacteriol.* 188, 6443–6448. doi: 10.1128/JB.00266-06
- Betteridge, D. J. (2000). What is oxidative stress? *Metab. Clin. Exp.* 49, 3–8. doi: 10.1016/S0026-0495(00)80077-3
- Binesse, J., Lindgren, H., Lindgren, L., Conlan, W., and Sjöstedt, A. (2015). Roles of reactive oxygen species-degrading enzymes of *Francisella tularensis* SCHU S4. *Infect. Immun.* 83, 2255–2263. doi: 10.1128/IAI.02488-14
- Bröms, J. E., Lavander, M., Meyer, L., and Sjöstedt, A. (2011). IglG and IglI of the *Francisella pathogenicity* island are important virulence determinants of *Francisella tularensis* LVS. *Infect. Immun.* 79, 3683–3696. doi: 10.1128/IAI.01344-10
- Bröms, J. E., Lavander, M., and Sjöstedt, A. (2009). A conserved alpha-helix essential for a type VI secretion-like system of *Francisella tularensis*. *J. Bacteriol.* 191, 2431–2446. doi: 10.1128/JB.01759-08
- Bröms, J. E., Sjöstedt, A., and Lavander, M. (2010). The role of the *Francisella tularensis* pathogenicity island in type VI secretion, intracellular survival, and modulation of host cell signaling. *Front. Microbiol.* 1:136. doi: 10.3389/fmicb.2010.00136
- Bryk, R., Griffin, P., and Nathan, C. (2000). Peroxynitrite reductase activity of bacterial peroxiredoxins. *Nature* 407, 211–215. doi: 10.1038/35025109
- Chong, A., and Celli, J. (2010). The *Francisella intracellular* life cycle: toward molecular mechanisms of intracellular survival and proliferation. *Front. Microbiol.* 1:138. doi: 10.3389/fmicb.2010.00138
- Conlan, J. W. (2011). Tularemia vaccines: recent developments and remaining hurdles. *Future Microbiol.* 6, 391–405. doi: 10.2217/fmb.11.22
- Edwards, J. A., Rockx-Brouwer, D., Nair, V., and Celli, J. (2010). Restricted cytosolic growth of *Francisella tularensis* subsp. *tularensis* by IFN-gamma activation of macrophages. *Microbiology* 156, 327–339. doi: 10.1099/mic.0.031716-0
- Farr, S. B., and Kogoma, T. (1991). Oxidative stress responses in *Escherichia coli* and *Salmonella typhimurium*. *Microbiol. Rev.* 55, 561–585.
- Flannagan, R. S., Cosio, G., and Grinstein, S. (2009). Antimicrobial mechanisms of phagocytes and bacterial evasion strategies. *Nat. Rev. Microbiol.* 7, 355–366. doi: 10.1038/nrmicro2128
- Fridovich, I. (1998). Oxygen toxicity: a radical explanation. *J. Exp. Biol.* 201, 1203–1209.
- Gavrillin, M. A., Bouakl, I. J., Knatz, N. L., Duncan, M. D., Hall, M. W., Gunn, J. S., et al. (2006). Internalization and phagosome escape required for *Francisella* to induce human monocyte IL-1 β processing and release. *Proc. Natl. Acad. Sci. U.S.A.* 103, 141–146. doi: 10.1073/pnas.0504271103
- Golovliov, I., Sjöstedt, A., Mokrievich, A., and Pavlov, V. (2003). A method for allelic replacement in *Francisella tularensis*. *FEMS Microbiol. Lett.* 222, 273–280. doi: 10.1016/S0378-1097(03)00313-6
- Griffin, A. J., Crane, D. D., Wehrly, T. D., and Bosio, C. M. (2015). Successful protection against tularemia in C57BL/6 mice is correlated with expansion of *Francisella tularensis*-specific effector T cells. *Clin. Vaccine Immunol.* 22, 119–128. doi: 10.1128/CVI.00648-14
- Hahn, J. S., Oh, S. Y., and Roe, J. H. (2002). Role of OxyR as a peroxide-sensing positive regulator in *Streptomyces coelicolor* A3(2). *J. Bacteriol.* 184, 5214–5222. doi: 10.1128/JB.184.19.5214-5222.2002
- Hartl, F. U., Bracher, A., and Hayer-Hartl, M. (2011). Molecular chaperones in protein folding and proteostasis. *Nature* 475, 324–332. doi: 10.1038/nature10317
- Hassan, H. M., and Fridovich, I. (1979). Paraquat and *Escherichia coli*. Mechanism of production of extracellular superoxide radical. *J. Biol. Chem.* 254, 10846–10852.
- Hogg, N., Darley-USmar, V. M., Wilson, M. T., and Moncada, S. (1992). Production of hydroxyl radicals from the simultaneous generation of superoxide and nitric oxide. *Biochem. J.* 281, 419–424. doi: 10.1042/bj2810419
- Honn, M., Lindgren, H., and Sjöstedt, A. (2012). The role of MglA for adaptation to oxidative stress of *Francisella tularensis* LVS. *BMC Microbiol.* 12:14. doi: 10.1186/1471-2180-12-14
- Hoopman, T. C., Liu, W., Joslin, S. N., Pybus, C., Brautigam, C. A., and Hansen, E. J. (2011). Identification of gene products involved in the oxidative stress response of *Moraxella catarrhalis*. *Infect. Immun.* 79, 745–755. doi: 10.1128/IAI.01060-10
- Kadzaev, K., Zingmark, C., Golovliov, I., Bolanowski, M., Shen, H., Conlan, W., et al. (2009). Identification of genes contributing to the virulence of *Francisella tularensis* SCHU S4 in a mouse intradermal infection model. *PLoS ONE* 4:e5463. doi: 10.1371/journal.pone.0005463
- Lindgren, H., Honn, M., Golovliov, I., Kadzaev, K., Conlan, W., and Sjöstedt, A. (2009). The 58-kilodalton major virulence factor of *Francisella tularensis* is required for efficient utilization of iron. *Infect. Immun.* 77, 4429–4436. doi: 10.1128/IAI.00702-09
- Lindgren, H., Shen, H., Zingmark, C., Golovliov, I., Conlan, W., and Sjöstedt, A. (2007). Resistance of *Francisella tularensis* strains against reactive nitrogen and oxygen species with special reference to the role of KatG. *Infect. Immun.* 75, 1303–1309. doi: 10.1128/IAI.01717-06
- Lindgren, H., Stenman, L., Tärnvik, A., and Sjöstedt, A. (2005). The contribution of reactive nitrogen and oxygen species to the killing of *Francisella tularensis* LVS by murine macrophages. *Microbes Infect.* 7, 467–475. doi: 10.1016/j.micinf.2004.11.020
- Lindgren, H., Stenmark, S., Chen, W., Tärnvik, A., and Sjöstedt, A. (2004). Distinct roles of reactive nitrogen and oxygen species to control infection with the facultative intracellular bacterium *Francisella tularensis*. *Infect. Immun.* 72, 7172–7182. doi: 10.1128/IAI.72.12.7172-7182.2004
- Ma, Z., Russo, V. C., Rabadi, S. M., Jen, Y., Catlett, S. V., Bakshi, C. S., et al. (2016). Elucidation of a mechanism of oxidative stress regulation in *Francisella tularensis* live vaccine strain. *Mol. Microbiol.* 101, 856–878. doi: 10.1111/mmi.13426
- Maddocks, S. E., and Oyston, P. C. (2008). Structure and function of the LysR-type transcriptional regulator (LTTR) family proteins. *Microbiology* 154, 3609–3623. doi: 10.1099/mic.0.2008/022772-0
- Man, S. M., Karki, R., Sasai, M., Place, D. E., Kesavardhana, S., Temirov, J., et al. (2016). IRGB10 liberates bacterial ligands for sensing by the AIM2 and Caspase-11-NLRP3 inflammasomes. *Cell* 167, 382–396.e17. doi: 10.1016/j.cell.2016.09.012
- Melillo, A. A., Bakshi, C. S., and Melendez, J. A. (2010). *Francisella tularensis* antioxidants harness reactive oxygen species to restrict macrophage signaling and cytokine production. *J. Biol. Chem.* 285, 27553–27560. doi: 10.1074/jbc.M110.144394
- Melillo, A. A., Mahawar, M., Sellati, T. J., Malik, M., Metzger, D. W., Melendez, J. A., et al. (2009). Identification of *Francisella tularensis* live vaccine strain CuZn superoxide dismutase as critical for resistance to extracellularly generated reactive oxygen species. *J. Bacteriol.* 191, 6447–6456. doi: 10.1128/JB.00534-09
- Meunier, E., Wallet, P., Dreier, R. F., Costanzo, S., Anton, L., Rühl, S., et al. (2015). Guanylate-binding proteins promote activation of the AIM2 inflammasome during infection with *Francisella novicida*. *Nat. Immunol.* 16, 476–484. doi: 10.1038/ni.3119
- Michán, C., Manchado, M., Dorado, G., and Pueyo, C. (1999). *In vivo* transcription of the *Escherichia coli* oxyR regulon as a function of growth phase and in response to oxidative stress. *J. Bacteriol.* 181, 2759–2764.
- Morgan, R. W., Christman, M. F., Jacobson, F. S., Storz, G., and Ames, B. N. (1986). Hydrogen peroxide-inducible proteins in *Salmonella typhimurium* overlap with heat shock and other stress proteins. *Proc. Natl. Acad. Sci. U.S.A.* 83, 8059–8063. doi: 10.1073/pnas.83.21.8059
- Murphy, M. P., Packer, M. A., Scarlett, J. L., and Martin, S. W. (1998). Peroxynitrite: a biologically significant oxidant. *Gen. Pharmacol.* 31, 179–186. doi: 10.1016/S0306-3623(97)00418-7
- Oyston, P. C., Sjöstedt, A., and Titball, R. W. (2004). Tularemia: bioterrorism defence renews interest in *Francisella tularensis*. *Nat. Rev. Microbiol.* 2, 967–978. doi: 10.1038/nrmicro1045

- Polsinelli, T., Meltzer, M. S., and Fortier, A. H. (1994). Nitric oxide-independent killing of *Francisella tularensis* by IFN-gamma-stimulated murine alveolar macrophages. *J. Immunol.* 153, 1238–1245.
- Pomposiello, P. J., and Demple, B. (2001). Redox-operated genetic switches: the SoxR and OxyR transcription factors. *Trends Biotechnol.* 19, 109–114. doi: 10.1016/S0167-7799(00)01542-0
- Rhee, S. G., Chae, H. Z., and Kim, K. (2005). Peroxiredoxins: a historical overview and speculative preview of novel mechanisms and emerging concepts in cell signaling. *Free Radic. Biol. Med.* 38, 1543–1552. doi: 10.1016/j.freeradbiomed.2005.02.026
- Schaible, U. E., and Kaufmann, S. H. (2004). Iron and microbial infection. *Nat. Rev. Microbiol.* 2, 946–953. doi: 10.1038/nrmicro1046
- Sjöstedt, A. (2006). Intracellular survival mechanisms of *Francisella tularensis*, a stealth pathogen. *Microbes Infect.* 8, 561–567. doi: 10.1016/j.micinf.2005.08.001
- Storz, G., Jacobson, F. S., Tartaglia, L. A., Morgan, R. W., Silveira, L. A., and Ames, B. N. (1989). An alkyl hydroperoxide reductase induced by oxidative stress in *Salmonella typhimurium* and *Escherichia coli*: genetic characterization and cloning of ahp. *J. Bacteriol.* 171, 2049–2055. doi: 10.1128/jb.171.4.2049-2055.1989
- Troxell, B., and Hassan, H. M. (2013). Transcriptional regulation by Ferric Uptake Regulator (Fur) in pathogenic bacteria. *Front. Cell. Infect. Microbiol.* 3:59. doi: 10.3389/fcimb.2013.00059
- Wei, Q., Minh, P. N., Dötsch, A., Hildebrand, F., Panmanee, W., Elfarash, A., et al. (2012). Global regulation of gene expression by OxyR in an important human opportunistic pathogen. *Nucleic Acids Res.* 40, 4320–4333. doi: 10.1093/nar/gks017
- Whitby, P. W., Morton, D. J., Vanwagoner, T. M., Seale, T. W., Cole, B. K., Mussa, H. J., et al. (2012). *Haemophilus influenzae* OxyR: characterization of its regulation, regulon and role in fitness. *PLoS ONE* 7:e50588. doi: 10.1371/journal.pone.0050588
- Zheng, M., Aslund, F., and Storz, G. (1998). Activation of the OxyR transcription factor by reversible disulfide bond formation. *Science* 279, 1718–1721. doi: 10.1126/science.279.5357.1718
- Zheng, M., Doan, B., Schneider, T. D., and Storz, G. (1999). OxyR and SoxRS regulation of fur. *J. Bacteriol.* 181, 4639–4643.

Conflict of Interest Statement: The authors declare that the research was conducted in the absence of any commercial or financial relationships that could be construed as a potential conflict of interest.

Copyright © 2017 Honn, Lindgren, Bharath and Sjöstedt. This is an open-access article distributed under the terms of the Creative Commons Attribution License (CC BY). The use, distribution or reproduction in other forums is permitted, provided the original author(s) or licensor are credited and that the original publication in this journal is cited, in accordance with accepted academic practice. No use, distribution or reproduction is permitted which does not comply with these terms.



Role of Glycosylation/Deglycosylation Processes in *Francisella tularensis* Pathogenesis

Monique Barel^{1,2,3*} and Alain Charbit^{1,2,3}

¹ Sorbonne Paris Cité, Bâtiment Leriche, Université Paris Descartes, Paris, France, ² Institut National de la Santé et de la Recherche Médicale, Institut Necker-Enfants Malades, INSERM U1151 -Team 11, Pathogenesis of Systemic Infections, Paris, France, ³ Centre National de la Recherche Scientifique, UMR8253, Paris, France

Francisella tularensis is able to invade, survive and replicate inside a variety of cell types. However, *in vivo* *F. tularensis* preferentially enters host macrophages where it rapidly escapes to the cytosol to avoid phagosomal stresses and to multiply to high numbers. We previously showed that human monocyte infection by *F. tularensis* LVS triggered deglycosylation of the glutamine transporter SLC1A5. However, this deglycosylation, specifically induced by *Francisella* infection, was not restricted to SLC1A5, suggesting that host protein deglycosylation processes in general might contribute to intracellular bacterial adaptation. Indeed, we later found that *Francisella* infection modulated the transcription of numerous glycosidase and glycosyltransferase genes in human macrophages and analysis of cell extracts revealed an important increase of N and O-protein glycosylation. In eukaryotic cells, glycosylation has significant effects on protein folding, conformation, distribution, stability, and activity and dysfunction of protein glycosylation may lead to development of diseases like cancer and pathogenesis of infectious diseases. Pathogenic bacteria have also evolved dedicated glycosylation machineries and have notably been shown to use these glycoconjugates as ligands to specifically interact with the host. In this review, we will focus on *Francisella* and summarize our current understanding of the importance of these post-translational modifications on its intracellular niche adaptation.

Keywords: glycosylation, host-pathogen interaction

OPEN ACCESS

Edited by:

Marina Santic,
University of Rijeka, Croatia

Reviewed by:

Jiri Stullik,
University of Defence, Czechia
Paul Edward Carlson,
Food and Drug Administration, USA

*Correspondence:

Monique Barel
Monique.barel@inserm.fr

Received: 13 January 2017

Accepted: 27 February 2017

Published: 21 March 2017

Citation:

Barel M and Charbit A (2017) Role of Glycosylation/Deglycosylation Processes in *Francisella tularensis* Pathogenesis. *Front. Cell. Infect. Microbiol.* 7:71. doi: 10.3389/fcimb.2017.00071

INTRODUCTION

Protein glycosylation is one of the most common post-translational modifications (PTM) of proteins, as present in all kingdoms of life. It consists in the covalent attachment of glycans onto amino acid side chains, this reaction being catalyzed by an enzyme. In eukaryotic cells, glycosylation has significant effects on protein folding, conformation, distribution, stability, and activity. Particularly, the sugar chains of glycoproteins are essential for maintaining the order of intercellular interactions among all differentiated cells in multicellular organisms. Therefore, alterations in the sugar chains may range from being essentially undetectable to a complete loss in particular functions (Varki, 1993). Indeed, dysfunction of protein glycosylation may lead to development of diseases like cancer and pathogenesis of infectious diseases (Moran et al., 2011). In the innate immune system, which is the major actor for protection against microbial

pathogens, several host glycoproteins have been shown to function as pattern recognition receptors (PRRs), involved in pathogen binding (Di Gioia and Zanoni, 2015). Cell-surface glycoproteins facing the extracellular environment are ideally located to facilitate this host–pathogen interaction. The receptors of the innate immune response i.e., Toll-like receptors (TLRs) and nucleotide oligomerization domain (NOD-like) receptors (NLRs) are glycoproteins. In the adaptive immune response, the major components, which include class I and class II major histocompatibility complex proteins, chemokine and cytokine receptors, and essentially all cytokines and chemokines are glycosylated (Opdenakker et al., 2016).

Bacterial pathogens have also evolved dedicated glycosylation machineries. When compared to higher organisms, bacteria are capable of producing an extraordinary amount of unique and diverse glycans, which are principally attached to the cell surface, and secreted molecules. Bacteria are able to use these glycoconjugates as a range of unique and specific ligands, which specifically interact with the host (Tytgat and de Vos, 2016). Bacteria are covered with various types of carbohydrate moieties. These surface-exposed bacterial structures are often called pathogen-associated molecular patterns (or PAMPS).

Oligosaccharides may either mediate “specific recognition” events or provide “modulation” of biological processes. For example, they may allow interaction of bacterial proteins with host-derived proteins or they may modulate bacteria- and/or host-related events (Bastos et al., 2017). All these events may be essential for bacterial colonization, its survival and the subsequent infection. Therefore, host immunization may be dependent on these PTM, whether mediated by the pathogen or by the host.

Francisella tularensis is a Gram-negative bacterium causing the zoonotic disease tularemia in a number of mammalian species, including humans (Sjöstedt, 2011). *F. tularensis* invades, survives and replicates inside a variety of cell types, including phagocytic and non-phagocytic cells of various species (Meibom and Charbit, 2010), as well as arthropod-derived cells (Santic et al., 2010). “*In vivo*,” *F. tularensis* preferentially enters host macrophages (Clemens et al., 2005), rapidly escapes to the cytosol where it actively multiplies (Case et al., 2014). While the cytoplasm was initially considered as a safe nutrient-replete haven (Ray et al., 2009), it is now clearly established that the host cytosol may be a harsh environment by depriving nutrients against invading bacteria (Abu Kwaik and Bumann, 2013; Zhang and Rubin, 2013). Conversely, invading intracellular pathogens may also “steal” nutrients of the host cell that, in turn, needs to adapt its metabolism to control its cytosolic content (Barel et al., 2015). Indeed, upon addition of gluconeogenic substrates, such as oxaloacetate and pyruvate, to the cell culture medium increased intracellular multiplication of *F. tularensis* LVS was observed, suggesting that these nutrients served as sources of glucose to feed multiplying bacteria.

We will herein summarize what is known about the glycosylation-deglycosylation processes occurring during *Francisella* infection, as observed from either the host or the pathogen.

HOST POINT OF VIEW

Francisella infection modifies numerous “glyco-genes” involved in glycosylation pathways in human macrophages. Indeed, using a glycan processing gene microarray (Chacko et al., 2011), we observed significant changes in the level of glycosyltransferase and glycosidase gene expression profiles in human THP-1 monocytes, infected for 24 h with *F. tularensis* LVS (Barel et al., 2016). Expression of eight genes, encoding four glycosyltransferases and four glycosidases, was down-regulated upon infection. These four glycosidase belonged to the EDEM family, which is involved in ER-associated degradation (ERAD). The expression of six genes was up-regulated upon infection, corresponding to five glycosyltransferases and one glycosidase. The up-regulated glycosyltransferases were involved either in *N*-glycosylation or in *O*-glycosylation of glycoproteins. The glycosidase gene whose expression was up-regulated, encoded the glycosidase HEXA, which is involved in the Hexosamine Biosynthetic Pathway (HBP) (Vaidyanathan et al., 2014).

Glycosylation occurred as soon as 1 h after entry of the bacteria into the cells. Only three proteins were found and characterized as carrying potential *N*-glycosylation residues, while nine proteins contained potential *O*-glycosylation residues. Among them, we characterized BiP/GRP78/HSPA5 protein, a member of the HSP70 heat shock protein family. BiP expression was increased both at transcription and translation level, by *F. tularensis* LVS infection immediately after binding to the cells. BiP glycosylation was also induced at early stage of infection. BiP being a key regulator of the UPR (Ni et al., 2009; Pfaffenbach and Lee, 2011), we hypothesized that the glycosylation-deglycosylation processes could be modified by *Francisella*. This could result in direct triggering of the UPR (including BiP) in infected cells with a decrease of the load of newly synthesized “abnormal” proteins. In addition, among the nine proteins containing potential *O*-glycosylation residues and being glycosylated by *Francisella* infection, we also found PRKCSH, the beta-subunit of glucosidase 2. This enzyme is acting upstream BiP, in the calnexin pathway, which is also involved in correcting misfolded proteins (Hetz et al., 2011).

Infection of human monocytes by *F. tularensis* LVS also triggered the deglycosylation of the glycosylated amino acid transporter SLC1A5 and other glycoproteins (Barel et al., 2012). Deglycosylation induced by *F. tularensis* LVS was maximum at 24 h when intracellular multiplication occurred and depended on the capacity of the bacteria to escape from the phagosomes (Barel et al., 2012). It was not an inhibition of glycosylation since tunicamycine had no inhibiting effect on this deglycosylation.

The enzymes involved in these glycosylation-deglycosylation mechanisms are still not characterized.

We tried to summarize the cascade of events triggered upon infection of macrophages by *Francisella* in the hypothetical model depicted in **Figure 1**. The transporter SLC1A5 was chosen as a prototypic glycosylated membrane protein. After its synthesis and translocation into the ER, the protein is transported to the Golgi where it is first glycosylated ① and, from there, addressed to the membrane via secretory vesicles. In the plasma membrane, SLC1A5 is present only as a glycosylated protein ② (Console

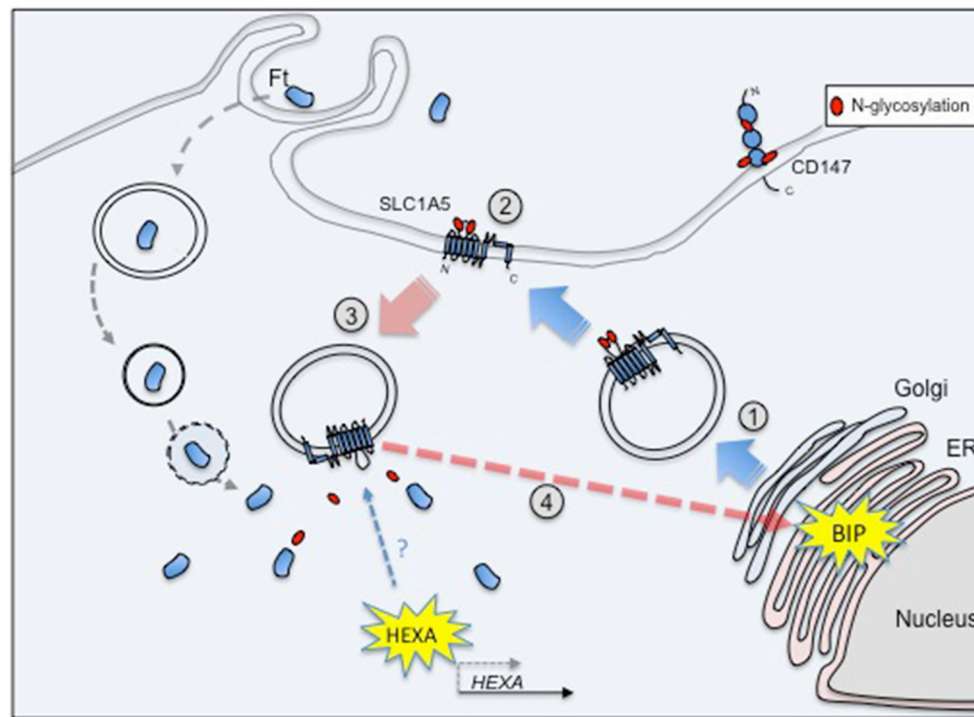


FIGURE 1 | SLC1A5 is glycosylated after passage into the Golgi ① and is exported to the membrane ②. Its endocytosis into the cytoplasm renders it available to glucosidases ③, e.g., HEXA, whose transcription level is increased upon *Francisella* infection. The deglycosylated form of SLC1A5 has been indeed localized only in the cytoplasm. In turn, these deglycosylated (and possibly misfolded) proteins could trigger the increase of BiP expression and its glycosylation ④.

et al., 2015). Upon re-entry into the cytoplasm via endocytosis, glycosylated SLC1A5 becomes available to glucosidases ③ such as HEXA (whose expression is induced upon *Francisella* infection). The deglycosylated form of SLC1A5 has been indeed localized only in the cytoplasm (Console et al., 2015). This deglycosylated form of the protein (possibly misfolded) could trigger increase of BiP expression and its glycosylation ④.

It is tempting to suggest that the intracellular survival of *Francisella* would be favored both by the control exerted on the UPR response of the host and by the availability of free oligosaccharides resulting from deglycosylation processes, that could serve as nutrients.

PATHOGEN POINT OF VIEW

A large number of bacterial proteins have been found to be glycosylated (Tan et al., 2015). They show a surprising degree of diversity, both within and between bacterial species. Protein glycosylation can be classified according to the glycosidic linkage. Attachment to the amide nitrogen of asparagine (Asn) is known as *N*-glycosylation, with that of serine or threonine (Ser/Thr) to the hydroxyl oxygen being known as *O*-glycosylation. *N*- and *O*-linked glycosylation may occur either through the action of an oligosaccharyltransferase (OST) or via the action of glycosyltransferases (GTs). OSTs substrates are lipid-linked oligosaccharides while the GTs substrates are

usually nucleotide-activated sugars. It was only very recently (Dankova et al., 2016) that the glycosylation machinery of *Francisella* was found to involve a variety of sugar biogenesis enzymes, glycosyltransferases, a flippase, and a protein-targeting oligosaccharyltransferase. As both type A and type B strains of *F. tularensis* subspecies expressed an *O*-linked protein glycosylation system, which utilizes core biosynthetic and assembly pathways, *O*-linked protein glycosylation may be a feature common to members of the *Francisella* genus (Egge-Jacobsen et al., 2011).

The initial attempts to elucidate the glycan repertoire of *Francisella* and their structures had failed because of the enzymatic and chemical release techniques used. Some proteins were found after transcriptional profiling of mutants. Indeed, FTT_0905 was characterized as a glycosylated Type IV pili protein, which is transcriptionally regulated by MglA. As MglA controls the expression of the *Francisella* pathogenicity island, FTT_0905 was considered as a new virulence factor (Brotcke et al., 2006). However, by mapping the glycoproteome of the FSC200 strain of *F. tularensis* subsp. *holarctica*, several candidate proteins were found that could be target for glycosylation as DsbA (FTH_1071), an uncharacterized protein FTH_0069, FopA, Tul4, and LemA (Balonova et al., 2010). In contrast, the PglA protein was identified as a targeting oligosaccharyltransferase because it is necessary for PilA glycosylation in *F. tularensis* (Egge-Jacobsen et al., 2011). Indeed, this protein undergoes multisite *O*-linked glycosylation, with a pentasaccharide of the structure

HexNac-Hex-Hex-HexNac-HexNac. PglA is highly conserved in *Francisella* genus, supporting the general feature of O-glycosylation. Then, the detailed characterization of the DsbA glycan and the putative role of the FTT0789–FTT0800 gene cluster in glycan biosynthesis were reported (Thomas et al., 2011). Indeed, these authors observed that the essential virulence factor DsbA migrated as multiple protein spots on two-dimensional electrophoresis gels. The protein was modified with a 1,156-Da glycan moiety in O-linkage. The glycan is a hexasaccharide, comprised of N-acetylhexosamines, hexoses, and an unknown monosaccharide. Loss of DsbA glycan modification was obtained by disruption of two genes within the FTT0789–FTT0800 putative polysaccharide locus, including a *galE* homolog (FTT0791) and one gene encoding a putative glycosyltransferase (FTT0798). As the mutants remained virulent in the murine model of subcutaneous tularemia, it indicated that glycosylation of DsbA does not play a major role in virulence under these conditions (Thomas et al., 2011). When defining the previously uncharacterized FTH_0069 protein as a novel glycosylated lipoprotein required for virulence, Balonova et al. (2012) also showed that the glycan structure modifying its two C-terminal peptides was identical to that of DsbA glycoprotein, as well as to one of the multiple glycan structures modifying the type IV pilin PilA. They therefore suggested a common biosynthetic pathway for the protein modification and a relationship between synthesis of the O-antigen and the glycan in the early steps of their biosynthetic pathways. Indeed, the *pglA* gene, encoding pilin oligosaccharyl transferase PglA, was involved in both pilin and general *F. tularensis* protein glycosylation.

In another study on activation of pulmonary inflammation after *F. tularensis* Schu S4 exposure (Walters et al., 2013), altered expression level of bacteria-specific mRNA transcripts was found. Among these transcripts, a hypothetical protein FTT_0797 was

characterized which shared homology with a glycosyl transferase. This protein is part of a gene cluster, which is thought to encode a polysaccharide additional to the lipopolysaccharide O antigen. Another protein, encoded by *FTS_1402*, was found to be involved in glycoprotein synthesis and to also contribute in part to LPS/capsule and/or Capsule Like Complex (CLC) production (Dankova et al., 2016). The resulting *FTS_1402* mutant presented more sensitivity to serum complement.

All these proteins are summarized in **Table 1**.

Concerning enzymes involved in degradation pathways, analysis of *F. tularensis* genomes showed a difference in the number of genes coding for proteins with such enzymatic activity (**Table 2**). Five genes were found in LVS, while only two genes were found in SchuS4 strain and only one gene in FSC200 strain. None of them was characterized.

ROLE OF POST-TRANSLATIONAL MODIFICATIONS (PTM) ON BACTERIA/HOST CELL PROTEINS

While two-third of all eukaryotic proteins are estimated to be glycosylated, the number of prokaryotic glycoproteins is still way behind understanding. This is mainly due to the enormous variability of their glycan structures and variations in the underlying glycosylation processes. In 2016, Schäffer and Messner (2016) combined glycan structural information with bioinformatic, genetic, biochemical and enzymatic data for in-depth analyses of glycosylation processes in prokaryotes. This study included the major classes of prokaryotic (i.e., bacterial and archaeal) glycoconjugates without any example on *Francisella*. Furthermore, in a very recent publication (Bastos et al., 2017), while *F. tularensis* was shown to exhibit the

TABLE 1 | Genes published involved in glycosylation pathway.

Published Gene	Gene Number (FTT)	Protein name	Characteristics	Function	References
FTT_0905		Type IV pili glycosylation protein	Glycosylated Type IV pilus	Virulence Factor	Brotcke et al., 2006
FTH_1071	Dsba	DsbA	Glycan Biosynthesis	Virulence Factor not affected when glycan is lost.	Thomas et al., 2011
FTH_0069			Putative Glycosylation		Balonova et al., 2010
fopA		FopA	Putative Glycosylation		Balonova et al., 2010
tul4		Tul4	Putative Glycosylation		Balonova et al., 2010
lemA		Lema	Putative Glycosylation		Balonova et al., 2010
pglA		PglA	Oligosaccharyltransferase	Pilin and Protein glycosylation	EGGE-JACOBSEN et al., 2011
FTT_0789		Ribulose-phosphate 3-epimerase	Glycan Biosynthesis		Thomas et al., 2011
FTT_0798		Glycosyl transferase family protein	Putative glycosyltransferase		Thomas et al., 2011
FTH_0069	FTT_1676	Hypothetical protein	Glycosylated lipoprotein	Virulence Factor	Balonova et al., 2012
FTT_0797		Glycosyl transferase family protein	Glycosyltransferase	Involved in O antigen glycosylation	Walters et al., 2013
FTS_1402	FTT_0793	ABC transporter	Putative glycan flippase	Involved in LPS and CLC product	Dankova et al., 2016

FTT, *Francisella tularensis* ssp. *tularensis*; FTH, *Francisella tularensis* ssp. *holarctica*; FTS, *Francisella tularensis* ssp. *tularensis*, FSC200 stain nomenclature.

TABLE 2 | Genes found in KEGG, with a putative deglycosylation function.

<i>Francisella tularensis</i>	Gene number	Name	Function
<i>Subsp. tularensis</i> SCHU S4	FTT_0928c	Beta-N-acetylhexosaminidase [EC:3.2.1.52]	Beta-glucosidase
	FTT_0412c	Pullulanase [EC:3.2.1.41]	PulB; pullulanase
<i>Subsp. holarctica</i> LVS (Live Vaccine Strain)	FTL_1282	Beta-N-acetylhexosaminidase [EC:3.2.1.52]	Beta-glucosidase-related glycosidase
	FTL_1052		Putative glycosidase
	FTL_0482	Pullulanase [EC:3.2.1.41]	Pullulanase
	AW21_68	Glycosyl hydrolase family 3 N terminal domain	Hypothetical protein
	AW21_1415	Glycosyl hydrolase family 3 N terminal domain	Hypothetical protein
<i>subsp. holarctica</i> FSC200	FTS_1254	Beta-N-acetylhexosaminidase [EC:3.2.1.52]	Glycosyl hydrolase family protein
<i>Subsp. novicida</i> U112	FTN_0911	Alpha-glucosidase [EC:3.2.1.20]	Glycosyl hydrolases family 31 protein
	FTN_0627	chitinase [EC:3.2.1.14]	Chitinase, glycosyl hydrolase family 18
	FTN_0806	Beta-N-acetylhexosaminidase [EC:3.2.1.52]	Glycosyl hydrolase family 3
	FTN_1474	bglX	Glycosyl hydrolase family 3

largest number of glycoproteins in common with *M. tuberculosis* (*Mtb*), by sharing 16% of its glycoproteome, none of the glycosylated proteins of *Francisella*, as well as none of the enzymes involved in glycosylation pathway, have been found to play a specific role in pathogenesis. At the opposite, in *M. tuberculosis*, glycosylation of HbN, a truncated hemoglobin protein, was demonstrated to be necessary for its maintainance at the bacterial membrane and wall (Arya et al., 2013). Mutation in its mannose glycan linkage disrupted the facilitation of *Mtb* and *M. smegmatis* entry within the macrophages. These data suggested that glycosylation processes allowed *Mtb* survival within the hazardous environment of macrophages and the establishment of long term persistent infection in the host (Dey and Bishai, 2014).

Of note, *Francisella* did not belong to the list of prokaryotes that catalyzed glycosylation of host cell proteins (Bastos et al., 2017). In contrast, *Legionella* was cited as targeting eEF1A through effect of the glucosyl transferase Lgt1, with as result, the killing of eukaryotic cells (Belyi et al., 2008).

CONCLUSION

While 146 examples of protein glycosylation were cited for *Francisella* and only 111 for *Helicobacter pylori* (Bastos et al., 2017), the importance of these PTM, observed in *Francisella* and those induced in the host, is still largely unknown, notably on the outcome of the infectious cycle. Indeed, a large correlation between glycosylation and bacterial pathogenicity has already been proven for various species e.g., *Campylobacter jejuni*,

REFERENCES

- Abu Kwaik, Y., and Bumann, D. (2013). Microbial quest for food *in vivo*: “Nutritional virulence” as an emerging paradigm. *Cell. Microbiol.* 15, 882–890. doi: 10.1111/cmi.12138
- Arya, S., Sethi, D., Singh, S., Hade, M. D., Singh, V., Raju, P., et al. (2013). Truncated hemoglobin, hbn, is post-translationally modified in

Legionella and enteropathogenic *Escherichia coli* (EPEC) (Lu et al., 2015).

Francisella infection modifies the unfolded protein response (UPR) (Barel et al., 2016) and manipulates autophagy (Miller and Celli, 2016). Both processes are involved in maintaining cellular homeostasis and helping destroy invading microorganisms. Glycosylation and deglycosylation could be involved in molecular mimicry of common host cell glycans therefore helping the bacteria to avoid immune recognition. At this stage, we have all the reasons to believe that the glycosylation-deglycosylation processes observed in THP-1 cells were originated from eukaryotic enzymes. However, we cannot formerly exclude that *Francisella* enzymes might also be involved. Glycans and glycan-binding receptors influence all stages of infection, starting from initial colonization of host epithelial surfaces to spreading in tissue and inducing inflammation or host-cell injury, which may results in clinical symptoms (Nizet and Esko, 2009). Therefore, knowledge of glycosylation pathways involved during *Francisella* infection remains fundamental for prevention and treatment strategies.

AUTHOR CONTRIBUTIONS

MB and AC wrote the review.

ACKNOWLEDGMENTS

INSERM, CNRS, and Université Paris Descartes Paris Cité Sorbonne supported these studies. The funders had no role in study design, data collection and analysis, decision to publish, or preparation of the manuscript.

Mycobacterium tuberculosis and modulates host-pathogen interactions during intracellular infection. *J. Biol. Chem.* 288, 29987–29999. doi: 10.1074/jbc.M113.507301

- Balonova, L., Hernychova, L., Mann, B. F., Link, M., Bilkova, Z., Novotny, M. V., et al. (2010). A multimethodological approach to identification of glycoproteins from the proteome of *Francisella tularensis*, an intracellular microorganism. *J. Proteome Res.* 9, 1995–2005. doi: 10.1021/pr9011602

- Balonova, L., Mann, B. F., Cervený, L., Alley, W. R., Chovancova, E., Forslund, A.-L., et al. (2012). Characterization of protein glycosylation in *Francisella tularensis* subsp. *holarctica*: identification of a novel glycosylated lipoprotein required for virulence. *Mol. Cell Proteomics* 11:M111.015016. doi: 10.1074/mcp.M111.015016
- Barel, M., Grall, N., and Charbit, A. (2015). *Pathogenesis of Francisella tularensis in Humans*. Hoboken, NJ: John Wiley & Sons, Inc.
- Barel, M., Harduin-Lepers, A., Portier, L., Slomianny, M.-C., and Charbit, A. (2016). Host glycosylation pathways and the unfolded protein response contribute to the infection by *Francisella*. *Cell. Microbiol.* 18, 1763–1781. doi: 10.1111/cmi.12614
- Barel, M., Meibom, K., Dubail, I., Botella, J., and Charbit, A. (2012). *Francisella tularensis* regulates the expression of the amino acid transporter SLC1A5 in infected THP-1 human monocytes. *Cell. Microbiol.* 14, 1769–1783. doi: 10.1111/j.1462-5822.2012.01837.x
- Bastos, P. A. D., da Costa, J. P., and Vitorino, R. (2017). A glimpse into the modulation of post-translational modifications of human-colonizing bacteria. *J. Proteomics* 152, 254–275. doi: 10.1016/j.jprot.2016.11.005
- Belyi, Y., Tabakova, L., Stahl, M., and Aktories, K. (2008). Lgt: a family of cytotoxic glucosyltransferases produced by *Legionella pneumophila*. *J. Bacteriol.* 190, 3026–3035. doi: 10.1128/JB.01798-07
- Brotcke, A., Weiss, D. S., Kim, C. C., Chain, P., Malfatti, S., Garcia, E., et al. (2006). Identification of MglA-regulated genes reveals novel virulence factors in *Francisella tularensis*. *Infect. Immun.* 74, 6642–6655. doi: 10.1128/IAI.01250-06
- Case, E. D. R., Chong, A., Wehrly, T. D., Hansen, B., Child, R., Hwang, S., et al. (2014). The *Francisella* O-antigen mediates survival in the macrophage cytosol via autophagy avoidance. *Cell. Microbiol.* 16, 862–877. doi: 10.1111/cmi.12246
- Chacko, B. K., Scott, D. W., Chandler, R. T., and Patel, R. P. (2011). Endothelial surface N-glycans mediate monocyte adhesion and are targets for anti-inflammatory effects of peroxisome proliferator-activated receptor γ ligands. *J. Biol. Chem.* 286, 38738–38747. doi: 10.1074/jbc.M111.247981
- Clemens, D. L., Lee, B. Y., and Horwitz, M. A. (2005). *Francisella tularensis* enters macrophages via a novel process involving pseudopod loops. *Infect. Immun.* 73, 5892–5902. doi: 10.1128/IAI.73.9.5892-5902.2005
- Console, L., Scalise, M., Tarmakova, Z., Coe, I. R., and Indiveri, C. (2015). N-linked glycosylation of human SLC1A5 (ASCT2) transporter is critical for trafficking to membrane. *Biochim. Biophys. Acta* 1853, 1636–1645. doi: 10.1016/j.bbamcr.2015.03.017
- Dankova, V., Balonova, L., Link, M., Straskova, A., Sheshko, V., and Stulik, J. (2016). Inactivation of *Francisella tularensis* gene encoding putative ABC transporter has a pleiotropic effect upon production of various glycoconjugates. *J. Proteome Res.* 15, 510–524. doi: 10.1021/acs.jproteome.5b00864
- Dey, B., and Bishai, W. R. (2014). Crosstalk between *Mycobacterium tuberculosis* and the host cell. *Semin. Immunol.* 26, 486–496. doi: 10.1016/j.smim.2014.09.002
- Di Gioia, M., and Zanoni, I. (2015). Toll-like receptor co-receptors as master regulators of the immune response. *Mol. Immunol.* 63, 143–152. doi: 10.1016/j.molimm.2014.05.008
- EGge-Jacobsen, W., Salomonsson, E. N., Aas, F. E., Forslund, A.-L., Winther-Larsen, H. C., Maier, J., et al. (2011). O-linked glycosylation of the pila pilin protein of *Francisella tularensis*: identification of the endogenous protein-targeting oligosaccharyltransferase and characterization of the native oligosaccharide. *J. Bacteriol.* 193, 5487–5497. doi: 10.1128/JB.00383-11
- Hetz, C., Martinon, F., Rodriguez, D., and Glimcher, L. H. (2011). The unfolded protein response: integrating stress signals through the stress sensor IRE1 α . *Physiol. Rev.* 91, 1219–1243. doi: 10.1152/physrev.00001.2011
- Lu, Q., Li, S., and Shao, F. (2015). Sweet talk: protein glycosylation in bacterial interaction with the host. *Trends Microbiol.* 23, 630–641. doi: 10.1016/j.tim.2015.07.003
- Meibom, K. L., and Charbit, A. (2010). The unraveling panoply of *Francisella tularensis* virulence attributes. *Curr. Opin. Microbiol.* 13, 11–17. doi: 10.1016/j.mib.2009.11.007
- Miller, C., and Celli, J. (2016). Avoidance and subversion of eukaryotic homeostatic autophagy mechanisms by bacterial pathogens. *J. Mol. Biol.* 428, 3387–3398. doi: 10.1016/j.jmb.2016.07.007
- Moran, A. P., Gupta, A., and Joshi, L. (2011). Sweet-talk: role of host glycosylation in bacterial pathogenesis of the gastrointestinal tract. *Gut* 60, 1412–1425. doi: 10.1136/gut.2010.212704
- Ni, M., Zhou, H., Wey, S., Baumeister, P., and Lee, A. Y. (2009). Regulation of PERK signaling and leukemic cell survival by a novel cytosolic isoform of the UPR regulator GRP78/BiP. *PLoS ONE* 4:e6868. doi: 10.1371/journal.pone.0006868
- Nizet, V., and Esko, J. (2009). “Chapter 39: Bacterial and viral infections,” in *Essentials of Glycobiology, 2nd Edn.*, eds R. D. Cummings, A. Varki, J. D. Esko, H. H. Freeze, P. Stanley, C. R. Bertozzi, G. W. Hart, and M. E. Etzler (Cold Spring Harbor, NY: Cold Spring Harbor Laboratory Press), 1–16.
- Opendakker, G., Proost, P., and Van Damme, J. (2016). Microbiomic and posttranslational modifications as preludes to autoimmune diseases. *Trends Mol. Med.* 22, 746–757. doi: 10.1016/j.molmed.2016.07.002
- Pfaffenbach, K. T., and Lee, A. S. (2011). The critical role of GRP78 in physiologic and pathologic stress. *Curr. Opin. Cell Biol.* 23, 150–156. doi: 10.1016/j.ceb.2010.09.007
- Ray, K., Marteyn, B., Sansonetti, P. J., and Tang, C. M. (2009). Life on the inside: the intracellular lifestyle of cytosolic bacteria. *Nat. Rev. Microbiol.* 7, 333–340. doi: 10.1038/nrmicro2112
- Santic, M., Al Khodor, S., and Abu Kwaik, Y. (2010). Cell biology and molecular ecology of *Francisella tularensis*. *Cell. Microbiol.* 12, 129–139. doi: 10.1111/j.1462-5822.2009.01400.x
- Schäffer, C., and Messner, P. (2016). Emerging facets of prokaryotic glycosylation. *FEMS Microbiol. Rev.* 41, 49–91. doi: 10.1093/femsre/fuw036
- Sjöstedt, A. (2011). Special topic on *Francisella tularensis* and tularemia. *Front. Cell. Infect. Microbiol.* 2:86. doi: 10.3389/fmicb.2011.00086
- Tan, F. Y. Y., Tang, C. M., and Exley, R. M. (2015). Sugar coating: bacterial protein glycosylation and host–microbe interactions. *Trends Biochem. Sci.* 40, 342–350. doi: 10.1016/j.tibs.2015.03.016
- Thomas, R. M., Twine, S. M., Fulton, K. M., Tessier, L., Kilmury, S. L. N., Ding, W., et al. (2011). Glycosylation of DsbA in *Francisella tularensis* subsp. *tularensis*. *J. Bacteriol.* 193, 5498–5509. doi: 10.1128/JB.00438-11
- Tytgat, H. L. P., and de Vos, W. M. (2016). Sugar coating the envelope: glycoconjugates for microbe–host crosstalk. *Trends Microbiol.* 24, 853–861. doi: 10.1016/j.tim.2016.06.004
- Vaidyanathan, K., Durning, S., and Wells, L. (2014). Functional O-GlcNAc modifications: implications in molecular regulation and pathophysiology. *Crit. Rev. Biochem. Mol. Biol.* 49, 140–163. doi: 10.3109/10409238.2014.884535
- Varki, A. (1993). Biological roles of oligosaccharides: all of the theories are correct. *Glycobiology* 3, 97–130. doi: 10.1093/glycob/3.2.97
- Walters, K.-A., Olsufka, R., Kuestner, R. E., Cho, J. H., Li, H., Zornetzer, G. A., et al. (2013). *Francisella tularensis* subsp. *tularensis* induces a unique pulmonary inflammatory response: role of bacterial gene expression in temporal regulation of host defense responses. *PLoS ONE* 8:e62412. doi: 10.1371/journal.pone.0062412
- Zhang, Y. J., and Rubin, E. J. (2013). Feast or famine: the host–pathogen battle over amino acids. *Cell. Microbiol.* 15, 1079–1087. doi: 10.1111/cmi.12140

Conflict of Interest Statement: The authors declare that the research was conducted in the absence of any commercial or financial relationships that could be construed as a potential conflict of interest.

Copyright © 2017 Barel and Charbit. This is an open-access article distributed under the terms of the Creative Commons Attribution License (CC BY). The use, distribution or reproduction in other forums is permitted, provided the original author(s) or licensor are credited and that the original publication in this journal is cited, in accordance with accepted academic practice. No use, distribution or reproduction is permitted which does not comply with these terms.



***Francisella tularensis* Susceptibility to Antibiotics: A Comprehensive Review of the Data Obtained *In vitro* and in Animal Models**

Yvan Caspar^{1,2*} and Max Maurin^{1,2}

¹ Laboratoire de Bactériologie-Hygiène Hospitalière, Département des agents infectieux, Centre National de Référence des *Francisella*, Institut de Biologie et de Pathologie, Centre Hospitalier Universitaire Grenoble Alpes, Grenoble, France,

² Université Grenoble Alpes, Centre National de la Recherche Scientifique, TIMC-IMAG, Grenoble, France

OPEN ACCESS

Edited by:

Jing-Ren Zhang,
Tsinghua University, China

Reviewed by:

Roger Derek Pechous,
University of Arkansas for Medical
Sciences, USA

Gregory T. Robertson,
Colorado State University, USA

*Correspondence:

Yvan Caspar
ycaspar@chu-grenoble.fr

Received: 25 January 2017

Accepted: 27 March 2017

Published: 11 April 2017

Citation:

Caspar Y and Maurin M (2017)
Francisella tularensis Susceptibility to
Antibiotics: A Comprehensive Review
of the Data Obtained *In vitro* and in
Animal Models.
Front. Cell. Infect. Microbiol. 7:122.
doi: 10.3389/fcimb.2017.00122

The antibiotic classes that are recommended for tularaemia treatment are the aminoglycosides, the fluoroquinolones and the tetracyclines. However, cure rates vary between 60 and 100% depending on the antibiotic used, the time to appropriate antibiotic therapy setup and its duration, and the presence of complications, such as lymph node suppuration. Thus, antibiotic susceptibility testing (AST) of *F. tularensis* strains remains of primary importance for detection of the emergence of antibiotic resistances to first-line drugs, and to test new therapeutic alternatives. However, the AST methods reported in the literature were poorly standardized between studies and AST data have not been previously evaluated in a comprehensive and comparative way. The aim of the present review was to summarize experimental data on antibiotic susceptibilities of *F. tularensis* obtained in acellular media, cell models and animal models since the introduction of fluoroquinolones in the treatment of tularaemia in 1989. We compiled MIC data of 33 antibiotics (including aminoglycosides, fluoroquinolones, tetracyclines, macrolides, β -lactams, chloramphenicol, rifampicin, and linezolid) against 900 *F. tularensis* strains (504 human strains), including 107 subsp. *tularensis* (type A), 789 subsp. *holarctica* (type B) and four subsp. *mediasiatica* strains, using various AST methods. Specific culture media were identified or confirmed as unsuitable for AST of *F. tularensis*. Overall, MICs were the lowest for ciprofloxacin (≤ 0.002 – 0.125 mg/L) and levofloxacin, and ranged from ≤ 0.016 to 2 mg/L for gentamicin, and 0.064 to 4 mg/L for doxycycline. No resistant strain to any of these antibiotics was reported. Fluoroquinolones also exhibited a bactericidal activity against intracellular *F. tularensis* and lower relapse rates in animal models when compared with the bacteriostatic compound doxycycline. As expected, lower MIC values were found for macrolides against type A and biovar I type B strains, compared to biovar II type B strains. The macrolides were more effective against *F. tularensis* grown in phagocytic cells than in acellular media.

Keywords: *Francisella tularensis*, antimicrobial susceptibility, MIC, MBC, intracellular, animal model, tularaemia, antibiotic therapy

SEARCH STRATEGY AND SELECTION CRITERIA

Data on antibiotic susceptibility testing (AST) of *Francisella tularensis*, both *in vitro* and in animal models, were collected from the English and French literature in the PubMed database, since the introduction of fluoroquinolones in the treatment of tularaemia in 1989 until December 2016. They were extracted using the key words “tularemia” and “*Francisella*” in order to achieve a broad screening of the entire body of literature on the subject since 1989. Only studies evaluating more than five *F. tularensis* strains were selected for analysis.

FRANCISELLA TULARENSIS AND TULAREMIA

F. tularensis, the etiological agent of tularaemia, is a Tier 1 biological threat agent according to the classification of the Centers for Disease Control and Prevention (Dennis et al., 2001). It was first isolated from ground squirrels in 1911 in Tulare County, California (USA), and from a human tularaemia case in 1914 in Ohio (USA) (McCoy and Chapin, 1912; Wherry and Lamb, 1914). The name “*Francisella tularensis*” was coined in 1959 to honor Dr. Edward Francis, who greatly contributed to improve the knowledge on human tularaemia (Francis et al., 1922; Francis, 1928; Rockwood, 1983). *Francisella tularensis* is currently divided into three subspecies: subsp. *tularensis* (type A strains), mainly found in North America; subsp. *holarctica* (type B strains) found throughout the northern hemisphere; and subsp. *mediasiatica* found in Central Asia (Olsufjev et al., 1959; Jellison and Owen, 1961; Olsufjev, 1970; Jellison, 1974; Olsufjev and Meshcheryakova, 1983). Debate continues on whether *Francisella novicida* is a fourth subspecies of *F. tularensis* or a separate species, but we agree with Johansson et al. in keeping *F. novicida* in a separate species because of its aquatic reservoir and very low virulence in humans (Busse et al., 2010; Huber et al., 2010; Johansson et al., 2010). Type B strains are also classically differentiated into three biovars (Kudelina and Olsufjev, 1980; Olsufjev and Meshcheryakova, 1982, 1983): biovar I (naturally susceptible to erythromycin) is found in Western Europe and North America; biovar II (naturally resistant to erythromycin) is found in Eastern Europe and Asia; and biovar japonica (susceptible to erythromycin but fermenting glycerol) is mainly found in Japan, although it has recently been described in China and Turkey (Kiliç et al., 2013; Wang et al., 2014). Biovar II strains are found in the Eastern part of Europe (Czech Republic, Finland, Georgia, Russia, Slovakia, Ukraine, Austria, Hungary, and Romania) (Vogler et al., 2009; Svensson et al., 2009b; Chanturia et al., 2011; Gyuranecz et al., 2012) and in Asia and both biovar I and II strains coexist in Germany, Switzerland and Scandinavia (Muller et al., 2013; Origgi et al., 2014; Maurin and Gyuranecz, 2016).

Although the *F. tularensis* genome displays very low variability, four distinct clades have been identified by pulse-field gel electrophoresis (PFGE) within type A strains in the United States (A.Ia, A.Ib, A.IIa, and A.IIb) with the A.Ib clade being

associated with a 24% mortality rate in humans (Kugeler et al., 2009). Type B strains have also been divided into several clades by whole genome sequencing. The four main clades include clade B.4 corresponding to North American strains, clade B.6 to biovar I Western European strains, clade B.12 to biovar II Eastern European strains, and clade B16 to strains belonging to biovar japonica (Fujita et al., 2008; Vogler et al., 2009; Kiliç et al., 2015; Karlsson et al., 2016).

F. tularensis is a Gram-negative, facultative intracellular coccobacillus (Broman et al., 2011). It is strictly aerobic, non-motile, non-toxicogenic, and non-spore-forming. It is a fastidious bacterium that may be grown in cysteine-enriched media, under 5% CO₂ atmosphere. The main virulence factor of *F. tularensis* corresponds to its ability to multiply within eukaryotic cells, especially in the cytosol of macrophages (Clemens and Horwitz, 2007). Virulence is associated with the presence of a duplicated pathogenicity island in the bacterial genome, encoding a type VI-like secretion system (Nano and Schmerk, 2007). However, the high variations in virulence observed among *F. tularensis* genotypes remain currently unexplained.

Human tularaemia is a zoonotic disease usually occurring as sporadic cases or small familial outbreaks (Tärnvik and Berglund, 2003; Bicakci and Parlak, 2008). However, a number of tularaemia outbreaks have been reported, including in the last two decades (Helvacı et al., 2000; Cerný, 2001; Feldman et al., 2001; Pérez-Castrillón et al., 2001; Reintjes et al., 2002; Christova et al., 2004; Payne et al., 2005; Celebi et al., 2006; Kantardjiev et al., 2006; Siret et al., 2006; Petersen et al., 2008; Akalın et al., 2009; Barut and Cetin, 2009; Svensson et al., 2009a; Hauri et al., 2010; Mailles et al., 2010; Larssen et al., 2011, 2014; Wang et al., 2011; Karlsson et al., 2013; Johansson et al., 2014; Mengelöglu et al., 2014). Humans may be infected with *F. tularensis* through direct contact with infected animals (manipulation of live or dead infected animals, animal bites or scratches), consumption of contaminated food or water, exposure to contaminated environments or through arthropod bites (Keim et al., 2007). *F. tularensis* can infect a large number of animal species, but lagomorphs and small rodents are considered key hosts for this pathogen (Gyuranecz et al., 2011; Maurin and Gyuranecz, 2016). This bacterium may also persist in water and soil environments for several months, which might be related to an ability to multiply in protozoa, such as amoebae (Abd et al., 2003; Keim et al., 2007; El-Etr et al., 2009; Broman et al., 2011). A terrestrial and an aquatic lifecycle have been described for this bacterium (Maurin and Gyuranecz, 2016). Arthropods, such as ticks and mosquitoes may be contaminated by *F. tularensis* from the animal or environmental reservoirs (Sjostedt, 2007; Maurin and Gyuranecz, 2016). Large tularaemia outbreaks have occurred, for which multiple sources of contamination and several *F. tularensis* clones were identified (Akalın et al., 2009; Barut and Cetin, 2009; Celebi et al., 2006; Cerný, 2001; Christova et al., 2004; Feldman et al., 2001; Hauri et al., 2010; Helvacı et al., 2000; Johansson et al., 2014; Kantardjiev et al., 2006; Karlsson et al., 2013; Larssen et al., 2011, 2014; Mailles et al., 2010; Mengelöglu et al., 2014; Payne et al., 2005; Pérez-Castrillón et al., 2001; Petersen et al., 2008; Reintjes et al., 2002; Siret et al., 2006; Svensson

et al., 2009a; Wang et al., 2011). Symptoms vary according to the infection route and classically correspond to six different clinical forms: ulceroglandular, glandular, oropharyngeal, oculoglandular, pneumonic and typhoidal (Tärnvik, 2007). Ulceroglandular and glandular forms are consecutive to skin inoculation of bacteria (e.g., through an arthropod bite or contact with infected animals). A regional lymphadenopathy develops with (ulceroglandular form) or without (glandular form) a skin ulcer at the inoculation site. When contamination occurs through the ocular conjunctiva, painful conjunctivitis with regional lymphadenopathy develops, which corresponds to oculoglandular tularaemia. The oropharyngeal form is characterized by pharyngitis with regional lymphadenopathy, usually occurring after consumption of contaminated meat or water. Pneumonic tularaemia results from airborne contamination or hematogenous spread of bacteria to the lungs and is characterized by unspecific symptoms, such as cough, fever, dyspnea and occasionally a mediastinal or hilar lymphadenopathy. The typhoidal form corresponds to systemic disease with neurological symptoms mimicking typhoid, often with *F. tularensis* bacteraemia, but without detection of any portal of entry of bacteria (especially no skin ulcer) and without symptoms of localized infection (especially no regional lymphadenopathy) (Tärnvik and Chu, 2007). Complications may occur, such as skin eruptions, abscess formation, lymph node suppuration with occasionally skin fistulisation, and secondary infectious locations due to hematogenous spread of bacteria (Tärnvik and Chu, 2007; Meric et al., 2008; Maurin et al., 2011; Erdem et al., 2014). Diagnosis is usually based on compatible clinical and epidemiological features, and positive serological tests. PCR is useful to detect *F. tularensis* DNA in various clinical samples, especially before specific antibodies can be detected (Tärnvik, 2007). Isolation of a *F. tularensis* strain from blood or tissue samples is obtained in <20% of patients, which makes antibiotic susceptibility testing (AST) of *F. tularensis* strains rare (Maurin et al., 2011).

The 2007 WHO guidelines for treatment of tularaemia are based on the 2001 consensus recommendations from Dennis et al. (2001). According to these publications, tularaemia treatment is mainly based on three antibiotic classes: the aminoglycosides, the fluoroquinolones and the tetracyclines, although many other antibiotic classes have been tested against *F. tularensis in vitro*. Here we have compiled all available experimental data on the evaluation of the activity of antibiotics against *F. tularensis in vitro*, in acellular and cell models, and *in vivo* in animal models to provide useful information for clinical microbiologists and physicians.

ANTIBIOTIC SUSCEPTIBILITY TESTING OF *F. TULARENSIS*

Antibiotic susceptibility testing (AST) of *F. tularensis* strains is usually not performed on a routine basis because: (1) isolation of the strain involved is only obtained in a few tularaemic patients (Maurin et al., 2011); (2) this procedure is at risk for the laboratory personnel handling cultures of this highly infectious pathogen and requires biosafety level 3 (BSL3) facilities (Tärnvik

and Chu, 2007); (3) acquired resistance to antibiotics has never been reported so far in clinical strains of *F. tularensis* (Tärnvik, 2007) and (4) *in vitro* data may not be predictive of treatment failure in tularaemia patients. However, reference laboratories have reported AST surveys for collections of human and animal strains of *F. tularensis* (Scheel et al., 1993; Ikäheimo et al., 2000; Johansson et al., 2000, 2002; García del Blanco et al., 2004; Tomaso et al., 2005; Urich and Petersen, 2008; Valade et al., 2008; Velinov et al., 2011; Yeşilyurt et al., 2011; Georgi et al., 2012; Hotta et al., 2013; Kiliç et al., 2013; Kreizinger et al., 2013; Origgi et al., 2014).

For this review, we collected *F. tularensis* AST results from all studies of more than five tularaemia cases, published in the literature since 1989. We obtained data from 898 *F. tularensis* strains isolated from humans (510 strains), animals (200 strains), arthropods (four strains), natural water samples (39 strains) and unknown sources (147). They included 107 type A, 789 type B and four *F. tularensis* subsp. *mediasiatica* strains (Table 1 and Table S1) (Scheel et al., 1993; Ikäheimo et al., 2000; Johansson et al., 2000, 2002; García del Blanco et al., 2004; Tomaso et al., 2005; Urich and Petersen, 2008; Valade et al., 2008; Velinov et al., 2011; Yeşilyurt et al., 2011; Georgi et al., 2012; Hotta et al., 2013; Kiliç et al., 2013; Kreizinger et al., 2013; Origgi et al., 2014). AST results were available for 33 antibiotics, although only some of them were tested in all studies (Tables 1–5 and Table S1). These antibiotics included four aminoglycoside compounds (gentamicin, streptomycin, amikacin and tobramycin), nine fluoroquinolones (ciprofloxacin, levofloxacin, moxifloxacin, ofloxacin, norfloxacin, grepafloxacin, sparfloxacin, trovafloxacin and gatifloxacin), three tetracyclines (tetracycline, doxycycline and tigecycline), four macrolides (erythromycin, azithromycin, roxithromycin and clarithromycin), one ketolide (telithromycin), nine β -lactams (ampicillin, amoxicillin + clavulanic acid, ceftazidime, piperacillin + tazobactam, ceftriaxone, cefepime, imipenem, meropenem and aztreonam), chloramphenicol, rifampicin, and linezolid.

MICs: Methods and Results

According to the Clinical and Laboratory Standards Institute (CLSI) and WHO guidelines, AST of *F. tularensis* strains should be performed using cation-adjusted Mueller-Hinton broth enriched with 2% defined growth supplement, such as Polyvitex[®] (referred to here as enriched caMHB), in order to fulfill the cysteine growth requirement of this bacterium (Tärnvik, 2007; CLSI. M45-A2, 2010). Adjustment of pH to 7.1 ± 0.1 is mandatory after addition of 2% growth supplement because it significantly reduces the pH of caMHB medium. The bacterial inoculum must be calibrated at 5×10^5 CFU/mL of final concentration. Culture media should be incubated for 48 h in ambient air, but incubation in 5% CO₂-enriched atmosphere may be needed for some strains, although it can lead to acidification of the culture medium and therefore overestimation of aminoglycoside and macrolide MICs, or underestimation of tetracyclines MICs (CLSI. M45-A2, 2010).

In the past three decades, three different methods for *F. tularensis* AST were most frequently reported in the literature: antibiotic agar dilution, broth microdilution and E-test strips.

TABLE 1 | Characteristics of *F. tularensis* strains included in this study and MICs for aminoglycosides (gentamicin and streptomycin), the tetracycline compound doxycycline and fluoroquinolones (ciprofloxacin and levofloxacin) according to the culture medium used and to the AST assay used.

Reference	Year(s)	Origin	Nb of strains Type/biovar	Culture medium	MIC (mg/L)									
					Gentamicin		Streptomycin		Doxycycline		Ciprofloxacin		Levofloxacin	
					Range	MIC ₉₀	Range	MIC ₉₀	Range	MIC ₉₀	Range	MIC ₉₀	Range	MIC ₉₀
BROTH MICRODILUTION														
Origi et al., 2014	1996–2013	Switzerland	19 B6 5 B12	caMHB + 2% IsoVitaléX	≤0.12–0.25	0.25	4	4	4	≤0.06	≤0.06	≤0.06	≤0.06	
Georgi et al., 2012	UNK	Europe	69 B	caMHB + 2% IsoVitaléX	≤0.12–0.25		4			≤0.06				
		North America	7 A	caMHB + 2% IsoVitaléX	≤0.25–0.5	0.5	≤0.5–2	2	2	≤0.031–0.125	0.063	≤0.031–0.125	0.063	
		Central Asia	4 ssp. <i>mediasiatica</i>	caMHB + 2% IsoVitaléX	≤0.25–0.5		≤2	≤2	≤2	0.031–0.125		≤0.031–0.063		
Ulrich and Petersen, 2008	1974–2005	North America	92 A	caMHB + 2% IsoVitaléX	0.03–0.5	0.25	0.25–4	2	2	0.004–0.06	0.06	0.015–0.12	0.06	
			77 B	caMHB + 2% IsoVitaléX	0.03–0.5	0.12	0.25–4	2	2	0.008–0.06	0.03	0.015–0.12	0.06	
E-TEST														
Johansson et al., 2000	1998	Sweden	7 B	Modified Thayer-Martin	0.5–1		0.25–0.5			0.008–0.015				
Hotta et al., 2013	1926–1989	Japan	36 B	Chocolate II agar	0.023–0.5	0.125	0.094–1.5	1	1	0.003–0.023	0.016			
Kreizinger et al., 2013	2003–2010	Hungary	29 B12	Modified Francis Agar	0.38–1	0.75	3–8	6	1	0.012–0.047	0.047	0.004–0.023	0.023	
Yeşilyurt et al., 2011	2009–2010	Turkey	39 B biovar II	GBCA	0.094–0.25	0.25	0.75–1.5	1.5		0.008–0.016	0.016	0.006–0.016	0.012	
Tomaso et al., 2005	1992–1998	Austrian	50 B biovar II	CHAB	0.094–2	0.75	0.75–8	3	2	0.004–0.125	0.032	0.008–0.047	0.032	
Ikäheimo et al., 2000	UNK	Finland	38 B	CHA + 2% Haemoglobin	0.38–1.5	1	0.25–4.0	4		0.008–0.023	0.016	0.008–0.023	0.016	
Kiliç et al., 2013	2009–2012	Turkey	249 B biovar II + 1 biovar <i>japonica</i>	CHAB	0.094–0.38	0.25	0.5–2	1.5	0.25	0.004–0.023	0.016	0.003–0.016	0.012	
Johansson et al., 2002	1996–2001	USA	8 A	MHII + 1% IsoVitaléX or CHAB	0.032–0.25		0.064–2			0.016–0.064				
Velinov et al., 2011	UNK	Bulgaria	16 B	caMHB + 2% IsoVitaléX	0.016–0.125	0.064	0.064–1	0.25	1	0.016–0.064	0.064	0.008–0.125	0.125	
			21 B biovar II	caMHB + 2% IsoVitaléX	0.064–0.5	0.125	0.25–2	1	2	0.002–0.06	0.047	0.016–0.125	0.094	
AGAR DILUTION														
Valade et al., 2008	1996–2005	France	71 B	MHII + 2% IsoVitaléX	0.03–0.5		<0.5–1			0.015–0.03				
Johansson et al., 2000	1998	Sweden	7B	Modified Thayer-Martin	1		0.5			0.03				

caMHB, cation-adjusted Mueller Hinton Broth; GBCA, glucose blood cysteine agar; MHII, Mueller Hinton II; CHA, cysteine heart agar; CHAB, cysteine heart agar enriched with blood; MIC₉₀, minimal inhibitory concentration that inhibits 90% of the strains; MIC range, range between the lowest and the highest MIC observed.

TABLE 2 | MIC and MIC₉₀ ranges of aminoglycosides, tetracyclines and fluoroquinolones against *F. tularensis*.

Antibiotics	MIC range (mg/L)	MIC ₉₀ range (mg/L)	CLSI breakpoint for susceptibility (mg/L)
Gentamicin	≤0.016–2	0.064–1	≤ 4
Streptomycin	≤0.064–8	0.25–6	≤ 8
Tetracycline	≤0.094–2	≤ 0.25- 1	≤ 4
Doxycycline	0.064–4	0.25–2	≤ 4
Ciprofloxacin	≤0.002–0.125	≤ 0.016–0.064	≤ 0.5
Levofloxacin	≤0.004–0.125	0.012–0.125	≤ 0.5
Chloramphenicol	≤0.023–4	≤ 0.25–2	≤ 8

Data are summarised from all studies selected for this review.

These techniques were poorly standardized between studies, including after CLSI guidelines were available (CLSI. M45-A2, 2010). Most particularly, growth media, incubation conditions (atmosphere and duration) and bacterial inocula used for *F. tularensis* AST greatly varied between studies. Therefore, the results obtained in these different studies should be compared with caution.

As for the broth microdilution method, a number of authors used Mueller-Hinton II broth supplemented with glucose, Ca²⁺ and Mg²⁺ ions, and ferric pyrophosphate (a medium referred to as modified MHII) in spite of the recommended enriched caMHB medium (Baker et al., 1985; García del Blanco et al., 2004; Origi et al., 2014). The use of MHII resulted in overestimation of the MICs of aminoglycosides and tetracyclines compared to caMHB (Table S1). The use of MHII for *F. tularensis* AST should be discouraged to avoid erroneous classification of some strains as resistant to aminoglycosides and/or tetracyclines using the CLSI breakpoints for susceptibility (concentration value threshold used for the categorization of a bacterial strain as susceptible, intermediately susceptible or resistant to an antibiotic). To date, antibiotic resistance reported in the literature for natural strains of *F. tularensis* have never been formally characterized by a reference laboratory. In the following paragraphs, the term resistant is applied to strain whose MICs are not classified as susceptible according to CLSI breakpoints for susceptibility, even though the mechanism of resistance has not been characterized. The MHII medium may also affect the activity of fluoroquinolones since ciprofloxacin MICs up to 0.25 mg/L were reported with this medium (Maurin et al., 2000; García del Blanco et al., 2004), while MICs for this antibiotic range from ≤ 0.002 to 0.125 mg/L (MIC₉₀, ≤ 0.016–0.047 mg/L) for all other studies reported (Table 1 and Table S1).

Several agar media were used for MIC determination using the E-test strip technique (Tables 1 and Table S1). MIC ranges observed with these different solid media were similar to each other and to those obtained with the broth microdilution method using enriched caMHB. No strain was classified as resistant to any of the drugs used for tularaemia treatment and for which CLSI breakpoints have been defined (i.e., gentamicin, streptomycin, ciprofloxacin, levofloxacin, tetracycline, doxycycline and chloramphenicol). Thus, the E-test strip methodology appears to be a convenient alternative for

TABLE 3 | MICs for the other aminoglycosides and fluoroquinolones evaluated against *F. tularensis*.

Reference	Origin	Nb of strains	Tobramycin		Amikacin		Moxifloxacin		Norfloxacin		Grepafloxacin		Trovafloxacin		Gatifloxacin		Sparfloxacin	
			Range	MIC ₉₀	Range	MIC ₉₀	Range	MIC ₉₀	Range	MIC ₉₀	Range	MIC ₉₀	Range	MIC ₉₀	Range	MIC ₉₀	Range	MIC ₉₀
BROTH MICRODILUTION																		
Georgi et al., 2012	Europe	69 B	≤0.5–2		2													
E-TEST																		
Yeşilyurt et al., 2011	Turkey	39 B biovar II	0.125–0.38	0.25	0.75–1	1	0.012–0.032	0.032										
Tomaso et al., 2005	Austria	50 B biovar II	0.19–3	0.75	1–16	4	0.016–0.19	0.125	0.023–0.19	0.125								
Ikäheimo et al., 2000	Finland	38 B	0.5–2	1.5							0.016–0.047	0.047	0.012–0.047	0.032				
Johansson et al., 2002	USA	8 A					0.032–0.125				0.008–0.125				0.016–0.125			
		16 B					0.032–0.125	0.125			0.016–0.125	0.064			0.008–0.064	0.064	0.008–0.064	0.064

TABLE 4 | MICs of tetracycline, tigecycline, macrolides (erythromycin, azithromycin) telithromycin, chloramphenicol, rifampicin and linezolid against *F. tularensis*.

Reference	Origin	Nb of strains Type/biovar	Tetracycline		Tigecycline		Erythromycin		Azithromycin		Telithromycin		Chloramphenicol		Rifampicin		Linezolid	
			Range	MIC ₉₀	Range	MIC ₉₀	Range	MIC ₉₀	Range	MIC ₉₀	Range	MIC ₉₀	Range	MIC ₉₀	Range	MIC ₉₀	Range	MIC ₉₀
BROTH MICRODILUTION																		
Origgi et al., 2014	Switzerland	19 B6 5 B12	≤0.25	≤0.25			2-8	4						≤2	≤2			
Georgi et al., 2012	Europe	69 B	≤0.125-2	1			1->16	>16					1-4	2	≤0.5-2			
	North America	7 A	≤0.125-0.5										1-4	≤0.5				
	Central Asia	4 ssp. <i>mediasiatica</i>	0.25-2										1-4					
Ulrich and Petersen, 2008	North America	92 A 77 B	0.25-2	1			0.5-4	2				0.5-4	2					
			0.12-2	1			0.5-2	0.5				0.5-4	2					
E-TEST MIC STRIPS																		
Johansson et al., 2000	Sweden	7 B					>256					0.25				0.5		
Hotta et al., 2013	Japan	36 B					0.094-1.5	1.5										
Kreizinger et al., 2013	Hungary	29 B12	0.19-0.72	0.5	0.094-0.19	0.19	>256	>256				0.5-1.5	1.5	0.5-2	1	12-48	32	
Yeşilyurt et al., 2011	Turkey	39 B biovar II	0.125-0.5	0.38	0.094-0.38	0.25	>256	>256				0.094-0.25	0.25	0.25-1	0.75	0.5-2	1.5	
Tomaso et al., 2005	Austria	50 B biovar II	0.125-0.75	0.75			4->256	>256				0.023-2	0.75	0.25-3	1.5			
Ikäheimo et al., 2000	Finland	38 B	0.094-0.5	0.38				>256	>256			0.125-0.5	0.38	0.094-0.38	0.25			
Kılıç et al., 2013	Turkey	249 B biovar II+ biovar <i>japonica</i>	0.094-0.5	0.38			1->256	>256				0.094-0.75	0.5	0.125-1	0.75			
Johansson et al., 2002	USA	8 A					0.125-1	0.125-2				0.5-1		0.25-2		2-4		
		16 B					0.125-1	1	0.064-2	1		0.25-1	1	0.125-1	1	4-16	8	
Velinov et al., 2011	Bulgaria	21 B biovar II					>256	>256				1-4	2					
AGAR DILUTION																		
Valade et al., 2008	France	71 B										0.125-0.25	0.25-2		0.015-0.5			
Johansson et al., 2000	Sweden	7 B										0.5-1			1			

TABLE 5 | MICs of beta-lactams against *F. tularensis*.

Reference	Origin	Nb of strains Type/biovar	MIC range (mg/L)								
			AMP	AMC	PIP/TAZ	CAZ	COX	FEP	IMI	MER	AZT
BROTH MICRODILUTION											
Georgi et al., 2012	Europe	69 B		64->64		>32				16->16	
E-TEST											
Hotta et al., 2013	Japan	34 B					0.047->256		0.047->32	0.094->32	0.75->256
Yeşilyurt et al., 2011	Turkey	39 B biovar II	>256	>256	>256	>256	>256	>256	>32		
Tomaso et al., 2005	Austria	50 B biovar II	>256		>256	>256	>32	>32	0.5->32	1.5->32	>256
Ikäheimo et al., 2000	Finland	38 B			>256	>256	>32		>32	>32	
Velinov et al., 2011	Bulgaria	21 B biovar II			>256		2-4				
AGAR DILUTION											
Scheel et al., 1993	Scandinavia	20 B				>32			>32	>32	>32

*if available, MIC₉₀ value corresponded every time to the highest value of MIC range. AMP, Ampicillin; AMC, Amoxicillin/Clavulanate; PIP/TAZ, Piperacillin/tazobactam; CAZ, Ceftazidime; COX, Ceftriaxone; FEP, Cefepime; IMI, Imipenem; MER, Meropenem; AZT, Aztreonam.

antibiotic susceptibility categorisation of *F. tularensis* strains compared to the more time-consuming and fastidious broth microdilution method. Moreover, this method is less risky for laboratory personnel because it does not require handling large volumes of liquid suspensions of *F. tularensis*. However, no study has compared AST results using MIC strips to those of the microdilution reference method using enriched caMHB. Standardization of agar media for *F. tularensis* AST would be beneficial for comparison of studies conducted in different laboratories.

A few studies have compared *F. tularensis* antibiotic susceptibilities when using the agar dilution technique with different solid media (Table 1 and Table S1). Blood cysteine agar should be avoided since it identified resistant strains of *F. tularensis* for gentamicin or streptomycin, which was never confirmed by characterizing the resistance mechanisms involved. For the Thayer Martin agar and enriched Mueller-Hinton agar, results were concordant with those of the broth microdilution and MIC strip assays. One study compared MIC results using the agar dilution method, the MIC strip method or the broth microdilution reference method. Unfortunately, results obtained with the reference method were not reproducible. The correlation of results obtained with either the agar dilution or MIC strip tests, using enriched Mueller Hinton agar, were 87% for doxycycline, 94% for ciprofloxacin, but only 42% for gentamicin. The agar dilution method poorly correlated with the broth microdilution method, with only 72% correlation for doxycycline, 68% for ciprofloxacin and 51% for gentamicin.

According to our previous comments on MIC methods, we excluded MIC values obtained with the broth microdilution method using modified MHII broth and those determined by the agar dilution method using blood cysteine agar plates (Table S1) MICs obtained with all other methods were recorded, although analyzed cautiously because of poor methodological standardization, as previously mentioned. The remaining 812 *F. tularensis* strains were categorized as susceptible to first-line antibiotics for tularaemia, including the aminoglycosides, the fluoroquinolones and the tetracyclines. MIC ranges and CLSI breakpoints for these antibiotics are shown in Table 2.

Aminoglycosides, Fluoroquinolones, and Doxycycline

Altogether, among antibiotic classes recommended for first-line treatment of tularaemia, ciprofloxacin displayed the lowest ranges for MICs (≤ 0.002 – 0.125 mg/L) and MIC₉₀ (≤ 0.016 – 0.064 mg/L) between studies. Gentamicin MICs ranged from ≤ 0.016 to 2 mg/L, and MIC₉₀ from 0.064 to 1 mg/L. The MIC and MIC₉₀ ranges for doxycycline were 0.064–4 mg/L and 0.25–2 mg/L, respectively (Table 1). Only slight differences in susceptibility to these antibiotics were observed between type A and type B strains of *F. tularensis*, or between various biovars or clades within type A and type B strains.

Among fluoroquinolones, ciprofloxacin and levofloxacin were the most active compounds *in vitro* (Table 1). All strains tested displayed MIC levels to these antibiotics at least 4-fold less than the CLSI breakpoint for susceptibility (Table 2). Moxifloxacin, norfloxacin, gatifloxacin, grepafloxacin, trovafloxacin and sparfloxacin were also effective against *F. tularensis in vitro* (Table 3), but the three latter antibiotics have been withdrawn from the market because of potential severe side effects.

As for the aminoglycosides, tobramycin and amikacin were evaluated in three studies, only against type B strains (Ikäheimo et al., 2000; Tomaso et al., 2005; Yeşilyurt et al., 2011). Tobramycin displayed MIC values (0.125–3 mg/L) close to those of gentamicin and streptomycin. Interestingly, Enderlin et al., reported in 1994 a cure rate with this antibiotic of only 50% but for a limited number of patients (3/6 patients) (Enderlin et al., 1994). Conversely, amikacin was less active *in vitro*, with MICs up to 16 mg/L (Table 3; Tomaso et al., 2005).

Thus all strains were confirmed as susceptible to the first-line antibiotics recommended for tularaemia treatment, with ciprofloxacin and levofloxacin showing the lowest MICs *in vitro*.

Macrolides

Erythromycin MICs are much higher for biovar II *F. tularensis* subsp. *holarctica* strains, than for biovar I strains of the same subspecies and for *F. tularensis* subsp. *tularensis* strains. Kudelina et al first described erythromycin-resistant strains of *F. tularensis*

as those able to grow on media containing up to 6400 mg/L of this antibiotic, while susceptible strains could be killed by 25 mg/L of this antibiotic (Kudelina and Olsufiev, 1980). In the literature, type B biovar II strains, which currently correspond to East European strains belonging to the B12 subclade, were all resistant to erythromycin with MIC > 256 mg/L using the E-test strip method (Table 4; Karlsson et al., 2016). Only Tomaso et al. reported one biovar II strain with an erythromycin MIC of only 4 mg/L, but this result can be questioned according to current literature (Tomaso et al., 2005). Using the broth microdilution method, all type B biovar II strains had erythromycin MICs of ≥ 32 mg/L (Table 1). In contrast, all type B biovar I strains displayed erythromycin MICs ≤ 8 mg/L using the broth microdilution method and ≤ 1 mg/L using MIC strips. Among erythromycin-susceptible *F. tularensis* strains, subtle differences in erythromycin MICs could be found in the literature between the US strains belonging either to type B biovar I (MIC range, 0.125–2 mg/L; MIC₉₀ range, 0.5–1 mg/L) or to type A (MIC range, 0.125–1 mg/L), and the West European type B biovar I strains (MIC range, 1–8 mg/L; MIC₉₀, 4 mg/L). This difference might be correlated with the B6 clade displaying higher MIC levels, or to methodological differences, such as incubation of media in ambient air vs. under 5% CO₂ atmosphere, the latter reducing the activity of the macrolides. The Japanese type B strains, including those formally identified as belonging to biovar japonica, displayed erythromycin MICs ranging from 0.094 to 1.5 mg/L.

According to the above data, a breakpoint for the biovar II definition might be set at erythromycin MIC ≥ 32 mg/L, in agreement with Kudelina's above-mentioned study (Kudelina and Olsufiev, 1980). Moreover, erythromycin resistance in type B biovar II strains has recently been correlated with the presence of a single mutation A2059C in the three copies of the *rrl* gene, encoding the 23S rRNA (Karlsson et al., 2016). Thus, determination of the *rrl* gene sequence provides a confirmatory identification of biovar II subtype.

Azithromycin MICs against *F. tularensis* were also determined in three studies, with the same dichotomy between biovar I and biovar II of type B strains. MIC ranges were similar to those observed for erythromycin (Table 4). Biovar II strains displayed azithromycin MICs > 256 mg/L, whereas MIC ranges were 0.064–2 mg/L for 16 type B and 0.125–2 mg/L for eight type A strains from the USA (Ikäheimo et al., 2000; Johansson et al., 2002; Yeşilyurt et al., 2011). Telithromycin, a ketolide compound, displayed MICs ranging from 0.125 to 0.25 mg/L with the agar dilution method against type B biovar I strains (Valade et al., 2008).

Thus, low MIC values are observed for macrolides and one ketolide against biovar I strains. No susceptibility breakpoints are currently defined by the CLSI for these antibiotics against *F. tularensis*, although they may represent useful therapeutic alternatives for infection related to biovar I strains, especially if first-line antibiotics are contraindicated. Further experimental data in animal models are needed for the *in vivo* evaluation of the activity of these compounds against *F. tularensis*. In contrast, the macrolides and ketolides are ineffective against biovar II strains.

Beta-Lactams

Many β -lactams have been tested *in vitro* against *F. tularensis*, although they are considered unreliable for treatment of tularaemia (Cross and Jacobs, 1993; Cross et al., 1995; Tarnvik, 2007; Maurin et al., 2011). In the literature, all the *F. tularensis* strains tested were resistant to penicillin A, ticarcillin and piperacillin, whether or not associated with a β -lactamase inhibitor, with MICs ≥ 64 mg/L (Table 5). In contrast, the cephalosporins, monobactams and carbapenems displayed larger MIC ranges. Although most *F. tularensis* strains displayed MICs higher than 32 mg/L to these β -lactams, a few strains displayed MICs lower than 1 mg/L (Table 5). In a study from Hotta et al., 30–60% of 36 Japanese strains displayed MICs lower than 1 mg/L for cefotaxime, ceftriaxone, ceftazidime, aztreonam, imipenem and meropenem (Hotta et al., 2013). Velinov et al. described 21 Bulgarian strains with a MIC range for ceftriaxone between 2 and 4 mg/L (Velinov et al., 2011). To date, two β -lactamase genes (*bla1* and *bla2*) have been identified in the LVS strain (with corresponding homologs in the Schu S4 strain), but the expression of recombinant LVS proteins in *Escherichia coli* only revealed the *bla2*_{LVS} gene to encode a functional β -lactamase (Bina et al., 2006). In 2012, Antunes et al. reported a class A β -lactamase (FTU-1) present in 14 strains belonging to all *F. tularensis* subspecies, including various type B strains from the USA, France, Japan, Russia, and Sweden (Antunes et al., 2012). Actually, the FTU-1 corresponds to the *bla2*_{LVS} gene, as evidenced by comparison of gene sequences (YP_513599.1 and FTT_0611c, respectively). This class A β -lactamase, which was partially inactivated by β -lactamase inhibitors, induced resistance to penicillin and a 4-fold increase in ceftazidime MIC when cloned and expressed in *E. coli*. This β -lactamase had no effect on other cephalosporins, monobactams and carbapenems (Bina et al., 2006; Antunes et al., 2012). The presence of the FTU-1/*bla2*_{LVS} gene is thus compatible with the cephalosporin-susceptibility phenotype observed in Japanese strains, whereas additional resistance mechanisms are probably involved in strains displaying resistance to cephalosporins, monobactams and carbapenems (Table 5). In 2008, Bina et al. characterized an AcrAB RND efflux system in the LVS strain, which conferred increased resistance to all beta-lactams tested in the study (i.e., ampicillin, carbenicillin and cefoperazone) but not to carbapenems (Bina et al., 2008). Thus, β -lactams are not recommended for the treatment of tularaemia.

Chloramphenicol

The reported chloramphenicol MICs range from ≤ 0.023 to 4 mg/L, with an MIC₉₀ range of 0.25–2 mg/L (Table 4). Chloramphenicol has been used occasionally (alone or in combination with other antibiotics) to treat patients with tularaemia meningitis, owing to its high distribution in brain tissue and cerebrospinal fluid (Tarnvik, 2007; Hofinger et al., 2009). Considering the MIC breakpoint of 8 mg/L, *F. tularensis* can be considered susceptible to chloramphenicol, but the clinical use of this antibiotic is currently restricted to meningitis because of potential severe bone marrow toxicity.

Rifampicin

Rifampicin is active *in vitro* against *F. tularensis* but with MICs ranging from ≤ 0.094 to 3 mg/L, and a MIC₉₀ range of 0.25–1.5 mg/L (Table 4). However, this antibiotic is not recommended for tularaemia treatment because of potential rapid selection of resistant mutants, as described by Johansson et al. (2000) and Tarnvik (2007). It has been used in combination with ciprofloxacin for treatment of an infected total knee arthroplasty, with resolution of symptoms only after addition of rifampicin and a successful outcome with this antibiotic combination (Cooper et al., 1999).

New Antibiotics

Among more recently developed antibiotics, tigecycline, a new glycylcycline, has been evaluated in two studies using the *E*-test method, with reported MICs (0.094–0.38 mg/L) and MIC₉₀ (0.19–0.25 mg/L) ranges lower than those determined in the same studies for tetracycline and doxycycline (Tables 1, 4) (Yeşilyurt et al., 2011; Kreizinger et al., 2013). No breakpoints are currently defined for *F. tularensis* susceptibility to tigecycline, but all tested strains displayed MICs ≤ 0.5 mg/L. Further studies are needed to evaluate tigecycline MICs using the microdilution reference method. Importantly, fresh medium (< 24 h) must be used to prevent overestimation of tigecycline MICs (Bradford et al., 2005). Tigecycline might be a suitable alternative to doxycycline for treatment of tularaemia, but its much broader antibacterial spectrum is a disadvantage due to a greater deleterious effect on the gut commensal flora.

Conflicting results were observed for linezolid, an oxazolidinone compound. The activity of this antibiotic is considered mainly restricted to Gram-positive bacteria, with a CLSI susceptibility breakpoint for the corresponding species set at ≤ 2 mg/L. However, MICs of 4–8 mg/L have been found for Gram-negative bacteria of the genera *Bacteroides*, *Moraxella* and *Pasteurella*, owing to the absence or low efficacy of efflux systems, or a high affinity of their ribosomes for linezolid (Livermore, 2003). As for *F. tularensis*, linezolid displayed MICs of 0.5–2 mg/L for 39 biovar II type B strains from Turkey, 2–4 mg/L for eight type A strains from the USA, and 4–16 mg/L for 16 type B strains from the USA, when using the *E*-test strip procedure. In contrast, MICs ranged from 12 to 48 mg/L for 29 Hungarian biovar II type B strains using the same technique, although such differences could be related to the use of different solid media for AST (Tables 1, 4). The relative susceptibility of *F. tularensis* to linezolid may be related to its small genome with a limited number of efflux systems, while MIC variations between strains may reflect variable expression of such efflux systems. This hypothesis needs to be further assessed on a larger panel of *F. tularensis* strains.

Conclusion

In conclusion, MIC data confirm that among the antibiotics recommended as first-line treatment of tularaemia, ciprofloxacin and levofloxacin display the lowest MIC ranges against *F. tularensis*. Gentamicin ranks second, while doxycycline has the highest MIC range with some strains displaying an MIC at 4 mg/L, which is the breakpoint for susceptibility (4 mg/L).

However, no resistant strains to any of these antibiotics have been characterized so far. Moreover, chloramphenicol is active and may be used in combination for rare meningitis due to *F. tularensis*. Azithromycin and telithromycin may be useful alternatives for infection related to biovar I strains of *F. tularensis* subsp. *holarctica*, when all first line antibiotics are contraindicated, but still require confirmation of their efficacy in animal models. Tigecycline and rifampicin are active *in vitro* and should be also further evaluated in animal models. Rifampicin may be an interesting antibiotic in association to fluoroquinolones for rare bone and joint infections.

MBCS AND OTHER BACTERICIDAL ASSAYS

A few *in vitro* studies have reported either MBC or time-kill kinetic experiments for *F. tularensis*. MBC testing is performed similarly to MIC testing using a broth microdilution method, but an aliquot of each well with no visible growth after 48 h incubation is plated on enriched chocolate agar media for CFU count determination. After 48 h incubation of the chocolate agar plates at 37°C, under 5% CO₂ atmosphere, CFU counting can determine the MBC, which is the lowest antibiotic concentration allowing 3-log or greater reduction of the primary bacterial inoculum.

Time-kill kinetic experiments determine CFU counts over time in antibiotics containing cultures, incubated for 48 h at 37°C, under 5% CO₂ atmosphere. Experiments are conducted using enriched caMHB medium, containing two, four or eight times the MIC of the tested antibiotic compound (Maurin et al., 2000; Caspar et al., 2014).

The MBCs of several antibiotics (ceftriaxone, streptomycin, amikacin, gentamicin, thiamphenicol, telithromycin, erythromycin, clarithromycin, rifampicin, ofloxacin, ciprofloxacin, pefloxacin, doxycycline, and cotrimoxazole) were determined against a single human strain of *F. tularensis* subsp. *holarctica* biovar I, using the modified MHII as the experimental medium (Maurin et al., 2000). MBCs were equal to MICs for ofloxacin and ciprofloxacin; 2-fold higher for the aminoglycosides (streptomycin, amikacin, and gentamicin), thiamphenicol, telithromycin, rifampicin, pefloxacin, and doxycycline; 4-fold higher for erythromycin; 16 times higher for cotrimoxazole; and 32 times higher for clarithromycin. Despite a MIC of 2 mg/L, a bactericidal effect was never observed with ceftriaxone against *F. tularensis*, although β -lactams are classically considered bactericidal drugs against most other bacteria susceptible to these compounds. The latter results reinforce prior statements that β -lactams and cotrimoxazole are not reliable for tularaemia treatment (Tarnvik, 2007). According to this work, most antibiotics tested could be considered as bactericidal against *F. tularensis*. However, it should be mentioned that the use of modified MH2 in these experiments may have influenced both the bacteriostatic and the bactericidal activity of antibiotics compared to caMHB, as previously discussed. Indeed, in that study, the MIC value for doxycycline was 8 mg/L, which is higher than usually found in other studies.

We recently evaluated MBCs for gentamicin and doxycycline against the LVS strain and two human strains of *F. tularensis* subsp. *holarctica* biovar I from France, using caMHB medium (Caspar et al., 2014). The MBC was 8-fold higher than the MIC for gentamicin (respectively, 2 and 0.25 mg/L) and could not be determined for doxycycline, which was mainly bacteriostatic (MIC = 0.25 mg/L) (Caspar et al., 2014). These data are more in agreement with the known bactericidal and bacteriostatic nature of these two antibiotics, respectively. Such a difference may participate to the lower relapse rates reported with gentamicin (Enderlin et al., 1994).

Finally, a third study measured the MBCs of ciprofloxacin, gentamicin and doxycycline against the LVS strain, using enriched caMHB medium (Aloni-Grinstein et al., 2015). The MBC/MIC ratios were measured at 1–2 for gentamicin and ≤ 4 for ciprofloxacin, confirming the bactericidal nature of these antibiotics against *F. tularensis*. The MBC/MIC ratio was equal to 4 for chloramphenicol. In contrast, the MBC/MIC ratio was ≥ 64 for doxycycline, demonstrating a bacteriostatic activity (Aloni-Grinstein et al., 2015).

In conclusion, MBC data investigated with suitable media for *F. tularensis* AST revealed a bactericidal activity for the aminoglycosides and the fluoroquinolones, but a bacteriostatic activity for doxycycline. These data should be further confirmed using a larger sample of *F. tularensis* strains.

CELL SYSTEMS

The activity of antibiotics against *F. tularensis* has rarely been evaluated in cell models. These models used either of the following cell systems: murine macrophage-like cell lines J774.1 or P388D1; kidney epithelial Vero cells from African green monkey; human cell lines, including lung epithelial A549 cells, pulmonary fibroblastic MRC5 cells, non-phagocytic kidney epithelial HEK 293 and THP-1 human monocytes; or human monocytes purified from buffy coat (Maurin et al., 2000; Golovliov et al., 2003; Madrid et al., 2013; Schmitt et al., 2013; Sutura et al., 2014). In these models, the multiplicity of infection (MOI, bacteria/eukaryotic cell ratios used for cell infection) varied between 10 and 3000 according to the *F. tularensis* strain used (i.e., *F. tularensis* subsp. *tularensis* SchuS4 strain, *F. tularensis* subsp. *holarctica* FSC200 strain, or LVS) and the nature of the eukaryotic cells. Cell infection usually occurs after 2–3 h of bacteria–cell contact. The penetration of bacteria within eukaryotic cells may be enhanced by centrifugation of infected cell monolayers (Maurin et al., 2000; Madrid et al., 2013; Schmitt et al., 2013; Sutura et al., 2014; Aloni-Grinstein et al., 2015). Then non-phagocytised bacteria are removed by adding gentamicin to the extracellular medium for 1–4 h, which is referred to as the gentamicin protection assay. The cell monolayers are then washed and incubated at 37°C in 5% CO₂ atmosphere, either in drug-free medium (growth control) or in the presence of the tested antibiotics. At various incubation times, cell monolayers are washed and lysed with detergents, and CFU counts in cell lysates are determined. Antibiotic activity is deduced from the ratio of CFU counts in antibiotic-containing cultures compared to the drug-free growth control.

Alternative methods for the evaluation of antibiotic activity against intracellular *F. tularensis* have been proposed. A dye-uptake assay based on the capacity of eukaryotic cells to internalize a vital dye has recently been reported. In this model, activity of antibiotics is deduced from their ability to inhibit bacterial growth within eukaryotic cells, preventing lysis of the cell monolayers. The term “minimal inhibitory extracellular concentration” (MIEC) was coined to define the minimal extracellular antibiotic concentration capable of preventing cytotoxic effects of *F. tularensis* multiplication (Sutura et al., 2014). The turnaround time of the dye uptake assay was 2 days compared to 4–5 days for the CFU count-based model. Cell mortality could also be evaluated by measuring lactate dehydrogenase activity in cell supernatants (Madrid et al., 2013). More recently, a qPCR assay was used to determine *F. tularensis* growth in Vero cells (Aloni-Grinstein et al., 2015). MIECs were determined after 24 h infection, with results comparable to those obtained with the CFU method (Aloni-Grinstein et al., 2015). However, qPCR may overestimate viable bacterial loads since it quantifies DNA from both viable and non-viable bacteria.

Fluoroquinolones

The intracellular activity of antibiotics against a French type B biovar I strain of *F. tularensis* (erythromycin MIC of 4 mg/L) was evaluated in a P388D1 murine macrophage-like cell model, using the CFU count methodology (Maurin et al., 2000). The results showed that ciprofloxacin and ofloxacin at 1 mg/L were the most potent compounds, with more than a 4- and 3-log reduction of bacterial inocula after only 48 h incubation of cultures, respectively (Maurin et al., 2000). In a systematic screening of FDA-approved drugs to identify compounds that may inhibit multiplication of biological threat agents, including *F. tularensis*, norfloxacin (50 μ M, i.e., 16 mg/L) exhibited 83% protection of cells against cytotoxicity of the SchuS4 strain in J774.1 murine macrophages, as determined by the supernatant's lactate dehydrogenase activity (Madrid et al., 2013). In a dye-uptake assay using MRC5 cells, MIECs and MICs were equal for ciprofloxacin, levofloxacin and moxifloxacin, suggesting good penetration of these antibiotics within *F. tularensis*-infected cells (Sutura et al., 2014).

Tetracyclines

In the P388D1 murine macrophage-like model, doxycycline at 4 mg/L only induced a 2-log reduction of bacterial inocula after 72 h incubation (Maurin et al., 2000). In the systematic screening assay of FDA-approved drugs, tetracycline completely protected infected cells from cytotoxicity of the SchuS4 strain at 50 μ M (22 mg/L), and minocycline induced 92% survival of infected cells at 23 mg/L (Madrid et al., 2013). In the dye uptake assay, MIECs were also equal to MIC for doxycycline, also demonstrating good penetration within infected cells. However, MIEC values were eight times higher for doxycycline (0.5 mg/L) compared to ciprofloxacin (0.064 mg/L) against the two biovar I type B strains evaluated in the study. In another study, the same ciprofloxacin MIEC was found for the LVS strain in Vero cells, as determined by both qPCR and CFU count methods,

but a lower MIEC (0.125–0.5 mg/L) was found for doxycycline (Aloni-Grinstein et al., 2015).

Aminoglycosides

In the P388D1 murine macrophage-like cell model, gentamicin at 3 mg/L was not bactericidal after 48 h incubation of cultures and only induced a 1-log reduction of the bacterial inoculum after 72 h incubation. When tested at 10 mg/L, a 2-log reduction of bacterial counts was observed after 48 h incubation and more than 3-log reduction after 72 h (Maurin et al., 2000). In another study using the attenuated LVS strain and the Vero cell line, gentamicin at 20 mg/L did not show any intracellular activity after 32 h incubation (Aloni-Grinstein et al., 2015). In the dye-uptake assay using MRC5 cells, the gentamicin MIEC after 48 h incubation of cultures was 2 mg/L against two French type B biovar I strains of *F. tularensis*, while the MICs of this antibiotic were, respectively, 0.25 and 0.5 mg/L for the same strains (Sutera et al., 2014). Delayed activity of gentamicin correlated with the slow penetration of this antibiotic within eukaryotic cells, usually detectable only after 48–72 h of antibiotic–cell contact.

The other aminoglycosides also penetrate slowly within eukaryotic cells. Amikacin and streptomycin, at 10 mg/L, only decreased *F. tularensis* inoculum by 1 log after 48 h, and 2 logs after 72 h (Maurin et al., 2000). In contrast, netilmicin did not prevent cell lysis in J774.1 cells infected with the SchuS4 strain (Madrid et al., 2013).

Macrolides/Lincosamides/Ketolides

Conflicting results have been reported between studies testing the intracellular form of *F. tularensis*, which may be due to the use of different cell types and bacterial strains. In P388D1 murine macrophage-like cells, erythromycin and clarithromycin at 4 mg/L exhibited no intracellular activity against a type B biovar I strain of *F. tularensis* displaying MICs of 4 and 8 mg/L in acellular media for these antibiotics, respectively. In contrast, telithromycin at 4 mg/L (MIC at 0.5 mg/L in acellular medium) was able to reduce the bacterial inoculum between two to three log₁₀ after 72 h (Maurin et al., 2000). Unlike telithromycin, the intracellular concentration of erythromycin and clarithromycin was probably not sufficient in this experiment to kill bacteria, as the extracellular concentration used was equal or superior to their MIC. In another study, a high concentration of erythromycin (50 μM, 37 mg/L) conferred full protection of J774.1 cell viability after infection with the SchuS4 type A strain (Madrid et al., 2013). In the same assay, clindamycin (50 μM, 21 mg/L) exhibited 83% protection of cells against the cytotoxic effect of *F. tularensis* proliferation (Madrid et al., 2013). In the dye uptake assay reported by Sutera et al., erythromycin MIECs were four times lower than MICs (respectively, 1–2 mg/L and 4–16 mg/L) for two French biovar I type B strains in MRC5 cells (Sutera et al., 2014). Altogether, these experiments show that erythromycin may be effective in preventing intracellular replication of type A and biovar I type B strains.

In another experiment reported by Ahmad et al., azithromycin (a C15 macrolide) showed complete killing of the LVS strain at 5 mg/L in murine macrophage J774.1 cells, although this antibiotic displays an MIC of 25 mg/L against this biovar II

type B strain (Ahmad et al., 2010). This result suggests a high bactericidal concentration of azithromycin within *F. tularensis*-infected J774.1 macrophages. This may not be true for all cell types since a previous experiment from Ahmad et al., demonstrated that azithromycin was fully bactericidal at only 25 mg/L against the LVS strain grown in human lung epithelial A549 cells (Ahmad et al., 2010).

Beta-Lactams

In the P388D1 murine macrophage-like model, β-lactams at 10 mg/L (penicillin G, amoxicillin, ceftriaxone) displayed no activity against intracellular *F. tularensis* (Maurin et al., 2000). Meropenem was ineffective against both intracellular and extracellular *F. tularensis* in the dye uptake assay (Sutera et al., 2014).

Other Antibiotics

In the P388D1 murine macrophage-like model, thiamphenicol at 4 mg/L displayed no intracellular activity. In contrast, rifampicin at 4 mg/L induced a 2-log reduction of bacterial inocula after 72 h incubation (Maurin et al., 2000). In the dye uptake assay using MRC5 cells, MIECs were close to MICs for rifampicin, also suggesting good penetration of this compound within *F. tularensis*-infected cells. However, MIEC values were 16 times higher than those of ciprofloxacin (1 vs. 0.064 mg/L, respectively) against the two biovar I type B strains tested for *F. tularensis* (Sutera et al., 2014). Interestingly, linezolid exhibited higher activity against intracellular than extracellular *F. tularensis*, suggesting its accumulation within MRC5 cells, with a MIEC of 1 mg/L and an MIC of 8 mg/L (Sutera et al., 2014). Finally, daptomycin was ineffective both intracellularly and extracellularly (Sutera et al., 2014).

Conclusion of Intracellular Activity of Antibiotics against Tularaemia

To summarize the data from the intracellular models, the fluoroquinolones ciprofloxacin, levofloxacin, moxifloxacin and ofloxacin displayed the lowest MIECs and the fastest bactericidal activity against intracellular *F. tularensis*, suggesting rapid and efficient concentration of these compounds within infected eukaryotic cells. The tetracyclines were less effective and mainly bacteriostatic against intracellular *F. tularensis*. The aminoglycosides displayed a bactericidal activity, but only after 48–72 h of antibiotic exposure of infected cells, which correlated with the slow intracellular accumulation of these basic compounds (Maurin and Raoult, 2001). Thus, the aminoglycosides are probably much more effective against the extracellular form of *F. tularensis* at the early stage of antibiotic treatment, while these antibiotics may also be active against intracellular *F. tularensis* after several days of treatment. Streptomycin and amikacin were slightly less effective than gentamicin at the same concentration, and netilmicin was ineffective. The beta-lactams and daptomycin were not effective in cell systems. In contrast, the activity of linezolid against intracellular *F. tularensis* should be further investigated both *in vitro* and *in vivo*.

Interestingly, in two studies, the macrolides erythromycin and azithromycin were found to be active against the intracellular form of type A and biovar I type B *F. tularensis* strains, which are naturally susceptible to these antibiotics. Azithromycin was also effective against the intracellular form of biovar II type B LVS strain, although naturally more resistant to macrolides, but only in phagocytic and fibroblastic cells. Indeed, the intracellular accumulation of the macrolides varies according to the eukaryotic cell type considered, with a lower accumulation in epithelial cells compared to phagocytic and fibroblast cells (Ahmad et al., 2010; Sutura et al., 2014). PK/PD studies have demonstrated the accumulation of azithromycin within human phagocytic and fibroblast cells, and in many human tissues, such as lungs, soft tissues, prostate and tonsils (McDonald and Pruul, 1991; Matzneller et al., 2013). The intracellular/extracellular azithromycin ratio in tissues is generally between 10 and 100, and can be >200 in polymorphonuclear (PMN) leukocytes, with probable large amounts of this antibiotic at the site of infection (Hand and Hand, 2001; Hall et al., 2002; Matzneller et al., 2013). The intracellular accumulation of erythromycin is lower, with intracellular/extracellular ratios generally between 1 and 10 in tissues and PMNs (McDonald and Pruul, 1991; Hand and Hand, 2001). The activity of azithromycin against intracellular *F. tularensis* warrants further evaluation of its activity in animal models. These experiments should be conducted using type A and type B strains, especially the type B biovar II strains.

ANIMAL MODELS

Although several animal models have been developed to study the pathogenesis of *F. tularensis* infection and vaccine efficacy, few of these models have evaluated *in vivo* antibiotic efficacy (Rick Lyons and Wu, 2007). This may be related to the absence of an optimal animal model mimicking human infection. In these models, antibiotic activity is usually deduced from the death rate and survival time of infected animals and the bacterial load in their organs (especially in the spleen) at the time of death or sacrifice, when treated with various antibiotic regimens compared to infected and untreated controls. BALB/c and C57BL/6 mice and guinea pigs are highly susceptible hosts to *F. tularensis* infection, but also to the LVS strain of *F. tularensis* subsp. *holarctica* and *F. novicida* strains, which have often been used as surrogates of *F. tularensis*, although they are much less virulent in humans (Stundick et al., 2013; Kingry and Petersen, 2014). Rabbits and Fisher 344 rats are less susceptible to *F. tularensis* infection and may better mimic human infection. However, variable immune responses to *F. tularensis* infection also exist between rat strains, with Sprague-Dawley being much more resistant than Fisher 344 rats (Raymond and Conlan, 2009). Results may also vary according to the route of infection, i.e., the intraperitoneal, intradermal, subcutaneous or intranasal routes for Fischer 344 rats (Stundick et al., 2013). Moreover, the “Animal Rule” states that experimental animal models should be developed using the true etiologic agent causing human disease. Thus, evaluation of antibiotic activity in Fisher 344 rats infected with virulent type A or type B strains would be more predictive of the clinical situation.

Few experiments have evaluated the activity of antibiotics in *F. tularensis*-infected animal models. However, interesting data have been obtained regarding the *in vivo* efficacy of antibiotics, and relapse rates according to delay in antibiotic therapy and treatment duration. Unfortunately, these models are highly heterogeneous with respect to the route of infection, the route of antibiotic administration, the antibiotic dose administered and the *F. tularensis* strain tested.

Fluoroquinolones and Doxycycline

In 1998, Russel et al. evaluated the effect of subcutaneous injection of doxycycline or ciprofloxacin on the median lethal dose (MLD) of the Schu S4 strain injected intraperitoneally to Porton outbred mice (Russell et al., 1998). The animals either received a 2-day antibiotic prophylaxis before the bacterial challenge, or were treated 48 h post-infection with 20 or 40 mg/kg twice a day, of doxycycline or ciprofloxacin for 10 days, and then were monitored for 24 days. Although the MLD was close to 1 CFU of the Schu S4 strain in untreated mice, full protection at the highest bacterial inoculum tested (8.8×10^6 CFU) was achieved by a 2-day prophylaxis with ciprofloxacin or doxycycline, and by 10 days of post-infection treatment with either of these antibiotics at 40 mg/kg twice a day. At this dosage, the serum concentrations were higher than $4 \times \text{MIC}$ for at least 12 h for ciprofloxacin, and $3 \times \text{MIC}$ for 9 h for doxycycline (Russell et al., 1998).

The *in vivo* efficacy of fluoroquinolones was confirmed in 2005, by Piercy et al. (2005). BALB/c mice were infected subcutaneously with 10^6 CFU of the Schu S4 strain and treated orally with 100 mg/kg of ciprofloxacin, gatifloxacin or moxifloxacin, from 6 h to 14 days post-infection. Survival rates at day 42 post-infection were 94, 100, and 100%, respectively, for these three antibiotics (Piercy et al., 2005).

In 2008, Klimpel et al. showed that a 13-day course of levofloxacin (5 mg/kg/day, intraperitoneally), starting 24 h following an intranasal challenge with 3 LD_{50} of *F. tularensis* Schu S4 strain, prevented death of all Balb/c mice (Klimpel et al., 2008). No bacteria were detectable in the spleen of the animals after 10 days of treatment, while very few were detected in the lungs at this time (Klimpel et al., 2008).

In 2012, Rotem et al. compared the efficacy of ciprofloxacin and doxycycline in Balb/c mice infected by inhalation of a 100-LD_{50} dose of *F. tularensis* LVS (10^5 CFU) or Schu S4 (10^2 CFU) strains (Rotem et al., 2012). Untreated controls died 5–7 days post-infection, whereas all LVS-infected mice were cured by intraperitoneal injection of ciprofloxacin (50 mg/kg bid) for 7 days or doxycycline (40 mg/kg bid) for 14 days, whether the antibiotic treatment was started at 24, 48, or 72 h post-infection (Rotem et al., 2012). *F. tularensis* LVS strain was undetectable by culture in the lungs, liver and spleen after completion of any of these treatments. In contrast, for animals infected with the Schu S4 strain, no death occurred when ciprofloxacin was administered 24 or 48 h post infection, while doxycycline only cured 90% of the animals even when administered 24 h post-infection (Rotem et al., 2012).

Treatment Delay

In the study from Russel et al., a 48-h prophylaxis with ciprofloxacin or doxycycline protected mice from a 3.7×10^6 CFU and 6.0×10^6 CFU challenge with the Schu S4 strain, respectively (Russell et al., 1998). In contrast, when antibiotic treatment was started 24 h post-infection, complete protection was only obtained against an intraperitoneal challenge with 880 CFU for ciprofloxacin and 100 CFU for doxycycline. Thus, antibiotic efficacy was dramatically reduced after only 24 h infection (Russell et al., 1998). In the study by Rotem et al., in which mice were infected via Schu S4 strain aerosols, no death occurred when ciprofloxacin was administered 24–48 h post infection, while a 30% mortality rate was observed when this antibiotic was administered 3 days post-infection (Rotem et al., 2012). Doxycycline only cured 90, 30, and 0% of the mice when started at 24, 48, and 72 h post-infection, respectively (Rotem et al., 2012). In the study reported by Piercy et al., the survival rates decreased dramatically (94, 67, and 0%) when ciprofloxacin was administered 6, 24, or 48 h post-infection, respectively (Piercy et al., 2005). In contrast, the survival rates were 100, 96, and 84% for gatifloxacin, and 100, 100, and 62% for moxifloxacin, respectively, showing the better therapeutic efficacy of these drugs compared to ciprofloxacin. In this study, the infectious dose was much higher than in that from Rotem et al. (10^6 CFU intraperitoneally vs. 10^2 CFU intranasally). Finally, in the Klimpel et al. study, full protection against the SchuS4 strain (99 CFU intraperitoneally) was observed for levofloxacin at 40 mg/kg/day, as long as the treatment delay did not exceed 72 h (Klimpel et al., 2008). If started at 72 h, bacterial load decreased approximately from 10^6 to 10 CFU per organ after 1 week of treatment. Delaying the treatment of more than 120 h resulted in the death of all infected mice (Klimpel et al., 2008).

Bactericidal Activity and Treatment Duration

In the Russel et al. study, when treatment was administered for 5 days rather than 10 days post-infection, the MLD was reduced from $> 8.8 \times 10^6$ CFU to 3.7×10^6 CFU for ciprofloxacin and 6.0×10^6 CFU for doxycycline (Russell et al., 1998). The protective effect of the antibiotic therapy also decreased when animals were treated with a lower dose (20 mg/kg bd rather than 40 mg/kg bd) of ciprofloxacin or doxycycline. Moreover, the authors reported that death occurred in 90% of animals after antibiotic treatment withdrawal, demonstrating that a 5-day course of antibiotic treatment was not sufficient to eradicate *F. tularensis* (Russell et al., 1998). Thus, in this study, the dose and length of the antibiotic therapy administered highly influenced the outcome of *F. tularensis* infection in animals (Russell et al., 1998).

Significant insight into relapses came from the study reported by Piercy et al. (2005). Among the nine groups tested (ciprofloxacin, moxifloxacin or gatifloxacin, initiated 6, 24, or 48 h post-infection), these authors showed that the administration of 7 days of dexamethasone to surviving mice in order to abolish their immune system resulted in 17–73% relapse rates depending on the treatment group. These findings suggested that quiescent

bacteria controlled by the immune system persisted in mice despite 14 days of fluoroquinolone therapy. Fluoroquinolones were thus not fully bactericidal when a high inoculum of *F. tularensis* was injected to the mice (e.g., subcutaneous injection of 10^6 CFU of the Schu S4 strain). Suppression of the immune system enabled latent bacteria to multiply and kill mice, even in the 6-h post-exposure treatment group (respectively, 36 and 42% mortality rates in the ciprofloxacin- and moxifloxacin-treated groups; Piercy et al., 2005).

Data from the study by Rotem et al. corroborated this hypothesis (Rotem et al., 2012). In their experiments with the virulent Schu S4 strain, no death occurred when ciprofloxacin was administered 24 or 48 h post-infection, while a 30% mortality rate was observed when this antibiotic was administered 3 days post-infection. In the latter case, bacteria were undetectable in organs at the time of antibiotic treatment withdrawal, while cultures were positive 3 days later for three out of 10 mice that died after antibiotic withdrawal. The extension of ciprofloxacin treatment duration from 7 to 10 days cured all animals, even when the antibiotic was administered 72 h post-infection. In contrast, when doxycycline was started 72 h post-infection, all animals had approximately 100 CFU/g of tissue (lungs, liver or spleen) at the end of treatment, after which the bacterial loads in organs increased in all mice until death. Extension of treatment from 14 to 21 days resulted in no cultivable bacteria in lungs, liver or spleen at the end of treatment, but all mice relapsed after 2 days of doxycycline withdrawal (Rotem et al., 2012). A different picture was observed with the LVS strain, which was below detectable level by culture in the lungs, liver and spleen after completion of any of the treatment regimens (ciprofloxacin for 7 days or doxycycline for 14 days, started 24, 48, and 72 h post-infection) in the mice sacrificed at the end of the treatment. However, 2 days after doxycycline treatment withdrawal, the LVS strain was detected in all organs, and bacterial loads gradually decreased to an undetectable level in the following 7 days and resulted in no death. Thus, although undetectable after doxycycline treatment, the attenuated LVS strain was not fully eradicated and regrowth of the bacteria was observed as soon as doxycycline was stopped, although it did not kill the mice. In contrast, re-emergence of bacteria did not occur for the ciprofloxacin group of LVS-infected mice after ciprofloxacin withdrawal.

Conclusions Drawn from Animal Model Data

Altogether, these data indicate that both ciprofloxacin and doxycycline are able to prevent tularaemia in mice when treatment is started 48 h before a challenge with *F. tularensis* SchuS4 strain. These antibiotics are also able to cure the disease and eradicate *F. tularensis* when administered post-infection at a concentration of 40 mg/kg or higher, for 5–10 days. Efficacy of the antibiotic treatment is highly correlated with the antibiotic dose administered, which is probably related to the duration over which serum concentrations of antibiotics are above the MIC values of the infecting strain.

However, when treatment was started 24–72 h post-infection, ciprofloxacin was superior to doxycycline: (1) in the study

conducted by Rotem et al., doxycycline was not able to cure all mice when infected with 10^2 CFU of the SchuS4 strain via the aerosol route, even when started at 24 h post-infection, while ciprofloxacin cured all mice when started either 24 or 48 h post-infection (Rotem et al., 2012); (2) relapse rates were higher for doxycycline as it was unable to fully eradicate the Schu S4 or LVS strains from the lungs, liver and spleen, even when administered for 14–21 days; (3) the time until antibiotic treatment initiation reduced doxycycline efficacy much more than for ciprofloxacin.

F. tularensis multiplies within the slightly acidic cytosol of eukaryotic cells, and a low pH may alter the activity of the basophilic antibiotics ciprofloxacin and doxycycline (Russell et al., 1998). Data obtained in animal models indicate that persistent bacteria may develop in hosts infected with *F. tularensis* when the antibiotic therapy administered has poor bactericidal activity or is too short in duration. These data suggest that long antibiotic treatment duration should be used in immunocompromised patients infected with *F. tularensis*. This could also be true for patients suffering from suppurated lymphadenopathy, who often experience relapses despite administration of ciprofloxacin for 14 days or doxycycline for 21 days.

Treatment must be initiated as soon as possible since antibiotic efficacy decreased significantly when treatment was delayed by 24–48 h post-infection. It should be noted that, because of diagnosis delays, antibiotics are often given several days to weeks after infection in patients suffering from tularaemia. Importantly, moxifloxacin efficacy was less impacted by treatment delay than ciprofloxacin and thus may represent an advantageous therapeutic option in case of late diagnosis. MIC values are close for moxifloxacin and ciprofloxacin.

GENERAL CONCLUSION AND PERSPECTIVES

Since the introduction of streptomycin in the mid-1950s, antibiotic treatment of human tularaemia has remained challenging. In most tularaemia endemic countries, human infections are now rare, and *F. tularensis* isolation is even rarer. Thus, AST data for isolated strains of *F. tularensis* may not reflect the true situation of current antibiotic resistance in this pathogen. Importantly, the analysis of AST methodological variations between studies shows an urgent need for international standardization. Following the CLSI guidelines, including using the appropriate experimental medium, bacterial inoculum and incubation time are mandatory, although some *F. tularensis* strains grow better or exclusively under 5% CO₂ atmosphere. The broth microdilution technique using enriched cMHB medium should be considered the reference method. As recommended by the CLSI, a final inoculum calibrated at 5×10^5 CFU/mL should be used, as a 10-fold higher or lower inoculum is associated to interpretation errors (Georgi et al., 2012). However, the modified Mueller-Hinton II liquid medium should not be used for *F. tularensis* AST to avoid reporting MICs that could categorize *F. tularensis* strains as resistant to aminoglycosides or doxycycline whereas such resistances have never been characterized so far in

this pathogen. From the data currently available, use of the CLSI broth microdilution method can be recommended to test large collections of *F. tularensis* strains in reference laboratories, while the E-test method would be more convenient for testing one or a few strains. However, the E-test MIC strip method, although more convenient to perform, still requires comparative studies with the reference method.

Altogether, available AST data indicate that the fluoroquinolones display the lowest MICs, are strongly and rapidly bactericidal in cell models and are highly effective in curing *F. tularensis* infection in infected mice when administered for at least 10 days. Among the fluoroquinolones, ciprofloxacin and levofloxacin have the lowest MICs. In contrast, doxycycline MICs are closer to the CLSI susceptibility breakpoint and this antibiotic is only bacteriostatic in cell models. In the mouse model, a 14-day course of doxycycline did not eradicate *F. tularensis* when treatment was started 72 h post-infection (Rotem et al., 2012). A 21-day course of treatment was still not fully effective to eradicate bacteria, whereas 10 days of ciprofloxacin treatment was effective. Therefore, doxycycline should be considered less effective than fluoroquinolones for treatment of tularaemia, which is consistent with higher therapeutic failure rates in humans observed with this antibiotic. Because antibiotic treatment is often administered several days after symptom onset in tularaemia patients, ciprofloxacin may be a better choice than doxycycline. Moreover, treatment duration with ciprofloxacin of at least 14 days should be recommended, while 3 weeks would be a minimum for doxycycline (Rotem et al., 2012). A longer duration of antibiotic treatment should probably be considered in case treatment is delayed longer than 2 weeks after symptom onset, especially if lymph node suppuration or other local or systemic complications have occurred. The aminoglycosides (especially gentamicin) also have low MICs. They are rapidly bactericidal in acellular media, but their intracellular bactericidal activity only takes place after 72 h of cell exposure owing to their slow penetration through the eukaryotic cell membrane. In the 1994 review by Enderlin et al., streptomycin was considered the most reliable treatment for human tularaemia, with almost no relapse after treatment removal (Enderlin et al., 1994). The aminoglycosides are still considered the most reliable treatment of severe tularaemia cases (e.g., the pneumonic and typhoidal forms of tularaemia, and all other systemic infections). Experimental data suggest that the combination of an aminoglycoside with a fluoroquinolone may currently be the most effective alternative in patients with severe tularaemia, especially to obtain a rapid bactericidal activity against extracellular and intracellular *F. tularensis*. However, one has always to remember that antimicrobial potency deduced from MIC values, MBC values, *in vitro* and *in vivo* bactericidal activity in animal models is only one of many factors (including pharmacokinetic and pharmacodynamic parameters, tolerability, plasma protein binding, tissue penetration, bactericidal activity, and contraindication) that may influence the decision of what drug to use in a clinical setting.

The macrolides (especially azithromycin) could be an alternative in patients infected with erythromycin-susceptible strains of *F. tularensis* (type A and type B biovar I) and in those

for whom the above first-line treatments are contraindicated, including young children and pregnant women. However, the macrolide-resistant type B biovar II strains are currently found in Eastern Europe and in Asia, and co-exist with biovar I strains in Germany, Switzerland and Scandinavia. The empirical use of a macrolide in tularaemia patients cannot be considered reliable in these areas. The use of a macrolide in patients with mild to moderate severity tularaemia is safer in Western Europe, where only type B biovar I strains cause human infections. In this context, quick discrimination between type B biovar I and II strains either by determination of erythromycin susceptibility (using MIC strips or sequencing of *rml* gene) or by detection of particular genetic markers (detection of RD23 deletion only found in West European strains) would be of particular interest (Dempsey et al., 2007; Pilo et al., 2009; Karlsson et al., 2016). Since these antibiotics mainly display a bacteriostatic activity against *F. tularensis*, they cannot be considered reliable to treat severe forms of tularaemia. Azithromycin combined with lymph node resection proved to be effective to cure a pregnant woman suffering from oropharyngeal tularaemia with no complications for the fetus (Dentan et al., 2013). Further *in vivo* data in animal models and humans are needed before azithromycin can be recommended as a reliable alternative for treatment of tularaemia.

Finally, the causes of the high relapse rates observed in tularaemia patients after administration of a fluoroquinolone or a tetracycline remain undetermined. Several hypotheses can be proposed, including low penetration of antibiotics in tissues and

eukaryotic cells *in vivo*; low susceptibility of bacteria *in vivo* especially because of low replication and persistence; inactivation of antibiotic activity *in vivo* owing to local conditions (e.g., acidic pH, enzymatic inactivation, etc.) and acquired resistance to antibiotics *in vivo* in patients under fluoroquinolone or tetracycline treatment. Further evaluation of such hypotheses in *in vitro* and *in vivo* experimental models is warranted.

AUTHOR CONTRIBUTIONS

YC has collected data on antibiotic susceptibility testing (AST) of *Francisella tularensis*, both *in vitro* and in animal models, from the English and French literature in the PubMed database, since the introduction of fluoroquinolones in the treatment of tularaemia in 1989 until December 2016. He has written the article. MM has participated to data analysis and corrected the text of the article.

FUNDING

The French National Reference Center for Tularemia is funded by Santé Publique France, the French Agency for Public Health.

SUPPLEMENTARY MATERIAL

The Supplementary Material for this article can be found online at: <http://journal.frontiersin.org/article/10.3389/fcimb.2017.00122/full#supplementary-material>

REFERENCES

- Abd, H., Johansson, T., Golovliov, I., Sandström, G., and Forsman, M. (2003). Survival and growth of *Francisella tularensis* in *Acanthamoeba castellanii*. *Appl. Environ. Microbiol.* 69, 600–606. doi: 10.1128/AEM.69.1.600-606.2003
- Ahmad, S., Hunter, L., Qin, A., Mann, B. J., and van Hoek, M. L. (2010). Azithromycin effectiveness against intracellular infections of *Francisella*. *BMC Microbiol.* 10, 123. doi: 10.1186/1471-2180-10-123
- Akalın, H., Helvacı, S., and Gedikoğlu, S. (2009). Re-emergence of tularemia in Turkey. *Int. J. Infect. Dis.* 13, 547–551. doi: 10.1016/j.ijid.2008.09.020
- Aloni-Grinshtein, R., Shifman, O., Lazar, S., Steinberger-Levy, I., Maoz, S., and Ber, R. (2015). A rapid real-time quantitative PCR assay to determine the minimal inhibitory extracellular concentration of antibiotics against an intracellular *Francisella tularensis* Live Vaccine Strain. *Front. Microbiol.* 6:1213. doi: 10.3389/fmicb.2015.01213
- Antunes, N. T., Frase, H., Toth, M., and Vakulenko, S. B. (2012). The class A β -Lactamase FTU-1 is native to *Francisella tularensis*. *Antimicrob. Agents Chemother.* 56, 666–671. doi: 10.1128/AAC.05305-11
- Baker, C. N., Hollis, D. G., and Thornsberry, C. (1985). Antimicrobial susceptibility testing of *Francisella tularensis* with a modified Mueller-Hinton broth. *J. Clin. Microbiol.* 22, 212–215.
- Barut, S., and Cetin, I. (2009). A tularemia outbreak in an extended family in Tokat Province, Turkey: observing the attack rate of tularemia. *Int. J. Infect. Dis.* 13, 745–748. doi: 10.1016/j.ijid.2008.12.002
- Bicakci, Z., and Parlak, M. (2008). A neglected cause of cervical lymphadenitis. Oropharyngeal tularemia. *Saudi Med. J.* 29, 1059–1061.
- Bina, X. R., Lavine, C. L., Miller, M. A., and Bina, J. E. (2008). The AcrAB RND efflux system from the live vaccine strain of *Francisella tularensis* is a multiple drug efflux system that is required for virulence in mice. *FEMS Microbiol. Lett.* 279, 226–233. doi: 10.1111/j.1574-6968.2007.01033.x
- Bina, X. R., Wang, C., Miller, M. A., and Bina, J. E. (2006). The Bla2 β -lactamase from the live-vaccine strain of *Francisella tularensis* encodes a functional protein that is only active against penicillin-class β -lactam antibiotics. *Arch. Microbiol.* 186, 219–228. doi: 10.1007/s00203-006-0140-6
- Bradford, P. A., Petersen, P. J., Young, M., Jones, C. H., Tischler, M., and O'Connell, J. (2005). Tigecycline MIC testing by broth dilution requires use of fresh medium or addition of the biocatalytic oxygen-reducing reagent oxyrase to standardize the test method. *Antimicrob. Agents Chemother.* 49, 3903–3909. doi: 10.1128/AAC.49.9.3903-3909.2005
- Broman, T., Thelaus, J., Andersson, A.-C., Backman, S., Wikstrom, P., Larsson, E., et al. (2011). Molecular detection of persistent *Francisella tularensis* Subspecies *holarctica* in natural waters. *Int. J. Microbiol.* 2011:851946. doi: 10.1155/2011/851946
- Busse, H.-J., Huber, B., Anda, P., Escudero, R., Scholz, H. C., Seibold, E., et al. (2010). Objections to the transfer of *Francisella novicida* to the subspecies rank of *Francisella tularensis*-response to Johansson et al. *Int. J. Syst. Evol. Microbiol.* 60, 1718–1720. doi: 10.1099/00207713-60-8-1718
- Caspar, Y., Sutura, V., Boisset, S., Denis, J.-N., and Maurin, M. (2014). Bis-indolic compounds as potential new therapeutic alternatives for tularaemia. *Front. Cell. Infect. Microbiol.* 4:24. doi: 10.3389/fcimb.2014.00024
- Celebi, G., Barüñü, F., Ayoğlu, F., Cinar, F., Karadenizli, A., Uğur, M. B., et al. (2006). Tularemia, a reemerging disease in northwest Turkey: epidemiological investigation and evaluation of treatment responses. *Jpn. J. Infect. Dis.* 59, 229–234.
- Cerný, Z. (2001). Changes of the epidemiology and the clinical picture of tularemia in Southern Moravia (the Czech Republic) during the period 1936–1999. *Eur. J. Epidemiol.* 17, 637–642. doi: 10.1023/A:1015551213151
- Chanturia, G., Birdsell, D. N., Kekelidze, M., Zhgenti, E., Babuadze, G., Tsertsvadze, N., et al. (2011). Phylogeography of *Francisella tularensis* subspecies *holarctica* from the country of Georgia. *BMC Microbiol.* 11:139. doi: 10.1186/1471-2180-11-139

- Christova, I., Velinov, T., Kantardjiev, T., and Galev, A. (2004). Tularaemia outbreak in Bulgaria. *Scand. J. Infect. Dis.* 36, 785–789. doi: 10.1080/00365540410021199
- Clemens, D. L., and Horwitz, M. A. (2007). Uptake and intracellular fate of *Francisella tularensis* in human macrophages. *Ann. N. Y. Acad. Sci.* 1105, 160–186. doi: 10.1196/annals.1409.001
- CLSI. M45-A2 (2010). *Methods for Antimicrobial Dilution and Disk Susceptibility Testing of Infrequently Isolated or Fastidious Bacteria; Approved Guideline-Second Edition*. M45A2. Wayne.
- Cooper, C. L., Caesele, P. V., Canvin, J., and Nicolle, L. E. (1999). Chronic prosthetic device infection with *Francisella tularensis*. *Clin. Infect. Dis.* 29, 1589–1591. doi: 10.1086/313550
- Cross, J. T., and Jacobs, R. F. (1993). Tularaemia: treatment failures with outpatient use of ceftriaxone. *Clin. Infect. Dis.* 17, 976–980. doi: 10.1093/clinids/17.6.976
- Cross, J. T., Schutze, G. E., and Jacobs, R. F. (1995). Treatment of tularaemia with gentamicin in pediatric patients. *Pediatr. Infect. Dis. J.* 14, 151–152. doi: 10.1097/00006454-199502000-00014
- Dempsey, M. P., Dobson, M., Zhang, C., Zhang, M., Lion, C., Gutiérrez-Martín, C. B., et al. (2007). Genomic deletion marking an emerging subclone of *Francisella tularensis* subsp. holarctica in France and the Iberian Peninsula. *Appl. Environ. Microbiol.* 73, 7465–7470. doi: 10.1128/AEM.00646-07
- Dennis, D. T., Inglesby, T. V., Henderson, D. A., Bartlett, J. G., Ascher, M. S., Eitzen, E., et al. (2001). Tularaemia as a biological weapon: medical and public health management. *JAMA* 285, 2763–2773. doi: 10.1001/jama.285.21.2763
- Dentan, C., Pavese, P., Pelloux, I., Boisset, S., Brion, J.-P., Stahl, J.-P., et al. (2013). Treatment of tularaemia in pregnant woman, France. *Emerging Infect. Dis.* 19, 996–998. doi: 10.3201/eid1906.130138
- El-Etr, S. H., Margolis, J. J., Monack, D., Robison, R. A., Cohen, M., Moore, E., et al. (2009). *Francisella tularensis* type A strains cause the rapid encystment of *Acanthamoeba castellanii* and survive in amoebal cysts for three weeks postinfection. *Appl. Environ. Microbiol.* 75, 7488–7500. doi: 10.1128/AEM.01829-09
- Enderlin, G., Morales, L., Jacobs, R. F., and Cross, J. T. (1994). Streptomycin and alternative agents for the treatment of tularaemia: review of the literature. *Clin. Infect. Dis.* 19, 42–47. doi: 10.1093/clinids/19.1.42
- Erdem, H., Ozturk-Engin, D., Yesilyurt, M., Karabay, O., Elaldi, N., Celebi, G., et al. (2014). Evaluation of tularaemia courses: a multicentre study from Turkey. *Clin. Microbiol. Infect.* 20, O1042–O1051. doi: 10.1111/1469-0691.12741
- Feldman, K. A., Enscoe, R. E., Lathrop, S. L., Matyas, B. T., McGuill, M., Schriefer, M. E., et al. (2001). An outbreak of primary pneumonic tularaemia on Martha's Vineyard. *N. Engl. J. Med.* 345, 1601–1606. doi: 10.1056/NEJMoa011374
- Francis, E. (1928). A Summary of Present Knowledge of Tularaemia. *Medicine* 7, 411–432.
- Francis, E., Mayne, B., and Lake, G. C. (1922). *Tularaemia Francis 1921 a New Disease of Man*. Washington, DC: Government Printing office.
- Fujita, O., Uda, A., Hotta, A., Okutani, A., Inoue, S., Tanabayashi, K., et al. (2008). Genetic diversity of *Francisella tularensis* subspecies holarctica strains isolated in Japan. *Microbiol. Immunol.* 52, 270–276. doi: 10.1111/j.1348-0421.2008.00036.x
- García del Blanco, N., Gutiérrez Martín, C. B., de la Puente Redondo, V. A., and Rodríguez Ferri, E. F. (2004). *In vitro* susceptibility of field isolates of *Francisella tularensis* subsp. holarctica recovered in Spain to several antimicrobial agents. *Res. Vet. Sci.* 76, 195–198. doi: 10.1016/j.rvsc.2003.12.002
- Georgi, E., Schacht, E., Scholz, H. C., and Splettstoesser, W. D. (2012). Standardized broth microdilution antimicrobial susceptibility testing of *Francisella tularensis* subsp. holarctica strains from Europe and rare *Francisella* species. *J. Antimicrob. Chemother.* 67, 2429–2433. doi: 10.1093/jac/dks238
- Golovliov, I., Baranov, V., Krocova, Z., Kovarova, H., and Sjöstedt, A. (2003). An attenuated strain of the facultative intracellular bacterium *Francisella tularensis* can escape the phagosome of monocytic cells. *Infect. Immun.* 71, 5940–5950. doi: 10.1128/IAI.71.10.5940-5950.2003
- Gyuranecz, M., Birdsell, D. N., Splettstoesser, W., Seibold, E., Beckstrom-Sternberg, S. M., Makrai, L., et al. (2012). Phylogeography of *Francisella tularensis* subsp. holarctica, Europe. *Emerg. Infect. Dis.* 18, 290–293. doi: 10.3201/eid1802.111305
- Gyuranecz, M., Rigó, K., Dán, A., Földvári, G., Makrai, L., Dénes, B., et al. (2011). Investigation of the ecology of *Francisella tularensis* during an inter-epizootic period. *Vector Borne Zoonotic Dis.* 11, 1031–1035. doi: 10.1089/vbz.2010.0091
- Hall, I. H., Schwab, U. E., Stacy Ward, E., Butts, J. D., Wolford, E. T., and Ives, T. J. (2002). Disposition and intracellular activity of azithromycin in human THP-1 acute monocytic cells. *Int. J. Antimicrob. Agents* 20, 348–360. doi: 10.1016/S0924-8579(02)00187-5
- Hand, W. L., and Hand, D. L. (2001). Characteristics and mechanisms of azithromycin accumulation and efflux in human polymorphonuclear leukocytes. *Int. J. Antimicrob. Agents* 18, 419–425. doi: 10.1016/S0924-8579(01)00430-7
- Hauri, A. M., Hofstetter, I., Seibold, E., Kaysser, P., Eckert, J., Neubauer, H., et al. (2010). Investigating an airborne tularaemia outbreak, Germany. *Emerging Infect. Dis.* 16, 238–243. doi: 10.3201/eid1602.081727
- Helvacı, S., Gedikoğlu, S., Akalin, H., and Oral, H. B. (2000). Tularaemia in Bursa, Turkey: 205 cases in ten years. *Eur. J. Epidemiol.* 16, 271–276. doi: 10.1023/A:1007610724801
- Hofinger, D. M., Cardona, L., Mertz, G. J., and Davis, L. E. (2009). Tularaemia meningitis in the united states. *Arch. Neurol.* 66, 523–527. doi: 10.1001/archneur.2009.14
- Hotta, A., Fujita, O., Uda, A., Sharma, N., Tanabayashi, K., Yamamoto, Y., et al. (2013). *In vitro* antibiotic susceptibility of *Francisella tularensis* isolates from Japan. *Jpn. J. Infect. Dis.* 66, 534–536. doi: 10.7883/yoken.66.534
- Huber, B., Escudero, R., Busse, H.-J., Seibold, E., Scholz, H. C., Anda, P., et al. (2010). Description of *Francisella hispaniensis* sp. nov., isolated from human blood, reclassification of *Francisella novicida* (Larson et al. 1955) Olsufiev et al. 1959 as *Francisella tularensis* subsp. novicida comb. nov. and emended description of the genus *Francisella*. *Int. J. Syst. Evol. Microbiol.* 60, 1887–1896. doi: 10.1099/ijs.0.015941-0
- Ikäheimo, I., Syrjälä, H., Karhukorpi, J., Schildt, R., and Koskela, M. (2000). *In vitro* antibiotic susceptibility of *Francisella tularensis* isolated from humans and animals. *J. Antimicrob. Chemother.* 46, 287–290. doi: 10.1093/jac/46.2.287
- Jellison, W. L. (1974). *Tularaemia in North America, 1930-1974*. University of Montana, University of Montana Foundation.
- Jellison, W. L., and Owen, C. R. (1961). *Tularaemia and Animal Populations Ecology and Epizootiology*. West Salem, Wis.
- Johansson, A., Berglund, L., Gothefors, L., Sjöstedt, A., and Tärnvik, A. (2000). Ciprofloxacin for treatment of tularaemia in children. *Pediatr. Infect. Dis. J.* 19, 449–453. doi: 10.1097/00006454-200005000-00011
- Johansson, A., Celli, J., Conlan, W., Elkins, K. L., Forsman, M., Keim, P. S., et al. (2010). Objections to the transfer of *Francisella novicida* to the subspecies rank of *Francisella tularensis*. *Int. J. Syst. Evol. Microbiol.* 60, 1717–1720. doi: 10.1099/ijs.0.022830-0
- Johansson, A., Lärkeryd, A., Widerström, M., Mörtberg, S., Myrtännäs, K., Ohrman, C., et al. (2014). A respiratory tularaemia outbreak caused by diverse clones of *Francisella tularensis*. *Clin. Infect. Dis.* 59, 1546–1553. doi: 10.1093/cid/ciu621
- Johansson, A., Urich, S. K., Chu, M. C., Sjöstedt, A., and Tärnvik, A. (2002). *In vitro* susceptibility to quinolones of *Francisella tularensis* subspecies *tularensis*. *Scand. J. Infect. Dis.* 34, 327–330. doi: 10.1080/00365540110080773
- Kantardjiev, T., Ivanov, I., Velinov, T., Padeshki, P., Popov, B., Nenova, R., et al. (2006). Tularaemia outbreak, Bulgaria, 1997–2005. *Emerging Infect. Dis.* 12, 678–680. doi: 10.3201/eid1204.050709
- Karlsson, E., Golovliov, I., Lärkeryd, A., Granberg, M., Larsson, E., Öhrman, C., et al. (2016). Clonality of erythromycin resistance in *Francisella tularensis*. *J. Antimicrob. Chemother.* 71, 2815–2823. doi: 10.1093/jac/dkw235
- Karlsson, E., Svensson, K., Lindgren, P., Byström, M., Sjödin, A., Forsman, M., et al. (2013). The phylogeographic pattern of *Francisella tularensis* in Sweden indicates a Scandinavian origin of Eurosiberian tularaemia. *Environ. Microbiol.* 15, 634–645. doi: 10.1111/1462-2920.12052
- Keim, P., Johansson, A., and Wagner, D. M. (2007). Molecular epidemiology, evolution, and ecology of *Francisella*. *Ann. N. Y. Acad. Sci.* 1105, 30–66. doi: 10.1196/annals.1409.011
- Kilic, S., Birdsell, D. N., Karagöz, A., Çelebi, B., Bakkaloglu, Z., Arikian, M., et al. (2015). Water as source of *Francisella tularensis* infection in humans, Turkey. *Emerg. Infect. Dis.* 21, 2213–2216. doi: 10.3201/eid2112.150634
- Kiliç, S., Çelebi, B., Acar, B., and Ataş, M. (2013). *In vitro* susceptibility of isolates of *Francisella tularensis* from Turkey. *Scand. J. Infect. Dis.* 45, 337–341. doi: 10.3109/00365548.2012.751125

- Kingry, L. C., and Petersen, J. M. (2014). Comparative review of *Francisella tularensis* and *Francisella novicida*. *Front. Cell. Infect. Microbiol.* 4:35. doi: 10.3389/fcimb.2014.00035
- Klimpel, G. R., Eaves-Pyles, T., Moen, S. T., Taormina, J., Peterson, J. W., Chopra, A. K., et al. (2008). Levofloxacin rescues mice from lethal intra-nasal infections with virulent *Francisella tularensis* and induces immunity and production of protective antibody. *Vaccine* 26, 6874–6882. doi: 10.1016/j.vaccine.2008.09.077
- Kreuzinger, Z., Makrai, L., Helyes, G., Magyar, T., Erdélyi, K., and Gyuranecz, M. (2013). Antimicrobial susceptibility of *Francisella tularensis* subsp. holarctica strains from Hungary, Central Europe. *J. Antimicrob. Chemother.* 68, 370–373. doi: 10.1093/jac/dks399
- Kudolina, R. I., and Olsufjev, N. G. (1980). Sensitivity to macrolide antibiotics and lincomycin in *Francisella tularensis* holarctica. *J. Hyg. Epidemiol. Microbiol. Immunol.* 24, 84–91.
- Kugeler, K. J., Mead, P. S., Janusz, A. M., Staples, J. E., Kubota, K. A., Chalcraft, L. G., et al. (2009). Molecular epidemiology of *Francisella tularensis* in the United States. *Clin. Infect. Dis.* 48, 863–870. doi: 10.1086/597261
- Larssen, K. W., Afset, J. E., Heier, B. T., Krogh, T., Handeland, K., Vikøren, T., et al. (2011). Outbreak of tularemia in central Norway, January to March 2011. *Euro Surveill.* 16:19828. Available online at: www.eurosurveillance.org/ViewArticle.aspx?ArticleId=19828
- Larssen, K. W., Bergh, K., Heier, B. T., Vold, L., and Afset, J. E. (2014). All-time high tularemia incidence in Norway in 2011: report from the national surveillance. *Eur. J. Clin. Microbiol. Infect. Dis.* 33, 1919–1926. doi: 10.1007/s10096-014-2163-2
- Livermore, D. M. (2003). Linezolid *in vitro*: mechanism and antibacterial spectrum. *J. Antimicrob. Chemother.* 51, ii9–ii16. doi: 10.1093/jac/dkg249
- Madrid, P. B., Chopra, S., Manger, I. D., Gilfillan, L., Keepers, T. R., Shurtleff, A. C., et al. (2013). A systematic screen of FDA-approved drugs for inhibitors of biological threat agents. *PLoS ONE* 8:e60579. doi: 10.1371/journal.pone.0060579
- Mailles, A., Madani, N., Maurin, M., Garin-Bastuji, B., and Vaillant, V. (2010). Unexpected increase of human and animal tularemia cases during winter 2007/2008 in France: emergence or short-lasting episode?. *Med. Mal. Infect.* 40, 279–284. doi: 10.1016/j.medmal.2009.11.006
- Matzner, P., Krasniqi, S., Kinzig, M., Sörgel, F., Hüttner, S., Lackner, E., et al. (2013). Blood, tissue, and intracellular concentrations of azithromycin during and after end of therapy. *Antimicrob. Agents Chemother.* 57, 1736–1742. doi: 10.1128/AAC.02011-12
- Maurin, M., and Gyuranecz, M. (2016). Tularemia: clinical aspects in Europe. *Lancet Infect. Dis.* 16, 113–124. doi: 10.1016/S1473-3099(15)00355-2
- Maurin, M., Mersali, N. F., and Raoult, D. (2000). Bactericidal activities of antibiotics against intracellular *Francisella tularensis*. *Antimicrob. Agents Chemother.* 44, 3428–3431. doi: 10.1128/AAC.44.12.3428-3431.2000
- Maurin, M., Pelloux, I., Brion, J. P., Banõ, J.-N. D., and Picard, A. (2011). Human tularemia in France, 2006–2010. *Clin. Infect. Dis.* 53, e133–e141. doi: 10.1093/cid/cir612
- Maurin, M., and Raoult, D. (2001). Use of aminoglycosides in treatment of infections due to intracellular bacteria. *Antimicrob. Agents Chemother.* 45, 2977–2986. doi: 10.1128/AAC.45.11.2977-2986.2001
- McCoy, G. W., and Chapin, C. W. (1912). Further observations on a plague-like disease of rodents with a preliminary note on the causative agent, bacterium tularensis. *J. Infect. Dis.* 10, 61–72. doi: 10.1093/infdis/10.1.61
- McDonald, P. J., and Pruul, H. (1991). Phagocyte uptake and transport of azithromycin. *Eur. J. Clin. Microbiol. Infect. Dis.* 10, 828–833. doi: 10.1007/BF01975835
- Mengelglu, Z., Duran, A., Hakyemez, I. N., Ocak, T., Kücükbayrak, A., Karadag, M., et al. (2014). Evaluation of patients with Tularemia in Bolu province in northwestern Anatolia, Turkey. *J. Infect. Dev. Ctries.* 8, 315–319. doi: 10.3855/jidc.3952
- Meric, M., Willke, A., Finke, E.-J., Grunow, R., Sayan, M., Erdogan, S., et al. (2008). Evaluation of clinical, laboratory, and therapeutic features of 145 tularemia cases: the role of quinolones in oropharyngeal tularemia. *APMIS* 116, 66–73. doi: 10.1111/j.1600-0463.2008.00901.x
- Muller, W., Hotzel, H., Otto, P., Karger, A., Bettin, B., Bocklisch, H., et al. (2013). German *Francisella tularensis* isolates from European brown hares (*Lepus europaeus*) reveal genetic and phenotypic diversity. *BMC Microbiol.* 13:61. doi: 10.1186/1471-2180-13-61
- Nano, F. E., and Schmerk, C. (2007). The francisella pathogenicity Island. *Ann. N. Y. Acad. Sci.* 1105, 122–137. doi: 10.1196/annals.1409.000
- Olsufjev, N. G., Emelyanova, O. S., and Dunayeva, T. N. (1959). Comparative study of strains of *B. tularensis* in the old and new world and their taxonomy. *J. Hyg. Epidemiol. Microbiol. Immunol.* 3, 138–149.
- Olsufjev, N. G. (1970). Taxonomy and characteristic of the genus *Francisella* Dorofeev, 1947. *J. Hyg. Epidemiol. Microbiol. Immunol.* 14, 67–74.
- Olsufjev, N. G., and Meshcheryakova, I. S. (1982). Intraspecific taxonomy of tularemia agent *Francisella tularensis* McCoy et Chapin. *J. Hyg. Epidemiol. Microbiol. Immunol.* 26, 291–299.
- Olsufjev, N. G., and Meshcheryakova, I. S. (1983). Subspecific Taxonomy of *Francisella tularensis* McCoy et Chapin 1912. *Int. J. Syst. Bacteriol.* 33, 872–874. doi: 10.1099/00207713-33-4-872
- Origi, F. C., Frey, J., and Pilo, P. (2014). Characterisation of a new group of *Francisella tularensis* subsp. holarctica in Switzerland with altered antimicrobial susceptibilities, 1996 to 2013. *Euro Surveill.* 19:20858. doi: 10.2807/1560-7917.ES2014.19.29.20858
- Payne, L., Arneborn, M., Tegnell, A., and Giesecke, J. (2005). Endemic tularemia, Sweden, 2003. *Emerging Infect. Dis.* 11, 1440–1442. doi: 10.3201/eid1109.041189
- Pérez-Castrillón, J. L., Bachiller-Luque, P., Martín-Luquero, M., Mena-Martín, F. J., and Herreros, V. (2001). Tularemia epidemic in Northwestern Spain: clinical description and therapeutic response. *Clin. Infect. Dis.* 33, 573–576. doi: 10.1086/322601
- Petersen, J. M., Carlson, J. K., Dietrich, G., Eisen, R. J., Coombs, J., Janusz, A. M., et al. (2008). Multiple *Francisella tularensis* subspecies and clades, tularemia outbreak, Utah. *Emerg. Infect. Dis.* 14, 1928–1930. doi: 10.3201/eid1412.080482
- Piercy, T., Steward, J., Lever, M. S., and Brooks, T. J. G. (2005). *In vivo* efficacy of fluoroquinolones against systemic tularemia infection in mice. *J. Antimicrob. Chemother.* 56, 1069–1073. doi: 10.1093/jac/dki359
- Pilo, P., Johansson, A., and Frey, J. (2009). Identification of *Francisella tularensis* cluster in central and Western Europe. *Emerg. Infect. Dis.* 15, 2049–2051. doi: 10.3201/eid1512.080805
- Raymond, C. R., and Conlan, J. W. (2009). Differential susceptibility of Sprague-Dawley and Fischer 344 rats to infection by *Francisella tularensis*. *Microb. Pathog.* 46, 231–234. doi: 10.1016/j.micpath.2009.01.002
- Reintjes, R., Dedushaj, I., Gjini, A., Jorgensen, T. R., Cotter, B., Liefucht, A., et al. (2002). Tularemia outbreak investigation in Kosovo: case control and environmental studies. *Emerg. Infect. Dis.* 8, 69–73. doi: 10.3201/eid0801.010131
- Rick Lyons, C., and Wu, T. H. (2007). Animal models of *Francisella tularensis* infection. *Ann. N. Y. Acad. Sci.* 1105, 238–265. doi: 10.1196/annals.1409.003
- Rockwood, S. (1983). Tularemia: what's in a name. *ASM News* 63–65.
- Rotem, S., Bar-Haim, E., Cohen, H., Elia, U., Ber, R., Shafferman, A., et al. (2012). Consequences of delayed ciprofloxacin and doxycycline treatment regimens against *Francisella tularensis* airway infection. *Antimicrob. Agents Chemother.* 56, 5406–5408. doi: 10.1128/AAC.01104-12
- Russell, P., Eley, S. M., Fulop, M. J., Bell, D. L., and Titball, R. W. (1998). The efficacy of ciprofloxacin and doxycycline against experimental tularemia. *J. Antimicrob. Chemother.* 41, 461–465. doi: 10.1093/jac/41.4.461
- Scheel, O., Hoel, T., Sandvik, T., and Berdal, B. P. (1993). Susceptibility pattern of scandinavian *Francisella tularensis* isolates with regard to oral and parenteral antimicrobial agents. *APMIS* 101, 33–36. doi: 10.1111/j.1699-0463.1993.tb00077.x
- Schmitt, D. M., O'Dee, D. M., Cowan, B. N., Birch, J. W.-M., Mazzella, L. K., Nau, G. J., et al. (2013). The use of resazurin as a novel antimicrobial agent against *Francisella tularensis*. *Front. Cell. Infect. Microbiol.* 3:93. doi: 10.3389/fcimb.2013.00093
- Siret, V., Barataud, D., Prat, M., Vaillant, V., Ansart, S., Le Coustumier, A., et al. (2006). An outbreak of airborne tularemia in France, August 2004. *Euro Surveill.* 11, 58–60.
- Sjostedt, A. (2007). Tularemia: history, epidemiology, pathogen physiology, and clinical manifestations. *Ann. N. Y. Acad. Sci.* 1105, 1–29. doi: 10.1196/annals.1409.009
- Stundick, M. V., Albrecht, M. T., Houchens, C. R., Smith, A. P., Dreier, T. M., and Larsen, J. C. (2013). Animal models for *Francisella tularensis* and *Burkholderia* species scientific and regulatory gaps toward approval of antibiotics under the FDA animal rule. *Vet. Pathol.* 50, 877–892. doi: 10.1177/030098513486812

- Sutera, V., Caspar, Y., Boisset, S., and Maurin, M. (2014). A new dye uptake assay to test the activity of antibiotics against intracellular *Francisella tularensis*. *Front. Cell. Infect. Microbiol.* 4:36. doi: 10.3389/fcimb.2014.00036
- Svensson, K., Back, E., Eliasson, H., Berglund, L., Granberg, M., Karlsson, L., et al. (2009a). Landscape epidemiology of tularemia outbreaks in Sweden. *Emerg. Infect. Dis.* 15, 1937–1947. doi: 10.3201/eid1512.090487
- Svensson, K., Granberg, M., Karlsson, L., Neubauerova, V., Forsman, M., and Johansson, A. (2009b). A real-time PCR array for hierarchical identification of francisella isolates. *PLoS ONE* 4:e8360. doi: 10.1371/journal.pone.0008360
- Tarnvik, A. (2007). *WHO Guidelines on Tularaemia*. Geneva: WHO/CDS/EPR/2007.7.
- Tärnvik, A., and Berglund, L. (2003). Tularaemia. *Eur. Respir. J.* 21, 361–373. doi: 10.1183/09031936.03.00088903
- Tärnvik, A., and Chu, M. C. (2007). New approaches to diagnosis and therapy of tularemia. *Ann. N. Y. Acad. Sci.* 1105, 378–404. doi: 10.1196/annals.1409.017
- Tomaso, H., Al Dahouk, S., Hofer, E., Spletstoesser, W. D., Treu, T. M., Dierich, M. P., et al. (2005). Antimicrobial susceptibilities of Austrian *Francisella tularensis* holarctica biovar II strains. *Int. J. Antimicrob. Agents* 26, 279–284. doi: 10.1016/j.ijantimicag.2005.07.003
- Urich, S. K., and Petersen, J. M. (2008). *In vitro* susceptibility of isolates of *Francisella tularensis* types A and B from North America. *Antimicrob. Agents Chemother.* 52, 2276–2278. doi: 10.1128/AAC.01584-07
- Valade, E., Vaissaire, J., Mérens, A., Hernandez, E., Gros, C., Doujet, C. L., et al. (2008). Susceptibility of 71 French isolates of *Francisella tularensis* subsp. holarctica to eight antibiotics and accuracy of the Etest[®] method. *J. Antimicrob. Chemother.* 62, 208–210. doi: 10.1093/jac/dkn146
- Velinov, K., Kantardjiev, T., Nicolova, M., and Kuzmanov, A. (2011). *In vitro* antimicrobial susceptibility of *Francisella tularensis* isolated in Bulgaria. *Probl. Infect. Parasit. Dis.* 39, 7–9.
- Vogler, A. J., Birdsell, D., Price, L. B., Bowers, J. R., Beckstrom-Sternberg, S. M., Auerbach, R. K., et al. (2009). Phylogeography of *Francisella tularensis*: global expansion of a highly fit clone. *J. Bacteriol.* 191, 2474–2484. doi: 10.1128/JB.01786-08
- Wang, Y., Hai, R., Zhang, Z., Xia, L., Cai, H., Liang, Y., et al. (2011). Genetic relationship between *Francisella tularensis* strains from China and from other countries. *Biomed. Environ. Sci.* 24, 310–314. doi: 10.3967/0895-3988.2011.03.015
- Wang, Y., Peng, Y., Hai, R., Xia, L., Li, H., Zhang, Z., et al. (2014). Diversity of *Francisella tularensis* Subsp. *holarctica* Lineages, China. *Emerg. Infect. Dis.* 20, 1191–1194. doi: 10.3201/eid2007.130931
- Wherry, W. B., and Lamb, B. H. (1914). Infection of man with bacterium tularensis. *J. Infect. Dis.* 15, 331–340. doi: 10.1093/infdis/15.2.331
- Yeşilyurt, M., Kılıç, S., Çelebi, B., Çelik, M., Gül, S., Erdoğan, F., et al. (2011). Antimicrobial susceptibilities of *Francisella tularensis* subsp. holarctica strains isolated from humans in the Central Anatolia region of Turkey. *J. Antimicrob. Chemother.* 66, 2588–2592. doi: 10.1093/jac/dkr338

Conflict of Interest Statement: The authors declare that the research was conducted in the absence of any commercial or financial relationships that could be construed as a potential conflict of interest.

Copyright © 2017 Caspar and Maurin. This is an open-access article distributed under the terms of the Creative Commons Attribution License (CC BY). The use, distribution or reproduction in other forums is permitted, provided the original author(s) or licensor are credited and that the original publication in this journal is cited, in accordance with accepted academic practice. No use, distribution or reproduction is permitted which does not comply with these terms.



Nramp1 and NrampB Contribute to Resistance against *Francisella* in *Dictyostelium*

Yannick Brenz¹, Denise Ohnezeit², Hanne C. Winther-Larsen³ and Monica Hagedorn^{4*}

¹ Department of Parasitology, Bernhard Nocht Institute for Tropical Medicine, Hamburg, Germany, ² Institute for Medical Microbiology, Hygiene and Virology, University Medical Center Hamburg-Eppendorf, Hamburg, Germany, ³ Centre for Integrative Microbial Evolution and Department of Pharmaceutical Biosciences, University of Oslo, Oslo, Norway, ⁴ Department of Life Sciences and Chemistry, Jacobs University, Bremen, Germany

The *Francisella* genus comprises highly pathogenic bacteria that can cause fatal disease in their vertebrate and invertebrate hosts including humans. In general, *Francisella* growth depends on iron availability, hence, iron homeostasis must be tightly regulated during *Francisella* infection. We used the system of the professional phagocyte *Dictyostelium* and the fish pathogen *F. noatunensis* subsp. *noatunensis* (*F.n.n.*) to investigate the role of the host cell iron transporters Nramp (natural resistance associated macrophage proteins) during *Francisella* infection. Like its mammalian ortholog, *Dictyostelium* Nramp1 transports iron from the phagosome into the cytosol, whereas the paralog NrampB is located on the contractile vacuole and controls, together with Nramp1, the cellular iron homeostasis. In *Dictyostelium*, Nramp1 localized to the *F.n.n.*-phagosome but disappeared from the compartment dependent on the presence of IgIC, an established *Francisella* virulence factor. In the absence of Nramp transporters the bacteria translocated more efficiently from the phagosome into the host cell cytosol, its replicative niche. Increased escape rates coincided with increased proteolytic activity in bead-containing phagosomes indicating a role of the Nramp transporters for phagosomal maturation. In the *nramp* mutants, a higher bacterial load was observed in the replicative phase compared to wild-type host cells. Upon bacterial access to the cytosol of wt cells, mRNA levels of bacterial iron uptake factors were transiently upregulated. Decreased iron levels in the *nramp* mutants were compensated by a prolonged upregulation of the iron scavenging system. These results show that Nramps contribute to host cell immunity against *Francisella* infection by influencing the translocation efficiency from the phagosome to the cytosol but not by restricting access to nutritional iron in the cytosol.

OPEN ACCESS

Edited by:

Thomas Henry,
Institut National de la Santé et de la
Recherche Médicale (INSERM),
France

Reviewed by:

Jeffrey Frelinger,
University of Arizona, United States
Salvatore Bozzaro,
University of Turin, Italy

*Correspondence:

Monica Hagedorn
m.hagedorn@jacobs-university.de

Received: 20 April 2017

Accepted: 09 June 2017

Published: 21 June 2017

Citation:

Brenz Y, Ohnezeit D,
Winther-Larsen HC and Hagedorn M
(2017) Nramp1 and NrampB
Contribute to Resistance against
Francisella in *Dictyostelium*.
Front. Cell. Infect. Microbiol. 7:282.
doi: 10.3389/fcimb.2017.00282

Keywords: *Dictyostelium*, *Francisella*, infection, iron transporter, Nramp

INTRODUCTION

Iron is essential for growth of virtually all organisms and is an important cofactor in many redox reactions. On the other hand, phagocytic cells can also use iron to act as a cofactor for generation of antimicrobial radicals. Therefore, host cells and intracellular bacterial pathogens are in a constant struggle for this nutrient. Consequently, iron uptake and homeostasis during infection is tightly regulated by both the host and the pathogen (Schaible and Kaufmann, 2004).

Members of the natural resistance associated macrophage protein (Nramp) family play an important regulatory role in cellular iron homeostasis. Nramps are transmembrane transporters of divalent metal ions, especially Fe^{2+} , Mn^{2+} , and Zn^{2+} , and widely distributed in prokaryotes and eukaryotes (Cellier et al., 1995; Courville et al., 2006; Nevo and Nelson, 2006). In mammals, two Nramp family members are present, Nramp1 (SLC11A1) and DMT-1 (SLC11A2 or Nramp2). Nramp1 is found on endosomal and lysosomal vesicles as well as phagosomal membranes in macrophages (Gruenheid et al., 1997; Searle et al., 1998), where it transports Fe^{2+} and Mn^{2+} from the phagosome into the cytosol dependent on a proton gradient (Buracco et al., 2015). Nramp1 was identified as part of the *Bcg/Ity/Lsh* locus in mice, which contributes to natural resistance against intracellular pathogens such as *Mycobacteria*, *Leishmania*, and *Salmonella* (Vidal et al., 1993, 1995). In humans, polymorphic variations of the *nramp1* gene are linked to tuberculosis (Wu et al., 2013), leprosy (Abel et al., 1998) and oropharyngeal tularemia (Somuk et al., 2016). In contrast, isoforms of DMT-1 are responsible for transferrin-independent iron uptake (Canonne-Hergaux et al., 1999) or recycling via endosomes (Gruenheid et al., 1999; Touret et al., 2003), and have been associated with microcytic anemia (Fleming et al., 1997; Canonne-Hergaux et al., 2000) and neurodegeneration (Salazar et al., 2008).

Dictyostelium discoideum is an amoeba, which is frequently used to dissect basic cellular processes (Muller-Taubenberger et al., 2013). In nature, *Dictyostelium* thrives on bacteria as a motile, single cell organism. However, when food is scarce, many amoebae aggregate to form a true multicellular organism that evolves further into a fruiting body harboring stress-resistant spores. The cycle closes when the spores are exposed to nutrients and single cells hatch from the spores. Most important for our study, at the single cell-stage, the amoeba is a professional phagocyte, and represents many features with cells of the innate immune system (Bozzaro, 2013; Zhang et al., 2016). Like macrophages, *Dictyostelium* can be infected with various pathogenic bacteria and is an established cellular infection model due to its homology to mammalian phagocytes, genetic tools and easy cultivation in the laboratory (Bozzaro and Eichinger, 2011). The genome of *Dictyostelium* comprises two *nramp* genes, *nramp1* and *nrampB*. Similar to its mammalian ortholog Nramp1 is localized on endolysosomal vesicles and is recruited to phagosomes and macropinosomes (Peracino et al., 2006). In contrast, NrampB is closer related to Nramp proteins from protists and fungi and the manganese transporters of proteobacteria. NrampB is localized at the contractile vacuole of the amoeba, a tubular network for the regulation of the cellular osmolarity, where it controls, synergistically with Nramp1, the cellular iron content (Peracino et al., 2013). Both Nramp1 and NrampB affect the replication of vacuole-dwelling bacteria in the amoeba as *Dictyostelium* knockout cell lines of either Nramp are more susceptible to *Legionella* and, in case of Nramp1, to *Mycobacteria* (Peracino et al., 2006, 2010, 2013).

The intracellular bacterium *Francisella tularensis* infects multiple host organisms of both invertebrate and vertebrate origin, and is the causative agent of potentially fatal tularemia

in humans (Keim et al., 2007; Foley and Nieto, 2010). Within host cells, infection by *F. tularensis* shows a biphasic course with the bacteria initially residing in a phagosome, which is followed by translocation and a replicative stage in the host cell cytosol (Golovliov et al., 2003; Clemens et al., 2004, 2009; Chong et al., 2008). As shown for other intracellular bacteria, *Francisella* growth depends highly on bioavailable iron in the host cell (Perez and Ramakrishnan, 2014; Perez et al., 2016), but iron also contributes to H_2O_2 -induced killing of *Francisella* (Lindgren et al., 2011). In contrast to vacuolar pathogens, little is known about the role of iron regulatory Nramp for *Francisella* and other cytosol-dwelling bacteria on the cellular level.

Iron acquisition in *F. tularensis* includes two uptake systems: the *Francisella* siderophore locus (*fsl*) system for ferric iron (Fe^{3+}) and the *feo* system for ferrous iron (Fe^{2+}) (Perez et al., 2016). Metabolically competent *Francisella* species including *F. noatunensis* subsp. *noatunensis* (*F.n.n.*) express the *feo*-factors FeoA and FeoB but only one protein (IucA/C) for Fe^{3+} uptake (Sridhar et al., 2012).

In this study, we used the established *Dictyostelium/F.n.n.* infection system (Lampe et al., 2016) to investigate the role of Nramp1 and NrampB during the infection with *Francisella*. We determined the localization of both Nramps during infection with *F.n.n.* and quantified the intracellular growth of the bacteria in the absence of the iron transporters. The influence of Nramp1 and NrampB on the phagosomal and cytosolic stages was determined by quantifying phagosomal escape of *F.n.n.* and bacterial mRNA levels of iron acquisition factors during infection. Our results suggest that Nramps contribute to resistance against *Francisella* infection by influencing the phagosomal stage of the bacteria rather than nutritional stress.

MATERIALS AND METHODS

Cells, Bacterial Strains, and Culture Conditions

Dictyostelium discoideum cells (Ax2) were cultured adherently in axenic HL5-C medium supplemented with 100 $\mu\text{g/ml}$ Pen/Strep (Hagedorn and Soldati, 2007). Prof. Salvatore Bozzaro (University of Torino, Italy) kindly provided confirmed knockout cell lines of Nramp1, NrampB and Nramp1/B (Peracino et al., 2006, 2013). Knockout cell lines had been generated by the authors (Peracino et al., 2006, 2013) using homologous recombination to replace the respective gene with the respective coding sequence disrupted by a blasticidin resistance cassette. Ax2 cells expressing Nramp1-GFP and NrampB-GFP were obtained by transformation with the plasmids pDEX-Nramp1::GFPC and pDEX-NrampB::GFPC, respectively [provided by Prof. Bozzaro, (Peracino et al., 2006, 2013)] and grown with 10–30 $\mu\text{g/ml}$ G418. Green (pKK289Km:*gfp*) and red (pKK289Km:*mCherry*) fluorescent *F.n.n.* wild-type and ΔiglC bacteria were cultivated in Eugon Broth (EB) shaking culture (100 rpm) at 22°C supplemented with 2 mM FeCl_3 and 15 $\mu\text{g/ml}$ Kanamycin (Lampe et al., 2016). The in-frame knockout of *iglC* was achieved via a suicide plasmid (pDMK2) containing the fused flanking regions (~1,100 bp each)

of *iglC* and a kanamycin resistance according to Lampe et al. (2016) and similar to other *Francisella* species (Lindgren et al., 2009). Results were verified by sequencing and qPCR confirmed no effects on neighboring genes *iglB* and *iglD* (Lampe et al., 2016). Iron depletion during *F.n.n.* cultivation was performed at 22°C using 100 µM 2,2'-dipyridyl (DP, Sigma-Aldrich) in EB as described by Brudal et al. (2013). In short, bacteria were incubated for 48 h until OD 1.5–2, diluted to OD 0.1 and grown for 24 h without FeCl₃. Subsequently, remaining iron was washed off with PBS (2x) and EB (+DP), the culture was diluted to OD 0.5 and grown for 24 h until OD 1.

Infection Assay

The infection of *Dictyostelium* cells with *F.n.n.* was performed as described (Lampe et al., 2016). *F.n.n.* bacteria were grown at 22°C in Eugon Broth supplemented with 2 mM FeCl₃ and 15 µg/ml Kanamycin until reaching the exponential growth phase. At least 24 h prior to infection, *Dictyostelium* cells were grown at 22°C in HL5-c medium without antibiotics in 25 or 75 cm² cell culture flasks. On infection day, *F.n.n.* equivalent to MOI 60 were centrifuged on a *Dictyostelium* monolayer of 80–100% confluency at 100 × g and 21°C for 30 min. After 5 min of additional time for phagocytosis, free bacteria were washed off with HL5-C without antibiotics and checked visually for remaining extracellular bacteria. Infected cells were seeded in HL5-C without antibiotics in 10 cm culture dishes at respective cell numbers (6 h post infection (hpi): 1 × 10⁷, 24 hpi: 4.5 × 10⁶, 48 hpi: 2 × 10⁶) and cultivated adherently at 22°C. At each timepoint, cells were resuspended, counted with a CASY Cell Counter and ~1 × 10⁶ cell were fixed with 4% paraformaldehyde (PFA) in Sørensen buffer for subsequent antibody staining and analysis via fluorescent microscopy or flow cytometry. For flow cytometry analysis, at least 4 × 10⁵ cells were quantified per sample using a FACSCalibur flow cytometer (Becton Dickinson) and analyzed according to Lampe et al. (2016) via FlowJo software v10. In short, dead cells and extracellular *F.n.n.* were excluded from analysis by gating only on living *Dictyostelium* cells using FSC/SSC. Infected and non-infected *Dictyostelium* populations were separated using SSC plotted as a function of green fluorescence (FL-1). The green fluorescence of intracellular *F.n.n.* was expressed as relative fluorescence units (RFU) per volume unit of cell culture (RFU/ml) as followed: the infection rate was multiplied with *Dictyostelium* cell number/ml to obtain infected cells/ml. This value was multiplied with the mean FL-1 value of *F.n.n.* only, which was calculated as mean FL-1 of infected cells - mean FL-1 of non-infected cells. All samples were analyzed with the same fluorescence detector settings. The resulting RFU/ml correlate with *F.n.n.* genome equivalents/ml as shown by Lampe et al. (2016).

Immunohistochemistry

Immunolabeling of PFA-fixed samples for microscopy (Hagedorn et al., 2006) and flow cytometry (Lampe et al., 2016) was performed as described. Monoclonal antibody against the putative copper transporter and endosomal marker p80 (Ravanel et al., 2001) was obtained from P. Cosson (University of Geneva, Switzerland) and used 1:10 in blocking solution (0.5%

FCS, 0.1% Triton in PBS). Rabbit polyclonal GFP-antibody (MBL International) was used at a dilution of 1:1,000 for microscopy and flow cytometry. Anti-rabbit and anti-mouse secondary antibodies from goat (Invitrogen) were coupled to AlexaFluor 488 and 568, respectively, and diluted 1:1,000. For quantitative microscopic analysis, a minimum of 100 bacteria was analyzed at each time-point. For statistical analysis of multiple groups to the wt control group over time, a repeated measures one-way ANOVA followed by Dunnett's *post-hoc* test was performed for each timepoint using Prism 7.0c software.

Microscopy

For live cell imaging, infected cells were resuspended in filtrated HL5-C and seeded in µ-Slide 8 well chambers (Ibidi) shortly before imaging. Microscopic analysis was performed at 21°C using a Zeiss LSM5 Live confocal microscope with a 100x Europlan apochromat oil immersion objective (N.A. 1.4) and a Diode-Laser 488, as well as a DPSS-Laser 561 [single track mode, 1 Airy unit, dual-band filter (500–545 band pass, 575 long pass)]. Image brightness and contrast were adjusted with ImageJ (Schneider et al., 2012) to whole images. A minimum of 100 bacteria were quantified at each timepoint except for *F.n.n.* Δ*iglC* at 2 hpi (50 bacteria). Imaging of PFA-fixed samples was performed with an Olympus IX81 confocal microscope equipped with an Olympus 100x UPlanSApo oil immersion objective (N.A. 1.4).

qRT-PCR of *F.n.n.* Iron Accumulation Genes

F.n.n. infected *Dictyostelium* cells or cultured bacteria were lysed with Trizol (Life Technologies). RNA extraction was performed using the PureLink RNA Mini Kit (Life Technologies) according to the manufacturer's instructions for Trizol extraction. For cDNA synthesis, the Maxima First Strand cDNA Synthesis Kit (Thermo Scientific) was applied according to the manufacturer's instructions. One microliter of 1:10 diluted cDNA was used for each sample as a template in a 10 µl reaction volume using LightCycler® 480 SYBR Green I Master mix (Roche) and a Rotor-Gene RG-3000 qPCR machine (Corbett Research). The thermal cycle conditions were as follows: 1 cycle at 95°C for 5 min; 40 cycles of amplification at 95°C for 30 s, 60°C for 30 s and 72°C for 30 s. A melting curve analysis was performed from 67–95°C with steps of 1°C. Samples of three infection experiments were run in duplicates. Gene-specific primer sequences of iron related genes (*feoA*, *feoB*, *iucA/C*) and reference genes (*ftsZ*, *polA*, *fopA*; Brudal et al., 2013) were designed with Primer3 software using contig data of *F.n.n.* (Sjodin et al., 2012) as a template and obtained from Brudal et al. (2013), respectively (Table S1). Results were analyzed using the ΔΔCt method and tested for statistical significance with a repeated measures one-way ANOVA followed by Dunnett's post test using the Prism 7.0c software.

Quantification of Proteolysis and pH in Bead Phagosomes

The phagosomal proteolysis and pH of *Dictyostelium* cell lines was quantified using fluorescently-labeled, 3 µm silica beads according to Sattler et al. (2013) with minor adaptations. In

short, latex beads were labeled with 0.15 mg of either DQ Green BSA (proteolysis-sensitive) or FITC (pH-sensitive) and Alexa 568 succinimidyl ester as a reference dye. Fluorescently labeled beads were added at a bead/cell ratio of 2:1 to a 90–100% confluent monolayer of *Dictyostelium* cells in a 96 well cell culture microplate μ Clear/black (Greiner). After short centrifugation (10 s, $300 \times g$, 22°C), cells were left 1 min for phagocytosis. Free beads were washed off and the fluorescence emission of intracellular beads was measured every 2 min for 2 h at 535 and 590 nm using an Infinite F200 fluorescence reader (Tecan). Filter settings for excitation/emission were as followed: 485(20)/535(25) for DQ Green/FITC and 550(10)/590(20) for Alexa568. To calculate the intraphagosomal pH from the 535/590 nm emission ratio, a calibration curve was prepared for each experiment using reference pH buffers in a range of pH 3 to 7. For comparison of the acidification and proteolysis profiles, linear regression lines were calculated for the timeframes of interest (proteolysis: linear range; covering ~ 25 datapoints each, acidification: $t = 0$ min to the minimal turning point (mtp), reneutralisation: mtp to $t = 120$ min; **Figure S4**) and the slopes were tested for significance using a one-way ANOVA followed by Dunnett's multiple comparison post test using the Prism 7.0c software.

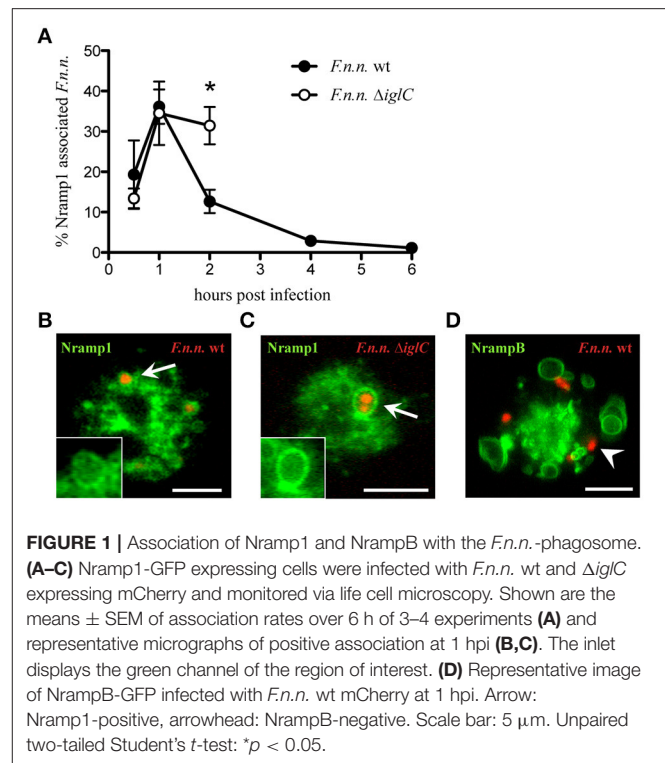
Survival Test of Exocytosed *F.n.n.*

Dictyostelium cells infected with either *F.n.n.* wt and $\Delta iglC$ were detached at 6 hpi and 1 ml cell culture including exocytosed bacteria was centrifuged at $500 \times g$ for 3 min to pellet cells but not bacteria. The supernatant was centrifuged at $5,000 \times g$ for 5 min and the bacterial pellet was dissolved in 100 μl HL5-C medium. 20 μl of undiluted and 1:50 diluted bacterial suspension was dropped on a chocolate agar plate and incubated for 1 week.

RESULTS

Nramp1 but Not NrampB Associates with *F.n.n.*-Containing Phagosomes

As transmembrane transporters of divalent metal ions, Nramp1 and NrampB change the ion composition of the compartment on which they are located. Thus, Nramp transporters could directly modify the environment of vacuolar bacteria. To investigate if Nramp1 and NrampB localize to the *F.n.n.*-phagosome (FP) in *Dictyostelium* cells, we infected amoeba expressing Nramp-GFP-fusion proteins with *F.n.n.* wild-type (wt) bacteria expressing mCherry. In addition, to monitor whether Nramp recruitment was actively manipulated by virulent *F.n.n.*, we compared Nramp1 association with wt bacteria as well an avirulent mutant strain lacking a major component of the pathogenicity island IglC (*F.n.n.* $\Delta iglC$). The proportion of Nramp-GFP associated FPs was quantified via life cell imaging in the early phase of infection (1–6 hpi). Until 1 hpi, wt and $\Delta iglC$ bacteria share similar association rates with Nramp1 at the FP (**Figures 1A–C**). However, whilst the association of wt *F.n.n.* with the iron transporter drops at 2 hpi, the avirulent mutant remains in an Nramp1-positive compartment. However, at 4 hpi, most *F.n.n.* $\Delta iglC$ are killed and exocytosed (**Figure S1**; Lampe et al., 2016) and not enough bacteria were available for reliable quantification. In contrast, wt



F.n.n. were not observed in NrampB-positive compartments at any time post infection (**Figure 1D**).

High Bacterial Load in *nramp* Knockout Cells

The localization of Nramp1 on the FP and the synergistic regulation of intracellular iron homeostasis by both Nramps (Peracino et al., 2013) led us to investigate the functional impact of Nramp1 and NrampB on *F.n.n.* infection. We infected *Dictyostelium* $\Delta nramp1$, $\Delta nrampB$ and $\Delta nramp1/B$ cells with GFP-expressing *F.n.n.* wt bacteria and compared the course of infection to *Dictyostelium* wt cells. The bacterial load was then monitored until 48 hpi quantifying bacteria by both fluorescence microscopy and flow cytometry.

Quantification of individual bacteria per cell by fluorescence microscopy showed a similar uptake of bacteria by wt and *nramp* knockout *Dictyostelium* cells (**Figures 2A–D**). However, from 24 hpi, the bacterial load per *Dictyostelium* cell was higher in the *nramp* deletion mutants. At 48 hpi, *nramp* mutants showed higher overall infection rates (wt: $13.6 \pm 3.8\%$, $\Delta nramp1$: $24.5 \pm 1.9\%$, $\Delta nrampB$: $40.7 \pm 7.8\%$, $\Delta nramp1/B$: $29.6 \pm 3.5\%$) and increased proportions of highly infected cells (more than 3 bacteria: wt: $20.4 \pm 12.5\%$, $\Delta nramp1$: $51.1 \pm 8.8\%$, $\Delta nrampB$: $57.4 \pm 6.7\%$, $\Delta nramp1/B$: $41.3 \pm 9.9\%$). The bacterial burden with more than 3 bacteria per cell over time is significantly higher in the *nramp* mutants indicating more bacterial growth at the single cell level.

To apply another approach to quantify *F.n.n.* growth we used quantitative flow cytometry and measured infection rate and bulk fluorescence of intracellular bacteria per volume over

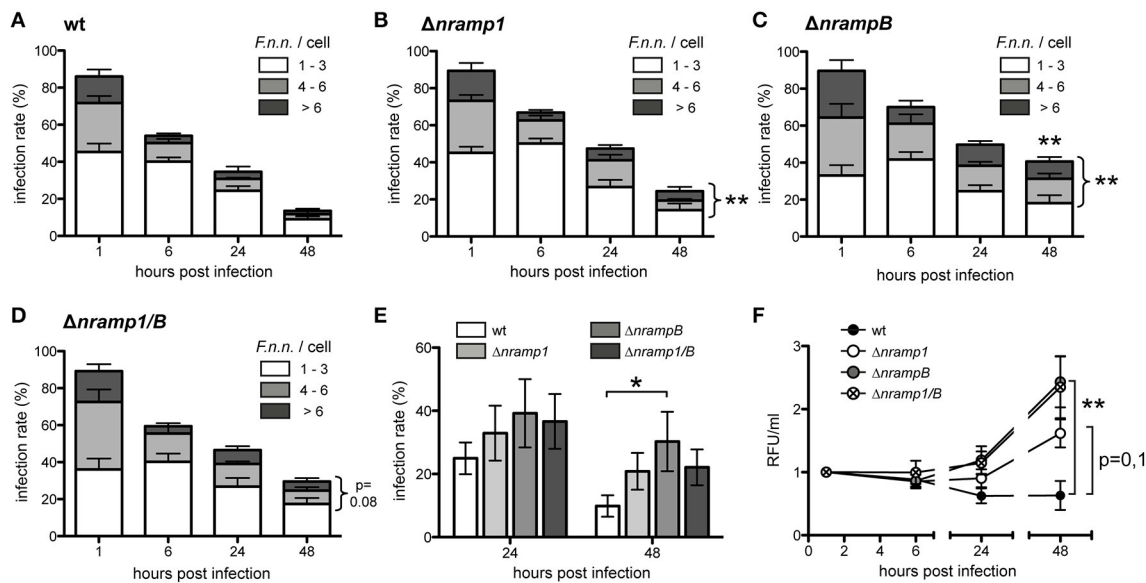


FIGURE 2 | Increased *F.n.n.* growth in the absence of Nramp1 and NrampB. **(A–D)** Infection rate and bacteria/cell of *Dictyostelium* wt **(A)**, $\Delta nramp1$ **(B)**, $\Delta nrampB$ **(C)** and $\Delta nramp1/B$ **(D)** cells infected with *F.n.n.* wt expressing GFP over 48 hpi. Number of *F.n.n.*/cell: 1–3 (white), 4–6 (gray), >6 (black). Shown are differences of the mean (\pm SEM, $n = 5$) analyzed for each timepoint with a repeated measures one-way ANOVA with Dunnett's post test: * $p < 0.05$, ** $p < 0.01$. **(E)** Infection rate of wt and *nramp* mutant cells infected with *F.n.n.* wt GFP at 24 and 48 hpi monitored via flow cytometry (mean \pm SEM, $n = 7$). **(F)** Relative bacterial fluorescence/ml in *Dictyostelium* wt and *nramp* knockout cells over 48 hpi (mean \pm SEM, $n = 7$). **(E,F)** Repeated measures one-way ANOVA with Dunnett's post-hoc test for each timepoint: * $p < 0.05$, ** $p < 0.01$.

48 h. Overall, the flow cytometry analysis recapitulated our results obtained by fluorescence microscopy. The infection rates of the *Dictyostelium nramp* mutants ($\Delta nramp1$: $20.84 \pm 5.8\%$, $\Delta nrampB$: $30.3 \pm 9.4\%$, $\Delta nramp1/B$: $22.1 \pm 5.7\%$) were higher in comparison to wt cells ($9.9 \pm 3.4\%$) at 48 hpi (**Figure 2E**). In principal, *Dictyostelium* cell growth can have an impact on the infection rate. However, the growth rates of the different cell lines were comparable over 48 h and could therefore not account for differing infection rates (**Figure S2**). The quantification of bacterial fluorescence (relative fluorescence units/ml) also showed higher bacterial loads in the mutant cell lines compared to wt cells (**Figure 2F**). This suggests that Nramp1 and NrampB contribute to resistance of the amoeboid host cell against *F.n.n.* growth.

F.n.n. Escapes the Phagosome More Efficiently in the Absence of Nramp Transporters

It seems most likely that Nramp1 and NrampB control bacterial replication by affecting the phagosomal stage of *F.n.n.* infection. Like *F. tularensis*, *F.n.n.* escapes the p80-positive phagosome in the late phagosomal stage in *Dictyostelium* (Lampe et al., 2016). Therefore, the endosomal protein p80, a putative copper transporter (Ravel et al., 2001), was applied as a marker for intraphagosomal vs. cytosolic bacteria phagosomal membranes (**Figures 3A,B**).

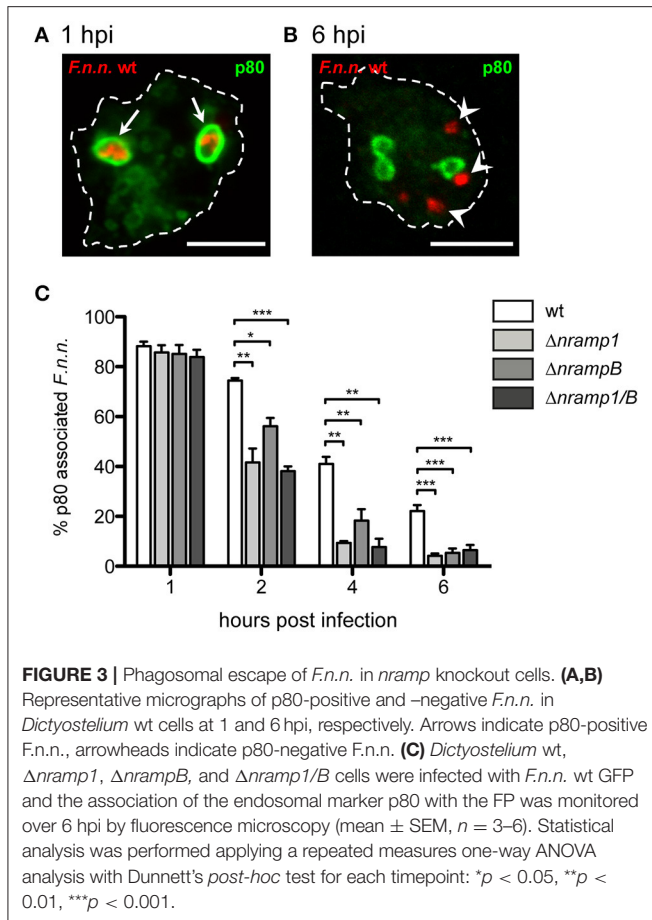
At 1 hpi, more than 80% of *F.n.n.* were localized in phagosomes of wt and *nramp* knockout cells (**Figure 3C**).

However, starting at 2 hpi, significantly less bacteria were located in p80-positive compartments in the *nramp* deletion mutants with a comparable total load of bacteria per cell between wild-type and mutant cells. This suggests that more bacteria translocate into the cytosol and reach the replicative, cytosolic phase in the *nramp* mutants, which results in a higher bacterial load per cell in the mutant strains at the late infection phase. Even though not statistically significant, in comparison to the $\Delta nrampB$ strain at 2 and 4 hpi, bacteria seem to escape more efficiently in the $\Delta nramp1$ cells. This transient delay of escape might highlight a rather indirect impact of NrampB, which is located at the contractile vacuole, in contrast to a direct impact of Nramp1 which is present at the *F.n.n.* vacuole.

F.n.n. Iron Transporters Are Upregulated in the *Dictyostelium nramp* Mutants

In principle, intracellular bacteria respond to limiting iron concentrations in their environment by upregulating the transcription of genes encoding for iron transporters (Rodriguez et al., 2002; Deng et al., 2006; Ledala et al., 2010). *F.n.n.* possesses two iron accumulation systems: the Feo system for uptake of soluble Fe^{2+} , represented by FeoA and FeoB, and the siderophor synthetase IucA/C for transport of insoluble Fe^{3+} . Members of both uptake systems (*feoA*, *iucA/C*) showed highly increased mRNA levels after depletion of iron during *in vitro* growth of *F.n.n.* (**Figure S3**).

We monitored mRNA levels of the iron accumulation genes *feoA*, *feoB* and *iucA/C* during infection of wt cells and normalized it to cultured bacteria (dotted line; **Figures 4A–C**). At 6 hpi,

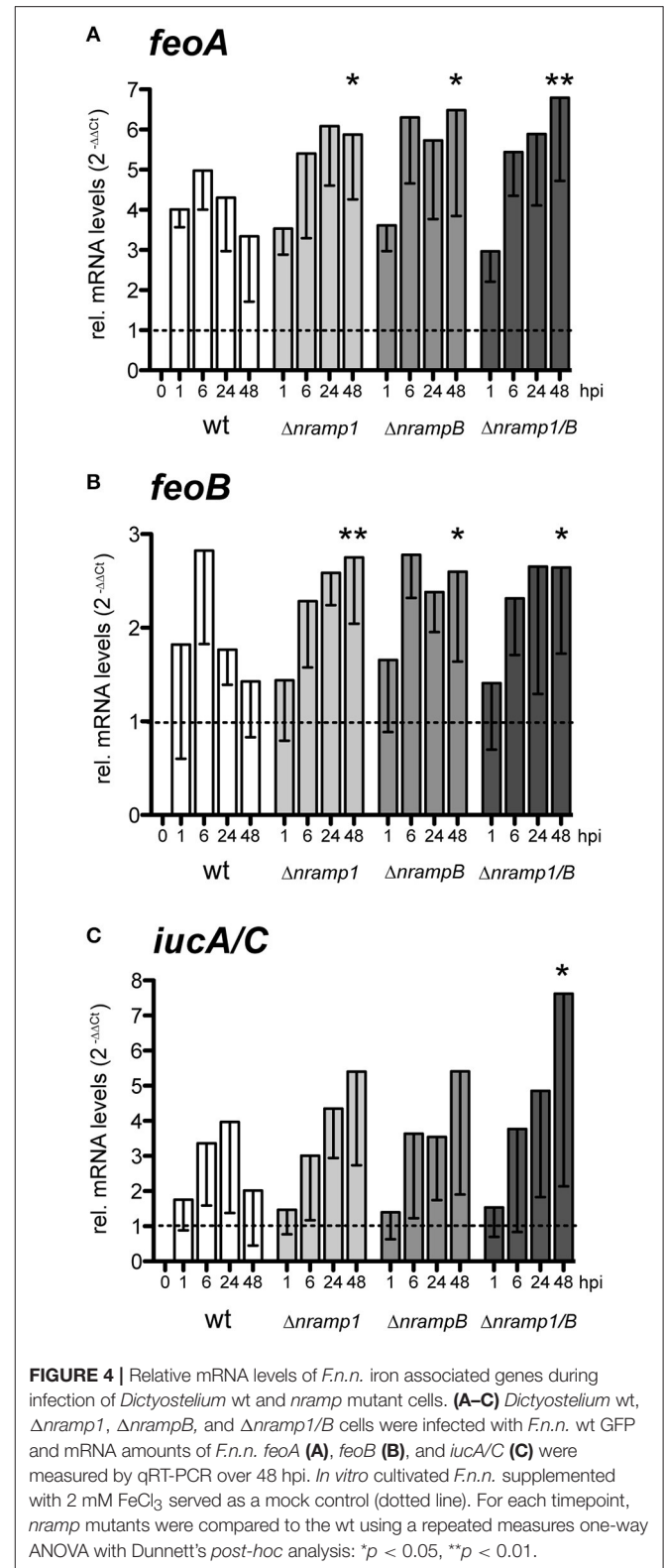


we observed an induction of all three genes, when most of the bacteria are entering the cytosolic growth phase. At later timepoints, mRNA levels of the entire gene set were still elevated in comparison to *in vitro* cultured bacteria but gradually decreased until 48 hpi. These observations suggest that *F.n.n.* relies on the uptake of external iron during the cytosolic growth phase in *Dictyostelium* cells.

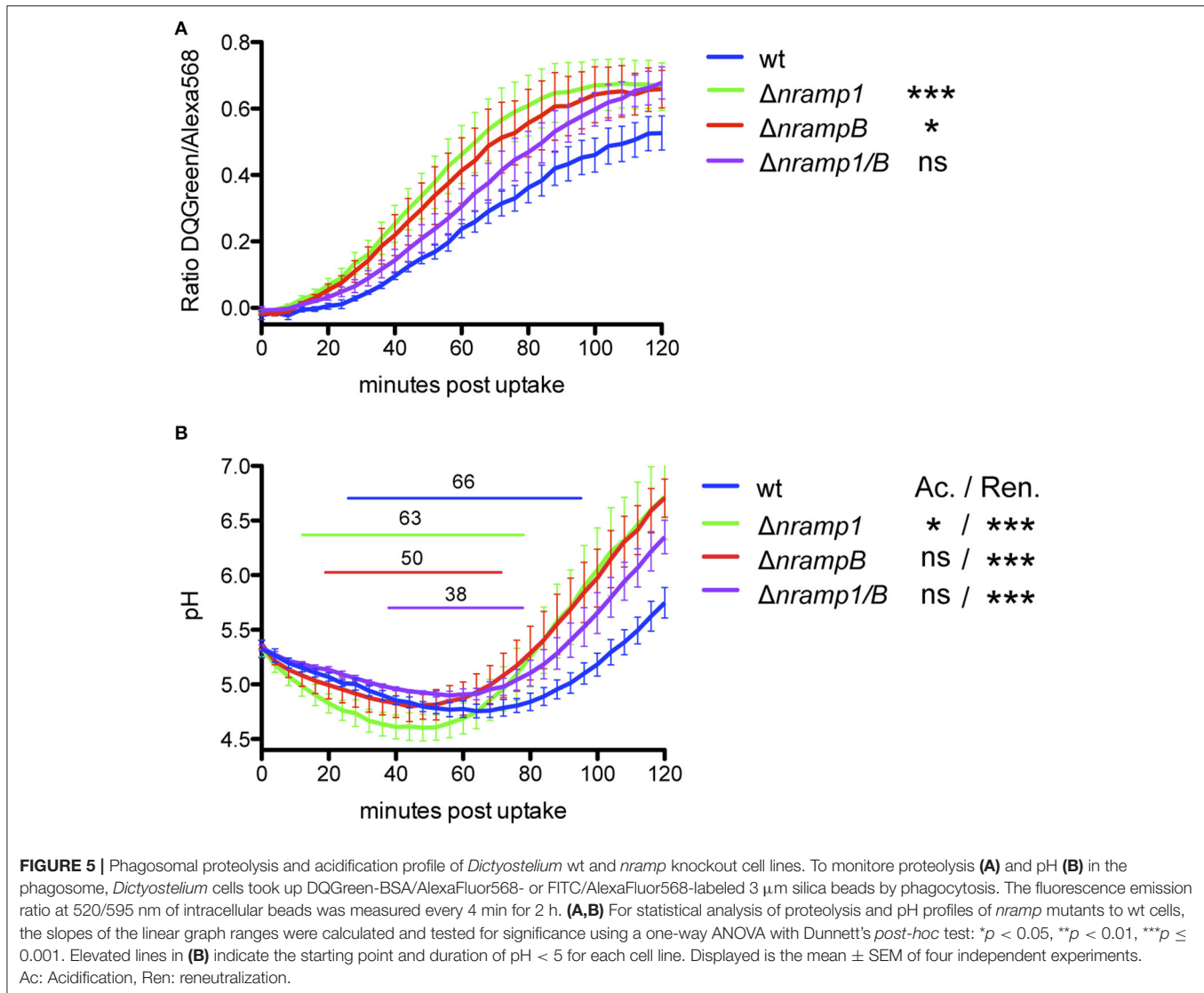
Peracino et al. (2013) observed that *nramp* mutants contain lower levels of intracellular, bioavailable iron. Accordingly, *F.n.n.* showed an increased induction of all iron related genes in the late infection phase of the *nramp* mutants compared to wt cells. Together, these results suggest that cytosolic *F.n.n.* experience an enhanced iron limitation in the absence of Nramp1 and NrampB, to which the bacteria respond by an upregulation of iron transporters.

Phagosomal Maturation Profiles Are Altered in *nramp* Mutants

Nramp1 is known to play a role in the maturation of phagosome-derived, pathogen-containing compartments during infection with bacteria such as *Salmonella* and *Mycobacteria* (Hackam et al., 1998; Govoni et al., 1999; Frehel et al., 2002). In *Dictyostelium*, phagosomal maturation is characterized by rapid lowering of the pH and delivery of proteolytic enzymes followed by the reneutralization of the compartment after 1–2 h via



recycling of the V-ATPase from the phagosomal membrane (Clarke et al., 2002, 2010). To investigate an impact of Nramp1 and NrampB on phagosomal maturation in our system, we



measured the phagosomal proteolysis and pH in wt and *nramp* mutant cell lines over 2 h using DQ Green BSA- (proteolysis-sensor) or FITC-labeled (pH-sensor) latex beads (Sattler et al., 2013).

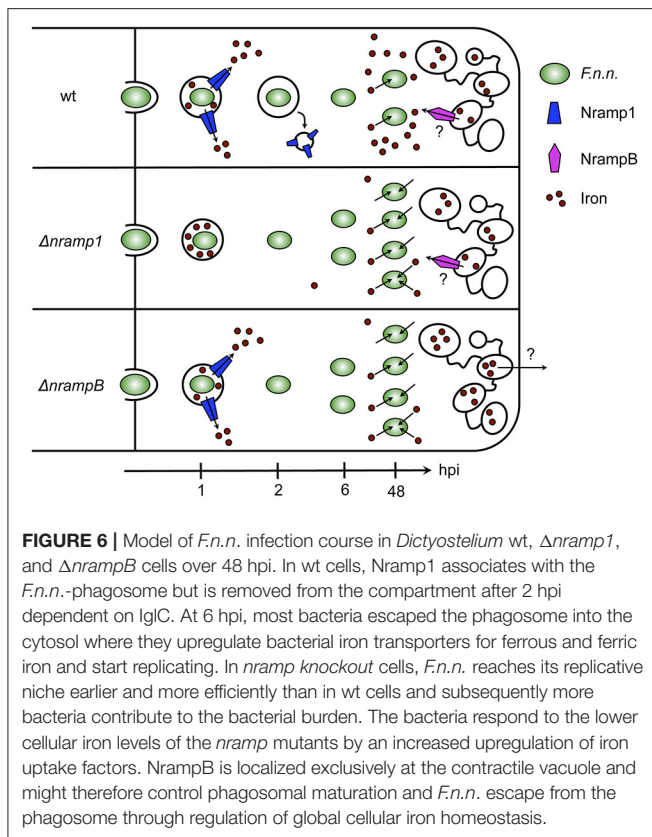
After phagocytosis of DQ Green BSA-labeled beads, we observe a significantly faster and stronger bulk proteolysis in *nramp* single mutants compared to *Dictyostelium* wt cells (Figure 5A, Figure S4). The double mutant shows an intermediate phenotype between wt and single mutant cell lines. All cell lines show an immediate decrease of the pH in the FITC-labeled bead containing phagosomes, which is significantly stronger in $\Delta nramp1$ compared to wt cells (Figure 5B, Figure S4). However, *nramp* mutants differ slightly in starting point and duration of acidification represented by a pH below 5 (indicated by the elevated line). An earlier ($\Delta nramp1$) or shorter ($\Delta nrampB$, $\Delta nramp1/B$) acidification below pH 5 coincided with a significantly faster reneutralization of the latex bead-containing phagosome compared to wt cells.

Together, these results indicate an impact of the Nramp transporters on phagosomal maturation of inert particles.

DISCUSSION

In this study, we showed that the iron transporters Nramp1 and NrampB contribute to resistance against *Francisella* in the *Dictyostelium/F.n.n.* model system. In mutants lacking either one or both of the Nramp transporter *F.n.n.* escaped its phagosome more efficiently resulting in higher bacterial burdens (summarized in Figure 6).

Iron is an essential nutritional factor for both the host and its pathogen and is tightly regulated by them during infection. This need for iron can also be used as a defense strategy against infection. For example, mammals can react against a bacterial infection by lowering serum iron levels (hypoferremia), which is also observed in humans during infection with *F. tularensis* (Pekarek et al., 1969; Kim et al., 2014).



The host iron transporter Nramp1 regulates iron homeostasis on the cellular level and contributes to resistance against vacuolar pathogens, like *Mycobacteria*, *Legionella* and *Leishmania* (Vidal et al., 1993, 1995; Frehel et al., 2002; Fritsche et al., 2012). Accordingly, in *Dictyostelium*, Nramp1 and NrampB also contribute to resistance against *Mycobacteria* and *Legionella* infection (Peracino et al., 2006, 2010, 2013).

Nramp function has only been investigated for bacteria thriving in vacuoles and the mechanism is still unknown. In general, two mechanisms are proposed to limit bacterial growth: the depletion of nutritional iron from the bacterial vacuole (Soldati and Neyrolles, 2012; Bozzaro et al., 2013) and to antagonize bacterial virulence strategies that are meant to block bactericidal activity in the phagosome (Hackam et al., 1998; Frehel et al., 2002; Cellier et al., 2007; Fritsche et al., 2012). The role of Nramps for cytosol-dwelling bacteria has not been well characterized on the cellular level. Therefore, we describe here the role of Nramp1 and NrampB for *Francisella* infection in the established *Dictyostelium/F. noatunensis* subsp. *noatunensis* model (Lampe et al., 2016).

We observed the transient recruitment of Nramp1 to the *F.n.n.* phagosome with a peak in association at 1 hpi followed by a fast decline. In contrast, the phagosome of avirulent *F.n.n.* $\Delta igIC$ bacteria remained Nramp1-positive until 2 hpi indicating a (direct or indirect) role of the type 6 secretion system for Nramp1 association with the phagosome during its maturation. In principle, this early loss of the membranous transporter could

be caused by phagosomal escape of wt bacteria. However, the association of *F.n.n.* wt with the phagosomal marker p80 remains stable between 1 and 2 hpi (Lampe et al., 2016), therefore cytosolic translocation of wt bacteria is unlikely to lead to the observed drop in Nramp1 association. It rather suggests an active retrieval of Nramp1 by *F.n.n.*

In contrast, *Legionella* pursues a different strategy in *Dictyostelium* to manipulate Nramp1 function. Nramp1 remains at the *Legionella* compartment until 24 hpi (Peracino et al., 2010). Peracino et al. suggest that *Legionella* reverses the transport direction of the iron transporter, thereby retaining essential iron in its replication niche. In contrast to Nramp1, NrampB was never observed at the *F.n.n.* phagosome suggesting that it has no direct effect on the ion composition of the bacterial compartment.

Using microscopy and flow cytometry, we observed increased bacterial loads in the late infection phase of both *Dictyostelium nramp* mutants. This shows that the Nramp transporters contribute to resistance against *Francisella* growth in *Dictyostelium*. Similarly, *L. pneumophila* and *M. avium* show increased bacterial growth in the absence of Nramp1 and, in case of *L. pneumophila*, NrampB.

As described, the infection with *Francisella* follows two phases, a phagosomal followed by a replicative, cytosolic stage. To determine if Nramp activity has an impact on the phagosomal stage we compared *F.n.n.* virulence in the phagosome between wt and *nramp* mutant cells by monitoring their phagosomal escape using the marker p80. We observed significantly higher escape rates in the absence of Nramp1 and NrampB suggesting that Nramp activity suppresses or delays phagosomal escape. As a result, more *F.n.n.* bacteria gain access to the cytosolic replication phase in the *nramp* mutants and contribute to *F.n.n.* growth. In accordance with our observation, *M. tuberculosis* ruptures the phagosome and gains access to the cytosol more efficiently in Nramp1-deficient macrophages (Simeone et al., 2015).

Mechanistically, the intraphagosomal environment, which is actively controlled by the pathogen has been suggested to influence the translocation rate of bacteria (Beauregard et al., 1997; Chong et al., 2008; Santic et al., 2008; Napier et al., 2012; Simeone et al., 2015). In accordance, during the infection of macrophages with *Mycobacteria* and *Salmonella*, Nramp1 promotes acidification and fusion with endosomal and lysosomal vesicles thereby generating a bactericidal environment for the pathogenic bacteria (Hackam et al., 1998; Govoni et al., 1999; Frehel et al., 2002; Jabado et al., 2003). In *Salmonella* infection, this effect could be replicated in Nramp1^{-/-} murine macrophages by using membrane-permeant iron chelators (Jabado et al., 2003). This led the authors to hypothesize that iron deprivation of the phagosome by Nramp1 counteracts the ability of the pathogen to manipulate phagosomal maturation and execute its virulence program. This is supported by studies in macrophages which showed no impact of Nramp1-deletion on phagosomal maturation of inert particles such as latex beads, non-pathogenic *Bacillus subtilis*, or dead *Mycobacteria*, but only for living pathogenic bacteria (Hackam et al., 1998; Frehel et al., 2002).

To investigate an impact of the Nramps on phagosomal maturation in our model system, we monitored the pH and

proteolysis in the phagosomes of *nramp* mutants via fluorescent bead analysis and compared it to wt cells. Our results showed only minor effects of the Nramps activity on the acidification profiles but a faster and stronger proteolysis inside the phagosome. The accelerated phagosomal maturation in the *nramp* mutants might trigger virulence strategies of the bacteria leading to their escape from the phagosome. Accordingly, several studies showed that phagosomal acidification of the *F. tularensis* phagosome is important for phagosomal escape (Chong et al., 2008; Santic et al., 2008; Clemens et al., 2009), whereas Clemens et al. observed no impact (Clemens et al., 2009). However, while our assay was performed with inert particles, living bacteria might encounter a different phagosomal maturation profile in the *nramp* mutants. Additionally, altered phagosomal maturation had no effect on cellular growth of *nramp* mutants in axenic medium and on non-pathogenic *Klebsiella* bacteria (Lelong et al., 2011), hence, the impact of these results on living *F.n.n.* should be interpreted with caution.

Besides a specific role of Nramp activity at the phagosome in our model system, a disturbed cellular iron homeostasis in the *nramp* mutants might be responsible for the early escape of *F.n.n.* from the phagosome. *Nramp* mutants demonstrate lower levels of bioavailable iron (Peracino et al., 2013), hence the cytosolic iron content of the host cell might be responsible for an early escape of the pathogen. This is supported by the increased *F.n.n.* translocation and similar phagosomal maturation of inert particles in both *nramp* knockout cell lines although NrampB is not localized at the phagosome. Additionally, the absence of an additive effect in the *nramp* double deletion mutant implies a common mechanism.

Upon access to the cytosol of *Dictyostelium* wt cells, *F.n.n.* upregulated gene transcription of its iron accumulation systems for Fe²⁺ (*feoA*, *feoB*) and Fe³⁺ (*iucA/C*). This indicates that iron, which *F.n.n.* needs for intracellular growth, is limited in the cytosol of *Dictyostelium*. *F.n.n.* is able to grow efficiently in the *nramp* mutants despite their decreased levels of bioavailable iron. This is accompanied by an increased upregulation of the iron accumulation genes in the late phase of infection. It would be interesting to monitor bacterial growth in *Dictyostelium* cells without external iron from the growth medium, however, dramatically decreased iron concentrations disturb basic cellular processes of the amoeba (Peracino et al., 2013).

Our results are consistent with a recent study (Powell and Frelinger, 2017) showing a critical role for Nramp1 during *F. tularensis* LVS infection *in vitro* in BMDMs and *in vivo* during pulmonary infection. In the early phase of infection (1 and 4 hpi), less bacteria were observed in BMDMs with a functional Nramp1 compared to BMDMs which express a non-functional Nramp1 protein. This correlated with an increased production of ROS in the presence of functional Nramp1. Additionally, less bacterial growth occurred in Nramp1⁺ BMDMs. *In vivo* studies revealed Nramp1⁺ B6 mice resistant to intranasal infection, however not for intradermal infection, and confirmed Nramp1 as a resistance factor for *Francisella* infection. Together, this indicates a protective role for Nramp1 during the early, phagosomal stage of *Francisella* similar to our results.

Our results stand in contrast to studies by Kovarova et al., who observed less *Francisella* growth in Bcg(s) mice lacking a functional Nramp1 protein (Kovarova et al., 2000). However, Fritsche et al. showed in RAW264.7 macrophages that Nramp1 modulates the expression of other iron transporters, which results in an increased iron content of cells without a functional Nramp1 (Fritsche et al., 2007). This additional iron source could boost *Francisella* growth in the cytosol and account for the contrasting phenotype in Bcg(s) mice.

Taken together with this study we highlight the ease with which the *Dictyostelium* system allows to dissect the role of host factors in *Francisella* infection. We show that Nramp-transporters protect the host cell from increased *Francisella* growth. Most importantly, Nramp1 or NrampB contribute to host resistance against *Francisella* infection rather by reducing the bacteria's translocation efficiency to their replicative niche than by restriction of nutritional iron in the cytosol.

AUTHOR CONTRIBUTION

YB, HW, and MH designed experiments and wrote the manuscript. YB and DO performed experiments.

ACKNOWLEDGMENTS

We would like to thank Barbara Peracino and Salvatore Bozzaro for their help and the generous gift of *nramp* knockout strains and Nramp1- and NrampB-GFP expression plasmids, Jason King for help with the manuscript and the German Research Foundation (SPP1580: H3474/6-1) for the funding of this project.

SUPPLEMENTARY MATERIAL

The Supplementary Material for this article can be found online at: <http://journal.frontiersin.org/article/10.3389/fcimb.2017.00282/full#supplementary-material>

Figure S1 | Survival test of exocytosed *F.n.n.* wt and $\Delta ig/C$. Supernatant of *Dictyostelium* cell cultures infected with *F.n.n.* wt (left) and $\Delta ig/C$ (right) at 6 hpi was tested for living *F.n.n.* on chocolate agar plates. Undiluted and 1:50 diluted bacterial suspensions were used ($n = 2$).

Figure S2 | Cell growth of *Dictyostelium* wt and *nramp* knockout cell lines during *F.n.n.* infection over 48 hpi ($n = 7 \pm$ SEM).

Figure S3 | Relative mRNA levels of *F.n.n.* iron uptake factors *FeoA* and *IucA/C* under iron limitation *in vitro*. Iron was sequestered in the *F.n.n.* growth medium via the iron chelator 2,2'-dipyridyl. *F.n.n.* grown with 2 mM FeCl₃ were used as a mock control. (*feoA*: $n = 4$, *iucA/C*: $n = 2$).

Figure S4 | Linear regression of the range of interest for the phagosomal proteolysis and pH profiles. **(A)** To compare bead-phagosome proteolysis of *nramp* mutant cell lines to wt cells, a linear regression function was calculated for the linear range of each cell line's proteolysis profile and displayed in the corresponding color. **(B,C)** Acidification **(B)** and RENEUTRALIZATION **(C)** of bead-containing phagosomes were compared for each cell line using the slope of the linear regression of $t = 0$ min to the minimal turning point (mtp) **(B)** and of the mtp to $t = 120$ min **(C)**. Ac: acidification, Ren: reneutralization. Slopes were tested for significance differences using a one-way ANOVA with Dunnett's *post-hoc* analysis. * $p < 0.05$, *** $p < 0.001$.

Table S1 | Primer sequences of *F.n.n.* reference and iron accumulation genes.

REFERENCES

- Abel, L., Sanchez, F. O., Oberti, J., Thuc, N. V., Hoa, L. V., Lap, V. D., et al. (1998). Susceptibility to leprosy is linked to the human NRAMP1 gene. *J. Infect. Dis.* 177, 133–145. doi: 10.1086/513830
- Beauregard, K. E., Lee, K. D., Collier, R. J., and Swanson, J. A. (1997). pH-dependent perforation of macrophage phagosomes by listeriolysin O from *Listeria monocytogenes*. *J. Exp. Med.* 186, 1159–1163. doi: 10.1084/jem.186.7.1159
- Bozzaro, S. (2013). The model organism *Dictyostelium discoideum*. *Methods Mol. Biol.* 983, 17–37. doi: 10.1007/978-1-62703-302-2_2
- Bozzaro, S., Buracco, S., and Peracino, B. (2013). Iron metabolism and resistance to infection by invasive bacteria in the social amoeba *Dictyostelium discoideum*. *Front. Cell Infect. Microbiol.* 3:50. doi: 10.3389/fcimb.2013.00050
- Bozzaro, S., and Eichinger, L. (2011). The professional phagocyte *Dictyostelium discoideum* as a model host for bacterial pathogens. *Curr. Drug Targets* 12, 942–954. doi: 10.2174/138945011795677782
- Brudal, E., Winther-Larsen, H. C., Colquhoun, D. J., and Duodu, S. (2013). Evaluation of reference genes for reverse transcription quantitative PCR analyses of fish-pathogenic Francisella strains exposed to different growth conditions. *BMC Res. Notes* 6:76. doi: 10.1186/1756-0500-6-76
- Buracco, S., Peracino, B., Cinquetti, R., Signoretto, E., Vollero, A., Imperiali, F., et al. (2015). *Dictyostelium* Nramp1, which is structurally and functionally similar to mammalian DMT1 transporter, mediates phagosomal iron efflux. *J. Cell Sci.* 128, 3304–3316. doi: 10.1242/jcs.173153
- Canonne-Hergaux, F., Fleming, M. D., Levy, J. E., Gauthier, S., Ralph, T., Picard, V., et al. (2000). The Nramp2/DMT1 iron transporter is induced in the duodenal mucosa of microcytic anemia mice but is not properly targeted to the intestinal brush border. *Blood* 96, 3964–3970.
- Canonne-Hergaux, F., Gruenheid, S., Ponka, P., and Gros, P. (1999). Cellular and subcellular localization of the Nramp2 iron transporter in the intestinal brush border and regulation by dietary iron. *Blood* 93, 4406–4417.
- Cellier, M. F., Courville, P., and Campion, C. (2007). Nramp1 phagocyte intracellular metal withdrawal defense. *Microbes Infect.* 9, 1662–1670. doi: 10.1016/j.micinf.2007.09.006
- Cellier, M., Prive, G., Belouchi, A., Kwan, T., Rodrigues, V., Chia, W., et al. (1995). Nramp defines a family of membrane proteins. *Proc. Natl. Acad. Sci. U.S.A.* 92, 10089–10093. doi: 10.1073/pnas.92.22.10089
- Chong, A., Wehrly, T. D., Nair, V., Fischer, E. R., Barker, J. R., Klose, K. E., et al. (2008). The early phagosomal stage of *Francisella tularensis* determines optimal phagosomal escape and *Francisella* pathogenicity island protein expression. *Infect. Immun.* 76, 5488–5499. doi: 10.1128/IAI.00682-08
- Clarke, M., Kohler, J., Arana, Q., Liu, T., Heuser, J., and Gerisch, G. (2002). Dynamics of the vacuolar H⁺-ATPase in the contractile vacuole complex and the endosomal pathway of *Dictyostelium* cells. *J. Cell Sci.* 115(Pt 14), 2893–2905.
- Clarke, M., Maddera, L., Engel, U., and Gerisch, G. (2010). Retrieval of the vacuolar H-ATPase from phagosomes revealed by live cell imaging. *PLoS ONE* 5:e8585. doi: 10.1371/journal.pone.0008585
- Clemens, D. L., Lee, B. Y., and Horwitz, M. A. (2004). Virulent and avirulent strains of *Francisella tularensis* prevent acidification and maturation of their phagosomes and escape into the cytoplasm in human macrophages. *Infect. Immun.* 72, 3204–3217. doi: 10.1128/IAI.72.6.3204-3217.2004
- Clemens, D. L., Lee, B. Y., and Horwitz, M. A. (2009). *Francisella tularensis* phagosomal escape does not require acidification of the phagosome. *Infect. Immun.* 77, 1757–1773. doi: 10.1128/IAI.01485-08
- Courville, P., Chaloupka, R., and Cellier, M. F. (2006). Recent progress in structure-function analyses of Nramp proton-dependent metal-ion transporters. *Biochem. Cell Biol.* 84, 960–978. doi: 10.1139/o06-193
- Deng, K., Blick, R. J., Liu, W., and Hansen, E. J. (2006). Identification of *Francisella tularensis* genes affected by iron limitation. *Infect. Immun.* 74, 4224–4236. doi: 10.1128/IAI.01975-05
- Fleming, M. D., Trenor, C. C. III., Su, M. A., Foernzler, D., Beier, D. R., Dietrich, W. F., et al. (1997). Microcytic anaemia mice have a mutation in Nramp2, a candidate iron transporter gene. *Nat. Genet.* 16, 383–386.
- Foley, J. E., and Nieto, N. C. (2010). Tularemia. *Vet. Microbiol.* 140, 332–338. doi: 10.1016/j.vetmic.2009.07.017
- Frehel, C., Canonne-Hergaux, F., Gros, P., and De Chastellier, C. (2002). Effect of Nramp1 on bacterial replication and on maturation of *Mycobacterium avium*-containing phagosomes in bone marrow-derived mouse macrophages. *Cell Microbiol.* 4, 541–556. doi: 10.1046/j.1462-5822.2002.00213.x
- Fritsche, G., Nairz, M., Libby, S. J., Fang, F. C., and Weiss, G. (2012). Slc11a1 (Nramp1) impairs growth of *Salmonella enterica* serovar typhimurium in macrophages via stimulation of lipocalin-2 expression. *J. Leukoc. Biol.* 92, 353–359. doi: 10.1189/jlb.1111554
- Fritsche, G., Nairz, M., Theurl, I., Mair, S., Bellmann-Weiler, R., Barton, H. C., et al. (2007). Modulation of macrophage iron transport by Nramp1 (Slc11a1). *Immunobiology* 212, 751–757. doi: 10.1016/j.imbio.2007.09.014
- Golovliov, I., Sjostedt, A., Mokrievid, A., and Pavlov, V. (2003). A method for allelic replacement in *Francisella tularensis*. *FEMS Microbiol. Lett.* 222, 273–280. doi: 10.1016/S0378-1097(03)00313-6
- Govoni, G., Canonne-Hergaux, F., Pfeifer, C. G., Marcus, S. L., Mills, S. D., Hackam, D. J., et al. (1999). Functional expression of Nramp1 *in vitro* in the murine macrophage line RAW264.7. *Infect. Immun.* 67, 2225–2232.
- Gruenheid, S., Canonne-Hergaux, F., Gauthier, S., Hackam, D. J., Grinstein, S., and Gros, P. (1999). The iron transport protein NRAMP2 is an integral membrane glycoprotein that colocalizes with transferrin in recycling endosomes. *J. Exp. Med.* 189, 831–841. doi: 10.1084/jem.189.5.831
- Gruenheid, S., Pinner, E., Desjardins, M., and Gros, P. (1997). Natural resistance to infection with intracellular pathogens: the Nramp1 protein is recruited to the membrane of the phagosome. *J. Exp. Med.* 185, 717–730. doi: 10.1084/jem.185.4.717
- Hackam, D. J., Rotstein, O. D., Zhang, W., Gruenheid, S., Gros, P., and Grinstein, S. (1998). Host resistance to intracellular infection: mutation of natural resistance-associated macrophage protein 1 (Nramp1) impairs phagosomal acidification. *J. Exp. Med.* 188, 351–364. doi: 10.1084/jem.188.2.351
- Hagedorn, M., Neuhaus, E. M., and Soldati, T. (2006). Optimized fixation and immunofluorescence staining methods for *Dictyostelium* cells. *Methods Mol. Biol.* 346, 327–338. doi: 10.1385/1-59745-144-4:327
- Hagedorn, M., and Soldati, T. (2007). Flotillin and RacH modulate the intracellular immunity of *Dictyostelium* to *Mycobacterium marinum* infection. *Cell Microbiol.* 9, 2716–2733. doi: 10.1111/j.1462-5822.2007.00993.x
- Jabado, N., Cuellar-Mata, P., Grinstein, S., and Gros, P. (2003). Iron chelators modulate the fusogenic properties of Salmonella-containing phagosomes. *Proc. Natl. Acad. Sci. U.S.A.* 100, 6127–6132. doi: 10.1073/pnas.0937287100
- Keim, P., Johansson, A., and Wagner, D. M. (2007). Molecular epidemiology, evolution, and ecology of *Francisella*. *Ann. N Y Acad. Sci.* 1105, 30–66. doi: 10.1196/annals.1409.011
- Kim, D. K., Jeong, J. H., Lee, J. M., Kim, K. S., Park, S. H., Kim, Y. D., et al. (2014). Inverse agonist of estrogen-related receptor gamma controls *Salmonella* typhimurium infection by modulating host iron homeostasis. *Nat. Med.* 20, 419–424. doi: 10.1038/nm.3483
- Kovarova, H., Hernychova, L., Hajduch, M., Sirova, M., and Macela, A. (2000). Influence of the bcg locus on natural resistance to primary infection with the facultative intracellular bacterium *Francisella tularensis* in mice. *Infect. Immun.* 68, 1480–1484. doi: 10.1128/IAI.68.3.1480-1484.2000
- Lampe, E. O., Brenz, Y., Herrmann, L., Repnik, U., Griffiths, G., Zingmark, C., et al. (2016). Dissection of *Francisella*-Host Cell Interactions in *Dictyostelium discoideum*. *Appl. Environ. Microbiol.* 82, 1586–1598. doi: 10.1128/AEM.02950-15
- Ledala, N., Sengupta, M., Muthaiyan, A., Wilkinson, B. J., and Jayaswal, R. K. (2010). Transcriptomic response of *Listeria monocytogenes* to iron limitation and Fur mutation. *Appl. Environ. Microbiol.* 76, 406–416. doi: 10.1128/AEM.01389-09
- Lelong, E., Marchetti, A., Gueho, A., Lima, W. C., Sattler, N., Molmeret, M., et al. (2011). Role of magnesium and a phagosomal P-type ATPase in intracellular bacterial killing. *Cell Microbiol.* 13, 246–258. doi: 10.1111/j.1462-5822.2010.01532.x
- Lindgren, H., Honn, M., Golovlev, I., Kadzhaev, K., Conlan, W., and Sjostedt, A. (2009). The 58-kilodalton major virulence factor of *Francisella tularensis* is required for efficient utilization of iron. *Infect. Immun.* 77, 4429–4436. doi: 10.1128/IAI.00702-09
- Lindgren, H., Honn, M., Salomonsson, E., Kuoppa, K., Forsberg, A., and Sjostedt, A. (2011). Iron content differs between *Francisella tularensis* subspecies *tularensis* and subspecies holarctica strains and correlates to their

- susceptibility to H₂O₂-induced killing. *Infect. Immun.* 79, 1218–1224. doi: 10.1128/IAI.01116-10
- Muller-Taubenberger, A., Kortholt, A., and Eichinger, L. (2013). Simple system-substantial share: the use of *Dictyostelium* in cell biology and molecular medicine. *Eur. J. Cell Biol.* 92, 45–53. doi: 10.1016/j.ejcb.2012.10.003
- Napier, B. A., Meyer, L., Bina, J. E., Miller, M. A., Sjostedt, A., and Weiss, D. S. (2012). Link between intraphagosomal biotin and rapid phagosomal escape in *Francisella*. *Proc. Natl. Acad. Sci. U.S.A.* 109, 18084–18089. doi: 10.1073/pnas.1206411109
- Nevo, Y., and Nelson, N. (2006). The NRAMP family of metal-ion transporters. *Biochim. Biophys. Acta* 1763, 609–620. doi: 10.1016/j.bbamcr.2006.05.007
- Pekarek, R. S., Bostian, K. A., Bartelloni, P. J., Calia, F. M., and Beisel, W. R. (1969). The effects of *Francisella tularensis* infection on iron metabolism in man. *Am. J. Med. Sci.* 258, 14–25. doi: 10.1097/0000441-196907000-00003
- Peracino, B., Balest, A., and Bozzaro, S. (2010). Phosphoinositides differentially regulate bacterial uptake and Nramp1-induced resistance to *Legionella* infection in *Dictyostelium*. *J. Cell Sci.* 123(Pt 23), 4039–4051. doi: 10.1242/jcs.072124
- Peracino, B., Buracco, S., and Bozzaro, S. (2013). The Nramp (Slc11) proteins regulate development, resistance to pathogenic bacteria and iron homeostasis in *Dictyostelium discoideum*. *J. Cell Sci.* 126(Pt 1), 301–311. doi: 10.1242/jcs.116210
- Peracino, B., Wagner, C., Balest, A., Balbo, A., Pergolizzi, B., Noegel, A. A., et al. (2006). Function and mechanism of action of *Dictyostelium* Nramp1 (Slc11a1) in bacterial infection. *Traffic* 7, 22–38. doi: 10.1111/j.1600-0854.2005.00356.x
- Perez, N., Johnson, R., Sen, B., and Ramakrishnan, G. (2016). Two parallel pathways for ferric and ferrous iron acquisition support growth and virulence of the intracellular pathogen *Francisella tularensis* Schu S4. *Microbiol. Open* 5, 453–468. doi: 10.1002/mbo3.342
- Perez, N. M., and Ramakrishnan, G. (2014). The reduced genome of the *Francisella tularensis* live vaccine strain (LVS) encodes two iron acquisition systems essential for optimal growth and virulence. *PLoS ONE* 9:e93558. doi: 10.1371/journal.pone.0093558
- Powell, D. A., and Frelinger, J. A. (2017). Efficacy of resistance to francisella imparted by ITY/NRAMP/SLC11A1 depends on route of infection. *Front. Immunol.* 8:206. doi: 10.3389/fimmu.2017.00206
- Ravanel, K., de Chasse, B., Cornillon, S., Benghezal, M., Zulianello, L., Gebbie, L., et al. (2001). Membrane sorting in the endocytic and phagocytic pathway of *Dictyostelium discoideum*. *Eur. J. Cell Biol.* 80, 754–764. doi: 10.1078/0171-9335-00215
- Rodriguez, G. M., Voskuil, M. I., Gold, B., Schoolnik, G. K., and Smith, I. (2002). *ideR*, An essential gene in mycobacterium tuberculosis: role of *IdeR* in iron-dependent gene expression, iron metabolism, and oxidative stress response. *Infect. Immun.* 70, 3371–3381. doi: 10.1128/IAI.70.7.3371-3381.2002
- Salazar, J., Mena, N., Hunot, S., Prigent, A., Alvarez-Fischer, D., Arredondo, M., et al. (2008). Divalent metal transporter 1 (DMT1) contributes to neurodegeneration in animal models of Parkinson's disease. *Proc. Natl. Acad. Sci. U.S.A.* 105, 18578–18583. doi: 10.1073/pnas.0804373105
- Santic, M., Asare, R., Skrobbonja, I., Jones, S., and Abu Kwaiq, Y. (2008). Acquisition of the vacuolar ATPase proton pump and phagosome acidification are essential for escape of *Francisella tularensis* into the macrophage cytosol. *Infect. Immun.* 76, 2671–2677. doi: 10.1128/IAI.00185-08
- Sattler, N., Monroy, R., and Soldati, T. (2013). Quantitative analysis of phagocytosis and phagosome maturation. *Methods Mol. Biol.* 983, 383–402. doi: 10.1007/978-1-62703-302-2_21
- Schaible, U. E., and Kaufmann, S. H. (2004). Iron and microbial infection. *Nat. Rev. Microbiol.* 2, 946–953. doi: 10.1038/nrmicro1046
- Schneider, C. A., Rasband, W. S., and Eliceiri, K. W. (2012). NIH Image to ImageJ: 25 years of image analysis. *Nat. Methods* 9, 671–675. doi: 10.1038/nmeth.2089
- Searle, S., Bright, N. A., Roach, T. I., Atkinson, P. G., Barton, C. H., Meloan, R. H., et al. (1998). Localisation of Nramp1 in macrophages: modulation with activation and infection. *J. Cell Sci.* 111(Pt 19), 2855–2866.
- Simeone, R., Sayes, F., Song, O., Groschel, M. I., Brodin, P., Brosch, R., et al. (2015). Cytosolic access of *Mycobacterium tuberculosis*: critical impact of phagosomal acidification control and demonstration of occurrence *in vivo*. *PLoS Pathog.* 11:e1004650. doi: 10.1371/journal.ppat.1004650
- Sjodin, A., Svensson, K., Ohrman, C., Ahlinder, J., Lindgren, P., Duodu, S., et al. (2012). Genome characterisation of the genus *Francisella* reveals insight into similar evolutionary paths in pathogens of mammals and fish. *BMC Genomics* 13:268. doi: 10.1186/1471-2164-13-268
- Soldati, T., and Neyrolles, O. (2012). Mycobacteria and the intraphagosomal environment: take it with a pinch of salt(s)! *Traffic* 13, 1042–1052. doi: 10.1111/j.1600-0854.2012.01358.x
- Somuk, B. T., Koc, S., Ates, O., Goktas, G., Soyalic, H., Uysal, I. O., et al. (2016). MBL, P2X7, and SLC11A1 gene polymorphisms in patients with oropharyngeal tularemia. *Acta Otolaryngol.* 136, 1168–1172. doi: 10.1080/00016489.2016.1186835
- Sridhar, S., Sharma, A., Kongshaug, H., Nilsen, F., and Jonassen, I. (2012). Whole genome sequencing of the fish pathogen *Francisella noatunensis* subsp. *orientalis* Toba04 gives novel insights into *Francisella* evolution and pathogenicity. *BMC Genomics* 13:598. doi: 10.1186/1471-2164-13-598
- Touret, N., Furuya, W., Forbes, J., Gros, P., and Grinstein, S. (2003). Dynamic traffic through the recycling compartment couples the metal transporter Nramp2 (DMT1) with the transferrin receptor. *J. Biol. Chem.* 278, 25548–25557. doi: 10.1074/jbc.M212374200
- Vidal, S. M., Malo, D., Vogan, K., Skamene, E., and Gros, P. (1993). Natural resistance to infection with intracellular parasites: isolation of a candidate for Bcg. *Cell* 73, 469–485. doi: 10.1016/0092-8674(93)90135-D
- Vidal, S., Tremblay, M. L., Govoni, G., Gauthier, S., Sebastiani, G., Malo, D., et al. (1995). The *Ity/Lsh/Bcg* locus: natural resistance to infection with intracellular parasites is abrogated by disruption of the Nramp1 gene. *J. Exp. Med.* 182, 655–666. doi: 10.1084/jem.182.3.655
- Wu, F., Zhang, W., Zhang, L., Wu, J., Li, C., Meng, X., et al. (2013). NRAMP1, VDR, HLA-DRB1, and HLA-DQB1 gene polymorphisms in susceptibility to tuberculosis among the Chinese Kazakh population: a case-control study. *Biomed. Res. Int.* 2013:484535. doi: 10.1155/2013/484535
- Zhang, X., Zhuchenko, O., Kuspa, A., and Soldati, T. (2016). Social amoebae trap and kill bacteria by casting DNA nets. *Nat. Commun.* 7:10938. doi: 10.1038/ncomms10938

Conflict of Interest Statement: The authors declare that the research was conducted in the absence of any commercial or financial relationships that could be construed as a potential conflict of interest.

Copyright © 2017 Brenz, Ohnezeit, Winther-Larsen and Hagedorn. This is an open-access article distributed under the terms of the Creative Commons Attribution License (CC BY). The use, distribution or reproduction in other forums is permitted, provided the original author(s) or licensor are credited and that the original publication in this journal is cited, in accordance with accepted academic practice. No use, distribution or reproduction is permitted which does not comply with these terms.



Isolation of *F. novicida*-Containing Phagosome from Infected Human Monocyte Derived Macrophages

Valentina Marecic¹, Olga Shevchuk^{2,3}, Mateja Ozanic¹, Mirna Mihelcic¹, Michael Steinert², Antonija Jurak Begonja³, Yousef Abu Kwaik⁴ and Marina Santic^{1*}

¹ Department of Microbiology and Parasitology, Faculty of Medicine, University of Rijeka, Rijeka, Croatia, ² Department of Microbiology, Institut für Mikrobiologie, Technische Universität Braunschweig and Helmholtz Center for Infection Research, Braunschweig, Germany, ³ Department of Biotechnology, University of Rijeka, Rijeka, Croatia, ⁴ Department of Microbiology and Immunology and Center for Predictive Medicine, Louisville, KY, United States

Francisella is a gram-negative bacterial pathogen, which causes tularemia in humans and animals. A crucial step of *Francisella* infection is its invasion of macrophage cells. Biogenesis of the *Francisella*-containing phagosome (FCP) is arrested for ~15 min at the endosomal stage, followed by gradual bacterial escape into the cytosol, where the microbe proliferates. The crucial step in pathogenesis of tularemia is short and transient presence of the bacterium within phagosome. Isolation of FCPs for further studies has been challenging due to the short period of time of bacterial residence in it and the characteristics of the FCP. Here, we will for the first time present the method for isolation of the FCPs from infected human monocytes-derived macrophages (hMDMs). For elimination of lysosomal compartment these organelles were pre-loaded with dextran coated colloidal iron particles prior infection and eliminated by magnetic separation of the post-nuclear supernatant (PNS). We encountered the challenge that mitochondria has similar density to the FCP. To separate the FCP in the PNS from mitochondria, we utilized iodophenylnitrophenyltetrazolium, which is converted by the mitochondrial succinate dehydrogenase into formazan, leading to increased density of the mitochondria and allowing separation by the discontinuous sucrose density gradient ultracentrifugation. The purity of the FCP preparation and its acquisition of early endosomal markers was confirmed by Western blots, confocal and transmission electron microscopy. Our strategy to isolate highly pure FCPs from macrophages should facilitate studies on the FCP and its biogenesis.

OPEN ACCESS

Edited by:

Albert Descoteaux,
Institut National de la Recherche
Scientifique, Canada

Reviewed by:

Mikhail A. Gavrilin,
The Ohio State University Columbus,
United States
Lee-Ann H. Allen,
University of Iowa, United States

*Correspondence:

Marina Santic
marina.santic@medri.uniri.hr

Received: 24 March 2017

Accepted: 20 June 2017

Published: 05 July 2017

Citation:

Marecic V, Shevchuk O, Ozanic M,
Mihelcic M, Steinert M, Jurak
Begonja A, Abu Kwaik Y and Santic M
(2017) Isolation of
F. novicida-Containing Phagosome
from Infected Human Monocyte
Derived Macrophages.
Front. Cell. Infect. Microbiol. 7:303.
doi: 10.3389/fcimb.2017.00303

Keywords: phagocytosis, organelle purification, pathogen-containing phagosomes, *Francisella*, human macrophages

INTRODUCTION

Intracellular bacteria invade eukaryotic cells, followed by subversion of endocytic pathway, which results in formation of membrane-bound phagosomes. They are able to modulate the membrane protein and lipid composition of phagosomes. This modulation is crucial for bacterial survival within the host cell because it either promotes the establishment of an intact replicative niche or allow the pathogen to escape to replication-permissive cytosol. Many intracellular bacterial pathogens have unique life cycles. Cytosolic bacteria, like *Shigella* (Ray et al., 2010) and *Listeria*

(Camejo et al., 2011) modulate the endosomal-lysosomal membrane-bound compartments and escape into the cytosol, which provides environment rich in nutrients. Intracellular bacteria, *Salmonella* (Steele-Mortimer, 2008; Malik-Kale et al., 2011), *Legionella* (Kagan and Roy, 2002; Shin and Roy, 2008; Isberg et al., 2009), and *Mycobacterium* spp. (Vergne et al., 2004) are intracellular bacterial pathogens that reside and replicate within host endomembrane system. These bacteria overcome the stressful conditions in membrane-bound vacuoles.

Francisella tularensis is a gram-negative, highly infectious bacterium. The bacterium causes the zoonotic disease tularemia. *F. tularensis* type A is a dangerous pathogen that constantly raises attention due to potential use as biological weapon. Interestingly, *Francisella novicida* shares many similarities to type A strain due to genome sequence, intracellular life cycle and infectivity.

F. tularensis can invade and multiply within a range of cell types (Buddingh and Womack, 1941; Shepard, 1959; Anthony L. S. et al., 1991; Ben Nasr et al., 2006; Lindemann et al., 2007), but *in vivo* its primary target are macrophages (Fortier et al., 1994). Within mammalian and arthropod-derived cells, *Francisella* resides in acidic vacuole prior to escape to the cytosol, where it replicates (Santic et al., 2009; Llewellyn et al., 2011). In contrast, within amoeba cells bacterium resides and replicates within non-acidified, membrane-bound vacuoles (Lauriano et al., 2004; Santic et al., 2008).

After entry, it is enclosed within a unique compartment. Intracellular proliferation is essential for *Francisella* virulence, and a lot of effort has been made on understanding of specific steps in the intracellular cycle of this bacterium. *Francisella* survival and proliferation strategies rely on entering in the initial phagosome along the endocytic pathway and physical escape to the cell cytosol, making this bacterium a typical cytosol-dwelling pathogen (Celli and Zahrt, 2013). Despite the fact that *Francisella* replicates in the cytosol of infected cells, short presence of the *Francisella* in the phagosome is necessary for productive multiplication.

Macrophage infection by *Francisella* begins with initial bacterial recognition at the cell membrane (Clemens et al., 2005). *Francisella* enters into macrophages by looping phagocytosis through cholesterol-rich membrane domains called “lipid rafts” with caveolin-1 (Clemens et al., 2004; Tamilselvam and Daefler, 2008; Moreau and Mann, 2013). Following uptake, *Francisella* resides within an initial vacuolar compartment, the *Francisella*-containing phagosome (FCP). Lipid raft-associated components are incorporated into the FCP during entry and the initial phase of intracellular infection of host cells (Tamilselvam and Daefler, 2008). Cholesterol, as a key structural and regulatory element for the integrity of lipid rafts, has an important role in *Francisella* internalization into macrophages (Tamilselvam and Daefler, 2008). FCP matures to an early endosome state regulated by Rab5, a protein that is critical for endosome-phagosome tethering and fusion (Alvarez-Dominguez et al., 1996; Jahraus et al., 1998; Duclos et al., 2000). The FCP consequently acquires late endosomal markers including CD63, LAMP-1, LAMP-2, and Rab7 (Clemens et al., 2004, 2009; Santic et al., 2005; Checroun et al., 2006; Chong et al., 2008; Wehrly et al., 2009). Eventually the late endosome becomes acidified upon acquisition of the

proton vATPase pump that imports hydrogen protons into the vacuole (Chong et al., 2008; Santic et al., 2008). The FCP does not accumulate any lysosomal markers, such as Cathepsin D, or lysosomal tracers (Anthony L. D. et al., 1991; Clemens et al., 2004; Santic et al., 2005; Bonquist et al., 2008). In order to evade lysosome-mediated killing, *Francisella* escapes from the FCP to the cytosol. Vacuolar escape by various strains of *F. tularensis* and *F. novicida* in macrophages and other cells types has been described (Golovliov et al., 2003; Clemens et al., 2004; Santic et al., 2005, 2008; Chong et al., 2008). However, the study of *Francisella* vacuolar escape kinetics has brought controversy to the field varying from the 15 min to 8 h post-infection (Golovliov et al., 2003; Clemens et al., 2004; Santic et al., 2005, 2008; Checroun et al., 2006; McCaffrey and Allen, 2006). However, these differences are likely due to variation in the host cells used, the *Francisella* species and the methodological approaches used by various studies (Golovliov et al., 2003; Clemens et al., 2004; Santic et al., 2005, 2008; Checroun et al., 2006; McCaffrey and Allen, 2006).

The survival and replication of *Francisella* in host cells depends on the expression of the *Francisella* pathogenicity island (FPI) proteins. FPI-deficient mutants fail in formation and maturation of FCP (Nano et al., 2004; Telepnev et al., 2005; McCaffrey and Allen, 2006; Qin and Mann, 2006; Chong et al., 2008, 2013; Broms et al., 2010; Napier et al., 2012; Steele et al., 2013). Moreover, inactivated *F. tularensis*, as well as FPI mutants *iglC* and *pdpC* are not capable to avoid the FCP suggesting that vacuolar escape is a *Francisella* mediated process. This was clearly demonstrated when vacuolar escape deficient mutant *pdpC* was paired on magnetic bead with wild type bacteria. Wild type *F. novicida* secreted effector proteins, which allowed both wild type and *pdpC* to escape the phagosome. Studies have shown that pathogen secrete the IglA-J, PdpA, C, E, DotU, and VgrG into the macrophage cytosol during the infection (Hare and Hueffer, 2014). However, another study shown that IglC, IglI and PdpE, but not IglA and IglG are secreted in a T6SS-dependent manner during infection (Broms et al., 2012). Another importance of phagosome formation is shown by the reduced ability of *Francisella* LVS (live vaccine strain) strain to grow in host cell cytosol after microinjection (Meyer et al., 2015). The brief time spent in the phagosome is a dynamic step during which *Francisella* must actively evade host antimicrobial defenses (Jones et al., 2012). *Francisella* phagosomal escape is requisite to intracellular proliferation and its essential in the *Francisella* intracellular life cycle (Lindgren et al., 2004; Santic et al., 2005; Bonquist et al., 2008; Barker et al., 2009; Wehrly et al., 2009; Broms et al., 2012).

Techniques for the isolation and analysis of phagosomes are important experimental tools in endocytosis and apoptosis research. Since 1969, most of the available methods are based on density gradient ultracentrifugation (Wetzel and Korn, 1969). Here we present a method for isolation of FCP from infected human monocyte-derived macrophages (hMDMs). The method is based on infection of human macrophages with *F. novicida*, followed by mechanical lysis and separation of intracellular organelles. Several adaptations of previously described method are included (Shevchuk et al., 2009; Shevchuk

and Steinert, 2013). For elimination of lysosomal compartment these organelles were loaded with dextran coated colloidal iron particles prior infection and eliminated by magnetic separation of post nuclear supernatant (PNS). The treatment of PNS with iodophenylnitrophenyltetrazolium (INT) salt was necessary to increase the density of mitochondria and fractionate it from FCP in a discontinuous sucrose density gradient.

MATERIALS AND METHODS

Cultivation of *F. novicida*

F. novicida (Birdsell et al., 2009) was grown on buffered charcoal-yeast extract (BCYE) agar at 37°C with 5% CO₂ atmosphere for 24 h.

Preparation of hMDMs from Blood of Healthy Human Donors

Human monocyte derived macrophages were differentiated from peripheral blood monocytes of healthy volunteers with no history of tularemia. Blood was diluted in ratio 1:2 with 0.9% saline, and 15 ml was applied on top of 7.5 ml of Ficoll-Hypaque (Ficoll-Paque; Pharmacia Fine Chemicals, USA). After 25 min of centrifugation at 300 × g, at room temperature (RT) the layer containing the mononuclear cell fraction was aspirated, transferred to a new tubes and centrifuged for additional 10 min at 300 × g at RT. Obtained monocytes were washed twice with 25 ml of 0.9% saline, resuspended in RPMI with glutamine (Bio Whittaker, Lonza, USA) supplemented with 20% FBS (Invitrogen, USA), and distributed in 6-well ultra-low attachment plates (Corning Life Sciences, USA). Serum starvation was performed to promote monocyte differentiation to macrophages (Santic et al., 2005; Ozanic et al., 2016). After 3 days of incubation at 37°C in 5% CO₂ the medium was replaced with 10% FBS RPMI, followed by replacement with 5% FBS RPMI (at day 6). At day 7 cells were scraped, collected and resuspended to desired concentration in RPMI with 1% FBS.

Preparation of Colloidal Iron Particles

Dextran-coated colloidal iron particles were prepared as follows. Equal volumes of 1.2 M FeCl₂ (10 ml) and 1.8 M FeCl₃ (10 ml) were mixed and agitated extensively while adding the same volume (10 ml) of 25% NH₃ dropwise. The suspension was divided in 5 ml aliquots and placed on a magnetic unit (Dyna, Thermo Fisher, USA). Precipitate was then collected on the bottom of the tubes and washed once with 5% NH₃, twice with ddH₂O and resuspend in 80 ml of 0.3 M HCl. Solution was magnetically stirred for 30 min. Dextran (4 g, 64 to 76 kDa, Sigma-Aldrich, USA) was added and solution was stirred for further 30 min. In study of distribution of colloidal iron particles within endosomal compartments, small aliquot of prepared colloidal iron was incubated with dextran-tetramethylrhodamine (1 mg/ml, 70 kDa, Sigma-Aldrich, USA) and stirred for 30 min. The samples were dialyzed against 5 l of cold water, changing water four times during 2 days. The final suspension was filtered through filter paper and was used immediately or stored at 4°C for maximum 3 months. The concentration of obtained iron solution was ~10 mg/ml (Rodriguez-Paris et al., 1993).

Preparation of Optiprep™ Density Gradients

OptiPrep gradients were prepared by mixing of two working solutions, 10 and 45% of OptiPrep (Sigma-Aldrich, USA) in HB buffer (0.5 mM Na₂EGTA, 20 mM HEPES, 250 mM Sucrose) in gradient mixer (Model #GM-40; C.B.S. Scientific Co, USA). Gradients were poured into polyallomer centrifuge tubes (9/16 × 3-3/4"; 14 × 95 mm; Beckman Coulter, USA) and used immediately or kept at 4°C overnight.

Infection of hMDMs with *F. novicida*

A total of 5·10⁷ hMDMs were seeded in 30 ml of RPMI supplemented with 1% FBS in 75 cm² cell culture flasks (TPP, Switzerland). Colloidal iron particles were added to a final concentration of 1 mg/ml, gently distributed 15 min before infection and left in the medium. The cells were infected with *F. novicida* at a multiplicity of infection (MOI) 10. In order to achieve synchronized infection, the cells were centrifuged immediately after infection at 100 × g for 3 min at RT. After 15 min of incubation at 37°C the cells were scraped, transferred to a 50 ml tube and centrifuged at 230 × g for 7 min at 4°C. Cells were washed twice in 30 ml of ice cold PBS and once in 10 ml of ice cold HB buffer.

Isolation of *F. novicida*-Containing Phagosome

For the isolation of FCP pellet of infected hMDMs was resuspended in 2 ml of cold HB buffer supplemented with EDTA-free protease inhibitor cocktail (Roche Diagnostic, Penzberg, Germany) according to manufacture protocol and with 5 mg/ml INT (Sigma-Aldrich, USA). The cells were mechanically disrupted in a Dura Grind stainless-steel homogenizer (Dounce Dura-Grind® Tissue Grinder; Braintree, Scientific, Inc.), transferred to a new tube and incubated with Benzonase (50 units/ml, Sigma-Aldrich, USA) for 7 min at 37°C. The nuclear and cell debris were removed by centrifugation at 110 × g for 5 min at 4°C. Obtained PNS was transferred to a new tubes and additional 2 ml of HB buffer with protease inhibitor cocktail was added to remaining pellet, carefully mixed and centrifuged at 100 × g for 3 min at 4°C. PNS was run through the MiniMACS column (OctoMACS™ Separation Unit; Miltenyi Biotec, Germany) to eliminate the lysosomal compartments loaded with colloidal iron. The flow through fraction was carefully applied on top of 8 ml of 10 to 45% OptiPrep gradient and centrifuged for 2 h in SW40 swing Rotor (Beckman Coulter, USA) at 100,000 × g at 4°C. After centrifugation, about 800 μl fractions were carefully collected from the top of gradient with cutted 1 ml tip. To analyze distribution of bacteria in gradient fractions, 10 μl of each fraction was diluted in 190 μl of ddH₂O and plated on BCYE square plates 120 × 120 mm (Greiner, Sigma-Aldrich, USA). After 2 days of incubation at 37°C the CFU of *F. novicida* were calculated.

Confocal Laser Scanning Microscopy

The hMDMs were infected with *F. novicida* at MOI 10. At 15 min after infection the cells were washed with PBS, fixed using 4% paraformaldehyde (PFA, Sigma-Aldrich, USA) for 30 min at

4°C and permeabilized with 0.5% Triton X-100 (Sigma-Aldrich, USA). The coverslips were incubated with mouse monoclonal anti *Francisella* antibodies (1:5,000), washed with PBS and incubated with Alexa Fluor 555 (1:4,000, Molecular probes, USA) secondary antibodies for 1 h at RT.

To study the integrity of isolated FCP, equal fractions of phagosomes were seeded onto 24-well coverslips and centrifuged at $200 \times g$ for 10 min at 4°C, followed by fixation with 4% PFA for 15 min at RT. Prepared samples were stained with 1 μ l/ml of propidium iodide (PI) (Serva, Germany) for 25 min in the dark. Control samples were permeabilized with methanol at -20°C for 5 min.

To study the labeling of endosomal compartments with dextran-tetramethylrhodamine coated colloidal iron, the hMDMs were seeded on coverslips. The cells were loaded with dextran-tetramethylrhodamine colloidal iron for 15 min. After 15 min the colloidal iron particles were left in the medium and the cells were additionally infected with *F. novicida* for 15 min at MOI 10 followed by centrifugation at $100 \times g$ for 3 min at RT. At 15 min after infection, and 30 min of colloidal iron particles load. the cells were washed, fixed and permeabilized as described above. The coverslips were incubated with mouse monoclonal anti *Francisella* antibodies (1:5,000), mouse monoclonal early endosome antigen (EEA1, 1:1,000, Bio Rad, USA), mouse monoclonal lysosome associated membrane protein 1 (Lamp-1, 1:1,000, Bio Rad, USA) and mouse monoclonal anti Cathepsin-D (1:1,000, BD Biosciences, USA). The coverslips were washed with PBS and incubated with donkey anti-goat Alexa Fluor 488 and goat anti-mouse Alexa Fluor 647 (1:4,000, Molecular probes, USA) secondary antibodies for 1 h at RT. All samples were mounted in Mowiol 4-88 (Sigma-Aldrich, USA) and analyses were performed on FV 1000 Olympus confocal microscope.

SDS-PAGE and Western Blot

For Western blot analysis, equal amount of fraction proteins was applied onto 10% SDS-PAGE. After separation, proteins were transferred to nitrocellulose membrane in Transfer Buffer (Tris Base, Glycine, Methanol, d_4H_2O) and blocked for 1 h at room temperature in 1x Tris Buffered Saline (TBS, Sigma-Aldrich, USA) with 0.1% (w/v) Tween-20 (TBST, Sigma-Aldrich, USA) and 3% (m/v) Bovine Serum Albumine (BSA, Sigma-Aldrich, USA). Monoclonal rabbit antibody against human Rab5 (1:1,000, Cell Signaling Technology, USA), rabbit antibody against mitochondrial apoptosis-inducing factor (AIF, 1:1,000, Cell Signaling Technology, USA), mouse monoclonal KDEL antibody (1:100, Santa Cruz Biotechnology, USA), antibody against Golgi matrix protein of 130 kDa (gm130, BD Biosciences, USA), mouse monoclonal EEA1 and Lamp-1 were used for overnight incubation in staining buffer (3% BSA in TBST). After washing three times for 10 min in TBST, secondary anti-rabbit IgG and anti-mouse IgG conjugated horseradish peroxidase antibodies (1:1,000, Cell Signaling Technology, USA) were added for 1 h at RT. Membrane was again washed three times for 10 min in TBST. Enhanced chemiluminescence detection reagents Luminal Enhancer Solution (GE Healthcare, UK) and Peroxide Solution (GE Healthcare, UK) were used for

visualization of the detected proteins by Bio Rad Chemi Doc XRR+ (Bio Rad Laboratories, USA).

Transmission Electron Microscopy

For transmission electron microscopy, the samples were transferred in 12-well cell culture plates (TPP, Switzerland). The samples were washed with 1x Sorensen buffer (TCS Biosciences Ltd., UK) and fixed using 2.5% glutaraldehyde (SPI Supplies, USA) for 45 min at 4°C. The post fixation was performed with 1% OsO₄ (SPI Supplies, USA) for 45 min at 4°C. The sample was dehydrated by ethanol series with increased concentration, embedded in epoxy resin (SPI Supplies, USA) and polymerized for 24–48 h at 60°C. Ultra-thin sections were cut and examined by Phillips Morgany transmission electron microscope.

Statistics

Statistical significances were determined using two-tailed Student's *t*-test. Statistical analyses were performed using Statistica (Statsoft) software version 12 or with GraphPad Prizm version 6.0 software. *P* < 0.001 were accepted as significantly different and were denoted by *.

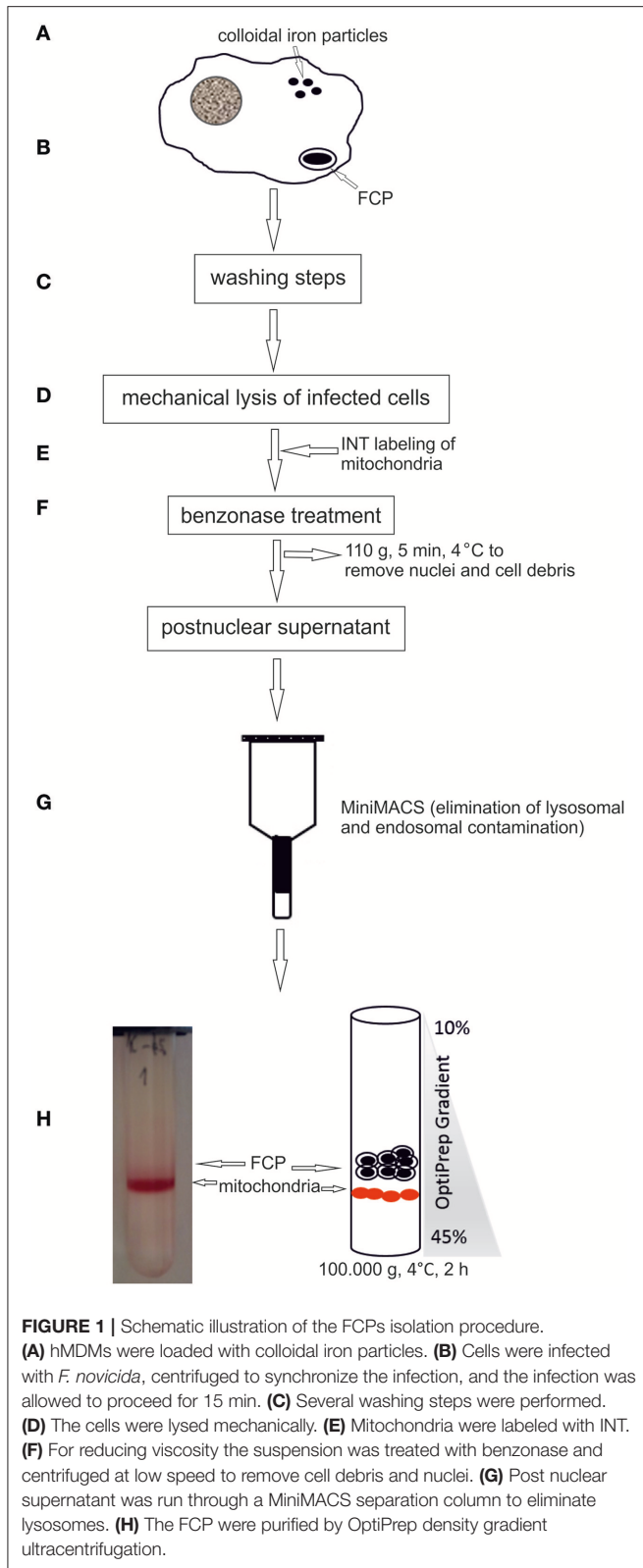
Ethics Statement

This study was carried out in accordance with the recommendations of Health Care Act Republic of Croatia (NN 158/08, 71/10, 139/10, 22/11, 84/11, 12/12, 35/12, 70/12 i 82/13), Act on the Protection of Patient's rights Republic of Croatia (NN 169/04, 37/08), was approved by the Ethical committee of Clinical Hospital Centre Rijeka as well as Ethical committee of Faculty of Medicine, with written informed consent from all subjects. All subjects gave written informed consent in accordance with the Declaration of Helsinki.

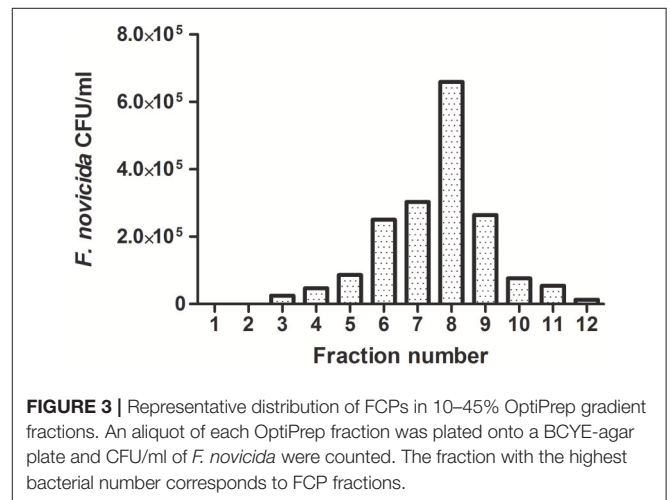
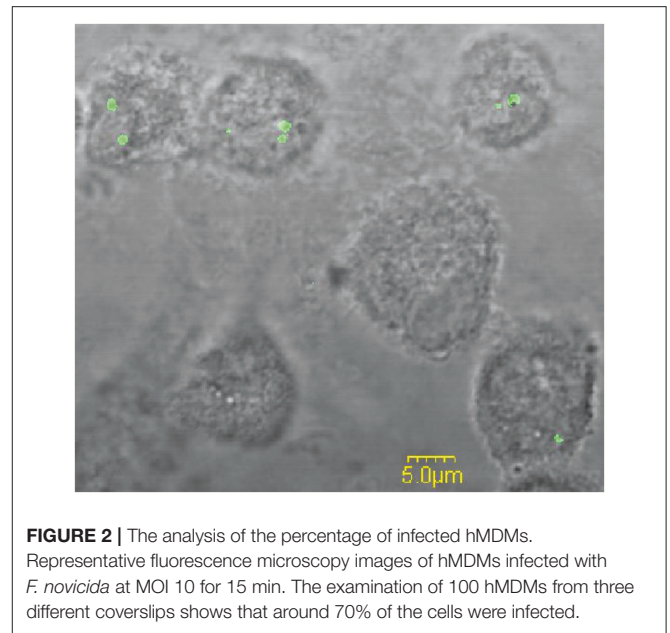
RESULTS

F. novicida-Containing Phagosome Isolated from Infected hMDMs

Following phagocytic uptake, *Francisella* resides within special vacuole-FCP and its formation is absolutely required for intracytoplasmic replication of bacteria (Checroun et al., 2006). Because of apparent importance of this organelle during establishment of infection we optimized the method of FCP isolation (**Figure 1**). Human macrophages were infected with *F. novicida* at multiplicity of infection 10 resulting in 70% of hMDMs infected with bacteria at 15 min after infection (**Figure 2**). Macrophages, free of extracellular bacteria were disrupted in a Dura Grind stainless-steel homogenizer by optimized number of strokes. The unbroken cells and nuclei were removed by centrifugation. Obtained PNS was treated with Benzonase, an enzyme mixture for nucleic acid degradation, which allows reduction of sample viscosity and allows the separation of FCP from other organelles in PNS. The distribution of *F. novicida* in the gradient after ultracentrifugation was determined by plating fractions onto BCYE agar plates and counting bacterial CFU/ml (**Figure 3**). Our results showed that the highest number of *F. novicida* was in fraction 8 and it



reached 6.5×10^5 CFU/ml (**Figure 3**). The fractions with highest number of bacteria were routinely proceeded for further analysis.



Separation of FCP from Subcellular Organelles

During isolation of bacterial vacuole, it is crucial to minimize artifacts caused by other organelles. The successful separation of FCP from subcellular organelles was assessed by Western blot and transmission electron microscopy.

For separation of FCP from mitochondria we treated the PNS with INT, which results in formation of formazan, a product of activity of mitochondrial succinate dehydrogenase. This step was necessary to increase the density of mitochondria and separate two organelles by ultracentrifugation. The distribution of early endosome markers Rab5 and EEA1, lysosomal marker Lamp-1 as well and mitochondrial marker AIF, Golgi marker gm130 and ER marker KDEL were assessed by WB. Rab5 and EEA1 were enriched in fractions with the highest number of bacteria

of the OptiPrep gradient, consistent with the accumulation of FCP in this fraction (Figure 4). AIF was enriched in fraction 10 of the OptiPrep gradient, confirming the presence of mitochondria in these fractions (Figure 4). Obtained results confirmed the separation of FCP from mitochondria by ultracentrifugation. Additionally, in gradient fractions formazan was visible after ultracentrifugation, and could be used as a marker for estimation of localization of bacterial fractions that were above this formazan circle (Figure 1). Further, our results showed that Golgi apparatus and endoplasmic reticulum are eliminated during the purification of the FCP and are not present in gradient fractions (Figure 4). The distribution of Lamp-1 in PNS before and after the magnetic separation, as well as in gradient fractions, was tested by Western blot (Figure 4). The results showed that lysosomes were present in PNS before magnetic separation and eliminated with this procedure.

To investigate the trafficking of the dextran coated colloidal iron particles within the endocytic pathways after infection of hMDMs with *F. novicida* the confocal microscopy was used. Our results showed that around 30% of dextran-tetramethylrhodamine colloidal iron particles colocalized with Lamp-1 and ~65% with Cathepsin-D (Figure 5B). In contrast, *F. novicida* colocalized with EEA1 (Figure 5A), indicating that most of colloidal iron does not interfere with early *F. novicida* phagosome.

In addition, human macrophages infected with *F. novicida* at MOI 10 at 15 min after infection and FCP within fractions were analyzed by transmission electron microscopy. At 15 min after infection bacteria were enclosed in intact phagosomes of infected hMDMs (Figure 6A). Low magnification TEM image of the FCP enriched fraction demonstrate the purity and small vesicle free fraction (Figure 6B). High magnification TEM image of the FCP enriched fraction revealed that single bacteria surrounded by per one-layer membrane were present (Figure 6C).

Integrity of the FCP Membrane after Isolation

The integrity of phagosomal membrane of isolated FCP was tested using PI by fluorescence microscopy. The fractions with the highest number of bacteria were used for this study. As a control sample, the isolated phagosomal fraction was permeabilized in order to allow the PI to penetrate inside the phagosome and stain the bacteria. This was considered as 100% of stained bacteria. Three coverslips were analyzed and the total stained bacteria in each sample were counted. This approach provided valuable information about the quality of the isolated FCP. Our results show that FCP membrane is intact on ~70% of the isolated phagosomal fractions ($P = 0.000001$; Figure 7).

DISCUSSION

It is essential for *Francisella* to replicate within host cells to successfully establish an infection and cause disease. Escape from the phagosome is an important step in *Francisella* life cycle since mutants deficient in escape are unable to cause productive infection (Chong et al., 2012). After invasion of the host cell, *Francisella* forms an endocytic membrane-bound phagosome. Bacteria must disrupt this phagosome and dislocate to the cytosol in order to replicate and spread from cell to cell (Clemens et al., 2004; Santic et al., 2005). However, these short-lived vacuoles can interact with the host vesicular trafficking, and can have important role for virulence and pathogenesis of *Francisella*. Due to importance of the phagosome in pathogenesis of tularemia we established a method for purification of FCP from infected human monocyte derived macrophages. To perform the separation of phagosome from infected cells, large cell number is necessary, making it challenging to use these approaches with human primary cells. For that reason, we

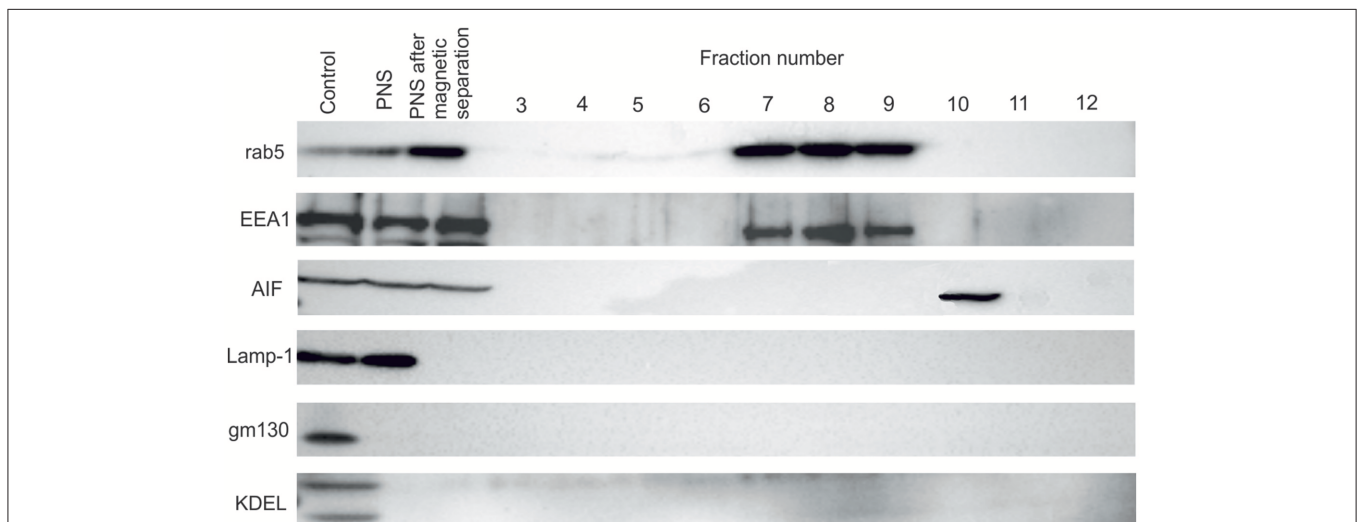
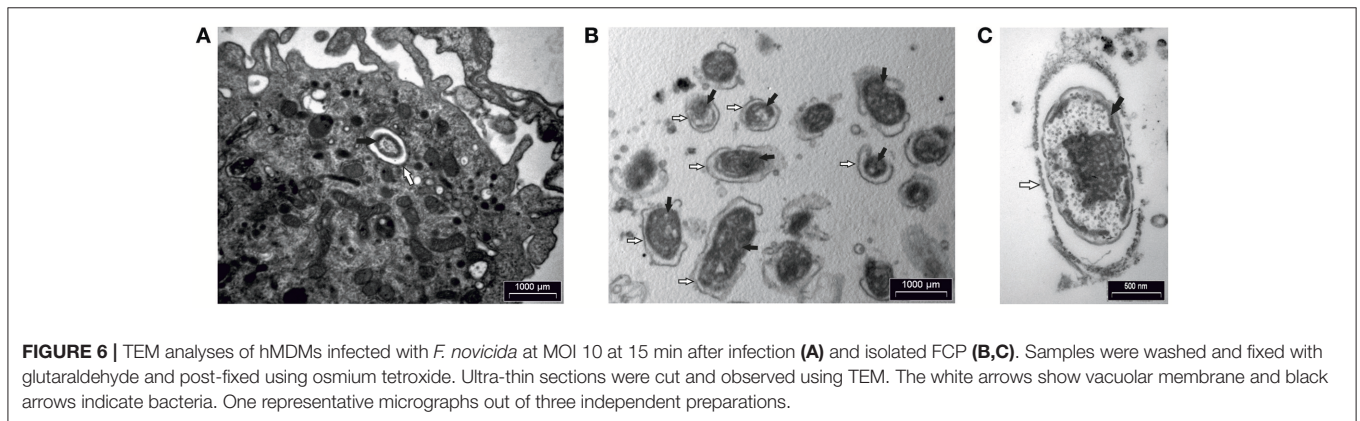
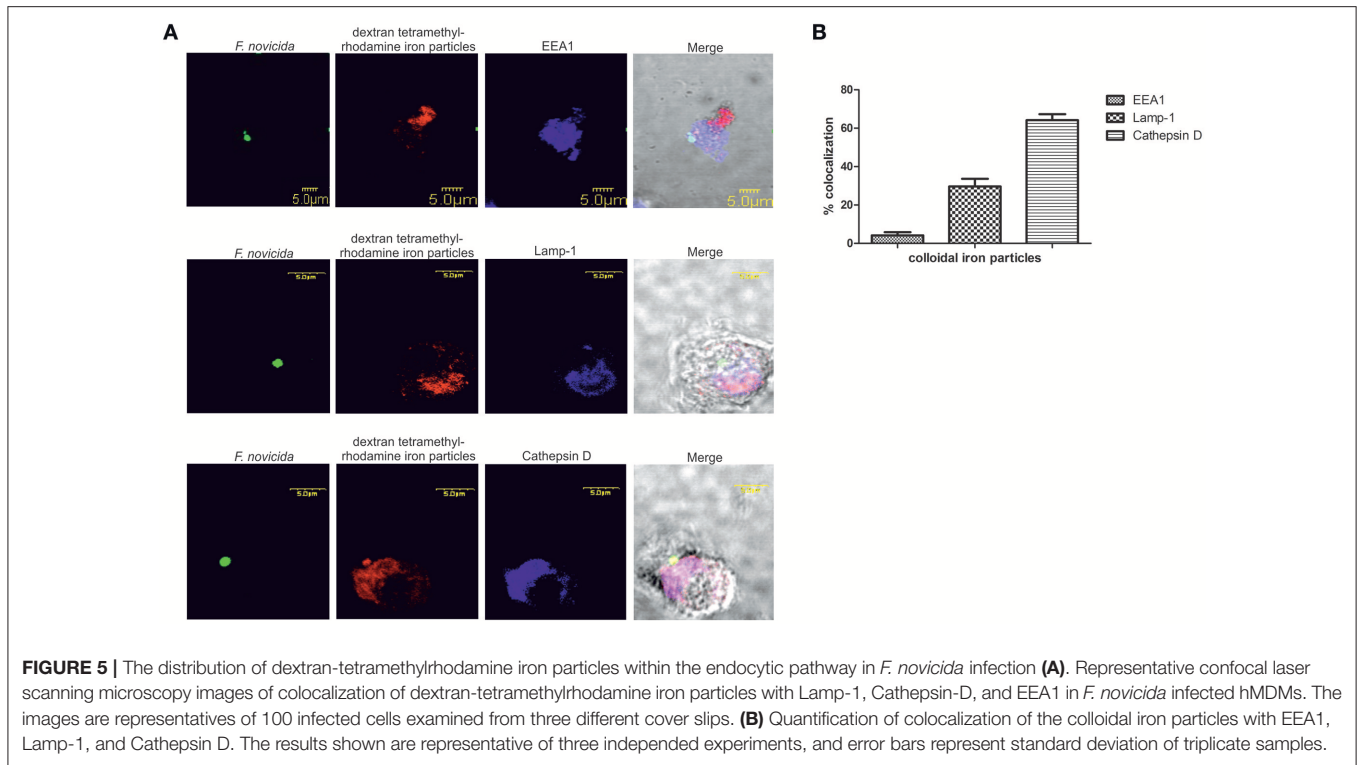
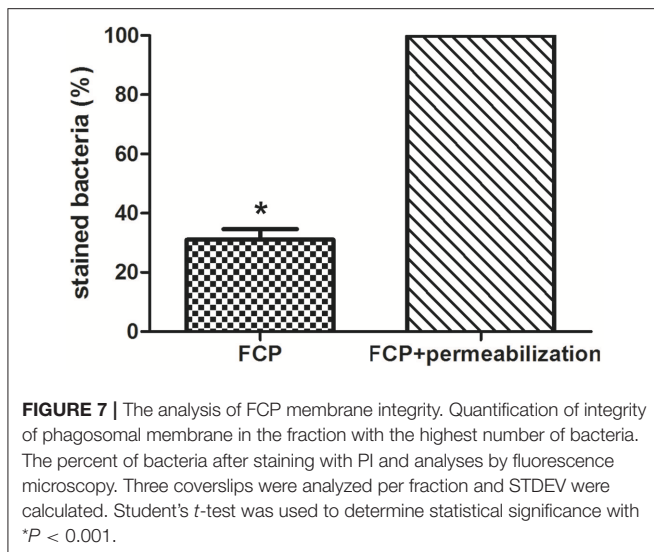


FIGURE 4 | Western blot analysis of OptiPrep fractions. Fractions 3 to 12 as well as PNS before and after magnetic separation were tested using the markers for the following compartments: early endosome (Rab5 and EEA1), lysosomes (Lamp-1), Golgi (gm130), mitochondria (AIF) and ER (KDEL). hMDMs lysate was used as a control.



pulled together the blood from different donors to obtain the necessary number of human macrophages. To ensure that we do not co-isolate the extracellular bacteria, intensive washing steps were included. In contrast to previously published protocols, the dextran coated iron particle were used for elimination of lysosomal and endosomal compartments prior infection (Shevchuk et al., 2009; Shevchuk and Steinert, 2013). With the use of confocal microscopy, we followed the trafficking of dextran-tetramethylrhodamine iron particles within hMDMs. The markers for early and late endosomes as well as lysosomes were used to document which endosomal compartments are labeled by colloidal iron. This is due to the specificity and rapidity of infection in comparison to other intracellular pathogens (Chong and Celli, 2010; Santic et al., 2010). Some of the most

interesting aspects of phagosome maturation depend on the ability of intracellular pathogens to bypass the normal maturation process. Attempts to purify these compartments represents a challenge when classical organelle enrichment techniques are used. To resolve this problem a combination of classical and improved methods for enrichment and pre-fractionation must be used. In previous published methods for isolation of *Legionella*-containing vacuole the 5–30% OptiPrep gradient was used (Shevchuk et al., 2009; Shevchuk and Steinert, 2013). During the establishment of phagosome isolation from *Dictyostelium discoideum* cells infected with *F. novicida*, different concentration of OptiPrep were tested (5–30, 5–35, 10–40, and 10–45%, data not shown). Optimization of OptiPrep gradient for successful isolation of FCP showed that the best separation of FCP was when



OptiPrep gradient 10–45% was used. In addition, the efficient removal of contaminants in the method of vacuole isolation is very important to achieve. Therefore, in order to separate two organelles with close density, mitochondria and FCP, we utilized an enzyme of the citrate cycle, the succinate dehydrogenase, located in the inner mitochondrial membrane. The INT added to the PNS is converted to formazan and increased the density of those organelles (Munujos et al., 1993). This phenomenon was used for separation of mitochondria from FCPs by discontinues ultracentrifugation method. In addition, Rab5 and EEA1, as markers for early endosomal compartment, were used to indicate the presence of FCP in OptiPrep fractions that was void of mitochondrial marker, AIF.

Isolation of bacteria-containing vacuoles (BCV) is of key importance for the understanding of these compartments, but technically is very challenging. During recent years, different groups have developed different protocols for isolation of BCV (reviewed in Herweg et al., 2015). The bacteria subvert endomembrane trafficking around the BCV and the communication around BCV and other host cell organelles has been described (Gagnon et al., 2002; Touret et al., 2005; Santos et al., 2015; Santos and Enninga, 2016).

Protocols for isolation of pathogen-containing vacuoles are based on subcellular/organelle fractionation based on physicochemical properties (Howe and Heinzen, 2008; He et al., 2012; Cheng et al., 2014). These protocols combine confocal fluorescence microscopy, Western blot and electron microscopy techniques providing the characterization of host cell compartments after infection with different intracellular pathogens. In addition, isolation of BCV can be based on immuno-affinity purification (Urwylers et al., 2010; Hoffmann et al., 2013; Vorwerk et al., 2015) or on FACS single cell enrichment by sorting bacteria and lysed host cells organelles (Becker et al., 2006; Pfortner et al., 2013; Surmann et al., 2014). Separation principles have been applied for isolation of latex

bead-phagosomes from macrophages (Desjardins et al., 1994) and *Dictyostelium* (Gotthardt et al., 2002). In the protocol for purification of *Legionella*-containing vacuole (LCV) from infected *D. discoideum* (Shevchuk et al., 2009; Urwylers et al., 2010; Finsel et al., 2013; Shevchuk and Steinert, 2013), or murine macrophage-like RAW 264.7 (Hoffmann et al., 2014) the immuno-magnetic separation using an anti-SidC antibody was performed, followed by 10–35% Histodenz density gradient centrifugation. Others established protocol for LCV isolation from U937 macrophages using 55–65% gradient (Bruckert and Abu Kwaik, 2015). Others and our studies show that the integrity of phagosome membrane is often compromised during the early time point of infection with *Francisella* (Santic et al., 2008; Chong et al., 2012; Ozanic et al., 2015; Rowe and Huntley, 2015). Besides the electron microscopy methods, fluorescence microscopy could be valuable method to check the integrity of the phagosomal membrane after its isolation (Lonnbro et al., 2008; Hoffmann et al., 2013, 2014; Bruckert and Abu Kwaik, 2015). Results from this study show that the phagosomal membrane is highly conserved 15 min after infection of hMDMs and only 30% of the analyzed fraction show some damage of the FCP. The FCP is presumably intact within 30 min after infection.

Many intracellular bacteria reside and replicate inside phagosomal compartment making protocol for vacuolar isolation easy to apply. In contrast, some intracellular pathogens show ability to escape from phagosome to directly use the cytoplasm as their replicative habitat (Ray et al., 2009). *Francisella* resides in phagosomes ~5–30 min after infection, making it more challenging for isolation of the phagosome from infected macrophages. After cytoplasmic replication, *Francisella* re-enters the endocytic pathways by autophagy (Checroun et al., 2006; Jones et al., 2012), and bacteria are found in autophagosomes by 24 h after infection. Our established method for isolation of FCP could be applied for the isolation of autophagosomes as well. The protocol presented here will enable future proteomic analyses analysis of those delicate intracellular compartments.

AUTHOR CONTRIBUTIONS

VM, OS, and MiS contributed in isolation of the vacuole and writing. MM and AJ participated in Western blot analyses. MO participated in electron microscopy analyses. MaS and YA participated in fluorescence analyses and writing.

FUNDING

This work is supported by a University Grants (No. 13.06.1.1.11. and No. 13.11.1.2.07), National Science Foundation (HRZZ, IP-2016-06-9003) and project RISK financed by European Regional Development Fund (ERDF). YA is supported by Public Health Service Award 1R01AI120244 and R21AI116517 from the National Institute of Health and by the Commonwealth of Kentucky Research Challenge Trust Fund.

REFERENCES

- Alvarez-Dominguez, C., Barbieri, A. M., Beron, W., Wandinger-Ness, A., and Stahl, P. D. (1996). Phagocytosed live *Listeria monocytogenes* influences Rab5-regulated *in vitro* phagosome-endosome fusion. *J. Biol. Chem.* 271, 13834–13843. doi: 10.1074/jbc.271.23.13834
- Anthony, L. D., Burke, R. D., and Nano, F. E. (1991). Growth of *Francisella* spp. in rodent macrophages. *Infect. Immun.* 59, 3291–3296.
- Anthony, L. S., Gu, M. Z., Cowley, S. C., Leung, W. W., and Nano, F. E. (1991). Transformation and allelic replacement in *Francisella* spp. *J. Gen. Microbiol.* 137, 2697–2703. doi: 10.1099/00221287-137-12-2697
- Barker, J. R., Chong, A., Wehrly, T. D., Yu, J. J., Rodriguez, S. A., Liu, J., et al. (2009). The *Francisella tularensis* pathogenicity island encodes a secretion system that is required for phagosome escape and virulence. *Mol. Microbiol.* 74, 1459–1470. doi: 10.1111/j.1365-2958.2009.06947.x
- Becker, D., Selbach, M., Rollenhagen, C., Ballmaier, M., Meyer, T. F., Mann, M., et al. (2006). Robust Salmonella metabolism limits possibilities for new antimicrobials. *Nature* 440, 303–307. doi: 10.1038/nature04616
- Ben Nasr, A., Haithcoat, J., Masterson, J. E., Gunn, J. S., Eaves-Pyles, T., and Klimpel, G. R. (2006). Critical role for serum opsonins and complement receptors CR3 (CD11b/CD18) and CR4 (CD11c/CD18) in phagocytosis of *Francisella tularensis* by human dendritic cells (DC): uptake of *Francisella* leads to activation of immature DC and intracellular survival of the bacteria. *J. Leukoc. Biol.* 80, 774–786. doi: 10.1189/jlb.1205755
- Birdsell, D. N., Stewart, T., Vogler, A. J., Lawaczek, E., Diggs, A., Sylvester, T. L., et al. (2009). *Francisella tularensis* subsp. novicida isolated from a human in Arizona. *BMC Res. Notes* 2:223. doi: 10.1186/1756-0500-2-223
- Bonquist, L., Lindgren, H., Golovliov, I., Guina, T., and Sjostedt, A. (2008). MglA and Igl proteins contribute to the modulation of *Francisella tularensis* live vaccine strain-containing phagosomes in murine macrophages. *Infect. Immun.* 76, 3502–3510. doi: 10.1128/IAI.00226-08
- Broms, J. E., Meyer, L., Sun, K., Lavander, M., and Sjostedt, A. (2012). Unique substrates secreted by the type VI secretion system of *Francisella tularensis* during intramacrophage infection. *PLoS ONE* 7:e50473. doi: 10.1371/journal.pone.0050473
- Broms, J. E., Sjostedt, A., and Lavander, M. (2010). The role of the *Francisella Tularensis* pathogenicity island in type VI secretion, intracellular survival, and modulation of host cell signaling. *Front. Microbiol.* 1:136. doi: 10.3389/fmicb.2010.00136
- Bruckert, W. M., and Abu Kwaiq, Y. (2015). Complete and ubiquitinated proteome of the Legionella-containing vacuole within human macrophages. *J. Proteome Res.* 14, 236–248. doi: 10.1021/pr500765x
- Buddingh, G. J., and Womack, F. C. (1941). Observations on the infection of chick embryos with Bacterium Tularensis, Brucella, and Pasteurella Pestis. *J. Exp. Med.* 74, 213–222. doi: 10.1084/jem.74.3.213
- Camejo, A., Carvalho, F., Reis, O., Leitao, E., Sousa, S., and Cabanes, D. (2011). The arsenal of virulence factors deployed by *Listeria monocytogenes* to promote its cell infection cycle. *Virulence* 2, 379–394. doi: 10.4161/viru.2.5.17703
- Celli, J., and Zahrt, T. C. (2013). Mechanisms of *Francisella tularensis* intracellular pathogenesis. *Cold Spring Harb. Perspect. Med.* 3:a010314. doi: 10.1101/cshperspect.a010314
- Checroun, C., Wehrly, T. D., Fischer, E. R., Hayes, S. F., and Celli, J. (2006). Autophagy-mediated reentry of *Francisella tularensis* into the endocytic compartment after cytoplasmic replication. *Proc. Natl. Acad. Sci. U.S.A.* 103, 14578–14583. doi: 10.1073/pnas.0601838103
- Cheng, Y., Liu, Y., Wu, B., Zhang, J. Z., Gu, J., Liao, Y. L., et al. (2014). Proteomic analysis of the *Ehrlichia chaffeensis* phagosome in cultured DH82 cells. *PLoS ONE* 9:e88461. doi: 10.1371/journal.pone.0088461
- Chong, A., and Celli, J. (2010). The francisella intracellular life cycle: toward molecular mechanisms of intracellular survival and proliferation. *Front. Microbiol.* 1:138. doi: 10.3389/fmicb.2010.00138
- Chong, A., Child, R., Wehrly, T. D., Rockx-Brouwer, D., Qin, A., Mann, B. J., et al. (2013). Structure-function analysis of DipA, a *Francisella tularensis* virulence factor required for intracellular replication. *PLoS ONE* 8:e67965. doi: 10.1371/journal.pone.0067965
- Chong, A., Wehrly, T. D., Child, R., Hansen, B., Hwang, S., Virgin, H. W., et al. (2012). Cytosolic clearance of replication-deficient mutants reveals *Francisella tularensis* interactions with the autophagic pathway. *Autophagy* 8, 1342–1356. doi: 10.4161/auto.20808
- Chong, A., Wehrly, T. D., Nair, V., Fischer, E. R., Barker, J. R., Klose, K. E., et al. (2008). The early phagosomal stage of *Francisella tularensis* determines optimal phagosomal escape and Francisella pathogenicity island protein expression. *Infect. Immun.* 76, 5488–5499. doi: 10.1128/IAI.00682-08
- Clemens, D. L., Lee, B. Y., and Horwitz, M. A. (2004). Virulent and avirulent strains of *Francisella tularensis* prevent acidification and maturation of their phagosomes and escape into the cytoplasm in human macrophages. *Infect. Immun.* 72, 3204–3217. doi: 10.1128/IAI.72.6.3204-3217.2004
- Clemens, D. L., Lee, B. Y., and Horwitz, M. A. (2005). *Francisella tularensis* enters macrophages via a novel process involving pseudopod loops. *Infect. Immun.* 73, 5892–5902. doi: 10.1128/IAI.73.9.5892-5902.2005
- Clemens, D. L., Lee, B. Y., and Horwitz, M. A. (2009). *Francisella tularensis* phagosomal escape does not require acidification of the phagosome. *Infect. Immun.* 77, 1757–1773. doi: 10.1128/IAI.01485-08
- Desjardins, M., Huber, L. A., Parton, R. G., and Griffiths, G. (1994). Biogenesis of phagolysosomes proceeds through a sequential series of interactions with the endocytic apparatus. *J. Cell Biol.* 124, 677–688. doi: 10.1083/jcb.124.5.677
- Duclos, S., Diez, R., Garin, J., Papadopoulou, B., Descoteaux, A., Stenmark, H., et al. (2000). Rab5 regulates the kiss and run fusion between phagosomes and endosomes and the acquisition of phagosome leishmanicidal properties in RAW 264.7 macrophages. *J. Cell Sci.* 113(Pt 19), 3531–3541.
- Finsel, I., Hoffmann, C., and Hilbi, H. (2013). Immunomagnetic purification of fluorescent Legionella-containing vacuoles. *Methods Mol. Biol.* 983, 431–443. doi: 10.1007/978-1-62703-302-2_24
- Fortier, A. H., Green, S. J., Polsinelli, T., Jones, T. R., Crawford, R. M., Leiby, D. A., et al. (1994). Life and death of an intracellular pathogen: *Francisella tularensis* and the macrophage. *Immunol. Ser.* 60, 349–361.
- Gagnon, E., Duclos, S., Rondeau, C., Chevet, E., Cameron, P. H., Steele-Mortimer, O., et al. (2002). Endoplasmic reticulum-mediated phagocytosis is a mechanism of entry into macrophages. *Cell* 110, 119–131. doi: 10.1016/S0092-8674(02)00797-3
- Golovliov, I., Baranov, V., Krocova, Z., Kovarova, H., and Sjostedt, A. (2003). An attenuated strain of the facultative intracellular bacterium *Francisella tularensis* can escape the phagosome of monocyctic cells. *Infect. Immun.* 71, 5940–5950. doi: 10.1128/IAI.71.10.5940-5950.2003
- Gotthardt, D., Warnatz, H. J., Henschel, O., Bruckert, F., Schleicher, M., and Soldati, T. (2002). High-resolution dissection of phagosome maturation reveals distinct membrane trafficking phases. *Mol. Biol. Cell* 13, 3508–3520. doi: 10.1091/mbc.E02-04-0206
- Hare, R. F., and Hueffer, K. (2014). *Francisella novicida* pathogenicity island encoded proteins were secreted during infection of macrophage-like cells. *PLoS ONE* 9:e105773. doi: 10.1371/journal.pone.0105773
- He, Y., Li, W., Liao, G., and Xie, J. (2012). Mycobacterium tuberculosis-specific phagosome proteome and underlying signaling pathways. *J. Proteome Res.* 11, 2635–2643. doi: 10.1021/pr300125t
- Herweg, J. A., Hansmeier, N., Otto, A., Geffken, A. C., Subbarayal, P., Prusty, B. K., et al. (2015). Purification and proteomics of pathogen-modified vacuoles and membranes. *Front. Cell. Infect. Microbiol.* 5:48. doi: 10.3389/fcimb.2015.00048
- Hoffmann, C., Finsel, I., and Hilbi, H. (2013). Pathogen vacuole purification from legionella-infected amoeba and macrophages. *Methods Mol. Biol.* 954, 309–321. doi: 10.1007/978-1-62703-161-5_18
- Hoffmann, C., Finsel, I., Otto, A., Pfaffinger, G., Rothmeier, E., Hecker, M., et al. (2014). Functional analysis of novel Rab GTPases identified in the proteome of purified Legionella-containing vacuoles from macrophages. *Cell. Microbiol.* 16, 1034–1052. doi: 10.1111/cmi.12256
- Howe, D., and Heinzen, R. A. (2008). Fractionation of the *Coxiella burnetii* parasitophorous vacuole. *Methods Mol. Biol.* 445, 389–406. doi: 10.1007/978-1-59745-157-4_25
- Isberg, R. R., O'connor, T. J., and Heidtman, M. (2009). The *Legionella pneumophila* replication vacuole: making a cosy niche inside host cells. *Nat. Rev. Microbiol.* 7, 13–24. doi: 10.1038/nrmicro1967
- Jahraus, A., Tjelle, T. E., Berg, T., Habermann, A., Storrie, B., Ullrich, O., et al. (1998). *In vitro* fusion of phagosomes with different endocytic organelles from J774 macrophages. *J. Biol. Chem.* 273, 30379–30390. doi: 10.1074/jbc.273.46.30379

- Jones, C. L., Napier, B. A., Sampson, T. R., Llewellyn, A. C., Schroeder, M. R., and Weiss, D. S. (2012). Subversion of host recognition and defense systems by *Francisella* spp. *Microbiol. Mol. Biol. Rev.* 76, 383–404. doi: 10.1128/MMBR.05027-11
- Kagan, J. C., and Roy, C. R. (2002). Legionella phagosomes intercept vesicular traffic from endoplasmic reticulum exit sites. *Nat. Cell Biol.* 4, 945–954. doi: 10.1038/ncb883
- Lauriano, C. M., Barker, J. R., Yoon, S. S., Nano, F. E., Arulanandam, B. P., Hassett, D. J., et al. (2004). MglA regulates transcription of virulence factors necessary for *Francisella tularensis* intra-macrophage and intramacrophage survival. *Proc. Natl. Acad. Sci. U.S.A.* 101, 4246–4249. doi: 10.1073/pnas.0307690101
- Lindemann, S. R., McLendon, M. K., Apicella, M. A., and Jones, B. D. (2007). An *in vitro* model system used to study adherence and invasion of *Francisella tularensis* live vaccine strain in nonphagocytic cells. *Infect. Immun.* 75, 3178–3182. doi: 10.1128/IAI.01811-06
- Lindgren, H., Golovliov, I., Baranov, V., Ernst, R. K., Telepnev, M., and Sjostedt, A. (2004). Factors affecting the escape of *Francisella tularensis* from the phagolysosome. *J. Med. Microbiol.* 53, 953–958. doi: 10.1099/jmm.0.45685-0
- Llewellyn, A. C., Jones, C. L., Napier, B. A., Bina, J. E., and Weiss, D. S. (2011). Macrophage replication screen identifies a novel *Francisella* hydroperoxide resistance protein involved in virulence. *PLoS ONE* 6:e24201. doi: 10.1371/journal.pone.0024201
- Lonnbro, P., Nordenfelt, P., and Tapper, H. (2008). Isolation of bacteria-containing phagosomes by magnetic selection. *BMC Cell Biol.* 9:35. doi: 10.1186/1471-2121-9-35
- Malik-Kale, P., Jolly, C. E., Lathrop, S., Winfree, S., Luterbach, C., and Steele-Mortimer, O. (2011). Salmonella - at home in the host cell. *Front. Microbiol.* 2:125. doi: 10.3389/fmicb.2011.00125
- McCaffrey, R. L., and Allen, L. A. (2006). *Francisella tularensis* LVS evades killing by human neutrophils via inhibition of the respiratory burst and phagosome escape. *J. Leukoc. Biol.* 80, 1224–1230. doi: 10.1189/jlb.0406287
- Meyer, L., Broms, J. E., Liu, X., Rottenberg, M. E., and Sjostedt, A. (2015). Microinjection of *Francisella tularensis* and *Listeria monocytogenes* reveals the importance of bacterial and host factors for successful replication. *Infect. Immun.* 83, 3233–3242. doi: 10.1128/IAI.00416-15
- Moreau, G. B., and Mann, B. J. (2013). Adherence and uptake of *Francisella* into host cells. *Virulence* 4, 826–832. doi: 10.4161/viru.25629
- Munujos, P., Coll-Canti, J., Gonzalez-Sastre, F., and Gella, F. J. (1993). Assay of succinate dehydrogenase activity by a colorimetric-continuous method using iodinitrotetrazolium chloride as electron acceptor. *Anal. Biochem.* 212, 506–509. doi: 10.1006/abio.1993.1360
- Nano, F. E., Zhang, N., Cowley, S. C., Klose, K. E., Cheung, K. K., Roberts, M. J., et al. (2004). A *Francisella tularensis* pathogenicity island required for intramacrophage growth. *J. Bacteriol.* 186, 6430–6436. doi: 10.1128/JB.186.19.6430-6436.2004
- Napier, B. A., Meyer, L., Bina, J. E., Miller, M. A., Sjostedt, A., and Weiss, D. S. (2012). Link between intraphagosomal biotin and rapid phagosomal escape in *Francisella*. *Proc. Natl. Acad. Sci. U.S.A.* 109, 18084–18089. doi: 10.1073/pnas.1206411109
- Ozanic, M., Marecic, V., Abu Kwaik, Y., and Santic, M. (2015). The divergent intracellular lifestyle of *Francisella tularensis* in evolutionarily distinct host cells. *PLoS Pathog.* 11:e1005208. doi: 10.1371/journal.ppat.1005208
- Ozanic, M., Marecic, V., Lindgren, M., Sjostedt, A., and Santic, M. (2016). Phenotypic characterization of the *Francisella tularensis* DeltapdpC and DeltaiglG mutants. *Microbes Infect.* 18, 768–776. doi: 10.1016/j.micinf.2016.07.006
- Pfortner, H., Wagner, J., Surmann, K., Hildebrandt, P., Ernst, S., Bernhardt, J., et al. (2013). A proteomics workflow for quantitative and time-resolved analysis of adaptation reactions of internalized bacteria. *Methods* 61, 244–250. doi: 10.1016/j.ymeth.2013.04.009
- Qin, A., and Mann, B. J. (2006). Identification of transposon insertion mutants of *Francisella tularensis* tularensis strain Schu S4 deficient in intracellular replication in the hepatic cell line HepG2. *BMC Microbiol.* 6:69. doi: 10.1186/1471-2180-6-69
- Ray, K., Bobard, A., Danckaert, A., Paz-Haftel, I., Clair, C., Ehsani, S., et al. (2010). Tracking the dynamic interplay between bacterial and host factors during pathogen-induced vacuole rupture in real time. *Cell. Microbiol.* 12, 545–556. doi: 10.1111/j.1462-5822.2010.01428.x
- Ray, K., Marteyn, B., Sansonetti, P. J., and Tang, C. M. (2009). Life on the inside: the intracellular lifestyle of cytosolic bacteria. *Nat. Rev. Microbiol.* 7, 333–340. doi: 10.1038/nrmicro2112
- Rodriguez-Paris, J. M., Nolte, K. V., and Steck, T. L. (1993). Characterization of lysosomes isolated from *Dictyostelium discoideum* by magnetic fractionation. *J. Biol. Chem.* 268, 9110–9116.
- Rowe, H. M., and Huntley, J. F. (2015). From the outside-in: the *Francisella tularensis* envelope and virulence. *Front. Cell. Infect. Microbiol.* 5:94. doi: 10.3389/fcimb.2015.00094
- Santic, M., Akimana, C., Asare, R., Kouokam, J. C., Atay, S., and Kwaik, Y. A. (2009). Intracellular fate of *Francisella tularensis* within arthropod-derived cells. *Environ. Microbiol.* 11, 1473–1481. doi: 10.1111/j.1462-2920.2009.01875.x
- Santic, M., Al-Khodori, S., and Abu Kwaik, Y. (2010). Cell biology and molecular ecology of *Francisella tularensis*. *Cell. Microbiol.* 12, 129–139. doi: 10.1111/j.1462-5822.2009.01400.x
- Santic, M., Asare, R., Skrobbonja, I., Jones, S., and Abu Kwaik, Y. (2008). Acquisition of the vacuolar ATPase proton pump and phagosome acidification are essential for escape of *Francisella tularensis* into the macrophage cytosol. *Infect. Immun.* 76, 2671–2677. doi: 10.1128/IAI.00185-08
- Santic, M., Molmeret, M., and Abu Kwaik, Y. (2005). Modulation of biogenesis of the *Francisella tularensis* subsp. novicida-containing phagosome in quiescent human macrophages and its maturation into a phagolysosome upon activation by IFN- γ . *Cell. Microbiol.* 7, 957–967. doi: 10.1111/j.1462-5822.2005.00529.x
- Santos, J. C., and Enninga, J. (2016). At the crossroads: communication of bacteria-containing vacuoles with host organelles. *Cell. Microbiol.* 18, 330–339. doi: 10.1111/cmi.12567
- Santos, S. B., Carvalho, C., Azeredo, J., and Ferreira, E. C. (2015). Correction: population dynamics of a salmonella lytic phage and its host: implications of the host bacterial growth rate in modelling. *PLoS ONE* 10:e0136007. doi: 10.1371/journal.pone.0136007
- Shepard, C. C. (1959). Nonacid-fast bacteria and HeLa cells: their uptake and subsequent intracellular growth. *J. Bacteriol.* 77, 701–714.
- Shevchuk, O., Batzilla, C., Hagele, S., Kusch, H., Engelmann, S., Hecker, M., et al. (2009). Proteomic analysis of Legionella-containing phagosomes isolated from *Dictyostelium*. *Int. J. Med. Microbiol.* 299, 489–508. doi: 10.1016/j.ijmm.2009.03.006
- Shevchuk, O., and Steinert, M. (2013). Isolation of pathogen-containing vacuoles. *Methods Mol. Biol.* 983, 419–429. doi: 10.1007/978-1-62703-302-2_23
- Shin, S., and Roy, C. R. (2008). Host cell processes that influence the intracellular survival of Legionella pneumophila. *Cell. Microbiol.* 10, 1209–1220. doi: 10.1111/j.1462-5822.2008.01145.x
- Steele, S., Brunton, J., Ziehr, B., Taft-Benz, S., Moorman, N., and Kawula, T. (2013). *Francisella tularensis* harvests nutrients derived via ATG5-independent autophagy to support intracellular growth. *PLoS Pathog.* 9:e1003562. doi: 10.1371/journal.ppat.1003562
- Steele-Mortimer, O. (2008). The Salmonella-containing vacuole - Moving with the times. *Curr. Opin. Microbiol.* 11, 38–45. doi: 10.1016/j.mib.2008.01.002
- Surmann, K., Michalik, S., Hildebrandt, P., Gierok, P., Depke, M., Brinkmann, L., et al. (2014). Comparative proteome analysis reveals conserved and specific adaptation patterns of *Staphylococcus aureus* after internalization by different types of human non-professional phagocytic host cells. *Front. Microbiol.* 5:392. doi: 10.3389/fmicb.2014.00392
- Tamilselvam, B., and Daefler, S. (2008). Francisella targets cholesterol-rich host cell membrane domains for entry into macrophages. *J. Immunol.* 180, 8262–8271. doi: 10.4049/jimmunol.180.12.8262
- Telepnev, M., Golovliov, I., and Sjostedt, A. (2005). *Francisella tularensis* LVS initially activates but subsequently down-regulates intracellular signaling and cytokine secretion in mouse monocytic and human peripheral blood mononuclear cells. *Microb. Pathog.* 38, 239–247. doi: 10.1016/j.micpath.2005.02.003
- Touret, N., Paroutis, P., Terebiznik, M., Harrison, R. E., Trombetta, S., Pypaert, M., et al. (2005). Quantitative and dynamic assessment of the contribution of the ER to phagosome formation. *Cell* 123, 157–170. doi: 10.1016/j.cell.2005.08.018
- Urwiler, S., Finsel, I., Ragaz, C., and Hilbi, H. (2010). Isolation of Legionella-containing vacuoles by immuno-magnetic separation. *Curr. Protoc. Cell Biol.* Chapter 3, Unit 3.34. doi: 10.1002/0471143030.cb0334s46

- Vergne, I., Chua, J., Singh, S. B., and Deretic, V. (2004). Cell biology of mycobacterium tuberculosis phagosome. *Annu. Rev. Cell Dev. Biol.* 20, 367–394. doi: 10.1146/annurev.cellbio.20.010403.114015
- Vorwerk, S., Krieger, V., Deiwick, J., Hensel, M., and Hansmeier, N. (2015). Proteomes of host cell membranes modified by intracellular activities of *Salmonella enterica*. *Mol. Cell. Proteomics* 14, 81–92. doi: 10.1074/mcp.M114.041145
- Wehrly, T. D., Chong, A., Virtaneva, K., Sturdevant, D. E., Child, R., Edwards, J. A., et al. (2009). Intracellular biology and virulence determinants of *Francisella tularensis* revealed by transcriptional profiling inside macrophages. *Cell. Microbiol.* 11, 1128–1150. doi: 10.1111/j.1462-5822.2009.01316.x
- Wetzel, M. G., and Korn, E. D. (1969). Phagocytosis of latex beads by *Acanthamoeba castellanii* (Neff). 3. Isolation of the phagocytic vesicles and their membranes. *J. Cell Biol.* 43, 90–104. doi: 10.1083/jcb.43.1.90
- Conflict of Interest Statement:** The authors declare that the research was conducted in the absence of any commercial or financial relationships that could be construed as a potential conflict of interest.
- Copyright © 2017 Marecic, Shevchuk, Ozanic, Mihelcic, Steinert, Jurak Begonja, Abu Kwaik and Santic. This is an open-access article distributed under the terms of the Creative Commons Attribution License (CC BY). The use, distribution or reproduction in other forums is permitted, provided the original author(s) or licensor are credited and that the original publication in this journal is cited, in accordance with accepted academic practice. No use, distribution or reproduction is permitted which does not comply with these terms.



Innate Immune Recognition: Implications for the Interaction of *Francisella tularensis* with the Host Immune System

Zuzana Krocova, Ales Macela and Klara Kubelkova*

Department of Molecular Pathology and Biology, Faculty of Military Health Sciences, University of Defence, Hradec Kralove, Czechia

The intracellular bacterial pathogen *Francisella tularensis* causes serious infectious disease in humans and animals. Moreover, *F. tularensis*, a highly infectious pathogen, poses a major concern for the public as a bacterium classified under Category A of bioterrorism agents. Unfortunately, research has so far failed to develop effective vaccines, due in part to the fact that the pathogenesis of intracellular bacteria is not fully understood and in part to gaps in our understanding of innate immune recognition processes leading to the induction of adaptive immune response. Recent evidence supports the concept that immune response to external stimuli in the form of bacteria is guided by the primary interaction of the bacterium with the host cell. Based on data from different *Francisella* models, we present here the basic paradigms of the emerging innate immune recognition concept. According to this concept, the type of cell and its receptor(s) that initially interact with the target constitute the first signaling window; the signals produced in the course of primary interaction of the target with a reacting cell act in a paracrine manner; and the innate immune recognition process as a whole consists in a series of signaling windows modulating adaptive immune response. Finally, the host, in the strict sense, is the interacting cell.

Keywords: innate immunity, intracellular bacteria, immune recognition, *Francisella tularensis*, signaling windows concept, spatiotemporal network

OPEN ACCESS

Edited by:

Anders Sjöstedt,
Umeå University, Sweden

Reviewed by:

Lee-Ann H. Allen,
University of Iowa, United States
Jacqueline Sharon,
Boston University, United States

*Correspondence:

Klara Kubelkova
klara.kubelkova@unob.cz

Received: 11 April 2017

Accepted: 29 September 2017

Published: 16 October 2017

Citation:

Krocova Z, Macela A and Kubelkova K
(2017) Innate Immune Recognition:
Implications for the Interaction of
Francisella tularensis with the Host
Immune System.
Front. Cell. Infect. Microbiol. 7:446.
doi: 10.3389/fcimb.2017.00446

INTRODUCTION

The mammalian immune system defends against a variety of microbial pathogens. The innate and the adaptive immune responses closely collaborate in developing the stage for protective immunity against microorganisms. Early recognition of invading microorganisms is provided by germline-encoded pattern recognition receptors (PRRs) that recognize conserved microbial components known as pathogen-associated molecular patterns (PAMPs). One of the best-characterized PRRs is the still-growing family of Toll-like receptors (TLRs), which are type I integral membrane proteins recognizing such PAMPs as lipopolysaccharide (TLR4), bacterial lipoproteins (TLR2), flagellin (TLR5), and/or CpG DNA (TLR9). The members of this PRRs family are located at cell surface membranes (TLR5, TLR11, TLR4, and the heterodimers of TLR2–TLR1 or TLR2–TLR6), binding to their respective ligands at the cell surface. Others (TLR3, TLR7–TLR8, TLR9, and TLR13) are expressed on endosomal membranes, where they sense microbial and host-derived nucleic acids.

TLR4 localizes to both the plasma membrane and the endosomes (see, for example, O'Neill et al., 2013). Ligand-induced dimerization of TLRs leads to signaling by almost all TLRs (except TLR3) using the adaptor protein myeloid differentiation primary response gene 88 (MyD88). MyD88 activates transcription factor NF- κ B signaling via serine-threonine kinases IRAK1 and IRAK2 (Warner and Núñez, 2013). For some TLRs, other adaptor proteins are needed to assemble the receptor signaling pathway. Mal (also known as TIR adaptor protein—TIRAP) is necessary to recruit Myd88 to TLR2 and TLR4 to ensure signaling via IRAKs. In the case of TLR4, the MyD88-dependent or MyD88-independent TRIF/TRAM (TIR domain-containing adaptor inducing IFN- β /TRIF-related adaptor molecule) signaling pathways can be activated by lipopolysaccharide (LPS) of Gram-negative bacteria. Ligation of LPS to TLR4 is facilitated by lipopolysaccharide binding protein (LBP) and CD14 (Lu et al., 2008).

Both macrophages (M ϕ) and dendritic cells (DC), which act as a dominant phagocytic and antigen processing and presentation component of the immune system, are equipped, in addition to TLRs, with numerous membrane-bound and cytosolic receptors that can detect microbes. Among them are complement receptors, C-type lectin receptors (CR), and Fc γ receptors (Fc γ R) at the cell membrane, as well as cytosolic nucleotide-binding and oligomerization domain (NOD)-like receptors (NLRs) or interferon-inducible protein, also known as absent in melanoma 2 (AIM2). NLRs and AIM2 constitute the pattern-recognition components of inflammasomes, which sense nucleotide sequences appearing in the cytosol (Kim et al., 2016; Man et al., 2016a). Upon binding a ligand, NLRs as well as AIM2 assemble multiprotein complexes called inflammasomes, which drive pyroptosis and proteolytic cleavage of the proinflammatory cytokines pro-IL-1 β and pro-IL-18. The NLRs and/or AIM2 proteins recruit the inflammasome adaptor protein ASC (apoptosis-associated speck-like protein containing a caspase recruitment domain), which in turn interacts with pro-caspase-1 leading to its activation. Once activated, caspase-1 promotes maturation of the proinflammatory cytokines interleukin (IL)-1 β and IL-18 (Jin and Xiao, 2015; Xiao, 2015). The general scheme of signaling pathways associated with ligation of PRRs is presented in **Figure 1**.

Serious infectious diseases in humans and animals caused by intracellular bacteria pose a major concern for the public because, to date, researchers have failed to develop effective vaccines. The reasons lie in the complicated pathogenesis and incomplete understanding of the innate immune recognition processes controlling the generation of immune responses. Knowledge regarding both the innate immune recognition of pathogens and the outfit of pathogens enabling the avoidance of defensive reactions by host cells at the beginning and, subsequently, of the

whole host immune system response are the keys to constructing efficient prophylactic tools. Recent evidence supports the concept that the immune response to external stimuli in the form of bacteria is guided by the primary interaction of the bacterium with the host cell. In this review, we provide the basic paradigms of the innate immune recognition concept arising from analyses of data obtained from the various *Francisella* models.

FRANCISELLA TULARENSIS—ETIOLOGICAL AGENT OF TULAREMIA

Francisella tularensis (*F. tularensis*) is one of the most virulent microorganisms currently known. *Francisellae* are Gram-negative intracellular bacteria causing the zoonotic systemic disease tularemia (Carvalho et al., 2014). Although, the severity of illness varies greatly depending upon which *Francisella* subspecies induces the disease, the taxonomy of the genus *Francisella* is in fact somewhat uncertain. Currently, there are four recognized species: *F. endosymbionts*, *F. philomiragia*, *F. novicida*, and *F. tularensis* with three subspecies (*tularensis*, *holarctica*, and *mediasiatica*; Duncan et al., 2013). The majority of tularemia cases are caused by Type A *F. tularensis* subsp. *tularensis* found exclusively in North America and Type B *F. tularensis* subsp. *holarctica* found throughout the northern hemisphere. A big unknown has long been the taxonomy of *F. novicida*, which is frequently used as a model microorganism to study the pathogenesis of *Francisella* infections. Based on genomic, virulence, pathogenic, clinical, and finally ecological differences, between *F. novicida* and *F. tularensis*, it was recently suggested that *F. novicida* and *F. tularensis* be maintained as separate species (Kingry and Petersen, 2014).

The morbidity and mortality of infection caused by different *F. tularensis* strains vary also according to the gateway of infection. The most dangerous is the pneumonic form of tularemia, followed by gastrointestinal, ulceroglandular, and oculoglandular forms. *Francisella* invades and replicates within phagocytic cell types, such as M ϕ and DC, as well as structural tissue cells, included hepatocytes, alveolar type II cells, or endothelial cells. For this reason, *F. tularensis* has been occasionally called a promiscuous intracellular pathogen (Hall et al., 2008). *F. tularensis* has been previously shown to infect and replicate in M ϕ , both *in vitro* and *in vivo* (Thorpe and Marcus, 1964a,b; Nutter and Myrvik, 1966; Fortier et al., 1994). The attenuated *F. tularensis* type B live vaccine strain (LVS) replicates exponentially in mouse and human DC (Bosio and Dow, 2005; Ben Nasr et al., 2006), and the strain *F. tularensis* Type A Schu S4 efficiently infects and replicates in human myeloid DC (Chase et al., 2009). The CD11b(high) M ϕ , DC, monocytes, and alveolar type II cells in murine lung were shown to be infected after intranasal infection with several strains of *F. tularensis* (Hall et al., 2008). Murine peritoneal M ϕ (F4/80⁺), neutrophils (Gr-1⁺CD11b⁺), and surprisingly almost all B1a B cells (CD19⁺CD5⁺CD11b⁺) have also been shown to be infected at different frequency after experimental intraperitoneal infection induced by LVS (Plzakova et al., 2014).

Abbreviations: AIM2, absent in melanoma 2; BCR, B cell receptor; CR, complement receptor; hMDMs, human monocyte-derived macrophages; LPS, lipopolysaccharide; LVS, live vaccine strain; MAIT cells, mucosa-associated invariant T cells; MyD88, myeloid differentiation primary response protein; NLRs, nucleotide-binding and oligomerization domain (NOD)-like receptors; PAMPs, pathogen-associated molecular patterns; PRRs, pattern recognition receptors; TLRs, Toll-like receptors.

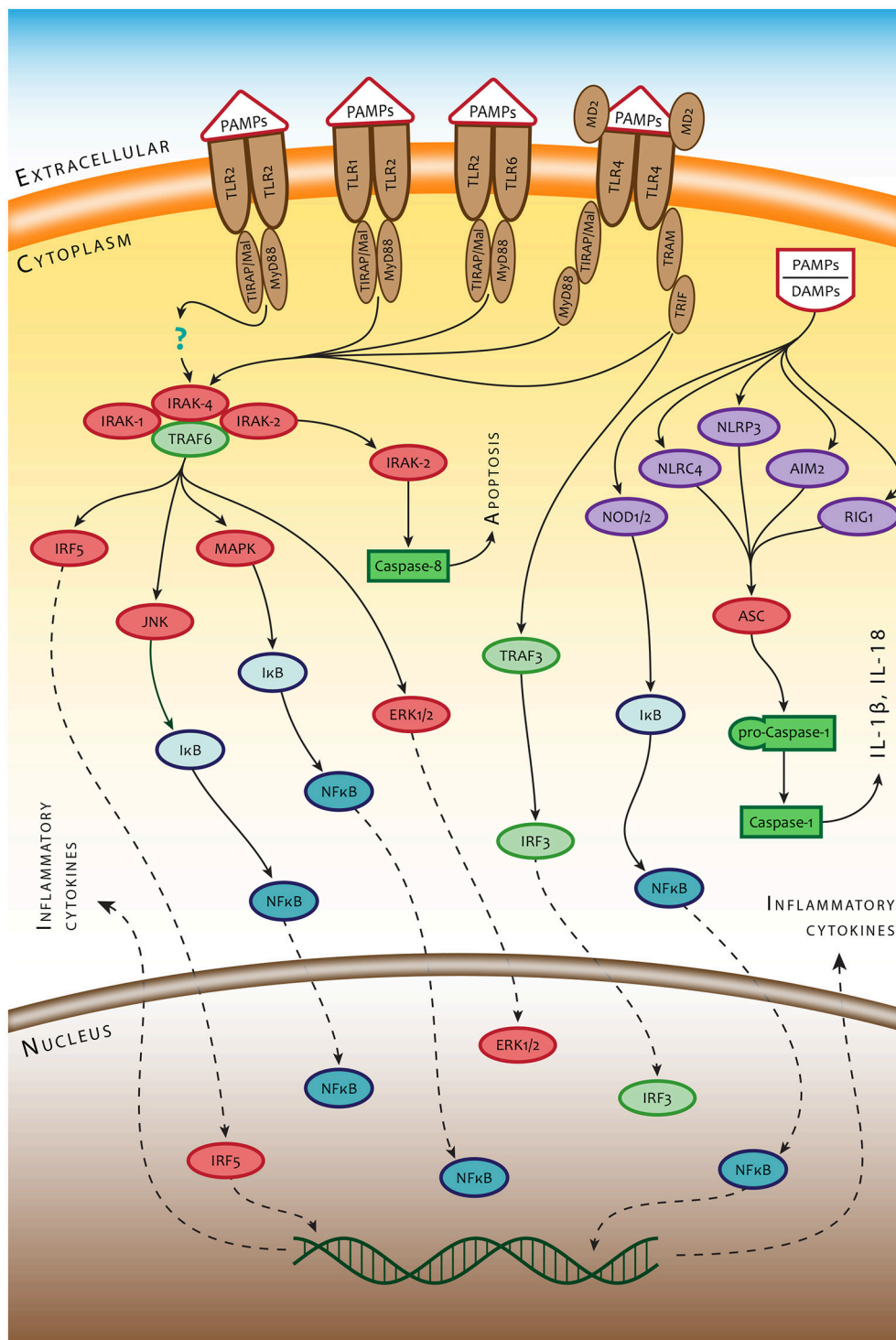


FIGURE 1 | Simplified scheme of innate immune recognition mediated by PRRs. TLR2/TLR1, TLR2/TLR6 heterodimers, and TLR2 homodimer are controlled mainly by the MyD88-dependent signaling pathway and/or the TRIF-dependent signaling pathway using sorting adaptors TIRAP/Mal and TRAM. MyD88 recruits IRAK4, IRAK1, IRAK2 and TRAF6 and induces inflammatory responses by activating NF- κ B, MAPK, and IRF5. TRIF recruits TRAF6 and TRAF3, which leads to activation of MAPK and NF- κ B. The signals from cell surface PRRs control the ultimate fate of the cell and production of intercellular signals inducing inflammatory response to infection. A different set of PRRs and amplification mechanisms operate in detecting bacteria inside the cytosol. Bacterial small nucleic acids secreted into the cytosol and bacterial mRNA are recognized by RNA-sensing RIG-1 or DNA-sensing Aim2 and NLRP3. Such structural components of bacteria as, for example, flagellin or peptidoglycan are recognized by NLRC4 and NOD1/2 receptors, respectively. Recognition of intracytosolic bacterial nucleic acids activates inflammasome(s) through the adaptor molecule ASC, which leads, in turn, to activation of caspase 1 and production of IL-1 beta (IL-1 β) and IL18.

The prophylaxis of tularemia infection is still problematic. The only vaccine, the live vaccine strain (LVS), is not authorized for human use. The current effort to construct a new *F. tularensis* vaccine is focused on developing both live attenuated and subunit vaccines. Live attenuated vaccine candidates are constructed by deleting genes involved mainly in metabolic and/or virulence pathways, which genes are necessary for *F. tularensis* intracellular replication and *in vivo* survival (Marohn and Barry, 2013). Subunit vaccine construction is oriented to *Francisella* molecular components that induce some degree of protection against lethal respiratory changes, for example surface proteins or lipoproteins administered with appropriate adjuvants or incorporated into liposomes (Putzova et al., 2016). A substantial challenge for vaccine development is to ascertain why *Francisella* seems to be immunologically silent for several days post infection. Vitally needed, therefore, is knowledge regarding host–pathogen interaction in general, and particularly during early stages of the innate immune response that modulate the induction, regulation, and expression of the adaptive immune response.

RECOGNITION AT THE HOST CELL MEMBRANE

As a Gram-negative bacterium, *F. tularensis* has LPS as a dominant component of its cellular surface. Similar to those of other Gram-negative bacteria, *F. tularensis* LPS is composed of lipid A, which anchors the LPS to the outer membrane, a core oligosaccharide attached to lipid A, 3-deoxy-D-manno-octulosonic acid (Kdo), and an O-polysaccharide (also known as O-antigen) which contains a varying number of tetrasaccharide repeating units (Gunn and Ernst, 2007). *Francisella* LPS also has many unusual characteristics, however, and these lead to unexpected consequences during innate immune recognition (Okan and Kasper, 2013). The LPS of gram-negative bacteria is generally recognized by TLR4/MD2, the PRR at the surface of a host cell, and induces a strong proinflammatory response (Maeshima and Fernandez, 2013; Park and Lee, 2013). One therefore could assume that TLR4 will be the dominant PRR recognizing *F. tularensis* at the cell membrane. Purified *F. tularensis* LPS has been shown, however, not to have an agonistic or antagonistic effect on the *Escherichia coli* LPS-induced activation of J774 cells and to have relatively weak endotoxic activity (Sandström et al., 1992; Ancuta et al., 1996; Telepnev et al., 2003; Hajjar et al., 2006). This has been somewhat surprising, because in a previous study the authors reported that TLR4-defective mice (C3H/HeJ strain) were more susceptible than wild-type mice to intradermal infection with LVS (Macela et al., 1996). The limited ability of *F. tularensis* LPS to signal via TLR4 might depend on some structural properties of the lipid A moiety, most likely related to the number and length of the acyl chain substituents and absence of phosphate moieties (Dueñas et al., 2006; Maeshima and Fernandez, 2013). In parallel, it was demonstrated that TLR4 does not contribute to resistance of mice to airborne type A *F. tularensis* infection or intradermal infection caused by LVS (Chen et al., 2004, 2005). Other studies also have demonstrated the inability of *F. tularensis* LPS to act

as either TLR agonists or antagonists (Ancuta et al., 1996; Hajjar et al., 2006). Nevertheless, some constituents of the bacterial body alone can function as TLR4 agonists. For example, the recombinant *F. tularensis* heat shock protein DnaK induced maturation of murine bone marrow-derived DC (demonstrated by an up-regulation of costimulatory molecules CD40, CD80, and CD86) and activated the production of proinflammatory cytokines (IL-6, TNF- α , and IL-12 p40, as well as low levels of IL-10) in a TLR4-dependent manner (Ashtekar et al., 2008). These findings may explain the observation (Macela et al., 1996) that TLR4-defective mice are more susceptible than wild-type mice to intradermal infection with LVS. Thus, TLR4 might, to some extent, be engaged in *Francisella* recognition at the cell membrane and, as a coreceptor, could modulate TLR2 signaling pathways downstream.

During the first decade of the twenty-first century, there appeared increasing evidence suggesting that TLR2 is involved in the recognition of *F. tularensis* on the surface of mouse innate immune system cells. TLR2 after ligation recognizes lipid-containing PAMPs such as lipoteichoic acid and di- and tri-acylated cysteine-containing lipopeptides, lipoarabinomannan from mycobacteria, or zymosan from yeast. The specific recognition of ligands by TLR2 is realized either in the form of TLR2 homodimer or as a heterodimer with TLR1 (recognizes tri-acylated lipopeptides) or TLR6 (recognizes the di-acylated ligand; Botos et al., 2011). Within *Francisella* models, TLR2 $^{-/-}$ mice had impaired bacterial clearance from livers, lungs, and spleens after intranasal challenge with a sublethal dose of *F. tularensis* LVS. Moreover, infected TLR2 $^{-/-}$ mice succumbed to a 10-fold lower challenge dose than did wild-type mice (Malik et al., 2006). Further studies documented that TLR2 of the mouse M ϕ and DC plays a significant role in the recognition of *F. tularensis* and functional activation of their antigen presenting function and controls the proinflammatory cytokine gene transcription (Katz et al., 2006; Li et al., 2006; Malik et al., 2006; Cole et al., 2007). DC from TLR2-deficient mice failed to produce IL-12p70 and did not co-stimulate liver lymphocytes for IFN- γ production in response to viable *F. tularensis* organisms (Hong et al., 2007). TLR2-dependent signaling appears to some extent to control *F. tularensis* infection and modulate inflammatory responses monitored by expression of proinflammatory cytokines and chemokines, such as TNF- α , IL-1 β , IL-6, M ϕ inflammatory protein 1 α , and M ϕ inflammatory protein 2 (Katz et al., 2006; Li et al., 2006; Malik et al., 2006; Abplanalp et al., 2009). TLR2 signaling seems to be dependent on new bacterial protein synthesis because the TLR2 agonist activity was abrogated when *F. tularensis* LVS organisms were heat- or formalin-killed or treated with chloramphenicol (Cole et al., 2007).

A substantial number of studies have identified TLR2 signaling as a critical event during the host innate immune response to *F. tularensis* infection. The data may indicate that, in a *Francisella* model, the TLR2 alone (perhaps as a homodimer—see for example Zheng et al., 2015; Udgate et al., 2016), rather than TLR2/TLR1 or TLR2/TLR6 heterodimers, play a critical role in *F. tularensis* recognition at the surface of immunocompetent cells (Abplanalp et al., 2009). Furthermore, a TLR2-independent pathway for activation of macrophages has also been identified

(Hong et al., 2007). Contrary to the majority of information, some data suggest that signals utilizing the adaptor protein MyD88 without the involvement of TLR2 are essential for controlling resistance to intradermal challenge with *F. tularensis* LVS but not for intra-macrophage bacterial multiplication (Collazo et al., 2006). Adaptor protein MyD88 is used by almost all TLRs (except TLR3) to activate the transcription factor NF- κ B (Lord et al., 1990). TIRAP/Mal (TIR domain-containing adaptor protein/MyD88-adaptor-like), an adaptor protein closely related to MyD88, is necessary to recruit Myd88 to TLR2 as well as to TLR4 (Hornig et al., 2001, 2002). In the context of other *Francisella* studies it was demonstrated that the molecular complex of TLR2/MyD88 (signaling through IRAKs; Arancibia et al., 2007) is indispensable for NF- κ B activation initiating macrophage proinflammatory cytokine production and, subsequently, protective innate immune responses in mice following challenge with attenuated as well as virulent *F. tularensis* strains (Collazo et al., 2006; Abplanalp et al., 2009; Cole et al., 2010; Russo et al., 2013).

Recognition of *Francisellae* at the host cell membrane is a fundamental step in its life cycle because it facilitates bacterial entry into host cells. This event is not exclusively a matter of TLRs. Such receptors as C-type lectin receptors, complement receptors (CR), and Fc-gamma receptors (Fc γ R) were shown in a specific situation to recognize either unopsonized or opsonized bacteria. The presence of natural opsonins in an experimental setup has a major role in the early phases of host-pathogen interactions and alters the intracellular fate of bacteria (Dai et al., 2013). Several models of *Francisella*-host cell interaction have identified the receptors engaged in the *Francisella* uptake at the host cells surface. The mannose receptor, one of the C-type lectin receptors (Balagopal et al., 2006; Schulert and Allen, 2006), the complement receptors CR3 (CD11b/CD18) in the case of M ϕ (Clemens et al., 2005; Balagopal et al., 2006; Geier and Celli, 2011), CR4 (CD11c/CD18) in the case of DC (Ben Nasr et al., 2006), and CR1/2 in the case of B cells (Plzakova et al., 2015), the scavenger receptor A (SRA) (Pierini, 2006; Geier and Celli, 2011), Fc γ Rs (Balagopal et al., 2006; Geier and Celli, 2011), and surface-exposed nucleolin with its bacterial ligand EF-Tu (Barel et al., 2008, 2010; Barel and Charbit, 2014) are involved in internalization of *Francisellae* into host cells.

Opsonization of *F. tularensis* Schu S4 strain with fresh serum or purified antibodies reoriented the interaction of bacteria with mouse bone marrow-derived M ϕ from the mannose receptor to the complement receptor CR3, the scavenger receptor A (SRA), and the Fc γ R (Geier and Celli, 2011). Experimental data demonstrated that opsonization of bacteria prior to engulfment by phagocytes substantially changes the intracellular fate of the bacteria and modulates parameters of the host APCs response to infection. CR3-mediated uptake of *Francisellae* negatively modulated maturation of the early *Francisella*-containing phagosome (FCP) and minimize phagosomal escape, whereas Fc γ R-dependent phagocytosis was associated with intensive superoxide production in the early FCP, a rapid, Fc γ R-mediated, NADPH oxidase-dependent oxidative burst, and restricted phagosomal escape (Geier and Celli, 2011). Serum opsonins modulate maturation of human monocyte-derived

immature DC and change their cytokine production profile in favor of IL-10 at the expense of IL-12 production (Ben Nasr et al., 2006). Efficient attachment and uptake of the highly virulent Type A *F. tularensis* subsp. *tularensis* strain Schu S4 by human monocyte-derived macrophages (hMDMs) require complement C3 opsonization and CR3. A complex cascade of events ending in uptake of *Francisellae* by phagocytes can initiate natural IgM binding to surface capsular and/or O-Ag polysaccharides of *F. tularensis*, a process activating classical complement cascade via C1q and promoting C3 opsonization of the bacterium and phagocytosis via CRs in a phagocyte-specific manner. CR1 (CD35) and CR3 (CD11b/CD18) have been observed to act in concert for phagocytosis of opsonized *F. tularensis* by human neutrophils, whereas CR3 and CR4 (CD11c/CD18) mediated uptake by hMDMs (Schwartz et al., 2012b). However, the CR3 engagement in an efficient uptake of *Francisellae* by hMDMs, in parallel, initiated CR3-TLR2 crosstalk leading to down-regulation of TLR2-dependent proinflammatory responses by inhibiting MAPK activation through outside-in signaling (Dai et al., 2013). Thus, such complex activation of several receptor signaling pathways influences the result of host-microbe interaction.

Taken together, the entry of *Francisellae* into host cells can be realized either by uptake of unopsonized or opsonized bacteria. In real *in vivo* situations, using natural infections, however, the uptake of opsonized bacteria is probably much more frequent than contact of host cells with unopsonized microbes. This latter mode of cell infection comes into play only during phagocytosis of whole infected cells by bystander phagocytes or during cytosolic transfer between macrophages via the process known as trogocytosis (Bourdonnay and Henry, 2016; Steele et al., 2016). Engagement of opsonophagocytic receptors alters the intracellular trafficking of *Francisella* by modulating the phagocytic pathways that restrict phagosomal escape and intracellular proliferation. Both can impact profoundly the final fate of *Francisella* in a host by modulating the intracellular recognition of *Francisella* in a cytosolic compartment of a host cell. These facts should be taken into account when designing *in vitro* experimental cell infection systems.

INNATE RECOGNITION AT INTRACELLULAR COMPARTMENTS

Uptake of *Francisella* by host cells is dependent on actin polymerization and functional microtubules in both phagocytic and nonphagocytic cells (Clemens and Horwitz, 2007; Lindemann et al., 2007). The mechanism of *Francisella* entry into host cells is dependent on the host cell type and the conditions under which the interaction with host cells takes place. One of the specific forms of entry is the formation of asymmetric, spacious pseudopod loops around live or killed bacteria (Clemens et al., 2005). More general mechanisms include macropinocytosis that had been demonstrated for the entry of *Francisella* LVS into type II alveolar epithelial cells or, rarely, during infection of macrophages with LVS (Clemens et al., 2005; Bradburne et al., 2013). Early after interaction with host

cell surface receptors *Francisella* is enclosed in a phagosome. There is no information available as to whether the bacteria are recognized during this stage of intracellular trafficking in spite of the fact that phagosomal PRRs recognize bacterial molecular markers (for example, phagosomal TLR9 has the capacity to recognize bacterial CpG motifs). The only information on intracellular colocalization of *Francisella* and TLR2 and MyD88 within macrophages suggests that *Francisella* LVS initiates signaling through TLR2 both at the cell surface and within the phagosome (Cole et al., 2007). The original engagement of the cell membrane PRRs and opsonophagocytic receptors on the cell surface, through which the mutual interaction of *Francisella* with a host cell is realized, produces the signals that dictate the fate of *Francisella* during intracellular trafficking (see, for example, Geier and Celli, 2011). Through modulation of phagosome biogenesis, *Francisella* escapes from its initial phagosome into the cytosol of a host macrophage.

Escape from the phagosome is the second fundamental step in the *Francisella* life cycle. This event is very dynamic, and experimental data has documented that phagosomal escape occurs within several tens of minutes to several hours post infection, depending upon the experimental setup (Golovliov et al., 2003; Clemens et al., 2004; Santic et al., 2005, 2008; Checroun et al., 2006). The cytosolic compartment of infected cells enables the proliferation of *Francisellae*. Once in the cytosol, however, the bacterial load is monitored by intracellular cytosolic DNA sensors, such as DNA-dependent activator of IFN-regulatory sensor (Takaoka et al., 2007), RIG-I (Ablasser et al., 2009), and/or AIM2 (Fernandes-Alnemri et al., 2009; Hornung et al., 2009; Jones et al., 2010), or by cytosolic nuclear oligomerization domain (NOD)-like receptors (NLRs) (Franchi et al., 2008, 2009). Both types of sensors are critical for innate defense by recognizing conserved structures of microorganisms. Upon sensing adequate ligands, these cytosolic PRRs trigger oligomerization of the inflammasome complex. Once completed, inflammasomes interact with 45-kDa pro-caspase 1, which undergoes auto-proteolytic processing that results in active caspase 1 (Thornberry et al., 1992; Miller et al., 1993; Ayala et al., 1994; Wilson et al., 1994). Subsequent cleavage of pro-IL-1 β and pro-IL-18 into their mature forms is critical for the host response to infection and is accompanied by caspase-1-dependent inflammatory cell death—pyroptosis (Man and Kanneganti, 2015).

Most information related to cytosolic recognition of *Francisella* has originated from *F. novicida* experimental models. Mice lacking AIM2, ASC, or caspase-1 are highly susceptible to infection and exhibit an increased bacterial burden compared with wild-type mice (Mariathasan et al., 2005; Fernandes-Alnemri et al., 2010; Jones et al., 2010). Macrophages from mice lacking AIM2 cannot sense cytosolic double-stranded DNA and fail to trigger inflammasome assembly. Immunofluorescence microscopy of macrophages infected with *Francisella* further revealed striking colocalization of bacterial DNA with endogenous AIM2 and inflammasome adaptor ASC (Jones et al., 2010). For the intracytosolic recognition of *Francisella*, therefore, the assembly of inflammasome and the accessibility of bacterial DNA or other molecular

components of the bacteria are key events. In the case of AIM2 inflammasome and *Francisella*, the critical role seems to be the integration of innate immune signaling. TLR2 signaling through MyD88 and NF- κ B in macrophages infected with *F. novicida* contributes to the rapid induction of inflammasome assembly and inflammasome functional activation (Jones and Weiss, 2011). How the recognizable bacterial components in the cytosol are produced is still under investigation. They can be produced directly in the cytosol or, alternatively, can originate from dead, partially destroyed bacteria released into the cytosol after fragmentation of the phagosomal membrane by live, fully active bacterial partners entrapped in a phagosome together with dead ones. For direct destruction of bacteria residing in the cytosol it can be argued that assembly and activation of the AIM2 inflammasome during infection with *F. novicida* requires transcription factor IRF1. The DNA sensor cGAS and its adaptor STING (Sun et al., 2013; Wu et al., 2013) induce type I interferon-dependent expression of IRF1. The IRF1 subsequently modulates the expression of guanylate-binding proteins (GBPs) that can ensure intracellular killing of bacteria and mediate cytosolic release of ligands for recognition by the AIM2 inflammasome (Man et al., 2015). Moreover, the interferon-inducible protein IRGB10 participates in the cytosolic destructive process of *F. novicida* by a mechanism requiring guanylate-binding proteins (Man et al., 2016b). Just because they are recognized by cytosolic DNA sensors does not necessarily mean that the bacteria will be killed; their product, cyclic dinucleotides, is sensed by STING directly and can initiate the innate immune response (see below).

Evidence of type I IFN involvement in the process of cytosolic recognition of *Francisella* by the inflammasome documents the need for multifold signal integration during adaptation of cells to recognize intracellular pathogens during primary interaction with host cells (Henry et al., 2007). Type I IFN signaling was observed to be necessary for activation of the inflammasome during infection with *F. novicida*. Production of type I IFN was coupled with recognition of cytosolic *F. novicida*. The process of *F. novicida* recognition was dependent on IRF-3 signaling and independent of signaling from RIG-I, MDA5, Nod1/2, and inflammasome adaptors. It was also independent of TLR signaling, which evidently demonstrated the intracytosolic recognition process (Henry et al., 2007). Production of type I IFN by BMDM after infection with *F. tularensis* LVS was observed to be dependent on STING, also known as MITA, MPYS, ERIS, and TMEM173. STING functions as both a direct cytosolic DNA sensor and an adaptor protein utilizing different molecular mechanisms (Ishikawa and Barber, 2008; Ishikawa et al., 2009). Downstream, STING activate transcription factors STAT6 and IRF3 through kinase TBK1 (Burdette and Vance, 2013). Signaling utilizing STING by cultured macrophages infected with LVS was required for type I IFN production, however, in parallel; a STING-dependent as well as a STING-independent signaling pathway were activated in *in vivo Francisella* infection models (Jin et al., 2011). The cyclic GMP-AMP synthase cGAS (Sun et al., 2013), as well as IFI214, a murine homolog of IFI16 (Unterholzner et al., 2010; Veeranki and Choubey, 2012), act as cytosolic DNA sensors and seem to be involved in the

sensing of intracytosolic *Francisella* DNA; both contribute to STING-dependent type I IFN response to high concentrations of cytosolic dsDNA (Storek et al., 2015). Moreover, as a direct innate immune sensor, STING alone can recognize cyclic dinucleotides (c-di-AMP and c-di-GMP), which are produced by bacteria, and mediate type I IFN cell response (Burdette et al., 2011; Barker et al., 2013).

To recapitulate and summarize the studies on intracytosolic recognition of *Francisella*, there are multiple intracytosolic signaling pathways that can, alone or in tandem, ensure the recognition of *Francisellae* localized in cytosolic compartment of a host cell. Reasons for these findings may be several. Unterholzner (2013) summarizes possible answers to the question of why so many receptors recognize DNA localized in the cytosol (nucleus) and induce an interferon response. First, receptors may have redundant functions. Further, DNA receptors may differ in their ligand specificity, different DNA receptors operate in different cell types, and/or receptors may act sequentially over time. Finally, some of the proposed DNA sensors may not be receptors. For our model of the intracellular pathogen *Francisella*, it can be concluded that at least two basic intracytosolic recognition processes are indispensable for expression of a proinflammatory response to infection. First, and in general, it is such recognition which results in the production of type I IFN needed for activation of IRFs. The second process is the expression of components and their assembly into inflammasome, by which the *Francisella* is recognized and the production of proinflammatory IL-1 β and IL-18 cytokines is ensured.

SIGNALING WINDOWS CONCEPT—SPATIOTEMPORAL NETWORK OF CELLULAR HOSTS

The emerging concept of signaling windows of innate immune recognition is based on the idea that there exist functional cellular immune response modules that temporarily, in spatiotemporal configuration, regulate innate immune recognition and sequentially modulate induction, regulation, and expression of the adaptive immune response. Intracellular pathogens such as *Francisella* are ideal models to construct realistic scenarios of innate immune recognition. Utilizing integrated approaches and analyzing the fate of mutual host cell–pathogen interaction, recent complex dynamic studies on immune cell networking have attempted to overcome the traditional static view on induction of immune cell signaling during induction of the immune response (see, for example, Nunes-Alves et al., 2014; Budak et al., 2015; Hotson et al., 2016; Rothchild et al., 2016). The *Francisella* experimental infection models provide sufficient information for attempting to construct the architecture of innate immune signaling windows. The basic paradigms of the signaling window concept define, in the strict sense, a cell as a decisive host of microbes and accept the idea of functional cellular modules of immune responses. The concept encompasses several basic assumptions: (1) There is a “jumble” of cellular hosts within a multicellular organism infected by bacteria. (2) Cellular hosts

create a four-dimensional net in the host organism. (3) Cellular hosts recognize and respond to interaction with the bacterium on spatiotemporal levels. (4) The host cell with which a microbe originally interacts forms the first signaling window. (5) Every spatiotemporal level opens a new signaling window. (6) The interplay among individual signaling windows ensures paracrine cytokine messages induced by microbial challenge. (7) Signaling windows integrate innate immune recognition signals. (8) PRRs cross-inhibition and interference of host and microbe signals influence the result of host–microbe interaction.

Macrophages and DC, which have been most utilized for studies on innate immune recognition, are not the only cells that recognize *Francisellae* in the context of the innate immune response. Moreover, TLRs are not the only cell surface receptors engaged in the innate immune recognition. *Francisella* infects phagocytic as well as nonphagocytic cells. Along with macrophages and DC, neutrophils (Löfgren et al., 1983; Hall et al., 2008), B cells (Plzakova et al., 2014), endothelial cells (Forestal et al., 2003), epithelial cells (Gentry et al., 2007; Lindemann et al., 2007), and/or hepatocytes (Law et al., 2011; Rennert et al., 2016) are all potential primary targets of *Francisella*. All these are permissive, and all are significant producers of signals representing the first signaling window. Neutrophils utilize a combination of NADPH oxidase-derived reactive oxygen species (ROS), antimicrobial peptides, and degradative enzymes to kill engulfed microorganisms for innate host defense (Kennedy and DeLeo, 2009). Phagocytosis of microorganisms leads very quickly to neutrophil apoptosis, which is known also as phagocytosis-induced cell death (Kobayashi et al., 2003). Tested strains of *Francisella*, however, inhibit the respiratory burst and profoundly prolong neutrophil lifespan (Schwartz et al., 2012a). In parallel, at the gene level, *Francisella* infection of neutrophils enhances expression of such neutrophil-specific survival factors as *cdk2* or *cdk7*, cytokine and chemokine genes that promote inflammation as well as neutrophil survival (*Il1b*, *Il1rn*, *Il6*, *osm*, *pbe1*, *cxcl1*, *Occl4*, *cxc4*). *Francisella* also has been shown to significantly affect expression of genes associated with cytosolic pattern recognition systems and inflammasome activation, as well as with early induction of *NLRP3* and *NOD2* followed by down-regulation of *AIM2*, *NAIP*, *PYCARDI*, and *NLRP1*. As in other cells that may be regarded as providing the cellular background of the first signaling window, *Francisella* escapes from the phagosome into the neutrophil cytosol (McCaffrey and Allen, 2006), where it might be recognized by inflammasomes or NOD-like receptors. B cells are engaged in the strong early protective response against *F. tularensis* LVS (Culkin et al., 1997). As early as 12 h post infection, peritoneal CD19(+) cells produce IFN- γ , IL-1 β , IL-4, IL-6, IL-12, IL-17, IL-23, and TNF- α (Plzakova et al., 2014). Mice deficient in mature B cells and antibodies (B-cell knockout mice) actually control primary sublethal infection but are 100-fold less well protected against a secondary lethal challenge (Elkins et al., 1999). Direct contact and entry of *Francisella* into B cells, depending on a given B cell subset, are mediated by B cell receptors (BCRs) with or without complement receptor CR1/2. In the B-1a cell subset, BCRs alone can ensure the internalization process, whereas BCRs on B-1b and B-2 cells require co-signaling

from the coreceptor containing CR1/2 in order to initiate *F. tularensis* engulfment (Plzakova et al., 2015). The production of IL-1 β by infected B cells suggests early cytosolic innate immune recognition after interaction of *Francisella* and B cell. At some stage of dissemination into various organs, *Francisella* must overcome the endothelial barrier in the microvasculature by one of three well-known mechanisms: transcellular, paracellular, or the so-called Trojan horse mechanism (i.e., crossing the barrier using infected phagocytes). To achieve this, *Francisella* readily adheres to the endothelial cell surface and uses Pile4 (type IV pili subunit) to interact with ICAM-1 molecule, adhere to the endothelial surface, and cross the endothelial barrier *in vivo* as well as *in vitro* (Bencurova et al., 2015). Endothelial as well as epithelial cells and hepatocytes produce a variety of cytokines at various levels after interaction with bacteria. This is just a reason for modulation of the functional profile of cells subsequently interacting with *Francisellae*, and in the suggested concept it corresponds to opening of the secondary signaling windows.

As part of innate immune response, moreover, unconventional T cell subsets might be engaged in innate immune recognition and constitute a bridge between innate and adaptive immune responses. This might be achieved through unconventionally presented byproducts or intermediates of bacterial metabolism secreted by the bacteria early after interaction with the host cells. Human V γ 9/V δ 2 T cells recognize specifically, in a non-MHC restricted manner, microbial isoprenoid precursor (*E*)-4-hydroxy-3-methyl-but-2-enyl pyrophosphate (HMB-PP), which is an intermediate of the microbial non-mevalonate pathway of isoprenoid biosynthesis utilized by most pathogenic Gram-negative and Gram-positive bacteria (Eberl and Jomaa, 2003; Eberl et al., 2003; Heuston et al., 2012). This molecule can function as a danger signal because HMB-PP is not present in higher eukaryotes, including humans (Sicard and Fournie, 2000; Morita et al., 2007). One of the consequences of the human V γ 9/V δ 2 T cells–pathogen interaction, and, in a broader sense, of their activation, is the rapid acquisition of antigen presenting cell characteristics that are reminiscent of mature DC (Moser and Eberl, 2011; Tyler et al., 2015), and in such way they can function as a primary signaling window. Concerning human tularemia, V γ 9/V δ 2 T cells expand after infection and comprise on average 30% of human peripheral blood T lymphocytes, thus suggesting some role in control of *F. tularensis* infection (Poquet et al., 1998). Experiments with co-culture of human V γ 9/V δ 2 T cells isolated from healthy donors with the THP-1 human monocyte cell line infected with *F. tularensis* has demonstrated the ability of V γ 9/V δ 2 T cells to recognize infection, to produce a whole range of cytokines and chemokines (including IL-1 β , IL-6, and IFN- γ , but not IL-10), and to limit bacterial proliferation in the culture (Rowland et al., 2012). Another unconventional T cell subset, mucosa-associated invariant T (MAIT) cells, also responds very early and intensively to *F. tularensis* infection. A murine *in vivo* model of sublethal *F. tularensis* LVS pulmonary infection demonstrated robust expansion of MAIT cells in the lungs during the early acute phase of infection. The MAIT cells recognized vitamin B metabolites in association with evolutionarily conserved MHC-related protein 1 (Kjær-Nielsen

et al., 2012), which possesses a unique antigen-binding cleft producing an antigen presenting function on this cell type (Huang et al., 2005). Because vitamin B biosynthesis pathways are unique to bacteria and yeast, MAIT cells may also constitute one of the primary signaling windows.

Knowing that the severity and time course of tularemia is, at least in an experimental setup, dependent on the route of infection, we can accept the view that these differences are due, at least in part, to the various types of original cellular hosts that convey primary interaction with the bacteria. Thus, the initial signals originating from different infected cell types might dictate the outcome of primary host cell–bacterium interaction, which in turn affects all subsequent events during the induction of immune responses. The cells that interact with the *Francisellae* in the first sequence create a timeframe for modulating the functional profile of cells that will interact with the bacterium in a secondary order. The intercellular contact is mediated by an integrated cytokine message produced by originally infected cellular “senders.” To our knowledge, the lifetime of infected cells in the case of macrophages is from 12 to 18 h post infection, depending on the experimental model (Libich, 1981). The transient bacteremia contributing to spreading *Francisellae* over the body begins 24–48 h post infection, which is thus the timeframe for changing the microenvironment for as yet uninfected cells. Cellular “receivers” located in a given microenvironment can thus respond accordingly. We hypothesize that the modulated functional profile of a secondarily reacting cell will be dependent on the type of cell that initiates the cytokine messages as well as on the expressed cell surface receptors able to recognize the cytokine messages and simultaneously (or subsequently) recognize incoming bacterium. The cytokine response of a cellular “receiver” of the same cell type as the cellular “sender,” whether infected or not, would necessarily be different from the message produced by the originally infected cell. Moreover, in the case of antigen presenting cells reacting in the secondary order, the recognition, handling, and processing the interacting bacteria might be quite different from the processes of the primary infected cells and could have a profound impact on the expression of the adaptive immune response. An example is the paracrine action of type I IFN, which changes the transcriptional response to innate immune recognition of *Francisellae* by infected primary human monocyte-derived macrophages and primary murine peritoneal macrophages but not by murine bone marrow-derived macrophages. This type I IFN-dependent modulated response of infected cells is synergistic with TLR2 transcriptional responses, partially TLR2-independent, but strictly MyD88-dependent, thus suggesting the supplementary action of co-receptor(s) (Richard et al., 2016). Alternatively, it could demonstrate the modulated function of cells reacting to *Francisellae* as a receiver of signals generated by cells infected in the primary order. An example can be seen in the signaling through IL-1 receptor of cells infected with *Francisellae* in a secondary order (Figure 2).

Thus, in our opinion, the data from the literature indicate that the differences in severity of tularemia depending on the route of infection can originate from differences in the local microenvironments and types of cells that are first infected

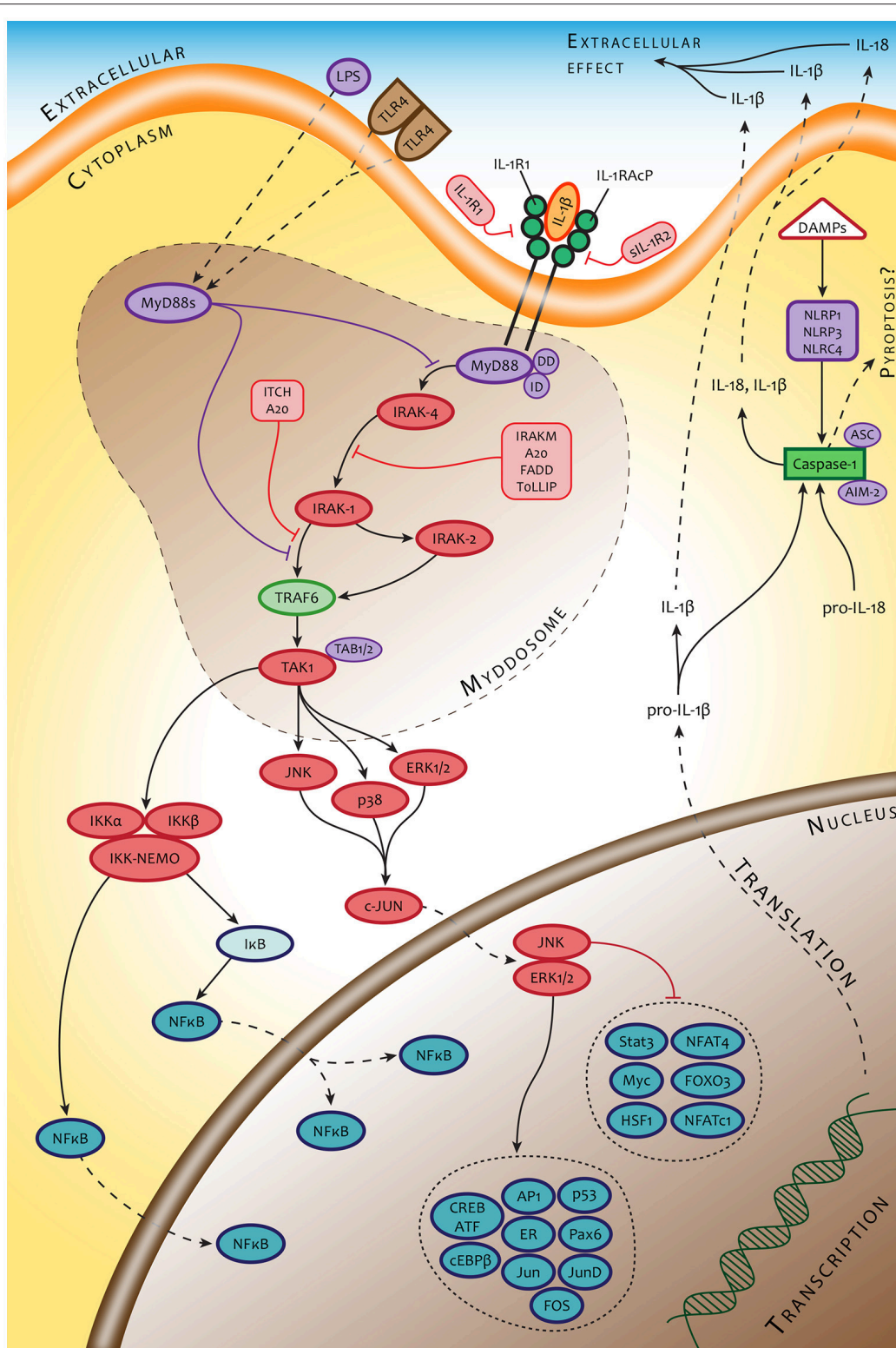


FIGURE 2 | An example of signaling pathways of cells interacting with *Francisella* in secondary order. The signaling pathways of these cells are modulated by signals originating from a primary responding cell (IL-1 β) or collateral signals from invading microbes (LPS).

with *Francisella*. As an example, the difference in LD50 after aerogenic and subcutaneous *F. tularensis* infection of mice is greater than six logarithms. Route of infection dominates over genetic background of recipients in the severity of illness. In the case of genetic background, the difference in LD50 for susceptible and resistant mice is less than three logarithms (Fortier et al., 1994). The reason for these differences can be seen in the different primary cellular hosts of *Francisellae*. Langerhans cells are primarily infected in dermis whereas alveolar macrophages are predominantly infected in the lungs. Such conclusion can also be deduced by comparing intranasal- vs. intradermal-induced murine tularemia (Roberts et al., 2014), which may be an example testifying to the concept proposed above.

The basic experiments with individual cell types and opsonizing bacteria have demonstrated not only the importance of responding cell type to primary interaction with *Francisella* but also the importance of type of expressed surface membrane receptor involved in the primary contact with the bacterium. Complement factors, such as ubiquitous opsonins in mammals, are critical factors mediating adhesion and subsequently internalization of *Francisellae* into host cells. The co-signaling from different surface receptors engaged in the adhesion of the bacterium modulates the response of host cells. There is an obvious dichotomy in macrophage response to interaction with C3 opsonized or unopsonized microbes, especially in relation to inflammatory response due to the interference of signaling pathways (Dai et al., 2013). Moreover, *Francisella* itself modulates the signaling pathways of infected cells. The data demonstrate, for example, that *F. tularensis* fails to induce production of proinflammatory cytokines or IFN- γ , inhibits increased expression of activation markers, including MHCII, on the surface of professional APCs, and suppresses activation of the inflammasome during early *Francisella* infection via targeting of TLR2-dependent signaling (Bosio and Dow, 2005; Bosio et al., 2007; Parsa et al., 2008; Chase et al., 2009; Dotson et al., 2013). There is uncertainty in the interpretation of these results, however, because much of this data was generated using different experimental setups and in different time proportions. Moreover, the majority of these studies were based on entirely artificial conditions not corresponding to *in vivo* situations (natural opsonization of bacteria and very high multiplicity, which is quite exceptional for natural infection). Some conclusions have been generalized according to the final fate of the eukaryotic host cell/organism–pathogen interaction using a traditional, more or less static experimental arrangement. To solve the general problem of innate immune recognition's involvement in the process of protective immunity induction, analyses are needed of the so-called social network of immune cells that participate in the early stages of infection.

To conclude the possible sequence of events during innate immune recognition of *Francisella* according to the emerging concept of signaling windows, we can formulate a minimum of four basic assumptions: (1) The first batch of signals, resulting from natural recognition of *Francisella* inside the multicellular organism, depends on the type of interacting cell and its surface receptor(s), which mediate(s) primary pathogen conjunction with the host cell. (2) *Francisella*–host cell interaction at the single-cell level corresponds to the concept of crosstalk between

innate immune receptors and integrates the signals into a prototypic signaling response corresponding to a particular cell type. (3) During the process of *Francisella* innate immune recognition, cells form a four-dimensional signaling network represented by signaling windows. This means that the concept reflects the spatiotemporal changes in the function of the individual cells that are engaged in immune recognition, which are caused by changing microenvironment over time. Integrated signals at the level of signaling windows generate a new signal for “opening” the additional signaling window. (4) Interference of host and microbe signals at a single-cell level can subvert and reprogram PPRs-mediated innate immune responses.

CONCLUSIONS AND PROSPECTS

Innate immune response constitutes the first line of defense against bacterial infection. Data collected from germ-free as well as specific pathogen free animal models of microbial pathogenesis demonstrate the dependency of induce and adaptive immunity on primary interaction between a microorganism and the host cell that the microbe first encounters. The innate immune recognition process plays a dominant role along with the intrinsic characteristics of the microorganism and host. The epigenetic reprogramming of innate immune cells, creating the hierarchy of immune response functional modules, is critical for inducing and regulating expression of the adaptive immune response. This process is extremely dynamic and the populations of individual cell types, whether infected or uninfected, change their functional characteristics depending on the local microenvironment modulated by the cells that were originally infected even at a distant place. If this is the case, then not all the cells of the same cell type in the body will respond to infection in an identical way at a given time. From this point of view, the cell, with its functional and secretion profile, rather than the host organism in its entirety, seems to be the primary microbe host (Kubelkova et al., 2016). In the case of *in vitro* *Francisella* models, the literature presents quite different conclusions concerning the outcome of *Francisella* innate immune recognition. Some studies provide evidence that *F. tularensis* LVS represses inflammasome activation, while other studies have demonstrated that *F. tularensis* LVS increases mRNA levels of proinflammatory cytokines and this is followed by increased protein secretion. Moreover, data from experiments with host-adapted *Francisella* LVS isolated from infected macrophages explain this heterogeneity of results by a “stealthy mode” of intra-host lifestyle (for a review, see Holland et al., 2016).

The host cells as well as invading *Francisellae* are affected by their “historical memory” and mutually generate, at any given time, an immediate microenvironment that should be respected in the generation of new infection models. In our experience, for example, germ-free mice infected subcutaneously with *F. tularensis* reacted differently to attenuated and virulent strains in comparison with specific-pathogen free mice. These mice, not having had contact with bacteria in ontogeny, can demonstrate the unique primary reaction of their immune systems to a pathogenic bacterium and can help us to understand the

processes that lead to the establishment of full-fledged protective immunity. To understand the innate immune response to infection we need to obtain multidimensional data sets providing comprehensive, cell-specific, and time-structured information on epigenetic reprogramming of innate immune cells that can provide us with the logic of interplay among immune cells.

AUTHOR CONTRIBUTIONS

All authors listed have made a substantial, direct, and intellectual contribution to the work, and approved it for publication.

REFERENCES

- Ablasser, A., Bauernfeind, F., Hartmann, G., Latz, E., Fitzgerald, K. A., and Hornung, V. (2009). RIG-I-dependent sensing of poly(dA:dT) through the induction of an RNA polymerase III-transcribed RNA intermediate. *Nat. Immunol.* 10, 1065–1072. doi: 10.1038/ni.1779
- Abplanalp, A. L., Morris, I. R., Parida, B. K., Teale, J. M., and Berton, M. T. (2009). TLR-dependent control of *Francisella tularensis* infection and host inflammatory responses. *PLoS ONE* 4:e7920. doi: 10.1371/journal.pone.0007920
- Ancuta, P., Pedron, T., Girard, R., Sandström, G., and Chaby, R. (1996). Inability of the *Francisella tularensis* lipopolysaccharide to mimic or to antagonize the induction of cell activation by endotoxins. *Infect. Immun.* 64, 2041–2046.
- Arancibia, S. A., Beltrán, C. J., Aguirre, I. M., Silva, P., Peralta, A. L., Malinarich, F., et al. (2007). Toll-like receptors are key participants in innate immune responses. *Biol. Res.* 40, 97–112. doi: 10.4067/S0716-97602007000200001
- Ashtekar, A. R., Zhang, P., Katz, J., Deivanayagam, C. C., Rallabhandi, P., Vogel, S. N., et al. (2008). TLR4-mediated activation of dendritic cells by the heat shock protein DnaK from *Francisella tularensis*. *J. Leukoc. Biol.* 84, 1434–1446. doi: 10.1189/jlb.0308215
- Ayala, J. M., Yamin, T. T., Egger, L. A., Chin, J., Kostura, M. J., and Miller, D. K. (1994). IL-1 beta-converting enzyme is present in monocytic cells as an inactive 45-kDa precursor. *J. Immunol.* 153, 2592–2599.
- Balagopal, A., MacFarlane, A. S., Mohapatra, N., Soni, S., Gunn, J. S., and Schlesinger, L. S. (2006). Characterization of the receptor-ligand pathways important for entry and survival of *Francisella tularensis* in human macrophages. *Infect. Immun.* 74, 5114–5125. doi: 10.1128/IAI.00795-06
- Barel, M., and Charbit, A. (2014). Detection of the interaction between host and bacterial proteins: eukaryotic nucleolin interacts with *Francisella elongation* factor Tu. *Methods Mol. Biol.* 1197, 123–139. doi: 10.1007/978-1-4939-1261-2_7
- Barel, M., Hovanessian, A. G., Meibom, K., Briand, J. P., Dupuis, M., and Charbit, A. (2008). A novel receptor-ligand pathway for entry of *Francisella tularensis* in monocyte-like THP-1 cells: interaction between surface nucleolin and bacterial elongation factor Tu. *BMC Microbiol.* 8:145. doi: 10.1186/1471-2180-8-145
- Barel, M., Meibom, K., and Charbit, A. (2010). Nucleolin, a shuttle protein promoting infection of human monocytes by *Francisella tularensis*. *PLoS ONE* 5:e14193. doi: 10.1371/journal.pone.0014193
- Barker, J. R., Koestler, B. J., Carpenter, V. K., Burdette, D. L., Waters, C. M., Vance, R. E., et al. (2013). STING-dependent recognition of cyclic di-AMP mediates type I interferon responses during *Chlamydia trachomatis* infection. *MBio* 4:e00018–e00013. doi: 10.1128/mBio.00018-13
- Bencurova, E., Kovac, A., Pulzova, L., Gyuranecz, M., Mlynarcik, P., Mucha, R., et al. (2015). Deciphering the protein interaction in adhesion of *Francisella tularensis* subsp. holarctica to the endothelial cells. *Microb. Pathog.* 81, 6–15. doi: 10.1016/j.micpath.2015.03.007
- Ben Nasr, A., Haithcoat, J., Masterson, J. E., Gunn, J. S., Eaves-Pyles, T., and Klimpel, G. R. (2006). Critical role for serum opsonins and complement receptors CR3 (CD11b/CD18) and CR4 (CD11c/CD18) in phagocytosis of

FUNDING

This work was supported by a Ministry of Defense of the Czech Republic—long-term organization development plan Medical Aspects of Weapons of Mass Destruction of the Faculty of Military Health Sciences, University of Defense.

ACKNOWLEDGMENTS

The authors would like to thank Martin Ondrej (University of Defence) for providing us with graphical cooperation on the manuscript figures.

- Francisella tularensis* by human dendritic cells (DC): uptake of *Francisella* leads to activation of immature DC and intracellular survival of the bacteria. *J. Leukoc. Biol.* 80, 774–786. doi: 10.1189/jlb.1205755
- Bosio, C. M., Bielefeldt-Ohmann, H., and Belisle, J. T. (2007). Active suppression of the pulmonary immune response by *Francisella tularensis* Schu4. *J. Immunol.* 178, 4538–4547. doi: 10.4049/jimmunol.178.7.4538
- Bosio, C. M., and Dow, S. W. (2005). *Francisella tularensis* induces aberrant activation of pulmonary dendritic cells. *J. Immunol.* 175, 6792–6801. doi: 10.4049/jimmunol.175.10.6792
- Botos, I., Segal, D. M., and Davies, D. R. (2011). The structural biology of Toll-like receptors. *Structure* 19, 447–459. doi: 10.1016/j.str.2011.02.004
- Bourdonnay, E., and Henry, T. (2016). Catch me if you can. *Elife* 5:e14721. doi: 10.7554/eLife.14721
- Bradburne, C. E., Verhoeven, A. B., Manyam, G. C., Chaudhry, S. A., Chang, E. L., Thach, D. C., et al. (2013). Temporal transcriptional response during infection of type II alveolar epithelial cells with *Francisella tularensis* Live Vaccine Strain (LVS) supports a general host suppression and bacterial uptake by macropinocytosis. *J. Biol. Chem.* 288, 10780–10791. doi: 10.1074/jbc.M112.362178
- Budak, G., Eren Ozsoy, O., Aydin Son, Y., Can, T., and Tuncbag, N. (2015). Reconstruction of the temporal signaling network in Salmonella-infected human cells. *Front. Microbiol.* 6:730. doi: 10.3389/fmicb.2015.00730
- Burdette, D. L., Monroe, K. M., Sotelo-Troha, K., Iwig, J. S., Eckert, B., Hyodo, M., et al. (2011). STING is a direct innate immune sensor of cyclic di-GMP. *Nature* 478, 515–518. doi: 10.1038/nature10429
- Burdette, D. L., and Vance, R. E. (2013). STING and the innate immune response to nucleic acids in the cytosol. *Nat. Immunol.* 14, 19–26. doi: 10.1038/ni.2491
- Carvalho, C. L., Lopes de Carvalho, I., Zé-Zé, L., Nuncio, M. S., and Duarte, E. L. (2014). Tularemia: a challenging zoonosis. *Comp. Immunol. Microbiol. Infect. Dis.* 37, 85–96. doi: 10.1016/j.cimid.2014.01.002
- Chase, J. C., Celli, J., and Bosio, C. M. (2009). Direct and indirect impairment of human dendritic cell function by virulent *Francisella tularensis* Schu S4. *Infect. Immun.* 77, 180–195. doi: 10.1128/IAI.00879-08
- Checroun, C., Wehrly, T. D., Fischer, E. R., Hayes, S. F., and Celli, J. (2006). Autophagy-mediated reentry of *Francisella tularensis* into the endocytic compartment after cytoplasmic replication. *Proc. Natl. Acad. Sci. U.S.A.* 103, 14578–14583. doi: 10.1073/pnas.0601838103
- Chen, W., KuoLee, R., Shen, H., Büsa, M., and Conlan, J. W. (2004). Toll-like receptor 4 (TLR4) does not confer a resistance advantage on mice against low-dose aerosol infection with virulent type A *Francisella tularensis*. *Microb. Pathog.* 37, 185–191. doi: 10.1016/j.micpath.2004.06.010
- Chen, W., KuoLee, R., Shen, H., Büsa, M., and Conlan, J. W. (2005). Toll-like receptor 4 (TLR4) plays a relatively minor role in murine defense against primary intradermal infection with *Francisella tularensis* LVS. *Immunol. Lett.* 97, 151–154. doi: 10.1016/j.imlet.2004.10.001
- Clemens, D. L., and Horwitz, M. A. (2007). Uptake and intracellular fate of *Francisella tularensis* in human macrophages. *Ann. N.Y. Acad. Sci.* 1105, 160–186. doi: 10.1196/annals.1409.001

- Clemens, D. L., Lee, B. Y., and Horwitz, M. A. (2004). Virulent and avirulent strains of *Francisella tularensis* prevent acidification and maturation of their phagosomes and escape into the cytoplasm in human macrophages. *Infect. Immun.* 72, 3204–3217. doi: 10.1128/IAI.72.6.3204-3217.2004
- Clemens, D. L., Lee, B. Y., and Horwitz, M. A. (2005). *Francisella tularensis* enters macrophages via a novel process involving pseudopod loops. *Infect. Immun.* 73, 5892–5902. doi: 10.1128/IAI.73.9.5892-5902.2005
- Cole, L. E., Laird, M. H., Seekatz, A., Santiago, A., Jiang, Z., Barry, E., et al. (2010). Phagosomal retention of *Francisella tularensis* results in TIRAP/Mal-independent TLR2 signaling. *J. Leukoc. Biol.* 87, 275–281. doi: 10.1189/jlb.0909619
- Cole, L. E., Shirey, K. A., Barry, E., Santiago, A., Rallabhandi, P., Elkins, K. L., et al. (2007). Toll-like receptor 2-mediated signaling requirements for *Francisella tularensis* live vaccine strain infection of murine macrophages. *Infect. Immun.* 75, 4127–4137. doi: 10.1128/IAI.01868-06
- Collazo, C. M., Sher, A., Meierovics, A. I., and Elkins, K. L. (2006). Myeloid differentiation factor-88 (MyD88) is essential for control of primary *in vivo* *Francisella tularensis* LVS infection, but not for control of intra-macrophage bacterial replication. *Microbes Infect.* 8, 779–790. doi: 10.1016/j.micinf.2005.09.014
- Culkin, S. J., Rhinehart-Jones, T., and Elkins, K. L. (1997). A novel role for B cells in early protective immunity to an intracellular pathogen, *Francisella tularensis* strain LVS. *J. Immunol.* 158, 3277–3284.
- Dai, S., Rajaram, M. V., Curry, H. M., Leander, R., and Schlesinger, L. S. (2013). Fine tuning inflammation at the front door: macrophage complement receptor 3-mediates phagocytosis and immune suppression for *Francisella tularensis*. *PLoS Pathog.* 9:e1005504. doi: 10.1371/journal.ppat.1003114
- Dotson, R. J., Rabadi, S. M., Westcott, E. L., Bradley, S., Catlett, S. V., Banik, S., et al. (2013). Repression of inflammasome by *Francisella tularensis* during early stages of infection. *J. Biol. Chem.* 288, 23844–23857. doi: 10.1074/jbc.M113.490086
- Dueñas, A. I., Aceves, M., Orduña, A., Díaz, R., Sánchez Crespo, M., and García-Rodríguez, C. (2006). *Francisella tularensis* LPS induces the production of cytokines in human monocytes and signals via Toll-like receptor 4 with much lower potency than *E. coli* LPS. *Int. Immunol.* 18, 785–795. doi: 10.1093/intimm/dxl015
- Duncan, D. D., Vogler, A. J., Wolcott, M. J., Li, F., Sarovich, D. S., Birdsell, D. N., et al. (2013). Identification and typing of *Francisella tularensis* with a highly automated genotyping assay. *Lett. Appl. Microbiol.* 56, 128–134. doi: 10.1111/lam.12022
- Eberl, M., Hintz, M., Reichenberg, A., Kollas, A. K., Wiesner, J., and Jomaa, H. (2003). Microbial isoprenoid biosynthesis and human gammadelta T cell activation. *FEBS Lett.* 544, 4–10. doi: 10.1016/S0014-5793(03)00483-6
- Eberl, M., and Jomaa, H. (2003). A genetic basis for human gammadelta T-cell reactivity towards microbial pathogens. *Trends Immunol.* 24, 407–409. doi: 10.1016/S1471-4906(03)00170-4
- Elkins, K. L., Bosio, C. M., and Rhinehart-Jones, T. R. (1999). Importance of B cells, but not specific antibodies, in primary and secondary protective immunity to the intracellular bacterium *Francisella tularensis* live vaccine strain. *Infect. Immun.* 67, 6002–6007.
- Fernandes-Alnemri, T., Yu, J. W., Datta, P., Wu, J., and Alnemri, E. S. (2009). AIM2 activates the inflammasome and cell death in response to cytoplasmic DNA. *Nature* 458, 509–513. doi: 10.1038/nature07710
- Fernandes-Alnemri, T., Yu, J. W., Juliana, C., Solorzano, L., Kang, S., Wu, J., et al. (2010). The AIM2 inflammasome is critical for innate immunity to *Francisella tularensis*. *Nat. Immunol.* 11, 385–393. doi: 10.1038/ni.1859
- Forestal, C. A., Benach, J. L., Carbonara, C., Italo, J. K., Lisinski, T. J., and Furie, M. B. (2003). *Francisella tularensis* selectively induces proinflammatory changes in endothelial cells. *J. Immunol.* 171, 2563–2570. doi: 10.4049/jimmunol.171.5.2563
- Fortier, A. H., Green, S. J., Polsinelli, T., Jones, T. R., Crawford, R. M., Leiby, D. A., et al. (1994). Life and death of an intracellular pathogen: *Francisella tularensis* and the macrophage. *Immunol. Ser.* 60, 349–361.
- Franchi, L., Park, J. H., Shaw, M. H., Marina-Garcia, N., Chen, G., Kim, Y. G., et al. (2008). Intracellular NOD-like receptors in innate immunity, infection and disease. *Cell. Microbiol.* 10, 1–8. doi: 10.1111/j.1462-5822.2007.01059.x
- Franchi, L., Warner, N., Viani, K., and Nuñez, G. (2009). Function of Nod-like receptors in microbial recognition and host defense. *Immunol. Rev.* 227, 106–128. doi: 10.1111/j.1600-065X.2008.00734.x
- Geier, H., and Celli, J. (2011). Phagocytic receptors dictate phagosomal escape and intracellular proliferation of *Francisella tularensis*. *Infect. Immun.* 79, 2204–2214. doi: 10.1128/IAI.01382-10
- Gentry, M., Taormina, J., Pyles, R. B., Yeager, L., Kirtley, M., Popov, V. L., et al. (2007). Role of primary human alveolar epithelial cells in host defense against *Francisella tularensis* infection. *Infect. Immun.* 75, 3969–3978. doi: 10.1128/IAI.00157-07
- Golovliov, I., Baranov, V., Krocova, Z., Kovarova, H., and Sjöstedt, A. (2003). An attenuated strain of the facultative intracellular bacterium *Francisella tularensis* can escape the phagosome of monocytic cells. *Infect. Immun.* 71, 5940–5950. doi: 10.1128/IAI.71.10.5940-5950.2003
- Gunn, J. S., and Ernst, R. K. (2007). The structure and function of *Francisella* lipopolysaccharide. *Ann. N.Y. Acad. Sci.* 1105, 202–218. doi: 10.1196/annals.1409.006
- Hajjar, A. M., Harvey, M. D., Shaffer, S. A., Goodlett, D. R., Sjöstedt, A., Edebro, H., et al. (2006). Lack of *in vitro* and *in vivo* recognition of *Francisella tularensis* subspecies lipopolysaccharide by Toll-like receptors. *Infect. Immun.* 74, 6730–6738. doi: 10.1128/IAI.00934-06
- Hall, J. D., Woolard, M. D., Gunn, B. M., Craven, R. R., Taft-Benz, S., Frelinger, J. A., et al. (2008). Infected-host-cell repertoire and cellular response in the lung following inhalation of *Francisella tularensis* Schu S4, LVS, or U112. *Infect. Immun.* 76, 5843–5852. doi: 10.1128/IAI.01176-08
- Henry, T., Brotcke, A., Weiss, D. S., Thompson, L. J., and Monack, D. M. (2007). Type I interferon signaling is required for activation of the inflammasome during *Francisella* infection. *J. Exp. Med.* 204, 987–994. doi: 10.1084/jem.20062665
- Heuston, S., Begley, M., Gahan, C. G., and Hill, C. (2012). Isoprenoid biosynthesis in bacterial pathogens. *Microbiology* 158, 1389–1401. doi: 10.1099/mic.0.051599-0
- Holland, K. M., Rosa, S. J., and Hazlett, K. R. (2016). *Francisella tularensis* - immune cell activator, suppressor, or stealthy evader: the evolving view from the petri dish. *J. Bioterror. Biodef.* 7:144. doi: 10.4172/2157-2526.1000144
- Hong, K. J., Wickstrum, J. R., Yeh, H. W., and Parmely, M. J. (2007). Toll-like receptor 2 controls the gamma interferon response to *Francisella tularensis* by mouse liver lymphocytes. *Infect. Immun.* 75, 5338–5345. doi: 10.1128/IAI.00561-07
- Hornig, T., Barton, G. M., Flavell, R. A., and Medzhitov, R. (2002). The adaptor molecule TIRAP provides signalling specificity for Toll-like receptors. *Nature* 420, 329–333. doi: 10.1038/nature01180
- Hornig, T., Barton, G. M., and Medzhitov, R. (2001). TIRAP: an adapter molecule in the Toll signaling pathway. *Nat. Immunol.* 2, 835–841. doi: 10.1038/ni0901-835
- Hornung, V., Ablasser, A., Charrel-Dennis, M., Bauernfeind, F., Horvath, G., Caffrey, D. R., et al. (2009). AIM2 recognizes cytosolic dsDNA and forms a caspase-1-activating inflammasome with ASC. *Nature* 458, 514–518. doi: 10.1038/nature07725
- Hotson, A. N., Gopinath, S., Nicolau, M., Khasanova, A., Finck, R., Monack, D., et al. (2016). Coordinate actions of innate immune responses oppose those of the adaptive immune system during *Salmonella* infection of mice. *Sci. Signal.* 9, ra4. doi: 10.1126/scisignal.aaa9303
- Huang, S., Gilfillan, S., Cella, M., Miley, M. J., Lantz, O., Lybarger, L., et al. (2005). Evidence for MR1 antigen presentation to mucosal-associated invariant T cells. *J. Biol. Chem.* 280, 21183–21193. doi: 10.1074/jbc.M501087200
- Ishikawa, H., and Barber, G. N. (2008). STING is an endoplasmic reticulum adaptor that facilitates innate immune signalling. *Nature* 455, 674–678. doi: 10.1038/nature07317
- Ishikawa, H., Ma, Z., and Barber, G. N. (2009). STING regulates intracellular DNA-mediated, type I interferon-dependent innate immunity. *Nature* 461, 788–792. doi: 10.1038/nature08476
- Jin, L., Hill, K. K., Filak, H., Mogan, J., Knowles, H., Zhang, B., et al. (2011). MPYS is required for IRF3 activation and type I IFN production in the response of cultured phagocytes to bacterial second messengers c-di-AMP and c-di-GMP. *J. Immunol.* 187, 2595–2601. doi: 10.4049/jimmunol.1100088
- Jin, T., and Xiao, T. S. (2015). Activation and assembly of the inflammasomes through conserved protein domain families. *Apoptosis* 20, 151–156. doi: 10.1007/s10495-014-1053-5

- Jones, C. L., and Weiss, D. S. (2011). TLR2 signaling contributes to rapid inflammasome activation during *F. novicida* infection. *PLoS ONE* 6:e20609. doi: 10.1371/journal.pone.0020609
- Jones, J. W., Kayagaki, N., Broz, P., Henry, T., Newton, K., O'Rourke, K., et al. (2010). Absent in melanoma 2 is required for innate immune recognition of *Francisella tularensis*. *Proc. Natl. Acad. Sci. U.S.A.* 107, 9771–9776. doi: 10.1073/pnas.1003738107
- Katz, J., Zhang, P., Martin, M., Vogel, S. N., and Michalek, S. M. (2006). Toll-like receptor 2 is required for inflammatory responses to *Francisella tularensis* LVS. *Infect. Immun.* 74, 2809–2816. doi: 10.1128/IAI.74.5.2809-2816.2006
- Kennedy, A. D., and DeLeo, F. R. (2009). Neutrophil apoptosis and the resolution of infection. *Immunol. Res.* 43, 25–61. doi: 10.1007/s12026-008-8049-6
- Kim, Y. K., Shin, J. S., and Nahm, M. H. (2016). NOD-like receptors in infection, immunity, and diseases. *Yonsei Med. J.* 57, 5–14. doi: 10.3349/ymj.2016.57.1.5
- Kingry, L. C., and Petersen, J. M. (2014). Comparative review of *Francisella tularensis* and *Francisella novicida*. *Front. Cell. Infect. Microbiol.* 4:35. doi: 10.3389/fcimb.2014.00035
- Kjer-Nielsen, L., Patel, O., Corbett, A. J., Le Nours, J., Meehan, B., Liu, L., et al. (2012). MRI presents microbial vitamin B metabolites to MAIT cells. *Nature* 491, 717–723. doi: 10.1038/nature11605
- Kobayashi, S. D., Braughton, K. R., Whitney, A. R., Voyich, J. M., Schwan, T. G., Musser, J. M., et al. (2003). Bacterial pathogens modulate an apoptosis differentiation program in human neutrophils. *Proc. Natl. Acad. Sci. U.S.A.* 100, 10948–10953. doi: 10.1073/pnas.1833375100
- Kubelkova, K., Benuchova, M., Kozakova, H., Sinkora, M., Krocova, Z., Pejchal, J., et al. (2016). Gnotobiotic mouse model's contribution to understanding host-pathogen interactions. *Cell. Mol. Life Sci.* 73, 3961–3969. doi: 10.1007/s00018-016-2341-8
- Law, H. T., Lin, A. E. S., Kim, Y., Quach, B., Nano, F. E., and Guttman, J. A. (2011). *Francisella tularensis* uses cholesterol and clathrin-based endocytic mechanisms to invade hepatocytes. *Sci. Rep.* 1:192. doi: 10.1038/srep00192
- Li, H., Nookala, S., Bina, X. R., Bina, J. E., and Re, F. (2006). Innate immune response to *Francisella tularensis* is mediated by TLR2 and caspase-1 activation. *J. Leukoc. Biol.* 80, 766–773. doi: 10.1189/jlb.0406294
- Libich, J. (1981). *Tularémie*. Prague: Avicenum.
- Lindemann, S. R., McLendon, M. K., Apicella, M. A., and Jones, B. D. (2007). An *in vitro* model system used to study adherence and invasion of *Francisella tularensis* live vaccine strain in nonphagocytic cells. *Infect. Immun.* 75, 3178–3182. doi: 10.1128/IAI.01811-06
- Löfgren, S., Tärnvik, A., Bloom, G. D., and Sjöberg, W. (1983). Phagocytosis and killing of *Francisella tularensis* by human polymorphonuclear leukocytes. *Infect. Immun.* 39, 715–720.
- Lord, K. A., Hoffman-Liebermann, B., and Liebermann, D. A. (1990). Nucleotide sequence and expression of a cDNA encoding MyD88, a novel myeloid differentiation primary response gene induced by IL6. *Oncogene* 5, 1095–1097.
- Lu, Y. C., Yeh, W. C., and Ohashi, P. S. (2008). LPS/TLR4 signal transduction pathway. *Cytokine* 42, 145–151. doi: 10.1016/j.cyto.2008.01.006
- Macela, A., Stulik, J., Hernychova, L., Kroca, M., Krocova, Z., and Kovarova, H. (1996). The immune response against *Francisella tularensis* live vaccine strain in Lps(n) and Lps(d) mice. *FEMS Immunol. Med. Microbiol.* 13, 235–238. doi: 10.1111/j.1574-695X.1996.tb00243.x
- Maeshima, N., and Fernandez, R. C. (2013). Recognition of lipid A variants by the TLR4-MD-2 receptor complex. *Front. Cell. Infect. Microbiol.* 3:3. doi: 10.3389/fcimb.2013.00003
- Malik, M., Bakshi, C. S., Sahay, B., Shah, A., Lotz, S. A., and Sellati, T. J. (2006). Toll-like receptor 2 is required for control of pulmonary infection with *Francisella tularensis*. *Infect. Immun.* 74, 3657–3662. doi: 10.1128/IAI.02030-05
- Man, S. M., and Kanneganti, T. D. (2015). Regulation of inflammasome activation. *Immunol. Rev.* 265, 6–21. doi: 10.1111/imr.12296
- Man, S. M., Karki, R., and Kanneganti, T. D. (2016a). AIM2 inflammasome in infection, cancer, and autoimmunity: role in DNA sensing, inflammation, and innate immunity. *Eur. J. Immunol.* 46, 269–280. doi: 10.1002/eji.201545839
- Man, S. M., Karki, R., Malireddi, R. K., Neale, G., Vogel, P., Yamamoto, M., et al. (2015). The transcription factor IRF1 and guanylate-binding proteins target activation of the AIM2 inflammasome by *Francisella* infection. *Nat. Immunol.* 16, 467–475. doi: 10.1038/ni.3118
- Man, S. M., Karki, R., Sasai, M., Place, D. E., Kesavardhana, S., Temirov, J., et al. (2016b). IRGB10 liberates bacterial ligands for sensing by the AIM2 and Caspase-11-NLRP3 inflammasomes. *Cell* 167, 382–396.e17. doi: 10.1016/j.cell.2016.09.012
- Mariathasan, S., Weiss, D. S., Dixit, V. M., and Monack, D. M. (2005). Innate immunity against *Francisella tularensis* is dependent on the ASC/caspase-1 axis. *J. Exp. Med.* 202, 1043–1049. doi: 10.1084/jem.20050977
- Marohn, M. E., and Barry, E. M. (2013). Live attenuated tularemia vaccines: recent developments and future goals. *Vaccine* 31, 3485–3491. doi: 10.1016/j.vaccine.2013.05.096
- McCaffrey, R. L., and Allen, L.-A. H. (2006). *Francisella tularensis* LVS evades killing by human neutrophils via inhibition of the respiratory burst and phagosome escape. *J. Leukoc. Biol.* 80, 1224–1230. doi: 10.1189/jlb.0406287
- Miller, D. K., Ayala, J. M., Egger, L. A., Raju, S. M., Yamin, T. T., Ding, G. J., et al. (1993). Purification and characterization of active human interleukin-1 beta-converting enzyme from THP.1 monocytic cells. *J. Biol. Chem.* 268, 18062–18069.
- Morita, C. T., Jin, C., Sarikonda, G., and Wang, H. (2007). Nonpeptide antigens, presentation mechanisms, and immunological memory of human Vγ2Vδ2 T cells: discriminating friend from foe through the recognition of prenyl pyrophosphate antigens. *Immunol. Rev.* 215, 59–76. doi: 10.1111/j.1600-065X.2006.00479.x
- Moser, B., and Eberl, M. (2011). γδ T-APCs: a novel tool for immunotherapy? *Cell. Mol. Life Sci.* 68, 2443–2452. doi: 10.1007/s00018-011-0706-6
- Nunes-Alves, C., Booty, M. G., Carpenter, S. M., Jayaraman, P., Rothchild, A. C., and Behar, S. M. (2014). In search of a new paradigm for protective immunity to TB. *Nat. Rev. Microbiol.* 12, 289–299. doi: 10.1038/nrmicr.03230
- Nutter, J. E., and Myrvik, Q. N. (1966). *In vitro* interactions between rabbit alveolar macrophages and Pasteurella tularensis. *J. Bacteriol.* 92, 645–651.
- Okan, N. A., and Kasper, D. L. (2013). The atypical lipopolysaccharide of *Francisella*. *Carbohydr. Res.* 378, 79–83. doi: 10.1016/j.carres.2013.06.015
- O'Neill, L. A., Golenbock, D., and Bowie, A. G. (2013). The history of Toll-like receptors - redefining innate immunity. *Nat. Rev. Immunol.* 13, 453–460. doi: 10.1038/nri3446
- Park, B. S., and Lee, J. O. (2013). Recognition of lipopolysaccharide pattern by TLR4 complexes. *Exp. Mol. Med.* 45:e66. doi: 10.1038/emmm.2013.97
- Parsa, K. V., Butchar, J. P., Rajaram, M. V., Cremer, T. J., Gunn, J. S., Schlesinger, L. S., et al. (2008). *Francisella* gains a survival advantage within mononuclear phagocytes by suppressing the host IFNγ response. *Mol. Immunol.* 45, 3428–3437. doi: 10.1016/j.molimm.2008.04.006
- Pierini, L. M. (2006). Uptake of serum-opsonized *Francisella tularensis* by macrophages can be mediated by class A scavenger receptors. *Cell. Microbiol.* 8, 1361–1370. doi: 10.1111/j.1462-5822.2006.00719.x
- Plzakova, L., Krocova, Z., Kubelkova, K., and Macela, A. (2015). Entry of *Francisella tularensis* into murine B Cells: the role of B cell receptors and complement receptors. *PLoS ONE* 10:e0132571. doi: 10.1371/journal.pone.0132571
- Plzakova, L., Kubelkova, K., Krocova, Z., Zarybnicka, L., Sinkorova, Z., and Macela, A. (2014). B cell subsets are activated and produce cytokines during early phases of *Francisella tularensis* LVS infection. *Microb. Pathog.* 75C, 49–58. doi: 10.1016/j.micpath.2014.08.009
- Poquet, Y., Kroca, M., Halary, F., Stenmark, S., Peyrat, M. A., Bonneville, M., et al. (1998). Expansion of Vγ9Vδ2 T cells is triggered by *Francisella tularensis*-derived phosphoantigens in tularemia but not after tularemia vaccination. *Infect. Immun.* 66, 2107–2114.
- Putzova, D., Senitkova, I., and Stulik, J. (2016). Tularemia vaccines. *Folia Microbiol.* 61, 495–504. doi: 10.1007/s12223-016-0461-z
- Rennert, K., Otto, P., Funke, H., Huber, O., Tomaso, H., and Mosig, A. S. (2016). A human macrophage-hepatocyte co-culture model for comparative studies of infection and replication of *Francisella tularensis* LVS strain and subspecies holarctica and mediasiatica. *BMC Microbiol.* 16:2. doi: 10.1186/s12866-015-0621-3
- Richard, K., Vogel, S. N., and Perkins, D. J. (2016). Type I interferon licenses enhanced innate recognition and transcriptional responses to *Francisella tularensis* live vaccine strain. *Innate Immun.* 22, 363–372. doi: 10.1177/1753425916650027
- Roberts, L. M., Tuladhar, S., Steele, S. P., Riebe, K. J., Chen, C. J., Cumming, R. I., et al. (2014). Identification of early interactions between *Francisella* and the host. *Infect. Immun.* 82, 2504–2510. doi: 10.1128/IAI.01654-13

- Rothchild, A. C., Sissons, J. R., Shafiani, S., Plaisier, C., Min, D., Mai, D., et al. (2016). MiR-155-regulated molecular network orchestrates cell fate in the innate and adaptive immune response to *Mycobacterium tuberculosis*. *Proc. Natl. Acad. Sci. U.S.A.* 113, E6172–E6181. doi: 10.1073/pnas.1608255113
- Rowland, C. A., Hartley, M. G., Flick-Smith, H., Laws, T. R., Eyles, J. E., and Oyston, P. C. (2012). Peripheral human $\gamma\delta$ T cells control growth of both avirulent and highly virulent strains of *Francisella tularensis* in vitro. *Microbes Infect.* 14, 584–589. doi: 10.1016/j.micinf.2012.02.001
- Russo, B. C., Brown, M. J., and Nau, G. J. (2013). MyD88-dependent signaling prolongs survival and reduces bacterial burden during pulmonary infection with virulent *Francisella tularensis*. *Am. J. Pathol.* 183, 1223–1232. doi: 10.1016/j.ajpath.2013.06.013
- Sandström, G., Sjöstedt, A., Johansson, T., Kuoppa, K., and Williams, J. C. (1992). Immunogenicity and toxicity of lipopolysaccharide from *Francisella tularensis* LVS. *FEMS Microbiol. Immunol.* 5, 201–210. doi: 10.1111/j.1574-6968.1992.tb05902.x
- Santic, M., Asare, R., Skrobonja, I., Jones, S., and Abu Kwaik, Y. (2008). Acquisition of the vacuolar ATPase proton pump and phagosomal acidification are essential for escape of *Francisella tularensis* into the macrophage cytosol. *Infect. Immun.* 76, 2671–2677. doi: 10.1128/IAI.00185-08
- Santic, M., Molmeret, M., Klose, K. E., Jones, S., and Kwaik, Y. A. (2005). The *Francisella tularensis* pathogenicity island protein IglC and its regulator MglA are essential for modulating phagosomal biogenesis and subsequent bacterial escape into the cytoplasm. *Cell. Microbiol.* 7, 969–979. doi: 10.1111/j.1462-5822.2005.00526.x
- Schulert, G. S., and Allen, L. A. (2006). Differential infection of mononuclear phagocytes by *Francisella tularensis*: role of the macrophage mannose receptor. *J. Leukoc. Biol.* 80, 563–571. doi: 10.1189/jlb.0306219
- Schwartz, J. T., Barker, J. H., Kaufman, J., Fayram, D. C., McCracken, J. M., and Allen, L. A. (2012a). *Francisella tularensis* inhibits the intrinsic and extrinsic pathways to delay constitutive apoptosis and prolong human neutrophil lifespan. *J. Immunol.* 188, 3351–3363. doi: 10.4049/jimmunol.1102863
- Schwartz, J. T., Barker, J. H., Long, M. E., Kaufman, J., McCracken, J., and Allen, L.-A. H. (2012b). Natural IgM mediates complement-dependent uptake of *Francisella tularensis* by human neutrophils via CR1 and CR3 in nonimmune serum. *J. Immunol.* 189, 3064–3077. doi: 10.4049/jimmunol.1200816
- Sicard, H., and Fournie, J. J. (2000). Metabolic routes as targets for immunological discrimination of host and parasite. *Infect. Immun.* 68, 4375–4377. doi: 10.1128/IAI.68.8.4375-4377.2000
- Steele, S., Radlinski, L., Taft-Benz, S., Brunton, J., and Kawula, T. H. (2016). Trogocytosis-associated cell to cell spread of intracellular bacterial pathogens. *Elife* 5:e10625. doi: 10.7554/eLife.10625
- Storek, K. M., Gertsvolf, N. A., Ohlson, M. B., and Monack, D. M. (2015). cGAS and Ifi204 cooperate to produce type I IFNs in response to *Francisella* infection. *J. Immunol.* 194, 3236–3245. doi: 10.4049/jimmunol.1402764
- Sun, L., Wu, J., Du, F., Chen, X., and Chen, Z. J. (2013). Cyclic GMP-AMP synthase is a cytosolic DNA sensor that activates the type I interferon pathway. *Science* 339, 786–791. doi: 10.1126/science.1232458
- Takaoka, A., Wang, Z., Choi, M. K., Yanai, H., Negishi, H., Ban, T., et al. (2007). DAI (DLM-1/ZBP1) is a cytosolic DNA sensor and an activator of innate immune response. *Nature* 448, 501–505. doi: 10.1038/nature06013
- Telepnev, M., Golovliov, I., Grundström, T., Tärnvik, A., and Sjöstedt, A. (2003). *Francisella tularensis* inhibits Toll-like receptor-mediated activation of intracellular signalling and secretion of TNF-alpha and IL-1 from murine macrophages. *Cell. Microbiol.* 5, 41–51. doi: 10.1046/j.1462-5822.2003.00251.x
- Thornberry, N. A., Bull, H. G., Calaycay, J. R., Chapman, K. T., Howard, A. D., Kostura, M. J., et al. (1992). A novel heterodimeric cysteine protease is required for interleukin-1 beta processing in monocytes. *Nature* 356, 768–774. doi: 10.1038/356768a0
- Thorpe, B. D., and Marcus, S. (1964a). Phagocytosis and intracellular fate of *Pasteurella tularensis*. II. *In vitro* studies with rabbit alveolar and guinea pig alveolar and peritoneal mononuclear phagocytes. *J. Immunol.* 93, 558–565.
- Thorpe, B. D., and Marcus, S. (1964b). Phagocytosis and intracellular fate of *Pasteurella tularensis*. I. *In vitro* studies with rabbit peritoneal mononuclear phagocytes. *J. Immunol.* 92, 657–663.
- Tyler, C. J., Doherty, D. G., Moser, B., and Eberl, M. (2015). Human V γ 9/V δ 2 T cells: innate adaptors of the immune system. *Cell. Immunol.* 296, 10–21. doi: 10.1016/j.cellimm.2015.01.008
- Udgata, A., Qureshi, R., and Mukhopadhyay, S., (2016). Transduction of functionally contrasting signals by two Mycobacterial PPE proteins downstream of TLR2 receptors. *J. Immunol.* 197, 1776–1787. doi: 10.4049/jimmunol.1501816
- Unterholzner, L. (2013). The interferon response to intracellular DNA: why so many receptors? *Immunobiology* 218, 1312–1321. doi: 10.1016/j.imbio.2013.07.007
- Unterholzner, L., Keating, S. E., Baran, M., Horan, K. A., Jensen, S. B., Sharma, S., et al. (2010). IFI16 is an innate immune sensor for intracellular DNA. *Nat. Immunol.* 11, 997–1004. doi: 10.1038/ni.1932
- Veeranki, S., and Choubey, D. (2012). Interferon-inducible p200-family protein IFI16, an innate immune sensor for cytosolic and nuclear double-stranded DNA: regulation of subcellular localization. *Mol. Immunol.* 49, 567–571. doi: 10.1016/j.molimm.2011.11.004
- Warner, N., and Núñez, G. (2013). MyD88: a critical adaptor protein in innate immunity signal transduction. *J. Immunol.* 190, 3–4. doi: 10.4049/jimmunol.1203103
- Wilson, K. P., Black, J. A., Thomson, J. A., Kim, E. E., Griffith, J. P., Navia, M. A., et al. (1994). Structure and mechanism of interleukin-1 beta converting enzyme. *Nature* 370, 270–275. doi: 10.1038/370270a0
- Wu, J., Sun, L., Chen, X., Du, F., Shi, H., Chen, C., et al. (2013). Cyclic GMP-AMP is an endogenous second messenger in innate immune signaling by cytosolic DNA. *Science* 339, 826–830. doi: 10.1126/science.1229963
- Xiao, T. S. (2015). The nucleic acid-sensing inflammasomes. *Immunol. Rev.* 265, 103–111. doi: 10.1111/imr.12281
- Zheng, H., Tan, Z., Zhou, T., Zhu, F., Ding, Y., Liu, T., et al. (2015). The TLR2 is activated by sporozoites and suppresses intrahepatic rodent malaria parasite development. *Sci. Rep.* 5:18239. doi: 10.1038/srep18239

Conflict of Interest Statement: The authors declare that the research was conducted in the absence of any commercial or financial relationships that could be construed as a potential conflict of interest.

Copyright © 2017 Krocova, Macela and Kubelkova. This is an open-access article distributed under the terms of the Creative Commons Attribution License (CC BY). The use, distribution or reproduction in other forums is permitted, provided the original author(s) or licensor are credited and that the original publication in this journal is cited, in accordance with accepted academic practice. No use, distribution or reproduction is permitted which does not comply with these terms.



The Multiple Localized Glyceraldehyde-3-Phosphate Dehydrogenase Contributes to the Attenuation of the *Francisella tularensis dsbA* Deletion Mutant

Ivona Pavkova^{1*}, Monika Kopeckova¹, Jana Klimentova¹, Monika Schmidt^{††}, Valeria Sheshko¹, Margarita Sobol², Jitka Zakova¹, Pavel Hozak^{2,3,4} and Jiri Stulik¹

¹ Department of Molecular Pathology, Faculty of Military Health Science, University of Defence, Hradec Kralove, Czechia,

² Department of Biology of the Cell Nucleus, Institute of Molecular Genetics ASCR v.v.i., Prague, Czechia, ³ Microscopy Centre-LM & EM, Institute of Molecular Genetics ASCR v.v.i., Prague, Czechia, ⁴ Division BIOCEV, Laboratory of Epigenetics of the Cell Nucleus, Institute of Molecular Genetics ASCR v.v.i., Vestec, Czechia

OPEN ACCESS

Edited by:

Jorge Eugenio Vidal,
Emory University, United States

Reviewed by:

Lee-Ann H. Allen,
University of Iowa, United States
Bradley D. Jones,
University of Iowa, United States

*Correspondence:

Ivona Pavkova
ivona.pavkova@unob.cz

† Present Address:

Monika Schmidt,
Department of Chemistry, Faculty of
Science, University of Hradec Kralove,
Hradec Kralove, Czechia

Received: 18 September 2017

Accepted: 22 November 2017

Published: 11 December 2017

Citation:

Pavkova I, Kopeckova M, Klimentova J, Schmidt M, Sheshko V, Sobol M, Zakova J, Hozak P and Stulik J (2017) The Multiple Localized Glyceraldehyde-3-Phosphate Dehydrogenase Contributes to the Attenuation of the *Francisella tularensis dsbA* Deletion Mutant. *Front. Cell. Infect. Microbiol.* 7:503. doi: 10.3389/fcimb.2017.00503

The DsbA homolog of *Francisella tularensis* was previously demonstrated to be required for intracellular replication and animal death. Disruption of the *dsbA* gene leads to a pleiotropic phenotype that could indirectly affect a number of different cellular pathways. To reveal the broad effects of DsbA, we compared fractions enriched in membrane proteins of the wild-type FSC200 strain with the *dsbA* deletion strain using a SILAC-based quantitative proteomic analysis. This analysis enabled identification of 63 proteins with significantly altered amounts in the *dsbA* mutant strain compared to the wild-type strain. These proteins comprise a quite heterogeneous group including hypothetical proteins, proteins associated with membrane structures, and potential secreted proteins. Many of them are known to be associated with *F. tularensis* virulence. Several proteins were selected for further studies focused on their potential role in tularemia's pathogenesis. Of them, only the gene encoding glyceraldehyde-3-phosphate dehydrogenase, an enzyme of glycolytic pathway, was found to be important for full virulence manifestations both *in vivo* and *in vitro*. We next created a viable mutant strain with deleted *gapA* gene and analyzed its phenotype. The *gapA* mutant is characterized by reduced virulence in mice, defective replication inside macrophages, and its ability to induce a protective immune response against systemic challenge with parental wild-type strain. We also demonstrate the multiple localization sites of this protein: In addition to within the cytosol, it was found on the cell surface, outside the cells, and in the culture medium. Recombinant GapA was successfully obtained, and it was shown that it binds host extracellular serum proteins like plasminogen, fibrinogen, and fibronectin.

Keywords: DsbA, SILAC, glyceraldehyde-3-phosphate dehydrogenase, *Francisella tularensis*, moonlighting

INTRODUCTION

Pathogenic bacteria produce a wide range of virulence factors whose activity, stability, and protease resistance depend on their correct folding through the formation of disulfide bonds between two cysteine thiol groups. The process of protein oxidative folding is achieved via the disulfide bond formation (Dsb) system and occurs within the periplasm in Gram-negative bacteria. The best characterized Dsb system is that of *Escherichia coli*. It is composed of two pathways: the oxidation pathway, with DsbA and DsbB proteins, and the isomerization pathway, with DsbC, DsbD, and DsbG proteins (Inaba, 2009). Inasmuch as there is growing evidence of extreme diversity in Dsb systems among bacteria (Bocian-Ostrzycka et al., 2015; Smith et al., 2016); however, the *E. coli* system should no longer be regarded as a universal model for bacteria. The key protein of this system—the non-specific disulfide oxidoreductase DsbA—introduces the disulfide bonds directly into extracytoplasmic proteins, including toxins, secretion systems, adhesins, or motility machines. Mutants with inactivated *dsbA* gene thus display attenuated virulence (Heras et al., 2009; Shouldice et al., 2011). Furthermore, a number of periplasmic proteins are also affected by the *dsbA* deletion, thereby reflecting the pleiotropic phenotype of relevant mutants.

Francisella tularensis is an intracellular, Gram-negative bacterium causing the zoonotic disease tularemia. Two *F. tularensis* subspecies are most associated with human disease: subsp. *tularensis* (type A) and subsp. *holarctica* (type B). Its low infectious dose, easy transfer, and extreme virulence cause *F. tularensis* to be a severe threat to human health, particularly because it can be misused as a bioterrorism agent. One gene of the *Francisella* genome encodes a protein with homology to DsbA: FtDsbA. This also is referred to as *Francisella* infectivity potentiator protein B (FipB) by Qin et al. (2011). Its significant role in virulence has been demonstrated in numerous previously published studies. In several respects, FtDsbA is unique from other known bacterial homologs. It is a glycosylated lipoprotein (Straskova et al., 2009; Thomas et al., 2011) with multiple functions, including not only oxidoreductase but also isomerase and chaperone activities (Straskova et al., 2009; Schmidt et al., 2013; Qin et al., 2014). It seems to be responsible for the introduction of disulfide bonds into various proteins, as well as for the repair of incorrectly formed disulfide bonds and protection of proteins from aggregation and misfolding. It is therefore assumed to influence the stability and function of diverse, predominantly extracytosolic proteins, many of which might directly mediate the *F. tularensis* virulence. Identification of proteins whose activity depends on DsbA can consequently reveal heretofore undetected virulence factors involved in molecular mechanisms of tularemia's pathogenesis. Accordingly, many of FtDsbA's substrates identified in previously published analyses are known virulence factors. In our earlier study using two distinct comparative proteomic approaches (two-dimensional gel electrophoresis and shotgun iTRAQ analysis), we were able to identify only nine proteins with abundances different in a *dsbA* mutant strain compared to the wild-type strain of *F. tularensis* LVS (Straskova et al., 2009). Several of

these were known virulence factors, such as DipA (Chong et al., 2013) or PdpE from the *Francisella* pathogenicity island (FPI) (Bröms et al., 2010). Two other studies applied more stringent trapping assays to look for the FtDsbA substrates in *F. tularensis* strains with *dsbA* gene mutations in regions responsible for the substrate binding (Ren et al., 2014; Qin et al., 2016). These approaches enabled the identification of far more proteins requiring FtDsbA for correct disulfide bond formation. Ren et al. (2014) found more than 50 FtDsbA substrates, including a number of known virulence factors (DipA, FopA, MipA, type IV pili component FTL_0359, and two FPI proteins: PdpE and PdpB). In addition, two novel hypothetical proteins, FTL_1548 and FTL_1709, were shown to be required for *F. tularensis* virulence. Even more potential FtDsbA substrates were identified by Qin et al. (2016). Again, several of them were known virulence factors. These include three FPI proteins (IglC, IglB, and PdpB). The marked discrepancy in number of proteins detected by our proteomic study compared to the trapping assays together with the availability of more advanced quantitative shotgun approaches led us to a decision to reanalyze the changes in membrane proteome induced by a lack of DsbA.

Here, we examined changes in membrane proteome caused by in-frame deletion of the *dsbA* gene in virulent type B strain of *F. tularensis* subsp. *holarctica* FSC200 (locus_tag FTS_1096). Using the highly sensitive stable isotope labeling with amino acids in cell culture (SILAC) technique, we succeeded in identifying 63 proteins with significantly altered abundance in the *dsbA* mutant strain. Fifteen proteins were further selected for elucidating their potential role in virulence, but only disruption of the gene encoding glyceraldehyde-3-phosphate dehydrogenase (GapA) resulted in attenuation of infection in the mouse model. Next, we provide a fundamental phenotypic characterization of the *gapA* deletion mutant strain, including experimental evidence of GapA's extracytosolic localization which provides convincing evidence of additional non-enzymatic functions of GapA in *F. tularensis*.

MATERIALS AND METHODS

Bacterial strains and Culture

The *F. tularensis* and *E. coli* strains used in this study are listed and described in **Table 1**. All *F. tularensis* strains were cultured on McLeod agar enriched with bovine hemoglobin (Becton Dickinson, Cockeysville, MD, USA) and IsoVitalEx (Becton Dickinson) and in liquid Chamberlain's medium at 37°C (Chamberlain, 1965), supplemented with tryptone (10 mg/mL) when indicated. *E. coli* strains were grown on Luria–Bertani (LB) agar and in LB broth at 37°C. Where appropriate, antibiotics were used at the following concentrations: chloramphenicol 2.5 µg/mL (*F. tularensis*) or 25 µg/mL (*E. coli*), polymyxin B 75 µg/mL, ampicillin 100 µg/mL, and penicillin 100 U/mL.

Construction of In-Frame Deletion Mutant *gapA* and Complementation

The DNA construct encoding in-frame deletion for the *gapA* gene with introduced restriction sites XhoI and SpeI (locus tag FTS_1117) was generated by overlapping PCR amplification

TABLE 1 | Bacterial strains and plasmids used in this study.

Strain/Plasmid	Genotype/Phenotype	Source/References
<i>F. tularensis</i>		
FSC200	<i>F. tularensis</i> subsp. <i>holarctica</i> ; clinical isolate	<i>Francisella</i> strain collection Johansson et al., 2000
dsbA	ΔFTS_1067/FSC200	Straskova et al., 2009
gapA	ΔFTS_1117/FSC200	This study
gapA-complemented	ΔFTS_1117/FSC200::FTS_1117	This study
<i>E. coli</i>		
Top10	F ⁻ <i>mcrA</i> Δ(<i>mrr-hsdRMS-mcrBC</i>), φ80 <i>lacZ</i> Δ <i>M15</i> Δ <i>lacX74</i> <i>recA1</i> <i>deoR</i> <i>araD139</i> (Δ <i>ara-leu</i>)7697 <i>galU</i> <i>galK</i> <i>rpsL</i> (Sm ^r) <i>endA1</i> <i>nupG</i>	Invitrogen
S17-1λpir	<i>recA</i> , <i>thi</i> , <i>pro</i> , <i>hsdR</i> ⁻ M ⁺ , <RP4:2-Tc:Mu:Km:Tn7>Tp ^R , Sm ^R	Simon et al., 1983
Plasmids		
pCR [®] 4.0-TOPO	TOPO-cloning vector. Amp ^R , Km ^R	Invitrogen
pDM4	Suicide plasmid. <i>sacB</i> ; <i>mobRP4</i> ; <i>oriR6K</i> ; Cm ^R	Milton et al., 1996

using the primers A–D shown in **Table 2**. The resulting DNA fragment was cloned into pCR4-TOPO vector (Invitrogen, Carlsbad, CA, USA) and verified by sequence analysis (ABI PRISM 3130xl, Applied Biosystems). Fragments from plasmids with verified inserts were cloned into pDM4 (**Table 1**), then introduced into *E. coli* S17-1λpir. The in-frame deletion mutant *gapA* was complemented *in cis* using a strategy similar to the in-frame deletion mutagenesis described above. Preparation of plasmid DNA, restriction enzyme digests, ligations, and transformations into *E. coli* all were performed essentially as described (Sambrook and Russel, 2001).

Proteomics

Metabolic Labeling, Membrane Fraction Preparation

F. tularensis was cultivated in Chamberlain's chemically defined medium (Chamberlain, 1965). The wild-type strain FSC200 was cultivated in the heavy variant of the medium containing isotopically labeled L-arginine hydrochloride [¹³C₆ ¹⁵N₄] and L-lysine hydrochloride [¹³C₆ ¹⁵N₂] (Sigma-Aldrich, Schnellendorf, Germany) in the same concentrations as in the light medium. The *dsbA* deletion mutant strain was grown in the light medium. Bacteria were cultivated in the corresponding media overnight at 36.8°C, 200 rpm. Overnight cultures were diluted 20 times with fresh media and again grown overnight. Bacteria were then pelleted, diluted with fresh media to OD_{600 nm} 0.1 and cultivated to OD_{600 nm} 0.8 (late exponential phase). Three biological replicates were prepared. Harvested and washed bacteria were suspended in phosphate-buffered saline (PBS, pH 7.4)

TABLE 2 | Sequences of primers used for creation of *F. tularensis* FSC200 *gapA* deletion mutant.

Gene	Primer designation	5'–3' Sequence
gapA (FTS_1117)	A	CTCGAGTATATAGCTTCGCAATTGA GTAA
	B	GCTCCGAAGTAACCATTAAATTGCAA CTCTCATTTT
	C	GCAATTAATGGTTACTCTCGGAGCTC TATAAACA
	D	ACTAGTATCTCATCCGCAACAAC ATAG

Restriction sites for selected endonucleases on primers A and D are in italic; complementary parts of primer B and C are underlined.

supplemented with protease inhibitor cocktail Complete EDTA-free (Roche Diagnostics, Germany) and benzonase (150 U/mL, Sigma-Aldrich), then disrupted in a French press (Thermo IEC, Needham Heights, MA, USA) by three passages at 16,000 PSI. Unbroken cells were removed by centrifugation at 6,000 × g for 30 min at 4°C. Protein concentration was determined using a bicinchoninic acid protein assay kit (Sigma-Aldrich). Corresponding light and heavy cell lysates were mixed in a 1:1 protein ratio and centrifuged at 120,000 × g for 30 min at 4°C in a Beckman TLA-100.3 fixed angle rotor (Beckman Instruments, Palo Alto, CA, USA). Supernatants were discarded and pellets (membrane-enriched fractions) were suspended in 50 mM Tris/HCl, pH 8.0, and pelleted again. Pellets were stored at –80°C until the mass spectrometry (MS) analysis.

Protein Digestion for Mass Spectrometry Analysis

The membrane pellets were dissolved in 50 mM ammonium bicarbonate with 5% (w/v) sodium deoxycholate (SDC), then incubated for 20 min on ice with intermittent vortexing. Protein concentration was then determined. Samples were then reduced with 10 mM dithiothreitol at 37°C for 60 min, alkylated with 20 mM iodoacetamide at room temperature for 30 min in darkness, and the unreacted iodoacetamide was quenched with additional 10 mM dithiothreitol at room temperature for 15 min. The samples were diluted with 50 mM ammonium bicarbonate to reduce the concentration of SDC to 0.5% and digested with sequencing grade trypsin (Promega, Madison, WI, USA) overnight at 37°C. SDC was removed using the modified phase transfer protocol (Masuda et al., 2008). Briefly, ethyl acetate was added and the digested product was acidified by trifluoroacetic acid (TFA) to a final concentration of ca 2% (v/v). The mixtures were vortexed vigorously for 1 min, centrifuged at 14,000 × g for 5 min, and the upper organic layer was removed. The extraction was repeated with a fresh portion of ethyl acetate. The aqueous phases were desalted on EmporeTM C18-SD (4 mm/1 mL) extraction cartridges (Sigma-Aldrich) and dried in a vacuum.

Peptide Separation and Mass Spectrometry Analysis

Liquid chromatography–mass spectrometry analysis was performed using the Ultimate 3000 RSLCnano System (Dionex, Sunnyvale, CA, USA) coupled online via a Nanospray Flex ion

source with a Q-Exactive mass spectrometer (Thermo Scientific, Bremen, Germany). Peptide mixtures were dissolved in 2% acetonitrile/0.05% TFA and 500 ng of each was loaded onto a capillary trap column (C18 PepMap100, 3 μm , 100 \AA , 0.075 \times 20 mm; Dionex) using 5 $\mu\text{L}/\text{min}$ of 2% acetonitrile/0.05% TFA for 5 min. They were then separated on a capillary column (C18 PepMap RSLC, 2 μm , 100 \AA , 0.075 \times 150 mm; Dionex) using a step linear gradient of mobile phase B (80% acetonitrile/0.1% formic acid) over mobile phase A (0.1% formic acid) from 4 to 34% B in 68 min and from 34 to 55% B in 21 min at flow rate of 300 nL/min. The column was kept at 40°C and the eluent was monitored at 215 nm. Spraying voltage was 1.75 kV and heated capillary temperature was 200°C. The mass spectrometer operated in the positive ion mode performing survey MS (at 350–1,650 m/z) and data-dependent MS/MS scans of the 10 most intense precursors with a dynamic exclusion window of 60 s and isolation window of 2.0 Da. MS scans were acquired with resolution of 70,000 from 3×10^6 accumulated charges; maximum fill time was 100 ms. Normalized collision energy for higher-energy collisional dissociation (HCD) fragmentation was 27 units. MS/MS spectra were acquired with resolution of 17,500 from 10^5 accumulated charges; maximum fill time was 100 ms. Each biological replicate was analyzed three times (total of nine measurements).

Protein Identification and Quantification

Database search and relative protein quantification were performed using Proteome Discoverer 1.3 (v. 1.3.0.339, Thermo Scientific) and the Mascot search algorithm. The reference proteome set of *F. tularensis* FSC200 was downloaded from UniProt/KB in March 2013 and merged with a common contaminants file downloaded from the MaxQuant web page (<http://www.maxquant.org/downloads.htm>). The merged database contained 1,671 sequences. The search parameters were as follows: digestion with trypsin, maximum two missed cleavages allowed, peptide mass tolerance of 10 ppm, fragment mass tolerance of 0.02 Da, fixed carbamidomethylation of cysteine, variable oxidation of methionine, and SILAC labels Arg10 and Lys8. The strict target value of false discovery rate (FDR) for a decoy database search of 0.01 was applied (high confidence). Only unique peptides were considered for quantification and the light-to-heavy ratios were normalized on protein median for each replicate. The quantification workflow was performed on two levels. On the first level, missing quantitative values were not considered and the maximum allowed fold change was set to 100. In the second level, extreme ratios were considered, the missing quantitative values were replaced by the minimum value detected (the detection threshold) and ratios above the maximum allowed fold change were used for quantification. The second-level quantification allowed for quantification of additional proteins (highlighted by asterisk in Table 3).

For relative protein quantification, only proteins with minimum of 1 quantified peptide per at least 6 measurements out of 9 were considered. Light-to-heavy ratios were converted to \log_2 and median was determined from the three measurements for each biological replicate. Mean, standard deviation, and the

t-statistic *p*-value were then evaluated from the three biological replicates. For further study, proteins showing absolute change larger than 1.5 and $p \leq 0.05$ were considered (see Table 3 and Supplementary Table 2). The mass spectrometry proteomics data have been deposited to the ProteomeXchange Consortium via the PRIDE (Vizcaíno et al., 2016) partner repository with the dataset identifier PXD007682.

Intracellular Replication and Invasion Assays

To generate bone marrow macrophages (BMMs), bone marrow cells were collected from dissected femurs of female BALB/c mice 6–10 weeks old and differentiated into macrophages in Dulbecco's Modified Eagle Medium (DMEM, Invitrogen) supplemented with 10% fetal bovine serum and 20% L929-conditioned medium for 6–7 days (Celli, 2008). The differentiated BMMs were seeded at concentration 5×10^5 cells/well in 24-well plates and infected the next day with *F. tularensis* strains at multiplicity of infection (MOI) 50:1 (bacteria/cell). To synchronize the infection, the infected cells were centrifuged at $400 \times g$ for 5 min and incubated at 37°C for 30 min. The extracellular bacteria were then removed by gentamicin treatment (5 $\mu\text{g}/\text{mL}$) for 30 min. For the proliferation assay, the infected BMMs were lysed at selected time points with 0.1% SDC. To determine the number of intracellular bacteria, the lysates were serially diluted and plated on McLeod agar. The human alveolar type II epithelial cell line A549 (ATCC[®] CCL-185[™]) was cultured in DMEM supplemented with 10% fetal bovine serum (Invitrogen). Infections were carried out as described by Lo et al. (2013). Briefly, the cells were infected with *F. tularensis* strains at MOI of 200 and incubated for 3 h. The extracellular bacteria were removed by gentamicin treatment, the cells were lysed at selected time points, then the cells were plated in serial dilution on McLeod agar.

Cell Viability and Cytotoxicity Assay

To follow the viability and cytotoxic effect of *F. tularensis* strains on BMMs, the cells were seeded in 96-well tissue culture plates at concentration 3×10^4 cells/well and allowed to adhere overnight. The next day, the BMMs were infected with bacterial cell suspensions at a MOI of 100:1 for 1 h. The extracellular bacteria were washed thoroughly away and the cells were incubated in DMEM medium at 37°C with 5% CO₂. The cell viability was observed in real time using a non-lytic bioluminescence RealTime-Glo[™] MT Cell Viability Assay (Promega, Madison, WI, USA). The cytotoxicity was assayed in parallel using fluorescence CellTox[™] Green Cytotoxicity Assay (Promega). The samples were processed and the luminescence and fluorescence were measured at indicated time points on a FLUOstar OPTIMA plate reader (BMG Labtech, Germany) according to the manufacturer's instructions.

Animal Studies

For survival studies, groups of at least five female BALB/c mice 6–8 weeks old were infected subcutaneously (s.c.) with the *gapA* mutant strain (using doses of 1.5×10^2 , 3×10^2 , 3×10^5 , and 3×10^7 cfu/mouse), the wild-type FSC200 strain (wt strain),

TABLE 3 | Proteins with significantly altered expression in *dsbA* mutant compared to the FSC200 wild-type strain detected by SILAC quantitative shotgun approach.

Accession ^a	FTS locus tag	Protein name ^a	up-/down- ^b	COG ^c	References
AFT93177	1495	Hypothetical protein, FTS_1495	up-	S	Straskova et al., 2009; Konecna et al., 2010; Ren et al., 2014; Qin et al., 2016
AFT93208	1538	Hypothetical protein FTS_1538	up-	S	Straskova et al., 2009; Konecna et al., 2010; Pávková et al., 2013; Ren et al., 2014
AFT93168	1485	Chitinase family 18 protein	up-	G	Kadzhaev et al., 2009; Straskova et al., 2009; Chung et al., 2014; Ren et al., 2014
AFT93368	1749	Hypothetical protein FTS_1749	up-	S	Ren et al., 2014; Qin et al., 2016
AFT92137	0123	Pyruvate phosphate dikinase	up-	G	
AFT92841	1034	D-alanyl-D-alanine carboxypeptidase	up-	M	Straskova et al., 2009; Ren et al., 2014; Qin et al., 2016
AFT92421	0495	Hypothetical protein FTS_0495	up-	S	Ren et al., 2014
AFT93021	1279	Hypothetical protein FTS_1279	up-	S	Straskova et al., 2009; Chong et al., 2013; Ren et al., 2014; Qin et al., 2016
AFT93404	1789	Siderophore biosynthesis protein	up-	P	Ramakrishnan et al., 2008; Pérez et al., 2016
AFT93162	1476	Glycerophosphoryl diester phosphodiesterase	up-	I	Konecna et al., 2010
AFT92351	0402	Hypothetical protein FTS_0402	up-	S	Ren et al., 2014
AFT92903	1117	Glyceraldehyde-3-phosphate dehydrogenase/erythrose-4-phosphate dehydrogenase	up-	G	Konecna et al., 2010; Qin et al., 2016; this study
AFT93160	1471	Catalase/peroxidase	up-	P	Lindgren et al., 2007; Qin et al., 2016
AFT93076	1361	Parvulin-like peptidyl-prolyl isomerase domain-containing protein	up-	O	Su et al., 2007
AFT92667	0815	Hypothetical protein FTS_0815	up-	S	Ren et al., 2014
AFT92381	0450	Hypothetical protein FTS_0450	up-	S	Brotcke et al., 2006; Brotcke and Monack, 2008; Wehrly et al., 2009
AFT92582	0702	FAD binding family protein	up-	C	Ren et al., 2014
AFT92713	0868	X-prolyl aminopeptidase 2	up-	E	Guina et al., 2007
AFT93339	1709	Elongation factor Tu	up-	J	Barel et al., 2008; Qin et al., 2016
AFT92546	0659	Hypothetical protein FTS_0659	up-	S	Straskova et al., 2009
AFT92986	1229	Hypothetical protein FTS_1229	up-	S	
AFT92133	0111/1139	Hypothetical FTS_0111	up-	S	Robertson et al., 2013; Bröms et al., 2016
AFT92684	0836	Isochorismatase hydrolase family protein	up-	Q	Pavkova et al., 2006; Su et al., 2007
AFT92956	1187	Hypothetical protein FTS_1187	up-	S	Wehrly et al., 2009; Qin et al., 2016
AFT92755	0920	Hypothetical protein FTS_0920	up-	S	Brotcke et al., 2006
AFT92560	0676	Hypothetical protein FTS_0676	up-	S	
AFT92796	0974	Hypothetical protein FTS_0974	up-*	S	Ren et al., 2014
AFT92765	0935	GTP-dependent nucleic acid-binding protein EngD	up-*	J	
AFT92195	0200	Hypothetical protein FTS_0200	down-	S	Dieppedale et al., 2011, 2013
AFT92865	1068	Hypothetical protein FTS_1068	down-	S	Straskova et al., 2009; Qin et al., 2011
AFT92060	0012	Inhibitor of RecA	down-	L	
AFT92481	0580	Sugar porter (SP) family protein	down-	G	
AFT93103	1397	Glycosyltransferase family protein	down-	M	Bandara et al., 2011
AFT92194	0199	von Willebrand factor type A domain-containing protein	down-	R,O	Dieppedale et al., 2011, 2013
AFT92732	0890	Protease, GTP-binding subunit	down-	J	Su et al., 2007
AFT92334	0381	Type IV pili, pilus assembly protein	down-	N,W	Salomonsson et al., 2011
AFT93371	1752	FOF1 ATP synthase subunit gamma	down-	C	
AFT92172	0175	LPS fatty acid acyltransferase	down-	M	McLendon et al., 2007
AFT92106	0079	Acyltransferase	down-	I	
AFT92933	1158	Ribonuclease HII	down-	L	Kadzhaev et al., 2009
AFT93108	1402	ABC transporter ATP-binding protein	down-	V	Dankova et al., 2016

(Continued)

TABLE 3 | Continued

Accession ^a	FTS locus tag	Protein name ^a	up-/down- ^b	COG ^c	References
AFT92145	0137	Hypothetical protein FTS_0137	down-	S	
AFT93370	1751	FOF1 ATP synthase subunit beta	down-	C	Qin et al., 2016
AFT93375	1756	FOF1 ATP synthase subunit C	down-	C	
AFT93243	1582	Drug: H ⁺ antiporter-1 (DHA1) family protein	down-	V	Su et al., 2007
AFT93130	1439	Excinuclease ABC, subunit A	down-	L	Su et al., 2007; Kadzhaev et al., 2009
AFT92197	0202	Hypothetical protein FTS_0202	down-	S	Dieppedale et al., 2011, 2013
AFT93269	1620	Nucleoside permease NUP family protein	down-	F	
AFT92502	0602	O-antigen flippase	down-	C	Dankova et al., 2016
AFT92502	1754	FOF1 ATP synthase subunit delta	down-	C	
AFT93369	1750	FOF1 ATP synthase subunit epsilon	down-	C	
AFT93467	1882	ATP-binding cassette (ABC) superfamily protein	down-	P,R	Asare and Abu Kwaik, 2010
AFT92984	1226	ATP-dependent RNA helicase	down-	L	
AFT93372	1753	FOF1 ATP synthase subunit alpha	down-	C	Qin et al., 2016
AFT92658	0799	Amino acid transporter	down-	E	Kadzhaev et al., 2009
AFT92817	1004	Radical SAM superfamily protein	down-	J	
AFT92323	0367	Hypothetical protein FTS_0367	down-	S	
AFT92497	0597	Membrane protein/O-antigen protein	down-	M	Kim et al., 2010
AFT93227	1562	Delta-aminolevulinic acid dehydratase	down-	H	
AFT92449	0533	Uracil-DNA glycosylase	down-	L	
AFT93102	1396	Glycosyltransferases group 1 family protein	down-	M	Weiss et al., 2007; Bandara et al., 2011; Thomas et al., 2011
AFT92105	0078	Acyltransferase	down-*	I	
AFT92192	0197	Uncharacterized protein FTS_0197	down-*	S	Dieppedale et al., 2011, 2013

^aAccession numbers and protein names according to NCBI (<https://www.ncbi.nlm.nih.gov>).

^bUp- or down-regulated proteins according to the following criteria: statistical significance $p < 0.05$; relative changes ≥ 1.5 for up-regulated or \leq for down regulated proteins. *Quantified by second-level quantification workflow (extreme ratios considered).

^cPredicted function of proteins by COG using the COGnitor program (<http://www.ncbi.nlm.nih.gov/COG/>). S, no functional prediction; G, carbohydrate metabolism and transport; M, cell wall structure and biogenesis and outer membrane; P, inorganic ion transport and metabolism; I, lipid metabolism; O, molecular chaperons and related functions; C, energy production and conversion; E, amino acid metabolism and transport; J, translation, ribosome structure, and biogenesis; N, secretion, motility, and chemotaxis; W, extracellular structure; L, replication, recombination, and repair; V, defense mechanisms; F, nucleotide transport and metabolism; Q, secondary metabolites biosynthesis, transport, and catabolism; H, coenzyme transport and metabolism; R, general function prediction only.

Genes encoding proteins highlighted in bold were inactivated using retargeted mobile group II introns and tested for potential attenuation in vivo.

and *gapA*-complemented strain (both at 10^2 cfu/mouse). Control groups of mice were inoculated with sterile saline only. Mice were housed in micro-isolator cages and fed sterilized water and food *ad libitum*. Infected mice were examined every day for signs of illness through 42 days. For protection studies, the mice were challenged s.c. 42 days post-infection with 3×10^2 cfu of the wt strain and monitored for survival for an additional 21 days. Three independent experiments were performed. For growth kinetics studies, groups of three BALB/c mice were infected with 3×10^2 cfu/mouse of wt strain, *gapA* mutant strain, or *gapA*-complemented strain. At 1, 3, 5, 7, 14, 21, 28, 35, and 42 days after infection, spleens and livers were aseptically removed, homogenized in 2 mL of PBS, and serial dilutions plated onto McLeod agar.

Preparation of the Whole-Cell Lysate, Crude Membrane Fraction, and Culture Filtrate Proteins

Bacteria were grown in Chamberlain's medium at 37°C until the late logarithmic phase (0.7–0.8 O.D.). To obtain whole-cell lysate, the bacteria were lysed in a French pressure cell and unbroken

cells and cell debris were removed by centrifugation. The pellet with membrane proteins was obtained by ultracentrifugation of the whole-cell lysate, then suspended in PBS as described previously. For the preparation of culture filtrate proteins (CFP), the bacteria were removed by centrifugation and the culture medium was vacuum-filtered through membranes (0.2 μ m pore; Merck Millipore, Billerica, MA, USA). The filtrate was then concentrated using Stirred Ultrafiltration Cell (8200, Millipore) with 5 kDa cut-off membrane from regenerated cellulose (Millipore) followed by diafiltration using Amicon Ultra 3K devices (Millipore) to further concentrate the protein sample and exchange the medium for 40 mM Tris/HCl (pH 7.3). The protein content was determined using a bicinchoninic acid assay.

2D Gel Electrophoresis and Immunodetection

Protein samples (150 μ g) were dissolved in rehydration buffer containing 1% (w/v) ASB-14 surfactant. Isoelectric focusing in the non-linear pH range of 3–10 and gradient 9–16% SDS-PAGE in the second dimension were performed as described previously (Straskova et al., 2009). Separated proteins were

electroblotted onto polyvinylidene difluoride membranes and the GapA protein was detected using a polyclonal rabbit anti-GapA antibody (Apronex, Vestec, Czech Republic). Swine anti-rabbit IgG/HRP (Dako, Glostrup, Denmark) was applied as secondary antibody. Chemiluminescence was detected using a BM Chemiluminescence Blotting Substrate (POD) according to the manufacturer's instructions (Roche Diagnostics, Mannheim, Germany).

Transmission Electron Microscopy

The overnight culture of wild-type strain bacteria (FSC200) grown in Chamberlain's medium was pelleted, washed in PBS, then fixed in a mixture of 3% formaldehyde plus 0.1% glutaraldehyde in 0.1 M Na/K phosphate buffer, pH 7.2–7.4 (Sørensen's buffer) in the ratio of 10:1 (v:v) for 30 min at room temperature. The fixed bacteria were centrifuged for 15 min at 7,300 rpm and the pellet was twice washed in ice-cold Sørensen's buffer. The pellet was then mixed with 2.5% agarose and centrifuged (25 min, 8,500 rpm, +37°C). The free aldehyde groups were quenched in 0.02 M glycine in Sørensen's buffer for 10 min. The sample was washed in Sørensen's buffer two times for 7 min each time. The samples were separated into two groups and processed for either LR White or Lowicryl HM20 resin embedding. "LR White" samples were dehydrated in 30, 50, 70, 90, and 96% ethanol for 7 min each, infiltrated in the mixtures of LR White with 96% ethanol (1:2 and 2:1 for 30 min each), then placed into LR White for overnight infiltration. All steps were carried out at +4°C. The next day, the samples were infiltrated in fresh LR White for 3 h at +4°C and polymerized by UV for 48 h at +4°C. "Lowicryl HM20" samples were dehydrated in 30% (30 min, +4°C), 50% (1 h, –20°C), 70% (1 h, –35°C), and 100% ethanol (two times for 1 h each time, –50°C), infiltrated in the mixtures of Lowicryl HM20 with 100% ethanol (1:1 and 2:1 for 1 h each, –50°C), placed into Lowicryl HM20 for 1 h (–50°C), then into fresh resin for overnight infiltration at –50°C. The next day, the temperature was elevated to –35°C and the samples were UV-polymerized for 24 h at –35°C and 72 h at room temperature.

Ultrathin sections (70 nm) were immunolabeled following a conventional protocol (Strádalová et al., 2008) and examined using Morgagni 268 (at 80 kV) and Tecnai G2 20 LaB6 (at 200 kV) transmission electron microscopes (FEI, Eindhoven, The Netherlands). The images were captured with Mega View III CCD and Gatan Model 894 UltraScan 1000 cameras. Multiple sections of repetitive immunogold labeling experiments were analyzed. Antibodies used for immunolabeling were primary rabbit anti-FTT antibody (dilution 1:25 to 1:100) and secondary goat anti-rabbit IgG (H + L) antibody coupled with 12 nm colloidal gold particles (Jackson ImmunoResearch Laboratories Inc., 111-205-144; dilution 1:30).

Expression and Purification of Recombinant GapA Protein

PCR was used to amplify the *F. tularensis* gapA gene with specific primers containing an NcoI site in the forward primer (5'-CCCCATGGGTTTAAATAAACTTTTCGCAAGATAA-3') and an XhoI site in the reverse primer (5'-GGCTCGAGTA

GAGCTCCGAAGTACTCT-3'). The gel-purified PCR products (Qiagen) were cloned into pET28b, resulting in the recombinant plasmid encoding GapA with a C-terminal histidine tag. The plasmid construct was verified by direct DNA sequencing. Expression vector pET-gapA was transformed into *E. coli* NiCo214(DE3)(NEB) cells for production and purification of recombinant protein. Cells were grown at 37°C to A600 of 0.6, and expression was subsequently induced using 1 mM IPTG for 4 h. Pelleted cells were lysed by sonication in lysis buffer (50 mM phosphate, 300 mM NaCl). The cell extract was clarified at 20,000 rpm for 30 min at 4°C, and supernatant was applied to a TALON column (Clontech) for purification of His-tagged GapA. Eluted fractions were verified by SDS-PAGE followed by Coomassie staining and immunoblotting for the presence of GapA.

Glyceraldehyde-3-Phosphate Dehydrogenase (GAPDH) Activity Assay

GAPDH activity measurement was conducted according to Pancholi and Fischetti (1992). The purified recombinant protein, whole-cell lysate, or fraction enriched in CFPs were mixed with 7 μ L glyceraldehyde-3-phosphate (50 mg/mL, substrate), 100 μ L NAD⁺ (10 mM), and assay buffer (40 mM triethanolamine, 50 mM Na₂HPO₄, and 5 mM EDTA, pH 8.6) in a final volume of 1 mL. Negative control assays were performed without the addition of substrate. The conversion of NAD⁺ to NADH was monitored spectrophotometrically at 340 nm at regular time intervals for a given time.

Binding Assays of GapA to Selected Human Proteins

Far-Western Assay

This method used for detection of GapA binding to human proteins fibrinogen, fibronectin, actin, and plasminogen was performed according to Egea et al. (2007). The proteins (5 μ g each, Sigma-Aldrich) were separated on a 12% SDS-PAGE and transferred to a PVDF membrane. The membrane was blocked in a solution of PBST [4 mM KH₂PO₄, 16 mM Na₂HPO₄, 115 mM NaCl (pH 7.4), 0.05% (v/v) Tween-20] and 5% (w/v) powdered milk for 1 h at room temperature. The membrane was incubated overnight with a purified recombinant GapA (0.5 μ g/mL) diluted in 10 mL binding buffer [100 mM NaCl, 20 mM Tris (pH 7.6), 0.5 mM EDTA, 10% (v/v) glycerol, 0.1% (v/v) Tween-20, 2% (w/v) powdered milk, 1 mM dithiothreitol] at 4°C and washed three times in the PBST. To visualize the interaction between GapA and selected proteins, the membrane was incubated with anti-GapA antibody diluted 1:1,000 in PBST with 5% (w/v) powdered milk for 16 h at 4°C and further processed using the ECL Select Western Blotting Detection Reagent according to the manufacturer's instructions (GE Healthcare Life Sciences).

Solid-phase Ligand-binding Assay

The human proteins (plasminogen, fibrinogen, fibronectin, and actin) (0.5 μ g/mL) diluted in 100 μ L PBS [4 mM KH₂PO₄, 16 mM Na₂HPO₄, 115 mM NaCl (pH 7.4)] were coated on 96-well microtiter plate overnight at room temperature. PBS buffer was changed for TBS blocking buffer [20 mM Tris-HCl, 150 mM NaCl, (pH 7.6)] with 1% (w/v) powdered bovine serum

albumin and incubated overnight at 4°C. The wells coated with proteins were incubated with purified recombinant GapA (0.125 µg/mL to 2 µg/mL) in TBS buffer with 1% bovine serum albumin for 3 h at room temperature. The plate was washed three times in TBS with 0.05% (v/v) Tween-20 and once in TBS buffer. The amount of GapA bound to these proteins was determined spectrophotometrically (450 nm) in an ELISA-based assay using anti-GapA antibody (1:10,000) followed by peroxidase-labeled donkey anti-rabbit anti-body (1:4000) and 3, 3', 5, 5'-tetramethylbenzidine (Sigma-Aldrich) as chromogenic substrate.

Ethics Statement

This study was carried out in accordance with the recommendations of the guidelines of the Animal Care and Use Ethical Committee of the Faculty of Military Health Sciences, University of Defence, Czech Republic. The protocol was approved by the Ethical Committee of the Faculty of Military Health Sciences, University of Defence, Czech Republic.

Statistical Analysis

All the experiments were performed at least three times and each sample in each separate experiment was processed at least in triplicate. Values are expressed as mean ± standard deviation (SD) and analyzed for significance using Student's two-tailed *t*-test. Differences were considered statistically significant at $p < 0.05$.

RESULTS

Semiquantitative Analysis of Membrane-Enriched Fractions of the *dsbA* Mutant and the Wild-Type Strain of Subsp. *holarctica* FSC200. Construction of Selected TargeTron Insertion Mutants and Their Testing for *in Vivo* Attenuation

In our previously published study (Straskova et al., 2009), using the combination of classical gel-based and iTRAQ quantitative shotgun proteome analyses, we had been able to identify only nine proteins with significantly altered abundance in membrane-enriched fractions of the *dsbA* mutant strain compared to its wild counterpart. Inasmuch as the DsbA protein of *F. tularensis* demonstrably plays a role in proper folding of other proteins, this number was evidently underestimated. That is why we decided to analyze and compare the two membrane proteomes (*dsbA* mutants strain vs. wt strain) using SILAC metabolic labeling. This approach enabled us to find a total of 63 proteins that were either significantly more (30) or less (35) abundant in response to deletion of the *dsbA* gene (Table 3). Therefore, in contrast to our previous study, the number of known DsbA-regulated proteins was significantly enlarged. This confirms the high sensitivity of the applied proteomic approach.

According to the Cluster of Orthologous Genes (COG) categories classification, the *dsbA* gene deletion resulted in broad changes within the bacterial proteome that included proteins from a diverse set of functional categories (Supplementary

Figure 3). The categories most represented involved poorly characterized proteins with unknown function (21) and proteins engaged in diverse metabolic processes (22). As seen in Table 3, most of the proteins affected by the *dsbA* gene deletion have previously been mentioned in the literature. Many of them are well-known virulence determinants; others have not been proven to play a direct role in the pathogenicity of tularemia infection. For the preliminary screening of new potential virulence factors dependent on DsbA oxidative folding, we successfully inactivated 15 genes encoding selected proteins (highlighted in bold in Table 3) using retargeted mobile group II introns as described previously (Rodriguez et al., 2009). The main criteria for the protein selection included lack of previously published data, known immunoreactive proteins (Kilmury and Twine, 2011; Chandler et al., 2015), and any evidence for association with virulence based on bioinformatics screening using NCBI or UniProt. All the data concerning the TargeTron insertion mutants, methodology, and results are summarized in the Supplementary Material. The prepared mutant strains were examined for their virulence potential in mice. Unfortunately, none of the tested mutant strains except for the strain with a targeted gene for glyceraldehyde-3-phosphate dehydrogenase (GapA, FTS_1117) revealed any signs of attenuation, as, similarly to the wt strain, all the challenged mice succumbed to infection around the 5th day. On the contrary, all the mice infected with the *gapA* insertion mutant (*gapAin*) in doses of 10^2 , 10^5 , and 10^7 CFU/mouse survived the 21st day of infection. Furthermore, the proliferation of *gapAin* mutant was significantly reduced both within the murine bone-marrow derived macrophages and monocyte-macrophage cell line J774.2 (Supplementary Figures 1A,B). However, the mutant strain revealed a significant growth defect also in Chamberlain's chemically defined medium (Supplementary Figure 2) which can contribute to the diminished replication and *in vivo* attenuation.

Preparation of In-Frame Deletion *gapA* Mutant

The *gapA* gene seems to be a part of a five-gene operon encoding genes of the glycolytic/gluconeogenic pathways. Therefore, the observed attenuation in the *gapAin* mutant may be partly due to the polar effect on downstream genes as the transposons are in general known to cause polar mutations, thereby preventing transcription of downstream genes in an operon. That is why we decided to target the gene by in-frame deletion mutagenesis. GAPDH plays a key role in glucose metabolism, and its gene is thus essential in many bacteria. We nevertheless succeeded in constructing an *F. tularensis* viable *gapA* deletion mutant strain. Additionally, a complementation mutant strain was prepared and used in most of the experiments to ensure the observed phenotype is really due to elimination of the *gapA* gene.

The *gapA* Deletion Mutant Is Viable, Retained the Ability to Enter the Host Cells but Revealed a Growth Defect *in Vitro*

We first tested the effect of *gapA* deletion on the mutant's growth in a chemically defined Chamberlain's medium. As seen in

Figure 1A, growth of the *gapA* mutant strain was comparable to that of the wt until the ninth to tenth hour of growth. Thereafter, growth of the mutant strain practically ceased, thereby indicating exhaustion of amino acids as an alternative energy source that the bacteria had used instead of glucose due to the disturbed glycolytic pathway (Raghunathan et al., 2010). Accordingly, when we supplemented the medium with tryptone as a rich source of amino acids the growth of the *gapA* mutant was almost comparable with that of the wt strain (**Figure 1B**). In the *gapA*in mutant strain, the growth defect was even greater, thus indicating the polar effect of the insertion mutagenesis (Supplementary Figures 1, 2). The course of growth in brain heart infusion medium of wt and *gapA* mutant strains revealed the same trend as seen in the standard Chamberlain's medium (data not shown).

Ability of *gapA* Mutant to Invade and Replicate within the Host Cells

Macrophages are believed to be the primary host cells for *F. tularensis in vivo*. To examine the ability of the *gapA* mutant to enter and replicate in macrophages, the BMMs were infected with the wt strain, the *gapA* mutant strain, and *gapA*-complemented strain at MOI 50:1 and numbers of intracellular bacteria were determined at 1, 6, 12, 24, and 48 h after infection (**Figure 2A**). Whereas, uptake of the *gapA* mutant seemed to be unaffected, the bacteria without the functional *gapA* gene revealed a significant defect in replication inside the BMMs. The numbers of bacteria did not change until 24 h post-infection. At that time, *gapA* bacteria started to replicate very slightly. Nevertheless, their intracellular amounts remained significantly reduced compared to those of the wt strain at 48 h. The same trend also was observed by immunofluorescence microscopy (data not shown).

Francisella has also been known to evade and replicate in non-phagocytic cells, such as epithelial cells. In a human alveolar epithelial cell line, the entry of *gapA* mutant bacteria also was comparable to that of the wt strain. The numbers of wt bacteria increased rapidly during the first 24 h and then stagnated until hour 48. In contrast, the *gapA* mutant strain replicated more slowly and showed a statistically significant growth defect at 24 h post-infection. The diminished growth continued to 48 h post-infection, at which time the number of microbes reached nearly the same level as that of the wild counterpart. The growth of bacteria was fully restored to wild-type levels by *gapA* complementation in both BMMs and A549, thereby demonstrating the contribution of the GapA protein to the ability of *F. tularensis* to replicate inside the host cell (**Figure 2B**).

We can conclude from this that the *gapA* mutant is able to invade and survive in both phagocytic and non-phagocytic cells. On the other hand, the *gapA* mutant exerts a significant replication defect that was far more pronounced in macrophages. However, we cannot exclude that this growth abolition can partly reflect the inability of the mutant strain to utilize glucose as main energy source and exhausted spare alternative intracellular sources of energy.

Effect of *gapA* Deletion on *F. tularensis* Cytotoxicity in BMMs

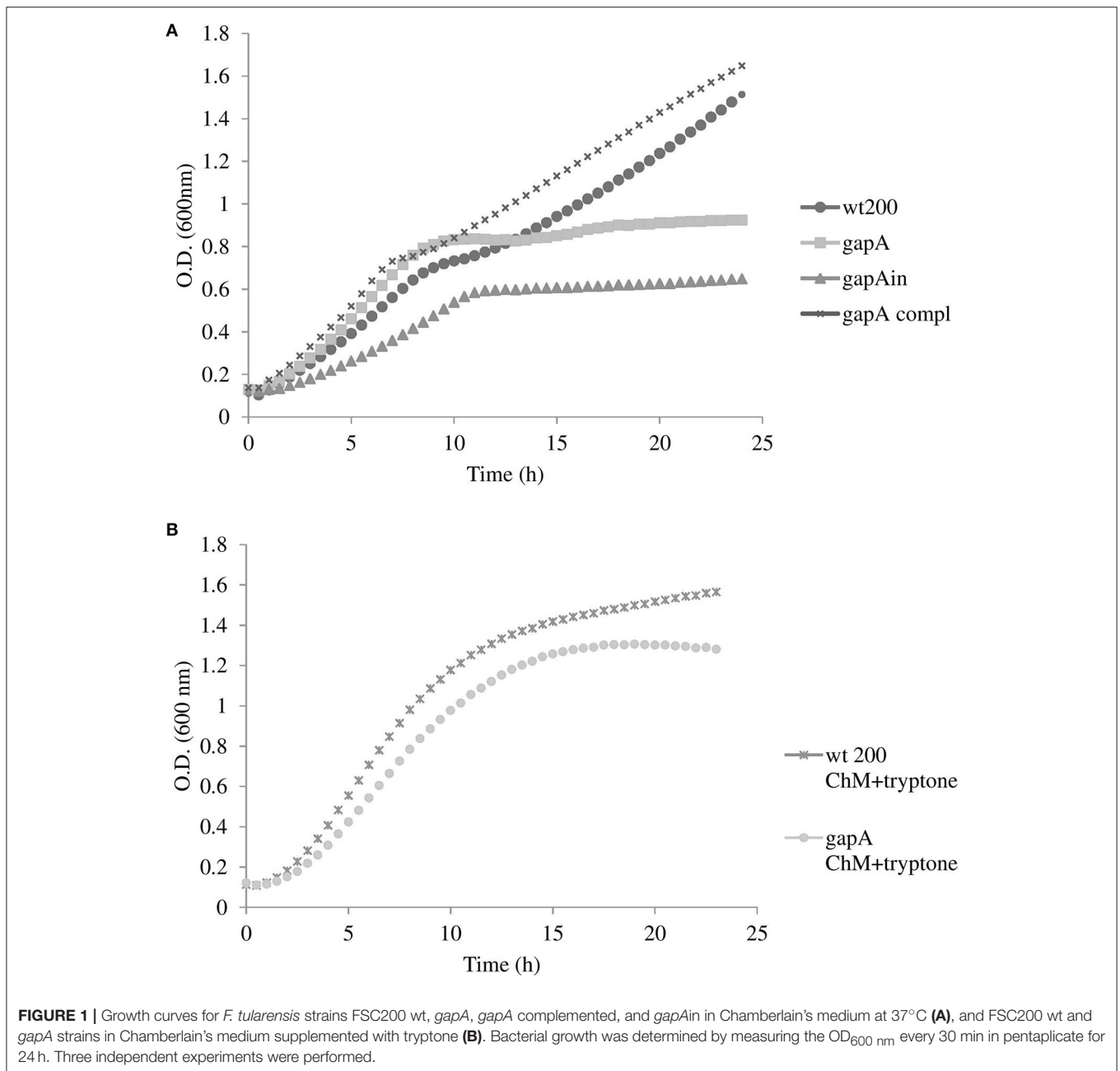
We also investigated the role of *gapA* gene deletion on host cell viability together with its cytopathogenic effects. We infected

BMMs with the wt strain or the *gapA* mutant and monitored the cell viability and cytotoxicity simultaneously over the 48 h time period using the commercial kits RealTime-Glo™ MT Cell Viability Assay and CellTox™ Green Cytotoxicity Assay (**Figure 2C**). Both these kits can be multiplexed and enable the monitoring of both parameters in real time. The luminescent viability assay determines the number of viable cells in culture by measuring the reducing potential of cells and thus metabolism. The fluorescent cytotoxicity assay measures changes in membrane integrity that occur as a result of cell death. At 2 h post-infection, the luminescence and fluorescence values were nearly the same in both infected and non-infected groups of cells. At 24 h after infection, both *F. tularensis* strains revealed a cytotoxic effect on BMMs that deepened over the next 24 h (to 48 h post-infection). The effect of the *gapA* mutant, however, was significantly less pronounced in comparison to that of the wt strain. The same trend could be observed also in cell viability. Taken together the deletion of *gapA* gene resulted in a strain with significantly less detrimental effects on cell membrane integrity and viability compared to the parental strain.

Effect of *gapA* Deletion on Virulence Attenuation and Protection in the Mouse Infection Model for Tularemia

Groups of at least five BALB/c mice were infected subcutaneously using different doses of the *gapA* mutant (1.5×10^2 , 3×10^2 , 3×10^5 , and 3×10^7) and then monitored for progression of the disease for 42 days (**Table 4**). The numbers of administered bacteria was confirmed by plating. The mice infected with wt FSC200 strain at doses 1.5×10^2 and 3×10^2 cfu died within 5–6 or 6–8 days, respectively. The *gapA* mutant, by contrast, showed a certain degree of attenuation as 60% of mice survived infection even with the highest dose of 3×10^7 cfu/mouse. Unfortunately, we could not reveal any dose dependence between the challenge dose and rate of survival, because there was no significant difference between the percentage of mice surviving the highest and lower doses: 56.7% of mice in the challenge with 3×10^5 cfu survived as did 66.7% of those infected with 3×10^2 cfu. At the lowest dose of 1.5×10^2 cfu, 76% of mice survived the infection. Complementation of the *gapA* mutant restored the virulence to the same levels as seen with the wt strain.

Those mice that survived administration of the *gapA* mutant strain were rechallenged s.c. with the full virulent wt FSC200 strain at day 42. All mice immunized with the four different doses of the *gapA* mutant survived the wt challenge and displayed no symptoms of tularemia disease during the following 3 weeks. Next, we evaluated the ability of the *gapA* mutant to disseminate through and persist within host tissues after s.c. infection. Groups of at least three BALB/c mice were inoculated subcutaneously with a dose of 3×10^2 cfu/mouse. The bacterial burdens were determined in the spleen and liver tissue homogenates at days 1, 3, 5, 7, 14, 28, 35, and 42 after infection (**Figure 3**). The numbers of wt and complemented strains increased rapidly in both organs from the first day and reached almost 10^{10} cfu in both organs. Mice infected with those two strains did not survive beyond day 5. On the other hand, the *gapA* mutant could be detected in all organs only from day 3. Thereafter, the



mutant bacteria replicated quite rapidly, reached the maximal burdens of $\sim 10^5$ cfu in the spleen and liver, then declined precipitously. By day 14, the bacteria had been completely eliminated from the liver. In the spleen, however, the initial quick decline ceased at day 14 and the bacteria persisted there at approximately the same levels of 10^2 cfu/spleen. After day 28 post-infection, those levels continued to decrease slowly. At day 42, the bacteria could still be detected in spleens of some inoculated mice in small amounts (<75 cfu). These data indicated that the *gapA* mutant is able to infect mice and to persist in infected organs, but its ability to replicate inside the host tissues is disrupted.

Localization of *F. Tularensis gapA* Protein

GAPDH is encoded in *F. tularensis* by a single gene, *gapA*. According to the PSORT-B program (<http://www.psорт.org/psортb/>), GapA is predicted to be a cytosolic protein. There is increasing evidence, however, of its extracytosolic localizations in other bacteria, often in connection with virulence. We thus decided to explore the localization of GapA in *F. tularensis* using various techniques. First, we analyzed whole-cell lysates, fractions enriched in membrane proteins, and CFPs representing the secreted proteins of *F. tularensis* by two-dimensional gel electrophoreses followed by western blot and immunodetection of GapA protein with polyclonal antibody. **Figure 4** shows that

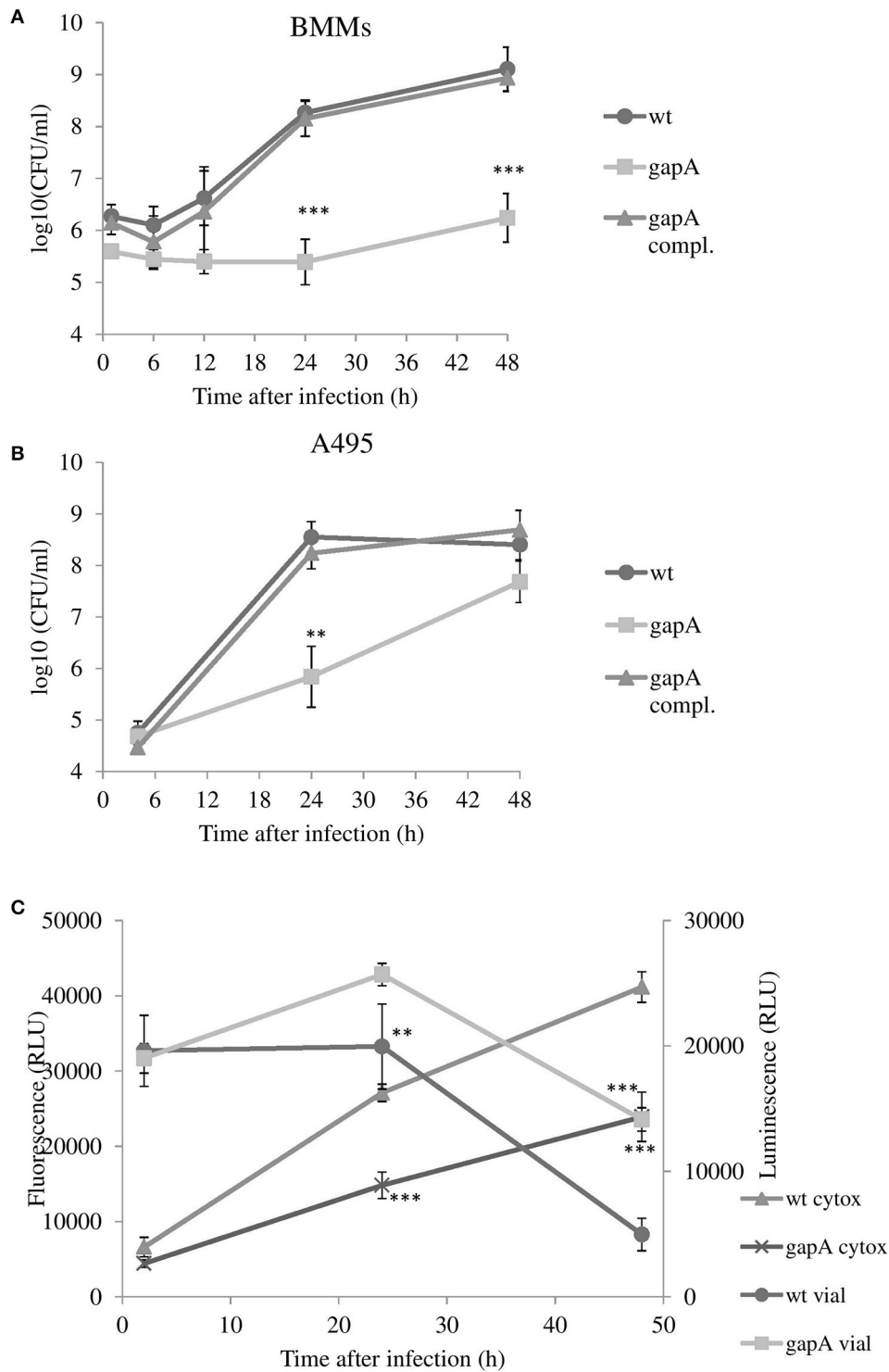


FIGURE 2 | *In vitro* invasion and proliferation of *gapA*, *gapA*-complemented, and wt FSC200 in bone marrow macrophages (BMMs) (A) and A549 cells (B). The cells were infected at MOI of 50:1 (BMM) or 200:1 (A549) with the indicated strains. BMMs were harvested at 1, 6, 12, 24, and 48 h and A549 at 4, 24, and 48 h post-infection. The numbers of bacteria recovered from the cells were counted as cfu. The data represent means \pm SD of three independent experiments performed in triplicate. (C) Viability of cells and induction of cytotoxicity determined in BMMs infected with *gapA* mutant or wild-type FSC 200 strains. At 2, 24, and 48 h the cells were assayed using RealTime-Glo™ MT Cell Viability Assay kit and CellTox™ Green Cytotoxicity Assay kit (Promega). Data are means \pm SD of triplicate samples and the results shown are representatives of three independent experiments. Asterisks indicate statistically significant differences; ***P* < 0.01; ****P* < 0.001 (comparing *gapA* with the wild-type FSC200 strain).

TABLE 4 | Survival of mice infected with *gapA*, *gapA*-complemented, and wild-type strain and protective efficacy of *gapA* mutant strain.

Strain	Inoculation dose (CFU) ^a	Time to death (day) ^b	% of survival ^c	wt FSC200 re-challenge dose (CFU) ^d	% of survival ^e
wt FSC200	3 × 10 ²	5–6	0	–	–
	1.5 × 10 ²	6–8	0	–	–
<i>gapA</i> complemented	3 × 10 ²	5–6	0	–	–
	1.5 × 10 ²	6–9	0	–	–
<i>gapA</i> mutant	3 × 10 ⁷	5–11	60%	3 × 10 ²	100%
	3 × 10 ⁵	5–11	56.7%	3 × 10 ²	100%
	3 × 10 ²	5–11	66.7%	3 × 10 ²	100%
	1.5 × 10 ²	8–14	76%	3 × 10 ²	100%

^aBALB/c mice were subcutaneously infected with the indicated inoculum dose indicated as CFU/mouse.

^bTime range in days when the mice died as consequence of infection.

^cPercentage of animals surviving infection by indicated *F. tularensis* strain.

^dMice that survived the infection with inoculation dose were challenged with wild-type FSC200 strain on day 42 and monitored for signs of infection for 21 days.

^ePercentage of animals immunized with different doses of *gapA* mutant that survived the rechallenge with wild-type strain FSC200.

GapA occurred in at least four charge variants in all tested fractions. Particularly noteworthy is that the immunodetection of GapA in CFPs revealed mass variants not detected in whole-cell lysates or membrane fractions. These data show for the first time the presence of GapA in other compartments besides the cytosol, post-translational modifications of this protein, and changes in the protein size that might be associated with the secretion process.

Further evidence of the GapA extracellular localization was obtained by the analysis of its catalytic activity. As seen in **Figure 5A**, the purified recombinant protein GapA is able to catalyze the NADH formation in the presence of the substrate glyceraldehyde-3-phosphate. As expected, the whole-cell lysates reported the GAPDH activity, as well. Furthermore, the CFPs also showed significant NADH formation coupled to glyceraldehyde-3-phosphate oxidation (**Figure 5B**). Unfortunately, due to problems with the solubility in reaction buffer, we were not able to demonstrate the catalytic activity of the fraction enriched in membrane proteins.

To define more precisely the cellular localization of GapA, we used *F. tularensis* FSC200 grown in Chamberlain's medium and processed for transmission electron microscopy. The immunolabeling experiments were performed on ultrathin sections as described in the section Materials and Methods. Electron microscopy revealed the presence of GapA protein mainly in the cytoplasm, which is consistent with its intracellular glycolytic function, and in the plasma membrane. In some cases, the protein appears in the cell wall, which might reflect the GapA trafficking to extracellular space (**Figure 6**).

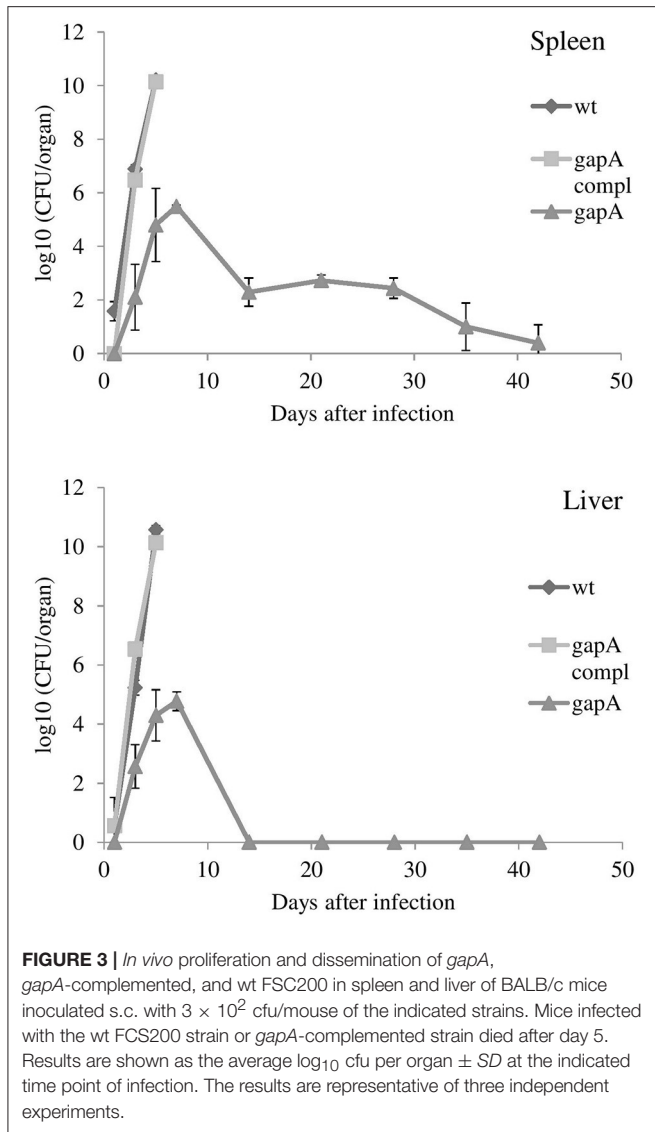
Binding of Recombinant GapA Protein to Host Proteins

Binding studies were performed to investigate the possible interaction of purified recombinant *F. tularensis* GapA with selected human proteins (plasminogen, fibrinogen, fibronectin, actin) known to interact with the GAPDH of other pathogens (summarized in Giménez et al., 2014). The results from far-western blot and solid-phase ligand-binding assays showed that purified GapA is able to bind to serum proteins plasminogen,

fibrinogen, and fibronectin (**Figures 7A,B**). On the other hand interaction with cytoskeletal protein actin could not be proved this way.

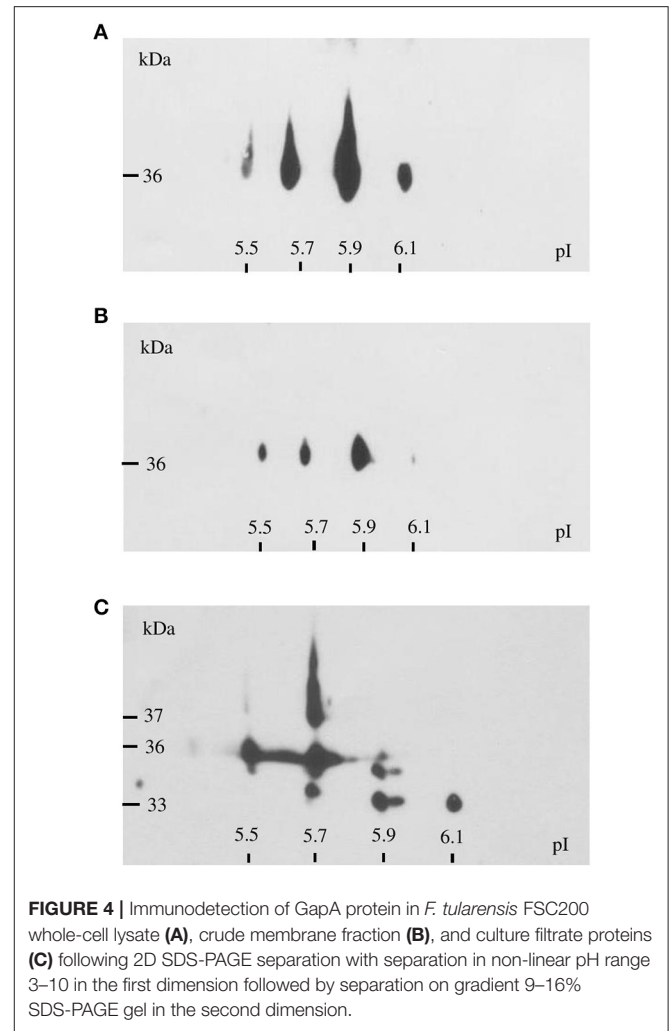
DISCUSSION

In general, the bacterial DsbA proteins catalyze the disulfide bond formation in a wide array of virulence factors essential for pathogenesis of bacteria, thus putting them at the center of interest as potential targets for the development of new therapeutic and prophylactic agents (Smith et al., 2016). During the past decade, several working groups, including our own, have studied intensively the DsbA protein of *F. tularensis* in its many aspects. The data have been presented in a number of publications (summarized by Rowe and Huntley, 2015). On the whole, FtDsbA ensures the correct folding of extracytosolic proteins through its oxidoreductase, isomerase, and probably also chaperone activities. The inactivation of the *dsbA* gene had a pleiotropic effect, resulting from the accumulation of a number of misfolded and thus dysfunctional and unstable proteins. This ultimately is reflected in reduced virulence in mice, as well as defects in intracellular survival and phagosomal escape. The two most recently published studies were directed to trapping and identification of FtDsbA substrates in order to detect new *F. tularensis* virulence factors (Ren et al., 2014); (Qin et al., 2016). In contrast to those studies, we provide here deeper insights into the complex proteome changes induced by the *dsbA* gene deletion. Using SILAC metabolic labeling, we were able to identify more than 60 proteins whose levels in the bacterial cells might be influenced directly or indirectly by the DsbA protein. The overlap of our analysis with both the trapping studies is quite limited, thus indicating far more extensive effect of the DsbA protein on other proteins and cellular processes mediated indirectly through the substrates. Only three proteins (hypothetical proteins FTS_1749 and FTS_1279 plus D-alanyl-D-alanine carboxypeptidase) were identified in common across the three studies. It should be noted, however, that even the two trapping studies overlapped in only 25 proteins. For example, Qin et al. (2016) presumed from their results that several components



of the FPI participating in the type VI secretion system (IglC, IglB, and PdpB) might be substrates of DsbA protein in subsp. *tularensis* (referred to here as FipB). This observation was not confirmed, however, by Ren et al. (2014). In our study, we detected significant elevation in only one FPI component (IglE), even though two of the aforementioned proteins (IglC and IglB) are quite abundant and detected reliably in the *Francisella* membranome (Pávková et al., 2005). One of the hypothetical proteins, FTS_0450, found to be elevated in the *dsbA* mutant is identical with FevR and might provide indirect evidence for changes in the secretion system. This transcriptional regulator is required for the expression of genes in the MglA/SspA regulon including all the *Francisella* pathogenicity island genes. Hence, the change of the FevR level can cause dysregulation in the FPI genes transcription, including in components of the type VI secretion system (Brotcke and Monack, 2008; Bröms et al., 2010).

In order to identify new candidates responsible for the *dsbA* mutant strain attenuation we inactivated 15 genes encoding



proteins whose DsbA dependent regulation has not been observed yet. Based on selection criteria we further focused on gene encoding cytosolic glycolytic enzyme, glyceraldehyde-3-phosphate dehydrogenase, whose level was significantly elevated in the *dsbA* mutant strain. This protein was previously shown to be immunoreactive, (Havlasová et al., 2005; Chandler et al., 2015; Straskova et al., 2015), and identified by proteomic analyses in fractions of enriched membrane proteins (Pávková et al., 2005) and CFPs (Konecna et al., 2010). These previous findings were in accordance with an increasing number of studies demonstrating additional activities of GAPDH not related to its primary metabolic function in both eukaryotic and prokaryotic cells. Many reports describe extracellular localization of GAPDH in Gram-positive (*Streptococcus* spp., *Mycoplasma pneumoniae*, *Listeria monocytogenes*, *Bacillus anthracis*) and several Gram-negative (*E. coli*, *Neisseria meningitidis*, *Brucella abortus*, *Edwardsiella tarda*) bacteria suggesting that this protein possesses other roles in addition to its glycolytic function including the involvement in host-pathogen interactions (summarized by Henderson and Martin, 2011; Giménez et al., 2014). Nevertheless, the gene encoding GAPDH is essential for survival of many

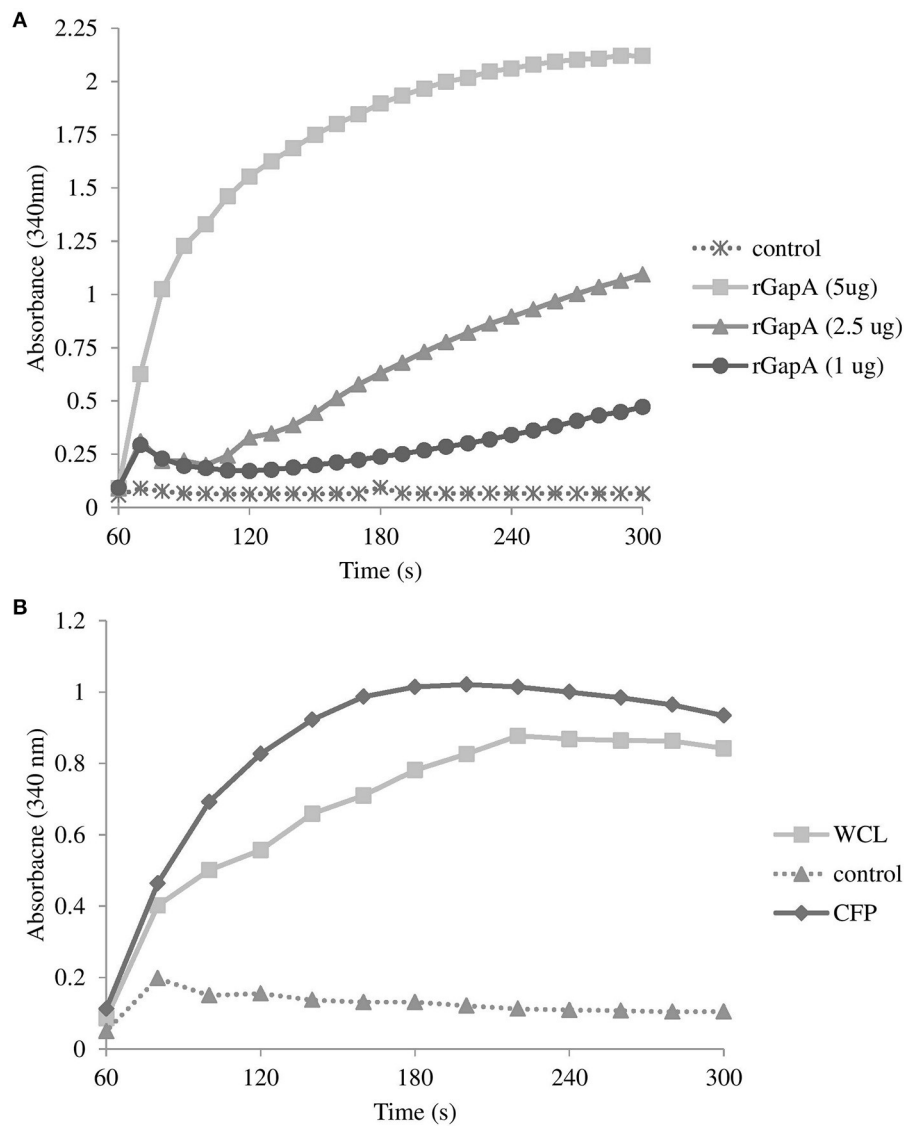


FIGURE 5 | Glyceraldehyde-3-phosphate dehydrogenase activity associated with purified recombinant GapA at concentrations 5, 2.5, and 1 μg **(A)**; whole-cell lysate and culture filtrate proteins (both 50 μg) from *F. tularensis* FSC200 **(B)** determined by the conversion of NAD^+ to NADH as described in the section Materials and Methods. Results shown from one experiment are representatives of two independent experiments.

bacteria, which limits the analysis of its role in pathogenic and virulence processes.

In *Francisella* spp., GAPDH is encoded by a single gene (*gapA*) and is highly conserved within the subspecies. As in other bacteria, its amino acid sequence shows no predicted signal sequence, membrane-spanning motif, or functional domain other than GAPDH NAD binding domain. Our experimental data show that GapA of *F. tularensis* subsp. *holarctica* FSC200 strain is an active enzyme able to catalyze the oxidative phosphorylation of glyceraldehyde-3-phosphate to 1,3-diphosphoglycerate in the presence of inorganic phosphate and NAD^+ , the sixth step of glycolysis. GapA had previously been regarded as non-essential for *Francisella* (Meibom and Charbit,

2010; Raghunathan et al., 2010). Here, we provide experimental evidence for this prediction inasmuch as the in-frame deletion of *gapA* resulted in a viable mutant strain with specific phenotype. The observed *gapA*-related phenotype was fully complemented in the *gapA*-complemented strain, indicating no polar effect of *gapA* gene deletion on surrounding genes. The glycolytic pathway is known to be complete in *F. tularensis*, but it is not critical for its intracellular survival and virulence inasmuch as the bacteria seem to prefer utilizing specific amino acids for energy production during the infection process (Raghunathan et al., 2010; Brissac et al., 2015). However, the *gapA* mutant revealed an obvious extracellular growth defect as it was able to grow in standard chemically defined Chamberlain's medium to the same extent as

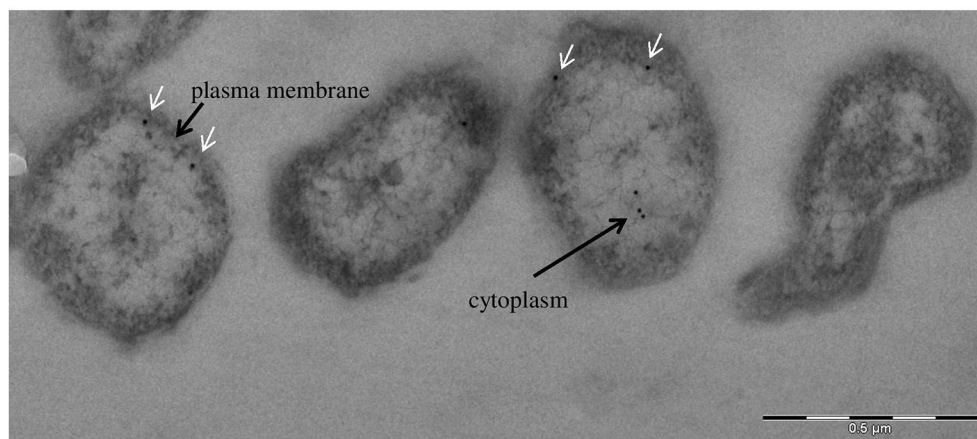
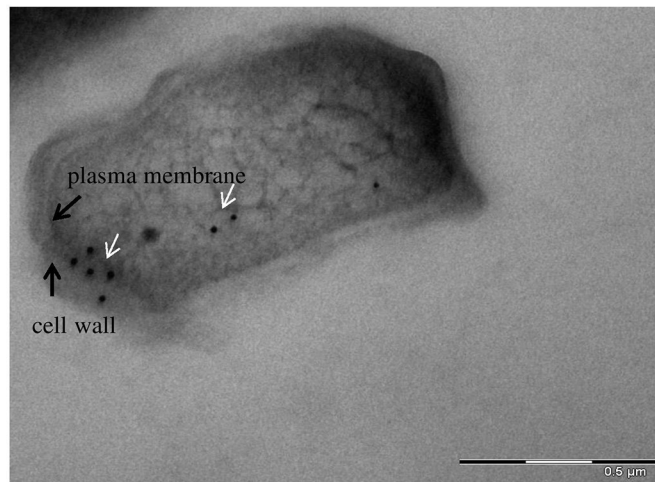


FIGURE 6 | Immunoelectron microscopy detection of glyceraldehyde-3-phosphate dehydrogenase: subcellular distribution of GapA in *F. tularensis* FSC200 grown in Chamberlain's medium. Cell cultures were fixed and processed as described in the section Materials and Methods. The GapA protein (white arrows) is detected in the bacteria's cytoplasm, plasma membrane, and cell wall.

does the wild-type strain only until exhaustion of the amino acids as alternative source of energy.

In several pathogenic bacteria like *Neisseria meningitidis* (Tunio et al., 2010) and *Streptococcus pyogenes* (Jin et al., 2005), the GAPDH was found to be required for optimal adhesion and subsequent invasion to host cells. This is not the case for the *F. tularensis* GapA as the entry of the *gapA* mutant into the cells was comparable to the parental strain in both the epithelial cell line and primary macrophages. The reduced bacterial numbers recovered from infected cells in the late stages of infection (24 h and later) can be associated with the disturbed glycolytic pathway (author note: the phagosomal escape in BMM's was not affected so far—data not shown). The consequence of this metabolic defect can also contribute to the attenuated phenotype of the *gapA* mutant in the mouse model of infection.

The alternative functions of metabolic enzymes in pathogenic bacteria are related to their cell surface display and/or secretion.

This localization enables the proteins to bind to host components and thus to participate in pathogenic processes. GAPDH has been found on the cell surface or even secreted in many Gram-positive (streptococci and staphylococci) and Gram-negative (e.g., *E. coli*, *N. meningitidis*, and *E. tarda*) bacteria, thereby facilitating the colonization and manipulation of host cells (summarized by Giménez et al., 2014). The relationship between extracellular localization of GAPDH and virulence has been revealed in several published studies. For example, only the pathogenic *E. coli* strains were able to secrete GAPDH into the culture medium (Egea et al., 2007). A mutant strain of *S. pyogenes* unable to export GAPDH from the cytosol to the cell surface revealed significant attenuation for virulence in the mouse model (Jin et al., 2011). Our previous proteomic analysis indicated extracellular localization of *F. tularensis* GapA, and in this study we verified this finding using several different approaches. Our data show that GapA occurs in various compartments involving

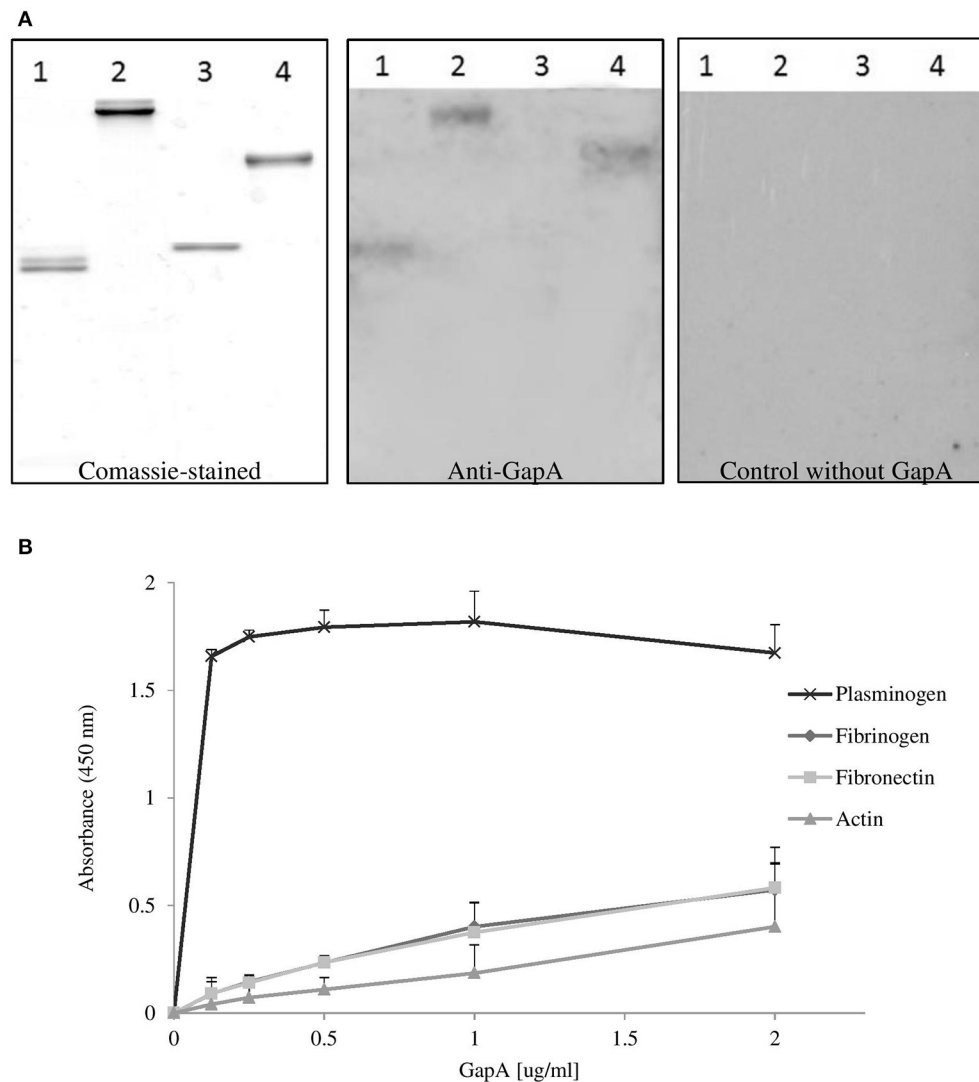


FIGURE 7 | Binding of *F. tularensis* GapA to selected host proteins. **(A)** Far-western analysis of GapA binding to PVDF-immobilized human proteins. The human proteins fibrinogen (lane 1), fibronectin (lane 2), actin (lane 3), plasminogen (lane 4) were separated on SDS-PAGE and the gel was either Coomassie blue-stained (first panel) or electroblotted. After the PVDF membrane had reacted with the recombinant GapA protein, it was incubated with anti-GapA antibodies and processed to visualize reactive bands (second panel). The third panel shows detection when the incubation with GapA was omitted. **(B)** Solid-phase binding assay of human proteins (plasminogen, fibrinogen, fibronectin, and actin) coated on 96-well microtiter plate and reacted with different concentrations of GapA. Data are presented as means \pm SD from three independent experiments.

the cytosol, cell wall, and extracellular medium. The possibility of cytosolic contamination of the fraction enriched in CFPs had previously been ruled out by exploring the lactate dehydrogenase activity (Konecna et al., 2010). On 2-D gels, the GapA could be detected in multiple spots that differ in isoelectric points. Several additional mass variants were found on 2-D gels with separated CFPs. The presence of multiple GAPDH variants on 2-D gels attributable to post-translational modifications has been widely reported in other microorganisms (Henderson and Martin, 2011; Giménez et al., 2014). The surface-localized or extracellularly secreted GAPDH of pathogenic bacteria is in general known to bind to a number of host proteins. The most commonly described

binding of bacterial GAPDH to human plasminogen, fibrinogen, or fibronectin plays a role in degradation of extracellular matrix proteins that facilitate bacterial dissemination within the host organism (summarized by Giménez et al., 2014). As *F. tularensis* is an intracellular pathogen we wanted to test whether its GAPDH homolog (GapA) has retained the ability to bind to those serum proteins. Using two *in vitro* systems, we could demonstrate the binding of GapA to selected host plasma components with strong preference for plasminogen compared to fibrinogen and fibronectin. However, further studies are needed to demonstrate the real meaning of these binding activities.

In conclusion, this extensive analysis of the *F. tularensis* subsp. *holarctica* membrane proteome enabled the discovery of a number of proteins that are directly or indirectly affected by the functional DsbA protein. These proteins are involved in various cellular processes and many of them might significantly contribute to the pleiotropic phenotype of *dsbA* mutant strain described in several previously published studies. In this study, we selected GAPDH of *F. tularensis* for further investigation as this protein is known to be multifunctional in other pathogenic bacteria and there is a growing evidence for its role in host-pathogen interaction. In this study we analyzed the basic features of *Francisella* GAPDH that are common for other bacterial homologs and indicate its multifunctional character. Accordingly we demonstrated the extracytosolic localization of *Francisella* GAPDH and its ability to bind several host serum proteins. Nevertheless it seems to be worth to perform further analysis on this protein. Next studies are underway to elucidate the real role of the secreted GAPDH of *F. tularensis*. They include the experimental manifestation of GapA secretion GapA into the cytoplasm of host cells and the detection and identification of potential intracellular interaction partners.

AUTHOR CONTRIBUTIONS

IP, JK, and JS designed the experiments; IP, JK, MK, MoS, VS, MaS, and JZ performed the experiments; IP, JK, MaS, and MK analyzed samples; IP, JK, MaS, PH, and JS interpreted the data; and IP, JK, and JS wrote the manuscript.

REFERENCES

- Asare, R., and Abu Kwaik, Y. (2010). Molecular complexity orchestrates modulation of phagosome biogenesis and escape to the cytosol of macrophages by *Francisella tularensis*. *Environ. Microbiol.* 12, 2559–2586. doi: 10.1111/j.1462-2920.2010.02229.x
- Bandara, A. B., Champion, A. E., Wang, X., Berg, G., Apicella, M. A., McLendon, M., et al. (2011). Isolation and mutagenesis of a capsule-like complex (CLC) from *Francisella tularensis*, and contribution of the CLC to *F. tularensis* virulence in mice. *PLoS ONE* 6:e19003. doi: 10.1371/journal.pone.019003
- Barel, M., Hovanessian, A. G., Meibom, K., Briand, J.-P., Dupuis, M., and Charbit, A. (2008). A novel receptor-ligand pathway for entry of *Francisella tularensis* in monocyte-like THP-1 cells: interaction between surface nucleolin and bacterial elongation factor Tu. *BMC Microbiol.* 8:145. doi: 10.1186/1471-2180-8-145
- Bocian-Ostrzycka, K. M., Grzeszczuk, M. J., Dziewit, L., and Jagusztyn-Krynicka, E. K. (2015). Diversity of the Epsilonproteobacteria Dsb (disulfide bond) systems. *Front. Microbiol.* 6:570. doi: 10.3389/fmicb.2015.00570
- Brissac, T., Ziveri, J., Ramond, E., Tros, F., Kock, S., Dupuis, M., et al. (2015). Gluconeogenesis, an essential metabolic pathway for pathogenic *Francisella*. *Mol. Microbiol.* 98, 518–534. doi: 10.1111/mmi.13139
- Bröms, J. E., Meyer, L., and Sjöstedt, A. (2016). A mutagenesis-based approach identifies amino acids in the N-terminal part of *Francisella tularensis* IglE that critically control Type VI system-mediated secretion. *Virulence* 8, 821–847. doi: 10.1080/21505594.2016.1258507
- Bröms, J. E., Sjöstedt, A., and Lavander, M. (2010). The role of the *Francisella Tularensis* pathogenicity island in type VI secretion, intracellular survival, and modulation of host cell signaling. *Front. Microbiol.* 1:136. doi: 10.3389/fmicb.2010.00136

FUNDING

This study/work was supported by the Ministry of Defence of the Czechia through the long-term organization development plan Medical Aspects of Weapons of Mass Destruction of the Faculty of Military Health Sciences, University of Defence and by The Specific Research grant of Ministry of Education, Youth and Sports of the Czech Republic No. SV/FVZ201603.

ACKNOWLEDGMENTS

We are very thankful to Maria Safarova and Lenka Luksikova for their technical assistance with mouse experiments, as well as Ivana Nováková for the excellent technical work with sample preparation for electron microscopy. We are thankful for the financial support TACR (TE01020118), project “BIOCEV–Biotechnology and Biomedicine Centre of the Academy of Sciences and Charles University” (CZ.1.05/1.1.00/02.0109) from the European Regional Development Fund, IMG (RVO:68378050). The electron microscopy data presented in this paper were produced at the Microscopy Centre—Electron Microscopy Core Facility, IMG ASCR, Prague, Czechia, supported by MEYS CR (LM2015062 Czech-BioImaging).

SUPPLEMENTARY MATERIAL

The Supplementary Material for this article can be found online at: <https://www.frontiersin.org/articles/10.3389/fcimb.2017.00503/full#supplementary-material>

- Brotcke, A., and Monack, D. M. (2008). Identification of fevR, a novel regulator of virulence gene expression in *Francisella novicida*. *Infect. Immun.* 76, 3473–3480. doi: 10.1128/IAI.00430-08
- Brotcke, A., Weiss, D. S., Kim, C. C., Chain, P., Malfatti, S., Garcia, E., et al. (2006). Identification of MglA-regulated genes reveals novel virulence factors in *Francisella tularensis*. *Infect. Immun.* 74, 6642–6655. doi: 10.1128/IAI.01250-06
- Celli, J. (2008). Intracellular localization of *Brucella abortus* and *Francisella tularensis* in primary murine macrophages. *Methods Mol. Biol.* 431, 133–145. doi: 10.1007/978-1-60327-032-8_11
- Chamberlain, R. E. (1965). Evaluation of live tularemia vaccine prepared in a chemically defined medium. *Appl. Microbiol.* 13, 232–235.
- Chandler, J. C., Sutherland, M. D., Harton, M. R., Molins, C. R., Anderson, R. V., Heaslip, D. G., et al. (2015). *Francisella tularensis* LVS surface and membrane proteins as targets of effective post-exposure immunization for tularemia. *J. Proteome Res.* 14, 664–675. doi: 10.1021/pr500628k
- Chong, A., Child, R., Wehrly, T. D., Rockx-Brouwer, D., Qin, A., Mann, B. J., et al. (2013). Structure-function analysis of DipA, a *Francisella tularensis* virulence factor required for intracellular replication. *PLoS ONE* 8:e67965. doi: 10.1371/journal.pone.0067965
- Chung, M.-C., Dean, S., Marakasova, E. S., Nwabueze, A. O., and van Hoek, M. L. (2014). Chitinases are negative regulators of *Francisella novicida* biofilms. *PLoS ONE* 9:e93119. doi: 10.1371/journal.pone.0093119
- Dankova, V., Balonova, L., Link, M., Straskova, A., Sheshko, V., and Stulik, J. (2016). Inactivation of *Francisella tularensis* gene encoding putative ABC transporter has a pleiotropic effect upon production of various glycoconjugates. *J. Proteome Res.* 15, 510–524. doi: 10.1021/acs.jproteome.5b00864
- Dieppedale, J., Gesbert, G., Ramond, E., Chhuon, C., Dubail, I., Dupuis, M., et al. (2013). Possible links between stress defense and the tricarboxylic acid (TCA) cycle in *Francisella* pathogenesis. *Mol. Cell. Proteomics* 12, 2278–2292. doi: 10.1074/mcp.M112.024794

- Dieppedale, J., Sobral, D., Dupuis, M., Dubail, I., Klimentova, J., Stulik, J., et al. (2011). Identification of a putative chaperone involved in stress resistance and virulence in *Francisella tularensis*. *Infect. Immun.* 79, 1428–1439. doi: 10.1128/IAI.01012-10
- Egea, L., Aguilera, L., Giménez, R., Sorolla, M. A., Aguilar, J., Badia, J., et al. (2007). Role of secreted glyceraldehyde-3-phosphate dehydrogenase in the infection mechanism of enterohemorrhagic and enteropathogenic *Escherichia coli*: interaction of the extracellular enzyme with human plasminogen and fibrinogen. *Int. J. Biochem. Cell Biol.* 39, 1190–1203. doi: 10.1016/j.biocel.2007.03.008
- Giménez, R., Aguilera, L., Ferreira, E., Aguilar, J., Baldoma, L., and Badia, J. (2014). “Glyceraldehyde-3-phosphate dehydrogenase as a moonlighting protein in bacteria,” in *Recent Advances in Pharmaceutical Sciences IV*, eds D. Munoz-Torrero, M. Vázquez-Carrera, and J. Estelrich (Kerala: Research Signpost), 165–180.
- Guina, T., Radulovic, D., Bahrami, A. J., Bolton, D. L., Rohmer, L., Jones-Isaac, K. A., et al. (2007). MglA regulates *Francisella tularensis* subsp. novicida (*Francisella novicida*) response to starvation and oxidative stress. *J. Bacteriol.* 189, 6580–6586. doi: 10.1128/JB.00809-07
- Havlasová, J., Hernychová, L., Brychta, M., Hubálek, M., Lenco, J., Larsson, P., et al. (2005). Proteomic analysis of anti-*Francisella tularensis* LVS antibody response in murine model of tularemia. *Proteomics* 5, 2090–2103. doi: 10.1002/ps.200401123
- Henderson, B., and Martin, A. (2011). Bacterial virulence in the moonlight: multitasking bacterial moonlighting proteins are virulence determinants in infectious disease. *Infect. Immun.* 79, 3476–3491. doi: 10.1128/IAI.00179-11
- Heras, B., Shouldice, S. R., Totsika, M., Scanlon, M. J., Schembri, M. A., and Martin, J. L. (2009). DSB proteins and bacterial pathogenicity. *Nat. Rev. Microbiol.* 7, 215–225. doi: 10.1038/nrmicro2087
- Inaba, K. (2009). Disulfide bond formation system in *Escherichia coli*. *J. Biochem.* 146, 591–597. doi: 10.1093/jb/mvp102
- Jin, H., Agarwal, S., Agarwal, S., and Pancholi, V. (2011). Surface export of GAPDH/SDH, a glycolytic enzyme, is essential for *Streptococcus pyogenes* virulence. *Mbio* 2, e00068-11. doi: 10.1128/mBio.00068-11
- Jin, H., Song, Y. P., Boel, G., Kochar, J., and Pancholi, V. (2005). Group A streptococcal surface GAPDH, SDH, recognizes uPAR/CD87 as its receptor on the human pharyngeal cell and mediates bacterial adherence to host cells. *J. Mol. Biol.* 350, 27–41. doi: 10.1016/j.jmb.2005.04.063
- Johansson, A., Berglund, L., Eriksson, U., Göransson, I., Wollin, R., Forsman, M., et al. (2000). Comparative analysis of PCR versus culture for diagnosis of ulceroglandular tularemia. *J. Clin. Microbiol.* 38, 22–26.
- Kadzaev, K., Zingmark, C., Golovliov, I., Bolanowski, M., Shen, H., Conlan, W., et al. (2009). Identification of genes contributing to the virulence of *Francisella tularensis* SCHU S4 in a mouse intradermal infection model. *PLoS ONE* 4:e5463. doi: 10.1371/journal.pone.0005463
- Kilmury, S. L. N., and Twine, S. M. (2011). The *Francisella tularensis* proteome and its recognition by antibodies. *Front. Microbiol.* 1:143. doi: 10.3389/fmicb.2010.00143
- Kim, T.-H., Sebastian, S., Pinkham, J. T., Ross, R. A., Blalock, L. T., and Kasper, D. L. (2010). Characterization of the O-antigen polymerase (Wzy) of *Francisella tularensis*. *J. Biol. Chem.* 285, 27839–27849. doi: 10.1074/jbc.M110.143859
- Konecna, K., Hernychova, L., Reichelova, M., Lenco, J., Klimentova, J., Stulik, J., et al. (2010). Comparative proteomic profiling of culture filtrate proteins of less and highly virulent *Francisella tularensis* strains. *Proteomics* 10, 4501–4511. doi: 10.1002/ps.201000248
- Lindgren, H., Shen, H., Zingmark, C., Golovliov, I., Conlan, W., and Sjöstedt, A. (2007). Resistance of *Francisella tularensis* strains against reactive nitrogen and oxygen species with special reference to the role of KatG. *Infect. Immun.* 75, 1303–1309. doi: 10.1128/IAI.01717-06
- Lo, K. Y.-S., Chua, M. D., Abdulla, S., Law, H. T., and Guttman, J. A. (2013). Examination of *in vitro* epithelial cell lines as models for *Francisella tularensis* non-phagocytic infections. *J. Microbiol. Methods* 93, 153–160. doi: 10.1016/j.mimet.2013.03.004
- Masuda, T., Tomita, M., and Ishihama, Y. (2008). Phase transfer surfactant-aided trypsin digestion for membrane proteome analysis. *J. Proteome Res.* 7, 731–740. doi: 10.1021/pr700658q
- McLendon, M. K., Schilling, B., Hunt, J. R., Apicella, M. A., and Gibson, B. W. (2007). Identification of LpxL, a late acyltransferase of *Francisella tularensis*. *Infect. Immun.* 75, 5518–5531. doi: 10.1128/IAI.01288-06
- Meibom, K. L., and Charbit, A. (2010). *Francisella tularensis* metabolism and its relation to virulence. *Front. Microbiol.* 1:140. doi: 10.3389/fmicb.2010.00140
- Milton, D. L., O’Toole, R., Horstedt, P., and Wolf-Watz, H. (1996). Flagellin A is essential for the virulence of *Vibrio anguillarum*. *J. Bacteriol.* 178, 1310–1319.
- Pancholi, V., and Fischetti, V. A. (1992). A major surface protein on group A streptococci is a glyceraldehyde-3-phosphate-dehydrogenase with multiple binding activity. *J. Exp. Med.* 176, 415–426. doi: 10.1084/jem.176.2.415
- Pávková, I., Brychta, M., Strašková, A., Schmidt, M., Macela, A., and Stulik, J. (2013). Comparative proteome profiling of host-pathogen interactions: insights into the adaptation mechanisms of *Francisella tularensis* in the host cell environment. *Appl. Microbiol. Biotechnol.* 97, 10103–10115. doi: 10.1007/s00253-013-5321-z
- Pávková, I., Hubálek, M., Zechovská, J., Lenco, J., and Stulik, J. (2005). *Francisella tularensis* live vaccine strain: proteomic analysis of membrane proteins enriched fraction. *Proteomics* 5, 2460–2467. doi: 10.1002/ps.200401213
- Pavkova, I., Reichelova, M., Larsson, P., Hubalek, M., Vackova, J., Forsberg, A., et al. (2006). Comparative proteome analysis of fractions enriched for membrane-associated proteins from *Francisella tularensis* subsp. tularensis and *F. tularensis* subsp. holarctica strains. *J. Proteome Res.* 5, 3125–3134. doi: 10.1021/pr0601887
- Pérez, N., Johnson, R., Sen, B., and Ramakrishnan, G. (2016). Two parallel pathways for ferric and ferrous iron acquisition support growth and virulence of the intracellular pathogen *Francisella tularensis* Schu S4. *Microbiologyopen* 5, 453–468. doi: 10.1002/mbo3.342
- Qin, A., Scott, D. W., Rabideau, M. M., Moore, E. A., and Mann, B. J. (2011). Requirement of the CXXC motif of novel *Francisella* infectivity potentiator protein B FipB, and FipA in virulence of *F. tularensis* subsp. tularensis. *PLoS ONE* 6:e24611. doi: 10.1371/journal.pone.0024611
- Qin, A., Zhang, Y., Clark, M. E., Moore, E. A., Rabideau, M. M., Moreau, G. B., et al. (2016). Components of the type six secretion system are substrates of *Francisella tularensis* Schu S4 DsbA-like FipB protein. *Virulence* 7, 882–894. doi: 10.1080/21505594.2016.1168550
- Qin, A., Zhang, Y., Clark, M. E., Rabideau, M. M., Millan Barea, L. R., and Mann, B. J. (2014). FipB, an essential virulence factor of *Francisella tularensis* subsp. tularensis, has dual roles in disulfide bond formation. *J. Bacteriol.* 196, 3571–3581. doi: 10.1128/JB.01359-13
- Raghunathan, A., Shin, S., and Daefler, S. (2010). Systems approach to investigating host-pathogen interactions in infections with the biothreat agent *Francisella*. Constraints-based model of *Francisella tularensis*. *BMC Syst. Biol.* 4:118. doi: 10.1186/1752-0509-4-118
- Ramakrishnan, G., Meeker, A., and Dragulev, B. (2008). fsIE Is necessary for siderophore-mediated iron acquisition in *Francisella tularensis* Schu S4. *J. Bacteriol.* 190, 5353–5361. doi: 10.1128/JB.00181-08
- Ren, G., Champion, M. M., and Huntley, J. F. (2014). Identification of disulfide bond isomerase substrates reveals bacterial virulence factors. *Mol. Microbiol.* 94, 926–944. doi: 10.1111/mmi.12808
- Robertson, G. T., Child, R., Ingle, C., Celli, J., and Norgard, M. V. (2013). IgE is an outer membrane-associated lipoprotein essential for intracellular survival and murine virulence of type A *Francisella tularensis*. *Infect. Immun.* 81, 4026–4040. doi: 10.1128/IAI.00595-13
- Rodriguez, S. A., Davis, G., and Klose, K. E. (2009). Targeted gene disruption in *Francisella tularensis* by group II introns. *Methods* 49, 270–274. doi: 10.1016/j.ymeth.2009.04.011
- Rowe, H. M., and Huntley, J. F. (2015). From the outside-in: the *Francisella tularensis* envelope and virulence. *Front. Cell. Infect. Microbiol.* 5:94. doi: 10.3389/fcimb.2015.00094
- Salomonsson, E. N., Forslund, A.-L., and Forsberg, A. (2011). Type IV Pili in *Francisella* - a virulence trait in an intracellular pathogen. *Front. Microbiol.* 2:29. doi: 10.3389/fmicb.2011.00029
- Sambrook, J., and Russel, D. (2001). *Molecular Cloning: A Laboratory Manual, 3rd Edn.* Cold Spring Harbor, NY: Cold Spring Harbor Laboratory.
- Schmidt, M., Klimentova, J., Rehulka, P., Straskova, A., Spidlova, P., Szotakova, B., et al. (2013). *Francisella tularensis* subsp. holarctica DsbA homologue: a

- thioredoxin-like protein with chaperone function. *Microbiol. Read. Engl.* 159, 2364–2374. doi: 10.1099/mic.0.070516-0
- Shouldice, S. R., Heras, B., Walden, P. M., Totsika, M., Schembri, M. A., and Martin, J. L. (2011). Structure and Function of DsbA, a key bacterial oxidative folding catalyst. *Antioxid. Redox Signal.* 14, 1729–1760. doi: 10.1089/ars.2010.3344
- Simon, R., Priefer, U., and Puhler, A. (1983). A broad host range mobilization system for *in vivo* genetic engineering: transposon mutagenesis in gram negative bacteria. *Nat. Biotechnol.* 1, 784–791. doi: 10.1038/nbt1183-784
- Smith, R. P., Paxman, J. J., Scanlon, M. J., and Heras, B. (2016). Targeting bacterial Dsb proteins for the development of anti-virulence agents. *Molecules* 21:811. doi: 10.3390/molecules21070811
- Strádalová, V., Gaplovská-Kyselá, K., and Hozák, P. (2008). Ultrastructural and nuclear antigen preservation after high-pressure freezing/freeze-substitution and low-temperature LR White embedding of HeLa cells. *Histochem. Cell Biol.* 130, 1047–1052. doi: 10.1007/s00418-008-0504-x
- Straskova, A., Pavkova, I., Link, M., Forslund, A.-L., Kuoppa, K., Noppa, L., et al. (2009). Proteome analysis of an attenuated *Francisella tularensis* dsbA mutant: identification of potential DsbA substrate proteins. *J. Proteome Res.* 8, 5336–5346. doi: 10.1021/pr900570b
- Straskova, A., Spidlova, P., Mou, S., Worsham, P., Putzova, D., Pavkova, I., et al. (2015). *Francisella tularensis* type B Δ dsbA mutant protects against type A strain and induces strong inflammatory cytokine and Th1-like antibody response *in vivo*. *Pathog. Dis.* 73:ftv058. doi: 10.1093/femspd/ftv058
- Su, J., Yang, J., Zhao, D., Kawula, T. H., Banas, J. A., and Zhang, J.-R. (2007). Genome-wide identification of *Francisella tularensis* virulence determinants. *Infect. Immun.* 75, 3089–3101. doi: 10.1128/IAI.01865-06
- Thomas, R. M., Twine, S. M., Fulton, K. M., Tessier, L., Kilmury, S. L. N., Ding, W., et al. (2011). Glycosylation of DsbA in *Francisella tularensis* subsp. *tularensis*. *J. Bacteriol.* 193, 5498–5509. doi: 10.1128/JB.00438-11
- Tunio, S. A., Oldfield, N. J., Ala'Aldeen, D. A., Wooldridge, K. G., and Turner, D. P. (2010). The role of glyceraldehyde 3-phosphate dehydrogenase (GapA-1) in *Neisseria meningitidis* adherence to human cells. *BMC Microbiol.* 10:280. doi: 10.1186/1471-2180-10-280
- Vizcaino, J. A., Csordas, A., Del-Toro, N., Dianes, J. A., Griss, J., Lavidas, I., et al. (2016). 2016 update of the PRIDE database and its related tools. *Nucleic Acids Res.* 44, 11033. doi: 10.1093/nar/gkw880
- Wehrly, T. D., Chong, A., Virtaneva, K., Sturdevant, D. E., Child, R., Edwards, J. A., et al. (2009). Intracellular biology and virulence determinants of *Francisella tularensis* revealed by transcriptional profiling inside macrophages. *Cell. Microbiol.* 11, 1128–1150. doi: 10.1111/j.1462-5822.2009.01316.x
- Weiss, D. S., Brotcke, A., Henry, T., Margolis, J. J., Chan, K., and Monack, D. M. (2007). *In vivo* negative selection screen identifies genes required for *Francisella* virulence. *Proc. Natl. Acad. Sci. U.S.A.* 104, 6037–6042. doi: 10.1073/pnas.0609675104

Conflict of Interest Statement: The authors declare that the research was conducted in the absence of any commercial or financial relationships that could be construed as a potential conflict of interest.

Copyright © 2017 Pavkova, Kopeckova, Klimentova, Schmidt, Sheshko, Sobol, Zakova, Hozak and Stulik. This is an open-access article distributed under the terms of the Creative Commons Attribution License (CC BY). The use, distribution or reproduction in other forums is permitted, provided the original author(s) or licensor are credited and that the original publication in this journal is cited, in accordance with accepted academic practice. No use, distribution or reproduction is permitted which does not comply with these terms.



Francisella tularensis Confronts the Complement System

Susan R. Brock and Michael J. Parmely*

Department of Microbiology, Molecular Genetics and Immunology, University of Kansas Medical Center, Kansas City, KS, United States

Francisella tularensis has developed a number of effective evasion strategies to counteract host immune defenses, not the least of which is its ability to interact with the complement system to its own advantage. Following exposure of the bacterium to fresh human serum, complement is activated and C3b and iC3b can be found covalently attached to the bacterial surface. However, the lipopolysaccharide and capsule of the *F. tularensis* cell wall prevent complement-mediated lysis and endow the bacterium with serum resistance. Opsonization of *F. tularensis* with C3 greatly increases its uptake by human neutrophils, dendritic cells and macrophages. Uptake occurs by an unusual looping morphology in human macrophages. Complement receptor 3 is thought to play an important role in opsonophagocytosis by human macrophages, and signaling through this receptor can antagonize Toll-like receptor 2-initiated macrophage activation. Complement C3 also determines the survival of infected human macrophages and perhaps other cell types. C3-opsonization of *F. tularensis* subsp. *tularensis* strain SCHU S4 results in greatly increased death of infected human macrophages, which requires more than complement receptor engagement and is independent of the intracellular replication by the pathogen. Given its entry into the cytosol of host cells, *F. tularensis* has the potential for a number of other complement-mediated interactions. Studies on the uptake C3-opsonized adenovirus have suggested the existence of a C3 sensing system that initiates cellular responses to cytosolic C3b present on invading microbes. Here we propose that C3 peptides enter the cytosol of human macrophages following phagosome escape of *F. tularensis* and are recognized as intruding molecular patterns that signal host cell death. With the discovery of new roles for intracellular C3, a better understanding of tularemia pathogenesis is likely to emerge.

Keywords: cell death, complement, C3, *Francisella tularensis*, macrophage

Francisella tularensis is the bacterial pathogen responsible for the infectious disease tularemia. While tularemia is relatively rare, infection via the respiratory route can be particularly life-threatening when not treated with appropriate antibiotics in a timely fashion (Stuart and Pullen, 1945; McCrumb, 1961; Dennis et al., 2001; Feldman et al., 2001). There are two subspecies of *F. tularensis* that account for the majority of infections in immunocompetent human beings. *F. tularensis* subsp. *tularensis* (type A) is considered the more virulent and will be the primary focus of this article. *F. tularensis* subsp. *holarctica* (type B) is also pathogenic in humans, but is less often associated with severe morbidity or mortality. *Francisella novicida* causes a tularemia-like disease in mice, but rarely infects human beings where disease is restricted to the immunocompromised (Kingry and Petersen, 2014). Following exposure to type A and type B *F. tularensis* by the pulmonary route,

OPEN ACCESS

Edited by:

Anders Sjöstedt,
Umeå University, Sweden

Reviewed by:

Mikhail A. Gavrilin,
The Ohio State University,
United States
Lee-Ann H. Allen,
University of Iowa, United States

*Correspondence:

Michael J. Parmely
mparmely@kumc.edu

Received: 31 October 2017

Accepted: 08 December 2017

Published: 19 December 2017

Citation:

Brock SR and Parmely MJ (2017)
Francisella tularensis Confronts the
Complement System.
Front. Cell. Infect. Microbiol. 7:523.
doi: 10.3389/fcimb.2017.00523

macrophages are among the first cells infected (Hall et al., 2008; Roberts et al., 2014; Steiner et al., 2017) and serve as an early and continuing replicative niche for the pathogen. Many receptors on the macrophage surface have been implicated in the uptake of *F. tularensis* (Clemens et al., 2005; Balagopal et al., 2006; Pierini, 2006; Schulert and Allen, 2006; Barel et al., 2008; Geier and Celli, 2011; Schwartz et al., 2012; Dai et al., 2013), but complement receptors, especially CR3, have consistently been found to be the primary mediators of enhanced uptake of serum-opsonized *F. tularensis* by human macrophages (Clemens et al., 2005; Schwartz et al., 2012; Dai et al., 2013). Once inside the cell, *F. tularensis* escapes the macrophage phagosome at a pace that varies with host species and replicates in the cytosol to high numbers (Golovliov et al., 2003; Clemens et al., 2004; Chong et al., 2008).

Macrophage death is a common outcome following *in vivo* infection with *F. tularensis* and partially explains the appearance of necrotic foci in the livers, lungs, spleens and lymph nodes in several mammalian species (Parmely et al., 2009). The mechanisms and significance of macrophage death depend on the (sub)species of *Francisella* studied (Mariathasan et al., 2005; Henry et al., 2007; Wickstrum et al., 2009). For example, *F. novicida* is a highly proinflammatory pathogen, which induces rapid cell death in mouse macrophages that limits the ability of the bacteria to replicate in the host (Mariathasan et al., 2005; Henry et al., 2007). When describing the lifecycle of type A and type B *F. tularensis*, it is not uncommon to attribute macrophage death to an uncharacterized signal associated with the extensive cytosolic replication of the pathogen. For example, Lai et al. reported on the effects of antibiotic treatment of J774.A1 macrophage-like cells infected with the *F. tularensis* Live Vaccine Strain (LVS) (Lai et al., 2001). Treating cultures with ciprofloxacin within the first 12 h of infection prevented both the replication of the bacteria and host cell death measured 24 h post-infection (PI). If ciprofloxacin treatment was delayed until 15 h PI, host cell death at 24 h PI was similar in magnitude to that of untreated, infected control cells. The authors concluded that intracellular bacterial replication was required for the induction of macrophage death. Recent studies performed in our laboratory with type A *F. tularensis* (Brock and Parmely, 2017) have questioned this interpretation. Intracellular replication of the SCHU S4 strain did not appear to be required for the induction of death in primary human macrophages.

During the course of these studies, we found that complement C3 played an important role in determining the survival of infected macrophages. Accordingly, in this article we review what is known about the interactions between *F. tularensis* and the complement system, discuss recent findings about the functions of intracellular complement, and propose new ways of thinking about the complement system in tularemia. Our primary focus will be on *F. tularensis* subsp. *tularensis*, although our use of

the designation *F. tularensis* reflects an effort to include relevant studies performed with subsp. *holartica* strains. We acknowledge this comes with the risk that future studies may prove some conclusions to be too inclusive.

EXTRACELLULAR COMPLEMENT ACTIVATION AND REGULATION

For detailed descriptions of complement activation, the reader is referred to several excellent reviews (Dunkelberger and Song, 2010; Ricklin et al., 2010; Noris and Remuzzi, 2013). There are three pathways of complement activation (**Figure 1**), all of which result in the proteolytic cleavage of complement component C3, an abundant serum protein. The classical and lectin pathways both generate a C3 convertase composed of the peptides C4b and C2a. Through the classical pathway, IgM and IgG antibodies, when bound to their respective antigens, bind C1q and initiate the assembly of the C1q_rs₂ complex. This complex cleaves C4 and C2 to produce a C3 convertase, designated C4bC2a. In the lectin pathway, the binding of certain carbohydrate patterns on microorganisms by either serum mannose-binding lectin (MBL) or ficolin proteins recruits and activates mannose-binding lectin-associated serine proteases (MASPs), which cleave C4 and C2 to generate the same C3 convertase. The alternative pathway is constitutively active with a low level “tick-over” of C3 in which an internal thioester bond is spontaneously hydrolyzed yielding C3(H₂O). Hydrolyzed C3 has a conformation similar to C3b (Chen et al., 2016) and can bind complement factor B (FB). Constitutively active factor D (FD) then cleaves FB, yielding an alternative pathway C3 convertase designated C3(H₂O)Bb. Like the C4b2a convertase, the alternative pathway convertase can cleave C3 to produce a bioactive short C3a peptide and a lengthier C3b peptide (**Figure 2**). C3a can serve as an anaphylatoxin. One of the primary functions of C3b is as a potent opsonin, which is attributed to its exposed thioester bond. Unless C3 has been spontaneously hydrolyzed by water, the C3b thioester can react with amine or hydroxyl groups. Formation of amide or ester linkages assures covalent attachment of C3b to nearby target surfaces, which makes them stable ligands for complement receptor-mediated uptake.

The alternative pathway also serves to amplify complement activation initiated by any of the three pathways by utilizing C3b as a focus for the formation of additional C3 convertases. Thus, C3b bound to a surface can form a complex with FB, which when cleaved by FD, becomes the new alternative pathway C3 convertase C3bBb. This amplification process results in increased localized activation of complement in proximity to susceptible microbial surfaces.

The binding of C3b to C3 convertases changes their specificity to C5-cleaving enzymes. Proteolysis of C5 produces the peptides C5a (another anaphylatoxin and potent chemotactic factor) and C5b, which initiates formation of the membrane attack complex. C5b binds C6, which then complexes with C7 and inserts into lipid membranes. The C5b67 complex then interacts with

Abbreviations: BMM, bone marrow-derived macrophage; CR, complement receptor; FB, factor B; FD, factor D; FI, factor I; HS, human serum; MDM, monocyte-derived macrophage; MOI, multiplicities of infection; PI, post-infection.

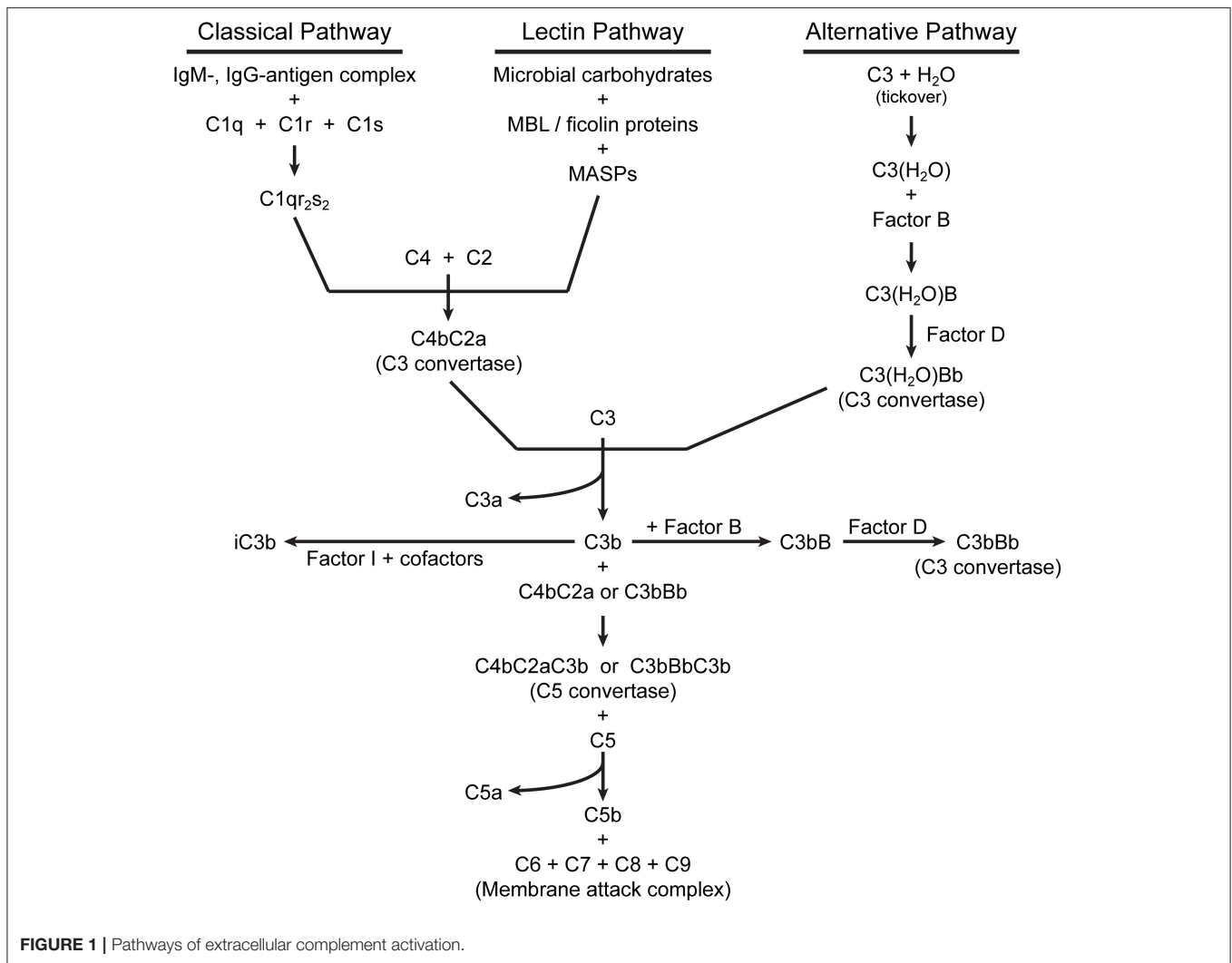


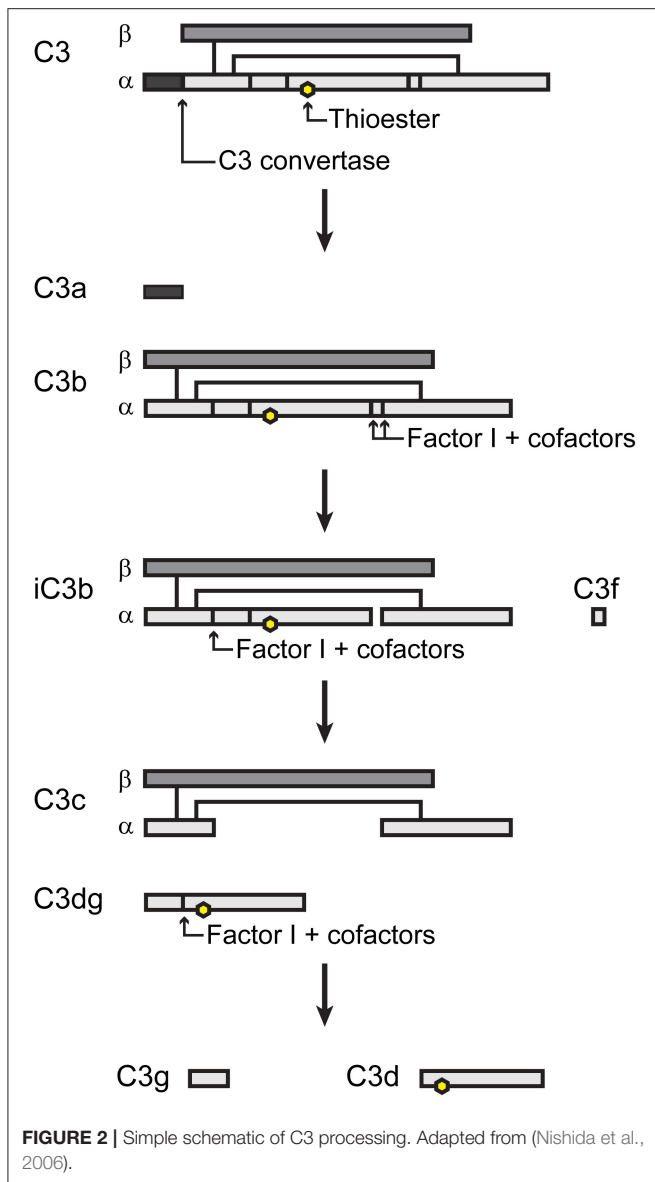
FIGURE 1 | Pathways of extracellular complement activation.

C8, followed by recruitment of multiple copies of C9, which polymerize to form a membrane pore, followed by rapid cell lysis.

Complement activation is tightly regulated by a variety of serum and membrane-bound proteins that control the three complement pathways (reviewed in Zipfel and Skerka, 2009; Noris and Remuzzi, 2013). The primary outcome is to limit host tissue damage that would result from unabated complement activation. Only two of these regulatory components will be mentioned here. Factor I (FI) is a serum protein that, along with certain cofactors, cleaves the alpha chain of C3b yielding inactivated C3b (iC3b) (Figure 2). The formation of iC3b terminates amplification of the complement cascade by preventing formation of additional C3 convertases and also halts C5 cleavage, which diminishes assembly of the membrane attack complex. However, iC3b retains its opsonic activity, albeit with different complement receptor specificity than that of C3b. Factor H (FH) serves as a co-factor for FI and also competes with FB binding to C3b, preventing formation of the alternative pathway C3 convertase.

CELL SURFACE RECEPTORS FOR C3

In addition to fluid phase complement factors, there are many membrane bound complement receptors that are important for complement regulation and complement-mediated clearance, phagocytosis and cellular signaling. Here we will discuss membrane bound complement receptors that have been shown to have important implications for *F. tularensis* virulence and host defense. For a comprehensive review of complement receptors, the reader is referred to two important reviews (Leslie, 2001; Zipfel and Skerka, 2009). Complement receptor 1 (CR1 or CD35) is expressed on leukocytes and erythrocytes and binds C3b (Table 1). In addition to its role in complement-mediated opsonophagocytosis, CR1 serves as a membrane-bound cofactor for FI, leading to conversion of C3b to iC3b. CR3 is a heterodimer of the membrane proteins CD11b and CD18 and is expressed on neutrophils, macrophages, follicular dendritic cells, eosinophils, basophils, NK cells and platelets. CR3 shows high affinity for iC3b, which facilitates phagocytosis of iC3b-bearing particles. While we will focus primarily on the opsonic activities of these



receptors, CR3 also plays a role in leukocyte trafficking to sites of infection and regulating cellular responses initiated by certain Toll-like receptors. CR4 is comprised of heterodimers of CD11c and CD18 and is expressed on monocytes and macrophages. CR4 also binds iC3b with high affinity.

Apart from the involvement of complement receptors in the uptake of *F. tularensis* by phagocytic cells, little research has investigated the role of other cell surface complement receptors and regulators. For example, tissue macrophages also express the complement receptor CR1g, which binds the beta chain of C3, allowing the receptor to phagocytize both C3b- and iC3b-opsonized particles. CR1g is important for the clearance of pathogens (Helmy et al., 2006; van Lookeren Campagne et al., 2007), but its role during *F. tularensis* infection has not been investigated. Mature B cells express CR2 (or CD21), which binds iC3b, C3dg and C3d peptides derived from FI-mediated cleavage

of iC3b. One report suggests that subsets of mouse B cells employ CR2 along with the B cell receptor for uptake of *F. tularensis* (Plzakova et al., 2015). CD46, CD55 and CD59 are expressed by most host cell types, regulate complement activation and protect host tissues from complement-mediated damage by aiding in the inactivation of C3, disrupting the C3 convertases or preventing the formation of the membrane attack complex, respectively. Whether or not these complement regulators play a role in *F. tularensis* virulence or host defense is unknown.

INTRACELLULAR ACTIONS OF COMPLEMENT

Based on phylogenetic studies and the presence of C3-like proteins in porifera (sponges), Elvington et al. have suggested that complement proteins served first to protect the intracellular space before evolving into a system for defending against pathogens at the cell membrane or in intercellular or intravascular domains of higher organisms (Elvington et al., 2016). Only recently have we begun to appreciate the extent to which complement mediates important intracellular functions (reviewed in Arbore et al., 2017; Liszewski et al., 2017).

Many cell types produce C3 (Lubbers et al., 2017) and maintain intracellular stores of the protein (Liszewski et al., 2013). Elvington et al. recently showed that intracellular C3 derives from a C3(H₂O) recycling pathway in which hydrolyzed, but not native, C3 is taken up from the extracellular environment (Elvington et al., 2017). After being loaded with C3(H₂O), Farage B lymphoma cells released ~80% of the C3(H₂O) back into the culture medium, suggesting that the cells processed the remainder as a source of bioactive C3 peptides (Liszewski et al., 2013; Elvington et al., 2017). Complement receptors CR1, CR2, CR3, and CD46 did not appear to be involved in the uptake of C3(H₂O) in this recycling pathway (Elvington et al., 2017).

Liszewski and colleagues have extensively documented mechanisms of C3 activation within cells (Liszewski et al., 2013). For example, cathepsin L can cleave C3 to form C3a and C3b within the lysosomes of human T cells. The resulting C3a mediates the tonic intracellular activation of its complement receptor C3aR on the lysosome membrane, leading to baseline mTOR activation necessary for T cell homeostasis. Inhibition of cathepsin L or siRNA inhibition of C3aR expression led to T cell apoptosis. Activation of T cells through their antigen receptors resulted in the transport of vesicles containing C3aR, C3 and cathepsin L to the cell surface. In an autocrine fashion, cleavage of C3 at the cell surface and binding of C3a and C3b to their respective receptors, C3aR and CD46, polarized the T cell to a Th1 phenotype (Liszewski et al., 2013; Kolev et al., 2015).

Intracellular activation of C3 is not limited to T cells. It has also been demonstrated in a variety of primary human cell types including monocytes, neutrophils, and B cells, as well as cultured human fibroblasts, ME-180 epithelial cells and umbilical vein endothelial cells (Liszewski et al., 2013). The proteases responsible for intracellular C3 cleavage vary among cell types.

TABLE 1 | Human complement receptors with known involvement in the uptake of serum-opsonized *F. tularensis*.

Complement receptor	Preferred ligand*	Cell expression*	Function in <i>F. tularensis</i> infection	References
CR1 (CD35)	C3b, C4b	Leukocytes (including neutrophils and macrophages) and erythrocytes	Uptake of serum-opsonized <i>F. tularensis</i> by human neutrophils	Schwartz et al., 2012
CR3 (CD11b, CD18)	iC3b	Neutrophils, macrophages, follicular dendritic cells, eosinophils, basophils, NK cells and platelets	Uptake of serum-opsonized <i>F. tularensis</i> by human neutrophils, macrophages and dendritic cells Crosstalk with TLR2-inhibition of TLR2-mediated inflammatory signaling	Clemens et al., 2005; Ben Nasr et al., 2006; Schwartz et al., 2012; Dai et al., 2013
CR4 (CD11c, CD18)	iC3b	Monocytes and macrophages	Uptake of serum-opsonized <i>F. tularensis</i> by macrophages and dendritic cells	Ben Nasr et al., 2006; Schwartz et al., 2012

*Receptor ligand specificity and cell expression obtained from Leslie (2001) and Zipfel and Skerka (2009).

While cathepsin L mediates activation of C3 in T cells and monocytes, it is not responsible for the C3 activation observed in lung epithelial cells (Liszewski et al., 2013). Both cathepsin L and cathepsin B contribute to C3 cleavage within human intestinal epithelial cells (Satyam et al., 2017). Factor H and FI can be taken up by cells and mediate intracellular cleavage of C3(H₂O) (Elvington et al., 2017). Factor H has also been shown to interact with cathepsin L to increase cleavage of endogenous C3 yielding iC3b (Martin et al., 2016). Clearly, additional studies are needed to form a complete understanding of the significance of intracellular complement activation and its potential relationship with host defense.

Tam and colleagues demonstrated that the presence of C3 peptides in the cytosol may also serve as molecular patterns that initiate danger signaling (Tam et al., 2014). A variety of C3-opsonized microbes, including both RNA and DNA non-enveloped viruses and the Δ *sifA* mutant of *Salmonella*, activated a NF- κ B-driven luciferase reporter when present in the cytosol. The reporter was not activated when cytosolic entry was prevented or when pathogens were not opsonized with C3. Latex beads opsonized with a mixture of purified C3, FB and FD also activated NF- κ B when transfected into HEK293T cells, suggesting that recognition of microbial patterns was not essential for this response. Signaling initiated by cytosolic C3 was independent of the signaling intermediates MyD88, TRIF, RIG-I, MDA5, Syk, and STING, but appeared to involve the mitochondrial antiviral signaling (MAVS) protein and TNF receptor-associated factor (TRAF). Cytosolic C3 sensing was observed in a variety of non-immune mammalian cell lines indicating that the proposed C3-detection pathway may be active in a number of cell types. However, it remains unknown whether macrophages sense cytosolic C3 in this manner. It should also be noted that these findings have not, as yet, been confirmed by other investigators and that a putative cytosolic C3 sensor has not yet been identified. This laboratory has identified tripartite motif-containing 21 (TRIM21) as a cytosolic sensor for IgG and IgM that also leads to the activation of NF- κ B and interferon regulatory factors (James et al., 2007; Mallery et al., 2010; McEwan et al., 2013). The notion that C3 peptides mediate similar intracellular surveillance is quite provocative and certainly worthy of further study.

COMPLEMENT ACTIVATION BY *F. TULARENSIS*

In the conventional sense, *F. tularensis* is relatively serum resistant, meaning that it can survive in human serum (HS) without succumbing to the lytic effects of complement (Lofgren et al., 1983; Sorokin et al., 1996). Serum resistance appears to be conferred by the lipopolysaccharide (LPS) and cell wall structure of *F. tularensis*, as evidence by the increased activation of complement (especially via the classical pathway) and susceptibility to serum-mediated lysis of LPS and capsule mutants (Sandstrom et al., 1988; Sorokin et al., 1996; Clay et al., 2008; Lindemann et al., 2011). It is possible that mutations in other *F. tularensis* genes similarly alter the density of iC3b deposition following serum opsonization. Additionally, growth of *F. tularensis* in different culture media, which can alter the expression of high molecular weight surface carbohydrates, can affect the extent of C3 deposition on the bacterial surface (Zarella et al., 2011). During opsonization of *F. tularensis* in HS, FH can bind to serum-opsonized *F. tularensis* (Ben Nasr and Klimpel, 2008), promoting the conversion of C3b to iC3b. This prevents the assembly of the membrane attack complex on the bacterial surface (Ben Nasr and Klimpel, 2008; Clay et al., 2008). *F. tularensis* may also express a surface CD59-like peptide (Madar et al., 2015), which may further hinder formation of the membrane attack complex by binding C8 or C9.

Several reports indicate that both the classical and alternative pathways are activated by *F. tularensis* (Ben Nasr and Klimpel, 2008; Clay et al., 2008) and include the observation that C1q is required for C3 deposition on the bacterium under certain conditions (Fulop et al., 1993; Clay et al., 2008; Schwartz et al., 2012). Natural IgM antibodies appear to play a role in complement activation by *F. tularensis* via the classical complement pathway (Sandstrom et al., 1988; Schwartz et al., 2012). Schwartz et al. showed that human serum (HS) from donors without a history of tularemia contained IgM antibodies that reacted with *F. tularensis* and mediated C3 deposition during the first 30 min of opsonization. Ben Nasr and Klimpel (2008) reported that, although the classical pathway was activated, they were unable to detect binding of serum IgM to *F. tularensis*. Balagopal et al. (2006) used immunofluorescence and ELISA to detect antibodies bound to *F. novicida* following opsonization of

the bacteria with HS. The differences between these reports may reflect the bacterial strains that were studied or the use of different techniques to detect antibody binding. Regardless, there appears to exist sufficient evidence to conclude that the classical pathway can mediate C3 opsonization of *F. tularensis*.

The classical pathway may be particularly important when serum opsonization occurs for periods of <30 min. Longer periods of incubation with serum may allow significant alternative pathway amplification and C3b deposition (Ben Nasr and Klimpel, 2008). We have found that uptake of *F. tularensis* SCHU S4 by human macrophages over 3 h is significantly reduced in C3-depleted HS compared to HS (Brock and Parmely, 2017). However, there is no difference in the level of SCHU S4 uptake during a 3-h incubation in C1q-depleted HS compared to HS (Brock and Parmely, unpublished). Likewise, Ben Nasr and Klimpel (2008) reported that EGTA chelation of Ca²⁺ ions necessary for classical pathway activation in HS delayed the deposition of iC3b on *F. tularensis* if opsonization was limited to 30 min. After 45 min of opsonization, there was no difference between the levels of iC3b deposition that occurred in HS and EGTA-treated HS (Ben Nasr and Klimpel, 2008). Conversely, treatment of HS with EDTA, which chelates both Ca²⁺ and Mg²⁺ and blocks both classical and alternative pathways, prevented any detectable iC3b deposition on SCHU S4 for at least 1 h (Ben Nasr and Klimpel, 2008). Thus, it appears that both the classical and alternative pathways can mediate complement activation during serum opsonization of *F. tularensis*.

COMPLEMENT-MEDIATED UPTAKE OF *F. TULARENSIS*

For a more comprehensive summary on the role of various cell surface receptors in the uptake of *F. tularensis*, the reader is referred to an excellent review by Moreau and Mann (Moreau and Mann, 2013). Our focus here will be limited to the receptors involved in complement-dependent uptake of *F. tularensis*.

Complement component C3 was first shown to be important for optimal uptake of *F. tularensis* by human monocyte-derived macrophages (MDMs) by replenishing C3-depleted serum with C3 protein (Clemens et al., 2005). This resulted in a C3 concentration-dependent uptake of bacteria. The importance of C3 in the uptake of *F. tularensis* has since been confirmed by several other groups (Dai et al., 2013; Brock and Parmely, 2017). Antibody blocking of CR3 with anti-CD11b and anti-CD18 reduced the uptake of HS-opsonized *F. tularensis* by human MDM (Clemens et al., 2005). Additional studies on blocking of complement receptors with antibodies have demonstrated that CR3 and CR4 are the predominant receptors involved in the uptake of HS-opsonized *F. tularensis* by human macrophages (Schulert and Allen, 2006; Schwartz et al., 2012). However, blocking antibodies often show relatively modest effects in this context. The use of siRNA to inhibit expression of CR3 in human MDM has also demonstrated that CR3 is an important receptor for the uptake of serum-opsonized SCHU S4 (Dai et al., 2013) and is consistent with the observation that C3 deposited on *F. tularensis* during HS opsonization is rapidly converted to iC3b.

Inactivated C3b, not C3b, is the primary ligand for CR3 and CR4. CR1 does not appear to play a significant role in the uptake of serum-opsonized *F. tularensis* by human MDM, based on antibody blocking of CR1 (Schwartz et al., 2012).

Another experimental approach for determining important receptor-ligand interactions in C3-mediated uptake of *F. tularensis* has involved heat inactivation of HS to block complement activation or selective depletion of individual complement components, both of which yield greater effects on uptake than receptor blocking with antibodies. Perhaps blocking antibodies lack the affinity required to compete with high affinity natural ligands. Alternatively, incomplete blocking by antibodies to CRs may indicate that other receptors also mediate uptake of serum-opsonized *F. tularensis*. For example, Class A scavenger receptors have been shown to bind iC3b (Goh et al., 2010) and have been implicated in the uptake of serum-opsonized *F. tularensis* (Pierini, 2006; Geier and Celli, 2011). Balagopal et al. (2006) suggested that Fcγ-receptors on human MDM could also contribute to uptake of serum-opsonized *F. novicida*. A role for CR1g in the uptake of serum-opsonized *F. tularensis* has not been investigated. CR1g is a complement receptor expressed on tissue macrophages which binds the beta chain of C3, allowing the receptor to phagocytize both C3b- and iC3b-opsonized particles. The receptor has been shown to be important for the clearance of pathogens (Helmy et al., 2006; van Lookeren Campagne et al., 2007). Thus, although our knowledge of all the receptors that mediate the uptake of serum-opsonized *F. tularensis* may be incomplete, iC3b and CR3 likely play dominant roles in *Francisella* opsonophagocytosis by macrophages.

Complement C3-mediated uptake of *F. tularensis* is not restricted to macrophages. Ben Nasr et al. showed that C3 is also required for increased uptake of *F. tularensis* by human monocyte-derived dendritic cells. Opsonization with C3-depleted HS resulted in levels of uptake similar to those observed with un-opsonized bacteria (Ben Nasr et al., 2006; Ben Nasr and Klimpel, 2008). Blocking with antibodies to CD11b and CD11c identified CR3 and CR4 as important for enhanced uptake by dendritic cells (Ben Nasr et al., 2006). By contrast, blocking Fc receptors had little effect (Ben Nasr et al., 2006). In similar receptor blocking studies, Schwartz et al. (2012) found that CR1 (CD35) and CR3 (CD11b) mediated uptake of HS-opsonized *F. tularensis* by human neutrophils (Schwartz et al., 2012). These studies illustrate that different cells utilize a range of complement receptors to phagocytize serum-opsonized *F. tularensis*.

EFFECTS OF COMPLEMENT ON *F. TULARENSIS* INFECTION OF MACROPHAGES

Complement C3-opsonization appears to have more effects than simply increasing the number of *F. tularensis* bacteria that are phagocytized. Clemens et al. showed that both non-opsonized and HS-opsonized *F. tularensis* LVS were taken up by a unique process, referred to as “looping phagocytosis,” which involved spacious, asymmetric pseudopod loops (Clemens et al., 2005, 2012). An O-antigen-deficient LVS mutant was also

phagocytized via looping in the absence of serum. However, the morphology of uptake of this serum-sensitive O-antigen mutant was altered in the presence of C7-deficient serum, which allowed for opsonization but prevented complement-mediated bacteriolysis (Clemens et al., 2012). C7-deficient serum promoted uptake of the mutant in very tight loops. As serum-sensitive O-antigen mutants support increased C3-deposition (Clay et al., 2008), the authors suggested that an increased interaction between bacterial surface bound C3 peptides and macrophage complement receptors likely led to closer physical interactions at the host-microbe interface (Clemens et al., 2012). An important unanswered question is whether this morphological change leads to different signaling in the host cell.

Geier and Celli demonstrated that CR3 was important in the uptake by mouse bone marrow-derived macrophages (BMM) of HS-opsonized SCHU S4 (Geier and Celli, 2011). Uptake of HS-opsonized SCHU S4 delayed the maturation of the phagosome as measured by the expression of LAMP-1. Baudino et al. have also reported a delay in phagosome maturation associated with the uptake of C3-opsonized apoptotic cells (Baudino et al., 2014). Uptake via CR3 decreased the proportion of SCHU S4 bacteria that escaped phagosomes measured at 30 min PI (Geier and Celli, 2011). However, differences between phagosome escape of HS-opsonized bacteria by wild-type BMM and CD11b-deficient BMM were lost by 45 min PI, suggesting the effect was only temporary.

Geier and Celli also concluded that HS-opsonization restricted the replication of the pathogen measured at 12 h PI. Our own studies with human macrophages indicate that intracellular replication rates of SCHU S4 in human macrophages are not affected by C3-opsonization (Brock and Parmely, 2017). SCHU S4 bacteria taken up in HS did not evidence any impaired ability to replicate to high densities within human primary macrophages. It should be noted that the time required for maximum *F. tularensis* escape from phagosomes appears to be greater in human THP-1 cells and primary macrophages (Clemens et al., 2004) than is observed in murine BMM (Geier and Celli, 2011), and this may explain some of the differences between these studies. Similarly, the percentage of HS-opsonized bacteria that ultimately do escape the phagosome appears to be higher in human macrophages (typically ~80%) (Clemens et al., 2004; Brock and Parmely, 2017) than mouse macrophages (typically ~55%) (Geier and Celli, 2011). Another distinction between these mouse and human studies is the use of human serum as the source of opsonins in both cases. This approach assumes that human C3 interacts with human and mouse complement receptors in a similar manner and that signaling from both species of receptors is also the same.

Dai et al. reported that the binding of C3-opsonized SCHU S4 to CR3 altered the human macrophage response to infection by suppressing inflammatory cytokine production induced by TLR2 (Dai et al., 2013). By comparing infection of MDM with SCHU S4 in C3-depleted and C3-replenished human serum, the investigators found that the presence of C3-opsonization decreased the phosphorylation of MAP kinases ERK and p38 and decreased levels of secreted TNF, IL-6 and IL-1 β .

Serum opsonization of SCHU S4 also resulted in less NF- κ B phosphorylation and nuclear translocation. Using siRNA to inhibit expression of CD11b or TLR2, they demonstrated that TLR2 activated pro-inflammatory responses to *F. tularensis* and that CR3 inhibited TLR2 signaling. CR3 inhibition of TLR2 signaling was mediated through phosphorylation of Lyn kinase.

These studies indicate that the binding and uptake of C3-opsonized *F. tularensis* has a number of effects beyond the promotion of phagocytosis. C3 mediates a different morphology of uptake, significant changes in early host cell signaling pathways, subtle changes in intracellular trafficking and even altered survival of infected macrophages (Brock and Parmely 2017), which will now be discussed in more detail.

C3 CONTROLS MACROPHAGE SURVIVAL DURING INFECTION WITH TYPE A *F. TULARENSIS*

While studying infections of human MDM with *F. tularensis* SCHU S4, we observed that large numbers of macrophages in infected cultures died by 24 h PI and that cell death was C3-dependent (Brock and Parmely, 2017). Death was rare among macrophages that had been infected in the presence of heat-inactivated or C3-depleted serum. Single cell analysis by confocal microscopy revealed that a high cytosolic bacterial burden was not required for C3-dependent macrophage death. Many cells that bore only a few bacteria died as long as uptake had been facilitated by the presence of fresh HS. Conversely, half of macrophages that contained more than 100 bacteria did not die by 24 h PI when bacteria were taken up in a C3-dependent fashion. Some MDM in cultures that had been infected with C3-opsonized SCHU S4 lacked any detectable bacteria, and very few of these bystander cells died. Acknowledging that differences in the extent of bacterial uptake existed between the two opsonization conditions, we equalized initial uptake of the pathogen in HS and C3-depleted HS by adjusting the multiplicities of infection (MOI). When initial uptake levels were equivalent, similar bacterial growth occurred under the two conditions, but macrophage death was only seen in the presence of C3. We concluded that high bacterial burden was neither necessary nor sufficient for cell death induction, which was confirmed by infections with the replication-deficient SCHU S4 Δ *purMCD* mutant. Despite its limited intracellular replication, the HS-opsonized Δ *purMCD* mutant strain escaped the phagosome and induced cell death at levels equivalent to those seen in wild type SCHU S4-infected cultures. C3-dependent uptake alone did not explain the induction of macrophage death, as shown by the failure of the phagosome escape-deficient mutant SCHU S4 Δ *fevR* to induce death of MDM, despite C3 opsonization. These findings suggest that two conditions need to be met for macrophage death. First, the cells must contain the pathogen. Second, uptake must occur in a C3-dependent fashion. While we do not yet know all of the details of this process, C3 appears to be emerging as an important factor in the induction of macrophage death that is so commonly seen in tularemia (Parmely et al., 2009).

The experiments of Tam et al. (2014) reviewed above provide a potential context for understanding how complement promotes macrophage death following infection with type A *F. tularensis*. This group demonstrated that cytosolic C3 peptides, likely in the form of C3b, can activate NF- κ B in a number of cell types. If this cellular response was initiated by the sensing of a cytosolic C3 peptide, as postulated by the authors, it would provide a reasonable hypothesis for explaining what we have observed during *F. tularensis* infections of human macrophages. Accordingly, we suggest that C3 peptides, including iC3b, are recognized in the cytosol of macrophages as molecular patterns and that the response to them is directed toward cell death, rather than NF- κ B activation, by type A *F. tularensis* (Figure 3). This pathogen has a well-established anti-inflammatory phenotype, which includes its ability to inhibit NF- κ B activation (Telepnev et al., 2003, 2005; Bosio et al., 2007; Butchar et al., 2008; Chase et al., 2009; Dotson et al., 2013; Bauler et al., 2014; Ghonime et al., 2015; Putzova et al., 2017). C3-dependent uptake of *F. tularensis* by CR3 further inhibits NF- κ B activation and pro-inflammatory gene expression in human macrophages (Dai et al., 2013).

Our prediction that C3 peptides induce macrophage death after SCHU S4 entry into the cytosol rests, in part, on studies with the phagosome escape SCHU S4 Δ *fevR* mutant. Strains deficient in *FevR* have been used by others to determine the importance of phagosome escape in various aspects of infection of and immunity to *F. tularensis* (Wehrly et al., 2009; Long et al., 2013). However, it should be noted that *FevR* is a global transcriptional regulator and controls the expression of a number of *F. tularensis* genes.

Our hypothesis would predict that C3 peptides enter the cytosol with *F. tularensis*. Human serum-opsonized *F. tularensis* bears covalently attached C3b and iC3b when it is taken up by cells, although the fate of these peptides during their extended stay in the phagosome is unknown. Phagosome escape by SCHU S4 in human macrophages is not complete until 8 h PI. In this context, it remains unclear whether the pathogen contributes more to macrophage death induction than simply transporting the relevant C3 peptides into the cytosol, but we expect that it does. Tam et al. (2014) were able to elicit a NF- κ B response in HEK293T cells by simply transfecting the cells with latex beads opsonized with the purified complement components C3, FB and FD. This would suggest that the NF- κ B response does not require a microbial component and that cytosolic C3 peptides may be sufficient for this response. Tam et al. (2014) did not report on the viability of the host cell following the transfection of C3 peptides into the cytosol. Thus, it remains to be determined if cytosolic C3 or cytosolic C3 fragments alone are sufficient to trigger macrophage death. Because both *F. tularensis* itself and CR3 engagement are capable of inhibiting NF- κ B activation (Telepnev et al., 2003; Dai et al., 2013; Putzova et al., 2017), we propose that the response to cytosolic C3 in *F. tularensis*-infected macrophages is diverted to a cell death pathway (Figure 3). This would explain the requirement for C3-opsonization and align our findings with the C3 sensing model proposed by Tam and colleagues.

Testing the hypothesis that cell death is initiated by the combined effects of C3 peptides and *F. tularensis* may be best

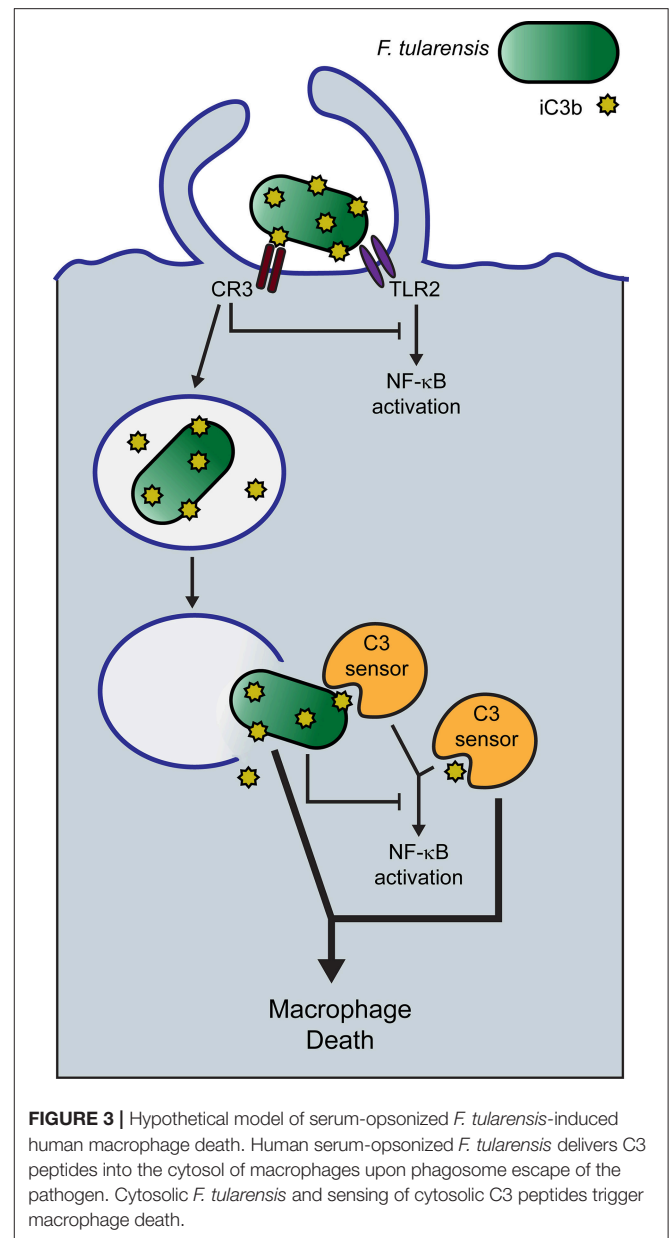


FIGURE 3 | Hypothetical model of serum-opsonized *F. tularensis*-induced human macrophage death. Human serum-opsonized *F. tularensis* delivers C3 peptides into the cytosol of macrophages upon phagosome escape of the pathogen. Cytosolic *F. tularensis* and sensing of cytosolic C3 peptides trigger macrophage death.

undertaken by the direct delivery of these components into the cytosol of macrophages by methods such as those described by Meyer et al. (2015) or Wu et al. (2015). These experimental approaches would allow one to isolate the effects of the cytosolic microenvironment from those stages of infection preceding phagosome escape and evaluate more precisely the nature of C3, the bacterial components and the host cell recognition process that combines to trigger macrophage death.

What role does CR3, which mediates the uptake of C3-opsonized SCHU S4 by human macrophages, play in signaling cell death? Two observations may be relevant. Dai et al. (2013) showed that human MDM infected with C3-opsonized SCHU S4 produced decreased amounts of IL-1 β , a finding we confirmed in our own studies (Brock and Parmely, 2017). Release of IL-1 β requires inflammasome-mediated caspase-1 activation, which

is not a characteristic of type A *F. tularensis* (Dotson et al., 2013; Ghonime et al., 2015). Thus, it is unlikely that CR3 binding of C3-opsonized SCHU S4 induces caspase-1-mediated pyroptosis in human macrophages as has been reported for mouse macrophages infected with *F. novicida* (Mariathasan et al., 2005; Henry et al., 2007; Peng et al., 2011). A second finding is also relevant. When we first infected human MDM at high MOI with SCHU S4 opsonized with C3-depleted serum and then infected these cells with C3-opsonized SCHU S4 $\Delta fevR$ mutant bacteria, the infected macrophages remained viable. Secondary infection with C3-opsonized wild type SCHU S4 resulted in macrophage death. Likewise, infection with C3-opsonized SCHU S4 $\Delta fevR$ alone also did not induce macrophage death, whereas C3-opsonized wild type SCHU S4 alone did. This illustrates that CR3 engagement is not a sufficient death signal, even in macrophages infected with high numbers of intracellular bacteria lacking C3 peptides. A reasonable explanation for these findings is that macrophage death requires both cytosolic *F. tularensis* and cytosolic C3 peptides. While it cannot be ruled out that CR3 signaling (Dai et al., 2013) contributes to macrophage death, there is also no reason to assume that CR3-mediated uptake of C3-opsonized *F. tularensis* is required for cell death induction. CR3 may simply be the most efficient receptor for assuring a high frequency of infected cells.

Although a putative C3 sensor remains to be characterized, two likely ligands—C3b and iC3b—are predicted by available information. First, Tam and his colleagues implied that the ligand was C3b by the few components—C3, FB and FD—that were required for opsonizing latex beads capable of activating NF- κ B following their transfection into cells (Tam et al., 2014). Second, when *F. tularensis* SCHU S4 is opsonized with HS, iC3b is the predominant peptide covalently attached to the organism (Ben Nasr and Klimpel, 2008; Clay et al., 2008; Brock and Parmely, 2017). This is consistent with the high levels of uptake of C3-opsonized *F. tularensis* by human macrophages being mediated by CR3 (Clemens et al., 2005; Schwartz et al., 2012; Dai et al., 2013), which shows high affinity for iC3b (Table 1).

Previous studies of mice infected with type A *F. tularensis* revealed a caspase-3-dependent pathway of macrophage death (Parmely et al., 2009; Wickstrum et al., 2009). However, to date, we have been unable to determine the cell death pathway activated by C3-opsonized SCHU S4 in human MDM. The extended period of time between infection with *F. tularensis* and macrophage death has suggested to some that a causal relationship exists between achieving a sufficient intracellular bacterial burden and cell death induction. However, recently published findings (Brock and Parmely, 2017) described above are inconsistent with this interpretation. If the kinetics of cell death reflects an apoptotic process, which can take up to 24 h (Saraste and Pulkki, 2000), then the delay in the appearance of overt signs of cell death (e.g., LDH release) may reflect the variability in apoptosis induction among individual cells, the

complex nature of signaling pathways or the lengthy degradative processes necessary for loss of membrane integrity leading to LDH release.

Francisella tularensis is likely to encounter the complement system quite early in infection, given the range of cells that produce complement components and the high concentrations of these components in body fluids, especially plasma, alveolar fluids and inflammatory exudates (Schenkein and Genco, 1978; Watford et al., 2000; Holers, 2014; Lubbers et al., 2017). Complement activation by extracellular microbial pathogens has traditionally been viewed as benefiting the host by mediating clearance, leukocyte chemotaxis and altered vascular permeability at sites of infection. However, this view needs to be balanced by recent reports that *F. tularensis* utilizes complement to its own advantage by avoiding many complement effector mechanisms, regulating innate immune cell activation and controlling host cell viability to promote its own survival, intracellular replication and dissemination. Caution is urged in considering therapeutic approaches to infection that might affect complement activation by *F. tularensis*. Clearly, the pathogen has a complicated and largely mysterious relationship with the complement system that deserves additional study to appreciate fully its role in tularemia pathogenesis.

ETHICS STATEMENT

This study was carried out in accordance with the recommendations of the human subjects research guidelines of the University of Kansas Medical Center Institutional Review Board with written informed consent from all subjects. All subjects gave written informed consent in accordance with the Declaration of Helsinki. The protocol was approved by the University of Kansas Medical Center Institutional Review Board.

AUTHOR CONTRIBUTIONS

SB and MP both contributed to the design, conception, and writing of this manuscript.

FUNDING

The laboratory of MP was funded by NIAID grant AI093921 from the National Institutes of Health and a Lied Basic Science Grant from the University of Kansas Medical Center Research Institute. SB was supported by a Biomedical Research Training Program grant from the University of Kansas Medical Center.

ACKNOWLEDGMENTS

The authors would like to thank Catharine Bosio, Jean Celli, and Lee-Ann Allen for providing *Francisella* strains which aided in this research.

REFERENCES

- Arbore, G., Kemper, C., and Kolev, M. (2017). Intracellular complement—the complex—in immune cell regulation. *Mol. Immunol.* 89, 2–9. doi: 10.1016/j.molimm.2017.05.012
- Balagopal, A., MacFarlane, A. S., Mohapatra, N., Soni, S., Gunn, J. S., and Schlesinger, L. S. (2006). Characterization of the receptor–ligand pathways important for entry and survival of *Francisella tularensis* in human macrophages. *Infect. Immun.* 74, 5114–5125. doi: 10.1128/IAI.00795-06
- Barel, M., Hovanessian, A. G., Meibom, K., Briand, J. P., Dupuis, M., and Charbit, A. (2008). A novel receptor–ligand pathway for entry of *Francisella tularensis* in monocyte-like THP-1 cells: interaction between surface nucleolin and bacterial elongation factor Tu. *BMC Microbiol.* 8:145. doi: 10.1186/1471-2180-8-145
- Baudino, L., Sardini, A., Ruseva, M. M., Fossati-Jimack, L., Cook, H. T., Scott, D., et al. (2014). C3 opsonization regulates endocytic handling of apoptotic cells resulting in enhanced T-cell responses to cargo-derived antigens. *Proc. Natl. Acad. Sci. U.S.A.* 111, 1503–1508. doi: 10.1073/pnas.1316877111
- Bauler, T. J., Chase, J. C., Wehrly, T. D., and Bosio, C. M. (2014). Virulent *Francisella tularensis* destabilize host mRNA to rapidly suppress inflammation. *J. Innate Immun.* 6, 793–805. doi: 10.1159/000363243
- Ben Nasr, A., Haithcoat, J., Masterson, J. E., Gunn, J. S., Eaves-Pyles, T., and Klimpel, G. R. (2006). Critical role for serum opsonins and complement receptors CR3 (CD11b/CD18) and CR4 (CD11c/CD18) in phagocytosis of *Francisella tularensis* by human dendritic cells (DC): uptake of *Francisella* leads to activation of immature DC and intracellular survival of the bacteria. *J. Leukoc. Biol.* 80, 774–786. doi: 10.1189/jlb.1205755
- Ben Nasr, A., and Klimpel, G. R. (2008). Subversion of complement activation at the bacterial surface promotes serum resistance and opsonophagocytosis of *Francisella tularensis*. *J. Leukoc. Biol.* 84, 77–85. doi: 10.1189/jlb.0807526
- Bosio, C. M., Bielefeldt-Ohmann, H., and Belisle, J. T. (2007). Active suppression of the pulmonary immune response by *Francisella tularensis* Schu4. *J. Immunol.* 178, 4538–4547. doi: 10.4049/jimmunol.178.7.4538
- Brock, S. R., and Parnely, M. J. (2017). Complement C3 as a prompt for human macrophage death during infection with *Francisella tularensis* strain SCHU S4. *Infect. Immun.* 85:e00424-17. doi: 10.1128/IAI.00424-17
- Butchar, J. P., Cremer, T. J., Clay, C. D., Gavrilin, M. A., Wewers, M. D., Marsh, C. B., et al. (2008). Microarray analysis of human monocytes infected with *Francisella tularensis* identifies new targets of host response subversion. *PLoS ONE* 3:e2924. doi: 10.1371/journal.pone.0002924
- Chase, J. C., Celli, J., and Bosio, C. M. (2009). Direct and indirect impairment of human dendritic cell function by virulent *Francisella tularensis* Schu S4. *Infect. Immun.* 77, 180–195. doi: 10.1128/IAI.00879-08
- Chen, Z. A., Pellarin, R., Fischer, L., Sali, A., Nilges, M., Barlow, P. N., et al. (2016). Structure of complement C3(H₂O) revealed by quantitative cross-linking/mass spectrometry and modeling. *Mol. Cell. Proteomics* 15, 2730–2743. doi: 10.1074/mcp.M115.056473
- Chong, A., Wehrly, T. D., Nair, V., Fischer, E. R., Barker, J. R., Klose, K. E., et al. (2008). The early phagosomal stage of *Francisella tularensis* determines optimal phagosomal escape and *Francisella* pathogenicity island protein expression. *Infect. Immun.* 76, 5488–5499. doi: 10.1128/IAI.00682-08
- Clay, C. D., Soni, S., Gunn, J. S., and Schlesinger, L. S. (2008). Evasion of complement-mediated lysis and complement C3 deposition are regulated by *Francisella tularensis* lipopolysaccharide O antigen. *J. Immunol.* 181, 5568–5578. doi: 10.4049/jimmunol.181.8.5568
- Clemens, D. L., Lee, B. Y., and Horwitz, M. A. (2004). Virulent and avirulent strains of *Francisella tularensis* prevent acidification and maturation of their phagosomes and escape into the cytoplasm in human macrophages. *Infect. Immun.* 72, 3204–3217. doi: 10.1128/IAI.72.6.3204-3217.2004
- Clemens, D. L., Lee, B. Y., and Horwitz, M. A. (2005). *Francisella tularensis* enters macrophages via a novel process involving pseudopod loops. *Infect. Immun.* 73, 5892–5902. doi: 10.1128/IAI.73.9.5892-5902.2005
- Clemens, D. L., Lee, B. Y., and Horwitz, M. A. (2012). O-antigen-deficient *Francisella tularensis* Live Vaccine Strain mutants are ingested via an aberrant form of looping phagocytosis and show altered kinetics of intracellular trafficking in human macrophages. *Infect. Immun.* 80, 952–967. doi: 10.1128/IAI.05221-11
- Dai, S., Rajaram, M. V., Curry, H. M., Leander, R., and Schlesinger, L. S. (2013). Fine tuning inflammation at the front door: macrophage complement receptor 3-mediate phagocytosis and immune suppression for *Francisella tularensis*. *PLoS Pathog.* 9:e1003114. doi: 10.1371/journal.ppat.1003114
- Dennis, D. T., Inglesby, T. V., Henderson, D. A., Bartlett, J. G., Ascher, M. S., Eitzen, E., et al. (2001). Tularemia as a biological weapon: medical and public health management. *JAMA* 285, 2763–2773. doi: 10.1001/jama.285.21.2763
- Dotson, R. J., Rabadi, S. M., Westcott, E. L., Bradley, S., Catlett, S. V., Banik, S., et al. (2013). Repression of inflammasome by *Francisella tularensis* during early stages of infection. *J. Biol. Chem.* 288, 23844–23857. doi: 10.1074/jbc.M113.490086
- Dunkelberger, J. R., and Song, W. C. (2010). Complement and its role in innate and adaptive immune responses. *Cell Res.* 20, 34–50. doi: 10.1038/cr.2009.139
- Elvington, M., Liszewski, M. K., and Atkinson, J. P. (2016). Evolution of the complement system: from defense of the single cell to guardian of the intravascular space. *Immunol. Rev.* 274, 9–15. doi: 10.1111/imr.12474
- Elvington, M., Liszewski, M. K., Bertram, P., Kulkarni, H. S., and Atkinson, J. P. (2017). A C3(H₂O) recycling pathway is a component of the intracellular complement system. *J. Clin. Invest.* 127, 970–981. doi: 10.1172/JCI89412
- Feldman, K. A., Ensore, R. E., Lathrop, S. L., Matyas, B. T., McGill, M., Schriefer, M. E., et al. (2001). An outbreak of primary pneumonic tularemia on Martha's Vineyard. *N. Engl. J. Med.* 345, 1601–1606. doi: 10.1056/NEJMoa011374
- Fulop, M., Webber, T., and Manchee, R. (1993). Activation of the complement system by *Francisella tularensis* lipopolysaccharide. *New Microbiol.* 16, 141–147.
- Geier, H., and Celli, J. (2011). Phagocytic receptors dictate phagosomal escape and intracellular proliferation of *Francisella tularensis*. *Infect. Immun.* 79, 2204–2214. doi: 10.1128/IAI.01382-10
- Ghonime, M. G., Mitra, S., Eldomany, R. A., Wewers, M. D., and Gavrilin, M. A. (2015). Inflammasome priming is similar for francisella species that differentially induce inflammasome activation. *PLoS ONE* 10:e0127278. doi: 10.1371/journal.pone.0127278
- Goh, J. W., Tan, Y. S., Dodds, A. W., Reid, K. B., and Lu, J. (2010). The class A macrophage scavenger receptor type I (SR-AI) recognizes complement iC3b and mediates NF- κ B activation. *Protein Cell* 1, 174–187. doi: 10.1007/s13238-010-0020-3
- Golovliov, I., Baranov, V., Krocova, Z., Kovarova, H., and Sjøstedt, A. (2003). An attenuated strain of the facultative intracellular bacterium *Francisella tularensis* can escape the phagosome of monocyte cells. *Infect. Immun.* 71, 5940–5950. doi: 10.1128/IAI.71.10.5940-5950.2003
- Hall, J. D., Woolard, M. D., Gunn, B. M., Craven, R. R., Taft-Benz, S., Frelinger, J. A., et al. (2008). Infected-host-cell repertoire and cellular response in the lung following inhalation of *Francisella tularensis* Schu S4, LVS, or U112. *Infect. Immun.* 76, 5843–5852. doi: 10.1128/IAI.01176-08
- Helmy, K. Y., Katschke, K. J. Jr., Gorgani, N. N., Kljavin, N. M., Elliott, J. M., Diehl, L., et al. (2006). CRiG: a macrophage complement receptor required for phagocytosis of circulating pathogens. *Cell* 124, 915–927. doi: 10.1016/j.cell.2005.12.039
- Henry, T., Brotcke, A., Weiss, D. S., Thompson, L. J., and Monack, D. M. (2007). Type I interferon signaling is required for activation of the inflammasome during *Francisella* infection. *J. Exp. Med.* 204, 987–994. doi: 10.1084/jem.20062665
- Holers, V. M. (2014). Complement and its receptors: new insights into human disease. *Annu. Rev. Immunol.* 32, 433–459. doi: 10.1146/annurev-immunol-032713-120154
- James, L. C., Keeble, A. H., Khan, Z., Rhodes, D. A., and Trowsdale, J. (2007). Structural basis for PRYSPRY-mediated tripartite motif (TRIM) protein function. *Proc. Natl. Acad. Sci. U.S.A.* 104, 6200–6205. doi: 10.1073/pnas.0609174104
- Kingry, L. C., and Petersen, J. M. (2014). Comparative review of *Francisella tularensis* and *Francisella novicida*. *Front. Cell. Infect. Microbiol.* 4:35. doi: 10.3389/fcimb.2014.00035
- Kolev, M., Dimeloe, S., Le Fric, G., Navarini, A., Arbore, G., Povolero, G. A., et al. (2015). Complement regulates nutrient influx and metabolic reprogramming during Th1 cell responses. *Immunity* 42, 1033–1047. doi: 10.1016/j.immuni.2015.05.024
- Lai, X. H., Golovliov, I., and Sjøstedt, A. (2001). *Francisella tularensis* induces cytopathogenicity and apoptosis in murine macrophages via a mechanism that requires intracellular bacterial multiplication. *Infect. Immun.* 69, 4691–4694. doi: 10.1128/IAI.69.7.4691-4694.2001

- Leslie, R. G. Q. (2001). "Complement Receptors," in *Encyclopedia of Life Sciences* (John Wiley & Sons, Ltd), 1–9. doi: 10.1038/npg.els.0000512
- Lindemann, S. R., Peng, K., Long, M. E., Hunt, J. R., Apicella, M. A., Monack, D. M., et al. (2011). *Francisella tularensis* Schu S4 O-antigen and capsule biosynthesis gene mutants induce early cell death in human macrophages. *Infect. Immun.* 79, 581–594. doi: 10.1128/IAI.00863-10
- Liszewski, M. K., Elvington, M., Kulkarni, H. S., and Atkinson, J. P. (2017). Complement's hidden arsenal: new insights and novel functions inside the cell. *Mol. Immunol.* 84, 2–9. doi: 10.1016/j.molimm.2017.01.004
- Liszewski, M. K., Kolev, M., Le Fric, G., Leung, M., Bertram, P. G., Fara, A. F., et al. (2013). Intracellular complement activation sustains T cell homeostasis and mediates effector differentiation. *Immunity* 39, 1143–1157. doi: 10.1016/j.immuni.2013.10.018
- Löfgren, S., Tärnvik, A., Bloom, G. D., and Sjöberg, W. (1983). Phagocytosis and killing of *Francisella tularensis* by human polymorphonuclear leukocytes. *Infect. Immun.* 39, 715–720.
- Long, M. E., Lindemann, S. R., Rasmussen, J. A., Jones, B. D., and Allen, L. A. (2013). Disruption of *Francisella tularensis* Schu S4 igII, igJ, and pdpC genes results in attenuation for growth in human macrophages and *in vivo* virulence in mice and reveals a unique phenotype for pdpC. *Infect. Immun.* 81, 850–861. doi: 10.1128/IAI.00822-12
- Lubbers, R., van Essen, M. F., van Kooten, C., and Trouw, L. A. (2017). Production of complement components by cells of the immune system. *Clin. Exp. Immunol.* 188, 183–194. doi: 10.1111/cei.12952
- Madar, M., Bencurova, E., Mlynarcik, P., Almeida, A. M., Soares, R., Bhide, K., et al. (2015). Exploitation of complement regulatory proteins by *Borrelia* and *Francisella*. *Mol. Biosyst.* 11, 1684–1695. doi: 10.1039/C5MB00027K
- Mallery, D. L., McEwan, W. A., Bidgood, S. R., Towers, G. J., Johnson, C. M., and James, L. C. (2010). Antibodies mediate intracellular immunity through tripartite motif-containing 21 (TRIM21). *Proc. Natl. Acad. Sci. U.S.A.* 107, 19985–19990. doi: 10.1073/pnas.1014074107
- Mariathasan, S., Weiss, D. S., Dixit, V. M., and Monack, D. M. (2005). Innate immunity against *Francisella tularensis* is dependent on the ASC/caspase-1 axis. *J. Exp. Med.* 202, 1043–1049. doi: 10.1084/jem.20050977
- Martin, M., Leffler, J., Smolag, K. I., Mytych, J., Björk, A., Chaves, L. D., et al. (2016). Factor H uptake regulates intracellular C3 activation during apoptosis and decreases the inflammatory potential of nucleosomes. *Cell Death Differ.* 23, 903–911. doi: 10.1038/cdd.2015.164
- McCrumb, F. R. (1961). Aerosol infection of man with *Pasteurella Tularensis*. *Bacteriol. Rev.* 25, 262–267.
- McEwan, W. A., Tam, J. C., Watkinson, R. E., Bidgood, S. R., Mallery, D. L., and James, L. C. (2013). Intracellular antibody-bound pathogens stimulate immune signaling via the Fc receptor TRIM21. *Nat. Immunol.* 14, 327–336. doi: 10.1038/ni.2548
- Meyer, L., Broms, J. E., Liu, X., Rottenberg, M. E., and Sjøstedt, A. (2015). Microinjection of *Francisella tularensis* and *Listeria monocytogenes* reveals the importance of bacterial and host factors for successful replication. *Infect. Immun.* 83, 3233–3242. doi: 10.1128/IAI.00416-15
- Moreau, G. B., and Mann, B. J. (2013). Adherence and uptake of *Francisella* into host cells. *Virulence* 4, 826–832. doi: 10.4161/viru.25629
- Nishida, N., Walz, T., and Springer, T. A. (2006). Structural transitions of complement component C3 and its activation products. *Proc. Natl. Acad. Sci. U.S.A.* 103, 19737–19742. doi: 10.1073/pnas.0609791104
- Noris, M., and Remuzzi, G. (2013). Overview of complement activation and regulation. *Semin. Nephrol.* 33, 479–492. doi: 10.1016/j.semnephrol.2013.08.001
- Parmely, M. J., Fischer, J. L., and Pinson, D. M. (2009). Programmed cell death and the pathogenesis of tissue injury induced by type A *Francisella tularensis*. *FEMS Microbiol. Lett.* 301, 1–11. doi: 10.1111/j.1574-6968.2009.01791.x
- Peng, K., Broz, P., Jones, J., Joubert, L. M., and Monack, D. (2011). Elevated AIM2-mediated pyroptosis triggered by hypercytotoxic *Francisella* mutant strains is attributed to increased intracellular bacteriolysis. *Cell. Microbiol.* 13, 1586–1600. doi: 10.1111/j.1462-5822.2011.01643.x
- Pierini, L. M. (2006). Uptake of serum-opsonized *Francisella tularensis* by macrophages can be mediated by class A scavenger receptors. *Cell. Microbiol.* 8, 1361–1370. doi: 10.1111/j.1462-5822.2006.00719.x
- Plzakova, L., Krocova, Z., Kubelkova, K., and Macela, A. (2015). Entry of *Francisella tularensis* into murine B cells: the role of B cell receptors and complement receptors. *PLoS ONE* 10:e0132571. doi: 10.1371/journal.pone.0132571
- Putzova, D., Panda, S., Härtlova, A., Stulík, J., and Gekara, N. O. (2017). Subversion of innate immune responses by *Francisella* involves the disruption of TRAF3 and TRAF6 signalling complexes. *Cell. Microbiol.* 19:e12769. doi: 10.1111/cmi.12769
- Ricklin, D., Hajishengallis, G., Yang, K., and Lambris, J. D. (2010). Complement: a key system for immune surveillance and homeostasis. *Nat. Immunol.* 11, 785–797. doi: 10.1038/ni.1923
- Roberts, L. M., Tuladhar, S., Steele, S. P., Riebe, K. J., Chen, C. J., Cumming, R. I., et al. (2014). Identification of early interactions between *Francisella* and the host. *Infect. Immun.* 82, 2504–2510. doi: 10.1128/IAI.01654-13
- Sandström, G., Löfgren, S., and Tärnvik, A. (1988). A capsule-deficient mutant of *Francisella tularensis* LVS exhibits enhanced sensitivity to killing by serum but diminished sensitivity to killing by polymorphonuclear leukocytes. *Infect. Immun.* 56, 1194–1202.
- Saraste, A., and Pulkki, K. (2000). Morphologic and biochemical hallmarks of apoptosis. *Cardiovasc. Res.* 45, 528–537. doi: 10.1016/S0008-6363(99)00384-3
- Satyam, A., Kannan, L., Matsumoto, N., Geha, M., Lapchak, P. H., Bosse, R., et al. (2017). Intracellular activation of complement 3 is responsible for intestinal tissue damage during mesenteric ischemia. *J. Immunol.* 198, 788–797. doi: 10.4049/jimmunol.1502287
- Schenkein, H. A., and Genco, R. J. (1978). Complement cleavage products in inflammatory exudates from patients with periodontal diseases. *J. Immunol.* 120, 1796–1796.
- Schulert, G. S., and Allen, L. A. (2006). Differential infection of mononuclear phagocytes by *Francisella tularensis*: role of the macrophage mannose receptor. *J. Leukoc. Biol.* 80, 563–571. doi: 10.1189/jlb.0306219
- Schwartz, J. T., Barker, J. H., Long, M. E., Kaufman, J., McCracken, J., and Allen, L. A. (2012). Natural IgM mediates complement-dependent uptake of *Francisella tularensis* by human neutrophils via complement receptors 1 and 3 in nonimmune serum. *J. Immunol.* 189, 3064–3077. doi: 10.4049/jimmunol.1200816
- Sorokin, V. M., Pavlovich, N. V., and Prozorova, L. A. (1996). *Francisella tularensis* resistance to bactericidal action of normal human serum. *FEMS Immunol. Med. Microbiol.* 13, 249–252. doi: 10.1111/j.1574-695X.1996.tb00246.x
- Steiner, D. J., Furuya, Y., Jordan, M. B., and Metzger, D. W. (2017). Protective role for macrophages in respiratory *Francisella tularensis* infection. *Infect. Immun.* 85:e00064-17. doi: 10.1128/IAI.00064-17
- Stuart, B. M., and Pullen, R. L. (1945). Tularemic pneumonia: review of American literature and report of 15 additional cases. *Am. J. Med. Sci.* 210, 223–236. doi: 10.1097/00000441-194508000-00013
- Tam, J. C., Bidgood, S. R., McEwan, W. A., and James, L. C. (2014). Intracellular sensing of complement C3 activates cell autonomous immunity. *Science* 345:1256070. doi: 10.1126/science.1256070
- Telepnev, M., Golovliov, I., Grundström, T., Tärnvik, A., and Sjøstedt, A. (2003). *Francisella tularensis* inhibits Toll-like receptor-mediated activation of intracellular signalling and secretion of TNF-alpha and IL-1 from murine macrophages. *Cell. Microbiol.* 5, 41–51. doi: 10.1046/j.1462-5822.2003.00251.x
- Telepnev, M., Golovliov, I., and Sjøstedt, A. (2005). *Francisella tularensis* LVS initially activates but subsequently down-regulates intracellular signaling and cytokine secretion in mouse monocyte and human peripheral blood mononuclear cells. *Microb. Pathog.* 38, 239–247. doi: 10.1016/j.micpath.2005.02.003
- van Lookeren Campagne, M., Wiesmann, C., and Brown, E. J. (2007). Macrophage complement receptors and pathogen clearance. *Cell. Microbiol.* 9, 2095–2102. doi: 10.1111/j.1462-5822.2007.00981.x
- Watford, W. T., Ghio, A. J., and Wright, J. R. (2000). Complement-mediated host defense in the lung. *Am. J. Physiol. Lung Cell. Mol. Physiol.* 279, L790–L798. doi: 10.1152/ajplung.2000.279.5.L790
- Wehrly, T. D., Chong, A., Virtaneva, K., Sturdevant, D. E., Child, R., Edwards, J. A., et al. (2009). Intracellular biology and virulence determinants of *Francisella tularensis* revealed by transcriptional profiling inside macrophages. *Cell. Microbiol.* 11, 1128–1150. doi: 10.1111/j.1462-5822.2009.01316.x
- Wickstrum, J. R., Bokhari, S. M., Fischer, J. L., Pinson, D. M., Yeh, H. W., Horvat, R. T., et al. (2009). *Francisella tularensis* induces extensive caspase-3 activation and apoptotic cell death in the tissues of infected mice. *Infect. Immun.* 77, 4827–4836. doi: 10.1128/IAI.00246-09

- Wu, Y. C., Wu, T. H., Clemens, D. L., Lee, B. Y., Wen, X., Horwitz, M. A., et al. (2015). Massively parallel delivery of large cargo into mammalian cells with light pulses. *Nat. Methods* 12, 439–444. doi: 10.1038/nmeth.3357
- Zarella, T. M., Singh, A., Bitsaktsis, C., Rahman, T., Sahay, B., Feustel, P. J., et al. (2011). Host-adaptation of *Francisella tularensis* alters the bacterium's surface-carbohydrates to hinder effectors of innate and adaptive immunity. *PLoS ONE* 6:e22335. doi: 10.1371/journal.pone.0022335
- Zipfel, P. F., and Skerka, C. (2009). Complement regulators and inhibitory proteins. *Nat. Rev. Immunol.* 9, 729–740. doi: 10.1038/nri2620

Conflict of Interest Statement: The authors declare that the research was conducted in the absence of any commercial or financial relationships that could be construed as a potential conflict of interest.

Copyright © 2017 Brock and Parmely. This is an open-access article distributed under the terms of the Creative Commons Attribution License (CC BY). The use, distribution or reproduction in other forums is permitted, provided the original author(s) or licensor are credited and that the original publication in this journal is cited, in accordance with accepted academic practice. No use, distribution or reproduction is permitted which does not comply with these terms.



Vaccine-Mediated Mechanisms Controlling Replication of *Francisella tularensis* in Human Peripheral Blood Mononuclear Cells Using a Co-culture System

Kjell Eneslätt¹, Igor Golovliov¹, Patrik Rydén² and Anders Sjöstedt^{1*}

¹ Department of Clinical Microbiology, Clinical Bacteriology, and Laboratory for Molecular Infection Medicine Sweden, Umeå University, Umeå, Sweden, ² Department of Mathematics and Mathematical Statistics, Umeå University, Umeå, Sweden

OPEN ACCESS

Edited by:

Jing-Ren Zhang,
Tsinghua University, China

Reviewed by:

Karsten R. O. Hazlett,
Albany Medical College, United States
Jingliang Su,
China Agricultural University, China

*Correspondence:

Anders Sjöstedt
anders.sjostedt@umu.se

Received: 08 November 2017

Accepted: 23 January 2018

Published: 07 February 2018

Citation:

Eneslätt K, Golovliov I, Rydén P and Sjöstedt A (2018) Vaccine-Mediated Mechanisms Controlling Replication of *Francisella tularensis* in Human Peripheral Blood Mononuclear Cells Using a Co-culture System. *Front. Cell. Infect. Microbiol.* 8:27. doi: 10.3389/fcimb.2018.00027

Cell-mediated immunity (CMI) is normally required for efficient protection against intracellular infections, however, identification of correlates is challenging and they are generally lacking. *Francisella tularensis* is a highly virulent, facultative intracellular bacterium and CMI is critically required for protection against the pathogen, but how this is effectuated in humans is poorly understood. To understand the protective mechanisms, we established an *in vitro* co-culture assay to identify how control of infection of *F. tularensis* is accomplished by human cells and hypothesized that the model will mimic *in vivo* immune mechanisms. Non-adherent peripheral blood mononuclear cells (PBMCs) were expanded with antigen and added to cultures with adherent PBMC infected with the human vaccine strain, LVS, or the highly virulent SCHU S4 strain. Intracellular numbers of *F. tularensis* was followed for 72 h and secreted and intracellular cytokines were analyzed. Addition of PBMC expanded from naïve individuals, i.e., those with no record of immunization to *F. tularensis*, generally resulted in little or no control of intracellular bacterial growth, whereas addition of PBMC from a majority of *F. tularensis*-immune individuals executed static and sometimes cidal effects on intracellular bacteria. Regardless of infecting strain, statistical differences between the two groups were significant, $P < 0.05$. Secretion of 11 cytokines was analyzed after 72 h of infection and significant differences with regard to secretion of IFN- γ , TNF, and MIP-1 β was observed between immune and naïve individuals for LVS-infected cultures. Also, in LVS-infected cultures, CD4 T cells from vaccinees, but not CD8 T cells, showed significantly higher expression of IFN- γ , MIP-1 β , TNF, and CD107a than cells from naïve individuals. The co-culture system appears to identify correlates of immunity that are relevant for the understanding of mechanisms of the protective host immunity to *F. tularensis*.

Keywords: *F. tularensis*, *in vitro* model, human immune response, IFN- γ , TNF, MIP-1 β , correlates of immunity

INTRODUCTION

Tularemia is a severe disease affecting many mammalian species and the etiological agent is the highly virulent bacterium, *Francisella tularensis* (Sjöstedt, 2007). Tularemia in humans is essentially always caused by either of two subspecies, *tularensis* (type A) and *holarctica* (type B), both of which are highly contagious. The former is distinctly more virulent with the potential to cause lethal disease, but there are also numerous descriptions of serious disease caused by type B strains. Tularemia is essentially confined to and reported from many countries of the Northern hemisphere. It is endemic in certain parts of Scandinavia and Turkey, but infrequently reported in most other countries of the world. A human vaccine strain exists, the live vaccine strain (LVS). Vaccination with LVS appears to have made an important contribution for prevention of laboratory-acquired infection, since the number of tularemia cases decreased very significantly among laboratory staff (Burke, 1977). However, despite the efficacious protection observed in the former group, only limited protection was observed when volunteers were subjected to aerosol infection with *F. tularensis* (reviewed by Conlan, 2011). In addition, a lack of understanding of the protective mechanisms has hampered its licensure. Therefore, more efficacious *Francisella* vaccines are needed and an essential basis for such work will be a thorough understanding of immune mechanisms conferring protection against tularemia.

A number of studies have characterized the human memory immune responses resulting from tularemia or tularemia vaccination (Tärnvik et al., 1985; Tärnvik, 1989; Karttunen et al., 1991; Surcel et al., 1991; Sjöstedt et al., 1992; Ericsson et al., 1994; Eneslätt et al., 2011, 2012). In accordance with the intracellular nature of the pathogen, most evidence indicates that cell-mediated immunity (CMI) is the predominant factor contributing to the protective efficacy of the tularemia vaccine (Tärnvik, 1989). The CMI is long-lasting and preserved for at least 25 years after vaccination or natural infection (Ericsson et al., 1994; Eneslätt et al., 2011, 2012). In fact, tularemia offers a unique model for studying the longevity of CMI in humans because it is such a rare disease; in most cases, therefore, re-exposure is very unlikely to be responsible for the persistence of immunity (Eneslätt et al., 2011).

CMI is critically required for efficacious protection against tularemia and, therefore, there is a need to obtain a detailed understanding of how this is effectuated in order to rationally develop future vaccines. Much evidence indicates that protection is carried out via a complex interaction of multiple T cell subsets and other immune mechanisms, rather than a unique immune mechanism (Elkins et al., 2007; De Pascalis et al., 2008, 2012, 2014; Shen et al., 2010; Cowley and Elkins, 2011; Eneslätt et al., 2011, 2012; Ryden et al., 2012). Therefore, simple proliferation assays will not be sufficient to fully delineate the effector mechanisms, but rather assays that closely mimic the *in vivo* situation will be required. Thus, more sophisticated models will be needed to elucidate the protective mechanisms and to identify putative correlates of protection, all of which will be necessary in order to assess vaccine candidates. In this regard,

substantial work with the aim to implement and validate *ex vivo* murine infection model systems has been performed to identify effector mechanisms of protective immune responses against *F. tularensis* (Cowley and Elkins, 2003; Cowley et al., 2005; Collazo et al., 2009; Elkins et al., 2011; De Pascalis et al., 2012, 2014; Mahawar et al., 2013; Griffin et al., 2015). Such assays, which measure immune-mediated inhibition of bacterial proliferation and their correlation to specific immunological parameters, allow direct assessments of protective immunity. The relevance of the identified correlates using these assays has to some extent been validated by demonstrating their important roles *in vivo* (Kurtz et al., 2013; Melillo et al., 2013, 2014). A limitation of most of the published work has been the use of the attenuated LVS strain and only few studies using fully virulent *F. tularensis* in the models have been performed (Mahawar et al., 2013; Griffin et al., 2015; Golovliov et al., 2017). An additional caveat is the lack of understanding of how relevant these putative protective correlates are for protection against tularemia in humans. Thus, and in conjunction with the aforementioned need to obtain a thorough understanding of immune mechanisms conferring protection against tularemia, there is a need to develop *in vitro* assays that can be used for the purpose of identifying human immune effector mechanisms that control *F. tularensis* replication and to determine if the mechanisms identified in animal models can be validated.

Previous studies have concluded that the *F. tularensis*-specific T cells are characterized by production of IFN- γ by both CD4 and CD8 T cells that express CCR7 or CD62L (Surcel et al., 1991; Eneslätt et al., 2011). In addition to IFN- γ , intracellular cytokine detection has demonstrated that the responding T cells also are characterized by expression of MIP-1 β and CD107a (Eneslätt et al., 2012). In the mouse model of tularemia, numerous studies have demonstrated the important roles of IFN- γ and TNF for the primary as well as the secondary protective immune responses (Anthony et al., 1989; Fortier et al., 1992; Leiby et al., 1992; Conlan et al., 1994; Elkins et al., 1996; Sjöstedt et al., 1996; Cowley et al., 2010). Work has been aimed to identify correlates of immunity by describing cytokine profiles that uniquely identify the proliferative responses of *F. tularensis*-immune individuals (Eneslätt et al., 2011, 2012). In one study, levels of MIP-1 β , IFN- γ , IL-10, and IL-5 discriminated vaccinees vs. naïve individuals (Eneslätt et al., 2012). Moreover, secretion of IL-17 has been identified as a characteristic cytokine of the *F. tularensis* memory response. However, if these cytokines are merely correlates of immunity, or also required for the control of infection is unknown.

Validation of tularemia vaccine candidates is challenging since the disease is rarely and irregularly occurring in most countries and therefore, the degree of protection achieved by vaccination will not be possible to evaluate as for most other vaccines (Sjöstedt, 2007). There are examples when human challenge studies have been performed to evaluate vaccine efficacy, e.g., malaria, influenza, and typhoid (Sauerwein et al., 2011; Shirley and McArthur, 2011), however, in view of the high virulence of respiratory infection with *F. tularensis*, it is highly unlikely that such studies will be ethically approved. In addition, correlates of protection conferred by CMI are difficult to identify and

absent for most intracellular infections. Collectively, all evidence indicates that the efficacy of a new tularemia vaccine, similar to vaccines protecting against other rarely occurring, serious infections, needs to be assessed as stipulated by the FDA Animal Rule (Snoy, 2010). It states that efficacy can be evaluated by use of animal models only, given that the protective mechanisms of the vaccine are well-understood and thereby can be extrapolated to the human situation. Thus, the implementation of the rule for tularemia vaccines will require that relevant animal models and correlates have been identified in these models, but also that models are established to characterize human correlates of immunity and protection. The latter will have to rely on bactericidal effects as surrogate measures of vaccine efficacy. To initiate the work needed to accomplish this, we here demonstrate that a novel assay based on infection of human adherent peripheral blood mononuclear cells (PBMCs) with either the LVS strain, or the highly virulent SCHU S4 strain, shows that infection can be controlled by the addition of non-adherent PBMC. In addition, the control of *F. tularensis* infection correlated with the expression of IFN- γ , MIP-1 β , TNF, and CD107a by CD4 T cells in LVS-infected cultures and with the secretion of IFN- γ and MIP-1 β in both LVS and SCHU S4-infected cultures.

MATERIALS AND METHODS

Bacterial Strains

Francisella tularensis LVS was originally obtained from the American Type Culture Collection (ATCC 29684). *F. tularensis* strain SCHU S4 (*F. tularensis* subsp. *tularensis*) was obtained from the *Francisella* Strain Collection of the Swedish Defense Research Agency, Umeå, Sweden. All bacteriological work related to the SCHU S4 strain was carried out in a biosafety level 3 facility certified by the Swedish Work Environment Authority. Before infection, bacteria were grown on modified GC-agar base at 37°C overnight. Formalin-killed bacteria were prepared by incubating LVS or SCHU S4 in 4% paraformaldehyde for 45 min at 37°C followed by three washes in PBS.

Blood Donors

Individuals included in the study had either (i) previously been vaccinated with LVS, henceforth designated vaccinees, or (ii) had no anamnestic data of LVS vaccination, tularemia, or occupational exposure to *F. tularensis*, henceforth designated naïve individuals. All vaccinees had been administered the same lot of LVS, designated NDBR 101, lot no. 11. The mean age and sex distribution of each group was for naïve individuals 38.2 \pm 12.9 years (3 females, 8 males) and for vaccinees 49.9 \pm 11.2 years (7 females, 4 males). Ethical approvals, 09-181M and 2016/335-31, were obtained from the Regional Ethical Review Board in Umeå, Sweden, and a written informed consent was obtained from all individuals included in the study.

PBMC Collection

Venous blood from donors was collected using CPT-tubes (Becton Dickinson, NJ, USA) and PBMC were prepared according to the manufacturer's recommendations. After washing with 10% of heat-inactivated fetal calf serum in RPMI

1640 (Invitrogen), cells were diluted in culture medium with 10% of heat-inactivated human serum in RPMI 1640. Cells were allowed to recover overnight; cell viability and the cell recovery rate were determined prior to subsequent functional assays.

Recall Stimulation and Lymphocyte Proliferation Assay (LPA)

PBMC were seeded at 2×10^5 cells/well in 200 μ L culture medium with 40 μ g/mL gentamicin per well in 96-well plates. Cells were stimulated with formalin-fixed LVS and SCHU S4 mixed in equal amounts (ffFt) at final concentrations of 0.1, 0.5 colony forming units (CFU)/PBMC, or without antigen and incubated for 5 days at 37°C in a humidified atmosphere with 5% CO₂. LPA was assessed by thymidine incorporation in triplicates as previously described (Ericsson et al., 1994).

Culture System to Assess Intracellular Bacterial Replication

PBMC obtained from naïve individuals or vaccinees were separated into adherent and non-adherent cell populations. The adherent population were incubated for 6 days in a 96-well plate at a density of 0.25×10^6 cells/ml and the non-adherent cells were stimulated with 0.5 ffFt/PBMC and incubated for 6 days at a density of 1×10^6 cells/ml. The non-adherent comprise a majority of morphologically similar cells, presumably lymphocytes. However, some of the cells showed an aberrant morphology and presumably were monocytes. Therefore, the non-adherent population also contained some antigen-presenting cells. After washing, adherent cells were infected with LVS or SCHU S4 at an MOI of 10:1 (bacterium-to-adherent cell) for 2 h, washed and incubated for 45 min with culture media containing 40 μ g/mL gentamicin. Following two washing steps, non-adherent cells were added at an effector/target ratio of 20:1, and cultures incubated for 72 h. Bacterial counts were determined by lysis of cultures and the number of CFU determined by plating. These MOIs and ratios were found to be optimal in preliminary experiments.

Multiplex Cytokine Analysis

Cell culture supernatants, 30 μ L/well, were collected from the same cell cultures as used for assessment of intracellular bacterial replication after 72 h of incubation and stored frozen at -80°C. The time point was chosen since levels of several cytokines increased in the supernatants between 24 and 72 h. The supernatants were analyzed using two custom-made multiplex kits and a Bio-Plex 200 system (BioRad Laboratories Inc., Hercules, CA, USA) according to the manufacturer's instructions. A 5-plex kit and 10-fold diluted supernatants were used to determine the levels of MIP-1 β , MCP-1, IL-6, IFN- γ , and TNF (high level cytokines), and a 6-plex kit in combination with two-fold diluted supernatants were used to measure IL-2, IL-5, IL-7, IL-10, IL-12(p70) and IL-13 (low level cytokines). These cytokines has previously been identified as those of most relevance after stimulation of PBMC from tularemia vaccinees with specific antigen derived from *F. tularensis* (Eneslätt et al., 2012). Estimated cytokine concentrations outside the range of

the standard curve were censored to the nearest standard value. Samples were analyzed in duplicate.

Flow Cytometry Analysis of Surface Markers and Intracellular Cytokine Staining

After 72 h of co-culture, non-adherent cells were transferred to a new plate and 5 μ g/mL of Brefeldin A was added. Four-hours later, plates were centrifuged for 3 min at 500 \times g and supernatants were removed. Cells were prepared for labeling with cell surface marker monoclonal antibodies (mAb) or conjugated intracellular cytokine mAb as recommended by BD Biosciences. The following mAb conjugates were used: CD3-APCCy7 (clone SK7, BD Biosciences), CD4-PE Texas red (clone S3.5, Caltag/Invitrogen), CD8-PerCPCy5.5 (clone SK1, BD Biosciences), IFN γ -FITC (clone 25723.11, BD Biosciences), MIP-1 β -PE (clone D21-1351, BD Biosciences), CD107a-APC (clone H4A3, BD Biosciences), TNF-Brilliant violet 421 (clone MAb11, BioLegend), IL17A-Alexa F700 (clone N49-653, BD Biosciences). Aqua Viability Dye (Molecular Probes/Invitrogen) was added to distinguish live and dead cells. Cells were acquired using an LSRII flow cytometer (BD Biosciences) with FACSDiva software (BD Biosciences). Results were analyzed using FlowJo software (Tree Star).

Data Analysis and Statistical Methods

Wilcoxon's rank-sum test or Student's *t*-test were used to identify significant differences ($P < 0.05$) between data sets. Spearman's rank correlation with a 0.05 significance level was used to test whether two variables were correlated. A significant correlation with a coefficient above 0.4 was considered a strong association, and above 0.7 a very strong association.

For vaccinated individuals, the cytokine levels (cl) were linearly dependent on the CFU (data not shown). Therefore, all cytokine concentrations were normalized as follows. For each cytokine, data (CFU and cl observations) from the vaccinees were selected and linear regression was used to model the relationship between CFU and expected cytokine levels (ecl), which resulted in a model $ecl = \alpha + \beta CFU$. This model was then used to calculate the *normalized cytokine levels* (ncl), where $ncl = cl + ecl$.

RESULTS

Optimization of Conditions for Intracellular Bacterial Assay

Adherent cells were infected with LVS or SCHU S4 at various MOIs of 1:1, 10:1, and 100:1 (bacteria:adherent cell). Maximal control of bacterial replication occurred when the MOI of 10:1 was used, although significant control also was observed for the other two MOIs. Since only one MOI could be used for practical reasons, the 10:1 ratio was chosen for all presented experiments. The ratio of effector vs. target cells was also investigated using a range from 1:1 to 25:1. Consistently, the ratio 20:1 was found to confer maximal control of bacterial replication.

Composition of Effector Cells Used in Assay of Intracellular Growth Inhibition

PBMC from naïve individuals and vaccinees were stimulated with specific *F. tularensis* antigen and after 6 days of culture, cells were characterized with regard to cell surface markers. 90–95% of the non-adherent cells were CD3⁺ cells and a majority of these, around 60%, were CD4⁺, whereas CD8⁺ T cells constituted between 20 and 30% with no differences between vaccinees and naïve individuals (Figure 1). Apart from the classical single-positive T cells, we identified significantly higher percentages of CD3⁺CD4⁻CD8⁻ cells in recall-stimulated cultures from vaccinees compared to naïve individuals [4.7% vs. 1.8% of CD3⁺ T cells (Figure 1)], whereas very few cells were CD3⁺CD4⁺CD8⁺ cells (<1% of CD3⁺ T cells). Among the CD3⁺CD4⁻CD8⁻ cells, >50% were $\gamma\delta$ ⁺ T cells, but with no differences among the groups (Figure 1).

Proliferative Responses to *F. tularensis* Antigens

In order to characterize the immune response of the individuals, PBMC were isolated from vaccinees or naïve individuals and their proliferative responses to recall stimulation with formalin-fixed *F. tularensis* antigen (fFt) were measured. The proliferative responses of PBMC from vaccinees were significantly higher ($P < 0.001$) than of PBMC from naïve individuals; this difference was seen irrespective of antigen concentration (Figure 2). Although PBMC from naïve individuals showed an increase in proliferation with increasing antigen concentration, this difference was not significant (Figure 2). The responses to a mitogen, ConA, were very similar between the two groups; 26,100 cpm \pm 10,600

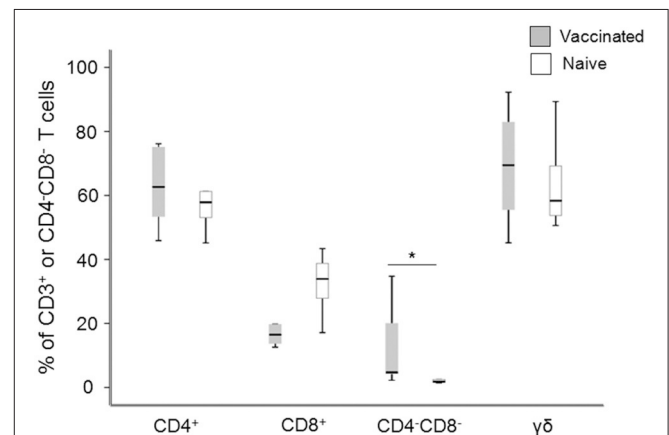
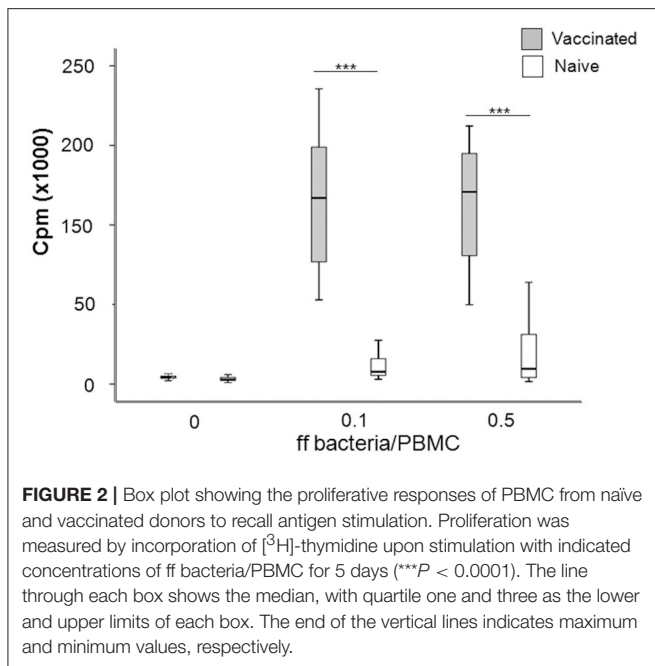


FIGURE 1 | Flow cytometry analysis of the composition of the non-adherent cells after 6 d of antigen stimulation. The values for the CD4⁺, CD8⁺, and CD4⁻CD8⁻ cells are expressed as percentages of the total number of CD3⁺ T cells and the values for $\gamma\delta$ T cells are expressed as percentages of the total number of CD4⁻CD8⁻ T cells. Levels of CD4⁻CD8⁻ T cells were significantly higher in vaccinees compared to naïve individuals (* $P < 0.05$). The line through each box shows the median, with quartile one and three as the lower and upper limits of each box. The end of the vertical lines indicates maximum and minimum values, respectively.



for naïve individuals vs. 21,300 cpm \pm 5,500 for vaccinees (Spearman's correlation coefficient $P > 0.60$).

In summary, the results showed that the immune individuals showed significantly higher *F. tularensis*-specific proliferative responses, as expected from their immune status.

Control of Intracellular Replication of *F. tularensis* and Cytokine Secretion by PBMC

We investigated the potential of PBMC to control the intracellular replication of SCHU S4 or LVS in cell cultures. To this end, non-adherent PBMC were stimulated with specific *F. tularensis* antigen for 6 days, counted and checked for viability, typically 80–95% viable cells, and thereafter added to cultures with LVS- or SCHU S4-infected, autologous, adherent PBMC using the aforementioned optimal MOI and target/effector ratios. The bacterial uptake was very similar regardless of whether the adherent cells originated from vaccinees or naïve individuals ($P > 0.84$). After 72 h of co-culture with target and effector cells, the number of intracellular bacteria was determined and the differences (\log_{10} CFU) in bacterial numbers in the cultures without non-adherent cells vs. the cultures with non-adherent cells were calculated. A representative experiment is shown in **Figure 3** illustrating that addition of non-adherent cells from a naïve individual did not confer any significant control of LVS (**Figure 3A**) or SCHU S4 bacteria (**Figure 3B**), whereas the addition of non-adherent cells from a vaccinee resulted in significant differences ($P < 0.001$), approximately 3 \log_{10} lower bacterial numbers, than in the absence of non-adherent cells (**Figures 3C,D**). When groups of individuals were analyzed, it was observed that there was highly significant control of bacterial replication in the presence vs. the absence of non-adherent

PBMC from vaccinees ($n = 11$); $P < 0.005$ for cultures with LVS-infected or SCHU S4-infected cells, whereas addition of non-adherent PBMC from naïve individuals ($n = 11$) did not result in significant control ($P > 0.05$) of bacterial numbers in any of the cultures (data not shown). Overall, the control exerted by PBMC from vaccinees was significantly greater vs. that executed by PBMC from naïve individuals, $P = 0.025$ for LVS-infected cultures and $P = 0.011$ for SCHU S4-infected cultures (**Figure 4**). Thus, control of intracellular bacterial replication correlated to the vaccination status of the donors.

Cytokine levels were determined for 11 cytokines and levels compared between cultures with PBMC from vaccinees vs. naïve individuals. No significant differences were observed for IL-2, IL-5, IL-7, IL-10, IL-12, or IL-13 between the two groups, regardless of whether the cultures had been infected with LVS or SCHU S4. IFN- γ , MIP-1 β , TNF, were consistently higher in LVS-infected cultures with PBMC from vaccinees vs. cultures with cells from naïve individuals ($P < 0.05$ for IFN- γ and TNF and $P < 0.01$ for MIP-1 β ; **Figure 5A**). Also, in SCHU S4-infected cultures, levels of IFN- γ and MIP-1 β were higher in vaccinees vs. naïve individuals, however, the differences were non-significant ($P > 0.05$; **Figure 5B**). Regardless of infecting strain, the levels of MCP-1 were significantly higher with PBMC from naïve individuals compared to PBMC from vaccinees ($P < 0.005$ with LVS, $P < 0.0005$ with SCHU-S4).

When absolute cytokine levels were normalized for CFUs, the normalized levels of IFN- γ , MIP-1 β , and TNF were significantly higher in both LVS- and SCHU S4-infected cultures with PBMC from vaccinees than with PBMC from naïve individuals ($P < 0.05$ for IFN- γ and MIP-1 β and $P < 0.01$ for TNF; **Figure 6**). IL-6 levels were significantly higher ($P < 0.01$) in SCHU S4-infected cultures with PBMC from vaccinees vs. naïve individuals (**Figure 6B**), whereas the levels of IL-6 did not differ in LVS-infected cultures (**Figure 6A**). Thus, levels of IFN- γ and MIP-1 β served as correlates of immunity, since they discriminated between vaccinees and naïve individuals.

Thus, the normalized cytokine levels more frequently demonstrated significant differences and also lower P -values between the groups (**Figure 6**), than did the actual cytokine levels in the supernatants, in particular with regard to the SCHU S4-infected cultures (**Figure 5**). This indicates that the bacterial numbers *per se* affect the cytokine levels.

Intracellular Cytokine Levels of T Cells in the Co-culture Assays

After 72 h of incubation, the non-adherent cells from LVS infected co-cultures were analyzed for intracellular cytokines by flow cytometry. CD3⁺CD4⁺ T cells from vaccinees showed significantly higher level of IFN- γ , MIP-1 β , TNF, and CD107a, but not IL-17, compared to the same cells from naïve individuals ($P < 0.05$; **Table 1**), but there were no significant differences between the two groups with regard to the CD3⁺CD8⁺ T cells (data not shown).

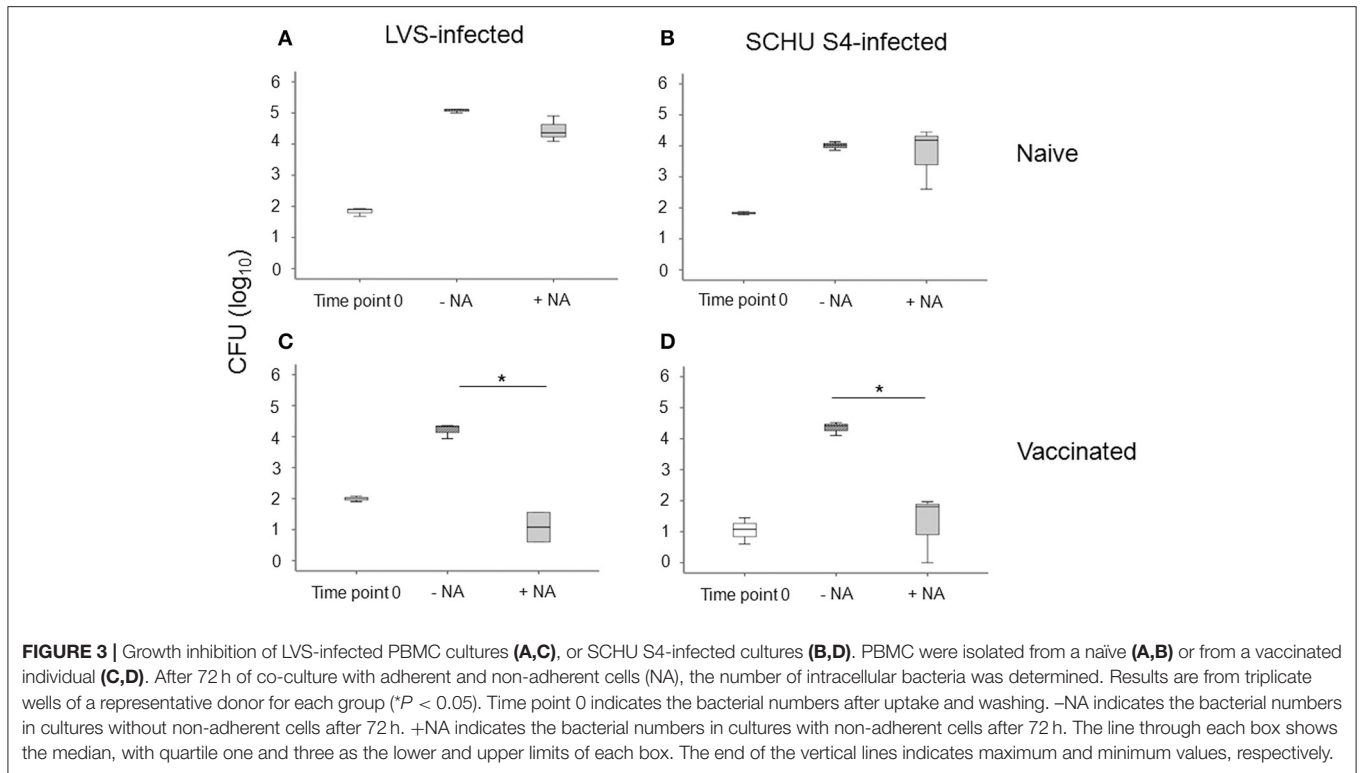


FIGURE 3 | Growth inhibition of LVS-infected PBMC cultures (A,C), or SCHU S4-infected cultures (B,D). PBMC were isolated from a naive (A,B) or from a vaccinated individual (C,D). After 72 h of co-culture with adherent and non-adherent cells (NA), the number of intracellular bacteria was determined. Results are from triplicate wells of a representative donor for each group ($*P < 0.05$). Time point 0 indicates the bacterial numbers after uptake and washing. -NA indicates the bacterial numbers in cultures without non-adherent cells after 72 h. +NA indicates the bacterial numbers in cultures with non-adherent cells after 72 h. The line through each box shows the median, with quartile one and three as the lower and upper limits of each box. The end of the vertical lines indicates maximum and minimum values, respectively.

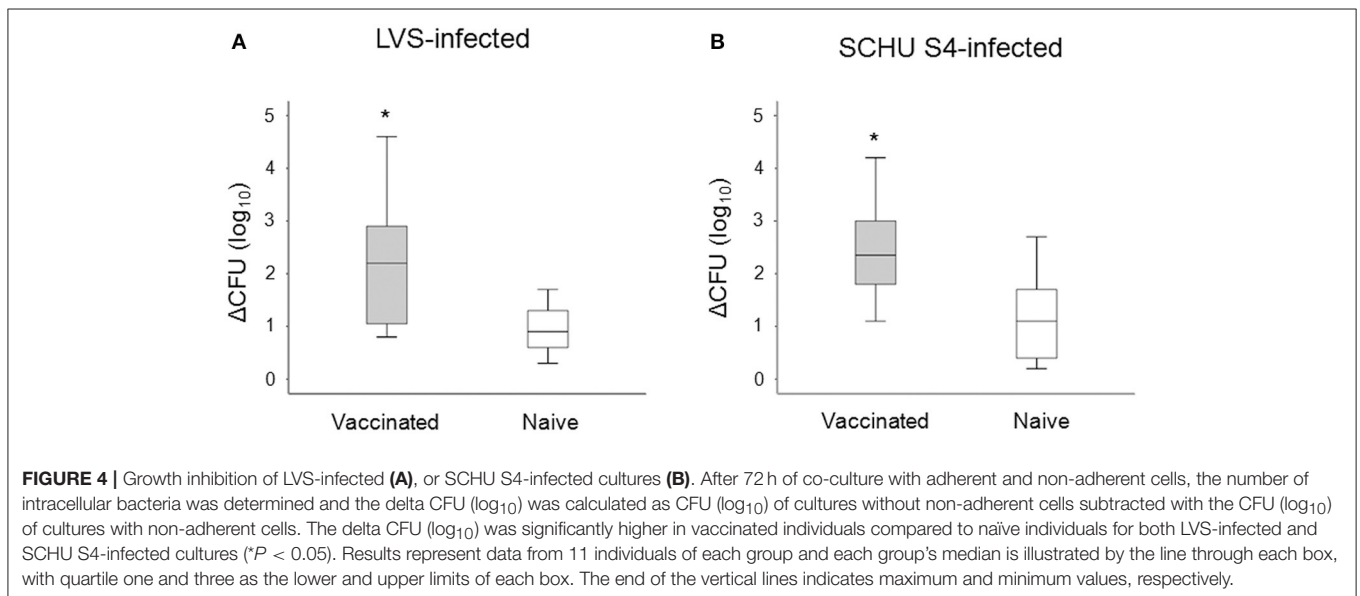
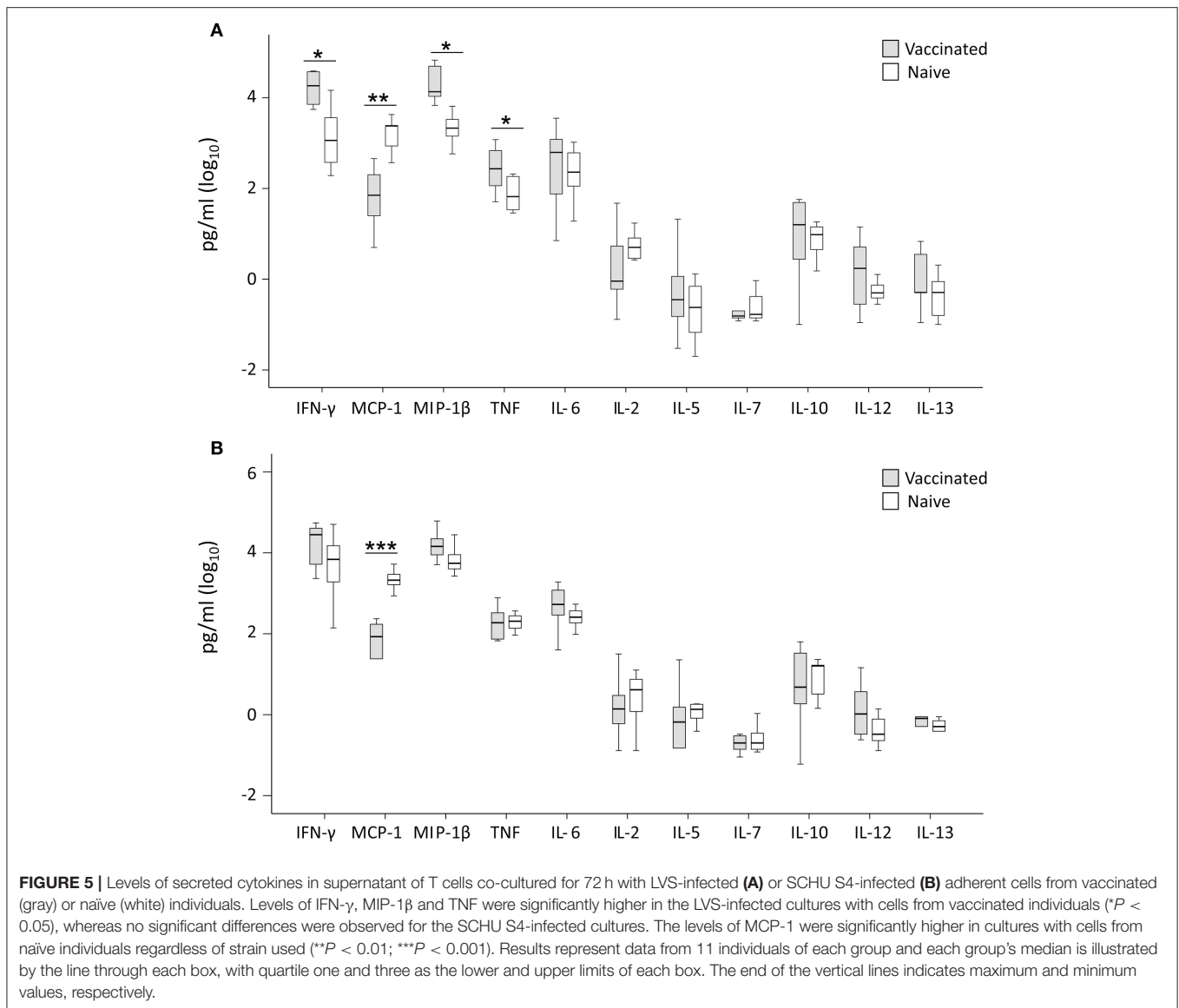


FIGURE 4 | Growth inhibition of LVS-infected (A), or SCHU S4-infected cultures (B). After 72 h of co-culture with adherent and non-adherent cells, the number of intracellular bacteria was determined and the delta CFU (\log_{10}) was calculated as CFU (\log_{10}) of cultures without non-adherent cells subtracted with the CFU (\log_{10}) of cultures with non-adherent cells. The delta CFU (\log_{10}) was significantly higher in vaccinated individuals compared to naive individuals for both LVS-infected and SCHU S4-infected cultures ($*P < 0.05$). Results represent data from 11 individuals of each group and each group's median is illustrated by the line through each box, with quartile one and three as the lower and upper limits of each box. The end of the vertical lines indicates maximum and minimum values, respectively.

DISCUSSION

Immunity against intracellular pathogens is often critically dependent on CMI. This hampers the identification of correlates of immunity and protection to such pathogens, since there are no validated methods for this identification. The lack of methods also hamper vaccine development, since they are required for the fulfillment of the Animal Rule. Moreover, since tularemia

is rather infrequently occurring in most parts of the world, human clinical trials will likely not confer sufficient statistical significance for validation of efficacy and the Animal Rule is likely the only option for licensing of future tularemia vaccines. This option is most likely applicable to biodefense agents and sporadically occurring diseases, both of which are relevant to tularemia. However, methodological developments will be required to overcome the obstacles before the requirements of the



Animal Rule can be fulfilled. These require that efficacy in animal models of relevance will be compared to a model that establishes human correlates of immunity and protection (Snoy, 2010). The latter will require bactericidal effects as surrogate measures of vaccine efficacy and we therefore sought to establish a model that would fulfill this criterion and the present study was designed accordingly.

A lack of correlates of immunity is not unique to tularemia, for example no validated method for identification of correlates exists for the extremely common disease tuberculosis (Nguipdop Djomo et al., 2013). Although patterns of polyfunctional cytokine-producing T cells have been proposed to correlate with tuberculosis vaccine efficacy (Derrick et al., 2011), these patterns are similar regardless of age, despite that vaccination with BCG confers better protection in children than in adults (Colditz et al., 1994; Kagina et al., 2010); thereby questioning

their relevance. Such polyfunctional T cells have been identified also for tularemia, e.g., during human recall responses after LVS vaccination, secretion of IL-12, IFN- γ , MCP-1, MIP-1 β , IL-17, and IL-22 have been identified, which served as immunospecific signatures and discriminated between immune and naïve individuals (Paranavitana et al., 2010; Eneslätt et al., 2012). Much work has been performed based on mouse models of tularemia in order to identify correlates of immunity (Cowley et al., 2007; Elkins et al., 2007; Cowley and Elkins, 2011; Ryden et al., 2012) and, again, secreted Th1-related cytokines, such as IFN- γ , TNF, and MCP-1, were observed and found to correlate to the protective efficacies obtained after immunization with attenuated mutants of *F. tularensis* subspecies *tularensis* (Ryden et al., 2012). In another study, the cytokine gene expression of leukocytes derived from lung, liver, and spleen was examined following immunization with variants of LVS that show variable protective

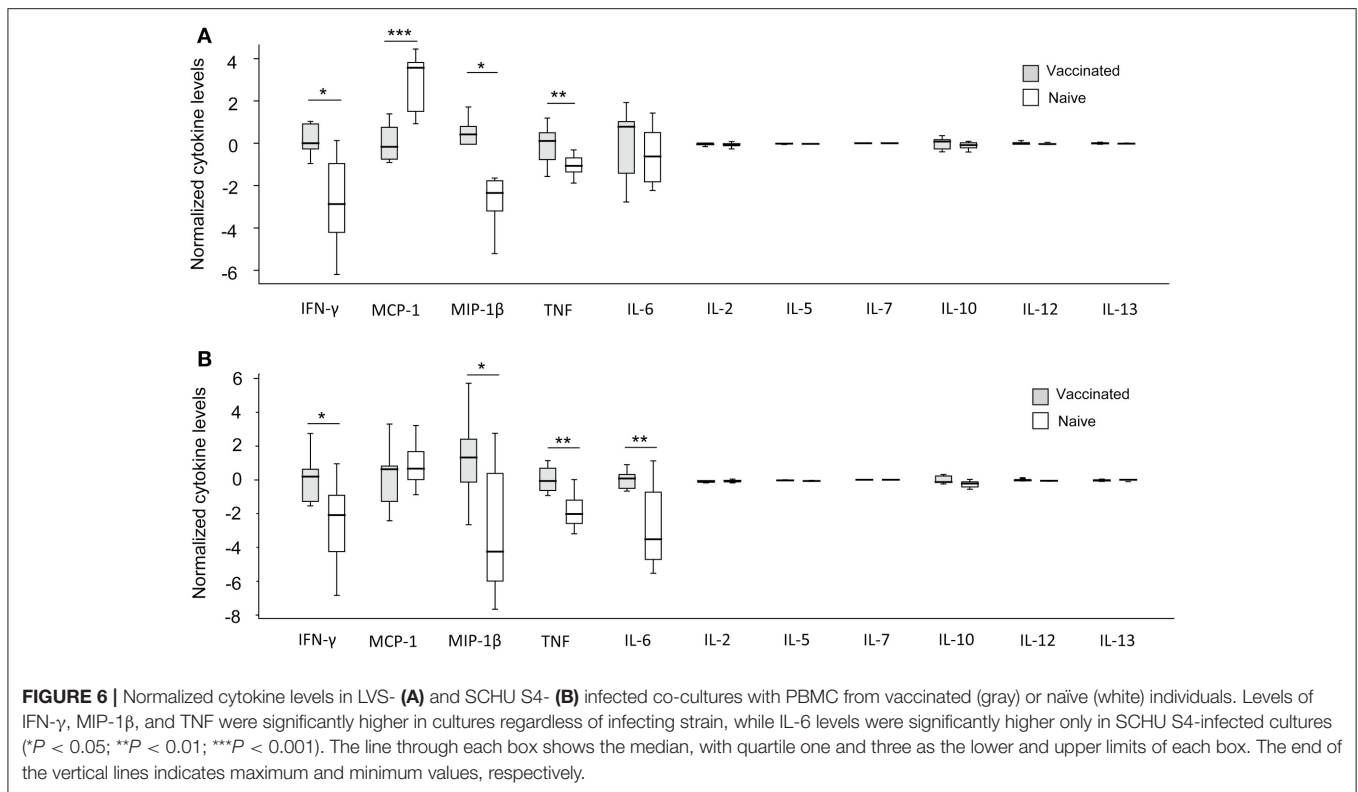


TABLE 1 | Intracellular cytokine level expression by CD4 T cells in co-culture assay.

	CD4 T cells				
	IFN- γ^a	IL-17	MIP-1 β	TNF	CD107a
Vaccinated	0.8 \pm 0.2 ^{b*}	0.3 \pm 0.1	2.5 \pm 0.6*	1.3 \pm 0.3*	1.4 \pm 0.3*
Naïve	0.3 \pm 0.1	0.2 \pm 0.0	0.2 \pm 0.0	0.4 \pm 0.0	0.4 \pm 0.1

^aIntracellular cytokine staining and flow cytometry analysis of cells were performed after 72 h of incubation in the co-culture assay infected with the LVS strain.

^bData represent mean percentages \pm SEM ($n = 8$).

* $P < 0.05$ vs. the group of naïve individuals.

efficacies. The overall pattern was complex when statistical models were developed to predict vaccine efficacy, however, several Th1 cytokine-associated factors were in combinations strongly predictive of protective efficacy, e.g., TNE, IFN- γ , T-bet, IL-27, and IL-12R β 2 (De Pascalis et al., 2014). In a recent study based on co-culture model using spleen cells from immunized mice, levels of nitric oxide, IFN- γ , IL-17, and GM-CSF strongly correlated with control of intramacrophage infection with SCHU S4 (Golovliov et al., 2017). Altogether, although some markers of immunity have been identified, their relevance for protection is generally poorly understood and there is a need of data that more directly demonstrate correlation to protection.

Francisella tularensis clearly is able to infect many cell types *in vivo*, however, the cumulative evidence indicates that the macrophage is a key target for the infection (Elkins et al., 2007). The present human co-culture system was established with

the aim to model *in vivo* interactions between infecting bacteria, their target host monocytic cells, and effector lymphocytes, with the assumption that bacterial replication would be restricted due to the interactions as has been shown in a murine co-culture system (Elkins et al., 2011). The non-adherent PBMC from immune individuals were stimulated with *F. tularensis* antigens to selectively expand antigen-specific, memory-immune T cells, whereas PBMC from naïve individuals were stimulated to control for nonspecific innate immunity and bystander effects. Cells from immune individuals generally showed efficient control of bacterial replication and, interestingly, this effect was essentially the same, whether or not the LVS strain or the SCHU S4 strain was used. In contrast, cells from naïve individuals showed minimal or no control of the *F. tularensis* infection. In view of this background, we hypothesized that the memory T-cell-mediated inhibition of intracellular *F. tularensis* observed in the co-culture model would correlate to the occurrence of Th1 cytokines and, thus, the latter would serve as correlates for protection to tularemia. Indeed, several pieces of evidence indicate that this, in fact, was the case. Thus, the present findings that normalized levels of IFN- γ , TNF, and MIP-1 β and absolute levels of IFN- γ and MIP-1 β in LVS-infected cultures correlated with the degree of protection observed in the cultures are in agreement with the hypothesis and are therefore of potential relevance as protective correlates. In addition, we previously demonstrated that IFN- γ and MIP-1 β were expressed by CD4⁺CD45RO⁺ and CD8⁺CD45RO⁺ human T cells (Eneslätt et al., 2012), the same cytokines expressed by CD4 T cells were also identified in the present study as discriminating between naïve and immune

individuals. It should be noted that the variation in cytokine levels within the groups of vaccinated or naïve individuals was substantial and in some instances rendered marked differences between the groups non-significant. Presumably, this is a reflection of the normal variation of an out-bred population. Interestingly, the variation within the groups was less marked with regard to the control of infection.

To identify human immune correlates of tularemia, several obstacles must be avoided, one of which is the almost complete absence of detectable levels of circulating cytokines in tularemia patients. In a previous study, sera were obtained from patients at five time points up to 4 weeks after onset of tularemia, but of eight cytokines studied, only IFN- γ was detected and only transiently on day two (Andersson et al., 2006). Moreover, if immunospecific signatures are identified by *in vitro* studies, it cannot be determined if they simply are correlates, or also provide mechanistic information. Thus, it will be important to complement such findings with assays, such as the co-culture model, that will provide mechanistic insights, thus fulfilling the requirements of the Animal Rule. An additional strength of the co-culture model is that similar murine models exist and they have been used to identify transcriptional signatures that discriminate *Francisella* vaccines of different efficacies and thus could serve as potential correlates of protection (De Pascalis et al., 2012, 2014; Mahawar et al., 2013; Griffin et al., 2015; Golovliov et al., 2017).

There is a multitude of evidence for the critical role of IFN- γ for immunity to *F. tularensis* (Anthony et al., 1989; Surcel et al., 1991; Fortier et al., 1992; Conlan et al., 1994; Elkins et al., 1996; Sjöstedt et al., 1996; Cowley et al., 2010) and this was further corroborated by our present findings, since the *in vitro* growth control detected in the co-culture model correlated to secretion of IFN- γ . Effector mechanisms have been much studied for the ability of macrophages to control *F. tularensis* infection in the murine model (Cowley and Elkins, 2011). IFN- γ activation of macrophages effectively restricts the intracellular multiplication of *F. tularensis* and this is conferred by mechanisms involving both reactive nitrogen species (RNS), such as NO, and reactive oxygen species (ROS), whereas their roles are less evident with regard to virulent strains (Lindgren et al., 2004a,b, 2007; Santic et al., 2005; Bönquist et al., 2008; Edwards et al., 2010; Mahawar et al., 2013; Griffin et al., 2015). We recently demonstrated, however, that NO strongly correlated with control of both LVS and SCHU S4 infection in a mouse co-culture model (Golovliov et al., 2017). The IFN- γ -mediated control of the closely related bacterium *F. novicida* is strictly dependent on the IFN- γ -inducible guanylate-binding proteins GBP2 and GBP5 (Man et al., 2015; Meunier et al., 2015) and this is also true for the LVS strain, but not for the SCHU S4 strain (Wallet et al., 2017). Thus, evidence from animal models indicate that the control of highly virulent strains is distinct from that of attenuated *F. tularensis* strains and demonstrate that the use of such strains in the co-culture models is necessary to identify relevant correlates of immunity and protection.

The effective control effectuated in the present co-culture model based on the highly virulent SCHU S4 strain is important, since it implicates that it should be possible to achieve human

vaccine-mediated immune responses that effectively control natural infections evoked by other strains of the highly virulent subspecies *tularensis*. In this regard, it is noteworthy that a likely limitation of the widely used mouse model for evaluation of *F. tularensis* vaccines is the exquisite susceptibility of mice, since regardless of route of infection; the lethal dose of virulent *F. tularensis* strains is one bacterium (Lyons and Wu, 2007).

A limitation of the present study was the exclusive use of PBMCs, since it is unknown how well these types of cells mimic the phenotypes of tissue-localized immune cells. In the mouse model, there is ample evidence that vaccination induces qualitatively distinct immune responses in different organs, for example, in a mouse model of tuberculosis, vaccination with BCG and then an intradermal boost with a recombinant antigen led to strong splenic Th1 T cell responses, whereas an intranasal boost resulted in efficacious control of an aerosol challenge, but weak splenic responses (Forbes et al., 2008). Likewise, a study on *Francisella* demonstrated that a variant of LVS conferred better protection against an intraperitoneal challenge after intranasal than after intradermal vaccination (De Pascalis et al., 2014). The results suggest that there are organ-specific qualitative differences between immune cells and, therefore, the route of immunization may be important to achieve optimal protection and also that the source of cells used in the *in vitro* systems matters. However, in the case of humans, there are few alternative cell sources and peripheral blood cells are the only readily available cell type. Accordingly, there are several examples of similar *in vitro* co-culture systems based on the use of peripheral blood cells developed for the use of evaluating vaccine efficacy and defining protective correlates against tuberculosis (Hoft et al., 2002; Parra et al., 2009; Berry et al., 2010; Bloom et al., 2012).

We and others have implemented logistic modeling to investigate the multivariate relations between the different types of correlates that can be identified *in vivo* and using co-culture systems, such as secreted cytokines, cytokine gene expression, bacterial numbers, lymphocyte stimulation indices etc. (Eneslätt et al., 2011, 2012; Ryden et al., 2012; De Pascalis et al., 2014). Previously, we implemented it to build models based on human *ex vivo* data that with the smallest number of features and the highest accuracy predicted the immune status of a donor (Eneslätt et al., 2011). Based on mouse data, a publication combined results from the co-culture method and gene expression *in vivo* and combining the two are likely desirable since they should have complementary properties (De Pascalis et al., 2014). By performing similar types of analyses based on data from multiple sources, we envision that it will be feasible to make inter-tissue and interspecies comparisons. This type of modeling may help to identify individual candidate correlates so that their relevance can be investigated in each of the systems (Kurtz et al., 2013; Melillo et al., 2013) with the ultimate aim that they will represent a rational strategy to evaluate vaccines by monitoring the correlates post-immunization as a first step to achieve the requirements of the Animal Rule.

Today, all licensed vaccines are based on correlates of protection derived from measures of humoral immunity and since many of them are based on relatively technically

straightforward assays utilizing serum, they are convenient to use (Nguipdop Djomo et al., 2013). The rational development of vaccines that predominantly trigger CMI will require the implementation of similarly simple methods to gauge the correlates; however, all of this work is still in its infancy and the present work on human correlates for tularemia is a first step to identify such correlates.

AUTHOR CONTRIBUTIONS

KE, AS: Conceived and designed the experiments; KE, IG: Performed the experiments; KE, IG, PR, AS: Analyzed the data; KE, PR, AS: Wrote the paper.

REFERENCES

- Andersson, H., Hartmanova, B., Back, E., Eliasson, H., Landfors, M., Naslund, L., et al. (2006). Transcriptional profiling of the peripheral blood response during tularemia. *Genes Immun.* 7, 503–513. doi: 10.1038/sj.gene.6364321
- Anthony, L. S., Ghadirian, E., Nestel, F. P., and Kongshavn, P. A. (1989). The requirement for gamma interferon in resistance of mice to experimental tularemia. *Microb. Pathog.* 7, 421–428. doi: 10.1016/0882-4010(89)90022-3
- Berry, M. P., Graham, C. M., McNab, F. W., Xu, Z., Bloch, S. A., Oni, T., et al. (2010). An interferon-inducible neutrophil-driven blood transcriptional signature in human tuberculosis. *Nature* 466, 973–977. doi: 10.1038/nature09247
- Bloom, C. I., Graham, C. M., Berry, M. P., Wilkinson, K. A., Oni, T., Rozakeas, F., et al. (2012). Detectable changes in the blood transcriptome are present after two weeks of antituberculosis therapy. *PLoS ONE* 7:e46191. doi: 10.1371/journal.pone.0046191
- Bönquist, L., Lindgren, H., Golovliov, I., Guina, T., and Sjöstedt, A. (2008). MglA and Igl proteins contribute to the modulation of *Francisella tularensis* live vaccine strain-containing phagosomes in murine macrophages. *Infect. Immun.* 76, 3502–3510. doi: 10.1128/IAI.00226-08
- Burke, D. S. (1977). Immunization against tularemia: analysis of the effectiveness of live *Francisella tularensis* vaccine in prevention of laboratory-acquired tularemia. *J. Infect. Dis.* 135, 55–60. doi: 10.1093/infdis/135.1.55
- Colditz, G. A., Brewer, T. F., Berkey, C. S., Wilson, M. E., Burdick, E., Fineberg, H. V., et al. (1994). Efficacy of BCG vaccine in the prevention of tuberculosis. Meta-analysis of the published literature. *JAMA* 271, 698–702. doi: 10.1001/jama.1994.03510330076038
- Collazo, C. M., Meierovics, A. I., De Pascalis, R., Wu, T. H., Lyons, C. R., and Elkins, K. L. (2009). T cells from lungs and livers of *Francisella tularensis*-immune mice control the growth of intracellular bacteria. *Infect. Immun.* 77, 2010–2021. doi: 10.1128/IAI.01322-08
- Conlan, J. W. (2011). Tularemia vaccines: recent developments and remaining hurdles. *Future Microbiol.* 6, 391–405. doi: 10.2217/fmb.11.22
- Conlan, J. W., Sjöstedt, A., and North, R. J. (1994). CD4+ and CD8+ T-cell-dependent and -independent host defense mechanisms can operate to control and resolve primary and secondary *Francisella tularensis* LVS infection in mice. *Infect. Immun.* 62, 5603–5607.
- Cowley, S. C., and Elkins, K. L. (2003). Multiple T cell subsets control *Francisella tularensis* LVS intracellular growth without stimulation through macrophage interferon gamma receptors. *J. Exp. Med.* 198, 379–389. doi: 10.1084/jem.20030687
- Cowley, S. C., Hamilton, E., Frelinger, J. A., Su, J., Forman, J., and Elkins, K. L. (2005). CD4⁺CD8⁺ T cells control intracellular bacterial infections both *in vitro* and *in vivo*. *J. Exp. Med.* 202, 309–319. doi: 10.1084/jem.20050569
- Cowley, S. C., Meierovics, A. I., Frelinger, J. A., Iwakura, Y., and Elkins, K. L. (2010). Lung CD4⁺CD8⁺ double-negative T cells are prominent producers of IL-17A and IFN- γ during primary respiratory murine infection with *Francisella tularensis* live vaccine strain. *J. Immunol.* 184, 5791–5801. doi: 10.4049/jimmunol.1000362

FUNDING

Grant support was obtained from the Swedish Medical Research Council (K2012-3469 and K2013-8621), Västerbottens läns landsting (Spjutspetsmedel, VLL-582571, Centrala ALF medel, VLL-463691 and VLL-733231), and the Medical Faculty, Umeå University, Umeå, Sweden. The work was performed in part at the Umeå Centre for Microbial Research (UCMR).

ACKNOWLEDGMENTS

Some of the results of the study were presented at the eight International Meeting on Tularemia, Opatija, Croatia, 2015.

- Cowley, S. C., Sedgwick, J. D., and Elkins, K. L. (2007). Differential requirements by CD4⁺ and CD8⁺ T cells for soluble and membrane TNF in control of *Francisella tularensis* live vaccine strain intramacrophage growth. *J. Immunol.* 179, 7709–7719. doi: 10.4049/jimmunol.179.11.7709
- Cowley, S., and Elkins, K. (2011). Immunity to *Francisella*. *Front. Microbiol.* 2:26. doi: 10.3389/fmicb.2011.00026
- De Pascalis, R., Chou, A. Y., Bosio, C. M., Huang, C. Y., Follmann, D. A., and Elkins, K. L. (2012). Development of functional and molecular correlates of vaccine-induced protection for a model intracellular pathogen, *Francisella tularensis* LVS. *PLoS Pathog.* 8:e1002494. doi: 10.1371/journal.ppat.1002494
- De Pascalis, R., Chou, A. Y., Ryden, P., Kennett, N. J., Sjöstedt, A., and Elkins, K. L. (2014). Models derived from *in vitro* analyses of spleen, liver, and lung leukocyte functions predict vaccine efficacy against the *Francisella tularensis* Live Vaccine Strain (LVS). *MBio* 5:e00936. doi: 10.1128/mBio.00936-13
- De Pascalis, R., Taylor, B. C., and Elkins, K. L. (2008). Diverse myeloid and lymphoid cell subpopulations produce gamma interferon during early innate immune responses to *Francisella tularensis* live vaccine strain. *Infect. Immun.* 76, 4311–4321. doi: 10.1128/IAI.00514-08
- Derrick, S. C., Yabe, I. M., Yang, A., and Morris, S. L. (2011). Vaccine-induced anti-tuberculosis protective immunity in mice correlates with the magnitude and quality of multifunctional CD4 T cells. *Vaccine* 29, 2902–2909. doi: 10.1016/j.vaccine.2011.02.010
- Edwards, J. A., Rockx-Brouwer, D., Nair, V., and Celli, J. (2010). Restricted cytosolic growth of *Francisella tularensis* subsp. *tularensis* by IFN- γ activation of macrophages. *Microbiology* 156(Pt 2), 327–339. doi: 10.1099/mic.0.031716-0
- Elkins, K. L., Cowley, S. C., and Bosio, C. M. (2007). Innate and adaptive immunity to *Francisella*. *Ann. N. Y. Acad. Sci.* 1105, 284–324. doi: 10.1196/annals.1409.014
- Elkins, K. L., Cowley, S. C., and Conlan, J. W. (2011). Measurement of macrophage-mediated killing of intracellular bacteria, including *Francisella* and mycobacteria. *Curr. Protoc. Immunol.* Chapter 14:Unit14.25. doi: 10.1002/0471142735.im1425s93
- Elkins, K. L., Rhinehart-Jones, T. R., Culkin, S. J., Yee, D., and Winegar, R. K. (1996). Minimal requirements for murine resistance to infection with *Francisella tularensis* LVS. *Infect. Immun.* 64, 3288–3293.
- Eneslätt, K., Normark, M., Björk, R., Rietz, C., Zingmark, C., Wolfrain, L. A., et al. (2012). Signatures of T cells as correlates of immunity to *Francisella tularensis*. *PLoS ONE* 7:e32367. doi: 10.1371/journal.pone.0032367
- Eneslätt, K., Rietz, C., Rydén, P., Stöven, S., House, R. V., Wolfrain, L. A., et al. (2011). Persistence of cell-mediated immunity three decades after vaccination with the live vaccine strain of *Francisella tularensis*. *Eur. J. Immunol.* 41, 974–980. doi: 10.1002/eji.201040923
- Ericsson, M., Sandstrom, G., Sjöstedt, A., and Tärnvik, A. (1994). Persistence of cell-mediated immunity and decline of humoral immunity to the intracellular bacterium *Francisella tularensis* 25 years after natural infection. *J. Infect. Dis.* 170, 110–114. doi: 10.1093/infdis/170.1.110
- Forbes, E. K., Sander, C., Ronan, E. O., McShane, H., Hill, A. V., Beverley, P. C., et al. (2008). Multifunctional, high-level cytokine-producing Th1 cells in the lung, but not spleen, correlate with protection against

- Mycobacterium tuberculosis* aerosol challenge in mice. *J. Immunol.* 181, 4955–4964. doi: 10.4049/jimmunol.181.7.4955
- Fortier, A. H., Polsinelli, T., Green, S. J., and Nacy, C. A. (1992). Activation of macrophages for destruction of *Francisella tularensis*: identification of cytokines, effector cells, and effector molecules. *Infect. Immun.* 60, 817–825.
- Golovliov, I., Lindgren, H., Eneslätt, K., Conlan, W., Mosnier, A., Henry, T., et al. (2017). An *in vitro* co-culture mouse model demonstrates efficient vaccine-mediated control of *Francisella tularensis* SCHU S4 and identifies nitric oxide as a predictor of efficacy. *Front. Cell. Infect. Microbiol.* 6:152. doi: 10.3389/fcimb.2016.00152
- Griffin, A. J., Crane, D. D., Wehrly, T. D., and Bosio, C. M. (2015). Successful protection against tularemia in C57BL/6 mice is correlated with expansion of *Francisella tularensis*-specific effector T cells. *Clin. Vaccine Immunol.* 22, 119–128. doi: 10.1128/CVI.00648-14
- Hoft, D. F., Worku, S., Kampmann, B., Whalen, C. C., Ellner, J. J., Hirsch, C. S., et al. (2002). Investigation of the relationships between immune-mediated inhibition of mycobacterial growth and other potential surrogate markers of protective *Mycobacterium tuberculosis* immunity. *J. Infect. Dis.* 186, 1448–1457. doi: 10.1086/344359
- Kagina, B. M., Abel, B., Scriba, T. J., Hughes, E. J., Keyser, A., Soares, A., et al. (2010). Specific T cell frequency and cytokine expression profile do not correlate with protection against tuberculosis after bacillus Calmette-Guérin vaccination of newborns. *Am. J. Respir. Crit. Care Med.* 182, 1073–1079. doi: 10.1164/rccm.201003-0334OC
- Karttunen, R., Surcel, H. M., Andersson, G., Ekre, H. P., and Herva, E. (1991). *Francisella tularensis*-induced *in vitro* gamma interferon, tumor necrosis factor alpha, and interleukin 2 responses appear within 2 weeks of tularemia vaccination in human beings. *J. Clin. Microbiol.* 29, 753–756.
- Kurtz, S. L., Foreman, O., Bosio, C. M., Anver, M. R., and Elkins, K. L. (2013). Interleukin-6 is essential for primary resistance to *Francisella tularensis* live vaccine strain infection. *Infect. Immun.* 81, 585–597. doi: 10.1128/IAI.01249-12
- Leiby, D. A., Fortier, A. H., Crawford, R. M., Schreiber, R. D., and Nacy, C. A. (1992). *In vivo* modulation of the murine immune response to *Francisella tularensis* LVS by administration of anticytokine antibodies. *Infect. Immun.* 60, 84–89.
- Lindgren, H., Golovliov, I., Baranov, V., Ernst, R. K., Telepnev, M., and Sjöstedt, A. (2004a). Factors affecting the escape of *Francisella tularensis* from the phagolysosome. *J. Med. Microbiol.* 53, 953–958. doi: 10.1099/jmm.0.45685-0
- Lindgren, H., Shen, H., Zingmark, C., Golovliov, I., Conlan, W., and Sjöstedt, A. (2007). Resistance of *Francisella tularensis* strains against reactive nitrogen and oxygen species with special reference to the role of KatG. *Infect. Immun.* 75, 1303–1309. doi: 10.1128/IAI.01717-06
- Lindgren, H., Stenmark, S., Chen, W., Tärnvik, A., and Sjöstedt, A. (2004b). Distinct roles of reactive nitrogen and oxygen species to control infection with the facultative intracellular bacterium *Francisella tularensis*. *Infect. Immun.* 72, 7172–7182. doi: 10.1128/IAI.72.12.7172-7182.2004
- Lyons, C. R., and Wu, T. H. (2007). Animal models of *Francisella tularensis* infection. *Ann. N. Y. Acad. Sci.* 1105, 238–265. doi: 10.1196/annals.1409.003
- Mahawar, M., Rabadi, S. M., Banik, S., Catlett, S. V., Metzger, D. W., Malik, M., et al. (2013). Identification of a live attenuated vaccine candidate for tularemia prophylaxis. *PLoS ONE* 8:e61539. doi: 10.1371/journal.pone.0061539
- Man, S. M., Karki, R., Malireddi, R. K., Neale, G., Vogel, P., Yamamoto, M., et al. (2015). The transcription factor IRF1 and guanylate-binding proteins target activation of the AIM2 inflammasome by *Francisella* infection. *Nat. Immunol.* 16, 467–475. doi: 10.1038/ni.3118
- Melillo, A. A., Foreman, O., Bosio, C. M., and Elkins, K. L. (2014). T-bet regulates immunity to *Francisella tularensis* live vaccine strain infection, particularly in lungs. *Infect. Immun.* 82, 1477–1490. doi: 10.1128/IAI.01545-13
- Melillo, A. A., Foreman, O., and Elkins, K. L. (2013). IL-12Rbeta2 is critical for survival of primary *Francisella tularensis* LVS infection. *J. Leukoc. Biol.* 93, 657–667. doi: 10.1189/jlb.1012485
- Meunier, E., Wallet, P., Dreier, R. F., Costanzo, S., Anton, L., Ruhl, S., et al. (2015). Guanylate-binding proteins promote activation of the AIM2 inflammasome during infection with *Francisella novicida*. *Nat. Immunol.* 16, 476–484. doi: 10.1038/ni.3119
- Nguipodp Djomo, P., Thomas, S., and Fine, P. (2013). *Correlates of Vaccine-Induced Protection: Methods and Implications*. Available online at: http://apps.who.int/iris/bitstream/10665/184288/1/WHO_IVB_13.01_eng.pdf
- Paranavitana, C., Zelazowska, E., DaSilva, L., Pittman, P. R., and Nikolich, M. (2010). Th17 cytokines in recall responses against *Francisella tularensis* in humans. *J. Interferon Cytokine Res.* 30, 471–476. doi: 10.1089/jir.2009.0108
- Parra, M., Yang, A. L., Lim, J., Kolibab, K., Derrick, S., Cadieux, N., et al. (2009). Development of a murine mycobacterial growth inhibition assay for evaluating vaccines against *Mycobacterium tuberculosis*. *Clin. Vaccine Immunol.* 16, 1025–1032. doi: 10.1128/CVI.00067-09
- Ryden, P., Twine, S., Shen, H., Harris, G., Chen, W., Sjöstedt, A., et al. (2012). Correlates of protection following vaccination of mice with gene deletion mutants of *Francisella tularensis* subspecies *tularensis* strain, SCHU S4 that elicit varying degrees of immunity to systemic and respiratory challenge with wild-type bacteria. *Mol. Immunol.* 54, 58–67. doi: 10.1016/j.molimm.2012.10.043
- Santic, M., Molmeret, M., and Abu Kwaik, Y. (2005). Modulation of biogenesis of the *Francisella tularensis* subsp. *novicida*-containing phagosome in quiescent human macrophages and its maturation into a phagolysosome upon activation by IFN- γ . *Cell. Microbiol.* 7, 957–967. doi: 10.1111/j.1462-5822.2005.00529.x
- Sauerwein, R. W., Roestenberg, M., and Moorthy, V. S. (2011). Experimental human challenge infections can accelerate clinical malaria vaccine development. *Nat. Rev. Immunol.* 11, 57–64. doi: 10.1038/nri2902
- Shen, H., Harris, G., Chen, W., Sjöstedt, A., Ryden, P., and Conlan, W. (2010). Molecular immune responses to aerosol challenge with *Francisella tularensis* in mice inoculated with live vaccine candidates of varying efficacy. *PLoS ONE* 5:e13349. doi: 10.1371/journal.pone.0013349
- Shirley, D. A., and McArthur, M. A. (2011). The utility of human challenge studies in vaccine development: lessons learned from cholera. *Vaccine* 2011, 3–13. doi: 10.2147/VDT.S23634
- Sjöstedt, A. (2007). Tularemia: history, epidemiology, pathogen physiology, and clinical manifestations. *Ann. N. Y. Acad. Sci.* 1105, 1–29. doi: 10.1196/annals.1409.009
- Sjöstedt, A., Eriksson, M., Sandström, G., and Tärnvik, A. (1992). Various membrane proteins of *Francisella tularensis* induce interferon-gamma production in both CD4+ and CD8+ T cells of primed humans. *Immunology* 76, 584–592.
- Sjöstedt, A., North, R. J., and Conlan, J. W. (1996). The requirement of tumour necrosis factor-alpha and interferon-gamma for the expression of protective immunity to secondary murine tularemia depends on the size of the challenge inoculum. *Microbiology* 142, 1369–1374. doi: 10.1099/13500872-142-6-1369
- Snoy, P. J. (2010). Establishing efficacy of human products using animals: the US food and drug administration's "animal rule." *Vet. Pathol.* 47, 774–778. doi: 10.1177/0300985810372506
- Surcel, H. M., Syrjala, H., Karttunen, R., Tapaninaho, S., and Herva, E. (1991). Development of *Francisella tularensis* antigen responses measured as T-lymphocyte proliferation and cytokine production (tumor necrosis factor β , γ interferon, and interleukin-2 and -4) during human tularemia. *Infect. Immun.* 59, 1948–1953.
- Tärnvik, A. (1989). Nature of protective immunity to *Francisella tularensis*. *Rev. Infect. Dis.* 11, 440–451. doi: 10.1093/clinids/11.3.440
- Tärnvik, A., Löfgren, M. L., Löfgren, S., Sandström, G., and Wolf-Watz, H. (1985). Long-lasting cell-mediated immunity induced by a live *Francisella tularensis* vaccine. *J. Clin. Microbiol.* 22, 527–530.
- Wallet, P., Benaoudia, S., Mosnier, A., Lagrange, B., Martin, A., Lindgren, H., et al. (2017). IFN- γ extends the immune functions of guanylate binding proteins to inflammasome-independent antibacterial activities during *Francisella novicida* infection. *PLoS Pathog.* 13:e1006630. doi: 10.1371/journal.ppat.1006630

Conflict of Interest Statement: The authors declare that the research was conducted in the absence of any commercial or financial relationships that could be construed as a potential conflict of interest.

Copyright © 2018 Eneslätt, Golovliov, Ryden and Sjöstedt. This is an open-access article distributed under the terms of the Creative Commons Attribution License (CC BY). The use, distribution or reproduction in other forums is permitted, provided the original author(s) and the copyright owner are credited and that the original publication in this journal is cited, in accordance with accepted academic practice. No use, distribution or reproduction is permitted which does not comply with these terms.



Tularemia in Germany—A Re-emerging Zoonosis

Mirko Faber¹, Klaus Heuner^{2,3}, Daniela Jacob³ and Roland Grunow^{3*}

¹ Gastrointestinal Infections, Zoonoses and Tropical Infections (Division 35), Department for Infectious Disease Epidemiology, Robert Koch Institute, Berlin, Germany, ² Working Group, Cellular Interactions of Bacterial Pathogens, Centre for Biological Threats and Special Pathogens, Division 2 (ZBS 2), Robert Koch Institute, Berlin, Germany, ³ Highly Pathogenic Microorganisms, Centre for Biological Threats and Special Pathogens, Division 2 (ZBS 2), Robert Koch Institute, Berlin, Germany

Tularemia, also known as “rabbit fever,” is a zoonosis caused by the facultative intracellular, gram-negative bacterium *Francisella tularensis*. Infection occurs through contact with infected animals (often hares), arthropod vectors (such as ticks or deer flies), inhalation of contaminated dust or through contaminated food and water. In this review, we would like to provide an overview of the current epidemiological situation in Germany using published studies and case reports, an analysis of recent surveillance data and our own experience from the laboratory diagnostics, and investigation of cases. While in Germany tularemia is a rarely reported disease, there is evidence of recent re-emergence. We also describe some peculiarities that were observed in Germany, such as a broad genetic diversity, and a recently discovered new genus of *Francisella* and protracted or severe clinical courses of infections with the subspecies *holarctica*. Because tularemia is a zoonosis, we also touch upon the situation in the animal reservoir and one-health aspects of this disease. Apparently, many pieces of the puzzle need to be found and put into place before the complex interaction between wildlife, the environment and humans are fully understood. Funding for investigations into rare diseases is scarce. Therefore, combining efforts in several countries in the framework of international projects may be necessary to advance further our understanding of this serious but also scientifically interesting disease.

Keywords: *Francisella tularensis*, tularemia, epidemiology, case report, one health, Germany, ecology, veterinary medicine

OPEN ACCESS

Edited by:

Marina Santic,
University of Rijeka, Croatia

Reviewed by:

John S. Gunn,
The Ohio State University,
United States
Lee-Ann H. Allen,
University of Iowa, United States

*Correspondence:

Roland Grunow
grunowr@rki.de

Received: 24 November 2017

Accepted: 31 January 2018

Published: 16 February 2018

Citation:

Faber M, Heuner K, Jacob D and
Grunow R (2018) Tularemia in
Germany—A Re-emerging Zoonosis.
Front. Cell. Infect. Microbiol. 8:40.
doi: 10.3389/fcimb.2018.00040

INTRODUCTION

Germany represents a low incidence region with regard to tularemia in humans caused by *Francisella tularensis*. We highlight some peculiarities of the pathogen as observed in Germany and describe the epidemiology, outbreaks and possible sources of infection, different clinical courses and aspects of diagnosis as well as underline the one-health aspect of tularemia considering this disease relevant for human, animal, and environmental health. Tularemia in Germany is described as an example for many other European countries with a similar epidemiological situation, and parallels might be helpful to initiate further research on national and international levels.

THE PATHOGEN

Tularemia is caused by infection with the facultative intracellular, gram-negative bacterium *Francisella tularensis* (Ellis et al., 2002; Sjöstedt, 2011). The most clinically relevant subspecies are *F. tularensis* ssp. *holarctica* distributed over the whole northern hemisphere and the more virulent ssp. *tularensis* which is almost exclusively found in North America and associated with lethal pulmonary infections (Ellis et al., 2002). Further species or subspecies of the genus *Francisella* have a low or unknown pathogenicity for humans (e.g., *F. tularensis* ssp. *novicida* and *F. tularensis* ssp. *mediasiatica* found in North America and Asia, respectively) (Ellis et al., 2002; Kingry and Petersen, 2014; Challacombe et al., 2017). Only recently, the presence of *F. tularensis* ssp. *holarctica* has been confirmed in the southern hemisphere (Eden et al., 2017).

In Germany, *F. tularensis* ssp. *holarctica* is the only subspecies known to cause disease in patients and animals. Only one other *Francisella* species, *Francisella* sp. isolate W12-1067 isolated from a water reservoir of a cooling tower of a hospital, has been found in Germany (Rydzewski et al., 2014). This isolate is ~89% identical to the chromosomal DNA of the published strain *F. guangzhouensis*, indicating that there may be additional, yet unidentified *Francisella* species present in Germany. Recently, a Chinese group proposed a strain related to *Francisella* sp. strain W12-1067 to represent a new genus called *Allofrancisella* (Qu et al., 2016). However, the identification of new *Francisella* species (Challacombe et al., 2017) and additional further research will reveal whether the proposal of a new genus can be confirmed and whether it is pathogenic for humans.

Studies on bacterial isolates from wild animals and humans revealed an unexpectedly high genetic diversity of *F. tularensis* ssp. *holarctica* in Germany (Gehring et al., 2013; Müller et al., 2013; Schulze et al., 2016). In a recent study the phylogenetic analysis of isolates from wild animals from the Berlin/Brandenburg region revealed three new subclades within the phylogenetic tree, subclade B.71 from a raccoon dog [*Nyctereutes procyonoides*], subclade B.74 from a red fox [*Vulpes vulpes*] and subclade B.75 from an Eurasian beaver [*Castor fiber albidus*] (Schulze et al., 2016). The genetic diversity is not only of academic interest: In the phylogenetic analysis, erythromycin-susceptible *F. tularensis* ssp. *holarctica* cluster with biovar I and erythromycin-resistant with biovar II. While biovar I is mainly found in Western Europe, biovar II occurs in Northern and Eastern Europe (Kudelina, 1973; Ellis et al., 2002; Svensson et al., 2009a; Vogler et al., 2009a,b; Karlsson et al., 2016). In a recent study, 94 isolates were susceptible to erythromycin, which defines biovar I (genotypes B.4 and B.6), while 34 were resistant (biovar II; genotype B.12). Both *Francisella* biovars are present in Germany (Tomaso et al., 2017). It is still under debate whether strains of genotype B.6 may have a higher pathogenic potential than strains belonging to the B.12 genotype (Gyuranecz et al., 2010; Origgi and Pilo, 2016; Hestvik et al., 2017; Kreizinger et al., 2017). There are further publications describing the phylogeographic pattern of *Francisella* in Europe (Vogler et al., 2009a; Gyuranecz et al., 2012; Karlsson et al., 2013; Origgi et al., 2014; Thelaus et al., 2014; Dwibedi et al., 2016).

The high genetic diversity observed in *F. tularensis* isolates suggests that additional *Francisella* pheno genotypes and remain to be discovered. Germany might represent a “melting pot,” a region where, within the postulated spread of the pathogen from east to west, strains are mixed, re-assorted and give rise to further variants with still unknown characteristics (Jusatz, 1952a, 1961; Chanturia et al., 2011; Dwibedi et al., 2016). Phylogenetic studies also revealed a spread of tularemia from Scandinavia to the south of Europe (Karlsson et al., 2013; Dwibedi et al., 2016). More research on phylogenetic relations and pathogenicity of specific isolates is required for a better understanding of how genetics correlates with environmental habitats, reservoirs, vectors, and transmission routes.

OCCURRENCE OF TULAREMIA IN GERMANY—PAST AND PRESENT

Historical publications describe the spread of tularemia from Eastern Europe to Western Europe, crossing the German geographical territory since the nineteenth century (Jusatz, 1952b). The cited early descriptions of tularemia assumed that the disease was already known under names such as “epidemic lymphadenitis,” “Plague-like lymphadenitis,” and “Influenza-like disease of water hole hunters.” A verification of such historic cases of lymphadenitis as tularemia would clarify the early occurrence and distribution of the disease in Europe.

More information is available for the time following the Second World War: a retrospective study revealed 687 cases reported from 1949 to 2005 (Grunow and Priebe, 2007), 515 of which were observed until 1959. This was attributed to the socio-economic situation after the war. The incidence of tularemia is known to increase during or after armed conflicts due to a decline in hygiene, housing conditions and food safety. This was also observed e.g., in Kosovo after the armed conflicts when two outbreaks of tularemia occurred in 2000–2002 with more than 500 confirmed cases in a region that had previously been likely to be non-endemic (Grunow et al., 2012). The suspected reason for these outbreaks was a strong increase in the population of small rodents due to crops left on the field. Beginning with the cold season, infected animals came in close contact with human dwellings and contaminated accessible food storages and unprotected drinking water sources. From 1960 to 2004, between 9 and 34 cases per 5-year intervals were reported in Germany, indicating a very low incidence or poor reporting activity despite the fact that tularemia was a notifiable disease in both East and West Germany during this period (Grunow and Priebe, 2007).

Today, tularemia is a notifiable disease in Germany according to the infection protection act of 2001. For surveillance purposes, a case is defined as a person with symptoms and laboratory confirmation of a recent *F. tularensis* infection, indicated by at least one of the four following methods: Antigen detection by e.g., enzyme immune assays or immunofluorescence assays; isolation of the living pathogen by cultivation; detection of specific nucleic acids, e.g., by polymerase chain reactions; or detection of specific antibodies with an increase of the titer in paired serum samples taken with a difference in time along the

clinical course or one clearly high titer of antibodies (http://www.rki.de/DE/Content/Infekt/IfSG/Falldefinition/Downloads/Falldefinitionen_des_RKI.pdf?__blob=publicationFile; <https://survstat.rki.de/default.aspx>).

Between 1 January 2002 and 31 December 2016, $n = 257$ cases of tularemia were notified in Germany (**Figure 1**), corresponding to a mean yearly incidence of 0.03 cases per 100,000 population (range: 0.00–0.05). In patients presenting with lymphadenitis and fever, tularemia is rarely considered as a differential diagnosis by clinicians and diagnostic laboratories, therefore it can be assumed that tularemia is subject to significant underdiagnosis and underreporting in Germany. Of the 257 cases reported, 217 were sporadic cases and 40 were part of case clusters. Age of the patients ranged from 1 to 87 years (mean: 46) and the male to female ratio was 2.06. While a median of three annual cases were notified from 2002 through 2006, a continuous increase with a maximum of 41 cases in 2016 was observed thereafter (**Figure 1**). It is unclear whether this increase is due to an actual increase in infection pressure and clinical cases or whether it is the result of increased awareness and more frequent testing. However, a relatively stable proportion of hospitalized cases suggests that the increase is not the result of a change in sensitivity of the surveillance system.

Tularemia is a clearly seasonal disease in Germany with most patients (68%) reporting symptom onset from July through November (**Figure 2**) when reservoir animal populations are peaking and frequent outdoor activities (such as hunting, farming, fishing, hiking etc.) facilitate contact between wildlife and humans. This is in concordance with the seasonal occurrence of tularemia cases in Europe (Hestvik et al., 2015). Imported cases only account for a small fraction of the total case load (28 of 227, 12.5%), peaking after the summer holiday season in August and after Christmas/New Year. It is remarkable that cases until and after 2001 were reported from almost all Federal States of Germany. Between 2002 and 2016 the highest mean annual incidences were recorded in parts of Saxony-Anhalt, Baden-Württemberg and Brandenburg (**Figure 3**).

Although there is large variability in the regional incidence of tularemia, long-term surveillance data indicate that the pathogen can be found all-over Germany. The variation in the number of reported cases from the different Federal States could be explained by (i) variations in actual disease incidence as a result of varying exposure risks or infection pressure or (ii) variations in diagnostic consideration of tularemia and reporting activity due to differences in awareness of health care workers for the disease. Indeed, serological studies indicate that most infections are not diagnosed and reported in Germany (Al Dahouk et al., 2003; Jenzora et al., 2008; Kaysser et al., 2008; Splettstoesser et al., 2009; Gehringer et al., 2013; Kuehn et al., 2013; Müller et al., 2013; Otto et al., 2014). Two cross-sectional studies have shown a relatively high seroprevalence; one population-representative study from 2004 with 6,617 sera and one study conducted in a small town in Baden-Württemberg in 2009 with 2,416 sera revealed positive results in 0.23% and 2.3% of the sera, respectively (Porsch-Ozcürümez et al., 2004; Splettstoesser et al., 2009). Serological studies in hunters as a putative population at high risk have shown a seroprevalence of up to 1.7% (Jenzora et al., 2008).

It can be concluded that *Francisella tularensis* has been endemic for centuries on the territory today known as Germany and has a wide-spread distribution among wildlife. In humans tularemia probably represents a re-emerging disease with a high proportion of undiagnosed cases. Better awareness and knowledge of the disease among health care personnel is required for a timely diagnosis and treatment of cases. More research is required for a better understanding of the burden of disease and public health impact of tularemia in Germany.

OUTBREAKS IN HUMANS AND SOURCES OF INFECTIONS

In Germany, outbreaks or clusters of tularemia occur rarely and are defined as at least two cases with an epidemiological link (such as a common source of exposure).

Between 2002 and 2016, 10 case clusters were reported. Except for two with a connection to situations in other countries and one large outbreak caused by grape must (unintentional contamination), the remaining eight clusters consisted of 2–10 cases and were associated with contact to wild animals, five of them in the context of hunting activities (Straube and Hess, 1986; Hofstetter et al., 2006; Schätzle and Schwenk, 2008; Hauri et al., 2010; Schubert et al., 2011; Kohlmann et al., 2014; Boone et al., 2015; Borde et al., 2017).

Five of the above clusters were reported in connection with consumption of or contact to infected hares. The largest one occurred in 2005 with a total of 10 affected hunters participating in a hare hunting event (Hofstetter et al., 2006; Hauri et al., 2010). For cases that were not part of clusters, tick bites have been suspected as the source of infection besides contact to hares (Lübbert et al., 2009; Boone et al., 2015; Borde et al., 2017). Indeed, prevalence studies in ticks in the south-west of Germany revealed presence of *Francisella* in 8% of 916 investigated *Ixodes ricinus* while *Dermacentor* species clustered with *Francisella* endosymbionts (Gehringer et al., 2013).

TULAREMIA IN ANIMALS

Tularemia case clusters in humans are often preceded by outbreaks in wildlife and detection of the pathogen in captured animals (Mörner, 1992; Splettstoesser et al., 2009); therefore much effort has been taken to describe the distribution of the pathogen in relevant reservoir animals. A serological study in various wildlife species in Brandenburg (the state surrounding the German capital Berlin), revealed a total of 101/1,353 positive sera (7.5%) in foxes (*Vulpes vulpes*), raccoon dogs (*Nyctereutes procyonoides*) and wild boar (*Sus scrofa*) (Kuehn et al., 2013). There is also serological evidence for *Francisella* infections in zoo animals: One seroconversion was documented in a hippo (*Hippopotamus amphibius*) between 2003 and 2004 (Kuehn et al., 2013). Other serological and bacteriological studies confirmed a high sero- and pathogen prevalence in wildlife including hares in Germany (Al Dahouk et al., 2003; Müller et al., 2013; Otto et al., 2014).

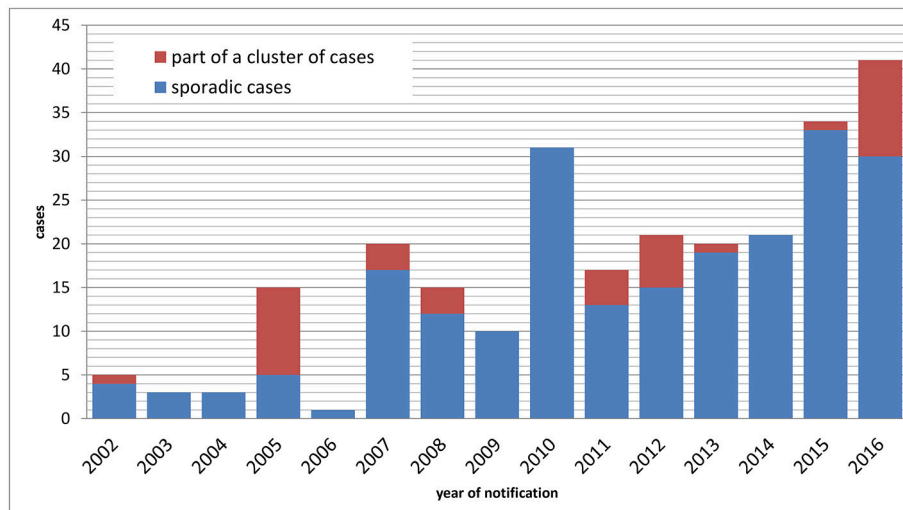


FIGURE 1 | Notified cases of tularemia (sporadic and non-sporadic cases) by year of notification, Germany, 2002–2016.

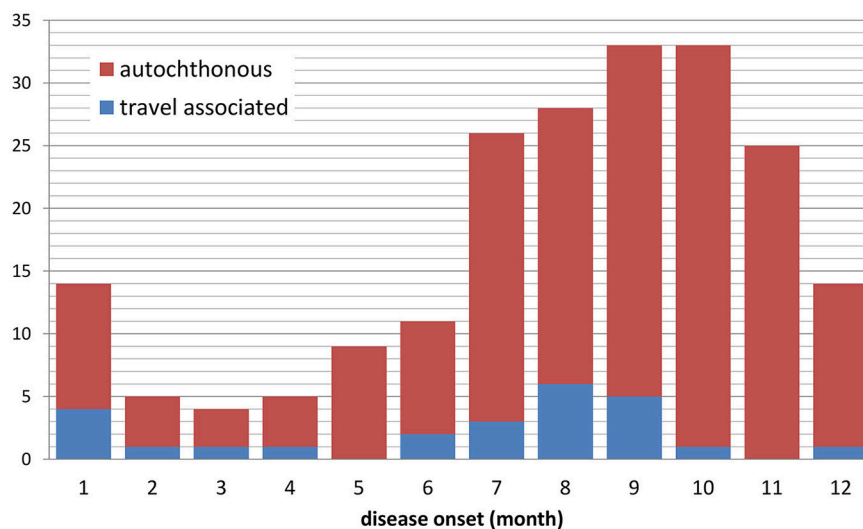


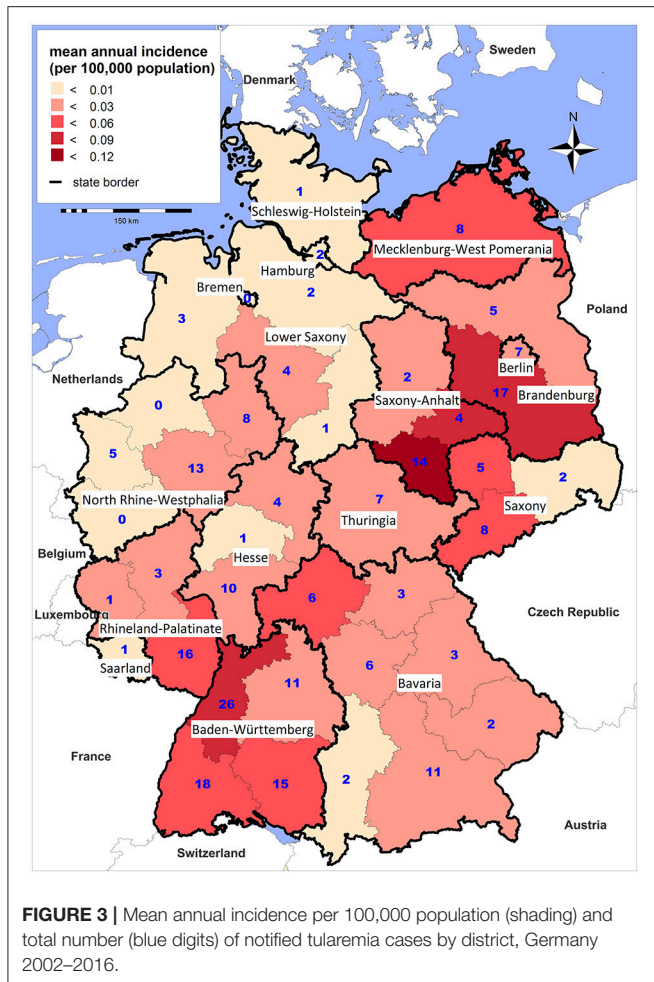
FIGURE 2 | Notified cases of tularemia with and without travel history by month of disease onset, Germany, 2002–2016 ($n = 207$ with available information).

In a recent study, 3 out of 29 animals (10%) examined were *F. tularensis* positive which was in good agreement with the results mentioned above, and the presence of *F. tularensis* in raccoon dogs and red foxes could be confirmed (Schulze et al., 2016). Thus *F. tularensis* was isolated from animal species not previously reported as natural hosts in Germany. In the case of a beaver deceased from tularemia in Brandenburg, it could be confirmed that animals with high bacterial load may act as local amplifiers in Germany (Otto et al., 2015; Schulze et al., 2016). qPCR analyses indicated that *F. tularensis* persisted in the aquatic environment during one climatic season, but apparently no longer (Schulze et al., 2016).

In 2004, an outbreak of tularemia occurred in semi-free-living common marmosets (*Callithrix jacchus*) (Mätz-Rensing et al., 2007). *F. tularensis* was identified as

the cause of a sudden die-off of 5 out of 62 animals. As all animals had been born at the facility, the outbreak was autochthonous meaning the source of infection was at the place where it occurred (Splettsjoesser et al., 2007). A subsequent study in rodents in central Germany identified bank voles (*Myodes glareolus*), water voles (*Arvicola terrestris*), field voles (*Microtus agrestis*), common voles (*Microtus arvalis*) and yellow-necked field mice (*Apodemus flavicollis*) as potential sources of *Francisella* infections (Kaysser et al., 2008; Gyuranecz et al., 2011; Gehringer et al., 2013). Classically known, but also previously rather neglected animals like foxes could be an indicator for the prevalence of the pathogen (Kuehn et al., 2013).

The conclusion from these observations is that *Francisella* is widely present in the environment in Germany and that a wide range of wild animals (such as hares and wild boars), but also



vectors (e.g., ticks as illustrated in the previous chapter) can be sources of infections in humans.

More research is needed to understand better the circumstances and mechanisms of a successful transmission of the pathogen from animal to animal and to humans. The main animal reservoir allowing the persistence and survival of *Francisella* in the wild is still unknown. Further research on this question is required. It would also be important to study changes in the ecosystems including populations of rodents and lagomorphs to understand better the impact of such changes on the prevalence of the pathogens in the wild and the occurrence of tularemia in humans.

DIAGNOSES AND CLINICAL ASPECTS OF TULAREMIA

F. tularensis ssp. *holarctica* causes usually a relatively mild form of tularemia in humans. The clinical manifestation of tularemia depends on the entry route of the bacterium into the organism and is defined by ulceroglandular or glandular form, oropharyngeal form, ocularglandular form and respiratory

form (WHO Guidelines on Tularaemia, 2007)¹. The primary common symptoms are fever and enlarged lymph nodes. The mean incubation time is 3–5 days with a range of 1–21 days. In the case of complications like suppuration, pneumonia and meningitis convalescence is often extended.

Among notified cases in Germany, the most frequent clinical presentations were glandular and ulceroglandular tularemia (Table 1). 7% of the patients presented with mixed forms and 14% could not be assigned (they typically only presented with fever (+ symptoms less typical for tularemia)). The latter could also represent typhoidal tularemia. Not all authors differentiate between “intestinal” and “oropharyngeal” forms of tularemia (WHO Guidelines on Tularaemia, 2007)¹. When symptoms of both forms were present, these are listed under “combination” in Table 1. Collecting additional clinical details during routine surveillance could be considered to allow for a more accurate classification of cases.

Of the 257 cases of tularemia reported in 2002–2016, 39 (15.2%) were confirmed using an antigen assay, 175 (68.1%) serologically, 35 (13.6%) by culture and 58 (22.6%) by PCR (some cases were confirmed by a combination of methods). Median time from the onset of symptoms until notification (which typically occurs within 2 days of diagnosis) was 32 days (inter quartile range: 20–56 days), indicating that diagnosis is often delayed.

The laboratory diagnosis is often based on the detection of specific serum antibodies and/or of the *F. tularensis* DNA in clinical samples, but also in fixed and paraffin-embedded samples usually available from the pathology (own experience) (Grunow et al., 2000, 2001, 2014; Schmitt et al., 2005; Splettsjoesser et al., 2005; Svensson et al., 2009b; Vogler et al., 2009b; Seibold et al., 2010; Jacob et al., 2011; Euler et al., 2012; Georgi et al., 2012; Sting et al., 2013; Chaignat et al., 2014; Becker et al., 2016; Challacombe et al., 2017). In addition, the isolation of the pathogen should be aimed at during an early stage of the disease for antibiotic sensitivity testing and further molecular-epidemiological investigation. The isolation of the pathogen was rarely successful when samples were obtained after initiation of an effective antibiotic treatment. On the other hand, we have seen that blood cultures taken early in the clinical course can lead to a successful isolation of the bacteria. Importantly, in the case of positive blood cultures with gram-negative bacteria, highly pathogenic bacterial organisms with extremely low infectious doses like *Brucella* or *Francisella* should be taken into consideration by the laboratory personnel and all following procedures should be carried out under appropriate biosafety conditions corresponding to BSL2 or BSL3 requirements (Directive 2000/54/EC <http://eur-lex.europa.eu/legal-content/EN/TXT/?uri=CELEX:32000L0054>). It should be noted that no natural resistances against first-line antibiotics have been described so far (Kudelina, 1973; Tomaso et al., 2005, 2017; Georgi et al., 2012; Karlsson et al., 2016). In Germany, the “Working Group of Competence and Treatment Centers for highly contagious and life-threatening diseases (STAKOB)” has developed recommendations for an adequate treatment

¹ http://apps.who.int/iris/bitstream/10665/43793/1/9789241547376_eng.pdf, last check February 2018.

TABLE 1 | Notified tularemia cases with laboratory confirmation by clinical presentation, Germany, 2002–2016 ($n = 257$).

Form	N	%
Glandular (lymphadenitis and not meeting criteria for other forms)	81	32
Ulceroglandular (lymphadenitis + skin ulcer)	46	18
Pneumonic (dyspnea or pneumonia)	29	11
Intestinal (diarrhea, vomiting or abdominal pain)	22	9
Oropharyngeal (lymphadenitis + tonsillitis, pharyngitis, stomatitis)	18	7
Oculoglandular (lymphadenitis + conjunctivitis)	3	1
Combination (meeting criteria of >1 form)	19	7
other (symptoms not meeting any of the above criteria, e.g., "only fever")	39	15
Total	257	100

of tularemia (http://www.rki.de/DE/Content/Kommissionen/Stakob/Stellungnahmen/Stellungnahme_Tularaemie.pdf?__blob=publicationFile).

Interestingly, we and others have diagnosed several tularemia patients with or without serious complications but with a prolonged time of recovery or even a recurrence of the disease after apparently adequate antibiotic treatment (Boone et al., 2015) (see case series below).

Case 1: We have reported a tularemia case in Germany who experienced a protracted clinical course over about 10 months (Grunow et al., 2015). The patient, a 22-year-old female, was living in an area in Germany where human cases of tularemia have been detected previously. The clinical history indicated a tick bite on the leg in June 2014. No further clinical signs occurred. In August 2014, the patient visited Turkey without any hints for an exposure risk. In mid-October, the patient became ill with fever and she also noted a vesiculo-papular rash. After treatment with ciprofloxacin over 5 days due to a simultaneous urinary tract infection, the patient recovered and was well. Early in December 2014, the patient experienced a unilateral cervical lymph node enlargement without other clinical symptoms and risk for exposure to *Francisella tularensis*. In mid-January 2015, the patient was hospitalized for further investigation. The Magnetic resonance imaging revealed an inflammatory liquefying lymph node on the right side and a lymphadenitis on the left side of the cervix. A lymph node extirpation was conducted and the biopsy of the enlarged lymph node revealed an abscess-forming granulomatous inflammation with giant cells. A tissue sample was tested positive for *F. tularensis* by 16S-rPCR and the markers *tul4* and *fopA* confirmed *F. tularensis*. The RD1-PCR identified subspecies *holarctica*. Isolation of the living pathogen was not successful. The patient was empirically treated with cefuroxime and metronidazole. She remained sub-febrile (37.3°C). After the diagnosis of tularemia the treatment was switched to oral doxycycline but the temperature did not decline. A further treatment with ciprofloxacin p.o. over 14 d cured the sub-febrile temperature. In February 2015, the patient was in good general condition without fever, but still showed

unilaterally enlarged lymph nodes and thickening of the cervical muscles, both painful on palpation. The site of the lymph node extirpation showed signs of delayed healing with secretion of a clear fluid (negative for *F. tularensis*). The vesiculo-papular exanthema in the cervical region and in the face was still visible. The serology at this time revealed an anti-*Francisella* titer of >100,000 by ELISA and a positive Western blot. After several ambulant controls, the patient was again hospitalized in March 2015 for further treatment with intravenous ciprofloxacin over 4 days and, after discharge from the hospital, further treatment with oral ciprofloxacin for an additional 11 days. In April 2015, out-patient control revealed secondary wound healing, good general condition, no fever and no enlarged lymph nodes.

Case 2: Another 68-year-old patient was described by H.L. Stich with a probable tick bite without cutaneous efflorescence and a time to diagnosis of about 8 weeks (Robert Koch-Institut, 2015). Because of a previously known neurological symptomatology, a neuro-somatic reason for the initial fever was assumed. After exclusion of this assumption, a detailed anamnesis including occupational information revealed that the patient had been a farmer for years and was also a hunter. This led to the assumption of a zoonotic infectious disease. The only sign of an infection was an elevated C-reactive protein (29.1 mg/l). Brucellosis and Q-fever were serologically excluded. Only 3 weeks after the first hospitalization, *F. tularensis* was considered and a clearly elevated antibody titer was detected. After this diagnosis, a specific treatment with doxycycline was initiated. The patient was discharged from the hospital after 4 weeks of therapy. Furthermore, it was revealed that 1 year before, four field hares infected with *F. tularensis* had been detected. This case shows that the consideration of differential diagnoses of tularemia might be hampered by other dominant clinical manifestations. In the case of pulmonary tularemia, lung cancer or tuberculosis are often the first choice of diagnoses. However, in the case of unclear fever and anamnestic information pointing toward contact with wild animals, tularemia should always be taken into diagnostic consideration.

Case 3: We described another 20-year-old female patient with a tick bite in her right hand occurring 5 months before consultation, followed by fever, chills and regional painful axillary lymphadenopathy (Lübbert et al., 2009). Interestingly, the empiric antibiotic treatment with doxycycline and ciprofloxacin had led to defervescence but no change in painful lymph node swelling. Surgical removal of a cubital lymph node was performed 3 months after the tick bite. 5 months after the tick bite laboratory findings were normal except for moderate elevation of C-reactive protein. Detection of specific serum antibodies against *F. tularensis* confirmed the suspected clinical diagnosis of ulceroglandular tularemia. The pathogen could not be detected by isolation or PCR. The histology of the removed painful axillary lymph node showed reticulocytic, abscess-forming lymphadenitis with a pseudotuberculosis type of granulomatosis and negative acid-fast staining. A complete recovery was achieved without renewed antibiotic treatment.

In 2016/2017 we have seen several additional cases with some peculiarities. An outbreak of tularemia with 6 serologically confirmed cases among 30 mostly volunteering participants

of a grape harvest in Rhineland-Palatinate which took place at the beginning of October 2016 was reported to ProMED (<http://www.promedmail.org/post/4647937>). 3–8 days after the activity, the affected individuals developed symptoms like high fevers, general malaise, and unilateral marked cervical lymphadenopathy suggesting an oropharyngeal route of infection. Interestingly, one patient showed symptoms of an oropharyngeal tularemia only 24 days after the exposure. Another patient experienced a severe clinical course of more than 2.5 months. Due to the absence of additional epidemiological hints, the diagnosis of tularemia was delayed. Three of the six patients were briefly hospitalized. An epidemiological outbreak investigation was initiated considering a broad range of environmental exposures and food-stuffs consumed during the event; the results have not been published yet.

The conclusion from these case reports is that *F. tularensis* ssp. *holarctica* can cause long-lasting clinical courses of disease. Tularemia can also occur as a recurrent disease over several months. In addition, the onset of an oro-pharyngeal tularemia can occur as late as 3 weeks after a relevant exposure. The pathologic mechanisms of a protracted course of tularemia are still unclear but an immune reaction to persistent antigens or pathogens appears a plausible explanation (Straube and Hess, 1986; Hanke et al., 2009; Lübbert et al., 2009; Capka et al., 2010; Dlugaiczyk et al., 2010; Fritzsich and Spletstoesser, 2010; Hauri et al., 2010; Potz-Biedermann et al., 2011; Bulut et al., 2013; Weile et al., 2013; Kohlmann et al., 2014; Guerpillon et al., 2016). The infection route often remains unclear and can be suggested only by a detailed anamnestic investigation. In late stages of the disease, especially after appropriate antibiotic treatment, living *Francisella* cannot be detected, but PCR investigation of tissue material and serology confirms the disease. Awareness of clinicians should be raised to consider tularemia in patients with enlarged lymph nodes and fever and a relevant exposure. This is even more important when atypical or very seldom clinical manifestations are seen like in pneumonic tularemia with lung nodules suggestive of malignancy, manifestation with uveitis or endocarditis (Terrada et al., 2016; Gaci et al., 2017; Odegaard et al., 2017).

ONE-HEALTH ASPECT OF TULAREMIA

Tularemia is a zoonotic disease. Cases of disease in humans and animals are notifiable in Germany and several other European countries. To understand the complexity of the disease, a close cooperation of veterinary medicine, human medicine, animal health and public health is crucial. Elevated risks of exposure or even outbreaks in humans are often preceded by observation of the disease in animals (Mörner, 1992; Spletstoesser et al., 2007, 2009; Gyuranecz et al., 2011; Grunow et al., 2012; Kuehn et al., 2013; Otto et al., 2014, 2015; Hestvik et al., 2015). Thus, a timely sharing of data concerning cases in animals with the public or the public health sector and awareness raising in outbreak situations could facilitate the early detection or prevention of cases in humans. The source of infection for human cases with tularemia often cannot be identified; however, in several cases, clues for an infection can be obtained through the anamnesis.

In very rare cases the source of infection can be verified. If not eliminated, the sources of infection can pose a high risk to other people. This can include e.g., drinking water contaminated by dead animals, freshly pressed juice from field fruits, fresh or frozen stored meat from infected animals. Unless direct identification of the infectious sources is done, transmission of bacteria by aerosols and dust, e.g., when cleaning barns or cutting grass could become a continuing event. As insect vectors can also transmit *Francisella*, knowledge of the prevalence in ticks, mosquitoes and possibly other insects is of interest. The investigation into sources of infection in sporadic cases and outbreaks and also the investigation of the prevalence of the pathogen in animals and environmental samples require a strong one-health approach in which specialists of animal health and of human health work together. This requires staff and financial resources which are often scarce. Compared to other infectious diseases, tularemia is rare and the burden of disease is relatively low. Thus, funders and decision makers are hesitant to allocate resources required to understand better the epidemiology of this disease and to prevent further cases. While the disease is rare, surveillance of human cases indicates a re-emergence with an approximately ten-fold increase of notified cases in Germany in a period of 15 years. Possible reasons include an increased presence of the pathogen in the environment and more frequent contact between humans and wildlife through leisure activities. However, an increased awareness of the disease and more frequent testing might have contributed to the continuous rise of notified cases.

Interactions between pathogen, the environment, its hosts and humans, render this interesting and potentially serious infectious disease a complex topic. In case of rare diseases like tularemia, utilizing international synergies, data, and expertise, ideally in internationally sponsored research projects, seems important to further advance prevention and control.

AUTHOR CONTRIBUTIONS

MF analyzed and described the surveillance data. RG is the head of the German Consultant Laboratory for Tularemia and in this function conducted laboratory diagnostics and epidemiological investigations and observed clinical cases which were summarized here together with the literature review. MF, KH, DJ, and RG drafted the manuscript. All authors have critically revised the manuscript.

FUNDING

This work was partially supported by the Health programme 2014-2020, through the Consumers, Health, Agriculture and Food Executive Agency (CHAFEA, European Commission); EMERGE Joint Action grant number: 677066.

ACKNOWLEDGMENTS

The authors would like to acknowledge Irene Schöneberg, Astrid Milde-Busch and Ulrike Grote for verification of tularemia case notifications.

REFERENCES

- Al Dahouk, S., Tomaso, H., Nöckler, K., Neubauer, H., and Frangoulidis, D. (2003). Laboratory-based diagnosis of brucellosis—a review of the literature. Part I: techniques for direct detection and identification of *Brucella* spp. *Clin. Lab.* 49, 487–505.
- Becker, S., Lochau, P., Jacob, D., Heuner, K., and Grunow, R. (2016). Successful re-evaluation of broth medium T for growth of *Francisella tularensis* ssp. and other highly pathogenic bacteria. *J. Microbiol. Methods* 121, 5–7. doi: 10.1016/j.mimet.2015.11.018
- Boone, I., Hassler, D., Nguyen, T., Spletstoesser, W. D., Wagner-Wiening, C., and Pfaff, G. (2015). Tularaemia in southwest Germany: three cases of tick-borne transmission. *Ticks Tick Borne Dis.* 6, 611–614. doi: 10.1016/j.ttbdis.2015.05.004
- Borde, J. P., Zange, S., Antwerpen, M. H., Georgi, E., Von Buttler, H., Kern, W. V., et al. (2017). Five cases of vector-borne *Francisella holarctica* infections in south-western Germany and genetic diversity. *Ticks Tick Borne Dis.* 8, 808–812. doi: 10.1016/j.ttbdis.2017.06.009
- Bulut, O. C., Dyckhoff, G., Spletstoesser, W., Nemeth, J., Klauschen, F., Penzel, R., et al. (2013). Unmasked: when a clinically malignant disease turns out infectious. a rare case of tularemia. *Int. J. Surg. Pathol.* 21, 76–81. doi: 10.1177/1066896912448424
- Capka, E., Roch, M., Ritter, M., and Stolzel, U. (2010). A 23-year-old patient with sore throat and cervical lymph node enlargement: a rare presentation of tularemia. *Internist* 51, 784–787. doi: 10.1007/s00108-009-2547-z
- Chaïgnat, V., Djordjevic-Spasic, M., Ruettger, A., Otto, P., Klimpel, D., Müller, W., et al. (2014). Performance of seven serological assays for diagnosing tularemia. *BMC Infect. Dis.* 14:234. doi: 10.1186/1471-2334-14-234
- Challacombe, J. F., Petersen, J. M., Gallegos-Graves, V., Hodge, D., Pillai, S., and Kuske, C. R. (2017). Whole-genome relationships among *Francisella* bacteria of diverse origins define new species and provide specific regions for detection. *Appl. Environ. Microbiol.* 83, e02589–e02516. doi: 10.1128/AEM.02589-16
- Chanturia, G., Birdsell, D. N., Kekelidze, M., Zhgenti, E., Babuadze, G., Tsertsvadze, N., et al. (2011). Phylogeography of *Francisella tularensis* subspecies *holarctica* from the country of Georgia. *BMC Microbiol.* 11:139. doi: 10.1186/1471-2180-11-139
- Đlugaiczak, J., Harrer, T., Zwerina, J., Traxdorf, M., Schwarz, S., Spletstoesser, W., et al. (2010). Oropharyngeal tularemia—a differential diagnosis of tonsillopharyngitis and cervical lymphadenitis. *Wien. Klin. Wochenschr.* 122, 110–114. doi: 10.1007/s00508-009-1274-8
- Dwivedi, C., Birdsell, D., Larkeryd, A., Myrtennas, K., Ohrman, C., Nilsson, E., et al. (2016). Long-range dispersal moved *Francisella tularensis* into Western Europe from the East. *Microb. Genom.* 2:e000100. doi: 10.1099/mgen.0.000100
- Eden, J. S., Rose, K., Ng, J., Shi, M., Wang, Q., Sintchenko, V., et al. (2017). *Francisella tularensis* ssp. *holarctica* in Ringtail Possums, Australia. *Emerg. Infect. Dis.* 23, 1198–1201. doi: 10.3201/eid2307.161863
- Ellis, J., Oyston, P. C., Green, M., and Titball, R. W. (2002). Tularemia. *Clin. Microbiol. Rev.* 15, 631–646. doi: 10.1128/CMR.15.4.631-646.2002
- Euler, M., Wang, Y., Otto, P., Tomaso, H., Escudero, R., Anda, P., et al. (2012). Recombinase polymerase amplification assay for rapid detection of *Francisella tularensis*. *J. Clin. Microbiol.* 50, 2234–2238. doi: 10.1128/JCM.06504-11
- Fritzsch, J., and Spletstoesser, W. D. (2010). Septic pneumonic tularaemia caused by *Francisella tularensis* subsp. *holarctica* biovar II. *J. Med. Microbiol.* 59, 1123–1125. doi: 10.1099/jmm.0.019893-0
- Gaci, R., Alauzet, C., Selton-Suty, C., Lozniewski, A., Pulcini, C., May, T., et al. (2017). *Francisella tularensis* endocarditis: two case reports and a literature review. *Infect. Dis.* 49, 128–131. doi: 10.1080/23744235.2016.1222546
- Gehring, H., Schacht, E., Maylaender, N., Zeman, E., Kaysser, P., Oehme, R., et al. (2013). Presence of an emerging subclone of *Francisella tularensis* *holarctica* in *Ixodes ricinus* ticks from south-western Germany. *Ticks Tick Borne Dis.* 4, 93–100. doi: 10.1016/j.ttbdis.2012.09.001
- Georgi, E., Schacht, E., Scholz, H. C., and Spletstoesser, W. D. (2012). Standardized broth microdilution antimicrobial susceptibility testing of *Francisella tularensis* subsp. *holarctica* strains from Europe and rare *Francisella* species. *J. Antimicrob. Chemother.* 67, 2429–2433. doi: 10.1093/jac/dks238
- Grunow, R., Ippolito, G., Jacob, D., Sauer, U., Rohleder, A., Di Caro, A., et al. (2014). Benefits of a European project on diagnostics of highly pathogenic agents and assessment of potential “dual use” issues. *Front. Public Health* 2:199. doi: 10.3389/fpubh.2014.00199
- Grunow, R., Joost, I., Serr, A., Yildiz, C., Kurz, P., Klee, S., et al. (2015). “Protracted course of human tularemia,” in *8th International Conference on Tularemia, Abstract S9-23* (Opatija), 131.
- Grunow, R., Kalaveshi, A., Kuhn, A., Mulliqi-Osmani, G., and Ramadani, N. (2012). Surveillance of tularaemia in Kosovo, 2001 to 2010. *Euro Surveill* 17, 20217. doi: 10.2807/ese.17.28.20217-en
- Grunow, R., and Priebe, H.-S. (2007). Tularämie – Zum Vorkommen in Deutschland, analyse auf der Basis der Meldedaten von 1949 bis 2006. *Epidemiol. Bull.* 7, 51–56.
- Grunow, R., Spletstoesser, W., McDonald, S., Otterbein, C., O'Brien, T., Morgan, C., et al. (2000). Detection of *Francisella tularensis* in biological specimens using a capture enzyme-linked immunosorbent assay, an immunochromatographic handheld assay, and a PCR. *Clin. Diagn. Lab. Immunol.* 7, 86–90. doi: 10.1128/CDLI.7.1.86-90.2000
- Grunow, R., Spletstosser, W., Hirsch, F. W., Kleemann, D., and Finke, E. J. (2001). Differential diagnosis of tularemia. *Dtsch. Med. Wochenschr.* 126, 408–413. doi: 10.1055/s-2001-12641
- Guerpillon, B., Boibieux, A., Guenne, C., Ploton, C., Ferry, T., Maurin, M., et al. (2016). Keep an ear out for *Francisella tularensis*: otomastoiditis cases after canyoneering. *Front. Med.* 3:9. doi: 10.3389/fmed.2016.00009
- Gyuranecz, M., Birdsell, D. N., Spletstoesser, W., Seibold, E., Beckstrom-Sternberg, S. M., Makrai, L., et al. (2012). Phylogeography of *Francisella tularensis* subsp. *holarctica*, Europe. *Emerg. Infect. Dis.* 18, 290–293. doi: 10.3201/eid1802.111305
- Gyuranecz, M., Rigo, K., Dan, A., Foldvari, G., Makrai, L., Denes, B., et al. (2011). Investigation of the ecology of *Francisella tularensis* during an inter-epizootic period. *Vector Borne Zoonotic Dis.* 11, 1031–1035. doi: 10.1089/vbz.2010.0091
- Gyuranecz, M., Szeredi, L., Makrai, L., Fodor, L., Meszaros, A. R., Szepe, B., et al. (2010). Tularemia of European brown hare (*Lepus europaeus*): a pathological, histopathological, and immunohistochemical study. *Vet. Pathol.* 47, 958–963. doi: 10.1177/0300985810369902
- Hanke, C. A., Otten, J. E., Berner, R., Serr, A., Spletstoesser, W., and Von Schnakenburg, C. (2009). Ulceroglandular tularemia in a toddler in Germany after a mosquito bite. *Eur. J. Pediatr.* 168, 937–940. doi: 10.1007/s00431-008-0862-3
- Hauri, A. M., Hofstetter, I., Seibold, E., Kaysser, P., Eckert, J., Neubauer, H., et al. (2010). Investigating an airborne tularemia outbreak, Germany. *Emerg. Infect. Dis.* 16, 238–243. doi: 10.3201/eid1602.081727
- Hestvik, G., Uhlhorn, H., Sodersten, F., Akerstrom, S., Karlsson, E., Westergren, E., et al. (2017). Tularaemia in European brown hares (*Lepus europaeus*) and mountain hares (*Lepus timidus*) Characterized by histopathology and immunohistochemistry: organ lesions and suggestions of routes of infection and shedding. *J. Comp. Pathol.* 157, 103–114. doi: 10.1016/j.jcpa.2017.06.003
- Hestvik, G., Warns-Petit, E., Smith, L. A., Fox, N. J., Uhlhorn, H., Artois, M., et al. (2015). The status of tularemia in Europe in a one-health context: a review. *Epidemiol. Infect.* 143, 2137–2160. doi: 10.1017/S0950268814002398
- Hofstetter, I., Eckert, J., Spletstoesser, W., and Hauri, A. M. (2006). Tularaemia outbreak in hare hunters in the Darmstadt-Dieburg district, Germany. *Euro. Surveill.* 11, E060119. doi: 10.2807/esw.11.03.02878-en
- Jacob, D., Wahab, T., Edvinsson, B., Peterzon, A., Boskani, T., Farhadi, L., et al. (2011). Identification and subtyping of *Francisella* by pyrosequencing and signature matching of 16S rDNA fragments. *Lett. Appl. Microbiol.* 53, 592–595. doi: 10.1111/j.1472-765X.2011.03158.x
- Jenzora, A., Jansen, A., Ranisch, H., Lierz, M., Wichmann, O., and Grunow, R. (2008). Seroprevalence study of *Francisella tularensis* among hunters in Germany. *FEMS Immunol. Med. Microbiol.* 53, 183–189. doi: 10.1111/j.1574-695X.2008.00408.x
- Jusatz, H. J. (1952a). Zweiter Bericht über das Vordringen der Tularämie nach Mittel- und Westeuropa in der Gegenwart. *Zeitschr. F. Hygiene* 134, 350–374.
- Jusatz, H. J. (1952b). “Tularaemia in Europe 1926–1951,” in *Welt-Seuchenatlas*, ed E. Rodenwaldt (Hamburg: Falk-Verlag).
- Jusatz, H. J. (1961). Dritter Bericht über das Vordringen der Tularämie nach Mittel- und Westeuropa im Zeitraum 1950–1960, *Zeitschr. F. Hygiene* 148, 69–93. doi: 10.1007/BF02151963
- Karlsson, E., Golovliov, I., Larkeryd, A., Granberg, M., Larsson, E., Ohrman, C., et al. (2016). Clonality of erythromycin resistance in *Francisella tularensis*. *J. Antimicrob. Chemother.* 71, 2815–2823. doi: 10.1093/jac/dkw235

- Karlsson, E., Svensson, K., Lindgren, P., Bystrom, M., Sjodin, A., Forsman, M., et al. (2013). The phylogeographic pattern of *Francisella tularensis* in Sweden indicates a Scandinavian origin of *EuroSiberian tularaemia*. *Environ. Microbiol.* 15, 634–645. doi: 10.1111/1462-2920.12052
- Kaysser, P., Seibold, E., Matz-Rensing, K., Pfeffer, M., Essbauer, S., and Spletstoesser, W. D. (2008). Re-emergence of tularemia in Germany: presence of *Francisella tularensis* in different rodent species in endemic areas. *BMC Infect. Dis.* 8:157. doi: 10.1186/1471-2334-8-157
- Kingry, L. C., and Petersen, J. M. (2014). Comparative review of *Francisella tularensis* and *Francisella novicida*. *Front. Cell. Infect. Microbiol.* 4:35. doi: 10.3389/fcimb.2014.00035
- Kohlmann, R., Wolf, P. J., and Gatermann, S. G. (2014). Pleuropulmonary tularemia in a 63-year-old hunter in Germany. *Dtsch. Med. Wochenschr.* 139, 534–537. doi: 10.1055/s-0033-1360076
- Kreizinger, Z., Erdelyi, K., Felde, O., Fabb, M., Sulyok, K. M., Magyar, T., et al. (2017). Comparison of virulence of *Francisella tularensis* ssp. *holarctica* genotypes B.12 and B.FTNF002-00. *BMC Vet. Res.* 13:46. doi: 10.1186/s12917-017-0968-9
- Kudalina, R. I. (1973). Change in the properties of the causative agent of tularemia due to erythromycin. *Zh. Mikrobiol. Epidemiol. Immunobiol.* 50, 98–101.
- Kuehn, A., Schulze, C., Kutzer, P., Probst, C., Hlinak, A., Ochs, A., et al. (2013). Tularamia seroprevalence of captured and wild animals in Germany: the fox (*Vulpes vulpes*) as a biological indicator. *Epidemiol. Infect.* 141, 833–840. doi: 10.1017/S0950268812001008
- Lübbert, C., Taege, C., Seufferlein, T., and Grunow, R. (2009). Prolonged course of tick-borne ulceroglandular tularemia in a 20-year-old patient in Germany—case report and review of the literature. *Dtsch. Med. Wochenschr.* 134, 1405–1410. doi: 10.1055/s-0029-1225296
- Mätz-Rensing, K., Floto, A., Schrod, A., Becker, T., Finke, E. J., Seibold, E., et al. (2007). Epizootic of tularemia in an outdoor housed group of cynomolgus monkeys (*Macaca fascicularis*). *Vet. Pathol.* 44, 327–334. doi: 10.1354/vp.44-3-327
- Mörner, T. (1992). The ecology of tularamia. *Rev. Sci. Tech.* 11, 1123–1130. doi: 10.20506/rst.11.4.657
- Müller, W., Hotzel, H., Otto, P., Karger, A., Bettin, B., Bocklich, H., et al. (2013). German *Francisella tularensis* isolates from European brown hares (*Lepus europaeus*) reveal genetic and phenotypic diversity. *BMC Microbiol.* 13:61. doi: 10.1186/1471-2180-13-61
- Odegaard, K., Boersma, B., and Keegan, J. (2017). Atypical Presentations of Tularemia. *S. D. Med.* 70, 207–209.
- Origg, F. C., Frey, J., and Pilo, P. (2014). Characterisation of a new group of *Francisella tularensis* subsp. *holarctica* in Switzerland with altered antimicrobial susceptibilities, 1996 to 2013. *Euro. Surveill.* 19:20858. doi: 10.2807/1560-7917.ES2014.19.29.20858
- Origg, F. C., and Pilo, P. (2016). *Francisella tularensis* clades B.FTN002-00 and B.13 are associated with distinct pathology in the European brown hare (*Lepus europaeus*). *Vet. Pathol.* 53, 1220–1232. doi: 10.1177/0300985816629718
- Otto, P., Chaignat, V., Klimpel, D., Diller, R., Melzer, F., Muller, W., et al. (2014). Serological investigation of wild boars (*Sus scrofa*) and red foxes (*Vulpes vulpes*) as indicator animals for circulation of *Francisella tularensis* in Germany. *Vector Borne Zoonotic Dis.* 14, 46–51. doi: 10.1089/vbz.2013.1321
- Otto, P., Kohlmann, R., Muller, W., Julich, S., Geis, G., Gatermann, S. G., et al. (2015). Hare-to-human transmission of *Francisella tularensis* subsp. *holarctica*, Germany. *Emerg. Infect. Dis.* 21, 153–155. doi: 10.3201/eid2101.131837
- Porsch-Ozcürümeç, M., Kischel, N., Priebe, H., Spletstosser, W., Finke, E. J., and Grunow, R. (2004). Comparison of enzyme-linked immunosorbent assay, Western blotting, microagglutination, indirect immunofluorescence assay, and flow cytometry for serological diagnosis of tularemia. *Clin. Diagn. Lab. Immunol.* 11, 1008–1015. doi: 10.1128/CDLI.11.6.1008-1015.2004
- Potz-Biedermann, C., Schwendemann, L., Schroppel, K., Sonnichsen, K., Schmidt, D., and Schaller, M. (2011). Ulceroglandular tularemia. *J. Dtsch. Dermatol. Ges.* 9, 806–808. doi: 10.1111/j.1610-0387.2011.07670.x
- Qu, P. H., Li, Y., Salam, N., Chen, S. Y., Liu, L., Gu, Q., et al. (2016). *Allofrancisella inopinata* gen. nov., sp. nov. and *Allofrancisella frigidiquae* sp. nov., isolated from water-cooling systems, and transfer of *Francisella guangzhouensis* Qu et al. 2013 to the new genus as *Allofrancisella guangzhouensis* comb. nov. *Int. J. Syst. Evol. Microbiol.* 66, 4832–4838. doi: 10.1099/ijsem.0.001437
- Robert Koch-Institut (2015). Tularämie als eine differentialdiagnostische Herausforderung—Ein Beispiel für eine fiebrige bakterielle Zoonose mit vieldeutiger Begleitsymptomatik. *Epidemiol. Bull.* 46, 491–492.
- Rydzewski, K., Schulz, T., Brzuszkiewicz, E., Holland, G., Luck, C., Fleischer, J., et al. (2014). Genome sequence and phenotypic analysis of a first German *Francisella* sp. isolate (W12-1067) not belonging to the species *Francisella tularensis*. *BMC Microbiol.* 14:169. doi: 10.1186/1471-2180-14-169
- Schätzle, W., and Schwenk, R. (2008). Three cases of tularamia in southern Baden-Wuerttemberg, Germany, November 2007. *Euro. Surveill.* 13, 8037. doi: 10.2807/ese.13.07.08037-en
- Schmitt, P., Spletstosser, W., Porsch-Ozcürümeç, M., Finke, E. J., and Grunow, R. (2005). A novel screening ELISA and a confirmatory Western blot useful for diagnosis and epidemiological studies of tularemia. *Epidemiol. Infect.* 133, 759–766. doi: 10.1017/S0950268805003742
- Schubert, A., Spletstoesser, W., and Bätzing-Feigenbaum, J. (2011). Tularamia in Berlin - two independent cases in travellers returning from central Anatolia, Turkey, February 2011. *Euro. Surveill.* 16:19860. doi: 10.2807/ese.16.18.19860-en
- Schulze, C., Heuner, K., Myrtennas, K., Karlsson, E., Jacob, D., Kutzer, P., et al. (2016). High and novel genetic diversity of *Francisella tularensis* in Germany and indication of environmental persistence. *Epidemiol. Infect.* 144, 3025–3036. doi: 10.1017/S0950268816001175
- Seibold, E., Maier, T., Kostrzewa, M., Zeman, E., and Spletstoesser, W. (2010). Identification of *Francisella tularensis* by whole-cell matrix-assisted laser desorption ionization-time of flight mass spectrometry: fast, reliable, robust, and cost-effective differentiation on species and subspecies levels. *J. Clin. Microbiol.* 48, 1061–1069. doi: 10.1128/JCM.01953-09
- Sjöstedt, A. (2011). Special topic on *Francisella tularensis* and tularemia. *Front. Microbiol.* 2:86. doi: 10.3389/fmicb.2011.00086
- Spletstoesser, W. D., Mätz-Rensing, K., Seibold, E., Tomaso, H., Al Dahouk, S., Grunow, R., et al. (2007). Re-emergence of *Francisella tularensis* in Germany: fatal tularamia in a colony of semi-free-living marmosets (*Callithrix jacchus*). *Epidemiol. Infect.* 135, 1256–1265. doi: 10.1017/S0950268807008035
- Spletstoesser, W. D., Piechotowski, I., Buckendahl, A., Frangoulidis, D., Kaysser, P., Kratzer, W., et al. (2009). Tularemia in Germany: the tip of the iceberg? *Epidemiol. Infect.* 137, 736–743. doi: 10.1017/S0950268808001192
- Spletstoesser, W. D., Tomaso, H., Al Dahouk, S., Neubauer, H., and Schuff-Werner, P. (2005). Diagnostic procedures in tularamia with special focus on molecular and immunological techniques. *J. Vet. Med. B. Infect. Dis. Vet. Public Health* 52, 249–261. doi: 10.1111/j.1439-0450.2005.00863.x
- Sting, R., Runge, M., Eisenberg, T., Braune, T., Müller, W., and Otto, P. H. (2013). Comparison of bacterial culture and polymerase chain reaction (PCR) for the detection of *F. tularensis* subsp. *holarctica* in wild animals. *Berl. Munch. Tierarztl. Wochenschr.* 126, 285–290. doi: 10.2376/0005-9366-126-285
- Straube, E., and Hess, C. (1986). Tularamia—report of 2 cases without detectable contact with animals. *Z. Gesamte Hyg.* 32, 580–581.
- Svensson, K., Back, E., Eliasson, H., Berglund, L., Granberg, M., Karlsson, L., et al. (2009a). Landscape epidemiology of tularamia outbreaks in Sweden. *Emerg. Infect. Dis.* 15, 1937–1947. doi: 10.3201/eid1512.090487
- Svensson, K., Granberg, M., Karlsson, L., Neubauerova, V., Forsman, M., and Johansson, A. (2009b). A real-time PCR array for hierarchical identification of *Francisella* isolates. *PLoS ONE* 4:e8360. doi: 10.1371/journal.pone.0008360
- Terrada, C., Azza, S., Bodaghi, B., Le Hoang, P., and Drancourt, M. (2016). Rabbit hunter uveitis: case report of tularemia uveitis. *BMC Ophthalmol.* 16:157. doi: 10.1186/s12886-016-0332-z
- Thelaus, J., Andersson, A., Broman, T., Backman, S., Granberg, M., Karlsson, L., et al. (2014). *Francisella tularensis* subspecies *holarctica* occurs in Swedish mosquitoes, persists through the developmental stages of laboratory-infected mosquitoes and is transmissible during blood feeding. *Microb. Ecol.* 67, 96–107. doi: 10.1007/s00248-013-0285-1
- Tomaso, H., Al Dahouk, S., Hofer, E., Spletstoesser, W. D., Treu, T. M., Dierich, M. P., et al. (2005). Antimicrobial susceptibilities of Austrian *Francisella tularensis holarctica* biovar II strains. *Int. J. Antimicrob. Agents* 26, 279–284. doi: 10.1016/j.ijantimicag.2005.07.003
- Tomaso, H., Hotzel, H., Otto, P., Myrtennas, K., and Forsman, M. (2017). Antibiotic susceptibility *in vitro* of *Francisella tularensis* subsp. *holarctica* isolates from Germany. *J. Antimicrob. Chemother.* 72, 2539–2543. doi: 10.1093/jac/dkx182

- Vogler, A. J., Birdsell, D., Price, L. B., Bowers, J. R., Beckstrom-Sternberg, S. M., Auerbach, R. K., et al. (2009a). Phylogeography of *Francisella tularensis*: global expansion of a highly fit clone. *J. Bacteriol.* 191, 2474–2484. doi: 10.1128/JB.01786-08
- Vogler, A. J., Birdsell, D., Wagner, D. M., and Keim, P. (2009b). An optimized, multiplexed multi-locus variable-number tandem repeat analysis system for genotyping *Francisella tularensis*. *Lett. Appl. Microbiol.* 48, 140–144. doi: 10.1111/j.1472-765X.2008.02484.x
- Weile, J., Seibold, E., Knabbe, C., Kaufmann, M., and Splettstoesser, W. (2013). Treatment of tularemia in patient with chronic graft-versus-host disease. *Emerg. Infect. Dis.* 19, 771–773. doi: 10.3201/eid1905.120377

Conflict of Interest Statement: The authors declare that the research was conducted in the absence of any commercial or financial relationships that could be construed as a potential conflict of interest.

Copyright © 2018 Faber, Heuner, Jacob and Grunow. This is an open-access article distributed under the terms of the Creative Commons Attribution License (CC BY). The use, distribution or reproduction in other forums is permitted, provided the original author(s) and the copyright owner are credited and that the original publication in this journal is cited, in accordance with accepted academic practice. No use, distribution or reproduction is permitted which does not comply with these terms.



Construction of a New Phage Integration Vector pFIV-Val for Use in Different *Francisella* Species

Hana Tlapák¹, Kristin Köppen¹, Kerstin Rydzewski¹, Roland Grunow² and Klaus Heuner^{1*}

¹ Division 2 (ZBS 2), Cellular Interactions of Bacterial Pathogens, Centre for Biological Threats and Special Pathogens, Robert Koch Institute, Berlin, Germany, ² Division 2 (ZBS 2), Highly Pathogenic Microorganisms, Centre for Biological Threats and Special Pathogens, Robert Koch Institute, Berlin, Germany

We recently identified and described a putative prophage on the genomic island FhaGI-1 located within the genome of *Francisella hispaniensis* AS02-814 (*F. tularensis* subsp. *novicida*-like 3523). In this study, we constructed two variants of a *Francisella* phage integration vector, called pFIV1-Val and pFIV2-Val (*Francisella* Integration Vector-tRNA^{Val}-specific), using the *attL/R*-sites and the site-specific integrase (FN3523_1033) of FhaGI-1, a chloramphenicol resistance cassette and a *sacB* gene for counter selection of transformants against the vector backbone. We inserted the respective sites and genes into vector pUC57-Kana to allow for propagation in *Escherichia coli*. The constructs generated a circular episomal form in *E. coli* which could be used to transform *Francisella spp.* where FIV-Val stably integrated site specifically into the tRNA^{Val} gene of the genome, whereas pUC57-Kana is lost due to counter selection. Functionality of the new vector was demonstrated by the successful complementation of a *Francisella* mutant strain. The vectors were stable *in vitro* and during host-cell infection without selective pressure. Thus, the vectors can be applied as a further genetic tool in *Francisella* research, expanding the present genetic tools by an integrative element. This new element is suitable to perform long-term experiments with different *Francisella* species.

Keywords: *Francisella tularensis*, integrative vector, pFIV-Val, genomic island, episomal, phage

OPEN ACCESS

Edited by:

Marina Santic,
University of Rijeka, Croatia

Reviewed by:

Roger Derek Pechous,
University of Arkansas for Medical
Sciences, United States
Janakiram Seshu,
University of Texas at San Antonio,
United States

*Correspondence:

Klaus Heuner
heuner@rki.de

Received: 27 October 2017

Accepted: 27 February 2018

Published: 14 March 2018

Citation:

Tlapák H, Köppen K, Rydzewski K,
Grunow R and Heuner K (2018)
Construction of a New Phage
Integration Vector pFIV-Val for Use in
Different *Francisella* Species.
Front. Cell. Infect. Microbiol. 8:75.
doi: 10.3389/fcimb.2018.00075

INTRODUCTION

Francisella tularensis, the causative agent of tularemia, is found in a wide range of wild animals and can infect humans, causing various clinical expressions ranging from skin lesions to severe pneumonia, depending on the route of infection (Ellis et al., 2002). Infections in humans are mostly associated with the highly virulent *F. tularensis* subsp. (*Ft.*) *tularensis* and the less virulent subspecies *Ft. holarctica* (*Fth*) (Keim et al., 2007). Opportunistic infections by other *Francisella* species such as *F. hispaniensis* (*Fhis*), *F. novicida* (*Fno*), and *F. philomiragia* (*Fph*) have been reported in individuals with compromised immune systems (Hollis et al., 1989; Clarridge et al., 1996; Whipp et al., 2003). Recently, a new *Francisella* species (*Francisella sp.* strain W12-1067) has been identified in an aquatic habitat in Germany (Rydzewski et al., 2014). Yet it is not clear if the new species will be grouped into the genus *Francisella* or into the new genus “*Allofrancisella*” (Qu et al., 2013, 2016; Challacombe et al., 2017a). So far it is not known if this species is able to infect humans.

We recently identified and described the genomic island (GI) FhaGI-1, located in the genome of *Fhis* AS02-814 (*Ft.* subsp. *novicida-like* 3523) that contains a putative prophage (Schunder et al., 2013). We could show that the GI integrates site specifically into the tRNA^{Val} gene of the genome and that it generates an episomal form in an integrase-dependent manner. Furthermore, we could demonstrate that small variants of FhaGI-1 are able to integrate site specifically into the genome of other *Francisella* species (Rydzewski et al., 2015). Therefore, we decided to create the first *Francisella* phage integration vector on the basis of this GI.

There are a number of tools to manipulate *Francisella* genetically. For the expression of genes and complementation *in trans*, there are several shuttle-vectors derived from the cryptic plasmid pFNL10. Although the second and third generation of these vectors are mostly stable without selective pressure, high copy numbers can still pose a problem (Norqvist et al., 1996; Pomerantsev et al., 2001; Maier et al., 2004; LoVullo et al., 2006). Vectors based on plasmids from *Fph* expand the repertoire of shuttle-vectors and make it possible to use more than one vector per organism (Le Pihive et al., 2009). Chromosomal integration is a way to circumvent the problems associated with high copy numbers. For many bacteria, integration systems based on the site-specific elements of bacteriophages have been described (Lee et al., 1991; Hoang et al., 2000; Lauer et al., 2002). In general, these vectors consist of the site-specific integrase of a bacteriophage together with its *attP*-site (Campbell, 2003), a resistance gene, and a multiple cloning site. For *Francisella* few chromosomal integration systems have been described so far. The existing systems are either based on allelic exchange or a mini-Tn7 vector. Both systems produce transformants that are stable without selective pressure, but they also require helper plasmids or multiple rounds of transformation and selection (Ludu et al., 2008; LoVullo et al., 2009a,b). Phage integration vectors have not been generated for *Francisella* since phages for this organism have not been described before (LoVullo et al., 2009a; Rydzewski et al., 2015). Further cryptic plasmids and a putative conjugative element have been described recently and may be used to generate further plasmids for *Francisella* in the future (Siddaramappa et al., 2014; Challacombe et al., 2017b).

Here we report the construction of two variants of a new phage integration vector pFIV-Val on the basis of the genomic island FhaGI-1 that replicate in *Escherichia coli* and integrate stably and site specifically into the genome of different *Francisella* species.

MATERIALS AND METHODS

Strains and Growth Conditions

Strains used in this study were *E. coli* (DH10B) One Shot[®] TOP 10 (Invitrogen) and various *Francisella* strains (see **Table 1**). The *iglC* mutant strain of *Fth* strain LVS was kindly provided by Anders Sjöstedt (Golovliov et al., 2003). For genes and abbreviations used, see **Table 1**.

E. coli was cultivated in Luria-Bertani (LB) medium or on LB agar. The antibiotic concentrations used for *E. coli* were chloramphenicol (Cm) 40 $\mu\text{g ml}^{-1}$ and kanamycin (Km) 40 $\mu\text{g ml}^{-1}$. *Francisella* strains were cultivated in medium T (Pavlovich

and Mishan'kin, 1987; Becker et al., 2016), on medium T-based agar plates (MT-KH agar: medium T containing 2.4 g l⁻¹ of activated charcoal, 14.3 g l⁻¹ of agar and 9.5 g l⁻¹ of hemoglobin), or on HCA agar (Brain Heart Infusion Agar [Liofilchem, Roseto degli Abruzzi, Italy] with 10% sheep blood). The antibiotic concentrations used for *Francisella* were 10 $\mu\text{g ml}^{-1}$ for chloramphenicol and 12 $\mu\text{g ml}^{-1}$ for kanamycin.

The human macrophage-like cell line U937 (ATCC CRL-1593.2) (growth medium RPMI 1640 + 10% FCS [purchased from PAA, Pasching, Austria]) was used to investigate the intracellular multiplication of *Francisella* strains. U937 cells were cultivated at 37°C and 5% CO₂.

Construction of Integration Vectors

Three different DNA constructs used to generate pFIV-Val vectors were generated by *in vitro* DNA synthesis. DNA synthesis and DNA sequence verification by DNA sequencing were performed by GeneCust (Dudelang, Luxembourg). The different constructs were then used to generate pFIV-Val vectors 1, 2, and pFIV1-*iglC*, using pUC57-Kana as the back-bone (for details, see **Table 1** and **Figure 1**). Construct 1: FhaGI-gfp-CmR is composed of 4,644 bp, exhibiting the tRNA^{Val} gene of FhaGI-1 (Rydzewski et al., 2015), followed by restriction sites for NotI, BclI, and SnaBI, a *gfp* gene with promoter from vector pKK289KmGFP (Bönquist et al., 2008), restriction sites for NotI and SacII, the GroES promoter of *Fth* LVS (pGroES) (Ericsson et al., 1997), the *iglA* promoter with the PigR response element (PRE, underlined bps in PRE*), (PRE*: AGCTGTATAA ACATTGTGTT ATTGGCGTTA TTAAGGTAAC TT) (Ramsey et al., 2015), the GroES promoter from strain *Francisella* sp. strain W12-1067 (Rydzewski et al., 2014), followed by a Cm resistance cassette (952 bp) with promoter GroES from vector pKK289KmGFP (Bönquist et al., 2008), the integrase of FhaGI-1 (FN3523_1033), and the phage integration site *attR* (47 bp) (Rydzewski et al., 2015).

We introduced the PRE* site into the pFIV-Val vector to introduce a promoter that should be active during intracellular replication of *Francisella*. It has been published that the PRE element is an activator sequence for the expression of virulence genes, including genes (e.g., *iglC*) present on the *Francisella* pathogenicity island (FPI), and that genes of the FPI are induced during intracellular replication of *Francisella* (Ramsey et al., 2015).

Construct 2: The sequence (2389 bp) of construct 2 (see **Figure 1**) is identical to the sequence of FhaGI-gfp-CmR except for the restriction sequences surrounding the *gfp* gene, designated MCS1 with restriction sites for NotI, BclI, SacI, AatII, and MCS2 with restriction sites for KpnI, EcoRV, NotI, and NcoI. Construct 3 (in pFIV2-Val): SacB-tRNA-MCS3 (2502 bp) is composed of the complete *sacB* gene (2007 bp) of *Bacillus subtilis* (Steinmetz et al., 1985), the tRNA^{Val} gene and a singular MCS3 including restriction sites for BclI, SacI, AatII, KpnI, EcoRV, NotI, and NcoI (**Figure 1**). In addition, the *iglC* gene of *Ft. holarctica* LVS (construct 4) was cloned into pFIV1-Val using SacI/NheI leading to pFIV1-*iglC* (**Figure 1**). The maps of pFIV-Val vectors are given in **Figure S1**.

TABLE 1 | Strains and genetic elements used in this study.

Strain (abbreviation)	Characteristics	References
<i>Francisella tularensis holarctica</i> LVS (<i>Fth</i> LVS)	Live vaccine strain	ATCC 29684
<i>Francisella tularensis holarctica</i> LVS FIV1-Val (<i>Fth</i> LVS FIV1-Val)	Strain containing vector FIV1-Val	This work
<i>Francisella tularensis holarctica</i> LVS FIV1-Val gfp (<i>Fth</i> LVS FIV1-Valgfp)	Strain containing vector FIV1-Val with additional <i>gfp</i> -gene	This work
<i>Francisella tularensis holarctica</i> LVS FIV2-Val (<i>Fth</i> LVS FIV2-Val)	Strain containing vector FIV2-Val	This work
<i>Francisella tularensis holarctica</i> LVS Δ iglC (<i>Fth</i> LVS Δ iglC)	<i>iglC</i> deletion mutant	Golovliov et al., 2003
<i>Francisella tularensis holarctica</i> LVS Δ iglC+FIV1-iglC (<i>Fth</i> LVS Δ iglC+FIV1-iglC)	<i>iglC</i> deletion mutant complemented with FIV1-iglC	This work
<i>Francisella tularensis holarctica</i> wild type	Isolated from beaver carcass	Schulze et al., 2016
<i>Francisella novicida</i> U112 (<i>Fno</i> U112)	Wild type strain	ATCC 15482
<i>Francisella novicida</i> U112 FIV1-Val (<i>Fno</i> U112 FIV1-Val)	Strain containing vector FIV1-Val	This work
<i>Francisella novicida</i> Fx1 (<i>Fno</i> Fx1)	Wild type strain	FSC 156
<i>Francisella</i> sp. strain W12-1067	Wild type strain	Rydzewski et al., 2014
<i>Francisella</i> W12-1067 FIV1-Val	Strain containing vector FIV1-Val	This work
<i>Francisella hispaniensis</i> (<i>Fhis</i>)	Wild type strain	Whipp et al., 2003

Gene name/genetic construct	Characteristics	References
Integrase (Int)	Site specific integrase of FhaGI-1 (FN3523_1033)	Rydzewski et al., 2015
pGroES	GroES promoter of <i>Ft. holarctica</i> LVS	Ericsson et al., 1997
pGroES (W12)	GroES promoter of strain <i>Francisella</i> sp. W12-1067	Rydzewski et al., 2014
PRE*	<i>iglA</i> promoter with P _{igR} response element (PRE)	Ramsey et al., 2015
<i>attL</i> -site (tRNA ^{Val})	General integration site for FhaGI-1	Rydzewski et al., 2015
<i>attB</i> (chromosomal); <i>attP</i> (episomal)	Phage attachment sites	Campbell, 2003
<i>attR</i> - site	Necessary for the formation of the episomal form of FhaGI-1	Rydzewski et al., 2015
<i>sacB</i>	<i>sacB</i> gene from <i>Bacillus subtilis</i> , coding for a secreted levansucrase	Steinmetz et al., 1985
CmR	Chloramphenicol resistance cassette, <i>Aeromonas hydrophila</i>	GenBank accession: AJ973195.1
KmR	Kanamycin resistance cassette	pUC57-Kana (GeneCust)

For the handling of pFIV-Val vectors in *E. coli* it is necessary to use chloramphenicol and kanamycin simultaneously to select for clones containing the whole vector. Otherwise, the episomal form, which is generated in *E. coli* will be lost, leading to strains containing only the ‘empty’ vector. This is because the episomal form (FIV-Val) is unable to integrate into the genome of *E. coli* or to replicate in *E. coli*. For further details, see Results and Discussion section.

DNA Techniques and PCR Analysis

Plasmid DNA for restriction digestion and PCR analysis was prepared using the Invisorb Plasmid Mini Two Kit (Stratagene, Berlin, Germany), and preparation of genomic DNA was done with the Blood & Tissue kit (Qiagen, Hilden, Germany). Restriction enzymes were purchased from New England BioLabs and used according to the manufacturer’s protocols (Frankfurt a. M., Germany). PCR was carried out using a Thermocycler TRIO-Thermoblock (Biometra, Göttingen, Germany) and the TopTaq DNA polymerase (Qiagen, Hilden, Germany). Analysis of *E. coli* transformants was done with primer pairs Fha-1^P/Fha-2** (for pFIV1-Val), SacB_R_out/Fha-2** (pFIV2-Val) and Fha-3*/Fha-4^P, for the presence of the complete construct and Fha-1^P/Fha-4^P (pFIV1-Val) and SacB_R_out/Fha-4^P (pFIV2-Val), for presence of the “empty” vector. The presence of the episomal form was shown using primer pair Fha-2**/Fha-3*. Integration

of the vectors into the genome of *Francisella* strains was shown using primer combinations Fha-1/Fha-2** and Fha-3*/Fha-4* (for integration into *Fth* LVS and *Fno* U112) and Fha-1^{W12}/Fha-2** and Fha-3*/Fha-4^{W12} (integration in *Francisella* sp. W12-1067). All mentioned primers are given in **Table 2**. In general, initial denaturation was performed at 94°C for 3 min and final extension was performed at 72°C for 10 min. The cycling conditions (35 cycles) were 94°C for 30 s, 57°C for 1 min and 72°C for 1 min, and ~ 100 ng of template DNA was used. Oligonucleotides were obtained from Eurofins MWG Operon (Ebersberg, Germany).

Transformation of Bacteria

Plasmid DNA was introduced into *E. coli* by thermal shock (30 min on ice, 30 s at 42°C, 2 min on ice) (Invitrogen). After transformation *E. coli* were incubated in LB medium for 1 h at 37°C and then plated onto agar containing 40 μg ml⁻¹ of chloramphenicol and 40 μg ml⁻¹ of kanamycin. Electroporation of *Francisella* strains was performed using a Gene Pulser system (Bio-Rad, Munich, Germany). Electroporation was done at 2.5 kV, 600 Ω and 25 μF. After transformation *Francisella* were incubated in medium T for 4 h at 37°C and then plated onto MT-KH or HCA agar plates containing 10 μg ml⁻¹ of chloramphenicol and when appropriate 5% sucrose.

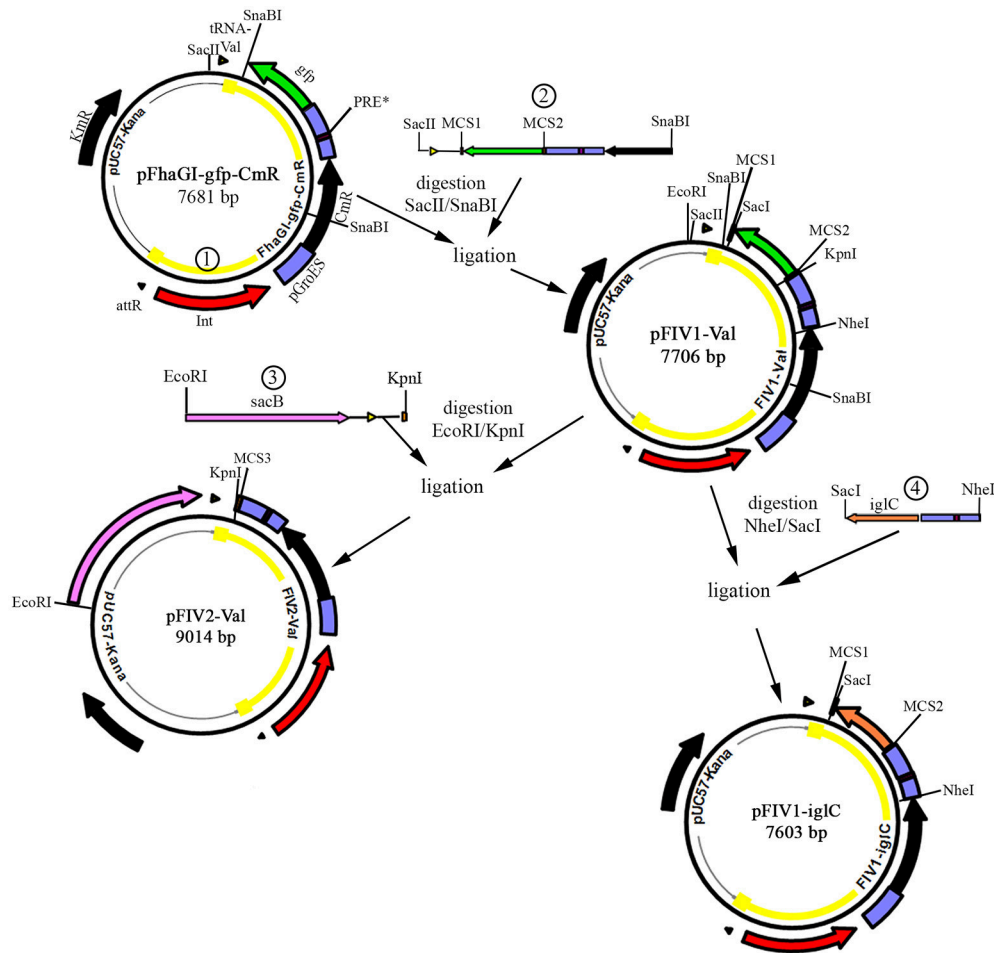


FIGURE 1 | Construction of FhaGI-1-derived vectors and cloning. Vector maps and restriction fragments for the construction of the different vector variants are shown. Antibiotic resistance cassettes for kanamycin (KmR) and chloramphenicol (CmR) are given in black; triangles represent tRNA-Val and *attR* and promoters are shown in blue; the integrase gene is shown in red; genes inserted into the MCS are shown in green (*gfp*) and orange (*ig1C*); the *SacB* gene is shown in pink; and the FIV-Val part of the vectors that integrates into the genome of *Francisella* transformants is highlighted by a yellow line. Restriction sites used in this study are indicated. Numbers indicate constructs (1–4) used for cloning, see also Materials and Methods section. Detailed vector maps with primer binding sites are given in **Figure S1**.

Testing the Stability of Vectors

To test the stability of the different vectors in *Francisella* transformants, they were cultured overnight in 3 ml of medium T with Cm ($5 \mu\text{g ml}^{-1}$). The next day 200 μl of the overnight culture were used to inoculate 3 ml of fresh medium T without antibiotics. Bacteria were passaged in this manner every 12 h. After 10 passages the optical density at 600 nm (OD_{600}) of the cultures was adjusted to 1, and cultures were diluted and plated on HCA agar with and without chloramphenicol to determine the number of bacteria still containing FIV-Val. Aliquots of the adjusted cultures were used for preparation of genomic DNA and for Western blot analysis. PCR analysis was performed to determine the presence of the integrated as well as the episomal form of FIV-Val.

SDS-PAGE and Immunoblotting

GFP detection was carried out by sodium dodecyl sulfate-polyacrylamide gel electrophoresis (SDS-PAGE) and Western blotting. The SDS-PAGE assay was performed as described previously (Laemmli, 1970). Equal amounts of aliquots of *Francisella* strains from stability testing (20 μl) were boiled for 10 min in Laemmli buffer. A total of 25 μl of the solution was loaded onto a 12% SDS polyacrylamide gel. Western blotting was carried out using a polyclonal anti-GFP antibody (A-11122, Thermo Fisher Scientific, Darmstadt, Germany) diluted in 1% milk-Tris-buffered saline (TBS) (1:1,000). A horseradish peroxidase-conjugated goat anti-rabbit antibody was used as secondary antibody (1:1,000). Visualization was done using ECL Western blotting substrate (Thermo Fisher Scientific) and X-ray film.

TABLE 2 | Primers used in this study.

Primer	T _m [°C]	Sequence 5' 3' (bp)	References
Fha-1	61.9	aatcactccaatagccagtagtaagga (27)	Rydzewski et al., 2015
Fha-1 ^{W12}	58.9	cttgcttcaatgactgggttttg (23)	This work
Fha-2**	60.1	attagcaatgagcttagctgttgc (26)	This work
SacB_R_out	58.9	ctacgcagacaacaatcaacgt (23)	This work
Fha-3*	59.3	ctgagaattaagccacttatcagaat (28)	Rydzewski et al., 2015
Fha-4*	63.4	gtaaaaccgcttggtcaacctatcag (27)	Rydzewski et al., 2015
Fha-4 ^{W12}	58.9	atccaggaatctttgtaggagct (23)	This work
M13U (Fha-1 ^P)	52.8	gtaaaacgacggccagt (17)	O'shaughnessy et al., 2003
M13R (Fha-4 ^P)	54.5	ggaacagctatgaccatg (19)	O'shaughnessy et al., 2003
iglC_U	58.4	actccgatcttactatgcagct (22)	This work
iglC_R	57.3	gcgagaccattcatgtgaga (20)	This work
RT-FIV-CmR-U	60.3	gaaagcggtagctggtgata (22)	This work
RT-FIV-CmR-R	60.3	gtgtagaactgccggaatcg (22)	This work
RT-FIV-CmR-TM	64.6	catgctctggagtgaataccacga (25)	This work
Ft-fopA-F	57.9	ttggcaaatctagcaggta (21)	Schulze et al., 2016
Ft-fopA-R	60.1	atctgtagtcaacactgttgaaca (26)	Schulze et al., 2016
Ft-fopA-TM	64.6	FAM- aagaccaccaccaatccaagca-BHQ-1 (25)	Schulze et al., 2016

Intracellular Replication in U937 Cells and Fluorescence Microscopy

For differentiation into macrophage-like cells, U937 cells were transferred into fresh RPMI medium containing 10% fetal calf serum (10% FCS), and PMA (phorbol-12-myristate-13-acetate, 1 mg/ml in dH₂O [P-8139; Sigma-Aldrich Chemie, Munich, Germany]) was added at a concentration of 1:20,000. After incubation for 36 h at 37°C and 5% CO₂, the supernatant was discarded and adherent cells were washed once with 10 ml of 0.2% EDTA in PBS. Cells were mechanically detached from the flask bottom and adjusted to 5 × 10⁵ cells/ml with RPMI + 10% FCS. To each well of a 24-well plate 1 ml of the cell suspension was added and incubated for 2 h at 37°C and 5% CO₂ for adhesion.

Overnight cultures of *Francisella* strains were diluted in plain RPMI medium, and the infection was done with a multiplicity of infection (MOI) of 10 (time point 0 h) for 2 h at 37°C and 5% CO₂. Cells were washed three times with RPMI and incubated with 50 μg ml⁻¹ of Gentamycin for 1 h to kill extracellular bacteria. Cells were washed again three times with RPMI and covered with 1 ml of RPMI. To determine the CFU at various time points of infection, coinfections of cells and bacteria were lysed by addition of 10 μl of 10% Saponin (S4521, Sigma-Aldrich Chemie) and serial dilutions were plated on HCA agar.

During the infection fluorescent images were obtained every 24 h using an inverse microscope (Carl Zeiss, Jena, Germany).

Copy Number

Copy numbers of FIV-Val were determined by qPCR-analysis. As target for the vector the *CmR* gene was used and as chromosomal reference the single copy gene *fopA*. Primers and hydrolysis probes are given in **Table 2**.

qPCRs were conducted in a total volume of 25 μl using the ABI 7500 Real Time PCR System and the TaqMan[®] Environmental Master Mix 2.0 (Applied Biosystems). Primers

and hydrolysis probes were used at a final concentration of 0.3 mM and 0.1 mM, respectively. 5 μl of target DNA were added to each reaction. For each vector three decimal dilutions of DNA (0.1; 0.01; 0.001 ng) were pipetted in duplicate. Reactions were initiated with an incubation at 95°C for 10 min followed by 40 cycles of 95°C for 15 s (denaturation) and 60°C for 60 s (annealing and elongation, detection). Copy numbers were calculated using the ΔCt method.

RESULTS AND DISCUSSION

Construction of pFIV-Val

Recently, we demonstrated that the *att*-sites of FhaGI-1 of *Fhis* AS02-814 in combination with the site-specific integrase are sufficient to generate the episomal form FIV-Val of the vector in *E. coli* and that after transformation into *Fth* LVS the element integrates site specifically into the tRNA-Val gene of transformants (Rydzewski et al., 2015). We now utilized this information to develop phage integration vectors to be used in *Francisella* research, with the idea that the constructs would be integrated site specifically and stable into the genome.

We constructed a first variation of the vector, called pFhaGI-gfp-CmR (7,681 bp) (**Figure 1** and **Figure S1A**). The construct was composed of the following elements (see also **Table 1**): (1) the *attL*-site (tRNA^{Val}) which is the general integration site for FhaGI-1; (2) a *gfp* gene flanked by restriction sites that serves as a place holder for the integration of future genes of interest (at this first stage) and as a control for gene expression during intracellular replication, (3) the *Fth* LVS GroES promoter; (4) the PRE* site that is used for the expression of genes during intracellular replication of *Francisella* in host cells; (5) the GroES promoter of strain *Francisella* sp. W12-1067 (pGroES-W12) for expression of genes in this species; (6) a chloramphenicol resistance marker for the selection process after transformation;

(7) the site-specific integrase which is necessary for generating the episomal form and the integration into the *attB*-site ($tRNA^{Val}$) of the acceptor strain (*Francisella* strain of interest) and the *attR*-site which is necessary for the formation of the episomal form of pFhaGI-gfp-CmR. For details, see also Materials and Methods. As a backbone, the plasmid pUC57-Kana was used to allow propagation of the construct in *E. coli*. Note, only the FhaGI-gfp-CmR construct (Figure 1 episomal form, marked in yellow) will be integrated site specifically into the genome of the acceptor strain (Rydzewski et al., 2015).

The construct was then introduced into *E. coli* by chemical transformation and plated on agar containing chloramphenicol and kanamycin. We isolated plasmid DNA from this strain and analyzed it for the presence of all three forms of pFhaGI-gfp-CmR using primer pairs 1^P/2^{**} and 3^{*}/4^P (pFIV-Val), 2^{**}/3^{*} (episomal form, FIV-Val), and 1^P/4^P (“empty” vector with *attB*-site) (Figures 2A,B). The PCRs confirmed that all three forms were present which means that the integrase is active in *E. coli*.

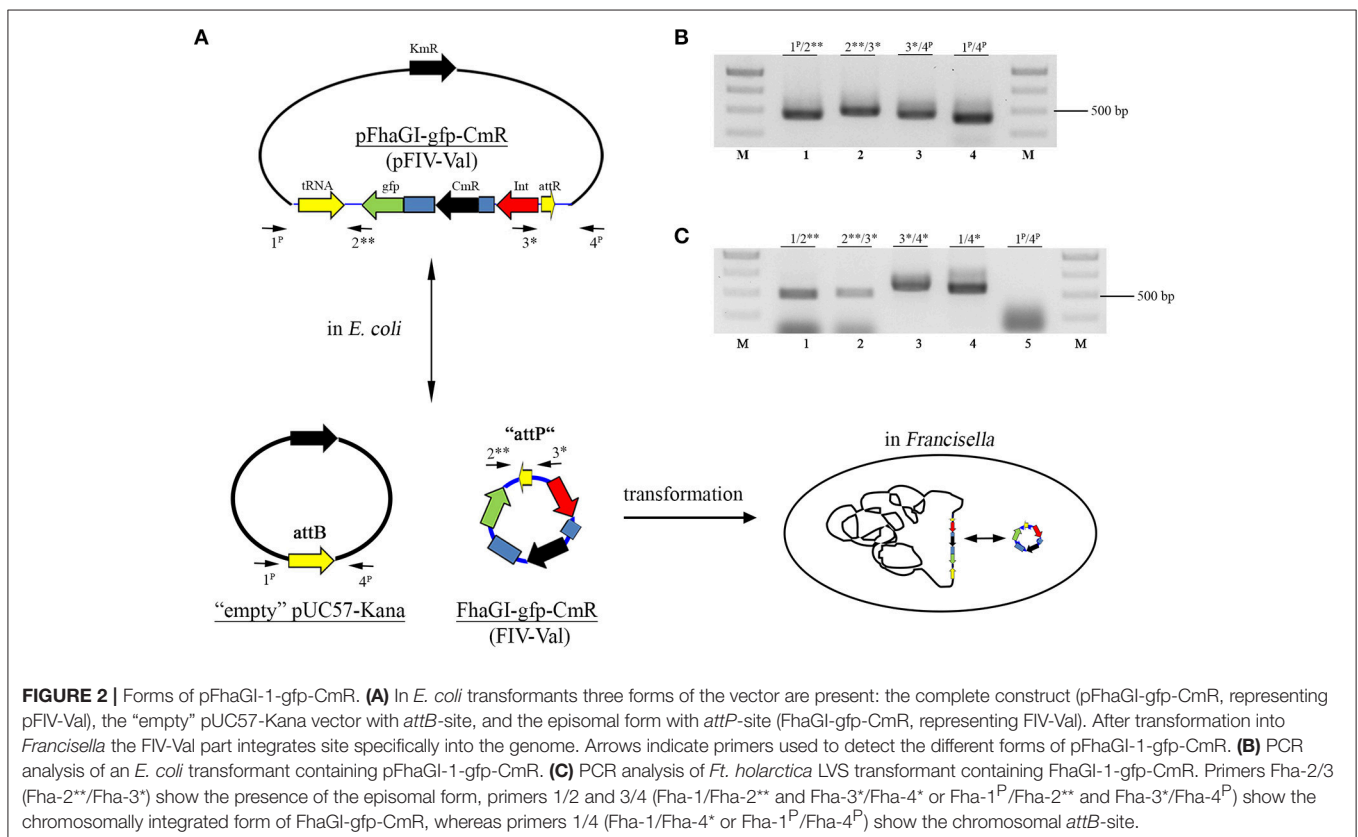
The plasmid preparation of pFhaGI-gfp-CmR was introduced into *Fth* LVS by electroporation and plated onto agar plates containing chloramphenicol. One hundred clones were picked and then transferred to plates containing kanamycin for negative selection against transformants still harboring the “empty” vector. Of the picked clones ~30% were kanamycin sensitive and, therefore, maintained only the desired construct (FhaGI-gfp-CmR), the episomal or genomically integrated form of pFhaGI-gfp-CmR (Figure 2A). The loss of the “empty” pUC57-Kana vector was also confirmed by PCR analysis (Figure 2C, lane

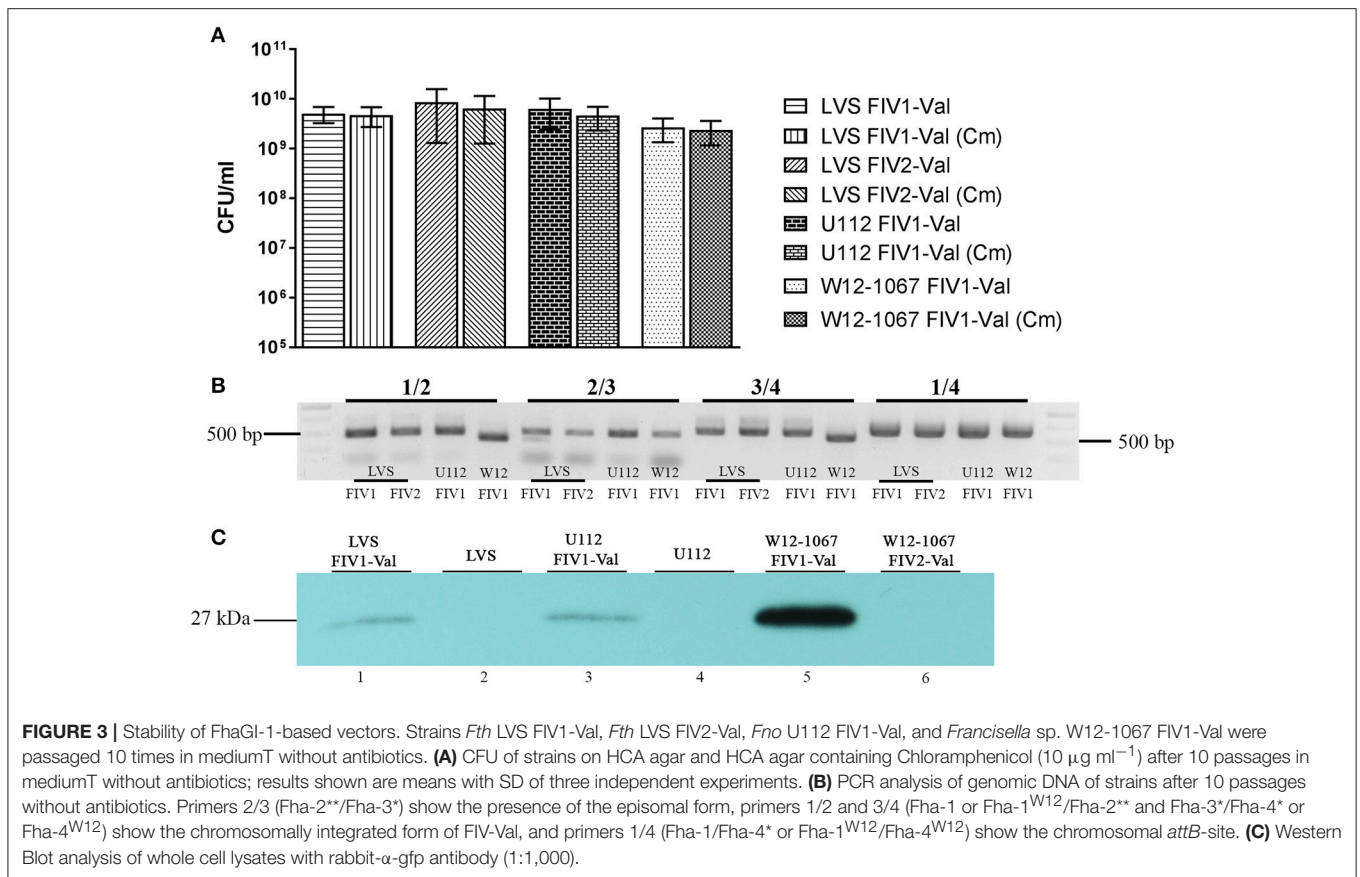
5). To test these clones for site-specific integration into the $tRNA^{Val}$ gene they were further analyzed by PCR using species specific (acceptor strain) primers (Figure 2C and Table 2). PCR confirmed that the construct was successfully integrated into the genome of *Fth* LVS (Figure 2C, lanes 1 and 3) and that the episomal form was also present (Figure 2C, lane 2). In addition, the PCR product of about 500 bp using primers 1/4^{*} (Figure 2C, lane 4) confirmed that after excision of FIV-Val, no copy of the GI is left in the genome (see also Rydzewski et al., 2015), indicating that the episomal form is not generated in a replicative way. The results demonstrated that the concept of a phage integration vector works at least in *Fth*.

Subsequently we optimized our vector by introducing an MCS on both sites of the *gfp* gene resulting in vector pFIV1-Val (7,706 bp) (Figure 1 and Figure S1B).

Functional Characterization of pFIV1-Val

An important characteristic of a vector is its stability without a selective pressure. To test the stability of FIV1-Val in *Fth* LVS without any selective pressure, we cultivated *Fth* LVS harboring FIV1-Val in medium T without antibiotics. After 10 passages, we plated cultures on HCA agar with and without chloramphenicol. As shown in Figure 3A, the CFU of tested strains on agar plates containing chloramphenicol was similar to that on agar without antibiotics, demonstrating that FIV1-Val remained stable without selective pressure. This was further verified by PCR analysis which confirmed the presence of the integrated as well as the episomal form of FIV1-Val (Figure 3B). To test if the gene



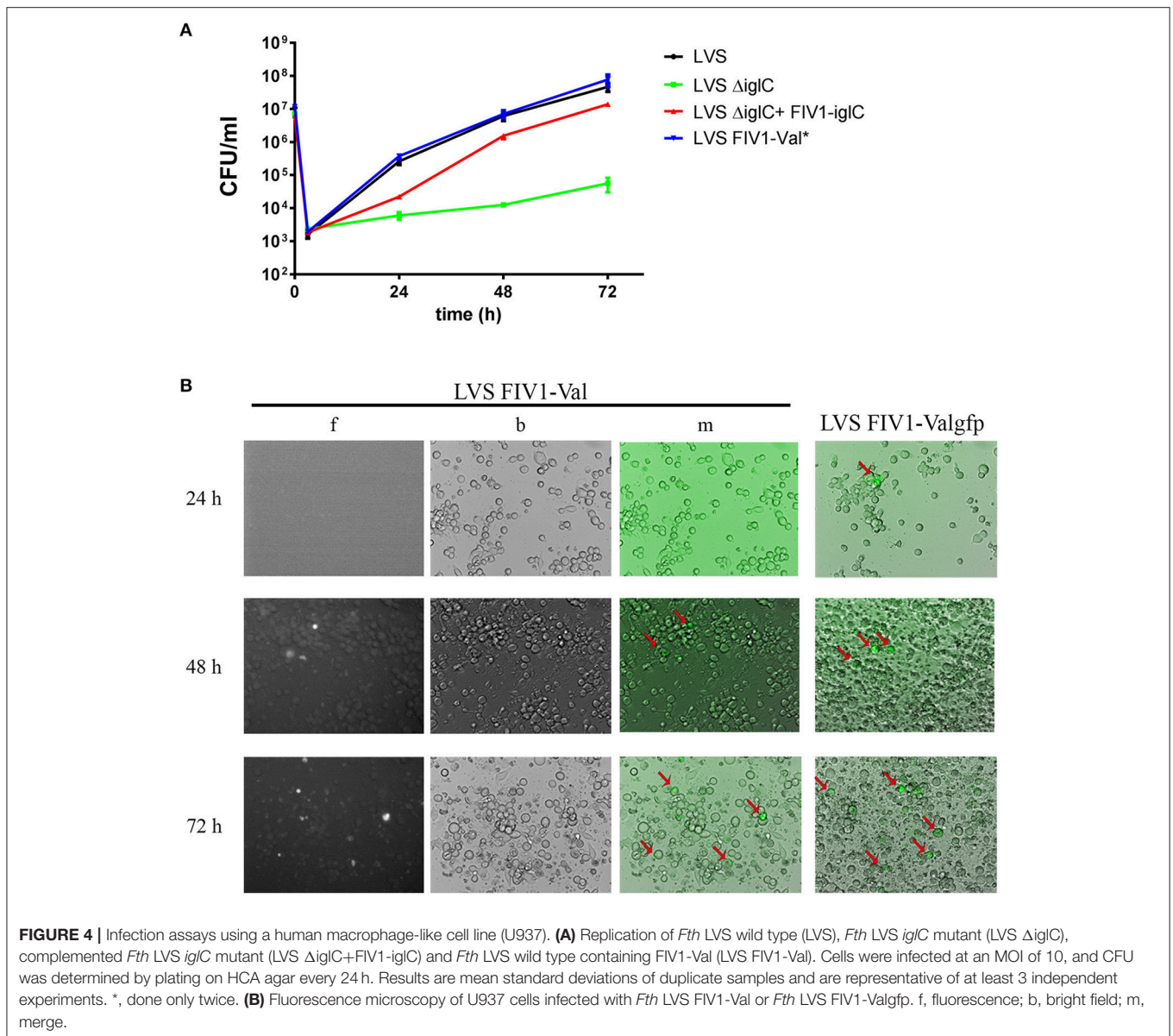


of interest (e.g., *gfp*) cloned into pFIV1-Val was expressed in the acceptor strain, Western Blot analysis using an anti-GFP antibody was performed. The results demonstrated that the *gfp* gene was expressed (Figure 3C, lane 1), indicating that the used promoter element of FIV-Val is active in *Fth*. The wild type control proves that although the observed band is rather faint it is not due to background binding of the antibody in the strain (Figure 3C, lane 2).

To demonstrate further that the integration vector is functional in *Francisella*, we used it to complement a specific mutant strain of *Fth*. We chose an *iglC* mutant strain of *Fth* LVS which is known to be unable to replicate within host cells (Golovliov et al., 2003). We cloned the *iglC* gene into pFIV1-Val, resulting in pFIV1-*iglC* (Figure 1). FIV1-*iglC* was then successfully integrated into the *iglC* mutant strain, leading to strain *Fth* LVS Δ *iglC*+FIV1-*iglC*. The site-specific integration of the construct was confirmed by PCR analysis (data not shown). Then we performed infection assays with this strain as well as the *Fth* LVS wild-type strain and *Fth* LVS FIV1-Val, using the human macrophage-like cell line U937 (Figure 4A). As expected, the *Fth* LVS wild-type strain replicated in the macrophages while the *iglC* mutant strain did not. The complemented *iglC* mutant strain was able to replicate in U937 cells nearly as well as the wild-type strain (Figure 4A). The nearly complete complementation of the *iglC* mutant might be due to the fact that both copies of the *iglC* gene present in the wild-type strain had

been inactivated (Golovliov et al., 2003; Lai et al., 2004) and that the expression of the gene from FIV1-Val was not high enough to complement both inactivated genes. However, the intracellular growth defect of the *iglC* mutant strain was complemented. In addition, we could demonstrate that the presence of FIV1-Val alone did not influence the intracellular replication of *Fth* LVS (Figure 4A). The results demonstrated that FIV-Val was stable without selective pressure and could be used to express genes of interest during intracellular replication of *Francisella* in host cells. In addition, since FIV-Val did not influence the ability of *Francisella* to replicate intracellularly in host cells, pFIV-Val can be used for successful complementation of specific mutant strains.

In a further infection assay, we verified whether we could visualize the expression of the *gfp* gene during intracellular replication of *Francisella*. Activity of the *gfp* gene of FIV1-Val during the infection of U937 cells was visualized using a fluorescence microscope. As shown in Figure 4B, the activity of the GFP was low but macrophages containing fluorescent *Fth* LVS FIV1-Val could be demonstrated after 48 h and the number of fluorescent cells increased after 72 h. The results corroborated that the gene of interest cloned into pFIV-Val is expressed during intracellular replication. LoVullo and colleagues observed a similarly low number of fluorescent cells when using a Tn7-based chromosomal integration system to insert a *gfp* gene into the genome of *Fth* LVS (LoVullo et al., 2009a). They attributed the



poor visualization to a multitude of factors including promoter strength and improper folding of the GFP. Another factor that might account for the rather weak fluorescent signal could be a low copy number of the gene. Experiments using a strain with an additional *gfp* gene cloned into pFIV1-Val (pFIV1-Valgfp) seemed to support the theory of low copy numbers. With this strain a fluorescent signal was visible after 24 h and overall there seemed to be more fluorescent cells (Figure 4B, lane LVS FIV1-Valgfp). Altogether these results further confirmed that FIV1-Val remains stable in *Fth* without selective pressure and that it can be used to manipulate *Fth* strains genetically.

Functionality Test of pFIV-Val in Other *Francisella* Species

To validate whether pFIV-Val could also be used in other *Francisella* species, we transformed *Fno* U112, *Fno* Fx1, and

Francisella sp. W12-1067 with pFIV-Val. For all three strains we verified the site-specific integration into the genome and the presence of the episomal form by PCR analysis (Figure 3B). We further analyzed *Fno* U112 and *Francisella* sp. W12-1067 for the stability of FIV1-Val (Figure 3A). In both species the construct remained stable integrated after 10 passages in medium T without antibiotics (Figure 3B, lanes U112 FIV1 and W12 FIV1, respectively). GFP activity in both strains was low but could be confirmed by Western-Blot analysis (Figure 3C, lanes 3 and 5). In *Francisella* sp. W12-1067 the amount of the GFP protein was higher than in both other species investigated, suggesting that the cloned promoter element is highly active in this *Francisella* species. However, the differences in GFP activity could be due to differences in vector copy number, expression or in protein stability (improper folding, LoVullo et al., 2009a). In our hands, similar results were also obtained

with plasmids harboring a pGroES-*gfp* gene (unpublished results).

We also successfully introduced pFIV-Val into a wild-type strain of *Fth* (isolated from a beaver, Schulze et al., 2016) (data not shown). These results show that pFIV1-Val is suitable as an integration vector in different species and strains of *Francisella*.

Further Improvements and Determination of the Copy Number of pFIV-Val

To simplify selection of FIV-Val-positive clones after transformation, we decided to employ the idea of a negative selection step and introduced the *sacB* gene of *Bacillus subtilis* into that part of pFIV1-Val which does not integrate into the genome of transformants. The *sacB* gene codes for a secreted levansucrase which is toxic for Gram-negative bacteria when expressed in the presence of sucrose (Steinmetz et al., 1983, 1985). Using the levansucrase, only one selection step of transformants is needed since clones still harboring the “empty” or complete vector will die in the presence of sucrose. The construct “SacB-tRNA-MCS3” was cloned into pFIV1-Val, leading to the second vector called pFIV2-Val (9,014 bp). In addition, to generate a standard cloning vector pFIV2-Val, the *gfp* gene has been deleted and a singular MCS 3 has been introduced instead (Figure 1 and Figure S1D).

After transformation of pFIV2-Val into *Fth* LVS and selection on agar plates containing chloramphenicol and sucrose, only FIV2-Val-positive clones with the integrated form of FIV2-Val could be detected by PCR analysis (Figure 3B and data not shown). This demonstrates that the selection on sucrose was very efficient, thus eliminating the need for a second selection step. FIV2-Val was tested for its stability as described for FIV1-Val. The vector remained stable without selective pressure (Figure 3B, lanes LVS FIV2). However, since the integrase is still located on the FIV2-Val part of the vector, the episomal (excised) form of FIV-Val is still generated and detectable (Figure 3B, primers 2/3). Earlier we could show that the integrase is sufficient for the excision of a small variant of FhaGI-1, but excision still occurred in *Fth* LVS of an element missing the site-specific integrase. This may be due to the presence of further integrases or RecA in the genome sequence of the acceptor strain (Lesic and Carniel, 2005; Rydzewski et al., 2015). We obtained a comparable result for a genomic island (LpcGI-2) of *Legionella pneumophila* in which a similar mechanism was used for the excision of the GI from the genome (Lautner et al., 2013).

First qPCR analyses to quantify the copy number of the FIV-Val constructs (see section Materials and Methods) suggest that the copy number of FIV-Val in *Fth* LVS was 3.6 for both FIV1-Val and FIV2-Val (see Table S1). The results demonstrated that FIV-Val behaves in *Francisella* like a low-copy vector.

CONCLUSION

In this study we constructed two variants of a new phage integration vector (pFIV1-Val and pFIV2-Val), derived from

FhaGI-1 of *Fhis* AS02-814 for the use in different *Francisella* species. Both constructs integrate site specifically into the genome of the acceptor species at the *attB*-site localized within the tRNA^{Val} gene and remain stable without selective pressure. The introduction of a levansucrase into pFIV2-Val simplified the selection process of FIV-Val-positive strains after transformation of the acceptor with pFIV-Val. qPCR analysis suggests that there are about 3.6 copies of FIV-Val in *Fth* LVS. We used pFIV1-Val to complement successfully an *iglC* mutant strain of *Fth* LVS and could demonstrate that an introduced ‘gene of interest’ (*gfp* gene) was active in three different *Francisella* species.

GFP activity was not high in *Fth*, but the advantage of pFIV-Val is the site-specific integration, the low copy number and the stability without any selective pressure. In contrast to other plasmids or integration systems, pFIV-Val can be used without the help of “helper-plasmids” and in combination with other expression vectors, since no origin of replication is present on FIV-Val. Furthermore, pFIV-Val is usable in different *Francisella* strains of *Fth* and *Fno* and also different *Francisella* species. Thus, our results demonstrate that FhaGI-1-derived vectors can be used as a further genetic tool in *Francisella* research. With this new integration vector we now are able to perform research (in the laboratory) on persistence and reservoir research with *Francisella* spp. in long-term experiments.

AUTHOR CONTRIBUTIONS

KH designed the study and RG provided facility and equipment. HT, KK, and KR performed the experiments. HT and KH wrote the paper.

ACKNOWLEDGMENTS

We would like to thank Ursula Erikli for copy-editing.

SUPPLEMENTARY MATERIAL

The Supplementary Material for this article can be found online at: <https://www.frontiersin.org/articles/10.3389/fcimb.2018.00075/full#supplementary-material>

Figure S1 | Detailed vector maps of FhaGI-derived vectors. Given are vector maps for the different versions of the vector. Antibiotic resistance cassettes for kanamycin (KmR) and chloramphenicol (CmR) are given in green; yellow triangles represent tRNA-Val and *attR* and promoters are shown in blue; the integrase gene is shown in red; the MCS is given in orange and the *SacB* gene is shown in pink; the FIV part of the vectors that integrates into the genome of *Francisella* transformants is highlighted by a yellow line; primer binding sites are indicated by blue arrows; and restriction sites of the MCS and others used in this study are indicated. Primer binding positions are given in the table below each map; restriction enzymes that do not cut the vectors are given in a list below each vector version. **(A)** Vector map of pFhaGI-gfp-CmR, **(B)** vector map of pFIV1-Val, **(C)** restriction digestion of the three pFIV-Val vectors with NheI/SacI. *, desired fragment; °, episomal form; [], empty vector; x, cut-out fragment, and **(D)** vector map of pFIV2-Val.

Table S1 | Data of qPCR analysis determining the copy number of FIV-Val.

REFERENCES

- Becker, S., Lochau, P., Jacob, D., Heuner, K., and Grunow, R. (2016). Successful re-evaluation of broth medium T for the growth of *Francisella tularensis* ssp. and other highly pathogenic bacteria. *J. Microbiol. Methods* 121, 5–7. doi: 10.1016/j.mimet.2015.11.018
- Bönquist, L., Lindgren, H., Golovliov, I., Guina, T., and Sjostedt, A. (2008). MglA and Igl proteins contribute to the modulation of *Francisella tularensis* live vaccine strain-containing phagosomes in murine macrophages. *Infect. Immun.* 76, 3502–3510. doi: 10.1128/IAI.00226-08
- Campbell, A. (2003). Prophage insertion sites. *Res. Microbiol.* 154, 277–282. doi: 10.1016/S0923-2508(03)00071-8
- Challacombe, J. F., Petersen, J. M., Gallegos-Graves, V., Hodge, D., Pillai, S., and Kuske, C. R. (2017a). Whole-Genome relationships among *Francisella* bacteria of diverse origins define new species and provide specific regions for detection. *Appl. Environ. Microbiol.* 83:e02589-16. doi: 10.1128/AEM.02589-16
- Challacombe, J. F., Pillai, S., and Kuske, C. R. (2017b). Shared features of cryptic plasmids from environmental and pathogenic *Francisella* species. *PLoS ONE* 12:e0183554. doi: 10.1371/journal.pone.0183554
- Clarridge, J. E. III., Raich, T. J., Sjostedt, A., Sandstrom, G., Darouiche, R. O., Shawa, R. M., et al. (1996). Characterization of two unusual clinically significant *Francisella* strains. *J. Clin. Microbiol.* 34, 1995–2000.
- Ellis, J., Oyston, P. C., Green, M., and Titball, R. W. (2002). Tularemia. *Clin. Microbiol. Rev.* 15, 631–646. doi: 10.1128/CMR.15.4.631-646.2002
- Ericsson, M., Golovliov, I., Sandstrom, G., Tarnvik, A., and Sjostedt, A. (1997). Characterization of the nucleotide sequence of the *groE* operon encoding heat shock proteins chaperone-60 and –10 of *Francisella tularensis* and determination of the T-cell response to the proteins in individuals vaccinated with *F. tularensis*. *Infect. Immun.* 65, 1824–1829.
- Golovliov, I., Sjostedt, A., Mokrievich, A., and Pavlov, V. (2003). A method for allelic replacement in *Francisella tularensis*. *FEMS Microbiol. Lett.* 222, 273–280. doi: 10.1016/S0378-1097(03)00313-6
- Hoang, T. T., Kutchma, A. J., Becher, A., and Schweizer, H. P. (2000). Integration-proficient plasmids for *Pseudomonas aeruginosa*: site-specific integration and use for engineering of reporter and expression strains. *Plasmid* 43, 59–72. doi: 10.1006/plas.1999.1441
- Hollis, D. G., Weaver, R. E., Steigerwalt, A. G., Wenger, J. D., Moss, C. W., and Brenner, D. J. (1989). *Francisella philomiragia* comb. nov. (formerly *Yersinia philomiragia*) and *Francisella tularensis* biogroup *novicida* (formerly *Francisella novicida*) associated with human disease. *J. Clin. Microbiol.* 27, 1601–1608.
- Keim, P., Johansson, A., and Wagner, D. M. (2007). Molecular epidemiology, evolution, and ecology of *Francisella*. *Ann. N. Y. Acad. Sci.* 1105, 30–66. doi: 10.1196/annals.1409.011
- Laemmli, U. K. (1970). Cleavage of structural proteins during the assembly of the head of bacteriophage T4. *Nature* 227, 680–685. doi: 10.1038/227680a0
- Lai, X. H., Golovliov, I., and Sjostedt, A. (2004). Expression of IglC is necessary for intracellular growth and induction of apoptosis in murine macrophages by *Francisella tularensis*. *Microb. Pathog.* 37, 225–230. doi: 10.1016/j.micpath.2004.07.002
- Lauer, P., Chow, M. Y., Loessner, M. J., Portnoy, D. A., and Calendar, R. (2002). Construction, characterization, and use of two *Listeria monocytogenes* site-specific phage integration vectors. *J. Bacteriol.* 184, 4177–4186. doi: 10.1128/JB.184.15.4177-4186.2002
- Lautner, M., Schunder, E., Herrmann, V., and Heuner, K. (2013). Regulation, integrase-dependent excision, and horizontal transfer of genomic islands in *Legionella pneumophila*. *J. Bacteriol.* 195, 1583–1597. doi: 10.1128/JB.01739-12
- Lee, C. Y., Buranen, S. L., and Ye, Z. H. (1991). Construction of single-copy integration vectors for *Staphylococcus aureus*. *Gene* 103, 101–105. doi: 10.1016/0378-1119(91)90399-V
- Le Pihive, E., Blaha, D., Chenavas, S., Thibault, F., Vidal, D., and Valade, E. (2009). Description of two new plasmids isolated from *Francisella philomiragia* strains and construction of shuttle vectors for the study of *Francisella tularensis*. *Plasmid* 62, 147–157. doi: 10.1016/j.plasmid.2009.07.001
- Lesic, B., and Carniel, E. (2005). Horizontal transfer of the high-pathogenicity island of *Yersinia pseudotuberculosis*. *J. Bacteriol.* 187, 3352–3358. doi: 10.1128/JB.187.10.3352-3358.2005
- LoVullo, E. D., Molins-Schneekloth, C. R., Schweizer, H. P., and Pavelka, M. S. Jr. (2009a). Single-copy chromosomal integration systems for *Francisella tularensis*. *Microbiology* 155, 1152–1163. doi: 10.1099/mic.0.022491-0
- LoVullo, E. D., Sherrill, L. A., and Pavelka, M. S. Jr. (2009b). Improved shuttle vectors for *Francisella tularensis* genetics. *FEMS Microbiol. Lett.* 291, 95–102. doi: 10.1111/j.1574-6968.2008.01440.x
- LoVullo, E. D., Sherrill, L. A., Perez, L. L., and Pavelka, M. S. Jr. (2006). Genetic tools for highly pathogenic *Francisella tularensis* subsp. *tularensis*. *Microbiology* 152, 3425–3435. doi: 10.1099/mic.0.29121-0
- Ludu, J. S., Nix, E. B., Duplantis, B. N., De Bruin, O. M., Gallagher, L. A., Hawley, L. M., et al. (2008). Genetic elements for selection, deletion mutagenesis and complementation in *Francisella* spp. *FEMS Microbiol. Lett.* 278, 86–93. doi: 10.1111/j.1574-6968.2007.00979.x
- Maier, T. M., Havig, A., Casey, M., Nano, F. E., Frank, D. W., and Zahrt, T. C. (2004). Construction and characterization of a highly efficient *Francisella* shuttle plasmid. *Appl. Environ. Microbiol.* 70, 7511–7519. doi: 10.1128/AEM.70.12.7511-7519.2004
- Norqvist, A., Kuoppa, K., and Sandstrom, G. (1996). Construction of a shuttle vector for use in *Francisella tularensis*. *FEMS Immunol. Med. Microbiol.* 13, 257–260. doi: 10.1111/j.1574-695X.1996.tb00248.x
- O'shaughnessy, J. B., Chan, M., Clark, K., and Ivanetich, K. M. (2003). Primer design for automated DNA sequencing in a core facility. *Biotechniques* 35, 118–121.
- Pavlovich, N. V., and Mishan'kin, B. N. (1987). [Transparent nutrient medium for culturing *Francisella tularensis*]. *Antibiot. Med. Biotechnol.* 32, 133–137.
- Pomerantsev, A. P., Golovliov, I. R., Ohara, Y., Mokrievich, A. N., Obuchi, M., Norqvist, A., et al. (2001). Genetic organization of the *Francisella* plasmid pFNL10. *Plasmid* 46, 210–222. doi: 10.1006/plas.2001.1548
- Qu, P. H., Chen, S. Y., Scholz, H. C., Busse, H. J., Gu, Q., Kampfer, P., et al. (2013). *Francisella guangzhouensis* sp. nov., isolated from air-conditioning systems. *Int. J. Syst. Evol. Microbiol.* 63, 3628–3635. doi: 10.1099/ijs.0.049916-0
- Qu, P. H., Li, Y., Salam, N., Chen, S. Y., Liu, L., Gu, Q., et al. (2016). *Allofrancisella inopinata* gen. nov., sp. nov. and *Allofrancisella frigidiquae* sp. nov., isolated from water-cooling systems, and transfer of *Francisella guangzhouensis* Qu et al. 2013 to the new genus *Allofrancisella guangzhouensis* comb. nov. *Int. J. Syst. Evol. Microbiol.* 66, 4832–4838. doi: 10.1099/ijsem.0.01437
- Ramsey, K. M., Osborne, M. L., Vvedenskaya, I. O., Su, C., Nickels, B. E., and Dove, S. L. (2015). Ubiquitous promoter-localization of essential virulence regulators in *Francisella tularensis*. *PLoS Pathog.* 11:e1004793. doi: 10.1371/journal.ppat.1004793
- Rydzewski, K., Schulz, T., Brzuszkiewicz, E., Holland, G., Luck, C., Fleischer, J., et al. (2014). Genome sequence and phenotypic analysis of a first German *Francisella* sp. isolate (W12-1067) not belonging to the species *Francisella tularensis*. *BMC Microbiol.* 14:169. doi: 10.1186/1471-2180-14-169
- Rydzewski, K., Tlapak, H., Niehaus, I. P., Dabrowski, P. W., Grunow, R., and Heuner, K. (2015). Identification and characterization of episomal forms of integrative genomic islands in the genus *Francisella*. *Int. J. Med. Microbiol.* 305, 874–880. doi: 10.1016/j.ijmm.2015.08.037
- Schulze, C., Heuner, K., Myrtennas, K., Karlsson, E., Jacob, D., Kutzer, P., et al. (2016). High and novel genetic diversity of *Francisella tularensis* in Germany and indication of environmental persistence. *Epidemiol. Infect.* 144, 3025–3036. doi: 10.1017/S0950268816001175
- Schunder, E., Rydzewski, K., Grunow, R., and Heuner, K. (2013). First indication for a functional CRISPR/Cas system in *Francisella tularensis*. *Int. J. Med. Microbiol.* 303, 51–60. doi: 10.1016/j.ijmm.2012.11.004
- Siddaramappa, S., Challacombe, J. F., Petersen, J. M., Pillai, S., and Kuske, C. R. (2014). Comparative analyses of a putative *Francisella* conjugative element. *Genome* 57, 137–144. doi: 10.1139/gen-2013-0231

- Steinmetz, M., Le Coq, D., Aymerich, S., Gonzy-Treboul, G., and Gay, P. (1985). The DNA sequence of the gene for the secreted *Bacillus subtilis* enzyme levansucrase and its genetic control sites. *Mol. Gen. Genet.* 200, 220–228. doi: 10.1007/BF00425427
- Steinmetz, M., Le Coq, D., Djemia, H. B., and Gay, P. (1983). [Genetic analysis of sacB, the structural gene of a secreted enzyme, levansucrase of *Bacillus subtilis* Marburg]. *Mol. Gen. Genet.* 191, 138–144. doi: 10.1007/BF00330901
- Whipp, M. J., Davis, J.M., Lum, G., De Boer, J., Zhou, Y., Bearden, S. W., et al. (2003). Characterization of a novicida-like subspecies of *Francisella tularensis* isolated in Australia. *J. Med. Microbiol.* 52, 839–842. doi: 10.1099/jmm.0.05245-0

Conflict of Interest Statement: The authors declare that the research was conducted in the absence of any commercial or financial relationships that could be construed as a potential conflict of interest.

Copyright © 2018 Tlapák, Köppen, Rydzewski, Grunow and Heuner. This is an open-access article distributed under the terms of the Creative Commons Attribution License (CC BY). The use, distribution or reproduction in other forums is permitted, provided the original author(s) and the copyright owner are credited and that the original publication in this journal is cited, in accordance with accepted academic practice. No use, distribution or reproduction is permitted which does not comply with these terms.



Population Genomics of *Francisella tularensis* subsp. *holarctica* and its Implication on the Eco-Epidemiology of Tularemia in Switzerland

Matthias Wittwer^{1,2*}, Ekkehard Altpeter³, Paola Pilo⁴, Sebastian M. Gygli^{5,6}, Christian Beuret¹, Frederic Foucault⁷, Rahel Ackermann-Gäumann^{1,8}, Urs Karrer^{6,9}, Daniela Jacob¹⁰, Roland Grunow¹⁰ and Nadia Schürch^{1,2}

¹ Spiez Laboratory, Federal Office for Civil Protection, Spiez, Switzerland, ² Swiss National Reference Center for *Francisella tularensis* (NANT), Spiez, Switzerland, ³ Swiss Federal Office of Public Health, Bern, Switzerland, ⁴ Department of Infectious Diseases and Pathobiology, Institute of Veterinary Bacteriology, University of Berne, Berne, Switzerland, ⁵ Swiss Tropical and Public Health Institute, Basel, Switzerland, ⁶ University of Basel, Basel, Switzerland, ⁷ Mabritec AG, Riehen, Switzerland, ⁸ Swiss National Reference Centre for Tick-Transmitted Diseases (NRZK), Spiez, Switzerland, ⁹ Cantonal Hospital Winterthur, Winterthur, Switzerland, ¹⁰ ZBS 2, Center for Biological Threats and Special Pathogens, Robert Koch Institute, Berlin, Germany

OPEN ACCESS

Edited by:

Jiri Stulik,
University of Defense, Czechia

Reviewed by:

Prabhu B. Patil,
Institute of Microbial Technology
(CSIR), India
Jason Sahl,
Northern Arizona University,
United States

*Correspondence:

Matthias Wittwer
matthias.wittwer@babs.admin.ch

Received: 21 December 2017

Accepted: 07 March 2018

Published: 22 March 2018

Citation:

Wittwer M, Altpeter E, Pilo P, Gygli SM, Beuret C, Foucault F, Ackermann-Gäumann R, Karrer U, Jacob D, Grunow R and Schürch N (2018) Population Genomics of *Francisella tularensis* subsp. *holarctica* and its Implication on the Eco-Epidemiology of Tularemia in Switzerland.
Front. Cell. Infect. Microbiol. 8:89.
doi: 10.3389/fcimb.2018.00089

Whole genome sequencing (WGS) methods provide new possibilities in the field of molecular epidemiology. This is particularly true for monomorphic organisms where the discriminatory power of traditional methods (e.g., restriction enzyme length polymorphism typing, multi locus sequence typing etc.) is inadequate to elucidate complex disease transmission patterns, as well as resolving the phylogeny at high resolution on a micro-geographic scale. In this study, we present insights into the population structure of *Francisella tularensis* subsp. *holarctica*, the causative agent of tularemia in Switzerland. A total of 59 *Fth* isolates were obtained from castor bean ticks (*Ixodes ricinus*), animals and humans and a high resolution phylogeny was inferred using WGS methods. The majority of the *Fth* population in Switzerland belongs to the west European B.11 clade and shows an extraordinary genetic diversity underlining the old evolutionary history of the pathogen in the alpine region. Moreover, a new B.11 subclade was identified which was not described so far. The combined analysis of the epidemiological data of human tularemia cases with the whole genome sequences of the 59 isolates provide evidence that ticks play a pivotal role in transmitting *Fth* to humans and other vertebrates in Switzerland. This is further underlined by the correlation of disease risk estimates with climatic and ecological factors influencing the survival of ticks.

Keywords: tularemia, whole genome sequencing (WGS), ticks, *Francisella tularensis* subsp. *holarctica*, ecology, epidemiology of infectious diseases, phylogenomics, canSNPs

INTRODUCTION

Classification of organisms according to inherent characteristics of their genome has become an indispensable principle in molecular biology. Over the years, progress in sequencing technologies led to an explosion in the amount of available sequencing data and an ever-increasing taxonomic resolution. This development culminated in the advent of massive parallel sequencing methods

that allow the classification and characterisation of an organism on a whole genome scale, opening new perspectives in molecular forensics, ecology, and epidemiology. The benefits of whole genome sequencing (WGS)-based classification are most pronounced when applied to genetically monomorphic organisms, for example *Mycobacterium tuberculosis* (Lee et al., 2015; Stucki et al., 2016), *Bacillus anthracis* (Girault et al., 2014) and *Francisella tularensis* (Dwivedi et al., 2016).

Tularaemia is caused by the gram negative, facultative intracellular bacterium *F. tularensis*. Due to its very low infective dose and high mortality when inhaled as aerosol, the organism is listed as a category A biothreat agent (Rotz et al., 2002). Two subspecies are responsible for most of the tularemia cases. *F. tularensis* subsp. *tularensis* (*Ftt*), and *F. tularensis* subsp. *holarctica* (*Fth*). In Europe, the less virulent *Fth* occurs and generally causes sporadic cases, of which the first were documented in the 1930s (Jusatz, 1961). *Fth*, however, occurs throughout the northern hemisphere. Since the late 1990s, case numbers are increasing and outbreaks exceeding 1,000 cases were reported in the Czech Republic, Hungary, Spain (Pérez-Castrillón et al., 2001), Sweden and Finland (Maurin and Gyuranecz, 2016). It is thought that in the United States the majority of *F. tularensis* infections are due to transmission from tick bites (Petersen et al., 2009) whereas in Europe, the situation is less clear. In Scandinavia, *Fth* is transmitted predominantly by mosquitoes and it is believed that the pathogen persists in an aquatic life cycle with mosquitoes, mosquito larvae and rodents (Desvars et al., 2015). The terrestrial lifecycle, with arthropods as reservoirs and small terrestrial rodents and lagomorphs, as susceptible hosts, is predominant in most European countries including Switzerland. In these countries, direct contact with infected rodents and lagomorphs seems to be the main route of infection. Concerning the transmission through arthropod vectors, the estimated percentage of tularaemia cases due to tick bites varies between 12% (Slovakia) and 26% (France) (Maurin and Gyuranecz, 2016). Since tularaemia is a notifiable disease in Switzerland, epidemiological data is collected from patient reports sent from the initial point of care to the health authorities. According to this information, tick bites could be associated with 47% of the tularaemia cases reported during the last 10 years. However, the quality of questionnaire-based data is often limited. Additionally, the confirmation of a causal connection between arthropod bites and tularaemia cases using a method providing adequate discriminative power has been lacking. In this study the epidemiology, routes of transmission, and phylo-geographic properties of tularaemia in Switzerland are delineated based on 59 sequenced genomes of *Fth* isolated from humans, animals and ticks (Table 1).

MATERIALS AND METHODS

Collection of Ticks

Between 2009 and 2015 a total of 120,000 questing ticks were collected at 165 collection sites throughout Switzerland by flagging low vegetation. Ticks were randomly identified based on morphological characteristics (Keirans, 1997) and immediately stored at -80°C . Subsequently, ticks were washed once in 75%

ethanol and twice in deionized water, dried on paper towels, and sorted into pools of 10 nymphs or 5 adult male or female *I. ricinus* ticks. Pooled samples were stored at -80°C until further processing (Gäumann et al., 2010).

Homogenization of Ticks

Tick homogenates were prepared from frozen tick pools of 10 nymphs or 5 adult female or male ticks as follows: 600 μl of cold PBS was added to each frozen tick pool. Samples were immediately homogenized using the TissueLyser system (Qiagen). Briefly, one 3-mm tungsten carbide bead (Qiagen) was added to each tube (collection microtubes; Qiagen), and tick pools were homogenized for 4 min at 30 Hz. After centrifuging the samples for 5 s at 3,220 g, supernatants were collected and split for further use: One 200 μl aliquot was used for DNA extraction and four 150 μl aliquots were immediately frozen in liquid nitrogen and stored at -80°C . To increase success rates of subsequent cultivation efforts, 40 μl glycerol (100%) was added as a cryoprotectant to two aliquots.

Screening of Tick Homogenates for the Presence of *Fth*

DNA was automatically extracted using a magnetic bead based protocol (QiaSymphony, QIAGEN). In total, 16,000 tick pools were screened for the presence of *Fth* using a one-step real-time RT-PCR assay based on the VNTR marker Ft-M19 (Byström et al., 2005). The Ft-M19 PCR positive samples were confirmed by an in-house real-time RT-PCR assay targeting the *fopA* gene (Table 2).

Isolation of *Fth* From Homogenized Tick Samples

Aliquots of the PCR positive samples were cultivated. Briefly, frozen aliquots were quickly thawed and 50 μl each was inoculated in 10 ml Broth Medium T (Becker et al., 2016), as well as streaked on Chocolate Agar PolyViteX (BioMérieux) and Thayer Martin VCNT Neisseria Selective Agar (Oxoid). Plates and liquid cultures were incubated at 37°C using GENBox C02 (BioMérieux) for 2–6 days. Presumptive *Fth* cultures were confirmed by real-time PCR as described above (*fopA*; Table 2).

DNA Isolation for WGS

All manipulations with live cultures were performed in a BSL 3 containment laboratory (approval number: A110502/3). Isolates of *Fth* were grown on Chocolate Agar PolyViteX (BioMérieux) for 2 days and colonies were harvested and suspended in 500 μl AVL Buffer (Qiagen). Lysates were heat inactivated for 15 min at 100°C and DNA was subsequently extracted using the EZ1 or the EZ1 Advanced robot (Qiagen) according to the manufacturer's instructions (EZ1, Tissue Kit, Bacteria Card, Qiagen).

Human Samples

In its function as the Swiss national reference center for tularemia in humans, the Spiez Laboratory maintains a culture collection of *Fth* isolates derived from routine clinical diagnostics. The patient and epidemiological data are collected by the Federal Office of

TABLE 1 | Overview of the 59 whole genome sequenced *Fth* strains from Switzerland used in this study.

Sample ID	Alternative ID	Source, year	Clade	Sequencing institute/ Sample provider	Length of assembly	Contigs	N50	Accession number	
FT 29	JF5340 ^a	Human, 2012	B.33	SL/IVB	1798068	102	26695	SAMN08108654	PKBF00000000
FT 31	JF5370 ^a	Human, 2012	B.33	SL/IVB, ADMED	1794649	100	27062	SAMN08108656	PKBD00000000
FT 65	JF5405 ^a	Hare, 2012	B.33	SL/IVB	1802560	102	27621	SAMN08108682	PKAE00000000
FT 66	JF5468 ^a	Hare, 2013	B.33	SL/IVB	1823931	98	27394	SAMN08108683	PKAD00000000
FT 70	JF5609	Monkey, 2014	B.33	SL/IVB	1823454	96	27316	SAMN08108687	PJZ000000000
FT 22	JF4456 ^a	Human, 2008	B.45	SL/IVB	1801181	95	27456	SAMN08108648	PKBL00000000
FT 32 ^b		Human, 2012	B.45	SL/IVB	1812310	95	27658	SAMN03774932	PKAX00000000
FT 41	FT6_D12	Tick, 2012	B.45	SL	1782791	96	26944	SAMN08108662	PKAK00000000
FT 56	JF5353 ^a	Marten, 2012	B.45	SL/IVB	1818006	97	27313	SAMN08108675	PKAC00000000
FT 67	JF5487	Hare, 2013	B.45	SL/IVB	1822695	96	27391	SAMN08108684	PJZY00000000
FT 71	JF5611	Hare, 2014	B.45	SL/IVB	1812653	98	27006	SAMN08108688	PKBP00000000
FT 14	JF3829	Lion Tamarin, 2004	B.46	SL/IVB	1801041	95	27712	SAMN08108642	PKBR00000000
FT 17	JF4128/FDC304 ^b	Human, 2008	B.46	SL/IVB	1778390	101	24282	SAMN08108644	PKBH00000000
FT 27	JF5141	Human, 2011	B.46	SL/IVB	1807038	109	26708	SAMN08108652	PKBG00000000
FT 28	JF5338	Human, 2012	B.46	SL/IVB	1788115	102	26847	SAMN08108653	PKBT00000000
FT 11	JF3821	Hare, 1997	B.49	SL/IVB	1801451	95	27456	SAMN08108640	PKBQ00000000
FT 16	JF4092	Hare	B.49	SL/IVB	1801566	95	27456	SAMN08108643	PKAQ00000000
FT 50		Human 2014	B.49	SL	1823626	96	27535	SAMN08108669	PKBO00000000
FT 18	JF4212/FDC305 ^b	Human, 2008	B.53	SL/IVB	1801159	95	27712	SAMN03773856	PKBB00000000
FT 36		Human, 2014	B.53	SL	1817604	96	27313	SAMN08108658	PKAS00000000
FT 48		Human, 2014	B.53	SL	1817319	96	27313	SAMN08108667	PKAJ00000000
FT 57	JF5369 ^a	Hare, 2012	B.53	SL/IVB	1809350	97	27005	SAMN08108676	PKAW00000000
FT 38	FT9C_G7 ^b	Tick, 2012	B.59	SL	1811355	96	27676	SAMN03774936	PKAU00000000
FT 42	FT11_B4	Tick, 2012	B.59	SL	1783150	96	26974	SAMN08108663	PKBI00000000
FT 45	FT8_F4	Tick, 2012	B.59	SL	1814235	96	27658	SAMN03774935	PKAO00000000
FT 46	FT8_B3	Tick, 2012	B.59	SL	1780077	95	26974	SAMN08108665	PKAN00000000
FT 26	JF5142	Human, 2011	B.61	SL/IVB	1800278	102	27104	SAMN08108651	PKAM00000000
FT 52	FT21_C4	Tick, 2013	B.61	SL	1801053	95	27456	SAMN08108671	PKAH00000000
FT 53	FT22_F9	Tick, 2013	B.61	SL	1801183	95	27456	SAMN08108672	PKBA00000000
FT 54	FT22_H4	Tick, 2013	B.61	SL	1801200	95	27456	SAMN08108673	PKAZ00000000
FT 59	JF5375 ^a	Hare, 2012	B.61	SL/IVB	1819651	97	27313	SAMN08108678	PKAY00000000
FT 37	FT14_F1	Tick, 2012	B.62	SL	1779923	96	26888	SAMN08108659	PKAV00000000
FT 39	FT14_C4	Tick, 2012	B.62	SL	1780016	96	26888	SAMN08108660	PKAT00000000
FT 40	FT17_C9	Tick, 2012	B.62	SL	1782242	96	26888	SAMN08108661	PJZW00000000
FT 43	FT16_B1 ^b	Tick, 2012	B.62	SL	1805387	95	27658	SAMN03774942	PKBU00000000
FT 44	FT16_E6	Tick, 2012	B.62	SL	1795991	96	27077	SAMN08108664	PKBV00000000
FT 47	FT16_G8 ^b	Tick, 2012	B.62	SL	1781679	96	26888	SAMN08108666	PKBS00000000
FT 75		Human, 2015	B.62	SL	1797368	95	27019	SAMN08108690	PKBM00000000
FT 08		Human, 2003	B.85	SL/IVB	1775380	133	21731	SAMN08108638	PKAG00000000
FT 10	JF3820 ^a	Hare, 1998	B.85	SL/IVB	1772027	102	23187	SAMN08108639	PKAB00000000
FT 13	JF3826 ^a	Marmoset, 1996	B.85	SL/IVB	1801174	95	27456	SAMN08108641	PKBK00000000
FT 20	JF4429/FDC310 ^b	Human, 2008	B.85	SL/IVB	1814653	96	27257	SAMN03773858	PKAP00000000
FT 60	JF5380 ^a	Hare, 2012	B.85	SL/IVB	1801233	95	27456	SAMN08108679	PKAL00000000
FT 68	JF5525	Hare, 2014	B.85	SL/IVB	1818684	96	27313	SAMN08108685	PKBY00000000
FT 24	JF5002	Human, 2011	B.87	SL/IVB	1786520	97	26974	SAMN08108649	PKBW00000000
FT 51		Human, 2014	B.87	SL	1820050	96	27535	SAMN08108670	PKBJ00000000
FT 55	JF5345	Mouse, 2012	B.87	SL/IVB	1825678	100	27313	SAMN08108674	PKBE00000000
FT 64	JF5410 ^a	Mouse, 2012	B.87	SL/IVB	1819162	96	27313	SAMN08108681	PJZX00000000
FT 07		Human, 2008	B.88	SL	1782483	96	26925	SAMN08108637	PKBN00000000

(Continued)

TABLE 1 | Continued

Sample ID	Alternative ID	Source, year	Clade	Sequencing institute/ Sample provider	Length of assembly	Contigs	N50	Accession number	
FT 25	JF5048	Human, 2011	B.88	SL/IVB	1797415	97	27104	SAMN08108650	PKBC00000000
FT 30	JF53461	Human, 2012	B.88	SL/IVB	1783341	96	27105	SAMN08108655	PKBX00000000
FT 19	JF4242/FDC306 ^b	Hare	B.89	SL/IVB	1801171	95	27712	SAMN03773857	PKAI00000000
FT 33		Human, 2013	B.89	SL	1820901	96	27535	SAMN08108657	PKAF00000000
FT 73		Human, 2015	B.89	SL	1797389	95	27712	SAMN08108689	PKAR00000000
FT 05		Human, 2008	B.90	SL/IVB	1797365	95	27456	SAMN08108636	PKAA00000000
FT 58	JF5374 ^a	Hare, 2014	B.90	SL/IVB	1819228	96	27313	SAMN08108677	MQVE00000000
FT 63	JF5393 ^a	Hare, 2012	B.90	SL/IVB	1824976	96	27435	SAMN08108680	MQVC00000000
FT 49		Human, 2014	B.91	SL	1822738	96	27535	SAMN08108668	MQVF00000000
FT 69	JF5597	Hare, 2014	B.91	SL/IVB	1818326	96	27313	SAMN08108686	MQVD00000000

SL, Spiez laboratory, Spiez, Switzerland; IVB, Institute of Veterinary Bacteriology, Bern, Switzerland; ADMED, Analyses et Diagnostics Medicaux, La Chaux de Fonds, Switzerland.

^aOriggi et al. (2014).

^bDwibedi et al. (2016).

TABLE 2 | PCR assays targeting the Francisella Outer Membrane Protein A used for *F. tularensis* ssp. screening.

Target		Sequence	Primer length
FopA-F	Forward primer	5'-CAAATCTAGCAGGTCAAGCAACAG-3'	24
FopA-R	Reverse primer	5'-CACTTGCTTGAACATTTCTAGATAGTTCA-3'	29
FopA-S	Probe	FAM-5'-TGCTTGGGATGTGGGTGGTGGTC-3'-BHQ1	23

Amplicon length = 270 bp.

Public Health according to the Epidemics Law and Ordinance (SR 818.101.126).

Animal Samples

Strains isolated from animals were selected from the strain collection of the Institute of Veterinary Bacteriology, Vetsuisse Bern, Switzerland, which is the national reference center for tularemia in animals.

Whole Genome Sequencing

The 59 *Fth* isolates were sequenced on the Illumina HiSeq 2500 platform using the TruSeq paired end chemistry for library preparation. The average read length was 126 bp and the average insert size was 350 bp (standard deviation = 87.593, lower quantile = 272, upper quantile = 488). Prior to the assembly the ~50,000,000 sequencing reads were quality trimmed with *Trimmomatic V0.32* (Bolger et al., 2014).

The quality trimmed reads were assembled using *SPAdes-3.10.1* (Bankevich et al., 2012) resulting in ~100 contigs with an average N50 of 27,000 bp. The coverage of the *Fth* genomes was >1,000 × in all samples. In order to use the pan genome pipeline *Roary* (Page et al., 2015), *gff3* annotation files were generated with *Prokka* (Seemann, 2014) using the Franco-Iberian *Fth* FTNF002-00 (NC_009749) strain as reference. Based on these *gff3* files, the core- and pan-genomes were inferred using *Roary* by applying a 95% *blastp* identity threshold. A given gene had to be present in 100% of the samples to be included into the core-genome. *Mafft* (Katoh et al., 2002) was used for core genome alignment. Ambiguously aligned

regions and Indels were removed from the *Mafft* alignment by *Gblocks* (Castresana, 2000) and *SEQfire* (Ajawatanawong et al., 2012). Maximum likelihood phylogenies were inferred with *PhyML* (Initial tree: BioNJ; Tree topology search: NNIs; Model of nucleotide substitution: TN93; Bootstrap replicates: 1000) (Guindon et al., 2010). Mutations in the sequenced strains relative to the reference genomes were identified with *breseq* (Deatherage and Barrick, 2014).

To designate the sequenced strains to the established canSNP node nomenclature the software canSNPer (Lärkeryd et al., 2014) was used. Naming of the novel subtypes found in this study is in agreement with the canSNP nomenclature scheme assigning an increasing ordinal number to each newly identified SNP. To implement the novel subtypes in the canSNPer tool, the text files containing the SNP positions and the tree topology were adjusted accordingly.

Calculation of average nucleotide identity using standard MUMmer algorithm (ANIm) from whole genome was done using a python program *pyani* (v0.2.4). Hierarchical cluster analysis of ANI correlation matrix was done using package *hclust* (R v3.4.3).

Spatial Statistics

Phylogeographic interpolation was performed with the R package *Phylin* (Tarroso et al., 2015). Calculation of spatial disease clusters was performed (carried out) with the R package *DCluster* (Hornik et al., 2003).

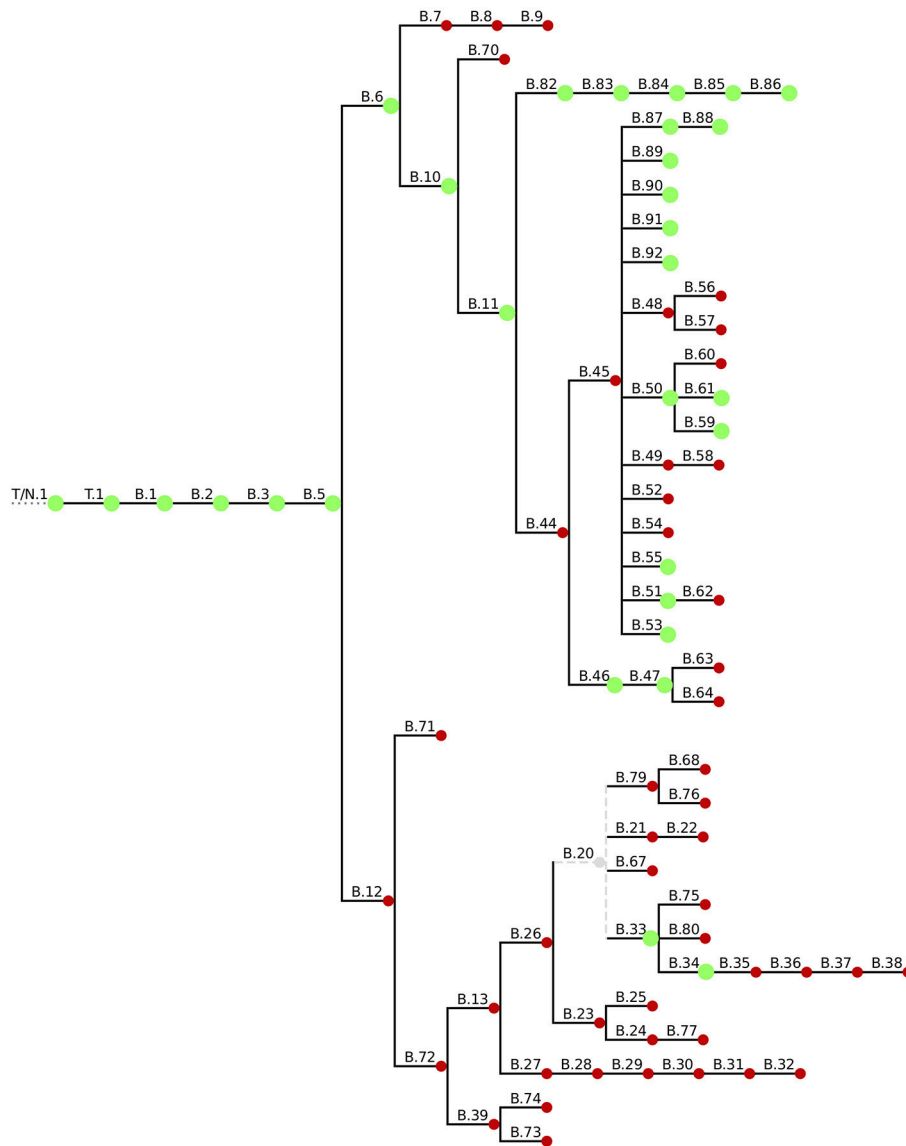


FIGURE 1 | Overview of the current canSNP typing scheme. Green blobs indicate the canSNP types found in the 59 sequenced Swiss *Fth* isolates.

RESULTS

Prevalence of *Fth* in Swiss Ticks

A total of 120,000 questing ticks were analyzed and only 25 tick homogenates were positive for *Fth* by PCR. This corresponds to a prevalence of ~0.02%.

Fourteen *Fth* isolates were successfully recovered from the 25 positive tick homogenates. The recovery from glycerol preserved samples was slightly improved and the isolation was often easier from Neisseria Agar than from Chocolate Agar due to reduced contaminating flora.

Phylogenetic Context of Swiss *Fth* Isolates

ANIm is a standard *in silico* method for bacterial species delimitation with a threshold value of 94–96%. Here, ANIm

was applied to validate that 59 isolates belong to *F. tularensis* subsp. *holarctica*. Whole genomes were compared to type strains: *F. tularensis* subsp. *tularensis* NIH B-38, *F. tularensis* subsp. *holarctica* FTNF002-00, *F. tularensis* subsp. *mediasiatica* FSC147, and *F. tularensis* subsp. *novicida* U112. In this small dataset, we found that an ANIm threshold of 99.5% could distinguish subspecies of *F. tularensis*. All 59 isolates showed >99.9% ANI identity to *F. tularensis* subsp. *holarctica* FTNF002-00 and *F. tularensis* subsp. *holarctica* FSC200.

To put the 59 Swiss *Fth* whole genome sequences in a global phylogenetic context we used a canonical SNP (canSNP) approach (Lärkeryd et al., 2014). According to this typing method, 54 strains (91.5%) were assigned to the B.11 clade, which is predominant in Western Europe including Switzerland (Pilo et al., 2009; Vogler et al., 2009; Dwibedi et al., 2016). Three animal

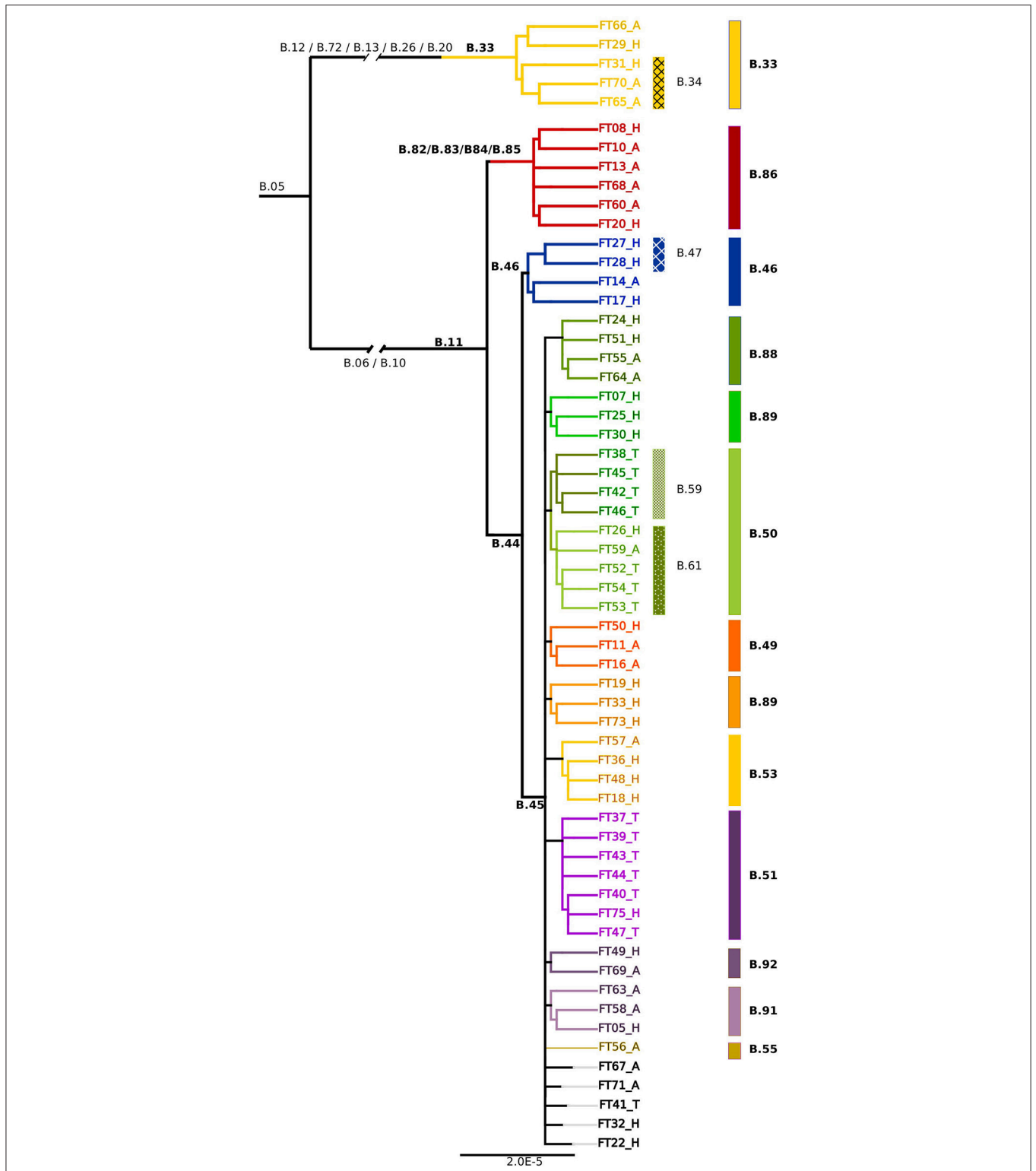
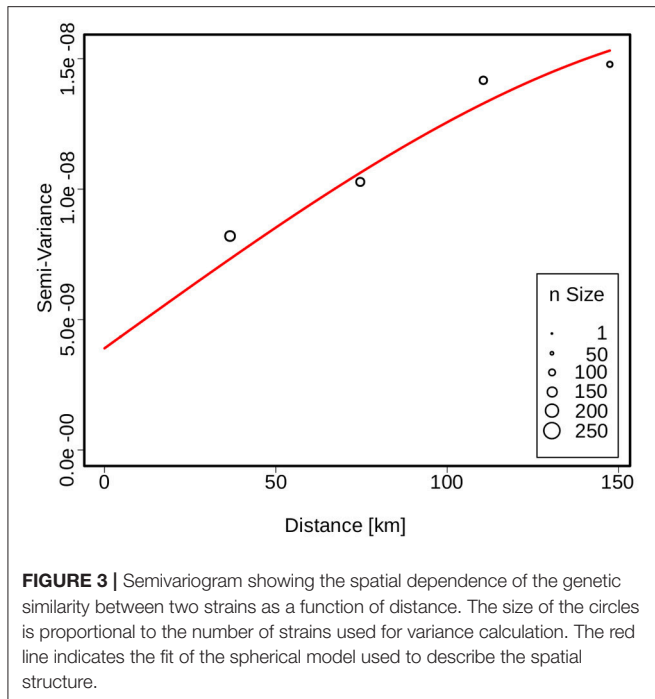


FIGURE 2 | Phylogenetic relationships based on the core genome alignment of 59 sequenced *Fth* strains. The clades and subclades are labeled according to the canSNP nomenclature. The ending letters of the tip labels indicate the source of the isolates (H, Human; A, Animal; T, Tick).



and two human isolates (11%) belong to the Northeast European B.12 clade (**Figure 1**).

To increase the phylogenetic resolution a core genome SNP analysis based on a 1477202bp alignment was applied and revealed a similar branching pattern of the B.11 clade as described in the European survey by Dwibedi et al. (2016). Clade B.45 was represented by 44 (18 human, 14 tick, 12 animal) and B.46 by four isolates (three human, 1 animal). In addition, six isolates (2 human, 4 animal) were assigned to a clade, which was previously represented by one Swiss isolate only. This novel B.11 subclade is distinguished by 5 SNPs (B.82/B.83/B.84/B.85/B.86; **Figure 2**).

Except of the clades B.48 and B.52 exclusively found in Spain, as well as the French B.54 clade, all subclades derived from B.45 were represented among the 59 sequenced isolates. In addition, five novel subclades deriving from B.45 could be identified (B.87/B.88, B.89, B.90, B.91, B.92; **Figure 2**).

The spatial dependence of the genetic variation among the isolates is represented by the semi-variogram shown in **Figure 3**. The good fit ($R^2 = 0.96$) of the applied spherical model clearly indicates a statistically significant dependence between genetic variation and geographic distance. The Kriging interpolation (Kriging, 1951), based on the model derived from the semi-variogram, shows that clade B.45 is spread over the majority of the Swiss territory below 1,500 m of altitude. The subclades of B.45 that show a higher spatial coherence are visible as focal hotspots (**Figure 4**). The clades B.46 and B.86 show a geographically more focused distribution (**Figure 5**). Three animal and one human isolate assigned to the Northeast European B.12 clade originated from areas close to the northern

and eastern Swiss border. One human isolate was isolated in central Switzerland.

Genetic Variation in the Swiss *Fth* Population

Breseq analysis revealed 259 polymorphisms within the 59 sequenced *Fth* genomes relative to the genome FTNF002-00. We identified 36 deletions, 28 insertions and 195 SNPs. Seventy-nine SNPs were non-synonymous. Of the 116 synonymous SNPs, 46 were located in coding regions of the genome. Regarding the mutations that were exclusively found in the newly defined B.86 subclade, 9 of the in total 17 SNPs were non-synonymous. Two non-synonymous mutations were found in genes associated with the heme (*hemA*) and cytochrome c (*FTA_0224*) biosynthesis. One mutation alters a member (*FTA_0090*) of the major facilitator superfamily (MFS) which is involved in the transport of small molecule substrates across all classes of organisms and plays an important role in sustaining the osmotic balance between the cytosol and the environment. The remaining 5 non-synonymous SNPs are found in genes coding for proteins involved in the carbohydrate (*FTA_0510*, *FTA_1026*, *FTA_1126*) and fatty-acid (*FTA_0617*) metabolism of *Fth* (**Table 3**).

All five strains assigned to the B.12 clade showed the SNPs in the *rrl* (23S rRNA) gene (A2059C and A453G) which were found to be responsible for the erythromycin resistance, which is characteristic for this clade (Karlsson et al., 2016). These findings are in agreement with the antibiotic susceptibility testing and MLVA typing results of Origgi et al. performed on the same isolates (Origgi et al., 2014).

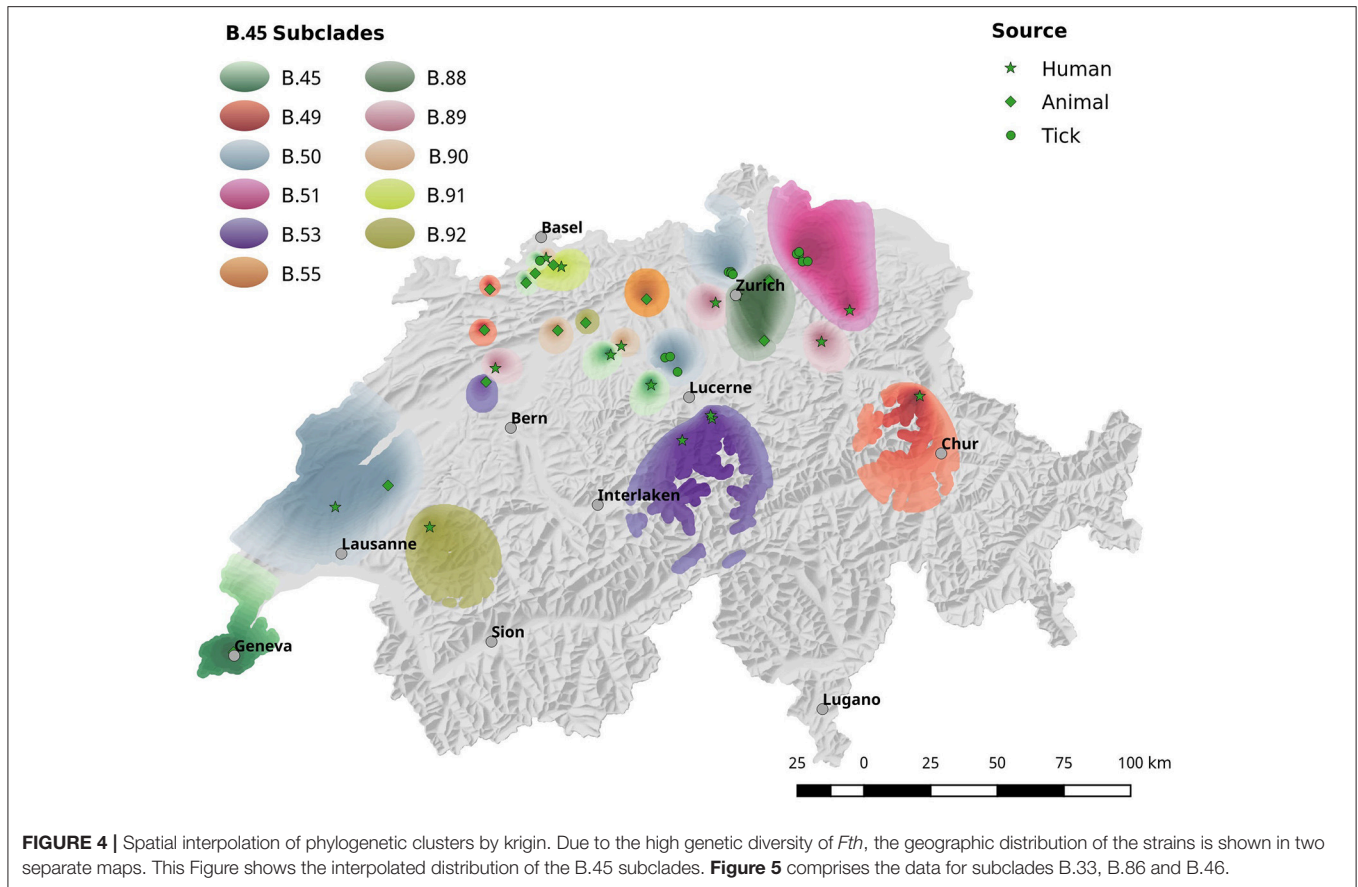
All genetic variations found in the core genome alignment with the strain FTNF00-002 as reference are included in a variant call file (vcf) as Supplementary Material (**Supplementary Table 1**).

Epidemiology of Tularemia in Switzerland

Since 2004, the incidence of tularemia in Switzerland has risen ~15-fold from 0.04 to 0.69 per 100,000 per year (**Figure 6**). With the exception of patients >75 years of age, males were generally more affected by tularemia. We observe a bimodal distribution of case numbers per age group with a narrow peak between 10 and 12 years of age and a broader peak spanning the ages from 27 to 75 years (**Figure 7**).

In agreement with a terrestrial lifecycle, *Fth* isolates from humans, animals and ticks are represented in the same terminal subclades. In subclade B.51, the tick derived isolates FT40/FT47 show no differences in the 1,474,944 bases core genome alignment with the human FT75 isolate. The same applies for the isolates FT05 (human) and FT58 (animal) in clade B.90.

The majority of the 276 patients reported an insect or arthropod bite prior to the occurrence of tularemia symptoms (33% tick-bite, 24% insects—total 57%). Contact with wild animals was assumed as the cause of 22% of the infections. In 23% of the cases, the source was unknown. The proportion of the cases with a suspected vector-borne source of tularemia infection correlated with the clinical manifestation of the disease.



The glandular/ulceroglandular type typically associated with the bite of a hematophagous arthropod was observed in 60% of the cases. The pulmonary type was represented in 24% and the abdominal/oropharyngeal type in 14% of the patients (**Figure 8**). Hence, 38% of the 276 reported infections can be attributed to direct or indirect contact with infected wild life.

Population corrected risk estimation on the spatial distribution of tularemia cases shows an uneven distribution. Areas with elevated relative risk are predominately located in the northeastern area of Switzerland (**Figure 9**). Our data suggest that ticks are the predominant source of infection in Switzerland. Therefore, we correlated the risk estimations with climatic as well as ecological factors known to influence the survival and vector competence of ticks. Relative humidity (RH) and saturation deficit (SD) are known to be of pivotal importance for tick abundance and survival. Consequently, we compared the surface normalized averages of waterlogging levels in areas with elevated risk for acquiring tularemia vs. low risk areas and found a highly significant effect of soil moisture (**Figures 10, 11**).

The reduction of biodiversity due to urbanization influences the competence of vectors by shifting the ratio of competent to non-competent hosts. Most of the regions with an elevated risk for acquiring tularemia are highly fragmented and show below average mesh sizes (**Figure 12**).

DISCUSSION

Prevalence, Genetic Diversity, and Population Genomics of Swiss *Fth* Isolates

The determined prevalence of 0.2‰ is low compared to other pathogens found in ticks (Oechslin et al., 2017) and confirms principally a previous smaller survey of the Swiss Army (Wicki et al., 2000).

The successful cultivation of *Fth* from ticks substantiate the role of *I. ricinus* as important vector of the pathogen. Furthermore, the availability of isolates was a prerequisite for the WGS inferred high-resolution phylogeny.

As described elsewhere (Origgi et al., 2014) the B.13 and B.11 strain are co-circulating in Switzerland with a predominance of the latter. Strikingly, the geographic origin of four of the five B.13 isolates is close to the northern and eastern Swiss border. Since the B.11 and B.13 strains are equally established in the German hare population (Müller et al., 2013) and B.13 prevails in Austria (Tomaso et al., 2005), our data suggests a sporadic intrusion of the B.13 strain from neighboring countries.

In accordance with recent publications regarding the dispersal of *Fth* in Europe (Dwibedi et al., 2016), Switzerland seems to harbor an exceptionally high genetic diversity of the pathogen compared to other European countries. The phylogenetic structure and proportion of the B.11 subclades derived from Swiss isolates are almost identical to the one reported in the

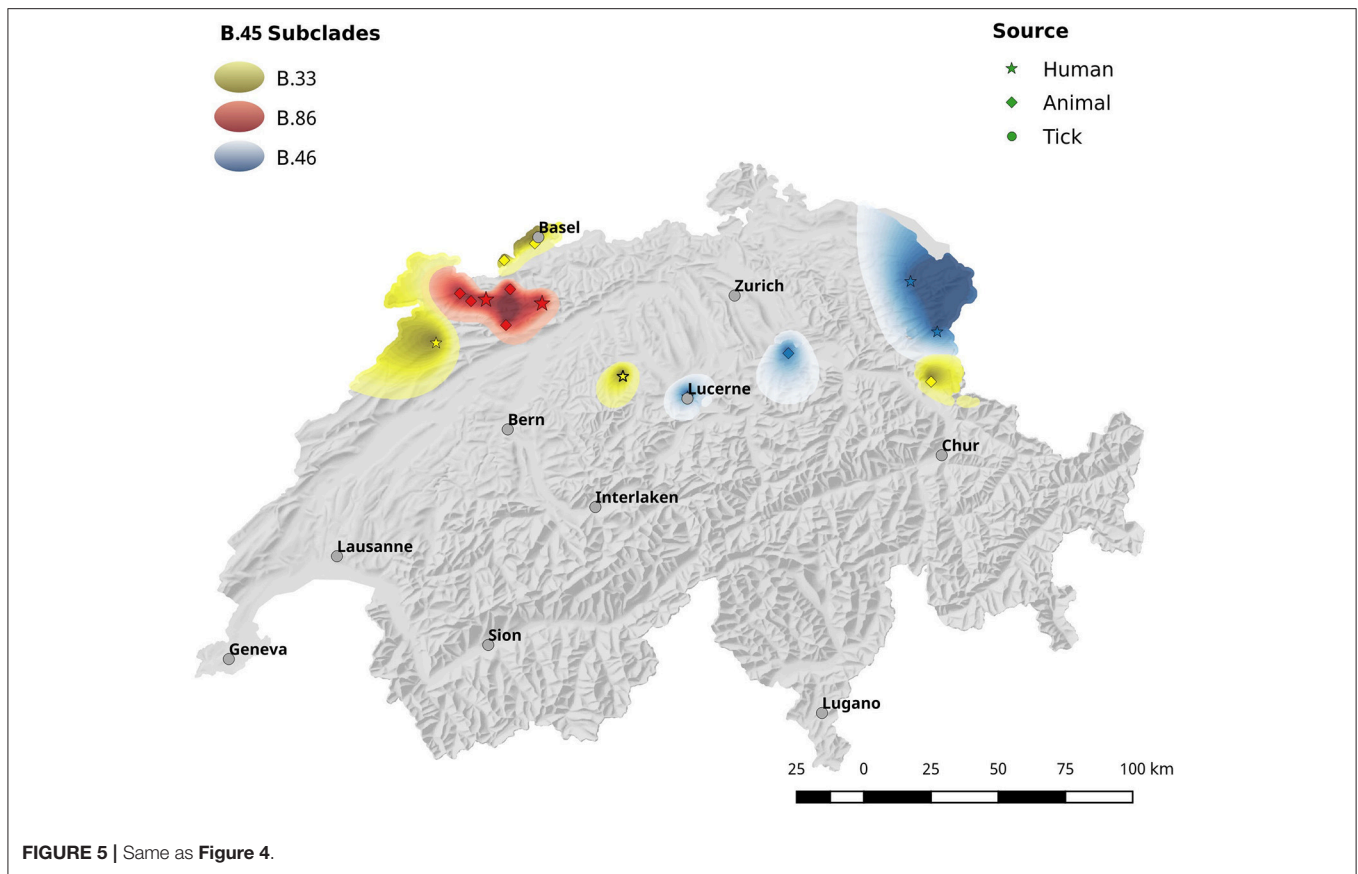


TABLE 3 | List of the non-synonymous SNPs identified with the *breseq* pipeline.

Position	Mutation	Annotation	Gene	Description
78116	C→T	V40I (GTT→ATT)	<i>FTA_0090</i> ←	Major facilitator family (MFS) transporter protein
207830	G→A	G61D (GGT→GAT)	<i>FTA_0224</i> →	Hypothetical membrane protein/putative cytochrome c-type biogenesis protein
468941	C→T	T425I (ACT→ATT)	<i>FTA_0510</i> →	Phosphoglucomutase/phosphomannomutase
563329	C→T	G221R (GGG→AGG)	<i>FTA_0617</i> ←	Acetyl-CoA acetyltransferase
944751	G→T	S162I (AGT→ATT)	<i>FTA_1026</i> →	Iron-containing alcohol dehydrogenase
1022282	G→T	R456M (AGG→ATG)	<i>FTA_1126</i> →	Phosphorylase family 2/alpha-beta hydrolase fold protein
1022285	A→G	D457G (GAC→GGC)	<i>FTA_1126</i> →	Phosphorylase family 2/alpha-beta hydrolase fold protein
1649613	A→C	I65R (ATA→AGA)	<i>hemA</i> ←	Glutamyl-tRNA reductase

The genomic positions correspond to the *FTNF002-00* strain (NC_009749.1).

European survey. In this aspect, Switzerland can be considered as a small-scale model for *Fth* population structure. Moreover, the identification of six additional B.11 subclades underlines the notion that the alpine region harbors an evolutionary older and highly diverse founder population (Dwivedi et al., 2016).

A major factor that is positively associated with the biodiversity of an ecosystem is the topographic complexity of a habitat (Zhou et al., 2015). Together with climate-related factors, topography is known to influence a wide array of environmental parameters including hydrology, nutrient dispersion, soil structure, and the microclimate. Furthermore, mountain ranges on the scale of the Swiss Alps form a relevant

barrier for animal migration. In this light, the observed diversity of the B.11 clade in Switzerland and the statistically significant correlation between genetic- and geographic distance may reflect small-scale topographic fragmentation of the habitat of the susceptible hosts and pathogen vectors.

Analysis of a Newly Identified B.11 Subclade

In agreement with the European survey, the B.45 subclade of B.11 was found to be the most successful subclade in Switzerland in terms of geographical distribution and prevalence. Noticeably,

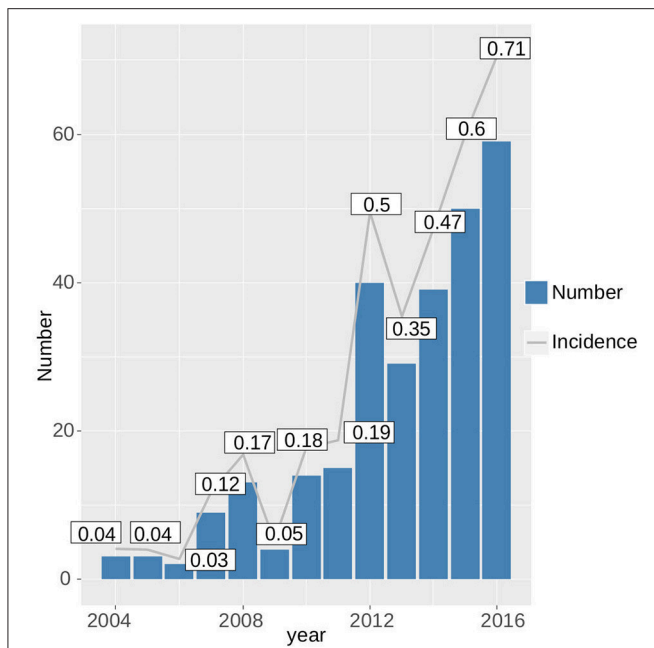


FIGURE 6 | Increase in the absolute case numbers and incidence of tularemia in Switzerland from 2004 to 2016.

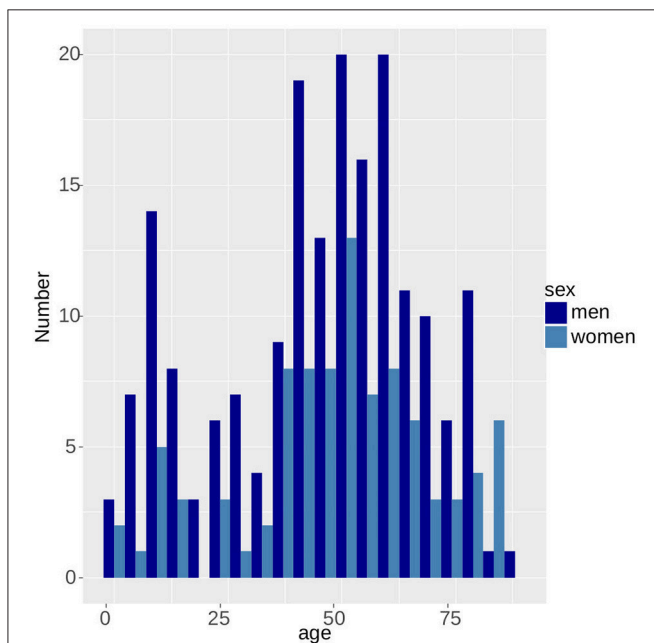


FIGURE 7 | Bimodal age distribution of tularemia patients. Men are more likely to be affected than women.

all of the 14 tick isolates from five different geographic regions were assigned to the B.45 clade, whereas B.46 and B.86 were solely comprised by human and animal isolates. One possible explanation for this observation could be that the strains of the B.45 subclade are better adapted to the arthropod vector and thus elevate the vector competence of the ticks, compared to ticks

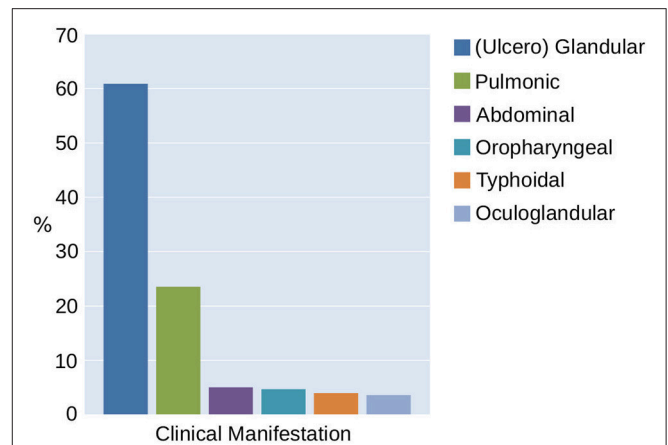
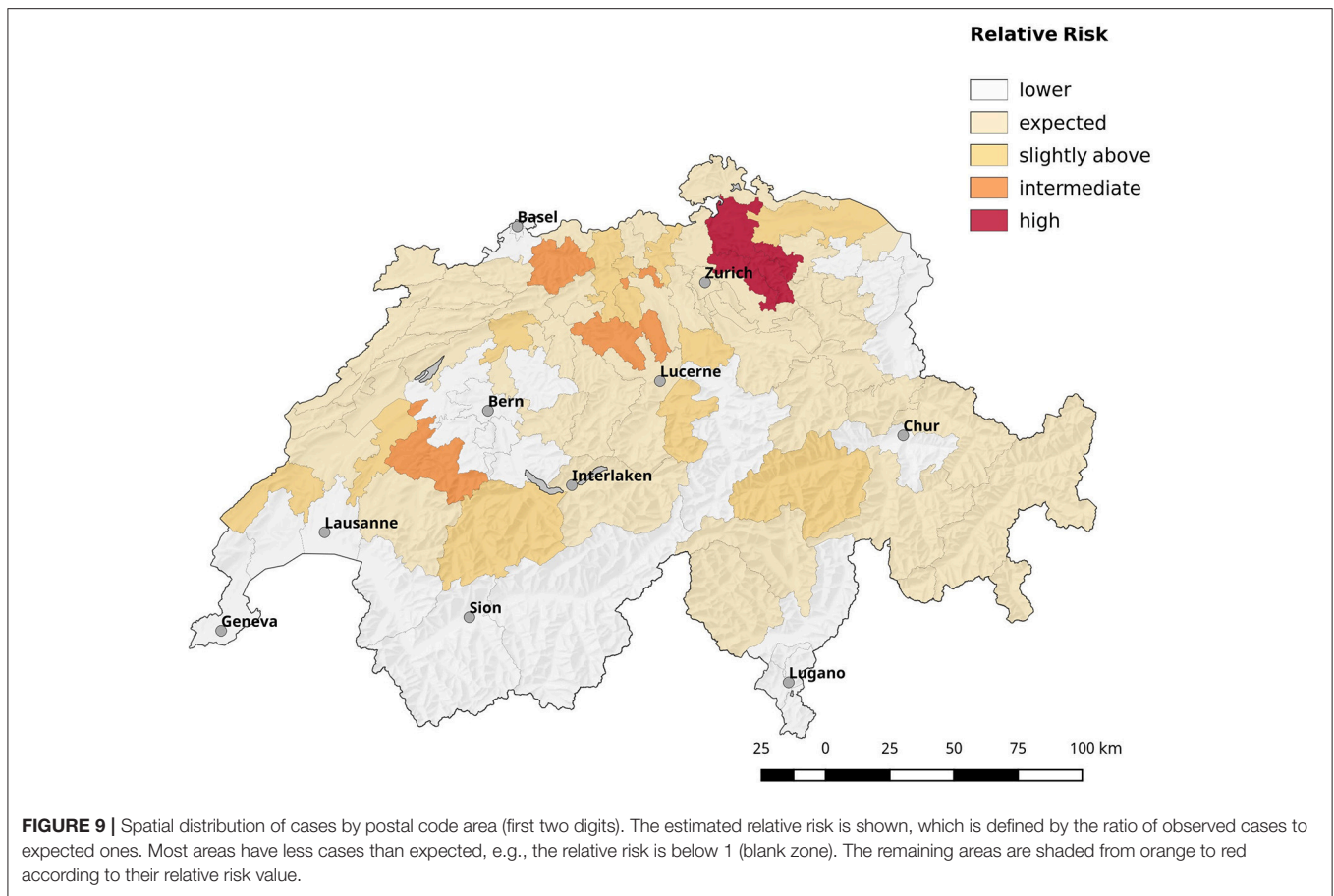


FIGURE 8 | Classification of tularemia in Switzerland between 2004 and 2016 according to the clinical manifestation.

carrying B.46/B.86 strains. A hint for this line of argumentation is provided by our *breseq* data. Seven non-synonymous SNPs were found exclusively in the B.86 subclade of B.11, which might modulate the function of proteins involved in intracellular survival. Members of the MFS are involved in the transport of small molecule substrates across all classes of organisms and play an important role in sustaining the osmotic balance between the cytosol and the environment. In *F. tularensis*, phagosomal transport proteins that are a sub-family of MFS were identified as factors essential for lethality to adult fruit flies (Akimana and Kwaik, 2011). Furthermore, members of the MFS class are discussed as a target for attenuation and vaccine development (Marohn et al., 2012). The tolerance to oxidative stress and the acquisition of iron are fundamental aspects for the survival of a pathogen in a host environment. Besides its pivotal role in cellular respiration, the iron containing porphyrin-ring heme is involved in the function of a variety of enzymes like catalases and nitric oxide synthase (Choby and Skaar, 2016). In this light, the non-synonymous mutation of *hemA* that is involved in the first steps of heme biosynthesis may affect the tolerance of clade B.86 strains to oxidative stress (Ezraty et al., 2017). Additionally, we identified a mutation in another component associated with the electron transport chain: cytochrome *c*-type biogenesis proteins are membrane-bound proteins that may play a role in the guidance of apocytochromes and heme groups for their covalent linkage by the cytochrome-*c*-heme lyase. In summary, the mutations of proteins involved in the adaptation to environmental conditions may modify the fitness of the B.86 subclade and may prevent persistence in ticks. This would lead to a diminished host range and thus restricted geographical dispersal. However, this interpretation should be treated with caution and needs to be substantiated further by functional studies.

Investigation of Eco-Epidemiological Aspects

According to the reported tularemia cases, ticks are the predominant vector for disease transmission in Switzerland



over the last 10 years. The importance of arthropod vectors is also reflected in the clinical manifestation of the disease where the glandular / ulcero glandular form prevails. These findings together with the sporadic occurrence and the low number of cases are in agreement with a terrestrial life cycle of *Fth* involving rodents, lagomorphs and ticks as main source for human infections. Despite the lacking evidence of a transovarial transmission of *Fth* in *Ixodes ricinus* (Genchi et al., 2015), it is known that the pathogen is propagated transracial from larvae to nymphs and adults in the 3-year life cycle of the vector. Therefore it was suggested that ticks can be regarded as a *de facto* reservoir of tularemia (Petersen et al., 2009; Foley and Nieto, 2010).

Our spatial data from tick, human, and vertebrate isolates, as well as from reported clinical cases suggest that the *Fth* population is not randomly distributed in Switzerland. The highest risk for acquiring tularemia coincides with regions where *Fth* was found in the ticks, a hint to the importance of their role as a biological niche for *Fth*. Since the initial tick survey was conducted with the aim to assess the prevalence of TBEV in all regions of Switzerland below 1,500 m altitude (Gäumann et al., 2010), the identification of *Fth* foci within the TBEV sample pool was not biased by the number of reported tularemia cases in a given region.

Analysis of Habitat Characteristics and Abiotic Factors Influencing the Tick Abundance

An important factor influencing the distribution of the pathogen in Switzerland is the complex topography of the country where 50% of the territory lays above an altitude of 1,000 m above sea level. Only one case of tularemia was reported in a patient living at 1,700 m altitude and contaminated water or food was suspected to be the source of infection (Ernst et al., 2015). In principle, the incidence of tularemia shows the same altitude dependence as was shown for borreliosis, where the prevalence of the pathogen in tick nymphs correlated negatively with altitude (Gern et al., 2008). There are multitudes of additional environmental parameters that are known to have an influence on the transmission dynamics of tick-borne pathogens. Abiotic factors like temperature, wind, RH and SD are recognized to be of pivotal importance for tick abundance and survival (Vial, 2009; Alonso-Carné et al., 2015). It was shown that a RH of 85% is required for the survival of *Ixodes ricinus* in its non-parasitic stage (Keymer et al., 2009). Studies, which assessed the usability of satellite-based remote sensing data as indices for geospatial disease monitoring, identified soil moisture as an important factor for the establishment of tick habitats (Beck et al., 2000; Barrios et al., 2012).

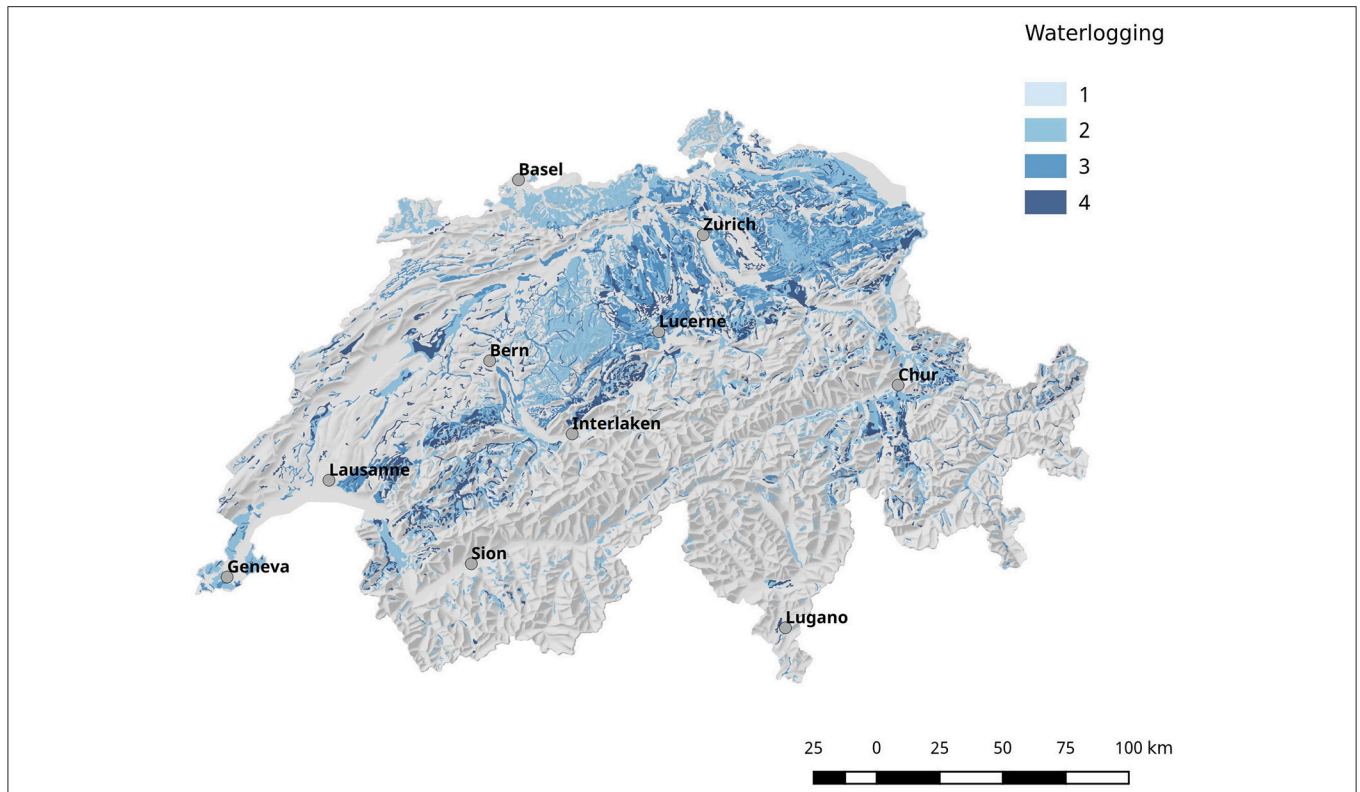


FIGURE 10 | Geographical overview of the water saturation of the soil (waterlogging). In general, the soil in the north-eastern part of Switzerland shows a higher degree of water saturation compared to other regions.

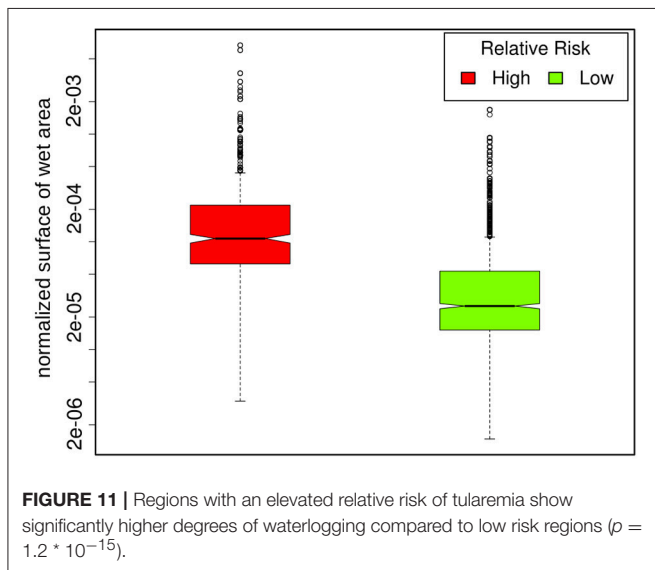


FIGURE 11 | Regions with an elevated relative risk of tularemia show significantly higher degrees of waterlogging compared to low risk regions ($p = 1.2 \cdot 10^{-15}$).

Comparing surface normalized averages of waterlogging levels in areas with elevated risk for acquiring tularemia vs. low-/expected risk areas, we find a highly significant effect of soil moisture (Figures 10, 11). Thus, the elevated prevalence of *Fth* in ticks and the higher incidence of tularemia in the northeastern

part of Switzerland may at least be partially explained by the above average soil moisture in this region, favoring tick survival during dry periods. Another observation that fits in this line of argumentation is the congruence of high-risk tularemia regions with areas of elevated risk of Tick Born Encephalitis (TBE) (Figure 13).

Habitat Fragmentation and Urbanization in Switzerland

Besides micro-climatic factors, anthropogenic changes of the ecosystem, and social factors are known to have a fundamental impact on the host-vector-pathogen dynamics (Bayles et al., 2013; Lou et al., 2014). As seen in other European countries, the fragmentation and urbanization of the Swiss landscape is on the rise which is reflected in a linear decrease of the “effective mesh size” during the last 70 years. The mesh size is a metric that describes the probability that two random points in the landscape can be connected without the interference of artificial structures, for example, transportation routes, buildings or developed land (Jaeger, 2000, 2006). The more barriers fragmenting the landscape, the lower the probability that two points are connected, and the lower the effective mesh size. In an ecological view, the mesh size can be interpreted as the probability that two animals of the same specie find each other in the landscape. Therefore, the reduction of the mesh size due to progressing landscape fragmentation may reach a limit where

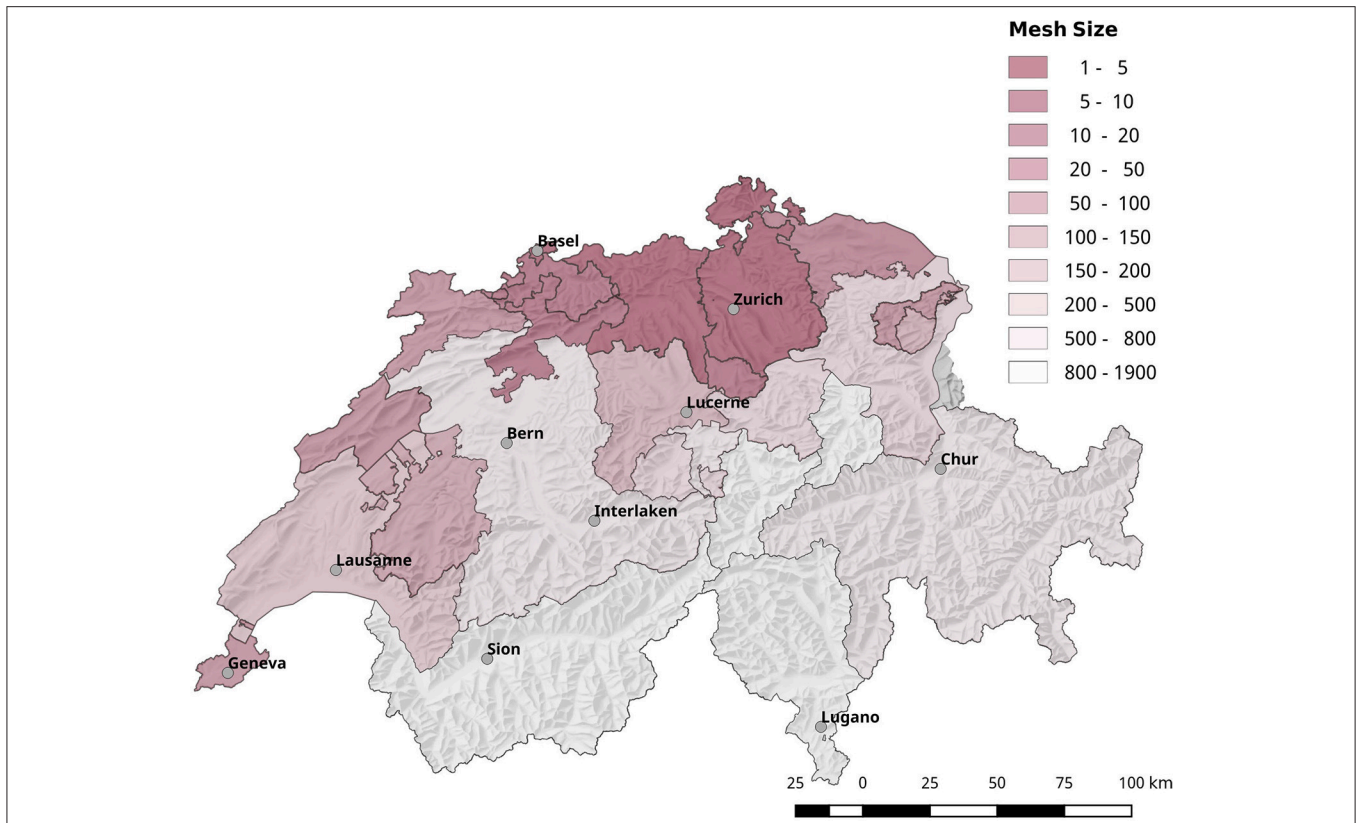


FIGURE 12 | Geographical overview of the degree of landscape fragmentation of the Swiss cantons. Most of the regions with a high risk for acquiring tularemia are also highly fragmented.

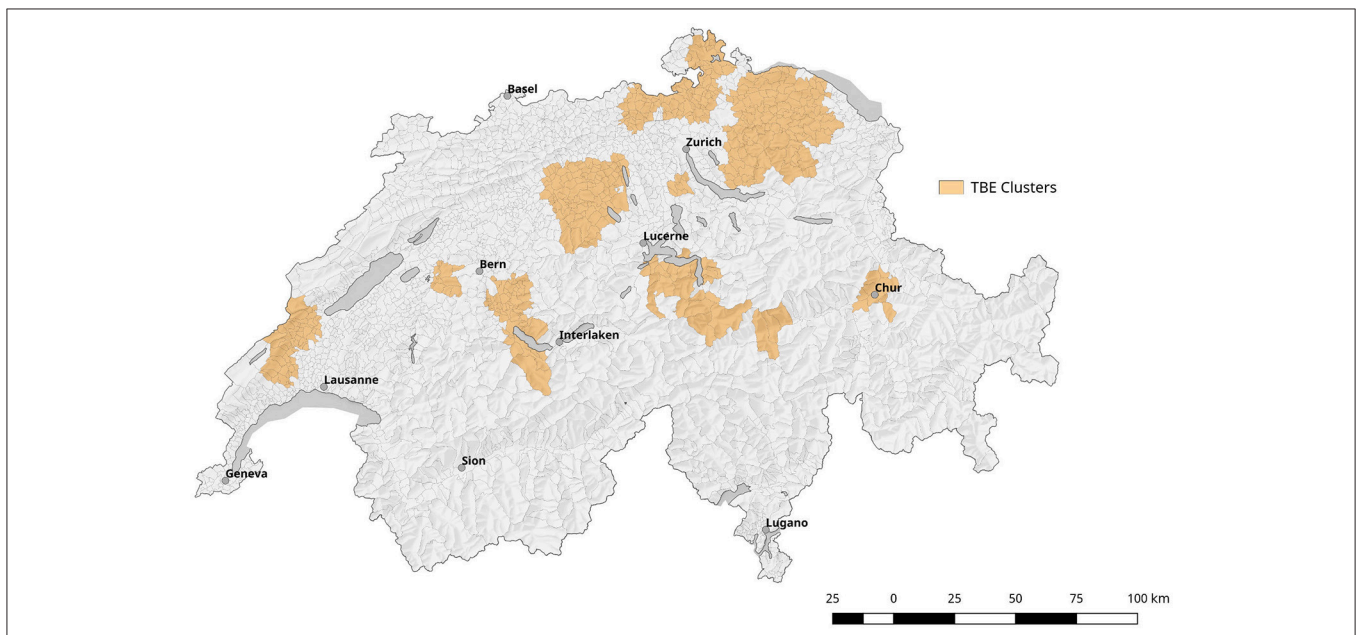


FIGURE 13 | Depiction of localized clusters of Tick borne encephalitis (TBE). It is based on information from the mandatory reporting system between 2007 and 2016.

a given species is no longer able to sustain a stable population, which reduces the biodiversity of the area (Di Giulio et al., 2009). Most of the regions with an elevated risk for acquiring tularemia are highly fragmented and show a below average mesh sizes (Figure 12). The reduction of biodiversity may alter the ratio of hosts vs. low or non-competent hosts, thereby reducing the pathogen dilution effect. A diminished pathogen dilution effect may in turn elevate the vector competence of the ticks and thus the probability of disease transmission (Schmidt and Ostfeld, 2001; Pfäffle et al., 2013; Dantas-Torres, 2015).

Risk Factors for Human Disease

The bimodal distribution of the tularemia cases per age group and the predominance of male patients is an indicator of social factors influencing the transmission probability of the disease and is in accordance with the incidence in other countries (Desvars et al., 2015). According to clinicians treating patients in the elevated risk areas, the peak in the age group of the 8–12 year old children is due to the joining of youth organizations like the scouts that are combing through the forests away from fixed paths seeking for adventure. The second peak with a maximum at 50 years reflects the demographic age structure of the Swiss population.

CONCLUSION

The combination of high-resolution whole genome phylogenies with epidemiological and ecological parameters allows a profound insight into the transmission modalities of tularemia. The exceptionally high genetic diversity of the Swiss *Fth* population allows us to study the population and disease dynamics of the pathogen in a small geographical context. In our work, we found evidence for the spatial correlation of disease incidence and ecological/anthropogenic factors that influence the survival and vector competence of the local tick population.

Based on these findings, we conclude that *I. ricinus* plays a pivotal role in the establishment of the disease in a given ecological niche and in sustaining the transmission cycle.

REFERENCES

- Ajawanawong, P., Atkinson, G. C., Watson-Haigh, N. S., Mackenzie, B., and Baldauf, S. L. (2012). SeqFIRE: a web application for automated extraction of indel regions and conserved blocks from protein multiple sequence alignments. *Nucleic Acids Res.* 40, W340–W347. doi: 10.1093/nar/gks561
- Akimana, C., and Kwaik, Y. A. (2011). Francisella-arthropod vector interaction and its role in patho-adaptation to infect mammals. *Front. Microbiol.* 2:34. doi: 10.3389/fmicb.2011.00034
- Alonso-Carné, J., García-Martín, A., and Estrada-Peña, A. (2015). Assessing the statistical relationships among water-derived climate variables, rainfall, and remotely sensed features of vegetation: implications for evaluating the habitat of ticks. *Exp. Appl. Acarol.* 65, 107–124. doi: 10.1007/s10493-014-9849-0
- Bankevich, A., Nurk, S., Antipov, D., Gurevich, A. A., Dvorkin, M., Kulikov, A. S., et al. (2012). SPAdes: a new genome assembly algorithm and its applications to single-cell sequencing. *J. Comput. Biol.* 19, 455–477. doi: 10.1089/cmb.2012.0021
- Barrios, J. M., Verstraeten, W. W., Maes, P., Clement, J., Aerts, J. M., Farifteh, J., et al. (2012). Remotely sensed vegetation moisture as explanatory variable of Lyme borreliosis incidence. *Int. J. Appl. Earth Obs. Geoinf.* 18, 1–12. doi: 10.1016/j.jag.2012.01.023
- Bayles, B. R., Evans, G., and Allan, B. F. (2013). Knowledge and prevention of tick-borne diseases vary across an urban-to-rural human land-use gradient. *Ticks Tick Borne Dis.* 4, 352–358. doi: 10.1016/j.ttbdis.2013.01.001
- Beck, L. R., Lobitz, B. M., and Wood, B. L. (2000). Remote sensing and human health: new sensors and new opportunities. *Emerg. Infect. Dis.* 6, 217–227. doi: 10.3201/eid0603.000301
- Becker, S., Lochau, P., Jacob, D., Heuner, K., and Grunow, R. (2016). Successful re-evaluation of broth medium T for growth of *Francisella tularensis* ssp. and other highly pathogenic bacteria. *J. Microbiol. Methods* 121, 5–7. doi: 10.1016/j.mimet.2015.11.018
- Bolger, A. M., Lohse, M., and Usadel, B. (2014). Trimmomatic: a flexible trimmer for Illumina sequence data. *Bioinformatics* 30:2114. doi: 10.1093/bioinformatics/btu170
- Byström, M., Böcher, S., Magnusson, A., Prag, J., and Johansson, A. (2005). Tularemia in Denmark: identification of a *Francisella tularensis* subsp. holarctica strain by real-time PCR and high-resolution typing by multiple-locus

AUTHOR CONTRIBUTIONS

MW analyzed the genomic data, performed the spatial statistics, and drafted the manuscript. EA compiled the epidemiological data and calculated the spatial relative disease risk. PP provided the animal isolates and expertise in the field of tularemia. SG performed the functional SNP analysis and provided the expertise in whole genome phylogeny. CB, RA-G designed and organized the tick sampling and provided expertise in tick borne diseases. UK provided the expertise in the clinical aspects of tularemia. DJ, RG gave theoretical and practical advice for bacterial isolation and provided expertise in the eco-epidemiology of tularemia. NS coordinated and supervised the presented work. All authors contributed to manuscript revision, read, and approved the submitted version.

ACKNOWLEDGMENTS

We like to thank Kerstin Myrtenäs from the Swedish Defense Research Agency (FOI) for fruitful discussions regarding the phylogeny of *Fth* and canSNP nomenclature. Furthermore, we thank the NBC Defense Laboratory 1 of the Swiss Armed Forces for the extensive tick sampling campaigns, ADMED (Analyses et Diagnostics Médicaux) for supplying DNA and last but certainly not least Sandra Paniga, Susanne Thomann, and Fritz Wüthrich for excellent technical assistance. This work was partially supported by the Health program 2014–2020, through the Consumers, Health, Agriculture and Food Executive Agency (CHAFEA, European Commission); EMERGE Joint Action grant number:677066.

SUPPLEMENTARY MATERIAL

The Supplementary Material for this article can be found online at: <https://www.frontiersin.org/articles/10.3389/fcimb.2018.00089/full#supplementary-material>

Supplementary Table 1 | Genetic variations found in the core genome alignment with the strain FTNF00–002.

- variable-number tandem repeat analysis. *J. Clin. Microbiol.* 43, 5355–5358. doi: 10.1128/JCM.43.10.5355-5358.2005
- Castresana, J. (2000). Selection of conserved blocks from multiple alignments for their use in phylogenetic analysis. *Mol. Biol. Evol.* 17, 540–552. doi: 10.1093/oxfordjournals.molbev.a026334
- Choby, J. E., and Skaar, E. P. (2016). Heme synthesis and acquisition in bacterial pathogens. *J. Mol. Biol.* 428, 3408–3428. doi: 10.1016/j.jmb.2016.03.018
- Dantas-Torres, F. (2015). Climate change, biodiversity, ticks and tick-borne diseases: the butterfly effect. *Int. J. Parasitol. Parasites Wildl.* 4, 452–461. doi: 10.1016/j.ijppaw.2015.07.001
- Deathage, D. E., and Barrick, J. E. (2014). Identification of mutations in laboratory-evolved microbes from next-generation sequencing data using breseq. *Methods Mol. Biol.* 1151, 165–188. doi: 10.1007/978-1-4939-0554-6_12
- Desvars, A., Furberg, M., Hjertqvist, M., Vidman, L., Sjöstedt, A., Rydén, P., et al. (2015). Epidemiology and ecology of Tularemia in Sweden, 1984–2012. *Emerg. Infect. Dis.* 21, 32–39. doi: 10.3201/eid2101.140916
- Di Giulio, M., Holderregger, R., and Tobias, S. (2009). Effects of habitat and landscape fragmentation on humans and biodiversity in densely populated landscapes. *J. Environ. Manage.* 90, 2959–2968. doi: 10.1016/j.jenvman.2009.05.002
- Dwibedi, C., Birdsell, D., Lärkeryd, A., Myrtenäs, K., Öhrman, C., Nilsson, E., et al. (2016). Long-range dispersal moved *Francisella tularensis* into Western Europe from the East. *Microb. Genomics* 2:e000100. doi: 10.1099/mgen.0.000100
- Ernst, M., Pilo, P., Fleisch, F., and Glisenti, P. (2015). Tularemia in the Southeastern Swiss Alps at 1,700 m above sea level. *Infection* 43, 111–115. doi: 10.1007/s15010-014-0676-3
- Ezraty, B., Gennaris, A., Barras, F., and Collet, J.-F. (2017). Oxidative stress, protein damage and repair in bacteria. *Nat. Rev. Microbiol.* 15, 385–396. doi: 10.1038/nrmicro.2017.26
- Foley, J. E., and Nieto, N. C. (2010). Tularemia. *Vet. Microbiol.* 140, 332–338. doi: 10.1016/j.vetmic.2009.07.017
- Gäumann, R., Mühlemann, K., Strasser, M., and Beuret, C. M. (2010). High-throughput procedure for tick surveys of tick-borne encephalitis virus and its application in a national surveillance study in Switzerland. *Appl. Environ. Microbiol.* 76, 4241–4249. doi: 10.1128/AEM.00391-10
- Genchi, M., Prati, P., Vicari, N., Manfredini, A., Sacchi, L., Clementi, E., et al. (2015). *Francisella tularensis*: no evidence for transovarial transmission in the tularemia tick vectors *Dermacentor reticulatus* and *Ixodes ricinus*. *PLoS ONE* 10:e0133593. doi: 10.1371/journal.pone.0133593
- Gern, L., Morán Cadenas, F., and Burri, C. (2008). Influence of some climatic factors on *Ixodes ricinus* ticks studied along altitudinal gradients in two geographic regions in Switzerland. *Int. J. Med. Microbiol.* 298, 55–59. doi: 10.1016/j.ijmm.2008.01.005
- Girault, G., Thierry, S., Cherchame, E., and Derzelle, S. (2014). Application of high-throughput sequencing : discovery of informative SNPs to Subtype *Bacillus anthracis*. *Adv. Biosci. Biotechnol.* 5, 669–677. doi: 10.4236/abb.2014.57079
- Guindon, S., Dufayard, J.-F., Lefort, V., Anisimova, M., Hordijk, W., and Gascuel, O. (2010). New algorithms and methods to estimate maximum-likelihood phylogenies: assessing the performance of PhyML 2.0. *Syst. Biol.* 59, 307–321. doi: 10.1093/sysbio/syq010
- Hornik, K., Leisch, F., Zeileis, A., Gómez-Rubio, V., Ferrándiz, J., and López, A. (2003). *Detecting Clusters of Diseases with R*. Available online at: <http://www.ci.tuwien.ac.at/Conferences/DSC-2003/> (Accessed June 19, 2017).
- Jaeger, J. (2000). Landscape division, splitting index, and effective mesh size: new measures of landscape fragmentation. *Landsc. Ecol.* 15, 115–130. doi: 10.1023/A:1008129329289
- Jaeger, J. (2006). *Degree of Landscape Fragmentation in Switzerland*. Federal Office for the Environment FOEN. DIV-8409-E
- Jusatz, H. J. (1961). “The geographical distribution of tularemia throughout the world, 1911–1959,” in *Welt-Suchen Atlas*, ed E. Rodenwaldt (Hamburg: Falk-Verlag), 7–12.
- Karlsson, E., Golovliov, I., Lärkeryd, A., Granberg, M., Larsson, E., Öhrman, C., et al. (2016). Clonality of erythromycin resistance in *Francisella tularensis*. *J. Antimicrob. Chemother.* 71, 2815–2823. doi: 10.1093/jac/dkw235
- Katoh, K., Misawa, K., Kuma, K.-I., and Miyata, T. (2002). MAFFT: a novel method for rapid multiple sequence alignment based on fast Fourier transform. *Nucleic Acids Res.* 30, 3059–3066. doi: 10.1093/nar/gkf436
- Keirans, J. E. (1997). Ticks of north-west Europe. By Paul D. Hillyard. *Med. Vet. Entomol.* 11, 102–103. doi: 10.1111/j.1365-2915.1997.tb00296.x
- Keymer, D. P., Lam, L. H., and Boehm, A. B. (2009). Biogeographic patterns in genomic diversity among a large collection of *Vibrio cholerae* isolates. *Appl. Environ. Microbiol.* 75, 1658–1666. doi: 10.1128/AEM.01304-08
- Krige, D. (1951). A statistical approach to some basic mine valuation problems on the Witwatersrand. *J. Chem. Metall. Min. Soc. South Afr.* 52, 201–203.
- Lärkeryd, A., Myrtenäs, K., Karlsson, E., Dwibedi, C. K., Forsman, M., Larsson, P. R., et al. (2014). CanSNPer: a hierarchical genotype classifier of clonal pathogens. *Bioinformatics* 30, 1762–1764. doi: 10.1093/bioinformatics/btu113
- Lee, R. S., Radomski, N., Proulx, J.-F., Levade, I., Shapiro, B. J., McIntosh, F., et al. (2015). Population genomics of *Mycobacterium tuberculosis* in the Inuit. *Proc. Natl. Acad. Sci. U.S.A.* 112, 13609–13614. doi: 10.1073/pnas.1507011112
- Lou, Y., Wu, J., and Wu, X. (2014). Impact of biodiversity and seasonality on Lyme-pathogen transmission. *Theor. Biol. Med. Model.* 11:50. doi: 10.1186/1742-4682-11-50
- Marohn, M. E., Santiago, A. E., Shirey, K. A., Lipsky, M., Vogel, S. N., and Barry, E. M. (2012). Members of the *Francisella tularensis* phagosomal transporter subfamily of major facilitator superfamily transporters are critical for pathogenesis. *Infect. Immun.* 80, 2390–2401. doi: 10.1128/IAI.00144-12
- Maurin, M., and Gyuranecz, M. (2016). Tularemia: clinical aspects in Europe. *Lancet Infect. Dis.* 16, 113–124. doi: 10.1016/S1473-3099(15)00355-2
- Müller, W., Hotzel, H., Otto, P., Karger, A., Bettin, B., Bocklisch, H., et al. (2013). German *Francisella tularensis* isolates from European brown hares (*Lepus europaeus*) reveal genetic and phenotypic diversity. *BMC Microbiol.* 13:61. doi: 10.1186/1471-2180-13-61
- Oechslin, C. P., Heutschi, D., Lenz, N., Tischhauser, W., Péter, O., Rais, O., et al. (2017). Prevalence of tick-borne pathogens in questing *Ixodes ricinus* ticks in urban and suburban areas of Switzerland. *Parasit. Vectors* 10:558. doi: 10.1186/s13071-017-2500-2
- Origi, F. C., Frey, J., and Pilo, P. (2014). Characterisation of a new group of *Francisella tularensis* subsp. holarctica in Switzerland with altered antimicrobial susceptibilities, 1996 to 2013. *Eurosurveillance* 19:20858. doi: 10.2807/1560-7917.ES2014.19.29.20858
- Page, A. J., Cummins, C. A., Hunt, M., Wong, V. K., Reuter, S., Holden, M. T. G., et al. (2015). Roary: rapid large-scale prokaryote pan genome analysis. *Bioinformatics* 30, 3691–3693. doi: 10.1093/bioinformatics/btv421
- Pérez-Castrillón, J. L., Bachiller-Luque, P., Martín-Luquero, M., Mena-Martín, F. J., and Herreros, V. (2001). Tularemia epidemic in Northwestern Spain: clinical description and therapeutic response. *Clin. Infect. Dis.* 33, 573–576. doi: 10.1086/322601
- Petersen, J. M., Mead, P. S., and Schriefer, M. E. (2009). *Francisella tularensis*: an arthropod-borne pathogen. *Vet. Res.* 40:7. doi: 10.1051/vetres:2008045
- Pfäffle, M., Littwin, N., Muders, S. V., and Petney, T. N. (2013). The ecology of tick-borne diseases. *Int. J. Parasitol.* 43, 1059–1077. doi: 10.1016/j.ijpara.2013.06.009
- Pilo, P., Johansson, A., and Frey, J. (2009). Identification of *Francisella tularensis* cluster in central and western Europe. *Emerg. Infect. Dis.* 15, 2049–2051. doi: 10.3201/eid1512.080805
- Rotz, L. D., Khan, A. S., Lillibridge, S. R., Ostroff, S. M., and Hughes, J. M. (2002). Public health assessment of potential biological terrorism agents. *Emerg. Infect. Dis.* 8, 225–230. doi: 10.3201/eid0802.010164
- Schmidt, K. A., and Ostfeld, R. S. (2001). Biodiversity and the dilution effect in disease ecology. *Ecology* 82, 609–619. doi: 10.1890/0012-9658(2001)082[0609:BATDEI]2.0.CO;2
- Seemann, T. (2014). Prokka: rapid prokaryotic genome Annotation 30, 2068–2069. doi: 10.1093/bioinformatics/btu153
- Stucki, D., Brites, D., Jeljeli, L., Coscolla, M., Liu, Q., Trauner, A., et al. (2016). *Mycobacterium tuberculosis* lineage 4 comprises globally distributed and geographically restricted sublineages. *Nat. Genet.* 48, 1535–1543. doi: 10.1038/ng.3704
- Tarroso, P., Velo-Anton, G., and Carvalho, S. B. (2015). *Phylin: Spatial Interpolation of Genetic Data*. Available online at: <https://cran.r-project.org/package=phylin>
- Tomaso, H., Al Dahouk, S., Hofer, E., Spletstoesser, W. D., Treu, T. M., Dierich, M. P., et al. (2005). Antimicrobial susceptibilities of Austrian *Francisella tularensis* holarctica biovar II strains. *Int. J. Antimicrob. Agents* 26, 279–284. doi: 10.1016/j.ijantimicag.2005.07.003

- Vial, L. (2009). Mise au point biological and ecological characteristics of soft ticks (ixodida: argasidae) and their impact for predicting tick and associated disease distribution. *Parasite* 16, 191–202. doi: 10.1051/parasite/2009163191
- Vogler, A. J., Birdsell, D., Price, L. B., Bowers, J. R., Beckstrom-Sternberg, S. M., Auerbach, R. K., et al. (2009). Phylogeography of *Francisella tularensis*: global expansion of a highly fit clone. *J. Bacteriol.* 191, 2474–2484. doi: 10.1128/JB.01786-08
- Wicki, R., Sauter, P., Mettler, C., Natsch, A., Enzler, T., Pusterla, N., et al. (2000). Swiss Army Survey in Switzerland to determine the prevalence of *Francisella tularensis*, members of the Ehrlichia phagocytophila genogroup, Borrelia burgdorferi sensu lato, and tick-borne encephalitis virus in ticks. *Eur. J. Clin. Microbiol. Infect. Dis.* 19, 427–432. doi: 10.1007/s100960000283
- Zhou, T., Chen, B.-M., Liu, G., Huang, F.-F., Liu, J.-G., Liao, W.-B., et al. (2015). Biodiversity of Jinggangshan Mountain: the importance of topography and geographical location in supporting higher biodiversity. *PLoS ONE* 10:e0120208. doi: 10.1371/journal.pone.0120208

Conflict of Interest Statement: The authors declare that the research was conducted in the absence of any commercial or financial relationships that could be construed as a potential conflict of interest.

Copyright © 2018 Wittwer, Altpeter, Pilo, Gygli, Beuret, Foucault, Ackermann-Gäumann, Karrer, Jacob, Grunow and Schürch. This is an open-access article distributed under the terms of the Creative Commons Attribution License (CC BY). The use, distribution or reproduction in other forums is permitted, provided the original author(s) and the copyright owner are credited and that the original publication in this journal is cited, in accordance with accepted academic practice. No use, distribution or reproduction is permitted which does not comply with these terms.



The Cynomolgus Macaque Natural History Model of Pneumonic Tularemia for Predicting Clinical Efficacy Under the Animal Rule

Tina Guina^{1*}, Lynda L. Lanning¹, Kristian S. Omland², Mark S. Williams¹, Larry A. Wolfrain¹, Stephen P. Heyse¹, Christopher R. Houchens³, Patrick Sanz¹ and Judith A. Hewitt¹

¹ National Institute of Allergy and Infectious Diseases, National Institutes of Health, Bethesda, MD, United States, ² Mergus Analytics, LLC, Jericho, VT, United States, ³ Biomedical Advanced Research and Development Authority, Department of Health and Human Services, Washington, DC, United States

OPEN ACCESS

Edited by:

Marina Santic,
University of Rijeka, Croatia

Reviewed by:

Sam Telford,
Tufts University, United States
Max Maurin,
Université Grenoble Alpes, France
Souhaila Al Khodor,
Sidra Medical and Research Center,
Qatar

*Correspondence:

Tina Guina
tina.guina@nih.gov

Received: 14 November 2017

Accepted: 16 March 2018

Published: 04 April 2018

Citation:

Guina T, Lanning LL, Omland KS, Williams MS, Wolfrain LA, Heyse SP, Houchens CR, Sanz P and Hewitt JA (2018) The Cynomolgus Macaque Natural History Model of Pneumonic Tularemia for Predicting Clinical Efficacy Under the Animal Rule. *Front. Cell. Infect. Microbiol.* 8:99. doi: 10.3389/fcimb.2018.00099

Francisella tularensis is a highly infectious Gram-negative bacterium that is the etiologic agent of tularemia in animals and humans and a Tier 1 select agent. The natural incidence of pneumonic tularemia worldwide is very low; therefore, it is not feasible to conduct clinical efficacy testing of tularemia medical countermeasures (MCM) in human populations. Development and licensure of tularemia therapeutics and vaccines need to occur under the Food and Drug Administration's (FDA's) Animal Rule under which efficacy studies are conducted in well-characterized animal models that reflect the pathophysiology of human disease. The Tularemia Animal Model Qualification (AMQ) Working Group is seeking qualification of the cynomolgus macaque (*Macaca fascicularis*) model of pneumonic tularemia under Drug Development Tools Qualification Programs with the FDA based upon the results of studies described in this manuscript. Analysis of data on survival, average time to death, average time to fever onset, average interval between fever and death, and bacteremia; together with summaries of clinical signs, necropsy findings, and histopathology from the animals exposed to aerosolized *F. tularensis* Schu S4 in five natural history studies and one antibiotic efficacy study form the basis for the proposed cynomolgus macaque model. Results support the conclusion that signs of pneumonic tularemia in cynomolgus macaques exposed to 300–3,000 colony forming units (cfu) aerosolized *F. tularensis* Schu S4, under the conditions described herein, and human pneumonic tularemia cases are highly similar. Animal age, weight, and sex of animals challenged with 300–3,000 cfu Schu S4 did not impact fever onset in studies described herein. This study summarizes critical parameters and endpoints of a well-characterized cynomolgus macaque model of pneumonic tularemia and demonstrates this model is appropriate for qualification, and for testing efficacy of tularemia therapeutics under Animal Rule.

Keywords: *Francisella tularensis*, pneumonic tularemia, cynomolgus macaque, non-human primate, animal model, Animal Rule, Animal Model Qualification

INTRODUCTION

Francisella tularensis is a highly infectious Gram-negative bacterium that is the etiologic agent of tularemia in animals and humans. Infections with highly virulent *F. tularensis* strains are lethal in 30–60% of individuals infected by the inhalation route if not treated with antibiotics, and *F. tularensis* strains have been weaponized for potential use as a biothreat agent (Stuart and Pullen, 1945; Hornick, 1998; Dennis et al., 2001). For these reasons, *F. tularensis* has been designated a Tier 1/Category A select agent by the Centers for Disease Control (CDC) and the National Institutes of Allergy and Infectious Diseases (NIAID), part of the National Institutes of Health (NIH). The natural incidence of pneumonic tularemia in the United States is very low (CDC, 2013). Hundreds of people have contracted tularemia in outbreaks in other countries, primarily in Eurasia (Dahlstrand et al., 1971; Christenson, 1984; Tarnvik et al., 1996; Ohara et al., 1998; Perez-Castrillon et al., 2001; Reintjes et al., 2002; Meka-Mechenko et al., 2003; Celebi et al., 2006). However, due to the sporadic nature of these outbreaks, it is not feasible to conduct clinical efficacy testing of tularemia vaccines and therapeutics in human populations. In the United States, tularemia medical countermeasures (MCM) efficacy studies can be conducted in accordance with the Animal Rule [21 CFR Parts 314 Subpart I and 21 CFR Part 601 Subpart H, Approval of New Drugs When Human Efficacy Studies Are Not Ethical or Feasible, and Food and Drug Administration (FDA, 2009, 2015)]. Drug or vaccine licensure under the Animal Rule requires availability of at least one well-characterized animal model displaying pathophysiology similar to disease in humans (FDA, 2009, 2015). Animal models are important components of preparedness as they are used for testing candidate MCM in response to public health emergencies (e.g., anthrax, Ebola, pandemic influenza).

FDA's Animal Model Qualification (AMQ) Program (FDA, 2017) under the Drug Development Tools Program is a regulatory pathway for qualification of animal models to be used for MCM efficacy testing and approval under the Animal Rule. A qualified animal model is product-independent and may be used for efficacy testing of multiple investigational drugs for the targeted disease or condition. A Tularemia Animal Model Qualification Working Group (AMQ WG) was established to integrate and analyze natural history studies to seek qualification of the cynomolgus macaque (*Macaca fascicularis*) model of pneumonic tularemia as a Drug Development Tool with the FDA. The intent for use of this model is demonstrating the efficacy of therapeutics for treatment and/or post-exposure prophylaxis of pneumonic tularemia. This model may be further refined for use in efficacy testing of tularemia vaccines.

Among non-human primates (NHPs), rhesus and cynomolgus macaques, African Green monkeys, and marmosets have been used in tularemia studies (Lyons and Wu, 2007). Recent studies (Glynn et al., 2015, and data described in this manuscript) demonstrated that the infectious dose and disease pathophysiology in cynomolgus macaques challenged with aerosolized *F. tularensis* strain Schu S4, closely resemble human pneumonic tularemia caused by *F. tularensis* subsp. *tularensis* (Type A) strains, the most severe and lethal form of

the disease. It is assumed that therapeutics and vaccines that show efficacy in the NHP model that reflects the most severe form of tularemia should also be efficacious against less severe forms of tularemia. *F. tularensis* Schu S4 is a highly virulent strain which caused febrile disease and other symptoms in volunteers after inhalation of <20 colony forming units (cfu) (Saslaw et al., 1961). It has been weaponized and used in human volunteer challenge studies and animal model development worldwide since the 1940's (Dennis et al., 2001; Lyons and Wu, 2007). Historically, rhesus macaques have been used in tularemia research, but currently available rhesus macaque colonies have been more resistant to infection with aerosolized Schu S4 when compared to cynomolgus macaques and humans (median lethal dose, LD₅₀ ~10⁵ cfu for rhesus, and LD₅₀ ~20 cfu for cynomolgus macaques; Saslaw et al., 1961; Glynn et al., 2015 and unpublished). For these reasons, the cynomolgus macaque was chosen for development of the pneumonic tularemia model in NHPs.

This manuscript describes the progression of pneumonic tularemia in cynomolgus macaques based on data collected in five natural history studies and one antibiotic efficacy study in which animals were exposed to aerosolized *F. tularensis* Schu S4. These previously unpublished studies were performed to develop and establish a NHP model of pneumonic tularemia for efficacy testing of therapeutics and vaccines at three sites including Battelle Biomedical Research Center (BBRC, West Jefferson, OH), Lovelace Respiratory Research Institute (LRRI, Albuquerque, NM), and the United States Army Medical Research Institute for Infectious Diseases (USAMRIID, Frederick, MD). Two natural history studies also included additional pathogenesis progression (serial pathology) study arms in which animals were euthanized for gross pathology examination and tissue analysis at specific days following challenge with *F. tularensis* to evaluate disease progression. Although the objectives and endpoints of all studies were similar, certain aspects of the individual study protocols (e.g., subject study inclusion and exclusion criteria) varied somewhat as the understanding of the model progressed over time. For example, one early study included groups of animals exposed to three target doses of 50, 500, and 5,000 cfu aerosolized *F. tularensis*, while all other studies targeted a 1,000 cfu exposure dose. Mortality, average time to death, average time to fever onset, average interval between fever and death, bacteremia, clinical signs, necropsy findings, and histopathology from the studies were analyzed and form the basis for the proposed cynomolgus macaque model parameters and endpoints. Telemetry data from four natural history studies and one antibiotic efficacy study was used for analyses of the core body temperature and for calculating onset of fever and hypothermia in individual animals and across studies. Tularemia AMQ WG recommendations on critical model parameters that are appropriate for use of this model for testing of MCMs under Animal Rule (see section Results) are based on the analysis of data from all six studies and comparison of the results with human cases of pneumonic tularemia from published literature. The manuscript describes suggested model inclusion and exclusion criteria, critical model parameters, model for calculation of onset of fever as the physiologic trigger for

initiation of therapy, and model endpoints. Data collected and analyzed to date support the conclusion that signs of pneumonic tularemia in cynomolgus macaques exposed to a target dose of 1,000 cfu (range 300–3,000 cfu) aerosolized *F. tularensis* Schu S4, under the conditions described herein, and human pneumonic tularemia cases are highly similar. Challenge doses lower than 300 cfu Schu S4 resulted in a wider range of symptoms, disease clinical course, survival rates and pathology outcomes, as was also observed in previous studies (Glynn et al., 2015, and data described in this manuscript). Analyses also support the use of fever onset as the physiologic trigger for initiation of therapeutic interventions during MCM efficacy testing.

MATERIALS AND METHODS

Test Animals and Study Inclusion Criteria

Cynomolgus macaques (*M. fascicularis*) of ~2 to ~7 years of age that originated from Indochina were obtained from commercial vendors in the United States. Animals were from colonies that originated with wild caught animals and were raised at the vendor facilities. Thirty-eight (38) female and forty (40) male animals were included in five natural history studies (Studies 1, 2, 3, 4, and 6; see **Table 1**). Two natural history study protocols (Studies 1 and 4) also included serial pathology study arms in which gross pathology and histopathology were evaluated on specific days after challenge with *F. tularensis* (**Table 1**), starting with Day 2 after challenge. Animals in the antibiotic efficacy study (Study 5) were administered either a vehicle or antibiotic solution intravenously (i.v.) after fever onset was determined. Because animals in the antibiotic efficacy study were treated differently than in natural history studies following fever onset, Study 5 data were used only for analyses of body temperature and fever onset, but not for analysis of survival time and biomarkers of disease progression. In natural history studies (Studies 1 through 4 and 6, **Table 1**), females were 2.3–7.7 years old and weighed 2.3–7.2 kg; males were 2.5–6.5 years old and weighed 2.6–7.4 kg. Nineteen animals (10 female, 9 male) included in the antibiotic efficacy study (Study 5, **Table 1**) were 3.0–7.0 years of age and weighed 2.5–4.0 kg. Macaques were prescreened and negative for prior exposure to *Mycobacterium tuberculosis*, *Klebsiella pneumoniae*, *Salmonella* sp., *Shigella* sp., simian immunodeficiency virus (SIV), simian retrovirus 1 and 2 (SRV1 and 2) and simian T-lymphotropic virus-1 (STLV-1), Macacine Herpesvirus 1 (Herpes B virus), and Simian Retrovirus (SRV1 and SRV2) prior to receipt at testing facilities. After arrival at testing facilities, animals were quarantined for at least 30 days before acceptance onto the studies. Previous exposure of animals to *F. tularensis* was examined by determination of anti-*F. tularensis* antibody titers using a tube agglutination test with *F. tularensis* antigen (BD, Franklin Lakes, NJ) at BBRC; or by ELISA, which measured binding of serum antibodies to the heat-inactivated whole cell preparation of *F. tularensis* subsp. *holarctica* Live Vaccine Strain (LVS) at LRRRI. Animals showing no humoral response to *F. tularensis* were included in the studies. In addition to these screens, macaques were also screened for previous exposure to *Trypanosoma cruzi* (via PCR and serology testing) and for infection with *Plasmodium* species in Study 5

(**Table 1**). Prior to release from quarantine, animals underwent a complete physical examination by a clinical veterinarian that included evaluation of a complete blood count (CBC), serum chemistry screen, and fecal ova and parasite determination. Only animals that were considered clinically healthy by veterinarian, including the above test results, were admitted onto the studies.

All available information for each animal as well as all pre-study activities (i.e., telemetry placement surgery, catheter placement surgery, antibiotic treatment, etc.) were recorded in individual animal case report forms (CRFs). Once an animal was placed onto a study, all individual animal information was captured in each laboratory's data systems and was presented in the study report in both individual and summary data formats. The CRF (animal receipt to study assignment) and the study data (from the time of animal study assignment to post-life assessments) comprised the totality of the information available for each individual animal before and throughout the study.

Ethics Statement

All studies presented in this manuscript were approved by the responsible institution's Institutional Animal Care and Use Committee (IACUC), and research was conducted in compliance with the Animal Welfare Act and other federal statutes and regulations relating to animals. Experiments involving animals adhered to principles stated in the Guide for the Care and Use of Laboratory Animals from the National Research Council. Studies were performed at institutions which are fully accredited by the Association for Assessment and Accreditation of Laboratory Animal Care International (AAALAC). Studies were performed under IACUC approved protocol numbers FY-09-012 (Study 1), 1026-G607612 (Study 2), 2741-G607612 (Study 3), FY-14-048 (Study 4), 3195-100050134 (Study 5), and AP09-002 (Study 6). Animal health prescreening and study inclusion/exclusion criteria are provided above. Macaques were pair housed up to about 1 week preceding telemetry surgery after which they were individually housed in stainless steel cages on racks equipped with automatic watering systems that met the specifications of The Guide for the Care and Use of Laboratory Animals, and the Animal Welfare Regulations (AWRs). Environmental humidity, temperature, and light/dark cycles (12-h each) in were controlled and monitored. Animals were fed commercially available fixed-formula diets formulated specifically for NHPs to provide the proper balance of nutrients, with additional nutritional supplementation (e.g., extra vegetables, fruit, PrimaLac, Ensure). To promote and enhance the psychological well-being, the macaques underwent enrichment according to the institutional Standard Operational Protocols (SOPs). After exposure, macaques were observed by laboratory personnel thrice daily with clinical signs and body weights monitoring. Analgesics buprenorphine (0.01 mg/kg), ketamine (20 mg/kg) were used prior to telemetry transponder implantation surgery. Buprenorphine (0.01 mg/kg), and in some cases flunixin meglumine (2 mg/kg), were used twice daily for 3 days after the surgery. Macaques were anesthetized with Telazol (1–6 mg/kg) prior to aerosol exposure and euthanasia. Isoflurane 3–5% was used for anesthesia induction and 0.5–3% for maintenance during inhalation exposure. Animals were

TABLE 1 | Summary of studies.

Study number	Study design	Animals in natural history study arm	Animals in pathogenesis progression study arm	Study site	Target challenge dose (cfu)	Data shown in figures and tables
1	Natural history	6 M, 6 F	8 M, 8 F	LRRI	1,000	Figures 2–6, Figure S1 Tables 2, 3, Table S1
2	Natural history	4 M, 5 F	na	BBRC	1,000	Figures 1–5, Figure S1 Tables 2, 3, Table S1
3	Natural history	5 M, 5 F	na	BBRC	1,000	Figures 2–5, Figure S1 Tables 2, 3, Table S1
4	Natural history	4 M, 4 F	8 M, 8 F	LRRI	1,000	Figures 2–5, Figure S1 Tables 2, 3, Table S1
5	Antibiotic efficacy, placebo control	5 M, 5 F (placebo) 4 M, 5 F (drug)	na	BBRC	1,000	Figures 3–5 Table 2, Table S1
6	Natural history, dose ranging	16 M, 12 F	na	USAMRIID	50, 500, 5,000	Figure 2 Table 3, Table S1

Cfu, colony forming units; M, male; F, female; na, not applicable; ST, Supporting Table; SF, Supporting Figure; LRRI, Lovelace Respiratory Research Institute; BBRC, Battelle Biomedical Research Center; USAMRIID, the United States Army Medical Research Institute for Infectious Diseases.

ethanized when moribund or at the end of the study following the American Veterinary Medical Association (AVMA) accepted methods of euthanasia.

***F. tularensis* Challenge Strain History and Provenance**

F. tularensis Schu S4 is a highly virulent strain which caused febrile disease and other symptoms in volunteers after inhalation of <20 cfu (Saslaw et al., 1961) and has been used in many historic studies in animal models (Lyons and Wu, 2007). SchuS4 was also administered in a low dose respiratory challenge study in humans investigating the safety and efficacy of the LVS of *F. tularensis* (Saslaw et al., 1961).

Aerosolized Schu S4 was used in the studies described in this manuscript. Source of challenge material was NIAID Schu S4 submaster cell bank [“Sublot 1,” stored at the Biodefense and Emerging Infections Research Resources Repository (BEI) under NR-10492], used for the preparation of challenge material. NR-10492 cell bank was manufactured following Good Manufacturing Practice (GMP) procedures by direct dilution of GMP-manufactured NIAID Schu S4 Master Cell Bank (BEI NR-28534), and characterized for its viability (cfu/ml); Gram stain, colony morphology, identity, purity, median lethal dose (LD₅₀) in BALB/c mice inoculated subcutaneously (s.c.), and LD₅₀ in New Zealand White Rabbits inoculated intranasally (i.n.), intravenously (i.v.), and s.c. The Master Cell Bank (BEI NR-28534) was originally propagated from the cell bank Lot No. 623-42 manufactured at the Salk Institute (Swiftwater, PA) in 1986. Cell bank Lot No. 623-42 was derived from a Schu S4 lot obtained from USAMRIID. Genomic sequences of NR-28534 and NR-10492 are publicly available at NCBI (accession numbers PRJNA270247 and PRJNA217349, respectively). Genome sequence annotation and analysis of NIAID cell banks NR-28534 and NR-10492 showed a single nucleotide polymorphism (SNP) in genomic DNA at location 1,767,864 of the published reference Schu S4 genome (GenBank number AJ749949.2)

which is located in intergenic region between open reading frames FTT_1698c (predicted formate dehydrogenase) and FTT_r08 (predicted 5S ribosomal RNA). NIAID cell banks NR-28534 and NR-10492 contain two copies of *Francisella* pathogenicity island (FPI) and are highly virulent in Fischer rats when administered by aerosol (LD₅₀ < 1 cfu, Hutt et al., 2017).

***F. tularensis* Challenge Material Preparation, Delivery, and Route of Administration**

F. tularensis Schu S4 was stored and used in Biosafety level 3 (BSL-3) laboratories following institutional SOPs and federal regulations for work with select agents. Animals were exposed to a target dose of 1,000 cfu aerosolized Schu S4 in aerosol particles of 1–3 microns mass median aerodynamic diameter (MMAD) in four natural history studies (Studies 1–4) and an antibiotic efficacy study (Study 5). Natural history Study 6 (Table 1) included three groups of animals, each exposed to target dose of 50, 500, or 5,000 cfu aerosolized Schu S4. For preparation of challenge material, individual Schu S4 colonies that were first grown on glucose cysteine blood agar (GCBA) at 37°C (at BBRC and LRRI) or the thawed material from the vials of bacterial stock stored at –80°C (at USAMRIID) were inoculated in liquid culture media for further propagation. Enriched Mueller Hinton II Broth supplemented with 0.1% glucose, and 2% IsoVitaleX, pH 7.0 was used at BBRC and USAMRIID, while Chamberlain’s broth (Chamberlain, 1965) was used for growth of *F. tularensis* at LRRI. Bacterial cultures were grown with aeration at 37°C until mid-log or early stationary phase of growth, after which they were suspended to a specific concentration (cfu/ml) in Brain Heart Infusion Broth (BHIB) at BBRC and LRRI, or enriched Mueller Hinton Broth (MHB) at USAMRIID to reach the desired target nebulizer mixture concentrations prior to aerosolization. Nebulizer mixtures used in animal exposures were analyzed by Gram stain, colony

morphology, purity, and viability by plating 10-fold dilutions onto GCBA plates.

Prior to challenge with *F. tularensis*, macaques were anesthetized and placed into the exposure chamber inside a Class III biological safety cabinet (BSC). *F. tularensis* Schu S4 was aerosolized by a 3-jet Collison nebulizer and delivered via a head-only inhalation exposure chamber in the BSC. Aerosol samples were collected from the exposure chamber using an all glass impinger (AGI) containing BHIB supplemented with anti-foam. Bacterial concentrations in the nebulizer and AGI were determined by spreading diluted samples on agar media. The bacterial suspension in the nebulizer was enumerated before and after aerosol generation. All plate cultures were visually inspected for colony morphology consistent with *F. tularensis*, and for lack of contamination. The temperature, relative humidity, and aerosol particle sizes were monitored during each exposure. The aerosol particle size distribution was determined based on samples collected from the exposure chamber and measured using an Aerodynamic Particle Sizer (APS) Spectrometer. Body plethysmography was used for measurement of the individual animal tidal volume, total accumulated tidal volume, and minute volume. The duration of the aerosol exposure was based upon an estimated Schu S4 concentration (cfu/ml) in aerosol determined in earlier studies and a cumulative minute volume measured for individual animals. Methods for the consistent delivery of the target challenge dose of *F. tularensis* were qualified during pre-challenge studies with *F. tularensis* Schu S4 aerosols and no animals, to calculate the spray factor necessary to achieve target doses of *F. tularensis* based on a fixed starting concentration of bacteria.

Clinical Observations and Histopathology

Animals were monitored for signs of disease including activity, body weight, morbidity, and mortality after the challenge for up to 14 days in Studies 2, 3, and 4, up to 28 days in studies 1 and 6, and up to 35 days after the challenge in the antibiotic efficacy Study 5. Telemetry transponders were implanted to measure physiologic parameters including core body temperature, respiration rate, systolic/diastolic pressure, and heart rate starting at 7–14 days before the challenge with *F. tularensis* and throughout the study. Core body temperature was measured in all studies, while respiration rate, systolic/diastolic pressure, and heart rate were measured in four of five natural history studies. Telemetry data were collected once for at least 30 s every 15 min. Body temperature data were summarized by hourly averages. Blood was collected for determination of bacteremia by plating on agar in all studies, and for hematology and clinical chemistry. Bacteremia and bacterial organ burdens were determined by plating on Chocolate II Agar or Thayer-Martin agar at 37°C. Organ burdens were typically determined by analysis of *F. tularensis* cell counts in organ lesions that were identified in course of gross pathology examination. Lesioned tissue was homogenized and plated on agar. The qPCR assay was used to detect bacterial DNA in animal blood in Studies 3 and 5. Briefly, nucleic acids were isolated from 100 μ L whole blood samples on an EasyMAG instrument

(bioMérieux, Durham, NC) and eluted into a final volume of 40 μ L. The purified nucleic acid samples were quantified as a number of DNA gene copies present in the samples using qPCR with *F. tularensis tul4* specific DNA primers (forward primer GCAGGTTTAGCGAGCTGTTCTAC; reverse primer ATGATGCAAAAGCTTCAGCTAAAG) and a minor groove binding probe (CTAGGGTTAGGTGGCTCT). The samples were analyzed on an ABI 7900HT instrument (Applied Biosystems, Carlsbad, CA) and the results were analyzed using Sequence Detection Systems (SDS) software. A linear regression was fit to the reference standard curve with cycle threshold (C_T) as the predictor and the logarithm of gene copies as the response.

Animals were humanely euthanized when moribund or at the end of the study. A complete necropsy was performed on all animals. External surfaces of the body, orifices, and the contents of the cranial, thoracic, and abdominal cavities were examined and all necropsy findings were recorded in descriptive terms including locations(s), size, shape, color, consistency, and number. Protocol-specified tissues were collected and organ bacterial burdens were evaluated from portions of tissues collected at necropsy, typically including spleen, liver, lungs, heart, brain, and various lymph nodes. All remaining tissues were fixed in 10% neutral buffered formalin. The fixed tissues were trimmed, embedded in paraffin, sectioned, and stained with hematoxylin and eosin for microscopic examination. An independent review of microscopic slides from these animals was performed by a blinded NIAID pathologist, to apply consistent terminology to the microscopic evaluation of tissues from animals in the natural history studies conducted at BBRC, LRRI, and USAMRIID.

Body Temperature Model, Fever Onset Determination, and Hypothermia Determination

Retrospectively after all studies were completed, body temperature recorded by telemetry (Studies 1–5; Study 6 had incomplete data) was modeled to evaluate a standardized approach to determining onset of fever; a similar framework was evaluated for determining morbidity, through onset of hypothermia. Hourly temperature readings during the period before exposure to the pathogen (“pre-exposure”) were modeled over time of day (24-h time transformed to a (0, 1] scale, i.e., midnight = 0, ..., 600 h = 6/24 = 0.25, ..., 2300 h = 23/24 = 0.9583) in the generalized additive models (GAM) framework. The smoothing function was a cyclic cubic spline to enforce smoothness over the midnight boundary. The data structure was accommodated through mixed effects: subject (nested in study and challenge date) and optionally study or challenge date (nested in study; Studies 1 and 5 included subsets of 6–10 subjects challenged on different dates 6–11 days apart) were included in the models as random effects on the intercept. Thus, the models comprise a GAM fixed effects component depicting the estimated population characteristic circadian rhythm of body temperature and a random effects component representing variation in baseline temperature due to subject, study, and challenge date. Model fitting was implemented using the gamm function in the

mgcv package in R; both Akaike's Information Criterion (AIC) and likelihood ratio tests were considered for model selection (Wood, 2017). AIC balances model complexity and fit with lower AIC-values indicating better support. AIC is reported as AIC differences (Δ AIC) with the best-supported model having Δ AIC = 0.00 and other models having positive Δ AIC. Models within 2 AIC units of the best-supported model (Δ AIC < 2.00) are considered to have good support while those more than 2 AIC units back (Δ AIC \geq 2.00) are considered to have poor support. Likelihood ratio tests are used only for nested pairs of models (Burnham and Anderson, 2003). Model predictions were appended to the full data set (i.e., pre- and post-exposure data) and differences from subject-specific predictions were taken as estimates of temperature elevation (or depression). Fever onset was determined as the first instance when temperature elevation was $\leq 1.5^\circ\text{C}$ over two or more consecutive hourly averages. Similarly, hypothermia was determined as the first instance when temperature depression was $\leq -1.5^\circ\text{C}$ over two or more consecutive hourly averages. Time to fever was analyzed using linear mixed effects models (Pinheiro and Bates, 2000) with candidate fixed effects predictors inhaled dose, weight, age (all centered and rescaled), and sex; inference was based on model selection using AIC and likelihood ratio tests. Study was included as a random effect. Time of hypothermia was simply described and not subject to any hypothesis tests.

RESULTS

Clinical Signs and Survival

Clinical signs of pneumonic tularemia in animals exposed to aerosolized *F. tularensis* Schu S4 typically started on Day 2 or 3 after challenge and included hunched posture, followed by lethargy, coughing, weakness, loss of appetite and weight loss, lower activity, labored breathing, and in some cases respiratory distress. Normal core body temperature followed a diurnal pattern immediately after the challenge until an increase over the baseline was observed in all animals starting on Day 2 or 3 (see an example in upper left in **Figure 1**). Hypothermia was often observed as animals succumbed to disease. Average respiratory rates remained near baseline levels for 2–3 days after challenge, and then increased above the baseline with an upward trend until macaques succumbed (lower right in **Figure 1**). Average animal heart rates remained near baseline during the first 2 days after challenge. Then heart rates increased to significantly greater than baseline average and were sustained during the next several days (upper right in **Figure 1**). Systolic and diastolic blood pressures remained steady until Day 3 after challenge when both began to decrease slightly. Their rate of decrease accelerated around Day 6, continuing downward until death about 3 days later (lower left in **Figure 1**).

An increase in total circulating white blood cells (WBC) typically started on Day 2 after challenge and peaked on Day 4 followed by a decrease and falling below baseline starting on Day 6 after challenge (**Figure S1**). The increase in WBC counts was due to a pronounced neutrophilia. Lymphocyte levels dropped precipitously below the normal range by Day 3–4 and remained low as the disease progressed. A marked

increase in the acute-phase C-reactive protein (CRP), a marker of inflammation, was observed in all animals, typically starting on Day 2 (**Figure S1**). CRP levels remained elevated until death. Serum biomarkers of tissue damage, lactate dehydrogenase (LDH), hepatic damage biomarkers aspartate aminotransferase (AST) and alanine aminotransferase (ALT), and kidney damage biomarker blood urea nitrogen (BUN) steadily increased with progression of tularemia, with significant increases in values over the pre-challenge baseline typically starting on Days 4 to 6 for LDH, Day 6 for AST and ALT, and Day 6 and later for BUN (not shown).

Survival of animals challenged with doses ranging 18–7,550 cfu *F. tularensis* Schu S4 in five natural history studies (Studies 1 through 4 and 6, **Table 1**) is shown in **Figure 2**. Among animals that were challenged with ~ 300 –3,000 cfu *F. tularensis* Schu S4, 44 out of 46 (95.7%) succumbed on Days 6 through 14, with two animals, each on a separate study, surviving the challenge. Challenge doses lower than 300 cfu Schu S4 resulted in a wider range of symptoms, disease clinical course, survival rates, and pathology outcomes, as it was also observed in previous studies (Glynn et al., 2015). A subset of animals challenged with doses above 3,000 cfu demonstrated faster disease progression and succumbed in 8 days or less (**Figure 2** and Glynn et al., 2015). The severe pneumonic tularemia disease model in which animals are exposed to doses above 3,000 cfu aerosolized *F. tularensis* would have a very short timeline between onset of disease and moribund state, with a narrow window for initiation of successful therapeutic treatment and demonstration of drug efficacy. Based on these results, Tularemia AMQ WG proposes a target challenge dose of 1,000 cfu aerosolized *F. tularensis* Schu S4 with 300–3,000 cfu tolerated dose range for the cynomolgus macaque model of pneumonic tularemia.

Bacteremia and Bacterial Organ Burden

The presence of *F. tularensis* Schu S4 in blood in animals in the five natural history studies was examined after plating on agar. Positive cultures were found in 32 out of 38 animals that were challenged with 300–3,000 cfu aerosolized Schu S4 on Study Days 2–8 (**Table S1**). Bacteremia has not been consistently detected on specific days after the challenge in these studies and was not correlated with the Schu S4 doses. The commonly used method of plating blood on agar plates is not highly sensitive for detection of bacteremia in models of tularemia. BBRC has developed and validated a qPCR method for measuring circulating bacterial genomes in the cynomolgus macaque based on amplification of a segment of the *F. tularensis* Schu S4 gene *tul4*. The qPCR assay was able to detect bacterial genomes in blood 1–4 days earlier when compared to the agar plating method in Study 3 (**Table S1**). In addition, the qPCR method detected bacterial genomes in blood of three animals which were not bacteremic based on agar plating results in this study (**Table S1**).

F. tularensis was also detected by agar plating in various organs including lungs, spleen, liver, mandibular and thoracic lymph nodes, and kidney in all challenged animals, with lungs showing the highest burdens of up to $\sim 10^8$ – 10^9 cfu *F. tularensis*/mg tissue in individual animals (not shown).

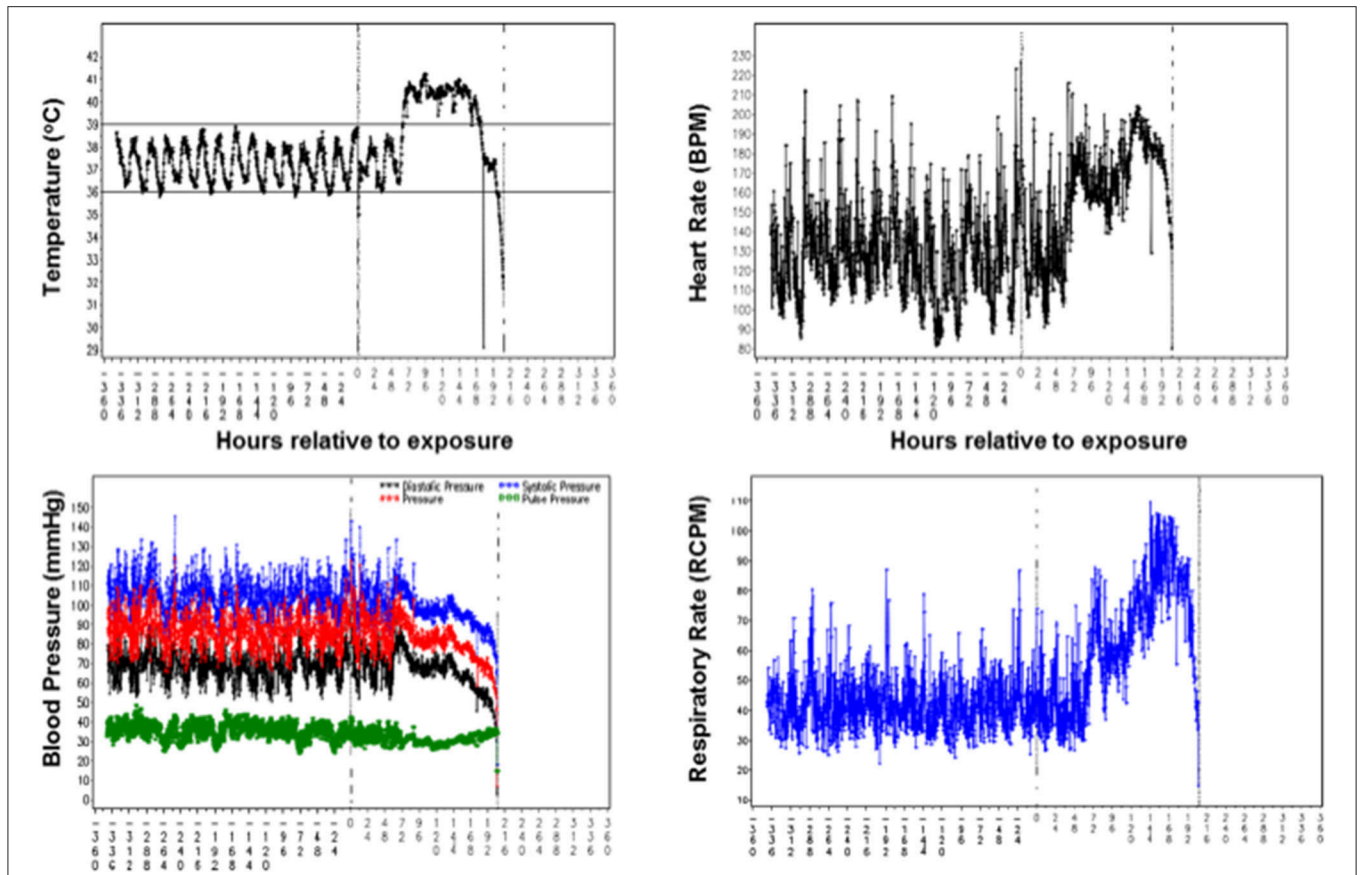


FIGURE 1 | Telemetry data of the core body temperature, heart rate, blood pressure, and respiratory rate recorded for a cynomolgus macaque exposed to 758 cfu *F. tularensis* in Study 2 (Table 1). Values on X axes in each graph represent time in hours before and after challenge with *F. tularensis* Schu S4 at 0 h.

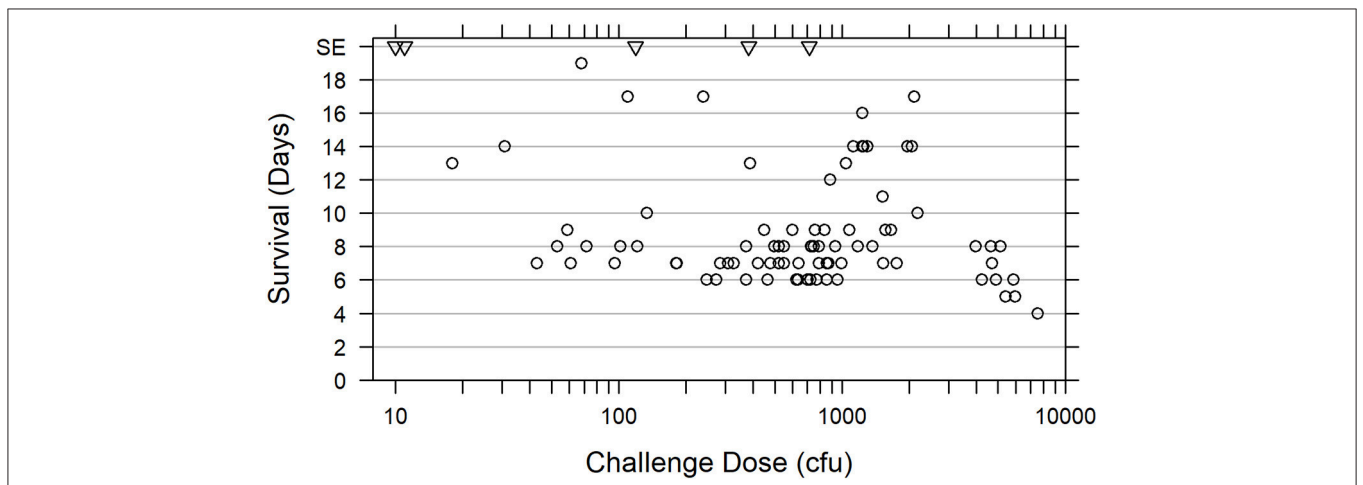


FIGURE 2 | Relationship between survival of cynomolgus macaques and *F. tularensis* Schu S4 challenge dose. Survival data are presented for 73 cynomolgus macaques challenged with 18 to 7,550 cfu aerosolized *F. tularensis* Schu S4 in five natural history studies (Studies 1 through 4 and Study 6, Table 1) (open circles). Data for two animals from the pathogenesis progression arm of Study 4 which succumbed prior to scheduled euthanasia are also included. Five animals that survived to the end of the study (SE) after exposure to 10, 11, 119, 382, or 714 cfu in four different studies, are also represented (triangles).

Model of Baseline Core Body Temperature

Fever was successfully used as a therapeutic trigger in human studies in which subjects were challenged with *F. tularensis* Schu S4 (Saslaw et al., 1961). A comprehensive analysis of core body temperature data recorded by telemetry was done to evaluate a standardized approach to determining onset of fever. Telemetry transponders were implanted to measure core body temperature starting at 7–14 days before the challenge with *F. tularensis* Schu S4 until the end of the study. Telemetry data from five natural history studies and one antibiotic efficacy study were analyzed to estimate baseline circadian rhythm of body temperature (see section Methods). Baseline core body temperature in one natural history study (Study 6) was markedly more variable than what was observed in the other studies (variance of residuals 0.351 compared to 0.146 or less for the other five studies), and telemetry recording in several animals in this study failed. The inconsistency in body temperature recordings that were the norm for other studies reported herein, and telemetry failure in several animals was likely an outcome of unsuccessful telemetry transponder surgery in Study 6. Due to lack of consistent baseline core body temperature data, animal body temperatures from this study were excluded from the remainder of the analysis. Data from the other five studies (four natural history studies, Studies 1 through 4, and one antibiotic efficacy study, Study 5) supported modeling random effects of subject nested in study but not challenge date. The models that included challenge date or excluded study had Akaike's Information Criterion differences (ΔAIC) = 1.9 to 4.7 (Table 2). Furthermore, likelihood ratio tests indicated study is a significant random effect (Model 2 vs. 4, test statistic 6.70, $p = 0.01$) but challenge date is not (Model 1 vs. 2, test statistic 0.00003, $p \approx 1$).

The GAM portion of the model was a parsimonious representation of baseline (pre-exposure) body temperature in the five included studies (adjusted $R^2 = 0.664$). Among the subjects across the five studies, modeled body temperature rose to about 38.0°C during the day and dropped to about 36.5°C at night (Figure 3). The standard deviation of the innermost residuals from the fitted model was 0.32°C implying that observed temperature was expected to be within 1.5°C of the subject-specific prediction about 99.99% of the time. Note that defining fever as two consecutive hourly readings $\geq 1.5^\circ\text{C}$ higher than the subject-specific prediction means that the probability of falsely determining fever is considerably $< 0.01\%$.

There were five instances in the pre-exposure period (two instances for one animal in Study 3 and three instances for one animal in Study 5) when hourly body temperature (T_b) was elevated 1.5°C or more above subject-specific baseline predictions but none occurred over consecutive hours or even within the same day; there were no instances when T_b was depressed 1.5°C or more below subject-specific predictions before exposure to *F. tularensis*.

Determination of Fever Onset

Among the 57 subjects included in this analysis (Studies 1 through 5, Table 1) that were challenged with Schu S4, all exhibited fever as defined above (core body temperature elevation $\geq 1.5^\circ\text{C}$ over two or more consecutive hourly averages)

TABLE 2 | Model selection for the random effects portion of the smooth model fit to pre-challenge data.

Model number	Random effects	Extra df	nIL	ΔAIC
1	Study, challenge date, subject	3	6,720.09	2.00
2	Study, subject	2	6,720.09	0.00
3	Challenge date, subject	2	6,721.05	1.91
4	Subject	1	6,723.44	4.70

Extra degrees of freedom (df) refers to the number of random effects. Negative log-likelihood (nIL) reflects goodness of fit with smaller values indicating better fit. AIC differences (ΔAIC) indicate the best-supported model having $\Delta AIC = 0.00$, models with $\Delta AIC < 2.00$ considered to have good support, and those with $\Delta AIC \geq 2.00$ considered to have poor support (Burnham and Anderson, 2003).

(Table S1). Fifty-four (54) subjects had computed fever onset between 40 and 70 h after challenge, one exhibited fever 26 h after challenge, and two others exhibited fever about 80 h after challenge. Mean time to fever across all studies was 57.3 h (standard deviation 8.6 h). Approximately 20% of the variance in time to fever was attributable to differences among studies and random effects coefficients (study-specific estimates of time to fever) ranged from 52.8 to 61.8 h. The 95% confidence interval for the fixed effect coefficient of that model was (52.4, 62.2). Fever onset was typically concurrent with or immediately followed clinical signs of disease in challenged animals. Fever preceded detection of bacteremia and was detected more often than bacteremia, similar to observations in humans with pneumonic tularemia. Therefore, fever is a more consistent biomarker of disease in pneumonic tularemia when compared to bacteremia.

Models that included effect of inhaled *F. tularensis* dose, weight, age, or sex on fever onset were not supported by the data (Figure 4). For the complete data set, AIC was lowest for the model that included age; the simple random effects model was nearly as well supported with $\Delta AIC = 0.60$. However, the effect of age was not strong (coefficient 1.47 h later for each additional year of age, 95% confidence interval $-0.33, 3.26$). Furthermore, noting the advanced age of seven subjects in Study 5 (aged 6 or 7 years; all 50 other subjects, including the 12 other subjects in that study, were aged 2–4 years), the influence of those older subjects was investigated by fitting the models to the data excluding subjects more than 4 years old. For that truncated data set, AIC is lower for the simple random effects model (model including age $\Delta AIC = 1.56$), meaning the truncated data do not strongly support including an age effect. While the coefficient for age remained positive, its 95% confidence interval broadly overlapped zero (1.26 h later for each additional year of age, 95% CI $-2.52, 5.07$). The age effect appeared spurious. Also for the complete data set, AIC for the model that included a fixed effect of inhaled dose was only 1.11 AIC units higher than the simple random effects model; however, the coefficient of the former model was positive (1.84 implying longer time to fever for higher inhaled doses) and its confidence interval included zero ($-2.27, 4.67$). These results showed that there was no strong effect of inhaled *F. tularensis* dose (43–2,182 cfu range), animal weight, age, or sex on fever onset in the studies presented herein.

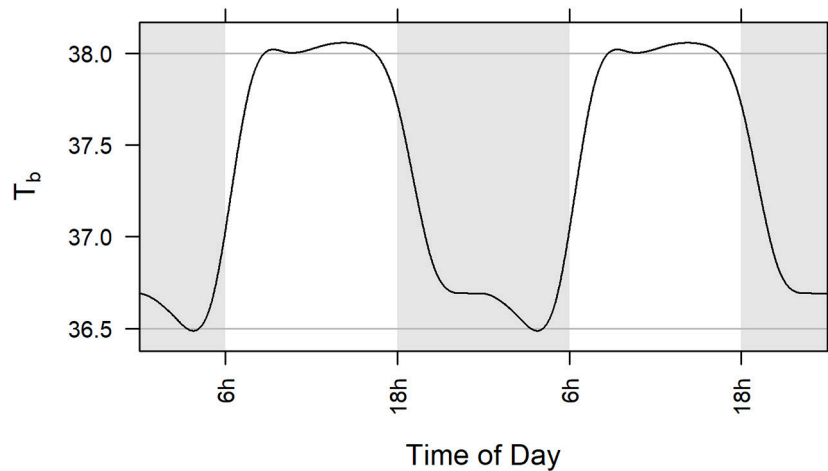


FIGURE 3 | Population level model (GAM) of circadian rhythm of body temperature in five studies illustrated over two 24-h cycles. Model is based on baseline core body temperature data of all subjects challenged with aerosolized *F. tularensis* in Studies 1, 2, 3, 4, and 5 (Table 1). Gray lines at 36.5 and 38.0°C represent a range of 1.5°C. Statistical methods used are described in section Materials and Methods.

Onset of Hypothermia and Morbidity

In studies described herein, animals were euthanized when they exhibited at least one protocol-defined euthanasia criterion, or at the scheduled termination of the study. Hypothermia was not included in protocol-defined euthanasia criteria in any of the six studies described. Onset of hypothermia was defined retrospectively after all studies were completed. Body temperature recorded by telemetry (Studies 1–5; Study 6 had incomplete data) was modeled to evaluate hypothermia as a tool for determining morbidity. Thirty-three (33) of the 57 subjects (Studies 1 through 5) were determined to have gone into hypothermia (Table S1), which was the first instance when temperature depression was $\leq -1.5^{\circ}\text{C}$ over two or more consecutive hourly averages. For five (5) subjects, time of hypothermia coincided with time of death (hypothermia determination at or 1 h before last telemetry recording). Twenty-six (26) other subjects survived for 3–57 h after hypothermia onset with steadily declining or irregular low body temperature (generally staying at least 1°C below subject-specific baseline) without ever recovering warmth. That left two subjects with indication of recovering warmth following hypothermia determination. In one case, body temperature rose above the subject's baseline again that evening through the next 4 days, even with periods of fever the following night, but it did not warm up on the third day when it was euthanized; that subject had unusually low baseline and was retrospectively flagged for large variance of residuals in the pre-exposure period. A second exception subject, which had not sustained fever more than about 24 h, regained warmth the morning after the hypothermia determination but then had low body temperature the following afternoon and was euthanized the day after that. A subset of animals (10 animals of 57; 17.5%) in all the analyzed studies (Studies 1 through 5) exhibited euthanasia criteria that indicated the onset of morbidity and mortality without meeting the criteria for onset of hypothermia. Examples of core body temperature

variation and onset of fever and hypothermia in individual animals are presented in Figure 5. Based on this analysis, we propose using hypothermia as a tool for determination of morbidity and inclusion of hypothermia in euthanasia criteria.

Pathology

Macroscopic Findings

The macroscopic findings observed during necropsy examination were similar regardless of the dose received, and/or the time-to-death following *F. tularensis* exposure. However, those animals receiving the lowest doses generally had less severe lesions affecting fewer organs. The most common lesions were observed in the lung, lymphoid tissues (spleen and lymph nodes), and liver.

Pulmonary findings typically affected all lung lobes, however, the caudal (inferior) lung lobe often appeared to have more severe changes. Findings in the lung included (but were not limited to) enlargement (failure to collapse), edema, mottled dark reddish-purple to black discoloration, fibrin on pleura, and randomly distributed, well-circumscribed to coalescing, tannish-white, firm to fluctuant foci. Additional thoracic findings include: blood-tinged, straw-colored pericardial fluid, and mediastinal edema.

Macroscopic findings in lymphoid tissues included enlargement and discoloration of lymph nodes and spleen and white/tan foci in the spleen. The most commonly affected lymph nodes were the mediastinal and tracheobronchial lymph nodes however similar lesions were observed in the mandibular, axillary, inguinal, and mesenteric lymph nodes. Splenic changes were also common but varied in severity between animals. The most noteworthy macroscopic lesion in the spleen consisted of tannish-white, flattened to slightly raised foci randomly dispersed throughout the parenchyma and capsular surface.

Hepatic changes included mild enlargement, dark red/brown color often with an accentuated lobular pattern. In some animals,

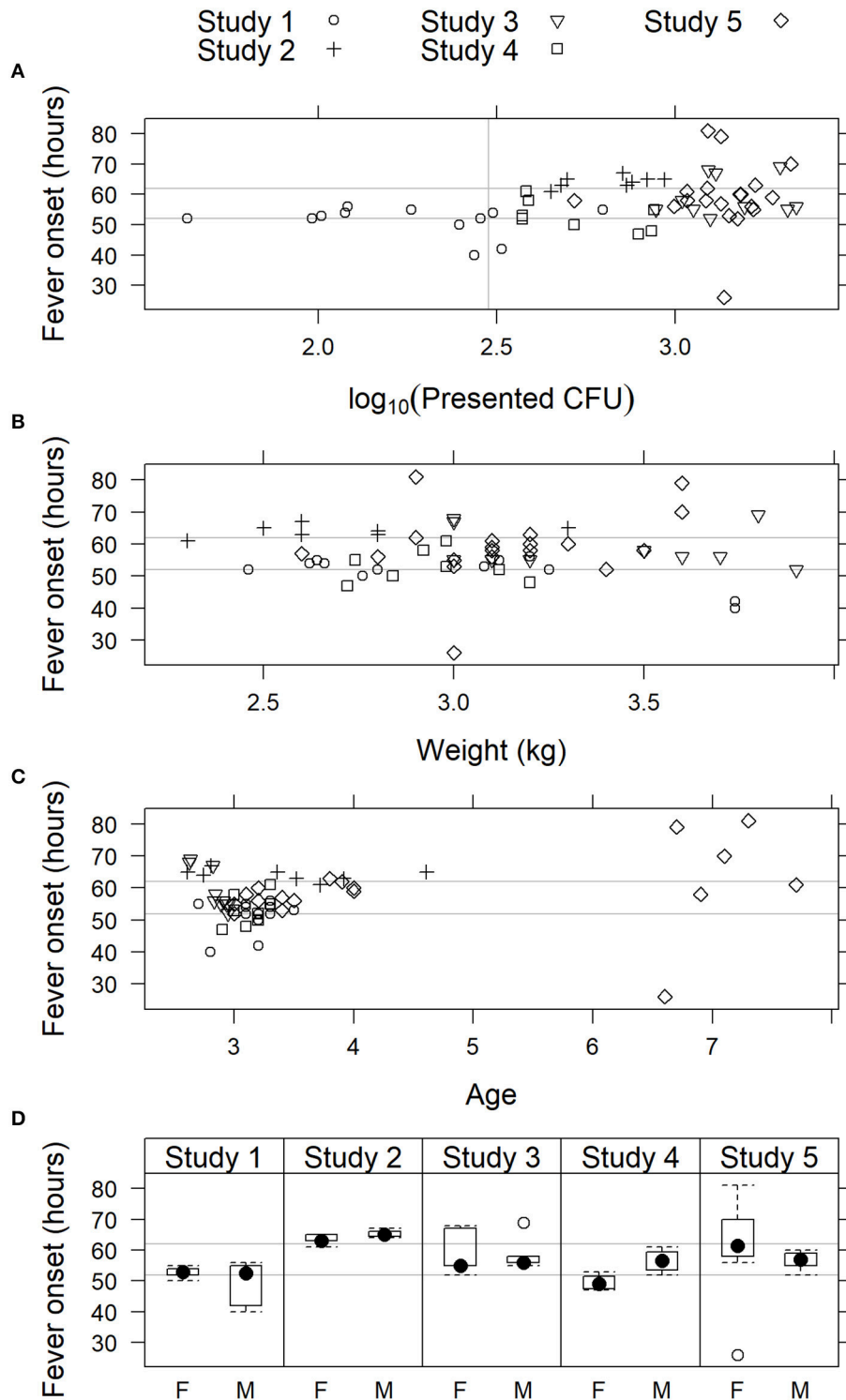


FIGURE 4 | Relationship of fever onset with physiological parameters in cynomolgus macaques exposed to 43 to 2,182 cfu *F. tularensis* Schu S4. In studies where fever onset was modeled, time of onset is plotted vs. (A) presented dose of *F. tularensis*; (B) body weight; (C) age; and (D) sex: female (F) or male (M). In (A–C), individual animals are represented by symbols, while sex data is presented as box and whiskers plots. Light gray horizontal lines represent the 95% confidence limits (52 and 62 h) of fever onset across all five studies.

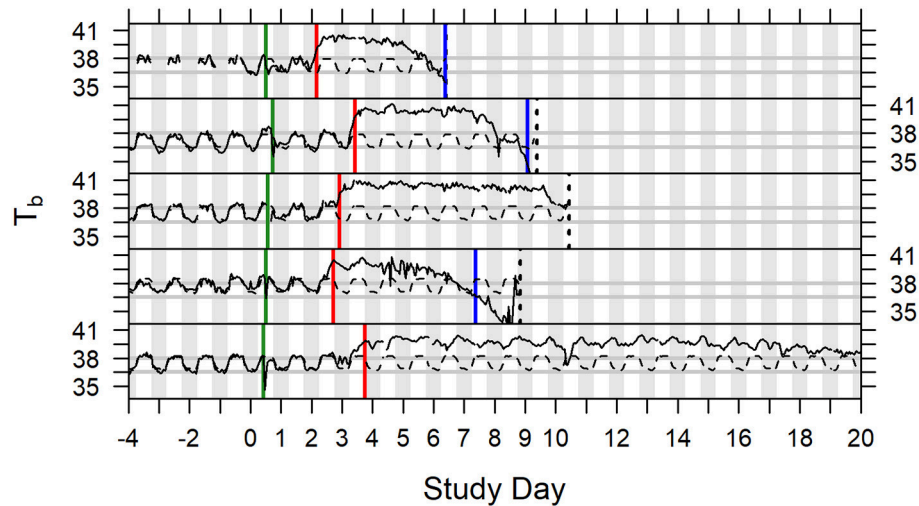


FIGURE 5 | Time series plots of body temperature for five animals depicted with subject specific model predictions of circadian rhythm, Study Days -4 through 19. Green vertical lines indicate exposure to aerosolized *F. tularensis* on Study Day 0. Red vertical lines indicate onset of fever. Blue vertical lines indicate onset of hypothermia. Dashed black vertical lines represent the time of death (the fifth subject illustrated survived to the end of the study).

randomly distributed, tannish-white foci were seen on the hepatic surface.

Histopathology

It is important to note that the tissue list for microscopic evaluation was different for each study. The only tissues evaluated microscopically in all animals from all studies were brain, liver, lung, tracheobronchial/bronchial lymph node, and spleen. In addition, the number and/or location of routine sections of lung processed to slide for microscopic evaluation were different for studies from each laboratory. Each laboratory handled the processing of pulmonary gross lesions in different ways.

In general, animals that received the lowest challenge doses had less severe lesions affecting fewer organs and tissues. The most common lesions were observed in the thoracic cavity, in the lung and mediastinal and tracheobronchial lymph nodes. Lesions were similar but varied in severity consisting of bronchiolar and alveolar inflammatory infiltrates of neutrophils and macrophages along with exudation of fibrin and protein-rich fluid, necrosis of infiltrating cells and pulmonary parenchyma, hypertrophy/hyperplasia of alveolar macrophages, and thrombi. Lesions were often associated with larger conducting airways and arterioles as well as randomly distributed, discrete inflammatory nodules which effaced alveolar and bronchiolar architecture. The latter was more common especially as the disease progresses. Pleural infiltrates with neutrophils and macrophages were also observed along with exudation of fibrin and protein-rich fluid and necrosis of infiltrating cells and pleural parenchyma. Lymphatic, perivascular and mural vascular infiltrates of neutrophils, macrophages, and exudation of fibrin were frequently observed along with necrosis of infiltrating cells. When present, these changes were also associated with perivascular edema and hemorrhage.

Hematopoietic and lymphoid tissues available for microscopic evaluation had inflammatory infiltrates, necrosis, hemorrhage, and/or edema similar to that observed in the lung. Affected lymph nodes had multifocal to coalescing areas of inflammatory infiltrates (neutrophil and macrophage), as well as edema and lymphoid follicle depletion. Infiltrating cells and lymphoid tissues were often in various stages of degeneration and necrosis. Lesions in the spleen included micronodular inflammatory infiltrates (neutrophil and macrophage), necrosis of red pulp and infiltrating cells, red pulp/lymph follicle depletion, and/or variable inflammation. As the disease progressed, splenic inflammation was accompanied by microthrombi in the splenic sinuses and trabecular vessels. In the most severely affected spleens, there was widespread necrosis of the red pulp and apoptosis and depletion of lymphocytes in the white pulp. In the bone marrow, micronodular inflammatory infiltrates (neutrophil and macrophage) were observed typically with necrosis of the infiltrating cells. In some animals, these infiltrates were accompanied by hemorrhage and myeloid hyperplasia.

The presence of micronodular inflammatory infiltrates was the primary change observed in affected livers from challenged animals. Inflammatory infiltrates (neutrophil and macrophage) were randomly distributed throughout the hepatic parenchyma with necrosis of infiltrating cells and in some cases adjacent hepatocytes. Inflammatory infiltrates were often accompanied by the presence of apoptotic cells in the hepatic sinusoids (likely hepatocytes, Kupffer cells) and/or intrasinusoidal fibrin microthrombi. Occasionally necrosis of small groups of hepatocytes and Kupffer cells were observed near sinusoids but not adjacent to areas of inflammatory infiltrate accumulations.

Few changes were observed in the kidney of challenged animals. These included hemorrhage, renal tubular degeneration,

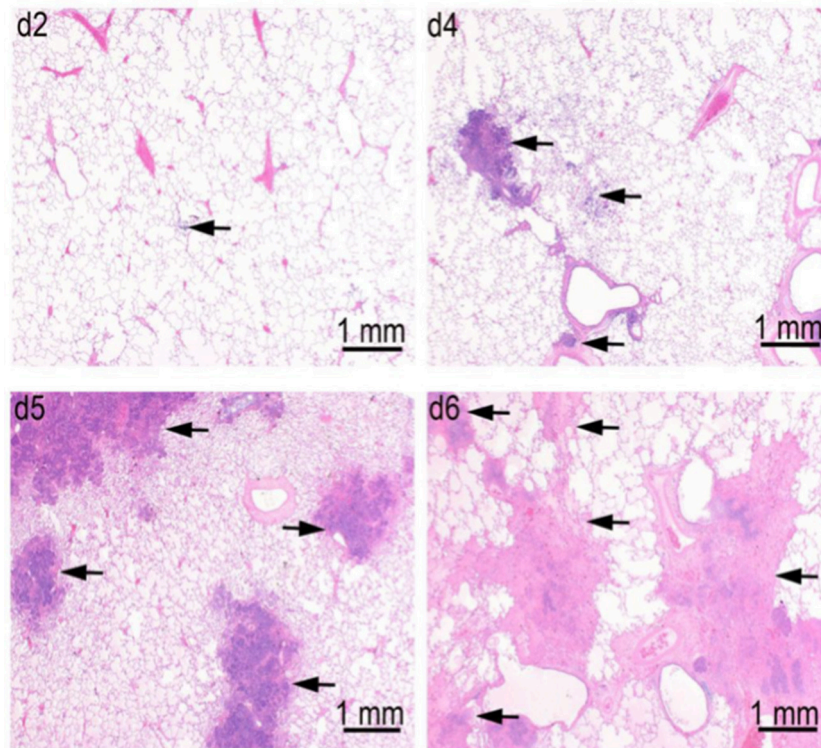


FIGURE 6 | Progression of lung lesions in cynomolgus macaques on Days 2 (d2), Day 4 (d4), Day 5 (d5), and Day 6 (d6) after challenge with aerosolized *F. tularensis* Schu S4. Data is shown for animals in the pathogenesis progression arm of Study 1 (Table 1). Arrows point to foci of inflammation and necrosis.

and foci of inflammatory infiltrates (neutrophils and macrophages) of minimal severity and low incidence.

Congestion and/or hemorrhage in the adrenal gland, pancreas, the urinary bladder mucosa, and throughout the gastrointestinal tract, when they occurred and were examined microscopically, were likely due to systemic *F. tularensis* infection. The most noteworthy gastrointestinal tract lesions were observed on the mucosal and, to a lesser extent, serosal surfaces of the pyloric stomach, ileocecal colic junction, and distal colon, suggestive of gastrointestinal-associated lymphoid tissue (GALT) hyperplasia, necrosis/inflammation, and/or hemorrhage.

In a pathogenesis progression arm of Study 1 (Table 1), the progression in severity of lesions in the lung, lymph nodes, spleen, and liver was clearly demonstrated. Pulmonary lesions progressed in severity from Day 2 through Day 6 post-challenge (Figure 6). Pulmonary lesions identified on Day 2 consisted of minimal to mild alveolar inflammatory infiltrates (neutrophil and macrophage), with fibrin exudation into the bronchioles and peribronchiolar alveoli. By Day 4, lesions had increased in severity, and were accompanied by inflammatory infiltrates of vessels (perivascular and mural), bronchioles, lymphatics, and pleura. By Days 5 and 6, all lesions increased in severity, and there was evidence of necrosis of infiltrating inflammatory cells and pulmonary parenchyma, with increased fibrin exudation and edema into alveoli. Inflammatory infiltration of the pleura

become extensive, and no longer only associated with the parenchymal foci.

Lymph nodes were affected in a similar manner with tracheobronchial and retropharyngeal lymph nodes affected first and most severely, followed by the mandibular lymph nodes. Initial lesions include micronodular inflammatory infiltrates of neutrophils and macrophages with fibrin exudates. By Days 5 and 6, necrosis of infiltrating cells and parenchyma had become so severe that some lymph nodes were left with only stromal framework. Comparable lesions were detected in the axillary lymph nodes by Days 5 and 6 in two animals, but no lesions were detected in inguinal and mesenteric lymph nodes. Inflammatory infiltrates in the red pulp of the spleen were observed on Day 2 and progressed to micronodules of neutrophils and histiocytes with necrosis by Day 4. By Days 5 and 6, these nodules expanded with increasing necrosis by Day 5 and 6. In some animals, foci of microthrombi formation in the splenic sinuses were observed at the latter time points. Liver lesions were not evident in any animals until Day 4, when randomly distributed foci of inflammatory infiltrates were observed. These micronodular lesions were more abundant by Day 5 and two animals developed widespread foci of sinusoidal microthrombi in the livers on Days 5 and 6.

A summary of tularemia-associated microscopic findings in the lungs of cynomolgus macaques challenged with aerosolized *F. tularensis* Schu 4 in natural history studies is shown in

Table 3. In summary, of the tissues available for microscopic evaluation, changes were noted in the lung (inflammatory infiltrates, fibrin, hemorrhage, edema, and/or necrosis), spleen (inflammatory infiltrates, fibrin, hemorrhage, and/or necrosis), lymph nodes (inflammatory infiltrates, necrosis, fibrin, edema, and/or hemorrhage), kidney (inflammatory infiltrates), sternal bone marrow (myeloid hyperplasia, inflammatory infiltrates and/or necrosis), and liver (inflammatory infiltrates and/or necrosis). Microscopic evaluation of tissues from animals in a pathogenesis progression study arm provided support for the progression of lesions in severity and incidence over time. Pulmonary inflammatory infiltrates comprised of neutrophils and macrophages, hemorrhage, fibrin exudation, necrosis (infiltrating cells, pleura, alveoli, bronchioles, vessels), and/or edema were prominent and present in the majority of animals from all studies. In affected animals, inflammatory infiltrates, hemorrhage, fibrin exudation, and/or necrosis were often observed in the thoracic lymph nodes (tracheobronchial and/or mediastinal) consistent with spread of bacteria from lymphatic drainage of infected pulmonary tissue. These lesions occurred in other lymph nodes (mandibular, axillary, mesenteric, and inguinal lymph nodes) but less frequently.

Microscopic evidence of septicemic spread of *F. tularensis* included nodular inflammatory infiltrates in the spleen (often accompanied by hemorrhage, fibrin exudation, and/or necrosis), liver (inflammatory infiltrates, necrosis and/or neutrophilic infiltrate), and sternal bone marrow (myeloid hyperplasia, micronodular inflammatory infiltrates, and/or necrosis).

Comparison of Pneumonic Tularemia in Cynomolgus Macaques and Humans

Clinical signs of pneumonic tularemia in cynomolgus macaques exposed to a target dose of 1,000 cfu (range 300–3,000 cfu) aerosolized *F. tularensis* Schu S4 and human pneumonic tularemia cases from published literature are highly similar (Table 4). In naturally occurring human cases, the infection route, time and dose are typically unknown and can only be estimated. For this reason, time to disease onset in human cases and animal studies is calculated from different starting points. The most frequently documented and typical clinical signs in both humans and the cynomolgus macaques were fever, detection of *F. tularensis* in blood or various organs (including lung, hilar lymph nodes, spleen, or liver), and change in heart and respiratory rates. Bacteremia was typically detected later than clinical signs and fever onset in both species (Table 4 and Table S1). It is difficult to compare bacteremia onset and bacterial burden after exposure to *F. tularensis* in human cases vs. animal models. In reported human cases, *F. tularensis* exposure doses, aerosolization parameters and exact time of exposure prior to onset of symptoms were unknown. In the studies reported herein, cynomolgus macaques were exposed to high doses of *F. tularensis* delivered in small particle aerosol, which resulted in severe disease and bacterial dissemination. Bacteremia in cynomolgus macaques exposed to 300–3,000 cfu aerosolized Schu S4 was observed starting on Day 4 after exposure (see

TABLE 3 | Summary of tularemia-associated microscopic findings in the lungs of cynomolgus macaques challenged with aerosolized *F. tularensis* Schu 4 in five natural history studies.

Number examined	Study 1*	Study 2	Study 3	Study 4*	Study 6	Total
	12 ^a	9 ^b	10	8	32	
Congestion	0	0	0	2	0	2
Edema, interstitium, intra-alveolar, and/or perivascular	1	9	10	8	31	59
Fibrin, intra-alveolar	0	8	10	5	30	53
Hemorrhage	12	2	0	2	20	36
Hyperplasia, bronchiolar	0	0	0	0	0	0
Inflammation, necrotizing, alveoli/bronchiole	0	2	0	0	0	2
Inflammation, necrotizing, vessels/perivascular	0	2	0	0	0	2
Inflammatory infiltrates, alveoli/bronchiole/bronchi, neutrophil, and macrophage ^c	12	7	10	8	30	67
Inflammatory infiltrate, intra-alveolar, macrophage	12	8	10	7	30	67
Inflammatory infiltrate, intra-alveolar, neutrophil	12	8	10	7	30	67
Inflammatory infiltrates, vessels/perivascular/mural, neutrophil, and macrophage	12	7	10	8	30	67
Necrosis, alveoli/bronchiole/bronchi	0	0	0	1	0	1
Pleura, inflammatory infiltrate, neutrophil, and/or macrophage with/without fibrin	11	9	10	9	25	64
Within normal limits	0	0	0	0	0	0

*Includes data from the pathogenesis progression arms of Studies 1 and 4 (see Table 1).

^aIncludes one animal that survived to study termination (Day 22).

^bOne animal was euthanized 2 days post-aerosol challenge due to complications from the telemetry unit surgery not due to illness from the challenge material. Therefore, the microscopic findings from this animal are not included in this summary table.

^cIn many sections presented for microscopic evaluation, necrosis of infiltrating cells and pulmonary parenchyma are prominent centrally with surrounding macrophages and exudated fibrin.

Table S1), mean day of death at 8.6 days post-exposure, whereas onset of fever, the first consistent sign of disease, occurred by Day 2–3 post-exposure. Bacteremia is likely a later disease stage event in both cynomolgus macaque model and human pneumonic tularemia disease cases. Bacteremia would not be detectable in patients soon after the antibiotic treatment is initiated, which may have also contributed to the low detection rates in human cases.

DISCUSSION

Based on the review and analysis of results of the studies described herein, we propose a set of critical parameters for the cynomolgus macaque (*M. fascicularis*) model of pneumonic tularemia to be used in the therapeutic efficacy studies as described in Table 5 and below. These criteria are currently under FDA review and may be revised upon final model qualification.

TABLE 4 | Natural course of pneumonic tularemia in human and cynomolgus macaque.

Disease symptoms and signs	Human ^a	Cynomolgus macaque ^b
Time course of disease	Approximately 2 weeks from onset of symptoms to death, with a range of 10–25 days	Typically 2–7 days from onset of fever to death
Body temperature	Fever can develop after a few days of illness (i.e., after 2–3 days after inhalation of a high dose of <i>F. tularensis</i> Schu S4)	Fever in 100% of cases (typically starting on Day 2–3 post-exposure)
<i>F. tularensis</i> detected	Positive in blood but not in all cases, positive in pharyngeal washings, sputum specimens, and gastric aspirates	Positive in blood but not in all cases, positive in lung, liver, spleen, and lymph nodes
Heart rate	Usually elevated but it can be slower than would be expected in the presence of high fever (pulse – temperature deficit)	Elevated (typically starting on Day 2 or 3 post-exposure)
Respiration rate	No change initially. Fulminant disease can rapidly progress to pneumonia and respiratory failure	Elevated (typically starting on Day 2 or 3 post-exposure)
Lung pathology	Pleural exudates, adhesions, and focal modular lesions can be found. Lobular pneumonia often involving all lobes is observed with areas of coagulation and caseous necrosis and sometimes cavitation. Microscopically, the exudate is composed of mononuclear cells with few lymphocytes, erythrocytes, epithelial cells, and plasma cells. The alveolar spaces are filled with exudate and sometimes fibrin. The alveolar septa are congested and may be necrotic. Blood vessels may show mononuclear infiltration, necrosis, and thrombosis. The perivascular lymphatics may be distended with a cellular or caseous exudate	Adhesions and discoloration of the lungs; fluid in the thoracic and abdominal cavities; necrotizing inflammation with variable amounts of hemorrhage and edema. The lesions were most consistent with a subacute necrotizing and suppurative bronchopneumonia with the most extensive lesions seen associated with larger airways and pulmonary arterioles and arteries. Abundant macrophages were present within neutrophilic or necrotic foci in the alveoli of lungs or surrounding liquefied necrotic centers forming caseating granulomas
Other findings	No specific clinical laboratory findings stand out. White blood count may reveal leukocytosis but not as elevated as would be expected for invasive bacterial disease. Increased CRP levels	Moderate leukocytosis on Day 2–3 followed by a drop after 48 h. Increase in CRP levels starting on Day 3

^aData from publications describing pneumonic tularemia in humans (Permar and MacLachlan, 1931; Blackford and Casey, 1941; Stuart and Pullen, 1945; McCrumb, 1961; Overholt et al., 1961; Saslaw et al., 1961; Hornick and Eigelsbach, 1966; Sawyer et al., 1966; Beisel, 1967; Beisel et al., 1967; Provenza et al., 1986; Syrjala, 1986; Penn and Kinasewitz, 1987; Tarnvik et al., 1989; Hoel et al., 1991; Scofield et al., 1992; Sjostedt et al., 1997; Dennis et al., 2001; Feldman et al., 2001; Haristoy et al., 2003; Lamps et al., 2004; Tarnvik and Chu, 2007; Penn, 2009; Fritsch and Spletstoeser, 2010; Thomas and Schaffner, 2010; Egan et al., 2011; Weber et al., 2012; Johansson et al., 2014).

^bReference is made to the disease signs in animals exposed to 300–3,000 cfu Schu S4 in natural history studies described in this manuscript.

The final qualification statement will be published on the FDA web site.

Animal Model Inclusion and Exclusion Criteria

Study animals need to fulfill defined inclusion criteria prior to challenge to be eligible for participation in the study. The following criteria are recommended for use in therapeutic efficacy studies: equal number of experimentally naïve males and females of Indochinese origin, aged between 3 and 7 years, weighing ≥ 2.5 kg. Animals of ~ 2 to ~ 7 years of age have been included in natural history studies described in this manuscript. There was no strong effect of animal sex, age, or weight on fever onset (see **Figure 4**), and no differences in disease progression or outcomes were observed in animals challenged with 309–2,182 cfu *F. tularensis* Schu S4 in natural history studies. However, we recommend including animals of 3–7 years of age and weighing ≥ 2.5 kg in therapeutics efficacy studies in which animals are subjected to additional pre-challenge and post-challenge procedures. Two-year old and younger animals are quite small (often < 2 kg) which increases both the anesthetic and surgical procedure risks, and decreases the blood volume available for analyses. In addition, smaller animals are at greater risk for dehydration and deteriorating condition because they have limited body reserve capacity.

Animals are to be healthy based on a clinical veterinary evaluation and history that reveals the absence of any clinically

relevant abnormality, which includes medical history, absence of viral, bacterial and parasitic infections, a physical examination, vital signs, ophthalmologic exam, the results of clinical chemistry, and hematology tests, and a urinalysis carried out within 30 days of challenge. In addition to clinically significant health issues, animal model study exclusion criteria consider any recent exposure to drugs or previous exposure to infectious agents, including *F. tularensis*, which may affect the course of infection and therapeutic efficacy study outcome. None of the studies included animal prescreening or examination of disease progression by lung radiography. We have aimed to develop and include model characterization methods that may be utilized by multiple research facilities, as some facilities may not have the necessary radiographic equipment in Biosafety level 3 laboratories. However, chest radiography may be considered as additional diagnostic methodology for use in animal prescreening in future studies.

Cynomolgus macaques that were used in the herein reported studies were obtained from Indochina. Recent publications describe the genetic heterogeneity of cynomolgus macaques obtained from Indochina, with some animals showing genetic evidence of interbreeding with rhesus macaques that started during the Pleistocene (Kanthaswamy et al., 2008). The bulk of cynomolgus macaques imported into the United States inhabit this active hybrid zone in Southeast Asia that includes Vietnam, Cambodia, Laos, and Burma. Consequently, Indochinese cynomolgus macaques exhibit much

TABLE 5 | Proposed critical parameters for the cynomolgus macaque (*Macaca fascicularis*) model of pneumonic tularemia.

Animal characteristics	Study inclusion criteria	Equal number of experimentally naive males and female of Indochinese origin Aged between 3 and 7 years, weighing ≥ 2.5 kg Healthy based on a clinical veterinary evaluation and history that reveals the absence of any clinically relevant abnormality ^a
	Study exclusion criteria	Any clinically significant (as deemed by the Clinical Veterinarian and Study Director) history of acute illness within 4 weeks of screening ^b Having evidence of previous exposure to <i>F. tularensis</i> or <i>Trypanosoma cruzi</i> Use of any antibiotic, antifungal, or antiparasitic within 14 days of challenge with <i>F. tularensis</i> Positive for a panel of viruses, bacteria, and parasites ^c Animals with increased white blood cell (WBC) counts or increased C-reactive protein (CRP) defined as a statistically significant increase over the corresponding reference range ^d
Challenge material	<i>F. tularensis</i> Schu S4 cell bank	Documented <i>F. tularensis</i> Schu S4 isolate history, provenance, and genomic DNA sequence corresponding to sequence of Schu S4 isolate described herein (BEI Cat. No. NR-10492, NCBI Accession #PRJNA217349) Documented cell bank identity, purity, viability, growth curve, and virulence in a small animal model (e.g., mouse, rat, or rabbit)
	Challenge material preparation	Growth in enriched Mueller-Hinton Broth (MHB) or Chamberlain's liquid medium that support <i>F. tularensis</i> Schu S4 growth Aerosol generator suspension is prepared using bacterial cultures in logarithmic phase of growth that were propagated from colonies of expected morphology
	Challenge material delivery	Delivery of 300–3,000 ^e cfu of <i>F. tularensis</i> Schu S4 in 1–5 μ m diameter aerosol particles using head-only exposure chamber Air volume inhaled by each animal is measured using methods such as plethysmography Concentration of viable aerosolized bacteria is measured during the exposure by enumerating the bacteria in an all-glass impinger Purity and colony morphology of challenge material delivered to each animal is confirmed Environmental conditions including air humidity and temperature during animal exposure are monitored and documented (>60% humidity in the exposure chamber is recommended)

Table contains critical parameters for the cynomolgus macaque model to be used in therapeutic efficacy studies as proposed by the Tularemia AMQ Working Group. Final model parameters may be modified upon FDA review.

^aIncludes a physical examination, medical history, vital signs, ophthalmologic exam, the results of clinical chemistry, and hematology tests, and a urinalysis carried out within 30 days of challenge.

^bIncluding asthma, or presence of cardiovascular, pulmonary, hepatic, renal, hematologic, gastrointestinal, endocrine, metabolic, immunologic, dermatologic, neurologic, or psychological disease; for example as assessed during the physical examination required for quarantine release. Current significant diarrhea, gastric stasis, or constipation.

^cPositive for Simian T Lymphotropic Virus (STLV-1), Simian Immunodeficiency Virus (SIV), Simian Retrovirus (SRV) Types 1 and 2, Macacine herpesvirus 1 (Herpes B virus), confirmed by currently accepted testing within 90 days of challenge. Positive *Salmonella*, *Shigella*, *Plasmodium*, and intestinal parasites, confirmed by currently accepted testing within 30 days of challenge. A positive TB test within 30 days of challenge.

^dUpon first recognition of either or both of these laboratory abnormalities, additional veterinary clinical evaluation of the animals including but not limited to additional physical examinations, additional blood draws for CRP- and WBC-value trends over time, WBC differentials and morphology, evaluation of other laboratory parameters (e.g., clinical chemistry) and the magnitude of the increases of CRP and WBC values should be conducted.

^eChallenge material dose range of 300–3,000 cfu *F. tularensis* Schu S4 is recommended based on similarities in disease progression and survival rates of cynomolgus macaques that were exposed to this dose range across all studies and performance sites, and the feasibility and the precision of delivery and quantification of 1,000 cfu Schu S4 challenge dose across all studies and performance sites.

greater genetic diversity than cynomolgus macaques from other geographic locations. Genetic evidence of natural interspecies admixture between cynomolgus and rhesus macaques in Indochina, leading to gene flow well beyond the hybrid zone, is well-documented (Kanthaswamy et al., 2013). This genetic diversity may account for differences in individual animal response and variations in disease and treatment outcomes. However, this model behaves consistently even with this genetic heterogeneity, such that drug efficacy can be extrapolated to a heterogeneous population of humans. In addition, age, weight, and sex of animals challenged with 300–3,000 cfu Schu S4 did not impact fever onset in studies described herein (see **Figure 4**).

Challenge Material Source, Preparation, and Delivery

To ensure the quality and reproducibility of exposures across the study, *F. tularensis* used for animal challenge is to be prepared from the cell banks generated from an isolate of a known history and provenance. Cell bank manufacture and storage, viability, morphology, and virulence in acceptable animal models of infection should be documented. The genomic DNA sequence of the *F. tularensis* Schu S4 cell bank used in studies described in this manuscript (BEI Cat. No. NR-10492, NCBI Accession #PRJNA217349) is identical, less a SNP, with previously published *F. tularensis* Schu S4 genomic DNA sequence (GenBank number AJ749949.2, Larsson et al., 2005).

A recent study comparing virulence of various *F. tularensis* strains in mice suggested that *F. tularensis* Schu S4 is not as highly virulent as *F. tularensis* clinical isolates, including an isolate (MA00-2987, Feldman et al., 2001; Matyas et al., 2007) from the blood of a fatal human case with pulmonary infection on Martha's Vineyard in year 2000 (Molins et al., 2014). We have performed full genome sequencing and compared DNA sequences of NIAID cell bank NR-10492 and the Schu S4 isolate used in the above referenced study (Molins et al., 2014). We also compared virulence of these two *F. tularensis* Schu S4 isolates side by side with the *F. tularensis* MA00-2987 in Fischer 344 rat model of pneumonic tularemia (Hutt et al., 2017). No rats ($n = 10/\text{group}$) that were exposed to target dose of 100 cfu aerosolized NIAID cell bank NR-10492 Schu S4 or MA00-2987 survived after 7 days post-exposure, while all rats exposed to aerosolized Schu S4 isolate that was used in Molins et al. (2014) survived through Day 21 post-exposure (manuscript in preparation). In addition, the less virulent Schu S4 isolate (Molins et al., 2014) had nine regions of difference in the genomic DNA sequence when compared to NIAID cell bank NR-10492, which may explain its reduced virulence in the rat model of pneumonic tularemia (manuscript in preparation). These results show that rigorous characterization of cell banks that are the source of infectious material is critical for successful animal model development.

A series of aerosol delivery qualification studies with sham aerosols (all steps taken except the animal exposure) were conducted at three performance sites (BBRC, LRRRI, and USAMRIID). These studies showed that delivery of aerosolized *F. tularensis* with acceptable cell viability and spray factor occurred when bacteria were grown to logarithmic phase prior to dilution into an aerosol generator mixture. There was no difference in disease progression and animal survival whether *F. tularensis* Schu S4 was grown in enriched MHB or Chamberlain's medium prior to exposure. *F. tularensis* was delivered in 1–5 μm diameter aerosol particles in the total volume of air that was estimated to contain the target dose of *F. tularensis* based on the minute inspiration volume recorded for each individual animal immediately prior to exposure using plethysmography. Viability and purity of aerosol generator mixture and delivered bacterial dose (samples collected in all-glass impinger) was analyzed by plating on agar after the exposure.

Animal Model Endpoints

The Tularemia AMQ WG intent is to qualify the natural history model of pneumonic tularemia in the cynomolgus macaque that will provide the basis for use of the model in evaluating the efficacy of antimicrobial therapeutics for the treatment and/or post-exposure prophylaxis of pneumonic tularemia under the Animal Rule. This model may also be used in the future for the development of vaccines for use in prevention of pneumonic tularemia. The Animal Rule states that the primary animal study endpoint has to be clearly related to the desired benefit in humans, such as the enhancement of survival or prevention of major morbidity (FDA, 2009, 2015). The Tularemia AMQ WG proposes that animal survival at a prospectively defined time point should be the primary endpoint

for therapeutic efficacy studies using the cynomolgus macaque model of pneumonic tularemia. This endpoint may differ in further refinement of this model for use in evaluation of vaccines efficacy.

Model secondary endpoints can consist of other critical model parameters/biomarkers that correlate with the disease progression and indicate that the model is functioning as expected across studies. We propose time to fever onset and bacteremia to be used as model secondary endpoints. Fever onset preceded clinical signs in animals across all studies reported in this manuscript. All 57 animals challenged with 300–3,000 cfu aerosolized *F. tularensis* Schu S4 in the natural history or therapeutic efficacy studies described herein exhibited onset of fever within 81 h, therefore, we propose that fever onset within this time frame in studies performed within the above described model parameters would serve as one of the indicators showing that the model is functioning as expected. In addition, we propose that fever onset be used as the trigger for initiation of treatment. Delay of treatment studies in which drug is administered at various time points after the onset of disease (in this case defined as the fever onset) may need to be performed to demonstrate drug therapeutic efficacy in advanced disease models. Hypothermia, defined as body temperature drop below the baseline (see **Figure 5** and accompanying text), may be indicative of the onset of morbidity in animal models of tularemia, as it was shown in a study that correlated hypothermia and survival of mice infected by *F. tularensis* (Molins et al., 2014). We propose to use hypothermia as one of the euthanasia criteria in future studies using this model.

Detection of bacteremia that correlates with challenge agent material is a common biomarker that is correlated with bacterial dissemination and disease progression. Unlike in infections with some other bacterial Tier 1 agents, bacteremia has not been consistently detected on specific days after challenge in the cynomolgus macaque model of pulmonary tularemia. This has also been observed in human cases of pulmonary tularemia, likely due to the relatively low levels of *F. tularensis* in blood during acute pneumonic tularemia (Saslaw et al., 1961).

Other potential model secondary endpoints examined by the Tularemia AMQ WG were hematology parameters and CRP levels. Changes in hematological parameters and CRP are non-specific indicators of disease. Results of the natural history studies described herein do not identify any hematological biomarkers of pneumonic tularemia. Although changes in hematology parameters are sometimes seen, none are identified as pathognomonic nor does there appear to be a characteristic pattern of change with pneumonic tularemia. Therefore, the WG believes the utility of these parameters is more applicable to inclusion or exclusion of animals onto therapeutic efficacy studies.

The results and analyses of the above described studies support the conclusion that signs of pneumonic tularemia in cynomolgus macaques exposed to 300–3,000 cfu of aerosolized *F. tularensis* Schu S4, under the conditions described herein, and human pneumonic tularemia cases are highly similar. The proposed *F. tularensis* Schu S4 challenge dose range resulted

in disease progression that would allow sufficient time for the initiation of therapeutic treatment after the onset of fever. Therefore, we propose that this model may be used for testing and development of tularemia therapeutics under Animal Rule. This model may also be further developed for use in efficacy testing of tularemia vaccines.

AUTHOR CONTRIBUTIONS

Conceived and designed the studies: TG, LL, MW, CH, PS, and JH. Analyzed the data: TG, LL, KO, MW, SH, CH, and JH. Wrote the paper: TG, LL, and KO.

FUNDING

This work was supported by NIH/NIAID contracts N01AI30061 and HHSN272201000003I to Battelle Biomedical Research Center (BBRC), HHSN266200500040C and HHSN266200400095I to Lovelace Respiratory Research Institute (LRRI), Interagency Agreement #Y1-AI-7282-01 to the United States Army Medical Research Institute for Infectious Diseases (USAMRIID), and HHSN272201500018C to Technical Resources International, Inc. (TRI).

ACKNOWLEDGMENTS

We are indebted to many excellent scientists and animal technicians who performed animal studies at BBRC, LRRI, and

USAMRIID, including Gabriel Meister, Katherine Brittingham, H. Carl Gelhaus, Kelly Jones, and Roy Barnewall at BBRC, Robert Sherwood, Michelle Valderas, Julie Hutt, Philip Kuehl, Julie Wilder, and Landon Westfall at LRRI, and Aysegül Nalca and Ondraya Frick at USAMRIID, who led the studies and provided many helpful suggestions during model development. We also thank Kristin DeBord (DHHS) for planning initial studies; Elizabeth Glaze, Blaire Osborn, and Dorte Jensen (NIAID) for thorough review of draft study reports and helpful suggestions; Edwin Nuzum, Marianne Baker (NIAID), and Richard Warren (consultant to BARDA) for valuable comments during discussions on critical model parameters.

SUPPLEMENTARY MATERIAL

The Supplementary Material for this article can be found online at: <https://www.frontiersin.org/articles/10.3389/fcimb.2018.00099/full#supplementary-material>

Figure S1 | Kinetics of changes in hematology and CRP-values in cynomolgus macaques after exposure to *F. tularensis*. The kinetics of changes in WBC counts (A), neutrophil counts (B), lymphocyte counts (C), and CRP plasma levels (D) in Studies 1, 2, 3, and 4 (Table 1) were plotted by study day. The data are plotted using a box and whiskers plot (Tukey method), where the dotted red vertical line represents the study day in which most animals developed fever (mean time to fever onset was 57 ± 8 h) and the shaded area for the hematology parameters represent the normal ranges in cynomolgus macaques.

Table S1 | Onset of fever, hypothermia and bacteremia. Onset of fever and hypothermia are shown for animals in four natural history studies (Study 1 through 4) and antibiotic efficacy study (Study 5). Bacteremia is shown for Studies 1 through 4.

REFERENCES

- Beisel, W. R. (1967). Neutrophil alkaline phosphatase changes in tularemia, sandfly fever, Q fever and noninfectious fevers. *Blood* 29, 257–268.
- Beisel, W. R., Bruton, J., Anderson, K. D., and Sawyer, W. D. (1967). Adrenocortical responses during tularemia in human subjects. *J. Clin. Endocrinol. Metab.* 27, 61–69.
- Blackford, S. D., and Casey, C. J. (1941). Pleuropulmonary tularemia. *Arch. Intern. Med.* 67, 43–71.
- Burnham, K. P. and Anderson, D. R. (2003). *Model Selection and Multimodel Inference: A Practical Information-Theoretic Approach, 2nd Edn*. Springer. doi: 10.1007/b97636
- CDC (2013). Tularemia - United States, 2001–2010. *MMWR Morb. Mortal. Wkly. Rep.* 62, 963–966.
- Celebi, G., Baruoñü, F., Ayoglu, F., Cinar, F., Karadenizli, A., Ugur, M. B., et al. (2006). Tularemia, a reemerging disease in northwest Turkey: epidemiological investigation and evaluation of treatment responses. *Jpn. J. Infect. Dis.* 59, 229–234.
- Chamberlain, R. E. (1965). Evaluation of live tularemia vaccine prepared in a chemically defined medium. *Appl. Microbiol.* 13, 232–235.
- Christenson, B. (1984). An outbreak of tularemia in the northern part of central Sweden. *Scand. J. Infect. Dis.* 16, 285–290.
- Dahlstrand, S., Ringertz, O., and Zetterberg, B. (1971). Airborne tularemia in Sweden. *Scand. J. Infect. Dis.* 3, 7–16.
- Dennis, D. T., Inglesby, T. V., Henderson, D. A., Bartlett, J. G., Ascher, M. S., Eitzen, E., et al. (2001). Tularemia as a biological weapon: medical and public health management. *JAMA* 285, 2763–2773. doi: 10.1001/jama.285.21.2763
- Egan, J. R., Hall, I. M., and Leach, S. (2011). Modeling inhalational tularemia: deliberate release and public health response. *Biosecur. Bioterror.* 9, 331–343. doi: 10.1089/bsp.2011.0004
- FDA (2017). *Animal Model Qualification Program*. Available online at: <https://www.fda.gov/drugs/developmentapprovalprocess/drugdevelopmenttoolsqualificationprogram/ucm284078.htm>
- FDA (2009). *Guidance for Industry: Animal Models – Essential Elements to Address Efficacy Under the Animal Rule*. FDA.
- FDA (2015). *Product Development Under the Animal Rule: Guidance for Industry*. FDA.
- Feldman, K. A., Ensore, R. E., Lathrop, S. L., Matyas, B. T., McGill, M., Schriefer, M. E., et al. (2001). An outbreak of primary pneumonic tularemia on Martha's Vineyard. *N. Engl. J. Med.* 345, 1601–1606. doi: 10.1056/NEJMoa011374
- Fritzsche, J., and Spletstoesser, W. D. (2010). Septic pneumonic tularemia caused by *Francisella tularensis* subsp. holarctica biovar II. *J. Med. Microbiol.* 59, 1123–1125. doi: 10.1099/jmm.0.019893-0
- Glynn, A. R., Alves, D. A., Frick, O., Erwin-Cohen, R., Porter, A., Norris, S., et al. (2015). Comparison of experimental respiratory tularemia in three nonhuman primate species. *Comp. Immunol. Microbiol. Infect. Dis.* 39, 13–24. doi: 10.1016/j.cimid.2015.01.003
- Haristoy, X., Lozniewski, A., Tram, C., Simeon, D., Bevanger, L., and Lion, C. (2003). *Francisella tularensis* bacteremia. *J. Clin. Microbiol.* 41, 2774–2776. doi: 10.1128/JCM.41.6.2774-2776.2003
- Hoel, T., Scheel, O., Nordahl, S. H., and Sandvik, T. (1991). Water- and airborne *Francisella tularensis* biovar palaeartica isolated from human blood. *Infection* 19, 348–350.
- Hornick, R. B. (1998). “Tularemia,” in *Bacterial Infections of Humans: Epidemiology and Control*, eds A. S. Evans and P. S. Brachman (New York, NY: Plenum Press), 823–837.
- Hornick, R. B., and Eigelsbach, H. T. (1966). Aerogenic immunization of man with live Tularemia vaccine. *Bacteriol. Rev.* 30, 532–538.
- Hutt, J. A., Lovchik, J. A., Dekonenko, A., Hahn, A. C., and Wu, T. H. (2017). The natural history of pneumonic tularemia in female fischer 344 rats after

- inhalational exposure to aerosolized *Francisella tularensis* subspecies *tularensis* strain SCHU S4. *Am. J. Pathol.* 187, 252–267. doi: 10.1016/j.ajpath.2016.09.021
- Johansson, A., Lärkeryd, A., Widerström, M., Mörtberg, S., Myrtännäs, K., Ohrman, C., et al. (2014). An outbreak of respiratory tularemia caused by diverse clones of *Francisella tularensis*. *Clin. Infect. Dis.* 59, 1546–1553. doi: 10.1093/cid/ciu621
- Kanthiswamy, S., Ng, J., Satkoski Trask, J., George, D. A., Kou, A. J., Hoffman, L. N., et al. (2013). The genetic composition of populations of cynomolgus macaques (*Macaca fascicularis*) used in biomedical research. *J. Med. Primatol.* 42, 120–131. doi: 10.1111/jmp.12043
- Kanthiswamy, S., Satkoski, J., George, D., Kou, A., Erickson, B. J., and Smith, D. G. (2008). Interspecies hybridization and the stratification of nuclear genetic variation of rhesus (*Macaca mulatta*) and Long-Tailed Macaques (*Macaca fascicularis*). *Int. J. Primatol.* 29, 1295–1311. doi: 10.1007/s10764-008-9295-0
- Lamps, L. W., Havens, J. M., Sjostedt, A., Page, D. L., and Scott, M. A. (2004). Histologic and molecular diagnosis of tularemia: a potential bioterrorism agent endemic to North America. *Mod. Pathol.* 17, 489–495. doi: 10.1038/modpathol.3800087
- Larsson, P., Oyston, P. C., Chain, P., Chu, M. C., Duffield, M., Fuxelius, H. H., et al. (2005). The complete genome sequence of *Francisella tularensis*, the causative agent of tularemia. *Nat. Genet.* 37, 153–159. doi: 10.1038/ng1499
- Lyons, R. C., and Wu, T. H. (2007). Animal models of *Francisella tularensis* infection. *Ann. N. Y. Acad. Sci.* 1105, 238–265. doi: 10.1196/annals.1409.003
- Matyas, B. T., Nieder, H. S., and Telford, S. R. III (2007). Pneumonic tularemia on Martha's Vineyard: clinical, epidemiologic, and ecological characteristics. *Ann. N. Y. Acad. Sci.* 1105, 351–377. doi: 10.1196/annals.1409.013
- McCrumb, F. R. (1961). Aerosol infection of man with pasteurella tularensis. *Bacteriol. Rev.* 25, 262–267.
- Meka-Mechenko, T., Aikimbayev, A., Kunitza, T., Ospanov, K., Temiralieva, G., Dernovaya, V., et al. (2003). Clinical and epidemiological characteristic of tularemia in Kazakhstan. *Przegl. Epidemiol.* 57, 587–591.
- Molins, C. R., Delorey, M. J., Yockey, B. M., Young, J. W., Belisle, J. T., Schriefer, M. E., et al. (2014). Virulence difference between the prototypic Schu S4 strain (A1a) and *Francisella tularensis* A1a, A1b, A2 and type B strains in a murine model of infection. *BMC Infect. Dis.* 14:67. doi: 10.1186/1471-2334-14-67
- Ohara, Y., Sato, T., and Homma, M. (1998). Arthropod-borne tularemia in Japan: clinical analysis of 1,374 cases observed between 1924 and 1996. *J. Med. Entomol.* 35, 471–473.
- Overholt, E. L., Tigertt, W. D., Kadull, P. J., Ward, M. K., Charkes, N. D., Rene, R. M., et al. (1961). An analysis of forty-two cases of laboratory-acquired tularemia. Treatment with broad spectrum antibiotics. *Am. J. Med.* 30, 785–806.
- Penn, R. L. (2009). “*Francisella tularensis* (Tularemia),” in *Mandell, Douglas, and Bennett's Principles and Practice of Infectious Diseases, 7th Edn.*, eds G. L. Mandel, J. E. Bennett, and R. Dolin (Philadelphia, PA: Elsevier; Churchill Livingstone), 2927–2937.
- Penn, R. L., and Kinasewitz, G. T. (1987). Factors associated with a poor outcome in tularemia. *Arch. Intern. Med.* 147, 265–268.
- Pérez-Castrillón, J. L., Bachiller-Luque, P., Martín-Luquero, M., Mena-Martín, F. J., and Herreros, V. (2001). Tularemia epidemic in northwestern Spain: clinical description and therapeutic response. *Clin. Infect. Dis.* 33, 573–576. doi: 10.1086/322601
- Permar, H. H., and MacLachlan, W. W. G. (1931). Tularemic pneumonia. *Ann. Intern. Med.* 5, 687–698.
- Pinheiro, J. C., and Bates, D. M. (2000). *Mixed-Effects Models in S and S-PLUS*. New York, NY: Springer.
- Provenza, J. M., Klotz, S. A., and Penn, R. L. (1986). Isolation of *Francisella tularensis* from blood. *J. Clin. Microbiol.* 24, 453–455.
- Reintjes, R., Dedushaj, I., Gjini, A., Jorgensen, T. R., Cotter, B., Lieftucht, A., et al. (2002). Tularemia outbreak investigation in Kosovo: case control and environmental studies. *Emerging Infect. Dis.* 8, 69–73. doi: 10.3201/eid0801.010131
- Saslaw, S., Eigelsbach, H. T., Prior, J. A., Wilson, H. E., and Carhart, S. (1961). Tularemia vaccine study. II. Respiratory challenge. *Arch. Intern. Med.* 107, 702–714. doi: 10.1001/archinte.1961.03620050068007
- Sawyer, W. D., Dangerfield, H. G., Hogge, A. L., and Crozier, D. (1966). Antibiotic prophylaxis and therapy of airborne tularemia. *Bacteriol. Rev.* 30, 542–550.
- Scotfield, R. H., Lopez, E. J., and McNabb, S. J. (1992). Tularemia pneumonia in Oklahoma, 1982–1987. *J. Okla. State Med. Assoc.* 85, 165–170.
- Sjostedt, A., Eriksson, U., Berglund, L., and Tarnvik, A. (1997). Detection of *Francisella tularensis* in ulcers of patients with tularemia by PCR. *J. Clin. Microbiol.* 35, 1045–1048.
- Stuart, B. M., and Pullen, R. L. (1945). Tularemic pneumonia: review of American literature and report of 15 additional cases. *Am. J. Med. Sci.* 210, 223–236. doi: 10.1097/00000441-194508000-00013
- Syrjala, H. (1986). Peripheral blood leukocyte counts, erythrocyte sedimentation rate and C-reactive protein in tularemia caused by the type B strain of *Francisella tularensis*. *Infection* 14, 51–54. doi: 10.1007/BF01644441
- Tarnvik, A., and Chu, M. C. (2007). New approaches to diagnosis and therapy of tularemia. *Ann. N. Y. Acad. Sci.* 1105, 378–404. doi: 10.1196/annals.1409.017
- Tarnvik, A., Henning, C., Falsen, E., and Sandstrom, G. (1989). Isolation of *Francisella tularensis* biovar palaeartica from human blood. *Eur. J. Clin. Microbiol. Infect. Dis.* 8, 146–150. doi: 10.1007/BF01963900
- Tarnvik, A., Sandstrom, G., and Sjostedt, A. (1996). Epidemiological analysis of tularemia in Sweden 1931–1993. *FEMS Immunol. Med. Microbiol.* 13, 201–204. doi: 10.1111/j.1574-695X.1996.tb00237.x
- Thomas, L. D., and Schaffner, W. (2010). Tularemia pneumonia. *Infect. Dis. Clin. North Am.* 24, 43–55. doi: 10.1016/j.idc.2009.10.012
- Weber, I. B., Turabelidze, G., Patrick, S., Griffith, K. S., Kugeler, K. J., and Mead, P. S. (2012). Clinical recognition and management of tularemia in Missouri: a retrospective records review of 121 cases. *Clin. Infect. Dis.* 55, 1283–1290. doi: 10.1093/cid/cis706
- Wood, S. N. (2017). *Generalized Additive Models: an Introduction with R*. Boca Raton, FL: CRC Press/Taylor & Francis Group.

Conflict of Interest Statement: KO is employed by Mergus Analytics, LLC, a subcontractor to TRI.

The other authors declare that the research was conducted in the absence of any commercial or financial relationships that could be construed as a potential conflict of interest.

Copyright © 2018 Guina, Lanning, Omland, Williams, Wolfrain, Heyse, Houchens, Sanz and Hewitt. This is an open-access article distributed under the terms of the Creative Commons Attribution License (CC BY). The use, distribution or reproduction in other forums is permitted, provided the original author(s) and the copyright owner are credited and that the original publication in this journal is cited, in accordance with accepted academic practice. No use, distribution or reproduction is permitted which does not comply with these terms.



Adaptive Immunity to *Francisella tularensis* and Considerations for Vaccine Development

Lydia M. Roberts¹, Daniel A. Powell² and Jeffrey A. Frelinger^{2*}

¹ Immunity to Pulmonary Pathogens Section, Laboratory of Bacteriology, Rocky Mountain Laboratories, National Institute of Allergy and Infectious Diseases (NIAID), National Institutes of Health (NIH), Hamilton, MT, United States, ² Department of Immunobiology and Valley Fever Center for Excellence, University of Arizona, Tucson, AZ, United States

Francisella tularensis is an intracellular bacterium that causes the disease tularemia. There are several subspecies of *F. tularensis* whose ability to cause disease varies in humans. The most virulent subspecies, *tularensis*, is a Tier One Select Agent and a potential bioweapon. Although considerable effort has made to generate efficacious tularemia vaccines, to date none have been licensed for use in the United States. Despite the lack of a tularemia vaccine, we have learned a great deal about the adaptive immune response that underlies protective immunity. Herein, we detail the animal models commonly used to study tularemia and their recapitulation of human disease, the field's current understanding of vaccine-mediated protection, and discuss the challenges associated with new vaccine development.

Keywords: *Francisella tularensis*, vaccine development, immune response, T cells, Antibodies

OPEN ACCESS

Edited by:

Anders Sjöstedt,
Umeå University, Sweden

Reviewed by:

Chandra Shekhar Bakshi,
New York Medical College,
United States
Girish Soorappa Kirimanjeswara,
Pennsylvania State University,
United States

*Correspondence:

Jeffrey A. Frelinger
jfrelin@email.arizona.edu

Received: 05 January 2018

Accepted: 23 March 2018

Published: 06 April 2018

Citation:

Roberts LM, Powell DA and
Frelinger JA (2018) Adaptive Immunity
to *Francisella tularensis* and
Considerations for Vaccine
Development.
Front. Cell. Infect. Microbiol. 8:115.
doi: 10.3389/fcimb.2018.00115

INTRODUCTION

Francisella tularensis is a Gram-negative intracellular bacterium and the causative agent of tularemia. *Francisella* can be transmitted by aerosol, breaks in the skin, ingestion of contaminated water, and bites of infected arthropods. Virulent, or Type A strains, of *F. tularensis* subspecies *tularensis* (*F. tularensis*) cause severe disease in both humans and other vertebrates, even infecting soil amoeba, at low exposure doses. The less virulent Type B *F. tularensis* subspecies *holartica* (*F. holartica*) strains also have a broad host range, but do not cause severe disease. While only 100–200 natural cases of tularemia are reported each year in the US, *F. tularensis* is a significant biothreat and has been weaponized (Christopher et al., 1997; Alibek and Handelman, 1999). Today, *Francisella* is categorized as a Tier 1 Select Agent due to its low infectious dose, ease of aerosolization, and ability to persist in the environment.

Ideally, there would be an efficacious vaccine for such a high consequence pathogen, however, no licensed vaccine for tularemia is available. The Live Vaccine Strain (LVS) was developed in the Soviet Union from *F. holartica* and provides limited protection (Eigelsbach and Downs, 1961). This vaccine is not currently licensed in the United States as the protection engendered is limited. Many recent attempts have been made to produce new vaccines against *Francisella*. While a successful vaccine has yet to be produced, the collective knowledge gained from these studies has provided many important insights into the immune response to *Francisella* vaccination and subsequent protection. Together, these data provide critical information as to the nature of protective immunity that must be provoked by future vaccine candidates.

Here, we discuss the animal models used to study the immune response to *Francisella* including their recapitulation of human disease and respective limitations. Next, we detail the adaptive

immune response and the effector functions that have been identified as protective. Finally, we address the challenges associated with developing effective tularemia vaccines.

CHARACTERISTICS OF HUMAN INFECTION

Tularemia presents in human patients in several forms dependent on exposure route and subspecies of the infecting strain. The most common presentation is ulceroglandular tularemia which is generally caused by an arthropod bite or skin abrasions (Tärnvik et al., 1996; Ohara et al., 1998). Bacteria will spread from this entry site through the lymphatic system to draining lymph nodes. From the lymph nodes, bacteria may disseminate to the periphery including the spleen, liver, lungs, kidneys, central nervous system, and skeletal muscle (Ellis et al., 2002). Ulceroglandular tularemia associated with subspecies *holarctica* is rarely fatal, with less than a 3% case mortality (Evans et al., 1985). Comparatively, pneumonic tularemia is caused by subspecies *tularensis* and carries a mortality rate ranging from 30 to 60% in the absence of therapeutic intervention (Gill and Cunha, 1997). Patients generally present with flu-like symptoms including chills, fever and headaches; diagnosis is achieved by selective culture, PCR, or serology (Burke, 1977; Carlsson et al., 1979; Koskela and Salminen, 1985; Syrjälä et al., 1986; Clarridge et al., 1996; Johansson et al., 2000). Treatment with antibiotics, like ciprofloxacin, is generally effective although β -lactam antibiotics are not due to a β -lactamase gene in *Francisella*. Convalescent patients have detectable antibody and T cell responses which are described in more detail later.

ANIMAL MODELS OF TULAREMIA

The 2002 “Animal Rule” (21 CFR 314.600-650 and 601.90) from the United States Food and Drug Administration (FDA) applies to development of novel *F. tularensis* therapeutics and vaccines given the highly pathogenic nature of human infection. The inability to ethically or appropriately test new therapies in humans requires efficacy testing in relevant animal model(s) prior to FDA licensure. Recently, a novel *Bacillus anthracis* vaccine was approved under the animal rule and several therapeutics for high consequence pathogens have been approved in the last decade after clinical efficacy was determined in appropriate animal models (Beasley et al., 2016; Park and Mitchel, 2016). There are multiple animal models for tularemia and their ability to recapitulate human disease is discussed below.

Mice

The mouse is the most commonly used animal to study tularemia due to its relatively low cost, well-characterized genetics, and available immunological tools. Most importantly, mouse infection with virulent *F. tularensis* recapitulates human disease. Like humans, mice are extremely susceptible to low doses (< 50 CFUs) of *F. tularensis*, developing disseminated disease that is asymptomatic for the first 2–3 days after inoculation (Shen et al., 2004; Pechous et al., 2008). Additionally, mice and humans

can be successfully vaccinated with *F. holarctica* LVS, but this protection only applies to low *F. tularensis* inoculum doses within a short timeframe post-vaccination (McCrum, 1961; Saslaw et al., 1961a; Chen et al., 2003; Conlan et al., 2005; Roberts et al., 2017). Mice are more resistant to *F. holarctica* than *F. tularensis* by certain routes of inoculation, yet extremely susceptible to *F. novicida* (Fortier et al., 1991; Conlan et al., 2003; Lauriano et al., 2004; Wu et al., 2005). Although the susceptibility of humans and mice differs greatly for *F. novicida* and there are some differences for *F. holarctica*, these discrepancies are not critical as they relate to the animal rule. The animal rule applies only to *F. tularensis*; therefore, the animal model used to test novel vaccines or therapeutics only needs to closely resemble human disease with *F. tularensis*. The BALB/c and C57Bl/6 mouse strains are the most prevalent in the literature for evaluating immune responses to *Francisella* although a variety of common laboratory mouse strains were tested in Shen et al. (2004). Initially, only BALB/c mice could survive *F. tularensis* challenge after immunization with LVS (Shen et al., 2004; Wu et al., 2005; KuoLee et al., 2007; Twine et al., 2012). More recently, C57Bl/6 mice were protected using a different strain of LVS (RML LVS) indicating the vaccinating strain utilized is critical for the development of protective immunity (Griffin et al., 2015).

Rats

Historically, white rats were used in tularemia studies and found to be more resistant to *F. tularensis* than mice when various inoculation routes were tested (Downs et al., 1947). More recently, Fisher 344 rats have been used and found to mimic human susceptibility to the various subspecies of *Francisella* (Ray et al., 2010). The *F. tularensis* intratracheal LD₅₀ for Fisher 344 rats is ~500 CFUs which is higher than the 10–15 CFUs that can cause lethal disease in humans (McCrum, 1961; Ray et al., 2010). Despite this moderate difference in susceptibility, pulmonary infection of rats does recapitulate human disease pathology (Francis and Callender, 1927; Dennis et al., 2001; Lamps et al., 2004; Guarner and Zaki, 2006; Hutt et al., 2017). *F. holarctica* LVS and *F. novicida* vaccine efficacy has been evaluated in Fisher 344 rats and found to protect against virulent challenge (Wu et al., 2009; Signarovitz et al., 2012; Chu et al., 2014). One argument for the use of rats as the preferred small animal model is their ability to be protected from high doses of pulmonary *F. tularensis* challenge (2×10^5 CFU) after *F. holarctica* LVS vaccination (Wu et al., 2009). While the ability to protect against high doses of *F. tularensis* is a primary goal in vaccine development, the rat's natural resistance to *F. tularensis* may overestimate the protective efficacy of a vaccine candidate as human studies have demonstrated poor or moderate protection with 10- to 100-fold lower challenge doses (McCrum, 1961; Hornick and Eigelsbach, 1966).

Rabbits

The use of rabbits as an animal model for tularemia has recently been revisited. Tularemia is also known as “rabbit fever” and rabbits are a natural host for *Francisella* species. Disease in the rabbit recapitulates human pathology and rabbits show similar susceptibility to the different subspecies of *Francisella*

like humans (Baskerville and Hambleton, 1976; Reed et al., 2011; Brown et al., 2015a). New Zealand White rabbits tolerate high doses of *F. holartica* LVS during oral, respiratory, or scarification vaccination, yet vaccinated animals do not survive *F. tularensis* challenge (Pasetti et al., 2008; Reed et al., 2014; Stinson et al., 2016). Similarly, type B vaccinated wild-caught cottontail rabbits had an extension in the mean time to death after type A challenge compared to unvaccinated animals but did not survive virulent secondary infection (Brown et al., 2015b). Defined *F. tularensis* mutants were partially protective against aerosol challenge with 50–500 LD₅₀ doses of wild-type *F. tularensis* in the New Zealand White rabbit suggesting the choice of vaccinating strain impacts protection (Reed et al., 2014). Overall, the rabbit is another appropriate small animal model for evaluating vaccine efficacy prior to non-human primate (NHP) or human studies.

Non-human Primates

Although NHP studies are more challenging and costly to conduct, this animal model also recapitulates tularemia pathology in humans. Importantly, NHPs mirror several aspects of human disease not observed in the rabbit, rat, or mouse. First, NHPs can develop skin lesions and lymphadenopathy (Nelson et al., 2010). Second, primates have V9 γ V28 T cells which expand after human infection, but are absent in small rodents (Sumida et al., 1992; Kroca et al., 2000). Several NHP species have been used in tularemia studies including African green monkeys, cynomolgus macaques, grivet monkeys, rhesus macaques, and marmosets (Hornick and Eigelsbach, 1966; Sawyer et al., 1966; Tulis et al., 1970; Baskerville et al., 1978; Hambleton et al., 1978; Nelson et al., 2009, 2010; Twenhafel et al., 2009; Chu et al., 2014; Glynn et al., 2015). Most NHP species have similar susceptibility to *F. tularensis* infection as humans with lethal infectious doses <100 CFUs (Nelson et al., 2009; Glynn et al., 2015). While the LD₅₀ for rhesus macaques was determined to be low (14 CFU) in the 1970's, a more recent study found they were remarkably resistant (lethal dose >2 \times 10⁵ CFU) (Day and Berendt, 1972; Glynn et al., 2015). The original study found the particle size affected the LD₅₀ with larger particles having higher LD₅₀ values (Day and Berendt, 1972). This factor could be contributing to the large difference in LD₅₀ values between the two studies. There have been a limited number of vaccine studies in NHP using either LVS or *F. novicida*. As observed in the mouse and rat, LVS vaccination can protect NHP during *F. tularensis* challenge (Eigelsbach et al., 1962; White et al., 1962; Hornick and Eigelsbach, 1966; Chu et al., 2014). To date, there is no consensus on the most appropriate NHP species to use for tularemia studies although there are clearly several candidates that mirror human disease.

Ultimately, studies in mice, rats, rabbits, and NHPs will likely be required to satisfy the Animal Rule for new tularemia vaccines or therapeutics. Mice, rats, and rabbits are particularly useful for evaluating vaccine efficacy and defining mechanisms of protection given their small size, available tools, and ability to recapitulate various aspects of human disease. A vaccine or therapeutic that is successful in small mammals, especially given the mouse's increased susceptibility to *F. tularensis*, is likely to have success in NHPs. Following confirmatory studies in NHPs

that indicate a high probability of success in humans, the FDA's Animal Rule will be satisfied.

IMMUNE RESPONSES TO FRANCISELLA

B Cells

Tularemia infection induces anti-*Francisella* antibodies in both mouse and man (Koskela and Herva, 1982; Koskela, 1985; Koskela and Salminen, 1985; Janovská et al., 2007). Many of these antibodies are directed against the LPS components, especially early in the infection, but many other immunogenic proteins have been described (Dreisbach et al., 2000; Eyles et al., 2007). It was reported that immunization of DBA/2 and C57Bl/6 with *F. holartica* LVS did not protect mice from lethal challenge with virulent *F. tularensis*. In contrast, vaccination of BALB/c or C3H/HeN mice were protected following identical vaccination (Twine et al., 2006b; Kilmury and Twine, 2010). Serum from C57Bl/6 and BALB/c were shown to recognize both shared and unique proteins from *Francisella*. It is not clear if this reflects an intrinsic difference in their B cell responses or a difference in the CD4 helper response. The proteins differentially recognized include outer membrane associated proteins as well as protein chain elongation factors (Twine et al., 2006a).

Antibodies against *Francisella* LPS have shown a protective capacity against lethal intradermal and intraperitoneal LVS challenge (Rhinehart-Jones et al., 1994; Culkin et al., 1997; Fulop et al., 2001; Stenmark et al., 2003; Sebastian et al., 2007). This protection is induced early after challenge and is driven by poly-specific IgM against the LPS components, though non-specific stimulation with monophosphoryl lipid A (MPL) could provide similar protection against LVS challenge (Cole et al., 2011). Given that intradermal vaccination with *F. holartica* LVS does not provide protection against *F. tularensis* intranasal challenge, and that intranasal vaccination protects against both routes of challenge suggests mucosal IgA could be involved (Conlan et al., 2005; Wu et al., 2005). IgA has been detected in the serum of both humans and mice as well as BAL from vaccinated mice (Koskela and Herva, 1982; Koskela, 1985; Koskela and Salminen, 1985; Lavine et al., 2007; Rawool et al., 2008). The protective effect of anti-*Francisella* antibodies (subclass undefined) has been shown to be independent of complement yet dependent on Fc receptors and phagocytosis (Kirimanjeswara et al., 2007).

Early treatments for *Francisella* centered around the use of immune serum (Francis and Felton, 1942; Foshay, 1950; Tärnvik, 1989). It is unclear whether this treatment was effective against pulmonary tularemia (Kirimanjeswara et al., 2008). In mice, serum transfer shows some protection against pulmonary *F. holartica* LVS and *F. novicida* infection (Pammit et al., 2006; Lu et al., 2007). Serum transfer from *F. holartica* LVS-immune animals provides no protection against *F. tularensis* pulmonary infection in BALB/c mice (Kirimanjeswara et al., 2008). In another model, convalescent serum from an *F. tularensis*-infected levofloxacin treated mouse was protective in BALB/c mice (Klimpel et al., 2008). The protection provided by antibody transfer was dependent on Fc γ R-mediated opsonophagocytosis as well as ADCC by Natural Killer cells (Kirimanjeswara et al., 2007; Sanapala et al., 2012). Additionally, it is important to note

that the protective ability of transferred serum is dependent on T cells in both the mouse and rat (Kirimanjeswara et al., 2008; Mara-Koosham et al., 2011). Therefore, the protection seen in these models is likely a consequence of an intact T cell response. Recently, nanoparticles incorporating lysates from either LVS or SchuS4, along with MPL have been shown to protect mice from lethal LVS challenge (Richard et al., 2017). This regime resulted in both an augmented T cell INF- γ response as well as an increased antibody response. The impact of these responses separately has not been determined.

While the ability to detect anti-*Francisella* antibodies is an indicator of previous exposure, antibody titers are poor predictors of a vaccine's protective efficacy in humans (Saslaw et al., 1961a,b). As a pathogen that prefers to replicate intracellularly, *Francisella* is typically inaccessible to the antibody response. However, the organism can be found extracellularly and thus antibodies could play a role in controlling infection (Forestal et al., 2007; Yu et al., 2008). The demonstration by several groups that T cells are required for immune sera to be protective suggests that antibodies buy the host time for the T cell response to appropriately develop. Further, B cells have been shown to play an important antibody-independent role during secondary *F. holartica* LVS infection as antigen-presenting cells and/or cytokine producers (Elkins et al., 1999). Therefore, while measuring the antibody response is a straightforward measure of *Francisella* exposure, vaccine development should focus on understanding the protective T cell response.

T Cells

$\alpha\beta$ T Cells

Decades of *Francisella* research have demonstrated the absolute requirement for T cells for the clearance of primary infections and protective immunity. Mice lacking T cells such as $\alpha\beta$ TCR^{-/-} or *nu/nu* mice develop a chronic *F. holartica* LVS infection that is eventually lethal (Elkins et al., 1993, 1996; Yee et al., 1996). Although naïve mice succumb to *F. tularensis* infection prior to the development of adaptive immunity, a convalescent model of *F. tularensis* infection shows $\alpha\beta$ TCR^{-/-} and SCID mice succumb to infection after antibiotic treatment is halted (Crane et al., 2012). T cells are also key mediators of protective immunity in both homotypic and heterotypic vaccination and challenge models (Yee et al., 1996; Chen et al., 2004; Conlan et al., 2005; Wu et al., 2005; Mara-Koosham et al., 2011; Roberts et al., 2016). Depletion of either CD4⁺ or CD8⁺ T cells in immune animals prior to *F. tularensis* challenge eliminates protective immunity in both BALB/c and C57Bl/6 mice with slight differences in mean time to death kinetics. Immune BALB/c mice lacking either CD4⁺ or CD8⁺ T cells have similar mean time to death whereas C57Bl/6 mice depleted of CD4⁺ T cells succumb to *F. tularensis* significantly faster than animals depleted of CD8⁺ T cells (Conlan et al., 2005; Roberts et al., 2016). These data indicate that both subsets of T cells are required for protective immunity with slightly different requirements depending on the mouse and vaccinating strain. The critical role of CD4⁺ T cells in C57Bl/6 mice is likely a consequence of the immune response being dominated by CD4⁺ T cells with at least 2-fold more cells during or after vaccination

compared to CD8⁺ (Cowley et al., 2005; Woolard et al., 2008; Barrigan et al., 2013; Griffin et al., 2015).

$\gamma\delta$ T Cells

While $\alpha\beta$ T cells are critical during primary and secondary infection with *Francisella*, $\gamma\delta$ T cells are dispensable. $\gamma\delta$ TCR^{-/-} mice are not more susceptible to primary intranasal or intradermal infection with *F. holartica* LVS (Yee et al., 1996; Markel et al., 2010). In a convalescent model of *F. tularensis*, $\gamma\delta$ TCR^{-/-} mice are not more susceptible than wild-type mice during the primary or secondary challenge (Crane et al., 2012). Together, $\gamma\delta$ T cells do not play a major role in resolving *Francisella* infection in the mouse. However, V γ 9/V δ 2 T cells comprise almost all peripheral $\gamma\delta$ T cells in infected humans and can make up one-third of all CD3⁺ T cells 1 month after infection (Sumida et al., 1992; Poquet et al., 1998). Purified $\gamma\delta$ T cells from some human patients are capable of controlling *F. holartica*-LVS replication in THP-1 cells by an IFN- γ -dependent mechanism (Rowland et al., 2012). There is evidence that $\gamma\delta$ T cells produce cytokines after infection (discussed below) and therefore are contributing to the immune response albeit at a lower level than other T cell subsets.

CD4⁻ CD8⁻ Double Negative T Cells

Mucosal associated invariant T cells (MAITs) are characterized by the lack of CD4 and CD8 expression and are MHC-related protein 1-restricted. Mice depleted of CD4⁺ and CD8⁺ T cells during *F. holartica* LVS infection are chronically infected suggesting this MAIT population controls bacterial burdens, but does not mediate clearance (Yee et al., 1996; Meierovics et al., 2013). MAITs are preferentially located in the lungs of intranasally inoculated mice, contribute to monocyte differentiation into dendritic cells, and support the response of CD4⁺ and CD8⁺ conventional T cells (Meierovics et al., 2013; Meierovics and Cowley, 2016). While it is clear MAITs play a role during attenuated *F. holartica* LVS infection, their contribution to virulent *Francisella* infection has not been evaluated.

Important T Cell Effector Functions

Identifying the effector function(s) necessary for controlling infection is a critical aspect of vaccine development. T cells from convalescent humans produce IFN- γ , TNF- α , IL-2, IL-17, and IL-22 indicating these cytokines are elicited by natural infection or vaccination and therefore should be further assessed for their role in protective immunity in animal models (Karttunen et al., 1991; Surcel et al., 1991; Ericsson et al., 1994; Salerno-Gonçalves et al., 2009; Paronavitana et al., 2010; Eneslätt et al., 2012). The requirement of the classical Th1 cytokines IFN- γ and TNF- α during murine *Francisella* infection has been demonstrated by multiple groups (Leiby et al., 1992; Sjöstedt et al., 1996; Collazo et al., 2006, 2009; Crane et al., 2012; Skyberg et al., 2013; Roberts et al., 2014). *F. holartica* LVS is highly susceptible to IFN- γ (Anthony et al., 1989; Fortier et al., 1992). *In vitro*, IFN- γ directly controls *F. holartica* LVS replication in peritoneal macrophages using a reactive-nitrogen dependent mechanism (Fortier et al., 1992). However, in alveolar macrophages, IFN- γ control of *F. holartica* LVS is reactive nitrogen and

TNF- α independent (Polsinelli et al., 1994). Further, pre-treatment of mouse or human macrophages with IFN- γ controls *F. tularensis* infection via reactive nitrogen and reactive oxygen independent mechanisms (Edwards et al., 2010). Together these data suggest the role of reactive nitrogen and oxygen species is cell-type dependent and another unknown mechanism to restrict intracellular growth exists. In another model of *in vitro* *F. tularensis* infection of mouse macrophages, treatment with IFN- γ alone after infection did not control bacterial replication (Roberts et al., 2016). Instead, both IFN- γ and TNF- α were required (Roberts et al., 2016); the mechanism(s) that underlie IFN- γ and TNF- α control of *F. tularensis* in BMMs has not yet been elucidated. However, the requirement for both effector cytokines for controlling bacterial replication indicate that a vaccine candidate should elicit poly-functional T cells to maximally control *F. tularensis* infection. IL-17A is also produced by CD4⁺, CD4⁻ CD8⁻ double negative, and $\gamma\delta$ T cells following pulmonary infection with *F. holartica* LVS, but absent when animals are peripherally inoculated (Woolard et al., 2008; Cowley et al., 2010; Markel et al., 2010). Mice deficient in IL-17 are more susceptible to primary infection with *F. holartica* LVS, yet IL-17 is dispensable during secondary infection with either *F. holartica* LVS or *F. tularensis* (Woolard et al., 2008; Lin et al., 2009; Cowley et al., 2010; Markel et al., 2010; Skyberg et al., 2013; Roberts et al., 2014).

The ability of CD4⁺ and CD8⁺ T cells to produce cytokines after vaccination or challenge has been evaluated using ELISPOT, ELISA, and intracellular cytokine staining. These tried and true methods are appropriate in many situations but are not a direct measure of a specific cell population's ability to control intracellular replication. One technique used by multiple laboratories to directly assess immune cell function is to co-culture infected bone marrow macrophages (BMMs) with a population of interest, e.g., CD4⁺ T cells. This technique has been used to determine whether specific cell populations are capable of mediating bacterial control and if so, what molecular mechanisms are required (Cowley and Elkins, 2003; Cowley et al., 2005; Collazo et al., 2009). Using this technique, groups have demonstrated that CD4⁺, CD8⁺, and MAIT cells control attenuated or virulent *Francisella* replication in macrophages, further underscoring the importance of these cell subsets during infection (Cowley and Elkins, 2003; Cowley et al., 2005; Collazo et al., 2009; Roberts et al., 2016). Although the control of bacterial replication is mostly dependent on IFN- γ , several groups have demonstrated a small, but significant degree of IFN- γ independent control of *F. holartica* LVS replication in macrophages (Cowley and Elkins, 2003; Collazo et al., 2009). IFN- γ -independent control of *Francisella* infection could be a result of cytotoxic activity. Unfortunately, the contribution of granzyme B and/or perforin has not been evaluated in *F. holartica* LVS or *F. tularensis* infection. Perforin does contribute to protection after *F. novicida* vaccination and was necessary for primed T cells to optimally control bacterial replication in macrophages (Sanapala et al., 2012). Co-culture assays have also been used to identify correlates of protection and vaccine efficacy (De Pascalis et al., 2012, 2014; Griffin et al., 2015; Golovliov et al., 2016; Roberts et al., 2016, 2017). Thus far, the identified correlates of protection are consistent with our understanding of protective

immunity and include classic Th1-associated responses (IFN- γ , IL-12, and T-bet) as well as IL-6, IL-18, SOCS-1, and iNOS (De Pascalis et al., 2012; Golovliov et al., 2016). Overall, the use of a co-culture system to define the mechanism of protection will likely be an important component of vaccine evaluation and is a useful *in vitro* system to screen vaccine candidates. Furthermore, co-culture assays can be used to determine the ability of human immune cells to control *F. tularensis* replication and confirm mechanisms of protection discovered in animal models.

Route of Vaccination and Influence on the Immune Response

The route of vaccination, bacterial strain, and mouse strain utilized has a strong influence on whether a vaccine candidate is deemed protective. For example, while mice vaccinated via the intradermal route with *F. holartica* LVS are protected only against subsequent intradermal challenge, no protection against pulmonary *F. tularensis* challenge is provided (Wu et al., 2005; KuoLee et al., 2007). Using another strain of *F. holartica* LVS, Anderson, et al. demonstrated BALB/c mice are protected from pulmonary *F. tularensis* challenge after subcutaneous vaccination (Anderson et al., 2010). Further, mice vaccinated intranasally are protected against challenge by either the intradermal or intranasal route, suggesting the location of the protective cell is important. When considering the development of protective T cell responses, it is therefore important to understand the localization of protective T cells. Tularemia is a disseminated disease, causing T cells to respond throughout the body during primary and secondary infection. Not surprisingly, the location of T cells during and after vaccination differs depending on the mouse strain and route of vaccination. A direct comparison was made between C57Bl/6 mice intradermally and intranasally vaccinated with *F. holartica* LVS. The CD4⁺ T cell response in the spleen and lung more rapidly expands after intradermal vaccination whereas T cells are only present in the bronchoalveolar lavage fluid after intranasal vaccination (Woolard et al., 2008). In a prime-boost model of intranasal *F. holartica* LVS vaccination in C57Bl/6 animals, the number of effector and cytokine-producing CD4⁺ T cells in the lung is significantly increased compared to prime only, whereas there is no difference in the spleen (Roberts et al., 2017). These data suggest multiple intranasal exposures specifically boost the number of T cells in the pulmonary compartment. In contrast, protection in immune BALB/c mice challenged intranasally with *F. tularensis* correlated with splenic activated and cytokine-producing CD4⁺ T cells as opposed to pulmonary T cells (Anderson et al., 2010). The difference in protective T cell location between BALB/c and C57Bl/6 is likely a mouse strain difference but highlights the importance of understanding the location of protective T cells in tularemia. Specifically, C57Bl/6 mice are not protected 90 days after a single LVS vaccination whereas BALB/c mice are (Anderson et al., 2010; Roberts et al., 2017).

T Cell Epitopes

F. holartica LVS is not licensed for use in the United States and it is unlikely that any live vaccine will be licensed for tularemia due to safety concerns. Generation of an acellular

vaccine will require the identification of epitopes recognized by the adaptive immune system combined with adjuvants that provoke the appropriate T cell response. The ability of a vaccine to provoke high avidity CD4⁺ T cells significantly improves vaccine efficacy (Roberts et al., 2016, 2017). While this system uses an epitope not present in *Francisella*, it serves as proof-of-concept that identifying this class of epitope is critical for future acellular vaccine development. Several CD4⁺ epitopes have been identified in the mouse, including the C57Bl/6 immunodominant epitope, LpnA_{86–99}, which comprises up to 20% of responding CD4⁺ T cells after LVS infection (Valentino et al., 2009, 2011). A computational approach was taken to identify CD8-restricted epitopes and a DNA-based vaccination containing the most prominent epitopes did protect during *F. holartica* LVS challenge (Rotem et al., 2014). Bioinformatics also identified *Francisella* peptides with predicted binding to human MHCI and MHCII (McMurry et al., 2007). The response to these peptides was then tested in PBMCs from humans previously infected with *F. tularensis* using ELISPOT and 39 novel epitopes were identified (McMurry et al., 2007). A comprehensive list of proteins recognized by convalescent human sera and *F. holartica* LVS-vaccinated mouse serum is presented in Kilmury and Twine (2010). This list is particularly useful because recognition of a protein by immune sera strongly suggests a T cell epitope is also present in that protein. In addition to being recognized by human sera, LpnA is recognized by sera from vaccinated NHP, rats, and mice suggesting T cell epitopes recognized by multiple species are present in this protein (Havlasová et al., 2002; Eyles et al., 2007; Chu et al., 2014). Given the diversity of MHC alleles across species and the requirements of the Animal Rule, *Francisella* proteins that evoke immune responses in mice, rats, NHPs, and humans like LpnA are attractive vaccine targets.

RATIONAL VACCINE DESIGN

Many labs have investigated potential vaccines by screening the ability of mutant *Francisella* strains that do not cause disease themselves to act as a live vaccine (reviewed in Conlan, 2011; Marohn and Barry, 2013). In many cases, these strains offer the same or enhanced protection compared to wild-type *F. holartica* LVS. Instead of targeting strains that are attenuated for growth as vaccine candidates, our lab has used a different approach. We found that *Francisella* infected macrophages produce prostaglandin E2 (PGE₂) that blunts the T cell IFN- γ response (Woolard et al., 2007, 2008). Mice treated with indomethacin to inhibit PGE₂ production had lower bacterial loads indicating the bacterium is manipulating the host immune response to its benefit. Therefore, instead of using a screen to find growth-attenuated bacteria, we identified an immune evasion trait of *Francisella* and selected mutants that were unable to suppress that particular immune response. When we screened a *F. novicida* mutant library, we found that mutants in the *clpB* gene were unable to induce PGE₂ secretion in infected macrophages (Woolard et al., 2013). Upon further study, we found that *F. holartica* LVS carrying mutations in this gene were attenuated *in vivo*, rarely produced disease, and protected

against a lethal wild-type *F. holartica* LVS challenge (Barrigan et al., 2013). Similarly, an *F. tularensis* $\Delta clpB$ mutant is also attenuated *in vivo* yet elicits a protective immune response during wild-type *F. tularensis* challenge (Conlan et al., 2010; Twine et al., 2012). The experiments described above clearly show that we can identify mutations that attenuate *Francisella* infection without directly affecting bacterial growth *in vitro*. Therefore, it is important to also consider mutations that target immune evasion mechanism(s) as potential vaccine candidates.

Although a live vaccine for tularemia may induce a protective immune response, safety concerns may ultimately prevent licensure. In lieu of live attenuated strains as vaccine candidates, several groups have investigated the use of acellular tularemia vaccines including glycoconjugate vaccines, purified outer membrane proteins, immune stimulating complexes, and cationic surfactant vesicles (Golovliov et al., 1995; Huntley et al., 2008; Cuccui et al., 2013; Richard et al., 2014, 2017). These acellular vaccines evoke partial protection when animals were challenged with *F. tularensis*. Identification of protective antigens will significantly improve the development of new acellular *Francisella* vaccines and should be a focus of future research.

Irrespective of the vaccine choice, an important consideration for its development will be the vaccination route(s). As discussed above, the route of vaccination influences the location and function of immune T cells (Woolard et al., 2008). The ability of *Francisella* species to cause disease via a variety of routes and the disseminated nature of tularemia suggests that the most effective vaccination strategy will provoke T cells in a variety of tissues. One mechanism to provoke multiple pools of protective T cells is to utilize a prime/boost strategy where one immunization is done via inhalation and one intradermally or subcutaneously. This approach will quantitatively improve the immune response while inducing memory T cells in multiple tissues.

Novel vaccine candidates are likely to be tested first in mice prior to moving to other small mammals and eventually NHPs. The mouse is the most rational choice for initial studies because of the immunological tools available to clearly define mechanisms of protection. To date, the identified mechanisms of protection are the same between mice, rats, and man therefore there is a high likelihood that results from a novel vaccine candidate will translate to humans. A final critical consideration for vaccine development is the requirement that a candidate be evaluated for its ability to protect against pulmonary infection with *F. tularensis*. While we have learned a great deal about the immune response during tularemia using homologous vaccine and challenge studies, challenge with *F. tularensis* is the most rigorous evaluation of a vaccine candidate's ability to elicit a protective immune response.

FUTURE CHALLENGES

Considerable progress has been made in understanding aspects of protective immunity to *Francisella*, yet important challenges remain. First, vaccines tested to-date only protect against low to moderate pulmonary challenges with *F. tularensis* in both mice and man (McCrumb, 1961; Saslaw et al., 1961a; Chen et al.,

2003; Conlan et al., 2005; Roberts et al., 2017). The difficulty protecting against higher respiratory doses may be a consequence of an insufficient T cell response and/or the unique ability of *F. tularensis* to inhibit the innate immune response (Bosio et al., 2007; Crane et al., 2013a,b; Gillette et al., 2014). Higher inoculum doses result in more bacteria interacting with target cells and potentially a more complete inhibition of innate immunity. Without the proper innate immune signals, T cells are not activated until bacterial loads are too high to overcome. Even with low inoculum doses, protective immunity to *F. tularensis* wanes quickly (Burke, 1977). Therefore, another challenge of vaccine development will be to provoke long-lasting central memory cells. The inability to protect mice against high challenge doses for long periods of time makes them an ideal model for testing vaccine candidates. Further, the genetic and immunological tools available for the mouse allow the protective immune response to be defined. Ultimately, success in multiple animal models will be required for approval of novel tularemia vaccines or therapeutics under the Animal Rule.

During the last 10 years there has been remarkable improvement in our understanding the immune response to *Francisella*. This has been accompanied by production of a wide

variety of potential vaccines, ranging from those developed using classical vaccinology, attenuated live bacteria, immunization using novel nanoparticles, and even LPS. Our own work has focused on better understanding protective immunity to *Francisella*, from defining mechanisms of immune evasion that can be modulated to more recent work identifying correlates of protection during *F. tularensis* challenge in immune animals (Woolard et al., 2007, 2008; Roberts et al., 2016, 2017). Even if live attenuated bacteria are never licensed for use, our understanding of immunity *Francisella*, and potentially other pulmonary bacterial pathogens have been greatly expanded.

AUTHOR CONTRIBUTIONS

All authors listed made substantial direct and intellectual contributions to the work and approved it for publication.

FUNDING

This research was supported in part by the Intramural Research Program of the National Institutes of Health, National Institute of Allergy of Infectious Diseases.

REFERENCES

- Alibek, K., and Handelman, S. (1999). *Biohazard: The Chilling True Story of the Largest Covert Biological Weapons Program in the World, Told from the Inside by the Man Who Ran It*. New York, NY: Random House.
- Anderson, R. V., Crane, D. D., and Bosio, C. M. (2010). Long lived protection against pneumonic tularemia is correlated with cellular immunity in peripheral, not pulmonary, organs. *Vaccine* 28, 6562–6572. doi: 10.1016/j.vaccine.2010.07.072
- Anthony, L. S., Ghadirian, E., Nestel, F. P., and Kongshavn, P. A. (1989). The requirement for gamma interferon in resistance of mice to experimental tularemia. *Microb. Pathog.* 7, 421–428. doi: 10.1016/0882-4010(89)90022-3
- Barrigan, L. M., Tuladhar, S., Brunton, J. C., Woolard, M. D., Chen, C. J., Saini, D., et al. (2013). Infection with *Francisella tularensis* LVS clpB leads to an altered yet protective immune response. *Infect. Immun.* 81, 2028–2042. doi: 10.1128/IAI.00207-13
- Baskerville, A., and Hambleton, P. (1976). Pathogenesis and pathology of respiratory tularaemia in the rabbit. *Br. J. Exp. Pathol.* 57, 339–347.
- Baskerville, A., Hambleton, P., and Dowsett, A. B. (1978). The pathology of untreated and antibiotic-treated experimental tularaemia in monkeys. *Br. J. Exp. Pathol.* 59, 615–623.
- Beasley, D. W. C., Brasel, T. L., and Comer, J. E. (2016). First vaccine approval under the FDA Animal Rule. *NPJ Vaccines* 1:16013. doi: 10.1038/npjvaccines.2016.13
- Bosio, C. M., Bielefeldt-Ohmann, H., and Belisle, J. T. (2007). Active suppression of the pulmonary immune response by *Francisella tularensis* Schu4. *J. Immunol.* 178, 4538–4547. doi: 10.4049/jimmunol.178.7.4538
- Brown, V. R., Adney, D. R., Bielefeldt-Ohmann, H., Gordy, P. W., Felix, T. A., Olea-Poppelka, F. J., et al. (2015a). Pathogenesis and immune responses of *Francisella Tularensis* strains in wild-caught cottontail rabbits (*Sylvilagus* spp.). *J. Wildl. Dis.* 51, 564–575. doi: 10.7589/2015-02-030
- Brown, V. R., Adney, D. R., Olea-Poppelka, F., and Bowen, R. A. (2015b). Prior inoculation with Type B Strains of *Francisella tularensis* provides partial protection against virulent type A strains in cottontail rabbits. *PLoS ONE* 10:e0140723. doi: 10.1371/journal.pone.0140723
- Burke, D. S. (1977). Immunization against tularemia: analysis of the effectiveness of live *Francisella tularensis* vaccine in prevention of laboratory-acquired tularemia. *J. Infect. Dis.* 135, 55–60. doi: 10.1093/infdis/135.1.55
- Carlsson, H. E., Lindberg, A. A., Lindberg, G., Hederstedt, B., Karlsson, K. A., and Agell, B. O. (1979). Enzyme-linked immunosorbent assay for immunological diagnosis of human tularemia. *J. Clin. Microbiol.* 10, 615–621.
- Chen, W., KuoLee, R., Shen, H., and Conlan, J. W. (2004). Susceptibility of immunodeficient mice to aerosol and systemic infection with virulent strains of *Francisella tularensis*. *Microb. Pathog.* 36, 311–318. doi: 10.1016/j.micpath.2004.02.003
- Chen, W., Shen, H., Webb, A., KuoLee, R., and Conlan, J. W. (2003). Tularemia in BALB/c and C57BL/6 mice vaccinated with *Francisella tularensis* LVS and challenged intradermally, or by aerosol with virulent isolates of the pathogen: protection varies depending on pathogen virulence, route of exposure, and host genetic background. *Vaccine* 21, 3690–3700. doi: 10.1016/S0264-410X(03)00386-4
- Christopher, G. W., Cieslak, T. J., Pavlin, J. A., and Eitzen, E. M. Jr. (1997). Biological warfare. A historical perspective. *JAMA* 278, 412–417. doi: 10.1001/jama.1997.03550050074036
- Chu, P., Cunningham, A. L., Yu, J. J., Nguyen, J. Q., Barker, J. R., Lyons, C. R., et al. (2014). Live attenuated *Francisella novicida* vaccine protects against *Francisella tularensis* pulmonary challenge in rats and non-human primates. *PLoS Pathog.* 10:e1004439. doi: 10.1371/journal.ppat.1004439
- Clarridge, J. E. 3rd, Raich, T. J., Sjøsted, A., Sandstrom, G., Darouiche, R. O., Shawar, R. M., et al. (1996). Characterization of two unusual clinically significant *Francisella* strains. *J. Clin. Microbiol.* 34, 1995–2000.
- Cole, L. E., Mann, B. J., Shirey, K. A., Richard, K., Yang, Y., Gearhart, P. J., et al. (2011). Role of TLR signaling in *Francisella tularensis*-LPS-induced, antibody-mediated protection against *Francisella tularensis* challenge. *J. Leukoc. Biol.* 90, 787–797. doi: 10.1189/jlb.0111014
- Collazo, C. M., Meierovics, A. I., De Pascalis, R., Wu, T. H., Lyons, C. R., and Elkins, K. L. (2009). T cells from lungs and livers of *Francisella tularensis*-immune mice control the growth of intracellular bacteria. *Infect. Immun.* 77, 2010–2021. doi: 10.1128/IAI.01322-08
- Collazo, C. M., Sher, A., Meierovics, A. I., and Elkins, K. L. (2006). Myeloid differentiation factor-88 (MyD88) is essential for control of primary *in vivo* *Francisella tularensis* LVS infection, but not for control of intra-macrophage bacterial replication. *Microbes Infect.* 8, 779–790. doi: 10.1016/j.micinf.2005.09.014
- Conlan, J. W. (2011). Tularemia vaccines: recent developments and remaining hurdles. *Future Microbiol.* 6, 391–405. doi: 10.2217/fmb.11.22

- Conlan, J. W., Chen, W., Shen, H., Webb, A., and Kuolee, R. (2003). Experimental tularemia in mice challenged by aerosol or intradermally with virulent strains of *Francisella tularensis*: bacteriological and histopathologic studies. *Microb. Pathog.* 34, 239–248. doi: 10.1016/S0882-4010(03)00046-9
- Conlan, J. W., Shen, H., Golovliov, I., Zingmark, C., Oyston, P. C., Chen, W., et al. (2010). Differential ability of novel attenuated targeted deletion mutants of *Francisella tularensis* subspecies tularensis strain SCHU S4 to protect mice against aerosol challenge with virulent bacteria: effects of host background and route of immunization. *Vaccine* 28, 1824–1831. doi: 10.1016/j.vaccine.2009.12.001
- Conlan, W. J., Shen, H., Kuolee, R., Zhao, X., and Chen, W. (2005). Aerosol-, but not intradermal-immunization with the live vaccine strain of *Francisella tularensis* protects mice against subsequent aerosol challenge with a highly virulent type A strain of the pathogen by an alphabeta T cell- and interferon gamma- dependent mechanism. *Vaccine* 23, 2477–2485. doi: 10.1016/j.vaccine.2004.10.034
- Cowley, S. C., and Elkins, K. L. (2003). Multiple T cell subsets control *Francisella tularensis* LVS intracellular growth without stimulation through macrophage interferon gamma receptors. *J. Exp. Med.* 198, 379–389. doi: 10.1084/jem.20030687
- Cowley, S. C., Hamilton, E., Frelinger, J. A., Su, J., Forman, J., and Elkins, K. L. (2005). CD4-CD8- T cells control intracellular bacterial infections both *in vitro* and *in vivo*. *J. Exp. Med.* 202, 309–319. doi: 10.1084/jem.20050569
- Cowley, S. C., Meierovics, A. I., Frelinger, J. A., Iwakura, Y., and Elkins, K. L. (2010). Lung CD4-CD8- double-negative T cells are prominent producers of IL-17A and IFN-gamma during primary respiratory murine infection with *Francisella tularensis* live vaccine strain. *J. Immunol.* 184, 5791–5801. doi: 10.4049/jimmunol.1000362
- Crane, D. D., Griffin, A. J., Wehrly, T. D., and Bosio, C. M. (2013a). B1a cells enhance susceptibility to infection with virulent *Francisella tularensis* via modulation of NK/NKT cell responses. *J. Immunol.* 190, 2756–2766. doi: 10.4049/jimmunol.1202697
- Crane, D. D., Ireland, R., Alinger, J. B., Small, P., and Bosio, C. M. (2013b). Lipids derived from virulent *Francisella tularensis* broadly inhibit pulmonary inflammation via toll-like receptor 2 and peroxisome proliferator-activated receptor α . *Clin. Vaccine Immunol.* 20, 1531–1540. doi: 10.1128/CVI.00319-13
- Crane, D. D., Scott, D. P., and Bosio, C. M. (2012). Generation of a convalescent model of virulent *Francisella tularensis* infection for assessment of host requirements for survival of tularemia. *PLoS ONE* 7:e33349. doi: 10.1371/journal.pone.0033349
- Cuccui, J., Thomas, R. M., Moule, M. G., D'Elia, R. V., Laws, T. R., Mills, D. C., et al. (2013). Exploitation of bacterial N-linked glycosylation to develop a novel recombinant glycoconjugate vaccine against *Francisella tularensis*. *Open Biol.* 3:130002. doi: 10.1098/rsob.130002
- Culkin, S. J., Rhinehart-Jones, T., and Elkins, K. L. (1997). A novel role for B cells in early protective immunity to an intracellular pathogen, *Francisella tularensis* strain LVS. *J. Immunol.* 158, 3277–3284.
- Day, W. C., and Berendt, R. F. (1972). Experimental tularemia in *Macaca mulatta*: relationship of aerosol particle size to the infectivity of airborne *Pasteurella tularensis*. *Infect. Immun.* 5, 77–82.
- Dennis, D. T., Inglesby, T. V., Henderson, D. A., Bartlett, J. G., Ascher, M. S., Eitzen, E., et al. (2001). Tularemia as a biological weapon: medical and public health management. *JAMA* 285, 2763–2773. doi: 10.1001/jama.285.21.2763
- De Pascalis, R., Chou, A. Y., Bosio, C. M., Huang, C. Y., Follmann, D. A., and Elkins, K. L. (2012). Development of functional and molecular correlates of vaccine-induced protection for a model intracellular pathogen, *F. tularensis* LVS. *PLoS Pathog.* 8:e1002494. doi: 10.1371/journal.ppat.1002494
- De Pascalis, R., Chou, A. Y., Ryden, P., Kennett, N. J., Sjostedt, A., and Elkins, K. L. (2014). Models derived from *in vitro* analyses of spleen, liver, and lung leukocyte functions predict vaccine efficacy against the *Francisella tularensis* Live Vaccine Strain (LVS). *MBio* 5:e00936. doi: 10.1128/mBio.00936-13
- Downs, C. M., Coriell, L. L., and Pinchot, G. B., Maumenee, E., Klauber, A., Chapman, S. S., et al. (1947). Studies on tularemia; the comparative susceptibility of various laboratory animals. *J. Immunol.* 56, 217–228.
- Dreisbach, V. C., Cowley, S., and Elkins, K. L. (2000). Purified lipopolysaccharide from *Francisella tularensis* live vaccine strain (LVS) induces protective immunity against LVS infection that requires B cells and gamma interferon. *Infect. Immun.* 68, 1988–1996. doi: 10.1128/IAI.68.4.1988-1996.2000
- Edwards, J. A., Rockx-Brouwer, D., Nair, V., and Celli, J. (2010). Restricted cytosolic growth of *Francisella tularensis* subsp. tularensis by IFN-gamma activation of macrophages. *Microbiology* 156, 327–339. doi: 10.1099/mic.0.031716-0
- Eigelsbach, H. T., and Downs, C. M. (1961). Prophylactic effectiveness of live and killed tularemia vaccines. I. Production of vaccine and evaluation in the white mouse and guinea pig. *J. Immunol.* 87, 415–425.
- Eigelsbach, H. T., Tulis, J. J., McGavran, M. H., and White, J. D. (1962). Live tularemia vaccine I. : host-parasite relationship in monkeys vaccinated intracutaneously or aerogenically. *J. Bacteriol.* 84, 1020–1027.
- Elkins, K. L., Bosio, C. M., and Rhinehart-Jones, T. R. (1999). Importance of B cells, but not specific antibodies, in primary and secondary protective immunity to the intracellular bacterium *Francisella tularensis* live vaccine strain. *Infect. Immun.* 67, 6002–6007.
- Elkins, K. L., Rhinehart-Jones, T., Nacy, C. A., Winegar, R. K., and Fortier, A. H. (1993). T-cell-independent resistance to infection and generation of immunity to *Francisella tularensis*. *Infect. Immun.* 61, 823–829.
- Elkins, K. L., Rhinehart-Jones, T. R., Culkin, S. J., Yee, D., and Winegar, R. K. (1996). Minimal requirements for murine resistance to infection with *Francisella tularensis* LVS. *Infect. Immun.* 64, 3288–3293.
- Ellis, J., Oyston, P. C., Green, M., and Titball, R. W. (2002). Tularemia. *Clin. Microbiol. Rev.* 15, 631–646. doi: 10.1128/CMR.15.4.631-646.2002
- Enesl tt, K., Normark, M., Bjork, R., Rietz, C., Zingmark, C., Wolfr m, L. A., et al. (2012). Signatures of T cells as correlates of immunity to *Francisella tularensis*. *PLoS ONE* 7:e32367. doi: 10.1371/journal.pone.0032367
- Ericsson, M., Sandstrom, G., Sjostedt, A., and Tarnvik, A. (1994). Persistence of cell-mediated immunity and decline of humoral immunity to the intracellular bacterium *Francisella tularensis* 25 years after natural infection. *J. Infect. Dis.* 170, 110–114. doi: 10.1093/infdis/170.1.110
- Evans, M. E., Gregory, D. W., Schaffner, W., and McGee, Z. A. (1985). Tularemia: a 30-year experience with 88 cases. *Medicine* 64, 251–269. doi: 10.1097/00005792-198507000-00006
- Eyles, J. E., Unal, B., Hartley, M. G., Newstead, S. L., Flick-Smith, H., Prior, J. L., et al. (2007). Immunodominant *Francisella tularensis* antigens identified using proteome microarray. *Proteomics* 7, 2172–2183. doi: 10.1002/pmic.200600985
- Forestal, C. A., Malik, M., Catlett, S. V., Savitt, A. G., Benach, J. L., Sellati, T. J., et al. (2007). *Francisella tularensis* has a significant extracellular phase in infected mice. *J. Infect. Dis.* 196, 134–137. doi: 10.1086/518611
- Fortier, A. H., Polsinelli, T., Green, S. J., and Nacy, C. A. (1992). Activation of macrophages for destruction of *Francisella tularensis*: identification of cytokines, effector cells, and effector molecules. *Infect. Immun.* 60, 817–825.
- Fortier, A. H., Slayter, M. V., Ziemba, R., Meltzer, M. S., and Nacy, C. A. (1991). Live vaccine strain of *Francisella tularensis*: infection and immunity in mice. *Infect. Immun.* 59, 2922–2928.
- Foshay, L. (1950). Tularemia. *Annu. Rev. Microbiol.* 4, 313–330. doi: 10.1146/annurev.mi.04.100150.001525
- Francis, E., and Callender, G. (1927). Tularemia: the microscopic changes of the lesions in man. *Arch. Pathol. Lab. Med.* 3, 577–607.
- Fulop, M., Mastroeni, P., Green, M., and Titball, R. W. (2001). Role of antibody to lipopolysaccharide in protection against low- and high-virulence strains of *Francisella tularensis*. *Vaccine* 19, 4465–4472. doi: 10.1016/S0264-410X(01)00189-X
- Francis, E., and Felton, L. D. (1942). Antitularemic serum. *Public Health Rep.* 57, 44–55. doi: 10.2307/4583978
- Gillette, D. D., Curry, H. M., Cremer, T., Ravneberg, D., Fatehchand, K., Shah, P. A., et al. (2014). Virulent type A *Francisella tularensis* actively suppresses cytokine responses in human monocytes. *Front. Cell. Infect. Microbiol.* 4:45. doi: 10.3389/fcimb.2014.00045
- Gill, V., and Cunha, B. A. (1997). Tularemia pneumonia. *Semin. Respir. Infect.* 12, 61–67.
- Glynn, A. R., Alves, D. A., Frick, O., Erwin-Cohen, R., Porter, A., Norris, S., et al. (2015). Comparison of experimental respiratory tularemia in three nonhuman primate species. *Comp. Immunol. Microbiol. Infect. Dis.* 39, 13–24. doi: 10.1016/j.cimid.2015.01.003
- Golovliov, I., Ericsson, M., Akerblom, L., Sandstrom, G., Tarnvik, A., and Sjostedt, A. (1995). Adjuvanticity of ISCOMs incorporating a T cell-reactive lipoprotein of the facultative intracellular pathogen *Francisella tularensis*. *Vaccine* 13, 261–267. doi: 10.1016/0264-410X(95)93311-V

- Golovliov, I., Lindgren, H., Eneslatt, K., Conlan, W., Mosnier, A., Henry, T., et al. (2016). An *in vitro* co-culture mouse model demonstrates efficient vaccine-mediated control of *Francisella tularensis* SCHU S4 and identifies nitric oxide as a predictor of efficacy. *Front. Cell. Infect. Microbiol.* 6:152. doi: 10.3389/fcimb.2016.00152
- Griffin, A. J., Crane, D. D., Wehrly, T. D., and Bosio, C. M. (2015). Successful protection against tularemia in C57BL/6 mice is correlated with expansion of *Francisella tularensis*-specific effector T cells. *Clin. Vaccine Immunol.* 22, 119–128. doi: 10.1128/CI.00648-14
- Guarner, J., and Zaki, S. R. (2006). Histopathology and immunohistochemistry in the diagnosis of bioterrorism agents. *J. Histochem. Cytochem.* 54, 3–11. doi: 10.1369/jhc.5R6756.2005
- Hambleton, P., Baskerville, A., Harris-Smith, P. W., and Bailey, N. E. (1978). Changes in whole blood and serum components of grivet monkeys with experimental respiratory *Francisella tularensis* infection. *Br. J. Exp. Pathol.* 59, 630–639.
- Havlasová, J., Hernychova, L., Halada, P., Pellantova, V., Krejsek, J., Stulik, J., et al. (2002). Mapping of immunoreactive antigens of *Francisella tularensis* live vaccine strain. *Proteomics* 2, 857–867. doi: 10.1002/1615-9861(200207)2:7<857::AID-PROT857>3.0.CO;2-L
- Hornick, R. B., and Eigelsbach, H. T. (1966). Aerogenic immunization of man with live Tularemia vaccine. *Bacteriol. Rev.* 30, 532–538.
- Huntley, J. F., Conley, P. G., Rasko, D. A., Hagman, K. E., Apicella, M. A., and Norgard, M. V. (2008). Native outer membrane proteins protect mice against pulmonary challenge with virulent type A *Francisella tularensis*. *Infect. Immun.* 76, 3664–3671. doi: 10.1128/IAI.00374-08
- Hutt, J. A., Lovchik, J. A., Dekonenko, A., Hahn, A. C., and Wu, T. H. (2017). The natural history of pneumonic Tularemia in female Fischer 344 rats after inhalational exposure to aerosolized *Francisella tularensis* subspecies Tularensis strain SCHU S4. *Am. J. Pathol.* 187, 252–267. doi: 10.1016/j.ajpath.2016.09.021
- Janovská, S., Pavkova, I., Reichelova, M., Hubaleka, M., Stulik, J., and Macela, A. (2007). Proteomic analysis of antibody response in a case of laboratory-acquired infection with *Francisella tularensis* subsp. tularensis. *Folia Microbiol.* 52, 194–198. doi: 10.1007/BF02932159
- Johansson, A., Berglund, L., Eriksson, U., Goransson, I., Wollin, R., Forsman, M., et al. (2000). Comparative analysis of PCR versus culture for diagnosis of ulceroglandular tularemia. *J. Clin. Microbiol.* 38, 22–26.
- Karttunen, R., Surcel, H. M., Andersson, G., Ekre, H. P., and Herva, E. (1991). *Francisella tularensis*-induced *in vitro* gamma interferon, tumor necrosis factor alpha, and interleukin 2 responses appear within 2 weeks of tularemia vaccination in human beings. *J. Clin. Microbiol.* 29, 753–756.
- Kilmury, S. L., and Twine, S. M. (2010). The *Francisella tularensis* proteome and its recognition by antibodies. *Front. Microbiol.* 1:143. doi: 10.3389/fmicb.2010.00143
- Kirmanjeswara, G. S., Golden, J. M., Bakshi, C. S., and Metzger, D. W. (2007). Prophylactic and therapeutic use of antibodies for protection against respiratory infection with *Francisella tularensis*. *J. Immunol.* 179, 532–539. doi: 10.4049/jimmunol.179.1.532
- Kirmanjeswara, G. S., Olmos, S., Bakshi, C. S., and Metzger, D. W. (2008). Humoral and cell-mediated immunity to the intracellular pathogen *Francisella tularensis*. *Immunol. Rev.* 225, 244–255. doi: 10.1111/j.1600-065X.2008.00689.x
- Klimpel, G. R., Eaves-Pyles, T., Moen, S. T., Taormina, J., Peterson, J. W., Chopra, A. K., et al. (2008). Levofloxacin rescues mice from lethal intra-nasal infections with virulent *Francisella tularensis* and induces immunity and production of protective antibody. *Vaccine* 26, 6874–6882. doi: 10.1016/j.vaccine.2008.09.077
- Koskela, P. (1985). Humoral immunity induced by a live *Francisella tularensis* vaccine. Complement fixing antibodies determined by an enzyme-linked immunosorbent assay (CF-ELISA). *Vaccine* 3, 389–391. doi: 10.1016/0264-410X(85)90129-X
- Koskela, P., and Herva, E. (1982). Cell-mediated and humoral immunity induced by a live *Francisella tularensis* vaccine. *Infect. Immun.* 36, 983–989.
- Koskela, P., and Salminen, A. (1985). Humoral immunity against *Francisella tularensis* after natural infection. *J. Clin. Microbiol.* 22, 973–979.
- Kroca, M., Tarnvik, A., and Sjostedt, A. (2000). The proportion of circulating gamma delta T cells increases after the first week of onset of tularaemia and remains elevated for more than a year. *Clin. Exp. Immunol.* 120, 280–284. doi: 10.1046/j.1365-2249.2000.01215.x
- KuoLee, R., Harris, G., Conlan, J. W., and Chen, W. (2007). Oral immunization of mice with the live vaccine strain (LVS) of *Francisella tularensis* protects mice against respiratory challenge with virulent type A *F. tularensis*. *Vaccine* 25, 3781–3791. doi: 10.1016/j.vaccine.2007.02.014
- Lamps, L. W., Havens, J. M., Sjostedt, A., Page, D. L., and Scott, M. A. (2004). Histologic and molecular diagnosis of tularemia: a potential bioterrorism agent endemic to North America. *Mod. Pathol.* 17, 489–495. doi: 10.1038/modpathol.3800087
- Lauriano, C. M., Barker, J. R., Yoon, S. S., Nano, F. E., Arulanandam, B. P., Hassett, D. J., et al. (2004). MglA regulates transcription of virulence factors necessary for *Francisella tularensis* intra-macrophage and intramacrophage survival. *Proc. Natl. Acad. Sci. U.S.A.* 101, 4246–4249. doi: 10.1073/pnas.0307690101
- Lavine, C. L., Clinton, S. R., Angelova-Fischer, I., Marion, T. N., Bina, X. R., Bina, J. E., et al. (2007). Immunization with heat-killed *Francisella tularensis* LVS elicits protective antibody-mediated immunity. *Eur. J. Immunol.* 37, 3007–3020. doi: 10.1002/eji.200737620
- Leiby, D. A., Fortier, A. H., Crawford, R. M., Schreiber, R. D., and Nacy, C. A. (1992). *In vivo* modulation of the murine immune response to *Francisella tularensis* LVS by administration of anticytokine antibodies. *Infect. Immun.* 60, 84–89.
- Lin, Y., Ritchea, S., Logar, A., Slight, S., Messmer, M., Rangel-Moreno, J., et al. (2009). Interleukin-17 is required for T helper 1 cell immunity and host resistance to the intracellular pathogen *Francisella tularensis*. *Immunity* 31, 799–810. doi: 10.1016/j.immuni.2009.08.025
- Lu, Z., Roche, M. I., Hui, J. H., Unal, B., Felgner, P. L., Gulati, S., et al. (2007). Generation and characterization of hybridoma antibodies for immunotherapy of tularemia. *Immunol. Lett.* 112, 92–103. doi: 10.1016/j.imlet.2007.07.006
- Mara-Koosham, G., Hutt, J. A., Lyons, C. R., and Wu, T. H. (2011). Antibodies contribute to effective vaccination against respiratory infection by type A *Francisella tularensis* strains. *Infect Immun* 79, 1770–1778. doi: 10.1128/IAI.00605-10
- Markel, G., Bar-Haim, E., Zahavy, E., Cohen, H., Cohen, O., Shafferman, A., et al. (2010). The involvement of IL-17A in the murine response to sub-lethal inhalational infection with *Francisella tularensis*. *PLoS ONE* 5:e11176. doi: 10.1371/journal.pone.0011176
- Marohn, M. E., and Barry, E. M. (2013). Live attenuated tularemia vaccines: recent developments and future goals. *Vaccine* 31, 3485–3491. doi: 10.1016/j.vaccine.2013.05.096
- McCrumb, F. R. (1961). Aerosol infection of man with *Pasteurella Tularensis*. *Bacteriol. Rev.* 25, 262–267.
- McMurry, J. A., Gregory, S. H., Moise, L., Rivera, D., Buus, S., and De Groot, A. S. (2007). Diversity of *Francisella tularensis* Schu4 antigens recognized by *T lymphocytes* after natural infections in humans: identification of candidate epitopes for inclusion in a rationally designed tularemia vaccine. *Vaccine* 25, 3179–3191. doi: 10.1016/j.vaccine.2007.01.039
- Meierovics, A. I., and Cowley, S. C. (2016). MAIT cells promote inflammatory monocyte differentiation into dendritic cells during pulmonary intracellular infection. *J. Exp. Med.* 213, 2793–2809. doi: 10.1084/jem.20160637
- Meierovics, A., Yankelevich, W. J., and Cowley, S. C. (2013). MAIT cells are critical for optimal mucosal immune responses during *in vivo* pulmonary bacterial infection. *Proc. Natl. Acad. Sci. U.S.A.* 110, E3119–E3128. doi: 10.1073/pnas.1302799110
- Nelson, M., Lever, M. S., Dean, R. E., Savage, V. L., Salguero, F. J., Pearce, P. C., et al. (2010). Characterization of lethal inhalational infection with *Francisella tularensis* in the common marmoset (*Callithrix jacchus*). *J. Med. Microbiol.* 59, 1107–1113. doi: 10.1099/jmm.0.020669-0
- Nelson, M., Lever, M. S., Savage, V. L., Salguero, F. J., Pearce, P. C., Stevens, D. J., et al. (2009). Establishment of lethal inhalational infection with *Francisella tularensis* (tularaemia) in the common marmoset (*Callithrix jacchus*). *Int. J. Exp. Pathol.* 90, 109–118. doi: 10.1111/j.1365-2613.2008.00631.x
- Ohara, Y., Sato, T., and Homma, M. (1998). Arthropod-borne tularemia in Japan: clinical analysis of 1,374 cases observed between 1924 and 1996. *J. Med. Entomol.* 35, 471–473. doi: 10.1093/jmedent/35.4.471
- Pammit, M. A., Raulie, E. K., Lauriano, C. M., Klose, K. E., and Arulanandam, B. P. (2006). Intranasal vaccination with a defined attenuated *Francisella novicida* strain induces gamma interferon dependent antibody-mediated protection against tularemia. *Infect. Immun.* 74, 2063–2071. doi: 10.1128/IAI.74.4.2063-2071.2006

- Paranavithana, C., Zelazowska, E., Dasilva, L., Pittman, P. R., and Nikolich, M. (2010). Th17 cytokines in recall responses against *Francisella tularensis* in humans. *J. Interferon Cytokine Res.* 30, 471–476. doi: 10.1089/jir.2009.0108
- Park, G. D., and Mitchel, J. T. (2016). Working with the U.S. Food and Drug Administration to obtain approval of products under the animal rule. *Ann. N Y Acad. Sci.* 1374, 10–16. doi: 10.1111/nyas.13126
- Pasetti, M. F., Cuberos, L., Horn, T. L., Shearer, J. D., Matthews, S. J., House, R. V., et al. (2008). An improved *Francisella tularensis* live vaccine strain (LVS) is well tolerated and highly immunogenic when administered to rabbits in escalating doses using various immunization routes. *Vaccine* 26, 1773–1785. doi: 10.1016/j.vaccine.2008.01.005
- Pechous, R. D., McCarthy, T. R., Mohapatra, N. P., Soni, S., Penoske, R. M., Salzman, N. H., et al. (2008). A *Francisella tularensis* Schu S4 purine auxotroph is highly attenuated in mice but offers limited protection against homologous intranasal challenge. *PLoS ONE* 3:e2487. doi: 10.1371/journal.pone.0002487
- Polsinelli, T., Meltzer, M. S., and Fortier, A. H. (1994). Nitric oxide-independent killing of *Francisella tularensis* by IFN-gamma-stimulated murine alveolar macrophages. *J. Immunol.* 153, 1238–1245.
- Poquet, Y., Kroca, M., Halary, F., Stenmark, S., Peyrat, M. A., Bonneville, M., et al. (1998). Expansion of Vgamma9 Vdelta2 T cells is triggered by *Francisella tularensis*-derived phosphoantigens in tularemia but not after tularemia vaccination. *Infect. Immun.* 66, 2107–2114.
- Rawool, D. B., Bitsaktsis, C., Li, Y., Gosselin, D. R., Lin, Y., Kurkure, N. V., et al. (2008). Utilization of Fc receptors as a mucosal vaccine strategy against an intracellular bacterium, *Francisella tularensis*. *J. Immunol.* 180, 5548–5557. doi: 10.4049/jimmunol.180.8.5548
- Ray, H. J., Chu, P., Wu, T. H., Lyons, C. R., Murthy, A. K., Guentzel, M. N., et al. (2010). The Fischer 344 rat reflects human susceptibility to *Francisella* pulmonary challenge and provides a new platform for virulence and protection studies. *PLoS ONE* 5:e9952. doi: 10.1371/journal.pone.0009952
- Reed, D. S., Smith, L., Dunsmore, T., Trichel, A., Ortiz, L. A., Cole, K. S., et al. (2011). Pneumonic tularemia in rabbits resembles the human disease as illustrated by radiographic and hematologic changes after infection. *PLoS ONE* 6:e24654. doi: 10.1371/journal.pone.0024654
- Reed, D. S., Smith, L. P., Cole, K. S., Santiago, A. E., Mann, B. J., and Barry, E. M. (2014). Live attenuated mutants of *Francisella tularensis* protect rabbits against aerosol challenge with a virulent type A strain. *Infect. Immun.* 82, 2098–2105. doi: 10.1128/IAI.01498-14
- Rhinehart-Jones, T. R., Fortier, A. H., and Elkins, K. L. (1994). Transfer of immunity against lethal murine *Francisella* infection by specific antibody depends on host gamma interferon and T cells. *Infect. Immun.* 62, 3129–3137.
- Richard, K., Mann, B. J., Qin, A., Barry, E. M., Ernst, R. K., and Vogel, S. N. (2017). Monophosphoryl lipid A enhances efficacy of a *Francisella tularensis* LVS-catanionic nanoparticle subunit vaccine against *F. tularensis* Schu S4 challenge by augmenting both humoral and cellular immunity. *Clin. Vaccine Immunol.* 24:e00574-16. doi: 10.1128/CI.00574-16
- Richard, K., Mann, B. J., Stocker, L., Barry, E. M., Qin, A., Cole, L. E., et al. (2014). Novel cationic surfactant vesicle vaccines protect against *Francisella tularensis* LVS and confer significant partial protection against *F. tularensis* Schu S4 strain. *Clin. Vaccine Immunol.* 21, 212–226. doi: 10.1128/CI.00738-13
- Roberts, L. M., Crane, D. D., Wehrly, T. D., Fletcher, J. R., Jones, B. D., and Bosio, C. M. (2016). Inclusion of epitopes that expand high-avidity CD4+ T cells transforms subprotective vaccines to efficacious immunogens against virulent *Francisella tularensis*. *J. Immunol.* 197, 2738–2747. doi: 10.4049/jimmunol.1600879
- Roberts, L. M., Davies, J. S., Sempowski, G. D., and Frelinger, J. A. (2014). IFN-gamma, but not IL-17A, is required for survival during secondary pulmonary *Francisella tularensis* live vaccine stain infection. *Vaccine* 32, 3595–3603. doi: 10.1016/j.vaccine.2014.05.013
- Roberts, L. M., Wehrly, T. D., Crane, D. D., and Bosio, C. M. (2017). Expansion and retention of pulmonary CD4+ T cells after prime boost vaccination correlates with improved longevity and strength of immunity against tularemia. *Vaccine* 35, 2575–2581. doi: 10.1016/j.vaccine.2017.03.064
- Rotem, S., Cohen, O., Bar-Haim, E., Bar-On, L., Ehrlich, S., and Shafferman, A. (2014). Protective immunity against lethal *F. tularensis* holarctica LVS provided by vaccination with selected novel CD8+ T cell epitopes. *PLoS ONE* 9:e85215. doi: 10.1371/journal.pone.0085215
- Rowland, C. A., Hartley, M. G., Flick-Smith, H., Laws, T. R., Eyles, J. E., and Oyston, P. C. (2012). Peripheral human gammadelta T cells control growth of both avirulent and highly virulent strains of *Francisella tularensis* in vitro. *Microbes Infect.* 14, 584–589. doi: 10.1016/j.micinf.2012.02.001
- Salerno-Gonçalves, R., Hepburn, M. J., Bavari, S., and Szein, M. B. (2009). Generation of heterogeneous memory T cells by live attenuated tularemia vaccine in humans. *Vaccine* 28, 195–206. doi: 10.1016/j.vaccine.2009.09.100
- Sanapala, S., Yu, J. J., Murthy, A. K., Li, W., Guentzel, M. N., Chambers, J. P., et al. (2012). Perforin- and granzyme-mediated cytotoxic effector functions are essential for protection against *Francisella tularensis* following vaccination by the defined *F. tularensis* subsp. novicida DeltafopC vaccine strain. *Infect. Immun.* 80, 2177–2185. doi: 10.1128/IAI.00036-12
- Saslaw, S., Eigelsbach, H. T., Prior, J. A., Wilson, H. E., and Carhart, S. (1961a). Tularemia vaccine study. II. Respiratory challenge. *Arch. Intern. Med.* 107, 702–714.
- Saslaw, S., Eigelsbach, H. T., Wilson, H. E., Prior, J. A., and Carhart, S. (1961b). Tularemia vaccine study. I. Intracutaneous challenge. *Arch. Intern. Med.* 107, 689–701.
- Sawyer, W. D., Dangerfield, H. G., Hogge, A. L., and Crozier, D. (1966). Antibiotic prophylaxis and therapy of airborne tularemia. *Bacteriol. Rev.* 30, 542–550.
- Sebastian, S., Dillon, S. T., Lynch, J. G., Blalock, L. T., Balon, E., Lee, K. T., et al. (2007). A defined O-antigen polysaccharide mutant of *Francisella tularensis* live vaccine strain has attenuated virulence while retaining its protective capacity. *Infect. Immun.* 75, 2591–2602. doi: 10.1128/IAI.01789-06
- Shen, H., Chen, W., and Conlan, J. W. (2004). Susceptibility of various mouse strains to systemically- or aerosol-initiated tularemia by virulent type A *Francisella tularensis* before and after immunization with the attenuated live vaccine strain of the pathogen. *Vaccine* 22, 2116–2121. doi: 10.1016/j.vaccine.2003.12.003
- Signarovitz, A. L., Ray, H. J., Yu, J. J., Guentzel, M. N., Chambers, J. P., Klose, K. E., et al. (2012). Mucosal immunization with live attenuated *Francisella novicida* U112DeltaiglB protects against pulmonary *F. tularensis* SCHU S4 in the Fischer 344 rat model. *PLoS ONE* 7:e47639. doi: 10.1371/journal.pone.0047639
- Sjöstedt, A., North, R. J., and Conlan, J. W. (1996). The requirement of tumour necrosis factor-alpha and interferon-gamma for the expression of protective immunity to secondary murine tularemia depends on the size of the challenge inoculum. *Microbiology* 142 (Pt 6), 1369–1374. doi: 10.1099/13500872-142-6-1369
- Skyberg, J. A., Rollins, M. F., Samuel, J. W., Sutherland, M. D., Belisle, J. T., and Pascual, D. W. (2013). Interleukin-17 protects against the *Francisella tularensis* live vaccine strain but not against a virulent *F. tularensis* type A strain. *Infect. Immun.* 81, 3099–3105. doi: 10.1128/IAI.00203-13
- Stenmark, S., Lindgren, H., Tärnvik, A., and Sjöstedt, A. (2003). Specific antibodies contribute to the host protection against strains of *Francisella tularensis* subspecies holarctica. *Microb. Pathog.* 35, 73–80. doi: 10.1016/S0882-4010(03)00095-0
- Stinson, E., Smith, L. P., Cole, K. S., Barry, E. M., and Reed, D. S. (2016). Respiratory and oral vaccination improves protection conferred by the live vaccine strain against pneumonic tularemia in the rabbit model. *Pathog. Dis.* 74:ftw079. doi: 10.1093/femspd/ftw079
- Sumida, T., Maeda, T., Takahashi, H., Yoshida, S., Yonaha, F., Sakamoto, A., et al. (1992). Predominant expansion of V gamma 9/V delta 2 T cells in a tularemia patient. *Infect. Immun.* 60, 2554–2558.
- Surcel, H. M., Syrjala, H., Karttunen, R., Tapaninaho, S., and Herva, E. (1991). Development of *Francisella tularensis* antigen responses measured as T-lymphocyte proliferation and cytokine production (tumor necrosis factor alpha, gamma interferon, and interleukin-2 and -4) during human tularemia. *Infect. Immun.* 59, 1948–1953.
- Syrjälä, H., Koskela, P., Ripatti, T., Salminen, A., and Herva, E. (1986). Agglutination and ELISA methods in the diagnosis of tularemia in different clinical forms and severities of the disease. *J. Infect. Dis.* 153, 142–145. doi: 10.1093/infdis/153.1.142
- Tärnvik, A. (1989). Nature of protective immunity to *Francisella tularensis*. *Rev. Infect. Dis.* 11, 440–451. doi: 10.1093/clinids/11.3.440
- Tärnvik, A., Ericsson, M., Golovliov, I., Sandstrom, G., and Sjöstedt, A. (1996). Orchestration of the protective immune response to intracellular bacteria: *Francisella tularensis* as a model organism. *FEMS Immunol. Med. Microbiol.* 13, 221–225. doi: 10.1111/j.1574-695X.1996.tb00242.x

- Tulis, J. J., Eigelsbach, H. T., and Kerpsack, R. W. (1970). Host-parasite relationship in monkeys administered live tularemia vaccine. *Am. J. Pathol.* 58, 329–336.
- Twenhafel, N. A., Alves, D. A., and Purcell, B. K. (2009). Pathology of inhalational *Francisella tularensis* spp. tularensis SCHU S4 infection in African green monkeys (*Chlorocebus aethiops*). *Vet. Pathol.* 46, 698–706. doi: 10.1354/vp.08-VP-0302-T-AM
- Twine, S. M., Petit, M. D., Shen, H., Mykytczuk, N. C., Kelly, J. F., and Conlan, J. W. (2006a). Immunoproteomic analysis of the murine antibody response to successful and failed immunization with live anti-*Francisella* vaccines. *Biochem. Biophys. Res. Commun.* 346, 999–1008. doi: 10.1016/j.bbrc.2006.06.008
- Twine, S. M., Shen, H., Kelly, J. F., Chen, W., Sjostedt, A., and Conlan, J. W. (2006b). Virulence comparison in mice of distinct isolates of type A *Francisella tularensis*. *Microb. Pathog.* 40, 133–138. doi: 10.1016/j.micpath.2005.12.004
- Twine, S., Shen, H., Harris, G., Chen, W., Sjostedt, A., Ryden, P., et al. (2012). BALB/c mice, but not C57BL/6 mice immunized with a DeltacpB mutant of *Francisella tularensis* subspecies tularensis are protected against respiratory challenge with wild-type bacteria: association of protection with post-vaccination and post-challenge immune responses. *Vaccine* 30, 3634–3645. doi: 10.1016/j.vaccine.2012.03.036
- Valentino, M. D., Hensley, L. L., Skrombolas, D., McPherson, P. L., Woolard, M. D., Kawula, T. H., et al. (2009). Identification of a dominant CD4 T cell epitope in the membrane lipoprotein Tul4 from *Francisella tularensis* LVS. *Mol. Immunol.* 46, 1830–1838. doi: 10.1016/j.molimm.2009.01.008
- Valentino, M. D., Maben, Z. J., Hensley, L. L., Woolard, M. D., Kawula, T. H., Frelinger, J. A., et al. (2011). Identification of T-cell epitopes in *Francisella tularensis* using an ordered protein array of serological targets. *Immunology* 132, 348–360. doi: 10.1111/j.1365-2567.2010.03387.x
- White, J. D., McGavran, M. H., Prickett, P. A., Tulis, J. J., and Eigelsbach, H. T. (1962). Morphologic and immunohistochemical studies of the pathogenesis of infection and antibody formation subsequent to vaccination of *Macaca irus* with an attenuated strain of *Pasteurella tularensis*: II. Aerogenic vaccination. *Am. J. Pathol.* 41, 405–413.
- Woolard, M. D., Barrigan, L. M., Fuller, J. R., Buntzman, A. S., Bryan, J., Manoil, C., et al. (2013). Identification of *Francisella novicida* mutants that fail to induce prostaglandin E(2) synthesis by infected macrophages. *Front. Microbiol.* 4:16. doi: 10.3389/fmicb.2013.00016
- Woolard, M. D., Hensley, L. L., Kawula, T. H., and Frelinger, J. A. (2008). Respiratory *Francisella tularensis* live vaccine strain infection induces Th17 cells and prostaglandin E2, which inhibits generation of gamma interferon-positive T cells. *Infect. Immun.* 76, 2651–2659. doi: 10.1128/IAI.01412-07
- Woolard, M. D., Wilson, J. E., Hensley, L. L., Jania, L. A., Kawula, T. H., Drake, J. R., et al. (2007). *Francisella tularensis*-infected macrophages release prostaglandin E2 that blocks T cell proliferation and promotes a Th2-like response. *J. Immunol.* 178, 2065–2074. doi: 10.4049/jimmunol.178.4.2065
- Wu, T. H., Hutt, J. A., Garrison, K. A., Berliba, L. S., Zhou, Y., and Lyons, C. R. (2005). Intranasal vaccination induces protective immunity against intranasal infection with virulent *Francisella tularensis* biovar A. *Infect. Immun.* 73, 2644–2654. doi: 10.1128/IAI.73.5.2644-2654.2005
- Wu, T. H., Zsemlye, J. L., Statom, G. L., Hutt, J. A., Schrader, R. M., Scrymgeour, A. A., et al. (2009). Vaccination of Fischer 344 rats against pulmonary infections by *Francisella tularensis* type A strains. *Vaccine* 27, 4684–4693. doi: 10.1016/j.vaccine.2009.05.060
- Yee, D., Rhinehart-Jones, T. R., and Elkins, K. L. (1996). Loss of either CD4+ or CD8+ T cells does not affect the magnitude of protective immunity to an intracellular pathogen, *Francisella tularensis* strain LVS. *J. Immunol.* 157, 5042–5048.
- Yu, J. J., Raulie, E. K., Murthy, A. K., Guentzel, M. N., Klose, K. E., and Arulanandam, B. P. (2008). The presence of infectious extracellular *Francisella tularensis* subsp. *novicida* in murine plasma after pulmonary challenge. *Eur. J. Clin. Microbiol. Infect. Dis.* 27, 323–325. doi: 10.1007/s10096-007-0434-x

Conflict of Interest Statement: The authors declare that the research was conducted in the absence of any commercial or financial relationships that could be construed as a potential conflict of interest.

Copyright © 2018 Roberts, Powell and Frelinger. This is an open-access article distributed under the terms of the Creative Commons Attribution License (CC BY). The use, distribution or reproduction in other forums is permitted, provided the original author(s) and the copyright owner are credited and that the original publication in this journal is cited, in accordance with accepted academic practice. No use, distribution or reproduction is permitted which does not comply with these terms.



Francisella tularensis D-Ala D-Ala Carboxypeptidase DacD Is Involved in Intracellular Replication and It Is Necessary for Bacterial Cell Wall Integrity

Petra Spidlova^{1*}, Pavla Stojkova¹, Vera Dankova¹, Iva Senitkova¹, Marina Santic², Dominik Pinkas³, Vlada Philimonenko^{3,4} and Jiri Stulik¹

¹ Department of Molecular Pathology and Biology, Faculty of Military Health Sciences, University of Defence, Hradec Kralove, Czechia, ² Department of Microbiology and Parasitology, Medical Faculty, University of Rijeka, Rijeka, Croatia, ³ Microscopy Center, Institute of Molecular Genetics ASCR v.v.i., Electron Microscopy Core Facility, Prague, Czechia, ⁴ Department of Biology of the Cell Nucleus, Institute of Molecular Genetics ASCR v.v.i., Prague, Czechia

OPEN ACCESS

Edited by:

Alain Charbit,
UMR8253 Institut Necker Enfants
Malades Centre de Médecine
Moléculaire (INEM), France

Reviewed by:

Max Maurin,
Université Grenoble Alpes, France
Nagendran Tharmalingam,
Alpert Medical School, United States

*Correspondence:

Petra Spidlova
petra.spidlova@unob.cz

Received: 27 November 2017

Accepted: 21 March 2018

Published: 10 April 2018

Citation:

Spidlova P, Stojkova P, Dankova V,
Senitkova I, Santic M, Pinkas D,
Philimonenko V and Stulik J (2018)
Francisella tularensis D-Ala D-Ala
Carboxypeptidase DacD Is Involved in
Intracellular Replication and It Is
Necessary for Bacterial Cell Wall
Integrity.
Front. Cell. Infect. Microbiol. 8:111.
doi: 10.3389/fcimb.2018.00111

D-alanyl-D-alanine carboxypeptidase, product of *dacD* gene in *Francisella*, belongs to penicillin binding proteins (PBPs) and is involved in remodeling of newly synthesized peptidoglycan. In *E. coli*, PBPs are synthesized in various growth phases and they are able to substitute each other to a certain extent. The DacD protein was found to be accumulated in fraction enriched in membrane proteins from severely attenuated *dsbA* deletion mutant strain. It has been presumed that the DsbA is not a virulence factor by itself but that its substrates, whose correct folding and topology are dependent on the DsbA oxidoreductase and/or isomerase activities, are the primary virulence factors. Here we demonstrate that *Francisella* DacD is required for intracellular replication and virulence in mice. The *dacD* insertion mutant strain showed higher sensitivity to acidic pH, high temperature and high osmolarity when compared to the wild-type. Eventually, transmission electron microscopy revealed differences in mutant bacteria in both the size and defects in outer membrane underlying its SDS and serum sensitivity. Taken together these results suggest DacD plays an important role in *Francisella* pathogenicity.

Keywords: *Francisella*, DacD, virulence, phagosomal escape, carboxypeptidase, penicillin binding proteins, membrane defects

INTRODUCTION

Bacteria possess many tools that enable them to resist unfriendly environments, such as hostile intracellular milieu and host immune response, in order to survive the effects of antimicrobial agents and, inter alia, changing ion concentration. Their cell wall and its structure protect them against these negative influences. However, these surface structures, such as lipopolysaccharide and peptidoglycan, are triggers for a host cell's primary immune response (Chandler and Ernst, 2017).

One key component of the bacterial cell wall is the middle segment called peptidoglycan layer, which is connecting link between outer and inner membrane in gram-negative bacteria. Peptidoglycan macromolecule, i.e., sacculus, consists of individual glycan chains crosslinked by short peptides (Egan et al., 2015). Peptidoglycan sacculus is responsible for maintaining bacterial

shape as well as providing mechanical strength to resist osmotic challenges (Vollmer et al., 2008a). The synthesis of peptidoglycan is divided into three steps with glycosyltransferases play an important role by polymerizing the glycan chains and DD-transpeptidases, that crosslink the peptides. Delivery of new material to the peptidoglycan layer occurs during transpeptidation. Because of this, there is need for some cleavage mechanisms to disrupt older layer and thus maintain the thickness of peptidoglycan. Cleavage is also required for cell division. This mechanism is ensured by peptidoglycan hydrolases (Vollmer et al., 2008b). Newly synthesized peptidoglycan is rich on pentapeptides, which are reduced to tetrapeptides by DD-carboxypeptidases. Some tetrapeptides are trimmed to tripeptides by LD-carboxypeptidases (Glauner and Hölte, 1990).

Penicillin binding proteins (PBPs) are components of peptidoglycan biosynthesis (Matsushashi, 1994). In *E. coli* 12 PBPs were identified. The first seven were named in order of their decreasing molecular weight (PBP 1a, 1b, 2, 3, 4, 5, 6; Spratt, 1975). The remaining five PBPs were described later: PBP 7 (Henderson et al., 1994), PBP 8 (Henderson et al., 1995), DacD (Baquero et al., 1996), AmpC and AmpH (Henderson et al., 1997), PBP 1c (Schiffer and Hölte, 1999). Generally, PBPs are divided to the two main categories of either (HMW) or low molecular weight (LMW). HMW's are involved in the synthesis of peptidoglycan and its incorporation into the sacculus, namely PBPs 1a, 1b, 1c, 2, and 3. LMW's *in vitro* biochemical capabilities have been already determined but *in vivo* functions are still remain unclear (Denome et al., 1999). Members of this class are PBPs 4, 5, 6, and 7, DacD, AmpC, and AmpH (Nelson and Young, 2001). PBPs are expressed in various cell growth phases and can substitute each other to a certain extent (Ghosh et al., 2008).

Our subject of interest is one of LWM PBPs with DD-carboxypeptidase activity DacD, product of *dacD* gene in *Francisella* (locus *FTS_1034* in FSC200 strain). In *E. coli* DacD, often denoted as PBP6b, is expressed in stationary phase (Baquero et al., 1996). Its amino acid sequence homology (48%) with PBP5 suggests its role in β -lactam resistance, but deletion of *dacD* did not change the β -lactam resistance (Sarkar et al., 2011). Some studies have shown its role in biofilm formation in *Salmonella enterica* and *E. coli* (Brambilla et al., 2014). Recently a study was published that indicated *E. coli* PBP6b as being most active and most abundant at a low pH (pH 5), which suggests its necessity for growth and maintenance of bacterial cell shape in an acidic environment (Peters et al., 2016).

The relationship between DacD and acidic pH resistance could be interesting in connection with intracellular pathogen such as *Francisella*, the causative agent of tularemia. It is assumed that this gram-negative bacterium is able to resist the acid environment in the phagosome, escape to the cytosol of host cell, replicate there, cause host cell death and re-infect next host cells (Celli and Zahrt, 2013). Here, we show that the mutant strain with inactivated gene coding for DD-carboxypeptidase DacD is unable to replicate inside host as effectively as the wild-type counterpart although it escapes more rapidly from phagosomes. Furthermore, the mutant bacteria are more sensitive to several stress stimuli and also demonstrate the defects in the membrane integrity and the cell shape. These results document the role

DacD in *Francisella* virulence contributing to the understanding of the mechanisms behind *Francisella* pathogenesis.

MATERIALS AND METHODS

Bacterial Strains, Plasmids, and Growth Conditions

Bacterial strains and plasmids used in this study are listed in **Table 1**. All work with *F. tularensis* subsp. *holarctica* FSC200 and derivative strains were conducted under BSL-2 containment. *Francisella* strains were cultured on McLeod agar plate enriched for bovine hemoglobin (Becton Dickinson, Cockeysville, MD, USA) and IsoVitalax (Becton Dickinson, Cockeysville, MD, USA) or grew in Chamberlain medium (Chamberlain, 1965) with shaking 200 rpm at 37°C. The *E. coli* strains were cultured in Luria Bertani (LB) broth medium or on LB agar plates. When appropriate, antibiotics were used at following concentration: kanamycin 20 μ g/ml (*F. tularensis*) or 50 μ g/ml (*E. coli*) (kanamycin sulfate, Serva, Heidelberg, Germany), ampicillin 100 μ g/ml (*E. coli*) (ampicillin Na-salt, Serva, Heidelberg, Germany).

All chemicals without the specified manufacturer were purchased from Sigma-Aldrich (St. Louis, MO, USA).

Targetron Insertional Mutagenesis

The TargetTron gene knockout system was used to generate the *dacD* mutant (Rodriguez et al., 2008) (Sigma-Aldrich, St. Louis, MO, USA). The primers used in plasmid construction are listed in Table S1. The PCR product was digested (*Hind*III-*Bsr*GI, NEB, Ipswich, MA, USA) then inserted into the *Francisella* targeting vector pKEK1140 (generously provided by Karl Klose, University of Texas at San Antonio, San Antonio, TX) to generate a TargetTron insertion plasmid (Rodriguez et al., 2008). Constructed plasmid DNA was introduced into the FSC200 strain by electroporation. The presence of the TargetTron insertion was determined by using an intron-specific EBS universal primer combined with a gene specific primer. Intron insertion of the targeted gene was determined by using gene-specific primers that amplified across the insertion site. Selected positive clones grew in Chamberlain medium at 37°C overnight then plated on McLeod agar plate (without kanamycin) and incubated at 37°C to remove the TargetTron temperature-sensitive plasmid. The insertion mutants were confirmed by using PCR with the gene-specific primers and denoted FSC200/*in dacD*.

Functional Complementation

The functional complementation in generating the *dacD* complemented strain included complementation *in trans* and *in cis*. A DNA fragment carrying the wild-type *dacD* gene was PCR amplified by using FSC200 genomic DNA as a template, employing primers DacD_pKK289_F and DacD_pKK289_R (Table S1). The final PCR product was sequenced, then cloned downstream of the GroES promoter by replacing the green fluorescence protein-encoding gene in the shuttle vector pKK289gfp (Bönquist et al., 2008). The constructed plasmid DNA pKK289dacD was introduced into the mutant strain FSC200/*in dacD* by electroporation. The strain complemented

TABLE 1 | Bacterial strains and plasmids used in this study.

Strain	Description	Source
<i>Francisella tularensis</i> FSC200	<i>Francisella tularensis</i> subsp. <i>holarctica</i> , wild-type, clinical isolate	<i>Francisella</i> Strain Collection (FSC) of the Swedish Defense Research Agency, Umeå, Sweden
FSC200/ <i>in dacD</i>	<i>dacD</i> (FTS_1034) insertion mutant strain	This study
FSC200/ <i>dacDtrans</i>	Insertion mutant strain complemented <i>in trans</i>	This study
FSC200/ <i>dacDcis</i>	Insertion mutant strain complemented <i>in cis</i>	This study
<i>E. coli</i> S17-1 λ pir	<i>Escherichia coli</i> donor strain for conjugation TpR SmR recA, thi, pro, hsdR-M+RP4: 2-Tc:Mu: Km Tn7 λ pir	Simon et al., 1983
<i>E. coli</i> XL1	<i>Escherichia coli</i> competent cell <i>recA1 endA1 gyrA96 thi-1 hsdR17 supE44 relA1 lac</i> [<i>F'</i> <i>proAB lacIq</i> Δ M15 Tn10 (Tet ^R)]	Stratagene
Plasmid	Description	Source
pCR4-TOPO	Cloning vector, pUC <i>ori</i> , P _{lac} , <i>lacZ</i> , Kan ^R , Amp ^R	Invitrogen
pDM4	<i>F. tularensis</i> suicide vector, <i>mob</i> _{RP4} , <i>ori</i> _{RP6K} , <i>sacB</i> , Cm ^R	Milton et al., 1996
pKK289KmGFP	<i>E. coli</i> / <i>F. tularensis</i> shuttle vector, Ft <i>ori</i> , p15a <i>ori</i> , Km ^R , groES promoter	Bönquist et al., 2008

in trans was denoted FSC200/*dacDtrans*. For complementation *in cis* the *dacD* gene with flanking regions was amplified by using primers DacDcis_F and DacDcis_R. The PCR product was inserted into pCR4.0 TOPO TA cloning vector (Invitrogen, Carlsbad, CA, USA) to facilitate sequencing (Institute of Microbiology, Prague, Czech Republic). Using *XhoI/XbaI* the fragment was cut out, and then inserted into pDM4 suicide vector (Milton et al., 1996) linearized by the same restriction endonucleases digestion (NEB, Ipswich, MA, USA) to generate the *dacDcis* plasmid. Conjugal mating between *E. coli* S17-1 λ pir donor strain (Simon et al., 1983) and *F. tularensis* FSC200/*in dacD* mutant strain followed by sucrose-selection led to the allelic exchange on the mutant strain chromosome and the resulting strain was denoted FSC200/*dacDcis*.

Isolation of Macrophages and *in Vitro* Proliferation

Mouse bone marrow cells were harvested from 6 to 10 weeks old, female BALB/c mice femur (Velaz, Czech Republic). The cavity of the femur was flushed out with DMEM (Invitrogen, Carlsbad, CA, USA) and bone marrow cells were collected. Washing bone marrow cells with pre-warmed DMEM two times then the cells were resuspended in BMMs medium [DMEM supplemented with 10% fetal bovine serum (FBS, Dominique Dutscher, Brumath, France) and 10% L929-conditioned medium as a source of macrophage colony stimulating factor] with appropriate antibiotics (50 U/ml penicillin, 50 μ g/ml streptomycin; Sigma-Aldrich, St. Louis, MO, USA). The cells were incubated at concentration of 6×10^6 cells per Petri dish for 1 week to differentiate into bone marrow-derived macrophages (BMMs). The day before infection, macrophages were seeded on tissue culture plates at the concentration of 5×10^5 cells per well in antibiotic-free DMEM supplemented with 10% fetal bovine serum. Following cultivation overnight, BMMs were infected with all four

bacterial strains (FSC200, FSC200/*in dacD*, FSC200/*dacDtrans*, and FSC200/*dacDcis*) at a multiplicity of infection (MOI) of 50. Actual infection doses were determined by plating serial dilutions of the culture inoculum. Infection started by centrifugation of plates for 5 min, $400 \times g$, and then the samples were incubated at 37°C, 5% CO₂ for 30 min. Extracellular bacteria were killed during incubation in DMEM with 5 μ g/ml gentamicin (Sigma-Aldrich, St. Louis, MO, USA) at 37°C, 5% CO₂ for 30 min. The cells were washed three times with pre-warmed PBS before adding the DMEM with 10% FBS without antibiotics. At set time points (1, 6, 24, and 48 h), infected cells were lysed by 0.1% sodium deoxycholate, and then the lysates were plated on McLeod agar plates in a serial dilution. The plates were incubated at 37°C, 5% CO₂ for 5 days. The number of viable intracellular bacteria was determined by colony forming units (CFU) counting.

Type II pulmonary epithelial cell line A549 (ATCC[®] CCL-185TM) was cultured in DMEM supplemented with 10% FBS at 37°C, 5% CO₂. Cell were seeded at a concentration of 1.5×10^5 cells/well and let to adhere overnight. Cells were infected at a MOI of 100. Infection started by centrifugation of plates for 5 min, $400 \times g$, and then the samples were incubated at 37°C, 5% CO₂ for 2 h. Extracellular bacteria were killed during incubation in DMEM with 25 μ g/ml gentamicin for 2 h at 37°C, 5% CO₂. The cells were washed three times with pre-warmed PBS before adding the DMEM with 10% FBS without antibiotics. At set time points (6, 24 and 48 h), the infected cells were lysed by 0.1% sodium deoxycholate, then the lysates were plated on McLeod agar plates in a serial dilution. The plates were incubated at 37°C, 5% CO₂ for 5 days. The number of viable intracellular bacteria was determined by colony forming units (CFU) counting.

Macrophage Cytotoxicity Assay

For cytotoxicity experiments, BMMs were seeded in 96-well tissue culture plates at a concentration of 2×10^4 cells/well and

allowed to adhere overnight at 37°C, 5% CO₂. The next day, the BMMs were infected with bacterial cell suspensions at an MOI of 50:1. Following 30 min incubation, the extracellular bacteria were killed by gentamicin (5 µg/ml, 30 min), which corresponds to time zero. At 0, 24, and 48 h postinfection, culture plates were centrifuged to pellet cells (300 × g, 3 min) and the supernatant was collected. The activity of lactate dehydrogenase (LDH) in the supernatant was measured according to manufacturer's instructions (PIERCE LDH Cytotoxicity Assay kit, Thermo Fisher Scientific, Waltham, MA, USA) as an absorbance at the wavelength of 490 nm using the Paradigm microplate reader (Beckman Coulter, Brea, CA, USA). As a positive control (representing 100% cell lysis), uninfected BMMs were lysed with 0.1% sodium deoxycholate. Sample absorbance values were expressed as a percentage of the positive-control value.

Infection of Mice

Groups of five, 6–10 weeks old female BALB/c mice (Velaz, Czech Republic) were challenged by subcutaneous route at the dose of 10 and 50 CFU/mouse for FSC200/*in dacD* mutant; 10 CFU/mouse for FSC200, complemented strains FSC200/*dacDtrans* and FSC200/*dacDcis*. Control group of mice was challenged with physiological saline solution. Mice were observed for 21 days for morbidity and mortality.

For bacterial dissemination study, mice were challenged by subcutaneous route at a dose of 10 CFU/mice for each tested strain. At set time points, 3 BALB/c mice were euthanized by carbon dioxide exposure. The liver, spleen, and lung were processed for plating to determine the presence of bacteria.

Standard and Stress Growth Kinetics

F. tularensis strains were grown overnight at 37°C in Chamberlain medium supplemented with kanamycin (20 µg/ml) when applicable. The cultures were diluted with fresh Chamberlain medium to OD₆₀₀ = 0.1. 200 µl aliquots of the diluted culture were transferred into a 96-well plate in pentaplicates with either the following stress conditions: pH 4.0, 3% NaCl, or 20 µM CuCl₂, then samples were incubated at 37°C for 24 h. For heat stress study, samples were incubated at 42°C for 24 h. The growth kinetics was determined by measuring the OD₆₀₀ every 10 min using a microplate reader FLUOstar Optima (BMG Labtech, Germany). Experiment was repeated three times.

SDS Sensitivity Assay

F. tularensis strains were grown overnight at 37°C in Chamberlain medium, when required the kanamycin (20 µg/ml) was added. The bacterial cultures were diluted with 5 ml of fresh Chamberlain medium to get a bacteria working solution at final concentration equal to 10⁸ bacteria/ml and SDS to a final concentration of 0.05% was added. The number of viable bacteria was determined by plating a serial dilution of bacterial cultures on McLeod plates at set time points (0, 1, 2, 3, and 4 h after SDS addition). Bacteria were enumerated after 72 h incubation at 37°C. Experiments were repeated independently three times and data represent the average of all experiments.

Transmission Electron Microscopy

BMMs were seeded in 24-well tissue culture plate at a concentration of 2 × 10⁵ cells/well and allowed to adhere overnight at 37°C, 5% CO₂. Next day, BMMs were infected with bacterial cell suspensions at a MOI of 50. At appropriate time intervals (10 min, 30 min, 1 and 6 h) BMMs were fixed with 3.8% paraformaldehyde for 30 min at RT and then neutralized with 50 mM NH₄Cl for 10 min at RT. Cells were quickly washed with Sörensen buffer (0.1 M sodium/potassium phosphate buffer, pH 7.3; SB) at 37°C, fixed with 2.5% glutaraldehyde in SB for 2 h, washed with SB, and postfixed with 1% OsO₄ solution in SB for 2 h. The cells were dehydrated in series of ethanol with increasing concentration, subsequently in propylene oxide, and embedded in mixture of Epon 812 substitute and Durcupan ACM (Sigma-Aldrich, St. Louis, MO, USA).

Bacteria cultured in Chamberlain medium were fixed with 2.5% glutaraldehyde in SB for 1 h, washed with SB, resuspended in small volume of SB and mixed with 2% agarose in 1:1 ratio at 37°C. After centrifugation, the pellet was chilled, cut, washed with SB and postfixed with 1% OsO₄ solution in SB for 2 h. The bacteria were dehydrated in series of ethanol with increasing concentration, subsequently in propylene oxide, and embedded in mixture of Epon 812 substitute and Durcupan ACM.

Polymerized blocks were cut into 80 nm ultrathin sections, collected on 200 mesh size copper grids, and stained with saturated aqueous solution of uranyl acetate for 4 min. The sections were examined in FEI Morgagni 268 transmission electron microscope (FEI, Eindhoven, The Netherlands) operated at 80 kV. The images were captured using Mega View III CCD camera (Olympus Soft Imaging Solutions, Münster, Germany).

For quantification of cell size differences, multiple random TEM images of wild-type and mutant cells taken at equal magnification of 11,000 x were used. Cell profiles were segmented using machine learning algorithms in ilastik software (Sommer et al., 2011), and areas determined in Fiji ImageJ (Schindelin et al., 2012). Total of 1,945 wild-type and 173 mutant cells were analyzed. Cell profiles exhibiting membrane defects were counted on the same images.

Serum Sensitivity Assay

Bactericidal assay was conducted with fresh human serum prepared from the whole blood of the anonymous healthy non-immune donors. Briefly, collected nonheparinized whole blood from donors was kept at room temperature for 1 h, then stored at 4°C for 30 min to allow blood to clot. The blood clot was removed by centrifugation at 500 × g for 30 min at 4°C. The serum fraction was collected, centrifuged at 500 × g for 5 min, aliquoted, and stored at –80°C until needed (no longer than 3 weeks). The bacteria from the McLeod agar plates were harvested and suspended into PBS. Normalized bacteria stock solution of OD₆₀₀ = 1.0 was used to make a working solution which contains 5 × 10⁷ bacteria in 1 ml of PBS. For each assay, 40 µl of bacteria working solution (containing 2 × 10⁶ bacteria) were added either to 160 µl of 100% serum (final concentration of 80%), or to 160 µl of 6.25% serum in PBS (final concentration of serum 5%), then the mixtures were incubated at 37°C for 90 min. One hundred

and sixty microliters of PBS was used as a positive control (100% survival). Lysis was stopped by incubating the tubes on ice for 5 min. Surviving bacteria were enumerated by plating 10-fold serial dilutions of each suspension. Experiment was performed in a triplicate.

Antibiotic Susceptibility Tests

For general tests with kanamycin, tetracycline (tetracycline hydrochloride, Zymo Research, Irvine, CA, USA), chloramphenicol, hygromycin B (Invitrogen, Carlsbad, CA, USA), gentamicin, polymyxin B sulfate, ampicillin, penicillin G (penicillin G sodium salt), and carbenicillin (Biolone, London, UK), we used gradient antibiotic plates (Szybalski and Bryson, 1952). For the determination of minimal inhibitory concentrations (MICs) for ampicillin, penicillin G, and carbenicillin broth macrodilution method was used.

SDS-PAGE and Western Blot

Francisella strains expressing variants of DacD were cultured in Chamberlain medium (37°C, 200 rpm), and harvested by centrifugation after reaching OD₆₀₀ of 1 (7,300 rpm, 10 min, 4°C). The cell pellets were washed with 50 mM Tris, pH 8 and resuspended in 50 mM Tris, pH 8 supplemented with protease inhibitor cocktail Complete Mini-EDTA free (Roche, Basel, Switzerland). Bacteria lysates were prepared using French press by three passages at 16,000 psi. Aliquots of lysates were separated on a one-dimensional SDS-PAGE and electroblotted onto PVDF membranes. Variants of DacD were detected by using a polyclonal rabbit anti FTS₁₀₃₄ serum (Moravian—Biotechnology, Brno, Czech Republic). As secondary antibody the polyclonal swine anti-rabbit IgG/HRP (Dako, Santa Clara, CA, USA) was used. Chemiluminescence detection was employed by using a BM Chemiluminescence Blotting Substrate (POD) while following the manufacturer's instructions (Roche, Basel, Switzerland).

Ethics Statement

All experiments using mice were performed in accordance with guidelines of the Animal Care and Use Ethical Committee of the Faculty of Military Health Sciences, University of Defense, Czech Republic. The research protocol was approved by this ethics committee under project no. 50-6/2016-684800. Experiments using human sera were conducted with the approval of Ethics Committee of University Hospital Hradec Kralove; reference no. 201710S10P and each volunteer provided written informed consent to participate in this study in accordance with regulatory guidelines.

Statistical Analysis

Statistical significances were analyzed by GraphPad Prism version 5 (GraphPad Software, La Jolla, CA, USA). The degree of significance was defined using two-way ANOVA followed by Bonferroni's multiple comparisons test or using Student's *t*-test depending on number of analyzed samples. In statistical analysis FSC200/*in dacD* mutant strain was compared to FSC200 strain. **P* < 0.05, ***P* < 0.01, ****P* < 0.001.

RESULTS

Construction of Mutant Strain and Functional Complementation

To better characterize the role of *F. tularensis* DacD protein, we generated a FSC200 *dacD* insertional mutant (for details see Figure S1) introducing the retargeted mobile group II intron, as described previously (Rodriguez et al., 2008). To complement the mutant, we either expressed *dacD in trans* from GroES promoter of pKK289Km (Bönquist et al., 2008) or using the allelic exchange to return the gene *dacD* back on the chromosome by replacing gene with introduced intron (complementation *in cis*). Western blot analysis was used to confirm that the DacD protein is missing in the mutant strain and that the protein is produced in complemented strains (Figure S2).

DacD Role in Intracellular Replication, Phagosomal Escape, and Cytopathogenicity

To address the role of DacD in virulence of *F. tularensis* we first studied the intracellular replication of FTS200/*in dacD* mutant strain inside murine bone-marrow derived macrophages (BMMs) and type II pulmonary epithelial A549 cell line. At 24 h post infection, the replication defects were obvious for both these types of cells. When compared to the wild-type FSC200 strain, the mutant bacteria showed significantly lower numbers of bacteria/ml (Figure 1). This defect was eliminated by complementation *in cis* but not by complementation *in trans*. The different situation has occurred 48 h after infection. It is evident that the defect in replication is still maintained in BMMs, whereas in A549 the FSC200/*in dacD* mutant strain proliferates comparable to WT. These results demonstrate the differences in requirement of DacD for intracellular proliferation and survival in BMMs and A549 cell line.

Transmission electron microscopy was used to further analyze the intracellular fate of the FSC200/*in dacD* mutant bacteria. The BMMs were infected by the wild-type and mutant bacteria, respectively. In four time intervals of infection, the percentage of bacteria in intact phagosome, damaged phagosome and in cell cytosol was calculated (Figure 2). Interestingly, we found out that mutant bacteria escape the phagosomes more rapidly than wild-type bacteria. The most significant differences were observed 1 h post infection. At this time only 11% of the mutant bacteria resided in damaged phagosomes vs. 51.5% of the wild-type, and 70 vs. 19.5% are found to be free in cytosol, respectively. This finding suggests that the inactivation of DacD impaired intracellular replication of mutant bacteria but it did not affect phagosomal escape. These data were confirmed by the analysis of colocalization of FSC200/*in dacD* bacteria-containing phagosomes with EEA1, LAMP1, and cathepsin D (data not shown).

To investigate the role of the DacD protein on *Francisella* cytopathogenic effects we infected BMMs with the wild-type FSC200 strain or the FSC200/*in dacD* mutant and measured the release of lactate dehydrogenase (LDH) into the cell supernatant. At the beginning of infection (time 0 h), the LDH level released

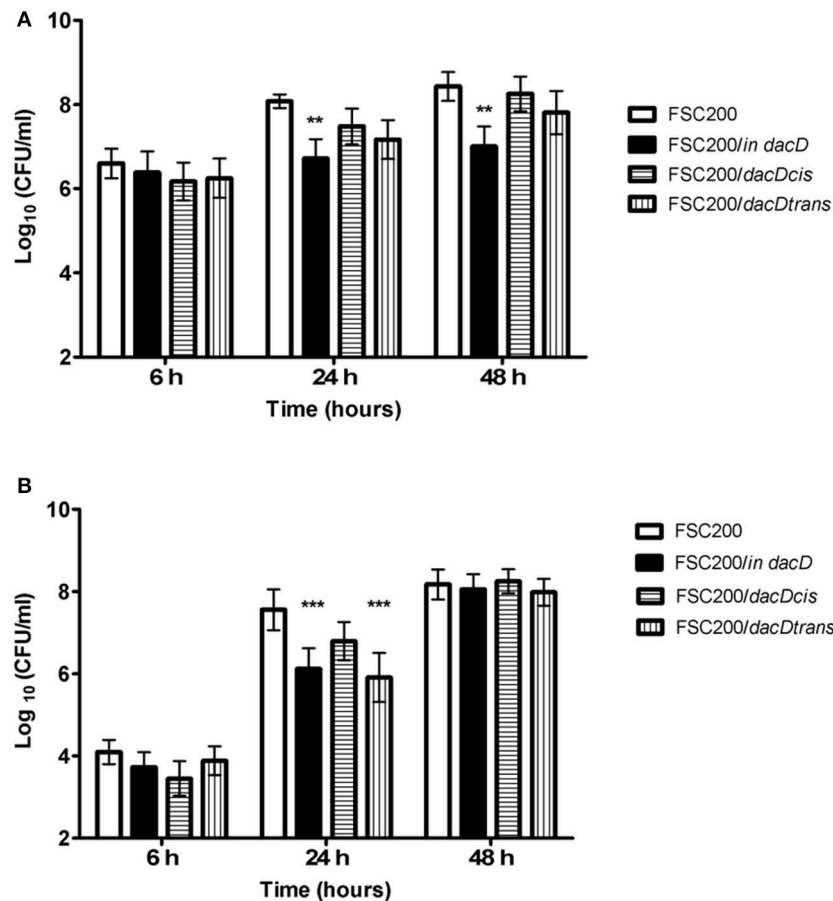


FIGURE 1 | Intracellular growth of the FSC200/*in dacD* mutant strain is affected. **(A)** Replication inside bone-marrow derived macrophages. FSC200/*in dacD* mutant strain shows significantly reduced proliferation inside BMMs 24 and 48 h post infection. **(B)** Replication inside A549 cell line. The significant defect in replication in A549 cell line is visible only at time interval 24 h post infection. At 48 h post infection the replication rate of all strains is the same. ** $P < 0.01$, *** $P < 0.001$.

from cells infected with the FSC200/*in dacD* mutant (~17%) was comparable to the LDH release detected in cells infected with the wild-type FSC200 strain (~15%; Figure S3). After 24 h of infection, the LDH levels increased to 49 and 38% for the FSC200/*in dacD* and parental FSC200 strains, respectively. At 48 h postinfection, the level of LDH release was 56% for the FSC200/*in dacD* mutant strain, which was almost the same as the LDH release detected for the wild-type FSC200 strain (53%). The LDH assay showed that the FSC200/*in dacD* mutant strain induces loss of host cell membrane integrity at similar levels as the wild-type strain.

Animal Studies

Taken into account that the mutant strain is deficient in intracellular replication, we further verified its attenuation in mouse model of infection. The course of mouse infection was followed for 21 days. Using the dose of 10^2 cfu of FSC200/*in dacD* resulted in the death of all mice tested (data not shown). By sequential dose reduction, we found out that the mutant strain is less lethal than wild-type strain for mice challenged by subcutaneous route at dose of 10 CFU/mouse (Figure 3A). The

increase of the mutant strain dose to 50 cfu led to the death of one animal (Figure 3B). So it is evident that opposite the wild-type strain, the FSC200/*in dacD* mutant is *in vivo* attenuated but it is not avirulent. The complementation *in cis* and *in trans* restored the wild-type phenotype with 6–8 days delay for the dose of 10 cfu and 3–7 days delay for the dose of 50 cfu when compared to the original wild-type strain.

The mutant attenuation was further corroborated by the analysis of bacteria dissemination in host tissues. The groups of three mice were challenged by subcutaneous route at the dose of 10 cfu/mouse for each tested strain. We followed the kinetics of infection by assessing the numbers of viable bacteria in the spleen, liver, and lung tissues at the post-infection time points. None of the mice infected with the wild-type FSC200 strain survived more than 5 days post infection, and mice infected with complemented strains dying gradually between day 7 and 14 post infection due to the rapid progression of disease. Contrary, mice infected with FSC200/*in dacD* survived the infection and the bacterial loads in target organs did not reach those for wild-type and complemented strains (Figure 4). For s.c. infection, the maximum replication of mutant strain inside tissues were

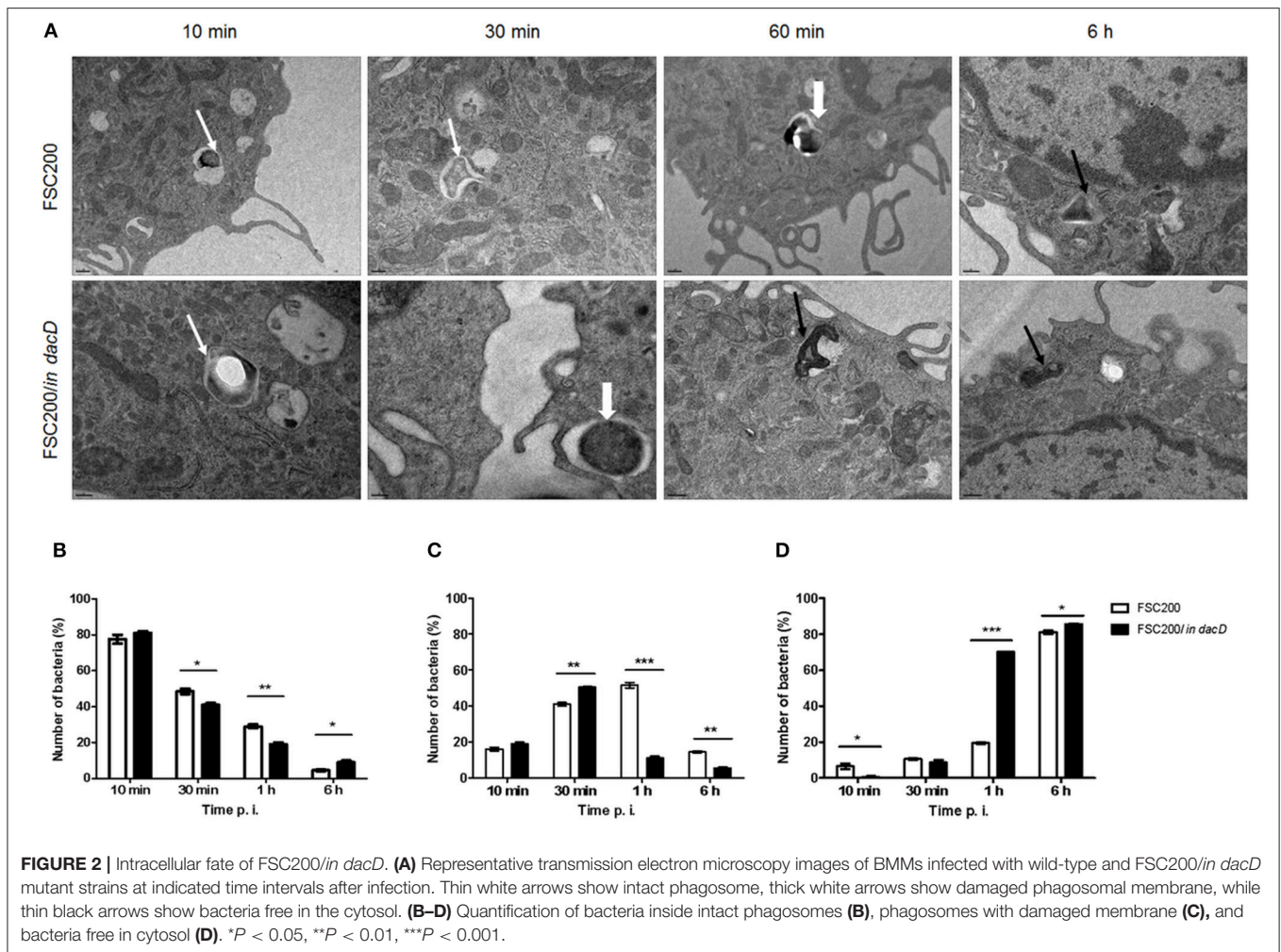


FIGURE 2 | Intracellular fate of FSC200/*in dacD*. **(A)** Representative transmission electron microscopy images of BMMs infected with wild-type and FSC200/*in dacD* mutant strains at indicated time intervals after infection. Thin white arrows show intact phagosome, thick white arrows show damaged phagosomal membrane, while thin black arrows show bacteria free in the cytosol. **(B–D)** Quantification of bacteria inside intact phagosomes **(B)**, phagosomes with damaged membrane **(C)**, and bacteria free in cytosol **(D)**. * $P < 0.05$, ** $P < 0.01$, *** $P < 0.001$.

detected on day 7. The FSC200/*in dacD* strain reached $\sim 10^6$ cfu/organ in case of spleen and liver but 10^4 cfu/organ in the lungs. After day 7, the number of mutant bacteria slowly decline, at day 21 mutant were totally cleared out of lung and for liver at day 28. However, mutant bacteria were not totally cleared out of spleen during whole observed time period. These results indicate that the FSC200/*in dacD* mutant is able to infect mice and persist in organs, but replicates less effectively than wild-type strain inside the host tissues.

Sensitivity of the FSC200/*in dacD* to Stress Stimuli

To address the role of DacD protein in adaptation to various stress stimuli, we compared the growth rate between wild-type strain and all the mutant strains. All tested strains grew in the media with four conditions as following: acid pH (pH 4), in high osmolarity (3% NaCl), in 42°C or CuCl₂-induced oxidative stress (Figure 5). As was expected the mutant strain was not able to resist high osmolarity, high temperature and low pH (Figures 5A–C). On the other hand the FSC200/*in dacD* mutant strain grew better than wild-type under the

oxidative stress conditions induced by the presence of 20 μ M CuCl₂ with the maximum of growth at 12 h interval, but afterwards the growth slowly drop down (Figure 5D). At standard cultivation conditions, the growth kinetics of wild-type and FSC200/*in dacD* mutant strain did not significantly differ (data not shown). With the exception of high osmolarity the complementation *in cis* restored fully wild-type phenotype, whereas the complementation *in trans* did not. Further, we studied the SDS sensitivity of the mutant strain. At 1 h after SDS addition no difference in bacterial growth was seen, but in later time intervals (2, 3, and 4 h) the significant difference in CFU count was observed (Figure 6). This result clearly indicates the membrane defects in FSC200/*in dacD* bacteria. Both complemented strains as well as wild-type strain resist the SDS during whole time interval tested.

FSC200/*in dacD* Shows Morphological Changes and Membrane Defects

To confirm membrane defects, we studied the morphology of mutant bacteria by using transmission electron microscopy. Comparing to the wild-type strain, the FSC200/*in dacD* bacteria

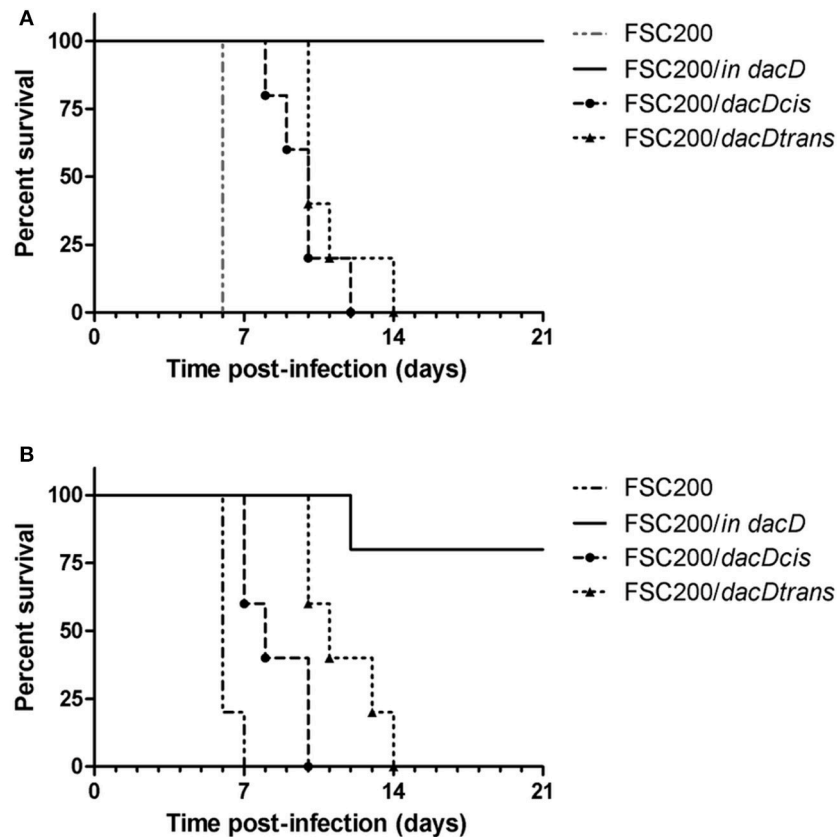


FIGURE 3 | Survival of mice after subcutaneous infection with FSC200/*in dacD*, complemented and wild-type strains. Mice were infected with a dose of 10 cfu/mouse (A) and 50 cfu/mouse (B) and were observed for 21 days and the deaths were recorded.

exerted larger size and discontinuous plasma membrane, as well (Figure 7). Morphological observation was supported by quantification. Mean area of cell profiles on ultrathin sections of mutant cells was nearly 10 times higher than in wild-type strain. Number of profiles membrane defects were visible on every third profile in mutant cells sections. Taken into account that the 80-nm thick section represents only a small fraction of the total cell volume, the total incidence of membrane defects in cell population would be much higher. These results demonstrate the necessity of DacD protein for the maintaining of bacterial membrane integrity and bacterial shape.

FSC200/*in dacD* Mutant Strain Sensitivity to Bactericidal Effect of Human Serum

The membrane defects can influence bacterial resistance to human serum. Therefore, we performed the serum bactericidal assay in which the wild-type, FSC200/*in dacD* mutant, both complemented mutant strains, and the FSC200/*wbtDEF::Cm* strain lacking LPS, were exposed to human nonimmune serum. The significant sensitivity of FSC200/*wbtDEF::Cm* strain to human serum on the one hand and the resistance of FSC200 on the other hand were consistent with previously published data (Dankova et al., 2016). The FSC200/*in dacD* mutant strain also exhibited some degree of sensitivity to complement-mediated lysis. In the case of 5% human serum 25% of mutant

bacteria were killed while using 80% human serum only 50% of bacteria survived (Figure 8). Both complemented strains showed resistance to effects of serum comparable to wild-type level.

Susceptibility to Antibiotics

Because the surface structures of FSC200/*in dacD* showed slight defects, the question arose as whether or not the mutant strain might be more sensitive to antibiotics, especially β -lactams. Using gradient antibiotic plates we tested susceptibility of FSC200, both complemented strains and FSC200/*in dacD* to kanamycin, tetracycline, chloramphenicol, hygromycin B, gentamicin, polymyxin B sulfate, ampicillin, penicillin G, and carbenicillin. From this experiment it seemed the resistance to β -lactams might be influenced because growth of the mutant strain was not as convincing as the other strains (data not shown). The susceptibility to tetracycline, chloramphenicol, hygromycin B, gentamicin, polymyxin B sulfate was not affected and was the same as for wild type and complemented strains. In case of kanamycin as expected the strain complemented *in trans* carrying the plasmid with a kanamycin cassette showed higher resistance to it. In order to check if there are differences in sensitivity to β -lactams, the broth macrodilution method for determination of MIC values was adopted. Nevertheless, in the concentration range tested (0–1,000 μ g/ml) no differences were detected.

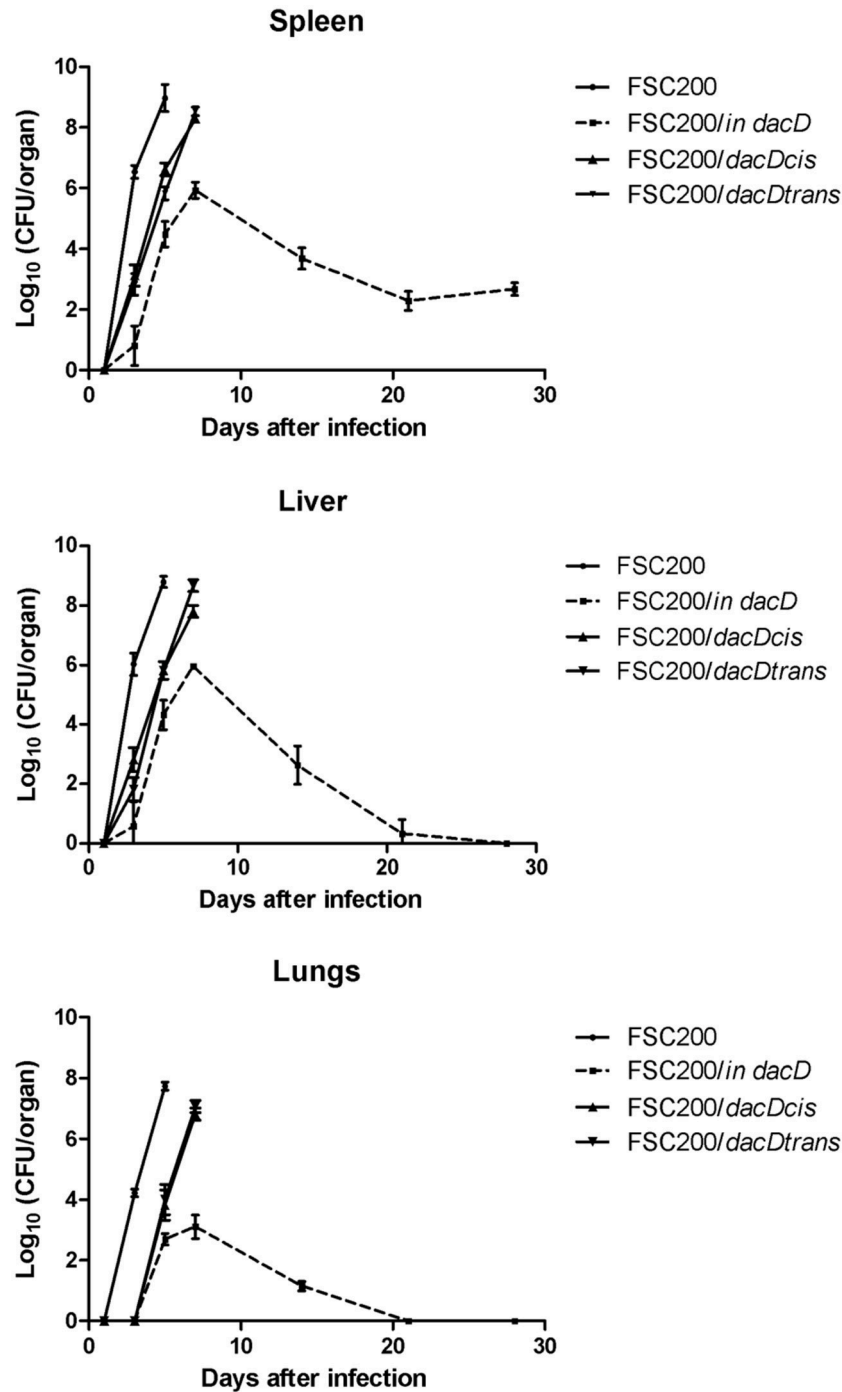


FIGURE 4 | Kinetics of FSC200/*in dacD* replication inside target host organs after s.c. infection. The groups of 3 BALB/c mice were infected s.c. with 10 CFU of the wild-type and mutant strains of *F. tularensis*. At the given time points, the numbers of bacteria in target organs were enumerated by CFU counts.

DISCUSSION

Bacterial cell wall and the peptidoglycan layer are necessary to maintain cell shape and prevent cell lysis. To synthesize or modify the peptidoglycan cell wall bacteria possess a machinery of enzymes. A small group of them forms PBPs. These enzymes

catalyze known biochemical reactions but the physiological role of the LMW PBPs still remains unclear (Ghosh et al., 2008). Here we aimed to address the role of DD-carboxypeptidase DacD, one of the LMW PBPs, in *Francisella*. This protein was identified as one of the proteins with altered abundance in membrane enriched fraction of *dsbA* deletion mutant strain compared to

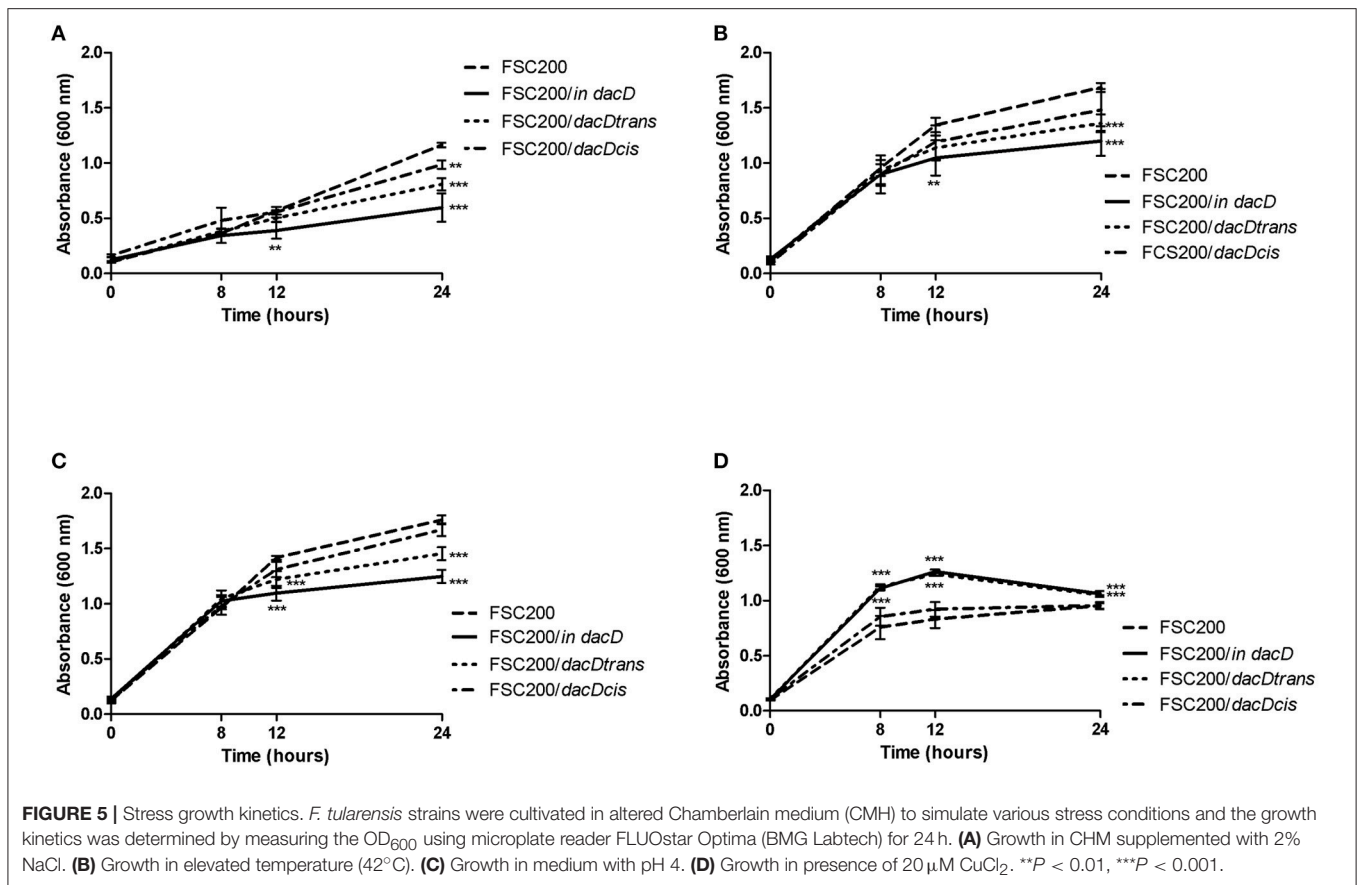


FIGURE 5 | Stress growth kinetics. *F. tularensis* strains were cultivated in altered Chamberlain medium (CMH) to simulate various stress conditions and the growth kinetics was determined by measuring the OD₆₀₀ using microplate reader FLUOstar Optima (BMG Labtech) for 24 h. **(A)** Growth in CHM supplemented with 2% NaCl. **(B)** Growth in elevated temperature (42°C). **(C)** Growth in medium with pH 4. **(D)** Growth in presence of 20 μM CuCl₂. **P < 0.01, ***P < 0.001.

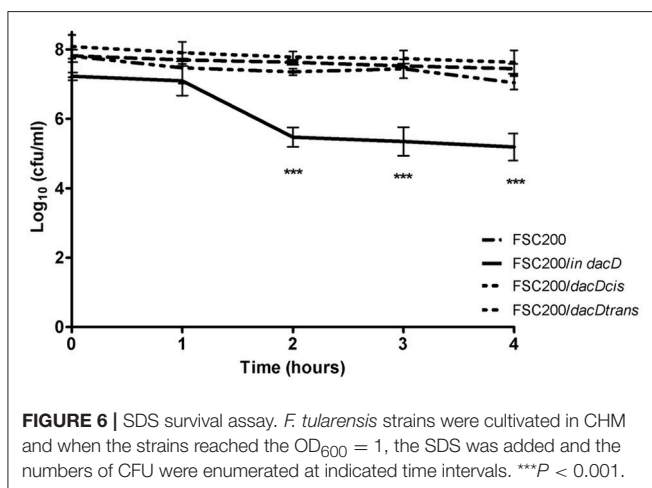


FIGURE 6 | SDS survival assay. *F. tularensis* strains were cultivated in CHM and when the strains reached the OD₆₀₀ = 1, the SDS was added and the numbers of CFU were enumerated at indicated time intervals. ***P < 0.001.

its wild counterpart (Pavkova et al., 2017). DsbA is believed to ensure the correct folding of many proteins, mainly virulence factors through its oxidoreductase and isomerase activities and thus DsbA indirectly promotes host cell binding, invasion, intracellular survival, or other virulence functions (Rowe and Huntley, 2015). As expected, we showed that the inactivation of DacD does not influence the viability of the mutant bacteria confirming the dispensability of this protein not only in *E. coli*, *S. enterica*, and *Streptomyces coelicolor*, but also in *F. tularensis*

(Brambilla et al., 2014; Rioseras et al., 2016). On the other hand we proved that the virulence of *Francisella* is affected by insertion inactivation of *dacD* gene. The mutant strain FSC200/*in dacD* showed defects in intracellular replication which was more pronounced in bone marrow derived macrophages. Previously, it was proposed in two comprehensive studies by Asare (Asare and Abu Kwaiq, 2010; Asare et al., 2010) that a transposon insertion mutant in the DacD homolog gene in *F. novicida* has decreased proliferation within *Drosophila melanogaster*-derived S2 cells. This phenomenon might be connected either with the replication defect or inability to escape the phagosome. TEM analysis revealed that in case of FSC200/*in dacD* mutant the phagosomal escape was not diminished. On the contrary, the mutant bacteria escaped the phagosome faster than wild-type bacteria but failed to replicate with the same kinetics as the wild-type strain. The same effect was observed for example in *F. novicida iglD* mutant (Santic et al., 2007). The authors assumed that the mutant was probably unable to modify the cytosol of macrophages to render it permissive to bacterial replication. Here, we speculate that the decreased resistance to acid environment might be the reason for rapid phagosomal escape of the FSC200/*in dacD* mutant. Noteworthy, there are discrepancies concerning phagosome acidification and some authors claim that *F. tularensis* does not require acidification of phagosome for the escape (Clemens et al., 2009).

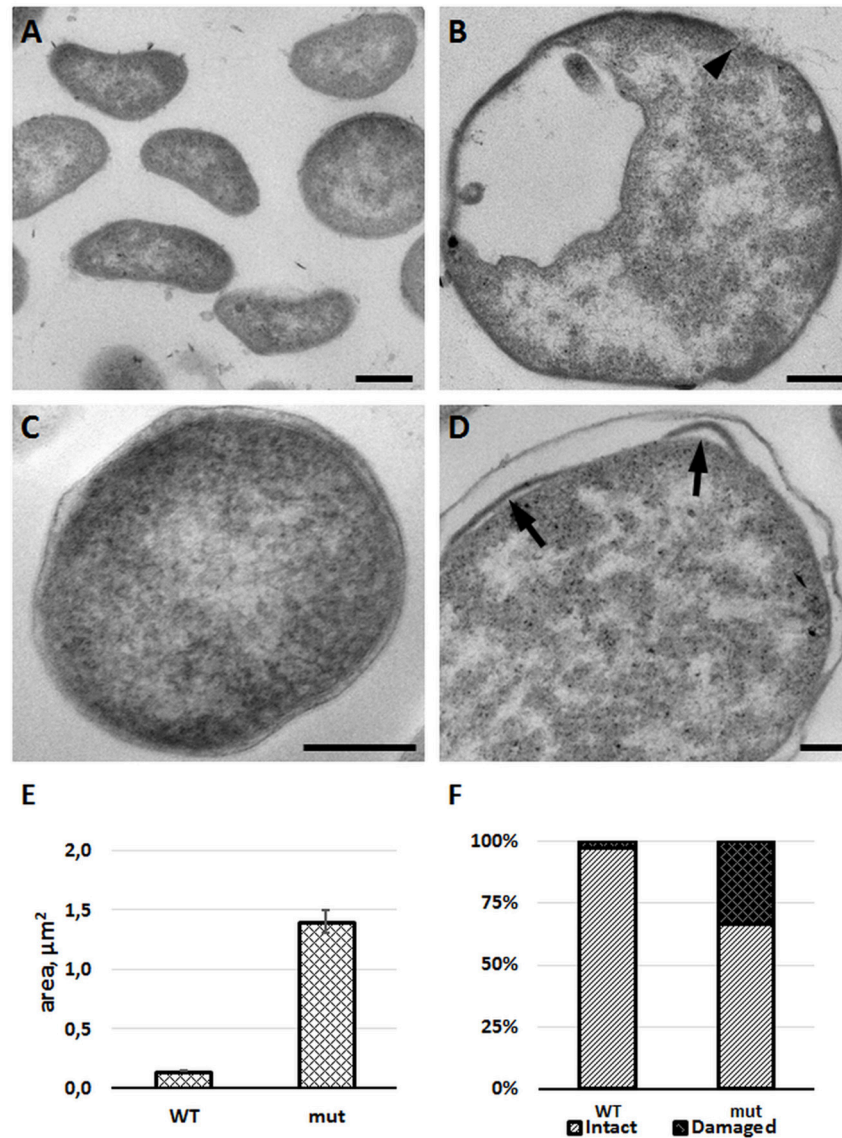


FIGURE 7 | FSC200/*in dacD* mutant bacteria differ in size when compared to the wild-type and exhibit membrane defects. *F. tularensis* FSC200 wild-type strain (**A,C**) and FSC200/*in dacD* mutant strain (**B,D**) were cultivated in CHM and then processed for transmission electron microscopy. Typical electron micrographs of ultrathin sections of bacteria in (**A,B**) at the same magnification illustrate size difference between wild-type and mutant strains. Wild-type cells possess intact membrane (**C**), while mutant cells exhibit discontinuous membrane (**B**, arrowhead) or membrane bulging (**D**, arrows). (**E**) Graph showing mean cell profiles area of wild-type and mutant bacteria on ultrathin sections; (**F**) Quantification of incidence of cell profiles with membrane defects on ultrathin sections. Bars: (**A,B**) 200 nm; (**C,D**) 100 nm.

So far only a few genes have been identified as being specifically required for cytosolic replication by *Francisella* (Brotcke et al., 2006; Fuller et al., 2008; Pechous et al., 2008; Alkhuder et al., 2009; Wehrly et al., 2009; Chong et al., 2012). Interestingly, mutants in all of these genes have also been strongly attenuated *in vivo*. This is not case of the FSC200/*in dacD* mutant that exhibits residual virulence. Nevertheless, the assessment of the viable mutant bacteria in target organs proved their lower numbers and gradual elimination with exception for spleen where survived during whole observed time interval.

The lack of functional DacD is also reflected by increased sensitivity to the bactericidal serum effect. The resistance of *Francisella* to this phenomenon has been attributed to LPS, so far (Sorokin et al., 1996). Thus, the explanation might be (i) that this effect is indirect or (ii) DacD might be involved in LPS biosynthesis, as well, but no evidence collected thus far have been able to support these hypotheses.

Recently it has been described that *E. coli* DacD is important for cell shape maintenance in acidic growth medium (Peters et al., 2016). The data we collected were in agreement as observations documented the mutant strain being unable to

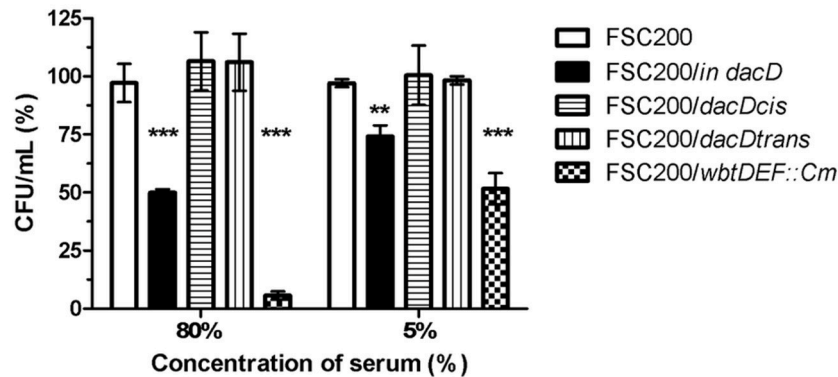


FIGURE 8 | Sensitivity to bactericidal effects of human serum. FSC200, FSC200/*in dacD*, FSC200/*dacDtrans*, FSC200/*dacDcis* and FSC200/*wbtDEF::Cm* strains were incubated with human nonimmune serum and their resistance/susceptibility was determined by CFU counts. FSC200/*wbtDEF::Cm* strain is highly susceptible to the effects of complement and the strain was used as a positive control for serum complement activity. ** $P < 0.01$, *** $P < 0.001$.

resist the acid pH as effectively as the wild-type strain and grew slowly in media with acid pH (pH 4). Similarly, the mutant bacteria had exerted the increased sensitivity to high temperature and high osmolarity. Nevertheless, these growth defects were not fully compensated by complementation *in trans*. Additionally, we demonstrate that the disruption of *dacD* gene results in insufficient resistance to surface active reagent SDS. This susceptibility as indicated by TEM analysis described membrane bulging. The discontinuous membrane may be associated with the defects in bacterial membrane integrity. The TEM quantification revealed the membrane defects may have over a third of the mutant population. The size of mutant bacteria were also altered, bacteria were almost 10 times larger when compared to the wild-type, which could suggest certain disproportion in peptidoglycan and outer membrane synthesis.

Assuming that the phenotype changes in the mutant strain might be a result of the polar effect on the genes flanking *dacD*, we have searched for alterations in their transcription. All monitored genes FTS_1038 through FTS_1032 are transcribed in the mutant, but the transcription level of FTS_1033 and FTS_1032 is lower than that in the wild-type (data not shown). In strain complemented *in cis* the transcription levels were those as for wild-type strain. However, the decreased transcription level of the FTS_1033 and FTS_1032 genes has also been observed in the strain complemented *in trans* with fully restored phenotype only in part of the tested assays. Therefore, we could assume that the changes in intramacrophage replication, attenuated phenotype in mouse model and the membrane defects are results of solely inactivation of *dacD* (complementation *in trans* restores the wild-type phenotype), but differences of mutant strain in resistance to acidic pH, high temperature and high osmolarity might be also the consequence of decreased transcription of downstream genes in the mutant (complementation *in trans* does not fully restore the wild-type phenotype).

As the DacD is enzyme connected with peptidoglycan layer modulation the higher susceptibility to especially β -lactams was considered. But in accordance with Sarkar et al. (2011) the

inactivation of DacD in *Francisella* did not change the β -lactam resistance similarly as was shown for *E. coli*. Furthermore, it is known that *F. tularensis* codes for functional β -lactamase, AmpG and metallo- β -lactamase family protein which hydrolyze β -lactam antibiotics (Biswas et al., 2008).

In conclusion, our results provide the evidence that the DacD protein has a role in *Francisella* pathogenesis. This is in agreement with previously published data where the expression of gene coding for FTT_1029 protein (DacD homolog in *F. tularensis* subsp. *tularensis* SchuS4 strain) was found to be up-regulated during intramacrophage growth (Wehrly et al., 2009) and where the FTT_1029 protein was described as virulence factor candidate (Wallqvist et al., 2015). In several recent publications DacD homologs were also identified as substrates for protein DsbA in *F. tularensis* subsp. *holarctica* LVS, *F. tularensis* subsp. *tularensis* SchuS4 and *F. tularensis* subsp. *holarctica* FSC200 (Ren et al., 2014; Qin et al., 2016; Pavkova et al., 2017; Spidlova et al., 2017) or as interacting partner of another virulence factor, TPR1 protein (FTL_0205) in *F. tularensis* subsp. *holarctica* LVS (Dieppedale et al., 2013).

AUTHOR CONTRIBUTIONS

PeS, MS, and JS conceived and designed the experiments. PeS, PaS, VD, IS, MS, DP, and VP performed the experiments. PeS, PaS, MS, DP, VP, and JS analyzed the data. PeS, PaS, MS, VP, and JS wrote the paper. All authors reviewed and approved the manuscript.

FUNDING

This work was supported by a Ministry of Defence of the Czech Republic—Long-term organization development plan Medical Aspects of Weapons of Mass Destruction of the Faculty of Military Health Sciences, University of Defence and by DTRA project No. D-CZ-10-00001. This work was supported in part by Croatian Science—Foundation under project IP-2016-06-9003. The Microscopy Centre—Electron Microscopy

CE, IMG AS CR is supported by the Czech-BioImaging large RI project (LM2015062 funded by MEYS CR) and by OP RDE (CZ.02.1.01/0.0/0.0/16_013/0001775 Modernization and support of research activities of the national infrastructure for biological and medical imaging Czech-BioImaging).

ACKNOWLEDGMENTS

We thank to Ake Forsberg for generously providing us with pKK289gfp shuttle vector and pDM4 suicide vector and to Karl Klose for providing us with pKEK1140 targeting vector. We would like to thank to Maria Safarova and Lenka Luksikova

for their excellent technical assistance. We thank Martin Capek from the Light Microscopy Core Facility, IMG ASCR, supported by the MEYS CR (LM2015062 Czech-BioImaging, LO1419 Biomodels for Health) for his help with quantification of TEM data. We thank to Sherry Mou for critical reading the manuscript.

SUPPLEMENTARY MATERIAL

The Supplementary Material for this article can be found online at: <https://www.frontiersin.org/articles/10.3389/fcimb.2018.00111/full#supplementary-material>

REFERENCES

- Alkhuder, K., Meibom, K. L., Dubail, I., Dupuis, M., and Charbit, A. (2009). Glutathione provides a source of cysteine essential for intracellular multiplication of *Francisella tularensis*. *PLoS Pathog.* 5:e1000284. doi: 10.1371/journal.ppat.1000284
- Asare, R., and Abu Kwaik, Y. (2010). Molecular complexity orchestrates modulation of phagosome biogenesis and escape to the cytosol of macrophages by *Francisella tularensis*. *Environ. Microbiol.* 12, 2559–2586. doi: 10.1111/j.1462-2920.2010.02229.x
- Asare, R., Akimana, C., Jones, S., and Abu Kwaik, Y. (2010). Molecular bases of proliferation of *Francisella tularensis* in arthropod vectors. *Environ. Microbiol.* 12, 2587–2612. doi: 10.1111/j.1462-2920.2010.02230.x
- Baquero, M. R., Bouzon, M., Quintela, J. C., Ayala, J. A., and Moreno, F. (1996). dacD, an *Escherichia coli* gene encoding a novel penicillin-binding protein (PBP6b) with DD-carboxypeptidase activity. *J. Bacteriol.* 178, 7106–7111. doi: 10.1128/jb.178.24.7106-7111.1996
- Biswas, S., Raoult, D., and Rolain, J.-M. (2008). A bioinformatic approach to understanding antibiotic resistance in intracellular bacteria through whole genome analysis. *Int. J. Antimicrob. Agents* 32, 207–220. doi: 10.1016/j.ijantimicag.2008.03.017
- Bönquist, L., Lindgren, H., Golovliov, I., Guina, T., and Sjöstedt, A. (2008). MglA and Igl proteins contribute to the modulation of *Francisella tularensis* live vaccine strain-containing phagosomes in murine macrophages. *Infect. Immun.* 76, 3502–3510. doi: 10.1128/IAI.00226-08
- Brambilla, L., Morán-Barrio, J., and Viale, A. M. (2014). Low-molecular-mass penicillin binding protein 6b (DacD) is required for efficient GOB-18 metallo- β -lactamase biogenesis in *Salmonella enterica* and *Escherichia coli*. *Antimicrob. Agents Chemother.* 58, 205–211. doi: 10.1128/AAC.01224-13
- Brotcke, A., Weiss, D. S., Kim, C. C., Chain, P., Malfatti, S., Garcia, E., et al. (2006). Identification of MglA-regulated genes reveals novel virulence factors in *Francisella tularensis*. *Infect. Immun.* 74, 6642–6655. doi: 10.1128/IAI.01250-06
- Celli, J., and Zahrt, T. C. (2013). Mechanisms of *Francisella tularensis* intracellular pathogenesis. *Cold Spring Harb. Perspect. Med.* 3:a010314. doi: 10.1101/cshperspect.a010314
- Chamberlain, R. E. (1965). Evaluation of live tularemia vaccine prepared in a chemically defined medium. *Appl. Microbiol.* 13, 232–235.
- Chandler, C. E., and Ernst, R. K. (2017). Bacterial lipids: powerful modifiers of the innate immune response. *F1000Res.* 6:F1000. doi: 10.12688/f1000research.11388.1
- Chong, A., Wehrly, T. D., Child, R., Hansen, B., Hwang, S., Virgin, H. W., et al. (2012). Cytosolic clearance of replication-deficient mutants reveals *Francisella tularensis* interactions with the autophagic pathway. *Autophagy* 8, 1342–1356. doi: 10.4161/auto.20808
- Clemens, D. L., Lee, B.-Y., and Horwitz, M. A. (2009). *Francisella tularensis* Phagosomal escape does not require acidification of the phagosome. *Infect. Immun.* 77, 1757–1773. doi: 10.1128/IAI.01485-08
- Dankova, V., Balonova, L., Link, M., Straskova, A., Sheshko, V., and Stulik, J. (2016). Inactivation of *Francisella tularensis* gene encoding putative ABC transporter has a pleiotropic effect upon production of various glycoconjugates. *J. Proteome Res.* 15, 510–524. doi: 10.1021/acs.jproteome.5b00864
- Denome, S. A., Elf, P. K., Henderson, T. A., Nelson, D. E., and Young, K. D. (1999). *Escherichia coli* mutants lacking all possible combinations of eight penicillin binding proteins: viability, characteristics, and implications for peptidoglycan synthesis. *J. Bacteriol.* 181, 3981–3993.
- Dieppedale, J., Gesbert, G., Ramond, E., Chhuon, C., Dubail, I., Dupuis, M., et al. (2013). Possible links between stress defense and the tricarboxylic acid (TCA) Cycle in *Francisella* Pathogenesis. *Mol. Cell. Proteomics* 12, 2278–2292. doi: 10.1074/mcp.M112.024794
- Egan, A. J. F., Biboy, J., van't Veer, I., Breukink, E., and Vollmer, W. (2015). Activities and regulation of peptidoglycan synthases. *Philos. Trans. R. Soc. Lond. B. Biol. Sci.* 370:20150031. doi: 10.1098/rstb.2015.0031
- Fuller, J. R., Craven, R. R., Hall, J. D., Kijek, T. M., Taft-Benz, S., and Kawula, T. H. (2008). RipA, a cytoplasmic membrane protein conserved among *Francisella* species, is required for intracellular survival. *Infect. Immun.* 76, 4934–4943. doi: 10.1128/IAI.00475-08
- Ghosh, A. S., Chowdhury, C., and Nelson, D. E. (2008). Physiological functions of D-alanine carboxypeptidases in *Escherichia coli*. *Trends Microbiol.* 16, 309–317. doi: 10.1016/j.tim.2008.04.006
- Glauner, B., and Höltje, J. V. (1990). Growth pattern of the murein sacculus of *Escherichia coli*. *J. Biol. Chem.* 265, 18988–18996.
- Henderson, T. A., Dombrosky, P. M., and Young, K. D. (1994). Artifacts processing of penicillin-binding proteins 7 and 1b by the OmpT protease of *Escherichia coli*. *J. Bacteriol.* 176, 256–259. doi: 10.1128/jb.176.1.256-259.1994
- Henderson, T. A., Templin, M., and Young, K. D. (1995). Identification and cloning of the gene encoding penicillin-binding protein 7 of *Escherichia coli*. *J. Bacteriol.* 177, 2074–2079. doi: 10.1128/jb.177.8.2074-2079.1995
- Henderson, T. A., Young, K. D., Denome, S. A., and Elf, P. K. (1997). AmpC and AmpH, proteins related to the class C beta-lactamases, bind penicillin and contribute to the normal morphology of *Escherichia coli*. *J. Bacteriol.* 179, 6112–6121. doi: 10.1128/jb.179.19.6112-6121.1997
- Matsuhashi, M. (1994). “Chapter 4: Utilization of lipid-linked precursors and the formation of peptidoglycan in the process of cell growth and division: membrane enzymes involved in the final steps of peptidoglycan synthesis and the mechanism of their regulation,” in *New Comprehensive Biochemistry*, eds J.-M. Ghuysen and R. Hakenbeck (Amsterdam: Elsevier), 55–71.
- Milton, D. L., O'Toole, R., Horstedt, P., and Wolf-Watz, H. (1996). Flagellin A is essential for the virulence of *Vibrio anguillarum*. *J. Bacteriol.* 178, 1310–1319.
- Nelson, D. E., and Young, K. D. (2001). Contributions of PBP 5 and DD-carboxypeptidase penicillin binding proteins to maintenance of cell shape in *Escherichia coli*. *J. Bacteriol.* 183, 3055–3064. doi: 10.1128/JB.183.10.3055-3064.2001
- Pavkova, I., Kopeckova, M., Klimentova, J., Schmidt, M., Sheshko, V., Sobol, M., et al. (2017). The multiple localized glyceraldehyde-3-phosphate dehydrogenase contributes to the attenuation of the *Francisella tularensis* dsbA deletion mutant. *Front. Cell. Infect. Microbiol.* 7:503. doi: 10.3389/fcimb.2017.00503
- Pechous, R. D., McCarthy, T. R., Mohapatra, N. P., Soni, S., Penoske, R. M., Salzman, N. H., et al. (2008). A *Francisella tularensis* Schu S4 purine auxotroph

- is highly attenuated in mice but offers limited protection against homologous intranasal challenge. *PLoS ONE* 3:e2487. doi: 10.1371/journal.pone.0002487
- Peters, K., Kannan, S., Rao, V. A., Biboy, J., Vollmer, D., Erickson, S. W., et al. (2016). The redundancy of peptidoglycan carboxypeptidases ensures robust cell shape maintenance in *Escherichia coli*. *MBio* 7:e00819-16. doi: 10.1128/mBio.00819-16
- Qin, A., Zhang, Y., Clark, M. E., Moore, E. A., Rabideau, M. M., Moreau, G. B., et al. (2016). Components of the type six secretion system are substrates of *Francisella tularensis* Schu S4 DsbA-like FipB protein. *Virulence* 7, 882–894. doi: 10.1080/21505594.2016.1168550
- Ren, G., Champion, M. M., and Huntley, J. F. (2014). Identification of disulfide bond isomerase substrates reveals bacterial virulence factors. *Mol. Microbiol.* 94, 926–944. doi: 10.1111/mmi.12808
- Rioseco, B., Yagüe, P., López-García, M. T., Gonzalez-Quinonez, N., Binda, E., Marinelli, F., et al. (2016). Characterization of SCO4439, a D-alanyl-D-alanine carboxypeptidase involved in spore cell wall maturation, resistance, and germination in *Streptomyces coelicolor*. *Sci. Rep.* 6:21659. doi: 10.1038/srep21659
- Rodriguez, S. A., Yu, J.-J., Davis, G., Arulanandam, B. P., and Klose, K. E. (2008). Targeted inactivation of *Francisella tularensis* genes by group II introns. *Appl. Environ. Microbiol.* 74, 2619–2626. doi: 10.1128/AEM.02905-07
- Rowe, H. M., and Huntley, J. F. (2015). From the outside-in: the *Francisella tularensis* envelope and virulence. *Front. Cell. Infect. Microbiol.* 5:94. doi: 10.3389/fcimb.2015.00094
- Santic, M., Molmeret, M., Barker, J. R., Klose, K. E., Dekanic, A., Doric, M., et al. (2007). A *Francisella tularensis* pathogenicity island protein essential for bacterial proliferation within the host cell cytosol. *Cell. Microbiol.* 9, 2391–2403. doi: 10.1111/j.1462-5822.2007.00968.x
- Sarkar, S. K., Dutta, M., Chowdhury, C., Kumar, A., and Ghosh, A. S. (2011). PBP5, PBP6 and DacD play different roles in intrinsic β -lactam resistance of *Escherichia coli*. *Microbiol. Read. Engl.* 157, 2702–2707. doi: 10.1099/mic.0.046227-0
- Schiffer, G., and Höltje, J. V. (1999). Cloning and characterization of PBP 1C, a third member of the multimodular class A penicillin-binding proteins of *Escherichia coli*. *J. Biol. Chem.* 274, 32031–32039. doi: 10.1074/jbc.274.45.32031
- Schindelin, J., Arganda-Carreras, I., Frise, E., Kaynig, V., Longair, M., Pietzsch, T., et al. (2012). Fiji: an open-source platform for biological-image analysis. *Nat. Methods* 9, 676–682. doi: 10.1038/nmeth.2019
- Simon, R., Priefer, U., and Pühler, A. (1983). A broad host range mobilization system for *in vivo* genetic engineering: transposon mutagenesis in gram negative bacteria. *Nat. Biotechnol.* 1, 784–791. doi: 10.1038/nbt1183-784
- Sommer, C., Strähle, C., Köthe, U., and Hamprecht, F. A. (2011). “ilastik: interactive learning and segmentation toolkit,” in *Proceedings of Eighth IEEE International Symposium on Biomedical Imaging (ISBI)* (Chigaco, IL), 230–233.
- Sorokin, V. M., Pavlovich, N. V., and Prozorova, L. A. (1996). *Francisella tularensis* resistance to bactericidal action of normal human serum. *FEMS Immunol. Med. Microbiol.* 13, 249–252. doi: 10.1111/j.1574-695X.1996.tb00246.x
- Spidlova, P., Senitkova, I., Link, M., and Stulik, J. (2017). Identification of two substrates of FTS₁₀₆₇ protein - An essential virulence factor of *Francisella tularensis*. *Acta Microbiol. Immunol. Hung.* 64, 37–49. doi: 10.1556/030.63.2016.013
- Spratt, B. G. (1975). Distinct penicillin binding proteins involved in the division, elongation, and shape of *Escherichia coli* K12. *Proc. Natl. Acad. Sci. U.S.A.* 72, 2999–3003. doi: 10.1073/pnas.72.8.2999
- Szybalski, W., and Bryson, V. (1952). Genetic studies on microbial cross resistance to toxic agents. I. Cross resistance of *Escherichia coli* to fifteen antibiotics. *J. Bacteriol.* 64,489–499.
- Vollmer, W., Blanot, D., and de Pedro, M. A. (2008a). Peptidoglycan structure and architecture. *FEMS Microbiol. Rev.* 32, 149–167. doi: 10.1111/j.1574-6976.2007.00094.x
- Vollmer, W., Joris, B., Charlier, P., and Foster, S. (2008b). Bacterial peptidoglycan (murein) hydrolases. *FEMS Microbiol. Rev.* 32, 259–286. doi: 10.1111/j.1574-6976.2007.00099.x
- Wallqvist, A., Memišević, V., Zavaljevski, N., Pieper, R., Rajagopala, S. V., Kwon, K., et al. (2015). Using host-pathogen protein interactions to identify and characterize *Francisella tularensis* virulence factors. *BMC Genomics* 16:1106. doi: 10.1186/s12864-015-2351-1
- Wehrly, T. D., Chong, A., Virtaneva, K., Sturdevant, D. E., Child, R., Edwards, J. A., et al. (2009). Intracellular biology and virulence determinants of *Francisella tularensis* revealed by transcriptional profiling inside macrophages. *Cell. Microbiol.* 11, 1128–1150. doi: 10.1111/j.1462-5822.2009.01316.x

Conflict of Interest Statement: The authors declare that the research was conducted in the absence of any commercial or financial relationships that could be construed as a potential conflict of interest.

The reviewer MM declared his involvement as a co-editor in the Research Topic with one of the authors MS, and confirmed the absence of any other collaboration.

Copyright © 2018 Spidlova, Stojkova, Dankova, Senitkova, Santic, Pinkas, Philimonenko and Stulik. This is an open-access article distributed under the terms of the Creative Commons Attribution License (CC BY). The use, distribution or reproduction in other forums is permitted, provided the original author(s) and the copyright owner are credited and that the original publication in this journal is cited, in accordance with accepted academic practice. No use, distribution or reproduction is permitted which does not comply with these terms.



The *Francisella* Type VI Secretion System

Daniel L. Clemens*, Bai-Yu Lee and Marcus A. Horwitz*

Division of Infectious Diseases, Department of Medicine, University of California, Los Angeles, Los Angeles, CA, United States

Francisella tularensis subsp. *tularensis* is an intracellular bacterial pathogen and the causative agent of the life-threatening zoonotic disease tularemia. The *Francisella* Pathogenicity Island encodes a large secretion apparatus, known as a Type VI Secretion System (T6SS), which is essential for *Francisella* to escape from its phagosome and multiply within host macrophages and to cause disease in animals. The T6SS, found in one-quarter of Gram-negative bacteria including many highly pathogenic ones, is a recently discovered secretion system that is not yet fully understood. Nevertheless, there have been remarkable advances in our understanding of the structure, composition, and function of T6SSs of several bacteria in the past few years. The system operates like an inside-out headless contractile phage that is anchored to the bacterial membrane via a baseplate and membrane complex. The system injects effector molecules across the inner and outer bacterial membrane and into host prokaryotic or eukaryotic targets to kill, intoxicate, or in the case of *Francisella*, hijack the target cell. Recent advances include an atomic model of the contractile sheath, insights into the mechanics of sheath contraction, the composition of the baseplate and membrane complex, the process of assembly of the apparatus, and identification of numerous effector molecules and activities. While *Francisella* T6SS appears to be an outlier among T6SSs, with limited or no sequence homology with other systems, its structure and organization are strikingly similar to other systems. Nevertheless, we have only scratched the surface in uncovering the mysteries of the *Francisella* T6SS, and there are numerous questions that remain to be answered.

Keywords: tularemia, *Francisella tularensis*, *Francisella* pathogenicity island, CryoElectron microscopy, atomic model, review

OPEN ACCESS

Edited by:

Thomas Henry,
INSERM Centre International de
Recherche en Infectiologie, France

Reviewed by:

Eric Cascales,
Aix-Marseille Université, France
Thibault Géry Sana,
Stanford University, United States

*Correspondence:

Daniel L. Clemens
dclemens@mednet.ucla.edu
Marcus A. Horwitz
mhorwitz@mednet.ucla.edu

Received: 02 January 2018

Accepted: 03 April 2018

Published: 23 April 2018

Citation:

Clemens DL, Lee B-Y and Horwitz MA
(2018) The *Francisella* Type VI
Secretion System.
Front. Cell. Infect. Microbiol. 8:121.
doi: 10.3389/fcimb.2018.00121

INTRODUCTION

Francisella tularensis subsp. *tularensis* is a Gram-negative bacterium that causes a serious and potentially fatal zoonotic infection, tularemia, in animals and humans (Ellis et al., 2002). *F. tularensis* has a relatively broad host-range and is capable of multiplying intracellularly in insects as well as in a wide range of mammals, including rabbits, rodents, beavers, and man. For mammals, *F. tularensis* is the most infectious bacterial pathogen known; the LD₅₀ in mice for a subcutaneous inoculation of the virulent SCHU S4 strain is 1–4 organisms (Bell et al., 1955), and in humans, as few as 10 organisms delivered subcutaneously or 25 organisms delivered by inhalation can lead to

life threatening infection (Saslaw et al., 1961a,b). Because of its high infectivity and lethality, the ease with which it can be cultured and dispersed, and the history of its use as a bioweapon, it is considered a potential agent of bioterrorism and is classified as a Tier 1 Select Agent. This has led to renewed interest and investigation of its cell biology and the pathogenic mechanisms underlying its remarkable infectivity.

INTRACELLULAR LIFE CYCLE OF *F. TULARENSIS*

Although *F. tularensis* infection has been demonstrated in many host cells, including alveolar epithelial cells, neutrophils, and hepatocytes, macrophages are infected early in infection and are important both as a major site of bacterial replication and in host defense against infection. We have shown that the bacteria are internalized by macrophages via a novel mechanism—looping phagocytosis (Clemens et al., 2005; Clemens and Horwitz, 2007; **Figure 1**), and that the O-antigen polysaccharide plays a role in the morphology of this process (Clemens et al., 2012). Following uptake, *F. tularensis* resides in a membrane-bound vacuole that acquires early endosomal markers, but resists maturation, as evidenced by its failure to fuse with secondary lysosomes and its only limited acquisition of cathepsin D and lysosome-associated membrane glycoproteins. Ultrastructurally, the *F. tularensis* phagosome acquires a unique, densely staining fibrillar coat that forms blebs and vesicles and subsequently fragments, with escape of the bacterium into the cytosol, where it replicates freely (Golovliov et al., 2003; Clemens et al., 2004; Clemens and Horwitz, 2007; Chong and Celli, 2010; **Figure 1**). *F. tularensis* subsp. *tularensis* (*F. tularensis*) is genetically closely related to the attenuated vaccine strain *F. tularensis* subsp. *holarctica* Live Vaccine Strain (LVS) and to *F. tularensis* subsp. *novicida* (also classified and hereafter referred to as *F. novicida*; Johansson et al., 2010) and it shares with them the same intracellular life-style. After extensive replication within the host cell, the bacteria induce apoptosis or pyroptosis, culminating in release of bacteria that can initiate another round of infection in host cells (Lai et al., 2001; Mariathasan et al., 2005) or spread from cell to cell by way of trogocytosis (Bourdonnay and Henry, 2016; Steele et al., 2016).

The host cell does have innate defenses that come into play. Macrophage guanylate binding proteins act downstream of Type I interferon receptors to bind to *F. tularensis*, facilitating lysis of the bacteria and release of bacterial DNA, which in turn activates the AIM2 inflammasome and Caspase 1, IL-1 β , and IL-18, leading to macrophage cell death and helping to control the infection (Henry et al., 2007; Weiss et al., 2007b; Man et al., 2015; Meunier et al., 2015).

Checroun et al. have shown, in mouse bone marrow-derived macrophages, that at late times after infection (> 20 h) a large percentage of *F. tularensis* LVS enter double-membraned, LC3-positive autophagic vacuoles (termed *Francisella*-containing vacuoles, FCVs) that are acidified, stain positively for LAMP-1 and cathepsin D and fuse with secondary lysosomes (Checroun et al., 2006). It is intriguing that the *F. tularensis* within the FCVs do not escape from these compartments via their Type

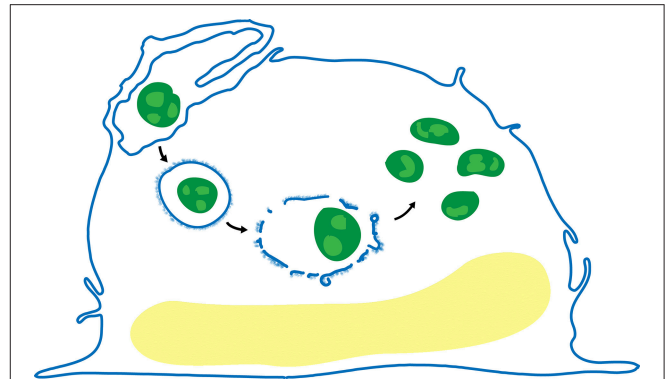


FIGURE 1 | Life cycle of *F. tularensis* in human macrophages. After uptake by looping phagocytosis (upper left), the bacteria (green) reside in a membrane bound vacuole that often acquires a densely staining fibrillar coat (post first arrow), which subsequently forms blebs and vesicles (post second arrow), and disintegrates. The bacteria escape the phagosome and replicate freely in the cytosol (post third arrow).

VI Secretion System (T6SS) apparatus as they do from their phagosome post ingestion. These autophagic FCVs may reflect an aspect of host control of the intracellular infection, rather than a feature of the *F. tularensis* intracellular life cycle that benefits the bacterium, since induction of autophagy promotes eradication of infection (Chiu et al., 2009).

THE FRANCISELLA PATHOGENICITY ISLAND

Gray et al. (2002) used transposon mutagenesis to identify five genetic loci in *F. novicida* whose disruption led to impaired intracellular growth in macrophages: *iglA*, *iglB*, *iglC*, *iglD*, and *clpB*. While the induction of IglC in the intramacrophage environment was appreciated from work by Golovliov et al. (1997) the relation of these genes to the gene clusters of other bacteria and their role in a secretion system was not recognized at this time. The existence of the Francisella Pathogenicity Island (FPI) was first reported by Nano et al. (2004), who described a large cluster of genes on an island of the *F. novicida* chromosome with a relatively low GC content that is required for intracellular growth in macrophages and for virulence in mice. This ~30-kb island encodes 18 genes, 14 of which have been shown to be essential for growth in macrophages; all, except for *pdpE* and *anmK*, are required for full virulence in mice (**Figure 2**; Bröms et al., 2010).

Because some proteins encoded on the FPI (such as VgrG and DotU) show clear homology to the core components of T6SSs of other Gram-negative bacteria, it was proposed that the FPI encoded a T6SS. Bioinformatic analysis of IglA and IglB suggested that they could be components of a T6SS apparatus, and de Bruin et al. showed that IglA was expressed as a soluble cytoplasmic protein under control of the MglA and MglB global regulators, with expression markedly increasing after macrophage infection, and that IglA expression was essential

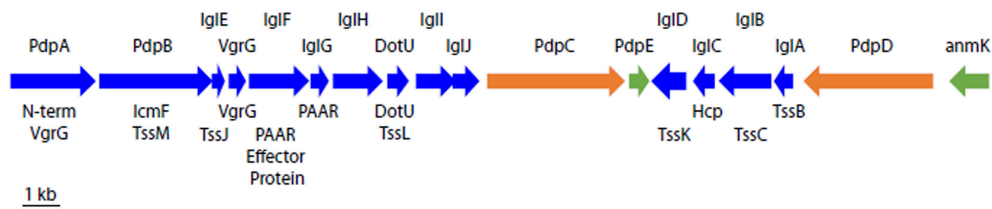


FIGURE 2 | Schematic organization of the T6SS gene cluster on the FPI. Names of *F. novicida* gene products are shown above and names of the corresponding canonical T6SS gene products (where known) are shown below. Gene products shown in blue are required for growth in macrophages and for virulence in animals; those in orange are required for full virulence in animals (Weiss et al., 2007a) but not for growth in macrophages; and those in green are not required for growth in macrophages or for virulence in animals (Bröms et al., 2010).

to intramacrophage growth of *F. novicida*. (de Bruin et al., 2007). While most proteins of the FPI have little or no sequence homology to T6SS proteins of other bacteria, for those whose structure has been determined to date, the proteins have shown striking structural homology to other T6SSs. For example, we have recently shown by CryoEM that the FPI proteins IgIA and IgIB assemble into long cylinders with strong structural homology to the sheaths of contractile phage tails (myophages), R-type pyocins, and the contractile sheaths of other bacterial T6SSs, despite the absence of sequence homology (Clemens et al., 2015).

There are two copies of the FPI present in *F. tularensis* and *F. tularensis* subsp. *holarctica* LVS, while *F. novicida* has a single copy (Bröms et al., 2010); additionally, *F. novicida* possesses a related genomic island named *Francisella novicida* island (Rigard et al., 2016). Because *F. novicida* has only a single copy of the FPI and is of low virulence for humans, it has served as a more tractable subspecies for study and it is widely used for investigations of the FPI.

TYPE VI SECRETION SYSTEMS

Type VI Secretion Systems (T6SSs) are recently identified large nanomachines encoded on gene clusters that function like an inside-out contractile phage tail to inject effector molecules across the inner and outer bacterial membrane and into host prokaryotic or eukaryotic targets in order to kill, intoxicate, or in the case of *Francisella*, hijack the target cell (Bingle et al., 2008; Cianfanelli et al., 2016b). T6SSs are very widespread among bacteria, being found in one quarter of sequenced Gram-negative bacteria, including many that are important plant, animal, and human pathogens (Bingle et al., 2008; Boyer et al., 2009). T6SSs resemble, and are thought to be evolutionarily related to, other Contractile Injection Systems (CISs): myophages (Leiman and Shneider, 2012), R-type pyocins (Ge et al., 2015), anti-feeding phage (Afp) (Heymann et al., 2013), and metamorphosis associated structures (MACs) (Shikuma et al., 2014). However, these contractile injection systems have undergone extensive divergence so that sequence homologies are often limited, and it is unclear which system evolved first. The T6SS differs from other CISs in that it is the only one that contracts inside the organism (Böck et al., 2017). The

T6SS remains within the intact bacterium when the apparatus contracts and injects its effectors across the bacterial inner and outer membranes and into the target cell. All other CISs, such as myophages, Afps, and MACs, are designated “eCISs” to indicate that they contract in the extracellular space following their release from the bacterium in which they were assembled (Böck et al., 2017).

CISs have in common several key components: a long contractile sheath, a tube that fits within the sheath tipped with a central spike/effector protein complex that is propelled by contraction of the sheath, and a baseplate complex (Leiman and Shneider, 2012). In addition to these components, T6SSs also include a membrane complex that anchors the baseplate to the membrane and allows passage of the central spike/effector complex and tube without compromise to the integrity of the host bacterial inner and outer membranes (Ho et al., 2014).

Canonical T6SSs have in common 13 conserved core subunits (designated “Type six secretion subunits, TssA–TssM, Table 1) encoded on gene clusters that assemble to form the apparatus. The discovery and general characteristics of the T6SS have been the subject of several excellent reviews (Ho et al., 2014; Basler, 2015; Cianfanelli et al., 2016b; Hood et al., 2017). The first clue to the existence of this new secretion system was the observation that Haemolysis coregulated protein (Hcp), which lacks a signal sequence, was secreted by *Vibrio cholerae* (Williams et al., 1996). In 2003, Bladergroen et al. (2003) identified a gene cluster essential for secretion in *Rhizobium leguminosarum* that encoded what subsequently became known as a T6SS. They showed that this gene cluster influenced the host range of the bacterium and hypothesized that it was involved in protein secretion. Similar gene clusters were identified in many other bacteria, including *V. cholerae*, and observed to include genes homologous to the Type 4 secretion membrane protein gene, *icmF* (Das and Chaudhuri, 2003). Evidence for the role of a similar gene cluster in virulence of the fish pathogen *Edwardsiella tarda* came from the work of Rao et al., who used transposon mutagenesis and proteomic analysis to identify five proteins important to *E. tarda* pathogenesis (Rao et al., 2004). While three of the five proteins were homologous with T3SS effector proteins, Rao et al. recognized that the other two, named EvpA and EvpC, were encoded with in a cluster of 8 genes (*evpA-H*) similar to those described for *R. leguminosarum*, *V. cholerae*, and other bacteria. Rao et al. noted that EvpA and EvpB show 25 and 30%

TABLE 1 | Essential T6SS proteins and their orthologues in *Francisella* and T4 Phage.

T6SS	Fn T6SS	T4 phage	Function
TssA	?	gp3/gp15	Assembly Chaperone and Tube/Sheath Cap
TssBC	IglAB	gp18	Sheath
Hcp	IglC	gp19	Tube
(Hcp)	(IglC)	gp48	Tube/Baseplate
(Hcp)	(IglC)	gp54	Tube/Baseplate
VgrG	VgrG and PdpA	gp5 and gp27	Spike complex
PAAR Protein	IglG (?)	gp5.4	Spike tip
PAAR Associated Effector Protein	IglF (?)	gp5.4	Effector
TssF	?	gp6	Baseplate
TssG	?	gp7/gp53	Baseplate
TssE	?	gp25	Baseplate
TssK	IglD	gp10* (Siphophage RBP)	Baseplate
TssJ	IglE	None	Membrane complex
TssL/DotU	DotU	None	Membrane complex
TssM/IcmF	PdpB	None	Membrane complex
ClpV	ClpB	None	Sheath disassembly

*TssK has no structural homolog in T4 phage baseplate, but TssK appears to occupy the same position in the baseplate as domain IV of gp10 (Nazarov et al., 2018). TssK has structural homology with Siphophage Receptor Binding Protein (RBP, Nguyen et al., 2017).

identity to *Francisella* IglA and IglB, respectively, that EvpC is homologous with Hcp, and that secretion of EvpC is blocked by disruption of either EvpA or EvpB, and they hypothesized that secretion of EvpC was not via the T3SS. Pukatzki et al. showed that the gene cluster in *V. cholerae* was essential for secretion of Hcp and VgrG (which also lacks a signal sequence) into the culture supernatant fluid and for the capacity of *V. cholerae* to kill *Dictyostelium discoideum* and J774 macrophages in a contact-dependent fashion (Pukatzki et al., 2006). Because addition of concentrated *V. cholerae* culture supernatants containing Hcp and VgrG proteins caused no cytotoxicity to *D. discoideum* amoebae, Pukatzki et al. proposed that the system was triggered by bacterium-eukaryotic cell contact and functioned to inject the secreted effector proteins into the eukaryotic cell cytosol; they named the system the Type 6 Secretion System (Pukatzki et al., 2006). A structural counterpart to these gene clusters was discovered using fluorescence microscopy and electron cryotomography (ECT) in intact *V. cholerae*, with visualization of the structure in both its extended and contracted states (Basler et al., 2012).

ROLE OF THE FRANCISELLA T6SS IN PHAGOSOMAL ESCAPE AND INTRACELLULAR REPLICATION

T6SSs play different roles in the biology of their host organisms depending upon the life style of that organism. In the

case of extracellular bacterial pathogens, such as *V. cholerae*, *Pseudomonas aeruginosa*, and enteropathogenic *E. coli*, the T6SSs primarily function in interbacterial warfare. For example, Basler et al. have shown that, in the case of *P. aeruginosa*, T6SS activity first occurring in prey species *V. cholerae* and *Acinetobacter baylyi* triggers reciprocal *P. aeruginosa* T6SS formation at the point of contact with the prey's T6SS with the result that the prey bacterium is killed in a "tit-for-tat" fashion (Basler et al., 2013). Some bacteria have several T6SSs, which may be regulated differently and secrete effectors with diverse functions and distinct target specificities (Bingle et al., 2008; Schwarz et al., 2010; Journet and Cascales, 2016). For example, *P. aeruginosa* has three T6SSs (H1-, H2-, and H3-T6SS). While H1-T6SS secretes toxins to counter other Gram-negative bacteria with T6SSs, H2-, and H3-T6SSs act on both prokaryotic and eukaryotic cells (Sana et al., 2016). In the case of the intracellular bacterial pathogen *F. tularensis* and other *Francisella*, the T6SS is required for phagosomal escape, intracytoplasmic replication in host cells, and virulence in animals (Lindgren et al., 2004; Nano et al., 2004; de Bruin et al., 2007; Bröms et al., 2010). Our structure-based mutagenesis studies of the *F. novicida* T6SS have demonstrated that mutations in the sheath proteins IglA and IglB that interfere with contraction of the sheath block T6SS secretion, phagosomal escape, and replication in human macrophage-like cells (Clemens et al., 2015). The T6SS of *Candidatus Amoebophilus asiaticus*, an obligate intracellular bacterial symbiont of amoebae, may serve a similar function in promoting phagosome escape for this organism (Böck et al., 2017).

All FPI genes that are required for phagosome escape and intracellular replication in macrophages are also required for full virulence in animals (Figure 2). However, while *pdpC* (Long et al., 2013) and *pdpD* (Ludu et al., 2008; Brodmann et al., 2017) are essential for full virulence in animals, their absence results in relatively minor defects in growth in macrophages. Virulence in animals may be highly sensitive to defects in intramacrophage growth, or perhaps PdpC and PdpD impact the innate immune response, which plays a greater role *in vivo* in animals than *in vitro* in macrophage cell culture. Interestingly, PdpD is present in *F. novicida* and the highly virulent Type A *F. tularensis*, but not in the less lethal Type B *F. tularensis* (Ludu et al., 2008).

T6SS CLASSIFICATION

T6SSs have been classified into three categories (T6SSⁱ⁻ⁱⁱⁱ, Table 2 and Figure 3) based on their genetic make-up, with T6SSⁱ encompassing canonical T6SSs of *Vibrio*, *Pseudomonas*, and Enteropathogenic *E. coli*; T6SSⁱⁱ representing *Francisella*; and T6SSⁱⁱⁱ comprised of *B. fragilis* and *Flavobacterium johnsoniae* (Russell et al., 2014b). Figure 3 shows the genetic relatedness of the large sheath unit (IglB, VipB, TssC) in bacteria with T6SS and, for comparison, the sheath subunits of Afp and R-pyocin. Similar maps have been made using the large sheath subunit (Rao et al., 2004), small sheath subunit (IglA, VipA, TssA) (Schwarz et al.,

TABLE 2 | Classification of T6SSs. T6SSⁱ⁻ⁱⁱ and T6SS^{iii-iv} belong to Gram-negative bacteria of taxonomically distinct subgroups.

Organism	Phylum	Class	T6SS Category
<i>Vibrio cholerae</i>	Gammaproteobacteria	Gammaproteobacteria	T6SS ⁱ
<i>Pseudomonas aeruginosa</i>	Gammaproteobacteria	Gammaproteobacteria	T6SS ⁱ
<i>Francisella tularensis</i>	Gammaproteobacteria	Gammaproteobacteria	T6SS ⁱⁱ
<i>Bacteroides fragilis</i>	Bacteroidetes	Bacteroidetes	T6SS ⁱⁱⁱ
<i>Flavobacterium johnsoniae</i>	Bacteroidetes	Flavobacteriia	T6SS ⁱⁱⁱ
<i>Ca. Amoebophilus asiaticus</i>	Bacteroidetes	Cytophagis	T6SS ^{iv}

2010), and the putative baseplate protein TssF (Journet and Cascales, 2016). While it is clear that this classification system reflects genetic and evolutionary relatedness, it is unclear whether these 3 categories correlate with structural or functional differences in the systems. For example, while the *F. tularensis* T6SS has been classified genetically as an outlier among T6SSs, every component of its apparatus whose structure has been determined thus far has shown striking structural homology to the structures of the canonical T6SS. On the other hand, a new T6SS^{iv} category (Table 2 and Figure 3) has recently been described in *Ca. A. asiaticus* (Böck et al., 2017) which is both genetically and structurally closer to eCIS, although it functions intracellularly like T6SSⁱ⁻ⁱⁱⁱ.

IDENTIFICATION OF ENVIRONMENTAL FACTORS THAT INDUCE ASSEMBLY OF THE *FRANCISELLA* T6SS

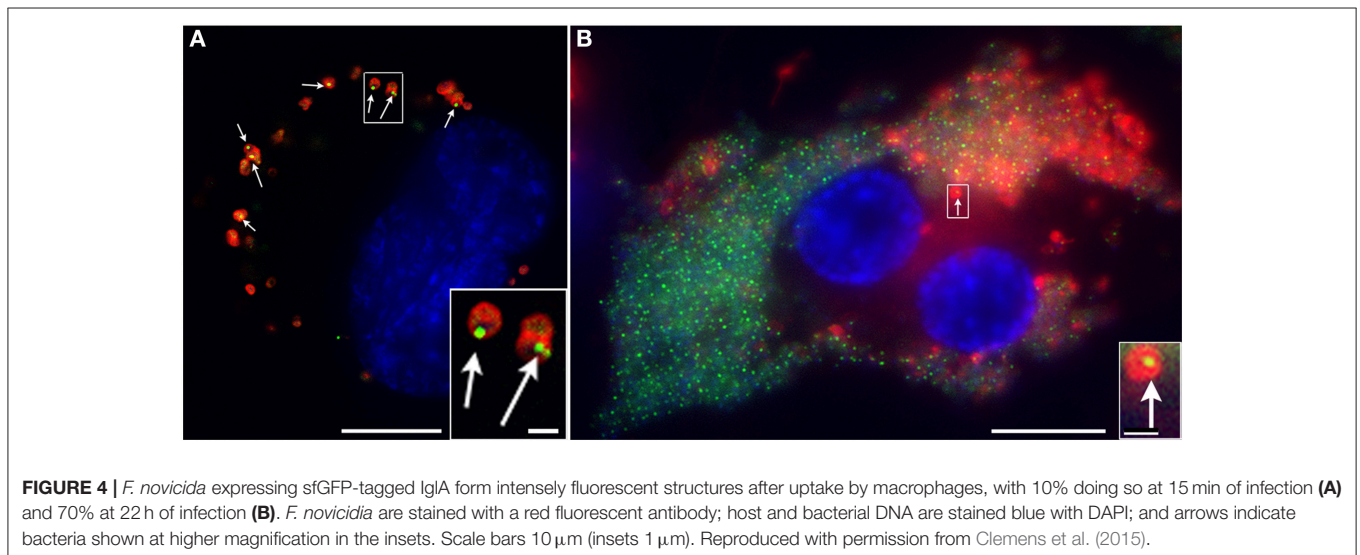
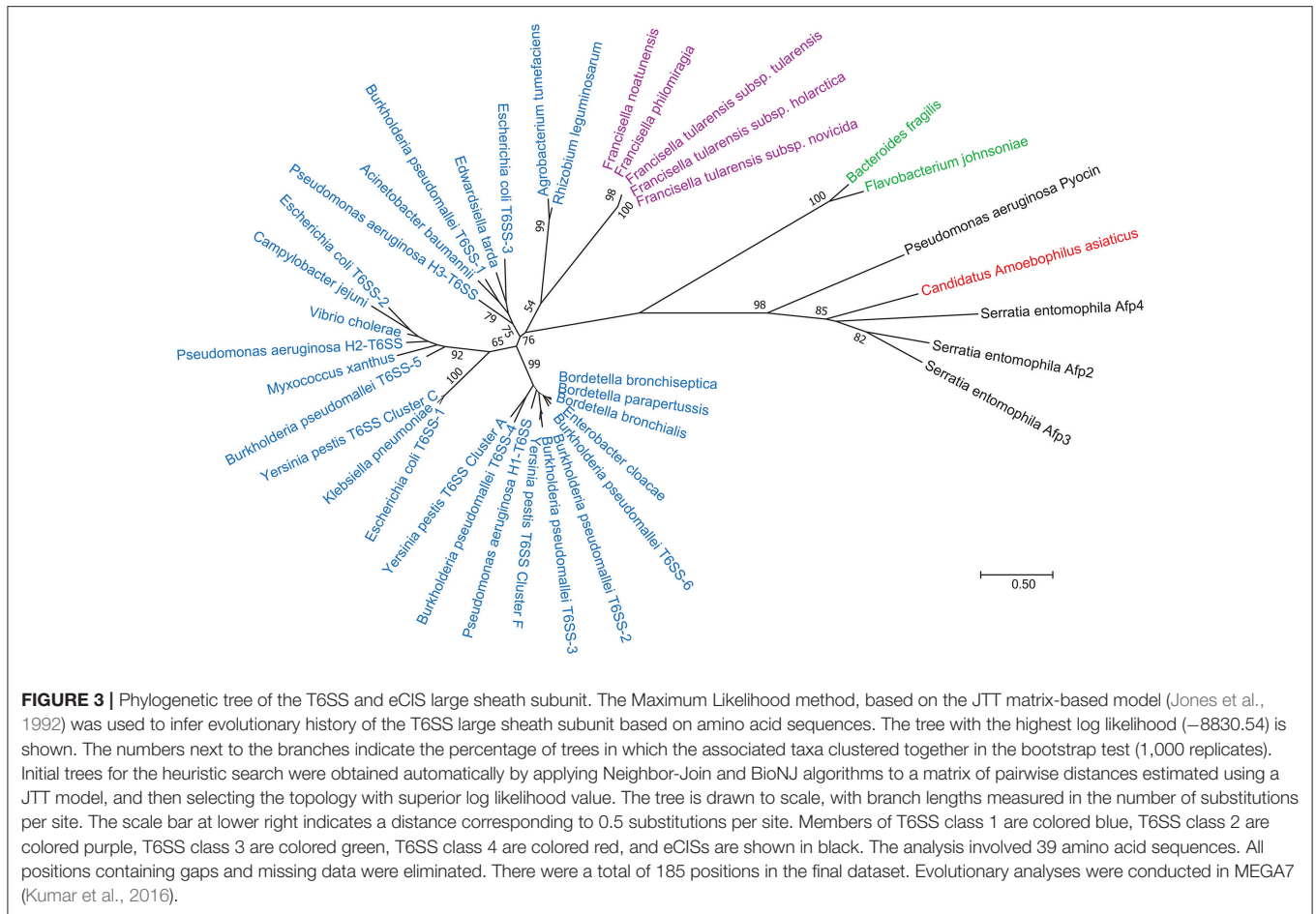
Golovliov et al. identified IglC as an *F. tularensis* protein that was induced by bacteria within macrophages or under oxidative stress (Golovliov et al., 1997); subsequently IglC was shown to be required for intracellular growth in macrophages (Lai et al., 2004) before its role in the T6SS was known. Other studies reported that FPI genes *iglA*, *iglB*, *iglC*, *pdpA*, and *pdpD* [and also *clpB*, a T6SS-related gene outside the FPI (Brodmann et al., 2017)] show increased expression in the intramacrophage environment (Wehrly et al., 2009). Activation of the stringent response by growth of *F. tularensis* SCHU S4 in culture medium with serine hydroxamate was recently shown to increase the expression of multiple FPI genes, including both copies of *iglA*, *iglB*, *iglC*, *iglD*, *pdpA*, and *pdpD* (Murch et al., 2017). Iron restriction, a condition associated with the intracellular environment, has been shown to increase expression of several FPI proteins, including IglC, IglD, IglA, and PdpB, and putative Fur boxes have been identified in front of *pdpB* and *iglC* (Deng et al., 2006). While oxidative stress, iron deprivation, and stringent response increase expression of FPI proteins, it has not been reported whether these maneuvers lead to increased T6SS assembly or secretion.

Whereas many T6SSs, such as those of *Vibrio*, the *Pseudomonas* H2-T6SS (Haapalainen et al., 2012; Decoin et al., 2014) and *Burkholderia*, show a basal level of secretion in broth culture, we have observed that *F. tularensis* LVS

and *F. novicida* do not (Clemens et al., 2015). This initially hampered structural and functional studies of the *Francisella* T6SS and the identification of additional proteins secreted by the system.

Preparation of *F. novicida* expressing IglA-sfGFP enabled us to search for *in vitro* conditions that induced formation of fluorescent structures within the bacteria. We found that the bacteria were not fluorescent when grown in standard broth culture, but that they rapidly acquired fluorescent foci after uptake by macrophages (Clemens et al., 2015; Figure 4). In addition, we found that bacteria placed on a microscope slide beneath a glass coverslip initially lacked fluorescent foci, but with time developed them (Figure 5). This was not due to evaporation and concentration of the culture medium, as bacteria continued to form fluorescent foci even when the coverslip was sealed with silicone. The nature of the coverslip stimulus sensed by *F. novicida* is unclear and may reflect a combination of factors, such as mechanical pressure from the coverslip and a decrease in oxygen tension. The use of gas permeable plastic coverslips instead of glass coverslips delays, but does not prevent, the formation of the fluorescent foci. We hypothesized that the induction of the T6SS within macrophages reflects a response by bacteria to conditions in the host cytoplasm that differ from those in standard broth culture medium. This prompted us to examine whether increasing the concentration of KCl would induce formation of fluorescent foci or T6SS secretion. We found that fluorescent foci did form in TSBC broth culture with 2.5 or 5% KCl (Figure 5), but not at lower concentrations, and that the formation of the fluorescent foci was accompanied by secretion of VgrG and IglC (Clemens et al., 2015).

While we did not observe in *F. novicida* the dynamic formation, contraction and disassembly of the T6SS described for *E. coli* or *V. cholerae*, this has recently been observed (Brodmann et al., 2017). Using improved instrumentation and image collection, Brodmann et al. (2017) have shown that *F. novicida* expressing IglA-sfGFP form dynamic sheaths that assemble, contract, and disassemble in a fashion similar to what has been shown for *V. cholerae* and *E. coli* (Figure 6). Dynamic assembly was observed both for free bacteria resuspended in phosphate buffered saline (Figure 6A) and for bacteria within mouse macrophages (Figure 6C), and sites of sheath assembly, contraction, and disassembly colocalized with ClpB-fluorescence (Figure 6C), which is thought to mediate sheath disassembly in *Francisella* (Brodmann et al., 2017). While the T6SSs of *Vibrio* and *Pseudomonas* typically assemble all over the cells, the T6SS of *F. novicida* forms exclusively at the poles, a site that may be better suited to puncturing phagosomal membranes (Brodmann et al., 2017), whereas locations all over the cell are required for optimal interbacterial targeting as seen in videos of *Vibrio*, *Pseudomonas*, and *E. coli* (Basler and Mekalanos, 2012; Basler et al., 2013; Brunet et al., 2013). As there is no tape measure protein in T6SS classes 1–3, the upper limit to the length of the sheath is the width of the bacterium. Therefore, sheaths that form at the poles can extend the length of the bacterium (~1 micron for *F. tularensis*), whereas



sheaths that form on the sides of the bacteria would be limited by the width of the bacteria (~ 0.5 micron). In the case of *V. cholerae*, the T6SS sheath contracts to 50% of its pre-contraction length (Wang et al., 2017); if the same holds true for *F. tularensis*,

then a 0.8 micron sheath could penetrate 0.4 microns into the area of contact with the phagosomal membrane, whereas a sheath that formed at the side would have a shorter penetration distance.

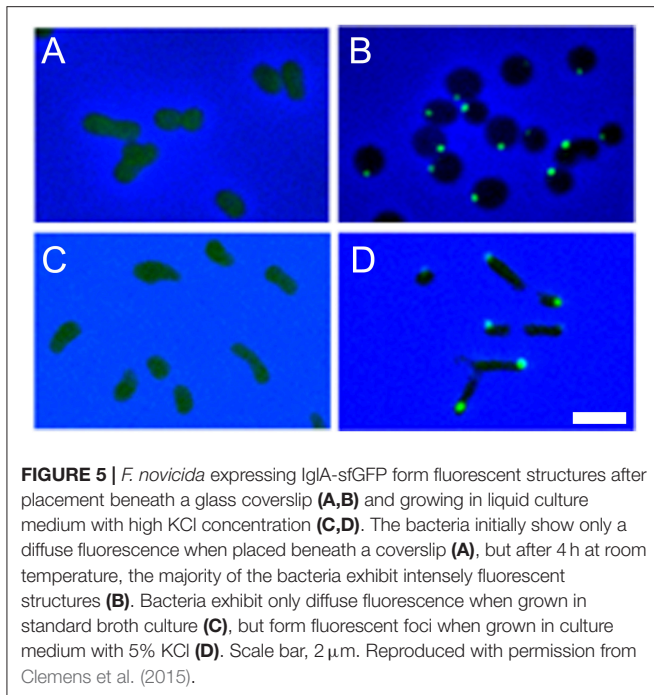


FIGURE 5 | *F. novicida* expressing IglA-sfGFP form fluorescent structures after placement beneath a glass coverslip (A,B) and growing in liquid culture medium with high KCl concentration (C,D). The bacteria initially show only a diffuse fluorescence when placed beneath a coverslip (A), but after 4 h at room temperature, the majority of the bacteria exhibit intensely fluorescent structures (B). Bacteria exhibit only diffuse fluorescence when grown in standard broth culture (C), but form fluorescent foci when grown in culture medium with 5% KCl (D). Scale bar, 2 μ m. Reproduced with permission from Clemens et al. (2015).

INDIVIDUAL COMPONENTS OF THE *FRANCISELLA* T6SS AND THEIR RELATION TO COMPONENTS OF OTHER CONTRACTILE SECRETION SYSTEMS

Structure and Composition of the *Francisella* T6SS Sheath

The essential feature common to all CISs is a long sheath that contracts to propel the tube and central spike across a membrane (Figure 7). In the case of myophage and all eCISs reported thus far, including R-pyocins, Afps, and MACs, the contractile sheath is composed of a single protein. In contrast, in canonical T6SSs, the sheath protein is a heterodimer of TssB and TssC, with TssB corresponding to the N-terminus and TssC corresponding to the C-terminus of the T4 phage gp18 sheath protein. In *Francisella*, IglA and IglB have limited sequence homology with TssB and TssC, respectively, and were shown to co-immunoprecipitate by de Bruin et al. (2007). Bröms et al. demonstrated interaction between IglA and IglB in a yeast-2-hybrid system and identified a conserved α -helical region of IglA critical to the IglA-IglB interaction and to phagosome escape and intracellular replication (Bröms et al., 2009).

T6SS sheaths have been purified and atomic models have been prepared for *F. novicida* (Clemens et al., 2015) and *V. cholerae* (Kudryashev et al., 2015) in their contracted configurations and for a contraction-defective *V. cholerae* sheath in its extended conformation (Wang et al., 2017). In the case of *F. novicida*, we determined the structure of the contracted sheath at 3.7 Å resolution by cryoEM (Clemens et al., 2015; Figure 8). We showed that the asymmetric unit of the sheath, the IglA/IglB heterodimer, is an α - β - α sandwich, with the central β sheet of

the sandwich formed by interdigitation of strands from both IglA and IglB. The IglA-IglB heterodimer shows remarkable structural homology with the gp18 and the R-pyocin sheath proteins despite only limited sequence homology (Clemens et al., 2015).

We found that the contracted T6SS sheath consists of disks of 6 IglA/IglB heterodimers (Figure 9) that stack in a helical configuration (Clemens et al., 2015) and the contracted sheath shows a similar helical rise and turn to the contracted sheaths of T4 phage (Leiman et al., 2004), R-pyocin (Ge et al., 2015), and *V. cholerae* T6SS (Kudryashev et al., 2015).

In the inner most layer of the contractile sheath of *F. novicida* (Clemens et al., 2015), an extensive interwoven meshwork of β -strands links the subunits of the sheath. Each disc of the sheath resembles the dancers in Matisse's "Dance," with each of the 6 heterodimers of the disk holding hands with its adjacent partners on the disk. Specifically, the N-terminal beta strand of IglA interacts with the C-terminal beta-strand of IglB of the adjacent heterodimer. These two parallel β -strands augment a two-stranded anti-parallel β -sheet near the C-terminus of IglB from the disc below, i.e., the disc closer to the baseplate, (Figure 10). This interlacing of strands produces an extensively interwoven 2-dimensional meshwork which plays a dominant role in holding the subunits of the sheath together. A similar interwoven β -sheet meshwork has also been identified in the *V. cholerae* T6SS sheath (Kudryashev et al., 2015), and in R-pyocin (Ge et al., 2015).

Although the prominent surface ridges of the *Francisella* T6SS sheath form a left-handed 6-start helix (Clemens et al., 2015) which is of opposite handedness to the surface ridges of T4 phage, R-pyocin, and *V. cholerae*, the β -strand connections between IglA/IglB heterodimers of adjacent rings in the interwoven meshwork in the inner layer of the sheath form a right-handed 6-start helix (Figure 9C) in common with the sheaths of R-pyocin (Figure 9D), T4 phage, and *V. cholerae* T6SS and other T6SSs.

Ge and colleagues recently developed an atomic model of the conformations of pre- and post-contraction R-pyocin (Ge et al., 2015). The extended sheath is a metastable conformation that is stabilized by interactions with the inner tube and all of the energy required for contraction of the sheath is stored within the pre-contraction state (Ge et al., 2015). During contraction, the R-pyocin sheath subunits move largely as rigid bodies, rotating 85° on an axis almost perpendicular to the main axis of the sheath, causing the sheath to widen and contract. The subunits of the sheath are held together during this profound change in quaternary conformation by the extensively interwoven mesh of β -strands (Figure 11). The rigid-body rotation of the subunits, while still being held by the interlaced β -strand meshwork, occurs by virtue of hinge-like action at the N- and C-terminal arms of the sheath subunits (Ge et al., 2015). If Matisse had drawn a ring of dancers performing a sheath contraction, the dancers of the extended sheath would be standing, holding hands in a tight circle with their hands at their sides. In the contracted conformation, they would be lying on their right sides in a circle on the floor, still holding hands but now with their (N-terminal) right arms outstretched beyond their heads and

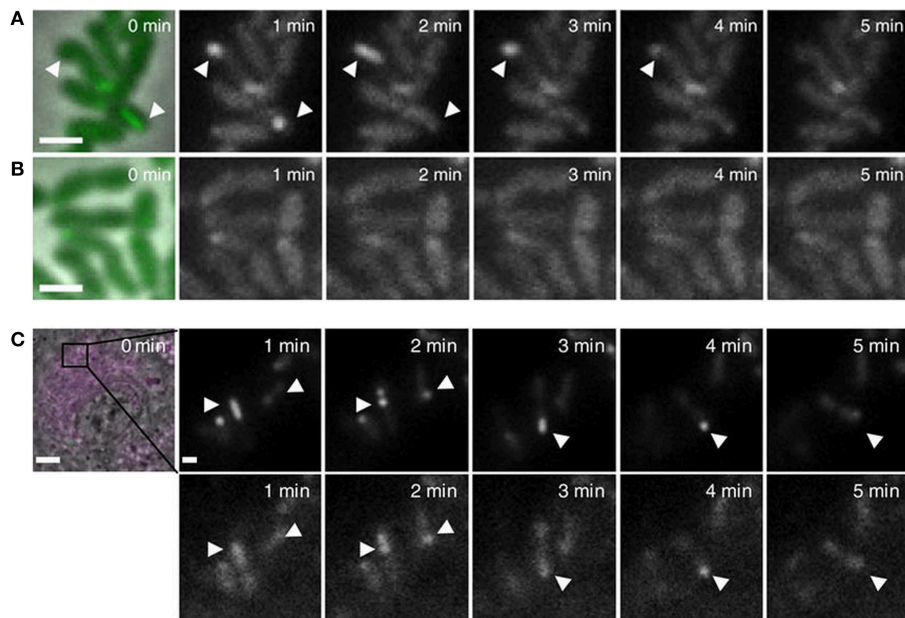
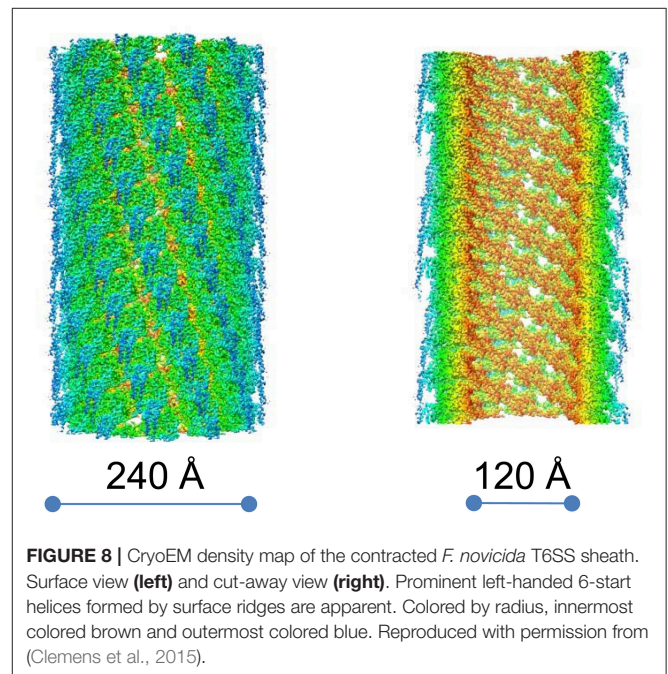
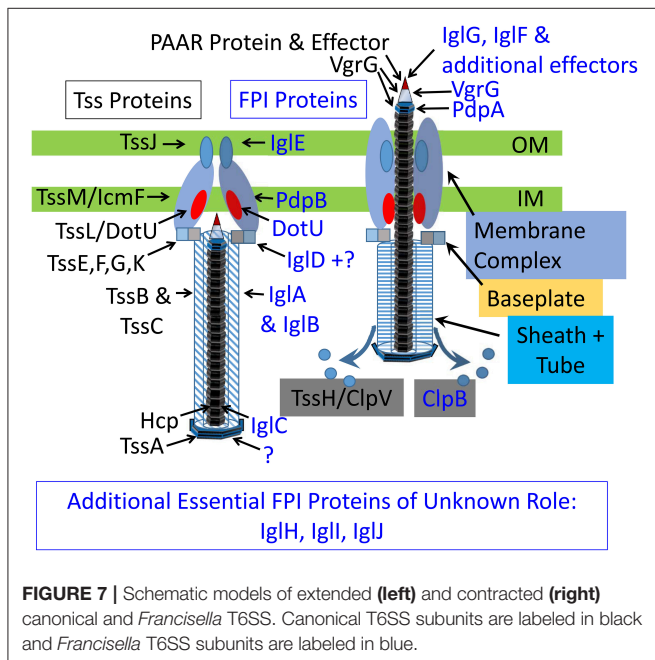


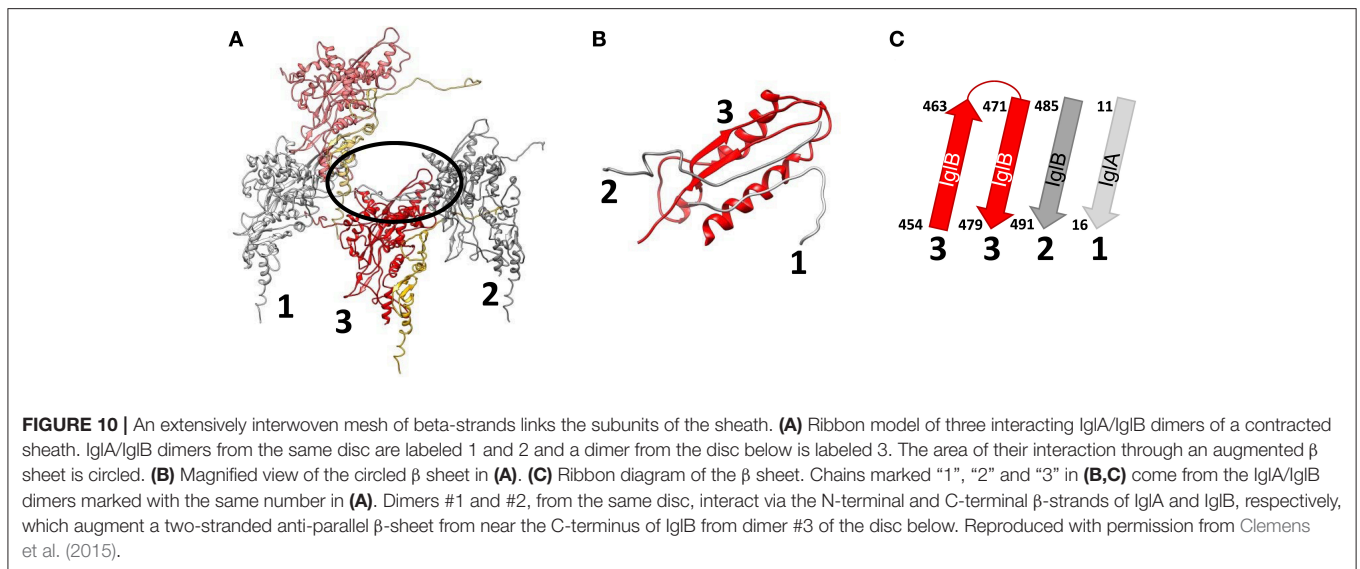
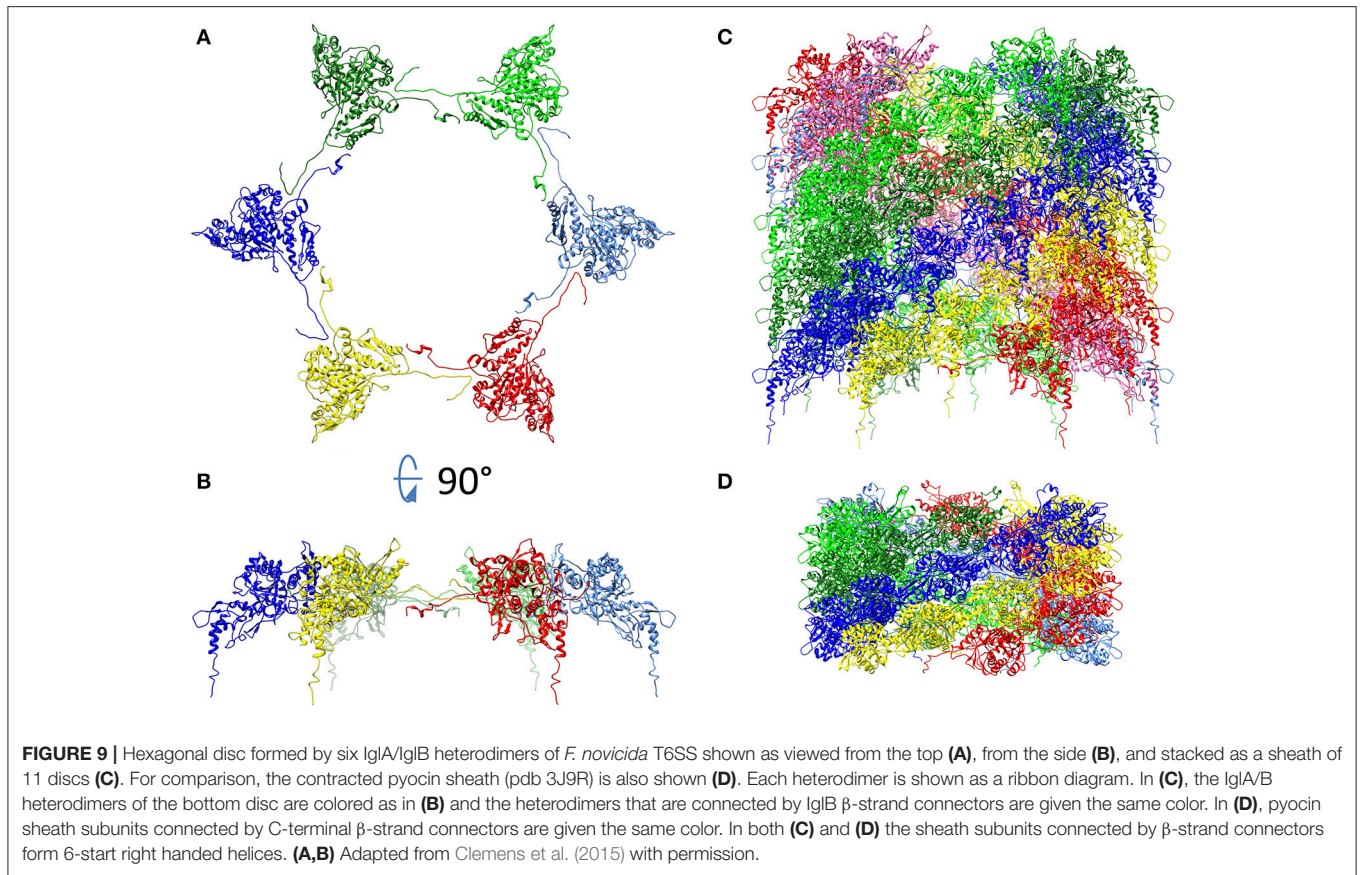
FIGURE 6 | (A,B) Live fluorescence microscopy shows dynamic formation and disassembly of IgA-sfGFP fluorescent structures in wild-type *F. novicida* (A) but not $\Delta pdpB$ *F. novicida* (B). Arrow heads indicate positions of fluorescent sheath assembly, contraction, and disassembly. Reproduced with permission from Brodmann et al. (2017). **(C)** Time-lapse images of unprimed wild-type BMDMs infected with *F. novicida* expressing IgA-sfGFP ClpB-mCherry2 for 1 h. First image shows merged phase contrast, GFP and mCherry channels with a $30 \times 30 \mu\text{m}$ field of view. Scale bar, $5 \mu\text{m}$. Close ups show GFP channel (upper panels) and mCherry channel (lower panels). Close ups show $5 \times 5 \mu\text{m}$ fields of view. Scale bar, $1 \mu\text{m}$. Arrowheads indicate positions of T6SS sheath assembly, contraction and location of sheath after contraction. Reproduced with permission from Brodmann et al. (2017).



their (C-terminal) left arms stretched beside their trunks. Thus, with contraction, the distance between partners in each ring increases, the diameter of the ring increases, and the rise between layers decreases. In the case of the canonical T6SS, contraction of the sheath rotates the sheath subunits outward, such that the

most peripheral domain becomes accessible for disassembly by the ClpV-ATPase (Kudryashev et al., 2015; Wang et al., 2017).

We have shown that the interwoven β -strand meshwork is essential to function of the T6SS. Deletion of either the N-terminal β -strand of IgIA or the C-terminal β -strand of IgIB



does not block formation of IgIA-IgIB heterodimers or formation of the fluorescent foci, but completely abolishes T6SS secretion and the capacity of the bacteria to escape their phagosome or to multiply intracellularly in macrophages (Clemens et al., 2015).

As hypothesized by Kudryashev et al. (2015) for the *V. cholerae* T6SS and shown by Taylor et al. (2016) in a pseudo-atomic model

of T4 phage, the interwoven meshwork of the sheath continues into the baseplate, providing a strong link between the sheath and the baseplate. The C-terminus of the T4 sheath initiator protein, gp25, and its T6SS orthologue, TssE, both have three β -strands that resemble the C-terminal “handshake” domain of the sheath protein and are available to interact with the C-terminal

β -strand of the sheath protein (gp18 or TssC, respectively) in the bottom disc of the sheath. Unfortunately, the corresponding baseplate protein in *Francisella* has not been identified. The β -strand meshwork has also been shown to be of critical importance for initiating and propagating sheath contraction. Basler's group has recently shown that insertion of 3–7 amino acids at residue 25, just after the VipA N-terminal (TssB) β -strand linker, blocks sheath contraction and allows the isolation of uncontracted sheaths with retained tube (Wang et al., 2017; Brackmann et al., 2018). CryoEM analysis of the non-contractile sheath revealed that the insertion led to altered connectivity between subunits, with the VipA N-terminal β -strand linker augmenting the 2 stranded anti-parallel β -strands of VipB of the adjacent heterodimer of the same disc, rather than of the disc below, as in the wild-type. The altered connectivity prevents contraction of the VipA-VipB mutant sheath because the VipA N-terminal β -strand is unable to stretch further to accommodate the conformational change required for sheath contraction. In their model, contraction is initiated by the baseplate pulling down on the N-terminal β -strand linkers of the first ring of the sheath, forcing a change in orientation of the subunits that propagates wave-like, ring-by-ring, from the baseplate to the last ring of the sheath (Wang et al., 2017; Brackmann et al., 2018).

SECRETED COMPONENTS OF THE T6SS

The IglC Tube

In all contractile injection systems, the contractile sheath wraps around a rigid central tube. In T4 phage, the tube is composed of gp19, which forms hexameric rings that stack to form the tube. The corresponding protein in canonical T6SS, Hcp, has sequence homology and structural homology to gp19. Interestingly, gp19 and Hcp show structural homology with the tube protein of non-contractile siphophage (Pell et al., 2009) (which lack a sheath), indicating an evolutionary linkage between contractile and non-contractile phage tail structures. In the case of myophage and siphophage, cargo of the phage tail delivery system (i.e., the tape measure protein and phage DNA) is injected into the target cell through the tube. For canonical T6SS, the effectors are associated (covalently or non-covalently) with VgrG at the tip of the tube rather than inside the tube. However, Hcp-associated effectors secreted inside the tube have also been demonstrated. For example, the *P. aeruginosa* Type 6 secreted effector proteins 1–4 (Tse1-4) bind the interior of the Hcp-1 hexameric ring and point mutations in Hcp-1 that disrupt this binding block secretion of these Tse proteins without interfering with Hcp-1 or VgrG secretion, consistent with the secretion of these effectors via the interior of the Hcp-1 tube (Silverman et al., 2013; Whitney et al., 2014). Similar Hcp-associated effector proteins may exist in other bacterial T6SSs, though none have been identified in *Francisella*.

The atomic structure of Hcp of canonical T6SS has been determined (Mougous et al., 2006), as has the structure of the inner tube of R-pyocin (Ge et al., 2015) and T4 phage gp19 (Taylor et al., 2016). The tube protein monomer assembles into hexameric rings that stack to form the tube. The tube is thought to serve as a scaffold for assembly of the sheath and, accordingly,

there is a one-to-one correspondence between sheath protein subunits and tube protein subunits. The atomic models of extended R-pyocin (Ge et al., 2015) and T4 phage tail (Taylor et al., 2016) show that the tube has the same helical rise and turn as the sheath. Consistent with a common evolutionary origin, the siphophage TP901-1 tube, R-pyocin tube, and T4 phage gp19 tube all have a similar helical turn and rise [22.4° and 38 Å for the siphophage TP901-1 tube (Bebeacqua et al., 2013), 18.3° and 38.4 Å for R-pyocin tube Ge et al., 2015, and 17.9° and 40.2 Å for T4 phage gp19 tube Taylor et al., 2016, respectively]. CryoEM analysis of the extended *V. cholerae* sheath-tube complex with the VipA N-terminal insertion also showed that the Hcp tube had the same helical turn and rise as the sheath (Wang et al., 2017). While T6SS Hcp hexamers have been seen to stack in solution as tubes without any helical turn, it seems more likely that—as with its evolutionary relatives—it assembles within bacteria with the same twist as the sheath.

In the case of pre-contraction pyocin, an attachment α -helix near the C-terminus of the pyocin sheath protein interacts via reciprocally charged residues on the surface of the tube monomer (Ge et al., 2015). A similar interaction between an α -helix of TssC sheath units and Hcp was recently observed by cryoET analysis of the *Myxococcus xanthus* pre-contraction T6SS (Chang et al., 2017) and the T6SS of *V. cholerae*, both by CryoET subtomogram averaging of the wild-type pre-contraction sheath and at atomic resolution by cryoEM of a contraction-defective extended mutant sheath (Wang et al., 2017). In the case of *F. novicida*, an α -helix (residues 424–437) similarly situated on the interior of the sheath near the C-terminus of IglB has a region of charge complementary to corresponding residues on the surface of IglC (Clemens et al., 2015). Additional studies are required to determine whether these residues of IglB and IglC interact and stabilize the pre-contraction sheath conformation.

While there is homology between eCIS and T6SS tube proteins, there are also important differences. eCIS tubes remain together following secretion, such that it is common in micrographs of R-pyocins (Higerd et al., 1969; Govan, 1974), MACs (Shikuma et al., 2014), and Afp structures to see naked tubes or tubes that have been partially ejected (Govan, 1974; Shikuma et al., 2014). In contrast, T6SS tubes typically dissociate following secretion, suggesting that interactions with the sheath proteins are required to stabilize the interactions between the tube proteins.

The X-ray crystal structure of recombinant *Francisella* IglC purified from *E. coli* (Sun et al., 2007) was shown to have striking structural homology with canonical Hcp despite the absence of sequence homology (de Bruin et al., 2011). However, the X-ray crystal structure of the recombinant *Francisella* IglC shows an N-terminal 32 residue extension that would block assembly of the monomers into hexagonal discs (de Bruin et al., 2011). We have found by mass spectrometry that secreted IglC still bears its N-terminus (i.e., it is not proteolytically cleaved off prior to secretion), which raises the possibility that the X-ray crystal structure of recombinant IglC might differ from that of native IglC. The structures of the native IglC monomer and of the assembled IglC tube remain to be determined.

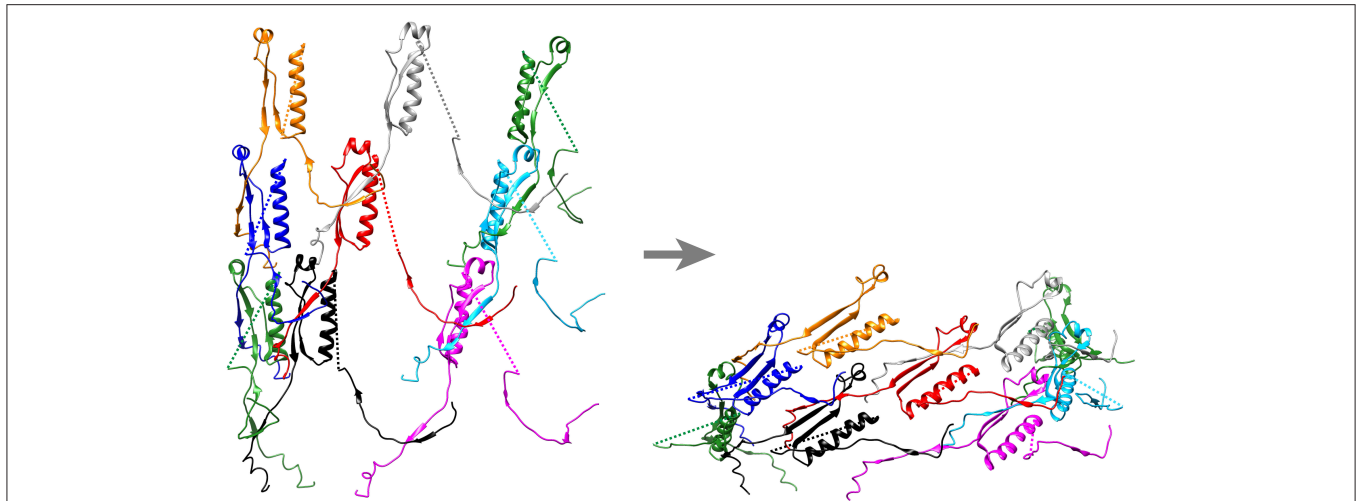


FIGURE 11 | Ribbon diagram of pre- and post-contraction R-pyocin illustrating how the extensively interwoven β -strand meshwork holds the subunits of the contractile sheath together during contraction. Shown are the interconnecting β -strand arms and the tube attachment α -helices of 9 sheath subunits (3 subunits on each of three strands) of the extended (**left**) and contracted (**right**) atomic models of R-pyocin, viewed from outside the sheath with the baseplate at the bottom. To facilitate visualization of the interwoven mesh, the majority of each sheath subunit has been deleted and replaced by a dashed line connecting the N- and C-terminal segments of each subunit. Corresponding sheath subunits are given the same colors in the extended and contracted diagrams. Diagrams were created using Chimera (Pettersen et al., 2004) and the PDB atomic models of extended (3j9c) and contracted (3j9r) R-pyocin (Ge et al., 2015).

The VgrG-PdpA Central Spike

In all CISs studied to date, the pre-contraction tube is tipped by a “central spike” protein complex that serves as a membrane-piercing needle. In T4 phage, the central spike complex is composed of two trimeric and one monomeric proteins: (gp27)₃, (gp5)₃, and (gp5.4)₁. T4 phage gp27 is a trimer that forms the central hub of the baseplate, acting as an adapter between the 6-fold rotational symmetry of the baseplate and tube and the 3-fold symmetry of gp5. T4 gp5 is a highly intertwined trimer with a long beta-helix roll that is rich in valine and glycine. Its N-terminal oligonucleotide/oligosaccharide-binding (OB)-fold domain interacts with gp27 and its C-terminal apex domain interacts with the tip of the spike, gp5.4, a monomeric PAAR-motif containing protein (Taylor et al., 2016). In canonical T6SSs, a trimeric VgrG (valine-glycine repeat) protein is a functional fusion with both sequence and structural homologies to the gp27-hub and gp5-spike proteins, and in the case of “evolved VgrGs”, there are C-terminal extensions corresponding to the spike tip gp5.4. For example, VgrG1 of *V. cholerae* has a wide N-terminal head domain that corresponds to gp27 and the N-terminal OB domains of gp5, a beta-helix spike domain that corresponds to the beta helix spike of gp5, and a large, 513 amino acid C-terminal actin-cross-linking effector domain (Pukatzki et al., 2007). In other T6SSs, separate PAAR-repeat proteins are orthologues of T4 phage gp5.4 (Shneider et al., 2013) and bind to the C-terminus of the VgrG trimer, where they complete the membrane piercing tip and also recruit additional effector proteins (Shneider et al., 2013). Different PAAR-containing effector proteins can partner with the same VgrG protein, providing flexibility in the effectors that are secreted (Cianfanelli et al., 2016a). A remarkably diverse range of T6SS effector proteins have been identified that can intoxicate or kill the target cell by a variety of mechanisms.

T6SS effector activities against bacteria include peptidoglycan hydrolases, phospholipases, pore forming proteins, and nucleases (Durand et al., 2014; Russell et al., 2014a), and those active against eukaryotic cells include cytoskeletal toxins [e.g., proteins causing ADP ribosylation of actin (Suarez et al., 2010) and actin cross-linking (Pukatzki et al., 2007)], and effectors that enhance uptake into epithelial cells (Sana et al., 2012), formation of multinucleated giant cells (Burtneck et al., 2011), inhibition of phagocytosis (Suarez et al., 2008), and red cell hemolysis (Böck et al., 2017).

Francisella VgrG protein has sequence homology with other VgrG proteins, but it is unusually short. Whereas, canonical VgrG proteins are typically 600–650 amino acids, *F. tularensis* VgrG is only 164 amino acid residues. Its short sequence and its appearance on EM negative staining suggest that it lacks both the N-terminal gp27-like head and any C-terminal effector extension. Indeed, bioinformatics modeling indicates that it even lacks the OB-fold of gp5. However, Eshraghi et al. have shown that PdpA is co-secreted with VgrG and co-immunoprecipitates with VgrG (Eshraghi et al., 2016). By TEM negative staining, PdpA resembles the cap on a VgrG needle (Eshraghi et al., 2016) and may functionally correspond to the gp27-like head domain and OB-fold domain of other VgrG proteins, providing an adaptor between the 3-fold symmetry of VgrG and the 6-fold symmetry of the tube and baseplate. In comparison with other VgrG proteins, the VgrG of *F. tularensis* and *F. novicida* is a truncated protein that lacks the N-terminal extensions of other VgrGs; PdpA may correspond to the missing N-terminal domains. Unlike canonical T6SSs, it is likely that the *Francisella* IgIc tube and the baseplate proteins interact with PdpA rather than with the truncated VgrG.

Additional Secreted Effector Proteins

In addition to IglC, VgrG, and PdpA, several additional proteins have been shown to be secreted by the *Francisella* T6SS in liquid culture medium and in macrophages. Bröms et al. systematically expressed each of the 17 proteins of the FPI as fusion proteins in *F. tularensis* LVS with β -lactamase so that proteins secreted into the macrophage cytosol would be detected by cleavage of fluorescent substrate (Bröms et al., 2012). The authors detected fluorescent signal in macrophage cytosol with the β -lactamase fused to IglE, IglC, VgrG, IglI, PdpE, PdpA, IglJ, and IglF. Detection of a positive β -lactamase fluorescent signal was not observed when the fusion proteins were expressed in $\Delta dotU$, $\Delta vgrG$, $\Delta iglC$, or $\Delta iglG$ LVS. Applying this method to *F. novicida* U112 required deletion of the FTN_1072 beta-lactamase gene. Fluorescent signal in the macrophage cytosol was observed with β -lactamase fused to IglE, IglC, PdpA, and PdpE, but not with VgrG, IglJ, IglF or IglI in the FTN_1072 deficient strain of *F. novicida*. The β -lactamase reporter is 29.5 kDa, which likely presents steric constraints and limitations on the proteins whose secretion can be detected by this assay system. As Nazarov et al. observed a 450 kDa cavity between the baseplate and the VgrG-PAAR protein complex of *V. cholerae* (Nazarov et al., 2018), there may be flexibility in the effector proteins that can be accommodated in assembly of the apparatus, and there may also be differences between *F. tularensis* LVS and *F. novicida* with regard to the effector proteins that are packed into this cavity. The observation of a positive fluorescence signal in the cytosol for IglE is intriguing, since IglE is generally thought to be an outer membrane lipoprotein corresponding to the membrane core complex protein, TssJ, rather than a secreted effector protein (Robertson et al., 2013; Nguyen et al., 2014). It is possible that IglE is released into the macrophage cytosol by a process of outer membrane blebbing when the *Francisella* replicate extensively in the host cell cytosol.

Rigard et al. used high KCl to induce T6SS secretion by *F. novicida* in liquid culture medium and demonstrated T6SS-dependent secretion of IglF and IglG (Rigard et al., 2016). Based on *in silico* analysis, they proposed that IglG is a PAAR-like protein that recruits IglF to the VgrG spike (Rigard et al., 2016). Eshraghi et al. compared proteins secreted by wild type and $\Delta dotU$ *F. novicida* in broth culture containing high KCl to identify T6SS proteins secreted in a T6SS-dependent fashion by mass spectrometry based proteomics. Their analysis identified five FPI encoded proteins—IglC, VgrG, PdpA, PdpC, and PdpD—and several proteins encoded on genes outside of the FPI (labeled OPI for “outside pathogenicity island”) as being secreted by the T6SS—OpiA, OpiB-1, and OpiB-3. Whereas, IglC, VgrG, and PdpA are all interdependent for secretion by the T6SS, disruption of genes encoding PdpC, PdpD, OpiA, or OpiB did not block secretion of the other proteins. Because *pdpC*, *pdpD*, and the *opi* genes can be disrupted without impacting secretion, they are presumed to encode effector functions. However, their actual biological functions are not known. While disruption of *iglC*, *pdpA*, or *vgrG* abolishes *F. novicida* growth in macrophages and virulence in animals, disruption of *pdpC* or *pdpD* has an intermediate effect, as these genes are required for virulence in animals, but they are not essential for intracellular growth in

macrophages (Ludu et al., 2008; Long et al., 2013). In the highly virulent *F. tularensis* SCHU S4 strain, disruption of both copies of *pdpC* caused a delay in phagosome escape and a modest decrease in intracellular growth in J774 mouse macrophages (Long et al., 2013). Following intranasal challenge, the *pdpC* double deletion mutant was able to disseminate to liver and spleen, but did not cause death and was ultimately cleared by mice (Long et al., 2013). Similarly, Uda et al. studied a SCHU strain of *F. tularensis* which has been attenuated by serial passage on artificial media (Uda et al., 2014). They restored full virulence by serial passage (9 passages) in mice and found that the only difference between the original attenuated strain and the virulent strain (“P9”) was a single nucleotide difference in one of the two copies of *pdpC*, such that the original strain expressed only truncated PdpC whereas the P9 strain with restored virulence expressed both a truncated and a full length PdpC (Uda et al., 2014). Uda et al. confirmed the importance of PdpC by disrupting both copies of *pdpC* in the P9 strain and showing that the $\Delta pdpC$ strain had reduced growth in mouse J774.1 macrophages and reduced virulence in mice, and that both attenuations were complemented with intact *pdpC*. Brodmann et al. recently demonstrated that *pdpC* and *pdpD* are not required for T6SS assembly in *F. novicida*, whereas *iglF*, *iglG*, *iglI*, and *iglJ* are required (Brodmann et al., 2017). Disruption of *pdpC* or *pdpD* genes markedly impaired phagosome escape and intracellular growth, but the defect was less severe than the defect resulting from disruption of *iglF*, *iglG*, *iglI*, or *iglJ* (Brodmann et al., 2017). Disruption of either *pdpC* or *pdpD* also impaired *F. novicida* virulence in mice, but the defect was less severe than disruption of the gene encoding the membrane complex protein, *pdpB* (Brodmann et al., 2017). On the other hand, disruption of both *pdpC* and *pdpD* resulted in *F. novicida* that were completely unable to escape their phagosome or cause disease in mice, i.e., defects as profound as that caused by $\Delta pdpB$ (Brodmann et al., 2017). In contrast, disruption of *pdpE* has no impact on phagosome escape in macrophages or virulence in mice in either *F. novicida* (Brodmann et al., 2017) or *F. tularensis* LVS (Bröms et al., 2011). Eshraghi et al. (2016) observed that disruption of *pdpD* or any of the *opi* genes, individually, had little or no impact on the capacity of *F. novicida* to multiply in macrophages. However, combined deletion of *pdpC*, *pdpD*, *opiA*, and *opiB* seriously impaired intracellular growth without impacting core T6SS secretion function. None of these genes are found in species outside of *Francisella* and their function remains unknown (Eshraghi et al., 2016). It is tempting to speculate that the effectors that are required for phagosome escape and intracellular growth include pore forming and phospholipase activities that could lead to formation of the characteristic fibrillar coat and phagosome escape.

Assuming that PdpA-VgrG-IglG correspond to the VgrG-PAAR protein complex of canonical T6SS, then IglF, PdpC, PdpD, OpiA, OpiB, PdpE, and possibly IglI may be additional effectors packaged within a ~450 kDa sized baseplate cavity similar to that described for *V. cholerae* (Nazarov et al., 2018). As the total mass of these monomeric proteins is 491–577 kDa (depending on which OpiA or OpiB proteins are packaged and whether or not IglI is included), it is possible that some, but not all, are packaged within an individual T6SS apparatus. *Francisella*

bacteria may preferentially package some effectors as opposed to others depending on environmental stimuli. Small effectors could fit within the IglC tube and almost all Hcp-associated effectors in other T6SSs are <20 kDa, which—for globular proteins—is a size that can fit within the 40 Å cavity of the Hcp tube (Whitney et al., 2014). However, other than VgrG and the presumed PAAR-like protein, IglG, none of the putative effectors listed in **Table 3** are <20 kDa. PdpE is 21.6 kDa, but attaching the 29.5 kDa β -lactamase fusion protein (Bröms et al., 2012), which is 43 Å in its smallest dimension, would sterically prevent it from fitting within the tube. Thus, the secreted β -lactamase signals for proteins, such as PdpE, observed by Bröms et al. (2012), would require packaging in the cavity between VgrG and the baseplate, rather than inside the tube. On the other hand, proteins for which Bröms et al. (2012) did not see a signal could conceivably fit within the tube in an unfolded or linear conformation, in a fashion analogous to the tape measure protein.

Baseplate Components

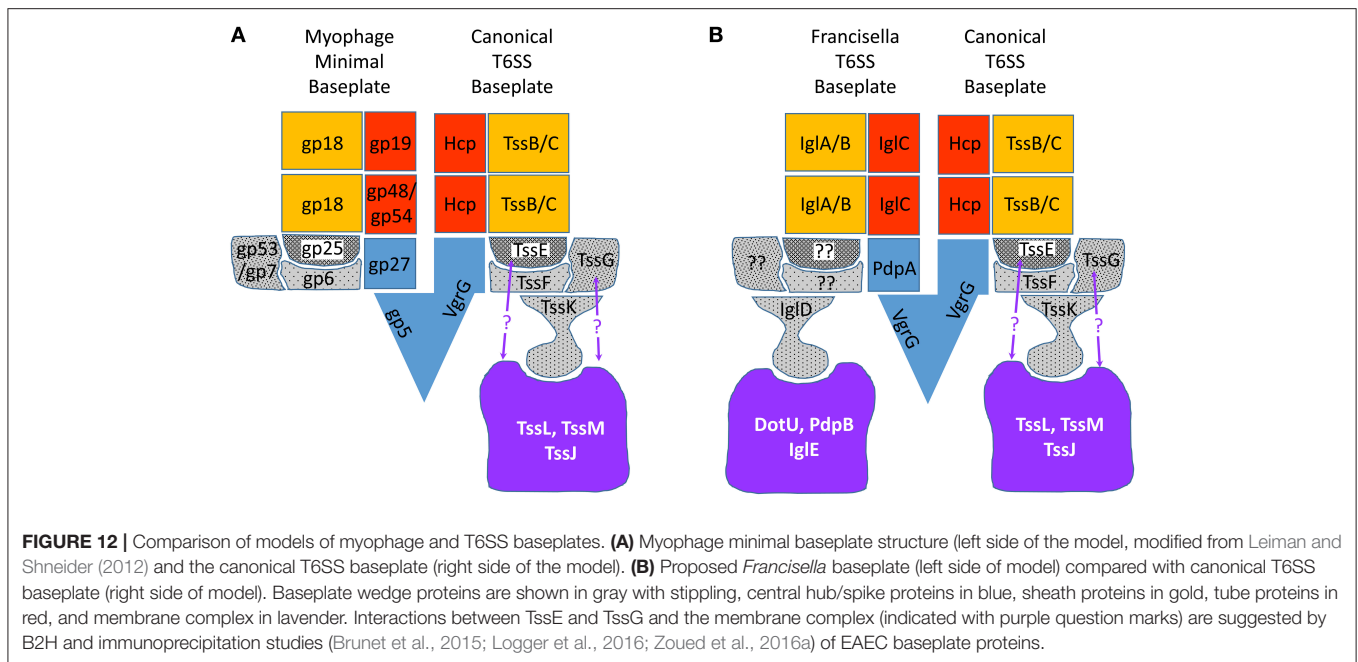
In all CISs, a baseplate serves as a platform for assembly of the tube and sheath. In T6SS, the baseplate has the additional function of anchoring the sheath to the membrane complex. In T4 phage, the baseplate is a highly complex structure made up of 145 polypeptide chains of 15 different proteins that assemble as six wedges around a central hub (Taylor et al., 2016). Other contractile phage, such as P2, have much less complex baseplate structures with only four different proteins: gpV (homologous to hub/spike proteins gp27 and gp5) and wedge components W (gp25-like sheath initiator), gpJ (gp6-like sheath platform) and gpI (gp53/gp7-like linker). This prompted Leiman and Shneider to propose the concept of a minimal tail tube structure with a simplified baseplate consisting of a central hub and three wedge proteins orthologous to gp6, gp25, and gp53/gp7 (Leiman and Shneider, 2012; **Figure 12**). Using the T4 baseplate nomenclature, the central hub of the minimal baseplate consists of the gp5-like spike and the gp27-like component that acts as an adaptor between the 3-fold symmetry of the gp5 spike and the 6-fold symmetry of the tail tube. Gp6, gp25, and gp53/gp7 proteins form a wedge and six wedges assemble to form a hexagonal baseplate that embraces the central hub. Gp25 is at the center of each wedge

and recruits sheath protein gp18 to initiate the polymerization of the sheath. Gp6 is a central component of each wedge, holding the wedges together and interacting with gp25 (at the center) and gp53/gp7 (at the periphery) of each wedge. Gp53/gp7, at the periphery of the wedge, interacts with tail fiber receptors and with gp6 (Leiman and Shneider, 2012).

Because the T6SS baseplate must fulfill the same functions as the phage baseplate, it is anticipated that it will show a structure similar to the myophage minimal baseplate, but with additional features that anchor it to the membrane complex (**Figure 12A**). As described above, VgrG of canonical T6SS is homologous to gp5 and gp27 and forms the hub of the baseplate. TssE shares homology with T4 baseplate protein gp25, the sheath initiator protein, but the assignment of other proteins to the T6SS baseplate are less clear. Brunet et al. developed Hcp Cys-substitution mutants of enteroaggregative *Escherichia coli* (EAEC) as a biochemical tool to report proper head-to-tail stacking of Hcp hexameric rings vs. improper tail-to-tail or head-head hexameric stacking, as assessed by SDS-PAGE and Western immunoblotting after *in vivo* oxidative cross-linking (Brunet et al., 2014). Since a functional baseplate is required as a platform for assembly of the tube of tailed bacteriophages, Brunet et al. reasoned that proper Hcp assembly could serve as a surrogate for functional T6SS baseplate assembly. Consistent with this hypothesis, they found that strains in which the baseplate hub VgrG was deleted, formed aberrant head-to-head and tail-to-tail Hcp interactions, whereas the parental EAEC formed only the correct head-to-tail Hcp multimers (Brunet et al., 2014). Interestingly, the sheath proteins TssB and TssC were not required for formation of the correct Hcp interactions. Using this assay, Brunet et al. demonstrated that 6 proteins—TssA, TssE, TssF, TssG, TssK, and VgrG—were required for formation of the correct Hcp interactions, suggesting that these 6 proteins are required for functional baseplate assembly (Brunet et al., 2015). Bioinformatic analysis showed secondary structural similarities between part of TssF and the P2 phage baseplate protein J and the corresponding T4 phage baseplate wedge protein gp6. Secondary structure similarities were also apparent between TssG and the P2 phage baseplate protein I (Brunet et al., 2015), which may correspond to T4 phage baseplate wedge protein gp53 or gp7 (Leiman and Shneider, 2012). Brunet et al. used bacterial-2-hybrid (B2H) analysis to show that TssF interacts with TssG and Hcp, and that TssG interacts with Hcp, TssC, TssE, and TssF. Immunoprecipitation pull-down studies of heterologously expressed protein lysates confirmed these interactions and also showed that TssF and TssG co-immunoprecipitated with TssE, and that VgrG pulled down TssF and TssG, and also pulled down TssE, -F, and -G (Brunet et al., 2015). In B2H analysis, TssK gave a positive signal when co-expressed with TssG and TssF, but not when expressed with either TssG or TssF alone, indicating the TssK interacts with the TssF-G complex. Genetic mutational analysis and fluorescence microscopy studies showed that EAEC expressing sfGFP-TssF or sfGFP-TssK formed discrete fluorescent foci near the inner membrane of both wild-type and $\Delta tssBC$ EAEC strains, consistent with the idea that the baseplate assembles on the membrane prior to sheath assembly. Indeed, in EAEC expressing both sfGFP-TssF or sfGFP-TssK and

TABLE 3 | Size of putative *Francisella* T6SS secreted proteins.

Putative effector proteins	Size (kDa)
VgrG	17.5
PdpA	95.3
IglG	18.3
IglF	67.9
IglI	44.6
PdpC	155.6
PdpD	140.7
PdpE	21.6
OpiA (FTN_0131)	50.7
OpiA-1 (FTN_1069)	91.2
OpiB-1 (FTN_1071)	54.9



mCherry-TssB, sheath elongation occurred after and at the site of the GFP-TssF or TssK focal fluorescence. In $\Delta tssK$ strains, sfGFP-TssF fluorescence was diffuse and no fluorescent foci formed, indicating that TssK is required for baseplate assembly. In $\Delta tssM$ EAEC strains, the sfGFP-TssF fluorescence was mostly diffuse, but some foci continued to form; these moved freely around the cytosol rather than appearing anchored to the membrane, consistent with the idea that the baseplate is anchored to the TssM-containing membrane complex (Brunet et al., 2015). Conversely, fluorescent foci of GFP-TssM form at the membrane even in $\Delta tssK$ and $\Delta tssF$ strains, consistent with the idea that membrane core complex formation precedes baseplate assembly. Since TssK interacts with cytoplasmic loops of TssL and TssM (Zoued et al., 2013), the data suggest a model in which the membrane complex forms first and recruits TssK, which in turn recruits the additional baseplate proteins TssE, -G, and -E (Brunet et al., 2015). Consistent with this model, Taylor et al. (2016) have recombinantly expressed TssE, -F, -G, and -K proteins and shown that they form a stable complex with an apparent stoichiometry of TssE₁F₂G₁K₃.

Since the baseplate connects the sheath to the membrane complex, it must form interactions with both, and these interactions have been examined by B2H analyses and immunoprecipitation studies. As noted above, TssE is thought to serve as a gp25-like sheath initiator and to anchor the sheath to the baseplate through an extension of the interwoven β -strand meshwork. B2H analyses and immunoprecipitation studies of EAEC T6SS have shown that TssE interacts with the cytosolic domain of TssL (Zoued et al., 2016a), suggesting that TssE interacts with the sheath, VgrG, and the membrane core complex. B2H and immunoprecipitation studies have shown that TssG interacts with the cytoplasmic loop of the inner membrane protein TssM (Brunet et al., 2015; Logger et al., 2016), and that

TssK interacts with both TssM and TssL (Zoued et al., 2013; Brunet et al., 2015; Logger et al., 2016; Nguyen et al., 2017).

The X-ray crystal structure of TssK shows a trimeric protein with an hourglass shape and three domains: a broad N-terminal shoulder, a thin neck, and a broad C-terminal head (Nguyen et al., 2017). The N-terminal shoulder domain is structurally and functionally similar to siphophage receptor binding protein (RBP) shoulder domains (Nguyen et al., 2017). Myophage such as T4 and P2 have no protein with sequence or structural homology with TssK. It is intriguing that, in evolution, T6SS has borrowed a structure from siphophage to provide a link between the baseplate and the membrane complex, a structure absent from phage. B2H studies show that the N-terminal shoulder domain interacts with the rest of the baseplate and that the C-terminal head interacts with the membrane complex. The connection between the C-terminal head domain and the neck is very flexible and this flexibility is hypothesized to allow TssK to maintain a stable link between the baseplate and the membrane complex during conformational changes accompanying contraction (Nguyen et al., 2017). In addition to linking the baseplate to the membrane complex, it has been reported that TssK interacts with TssC in Enteroaggregative *E. coli* (EAEC) (Zoued et al., 2013), suggesting that it may also help link the sheath to the baseplate. However, cryoET of the *M. xanthus* T6SS shows a distance of 300 Å between the sheath and the membrane complex (Chang et al., 2017), which is more than twice the 110 Å length of TssK (Nguyen et al., 2017). While it might be envisioned that TssK oligomerization could bridge this distance, in siphophage the RBP shoulder domains all lie in the same plane of the baseplate, perpendicular to the main axis of the sheath (Legrand et al., 2016).

T6SS baseplate structures have been observed at low resolution by cryoET of intact *M. xanthus* (Chang et al.,

2017) and at a finer 8.0 Å resolution by cryoEM of isolated sheath-baseplate complexes from contraction-defective VipA-N3 *V. cholerae* (Nazarov et al., 2018), but the resolution has not been sufficient to assign proteins definitively to the observed electron densities in the baseplate. Nazarov and colleagues observed a central spike surrounded by six structures similar to the phage baseplate wedges, but with an additional density hanging down from each wedge in a position suited to connect to the membrane core complex. They were able to fit the X-ray crystal structure of VgrG₃ and PAAR monomer to their central spike electron density, and use the protein density volume-to-mass coefficient to estimate a combined mass for the proteins in the baseplate wedge of 191.2 kDa, which is a good match to the calculated mass of 189.2 kDa, based on amino acid sequence, for a wedge complex consisting of TssE₁F₂G₁ (Nazarov et al., 2018). Nazarov et al. determined the structure of the “connector protein” densities hanging down from each wedge to a resolution of 10 Å and observed a good fit with the X-ray crystal structure of the shoulder and neck domains of EAEC TssK trimer determined by Nguyen et al. The head domain was not resolved, presumably because of its flexibility. Nazarov et al. observed that the putative TssK₃ “connector proteins” are situated in the T6SS baseplate in a position corresponding to that of domain IV of the trimeric gp10 proteins at the periphery of the T4 phage baseplate. Whereas, domain IV of gp10₃ connects gp7 in the T4 phage baseplate to the tail fiber network, TssK₃ in the T6SS baseplate would connect TssG to the membrane complex (Nazarov et al., 2018). In their model, the VgrG/PAAR central spike complex is surrounded by a spacious cavity that can accommodate up to ~450 kDa of effector proteins (Nazarov et al., 2018). This model is consistent with TssK interactions with baseplate proteins, TssF and TssG, and with membrane complex proteins, TssL and TssM, but not with TssK interactions with the sheath (Figure 12). In addition, while the model is consistent with TssE interacting with both the sheath and with TssF and TssG, it is difficult to visualize interactions between the membrane complex and TssE or TssG (Figure 12). While it is possible that this could reflect differences between baseplates of EAEC and *V. cholerae*, it is also possible that some protein-protein interactions observed in B2H systems and pull-down studies do not reflect interactions in an assembled sheath. After all, Hcp can form aberrant head-to-head and tail-to-tail interactions that do not reflect its interactions in an assembled T6SS.

The *Francisella* T6SS Baseplate

While IglD shows extremely limited homology with TssK and is assumed to be part of the baseplate, the FPI proteins that correspond to TssE, TssF, and TssG remain to be determined and the structure of the *Francisella* T6SS baseplate is unknown (Figure 12B). It is noteworthy that the spacious cavity surrounding the *V. cholerae* T6SS central spike could accommodate multiple effector proteins identified by Eshraghi et al. (2016).

Membrane Complex

Canonical T6SSs have a membrane complex that creates a channel spanning the inner and outer membranes. The

membrane complex functions to anchor the T6SS to the membrane and allows secretion to occur without loss of membrane integrity (Ho et al., 2014). The membrane complex is a key feature that differentiates T6SSs from other CISs, which, functioning extracellularly, have no need for such a structure. In the case of canonical T6SS, two integral inner membrane proteins—TssM and TssL—and one outer membrane lipoprotein, TssJ, have been identified as components of the membrane complex (Ma et al., 2009; Felisberto-Rodrigues et al., 2011; Durand et al., 2012). TssL and TssM have homology with the inner membrane proteins, DotU and IcmF, respectively, of the Type 4 Secretion System (Ma et al., 2009; Durand et al., 2012), suggesting that these components were inherited from the T4SS during evolution of the T6SS.

The X-ray crystal structures of some of the soluble cytosolic domains of the membrane complex have been determined. In addition, the TssJLM proteins of EAEC have been co-expressed as an epitope-tagged protein complex in *E. coli* BL21, allowing affinity purification of the recombinant TssJLM complex and determination of its structure at 11 Å resolution by TEM analysis of negatively stained particles (Durand et al., 2015). The 1.7 MDa particles exhibited 5-fold symmetry and consisted of 30 polypeptide chains, with 5 dimers of TssJLM heterotrimers. The integral inner membrane protein TssM interacts with TssJ via its C-terminal periplasmic domain, and it interacts with TssL via its cytoplasmic domain (Zheng and Leung, 2007; Ma et al., 2009, 2012; Felisberto-Rodrigues et al., 2011; Rao et al., 2011; Durand et al., 2015). Structural analysis and chemical modification studies with a membrane impermeant reagent are consistent with a model in which the complex undergoes a conformational change during secretion, with the tip of the complex opening akin to the way the leaves of a camera shutter move to form an aperture, thereby allowing passage of the tube and spike complex (Durand et al., 2015).

Stable interaction between a membrane complex with 5-fold symmetry and a baseplate with 6-fold symmetry is problematic. The attachments between sheath, baseplate, and membrane complex must have a strength comparable to that conferred by the interwoven meshwork (“handshakes”) that holds the sheath together during contraction (Kudryashev et al., 2015). However, as the TssJLM proteins were overexpressed in the absence of other components of the T6SS, it is possible that the symmetry of the purified complex differs from that of the *in situ* structure. Noting that TssA interacts with TssJM prior to recruitment of TssL, Cascales group has suggested that the star-shaped, dodecameric TssA acts as a chaperone that imposes a 6-fold symmetry onto the TssJLM membrane complex as it forms (Zoued et al., 2017).

The *Francisella* T6SS Membrane Complex

Based on limited sequence homologies, mutational analysis, immunoprecipitation and B2H analyses, IglE, DotU, and PdpB have been proposed as orthologues of TssJ, TssL, and TssM, respectively (Robertson et al., 2013; Nguyen et al., 2014). Although *F. novicida* DotU shows only 15% identity to TssL, X-ray crystallography of the *F. novicida* DotU soluble domain (Robb et al., 2012) shows structural homology to the soluble TssL domain of EAEC (Durand et al., 2012). PdpB shows only 18%

identity to TssM/IcmF of *V. cholerae*, but appears functionally to resemble TssM/IcmF because it is an inner membrane protein that interacts both with DotU and with the outer membrane lipoprotein, IglE. Although IglE has no sequence homology with TssJ, it undergoes palmitoylation at a cysteine residue that anchors it to the outer membrane and replacement of this cysteine with a glycine abolishes both palmitoylation and multiplication of the bacteria in macrophages (Nguyen et al., 2014). Consistent with IglE being the orthologue of TssJ, B2H screening and immunoprecipitation studies demonstrate that IglE interacts with the periplasmic C-terminus of PdpB (Nguyen et al., 2014).

While there is good evidence that IglE, DotU, and PdpB contribute to the membrane complex of *Francisella*, there may be additional proteins within or outside of the FPI that contribute to the membrane complex. For example, in some cases it has been shown that the T6SS membrane complex is inserted and anchored into the membrane in concert with additional proteins that have peptidoglycan binding and degrading activities (Aschtgen et al., 2010; Weber et al., 2016; Santin and Cascales, 2017). As *Francisella* has an extensive capsule that could present a barrier to T6SS operation, it is tempting to speculate that similar peptidoglycan and capsule binding and degrading proteins might be recruited to the *Francisella* membrane complex.

FPI Proteins of Unknown Function

Several proteins of the FPI are essential for intracellular growth and virulence of *Francisella* in animals, yet their specific role has not been determined. These proteins may correspond to key components of canonical T6SS, such as the chaperone protein TssA, or baseplate proteins TssE, TssF, and TssG, whose corresponding proteins in *Francisella* have not yet been identified.

NON-FPI COMPONENTS

ClpV

An essential component present in all canonical T6SSs is a ClpV ATPase that functions to disassemble the contracted sheath and enable dynamic recycling for repeated rounds of firing, disassembly and reassembly. Myophage, R-pyocins, Afps, and MACs have no requirement for a gene corresponding to ClpV because their contractile apparatus contracts once and is not recycled. The *Francisella* T6SS is an outlier in that none of the genes within the FPI gene cluster encode a ClpV ATPase. However, Brodmann *et al.* recently demonstrated that *F. novicida* employs ClpB ATPase, encoded outside of the FPI, to disassemble its contracted T6SS sheath (Brodmann et al., 2017). In live fluorescence imaging, ClpB-mCherry fluorescence colocalizes with sites of IglA-sfGFP sheath assembly, contraction, and disassembly, as shown in **Figure 6C** (Brodmann et al., 2017). Canonical T6SSs have a conserved sequence on their sheath protein, an α -helical region at the N-terminus of VipB which includes a consensus sequence “LLDEIM” (residues 19–24 of the *V. cholerae* TssC homolog, VipB) that is bound by the ClpV ATPase (Pietrosiuk et al., 2011). However, *F. tularensis* IglB has no similar α -helical region or consensus sequence. The sheath

sequence recognized by ClpB ATPase has not been determined, but presumably is more exposed and accessible to binding in the contracted than in the pre-contracted sheath conformation.

Antennae

Contractile injection systems are thought to function in a contact dependent fashion, with sheath contraction occurring upon interaction between the system and the target surface. In the case of myophage, receptor binding proteins are connected via tail fibers to the baseplate (Bartual et al., 2010). R-pyocins (Higerd et al., 1969), MACs (Shikuma et al., 2014), and Afps (Heymann et al., 2013) have been shown to have similar tail-fiber structures connecting to their baseplates. It is thought that interaction between the tail fiber receptor and its ligand triggers conformational changes in the baseplate that in turn lead to opening of the baseplate and sheath contraction. For T6SS, ECT of intact *M. xanthus* bacteria has visualized tail fiber-like antennae with terminal bulbs suggestive of receptor binding proteins (Chang et al., 2017). The genes encoding these structures are not known and most likely reside outside of the T6SS gene cluster as no genes homologous to tail fiber proteins are present within the *M. xanthus* T6SS gene cluster (Chang et al., 2017). In addition, as connections between the antennae and the T6SS baseplate or membrane complex have not been visualized, it is unclear whether the observed antennae are truly T6SS elements.

Because *F. tularensis* T6SS functions to mediate phagosome escape, it is tempting to speculate that it possesses similar antennae-like sensors that interact with molecules within the host phagosome or on the phagosomal membrane to trigger contraction.

The T6SS Assembly Process

The sequence of events involved in assembly of canonical T6SS has been dissected by genetic mutational analysis and fluorescence studies in EAEC (Brunet et al., 2015; Zoued et al., 2016b). These studies have revealed that assembly of the T6SS begins with recruitment of TssM to TssJ. TssA, acting as a chaperone, then binds to the TssMJ prior to recruitment of TssL and formation of the membrane complex. As noted above, the TssA complex, with its 6-fold symmetry, could impose a similar symmetry during assembly of the TssJLM membrane complex (Zoued et al., 2017). The baseplate then assembles at the site of the membrane complex and polymerization of the sheath and tube follows (Brunet et al., 2015), again with a requirement for TssA acting as a chaperone to ensure proper assembly, though TssA does not become a part of the final assembled baseplate (Zoued et al., 2017). Polymerization of the sheath and tube then occur, and it has been shown that TssA is required for proper stacking of Hcp hexamers and for extension of the sheath, leading to the hypothesis that the star shaped TssA complex acts as a chaperone to ensure proper assembly of each new hexagonal layer of the tube and extended sheath (Zoued et al., 2017). As the tube and sheath assemble, the TssA complex remains associated with the distal end of the sheath (Zoued et al., 2016b). In the final extended sheath, TssA may function in a fashion analogous to the T4 phage gp3/gp15 tube/sheath terminator proteins, serving to stabilize the extended sheath and ensure proper expulsion of the tube during

contraction (Zoued et al., 2016b). CryoEM of extended sheaths from the contraction-defective VipA-N3 expressing strain of *V. cholerae* by Basler's group revealed cap-like structures at the distal end of the sheaths (resolved at 7.5 Å) with a star-like configuration and an estimated mass of 540 kDa, consistent with either dodecameric TssA or an unusual configuration of the terminal VipA/B sheath subunits (Nazarov et al., 2018). An alternative model has been proposed by Planamente et al., who also observed dodecameric rings of *Pseudomonas* TssA1 at the ends of T6SS sheaths, demonstrated interaction of TssA1 with TssK1 and TssF1 by pull-down experiments, and noted sequence similarity between the TssA1 and the C-terminus of gp6, leading them to propose a gp6-like role for the *Pseudomonas* TssA1 in the baseplate (Planamente et al., 2016). However, TssA of EAEC lacks the gp6-like domain found in *Pseudomonas* TssA1, and whereas TssA is essential to EAEC T6SS assembly and function, TssA1 is not essential to *Pseudomonas* T6SS function, suggesting that EAEC TssA and *Pseudomonas* TssA1 have different structures and functions (Zoued et al., 2017).

While it is likely that the *Francisella* T6SS is assembled in a similar fashion, the *Francisella* orthologue to TssA of EAEC has not been identified.

REFERENCES

- Aschtgen, M. S., Gavioli, M., Dessen, A., Llobès, R., and Cascales, E. (2010). The SciZ protein anchors the enteroaggregative *Escherichia coli* Type VI secretion system to the cell wall. *Mol. Microbiol.* 75, 886–899. doi: 10.1111/j.1365-2958.2009.07028.x
- Bartual, S. G., Otero, J. M., Garcia-Doval, C., Llamas-Saiz, A. L., Kahn, R., Fox, G. C., et al. (2010). Structure of the bacteriophage T4 long tail fiber receptor-binding tip. *Proc. Natl. Acad. Sci. U.S.A.* 107, 20287–20292. doi: 10.1073/pnas.1011218107
- Basler, M. (2015). Type VI secretion system: secretion by a contractile nanomachine. *Philos. Trans. R. Soc. Lond. B Biol. Sci.* 370:20150021. doi: 10.1098/rstb.2015.0021
- Basler, M., Ho, B. T., and Mekalanos, J. J. (2013). Tit-for-tat: type VI secretion system counterattack during bacterial cell-cell interactions. *Cell* 152, 884–894. doi: 10.1016/j.cell.2013.01.042
- Basler, M., and Mekalanos, J. J. (2012). Type 6 secretion dynamics within and between bacterial cells. *Science* 337, 815–815. doi: 10.1126/science.1222901
- Basler, M., Pilhofer, M., Henderson, G. P., Jensen, G. J., and Mekalanos, J. J. (2012). Type VI secretion requires a dynamic contractile phage tail-like structure. *Nature* 483, 182–186. doi: 10.1038/nature10846
- Bebecua, C., Lai, L., Vegge, C. S., Brøndsted, L., Van Heel, M., Veesler, D., et al. (2013). Visualizing a complete Siphoviridae member by single-particle electron microscopy: the structure of lactococcal phage TP901-1. *J. Virol.* 87, 1061–1068. doi: 10.1128/JVI.02836-12
- Bell, J. F., Owen, C. R., and Larson, C. L. (1955). Virulence of *Bacterium tularensis*. I. A study of the virulence of *Bacterium tularensis* in mice, guinea pigs, and rabbits. *J. Infect. Dis.* 97, 162–166. doi: 10.1093/infdis/97.2.162
- Bingle, L. E., Bailey, C. M., and Pallen, M. J. (2008). Type VI secretion: a beginner's guide. *Curr. Opin. Microbiol.* 11, 3–8. doi: 10.1016/j.mib.2008.01.006
- Bladergroen, M. R., Badelt, K., and Spaink, H. P. (2003). Infection-blocking genes of a symbiotic *Rhizobium leguminosarum* strain that are involved in temperature-dependent protein secretion. *Mol. Plant Microbe Interact.* 16, 53–64. doi: 10.1094/MPMI.2003.16.1.53
- Böck, D., Medeiros, J. M., Tsao, H. F., Penz, T., Weiss, G. L., Aistleitner, K., et al. (2017). *In situ* architecture, function, and evolution of a contractile injection system. *Science* 357, 713–717. doi: 10.1126/science.aa n7904

SUMMARY

Clearly, we have come a long way in our understanding of the *Francisella* T6SS, yet much remains to be determined. Key unresolved issues include: (a) the protein composition and structure of the baseplate, (b) the intracellular signals that trigger contraction, (c) the receptors that sense these signals, (d) the signal transduction mechanism, (e) an atomic model of the baseplate and membrane complex, (f) the atomic structure of the extended sheath, and (g) identification of the functions of the secreted components and an understanding of how they promote phagosome escape and intracellular replication.

AUTHOR CONTRIBUTIONS

All authors listed have made a substantial, direct and intellectual contribution to the work, and approved it for publication.

ACKNOWLEDGMENTS

The authors were supported by NIH Grants AI065359 and AI123630.

- Bourdonnay, E., and Henry, T. (2016). Catch me if you can. *Elife* 5:e14721. doi: 10.7554/eLife.14721
- Boyer, F., Fichant, G., Berthod, J., Vandenbrouck, Y., and Attree, I. (2009). Dissecting the bacterial type VI secretion system by a genome wide in silico analysis: what can be learned from available microbial genomic resources? *BMC Genomics* 10:104. doi: 10.1186/1471-2164-10-104
- Brackmann, M., Wang, J., and Basler, M. (2018). Type VI secretion system sheath inter-subunit interactions modulate its contraction. *EMBO Rep.* 19, 225–233. doi: 10.15252/embr.201744416
- Brodmann, M., Dreier, R. F., Broz, P., and Basler, M. (2017). *Francisella* requires dynamic type VI secretion system and ClpB to deliver effectors for phagosomal escape. *Nat. Commun.* 8:15853. doi: 10.1038/ncomms15853
- Bröms, J. E., Lavander, M., Meyer, L., and Sjöstedt, A. (2011). IglG and IglI of the *Francisella* pathogenicity island are important virulence determinants of *Francisella tularensis* LVS. *Infect. Immun.* 79, 3683–3696. doi: 10.1128/IAI.01344-10
- Bröms, J. E., Lavander, M., and Sjöstedt, A. (2009). A conserved alpha-helix essential for a type VI secretion-like system of *Francisella tularensis*. *J. Bacteriol.* 191, 2431–2446. doi: 10.1128/JB.01759-08
- Bröms, J. E., Meyer, L., Sun, K., Lavander, M., and Sjöstedt, A. (2012). Unique substrates secreted by the type VI secretion system of *Francisella tularensis* during intramacrophage infection. *PLoS ONE* 7:e50473. doi: 10.1371/journal.pone.0050473
- Bröms, J. E., Sjöstedt, A., and Lavander, M. (2010). The role of the *Francisella tularensis* pathogenicity island in Type VI secretion, intracellular survival, and modulation of host cell signaling. *Front. Microbiol.* 1:136. doi: 10.3389/fmicb.2010.00136
- Brunet, Y. R., Espinosa, L., Harchouni, S., Mignot, T., and Cascales, E. (2013). Imaging type VI secretion-mediated bacterial killing. *Cell Rep.* 3, 36–41. doi: 10.1016/j.celrep.2012.11.027
- Brunet, Y. R., Héning, J., Celia, H., and Cascales, E. (2014). Type VI secretion and bacteriophage tail tubes share a common assembly pathway. *EMBO Rep.* 15, 315–321. doi: 10.1002/embr.201337936
- Brunet, Y. R., Zoued, A., Boyer, F., Douzi, B., and Cascales, E. (2015). The Type VI secretion TssEFGK-VgrG phage-like baseplate is recruited to the TssJLM membrane complex via multiple contacts and serves as assembly platform for tail tube/sheath polymerization. *PLoS Genet.* 11:e1005545. doi: 10.1371/journal.pgen.1005545

- Burtneck, M. N., Brett, P. J., Harding, S. V., Ngugi, S. A., Ribot, W. J., Chantratita, N., et al. (2011). The cluster 1 type VI secretion system is a major virulence determinant in *Burkholderia pseudomallei*. *Infect. Immun.* 79, 1512–1525. doi: 10.1128/IAI.01218-10
- Chang, Y. W., Rettberg, L. A., Ortega, D. R., and Jensen, G. J. (2017). *In vivo* structures of an intact type VI secretion system revealed by electron cryotomography. *EMBO Rep.* 18, 1090–1099. doi: 10.15252/embr.201744072
- Checroun, C., Wehrly, T. D., Fischer, E. R., Hayes, S. F., and Celli, J. (2006). Autophagy-mediated reentry of *Francisella tularensis* into the endocytic compartment after cytoplasmic replication. *Proc. Natl. Acad. Sci. U.S.A.* 103, 14578–14583. doi: 10.1073/pnas.0601838103
- Chiu, H. C., Soni, S., Kulp, S. K., Curry, H., Wang, D., Gunn, J. S., et al. (2009). Eradication of intracellular *Francisella tularensis* in THP-1 human macrophages with a novel autophagy inducing agent. *J. Biomed. Sci.* 16:110. doi: 10.1186/1423-0127-16-110
- Chong, A., and Celli, J. (2010). The *Francisella* intracellular life cycle: toward molecular mechanisms of intracellular survival and proliferation. *Front. Microbiol.* 1:138. doi: 10.3389/fmicb.2010.00138
- Cianfanelli, F. R., Alcoforado Diniz, J., Guo, M., De Cesare, V., Trost, M., and Coulthurst, S. J. (2016a). VgrG and PAAR proteins define distinct versions of a functional type VI secretion system. *PLoS Pathog.* 12:e1005735. doi: 10.1371/journal.ppat.1005735
- Cianfanelli, F. R., Monlezun, L., and Coulthurst, S. J. (2016b). Aim, load, fire: the type VI secretion system, a bacterial nanoweapon. *Trends Microbiol.* 24, 51–62. doi: 10.1016/j.tim.2015.10.005
- Clemens, D. L., Ge, P., Lee, B. Y., Horwitz, M. A., and Zhou, Z. H. (2015). Atomic structure of T6SS reveals interlaced array essential to function. *Cell* 160, 940–951. doi: 10.1016/j.cell.2015.02.005
- Clemens, D. L., and Horwitz, M. A. (2007). Uptake and intracellular fate of *Francisella tularensis* in human macrophages. *Ann. N. Y. Acad. Sci.* 1105, 160–186. doi: 10.1196/annals.1409.001
- Clemens, D. L., Lee, B. Y., and Horwitz, M. A. (2004). Virulent and avirulent strains of *Francisella tularensis* prevent acidification and maturation of their phagosomes and escape into the cytoplasm in human macrophages. *Infect. Immun.* 72, 3204–3217. doi: 10.1128/IAI.72.6.3204-3217.2004
- Clemens, D. L., Lee, B. Y., and Horwitz, M. A. (2005). *Francisella tularensis* enters macrophages via a novel process involving pseudopod loops. *Infect. Immun.* 73, 5892–5902. doi: 10.1128/IAI.73.9.5892-5902.2005
- Clemens, D. L., Lee, B. Y., and Horwitz, M. A. (2012). O-antigen-deficient *Francisella tularensis* Live Vaccine Strain mutants are ingested via an aberrant form of looping phagocytosis and show altered kinetics of intracellular trafficking in human macrophages. *Infect. Immun.* 80, 952–967. doi: 10.1128/IAI.05221-11
- Das, S., and Chaudhuri, K. (2003). Identification of a unique IAHP (IcmF associated homologous proteins) cluster in *Vibrio cholerae* and other proteobacteria through in silico analysis. *In Silico Biol.* 3, 287–300.
- de Bruin, O. M., Duplantis, B. N., Ludu, J. S., Hare, R. F., Nix, E. B., Schmerk, C. L., et al. (2011). The biochemical properties of the *Francisella* pathogenicity island (FPI)-encoded proteins IglA, IglB, IglC, PdpB and DotU suggest roles in type VI secretion. *Microbiology* 157, 3483–3491. doi: 10.1099/mic.0.052308-0
- de Bruin, O. M., Ludu, J. S., and Nano, F. E. (2007). The *Francisella* pathogenicity island protein IglA localizes to the bacterial cytoplasm and is needed for intracellular growth. *BMC Microbiol.* 7:1. doi: 10.1186/1471-2180-7-1
- Decoin, V., Barbey, C., Bergeau, D., Latour, X., Feuilloley, M. G. J., Orange, N., et al. (2014). A type VI secretion system is involved in *Pseudomonas fluorescens* bacterial competition. *PLoS ONE* 9:e89411. doi: 10.1371/journal.pone.0089411
- Deng, K., Blick, R. J., Liu, W., and Hansen, E. J. (2006). Identification of *Francisella tularensis* genes affected by iron limitation. *Infect. Immun.* 74, 4224–4236. doi: 10.1128/IAI.01975-05
- Durand, E., Cambillau, C., Cascales, E., and Journet, L. (2014). VgrG, Tae, Tle, and beyond: the versatile arsenal of Type VI secretion effectors. *Trends Microbiol.* 22, 498–507. doi: 10.1016/j.tim.2014.06.004
- Durand, E., Nguyen, V. S., Zoued, A., Logger, L., Pêhau-Arnaudet, G., Aschtgen, M.-S., et al. (2015). Biogenesis and structure of a type VI secretion membrane core complex. *Nature* 523, 555–560. doi: 10.1038/nature14667
- Durand, E., Zoued, A., Spinelli, S., Watson, P. J., Aschtgen, M. S., Journet, L., et al. (2012). Structural characterization and oligomerization of the TssL protein, a component shared by bacterial type VI and type IVb secretion systems. *J. Biol. Chem.* 287, 14157–14168. doi: 10.1074/jbc.M111.3.38731
- Ellis, J., Oyston, P. C., Green, M., and Titball, R. W. (2002). Tularemia. *Clin. Microbiol. Rev.* 15, 631–646. doi: 10.1128/CMR.15.4.631-646.2002
- Eshraghi, A., Kim, J., Walls, A. C., Ledvina, H. E., Miller, C. N., Ramsey, K. M., et al. (2016). Secreted effectors encoded within and outside of the *Francisella* pathogenicity island promote intramacrophage growth. *Cell Host Microbe* 20, 573–583. doi: 10.1016/j.chom.2016.10.008
- Felisberto-Rodrigues, C., Durand, E., Aschtgen, M. S., Blangy, S., Ortiz-Lombardia, M., Douzi, B., et al. (2011). Towards a structural comprehension of bacterial type VI secretion systems: characterization of the TssJ-TssM complex of an *Escherichia coli* pathovar. *PLoS Pathog.* 7:e1002386. doi: 10.1371/journal.ppat.1002386
- Ge, P., Scholl, D., Leiman, P. G., Yu, X., Miller, J. F., and Zhou, Z. H. (2015). Atomic structures of a bactericidal contractile nanotube in its pre- and postcontraction states. *Nat. Struct. Mol. Biol.* 22, 377–382. doi: 10.1038/nsmb.2995
- Golovliov, I., Baranov, V., Krocova, Z., Kovarova, H., and Sjöstedt, A. (2003). An attenuated strain of the facultative intracellular bacterium *Francisella tularensis* can escape the phagosome of monocytic cells. *Infect. Immun.* 71, 5940–5950. doi: 10.1128/IAI.71.10.5940-5950.2003
- Golovliov, I., Ericsson, M., Sandström, G. G., Tärnvik, A., and Sjöstedt, A. (1997). Identification of proteins of *Francisella tularensis* induced during growth in macrophages and cloning of the gene encoding a prominently induced 23-kilodalton protein. *Infect. Immun.* 65, 2183–2189.
- Govan, J. R. (1974). Studies on the pyocins of *Pseudomonas aeruginosa*: morphology and mode of action of contractile pyocins. *J. Gen. Microbiol.* 80, 1–15. doi: 10.1099/00221287-80-1-1
- Gray, C. G., Cowley, S. C., Cheung, K. K., and Nano, F. E. (2002). The identification of five genetic loci of *Francisella novicida* associated with intracellular growth. *FEMS Microbiol. Lett.* 215, 53–56. doi: 10.1111/j.1574-6968.2002.tb11369.x
- Haapalainen, M., Mosorin, H., Dorati, F., Wu, R. F., Roine, E., Taira, S., et al. (2012). Hcp2, a secreted protein of the phytopathogen *Pseudomonas syringae* pv. tomato DC3000, is required for fitness for competition against bacteria and yeasts. *J. Bacteriol.* 194, 4810–4822. doi: 10.1128/JB.00611-12
- Henry, T., Brotcke, A., Weiss, D. S., Thompson, L. J., and Monack, D. M. (2007). Type I interferon signaling is required for activation of the inflammasome during *Francisella* infection. *J. Exp. Med.* 204, 987–994. doi: 10.1084/jem.20062665
- Heymann, J. B., Bartho, J. D., Rybakova, D., Venugopal, H. P., Winkler, D. C., Sen, A., et al. (2013). Three-dimensional structure of the toxin-delivery particle antifeeding prophage of *Serratia entomophila*. *J. Biol. Chem.* 288, 25276–25284. doi: 10.1074/jbc.M113.456145
- Higerd, T. B., Baechler, C. A., and Berk, R. S. (1969). Morphological studies on relaxed and contracted forms of purified pyocin particles. *J. Bacteriol.* 98, 1378–1389.
- Ho, B. T., Dong, T. G., and Mekalanos, J. J. (2014). A view to a kill: the bacterial type VI secretion system. *Cell Host Microbe* 15, 9–21. doi: 10.1016/j.chom.2013.11.008
- Hood, R. D., Peterson, S. B., and Mougou, J. D. (2017). From striking out to striking gold: discovering that type VI secretion targets bacteria. *Cell Host Microbe* 21, 286–289. doi: 10.1016/j.chom.2017.02.001
- Johansson, A., Celli, J., Conlan, W., Elkins, K. L., Forsman, M., Keim, P. S., et al. (2010). Objections to the transfer of *Francisella novicida* to the subspecies rank of *Francisella tularensis*. *Int. J. Syst. Evol. Microbiol.* 60, 1718–1720. doi: 10.1099/ijs.0.022830-0
- Jones, D. T., Taylor, W. R., and Thornton, J. M. (1992). The rapid generation of mutation data matrices from protein sequences. *Comput. Appl. Biosci.* 8, 275–282. doi: 10.1093/bioinformatics/8.3.275
- Journet, L., and Cascales, E. (2016). The type VI secretion system in *Escherichia coli* and related species. *EcoSal Plus* 7, 1–20. doi: 10.1128/ecosalplus.ESP-0009-2015
- Kudryashev, M., Wang, R. Y., Brackmann, M., Scherer, S., Maier, T., Baker, D., et al. (2015). Structure of the type VI secretion system contractile sheath. *Cell* 160, 952–962. doi: 10.1016/j.cell.2015.01.037
- Kumar, S., Stecher, G., and Tamura, K. (2016). MEGA7: molecular evolutionary genetics analysis version 7.0 for bigger datasets. *Mol. Biol. Evol.* 33, 1870–1874. doi: 10.1093/molbev/msw054

- Lai, X. H., Golovliov, I., and Sjöstedt, A. (2001). *Francisella tularensis* induces cytopathogenicity and apoptosis in murine macrophages via a mechanism that requires intracellular bacterial multiplication. *Infect. Immun.* 69, 4691–4694. doi: 10.1128/IAI.69.7.4691-4694.2001
- Lai, X. H., Golovliov, I., and Sjöstedt, A. (2004). Expression of IglC is necessary for intracellular growth and induction of apoptosis in murine macrophages by *Francisella tularensis*. *Microb. Pathog.* 37, 225–230. doi: 10.1016/j.micpath.2004.07.002
- Legrand, P., Collins, B., Blangy, S., Murphy, J., Spinelli, S., Gutierrez, C., et al. (2016). The atomic structure of the phage Tuc2009 baseplate tripod suggests that host recognition involves two different carbohydrate binding modules. *mBio* 7:e01781-15. doi: 10.1128/mBio.01781-15
- Leiman, P. G., Chipman, P. R., Kostyuchenko, V. A., Mesyanzhinov, V. V., and Rossmann, M. G. (2004). Three-dimensional rearrangement of proteins in the tail of bacteriophage T4 on infection of its host. *Cell* 118, 419–429. doi: 10.1016/j.cell.2004.07.022
- Leiman, P. G., and Shneider, M. M. (2012). Contractile tail machines of bacteriophages. *Adv. Exp. Med. Biol.* 726, 93–114. doi: 10.1007/978-1-4614-0980-9_5
- Lindgren, H., Golovliov, I., Baranov, V., Ernst, R. K., Telepnev, M., and Sjöstedt, A. (2004). Factors affecting the escape of *Francisella tularensis* from the phagolysosome. *J. Med. Microbiol.* 53, 953–958. doi: 10.1099/jmm.0.45685-0
- Logger, L., Aschtgen, M. S., Guérin, M., Cascales, E., and Durand, E. (2016). Molecular dissection of the interface between the type VI secretion TssM cytoplasmic domain and the TssG baseplate component. *J. Mol. Biol.* 428, 4424–4437. doi: 10.1016/j.jmb.2016.08.032
- Long, M. E., Lindemann, S. R., Rasmussen, J. A., Jones, B. D., and Allen, L. A. (2013). Disruption of *Francisella tularensis* Schu S4 iglI, iglJ, and pdpC genes results in attenuation for growth in human macrophages and *in vivo* virulence in mice and reveals a unique phenotype for pdpC. *Infect. Immun.* 81, 850–861. doi: 10.1128/IAI.00822-12
- Ludu, J. S., de Bruin, O. M., Duplantier, B. N., Schmerk, C. L., Chou, A. Y., Elkins, K. L., et al. (2008). The *Francisella* pathogenicity island protein PdpD is required for full virulence and associates with homologues of the type VI secretion system. *J. Bacteriol.* 190, 4584–4595. doi: 10.1128/JB.00198-08
- Ma, L. S., Lin, J. S., and Lai, E. M. (2009). An IcmF family protein, ImpLM, is an integral inner membrane protein interacting with ImpKL, and its walker a motif is required for type VI secretion system-mediated Hcp secretion in *Agrobacterium tumefaciens*. *J. Bacteriol.* 191, 4316–4329. doi: 10.1128/JB.00029-09
- Ma, L. S., Narberhaus, F., and Lai, E. M. (2012). IcmF family protein TssM exhibits ATPase activity and energizes type VI secretion. *J. Biol. Chem.* 287, 15610–15621. doi: 10.1074/jbc.M111.301630
- Man, S. M., Karki, R., Malireddi, R. K., Neale, G., Vogel, P., Yamamoto, M., et al. (2015). The transcription factor IRF1 and guanylate-binding proteins target activation of the AIM2 inflammasome by *Francisella* infection. *Nat. Immunol.* 16, 467–475. doi: 10.1038/ni.3118
- Mariathasan, S., Weiss, D. S., Dixit, V. M., and Monack, D. M. (2005). Innate immunity against *Francisella tularensis* is dependent on the ASC/caspase-1 axis. *J. Exp. Med.* 202, 1043–1049. doi: 10.1084/jem.20050977
- Meunier, E., Wallet, P., Dreier, R. F., Costanzo, S., Anton, L., Rühl, S., et al. (2015). Guanylate-binding proteins promote activation of the AIM2 inflammasome during infection with *Francisella novicida*. *Nat. Immunol.* 16, 476–484. doi: 10.1038/ni.3119
- Mougous, J. D., Cuff, M. E., Raunser, S., Shen, A., Zhou, M., Gifford, C. A., et al. (2006). A virulence locus of *Pseudomonas aeruginosa* encodes a protein secretion apparatus. *Science* 312, 1526–1530. doi: 10.1126/science.1128393
- Murch, A. L., Skipp, P. J., Roach, P. L., and Oyston, P. C. F. (2017). Whole genome transcriptomics reveals global effects including up-regulation of *Francisella* pathogenicity island gene expression during active stringent response in the highly virulent *Francisella tularensis* subsp. *tularensis* SCHU S4. *Microbiology* 163, 1664–1679. doi: 10.1099/mic.0.000550
- Nano, F. E., Zhang, N., Cowley, S. C., Klose, K. E., Cheung, K. K., Roberts, M. J., et al. (2004). A *Francisella tularensis* pathogenicity island required for intramacrophage growth. *J. Bacteriol.* 186, 6430–6436. doi: 10.1128/JB.186.19.6430-6436.2004
- Nazarov, S., Schneider, J. P., Brackmann, M., Goldie, K. N., Stahlberg, H., and Basler, M. (2018). Cryo-EM reconstruction of type VI secretion system baseplate and sheath distal end. *EMBO J.* 37:e97103. doi: 10.15252/embj.201797103
- Nguyen, J. Q., Gilley, R. P., Zogaj, X., Rodriguez, S. A., and Klose, K. E. (2014). Lipidation of the FPI protein IglE contributes to *Francisella tularensis* ssp. *novicida* intramacrophage replication and virulence. *Pathog. Dis.* 72, 10–18. doi: 10.1111/2049-632X.12167
- Nguyen, V. S., Logger, L., Spinelli, S., Legrand, P., Huyen Pham, T. T., Nhung Trinh, T. T., et al. (2017). Type VI secretion TssK baseplate protein exhibits structural similarity with phage receptor-binding proteins and evolved to bind the membrane complex. *Nat. Microbiol.* 2:17103. doi: 10.1038/nmicrobiol.2017.103
- Pell, L. G., Kanelis, V., Donaldson, L. W., Lynne Howell, P. L., and Davidson, A. R. (2009). The phage λ major tail protein structure reveals a common evolution for long-tailed phages and the type VI bacterial secretion system. *Proc. Natl. Acad. Sci. U.S.A.* 106, 4160–4165. doi: 10.1073/pnas.0900044106
- Petersen, E. F., Goddard, T. D., Huang, C. C., Couch, G. S., Greenblatt, D. M., Meng, E. C., et al. (2004). UCSF Chimera—a visualization system for exploratory research and analysis. *J. Comput. Chem.* 25, 1605–1612. doi: 10.1002/jcc.20084
- Pietrosiuk, A., Lenherr, E. D., Falk, S., Bönemann, G., Kopp, J., Zentgraf, H., et al. (2011). Molecular basis for the unique role of the AAA+ chaperone ClpV in type VI protein secretion. *J. Biol. Chem.* 286, 30010–30021. doi: 10.1074/jbc.M111.253377
- Planamente, S., Salih, O., Manoli, E., Albesa-Jové, D., Freemont, P. S., and Filloux, A. (2016). TssA forms a gp6-like ring attached to the type VI secretion sheath. *EMBO J.* 35, 1613–1627. doi: 10.15252/embj.201694024
- Pukatzki, S., Ma, A. T., Revel, A. T., Sturtevant, D., and Mekalanos, J. J. (2007). Type VI secretion system translocates a phage tail spike-like protein into target cells where it cross-links actin. *Proc. Natl. Acad. Sci. U.S.A.* 104, 15508–15513. doi: 10.1073/pnas.0706532104
- Pukatzki, S., Ma, A. T., Sturtevant, D., Krastins, B., Sarracino, D., Nelson, W. C., et al. (2006). Identification of a conserved bacterial protein secretion system in *Vibrio cholerae* using the Dictyostelium host model system. *Proc. Natl. Acad. Sci. U.S.A.* 103, 1528–1533. doi: 10.1073/pnas.0510322103
- Rao, P. S., Yamada, Y., Tan, Y. P., and Leung, K. Y. (2004). Use of proteomics to identify novel virulence determinants that are required for *Edwardsiella tarda* pathogenesis. *Mol. Microbiol.* 53, 573–586. doi: 10.1111/j.1365-2958.2004.04123.x
- Rao, V. A., Shepherd, S. M., English, G., Coulthurst, S. J., and Hunter, W. N. (2011). The structure of *Serratia marcescens* Lip, a membrane-bound component of the type VI secretion system. *Acta Crystallogr. D Biol. Crystallogr.* 67, 1065–1072. doi: 10.1107/S0907444911046300
- Rigard, M., Bröms, J. E., Mosnier, A., Hologne, M., Martin, A., Lindgren, L., et al. (2016). *Francisella tularensis* IglG belongs to a novel family of PAAR-like T6SS proteins and harbors a unique N-terminal extension required for virulence. *PLoS Pathog.* 12:e1005821. doi: 10.1371/journal.ppat.1005821
- Robb, C. S., Nano, F. E., and Boraston, A. B. (2012). The structure of the conserved type six secretion protein TssL (DotU) from *Francisella novicida*. *J. Mol. Biol.* 419, 277–283. doi: 10.1016/j.jmb.2012.04.003
- Robertson, G. T., Child, R., Ingle, C., Celli, J., and Norgard, M. V. (2013). IglE is an outer membrane-associated lipoprotein essential for intracellular survival and murine virulence of type A *Francisella tularensis*. *Infect. Immun.* 81, 4026–4040. doi: 10.1128/IAI.00595-13
- Russell, A. B., Peterson, S. B., and Mougous, J. D. (2014a). Type VI secretion system effectors: poisons with a purpose. *Nat. Rev. Microbiol.* 12, 137–148. doi: 10.1038/nrmicro3185
- Russell, A. B., Wexler, A. G., Harding, B. N., Whitney, J. C., Bohn, A. J., Goo, Y. A., et al. (2014b). A type VI secretion-related pathway in *Bacteroidetes* mediates interbacterial antagonism. *Cell Host Microbe* 16, 227–236. doi: 10.1016/j.chom.2014.07.007
- Sana, T. G., Berni, B., and Blevess, S. (2016). The T6SSs of *Pseudomonas aeruginosa* Strain PAO1 and Their effectors: beyond bacterial-cell targeting. *Front. Cell. Infect. Microbiol.* 6:61. doi: 10.3389/fcimb.2016.00061
- Sana, T. G., Hachani, A., Bucior, I., Soscia, C., Garvis, S., Termine, E., et al. (2012). The second type VI secretion system of *Pseudomonas aeruginosa* strain PAO1 is regulated by quorum sensing and Fur and modulates internalization

- in epithelial cells. *J. Biol. Chem.* 287, 27095–27105. doi: 10.1074/jbc.M112.376368
- Santin, Y. G., and Cascales, E. (2017). Domestication of a housekeeping transglycosylase for assembly of a Type VI secretion system. *EMBO Rep.* 18, 138–149. doi: 10.15252/embr.201643206
- Saslaw, S., Eigelsbach, H. T., Prior, J. A., Wilson, H. E., and Carhart, S. (1961a). Tularemia vaccine study. I: intracutaneous challenge. *Arch. Intern. Med.* 107, 121–133. doi: 10.1001/archinte.1961.03620050055006
- Saslaw, S., Eigelsbach, H. T., Prior, J. A., Wilson, H. E., and Carhart, S. (1961b). Tularemia vaccine study. II. respiratory challenge. *Arch. Intern. Med.* 107, 702–714. doi: 10.1001/archinte.1961.03620050068007
- Schwarz, S., West, T. E., Boyer, F., Chiang, W. C., Carl, M. A., Hood, R. D., et al. (2010). Burkholderia type VI secretion systems have distinct roles in eukaryotic and bacterial cell interactions. *PLoS Pathog.* 6:e1001068. doi: 10.1371/journal.ppat.1001068
- Shikuma, N. J., Pilhofer, M., Weiss, G. L., Hadfield, M. G., Jensen, G. J., and Newman, D. K. (2014). Marine tubeworm metamorphosis induced by arrays of bacterial phase tail-like structures. *Science* 343, 529–533. doi: 10.1126/science.1246794
- Shneider, M. M., Buth, S. A., Ho, B. T., Basler, M., Mekalanos, J. J., and Leiman, P. G. (2013). PAAR-repeat proteins sharpen and diversify the type VI secretion system spike. *Nature* 500, 350–353. doi: 10.1038/nature12453
- Silverman, J. M., Agnello, D. M., Zheng, H., Andrews, B. T., Li, M., Catalano, C. E., et al. (2013). Haemolysin coregulated protein is an exported receptor and chaperone of type VI secretion substrates. *Mol. Cell* 51, 584–593. doi: 10.1016/j.molcel.2013.07.025
- Steele, S., Radlinski, L., Taft-Benz, S., Brunton, J., and Kawula, T. H. (2016). Trogocytosis-associated cell to cell spread of intracellular bacterial pathogens. *Elife* 5:e10625. doi: 10.7554/eLife.10625
- Suarez, G., Sierra, J. C., Erova, T. E., Sha, J., Horneman, A. J., and Chopra, A. K. (2010). A type VI secretion system effector protein, VgrG1, from *Aeromonas hydrophila* that induces host cell toxicity by ADP ribosylation of actin. *J. Bacteriol.* 192, 155–168. doi: 10.1128/JB.01260-09
- Suarez, G., Sierra, J. C., Sha, J., Wang, S., Erova, T. E., Fadl, A. A., et al. (2008). Molecular characterization of a functional type VI secretion system from a clinical isolate of *Aeromonas hydrophila*. *Microb. Pathog.* 44, 344–361. doi: 10.1016/j.micpath.2007.10.005
- Sun, P., Austin, B. P., Schubot, F. D., and Waugh, D. S. (2007). New protein fold revealed by a 1.65 Å resolution crystal structure of *Francisella tularensis* pathogenicity island protein IglC. *Protein Sci.* 16, 2560–2563. doi: 10.1110/ps.073177307
- Taylor, N. M., Prokhorov, N. S., Guerrero-Ferreira, R. C., Shneider, M. M., Browning, C., Goldie, K. N., et al. (2016). Structure of the T4 baseplate and its function in triggering sheath contraction. *Nature* 533, 346–352. doi: 10.1038/nature17971
- Uda, A., Sekizuka, T., Tanabayashi, K., Fujita, O., Kuroda, M., Hotta, A., et al. (2014). Role of pathogenicity determinant protein C (PdpC) in determining the virulence of the *Francisella tularensis* subspecies tularensis SCHU. *PLoS ONE* 9:e89075. doi: 10.1371/journal.pone.0089075
- Wang, J., Brackmann, M., Castaño-Diez, D., Kudryashev, M., Goldie, K. N., Maier, T., et al. (2017). Cryo-EM structure of the extended type VI secretion system sheath-tube complex. *Nat. Microbiol.* 2, 1507–1512. doi: 10.1038/s41564-017-0020-7
- Weber, B. S., Hennon, S. W., Wright, M. S., Scott, N. E., de Berardinis, V., Foster, L. J., et al. (2016). Genetic dissection of the type VI secretion system in *Acinetobacter* and identification of a novel peptidoglycan hydrolase, TagX, required for its biogenesis. *MBio* 7:e01253-16. doi: 10.1128/mBio.01253-16
- Wehrly, T. D., Chong, A., Virtaneva, K., Sturdevant, D. E., Child, R., Edwards, J. A., et al. (2009). Intracellular biology and virulence determinants of *Francisella tularensis* revealed by transcriptional profiling inside macrophages. *Cell. Microbiol.* 11, 1128–1150. doi: 10.1111/j.1462-5822.2009.01316.x
- Weiss, D. S., Brotcke, A., Henry, T., Margolis, J. J., Chan, K., and Monack, D. M. (2007a). *In vivo* negative selection screen identifies genes required for *Francisella* virulence. *Proc. Natl. Acad. Sci. U.S.A.* 104, 6037–6042. doi: 10.1073/pnas.0609675104
- Weiss, D. S., Henry, T., and Monack, D. M. (2007b). *Francisella tularensis*: activation of the inflammasome. *Ann. N. Y. Acad. Sci.* 1105, 219–237. doi: 10.1196/annals.1409.005
- Whitney, J. C., Beck, C. M., Goo, Y. A., Russell, A. B., Harding, B. N., De Leon, J. A., et al. (2014). Genetically distinct pathways guide effector export through the type VI secretion system. *Mol. Microbiol.* 92, 529–542. doi: 10.1111/mmi.12571
- Williams, S. G., Varcoe, L. T., Attridge, S. R., and Manning, P. A. (1996). *Vibrio cholerae* Hcp, a secreted protein coregulated with HlyA. *Infect. Immun.* 64, 283–289.
- Zheng and Leung, K. Y. (2007). Dissection of a type VI secretion system in *Edwardsiella tarda*. *Mol. Microbiol.* 66, 1192–1206. doi: 10.1111/j.1365-2958.2007.05993.x
- Zoued, A., Cassaro, C. J., Durand, E., Douzi, B., España, A. P., Cambillau, C., et al. (2016a). Structure-function analysis of the TssL cytoplasmic domain reveals a new interaction between the type VI secretion baseplate and membrane complexes. *J. Mol. Biol.* 428, 4413–4423. doi: 10.1016/j.jmb.2016.08.030
- Zoued, A., Durand, E., Bebeacua, C., Brunet, Y. R., Douzi, B., Cambillau, C., et al. (2013). TssK is a trimeric cytoplasmic protein interacting with components of both phage-like and membrane anchoring complexes of the type VI secretion system. *J. Biol. Chem.* 288, 27031–27041. doi: 10.1074/jbc.M113.499772
- Zoued, A., Durand, E., Brunet, Y. R., Spinelli, S., Douzi, B., Guzzo, M., et al. (2016b). Priming and polymerization of a bacterial contractile tail structure. *Nature* 531, 59–63. doi: 10.1038/nature17182
- Zoued, A., Durand, E., Santin, Y. G., Jounet, L., Roussel, A., Cambillau, C., et al. (2017). TssA: the cap protein of the type VI secretion system tail. *Bioessays* 39:1600262. doi: 10.1002/bies.201600262

Conflict of Interest Statement: The authors declare that the research was conducted in the absence of any commercial or financial relationships that could be construed as a potential conflict of interest.

Copyright © 2018 Clemens, Lee and Horwitz. This is an open-access article distributed under the terms of the Creative Commons Attribution License (CC BY). The use, distribution or reproduction in other forums is permitted, provided the original author(s) and the copyright owner are credited and that the original publication in this journal is cited, in accordance with accepted academic practice. No use, distribution or reproduction is permitted which does not comply with these terms.



Environmental Surveillance of Zoonotic *Francisella tularensis* in the Netherlands

Ingmar Janse*, Rozemarijn Q. J. van der Plaats, Ana Maria de Roda Husman and Mark W. J. van Passel

Zoonoses and Environmental Microbiology, Centre for Infectious Diseases Control, National Institute for Public Health and the Environment, Bilthoven, Netherlands

OPEN ACCESS

Edited by:

Anders Sjöstedt,
Umeå University, Sweden

Reviewed by:

Sam Telford,
Tufts University, United States
Mats Forsman,
Swedish Defence Research Agency,
Sweden

*Correspondence:

Ingmar Janse
ingmar.janse@rivm.nl

Received: 16 January 2018

Accepted: 18 April 2018

Published: 08 May 2018

Citation:

Janse I, van der Plaats RQJ, de Roda Husman AM and van Passel MWJ (2018) Environmental Surveillance of Zoonotic *Francisella tularensis* in the Netherlands.
Front. Cell. Infect. Microbiol. 8:140.
doi: 10.3389/fcimb.2018.00140

Tularemia is an emerging zoonosis caused by the Gram-negative bacterium *Francisella tularensis*, which is able to infect a range of animal species and humans. Human infections occur through contact with animals, ingestion of food, insect bites or exposure to aerosols or water, and may lead to serious disease. *F. tularensis* may persist in aquatic reservoirs. In the Netherlands, no human tularemia cases were notified for over 60 years until in 2011 an endemic patient was diagnosed, followed by 17 cases in the 6 years since. The re-emergence of tularemia could be caused by changes in reservoirs or transmission routes. We performed environmental surveillance of *F. tularensis* in surface waters in the Netherlands by using two approaches. Firstly, 339 samples were obtained from routine monitoring -not related to tularemia- at 127 locations that were visited between 1 and 8 times in 2015 and 2016. Secondly, sampling efforts were performed after reported tularemia cases (n = 8) among hares or humans in the period 2013–2017. *F. tularensis* DNA was detected at 17% of randomly selected surface water locations from different parts of the country. At most of these positive locations, DNA was not detected at each time point and levels were very low, but at two locations contamination was clearly higher. From 7 out of the 8 investigated tularemia cases, *F. tularensis* DNA was detected in at least one surface water sample collected after the case. By using a protocol tailored for amplification of low amounts of environmental DNA, 10 gene targets were sequenced. Presence of *F. tularensis* subspecies *holarctica* was confirmed in 4 samples, and in 2 of these, clades B.12 and B.6 were identified. This study shows that for tularemia, information regarding the spatial and temporal distribution of its causative agent could be derived from environmental surveillance of surface waters. Tracking a particular strain in the environment as source of infection is feasible and could be substantiated by genotyping, which was achieved in water samples with only low levels of *F. tularensis* present. These techniques allow the establishment of a link between tularemia cases and environmental samples without the need for cultivation.

Keywords: *Francisella tularensis* *holarctica*, tularemia, environmental surveillance, surface water, case-related sampling, genotyping, subclades, zoonosis

INTRODUCTION

Tularemia is a zoonosis with a human, animal and environmental component. The disease is caused by the Gram-negative bacterium *Francisella tularensis*, which is able to infect different species of animals besides humans. Disease in humans and animals is mostly caused by subspecies *tularensis* (type A) and *holarctica* (type B) (Hestvik et al., 2015). The infectious dose is very low and infection can cause many different symptoms, ranging from fever and skin ulcers to life-threatening pneumonia. Human infections occur through direct contact with infected animals, ingestion of food or water, insect bites or exposure to aerosols or water (WHO, 2007). Disease incidence due to infections with subspecies *holarctica* has been shown to be higher near lakes and rivers (Desvars et al., 2015). *F. tularensis* has been detected in various types of surface waters and sediments (Petersen et al., 2009; Broman et al., 2011; Janse et al., 2017) where the bacterium can be hosted by free-living protozoa and may reside in biofilms (Abd et al., 2003; Sinclair et al., 2008; van Hoek, 2013).

In the Netherlands, a patient was diagnosed with tularemia in 2011, which was the first indigenous case since 1953 (Maraha et al., 2013). Since then, occasional human cases (17 in total) have been reported. Also, after surveillance of dead hares started in 2011 (Janse et al., 2017), several *Francisella*-infected hares were identified in the same period. These human and hare tularemia cases from 2011 to 2017 occurred dispersed in time and space (van de Wetering et al., 2015; Pijnacker et al., 2016; Janse et al., 2017; Zijlstra et al., 2017), which suggests a widespread occurrence and the existence of an endemic cycle of the pathogen. In 2015, environmental surveillance following a tularemia epizootic among hares in Friesland (northern Netherlands) revealed the presence of *F. tularensis* DNA in surface water and sediments (Janse et al., 2017). Surveillance data can be used to signal potential public health threats, but also to better understand the environmental components that may drive changes in the abundance of pathogenic microbes. The apparent re-emergence of tularemia could be caused by changes in the numbers or genotypes of *F. tularensis*, and by changes in transmission routes to humans or animals. In turn, such changes could be caused by changes in host populations or the environment as a result of altered land and water usage or climate. The effects of variations in reservoirs and transmission routes could be noticeable on a local scale. Biogeographical data of presence and absence may point to habitat features that could benefit growth and/or persistence of *F. tularensis*.

We performed an environmental surveillance to gain insight into the distribution of *F. tularensis* in surface waters throughout the Netherlands. Surface water samples were obtained from monitoring programs not related to disease, as well as from location-specific sampling efforts performed after reported tularemia cases among hares or humans. Presence of *F. tularensis* DNA in surface waters was investigated and genotyping was performed to confirm the presence of *F. tularensis* subspecies *holarctica* and to further identify subclades.

MATERIALS AND METHODS

Sample Collection and Processing

Two different environmental surveillance approaches were used to obtain three sets of surface water samples. The first approach used water samples from locations which had not been selected based on signals indicating the presence of tularemia. Based on this approach, two sets of samples were obtained. The first set (set I) of 160 samples was collected at 51 locations in 2015 by Rijkswaterstaat (RWS, the executive agency of the Ministry of Infrastructure and Water management of the Netherlands) for a research project not related to tularemia. Samples were collected from week 17 to 40 (not evenly spread) and the number of samples per location ranged between 1 and 8 (Table 1). Surface waters included mostly freshwater, but also several brackish and saltwater locations. The second set (set II) consisted of 179 surface water samples collected at 76 locations by 9 Dutch water boards in 2016. Samples were collected from week 15 to 44 (not evenly spread) and the number of samples per location ranged between 1 and 6 (Table 1). Surface waters included only freshwater and sites were chosen from the routine monitoring program for surface water quality by the cooperating water boards. Selection criteria were locations spanning diverse water types, including small water bodies, and locations where sampling was repeated in order to include temporal variation. The selection of sampling sites was unrelated to tularemia cases, although two locations in Friesland (northern Netherlands) had a geographical link with tularemia as they were situated in an area where a hare epizootic occurred in the previous year (Janse et al., 2017). However, these samples were collected almost a year after the peak of this outbreak.

In the second environmental surveillance approach, sampling was performed near locations of notified tularemia cases in humans or hares. Based on this approach, a third set of 130 samples (set III) was collected in 8 different geographical regions in the period from 2013 to 2017 (Table 1). Locations for casus-related sampling were selected as follows. In the Netherlands, tularemia is a notifiable disease in humans since November 2016, but in the preceding period, cases were also monitored (Janse et al., 2017). In the period from 2015 to 2017, there were several human tularemia cases with a potential environmental infection source. In the same period, dead hares were also investigated for tularemia, which resulted in the recognition of several confirmed tularemia cases. Eight of these human or hare signals which could be linked to a possible exposure site were followed up by the collection of between 4 and 77 surface water samples (Table 1). Indications for sampling locations based on human cases ranged from the home address of a patient who had not had direct contact with water to an obvious exposure during a mud run event (Zijlstra et al., 2017). Sampling locations based on tularemia confirmed in dead hares was based on the finding location of these hares. After 5 cases, samples were collected at one single time point, whereas after 3 cases follow-up sampling was carried out as well (Table 1). A follow-up sample collected at Maarsseveen (MV) was included because a second human tularemia case possibly linked to environmental exposure had been recognized in the same area. In Friesland (FL) and in

TABLE 1 | Surface water samples collected for environmental surveillance.

	Samples		Locations								
			Total	Frequency (number of time points)							
				1	2	3	4	5	6	7	8
I (2015)		160	51	11	9	13	10		5	2	1
II (2016)		179	76	19	29	24			5		
III (2013-17)	MB (2013)	4	4	4							
	FL (2015)	77	42	26	4	8	2	2			
	MV (2015)	5	4	3	1						
	ZL (2015)	5	5	5							
	HB (2016)	14	14	14							
	FP (2016)	8	7	6	1						
	LB (2016)	5	5	5							
	RH (2017)	9	9	9							

The table displays for each dataset (I, II and III) the total number of samples, the total number of locations where these were collected and the number of locations where sampling was repeated between 1 to 8 time points.

the Flevopolder (FP), follow-up samples were collected because of the relatively high levels of *F. tularensis* DNA in the first surface water samples. Most results from the Friesland cluster were described in an earlier communication (Janse et al., 2017), but the current report includes additional samples from a wider area.

Water samples collected in 1 L flasks were transported to the laboratory. Water was filtered using Tuffryn membrane filters (Pall Life Sciences, Ann Arbor, USA) with a pore size of 0.45 μ m until they clogged, after which the filters were stored at -20° . DNA was extracted from the filters by using the PowerWater DNA extraction kit (Qiagen, Hilden, Germany) according to the manufacturer's recommendations.

Detection of *F. tularensis* DNA

To detect *F. tularensis* DNA, both undiluted and 10x diluted extracts were analyzed in triplicate by using qPCR (Janse et al., 2010). This multiplex assay includes multi-copy signature sequence *ISFtu2* and single-copy gene *fopA* for the detection of *F. tularensis* species. Subspecies *holarctica*, *tularemia*, *novicida* and *mediasiatica* are all detected. Marker (*pdpD*) for differentiation between subtypes A (*F. tularensis tularensis*) and B (*F. tularensis holarctica*) was not included in the assay because subtype A is not encountered in Europe and it was not detected in surface water samples analyzed previously (Janse et al., 2017). To enable comparison of DNA levels between samples that can also be easily visualized, positive qPCR results were binned into 5 categories as follows. Level 1 = *ISFtu2* detected 1 or 2 out of 3; Level 2 = *ISFtu2* detected 3 out of 3; Level 3 = *ISFtu2* detected 3 out of 3 and Cq value < 33; Level 4 = *ISFtu2* detected 3 out of 3 and *fopA* detected 1 or 2 out of 3; Level 5 = Both *ISFtu2* and *fopA* detected 3 out of 3. Binning was based on the fact that increasing amounts of *F. tularensis* gDNA subsequently increase the chance of detecting target in each replicate reaction, result in lower Cq values and increase detection of single-copy target *fopA* in addition to multicopy target *ISFtu2*.

Sequence Analysis

Primers were used for amplification of *F. tularensis* DNA for subsequent sequence analysis. Sequences that were targeted included the genes used for the detection (*ISFtu2* and *fopA*), and a selection of 8 additional genes which could be used for the differentiation of subclades. Gene selection was based on studies developing genotyping assays (Svensson et al., 2009; Vogler et al., 2009; Birdsell et al., 2014). Primers for the amplification of *ISFtu2* and *fopA* had been described previously (Janse et al., 2010) and spanned larger gene fragments (524 and 428 bp, respectively) than those used for qPCR detection (89 and 115 bp, respectively). Novel oligonucleotides were designed using the software package Visual Oligonucleotide Modeling Platform (DNA software Inc. Ann Arbor, USA) for application in a multiplex mixture of 20 primers and amplifying a region of between 250 and 350 basepairs. Gene targets, primer sequences and amplicon sizes are displayed in Supplemental Table S1.

Sequences were amplified by using a two-step protocol. In the first step, amplification was performed by using the SSO pre-amplification kit (Bio-Rad, California, USA) in reactions containing all 20 primers mixed at a final concentration of 50 nM each. Thermocycling conditions were as follows: 95°C for 3 min, 14 cycles at 95°C for 15 s, 56°C for 240 s. Thermocycling reactions were carried out in a C1000 Touch combined with a S1000 Thermal Cycler (Bio-Rad, California, USA). Subsequently, primers were removed by incubation with 0.6 U/ μ l final concentration Exonuclease I (New England Biolabs, Massachusetts, USA) 37°C for 30 min, followed by enzyme inactivation at 80°C for 15 min. The reaction was diluted 5x in Tris-EDTA buffer solution and these amplified materials were used for a second step during which each target sequence was amplified in a separate PCR reaction. The Qiagen multiplex PCRkit (Qiagen, Hilden, Germany) was used for this amplification, primers were present at a final concentration of 200 nM. Thermocycling conditions were as follows: 95°C for 15 min, 35 cycles at 94°C for 30 s, 57°C for 90 s, and 72°C

for 90 s, followed by a final step at 72°C for 10 min. Quality and quantity of PCR products were inspected on the Agilent 2100 Bioanalyzer instrument using the DNA 1000 kit (Agilent Technologies, Eindhoven, the Netherlands). To prevent cross-contamination between samples, rigorous PCR protocols were applied. Moreover, materials from control strains were utilized at low concentrations and control materials and environmental samples were processed in separate experiments. PCR products were purified by using ExoSAP-IT (USB, Cleveland, USA) and Sanger sequencing of both strands was performed by Baseclear (Leiden, the Netherlands). Sequences were deposited in Genbank under accession numbers MH156230-MH156254. Strand assembly, identification of genomes containing similar sequences by using BLAST, genome retrieval from NCBI and sequence alignment was carried out using CLCbio software (Qiagen, Hilden, Germany). The CanSNPer program (Lärkeryd et al., 2014) was used for nomenclature of the canonical SNPs with strain OSU18 (accession CP000437) as reference genome. As a positive control for amplification and sequencing of gene targets, we used strains LVS, *F. tularensis holarctica* clade B.12 (subclade B.23) and Ft7, *F. tularensis holarctica* clade B.6, which has been isolated from a Spanish patient.

RESULTS

Two different approaches were used for environmental surveillance for *F. tularensis* in the Netherlands. For the first approach, sampling locations were selected independent of recent tularemia cases. A total of 339 surface water samples were collected from 51 locations in 2015 (set I) and from 76 locations in 2016 (set II). The frequency of sampling at each location varied between 1 and 8 (Table 1). *F. tularensis* DNA was detected by using qPCR and different levels of contamination were recognized by binning positive results into 5 categories of increasing DNA concentrations (Figure 1 and Table 2). *F. tularensis* DNA was detected at 22 out of the 127 randomly selected surface water locations (17%) in different parts of the country. Positive locations included three brackish or saltwater locations (Figure 1, D, E, P). The level detected was highest at two locations (Figure 1 and Table 2, A and B), with at location A detection of the single-copy gene target *fopA* in addition to the detection of multi-copy signature sequence *ISFtu2* (Janse et al., 2010). At three locations which were sampled more than once (i.e., all but the smallest symbols in Figure 1), *F. tularensis* DNA was detected at all 3 (location D) or 2 (location A and R) time-points (Table 2 and Figure 1). In contrast, most of the positive locations that were sampled repeatedly included at least one time point when *F. tularensis* was not detected. This was true when samples had been collected at 6 (locations E and L), 3 (locations B, G, I, J, K, S) or 2 (locations C, F, H, M, N, O, P, Q, T, U) time-points (Figure 1 and Table 2). There was no significant correlation between the time of the year samples were collected and detection of *F. tularensis* DNA (data not shown).

For the second approach, a total of 127 surface water samples were collected following reported tularemia cases in hares or

humans with a possible environmental source of the infection. In 7 out of 8 of such tularemia case-related sampling efforts, *F. tularensis* DNA was detected at one or more surface water locations (Figure 2 and Tables 1, 3). *F. tularensis* DNA was detected even though the period between suspected infection and sample collection could be up to 6 weeks (Table 3). *F. tularensis* DNA was not detected in samples collected more than 2 months after a case in the South-East of the Netherlands in 2013 (MB; Table 1, Figure 2). On the other hand, it was detected in the South-West, where samples were collected one year after tularemia cases were reported from the area (ZL; Tables 1, 3, Figure 2). Higher DNA levels, including levels permitting the detection of single-copy gene *fopA*, were found after 3 tularemia cases: FL, FP and LB (Table 3 and Figure 2).

Sample collection at most locations was not repeated, with two exceptions. During the hare epizootic in Friesland mentioned above, initial sampling at several locations was followed by a second sample collection after 1 month, and locations both from within the epizootic area and from more distant locations were sampled at monthly intervals for 3 months after the epizootic had ceased. Also, after detection of *F. tularensis* DNA in surface water linked to a tularemia case with suspected environmental exposure, a follow-up sample was collected 1 month later (Table 3, FL and FP). At those locations with relatively high *F. tularensis* levels detected in the initial samples (Table 3, FL-B2, FL-B3, FL-D1 and FP-E), *F. tularensis* DNA was again detected in the follow-up sample. However, after the hare epizootic in Friesland ended, *F. tularensis* was no longer detected (Figure 1 and Tables 2, 3).

In order to confirm the presence of *F. tularensis* subspecies *holarctica*, and to enable typing to subclade level (Svensson et al., 2009; Vogler et al., 2009), sequences were obtained from DNA amplified from selected surface water samples. These samples included sample A from set II (Figure 1 and Table 2) and FL-B3, FL-D1, FP-E, LB-D from set III (Figure 2 and Table 3). Ten DNA targets (Supplemental Table S1) were sequenced from samples A and FL-D1, whereas from samples FL-B3, FP-E, and LB-D only target sequence *ISFtu2* was sequenced.

Sequence similarities between gene targets amplified from water samples and from two reference strains (Ft7 and LVS) were investigated and compared to reference sequences. Sequences from gene target *ISFtu2* amplified from samples FL-D1, FL-B3, and LB-D were identical and matched those of *F. tularensis holarctica* strains while they had mismatches with *ISFtu2* sequences from other *F. tularensis* substrains. In contrast, *ISFtu2* sequences amplified from samples A and FP-E were very different from the other samples (13 and 11% mismatches, respectively). BLAST analysis showed for samples A and FP-E highest similarity with genomes from *F. hispaniensis* (Huber et al., 2010) (6.1 and 4.7%, respectively) and *Francisella uliginis* sp. nov. (Challacombe et al., 2017) (6.7% and 5.9% mismatches, respectively). Sequences from gene target *fopA* amplified from samples FL-B3, FL-D1 and A were identical and matched those of *F. tularensis holarctica* and *F. tularensis novicida* strains. All sequences from gene

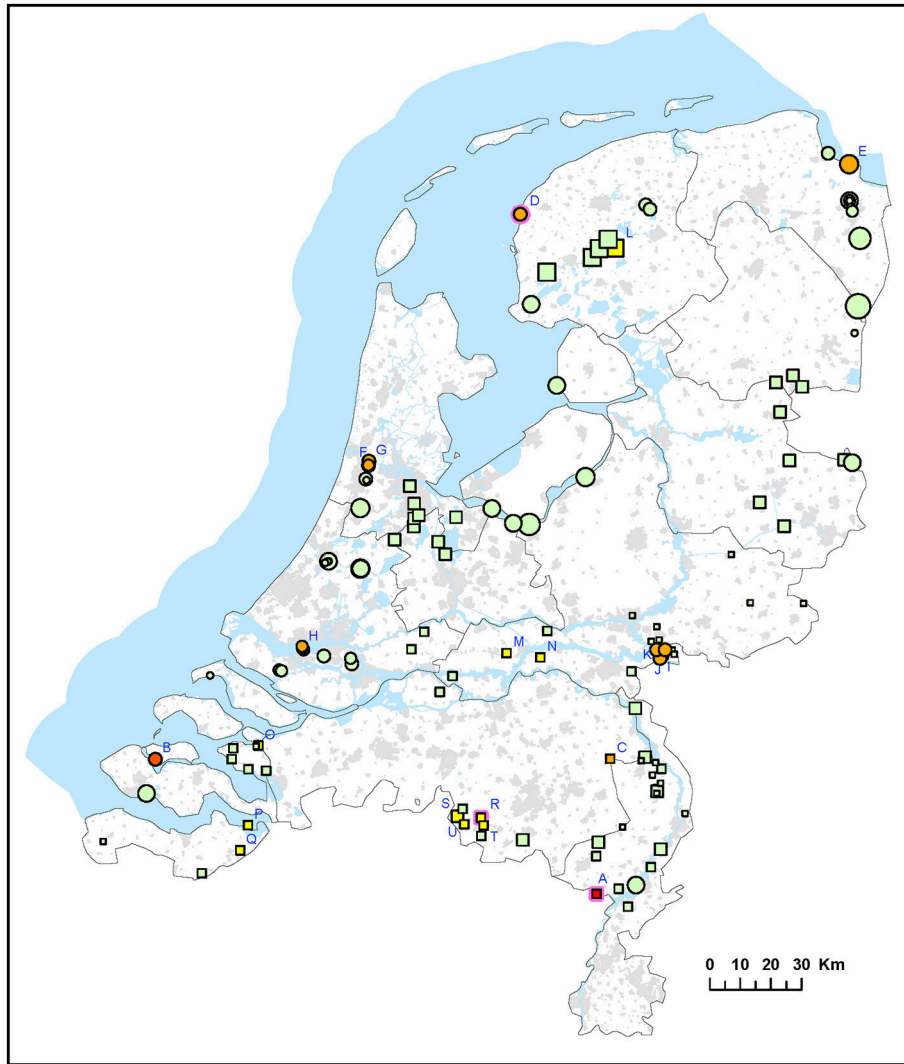


FIGURE 1 | Occurrence of *F. tularensis* in surface waters in the Netherlands. Circles represent samples collected in 2015 (sample set I) and squares represent samples collected in 2016 (sample set II). Symbol sizes correlate to the number of repeated samples obtained from a particular location (range 1-8). Colors refer to the level of *F. tularensis* DNA in the samples and ranges from 0 (DNA not detected) to 5 (highest level). Green = 0, yellow = 1, light orange = 2, dark orange = 3, light red = 4, bright red = 5. The level was based on the detection of multicopy target *ISFtu2* and singlecopy target *fopA* in triplicate qPCR measurements. When sampling was repeated, symbol color was based on the time-point with the highest DNA level. A pink halo indicates that *F. tularensis* DNA was detected at each time-point. Blue capitals cross-reference to **Table 2** which gives more details on the water samples in which *F. tularensis* was detected.

targets *putA*, FTH_0021, *pdpC1*, *ribA*, FTH_0165, FTH_1370, *aroA*, and *gph-lysR* (Supplemental Table S1) amplified from samples FL-D1 and A matched with *F. tularensis holarctica* strains. Several sequence positions had mismatches with all other *F. tularensis* species and subspecies and were thereby exclusive for *F. tularensis holarctica*. Sequence variation between *F. tularensis holarctica* strains at particular positions was used to identify subclades (Svensson et al., 2009; Lärkeryd et al., 2014). In sample FL-D1, the derived base G in target *pdpC1* (position 107819 in strain OSU18, accession CP000437) points to the presence of *F. tularensis holarctica* clade B.12 (subclade B.20). Similarly, in sample A, *F. tularensis holarctica* could be classified as clade B.6(indel Ftind49) based on a 9 bp deletion

TGGCAATTT (position 1339960–68 in strain OSU18, accession CP000437).

DISCUSSION

Spatial and Temporal Variation

F. tularensis appeared to be present at various locations throughout the Netherlands, including freshwater, brackish water and saltwater. Locations could be identified where occurrence was more prominent, as evidenced from higher levels of *F. tularensis* DNA detected and recurring detection when sampling was repeated. Most of these locations were derived from case-related surveillance (**Figure 2** and **Table 3**). Case-unrelated

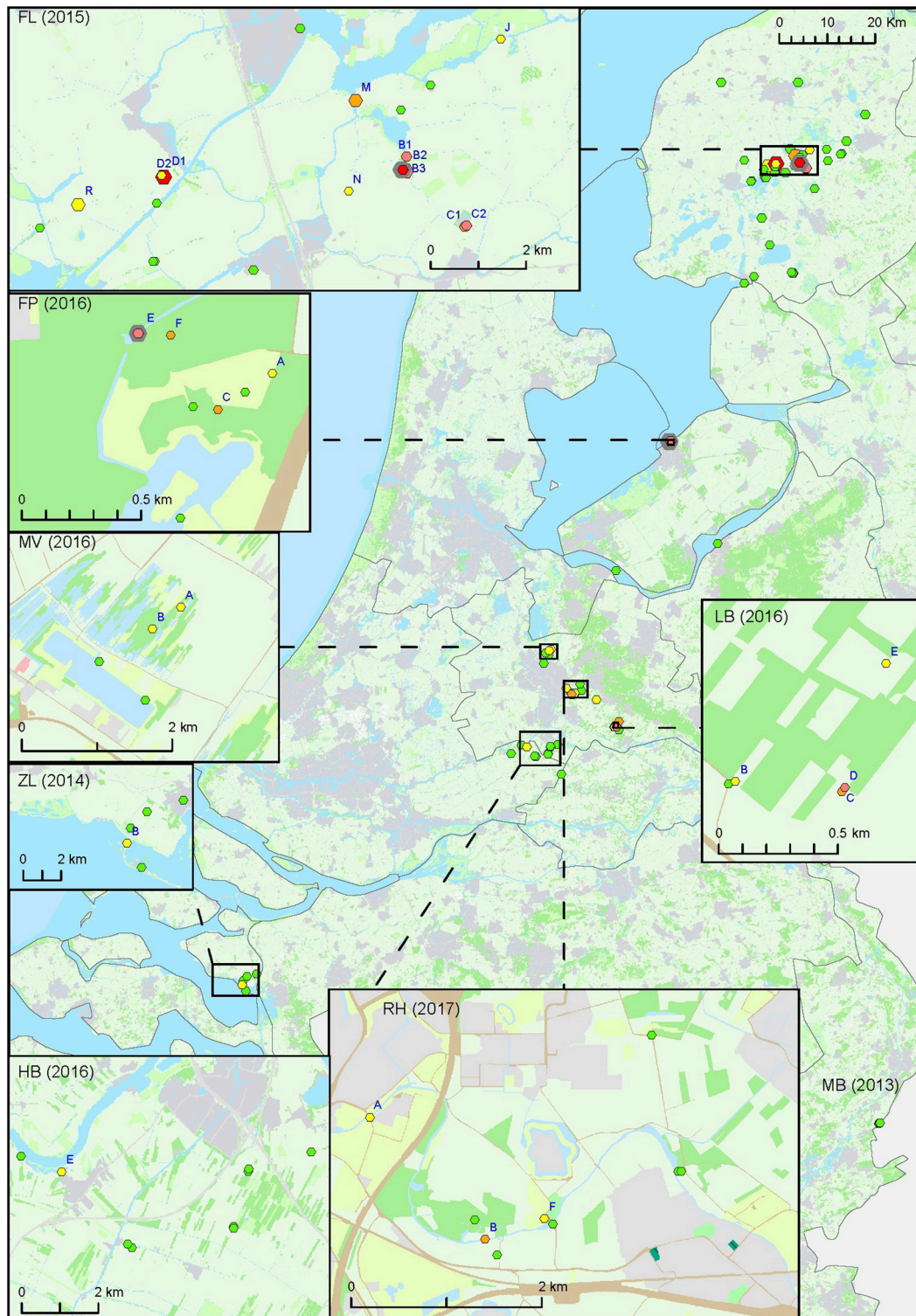


FIGURE 2 | Occurrence of *F. tularensis* in surface waters in the Netherlands following tularemia cases in humans or hares. Samples were collected between 2013 and 2017 (sample set III). Symbol sizes correlate to the number of repeated samples obtained from a particular location (range 1-8). Colors refer to the level of *F. tularensis* DNA in the samples and ranges from 0 (DNA not detected) to 5 (highest level). Green = 0, yellow = 1, light orange = 2, dark orange = 3, light red = 4, bright red = 5. The level was based on the detection of multicopy target *ISFtu2* and singlecopy target *fopA* in triplicate qPCR measurements. When sampling was repeated, symbol color was based on the time-point with the highest DNA level. A pink halo indicates that *F. tularensis* DNA was detected at each time-point. Blue capitals cross-reference to **Table 3** which gives more details on tularemia cases and water samples in which *F. tularensis* was detected.

TABLE 3 | *F. tularensis* DNA in surface water samples collected at locations with a history of tularemia cases.

case				surface water samples												
Infected host	Insert Figure 2	Year	Week	Year	Code sample	Week	Ft									
hare	FL ^a	2015	7–20 ^b	2015	FL-B1	16	4	22	0							
					FL-B2	16	4	22	2	31	0	34	0	37	0	
					FL-B3	16	5	22	4							
					FL-C1	16	2	22	0							
					FL-C2	16	4	22	0							
					FL-D1	16	5	22	2	31	1	34	0	37	0	
					FL-J			22	1							
					FL-M			22	2	31	0	34	0	37	0	
					FL-N			22	1							
					FL-R			22	1	31	0	34	0	37	0	
human	FP ^a	2016	35	2016	FP-A	40	1									
					FP-C	40	2									
					FP-E	40	4	44	4							
					FP-F	40	2									
human	MV	2015	33	2015	MV-A	39	1									
					MV-B	39	1									
hare human	LB	2016	3, 41 10	2016	LB-B	44	1									
					LB-C	44	2									
					LB-D	44	4									
					LB-E	44	1									
hare human	HB	2014	15	2016	HB-M	25	2									
					HB-N	25	1									
		2016	19		HB-E	25	1									
hare	RH	2017	20	2017	RH-A	25	1									
					RH-B	25	2									
					RH-F	25	1									
hare human	ZL	2014	9–14 ^c 9–14 ^c	2015	ZL-B	22	1									

Numbers refer to the level of *F. tularensis* DNA detected in the samples, ranging from 0 (not detected) to 5 (highest level).

^aCase references; FL: (Janse et al., 2017), FP: (Zijlstra et al., 2017).

^bMultiple hares were found during this period.

^cOnly month in which case occurred is known.

surveillance yielded only two such locations with relatively high *F. tularensis* contamination (A and B, **Figure 1**, **Table 2**).

It is not possible to conclude absence of *F. tularensis* at a particular location. This is illustrated by the fluctuation of presence and absence between subsequent time points, which was often observed at locations with low levels of *F. tularensis* (**Tables 2**, **3**). Nevertheless, at several locations a presence of *F. tularensis* could be considered less likely as its DNA was not detected, including after repeated sampling. No common habitat features were identified for locations with different levels of *F. tularensis* contamination. Previous research had suggested a more likely *F. tularensis* occurrence in smaller water bodies such as ditches, since *F. tularensis* DNA was not detected in samples from lakes and larger canals (Janse et al., 2017). However, since

the selection of sampling locations for that study was largely based on finding sites of tularemia confirmed dead hares, smaller water bodies in rural areas were more frequently investigated. The selection of case related sampling locations (set III) in the current study was subject to a similar bias. Although 5 sampling locations were also based on human cases, the two tularemia patients with an obvious surface water exposure (swimming and a mud run) had had contact with small water bodies. The different approach used for the selection of locations for sample sets I and II in this study yielded a more diverse array of surface waters. Results from these 127 locations showed that *F. tularensis* DNA can be detected in large water bodies, including at the banks of lakes (B, **Figure 1**) and at sea shores (D, E, **Figure 1**).

The occurrence of *F. tularensis* in diverse aquatic environments, possibly involving biofilms, has been reported before (Sinclair et al., 2008; Petersen et al., 2009; Broman et al., 2011; van Hoek, 2013). Its widespread occurrence suggests diverse roles in aquatic ecosystems, which may also differ between strains and relate to their ability to associate with unicellular eukaryotes (Duodu et al., 2012). In addition, at least some of the distribution of *F. tularensis* may be explained by transient contamination by shedding from infected animals. Animals with a high bacterial load may act as amplifiers contaminating the local environment (Broman et al., 2011; Rossow et al., 2014; Schulze et al., 2016). Such contamination will be difficult to verify as tularemia in wild animals will largely go unnoticed. For instance, in the Netherlands, only hares that died from tularemia have a slight chance of being noted.

Besides surface waters, infected animals such as rodents could also contaminate local (open) water supplies. Therefore, small, uncontrolled private supplies could be potential exposure routes for tularemia. In Sweden and Turkey, consumption of untreated drinking water from private wells and small community supplies has been identified as source of infection (Karadenizli et al., 2015; Lindhusen Lindhé et al., 2018).

Environmental Surveillance

Presence of *F. tularensis* in surface water may imply health risks. Tularemia incidence was shown to correlate with the presence of aquatic habitats (Desvars et al., 2015). Also, the occurrence of *F. tularensis* in surface water and sediment has been associated with human tularemia outbreaks (Broman et al., 2011). However, it is not possible to infer or predict infection risk or tularemia incidence based on our results of *F. tularensis* DNA levels in surface water. This is due to several factors, such as a limited number of cases and samples, variable time-periods between cases and sampling and absence of information about viability and infectivity of *F. tularensis* detected by using qPCR. Nevertheless, data from the environmental surveillance approach independent of tularemia cases (Figure 1 and Table 2) could be used to identify locations harboring higher levels of *F. tularensis*, which could be useful to focus research of tularemia incidence in relation to occurrence of *F. tularensis*.

Our data support the feasibility of tracking possible sources of environmental exposure. It was more likely to detect *F. tularensis* in surface water samples obtained following a tularemia case (set III) compared with case-unrelated samples (set I and II). Positive samples were obtained from 7 out of 8 (88%) case-related sampling efforts, while from randomly collected samples only 17% of the locations (and 10% of the samples) were positive. These figures can only be used to illustrate these differences, as the datasets differ too much in numbers of samples (Table 1) and definition of locations (Figures 1, 2) to support quantitative comparisons.

A detailed environmental investigation following a reported case could point to the most likely source of infection on a local scale. For instance, several locations that were investigated in relation to the FP case clearly showed different levels of *F. tularensis* contamination (Figure 2 and Table 3). Findings from the outbreak among hares in Friesland also showed that

detection of *F. tularensis* following tularemia cases is limited to a geographical area and time period (Figure 2 and Table 3) (Janse et al., 2017). This is also congruent with a study in Germany where *F. tularensis* DNA was detected in surface water samples after animal tularemia cases, but not at distant sites or in the following year (Schulze et al., 2016). These findings support the identification of a particular strain as the source of infection if retrieved from surface water samples collected after tularemia cases. A link between source and case could be substantiated by genotyping, which can be done using cultivated isolates (Karadenizli et al., 2015), but if these are not available also by directly analyzing water samples (see below).

Genotyping *F. tularensis holarctica* in Surface Waters

Presence of *F. tularensis holarctica* in samples FL-D1, FL-B3 and LB-D was confirmed by the amplified IS*Ftu2* sequences, which differ at several positions from other subspecies. One useful signature is a deletion TAG which corresponds to *Francisella tularensis tularensis* strain SCHU S4 (accession AJ749949) position 103552–103554. In contrast, IS*Ftu2* sequences from samples FP-E and A had a low similarity to those from *F. tularensis holarctica* and were likely amplified from an unknown and abundant environmental strain. Inspection of primer binding sites in the most similar genome from *Francisella hispaniensis* strain FSC454 (accession CP018093), revealed only 1 mismatch with both the forward and reverse primers used for IS*Ftu2* amplification. Therefore, it is likely that DNA from a similar strain present in higher numbers than *F. tularensis holarctica* was amplified preferentially, thereby preventing amplification of IS*Ftu2* from *F. tularensis holarctica*. This illustrates that it is important to be aware of the primer matches with (hitherto unknown) related non-target organism (Ahlander et al., 2012; Challacombe et al., 2017). For future studies encompassing sequencing of IS*Ftu2* from *F. tularensis holarctica* in environmental samples, it is advisable to adjust sequencing primers to make them more selective. Inspection of the primers used for detection of *F. tularensis* confirmed that the specificity of the qPCR detection of *F. tularensis* was not compromised by the presence of this environmental strain, as the reverse primer and probe had respectively 7 and 4 mismatches with these sequences (data not shown). Therefore, the *Francisella spp.* of indirect relevance to tularemia ecology and epidemiology that were detected in two of the samples did not impact the qPCR detection of *F. tularensis* in our environmental surveillance. The other gene targets from which sequences were obtained, i.e., all targets for samples FL-D (set III) and A (set I) and targets *fopA* and *FTH_0165* for sample FL-B3 (set III), all confirmed the presence of *F. tularensis holarctica* in the water samples. Sequences were identical to sequences derived from *F. tularensis holarctica* genomes, and there were several sequence positions which differed from all other *Francisella* strains. In summary, sequencing confirmed the presence of *F. tularensis holarctica* in 4 water samples that were investigated in more detail. These samples were derived both from case-related and unrelated surveillance efforts. Presence of *F. tularensis holarctica* was not confirmed in sample FP-E, but this was probably due to the fact that only target IS*Ftu2* was inspected for this sample. More

extensive sequencing efforts, as was carried out for sample A, would likely identify *F. tularensis holarctica*.

Investigation of all gene targets as was carried out with samples FL-D1 and A, permitted differentiation between locations by typing to the subclade level (respectively clade B.12, SNP B.20 and clade B.6, indel Ftind49). The identification of *F. tularensis holarctica* clade B.6 supports the possibility of surface water as source of infection of the first endemic case from 2011, since a clinical isolate obtained from this patient was classified as this Franco-Iberian subclone (Maraha et al., 2013).

Because the methods used only reveal dominant sequences, the presence of other subclades in a sample cannot be ruled out. Considerable genomic diversity of *F. tularensis* has been shown in e.g., Scandinavian countries and Germany (Karlsson et al., 2013; Schulze et al., 2016), and similar diversity may occur in the Netherlands. A more detailed investigation of *F. tularensis* diversity, including less abundant genotypes, would require different protocols however, including clonal purification of DNA targets and NGS sequencing methods. We showed that it is possible to perform such genotyping in samples in which only low levels of *F. tularensis* were detected. This prevents the need for isolation of strains from the environment, which can be very difficult because of low absolute and relative numbers of *F. tularensis* and abundant competing bacteria able to grow in isolation media. By applying these techniques to tissue samples or isolated strains derived from patients or animals, it will be possible to establish a link between tularemia cases and environmental samples.

CONCLUSIONS

This study shows that for tularemia, valuable information regarding the spatial and temporal distribution of its causative agent could be derived from environmental surveillance. The significance of detectable levels of *F. tularensis* in surface waters in terms of infection risks requires more immediate and extensive monitoring data to relate to information about tularemia cases. Tracking a particular strain as source of infection from an environmental source is feasible and could be substantiated by genotyping, which was shown to be possible

directly on water samples with only low levels of *F. tularensis* present.

AUTHOR CONTRIBUTIONS

IJ designed the study, carried out sampling, analyzed data and wrote the manuscript. RP performed the experiments and contributed to the design of the study. AR provided intellectual input. MP contributed to design of the study and intellectual input. All authors contributed to manuscript revision, read and approved the submitted version.

FUNDING

Parts of the work were funded by STOWA (Foundation of Applied Water Research) project number 443.334, the Netherlands and by the RIVM-CIB outbreak response emergency funding.

ACKNOWLEDGMENTS

We thank Edwin Kardinaal from KWR (Water Recycle Institute), the Netherlands, for sharing surface water samples. We thank the following Dutch water boards and water authorities for their efforts and cooperation: Den Dommel, Hollandse delta, Hunze en Aa's, Peel en Maasvallei, Rivierenland, Rijkswaterstaat, Rijnland, Roer en Overmaas, Scheldestromen, Vechtstromen, Waternet, Wetterskip Fryslan, Wrij, Rijn en IJssel. We thank Jolianne M. Rijks from the Dutch Wildlife Health Centre, University Utrecht, for supplying details of tularemia infected hares and Ewout Fanoy from RIVM for supplying timely information on human tularemia cases. The reviewers are acknowledged for their valuable comments.

SUPPLEMENTARY MATERIAL

The Supplementary Material for this article can be found online at: <https://www.frontiersin.org/articles/10.3389/fcimb.2018.00140/full#supplementary-material>

REFERENCES

- Abd, H., Johansson, T., Golovliov, I., Sandstrom, G., and Forsman, M. (2003). Survival and growth of *Francisella tularensis* in *Acanthamoeba castellanii*. *Appl. Environ. Microbiol.* 69, 600–606. doi: 10.1128/AEM.69.1.600-606.2003
- Ahlinder, J., Ohrman, C., Svensson, K., Lindgren, P., Johansson, A., Forsman, M., et al. (2012). Increased knowledge of *Francisella* genus diversity highlights the benefits of optimised DNA-based assays. *BMC Microbiol.* 12:220. doi: 10.1186/1471-2180-12-220
- Birdsell, D. N., Vogler, A. J., Buchhagen, J., Clare, A., Kaufman, E., Naumann, A., et al. (2014). TaqMan real-time PCR assays for single-nucleotide polymorphisms which identify *Francisella tularensis* and its subspecies and subpopulations. *PLoS ONE* 9:e107964. doi: 10.1371/journal.pone.0107964
- Broman, T., Thelaus, J., Andersson, A. C., Backman, S., Wikstrom, P., Larsson, E., et al. (2011). Molecular detection of persistent *Francisella tularensis* subspecies *holarctica* in natural waters. *Int. J. Microbiol.* 2011:851946. doi: 10.1155/2011/851946
- Challacombe, J. F., Petersen, J. M., Gallegos-Graves, V., Hodge, D., Pillai, S., and Kuske, C. R. (2017). Whole-genome relationships among *Francisella* bacteria of diverse origins define new species and provide specific regions for detection. *Appl. Environ. Microbiol.* 83:e02589-16. doi: 10.1128/AEM.02589-16
- Desvars, A., Furberg, M., Hjertqvist, M., Vidman, L., Sjostedt, A., Ryden, P., et al. (2015). Epidemiology and ecology of tularemia in Sweden, 1984–2012. *Emerging Infect. Dis.* 21, 32–39. doi: 10.3201/eid2101.140916
- Duodu, S., Larsson, P., Sjodin, A., Forsman, M., and Colquhoun, D. J. (2012). The distribution of *Francisella*-like bacteria associated with coastal waters in Norway. *Microb. Ecol.* 64, 370–377. doi: 10.1007/s00248-012-0023-0
- Hestvik, G., Warns-Petit, E., Smith, L. A., Fox, N. J., Uhlhorn, H., Artois, M., et al. (2015). The status of tularemia in Europe in a one-health context: a review. *Epidemiol. Infect.* 143, 2137–2160. doi: 10.1017/S0950268814002398

- Huber, B., Escudero, R., Busse, H. J., Seibold, E., Scholz, H. C., Anda, P., et al. (2010). Description of *Francisella hispaniensis* sp. nov., isolated from human blood, reclassification of *Francisella novicida* (Larson et al. 1955) Olsufiev et al. 1959 as *Francisella tularensis* subsp. *novicida* comb. nov. and emended description of the genus *Francisella*. *Int. J. Syst. Evol. Microbiol.* 60, 1887–1896. doi: 10.1099/ijs.0.015941-0
- Janse, I., Hamidjaja, R. A., Bok, J. M., and Van Rotterdam, B. J. (2010). Reliable detection of *Bacillus anthracis*, *Francisella tularensis* and *Yersinia pestis* by using multiplex qPCR including internal controls for nucleic acid extraction and amplification. *BMC Microbiol.* 10:314. doi: 10.1186/1471-2180-10-314
- Janse, I., Maas, M., Rijks, J. M., Koene, M., Van Der Plaats, R. Q., Engelsma, M., et al. (2017). Environmental surveillance during an outbreak of tularaemia in hares, the Netherlands, 2015. *Euro Surveill.* 22:30607. doi: 10.2807/1560-7917.ES2017.22.35.30607
- Karadenizli, A., Forsman, M., Simsek, H., Taner, M., Ohrman, C., Myrtennas, K., et al. (2015). Genomic analyses of *Francisella tularensis* strains confirm disease transmission from drinking water sources, Turkey, 2008, 2009 and 2012. *Euro Surveill.* 20:21136. doi: 10.2807/1560-7917.ES2015.20.21.21136
- Karlsson, E., Svensson, K., Lindgren, P., Bystrom, M., Sjodin, A., Forsman, M., et al. (2013). The phylogeographic pattern of *Francisella tularensis* in Sweden indicates a Scandinavian origin of *Eurosiberian tularaemia*. *Environ. Microbiol.* 15, 634–645. doi: 10.1111/1462-2920.12052
- Lärkeryd, A., Myrtennas, K., Karlsson, E., Dwibedi, C. K., Forsman, M., Larsson, P., et al. (2014). CanSNPer: a hierarchical genotype classifier of clonal pathogens. *Bioinformatics* 30, 1762–1764. doi: 10.1093/bioinformatics/btu113
- Lindhusen Lindhé, E., Hjertqvist, M., and Wahab, T. (2018). Outbreak of tularaemia connected to a contaminated well in the Västra Götaland region in Sweden. *Zoonoses Public Health* 65, 142–146. doi: 10.1111/zph.12382
- Maraha, B., Hajer, G., Sjodin, A., Forsman, M., Paaauw, A., Roeselers, G., et al. (2013). Indigenous infection with *Francisella tularensis* holarctica in The Netherlands. *Case Rep. Infect. Dis.* 2013:916985. doi: 10.1155/2013/916985
- Petersen, J. M., Carlson, J., Yockey, B., Pillai, S., Kuske, C., Garbalena, G., et al. (2009). Direct isolation of *Francisella* spp. from environmental samples. *Lett. Appl. Microbiol.* 48, 663–667. doi: 10.1111/j.1472-765X.2009.02589.x
- Pijnacker, R., Koene, M., Rijks, J. M., Swaan, C., Maas, M., De Rosa, M., et al. (2016). Tularaemia in Nederland, terug van weggeweest? *Ned. Tijdschr. voor Medische Microbiol.* 24, 65–68.
- Rosow, H., Forbes, K. M., Tarkka, E., Kinnunen, P. M., Hemmila, H., Huitu, O., et al. (2014). Experimental Infection of voles with *Francisella tularensis* indicates their amplification role in tularaemia outbreaks. *PLoS ONE* 9:e108864. doi: 10.1371/journal.pone.0108864
- Schulze, C., Heuner, K., Myrtennas, K., Karlsson, E., Jacob, D., Kutzer, P., et al. (2016). High and novel genetic diversity of *Francisella tularensis* in Germany and indication of environmental persistence. *Epidemiol. Infect.* 144, 3025–3036. doi: 10.1017/S0950268816001175
- Sinclair, R., Boone, S. A., Greenberg, D., Keim, P., and Gerba, C. P. (2008). Persistence of category a select agents in the environment. *Appl. Environ. Microbiol.* 74, 555–563. doi: 10.1128/AEM.02167-07
- Svensson, K., Granberg, M., Karlsson, L., Neubauerova, V., Forsman, M., and Johansson, A. (2009). A real-time PCR array for hierarchical identification of *Francisella* isolates. *PLoS ONE* 4:e8360. doi: 10.1371/journal.pone.0008360
- van de Wetering, D., Oliveira Dos Santos, C., Wagelaar, M., De Kleuver, M., Koene, M. G., Roest, H. I., et al. (2015). A cluster of tularaemia after contact with a dead hare in the Netherlands. *Neth. J. Med.* 73, 481–482.
- van Hoek, M. L. (2013). Biofilms: an advancement in our understanding of *Francisella* species. *Virulence* 4, 833–846. doi: 10.4161/viru.27023
- Vogler, A. J., Birdsell, D., Price, L. B., Bowers, J. R., Beckstrom-Sternberg, S. M., Auerbach, R. K., et al. (2009). Phylogeography of *Francisella tularensis*: global expansion of a highly fit clone. *J. Bacteriol.* 191, 2474–2484. doi: 10.1128/JB.01786-08
- WHO (2007). *WHO Guidelines on Tularaemia*. Geneva: World Health Organization.
- Zijlstra, M., Hulsker, C. C. C., Fanoy, E. B., Pijnacker, R., Kraaijeveld, A., Koene, M. G. J., et al. (2017). Tularaemia in a boy following participation in a mud race. *Ned. Tijdschr. Geneesk.* 160:D1180.

Conflict of Interest Statement: The authors declare that the research was conducted in the absence of any commercial or financial relationships that could be construed as a potential conflict of interest.

Copyright © 2018 Janse, van der Plaats, de Roda Husman and van Passel. This is an open-access article distributed under the terms of the Creative Commons Attribution License (CC BY). The use, distribution or reproduction in other forums is permitted, provided the original author(s) and the copyright owner are credited and that the original publication in this journal is cited, in accordance with accepted academic practice. No use, distribution or reproduction is permitted which does not comply with these terms.



Live Attenuated Tularemia Vaccines for Protection Against Respiratory Challenge With Virulent *F. tularensis* subsp. *tularensis*

Qingmei Jia* and Marcus A. Horwitz*

Division of Infectious Diseases, Department of Medicine, 37-121 Center for Health Sciences, School of Medicine, University of California, Los Angeles, Los Angeles, CA, United States

Francisella tularensis is the causative agent of tularemia and a Tier I bioterrorism agent. In the 1900s, several vaccines were developed against tularemia including the killed “Foshay” vaccine, subunit vaccines comprising *F. tularensis* protein(s) or lipoproteins(s) in an adjuvant formulation, and the *F. tularensis* Live Vaccine Strain (LVS); none were licensed in the U.S.A. or European Union. The LVS vaccine retains toxicity in humans and animals—especially mice—but has demonstrated efficacy in humans, and thus serves as the current gold standard for vaccine efficacy studies. The U.S.A. 2001 anthrax bioterrorism attack spawned renewed interest in vaccines against potential biowarfare agents including *F. tularensis*. Since live attenuated—but not killed or subunit—vaccines have shown promising efficacy and since vaccine efficacy against respiratory challenge with less virulent subspecies *holarctica* or *F. novicida*, or against non-respiratory challenge with virulent subsp. *tularensis* (Type A) does not reliably predict vaccine efficacy against respiratory challenge with virulent subsp. *tularensis*, the route of transmission and species of greatest concern in a bioterrorist attack, in this review, we focus on live attenuated tularemia vaccine candidates tested against respiratory challenge with virulent Type A strains, including homologous vaccines derived from mutants of subsp. *holarctica*, *F. novicida*, and subsp. *tularensis*, and heterologous vaccines developed using viral or bacterial vectors to express *F. tularensis* immunoprotective antigens. We compare the virulence and efficacy of these vaccine candidates with that of LVS and discuss factors that can significantly impact the development and evaluation of live attenuated tularemia vaccines. Several vaccines meet what we would consider the minimum criteria for vaccines to go forward into clinical development—safety greater than LVS and efficacy at least as great as LVS, and of these, several meet the higher standard of having efficacy \geq LVS in the demanding mouse model of tularemia. These latter include LVS with deletions in *purMCD*, *sodB_{FT}*, *capB* or *wzy*; LVS Δ *capB* that also overexpresses Type VI Secretion System (T6SS) proteins; FSC200 with a deletion in *clpB*; the single deletional *purMCD* mutant of *F. tularensis* SCHU S4, and a heterologous prime-boost vaccine comprising LVS Δ *capB* and *Listeria monocytogenes* expressing T6SS proteins.

Keywords: tularemia, *Francisella tularensis*, tularemia vaccine, live attenuated vaccine, bioterrorism, homologous vaccine, heterologous vaccine, prime-boost vaccine

OPEN ACCESS

Edited by:

Joseph Wayne Conlan,
National Research Council Canada
(NRC-CNRC), Canada

Reviewed by:

Larry Schlesinger,
The Ohio State University,
United States
Petra Oyston,
Defence Science and Technology
Laboratory, United Kingdom

*Correspondence:

Qingmei Jia
qjia@mednet.ucla.edu
Marcus A. Horwitz
mhorwitz@mednet.ucla.edu

Received: 09 January 2018

Accepted: 24 April 2018

Published: 15 May 2018

Citation:

Jia Q and Horwitz MA (2018) Live Attenuated Tularemia Vaccines for Protection Against Respiratory Challenge With Virulent *F. tularensis* subsp. *tularensis*. *Front. Cell. Infect. Microbiol.* 8:154. doi: 10.3389/fcimb.2018.00154

INTRODUCTION

Francisella tularensis, the causative agent of tularemia, was originally named *Bacterium tularensis* by McCoy and Chapin in 1911, who discovered it as the causative agent of a “plague like disease” prevalent among the ground squirrels in Tulare County, California (McCoy GW, 1912; Francis, 1925). The bacterium was designated as *Pasteurella tularensis* in 1920’s and later renamed *Francisella tularensis* in honor of the contributions made by Dr. Edward Francis among others (Francis, 1928; Weinberg, 2004; Sjostedt, 2007). Several vaccine strategies were developed in the 1900s against virulent *F. tularensis* infection, including killed whole cell vaccines, subunit vaccines, and live attenuated homologous vaccines (Wayne Conlan and Oyston, 2007). A killed whole cell vaccine, the earliest vaccine developed against tularemia and referred to as the “Foshay” vaccine (Foshay, 1932; Foshay et al., 1942), was prepared from phenolized liquid culture and was not highly protective against subsequent systemic and aerosol challenge with highly virulent strains of *F. tularensis* in mice, guinea pigs, rabbits, and humans (Foshay, 1932; Foshay et al., 1942; Kadull et al., 1950; Vanmetre and Kadull, 1959; Eigelsbach and Downs, 1961; Saslaw et al., 1961a,b). Subunit vaccines comprising *F. tularensis* protein(s) or lipoproteins(s) in an adjuvant formulation also failed to demonstrate strong protective immunity against virulent non-Type A or Type A *F. tularensis* in animal models (Sjostedt et al., 1992b; Golovliov et al., 1995; Fulop et al., 2001; Conlan et al., 2002). Live attenuated homologous vaccines showed greater promise. The earliest live attenuated homologous tularemia vaccine, Live Vaccine Strain or LVS, derived from a virulent isolate of *F. tularensis* subsp. *holarctica* (Type B), was developed by U.S.A. and Russian scientists in the 1950s (Eigelsbach and Downs, 1961). However, LVS retained considerable virulence in animals and provided incomplete protection to humans challenged with *F. tularensis* subsp. *tularensis* (Type A) by aerosol, the route of transmission of greatest concern in a bioterrorist attack (Saslaw et al., 1961a; Hornick and Eigelsbach, 1966; Fortier et al., 1991). The fundamental mechanism of LVS attenuation is not fully understood, although *pilA* and FTT0918 have been identified as contributing to LVS virulence (Salomonsson et al., 2009). The LVS vaccine has not been licensed in the U.S.A.^{1,2} or in the European Union³.

Until 2001, few researchers were actively working on vaccine development against tularemia. However, in the wake of the September 11, 2001 terrorist attack on the World Trade Center and the U.S.A. anthrax bioterrorism attack 1 week later, there has been renewed interest in vaccine development against

tularemia and other potential biowarfare agents. This has been accompanied by a substantial increase in publications on development of tularemia vaccines, mostly on live attenuated vaccine candidates, including defined mutants of *F. tularensis* subsp. *holarctica* (Bakshi et al., 2006, 2008; Pechous et al., 2006, 2008; Li et al., 2007; Sebastian et al., 2007, 2009; Meibom et al., 2008; Sammons-Jackson et al., 2008; Santiago et al., 2009; Jia et al., 2010; Zarrella et al., 2011; Kim et al., 2012; Schmitt et al., 2012; Barrigan et al., 2013; Golovliov et al., 2013; Mahawar et al., 2013; Straskova et al., 2015; Suresh et al., 2015), *F. novicida* (Pammit et al., 2006; Tempel et al., 2006; Mohapatra et al., 2007; Quarry et al., 2007; Kanistanon et al., 2008; West et al., 2008; Cong et al., 2009; Sanapala et al., 2012; Signarovitz et al., 2012; Chu et al., 2014; Cunningham et al., 2014), and subsp. *tularensis* (Twine et al., 2005, 2012; Qin et al., 2008, 2009; Conlan et al., 2010; Michell et al., 2010; Shen et al., 2010; Ireland et al., 2011; Rockx-Brouwer et al., 2012; Reed et al., 2014; Santiago et al., 2015), but also on live attenuated heterologous vaccines expressing *F. tularensis* proteins (Jia et al., 2009; Kaur et al., 2012; Banik et al., 2015) and recombinant LVS vaccines expressing *F. tularensis* proteins (Jia et al., 2013, 2016). Some of these vaccine candidates have been reviewed elsewhere (Conlan, 2011; Marohn and Barry, 2013; Elkins et al., 2016). Because vaccine efficacy against respiratory challenge with subsp. *holarctica* or against non-respiratory challenge with subsp. *tularensis* does not reliably predict vaccine efficacy against respiratory challenge with subsp. *tularensis* (Conlan, 2011; Marohn and Barry, 2013), as noted the route of transmission and species of greatest concern in a bioterrorist attack, in this review, we focus on live attenuated vaccines that have been tested against respiratory challenge with virulent *F. tularensis* subsp. *tularensis*—the SCHU S4 strain originally isolated from a human ulcer in 1941 (Eigelsbach et al., 1951) or FSC033 (*Francisella* Strain Collection from Swedish Defense Research Agency, Sweden) originally isolated from a squirrel in Georgia (Forsman et al., 1994).

TULAREMIA AND *F. TULARENSIS*

Tularemia occurs in nature as a fatal bacteremia of various rodents and other animals, such as rabbits, and is transmitted to humans as an accidental infection (Francis, 1925). Depending primarily on the route of transmission, there are several clinical forms of tularemia, including ulceroglandular and glandular tularemia caused by an arthropod bite or skin contact with an infected animal; oculoglandular tularemia caused by direct infection of the eye; oropharyngeal tularemia caused by ingestion of water contaminated by infected rodents or other animals or consumption of under-cooked meat from an infected animal; typhoidal tularemia from any mode of transmission; and pneumonic tularemia caused by inhalation of aerosolized bacteria. Typhoidal and pneumonic tularemia are the most dangerous forms as they carry a high fatality rate—30–60% if untreated (Dennis et al., 2001; Matyas et al., 2007). Because *F. tularensis* is one of the most pathogenic human pathogens known and can be spread by aerosol transmission to cause highly fatal pneumonic tularemia, it is classified as a Tier 1 select agent

¹Centers for Disease Control and Prevention, Tularemia Prevention, <https://www.cdc.gov/tularemia/prevention/index.html>, October 26, 2015.

²U. S. Food and Drug Administration, Vaccines Licensed for Use in the United States, <https://www.fda.gov/BiologicsBloodVaccines/Vaccines/ApprovedProducts/ucm093833.htm>, 02/14/2018.

³European Medicines Agency. EMA/CHMP Guidance document on use of medicinal products for the treatment and prophylaxis of biological agents that might be used as weapons of bioterrorism, http://www.ema.europa.eu/docs/en_GB/document_library/Regulatory_and_procedural_guideline/2010/01/WC500049399.pdf, 18 November 2014.

of bioterrorism, i.e., among the most likely pathogens to be deliberately used in a bioterrorist attack. In fact, Japan, the U.S.A., and the U.S.S.R. have stockpiled *F. tularensis* as a bioweapon in the past (Harris, 1992; Christopher et al., 1997; Alibek, 1999). *F. tularensis* subsp. *tularensis* (Type A), prevalent in North America, is the most virulent subsp.; intracutaneous challenge or inhalation of as few as 10–50 colony forming units (CFU) (SCHU S4 strain) is able to cause clinical tularemia in humans (McCrum, 1961; Saslaw et al., 1961a,b). *F. tularensis* subsp. *holarctica* (Type B), found in Europe, Asia and North America, is less virulent than subsp. *tularensis*. Subsp. *mediasiatica*, found in the Central Asia and the former USSR, is of similar virulence to subsp. *holarctica* (Sjostedt, 2007). *F. novicida*, genetically closely related to *F. tularensis* and frequently referred to as subsp. *novicida* (Rohmer et al., 2007; Huber et al., 2010), is currently classified as a separate species (Johansson et al., 2010; Kingry and Petersen, 2014). *F. novicida* shows low virulence in experimental models, occasionally causes disease in immunocompromised individuals, and has been isolated from patients with various clinical entities in the U.S.A., Canada, Australia, and Spain (Bernard et al., 1994; WHO, 2007).

BIOLOGY AND PATHOGENESIS OF EXPERIMENTAL TULAREMIA AND THE HOST RESPONSE

F. tularensis is a facultative intracellular pathogen that is capable of infecting multiple types of eukaryotic cells, including macrophages. Using a human macrophage-like cell line (THP-1), Clemens et al. showed that *F. tularensis* subsp. *tularensis* SCHU S4 and subsp. *holarctica* LVS enter human macrophages via a unique complement-dependent process termed looping phagocytosis; then enter a unique fibrillar-coated phagosome; and finally exit the phagosome to multiply freely in the cytoplasm using a Type VI Secretion System (T6SS) (Clemens et al., 2004, 2005, 2015; Clemens and Horwitz, 2007). In addition to the macrophage, *F. tularensis* can infect alveolar type II epithelial cells, neutrophils, dendritic cells, and others (Metzger et al., 2007). Studies on the pathogenesis of experimental tularemia were mostly conducted in mice and to a lesser extent in Fisher rats and non-human primates (Jemski, 1981; Lyons and Wu, 2007; Hutt et al., 2017). Upon i.d. or aerosol infection, *F. tularensis* quickly disseminates systemically to spleen, liver, lung, lymph nodes, and bone marrow, and multiplies in these organs (Conlan et al., 2003; Fritz et al., 2014). As with many other intracellular pathogens, *F. tularensis* does not produce a toxin to cause tissue damage. Instead, *F. tularensis* damages tissues by invasion and destruction. Multiplication of *F. tularensis*, especially subsp. *tularensis*, in the tissues fails to trigger—but rather actively suppresses—innate immune responses in humans, which likely contributes to its enhanced pathogenicity (Bosio et al., 2007; Gillette et al., 2014). Although various immune responses to LVS vaccination and *F. tularensis* infection have been identified in animal models, correlates of protection are still not known. Both LVS vaccination and subsp. *tularensis* infection induce antibody responses. In the mouse, LVS vaccination induces *F. tularensis* antigen specific humoral (antibodies

and B cells) and cellular (both CD4+ and CD8+ T cells) immune responses. While T-cell mediated immune responses are important for control of primary *Francisella* infection or vaccine-induced protection, antibodies may also provide prophylactic and therapeutic protection against pulmonary infection with low virulence *F. tularensis*, strains (Elkins et al., 2007; Metzger et al., 2007; Cole et al., 2009). Protective immunity induced by natural infection with *F. tularensis* or vaccination with LVS in humans depends primarily upon cell-mediated Th1-type immune responses, including interferon-gamma (IFN- γ), tumor necrosis factor-alpha (TNF- α), and interleukin-12 (IL-12) (Karttunen et al., 1987; Tarnvik, 1989; Sjostedt et al., 1992a; Ericsson et al., 1994, 2001).

THE LVS VACCINE IN HUMAN STUDIES

The LVS vaccine was studied for safety and efficacy in small numbers of individuals in the 1960s. Saslaw et al. showed that individuals vaccinated with LVS intradermally (i.d., via multiple punctures) develop local lesions manifested by erythema (~1 cm in diameter) followed by non-tender papules that fade rapidly with no fever or systemic reactions (Saslaw et al., 1961a). Hornick et al. showed that among persons exposed to aerosolized LVS, 90% of individuals that inhaled 10^8 LVS exhibited mild typhoidal tularemia and 80% had temperature elevations of $>100^\circ\text{F}$; symptoms and signs were milder when the inhalation dose was reduced to 10^6 (Hornick and Eigelsbach, 1966). Saslaw et al. further showed that i.d. vaccination of humans with LVS induced incomplete protection (3 of 18 persons developed disease vs. 8 of 10 nonvaccinated controls) against aerosol challenge with 10–53 CFU of subsp. *tularensis* SCHU S4 strain; in contrast, in a separate part of the study, the Foshay vaccine was not protective as there was no significant difference in the incidence of disease between the vaccinated and unvaccinated groups after aerosol challenge with similar doses of subsp. *tularensis* SCHU S4 strain (Saslaw et al., 1961a). Hornick and Eigelsbach demonstrated that individuals vaccinated with 10^6 or 10^8 CFU LVS by aerosol were well protected (none required antibiotic treatment) against a high dose challenge with aerosolized SCHU S4 (25,000 CFU, 500–2,500 minimum infective doses) 4–6 months post-vaccination. Similarly vaccinated volunteers were better protected than individuals immunized with a lower dose of LVS (10^4 CFU) by aerosol or vaccinated i.d. by acupuncture; 46% of the latter group required antibiotic treatment vs. 89% of unvaccinated controls (Hornick and Eigelsbach, 1966). Hornick et al. also demonstrated that oral vaccination with LVS provided incomplete protection against aerosol challenge with SCHU S4 (Hornick et al., 1966). However, the i.d. route, but not the aerosol or oral route, has been regularly used for humans in the U.S.A. Saslaw and Carhart found that the greater efficacy of the live LVS vaccine than the Foshay killed vaccine was not related to antibody titers (Saslaw and Carhart, 1961). Recently, a new lot of LVS manufactured under modern GMP conditions has been studied in animals and in two human clinical trials to evaluate its safety, reactogenicity, and immunogenicity (Pasetti et al., 2008; El Sahly et al., 2009; Mulligan et al., 2017). In a Phase I study, Sahly et al. reported that individuals vaccinated with LVS by scarification or subcutaneously (s.c.)

frequently experienced \geq grade 2 (interfering with activity) systemic complaints, especially headache and fatigue; many experienced erythema and induration at the injection site of which \sim one-third had \geq grade 2 erythema (≥ 30 mm) and induration (≥ 15 mm). Of note, some individuals, especially those vaccinated by scarification, developed transient lymphangitis and papular satellite lesions surrounding the infection site. High dose scarification vaccination induced serologic immune responses and scarification and to a lesser extent s.c. vaccination induced high IFN- γ responses (El Sahly et al., 2009). In a Phase II study, Mulligan et al. compared the new lot of LVS to the existing USAMRIID LVS vaccine (Mulligan et al., 2017). They found that both vaccines appeared safe. Injection site reactogenicity was deemed generally mild and similar for the two vaccines; severe vaccine site reactions (erythema or induration > 5 cm) occurred in 4.4 and 3.5% of vaccinees administered the new lot and USAMRIID vaccines, respectively. Similar percentages of the vaccinees administered the new lot or USAMRIID vaccine experienced severe (2 and 3%, respectively) or moderate (24 and 22%, respectively) systemic reactions. Both vaccines resulted in similar (94%) rates of seroconversion.

Thus, while LVS retains residual toxicity, it has demonstrated substantial albeit incomplete protection in humans against aerosol challenge with virulent subsp. *tularensis* SCHU S4. Although LVS has not been licensed for use in the U.S.A. and European Union, it is the only vaccine that has been shown to be reasonably safe and efficacious in humans. There is a general consensus that any vaccine that warrants further consideration as a human vaccine needs to be safer than LVS while providing protection comparable to or greater than that provided by LVS against aerosolized fully virulent *F. tularensis* subsp. *tularensis*. Because LVS retains significant virulence in animals, has toxicity in humans, and provides incomplete protection against aerosol challenge with SCHU S4, there has been great interest since 2001 in developing alternative vaccines—these are reviewed below and summarized in **Tables 1–5**. We focus here on vaccines that have been tested against subsp. *tularensis* SCHU S4 respiratory challenge and compared with LVS for efficacy and virulence.

LIVE ATTENUATED SUBSP. *HOLARCTICA* VACCINE CANDIDATES

Various mutant strains of subsp. *holarctica*, mainly in the background of LVS, have been developed, including mutants that have a lesion in a pathway or gene involved in nutrient metabolism (*purMCD*), response to oxidant stress (*sodB*, *emrA1*), the heat shock response (*clpB*), putative capsular synthesis (*capB*), membrane integrity (FTL_0325, FTL_0057, *wbtA*, *wzy*), transcription (*mgla*), disulfide bond formation (*dsbA*), and other functions (Bakshi et al., 2006, 2008; Pechous et al., 2006, 2008; Meibom et al., 2008; Sebastian et al., 2009; Jia et al., 2010, 2013; Kim et al., 2012; Barrigan et al., 2013; Golovliov et al., 2013; Mahawar et al., 2013; Straskova et al., 2015; Suresh et al., 2015). Some of these strains have demonstrated significant attenuation by the intranasal (i.n.) route, and importantly, provided immune protection against respiratory challenge with virulent subsp.

tularensis SCHU S4 strain (**Table 1**). The SCHU S4 strain of *F. tularensis* subsp. *tularensis* is used almost exclusively in vaccine testing. Of note, although the virulence of LVS in BALB/c mice is similar to that in C57BL mice, with an estimated LD₅₀ in both strains of $< 10^3$ CFU by the i.n. route, $< 10^1$ CFU by the intraperitoneal (i.p.) route, and $> 10^7$ CFU by the intradermal (i.d.) route (Saslaw et al., 1961a; Hornick and Eigelsbach, 1966; Fortier et al., 1991; Jia et al., 2009), the protective immunity induced by LVS is different in these two mouse strains (Chen et al., 2003). BALB/c mice immunized with LVS are protected against systemic challenge with both subsp. *tularensis* and subsp. *holarctica* strains; C57BL mice immunized with LVS are protected against systemic challenge with only the subsp. *holarctica* strain (Chen et al., 2003).

Nutrient Metabolic Mutant

Pechous et al. constructed an LVS mutant with a deletion in the *purMCD* purine biosynthetic locus, LVS Δ *purMCD*, by allelic exchange (Pechous et al., 2006), and complemented the Δ *purMCD* strain *in trans* with wild type *purMCD*. The authors showed that the LVS Δ *purMCD* mutant is defective for growth in medium containing limiting concentrations of purines and is defective for intra-macrophage growth, as it escapes from the phagosome but fails to replicate in the cytosol. The Δ *purMCD* mutant is significantly attenuated in BALB/c mice with an LD₅₀ $> 5 \times 10^6$ by the i.p. route (vs. $< 10^1$ CFU for LVS). 100% of BALB/c mice immunized i.p. with 5×10^4 – 5×10^6 CFU of the LVS Δ *purMCD* mutant and challenged 21 days later i.p. with parental LVS (5×10^1 – 5×10^3) survived the challenge, while 40% of naïve mice survived the challenge (Pechous et al., 2006). The authors further tested the efficacy of LVS Δ *purMCD*, with or without boosting, against respiratory challenge with SCHU S4 and compared it with LVS. In contrast to the result after challenge of the immunized mice with LVS i.p., mice immunized i.n. once with LVS Δ *purMCD* were not protected (0% survival) against i.n. challenge with SCHU S4, similar to sham-immunized mice, whereas mice immunized i.n. once with LVS had 100% survival. However, the protection was increased to the levels induced by LVS following a homologous booster vaccination (**Table 1**, *Nutrient metabolic mutant*) (Pechous et al., 2008). These studies underscore the fact that protection against challenge with subsp. *holarctica* LVS is not predictive of protection against challenge with subsp. *tularensis* SCHU S4, especially when the vaccination and challenge routes are different, in this case i.p./i.p. vs. i.n./i.n.

Oxidative Stress Response Mutants

Several oxidant mutants of LVS have been reported (Lenco et al., 2005; Bakshi et al., 2006, 2008; Buchan et al., 2009; Melillo et al., 2009; Honn et al., 2012, 2017; Ma et al., 2014; Suresh et al., 2015; Saha et al., 2017) among which LVS mutants with a point mutation in *sodB* (FTL_1791), encoding an iron superoxide dismutase (*sodB_{FT}*), with a transposon insertion in a putative gene for the EmrA1 (FTL_0687) secretion protein (*emrA1*), or with a deletion in *dsbA*, encoding a disulfide oxidoreductases protein family homolog (Δ *dsbA*/FSC200), have been tested in mice for their efficacy against respiratory challenge with SCHU S4 (Bakshi et al., 2006, 2008; Straskova et al., 2015; Suresh et al., 2015).

TABLE 1 | *F. tularensis* subsp. *holarctica* mutants: Protection against subsp. *tularensis* SCHU S4 respiratory challenge.

Vaccine ^a	Host strain	Vaccine route, dose (CFU) ^b	Boost (route)	LVS control (route)	Interval (days) ^c	SCHU S4 challenge route, dose (CFU)	% Survival post-challenge (MST, days) ^d			References
							Vaccine	LVS	Sham	
NUTRIENT METABOLIC MUTANT										
LVS $\Delta purMCD$	BALB/c	i.n., 10^6	No	Yes (i.n.)	42	i.n., 100	0 (6)	100 (21)	0 (5)	Pechous et al., 2008
						i.n., 2000	0 (5)	0 (7)	0 (5)	
	BALB/c	i.n., 10^6	Yes (i.n.)	Yes (i.n.)	21	i.n., 100	100 (21)	100 (21)	0 (5)	Pechous et al., 2008
						i.n., 2000	33 (17)	33 (11)	0 (5)	
OXIDATIVE STRESS RESPONSE MUTANTS										
LVS $\Delta sodB_{Ft}$	C57BL/6	i.n., 5×10^3	No	Yes (i.n.)	21	i.n., 14	40	0 (12)	0 (7)	Bakshi et al., 2006, 2008
	C57BL/6	i.n., 5×10^2	Yes (i.n.)	Yes (i.n.)	21	i.n., 103	42	0 (15)	0 (6)	
emrA1	C57BL/6	i.n., 10^6	No	No	21	i.n., 32	0 (8)	ND	0 (6)	Suresh et al., 2015
		i.n., 10^6	Yes (i.n.)	No	21	i.n., 38	0 (9)	ND	0 (6)	Suresh et al., 2015
		i.d., 10^6	Yes (i.d.)	No	21	i.n., 17	0 (10)	ND	0 (7)	Suresh et al., 2015
		i.d., 10^6	Yes (i.n.)	No	21	i.n., 17	0 (10)	ND	0 (7)	Suresh et al., 2015
		i.n., 10^3	Yes (i.d.)	No	21	i.n., 23	20	ND	0 (6)	Suresh et al., 2015
		i.d., 10^3	Yes (i.n.)	No	21	i.n., 24	20	ND	0 (6)	Suresh et al., 2015
$\Delta dsbA/FSC200$	BALB/c	i.n., 10^2	No	No	28	i.n., 100	0	ND	0 (5)	Straskova et al., 2015
		i.n., 10^3	No	No	28	i.n., 100	0	ND	0 (5)	Straskova et al., 2015
		i.n., 10^4	No	No	28	i.n., 100	20	ND	0 (5)	Straskova et al., 2015
		i.n., 10^5	No	No	28	i.n., 100	30	ND	0 (5)	Straskova et al., 2015
		i.n., 10^6	No	No	28	i.n., 100	50	ND	0 (5)	Straskova et al., 2015
HEAT SHOCK PROTEIN MUTANTS										
LVS $\Delta clpB$	BALB/c	i.d., 10^5	No	No	42	i.n. 40	0 (~12)	ND	0 (5)	Golovliov et al., 2013
FSC200 $\Delta clpB$	BALB/c	i.d., 10^5	No	Yes (i.d.)	42	i.n. 86	40	0	0 (5)	Golovliov et al., 2013
CAPSULAR AND MEMBRANE MUTANTS										
LVS $\Delta capB$	BALB/c	i.d., 10^6	No	Yes (i.d.)	42	Aero., 10	0 (10)	67 (16)	0 (5)	Jia et al., 2010
		i.n., 10^5	No	Yes (i.n.)	42	Aero. 10	100 (21)	100 (21)	0 (5)	Jia et al., 2010
rLVS $\Delta capB$ /IglA	BALB/c	i.d., 10^6	No	Yes (i.d.)	42	Aero., 10	50 (16)	63 (17)	0 (5)	Jia et al., 2013
rLVS $\Delta capB$ /IglC	BALB/c	i.d., 10^6	No	Yes (i.d.)	42	Aero., 10	40 (14)	63 (17)	0 (5)	Jia et al., 2013
rLVS $\Delta capB$ /IglABC	BALB/c	i.d., 10^6	No	Yes (i.d.)	42	i.n., 16–31	0	50	0 (4)	Jia et al., 2016
		i.d., 10^6	Yes (i.d.)	Yes (i.d.)	42	i.n., 10	50	50–75	0 (4)	Jia et al., 2018
		i.n., 10^6	Yes (i.n.)	Yes (i.d.)	42	i.n., 6–10	83–100	50–75	0 (4)	Jia et al., 2018
LVS:: Δwzy	BALB/c	i.n., 3.5×10^6	Yes (i.n.)	Yes (i.n.)	28	i.n., 8	84	100	0 (6)	Kim et al., 2012
LVS::wbtA-OPS-TT*	BALB/c	i.n., 1.5×10^7	Yes (i.n.)	No	28	i.n., 10	40 (15)	ND	20 (7)	Sebastian et al., 2009
LVS:: $\Delta wbtA$	BALB/c	i.n., 3.7×10^6	Yes (i.n.)	Yes (i.n.)	28	i.n., 8	0	100	0 (6)	Kim et al., 2012
FTL_0057	BALB/c	i.n., 10^7	No	No	30	i.n., 100	100	ND	0 (6)	Mahawar et al., 2013
FTL_0325	BALB/c	i.n., 10^7	No	No	30	i.n., 100	100	ND	0 (6)	Mahawar et al., 2013
OTHER MUTANTS										
LVS FTL0552 (pmrA)	BALB/c	i.n., 10^5	No	No	30	i.n., 100	30	ND	0 (6)	Sammons-Jackson et al., 2008
		i.n., 10^5	Yes (i.n.)	No	30	i.n., 100	40	ND	0 (6)	Sammons-Jackson et al., 2008
	C57BL/6	i.n., 10^4	No	No	30	i.n., 100	0 (9)	ND	0 (7)	Sammons-Jackson et al., 2008
	C57BL/6	i.n., 10^4	Yes (i.n.)	No	30	i.n., 100	0 (16)	ND	0 (7)	Sammons-Jackson et al., 2008
FTL_0291	BALB/c	i.n., 10^7	No	No	30	i.n., 100	100	ND	0 (6)	Mahawar et al., 2013
FTL_0304	BALB/c	i.n., 10^7	No	No	30	i.n., 100	0 (12)	ND	0 (6)	Mahawar et al., 2013

^aVaccine: *, animals vaccinated simultaneously with LVS::wbtA and OPS-TT [LVS O-polysaccharide (OPS) conjugated with-tetanus toxoid (TT)]. ^bVaccine route, dose: i.n., intranasal; i.d., intradermal. ^cInterval: Interval between the only or the last vaccination and challenge. ^d% Survival: % survival post-challenge in animals immunized with the vaccine candidate (vaccine), LVS control (LVS), or PBS or unvaccinated control (Sham); MST, Mean/Median Survival Time; ND, not determined.

TABLE 2 | *F. novicida* mutants: Protection against *F. tularensis* subsp. *tularensis* challenge.

Vaccine	Host strain ^a	Vaccine route, dose (CFU) ^b	Boost (route)	LVS control (route)	Interval (days) ^c	SCHU S4 challenge route, dose (CFU or LD ₅₀) ^d	% Survival post-challenge (MST, days) ^e			References
							Vaccine	LVS	Sham	
U112	BALB/c	i.d., 100	No	Yes (i.d.)	56	Aerosol, 10 ⁸	0 (5)	0 (6)	0 (5)	Shen et al., 2004
U112	BALB/c	i.d., 100	No	Yes (i.d.)	56	i.d., 350 ⁸	0 (5)	100 (>21)	0 (6)	
U112	Rats	i.t., 10 ⁷	No	No	30	i.t., 25 LD ₅₀	100	ND	0 (10)	Signarovitz et al., 2012
		p.o., 10 ⁷	No	No	30	i.t., 25 LD ₅₀	50	ND	0 (10)	Signarovitz et al., 2012
Δ <i>iglB</i> (KKF235)	C57BL/6	p.o., 10 ³	No	No	21	i.n., 25	67	ND	0 (6)	Cong et al., 2009
	C57BL/6	p.o., 10 ³	No	No	21	i.n., 50	10	ND		Cong et al., 2009
	C57BL/6	p.o., 10 ³	Yes (p.o.)	No	21	i.n., 52	40	ND		Cong et al., 2009
Δ <i>iglB</i>	Rats	i.t., 10 ⁷	No	No	30	i.t., 1.25 × 10 ⁴ *	50	ND	0 (10)	Signarovitz et al., 2012
		p.o., 10 ⁷	No	No	30	i.t., 1.25 × 10 ⁴ *	50	ND	0 (10)	Signarovitz et al., 2012
Δ <i>iglB</i> :: <i>fljB</i>	BALB/c	p.o., 10 ⁷	No	No	30	i.t., 1.25 × 10 ⁴ *	83	ND		Cunningham et al., 2014
	Rats	p.o., 10 ⁷	No	No	30	i.t., 1.25 × 10 ⁴ *	88	ND		Cunningham et al., 2014
<i>Fn iglD</i>	BALB/c	i.n., ~10 ⁹	No	No	30	i.n., 10 ³	0	ND	0	Chu et al., 2014
	Rats	p.o., 10 ⁷	No	No	30	i.t., 10 ⁴	83	ND	17	Chu et al., 2014
	Rats	i.t., 10 ⁵	No	No	30	i.t., 10 ⁴	100	ND	25	Chu et al., 2014
	Rats	i.t., 10 ⁷	No	No	30	i.t., 10 ⁴	83	ND	25	Chu et al., 2014
	NHP	t.b., 10 ⁸	No	Yes (s.c.)	30	Aerosol, (2,500–5,000)	83	100	0 (8)	Chu et al., 2014
Δ <i>pmrA</i>	BALB/c	i.n. (10 ⁶)	No	No	35	i.n., 100	Not protected	ND	ND	Mohapatra et al., 2007

^aHost strain: Mice: BALB/c or C57BL/6 mice; Rats: Fisher rats; NHP: non-human primates, cynomolgus macaques.

^bVaccine route: intranasal (i.n.); oral (p.o.); intratracheal (i.t.); via bronchoscopy (t.b.).

^cInterval: interval between the only or the last vaccination and challenge.

^dSCHU S4 challenge route (dose, CFU of LD₅₀): §challenged with subsp. *tularensis* FSC 033 strain; *, 1.25 × 10⁴ CFU, approximately 25 LD₅₀ in rats.

^e% Survival post-challenge: % survival post-challenge in animals immunized with the vaccine candidate (vaccine), LVS control (LVS), or PBS or unvaccinated control (Sham). MST, mean/median survival time. ND; not determined.

Both *sodB_{Ft}* and *emrA1* LVS mutants are sensitive to oxidative stress and are more attenuated than the parental LVS in mice; C57BL/6 and BALB/c mice infected i.n. with 1 × 10⁴ CFU of the *sodB_{Ft}* mutant of LVS had 83 and 60% survival, respectively, while C57BL/6 and BALB/c mice infected i.n. with 1 × 10⁴ CFU parental LVS had 8.3 and 0% survival, respectively (Bakshi et al., 2006). C57BL/6 mice immunized i.n. with 5 × 10³ *sodB_{Ft}* mutant and 21 days later challenged i.n. with 14 CFU SCHU S4 had 40% survival, significantly greater than that of naïve mice (0% survival) and mice immunized i.n. with 5 × 10³ LVS (0% survival). The protection was similar following administration of a homologous booster vaccination (42% survival) against i.n. challenge with 103 CFU of SCHU S4 (Table 1, *Oxidative stress response mutants*) (Bakshi et al., 2008). It is noted that the i.n. vaccination doses for the *sodB_{Ft}* mutant and LVS were both close to the LD₅₀ i.n. and the interval between the last immunization and challenge was only 21 days.

The *emrA1* mutant of LVS is more attenuated than the *sodB_{Ft}* mutant of LVS in mice, with an LD₅₀ > 10⁶ i.n. in C57BL/6 mice (Ma et al., 2014). However, mice immunized with 1 × 10⁶ *emrA1* and challenged 21 days later i.n. with 32 CFU of the heterologous subsp. *tularensis* SCHU S4 strain had 0% survival; mice homologously primed-boosted with 1 × 10⁶ *emrA1* via the i.n. or the i.d. route or both routes alternately (i.d./i.n., or i.n./i.d.) and challenged 21 days later had 0–20% survival, similar

to naïve mice (Table 1, *Oxidative stress response mutants*). It is noted that mice immunized with *emrA1* had 100% survival after i.n. challenge with the homologous parental LVS strain at doses up to 1 × 10⁸ CFU LVS (Suresh et al., 2015). Thus, the vaccine was poorly protective against SCHU S4 but highly protective against LVS. These results suggest that over attenuation of LVS resulted in a significant reduction in protective immunity. Importantly, these results once again show that efficacy against respiratory challenge with subsp. *holartica* LVS does not predict efficacy against respiratory challenge with subsp. *tularensis* SCHU S4 (see Summary and Discussion).

The *dsbA* mutant of FSC200 (a fully virulent Type B strain genetically similar to LVS, with LD₁₀₀ < 5 CFU i.d. and i.p. in mice), Δ*dsbA*/FSC200, administered i.n. has also shown dose-dependent protection against i.n. challenge with SCHU S4 (Table 1, *Oxidative stress response mutants*) (Straskova et al., 2015).

Heat Shock Protein Mutants

Several *F. tularensis* Type B (LVS and FSC200) mutants defective in heat shock chaperone protein ClpB, which is involved in the response to oxidative, ethanol, and acid stresses, have been reported (Meibom et al., 2008; Golovliov et al., 2013). LVS ClpB (FTL_0094) has 98–100% identity to ClpB in other *F. tularensis* strains (Meibom et al., 2008). The *clpB* mutant strains derived

TABLE 3 | *F. tularensis* subsp. *tularensis* SCHU S4 mutants: Protection against SCHU S4 respiratory challenge.

Vaccine	Host strain ^a	Vaccine route, dose (CFU)	Boost (route)	LVS control (route)	Interval (days) ^b	SCHU S4 challenge route, dose (CFU or LD ₅₀) ^c	% Survival post-challenge (MST, days) ^d			References
							Vaccine	LVS	Sham	
NUTRIENT METABOLIC MUTANTS										
$\Delta purMCD$	BALB/c	i.n., 10 ⁴	No	Yes (i.n.)	42	i.n., 100	14 (11)	100 (21)	0 (5)	Pechous et al., 2008
		i.n., 10 ⁴	No	Yes (i.n.)	42	i.n., 2000	0 (6)	0 (7)	0 (5)	Pechous et al., 2008
		i.n., 10 ⁴	Yes (i.n.)	Yes (i.n./i.n.)	21	i.n., 100	71 (18)	100 (21)	0 (5)	Pechous et al., 2008
		i.n., 10 ⁴	Yes (i.n.)	Yes (i.n./i.n.)	21	i.n., 2000	0 (7)	33 (11)	0 (5)	Pechous et al., 2008
		i.d., 10 ¹⁻⁶	No	No	21	i.n., 500	0 (6-8)	ND	0 (6)	Pechous et al., 2008
		i.n., 10 ¹⁻⁶	No	No	21	i.n., 500	0 (6-11)	ND	0 (6)	Pechous et al., 2008
$\Delta FTT1019c$ (<i>guaA</i>)	C57BL/6	i.n., 7 × 10 ⁵	No	No	28	i.n., 100	0 (4)	ND	0 (4)	Santiago et al., 2015
$\Delta FTT1317c$ (<i>guaB</i>)	C57BL/6	i.n., 1 × 10 ⁹	No	No	28	i.n., 95	0 (6)	ND	0 (4)	Santiago et al., 2015
		i.n., 6 × 10 ⁷	Yes (i.n.)	No	28	i.n., 100	0 (4)	ND	0 (4)	Santiago et al., 2015
$\Delta FTT1019c, \Delta FTT1317c$ (<i>guaA, guaB</i>)	C57BL/6	i.n., 1 × 10 ⁸	Yes (i.n.)	No	28	i.n., 100	0 (4)	ND	0 (4)	Santiago et al., 2015
$\Delta guaBA$	Rabbits	i.d., 10 ⁹	No	Yes (i.d.)	30	Aero., 40 LD ₅₀	27 (7)*	0 (7)	0 (5)	Reed et al., 2014
$\Delta aroD$	Rabbits	i.d., 10 ⁹	No	Yes (i.d.)	30	Aero., 40 LD ₅₀	36 (7)*	0 (7)	0 (5)	Reed et al., 2014
HEAT SHOCK PROTEIN MUTANTS										
$\Delta clpB$	BALB/c	i.d., 10 ⁵	No	Yes (i.d.)	42	Aero., 20	60 (28)	0 (8)	0 (5)	Conlan et al., 2010
	BALB/c	i.d., 10 ⁵	Yes (p.o.)	Yes (i.d./p.o)	42	Aero., 20	20 (11)	0 (8)	0 (5)	Conlan et al., 2010
	C3H/HeN	i.d., 10 ⁵	No	Yes (i.d.)	42	Aero., 20	0 (10)	0 (11)	0 (5)	Conlan et al., 2010
	C3H/HeN	i.d., 10 ⁵	Yes (p.o.)	Yes (i.d./p.o)	42	Aero., 20	0 (16)	0 (7)	0 (6)	Conlan et al., 2010
	BALB/c	p.o., 10 ⁸	No	Yes (p.o.)	42	Aero., 20	40 (16)	0 (5)	0 (5)	Conlan et al., 2010
	BALB/c	p.o., 10 ⁸	Yes (p.o.)	Yes (p.o./p.o)	42	Aero., 20	20 (11)	0 (7)	0 (5)	Conlan et al., 2010
	C3H/HeN	p.o., 10 ⁸	No	Yes (p.o.)	42	Aero., 20	0 (12)	0 (5)	0 (5)	Conlan et al., 2010
	C3H/HeN	p.o., 10 ⁸	Yes (p.o.)	Yes (p.o./p.o)	42	Aero., 20	60 (28)	0 (7)	0 (5)	Conlan et al., 2010
	BALB/c	i.d., 10 ⁵	No	Yes (i.d.)	42	i.n., 10	100	30	0 (~5)	Shen et al., 2010
	BALB/c	i.d., 10 ⁵	No	Yes (i.d.)	42	i.n., 100	80	0	0 (~5)	Shen et al., 2010
	BALB/c	i.d., 10 ⁵	No	Yes (i.d.)	42	i.n., 1000	20	0	0 (~5)	Shen et al., 2010
	BALB/c	i.d., 10 ⁵	No	No	42	i.n., 100	~75	ND	0 (~5)	Twine et al., 2012
	C57BL/6	i.d., 10 ⁵	No	No	42	i.n., 100	0	ND	0 (5)	Twine et al., 2012
	BALB/c	i.d., 10 ³	No	No	42	i.n., 105	~100	ND	0 (5)	Golovliov et al., 2013
	BALB/c	i.d., 10 ⁵	No	No	42	i.n., 105	~80	ND	0 (5)	Golovliov et al., 2013
	BALB/c	i.d., 10 ⁷	No	No	42	i.n., 105	~60	ND	0 (5)	Golovliov et al., 2013
BALB/c	i.d., 10 ⁵	No	No	42	i.n., 40	100	ND	0 (~5)	Golovliov et al., 2013	
$\Delta clpB \Delta capB$	BALB/c	i.d., 10 ⁷	No	Yes (i.d.)	42	Aero., 100	≤ 20	0	ND	Golovliov et al., 2013
CAPSULAR MUTANT										
$\Delta FTT0918 \Delta capB$	BALB/c	i.d., 10 ³	No	Yes (i.d.)	42	Aero., 2	40 (8)	0 (8)	0 (5)	Conlan et al., 2010
		i.d., 10 ³	Yes (p.o.)	Yes (i.d./p.o)	42	Aero., 2	0 (8)	0 (8)	0 (5)	Conlan et al., 2010
		p.o., 10 ⁸	No	Yes (p.o.)	42	Aero., 2	0 (5)	0 (5)	0 (5)	Conlan et al., 2010
		p.o., 10 ⁸	Yes (p.o.)	Yes (i.d./p.o.)	42	Aero., 2	0 (8)	0 (7)	0 (5)	Conlan et al., 2010

(Continued)

TABLE 3 | Continued

Vaccine	Host strain ^a	Vaccine route, dose (CFU)	Boost (route)	LVS control (route)	Interval (days) ^b	SCHU S4 challenge route, dose (CFU or LD ₅₀) ^c	% Survival post-challenge (MST, days) ^d			References
							Vaccine	LVS	Sham	
	C3H/HeN	i.d., 10 ³	No	Yes (i.d.)	42	Aero., 20	0 (5)	0 (11)	0 (5)	Conlan et al., 2010
		i.d., 10 ⁵	Yes (p.o.)	Yes (i.d./p.o.)	42	Aero., 20	50 (17)	0 (7)	0 (6)	Conlan et al., 2010
		p.o., 10 ⁸	No	Yes (p.o.)	42	Aero., 20	0 (5)	0 (5)	0 (5)	Conlan et al., 2010
		p.o., 10 ⁸	Yes (p.o.)	Yes (p.o./p.o.)	42	Aero., 20	0 (5)	0 (7)	0 (6)	Conlan et al., 2010
LIPOPROTEIN MUTANTS										
ΔFTT1103	C57BL/6	i.n., 3 × 10 ⁷	No	No	32	i.n., 68	100	ND	0 (5)	Qin et al., 2009
		i.n., 1 × 10 ⁸	No	No	32	i.n., 37	100	ND	0 (5)	Qin et al., 2009
		i.n., 3 × 10 ⁸	No	No	32	i.n., 68	50 (18)	ND	0 (5)	Qin et al., 2009
	BALB/c	i.n., 1 × 10 ⁸	No	No	33	i.n., 95	75 (21)	ND	0 (5)	Qin et al., 2009
ΔFTT1103 (<i>fipB</i>)	Rabbits	i.d., 10 ⁹	No	Yes (i.d.)	30	Aero., 40 LD ₅₀	0 (6)	0 (7)	0 (5)	Reed et al., 2014
OTHER MUTANTS										
ΔFTT0918	BALB/c	i.d., 10 ⁵	No	Yes (i.d.)	63	Aero., 10*	33 (15)	0 (7)	0 (5)	Twine et al., 2005
Δ <i>iglC</i>	BALB/c	i.d., 10 ⁷	No	Yes (i.d.)	63	Aero., 10*	0 (6)	0 (7)	0 (5)	Twine et al., 2005
Δ <i>iglC</i>	BALB/c	i.d., 10 ⁵	No	Yes (i.d.)	42	Aero., 20	0 (6)	0 (8)	0 (5)	Conlan et al., 2010
	BALB/c	p.o., 10 ⁸	No	Yes (p.o.)	42	Aero., 20	0 (5)	0 (5)	0 (5)	Conlan et al., 2010
	C3H/HeN	i.d., 10 ⁵	No	Yes (i.d.)	42	Aero., 20	0 (5)	0 (11)	0 (5)	Conlan et al., 2010
	C3H/HeN	p.o., 10 ⁸	No	Yes (p.o.)	42	Aero., 20	0 (5)	0 (5)	0 (5)	Conlan et al., 2010
ΔFTT0369c	BALB/c	i.d., 50	No	No	45	i.n., 10	90	ND	0 (5)	Rockx-Brouwer et al., 2012
		i.n., 10	No	No	45	i.n., 10	80	ND	0 (5)	Rockx-Brouwer et al., 2012
ΔFTT1676	BALB/c	i.d., 50	No	No	45	i.n., 10	100	ND	0 (5)	Rockx-Brouwer et al., 2012
		i.n., 10	No	No	45	i.n., 10	~50	ND	0 (5)	Rockx-Brouwer et al., 2012
ΔFTT0369	BALB/c	i.d., 50	No	No	45	i.n., 10	60	ND	0 (5)	Rockx-Brouwer et al., 2012
ΔFTT1676		i.n., 10	No	No	45	i.n., 10	10	ND	0 (5)	Rockx-Brouwer et al., 2012

^aHost strain: Mice: BALB/c, C57BL/6, or C3H/HeN mice; Rabbits: New Zealand White rabbits.

^bInterval: time between the only or the last vaccination and challenge.

^cSCHU S4 challenge route: *challenged with subsp. *tularensis* (Type A) FSC033 strain.

^dSurvival: % survival after challenge of mice immunized with the vaccine candidate (vaccine), LVS control (LVS), or no vaccine or PBS control (Sham). MST, mean/median survival time; *Time to death does not include survivors; ND, not determined.

from subsp. *holarctica* LVS and FSC200 and subsp. *tularensis* SCHU S4 are attenuated when delivered by i.d., i.p., or oral routes; they have been tested as vaccine candidates against respiratory challenge with SCHU S4 (Meibom et al., 2008; Conlan et al., 2010; Shen et al., 2010; Twine et al., 2012; Golovliov et al., 2013; Ryden et al., 2013). Specifically, the LD₅₀ for the LVS Δ*clpB* (transposon insertional mutant) is >10⁷ CFU i.p. in BALB/c mice (vs. <10¹ CFU for LVS) and the LD₅₀ for FSC200 Δ*clpB* (deletional mutant) is >1 × 10⁵ CFU i.n. for BALB/c mice (vs. ~10³ CFU for LVS); however, FSC200 Δ*clpB* replicated to higher numbers at the intradermal vaccination site and was more lethal than LVS in SCID mice (Meibom et al., 2008; Golovliov et al., 2013). C57BL/6J (B6) mice immunized i.n. with 5 × 10⁴ LVS Δ*clpB* and challenged 28 or 120 days later with 5 × 10³ parental LVS i.n. (~5 LD₅₀) had 100% survival, the same as mice immunized with 5 × 10² LVS i.n.; all naïve mice died by day 7 (Barrigan et al., 2013). In a separate study, BALB/c mice

immunized i.d. with 10⁵ CFU LVS Δ*clpB* and challenged 6 weeks later i.n. with 40 CFU SCHU S4 had 0% survival (Golovliov et al., 2013). BALB/c mice immunized i.d. with 10⁵ CFU FSC200 Δ*clpB* and challenged 6 weeks later i.n. with 86 CFU SCHU S4 had ~40% survival vs. 0% for mice immunized i.d. with LVS (Golovliov et al., 2013). Both FSC200 Δ*clpB* and LVS Δ*clpB* mutants were generally less protective than a SCHU S4 Δ*clpB* mutant against i.n. challenge with SCHU S4 (Table 1, Table 3, Heat shock protein mutants), although the latter strain has only a single deletional mutation and thus presents safety issues (see Summary and Discussion).

Putative Capsular and Membrane Mutants

F. tularensis Type B mutants defective in genes involved in putative capsular and membrane synthesis are highly attenuated in mice, including LVS mutants defective in *capBCA* (FTT0806, FTT0805, and FTT0798, respectively), *wzy*, *wbtA*, FTL_0057,

TABLE 4 | Live attenuated heterologous vaccine candidates: Protection against SCHU S4 respiratory challenge.

Prime vaccine	Host strain	Prime route, dose (CFU)	Boost (vaccine, route) ^a	LVS control (route) ^b	Interval (days) ^c	SCHU S4 challenge route, dose (LD ₅₀)	% Survival post-challenge (MST, days) ^d			References
							Vaccine	LVS	Sham	
HETEROLOGOUS STANDALONE VACCINES										
Lm <i>ΔactA</i> (LmV)	BALB/c	i.d., 10 ⁶	Yes (LmV × 1, i.d.)	Yes (i.d.)	42	Aerosol, 1	38	88	50	Jia et al., 2009
		i.d., 10 ⁶	Yes (LmV × 1, i.d.)	Yes (i.d.)	42	Aerosol, 10	38	88	0	Jia et al., 2009
rLm/iglC	BALB/c	i.d., 10 ⁶	Yes (rLm/iglC × 1, i.d.)	Yes (i.d.)	42	Aerosol, 1	100	88	50	Jia et al., 2009
		i.d., 10 ⁶	Yes (rLm/iglC × 1, i.d.)	Yes (i.d.)	42	Aerosol, 10	75	88	0 (6)	Jia et al., 2009
rLm/katG	BALB/c	i.d., 10 ⁶	Yes (rLm/katG × 1, i.d.)	Yes (i.d.)	42	Aerosol, 1	88	88	50	Jia et al., 2009
		i.d., 10 ⁶	Yes (rLm/katG × 1, i.d.)	Yes (i.d.)	42	Aerosol, 10	25	88	0 (6)	Jia et al., 2009
HOMOLOGOUS PRIME AND HETEROLOGOUS BOOST VACCINES										
LVS <i>ΔcapB</i>	BALB/c	i.d., 10 ⁶	Yes (rLm/iglC × 1, i.d.)	Yes (i.d.)	42	Aerosol, 10	75 (19)	63 (17)	0 (5)	Jia et al., 2013
rLVS <i>ΔcapB</i> /iglC	BALB/c	i.d., 10 ⁶	Yes (rLm/iglC × 1, i.d.)	Yes (i.d.)	42	Aerosol, 10	75 (20)	63 (17)	0 (5)	Jia et al., 2013
rLVS <i>ΔLPS</i> /iglC	BALB/c	i.d., 10 ⁶	Yes (rLm/iglC × 1, i.d.)	Yes (i.d.)	42	Aerosol, 3	63 (16)	100 (21)	0 (4)	Jia et al., 2013
rLVS <i>ΔLPS</i> /iglC	BALB/c	i.d., 10 ⁶	Yes (rLm/iglC × 2, i.d.)	Yes (i.d.)	42	Aerosol, 3	100 (21)	100 (21)	0 (4)	Jia et al., 2013
rLVS <i>ΔLPS</i> /iglC	BALB/c	i.d., 10 ⁶	Yes (rLm/iglC × 1, i.d.)	Yes (i.d.)	42	Aerosol, 10	38 (11)	100 (21)	0 (4)	Jia et al., 2013
rLVS <i>ΔLPS</i> /iglC	BALB/c	i.d., 10 ⁶	Yes (rLm/iglC × 2, i.d.)	Yes (i.d.)	42	Aerosol, 10	63 (15)	100 (21)	0 (4)	Jia et al., 2013

^aBoost: Heterologous standalone vaccines: mice were primed at Week 0 and boosted once (× 1) at Week 4 with Lm vector (LmV) or LmV expressing *F. tularensis* IglC (rLm/iglC) or KatG (rLm/katG); Homologous prime and heterologous boost vaccines: mice were primed at Week 0 with LVS *ΔcapB* or LVS *ΔcapB* overexpressing IglC (rLVS *ΔcapB*/iglC) or LVS *ΔLPS* overexpressing IglC (rLVS *ΔLPS*/iglC), and boosted with rLm/iglC once (× 1) at Week 4 or twice (× 2) at Weeks 3 and 6.

^bLVS control: in heterologous standalone vaccine studies, LVS was given i.d. twice at Weeks 0 and 4; in homologous prime-heterologous boost studies, LVS was given once at Week 4.

^cInterval: Time between the only or the last immunization and the challenge.

^dSurvival, % survival after challenge of mice immunized with the vaccine candidate (vaccine), LVS control (LVS), or no vaccine or PBS control (Sham). MST: Mean Survival Time.

and FTL_0325 (Table 1, Capsular and membrane mutants) (Sebastian et al., 2007; Su et al., 2007, 2011; Weiss et al., 2007; Jia et al., 2010; Michell et al., 2010; Kim et al., 2012; Mahawar et al., 2013). We have constructed and characterized a defined LVS mutant with an antibiotic resistance marker-free deletion in *capB* (FTL_1416) (LVS *ΔcapB*) as a vaccine candidate and shown that LVS *ΔcapB* is resistant to serum killing, out-competed for growth by its parental LVS in infected human macrophage cells, and significantly more attenuated (>10,000-fold) than LVS administered i.n. in mice (Jia et al., 2010). BALB/c mice immunized with LVS *ΔcapB* i.n. or i.d. develop humoral and

cellular immune responses comparable to LVS and induce full protection (100% survival) against i.n. challenge 4 or 8 weeks later with the parental LVS vaccine (~5 LD₅₀). Most importantly, while the vaccine was poorly protective when administered i.d., mice immunized with LVS *ΔcapB* i.n. were highly protected (100% survival) against an aerosol challenge 6 weeks later with 10 × LD₅₀ *F. tularensis* SCHU S4 (Table 1, Capsular and membrane mutant) (Jia et al., 2010). In subsequent studies, we constructed several rLVS *ΔcapB* strains over-expressing T6SS proteins IglA (rLVS *ΔcapB*/iglA) or IglC (rLVS *ΔcapB*/iglC) or a fusion protein comprising immunoprotective domains of IglA,

TABLE 5 | Attenuation and protective efficacy against SCHU S4 respiratory challenge of *F. tularensis* vaccine candidates relative to LVS.

Vaccine ^a	LD ₅₀ in mice (route, strain)	Efficacy ≥ LVS in mice against respiratory challenge with SCHU S4 (host strain) ^b			Vaccination—challenge interval (days) and other comments	References
		i.d.	i.n.	p.o.		
LVS	~10 ³ (i.n. BALB/c) >10 ⁷ (i.d. BALB/c) >10 ⁸ (p.o., C3H/HeN)				Toxicity	Fortier et al., 1991; Jia et al., 2009; Conlan et al., 2010
MORE ATTENUATED THAN LVS						
LVS Δ purMCD	>10 ⁶ (i.n. BALB/c)		Yes with boost (BALB/c)		21	Pechous et al., 2008
LVS <i>sodB</i> _{Ft}	>10 ⁴ (i.n. C57BL/6) >10 ⁴ (i.n. BALB/c)		Yes (C57BL/6)		21	Bakshi et al., 2006, 2008
FSC200 Δ c1pB	>10 ⁵ (i.n. BALB/c)	Yes (BALB/c)			42; Less attenuated than LVS in SCID mice	Golovliov et al., 2013
LVS Δ capB	>10 ⁷ (i.n. BALB/c) >10 ⁸ (i.d. BALB/c)	No (BALB/c)	Yes (BALB/c)		42; Need i.n. vaccination	Jia et al., 2010, 2013, 2016
LVS Δ capB /iglA		Yes (BALB/c)			42	Jia et al., 2013
LVS Δ capB /iglC		Yes (BALB/c)			42	Jia et al., 2013
LVS Δ capB /iglABC		Yes (BALB/c)	Yes (BALB/c)		42	Jia et al., 2016, 2018
LVS::wzy	>10 ⁷ (i.n. BALB/c)		Yes (BALB/c)		28	Kim et al., 2012
LVS::wbtA	>10 ⁷ (i.n. BALB/c)		No (BALB/c)		28	Sebastian et al., 2007; Kim et al., 2012
Fn Δ iglD	>9.7 × 10 ⁸ (i.n. BALB/c)				30; No protection in BALB/c mice; relevant efficacy to LVS in mice and rats not known; efficacy in NHP equivalent to LVS	Chu et al., 2014
SCHU S4 Δ purMCD	>10 ⁶ (i.d. BALB/c) >10 ⁶ (i.n. BALB/c)		Yes with boost (BALB/c)		21; Single deletion	Pechous et al., 2008
SchuS4 Δ gurBA	>10 ⁸ (i.n. C57BL/6)				30; Efficacious in rabbits; single deletion	Reed et al., 2014; Santiago et al., 2015
SCHU S4 Δ fipB	>10 ¹⁰ (i.n. C57BL/6)				30; Less efficacious than LVS in rabbits; single deletion	Qin et al., 2009; Reed et al., 2014
SCHU S4 Δ iglC	>10 ⁸ (i.d. BALB/c)				42 or 63; Not efficacious; single deletion	Twine et al., 2005; Conlan et al., 2010
LVS Δ capB + rLm/iglC	>10 ⁷ (i.d. BALB/c) for both vaccines	Yes (BALB/c)			42	Jia et al., 2009, 2013
LVS Δ capB/iglC + rLm/iglC	>10 ⁷ (i.d. BALB/c) for both vaccines	Yes (BALB/c)			42	Jia et al., 2009, 2013
VIRULENCE EQUIVALENT TO LVS						
SCHU S4 Δ c1pB	>10 ⁷ (i.d. BALB/c)	Yes (BALB/c)		Yes (BALB/c)	42; Single deletion	Conlan et al., 2010; Shen et al., 2010
SCHU S4 Δ c1pB Δ capB	>10 ⁷ (i.d. BALB/c)	Yes (BALB/c)			42; Survival ≤20%	Golovliov et al., 2013
LESS ATTENUATED THAN LVS						
SCHU S4 Δ FTT0918	~10 ⁵ (i.d. BALB/c)	Yes (BALB/c)			42; More virulent than LVS in mice	Twine et al., 2005
SCHU S4 Δ FTT0918 Δ capB	≥10 ⁷ (i.d. BALB/c) ~10 ³ (i.d. C3H/HeN)	Yes (BALB/c)		Yes (C3H/HeN)	42; Protection in C3H mice ≥ LVS with i.d. prime and oral boost; more virulent than LVS in C3H mice	Conlan et al., 2010
VIRULENCE NOT COMPARED WITH LVS						
SchuS4 Δ aroD	Not available				21; More protective than LVS in rabbits; single deletion	Reed et al., 2014

^aVaccine: Only vaccines that were tested against subsp. *tularensis* (Type A) respiratory challenge and compared with LVS are listed.

^bEfficacy relative to LVS: Percentage survival was used to compare the protective efficacy against respiratory challenge with a subsp. *tularensis* Type A strain between animals immunized with the vaccine candidate and animals immunized with LVS. Statistical significance was not available from some of the reported studies.

IgIb, and IgIc (rLVS $\Delta capB/iglABC$) and evaluated their capacity to protect against i.n. challenge (more consistent route than aerosol challenge) with *F. tularensis* SCHU S4. BALB/c mice immunized once i.d. with rLVS $\Delta capB/iglC$ or rLVS $\Delta capB/iglA$ had a significantly greater survival rate (40 and 50%, respectively) than mice immunized with the parental LVS $\Delta capB$ vector (0% survival, $p = 0.09$ and 0.01 , respectively), which was not significantly different from that of the LVS-immunized mice (63% survival) (**Table 1**, *Capsular and membrane mutant*) (Jia et al., 2013). In separate studies, mice homologously primed-boosted with rLVS $\Delta capB/iglABC$ i.n. three times at Weeks 0, 4, and 8 or twice at Weeks 4 and 8 and challenged i.n. at Week 14 with a lethal dose of SCHU S4 had 83–100% survival—greater than LVS i.d. vaccination—while all the naïve mice died at day 4 post-challenge. Mice homologously primed-boosted i.d. with rLVS $\Delta capB/iglABC$ twice or three times had survival equivalent to LVS-immunized mice (**Table 1**, *Capsular and membrane mutants*) (Jia et al., 2016, 2018).

Kim et al. constructed *wzy* (O-antigen polymerase) (LVS:: Δwzy) and *wbtA* (LVS:: $\Delta wbtA$) deletion mutants of LVS; both were significantly attenuated in mice (Kim et al., 2012). BALB/c mice immunized i.n. with LVS:: Δwzy , but not with LVS:: $\Delta wbtA$, were highly protected against i.n. challenge 4 weeks later with 8 CFU SCHU S4, similar to LVS i.n. immunized mice (**Table 1**, *Capsular and membrane mutants*) (Kim et al., 2012). Mahawa et al. developed LVS mutants defective in a conserved hypothetical membrane protein (FTL_0057) or in an outer membrane protein A-like family protein (FTL_0325). BALB/c mice immunized i.n. with FTL_0057 or FTL_0325 mutants of LVS were highly protected against i.n. challenge with SCHU S4; however, their efficacy relevant to LVS was not studied (**Table 1**, *Capsular and membrane mutants*) (Mahawar et al., 2013).

Other subsp. *holarctica* Mutants

Subsp. *holarctica* LVS mutants deficient in FTL_0552 (a transcriptional response regulation gene, *pmrA*), FTL_0291, or FTL_0304 also have shown attenuated phenotypes and protective efficacy against i.n. challenge with SCHU S4 in murine models. However, these mutants were not compared for efficacy with the parental LVS vaccine (**Table 1**, *Other mutants*) (Sammons-Jackson et al., 2008; Mahawar et al., 2013).

LIVE ATTENUATED *F. NOVICIDA* VACCINE CANDIDATES

F. novicida vaccine candidates have been constructed by deleting genes involved in the purine biosynthesis pathway (*purA* and *purF*), the T6SS (*iglB*, *iglC*, *pdpB*, and *iglD*), the response regulator (*pmrA*), or in other activities. A complete list of the *F. novicida* mutants can be found in a review article written by Pechous et al. (2009). However, only a few of the *F. novicida* mutants, including mutants with a deletion in *purE*, *purA*, *iglB*, *iglD*, or *pmrA*, have been tested against challenge with virulent SCHU S4, and even fewer against respiratory challenge with SCHU S4. In one study, BALB/c mice immunized i.p., but not

s.c., with *F. novicida* U112 $\Delta purF$::cm were partially protected against i.p. challenge with the homologous U112 strain, but not against challenge with the heterologous SCHU S4 strain; a similar mutant, U112 $\Delta purA$::cm, was not protective against either U112 or SCHU S4 challenge (Quarry et al., 2007). Two *F. novicida* U112 *iglB* deletion mutants, U112 $\Delta iglB$ and U112 $\Delta iglB$::fljB (expressing one domain D of the *Salmonella typhimurium* FljB flagellin, reportedly a TLR5 agonist), administered orally, have been shown to partially protect against i.n. or intratracheal (i.t.) challenge with SCHU S4 in mice and Fisher rats; however, efficacy was not compared with LVS (**Table 2**; Cong et al., 2009; Signarovitz et al., 2012; Cunningham et al., 2014). An *F. novicida* mutant with a deletion in *iglD* (Fn IglD), although not protective in a murine model of tularemia, has demonstrated protection against i.t. challenge with SCHU S4 in the more resistant Fisher rat model and in the non-human primate model of tularemia (see below for details) (Chu et al., 2014). Another *F. novicida* mutant with a deletion in an orphan response regulator gene *pmfA* was protective against homologous U112 but not against heterologous SCHU S4 challenge (**Table 2**; Mohapatra et al., 2007). Other studies also have shown that *F. novicida* and its derivative mutants can induce protective immunity against homologous respiratory challenge with wild-type *F. novicida*; however, these mutants have not been shown capable of inducing protection against respiratory challenge with subsp. *tularensis* in murine models of pneumonic tularemia by traditional i.d. or i.n. routes (Pammit et al., 2006; Sanapala et al., 2012).

T6SS Mutant

The Francisella pathogenicity island (FPI) proteins, including IglD, are required for bacterial phagosome escape, intracellular replication, and virulence, and are components of a T6SS apparatus (Clemens et al., 2015). Chu et al. reported on the protective immunity induced by *iglD* deletion mutants of subsp. *tularensis* (Ftt *iglD*) and *F. novicida* (Fn *iglD*) in murine, Fischer rat, and non-human primate models of pneumonic tularemia (Chu et al., 2014). Ftt *iglD* and Fn *iglD* are defective for intramacrophage replication and attenuated in mice (the LD₅₀ for Fn *iglD* is 9.7×10^8 CFU i.n. in BALB/c mice vs. $\sim 10^3$ CFU for LVS). Mice immunized i.n. with Fn *iglD* were fully protected against subsequent homologous challenge with 10^3 CFU of the parental *F. novicida* U112 strain; however, mice immunized i.n. with Fn *iglD* or Ftt *iglD* were not protected against respiratory challenge with the heterologous subsp. *tularensis* SCHU S4 strain. Arguing that the mouse may be too sensitive to tularemia, Chu et al. evaluated the Fn *iglD* vaccine in the Fischer rat, an animal model that has been shown to be more resistant to various *Francisella* subspecies than mice and non-human primates. Fischer rats vaccinated with Fn *iglD* orally or i.t. and challenged i.t. 30 days later with subsp. *tularensis* SCHU S4 had 83–100% survival post-challenge vs. 17–25% survival post-challenge for naïve rats. Of note, Fn *iglD* was not compared with LVS for efficacy in the murine and rat models. Cynomolgus macaques vaccinated with 10^8 CFU Fn *iglD* via bronchoscopy and challenged via head-only aerosol inhalation 30 days later with $\sim 2,500$ – $5,000$ CFU SCHU S4 had 83% survival, somewhat less than those immunized s.c. with 10^8 CFU LVS (100% survival);

mock vaccinated animals died 7–13 days post-challenge (Table 2; Chu et al., 2014).

LIVE ATTENUATED SUBSP. *TULARENSIS* VACCINE CANDIDATES

Because subsp. *tularensis* and subsp. *holarctica* differ in genetic organization, antigen expression, and disease pathogenesis, it was hypothesized that attenuated mutants on the background of subsp. *tularensis* may offer better protection against respiratory challenge with the parental subsp. *tularensis* than mutants derived from subsp. *holarctica* (Conlan et al., 2003; Wu et al., 2005). Thus, a series of mutants have been generated in the SCHU S4 background with mutations previously shown to attenuate LVS and tested in murine, rabbit, and non-human primate models of pneumonic tularemia (Twine et al., 2005, 2012; Pechous et al., 2008; Qin et al., 2008, 2009; Conlan et al., 2010; Michell et al., 2010; Shen et al., 2010; Rockx-Brouwer et al., 2012; Reed et al., 2014; Santiago et al., 2015). Summarized below are some SCHU S4 mutants that have been tested against respiratory SCHU S4 challenge.

Nutrient Metabolic Mutants

Based on the capacity of the attenuated LVS $\Delta purMCD$ mutant to induce protective immunity, Pechous et al. generated a defined subsp. *tularensis* SCHU S4 $\Delta purMCD$ mutant and showed that it is significantly more attenuated in mice when delivered by the i.d. ($LD_{50} > 10^6$ CFU) and i.n. ($LD_{50} > 10^6$ CFU) routes than its parental SCHU S4 strain ($LD_{50} < 10$ CFU i.n. or i.d.) (Pechous et al., 2008). However, mice immunized i.n. with SCHU S4 $\Delta purMCD$ had tissue damage in the lung and were protected no better than mice vaccinated with LVS or with an analogous LVS $\Delta purMCD$ mutant. BALB/c mice immunized once i.n. with 10^4 CFU SCHU S4 $\Delta purMCD$, 10^6 CFU LVS $\Delta purMCD$ or 10^2 CFU LVS and challenged 42 days later i.n. with 100 CFU SCHU S4 had 14, 0, and 100% survival, respectively; mice immunized twice i.n. with the same vaccines had 71, 100, and 100% survival after i.n. challenge with 100 CFU SCHU S4 (Results for SCHU S4 mutant and LVS shown in Table 3, *Nutrient metabolic mutants*) (Pechous et al., 2008); thus homologous i.n. boosting substantially improved the efficacy of the SCHU S4 $\Delta purMCD$ vaccine. Several other SCHU S4 mutants that are deficient in nutrient metabolic enzymes have also been tested against respiratory challenge with SCHU S4 in a murine or rat model (Table 3, *Nutrient metabolic mutants*) (Reed et al., 2014; Santiago et al., 2015).

Heat Shock Mutants

A defined SCHU S4 *clpB* mutant (SCHU S4 $\Delta clpB$) has been studied extensively for its capacity to induce protective immunity in BALB/c, C3H/HeN, and C57BL/6 mice (Conlan et al., 2010; Shen et al., 2010; Twine et al., 2012; Golovliov et al., 2013). Conlan et al. immunized BALB/c mice or C3H/HeN mice with 1×10^5 CFU i.d. or 1×10^8 CFU orally (p.o.) with LVS or SCHU S4 $\Delta clpB$, boosted or did not boost p.o., and challenged the mice 6 weeks later by aerosol with 20 CFU of the parental SCHU S4 strain. Unvaccinated mice served as controls. BALB/c mice

immunized i.d. or orally with SCHU S4 $\Delta clpB$ had 60 and 40% survival, respectively, significantly greater than those of naïve mice (0% survival) and mice immunized with LVS (0% survival), whereas C3H/HeN mice immunized i.d. or orally with the same vaccine had 0% survival. Boosting i.d. immunized BALB/c and C3H/HeN mice p.o. at week 8 did not improve the survival of mice against SCHU S4 challenge; boosting orally immunized C3H/HeN, but not BALB/c mice, with SCHU S4 $\Delta clpB$ did improve protection against SCHU S4 challenge (Conlan et al., 2010). Others also showed similar protective immunity of SCHU S4 $\Delta clpB$ in BALB/c but not in C57BL/6 mice (Shen et al., 2010; Twine et al., 2012; Golovliov et al., 2013). Introducing a second deletional mutation—one in *capB*—to SCHU S4 $\Delta clpB$ (SCHU S4 $\Delta clpB\Delta capB$) appeared to reduce its capacity to induce protective immunity against respiratory challenge with parental SCHU S4 (Golovliov et al., 2013; Table 3, *Heat shock protein mutants*).

Putative Capsular Mutants

Defined subsp. *tularensis* SCHU S4 mutants with a single deletion in *capB* ($\Delta capB::Cam$) or double deletions in *FTT0918* and *capB* ($\Delta FTT0918\Delta capB$) have been developed by Michell and Conlan et al. and evaluated as vaccine candidates (Conlan et al., 2010; Michell et al., 2010). Michell et al. showed that the s.c. median lethal dose for SCHU S4 $\Delta capB::Cam$, a single *capB* deletion mutant with a chloramphenicol resistance cassette (Cam) inserted at the deleted *capB* locus, is $>1.6 \times 10^6$ CFU in BALB/c mice. The level of protection afforded by s.c. immunization with 10^4 SCHU S4 $\Delta capB::Cam$ is comparable to that of s.c. immunization with 10^4 CFU LVS against systemic (s.c.) challenge with 10^3 SCHU S4 56 days later. The SCHU S4 $\Delta capB::Cam$ vaccine was not tested against respiratory challenge (Michell et al., 2010). Conlan et al. showed that SCHU S4 $\Delta FTT0918\Delta capB$ administered i.d. is as attenuated as LVS in BALB/c mice ($LD_{50} \geq 10^7$ CFU) but more virulent than LVS in C3H/HeN mice ($LD_{50} < 10^5$ CFU vs. $LD_{50} > 10^5$ CFU for LVS). In a virulence study, BALB/c and C3H/HeN mice infected orally with 10^8 CFU SCHU S4 $\Delta FTT0918\Delta capB$ had 80% (12/15) and 60% (9/15) survival, respectively (Conlan et al., 2010). In a study summarized in Table 3, *Capsular mutant*, BALB/c or C3H/HeN mice were not immunized, or immunized i.d. with 10^3 CFU or orally with 10^8 CFU $\Delta FTT0918\Delta capB$ or LVS, homologously boosted or not boosted orally, and challenged by aerosol 6 weeks later with 20 CFU SCHU S4. BALB/c mice immunized i.d. or orally with $\Delta FTT0918\Delta capB$ had 40 and 0% survival, respectively, after SCHU S4 aerosol challenge whereas none of the C3H/HeN mice immunized i.d. or orally with $\Delta FTT0918\Delta capB$ survived the challenge; nor did the naïve mice or mice immunized i.d. or orally with LVS. Homologous boosting orally did not significantly improve the protection against aerosol challenge with SCHU S4 except that C3H/HeN mice immunized i.d. and boosted orally with $\Delta FTT0918\Delta capB$ had improved survival (50% vs. 0% without boosting) (Conlan et al., 2010). In an earlier study, Twine et al. showed that the SCHU S4 FTT0918 single deletional mutant (SCHU S4 $\Delta FTT0918$) had an i.d. LD_{50} of $\sim 10^5$ CFU and was thus 10-fold more virulent than LVS in BALB/c mice. BALB/c mice immunized i.d. with

10^5 Δ FTT0918 and challenged i.n. 9 weeks later with 10 CFU FSC 033 had 33% survival, while LVS-immunized mice had 0% survival after aerosol FSC033 challenge (Table 3, *Other mutants*) (Twine et al., 2005). The results of these studies suggest that single deletional mutants in the background of SCHU S4, although more attenuated than the parental SCHU S4 strain, are generally still more virulent than LVS. Introducing a second major attenuating deletion attenuates the mutant further but diminishes its capacity to induce protective immunity such that it is comparable to or less protective than LVS vaccination against virulent subsp. *tularensis* challenge.

Lipoprotein Mutants

Qin et al. initially reported a subsp. *tularensis* SCHU S4 mutant with a transposon insertion at the FTT1103 locus (encoding a hypothetical lipoprotein); subsequently, they generated a defined subsp. *tularensis* SCHU S4 FTT1103 deletion mutant (SCHU S4 Δ FTT1103) (Qin et al., 2009, 2011). SCHU S4 Δ FTT1103 is highly attenuated in mice with an LD₅₀ > 10¹⁰ i.n., and > 10⁶ i.p., s.c., or i.v.. C57BL/6 mice immunized once i.n. with 3 × 10⁷, 1 × 10⁸, or 3 × 10⁸ SCHU S4 Δ FTT1103 and challenged i.n. 32 days later with 37–68 CFU SCHU S4 had 100%, 100% and 50% survival post-challenge; BALB/c mice immunized i.n. with 1 × 10⁸ SCHU S4 Δ FTT1103 and challenged i.n. 33 days later with 95 CFU of the parental SCHU S4 strain had 75% survival post-challenge; however, there was no LVS control included in this study (Table 3, *Lipoprotein mutants*) (Qin et al., 2009, 2011). Recently, Reed et al. evaluated the vaccine efficacy of SCHU S4 Δ FTT1103 along with several other SCHU S4 mutants in a rabbit model (Reed et al., 2014). New Zealand White (NZW) rabbits were vaccinated via scarification with PBS, LVS, SCHU S4 Δ fibB (FTT1103), SCHU S4 Δ guaBA, or SCHU S4 Δ aroD; 30 days later, the animals were challenged with 1,000–10,000 CFU (~40–400 LD₅₀) of aerosolized SCHU S4 and monitored for signs of illness and survival. Animals vaccinated with SCHU S4 Δ guaBA or SCHU S4 Δ aroD had 27 and 36% survival, respectively (Table 3, *Nutrient metabolic mutants*); none of the mock-, LVS-, and Δ fibB-vaccinated animals survived the SCHU S4 challenge (Table 3, *Lipoprotein mutants*) (Reed et al., 2014).

Other subsp. *tularensis* Mutants

Other subsp. *tularensis* mutants, including SCHU S4 mutants with a single deletion in FTT0918, *iglC*, FTT0369, or FTT1676, or double deletions in FTT0369 and FTT1676 have also been reported; some have shown protection against i.n. challenge with SCHU S4 (Table 3, *Other mutants*) (Twine et al., 2005; Conlan et al., 2010; Rockx-Brouwer et al., 2012).

OTHER LIVE ATTENUATED RECOMBINANT VACCINE CANDIDATES

Other live attenuated recombinant vaccine candidates have been developed by using heterologous vectors—adenovirus, Tobacco Mosaic Virus, and *Listeria monocytogenes* (Lm), or a homologous LVS mutant (LVS Δ capB or LVS Δ LPS) vector to express/overexpress *F. tularensis* antigens (Jia et al., 2009, 2013, 2016; Kaur et al., 2012; Banik et al., 2015). Among these vaccines, some of the Lm-, LVS Δ capB-, and LVS Δ LPS-vectored

vaccines were tested against respiratory challenge with subsp. *tularensis* SCHU S4 and these are summarized in Table 4. We constructed seven recombinant Lm (rLm) vaccines using Lm Δ actA (a live attenuated *actA* deficient mutant) as a vector to express *F. tularensis* proteins, including T6SS protein IglC, metabolic enzymes AcpA, KatG, and Pld, and other proteins including bacterioferritin (Bfr), DnaK, and GroEL, and tested their protective immunity against LVS i.n. challenge in BALB/c mice. Among the seven rLm vaccines constructed, two of them, rLm/*iglC* and rLm/*katG*, were further tested for their efficacy against aerosol challenge with subsp. *tularensis* SCHU S4 (Jia et al., 2009). BALB/c mice were sham-immunized, or primed-boosted i.d. with Lm Δ actA (vector control), rLm/*iglC*, rLm/*katG* (heterologous vaccines), or the LVS control, and challenged six weeks later with 1 × LD₅₀ or 10 × LD₅₀ aerosolized SCHU S4. Mice primed-boosted with rLm/*iglC* had a greater survival rate (100 and 75% post-aerosol challenge with 1 × and 10 × LD₅₀ SCHU S4, respectively) than sham-immunized mice or mice immunized with the vector control, and the survival rates were comparable to that of LVS-immunized mice (87.5%). Mice immunized with rLm/*katG* also showed greater survival than sham-immunized animals (Table 4, *Heterologous standalone vaccines*) (Jia et al., 2009). In subsequent studies, mice primed at Week 0 with LVS Δ capB or rLVS Δ capB/IglC (prime vaccines homologous to *F. tularensis*), boosted at Week 4 with heterologous vaccine rLm/*iglC*, and subsequently challenged at Week 10 with 10x LD₅₀ aerosolized SCHU S4 had a significantly greater survival rate (75%) than sham-immunized mice (0%) ($p < 0.0001$), and the survival rate was greater than that of the LVS-immunized mice (62.5%) (Jia et al., 2013). Mice primed-boosted with rLVS Δ LPS/IglC—rLm/*iglC* (1 or 2 boosts) and subsequently challenged with 3 × or 10 × LD₅₀ aerosolized SCHU S4 also had significantly greater survival rates than sham-immunized mice and mice immunized with the prime vaccine only (Table 4, *Homologous prime and heterologous boost vaccines*) (Jia et al., 2013).

SUMMARY AND DISCUSSION

The vaccines summarized here include deletional mutants of subsp. *holarctica* LVS or FSC200 (Table 1), *F. novicida* U112 (Table 2), and subsp. *tularensis* SCHU S4 (Table 3), and homologous LVS mutants overexpressing *F. tularensis* antigens and heterologous vectors expressing *F. tularensis* antigens (Table 4). The unlicensed LVS vaccine, the only vaccine available in the U.S.A., has shown substantial albeit incomplete efficacy in humans but retains residual toxicity. As noted, it would seem reasonable to expect that any vaccine warranting further consideration as a human vaccine satisfy the following two criteria: 1) the vaccine is safer than LVS; and 2) the vaccine provides protection equivalent to or greater than LVS against respiratory challenge with subsp. *tularensis* SCHU S4 in appropriate animal models. The data summarized here show that it is relatively easy to generate genetically defined mutants that are safer than LVS so as to meet the first criterion; however, it is difficult to control the balance between attenuation and protection so as to meet the second criterion simultaneously. Practically speaking, among the vaccine candidates summarized

here, only a few meet both criteria. Often, the LVS-derived vaccine candidates need either prime-boost vaccination or intranasal administration in order to provide very high-level protective immunity.

With respect to the relative efficacies of vaccine candidates, in many cases, vaccines and challenge strains have been tested under different conditions, e.g., different preparations of vaccine and challenge strains; different routes of vaccine administration (mucosal vs. systemic); different immunization-challenge intervals (typically ranging from 3 to 6 weeks); different routes and doses of challenge strain (less virulent subsp. *holarctica* or *F. novicida* vs. highly virulent subsp. *tularensis* SCHU S4); and different animal models (mice, rats, rabbits, or non-human primates), making it difficult to compare their relative efficacies. Of course, head-to-head comparisons are the most reliable way to compare vaccine candidates, but except for comparisons with LVS—the only vaccine tested and shown protective in humans and effectively the current gold standard—this is rarely done. We summarize vaccines that were tested against respiratory challenge with SCHU S4 and compared with LVS for efficacy in **Table 5** and discuss factors that affect vaccine efficacy below.

Vaccine and Challenge Strain Stock Preparation

As summarized in **Tables 1–4**, some studies used LVS as a positive control to evaluate the efficacy of various vaccines against respiratory challenge with SCHU S4 strains. It is interesting that while the median/mean survival time for unvaccinated or sham-immunized mice fell between 4 and 6 days post-respiratory SCHU S4 challenge in most studies, the immunity induced by LVS varied significantly in these studies. Of note, some vaccine strains were produced on solid agar while others in broth medium. Eigelsbach et al. conducted a study on virulence and immunogenicity of live vaccine strains. The study showed that LVS harvested from modified casein partial hydrolysate medium (MCPH) appeared more virulent and immunogenic in mice than LVS harvested from glucose cysteine hemin agar (GCHA); however, LVS prepared from GCHA and MCPH induced comparable protection in guinea pigs (Eigelsbach and Downs, 1961). While it is impossible to compare vaccines among different studies, it would be helpful to include LVS prepared using a standardized method as a positive control in efficacy studies.

Mucosal vs. Systemic Route of Vaccine Administration

As noted above, several live attenuated vaccine candidates induce more potent protective immunity against respiratory challenge with subsp. *tularensis* SCHU S4 when administered by the mucosal respiratory route (e.g., i.n., aerosol, or intratrachea), or by the mucosal oral route than by a traditional systemic route (i.d., s.c., or i.p.) (Hornick and Eigelsbach, 1966; Conlan et al., 2005; Wu et al., 2005; Pechous et al., 2008; Jia et al., 2010, 2013), with a few exceptions (Rockx-Brouwer et al., 2012). In one study, an alternative mucosal (i.e., oral) route for delivery of *F. novicida*-derived vaccine candidates showed greater protective immunity than the i.n. route against respiratory challenge with the virulent

SCHU S4 strain (Cong et al., 2009). The i.n. route raises some additional safety concerns; that said, the current live attenuated flu vaccine administered i.n. has an excellent safety record (Pavot et al., 2012).

Interval Between Vaccination and Challenge

As summarized in **Tables 1–4**, intervals between the last or the only vaccination and challenge ranged between 3 and 6 weeks in different studies. Eigelsbach and Downs investigated the effect of the vaccination-challenge interval on the immunity of LVS in mice and guinea pigs (Eigelsbach and Downs, 1961). Albino mice (Webster) vaccinated with LVS s.c. 15–30 days prior to challenge with 10^3 CFU of SCHU S4 s.c. had a higher survival rate (68–88%) than mice vaccinated 60 days prior to challenge (49–56%). This difference was appreciably greater in guinea pigs. Guinea pigs (Harley) vaccinated 15 days prior to challenge had 45% survival vs. 5% survival for those vaccinated 30 days prior to challenge. LVS administered i.d. or i.n. to mice was cleared from all the infected organs by 3 weeks (Jia et al., 2010). Thus, it would be helpful to challenge animals at a longer interval, i.e., more than 3 weeks, to minimize the effect of non-specific immunity and to allow evaluation of various vaccines under more rigorous conditions.

Hypo- and Hyper- Attenuation of Vaccines

Some mutants of subsp. *holarctica* LVS (i.e., LVS Δ *purMCD*, LVS *sodB_K*, LVS Δ *capB*, LVS Δ *capB/iglA*, LVS Δ *capB/iglABC*, and LVS Δ *wzy*) and subsp. *tularensis* SCHU S4 (SCHU S4 Δ *purMCD*, SCHU S4 Δ *clpB*, SCHU S4 Δ *clpB* Δ *capB*) show significant attenuation and promising protective immunity against respiratory challenge in a murine model (**Table 5**) (Bakshi et al., 2006, 2008; Pechous et al., 2008; Qin et al., 2009; Sebastian et al., 2009; Jia et al., 2010, 2013, 2016; Shen et al., 2010; Kim et al., 2012; Rockx-Brouwer et al., 2012; Twine et al., 2012; Golovliov et al., 2013; Marohn and Barry, 2013; Straskova et al., 2015); other mutants, however, are either hypo- or hyper- attenuated, rendering them either poorly immunogenic or too virulent to use. LVS-derived vaccine candidates have deletions of at least three major virulence genes including two that were lost in the generation of the parental LVS strain (Salomonsson et al., 2009). Most immunoprotective SCHU S4 mutants, however, are single deletional mutants, raising the concern that they are only one mutation away from reversion to virulence, as seen with viral pathogens (Jia et al., 1999; Zhou et al., 2016). Therefore, a second major attenuating deletion is generally thought necessary—this typically markedly reduces their capacity to induce protective immunity. For example, the SCHU S4 Δ *clpB* mutant is highly attenuated ($LD_{50} > 10^7$ i.d.) and protective against respiratory challenge with ≤ 100 CFU SCHU S4 (40–100% of immunized BALB/c mice survived challenge)—more protective than LVS. However, introduction of a second major attenuating deletion in various genes (*pmrA*, *relA*, *capB*, *wbtC*, *ggt*, or *fupA*) significantly reduces its capacity to induce protective immunity against SCHU S4 challenge (<20% of mice immunized with the double deletional mutants survived SCHU S4 challenge) (**Table 3**, Heat shock protein mutants) (Golovliov et al., 2013). Another example is a SCHU S4 mutant with a

single deletion in FTT0369c or FTT1676; these show significant protection against respiratory challenge with SCHU S4; however, a double deletion in both FTT0369c and FTT1676 significantly reduces the vaccine's capacity to induce protective immunity (**Table 3, Other mutants**) (Rockx-Brouwer et al., 2012).

Vaccine Genetic Background

Vaccines have been generated in the background of subsp. *holarctica*, subsp. *tularensis*, *F. novicida*, and heterologous vectors. The subsp. *holarctica* LVS strain is the only vaccine tested and shown efficacious in humans against virulent SCHU S4 challenge; however, its residual toxicity in humans and unknown attenuation mechanism may have presented obstacles to its licensure. LVS-derived vaccines are safer than LVS and retain the large antigen pool that might be required for protection against heterologous challenge with the virulent subsp. *tularensis* strain. However, a booster or intranasal vaccination route are generally required for enhanced vaccine-induced protection (**Table 1**). *F. novicida* is less virulent than LVS in mice, guinea pigs, rabbits and Fisher rats, and rarely infects humans (so far only 12 cases have been documented) (Kingry and Petersen, 2014). However, in contrast to LVS, *F. novicida* differs from *F. tularensis* in the mechanism of pathogenicity; they differ in cell surface structure, means of cellular entry, types of cells infected *in vivo*, and ability to evade host immune responses (Kingry and Petersen, 2014). The *F. novicida* parental strain and its derivatives have not shown efficacy against respiratory challenge with SCHU S4 in mice and guinea pigs by i.d. or i.n. route; the protective immunity induced by the i.t. or oral route against i.t. challenge with SCHU S4 in Fisher rats was not compared with that of LVS (**Table 2**). The subsp. *tularensis*-derived vaccines are generally more efficacious than LVS against homologous challenge with SCHU S4. However, this may be true only for SCHU S4-derived vaccines with a single deletion. A second major attenuating deletion significantly reduces vaccine efficacy (**Table 3**). The vaccines constructed using a heterologous vector (i.e., *Listeria monocytogenes*) have a much more limited antigen pool, need multiple vaccinations, and are less efficacious than LVS (**Table 4**).

The impact of vaccine genetic background on vaccine efficacy is also evident in comparisons of vaccines derived from different subspecies but comprising the same deletional gene mutation. For example, some gene deletional mutants in the LVS background are both highly attenuated and able to induce protective immunity against SCHU S4 challenge, but this may not be true of the same deletion in the *F. novicida* or SCHU S4 background. An LVS mutant with a deletion in *purMCD*, LVS $\Delta purMCD$, is both highly attenuated and able to induce protection against virulent SCHU S4 i.n. challenge; protective immunity is similar to that induced by LVS i.n. vaccination. However, an attenuated SCHU S4 with the same deletion, SCHU S4 $\Delta purMCD$, provides limited protection against SCHU S4 challenge, less than that induced by LVS vaccination (Pechous et al., 2006, 2008). Attenuated *F. novicida* mutants with similar deletions, $\Delta purCD$ and $\Delta purM$, are not able to induce protection against the homologous wild-type strain challenge (Tempel et al., 2006; Quarry et al., 2007). The same findings have been reported for *guaA*, *guaB*, and *guaBA* mutants (Santiago et al.,

2009, 2015). In contrast, *clpB* deletional mutants in the subsp. *tularensis* (SCHU S4) background induced full protection against respiratory challenge with the parent SCHU S4; a mutant with the same deletion in LVS showed no protection (Golovliov et al., 2013). Hence, the vaccine's genetic background is an important determinant of the vaccine's attenuation and protective efficacy.

Animal Model

Various animal models—mice, rats, rabbits, guinea pigs, and non-human primates—have been used to study tularemia vaccine efficacy as reviewed recently by Elkins et al. (2016); however, they differ in their sensitivity to the highly virulent SCHU S4 strain and in vaccine-induced protective immunity against SCHU S4 challenge. Mice, guinea pigs, rabbits, and primates are more sensitive to SCHU S4 than rats (White rats and Fisher rats). The LD₅₀ for SCHU S4 by a systemic route (s.c. or i.d.) is 1 CFU in mice, 1 CFU in guinea pigs, 1 CFU in rabbits, and >10⁸ CFU (s.c.) in White rats; the LD₅₀ of SCHU S4 by the respiratory route is 1-3 CFU in mice (i.n.), 1 CFU in cynomolgus macaques (aerosol), and >5 × 10² CFU in Fisher rats (intratracheal); in humans, as few as 10–50 CFU SCHU S4 can cause clinical tularemia (Eigelsbach et al., 1951; McCrumb, 1961; Saslaw et al., 1961a,b; Schricker et al., 1972; Kostiala et al., 1975; Jemski, 1981; Conlan et al., 2003; Barker and Klose, 2007; Lyons and Wu, 2007; Raymond and Conlan, 2009; Wu et al., 2009; Ray et al., 2010; Chu et al., 2014; Kingry and Petersen, 2014; Hutt et al., 2017; Nguyen et al., 2017). Mice, rats, guinea pigs, and primates also differ in the degree of vaccine-induced protective immunity against virulent SCHU S4 challenge. Mice, guinea pigs, and humans vaccinated with the Foshay-killed vaccine were not protected against aerosol challenge with SCHU S4, while White rats were protected (Lyons and Wu, 2007). Furthermore, different strains within species show substantial variability in their susceptibility to challenge and the degree of vaccine-induced protection. LVS-immunized BALB/c mice are more resistant than LVS-immunized C57BL/6 mice to low dose aerosol or high dose i.d. challenge with virulent subsp. *tularensis* FSC 033 strain (Chen et al., 2003); however, C57BL/6 mice clear subsp. *tularensis* SCHU S4 infection more rapidly (Fritz et al., 2014). White rats and Fisher rats are more resistant to SCHU S4 challenge than Sprague–Dawley rats (Lyons and Wu, 2007; Raymond and Conlan, 2009). African green monkeys and cynomolgus monkeys are more sensitive to SCHU S4 aerosol challenge than Rhesus monkeys, with an aerosol lethal dose of 40, 32, and 2.8 × 10⁵ CFU, respectively (Glynn et al., 2015). In addition, recent studies show that vaccines inducing strong protective immunity in one animal model may not do so in another model. For example, *guaBA*, *aroD*, and *fipB* (FTT1103) mutants have been tested in both mice and rabbits (Qin et al., 2009; Santiago et al., 2009, 2015; Reed et al., 2014). While the SCHU S4 $\Delta guaB$ and $\Delta guaA$ mutants, administered via scarification, induce partial protective immunity against respiratory SCHU S4 challenge in the New Zealand rabbit model, they do not do so in C57BL mice (Reed et al., 2014; Santiago et al., 2015). In contrast, the SCHU S4 $\Delta fibB$ (FTT1103) mutant, while fully protective in C57BL mice and partially protective in BALB/c mice, showed no protection against SCHU S4 challenge in the rabbit model (Qin et al.,

2009; Reed et al., 2014). Other reports have reported differences in protective immunity conferred by the same vaccine in the murine and Fisher rat models (Cong et al., 2009; Signarovitz et al., 2012; Chu et al., 2014). These findings highlight the impact of animal model on the outcomes of preclinical vaccine efficacy studies.

The low natural incidence of tularemia renders field trials of efficacy unfeasible, and ethical considerations make it unlikely that tularemia vaccines will ever again be tested for efficacy in human challenge studies. In such situations, the FDA has promulgated the Animal Rule, whereby a drug or vaccine may be licensed on the basis of efficacy in relevant animal models. That raises the question as to which animal models are most relevant. If a vaccine is ineffective in the highly sensitive mouse model, are efficacy studies in the relatively resistant Fisher rat model an acceptable substitute? Proponents of this rat model would argue that the susceptibility of the Fisher rat to various *F. tularensis* strains more closely approximates that of humans than the mouse. Be it as it may, from the standpoint of efficacy, a vaccine that is efficacious in the most sensitive animal models would seem to be a more reliable one for humans, who likely have varying susceptibility to infection depending upon numerous host variables, than a vaccine efficacious only in relatively resistant models.

CONCLUSION

Since 2001, several promising live attenuated vaccine candidates have been developed that meet what would seem to be minimal criteria for a new human vaccine—safety greater than LVS and protective efficacy equivalent to or greater than LVS against respiratory challenge with subsp. *tularensis* SCHU S4 in appropriate animal models (Table 5). Some of these vaccines additionally demonstrate efficacy comparable to or greater than that of LVS against SCHU S4 respiratory

challenge in the demanding mouse model. Vaccines meeting this higher standard include LVS mutants (LVS Δ purMCD, LVS *sodB_{Fl}*, LVS Δ capB, and LVS::wzy), another *F. tularensis* type B mutant (FSC200 Δ clpB), LVS Δ capB overexpressing *F. tularensis* T6SS proteins (LVS Δ capB/IglA, IglC or IglABC), a LVS Δ capB-rLm/IglC heterologous prime-boost vaccine, and a single deletional SCHU S4 mutant (Δ purMCD). Another single deletional SCHU S4 mutant, SCHU S4 Δ clpB, and a double deletional SCHU S4 mutant, SCHU S4 Δ clpB Δ capB demonstrates efficacy greater than LVS but its attenuation is equivalent to LVS. That these SCHU S4 mutants contain only one major attenuating deletion raises a safety concern, namely reversion to virulence. A second major attenuating deletion would alleviate this concern, but retaining efficacy upon the introduction of a second major attenuating mutation has been a major challenge for single deletional SCHU S4 mutant vaccines. The efficacy of the new vaccines has typically been greatest when administered by the intranasal or another respiratory route, but administering vaccines by this route raises additional safety issues. Nevertheless, vaccines that are safer than LVS and at least as efficacious, including by the i.d. route, have been developed, and they are promising candidates for going forward into more advanced animal studies such as in the non-human primate model and human safety trials.

AUTHOR CONTRIBUTIONS

QJ and MAH wrote the article. The comments in this article represent the opinions of both QJ and MAH.

ACKNOWLEDGMENTS

This study was supported by National Institutes of Health grant AI101189.

REFERENCES

- Alibek, K. (1999). *Biohazard: The Chilling True Story of the Largest Covert Biological Weapons Program in the World, Told From the Inside by the Man Who Ran It*. New York, NY: Random House, Inc.
- Bakshi, C. S., Malik, M., Mahawar, M., Kirimanjeswara, G. S., Hazlett, K. R., Palmer, L. E., et al. (2008). An improved vaccine for prevention of respiratory tularemia caused by *Francisella tularensis* SchuS4 strain. *Vaccine* 26, 5276–5288. doi: 10.1016/j.vaccine.2008.07.051
- Bakshi, C. S., Malik, M., Regan, K., Melendez, J. A., Metzger, D. W., Pavlov, V. M., et al. (2006). Superoxide dismutase B gene (*sodB*)-deficient mutants of *Francisella tularensis* demonstrate hypersensitivity to oxidative stress and attenuated virulence. *J. Bacteriol.* 188, 6443–6448. doi: 10.1128/JB.00266-06
- Banik, S., Mansour, A. A., Suresh, R. V., Wykoff-Clary, S., Malik, M., McCormick, A. A., et al. (2015). Development of a multivalent subunit vaccine against tularemia using Tobacco Mosaic Virus (TMV) based delivery system. *PLoS ONE* 10:e0130858. doi: 10.1371/journal.pone.0130858
- Barker, J. R., and Klose, K. E. (2007). Molecular and genetic basis of pathogenesis in *Francisella tularensis*. *Ann. N. Y. Acad. Sci.* 1105, 138–59. doi: 10.1196/annals.1409.010
- Barrigan, L. M., Tuladhar, S., Brunton, J. C., Woolard, M. D., Chen, C. J., Saini, D., et al. (2013). Infection with *Francisella tularensis* LVS clpB leads to an altered yet protective immune response. *Infect. Immun.* 81, 2028–2042. doi: 10.1128/IAI.00207-13
- Bernard, K., Tessier, S., Winstanley, J., Chang, D., and Borczyk, A. (1994). Early recognition of atypical *Francisella tularensis* strains lacking a cysteine requirement. *J. Clin. Microbiol.* 32, 551–553.
- Bosio, C. M., Bielefeldt-Ohmann, H., and Belisle, J. T. (2007). Active suppression of the pulmonary immune response by *Francisella tularensis* Schu4. *J. Immunol.* 178, 4538–4547. doi: 10.4049/jimmunol.178.7.4538
- Buchan, B. W., McCaffrey, R. L., Lindemann, S. R., Allen, L. A. H., and Jones, B. D. (2009). Identification of migR, a regulatory element of the *Francisella tularensis* live vaccine strain iglABCD virulence operon required for normal replication and trafficking in macrophages. *Infect. Immun.* 77, 2517–2529. doi: 10.1128/IAI.00229-09
- Chen, W., Shen, H., Webb, A., KuoLee, R., and Conlan, J. W. (2003). Tularemia in BALB/c and C57BL/6 mice vaccinated with *Francisella tularensis* LVS and challenged intradermally, or by aerosol with virulent isolates of the pathogen: protection varies depending on pathogen virulence, route of exposure, and host genetic background. *Vaccine* 21, 3690–3700. doi: 10.1016/S0264-410X(03)00386-4
- Christopher, G. W., Cieslak, T. J., Pavlin, J. A., and Eitzen, E. M. Jr. (1997). Biological warfare. A historical perspective. *JAMA* 278, 412–417.
- Chu, P., Cunningham, A. L., Yu, J. J., Nguyen, J. Q., Barker, J. R., Lyons, C. R., et al. (2014). Live attenuated *Francisella novicida* vaccine protects against *Francisella*

- tularensis* pulmonary challenge in rats and non-human primates. *PLoS Pathog.* 10:e1004439. doi: 10.1371/journal.ppat.1004439
- Clemens, D. L., Ge, P., Lee, B. Y., Horwitz, M. A., and Zhou, Z. H. (2015). Atomic structure of T6SS reveals interlaced array essential to function. *Cell* 160, 940–951. doi: 10.1016/j.cell.2015.02.005
- Clemens, D. L., and Horwitz, M. A. (2007). Uptake and intracellular fate of *Francisella tularensis* in human macrophages. *Ann. N. Y. Acad. Sci.* 1105, 160–186. doi: 10.1196/annals.1409.001
- Clemens, D. L., Lee, B. Y., and Horwitz, M. A. (2004). Virulent and avirulent strains of *Francisella tularensis* prevent acidification and maturation of their phagosomes and escape into the cytoplasm in human macrophages. *Infect. Immun.* 72, 3204–3217. doi: 10.1128/IAI.72.6.3204-3217.2004
- Clemens, D. L., Lee, B. Y., and Horwitz, M. A. (2005). *Francisella tularensis* enters macrophages via a novel process involving pseudopod loops. *Infect. Immun.* 73, 5892–5902. doi: 10.1128/IAI.73.9.5892-5902.2005
- Cole, L. E., Yang, Y., Elkins, K. L., Fernandez, E. T., Qureshi, N., Shlomchik, M. J., et al. (2009). Antigen-specific B-1a antibodies induced by *Francisella tularensis* LPS provide long-term protection against *F. tularensis* LVS challenge. *Proc. Natl. Acad. Sci. U.S.A.* 106, 4343–4348. doi: 10.1073/pnas.0813411106
- Cong, Y., Yu, J. J., Guentzel, M. N., Berton, M. T., Seshu, J., Klose, K. E., et al. (2009). Vaccination with a defined *Francisella tularensis* subsp. novicida pathogenicity island mutant (DeltaiglB) induces protective immunity against homotypic and heterotypic challenge. *Vaccine* 27, 5554–5561. doi: 10.1016/j.vaccine.2009.07.034
- Conlan, J. W. (2011). Tularemia vaccines: recent developments and remaining hurdles. *Future Microbiol.* 6, 391–405. doi: 10.2217/fmb.11.22
- Conlan, J. W., Chen, W., Shen, H., Webb, A., and KuoLee, R. (2003). Experimental tularemia in mice challenged by aerosol or intradermally with virulent strains of *Francisella tularensis*: bacteriologic and histopathologic studies. *Microb. Pathog.* 34, 239–248. doi: 10.1016/S0882-4010(03)00046-9
- Conlan, J. W., Shen, H., Golovliov, I., Zingmark, C., Oyston, P. C., Chen, W., et al. (2010). Differential ability of novel attenuated targeted deletion mutants of *Francisella tularensis* subspecies tularensis strain SCHU S4 to protect mice against aerosol challenge with virulent bacteria: effects of host background and route of immunization. *Vaccine* 28, 1824–1831. doi: 10.1016/j.vaccine.2009.12.001
- Conlan, J. W., Shen, H., Webb, A., and Perry, M. B. (2002). Mice vaccinated with the O-antigen of *Francisella tularensis* LVS lipopolysaccharide conjugated to bovine serum albumin develop varying degrees of protective immunity against systemic or aerosol challenge with virulent type A and type B strains of the pathogen. *Vaccine* 20, 3465–3471. doi: 10.1016/S0264-410X(02)00345-6
- Conlan, W. J., Shen, H., Kuolee, R., Zhao, X., and Chen, W. (2005). Aerosol-, but not intradermal-immunization with the live vaccine strain of *Francisella tularensis* protects mice against subsequent aerosol challenge with a highly virulent type A strain of the pathogen by an alphabeta T cell- and interferon gamma- dependent mechanism. *Vaccine* 23, 2477–2485. doi: 10.1016/j.vaccine.2004.10.034
- Cunningham, A. L., Dang, K. M., Yu, J. J., Guentzel, M. N., Heidner, H. W., Klose, K. E., et al. (2014). Enhancement of vaccine efficacy by expression of a TLR5 ligand in the defined live attenuated *Francisella tularensis* subsp. novicida strain U112DeltaiglB::fljB. *Vaccine* 32, 5234–5240. doi: 10.1016/j.vaccine.2014.07.038
- Dennis, D. T., Inglesby, T. V., Henderson, D. A., Bartlett, J. G., Ascher, M. S., Eitzen, E., et al. (2001). Tularemia as a biological weapon: medical and public health management. *JAMA* 285, 2763–2773. doi: 10.1001/jama.285.2.2763
- Eigelsbach, H. T., Braun, W., and Herring, R. D. (1951). Studies on the variation of *Bacterium tularensis*. *J. Bacteriol.* 61, 557–569.
- Eigelsbach, H. T., and Downs, C. M. (1961). Prophylactic effectiveness of live and killed tularemia vaccines. I. Production of vaccine and evaluation in the white mouse and guinea pig. *J. Immunol.* 87, 415–425.
- Elkins, K. L., Cowley, S. C., and Bosio, C. M. (2007). Innate and adaptive immunity to *Francisella*. *Ann. N. Y. Acad. Sci.* 1105, 284–324. doi: 10.1196/annals.1409.014
- Elkins, K. L., Kurtz, S. L., and De Pascalis, R. (2016). Progress, challenges, and opportunities in *Francisella* vaccine development. *Expert Rev. Vaccines* 15, 1183–1196. doi: 10.1586/14760584.2016.1170601
- El Sahly, H. M., Atmar, R. L., Patel, S. M., Wells, J. M., Cate, T., Ho, M., et al. (2009). Safety, reactogenicity and immunogenicity of *Francisella tularensis* live vaccine strain in humans. *Vaccine* 27, 4905–4911. doi: 10.1016/j.vaccine.2009.06.036
- Ericsson, M., Kroca, M., Johansson, T., Sjostedt, A., and Tarnvik, A. (2001). Long-lasting recall response of CD4+ and CD8+ alphabeta T cells, but not gamma delta T cells, to heat shock proteins of *Francisella tularensis*. *Scand J. Infect. Dis.* 33, 145–152. doi: 10.1080/003655401750065562
- Ericsson, M., Sandstrom, G., Sjostedt, A., and Tarnvik, A. (1994). Persistence of cell-mediated immunity and decline of humoral immunity to the intracellular bacterium *Francisella tularensis* 25 years after natural infection. *J. Infect. Dis.* 170, 110–114. doi: 10.1093/infdis/170.1.110
- Forsman, M., Sandstrom, G., and Sjostedt, A. (1994). Analysis of 16S ribosomal DNA sequences of *Francisella* strains and utilization for determination of the phylogeny of the genus and for identification of strains by PCR. *Int. J. Syst. Bacteriol.* 44, 38–46. doi: 10.1099/00207713-44-1-38
- Fortier, A. H., Slayter, M. V., Ziemba, R., Meltzer, M. S., and Nacy, C. A. (1991). Live vaccine strain of *Francisella tularensis*: infection and immunity in mice. *Infect. Immun.* 59, 2922–2928.
- Foshay, L. (1932). Prophylactic vaccination against tularemia. *Am. J. Clin. Pathol.* 2, 7–10.
- Foshay, L., Hesselbrock, W. H., Wittenberg, H. J., and Rodenberg, A. H. (1942). Vaccine Prophylaxis against Tularemia in Man. *Am. J. Public Health Nation's Health* 32, 1131–1145.
- Francis, E. (1925). Tularemia. *JAMA* 84, 1243–1250. doi: 10.1001/jama.1925.02660430001001
- Francis, E. (1928). A summary of present knowledge of tularaemia. *J. Clin. Endocrinol.* 7, 411–432.
- Fritz, D. L., England, M. J., Miller, L., and Waag, D. M. (2014). Mouse models of aerosol-acquired tularemia caused by *Francisella tularensis* types A and B. *Comp. Med.* 64, 341–50.
- Fulop, M., Mastroeni, P., Green, M., and Titball, R. W. (2001). Role of antibody to lipopolysaccharide in protection against low- and high-virulence strains of *Francisella tularensis*. *Vaccine* 19, 4465–4472. doi: 10.1016/S0264-410X(01)00189-X
- Gillette, D. D., Curry, H. M., Cremer, T., Ravneberg, D., Fatehchand, K., Shah, P. A., et al. (2014). Virulent Type A *Francisella tularensis* actively suppresses cytokine responses in human monocytes. *Front. Cell. Infect. Microbiol.* 4:45. doi: 10.3389/fcimb.2014.00045
- Glynn, A. R., Alves, D. A., Frick, O., Erwin-Cohen, R., Porter, A., Norris, S., et al. (2015). Comparison of experimental respiratory tularemia in three nonhuman primate species. *Comp. Immunol. Microbiol. Infect. Dis.* 39, 13–24. doi: 10.1016/j.cimid.2015.01.003
- Golovliov, I., Ericsson, M., Akerblom, L., Sandstrom, G., Tarnvik, A., and Sjostedt, A. (1995). Adjuvant activity of ISCOMs incorporating a T cell-reactive lipoprotein of the facultative intracellular pathogen *Francisella tularensis*. *Vaccine* 13, 261–267. doi: 10.1016/0264-410X(95)93311-V
- Golovliov, I., Twine, S. M., Shen, H., Sjostedt, A., and Conlan, W. (2013). A DeltaiglB mutant of *Francisella tularensis* subspecies holarctica strain, FSC200, is a more effective live vaccine than *F. tularensis* LVS in a mouse respiratory challenge model of tularemia. *PLoS ONE* 8:e78671. doi: 10.1371/journal.pone.0078671
- Harris, S. (1992). Japanese biological warfare research on humans: a case study of microbiology and ethics. *Ann. N. Y. Acad. Sci.* 666, 21–52. doi: 10.1111/j.1749-6632.1992.tb38021.x
- Honn, M., Lindgren, H., Bharath, G. K., and Sjostedt, A. (2017). Lack of OxyR and KatG results in extreme susceptibility of *Francisella tularensis* LVS to oxidative stress and marked attenuation *in vivo*. *Front. Cell. Infect. Microbiol.* 7:14. doi: 10.3389/fcimb.2017.00014
- Honn, M., Lindgren, H., and Sjostedt, A. (2012). The role of MglA for adaptation to oxidative stress of *Francisella tularensis* LVS. *BMC Microbiol.* 12:14. doi: 10.1186/1471-2180-12-14
- Hornick, R. B., Dawkins, A. T., Eigelsbach, H. T., and Tulis, J. J. (1966). Oral tularemia vaccine in man. *Antimicrob. Agents Chemother.* 6, 11–14.
- Hornick, R. B., and Eigelsbach, H. T. (1966). Aerogenic immunization of man with live Tularemia vaccine. *Bacteriol. Rev.* 30, 532–538.
- Huber, B., Escudero, R., Busse, H. J., Seibold, E., Scholz, H. C., Anda, P., et al. (2010). Description of *Francisella hispaniensis* sp. nov., isolated from human blood, reclassification of *Francisella novicida* (Larson et al. 1955) Olsufiev

- et al. 1959 as *Francisella tularensis* subsp. novicida comb. nov and emended description of the genus *Francisella*. *Int. J. Syst. Evol. Microbiol.* 60, 1887–1896. doi: 10.1099/ijs.0.015941-0
- Hutt, J. A., Lovchik, J. A., Dekonenko, A., Hahn, A. C., and Wu, T. H. (2017). The natural history of pneumonic tularemia in female Fischer 344 rats after inhalational exposure to aerosolized *Francisella tularensis* subspecies *tularensis* strain SCHU S4. *Am. J. Pathol.* 187, 252–267. doi: 10.1016/j.ajpath.2016.09.021
- Ireland, P. M., LeButt, H., Thomas, R. M., and Oyston, P. C. (2011). A *Francisella tularensis* SCHU S4 mutant deficient in gamma-glutamyltransferase activity induces protective immunity: characterization of an attenuated vaccine candidate. *Microbiology* 157, 3172–3179. doi: 10.1099/mic.0.052902-0
- Jemski, J. V. (1981). Respiratory tularemia: comparison of selected routes of vaccination in Fischer 344 rats. *Infect. Immun.* 34, 766–772.
- Jia, Q., Bowen, R., Dillon, B. J., Maslesa-Galić, S., Chang, B. T., Kaidi, A. C., et al. (2018). Single vector platform vaccine protects against lethal respiratory challenge with Tier 1 select agents of anthrax, plague, and tularemia. *Sci Rep.* 8:7009. doi: 10.1038/s41598-018-24581-y
- Jia, Q., Bowen, R., Lee, B. Y., Dillon, B. J., Maslesa-Galic, S., and Horwitz, M. A. (2016). *Francisella tularensis* Live Vaccine Strain deficient in capB and overexpressing the fusion protein of IglA, IglB, and IglC from the bfr promoter induces improved protection against *F. tularensis* respiratory challenge. *Vaccine* 34, 4969–78. doi: 10.1016/j.vaccine.2016.08.041
- Jia, Q., Bowen, R., Sahakian, J., Dillon, B. J., and Horwitz, M. A. (2013). A heterologous prime-boost vaccination strategy comprising the *Francisella tularensis* live vaccine strain capB mutant and recombinant attenuated *Listeria monocytogenes* expressing *F. tularensis* IglC induces potent protective immunity in mice against virulent *F. tularensis* aerosol challenge. *Infect. Immun.* 81, 1550–1561. doi: 10.1128/IAI.01013-12
- Jia, Q., Lee, B. Y., Bowen, R., Dillon, B. J., Som, S. M., and Horwitz, M. A. (2010). A *Francisella tularensis* live vaccine strain (LVS) mutant with a deletion in capB, encoding a putative capsular biosynthesis protein, is significantly more attenuated than LVS yet induces potent protective immunity in mice against *F. tularensis* challenge. *Infect. Immun.* 78, 4341–4355. doi: 10.1128/IAI.00192-10
- Jia, Q., Lee, B. Y., Clemens, D. L., Bowen, R. A., and Horwitz, M. A. (2009). Recombinant attenuated *Listeria monocytogenes* vaccine expressing *Francisella tularensis* IglC induces protection in mice against aerosolized Type A *F. tularensis*. *Vaccine* 27, 1216–1229. doi: 10.1016/j.vaccine.2008.12.014
- Jia, Q., Ohka, S., Iwasaki, K., Tohyama, K., and Nomoto, A. (1999). Isolation and molecular characterization of a poliovirus type 1 mutant that replicates in the spinal cords of mice. *J. Virol.* 73, 6041–6047.
- Johansson, A., Celli, J., Conlan, W., Elkins, K. L., Forsman, M., Keim, P. S., et al. (2010). Objections to the transfer of *Francisella novicida* to the subspecies rank of *Francisella tularensis*. *Int. J. Syst. Evol. Microbiol.* 60, 1717–1718. doi: 10.1099/ijs.0.022830-0
- Kadull, P. J., Reames, H. R., Coriell, L. L., and Foshay, L. (1950). Studies on tularemia. V. Immunization of man. *J. Immunol.* 65, 425–435.
- Kanistanon, D., Hajjar, A. M., Pelletier, M. R., Gallagher, L. A., Kalthorn, T., Shaffer, S. A., et al. (2008). A *Francisella* mutant in lipid A carbohydrate modification elicits protective immunity. *PLoS Pathog.* 4:e24. doi: 10.1371/journal.ppat.0040024
- Karttunen, R., Andersson, G., Ekre, H. P., Jutinen, K., Surcel, H. M., Syrjala, H., et al. (1987). Interleukin 2 and gamma interferon production, interleukin 2 receptor expression, and DNA synthesis induced by tularemia antigen *in vitro* after natural infection or vaccination. *J. Clin. Microbiol.* 25, 1074–1078.
- Kaur, R., Chen, S., Arevalo, M. T., Xu, Q., Chen, Y., and Zeng, M. (2012). Protective immunity against tularemia provided by an adenovirus-vectored vaccine expressing Tul4 of *Francisella tularensis*. *Clin. Vaccine Immunol.* 19, 359–364. doi: 10.1128/CAI.05384-11
- Kim, T. H., Pinkham, J. T., Heninger, S. J., Chalabaev, S., and Kasper, D. L. (2012). Genetic modification of the O-polysaccharide of *Francisella tularensis* results in an avirulent live attenuated vaccine. *J. Infect. Dis.* 205, 1056–1065. doi: 10.1093/infdis/jir620
- Kingry, L. C., and Petersen, J. M. (2014). Comparative review of *Francisella tularensis* and *Francisella novicida*. *Front. Cell. Infect. Microbiol.* 4:35. doi: 10.3389/fcimb.2014.00035
- Kostiala, A. A., McGregor, D. D., and Logie, P. S. (1975). Tularemia in the rat. I. The cellular basis on host resistance to infection. *Immunology* 28, 855–869.
- Lenco, J., Pavkova, I., Hubalek, M., and Stulik, J. (2005). Insights into the oxidative stress response in *Francisella tularensis* LVS and its mutant DeltaiglC1+2 by proteomics analysis. *FEMS Microbiol. Lett.* 246, 47–54. doi: 10.1016/j.femsle.2005.03.040
- Li, J., Ryder, C., Mandal, M., Ahmed, F., Azadi, P., Snyder, D. S., et al. (2007). Attenuation and protective efficacy of an O-antigen-deficient mutant of *Francisella tularensis* LVS. *Microbiology* 153, 3141–3153. doi: 10.1099/mic.0.2007/006460-0
- Lyons, R. C., and Wu, T. H. (2007). Animal models of *Francisella tularensis* infection. *Ann. N. Y. Acad. Sci.* 1105, 238–265. doi: 10.1196/annals.1409.003
- Ma, Z., Banik, S., Rane, H., Mora, V. T., Rabadi, S. M., Doyle, C. R., et al. (2014). EmrA1 membrane fusion protein of *Francisella tularensis* LVS is required for resistance to oxidative stress, intramacrophage survival and virulence in mice. *Mol. Microbiol.* 91, 976–995. doi: 10.1111/mmi.12509
- Mahawar, M., Rabadi, S. M., Banik, S., Catlett, S. V., Metzger, D. W., Malik, M., et al. (2013). Identification of a live attenuated vaccine candidate for tularemia prophylaxis. *PLoS ONE* 8:e61539. doi: 10.1371/journal.pone.0061539
- Marohn, M. E., and Barry, E. M. (2013). Live attenuated tularemia vaccines: recent developments and future goals. *Vaccine* 31, 3485–3491. doi: 10.1016/j.vaccine.2013.05.096
- Matyas, B. T., Nieder, H. S., and Telford, S. R., 3rd (2007). Pneumonic tularemia on Martha's Vineyard: clinical, epidemiologic, and ecological characteristics. *Ann. N. Y. Acad. Sci.* 1105, 351–377. doi: 10.1196/annals.1409.013
- McCoy GW, C. C. (1912). Further observations on a plaguelike disease of rodents with a preliminary note on the causative agent *Bacterium tularensis*. *J. Infect. Dis.* 10, 61–72. doi: 10.1093/infdis/10.1.61
- McCrumb, F. R. (1961). Aerosol infection of man with *Pasteurella tularensis*. *Bacteriol. Rev.* 25, 262–267.
- Meibom, K. L., Dubail, I., Dupuis, M., Barel, M., Lenco, J., Stulik, J., et al. (2008). The heat-shock protein ClpB of *Francisella tularensis* is involved in stress tolerance and is required for multiplication in target organs of infected mice. *Mol. Microbiol.* 67, 1384–401. doi: 10.1111/j.1365-2958.2008.06139.x
- Melillo, A. A., Mahawar, M., Sellati, T. J., Malik, M., Metzger, D. W., Melendez, J. A., et al. (2009). Identification of *Francisella tularensis* live vaccine strain CuZn superoxide dismutase as critical for resistance to extracellularly generated reactive oxygen species. *J. Bacteriol.* 191, 6447–6456. doi: 10.1128/JB.00534-09
- Metzger, D. W., Bakshi, C. S., and Kirimanjeswara, G. (2007). Mucosal immunopathogenesis of *Francisella tularensis*. *Ann. N. Y. Acad. Sci.* 1105, 266–283. doi: 10.1196/annals.1409.007
- Michell, S. L., Dean, R. E., Eyles, J. E., Hartley, M. G., Waters, E., Prior, J. L., et al. (2010). Deletion of the *Bacillus anthracis* capB homologue in *Francisella tularensis* subspecies *tularensis* generates an attenuated strain that protects mice against virulent tularemia. *J. Med. Microbiol.* 59, 1275–1284. doi: 10.1099/jmm.0.018911-0
- Mohapatra, N. P., Soni, S., Bell, B. L., Warren, R., Ernst, R. K., Muszynski, A., et al. (2007). Identification of an orphan response regulator required for the virulence of *Francisella* spp. and transcription of pathogenicity island genes. *Infect. Immun.* 75, 3305–3314. doi: 10.1128/IAI.00351-07
- Mulligan, M. J., Stapleton, J. T., Keitel, W. A., Frey, S. E., Chen, W. H., Roupael, N., et al. (2017). Tularemia vaccine: safety, reactogenicity, “Take” skin reactions, and antibody responses following vaccination with a new lot of the *Francisella tularensis* live vaccine strain - A phase 2 randomized clinical Trial. *Vaccine* 35, 4730–4737. doi: 10.1016/j.vaccine.2017.07.024
- Nguyen, J. Q., Zogaj, X., Adelani, A. A., Chu, P., Yu, J. J., Arulanandam, B. P., et al. (2017). Intratracheal inoculation of Fischer 344 rats with *Francisella tularensis*. *J. Vis. Exp.* 127:e56123. doi: 10.3791/56123
- Pammit, M. A., Raulie, E. K., Lauriano, C. M., Klose, K. E., and Arulanandam, B. P. (2006). Intranasal vaccination with a defined attenuated *Francisella novicida* strain induces gamma interferon-dependent antibody-mediated protection against tularemia. *Infect. Immun.* 74, 2063–2071. doi: 10.1128/IAI.74.4.2063-2071.2006
- Pasetti, M. F., Cuberos, L., Horn, T. L., Shearer, J. D., Matthews, S. J., House, R. V., et al. (2008). An improved *Francisella tularensis* live vaccine strain (LVS) is well tolerated and highly immunogenic when administered to rabbits in escalating doses using various immunization routes. *Vaccine* 26, 1773–1785. doi: 10.1016/j.vaccine.2008.01.005

- Pavot, V., Rochereau, N., Genin, C., Verrier, B., and Paul, S. (2012). New insights in mucosal vaccine development. *Vaccine* 30, 142–154. doi: 10.1016/j.vaccine.2011.11.003
- Pechous, R., Celli, J., Penoske, R., Hayes, S. F., Frank, D. W., and Zahrt, T. C. (2006). Construction and characterization of an attenuated purine auxotroph in a *Francisella tularensis* live vaccine strain. *Infect. Immun.* 74, 4452–4461. doi: 10.1128/IAI.00666-06
- Pechous, R. D., McCarthy, T. R., Mohapatra, N. P., Soni, S., Penoske, R. M., Salzman, N. H., et al. (2008). A *Francisella tularensis* Schu S4 purine auxotroph is highly attenuated in mice but offers limited protection against homologous intranasal challenge. *PLoS ONE* 3:e2487. doi: 10.1371/journal.pone.0002487
- Pechous, R. D., McCarthy, T. R., and Zahrt, T. C. (2009). Working toward the future: insights into *Francisella tularensis* pathogenesis and vaccine development. *Microbiol. Mol. Biol. Rev.* 73, 684–711. doi: 10.1128/MMBR.00028-09
- Qin, A., Scott, D. W., and Mann, B. J. (2008). *Francisella tularensis* subsp. *tularensis* Schu S4 disulfide bond formation protein B, but not an RND-type efflux pump, is required for virulence. *Infect. Immun.* 76, 3086–3092. doi: 10.1128/IAI.00363-08
- Qin, A., Scott, D. W., Rabideau, M. M., Moore, E. A., and Mann, B. J. (2011). Requirement of the CXXC motif of novel *Francisella* infectivity potentiator protein B FipB, and FipA in virulence of *F. tularensis* subsp. *tularensis*. *PLoS ONE* 6:e24611. doi: 10.1371/journal.pone.0024611
- Qin, A., Scott, D. W., Thompson, J. A., and Mann, B. J. (2009). Identification of an essential *Francisella tularensis* subsp. *tularensis* virulence factor. *Infect. Immun.* 77, 152–61. doi: 10.1128/IAI.01113-08
- Quarry, J. E., Isherwood, K. E., Michell, S. L., Diaper, H., Titball, R. W., and Oyston, P. C. (2007). A *Francisella tularensis* subspecies *novicida* purF mutant, but not a purA mutant, induces protective immunity to tularemia in mice. *Vaccine* 25, 2011–2018. doi: 10.1016/j.vaccine.2006.11.054
- Ray, H. J., Chu, P., Wu, T. H., Lyons, C. R., Murthy, A. K., Guentzel, M. N., et al. (2010). The Fischer 344 rat reflects human susceptibility to *Francisella* pulmonary challenge and provides a new platform for virulence and protection studies. *PLoS ONE* 5:e9952. doi: 10.1371/journal.pone.0009952
- Raymond, C. R., and Conlan, J. W. (2009). Differential susceptibility of Sprague-Dawley and Fischer 344 rats to infection by *Francisella tularensis*. *Microb. Pathog.* 46, 231–234. doi: 10.1016/j.micpath.2009.01.002
- Reed, D. S., Smith, L. P., Cole, K. S., Santiago, A. E., Mann, B. J., and Barry, E. M. (2014). Live attenuated mutants of *Francisella tularensis* protect rabbits against aerosol challenge with a virulent type A strain. *Infect. Immun.* 82, 2098–2105. doi: 10.1128/IAI.01498-14
- Rockx-Brouwer, D., Chong, A., Wehrly, T. D., Child, R., Crane, D. D., Celli, J., et al. (2012). Low dose vaccination with attenuated *Francisella tularensis* strain SchuS4 mutants protects against tularemia independent of the route of vaccination. *PLoS ONE* 7:e37752. doi: 10.1371/journal.pone.0037752
- Rohmer, L., Fong, C., Abmayr, S., Wasnick, M., Larson Freeman, T. J., Radey, M., et al. (2007). Comparison of *Francisella tularensis* genomes reveals evolutionary events associated with the emergence of human pathogenic strains. *Genome Biol.* 8:R102. doi: 10.1186/gb-2007-8-6-r102
- Ryden, P., Twine, S., Shen, H., Harris, G., Chen, W., Sjostedt, A., et al. (2013). Correlates of protection following vaccination of mice with gene deletion mutants of *Francisella tularensis* subspecies *tularensis* strain, SCHU S4 that elicit varying degrees of immunity to systemic and respiratory challenge with wild-type bacteria. *Mol. Immunol.* 54, 58–67. doi: 10.1016/j.molimm.2012.10.043
- Saha, S. S., Hashino, M., Suzuki, J., Uda, A., Watanabe, K., Shimizu, T., et al. (2017). Contribution of methionine sulfoxide reductase B (MsrB) to *Francisella tularensis* infection in mice. *FEMS Microbiol. Lett.* 364:fnw260. doi: 10.1093/femsle/fnw260
- Salomonsson, E., Kuoppa, K., Forslund, A. L., Zingmark, C., Golovliov, I., Sjostedt, A., et al. (2009). Reintroduction of two deleted virulence loci restores full virulence to the live vaccine strain of *Francisella tularensis*. *Infect. Immun.* 77, 3424–3431. doi: 10.1128/IAI.00196-09
- Sammons-Jackson, W. L., McClelland, K., Manch-Citron, J. N., Metzger, D. W., Bakshi, C. S., Garcia, E., et al. (2008). Generation and characterization of an attenuated mutant in a response regulator gene of *Francisella tularensis* live vaccine strain (LVS). *DNA Cell Biol.* 27, 387–403. doi: 10.1089/dna.2007.0687
- Sanapala, S., Yu, J. J., Murthy, A. K., Li, W., Guentzel, M. N., Chambers, J. P., et al. (2012). Perforin- and granzyme-mediated cytotoxic effector functions are essential for protection against *Francisella tularensis* following vaccination by the defined *F. tularensis* subsp. *novicida* DeltafopC vaccine strain. *Infect. Immun.* 80, 2177–2185. doi: 10.1128/IAI.00036-12
- Santiago, A. E., Cole, L. E., Franco, A., Vogel, S. N., Levine, M. M., and Barry, E. M. (2009). Characterization of rationally attenuated *Francisella tularensis* vaccine strains that harbor deletions in the *guaA* and *guaB* genes. *Vaccine* 27, 2426–2436. doi: 10.1016/j.vaccine.2009.02.073
- Santiago, A. E., Mann, B. J., Qin, A., Cunningham, A. L., Cole, L. E., Grassel, C., et al. (2015). Characterization of *Francisella tularensis* Schu S4 defined mutants as live-attenuated vaccine candidates. *Pathogens Dis.* 73:ftv036. doi: 10.1093/femspd/ftv036
- Saslaw, S., and Carhart, S. (1961). Studies with tularemia vaccines in volunteers. III. Serologic aspects following intracutaneous or respiratory challenge in both vaccinated and nonvaccinated volunteers. *Am. J. Med. Sci.* 241, 689–699.
- Saslaw, S., Eigelsbach, H. T., Prior, J. A., Wilson, H. E., and Carhart, S. (1961a). Tularemia vaccine study. II. Respiratory challenge. *Arch. Intern. Med.* 107, 702–714. doi: 10.1001/archinte.1961.03620050068007
- Saslaw, S., Eigelsbach, H. T., Wilson, H. E., Prior, J. A., and Carhart, S. (1961b). Tularemia vaccine study. I. Intracutaneous challenge. *Arch. Intern. Med.* 107, 689–701. doi: 10.1001/archinte.1961.03620050055006
- Schmitt, D. M., O'Dee, D. M., Horzempa, J., Carlson, P. E. Jr., Russo, B. C., Bales, J. M., et al. (2012). A *Francisella tularensis* live vaccine strain that improves stimulation of antigen-presenting cells does not enhance vaccine efficacy. *PLoS ONE* 7:e31172. doi: 10.1371/journal.pone.0031172
- Schricker, R. L., Eigelsbach, H. T., Mitten, J. Q., and Hall, W. C. (1972). Pathogenesis of tularemia in monkeys aerogenically exposed to *Francisella tularensis* 425. *Infect. Immun.* 5, 734–744.
- Sebastian, S., Dillon, S. T., Lynch, J. G., Blalock, L. T., Balon, E., Lee, K. T., et al. (2007). A defined O-antigen polysaccharide mutant of *Francisella tularensis* live vaccine strain has attenuated virulence while retaining its protective capacity. *Infect. Immun.* 75, 2591–602. doi: 10.1128/IAI.01789-06
- Sebastian, S., Pinkham, J. T., Lynch, J. G., Ross, R. A., Reinap, B., Blalock, L. T., et al. (2009). Cellular and humoral immunity are synergistic in protection against types A and B *Francisella tularensis*. *Vaccine* 27, 597–605. doi: 10.1016/j.vaccine.2008.10.079
- Shen, H., Chen, W., and Conlan, J. W. (2004). Mice sublethally infected with *Francisella novicida* U112 develop only marginal protective immunity against systemic or aerosol challenge with virulent type A or B strains of *F. tularensis*. *Microb. Pathog.* 37, 107–110. doi: 10.1016/j.micpath.2004.04.005
- Shen, H., Harris, G., Chen, W., Sjostedt, A., Ryden, P., and Conlan, W. (2010). Molecular immune responses to aerosol challenge with *Francisella tularensis* in mice inoculated with live vaccine candidates of varying efficacy. *PLoS ONE* 5:e13349. doi: 10.1371/journal.pone.0013349
- Signarovitz, A. L., Ray, H. J., Yu, J. J., Guentzel, M. N., Chambers, J. P., Klose, K. E., et al. (2012). Mucosal immunization with live attenuated *Francisella novicida* U112DeltaiglB protects against pulmonary *F. tularensis* SCHU S4 in the Fischer 344 rat model. *PLoS ONE* 7:e47639. doi: 10.1371/journal.pone.0047639
- Sjostedt, A. (2007). Tularemia: history, epidemiology, pathogen physiology, and clinical manifestations. *Ann. N. Y. Acad. Sci.* 1105, 1–29. doi: 10.1196/annals.1409.009
- Sjostedt, A., Eriksson, M., Sandstrom, G., and Tarnvik, A. (1992a). Various membrane proteins of *Francisella tularensis* induce interferon-gamma production in both CD4+ and CD8+ T cells of primed humans. *Immunology* 76, 584–592.
- Sjostedt, A., Sandstrom, G., and Tarnvik, A. (1992b). Humoral and cell-mediated immunity in mice to a 17-kilodalton lipoprotein of *Francisella tularensis* expressed by *Salmonella typhimurium*. *Infect. Immun.* 60, 2855–2862.
- Straskova, A., Spidlova, P., Mou, S., Worsham, P., Putzova, D., Pavkova, I., et al. (2015). *Francisella tularensis* type B DeltadsBA mutant protects against type A strain and induces strong inflammatory cytokine and Th1-like antibody response *in vivo*. *Pathogens Dis.* 73:ftv058. doi: 10.1093/femspd/ftv058
- Su, J., Asare, R., Yang, J., Nair, M. K., Mazurkiewicz, J. E., Abu-Kwaik, Y., et al. (2011). The capBCA locus is required for intracellular growth of *Francisella tularensis* LVS. *Front. Microbiol.* 2:83. doi: 10.3389/fmicb.2011.00083

- Su, J., Yang, J., Zhao, D., Kawula, T. H., Banas, J. A., and Zhang, J. R. (2007). Genome-wide identification of *Francisella tularensis* virulence determinants. *Infect. Immun.* 75, 3089–3101. doi: 10.1128/IAI.01865-06
- Suresh, R. V., Ma, Z., Sunagar, R., Bhatti, V., Banik, S., Catlett, S. V., et al. (2015). Preclinical testing of a vaccine candidate against tularemia. *PLoS ONE* 10:e0124326. doi: 10.1371/journal.pone.0124326
- Tarnvik, A. (1989). Nature of protective immunity to *Francisella tularensis*. *Rev. Infect. Dis.* 11, 440–451. doi: 10.1093/clinids/11.3.440
- Tempel, R., Lai, X. H., Crosa, L., Kozlowicz, B., and Heffron, F. (2006). Attenuated *Francisella novicida* transposon mutants protect mice against wild-type challenge. *Infect. Immun.* 74, 5095–5105. doi: 10.1128/IAI.00598-06
- Twine, S., Bystrom, M., Chen, W., Forsman, M., Golovliov, I., Johansson, A., et al. (2005). A mutant of *Francisella tularensis* strain SCHU S4 lacking the ability to express a 58-kilodalton protein is attenuated for virulence and is an effective live vaccine. *Infect. Immun.* 73, 8345–8352. doi: 10.1128/IAI.73.12.8345-8352.2005
- Twine, S., Shen, H., Harris, G., Chen, W., Sjostedt, A., Ryden, P., et al. (2012). BALB/c mice, but not C57BL/6 mice immunized with a DeltaclpB mutant of *Francisella tularensis* subspecies tularensis are protected against respiratory challenge with wild-type bacteria: association of protection with post-vaccination and post-challenge immune responses. *Vaccine* 30, 3634–3645. doi: 10.1016/j.vaccine.2012.03.036
- Vanmetre, T. E., and Kadull, P. J. (1959). Laboratory-acquired tularemia in vaccinated individuals - a report of 62 Cases. *Ann. Intern. Med.* 50, 621–632. doi: 10.7326/0003-4819-50-3-621
- Wayne Conlan, J., and Oyston, P. C. (2007). Vaccines against *Francisella tularensis*. *Ann. N. Y. Acad. Sci.* 1105, 325–350. doi: 10.1196/annals.1409.012
- Weinberg, A. N. (2004). Commentary: Wherry WB, Lamb BH. Infection of man with Bacterium tularensis. *J Infect Dis* 15, 331–40. *J. Infect. Dis.* 189, 1317–1320. doi: 10.1086/382546
- Weiss, D. S., Brotcke, A., Henry, T., Margolis, J. J., Chan, K., and Monack, D. M. (2007). In vivo negative selection screen identifies genes required for *Francisella virulence*. *Proc. Natl. Acad. Sci. U.S.A.* 104, 6037–6042. doi: 10.1073/pnas.0609675104
- West, T. E., Pelletier, M. R., Majure, M. C., Lembo, A., Hajjar, A. M., and Skerrett, S. J. (2008). Inhalation of *Francisella novicida* Delta mglA causes replicative infection that elicits innate and adaptive responses but is not protective against invasive pneumonic tularemia. *Microbes Infect.* 10, 773–780. doi: 10.1016/j.micinf.2008.04.008
- WHO (2007). *WHO Guidelines on Tularaemia*. WHO Press, World Health Organization, Switzerland. Available online at: <https://www.cdc.gov/tularemia/resources/whotularemiamanual.pdf>
- Wu, T. H., Hutt, J. A., Garrison, K. A., Berliba, L. S., Zhou, Y., and Lyons, C. R. (2005). Intranasal vaccination induces protective immunity against intranasal infection with virulent *Francisella tularensis* biovar A. *Infect. Immun.* 73, 2644–2654. doi: 10.1128/IAI.73.5.2644-2654.2005
- Wu, T. H., Zsemlye, J. L., Statom, G. L., Hutt, J. A., Schrader, R. M., Scrymgeour, A. A., et al. (2009). Vaccination of Fischer 344 rats against pulmonary infections by *Francisella tularensis* type A strains. *Vaccine* 27, 4684–4693. doi: 10.1016/j.vaccine.2009.05.060
- Zarella, T. M., Singh, A., Bitsaktis, C., Rahman, T., Sahay, B., Feustel, P. J., et al. (2011). Host-adaptation of *Francisella tularensis* alters the bacterium's surface-carbohydrates to hinder effectors of innate and adaptive immunity. *PLoS ONE* 6:e22335. doi: 10.1371/journal.pone.0022335
- Zhou, B., Meliopoulos, V. A., Wang, W., Lin, X., Stucker, K. M., Halpin, R. A., et al. (2016). Reversion of cold-adapted live attenuated influenza vaccine into a pathogenic virus. *J. Virol.* 90, 8454–8463. doi: 10.1128/JVI.00163-16

Conflict of Interest Statement: The authors declare inventors on patents describing tularemia vaccines that are owned by UCLA.

Copyright © 2018 Jia and Horwitz. This is an open-access article distributed under the terms of the Creative Commons Attribution License (CC BY). The use, distribution or reproduction in other forums is permitted, provided the original author(s) and the copyright owner are credited and that the original publication in this journal is cited, in accordance with accepted academic practice. No use, distribution or reproduction is permitted which does not comply with these terms.



Galleria mellonella Reveals Niche Differences Between Highly Pathogenic and Closely Related Strains of *Francisella* spp.

Johanna Thelaus*, Eva Lundmark, Petter Lindgren, Andreas Sjödin and Mats Forsman

Swedish Defence Research Agency (FOI), Umeå, Sweden

Francisella tularensis, a highly virulent bacteria that causes the zoonotic disease tularemia, is considered a potential agent of biological warfare and bioterrorism. Although the host range for several species within the *Francisella* is known, little is known about the natural reservoirs of various *Francisella* species. The lack of knowledge regarding the environmental fates of these pathogens greatly reduces the possibilities for microbial risk assessments. The greater wax moth (*Galleria mellonella*) is an insect of the order *Lepidoptera* that has been used as an alternative model to study microbial infection during recent years. The aim of this study was to evaluate *G. mellonella* as a model system for studies of human pathogenic and closely related opportunistic and non-pathogenic strains within the *Francisella* genus. The employed *G. mellonella* larvae model demonstrated differences in lethality between human pathogenic and human non-pathogenic or opportunistic *Francisella* species. The *F. novicida*, *F. hispaniensis* and *F. philomiragia* strains were significantly more virulent in the *G. mellonella* model than the strains of human pathogens *F. t. holarctica* and *F. t. tularensis*. Our data show that *G. mellonella* is a possible *in vivo* model of insect immunity for studies of both opportunistic and virulent lineages of *Francisella* spp., that produces inverse results regarding lethality in *G. mellonella* and incapacitating disease in humans. The results provide insight into the potential host specificity of *F. tularensis* and closely related members of the same genus, thus increasing our present understanding of *Francisella* spp. ecology.

Keywords: tularemia, *Francisella tularensis*, *Galleria mellonella*, virulence, host specificity, lethality, ecology

OPEN ACCESS

Edited by:

Anders Sjöstedt,
Umeå University, Sweden

Reviewed by:

Richard Titball,
University of Exeter, United Kingdom
Siouxie Wiles,
University of Auckland, New Zealand

*Correspondence:

Johanna Thelaus
johanna.thelaus@foi.se

Received: 06 March 2018

Accepted: 15 May 2018

Published: 05 June 2018

Citation:

Thelaus J, Lundmark E, Lindgren P,
Sjödin A and Forsman M (2018)
Galleria mellonella Reveals Niche
Differences Between Highly
Pathogenic and Closely Related
Strains of *Francisella* spp.
Front. Cell. Infect. Microbiol. 8:188.
doi: 10.3389/fcimb.2018.00188

INTRODUCTION

Francisella tularensis is a highly virulent bacteria that causes the zoonotic disease tularemia. This pathogen is considered a potential agent of biological warfare and bioterrorism. As such, it is classified as a Tier 1 select agent (Federal Register, 2012). Three subspecies of *F. tularensis* are commonly accepted: *F. t. holarctica*, *F. t. tularensis* and *F. t. mediasiatica* (Sjöstedt, 2015). Both *F. tularensis* subspecies *holarctica* and subspecies *tularensis* cause disease in humans (Penn, 2010). However, information on the virulence of *F. t. mediasiatica*, which is primarily found in Central Asia, in humans is limited (Timofeev et al., 2017). Besides *F. tularensis*, the genus *Francisella* also includes opportunistic pathogens that only cause disease in immunocompromised humans (i.e.,

F. novicida, *F. hispaniensis* and *F. philomiragia*; Larson et al., 1955; Olsufjev et al., 1959; Hollis et al., 1989; Huber et al., 2010; Penn, 2010; Aravena-Román et al., 2015). There is an ongoing debate about whether *F. novicida* should be classified as a separate *Francisella* species or as a subspecies of *F. tularensis* (Busse et al., 2010; Johansson et al., 2010). The facts that *F. novicida* infections are uncommon in humans and that infections have only occurred in immunocompromised individuals or people with underlying health problems reflect that *F. novicida* is indeed an opportunistic pathogen (Kingry and Petersen, 2014). In addition, the genus *Francisella* includes fish pathogens (i.e., *F. noatunensis*, *F. haliotica*) (Ottem et al., 2008; Brevik et al., 2011), endosymbionts of ticks and ciliates (i.e., *F. persica* and *F. endociliophora*) (Sjödin et al., 2014; Larson et al., 2016), and species with unknown niche preferences, i.e., species isolated from brackish water, air conditioning systems and cooling towers (*F. salina*, *F. uliginis*, *F. frigiditurris*, and *Allofrancisella* spp.; Qu et al., 2013, 2016; Challacombe et al., 2017). Thus, representatives of the *Francisella* genus inhabit diverse ecological niches. Rapid developments in high-throughput sequencing technologies during the last years have increased knowledge on the diversity of *Francisella* and its genetic neighbors (Sjödin et al., 2012; Challacombe et al., 2017).

Although previous research has identified the host preferences of several *Francisella* species, little is known about the natural reservoirs of these different *Francisella* species. This lack of knowledge concerning environmental dynamics greatly reduces the possibilities for microbial risk assessments of *Francisella* pathogens. However, the increase in genus diversity knowledge is pivotal to discriminating pathogenic from non-pathogenic strains. This could improve environmental bio-surveillance and epidemiological studies that rely on complex sample matrices which are plagued by false positive signals originating from both non-pathogenic *Francisella* species and close genetic neighbors. Still, studies of these newly defined organisms are challenged by the difficulties in culturing these strains in the laboratory.

The greater wax moth (*Galleria mellonella*) is an insect of the order *Lepidoptera* that has been introduced as an alternative model to study microbial infection during recent years (Tsai et al., 2016). When compared to traditional murine models, *G. mellonella* larvae are cheaper and easier to maintain. Furthermore, *G. mellonella* can survive temperatures between 25 and 37°C, which enables researchers to investigate the host-associated replication of human pathogens. Although there are major differences between the immune systems of humans and insects, the innate immune responses of insects and vertebrates share a cellular and a humoral component (Kavanagh and Reeves, 2004; Browne et al., 2013). *G. mellonella* has been used as an infection model to study bacterial and fungal infections, as well as to evaluate the efficacy of antimicrobial substances (Johnson et al., 2015; Tsai et al., 2016; Barnoy et al., 2017; Meir et al., 2018). Additionally, a *G. mellonella* infection model has been established for the *F. t. holarctica* live vaccine strain (LVS) (Aperis et al., 2007).

The aim of this study was to evaluate whether *G. mellonella* can be used as a model system to differentiate human pathogenic strains from closely related opportunistic and non-pathogenic

TABLE 1 | *Francisella* strains included in the study.

Strain	FSC number	References
<i>F. t. holarctica</i> LVS	458	Isolated from vaccine ampoule, no NDBR 101, Pasturella tularensis Vaccine Live, lot no 11, 1964, The National Drug Company, Philadelphia, USA
<i>F. t. holarctica</i>	200	Svensson et al., 2012
<i>F. t. tularensis</i> SchuS4	237	Larsson et al., 2005
<i>F. t. mediasiatica</i>	147	Larsson et al., 2009
<i>F. novicida</i>	040	Larson et al., 1955; Rohmer et al., 2007
<i>F. hispaniensis</i>	454	Huber et al., 2010
<i>F. philomiragia</i>	037	Sjödin et al., 2012
<i>F. endociliophora</i>	1006	Sjödin et al., 2014

strains within the *Francisella* genus. We show unexpected differences in lethality between human-pathogenic and human non-pathogenic or opportunistic *Francisella* species in the *G. mellonella* larvae model. Thus, the results demonstrate the importance of including non-pathogenic genetic neighbors when evaluating new model systems and suggest niche differences between highly pathogenic and closely related strains of *Francisella*.

MATERIALS AND METHODS

Bacterial Strains Growth Conditions

All *Francisella* strains used in this study (Table 1) were cultured on GCII agar containing 1% hemoglobin and 1% IsoVitaleX (World Health Organization, 2007), and complemented with 50 µg/mL ampicillin, 100 µg/mL polymyxin B and 25 µg/mL vancomycin. The cultures were incubated at 37°C (5% CO₂), except for *F. endociliophora*, which was incubated at 22°C. Laboratory work with FSC200, FSC147, and FSC237 were performed at a Biosafety level 3 (BSL3) laboratory.

Preparation of Inocula for Infections

Bacteria were suspended in PBS solution to a final count of 1×10^9 bacteria/mL as determined by optical density (OD₆₀₀) measurements, and further diluted to give inocula of 10⁸, 10⁶, and 10⁴ bacteria/mL. The actual infectious dose was confirmed by plating serial dilutions for an analysis of colony forming units (CFU).

Bacterial Growth Experiments

Bacteria were suspended in PBS solution to a final count of 10⁵ bacteria/mL. Growth rate experiments were performed on solid agar plates where one µl of bacterial suspension were applied in eight technical replicates. Growth was monitored at 18, 32, and 48 h and scored when bacterial colonies were visible to the eye.

Infection of *G. mellonella*

G. mellonella larvae in the final larval stage (Vivara/CJ Wildbird Foods Ltd., Shrewsbury, UK) were stored in the dark at 14°C. To assess the differences between bacterial concentrations, 10 µl of the different dilutions described above were injected into the

hemocoel of larvae via the last left proleg. After injection, the larvae were incubated in Petri dishes at 37° or 22°C for 9 days. Ten randomly chosen larvae from each group were used to evaluate virulence, and the number of dead larvae was scored every day. Larvae were considered dead when they did not turn after being turned onto their back. All experiments were repeated three times with different batches of larvae. Untreated larvae and larvae injected with PBS were used as controls in all experiments. Upon death or at the end of the experiment, hemolymph was collected from larvae into 1.5 ml Eppendorf tubes for immediate analysis of viable counts or stored at -80°C for confirmative real-time PCR analysis.

Confirmative Culture and Real-Time PCR

To evaluate the tissue burden of *Francisella* spp. (for FSC200, FSC040, FSC454, and FSC037) in *G. mellonella*, the hemolymph collected from infected larvae was serially diluted and plated onto agar plates as described above. In order to confirm that larval death was caused by *Francisella* sp., all hemolymph samples were screened for the presence of *Francisella* specific DNA using real-time PCR with the primers Fra_ISFtu2_F CCCTGATTACAGAAGTC and Fra_ISFtu2_R CTTGGTTATCATCTTTATCATATC and probe Fra_ISFtu2 TGATTCAACAATAGCAAGAGCACAT (for FSC 458, 200, 237, 147, and 040) modified from Versage et al. (2003), and the primers GF1_F AACTGGCTGACCTTCAGCAT and GF1_R GTGGTCGTGGTAAAGCTGGT and GF1 probe CCGATTAGGCTTTCTGCTACTTCACGA (Sjödín, unpublished) (for FSC 037, 454, and 1006). No DNA extraction was performed prior to the PCR, however, all samples were diluted 1/10 in water to avoid inhibition of the PCR process.

Each reaction mixture comprised 1 µl diluted larval hemolymph, 12.5 µl PerfeCTa qPCR ToughMix (Quantabio, Beverly, MA), 0.625 µl of each primer (20 pM), 0.5 µl of probe (5 pM) and MiliQ water to a total volume of 25 µl. An initial denaturation at 98°C for 2 min was followed by 45 cycles of 98°C for 5 s and 60°C for 5 s on an iCycler (Bio-Rad, Hercules, CA). Larval hemolymph samples spiked with *F. t. holarctica* LVS concentrations ranging from 10⁴ to 10⁹ CFU per mL were analyzed in duplicates to test the limit of detection and generate a standard curve for assessing target DNA concentrations. The standard curve was evaluated with FRA_ISFtu2 primerpair and probe and the GF1 primerpair and probe.

Statistical Analysis

The Kaplan-Meier estimator was used to estimate the survival function of *G. mellonella* larvae. An event was defined as a dead larva meeting the requirement of a positive PCR measurement (ct < 35,97 (GF1) and ct < 29,94 (Fra_ISFtu2), corresponding to 10⁵ cfu/ml. Observations of dead larvae with a negative PCR measurement (ct > 35,97 (GF1) and ct > 29,94 (Fra_ISFtu2)) as well as observations of larvae that had started pupation were considered censored at the time of death and the time of pupation, respectively. The log rank test was used to compare survival functions between groups (i.e., different *Francisella* species). Analyses for each infectious dose at 37°C as well as for the infectious dose of 10⁶ bacteria/mL at 22°C were performed. In addition, we tested the difference in survival

functions between strains at 37°C when controlled for the infectious dose effect. The control group was omitted from this analysis due to discrepancy in infectious dose. In each analysis, multiple adjustments were performed using the Tukey-Kramer method, with adjusted *p*-values < 0.05 considered statistically significant. The survival analysis was performed using the PROC LIFETEST in SAS[®] version 9.4 (SAS Institute, Cary, NC). For details see experimental data and sourcecode deposited at figshare (DOI code: 10.6084/m9.figshare.6154919 and DOI data: 10.6084/m9.figshare.6154928).

Phylogenetic Study of *Francisella* Species

Sequence files for all publicly available *Francisella* genomes were downloaded from NCBI (Jan 26, 2018). All of the sequences were aligned using progressiveMauve (Darling et al., 2010), and the multiple alignment was transformed to a common coordinate system (Lärkeryd et al., 2014) before it was imported into MEGA7 (Kumar et al., 2016) to construct a neighbor-joining tree. All analysis steps except tree generation were performed using snakemake (Köster and Rahmann, 2012) and Bioconda.

RESULTS

G. mellonella Mortality Depends on Both *Francisella* Species and Temperature

Infection of *Galleria mellonella* with *Francisella* strains resulted in larval death (Figure 1). We infected *G. mellonella* with samples containing 10⁴, 10⁶ or 10⁸ bacteria/mL, resulting in actual infectious doses of 10², 10⁴ and 10⁶ bacteria per larva (low, intermediate and high dose, respectively. see Figures 1A–C).

At a temperature of 37°C, *G. mellonella* larvae were generally more sensitive to the opportunistic *F. novicida*, *F. hispaniensis*, and *F. philomiragia* strains than the other tested strains (Figure 1). This difference was found to be significant (*p* < 0.001 for all such pairwise combinations) when controlling for infectious dose (Supplementary Table 1, column E). The highest infectious doses of the opportunistic strains resulted in extensive larval death within 3 days while the majority of larvae died within 6–9 days after being injected with the highest infectious doses of the *F. tularensis* strains (*tularensis*, *holarctica*, and *mediasiatica*). The survival proportion of larvae infected with the highest infectious dose of *F. endociliophora* was approximately 0.6 at the end of the experiment (Figure 1C), while larvae infected with the lowest and intermediate infectious doses were not affected. At an intermediate infectious dose, wild-type *F. t. holarctica* was significantly more virulent than the *F. t. holarctica* LVS (Figure 1B, Supplementary Table 1 column B). This difference was not observed for the lowest or highest infectious dose (Figures 1A,C, Supplementary Table 1 column A and C).

Francisella infection of *G. mellonella* was also temperature-dependent, as higher larval survival proportions were noted when the experiment was performed at 22°C (Figure 2) than when the experiment was performed at 37°C (Figure 1). This trend was noted for all strains at the intermediate infectious dose.

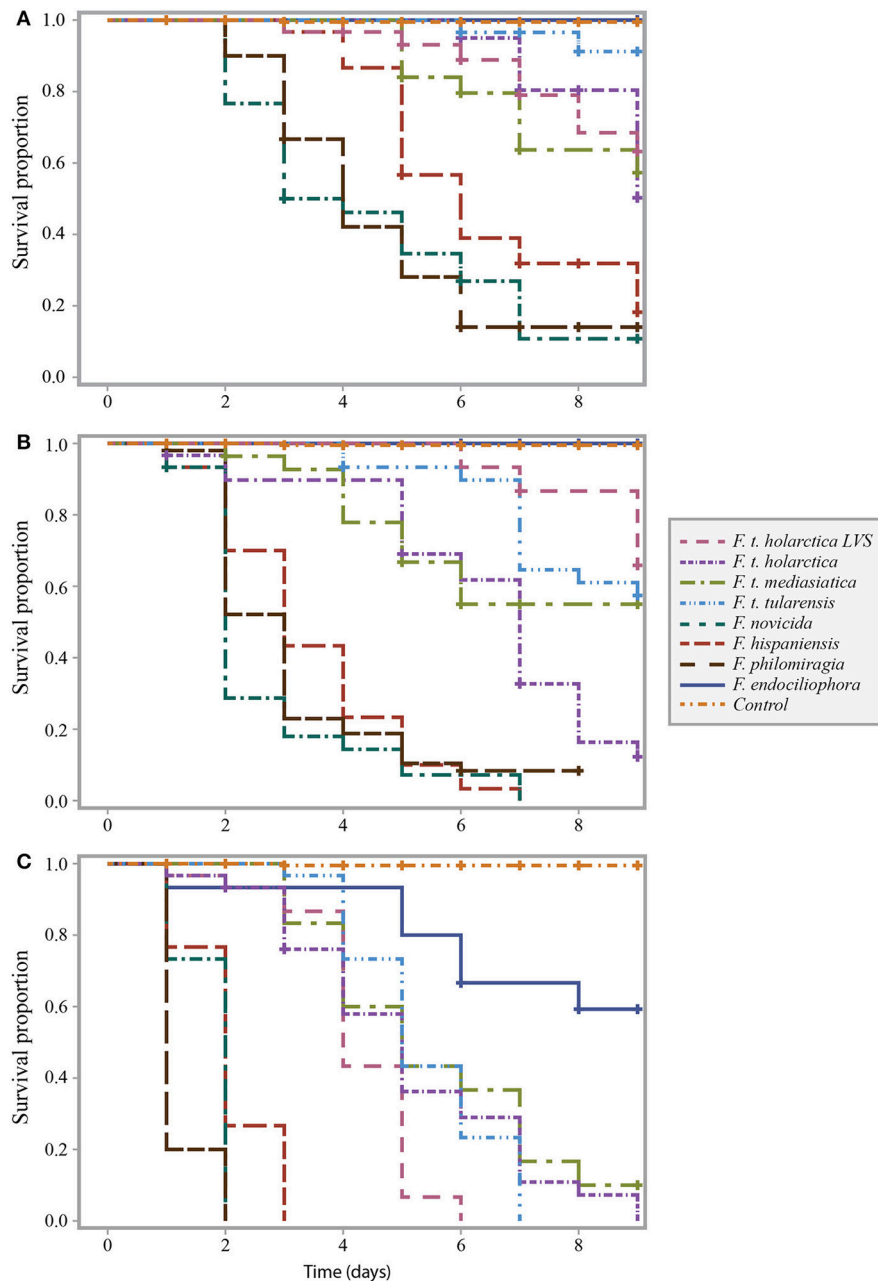


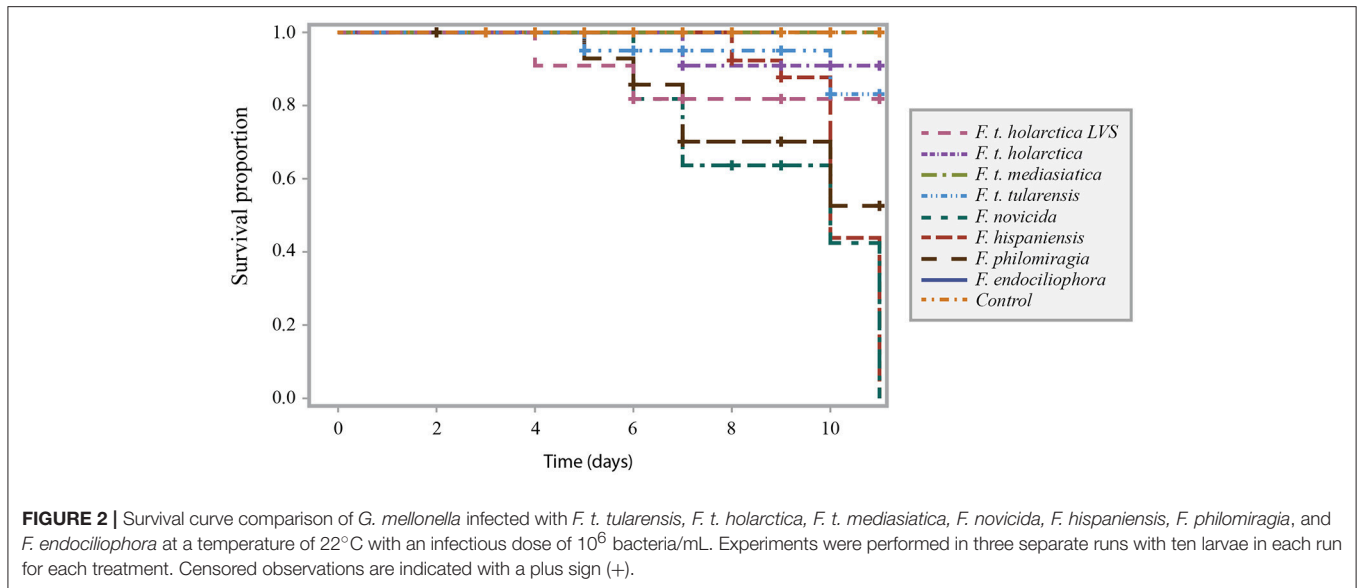
FIGURE 1 | Survival curve comparison of *G. mellonella* infected with *F. t. tularensis*, *F. t. holarctica*, *F. t. mediasiatica*, *F. novicida*, *F. hispaniensis*, *F. philomiragia*, and *F. endociliophora* at a temperature of 37°C with an infectious dose of (A) 10^4 bacteria/mL, (B) 10^6 bacteria/mL, and (C) 10^8 bacteria/mL. Experiments were performed in three separate runs with ten larvae in each run for each treatment. Censored observations are indicated with a plus sign (+).

***Francisella* spp. Infect *G. mellonella* With a Small Infectious Dose and Grow to High Bacterial Count**

The bacterial load of *Francisella* spp. in *G. mellonella* hemolymph upon larval death reached approximately 10^{10} CFU/mL for *F. t. holarctica*, *F. novicida* and *F. hispaniensis* (Figure 3). Based on the assumption that each larvae contains 35 μ L of hemolymph, the initial 10^4 bacteria introduced upon infection

(intermediate dose) reached 3.5×10^8 bacteria per larva at the time of larval death. However, the bacterial load of *F. philomiragia* in hemolymph upon larval death was noticeably lower than what was observed for other *Francisella* species, not exceeding 10^8 CFU/mL, which corresponds to 3.5×10^6 bacteria per larva at the time of death (Figure 3).

Taken together, these results suggest that the bacterial load increased by 10^4 over 2 days in samples infected with *F. novicida*



and *F. hispaniensis*, by 10^4 over 5 days in samples infected with *F. t. holarctica*, and 10^2 over 2 days in samples infected with *F. philomiragia*. No increase in the bacterial load of *F. endociliophora* in larval hemolymph was observed during the 9-day experiment (data not shown).

Differences in Growth Rate Between *Francisella* Strains on Laboratory Culture Media

Growth of *F. hispaniensis* and *F. philomiragia* was observed after 18h incubation on solid agar media (**Supplementary Figure 1**). At 32h colonies of the *F. t. tularensis*, the *F. t. mediasiatica* and the *F. novicida* strains were visible. However, colonies of *F. t. holarctica* and *F. t. holarctica* LVS were not visible until the 48h time point. *F. endociliophora* was not included in the growth experiment since the strain does not grow at 37°C.

Host Specificity of *Francisella* Species

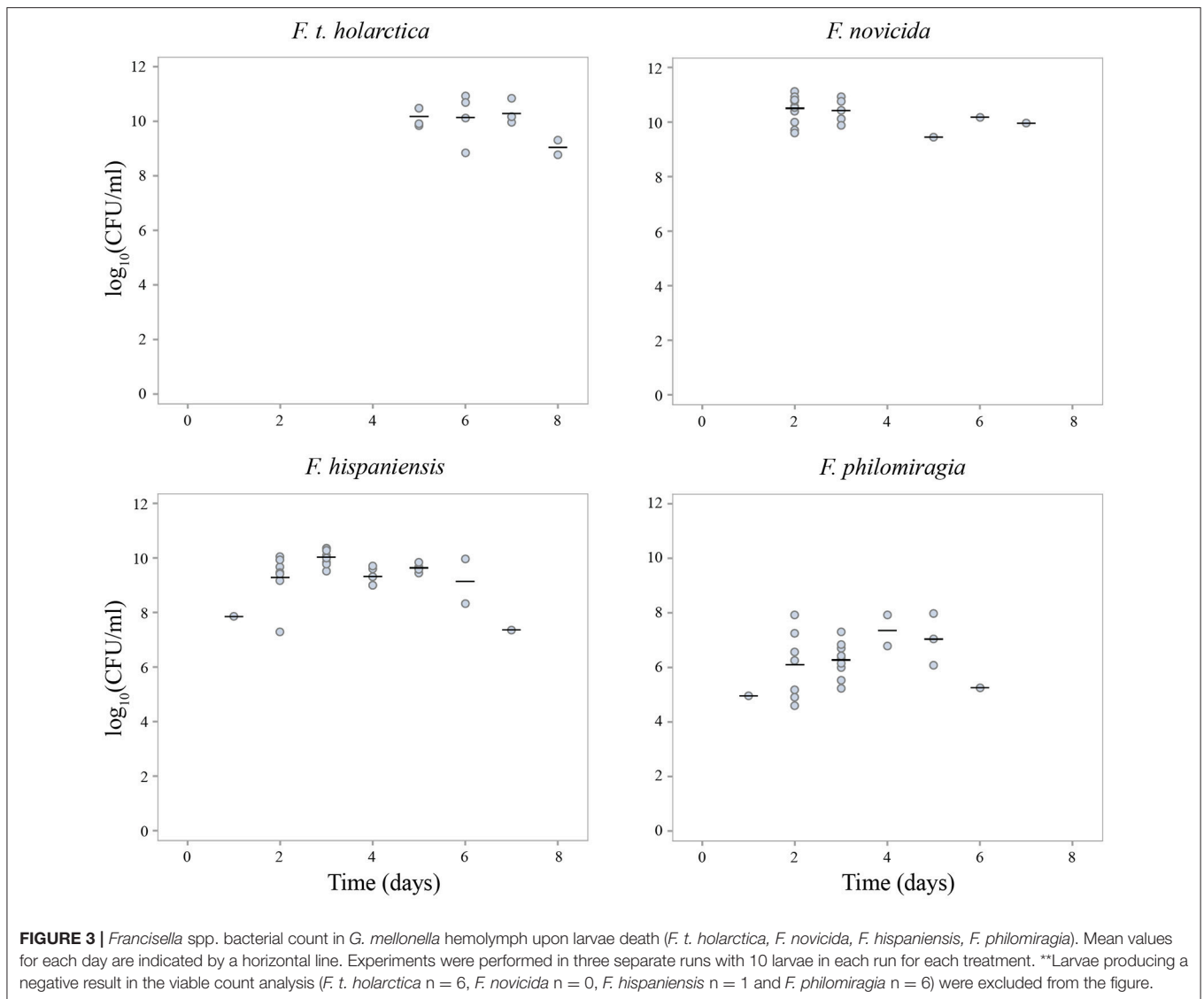
The relevance of *G. mellonella* as a model system to differentiate human pathogenic strains from closely related opportunistic and non-pathogenic strains within the *Francisella* genus was evaluated by comparing lethality in *G. mellonella* (this study) with previously published data describing *Francisella* lethality in mice and severity of disease in humans (previously published studies and epidemiological data, respectively, **Figure 4**). The lethality of different *Francisella* strains in *G. mellonella* (this study) and mice were ranked as either high lethality (red), intermediate lethality (orange) and non-lethal (green). Similarly, the severity of disease caused by *Francisella* strains in humans was scored as incapacitating disease in humans (red), causing disease only in humans with a compromised immune response or underlying health defects (yellow), and non-virulent (green) (**Figure 4**). Our data show an inverse relationship, as the opportunistic pathogens in humans (*F. novicida*, *F. hispaniensis*, and *F. philomiragia*) are highly lethal in *G. mellonella* (**Figure 4**), while the human

pathogens (*F. t. tularensis* and *F. t. holarctica*) show intermediate lethality in *G. mellonella*. *F. endociliophora* does not cause disease in either humans or *G. mellonella*.

DISCUSSION

Our *G. mellonella* model identified differences in lethality between *Francisella* species that do not correspond to severity of disease in humans as shown by available epidemiological and experimental data. The *F. novicida*, *F. hispaniensis* and *F. philomiragia* strains were significantly more lethal in the *G. mellonella* model than the *F. t. holarctica* and *F. t. tularensis* strains that represent human pathogens. The results provide insight into the potential host specificity of *F. tularensis* and reflect different adaptation to an insect host (*G. mellonella*) between *F. tularensis* and its near-neighbours. Arthropode borne transmission of human pathogenic *F. tularensis* species is widely documented and vectors considered significant for the transmission of *F. tularensis* to humans are hard tick, mosquito, deer-fly, and horse-fly (Petersen et al., 2009; Pilo, 2018). Our findings suggest that although phylogenetically close to the human pathogenic strains, the *F. novicida*, *F. hispaniensis*, and *F. philomiragia* are more adapted for rapid growth in the insect host model.

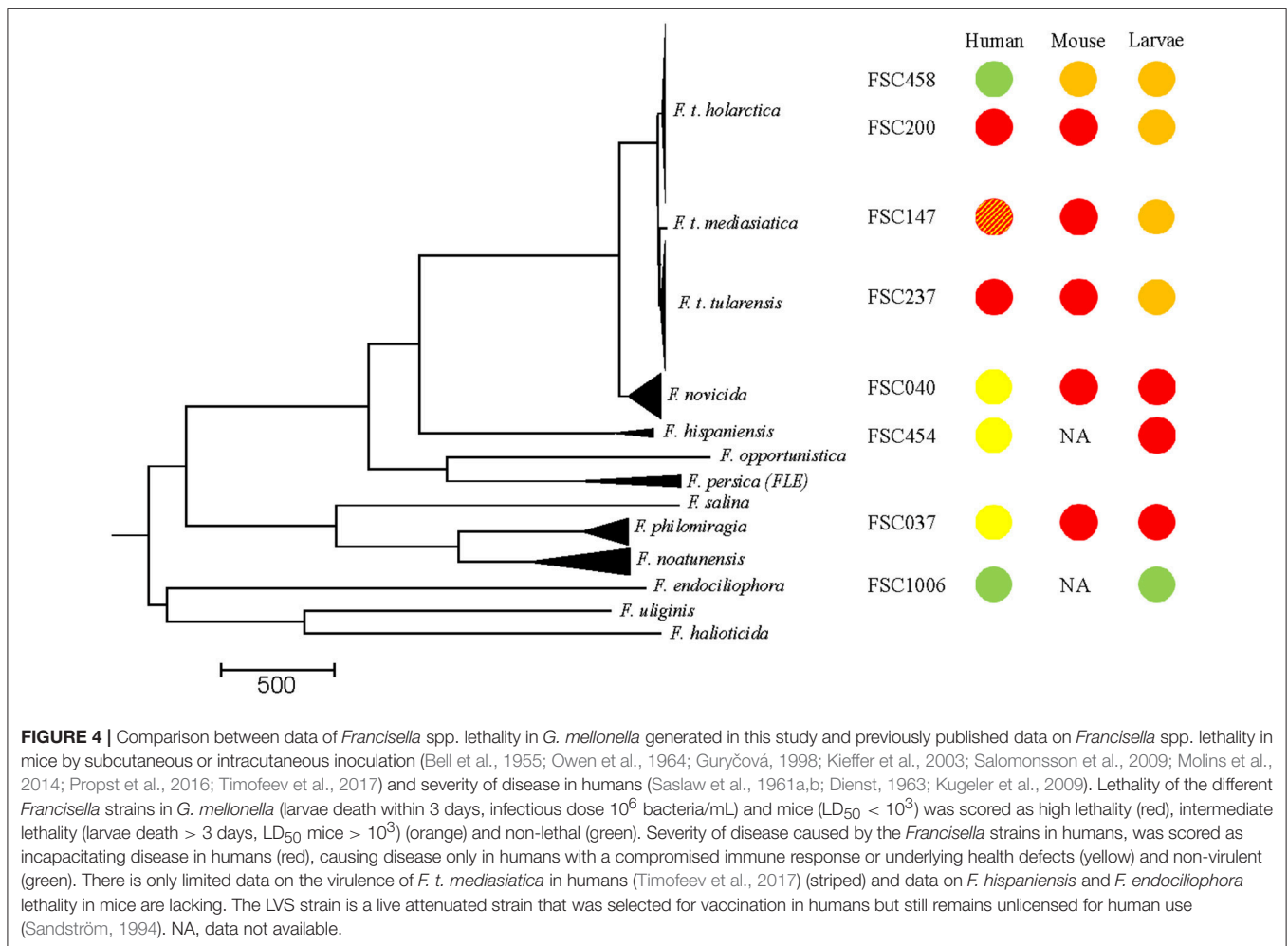
The strains investigated in this study were separated into three lineages (**Figure 4**), i.e., the *F. tularensis* lineage (*F. t. tularensis*, *F. t. mediasiatica*, *F. t. holarctica*, and *F. t. holarctica* LVS), the more diverse group comprising animal and opportunistic human pathogens associated with water environments (*F. novicida*, *F. hispaniensis*, and *F. philomiragia*) and a lineage containing only *F. endociliophora*, a recently identified endosymbiont of the marine ciliate *Euplotes raikovi*. We can only provide speculative explanations for the inverse result of the first and second *Francisella* lineages in humans and *G. mellonella* as knowledge of *Francisella* spp. virulence mechanisms has mainly been restricted



to studies of *F. t. holarctica*, *F. t. tularensis* and *F. novicida*. Strains in the first lineage (*F. tularensis*), are characterized by selective genome reduction, which has resulted in deletions of metabolic pathway components (i.e., genes involved in amino acid biosynthesis) as a specialized intracellular parasite can acquire the nutrients required for growth and replication upon infecting a host (Larsson et al., 2005, 2009). In comparison, the second lineage of opportunistic strains and specifically, the extensively studied species *F. novicida*, are more metabolically versatile, less fastidious and show higher growth rates (Owen et al., 1964; Rohmer et al., 2007). In addition *F. novicida* elicits a different immune response in the mammalian host than *F. t. tularensis* and *F. t. holarctica*, causing disease only in immunocompromised persons (Kingry and Petersen, 2014). Our results corroborate previous studies that have shown vigorous growth of *F. novicida* in hemocytes (Santic et al., 2009). Studies of *F. novicida* within arthropod cells identified similar molecular mechanisms of pathogenesis, i.e., intracellular trafficking, as

in mammalian cells (Ozanic et al., 2015), but the species nevertheless utilizes different virulence factors for proliferation in mammal and arthropod cells (Read et al., 2008; Santic et al., 2009; Åhlund et al., 2010).

A distinguishing feature of *F. tularensis* is its ability to evade the host immune response in mammals (Sjöstedt, 2006). *F. tularensis* maintain a low immunological profile early during the infection process by evading immune system surveillance, and only later replicate within the relatively protective environment of the host cell cytoplasm (Jones et al., 2014; Steiner et al., 2014). One important factor in *F. tularensis* immune evasion is an atypical lipopolysaccharide (LPS) that exhibits very low endotoxicity and stimulation of inflammatory pathways (Hajjar et al., 2006). In contrast, *F. novicida* exhibits a structurally and antigenically different LPS which elicits an inflammatory response (Jones et al., 2014). Since the growth of *Francisella* in hemocytes and macrophages shares many similarities, it is possible that the pathways of the *G. mellonella*



humoral immune response (Browne et al., 2013; Tsai et al., 2016) differ from those in humans regarding early detection of *Francisella* species, and that the difference in lethality observed in our experiments (Figure 3) rather reflects growth rate differences (Supplementary Figure 1), with the metabolically versatile opportunistic *Francisella* strains having an advantage in *G. mellonella*.

The growth of *F. philomiragia* was most detrimental to the host (*G. mellonella*). The larvae succumbed at a lower bacterial load than what was observed for the other strains tested in this study. A more detrimental effect from growth of *F. philomiragia*, in comparison with *F. tularensis* ssp. and *F. novicida*, was also reported in the ciliate *T. pyriformis* (Thelaus et al., 2009). Virulence factors in *F. philomiragia* have been less studied, but based on the genome sequence, this species is likely to express similar proteins as *F. tularensis* and *F. novicida* (Zeytun et al., 2012). Previous studies have shown that *F. philomiragia* can infect and grow in macrophages, lung, and liver cells as well as in *T. pyriformis* and *G. mellonella* (Thelaus et al., 2009; Propst et al., 2016). This suggests that *F. philomiragia*, like *F. tularensis* ssp. and *F. novicida*, can infect and proliferate in many hosts and cell types. Although *F. philomiragia* stands out as the most

aggressive strain in our experiments, all of the opportunistic strains resulted in *G. mellonella* death significantly faster than the three *F. tularensis* strains tested.

Finally, the third lineage, which includes only the endosymbiont *F. endociliophora*, represents a specific niche that is restricted to growth in a ciliate host and at lower temperature compared to the other strains tested (Sjödin et al., 2014). In contrast to the *F. tularensis* and opportunistic strains, no growth of *F. endociliophora* in *G. mellonella* was recorded. This is in line with the high degree of host restriction that is characteristic to primary endosymbionts, as well as the adaptation to host growth rates, which ensures that bacteria are transferred during host cell division (Fokin, 2004). Interestingly, *F. endociliophora* branch early in the phylogenetic tree of the *Francisella* genus (Figure 4) but display a more specialized lifestyle than the more recently branching *Francisella* species that are characterized by the ability to replicate in a broad range of hosts.

We only detected a significant difference in the lethality between wild-type *F. t. holarctica* and the live vaccine strain (LVS) at the intermediate infectious dose. No difference in lethality between these two strains was found in the

G. mellonella system when the results were corrected for dose (Supplementary Table 1, column E). It could be speculated that the doses might have affected this result, with the highest dose too high to allow differentiation of the two strains, and the lower dose may have revealed differences if the study duration was extended. This should be considered in any further experiments.

Larval death following infection was less pronounced at 22°C than at 37°C for all of the tested strains, and the difference between the *F. tularensis* and opportunistic strains was less pronounced at 22°C. It is possible that prolonged incubation would have revealed lethality differences between strains. However, *G. mellonella* larvae have been reported to survive incubation at 37°C but prolonged incubation at this temperature may induce heat stress that renders the larvae more sensitive to infection. Thus, it is plausible that the effect of temperature on larval survival can be explained by incubation at 37°C representing a temperature that is close to the upper limit for *G. mellonella* larvae.

In 2007, Aperis et al. introduced *G. mellonella* as a model host for studies of LVS and antibacterial agent efficacy (Aperis et al., 2007). In addition, Propst and colleagues compared different model systems, including *G. mellonella* to clarify the use of *F. philomiragia* as a model for studies of *Francisella* (Propst et al., 2016). These previous studies, along with our data, show that *Francisella* spp. strains multiply in, and eventually kill, *G. mellonella* larvae, which proves their utility as a model for virulence studies. This in line with numerous studies of *G. mellonella* as a model for bacterial virulence, the majority of which present good correspondence regarding bacterial pathogenicity in humans and *G. mellonella* (Sprynski et al., 2014; Tsai et al., 2016). Our data clearly show that the strains that cause incapacitating disease in humans are not as efficient in replicating in the larval host model as the *F. novicida*, *F. hispaniensis*, and *F. philomiragia* strains. Thus, *Francisella* spp. lethality in *G. mellonella* is not reflective of severity of disease in humans. This in line with a study of pathogenic *Escherichia coli* (causing urosepsis) in *G. mellonella* that conclude that the larval lethality model cannot be a substitute for the murine sepsis model (Johnson et al., 2015). On the other hand, Mukherjee et al. report on *G. mellonella* as a model system that reflects severity of disease of human pathogenic and non pathogenic environmental strains of *Listeria* spp. (Mukherjee et al., 2010). In addition, pathogenic *Yersinia enterocolitica* cause lethality in *G. mellonella* but other environmental strains of *Yersinia* showed high variability in insecticidal potential (Fuchs et al., 2008). Although, the innate immune responses of insects and vertebrates share a cellular and a humoral component, the evolutionary distance between insect and murine models makes it clear that many host-specific phenomena are likely to exist (Scully and Bidochka, 2006). The *G. mellonella* model may or may not result in a bias toward genes relevant for evading insect immunity. This will ultimately depend on the evolutionary history and ecological niche of the bacterial pathogen studied. A possible adaptation of the bacteria to an insect host would be reflected in the *G. mellonella* model system.

A limitation of *G. mellonella* as a model is the lack of standardization that results in unknown variation between sources that may interfere with the experimental outcome. This

variation limit the possibility to directly compare data from studies performed at different laboratories. The data presented here were generated using three different batches of *G. mellonella* from the same source (Vivaria). In addition, we performed control experiments with two strains (*F. t. holarctica* LVS and *F. novicida*) using larvae from an alternative source (TruLarv™ BioSystems Technology Ltd, UK). Infection of larvae from both sources with the two strains produced similar lethality results, but larval death in the TruLarv™ system occurred 2 days later than in the Vivaria system (data not shown). This result highlights the need for comparative studies in the search for consistent model systems.

The *G. mellonella* data presented here illustrate possible niche differences of *Francisella* species and contribute to the effort to understand pathogenic *F. tularensis* spp. in the context of near genetic neighbors. Larvae or insects may play a role as hosts for the replication of opportunistic human pathogens often associated with environmental samples and water. Accordingly, *G. mellonella* is a possible *in vivo* model of insect immunity that can be used for studies of both opportunistic and virulent lineages of *Francisella* spp., that produces inverse results regarding lethality in *G. mellonella* and incapacitating disease in humans. Further studies are needed in order to detangle the specific mechanism that render *Francisella* spp. strains lethal to *G. mellonella*.

AUTHOR CONTRIBUTIONS

JT designed the study, performed experiments and drafted the manuscript. EL performed experiments and contributed to the design of the study. PL contributed to the design of the study and performed the statistical analyses. AS performed the phylogenetic analysis. MF contributed to the design of the study and writing of the manuscript. All authors contributed to manuscript revision, as well as read and approved the submitted version.

FUNDING

This work was supported by the Swedish Ministry of Defense (A4042).

ACKNOWLEDGMENTS

The authors would like to thank Cecilia Ylinenjärvi for her laboratory work and Dr. Joann L Prior and her team at the Defence Science and Technology Laboratory (Dstl, United Kingdom) for introduction to the laboratory model of *Galleria mellonella*.

SUPPLEMENTARY MATERIAL

The Supplementary Material for this article can be found online at: <https://www.frontiersin.org/articles/10.3389/fcimb.2018.00188/full#supplementary-material>

Supplementary Figure 1 | Growth rate of *Francisella* spp. strains (*F. t. tularensis*, *F. t. holarctica*, *F. t. mediasiatica*, *F. t. holarctica* LVS, *F. hispaniensis*, *F.*

philomiragia, and *F. novicida*) at 37°C on laboratory media. Bacteria was seeded onto agar plates in eight technical replicates and growth was monitored at 0, 18, 32, and 48 h. Growth was scored when bacterial colonies were visible to the eye.

Supplementary Table 1 | *P*-values obtained from the log rank test for comparison of strains concerning survival estimates at (A) 37°C and

infectious dose of 10⁴ bacteria/mL, (B) 37°C and infectious dose of 10⁶ bacteria/mL, (C) 37°C and infectious dose of 10⁸ bacteria/mL, (D) 22°C and infectious dose of 10⁶ bacteria/mL and (E) 37°C controlled for infectious dose. The *p*-values are adjusted for multiple testing according to the Tukey-Kramer method.

REFERENCES

- Åhlund, M. K., Rydén, P., Sjöstedt, A., and Stöven, S. (2010). Directed screen of *Francisella novicida* virulence determinants using *Drosophila melanogaster*. *Infect. Immun.* 78, 3118–3128. doi: 10.1128/IAI.00146-10.
- Aperis, G., Burgwyn Fuchs, B., Anderson, C. A., Warner, J. E., Calderwood, S. B., and Mylonakis, E. (2007). *Galleria mellonella* as a model host to study infection by the *Francisella tularensis* live vaccine strain. *Microbes Infect.* 9, 729–734. doi: 10.1016/j.micinf.2007.02.016
- Aravena-Román, M., Merritt, A., and Inglis, T. J. J. (2015). First case of *Francisella* bacteraemia in Western Australia. *New Microbes New Infect.* 8, 75–77. doi: 10.1016/j.nmni.2015.10.004
- Barnoy, S., Gancz, H., Zhu, Y., Honnold, C. L., Zurawski, D. V., and Venkatesan, M. M. (2017). The *Galleria mellonella* larvae as an *in vivo* model for evaluation of *Shigella* virulence. *Gut Microbes* 8, 335–350. doi: 10.1080/19490976.2017.1293225
- Bell, J. F., Owen, C. R., and Larson, C. L. (1955). Virulence of *Bacterium tularensis*. I. A study of the virulence of *Bacterium tularensis* in mice, guinea pigs, and rabbits. *J. Infect. Dis.* 97, 162–166.
- Brevik, O. J., Ottem, K. F., Kamaishi, T., Watanabe, K., and Nylund, A. (2011). *Francisella haliotidica* sp. nov., a pathogen of farmed giant abalone (*Haliotis gigantea*) in Japan. *J. Appl. Microbiol.* 111, 1044–1056. doi: 10.1111/j.1365-2672.2011.05133.x.
- Browne, N., Heelan, M., and Kavanagh, K. (2013). An analysis of the structural and functional similarities of insect hemocytes and mammalian phagocytes. *Virulence* 4, 597–603. doi: 10.4161/viru.25906.
- Busse, H.-J., Huber, B., Anda, P., Escudero, R., Scholz, H. C., Seibold, E., et al. (2010). Objections to the transfer of *Francisella novicida* to the subspecies rank of *Francisella tularensis* - response to Johansson et al. *Int. J. Syst. Evol. Microbiol.* 60, 1718–1720. doi: 10.1099/00207713-60-8-1718
- Challacombe, J. F., Petersen, J. M., Gallegos-Graves, L. V., Hodge, D., Pillai, S., and Kuske, C. R. (2017). Whole-genome relationships among *Francisella* bacteria of diverse origins define new species and provide specific regions for detection. *Appl. Environ. Microbiol.* 83, AEM.02589–02516. doi: 10.1128/AEM.02589-16.
- Darling, A. E., Mau, B., and Perna, N. T. (2010). ProgressiveMauve: multiple genome alignment with gene gain, loss and rearrangement. *PLoS ONE* 5:e11147. doi: 10.1371/journal.pone.0011147
- Dienst, F. J. (1963). Tularemia — a perusal of three hundred thirty-nine cases. *J. La State Med. Soc.* 115, 114–127.
- Federal Register (2012). Possession, Use, and Transfer of Select Agents and Toxins; Biennial Review; Final Rule. *Fed. Regist. U.S. Dep. Heal. Hum. Serv.* 77, 61084–61115.
- Fokin, S. I. (2004). Bacterial endosymbionts of Ciliophora and their interactions with the host cell. *Int. Rev. Cytol.* 236, 181–249. doi: 10.1016/S0074-7696(04)36005-5.
- Fuchs, T. M., Bresolin, G., Marcinowski, L., Schachtner, J., and Scherer, S. (2008). Insecticidal genes of *Yersinia* spp.: Taxonomical distribution, contribution to toxicity towards *Manduca sexta* and *Galleria mellonella*, and evolution. *BMC Microbiol.* 8:214. doi: 10.1186/1471-2180-8-214
- Guryčová, D. (1998). First isolation of *Francisella tularensis* subsp. *tularensis* in Europe. *Eur. J. Epidemiol.* 14, 797–802. doi: 10.1023/A:1007537405242
- Hajjar, A. M., Harvey, M. D., Shaffer, S. A., Goodlett, D. R., Sjöstedt, A., Edebro, H., et al. (2006). Lack of *in vitro* and *in vivo* recognition of *Francisella tularensis* subspecies lipopolysaccharide by Toll-like receptors. *Infect. Immun.* 74, 6730–6738. doi: 10.1128/IAI.00934-06
- Hollis, D. G., Weaver, R. E., Steigerwalt, A. G., Wenger, J. D., Moss, W. C., and Brenner, D. J. (1989). *Francisella philomiragia* comb. nov. (formerly *Yersinia philomiragia*) and *Francisella tularensis* biogroup *novicida* (formerly *Francisella novicida*) associated with human disease. *J. Clin. Microbiol.* 27, 1601–1608.
- Huber, B., Escudero, R., Busse, H.-J., Seibold, E., Scholz, H. C., Anda, P., et al. (2010). Description of *Francisella hispaniensis* sp. nov., isolated from human blood, reclassification of *Francisella novicida* (Larson et al. 1955) Olsufiev et al. 1959 as *Francisella tularensis* subsp. *novicida* comb. nov. and emended description of the genus *Franc.* *Int. J. Syst. Evol. Microbiol.* 60, 1887–1896. doi: 10.1099/ijls.0.015941-0
- Johansson, A., Celli, J., Conlan, W., Elkins, K. L., Forsman, M., Keim, P. S., et al. (2010). Objections to the transfer of *Francisella novicida* to the subspecies rank of *Francisella tularensis*. *Int. J. Syst. Evol. Microbiol.* 60, 1717–1718. doi: 10.1099/ijls.0.022830-0.
- Johnson, J. R., Porter, S., Johnston, B., Kuskowski, M. A., Spurbeck, R. R., Mobley, H. L. T., et al. (2015). Host Characteristics and bacterial traits predict experimental virulence for *Escherichia coli* bloodstream isolates from patients with urosepsis. *Open Forum Infect. Dis.* 2. doi: 10.1093/ofid/ofv083
- Jones, B. D., Faron, M., Rasmussen, J. A., and Fletcher, J. R. (2014). Uncovering the components of the *Francisella tularensis* virulence stealth strategy. *Front. Cell. Infect. Microbiol.* 4:32. doi: 10.3389/fcimb.2014.00032
- Kavanagh, K., and Reeves, E. P. (2004). Exploiting the potential of insects for *in vivo* pathogenicity testing of microbial pathogens. *FEMS Microbiol. Rev.* 28, 101–112. doi: 10.1016/j.femsre.2003.09.002
- Kieffer, T. L., Cowley, S., Nano, F. E., and Elkins, K. L. (2003). *Francisella novicida* LPS has greater immunobiological activity in mice than *F. tularensis* LPS, and contributes to *F. novicida* murine pathogenesis. *Microbes Infect.* 5, 397–403. doi: 10.1016/S1286-4579(03)00052-2
- Kingry, L. C., and Petersen, J. M. (2014). Comparative review of *Francisella tularensis* and *Francisella novicida*. *Front. Cell. Infect. Microbiol.* 4:35. doi: 10.3389/fcimb.2014.00035
- Köster, J., and Rahmann, S. (2012). Snakemake—a scalable bioinformatics workflow engine. *Bioinformatics* 28, 2520–2522. doi: 10.1093/bioinformatics/bts480
- Kugeler, K. J., Mead, P. S., Janusz, A. M., Staples, J. E., Kubota, K. A., Chalcraft, L. G., et al. (2009). Molecular Epidemiology of *Francisella tularensis* in the United States. *Clin. Infect. Dis.* 48, 863–870. doi: 10.1086/597261
- Kumar, S., Stecher, G., and Tamura, K. (2016). MEGA7: molecular evolutionary genetics analysis version 7.0 for bigger datasets. *Mol. Biol. Evol.* 33, 1870–1874. doi: 10.1093/molbev/msw054
- Lärkeryd, A., Myrtenäs, K., Karlsson, E., Dwibedi, C. K., Forsman, M., Larsson, P., et al. (2014). CanSNPer: a hierarchical genotype classifier of clonal pathogens. *Bioinformatics* 30, 1762–1764. doi: 10.1093/bioinformatics/btu113
- Larson, C., Wicht, W., and Jellison, W. (1955). A new organism resembling *P. tularensis* isolated from water. *Public Health Rep.* 70, 253–258.
- Larson, M. A., Nalbantoglu, U., Sayood, K., Zentz, E. B., Cer, R. Z., Iwen, P. C., et al. (2016). Reclassification of *Wolbachia persica* as *Francisella persica* comb. nov. and emended description of the family Francisellaceae. *Int. J. Syst. Evol. Microbiol.* 66, 1200–1205. doi: 10.1099/ijsem.0.000855
- Larsson, P., Elfsmark, D., Svensson, K., Wikström, P., Forsman, M., Brettn, T., et al. (2009). Molecular evolutionary consequences of niche restriction in *Francisella tularensis*, a facultative intracellular pathogen. *PLoS Pathog.* 5:e1000472. doi: 10.1371/journal.ppat.1000472
- Larsson, P., Oyston, P. C., Chain, P., Chu, M. C., Duffield, M., Fuxelius, H. H., et al. (2005). The complete genome sequence of *Francisella tularensis*, the causative agent of tularemia. *Nat. Genet.* 37, 153–159. doi: 10.1038/ng1499
- Meir, M., Grosfeld, T., and Barkan, D. (2018). Establishment and validation of *Galleria mellonella* as a novel model organism to study *Mycobacterium abscessus* infection, pathogenesis and treatment. *Antimicrob. Agents Chemother.* 62:e02539-17. doi: 10.1128/AAC.02539-17
- Molins, C. R., Delorey, M. J., Yockey, B. M., Young, J. W., Belisle, J. T., Schriefer, M. E., et al. (2014). Virulence difference between the prototypic Schu S4 strain (A1a) and *Francisella tularensis* A1a, A1b, A2 and type B strains in

- a murine model of infection. *BMC Infect. Dis.* 14:67. doi: 10.1186/1471-2334-14-67.
- Mukherjee, K., Altincicek, B., Hain, T., Domann, E., Vilcinskas, A., and Chakraborty, T. (2010). *Galleria mellonella* as a model system for studying *Listeria pathogenesis*. *Appl. Environ. Microbiol.* 76, 310–317. doi: 10.1128/AEM.01301-09.
- Olsufjev, N. G., Emelyanova, O. S., and Dunaeva, T. N. (1959). Comparative study of strains of *B. tularensis* in the Old and New World and their taxonomy. *Hyg. Epidemiol. Microbiol. Immunol.* 3, 138–149.
- Ottem, K. F., Nylund, A., Karlsbakk, E., Friis-Møller, A., and Kamaishi, T. (2008). Elevation of *Francisella philomiragia* subsp. *noatunensis* Mikalsen et al. (2007) to *Francisella noatunensis* comb. nov. [syn. *Francisella piscicida* Ottem et al. (2008) syn. nov.] and characterization of *Francisella noatunensis* subsp. *orientalis* subsp. nov. *J. Appl. Microbiol.* 106, 1231–1243. doi: 10.1111/j.1365-2672.2008.04092.x
- Owen, C. R., Buker, E. O., Jellison, W. L., Lackman, D. B., and Bell, J. F. (1964). Comparative studies of *Francisella tularensis* and *Francisella novicida*. *J. Bacteriol.* 87, 676–683.
- Ozanic, M., Marecic, V., Abu Kwaik, Y., and Santic, M. (2015). The divergent intracellular lifestyle of *Francisella tularensis* in evolutionarily distinct host cells. *PLoS Pathog.* 11:e1005208. doi: 10.1371/journal.ppat.1005208
- Penn, R. (2010). “*Francisella tularensis* (Tularemia),” in *Mandell, Douglas and Bennett’s Principles and Practice of Infectious Diseases*, eds G. L. Mandell, J. E. Bennet, and R. Dolbin (Philadelphia PA: Elsevier Churchill, Livingstone), 2927–2937.
- Petersen, J. M., Mead, P. S., and Schriefer, M. E. (2009). *Francisella tularensis*: an arthropod-borne pathogen. *Vet. Res.* 40:7. doi: 10.1051/vetres:2008045
- Pilo, P. (2018). Arthropod Infection Models for *Francisella tularensis*. *Curr. Clin. Microbiol. Reports* 5, 10–17. doi: 10.1007/s40588-018-0084-z
- Propst, C. N., Pylpko, S. L., Blower, R. J., Ahmad, S., Mansoor, M., and van Hoek, M. L. (2016). *Francisella philomiragia* Infection and Lethality in Mammalian Tissue Culture Cell Models, *Galleria mellonella*, and BALB/c Mice. *Front. Microbiol.* 7:696. doi: 10.3389/fmicb.2016.00696
- Qu, P.-H., Chen, S.-Y., Scholz, H. C., Busse, H.-J., Gu, Q., Kämpfer, P., et al. (2013). *Francisella guangzhouensis* sp. nov., isolated from air-conditioning systems. *Int. J. Syst. Evol. Microbiol.* 63, 3628–3635. doi: 10.1099/ijs.0.049916-0
- Qu, P.-H., Li, Y., Salam, N., Chen, S.-Y., Liu, L., Gu, Q., et al. (2016). *Allofrancisella inopinata* gen. nov., sp. nov. and *Allofrancisella frigidaquae* sp. nov., isolated from water-cooling systems, and transfer of *Francisella guangzhouensis* Qu et al. 2013 to the new genus as *Allofrancisella guangzhouensis* comb. nov. *Int. J. Syst. Evol. Microbiol.* 66, 4832–4838. doi: 10.1099/ijsem.0.001437
- Read, A., Vogl, S. J., Hueffer, K., Gallagher, L. A., and Happ, G. M. (2008). *Francisella* genes required for replication in mosquito cells. *J. Med. Entomol.* 45, 1108–1116. doi: 10.1603/0022-2585(2008)45:1108:FGRFRI2.0.CO;2
- Rohmer, L., Fong, C., Abmayr, S., Wasnick, M., Larson Freeman, T. J., Radey, M., et al. (2007). Comparison of *Francisella tularensis* genomes reveals evolutionary events associated with the emergence of human pathogenic strains. *Genome Biol.* 8:R102. doi: 10.1186/gb-2007-8-6-r102
- Salomonsson, E., Kuoppa, K., Forslund, A. L., Zingmark, C., Golovliov, I., Sjöstedt, A., et al. (2009). Reintroduction of two deleted virulence loci restores full virulence to the live vaccine strain of *Francisella tularensis*. *Infect. Immun.* 77, 3424–3431. doi: 10.1128/IAI.00196-09
- Sandström, G. (1994). The tularaemia vaccine. *J. Chem. Technol. Biotechnol.* 59, 315–320. doi: 10.1002/jctb.280590402
- Santic, M., Akimana, C., Asare, R., Kouokam, J. C., Atay, S., and Kwaik, Y. A. (2009). Intracellular fate of *Francisella tularensis* within arthropod-derived cells. *Environ. Microbiol.* 11, 1473–1481. doi: 10.1111/j.1462-2920.2009.01875.x
- Saslaw, S., Eigelsbach, H. T., Prior, J. A., Wilson, H. E., and Carhart, S. (1961a). Tularemia vaccine study. I. Intracutaneous challenge. *Arch. Intern. Med.* 107, 689–701. doi: 10.1001/archinte.1961.03620050055006
- Saslaw, S., Eigelsbach, H. T., Prior, J. A., Wilson, H. E., and Carhart, S. (1961b). Tularemia vaccine study. II. Respiratory challenge. *Arch. Intern. Med.* 107, 702–714.
- Scully, L. R., and Bidochka, M. J. (2006). Developing insect models for the study of current and emerging human pathogens. *FEMS Microbiol. Lett.* 263, 1–9. doi: 10.1111/j.1574-6968.2006.00388.x
- Sjödin, A., Öhrman, C., Bäckman, S., Lärkeryd, A., and Granberg, M., Lundmark, E., et al. (2014). Complete genome sequence of *Francisella endociliophora* strain FSC1006, isolated from a laboratory culture of the marine ciliate *Euplotes raikovi*. *Genome Announc.* 2, 6–7. doi: 10.1128/genomeA.01227-14. Copyright
- Sjödin, A., Svensson, K., Öhrman, C., Ahlinder, J., Lindgren, P., Duodu, S., et al. (2012). Genome characterisation of the genus *Francisella* reveals insight into similar evolutionary paths in pathogens of mammals and fish. *BMC Genomics* 13:268. doi: 10.1186/1471-2164-13-268
- Sjöstedt, A. (2006). Intracellular survival mechanisms of *Francisella tularensis*, a stealth pathogen. *Microbes Infect.* 8, 561–567. doi: 10.1016/j.micinf.2005.08.001
- Sjöstedt, A. B. (2015). “Francisellaceae fam. nov.,” in *Bergey’s Manual of Systematics of Archaea and Bacteria*, eds G. Garrity, J. Don, N. Krieg, and J. Staley (Chichester: John Wiley & Sons, Ltd), 1–2.
- Sprynski, N., Valade, E., and Neulat-Ripoll, F. (2014). *Galleria mellonella* as an Infection Model for Select Agents. New York, NY: Humana Press.
- Steiner, D. J., Furuya, Y., and Metzger, D. (2014). Host-pathogen interactions and immune evasion strategies in *Francisella tularensis* pathogenicity. *Infect. Drug Resist.* 7, 239–251. doi: 10.2147/IDR.S53700
- Svensson, K., Sjödin, A., Bystrom, M., Granberg, M., Brittnacher, M. J., Rohmer, L., et al. (2012). Genome Sequence of *Francisella tularensis* subspecies holarctica Strain FSC200, Isolated from a Child with Tularemia. *J. Bacteriol.* 194, 6965–6966. doi: 10.1128/JB.01040-12
- Thelaus, J., Andersson, A., Mathisen, P., Forslund, A.-L., Noppa, L., and Forsman, M. (2009). Influence of nutrient status and grazing pressure on the fate of *Francisella tularensis* in lake water. *FEMS Microbiol. Ecol.* 67, 69–80. doi: 10.1111/j.1574-6941.2008.00612.x
- Timofeev, V., Bakhteeva, I., Titareva, G., Kopylov, P., Christiany, D., Mokrievich, A., et al. (2017). Russian isolates enlarge the known geographic diversity of *Francisella tularensis* subsp. *mediasiatica*. *PLoS ONE* 12:e0183714. doi: 10.1371/journal.pone.0183714
- Tsai, C. J.-Y., Loh, J. M. S., and Proft, T. (2016). *Galleria mellonella* infection models for the study of bacterial diseases and for antimicrobial drug testing. *Virulence* 7, 214–229. doi: 10.1080/21505594.2015.1135289
- Versage, J. L., Severin, D. D., Chu, M. C., and Petersen, J. M. (2003). Development of a multitarget real-time TaqMan PCR assay for enhanced detection of *Francisella tularensis* in complex specimens. *J. Clin. Microbiol.* 41, 5492–5499. doi: 10.1128/JCM.41.12.5492-5499.2003
- World Health Organization, WHO (2007). *WHO Guidelines on Tularaemia*. Geneva: WHO Press.
- Zeytun, A., Malfatti, S. A., Vergez, L. M., Shin, M., Garcia, E., and Chain, P. S. G. (2012). Complete genome sequence of *Francisella philomiragia* ATCC 25017. *J. Bacteriol.* 194, 3266–3265. doi: 10.1128/JB.00413-12

Conflict of Interest Statement: The authors declare that the research was conducted in the absence of any commercial or financial relationships that could be construed as a potential conflict of interest.

Copyright © 2018 Thelaus, Lundmark, Lindgren, Sjödin and Forsman. This is an open-access article distributed under the terms of the Creative Commons Attribution License (CC BY). The use, distribution or reproduction in other forums is permitted, provided the original author(s) and the copyright owner are credited and that the original publication in this journal is cited, in accordance with accepted academic practice. No use, distribution or reproduction is permitted which does not comply with these terms.



Further Characterization of the Capsule-Like Complex (CLC) Produced by *Francisella tularensis* Subspecies *tularensis*: Protective Efficacy and Similarity to Outer Membrane Vesicles

Anna E. Champion¹, Aloka B. Bandara¹, Nrusingh Mohapatra¹, Kelly M. Fulton², Susan M. Twine² and Thomas J. Inzana^{1,3*}

¹ Department of Biomedical Sciences and Pathobiology, Virginia-Maryland College of Veterinary Medicine, Virginia Tech, Blacksburg, VA, United States, ² Institute for Biological Sciences, National Research Council Canada, Ottawa, ON, Canada, ³ Virginia Tech Carilion School of Medicine, Roanoke, VA, United States

OPEN ACCESS

Edited by:

Anders Sjöstedt,
Umeå University, Sweden

Reviewed by:

Jason Holt Barker,
University of Iowa, United States
Karsten R. O. Hazlett,
Albany Medical College, United States

*Correspondence:

Thomas J. Inzana
tinzana@vt.edu

Received: 12 January 2018

Accepted: 09 May 2018

Published: 15 June 2018

Citation:

Champion AE, Bandara AB, Mohapatra N, Fulton KM, Twine SM and Inzana TJ (2018) Further Characterization of the Capsule-Like Complex (CLC) Produced by *Francisella tularensis* Subspecies *tularensis*: Protective Efficacy and Similarity to Outer Membrane Vesicles. *Front. Cell. Infect. Microbiol.* 8:182. doi: 10.3389/fcimb.2018.00182

Francisella tularensis is the etiologic agent of tularemia, and subspecies *tularensis* (type A) is the most virulent subspecies. The live vaccine strain (LVS) of subspecies *holarctica* produces a capsule-like complex (CLC) that consists of a large variety of glycoproteins. Expression of the CLC is greatly enhanced when the bacteria are subcultured in and grown on chemically defined medium. Deletion of two genes responsible for CLC glycosylation in LVS results in an attenuated mutant that is protective against respiratory tularemia in a mouse model. We sought to further characterize the CLC composition and to determine if a type A CLC glycosylation mutant would be attenuated in mice. The CLCs isolated from LVS extracted with 0.5% phenol or 1 M urea were similar, as determined by gel electrophoresis and Western blotting, but the CLC extracted with urea was more water-soluble. The CLC extracted with either 0.5% phenol or 1 M urea from type A strains was also similar to the CLC of LVS in antigenic properties, electrophoretic profile, and by transmission electron microscopy (TEM). The solubility of the CLC could be further enhanced by fractionation with Triton X-114 followed by N-Lauroylsarcosine detergents; the largest (>250 kDa) molecular size component appeared to be an aggregate of smaller components. Outer membrane vesicles/tubules (OMV/T) isolated by differential centrifugation and micro-filtration appeared similar to the CLC by TEM, and many of the proteins present in the OMV/T were also identified in soluble and insoluble fractions of the CLC. Further investigation is warranted to assess the relationship between OMV/T and the CLC. The CLC conjugated to keyhole limpet hemocyanin or flagellin was highly protective against high-dose LVS intradermal challenge and partially protective against intranasal challenge. A protective response was associated with a significant rise in cytokines IL-12, IL-10, and IFN- γ . However, a type A CLC glycosylation mutant remained virulent in BALB/c mice, and immunization with the CLC did not protect mice against high dose respiratory challenge with type A strain SCHU S4.

Keywords: *Francisella tularensis*, virulence factors, capsule-like complex, outer membrane vesicles, protection, immune response

INTRODUCTION

Francisella tularensis, the etiologic agent of tularemia, is a Gram-negative coccobacillus capable of causing severe disease in animals and humans (Olsufjev, 1966). Infection can occur through several routes, which include the lungs (inhalation), ingestion of contaminated water or food (gastrointestinal), or a break in the skin and mucous membranes (ulcero-glandular) (Keim et al., 2007; Sjöstedt, 2007). *F. tularensis* is classified as a Tier I select agent by the U.S. Center for Disease Control due to its ease of dispersal, persistence in the environment, and its high infectivity and potential lethality (Dennis et al., 2001). *F. tularensis* subspecies *tularensis* (type A) is the most virulent biotype and found predominately in North America. Subspecies *tularensis* is capable of causing lethal disease in up to 30% of untreated cases with as few as 10 organisms (via inhalation) (McCrum, 1961; Brooks and Buchanan, 1970). *F. tularensis* subspecies *holarctica* (type B), is less virulent for humans, but is responsible for most tularemia outbreaks in Europe and can cause death if untreated (Chen et al., 2003; Kantardjiev et al., 2006). Research over the last decade has expanded our understanding of the pathogenesis of this facultative intracellular pathogen and progress has been made on development of a vaccine (Jones et al., 2014; Sunagar et al., 2016). Currently there is no approved, licensed vaccine for tularemia. However, a live attenuated strain of subspecies *holarctica* was developed by researchers in the Soviet Union, and modified by U.S. investigators. This attenuated strain, later referred to as the live vaccine strain (LVS), conferred protection against aerosol challenge with virulent type A strains (Saslaw et al., 1961). Although LVS induces improved protection compared to killed strains, it is still not adequately protective against high dose respiratory exposure. Due to the need for improved protection, the potential for virulence in some immune-compromised individuals, and concern over the strain's stability (phase variable gray variants readily develop and are not protective), LVS is not approved for use as a vaccine to the public. Given the intracellular nature of *F. tularensis* and the success of LVS as a vaccine, a live attenuated type A strain with a defined mutation would logically be expected to be the most efficacious to induce protective immunity against infection. Targeted mutations that have been successful in attenuating *F. tularensis* have included surface components such as the lipopolysaccharide (LPS) and some outer membrane proteins (OMPs) (Thomas et al., 2007; Meibom et al., 2009; Qin et al., 2009; Reed et al., 2014), and the *Francisella* pathogenicity island (FPI) (Ozanic et al., 2016).

Investigation of the surface components of *F. tularensis* has markedly increased over the past 10–15 years. Some of the known surface components include LPS, O-antigen capsule, pili, several outer membrane proteins, outer membrane vesicles and tubes (OMV/T), and the capsule-like complex (CLC). The LPS has been the most thoroughly studied surface antigen, and its role in virulence and resistance to complement-mediated bactericidal activity is well-documented (Hartley et al., 2004; Li et al., 2007; Raynaud et al., 2007; Sebastian et al., 2007). Deletion of the O-antigen in types A and B strains results in a highly attenuated mutant that confers protection against

challenge with type B strains, but not type A infection (Li et al., 2007; Raynaud et al., 2007; Sebastian et al., 2007; Thomas et al., 2007). In addition, a capsule comprised of O-antigen sugars is present in types A and B strains, and is necessary for intracellular growth (Apicella et al., 2010). While an O-antigen capsule-deficient mutant is attenuated, this mutant also does not provide adequate protection against type A *F. tularensis* (Apicella et al., 2010; Lindemann et al., 2011). OMV, common to Gram-negative bacteria, are also produced by *Francisella* spp., but the majority of that work has been described in *F. novicida* (Pierson et al., 2011; McCaig et al., 2013), a more distant subspecies of *F. tularensis*. Several proteins recognized as virulence factors, such as FopB, TolC, GroEL, as well as the FPI proteins IglABC and PdpAB, are also present in the OMV (Nano et al., 2004; Oyston, 2008; Pierson et al., 2011). Furthermore, *F. novicida* OMV have successfully been used as a vaccine against challenge with *F. novicida*, but that does not indicate that OMVs would protect against the more virulent *F. tularensis* type A and B strains (Pierson et al., 2011). However, Huntley et al. (2008) have shown that outer membranes consisting of native OMPs provide limited protection of mice against challenge with 40 colony forming units (CFU) of type A strain SCHU S4. Golovliov *et al.* reported that a capsular/vesicular material surrounds phagocytized *F. tularensis* and that this material could be shed during infection as a way of masking the bacteria from the host (Golovliov et al., 2003).

Another novel surface component that has been identified in *F. tularensis* is the CLC (Bandara et al., 2011). The CLC appears as an electron dense material around the cell surface when visualized by transmission electron microscopy (TEM), and its presence requires subculture under specific growth conditions and components (Cherwonogrodzky et al., 1994). After semi-purification, the CLC was found to consist of about 10% carbohydrate that is predominately glucose, galactose, and mannose (Bandara et al., 2011). However, the CLC appears to contain many proteinase-resistant proteins, glycoproteins, and possibly a high molecular size (HMS) carbohydrate/glycoprotein that presents as multiple bands or a diffuse banding between 150 and 250-kDa (Bandara et al., 2011). Identification of novel glycoproteins, or the presence of previously identified *F. tularensis* glycoproteins, such as DsbA or the Pil proteins, in the CLC has not yet been established. The production of HMS carbohydrate was also found to be dependent on growth in medium that mimicked growth factors present in the host (Brain Heart Infusion, BBL) (Zarrella et al., 2011). A definitive link between the HMS carbohydrate, described by Zarrella et al., and the CLC has yet to be established (Zarrella et al., 2011). The locus responsible for glycosylation of some proteins (FTT0789-FTT0800), such as DsbA, in *F. tularensis* type A and B strains is also responsible for glycosylation of the CLC (Larsson et al., 2005; Bandara et al., 2011) (Balonova et al., 2010; Thomas et al., 2011). We previously demonstrated that when two glycosyl transferases (FTT0798-99) in this locus were deleted in LVS (Bandara et al., 2011) or *F. novicida* (Freudenberger Catanzaro et al., 2017), CLC production was significantly diminished and both species were highly attenuated. In LVS, and to a lesser extent *F. novicida*, the CLC-deficient strains were protective against challenge with the parent strain.

TABLE 1 | *Francisella tularensis* bacterial strains used in this study.

Strain	LPS/O-antigen	O-antigen capsule	CLC	Attenuated	Source
LVS	+	+	+	N	May Chu, CDC
LVS_P10 ^a	+	+	+++	N	Bandara et al., 2011
LVSΔ1423-22_P10 ^a	+	+	–	Y	Bandara et al., 2011
Wbt _{G191V}	–	–	+	Y	Li et al., 2007
Wbt _{G191V} _P10 ^a	–	–	+++	Y	Bandara et al., 2011
Wbt _{G191V} Δ1423-22_P10 ^a	–	–	–	Y	Bandara et al., 2011
SCHU S4_P10 ^a	+	+	+++	N	Mark Wolcott, USAMRIID
SCHU S4Δ0798/0799_P10 ^a	+	+	–	N	This work
TI0902	+	+	+	N	Inzana et al., 2004
TI0902_P10 ^a	+	+	+++	N	This work
TIGB03	–	+	+	Y	Modise et al., 2012
TIGB03[wbtk+]	+	+	+	N	This work

^aThe suffix P10 indicates the strain has been subcultured daily for 10 days in Chamberlain's defined medium (CDM) broth followed by culture on CDM agar at 32°C for several days to enhance expression of CLC.

Further identification of the many individual components of the CLC could result in a better understanding of the CLC's role in virulence and help elucidate potential genetic targets that could be useful for vaccine development. In this work we further characterized the *F. tularensis* CLC from both type A and LVS strains through enhancing solubility, further compositional analysis, and comparison to OMV/T. Immunization of mice with the CLC conjugated to protein stimulated a selective cytokine response and was protective against LVS challenge. However, a CLC glycosylation mutant of type A *F. tularensis* remained virulent in mice, and immunization of mice with the CLC did not provide adequate protection against respiratory challenge with SCHU S4. Further analysis of the CLC and its components could prove advantageous in elucidating the role of CLC in pathogenesis.

MATERIALS AND METHODS

Bacterial Strains and Growth Conditions

The bacterial strains used and their sources are listed in Table 1. LVS mutants lacking LPS O-antigen were used for CLC isolation and characterization to eliminate contamination of CLC extracts with O-antigen sugars. *F. tularensis* strains were cultured from frozen stock suspensions onto brain heart infusion agar (BHIA) (Becton-Dickinson, Franklin Lakes, NJ) supplemented with 0.1% L-cysteine hydrochloride monohydrate (Sigma-Aldrich, St. Louis, MO) (BHIA), Chamberlain's defined medium (CDM) (Cherwonogrodzky et al., 1994) with 1.5% glucose, or Modified Mueller Hinton (MH) medium supplemented with 0.1% glucose, 0.025% ferric pyrophosphate, and 2% IsoVitalEx (Becton-Dickinson), and incubated at 37°C in 6% CO₂, unless otherwise stated. Supplemented BHI medium was the standard medium used to routinely culture *F. tularensis*. Supplemented CDM medium was used to enhance CLC production, as described (Bandara et al., 2011). Supplemented MH medium was used based on evidence that *F. tularensis* grown in MHB medium lacks the cell surface HMS carbohydrates/glycoproteins that

are expressed by bacteria grown in BHI medium and during growth in mammalian hosts (Zarrella et al., 2011). For culture in broth, *F. tularensis* strains were grown with shaking (175 rpm) in BHI broth (BHIB) at 37°C, or CDM broth (CDMB) at 32°C. For selection of recombinant strains 15 μg kanamycin (Kan)/ml was added to the stated medium. For enhancement of surface CLC, the bacteria were subcultured in CDMB daily for 10 consecutive passages and indicated by the extension "P10" on the strain name. For CLC preparation, CDMB-subcultured *F. tularensis* was grown on CDM agar (CDMA) in 150-mm × 15-mm petri dishes, and incubated at 32°C in 6% CO₂ for 5 days. All experiments with LVS and mutants were carried out in biosafety level (BSL)-2 facilities in an approved biosafety cabinet. All experiments with type A strains TI0902 and SCHU S4 were carried out in a biosafety level-3 (BSL-3) facility in an approved biosafety cabinet in the college's infectious disease unit (IDU). All investigators working with select agents have FBI and CDC clearance and approval. The current CDC approval number for the BSL3/ABSL3 facility of the IDU is C20111027-1280.

Mutagenesis of the Type A CLC Glycosylation Locus

The suicide vector pJC84 (generously provided by Jean Celli, Washington State University, Pullman, WA) was used to generate an in-frame deletion of FTT_0798 and 0799 genes in the *F. tularensis* strain SCHU S4. The deletion construct of these genes was carried out as described (Mohapatra et al., 2013). In brief, PCR amplified products of about 1100 bp of an upstream region (forward primer—ACG CGT CGA CGA AGT ATT TAA AAG GAT ATT TTC ACG TAG and reverse primer—CGC GGA TCC ATT TAC CTT AAG AGT ATT AAT CTT TAA ATA AGA AG) and downstream region (forward primer—CGC GGA TCC AAA ATT TTA AGG AAT GAA ATG AAA ACC T and reverse primer—TCC CCC CGG GCT TTC TGT GCA AAT ATT TAC AAA GG) of FTT_0798 and 0799 was cloned into the pJC84 plasmid using suitable restriction sites. All plasmid constructs were verified by sequencing, and glycerol stocks were

frozen at -80°C for further use. The deletion constructs were transformed into SCHU S4 by electroporation as described (McRae et al., 2010). Kanamycin-resistant transformants were tested for integration of the allelic replacement plasmid using suitable primer combinations (forward primer—CTA GCT AGC AGG AGA CAT GAA CGA TGA ACA TC, reverse primer—GGG ACG TCG GAT TCA CCT TTA TGT TGA TAA G and forward primer—ATC AGC TCA CTC AAA GGC GG and reverse primer—GGG ACG TCG ATT AAG CAT TGG TAA CTG TCA GAC C). The positive clones were subjected to sucrose counter selection as described (McRae et al., 2010). Sucrose-resistant clones were patched on MH-kanamycin agar to verify loss of the kanamycin-resistance marker, and colony PCR was performed to detect clones with allelic replacement within the correct chromosomal locus using FTT_0798 and 0799 gene specific primers, which are identical to primers used for detection of FTL_1422 and FTL_1423 from LVS (Bandara et al., 2011). Mutagenesis of the glycosylation locus in one clone (SCHU S4 Δ 0798-99) was confirmed by the loss of carbohydrate content using the anthrone assay (Scott and Melvin, 1953) as previously described (Freudenberger Catanzaro et al., 2017).

CLC Extraction

To avoid the presence of O-antigen sugars in CLC extracts, LVS O-antigen mutant WbtI_{G191V}_P10 (Li et al., 2007) was used for most CLC extractions. To enhance for CLC expression, the bacteria were subcultured daily for 10 days in CDMB at 37°C with shaking, and then grown on CDMA for 5 days with 6% CO_2 at 32°C , as previously described (Bandara et al., 2011). For some experiments, the cells were also grown on BHI or MH agar. To determine if solubility of the CLC could be improved, the bacteria were extracted with a variety of chaotropic agents. The bacteria were scraped off the plates, and gently washed twice with 10 mM HEPES (4-(2-hydroxyethyl)-1-piperazineethanesulfonic acid) before extraction of the CLC. The bacteria were suspended to 2×10^{10} (CFU)/ml, determined spectrophotometrically, pelleted by centrifugation, and suspended in 1 ml of various chaotropic agents (e.g., low/high pH, urea, phenol, guanidine, neutral buffers) for 15 min at room temperature to determine the extraction buffer that maximized solubility of the CLC (Supplementary Table 1). The bacteria were removed by centrifugation and acidic samples were adjusted to pH 7 with 5N NaOH to avoid protein degradation. Supernatants were either used directly or excess ethanol was added to precipitate large molecular size components. Urea (1 M) was determined to be the most effective extraction buffer, and therefore all CLC extractions described in this study utilized 1 M urea or 0.5% phenol, as described previously (Bandara et al., 2011). Briefly, the bacteria were scraped off two agar plates with 20 mls of 1 M urea or 0.5% phenol. The suspended cells were incubated at room temperature for 15 min, harvested by centrifugation ($10,000 \times g$ for 15 min), and the supernatant retained. The wet weight of the cell pellets was determined, and the CLC volumes adjusted based on the mass between parent and mutant strains to normalize the extracts. For type A strains extractions were carried out in a BLS-3 facility and complete loss of cell viability was verified before removal of any material from

the BSL-3 laboratory. After urea-extracted supernatants were harvested, sodium acetate was added to a final concentration of 30 mM and the CLC was precipitated with 5 volumes of cold 95% ethanol. A portion of this crude supernatant was concentrated 5- to 10-fold by ultrafiltration through a 100-kDa Centriprep filter (Millipore, Darmstadt, Germany).

For some experiments, WbtI_{G191V}_P10 was grown in CDM, BHI, or MH broth (100 ml) with shaking at 180 rpm at 32 or 37°C . The broth cultures were grown to 10^9 CFU/ml, determined spectrophotometrically and confirmed by viable plate count. The cells were removed by centrifugation ($10,000 \times g$ for 15 min), and 5 volumes of 95% ethanol were added to the supernatant and held at -20°C overnight. The resulting precipitate was harvested and resuspended in 5–10 ml of sterile water and lyophilized. The cell pellet was resuspended in 20 ml of 1 M urea and extracted for CLC, as described above.

Electrophoretic Analysis of CLC

Ten μl of CLC extract was analyzed by sodium dodecyl sulfate-polyacrylamide gel electrophoresis (SDS-PAGE) on either 4–8% NuPAGE or 4–12% NuPAGE gels (Invitrogen, Grand Island, NY). The gels were stained with either the SilverSnap kit (Pierce, Rockford, IL) or by StainsAll/silver stain (Sigma), as described (Bandara et al., 2011). Carbohydrate in the gels developed with StainsAll/silver appeared as blue bands, proteins were pink, lipids yellow, and glycoproteins appeared purple. Unmodified, ionic proteins are not stained and appear white, or are negatively stained by StainsAll/silver stain. To avoid interference by LPS O-antigen, only extracts from O-antigen mutants were examined by gel electrophoresis. As a control, excess 95% cold ethanol was added to media without bacterial growth and the precipitate was solubilized and analyzed as described above.

For fractionation analysis, 100 μg (lyophilized weight) of urea-extracted CLC from O-antigen mutant WbtI_{G191V}_P10 was electrophoresed through the Gel Elution Liquid Fraction Entrapment Electrophoresis (GELFREE) 8100 (Expedeon, San Diego, CA) protein fractionation system. This system uses cartridges to fractionate proteins over a mass range of 3.5–500 kDa into user-selectable, liquid phase molecular weight fractions. Urea-extracted CLC was desalted by Zeba spin desalting columns (7K MWCO) (Pierce) prior to fractionation and lyophilized. The desalted CLC (100 μg) was resuspended in 112 μl sterile distilled water, and 8 μl of 1 M DTT (dithiothreitol) and 30 μl of provided sample buffer was added. The sample was heated at 50°C for 10 min, cooled to room temperature, and fractionated into 12 fractions following the manufactures' instructions for the high molecular size 5% tris-acetate cartridge. Each fraction was then analyzed by SDS-PAGE.

To resolve insolubility issues that commonly occurred following concentration of even the urea-extracted CLC, purified CLC from WbtI_{G191V}_P10 and WbtI_{G191V} Δ 1423-22_P10 was fractionated using the detergents Triton X-114 and *N*-Lauroylsarcosine (sarkosyl) (Bordier, 1981). Samples from O-antigen and O-antigen/CLC mutants were normalized to equivalent amounts of wet weight because normalization based on protein content would be inaccurate due to substantial differences in glycosylation of CLC between the different

mutants. Due to incubation on plates for several days, a viable plate count for bacterial cell numbers would also be inaccurate. Equal amounts (5 mg) of lyophilized, urea-extracted CLC from the O-antigen mutant and the CLC-deficient mutants were suspended in 5 ml of distilled water and Triton X-114 (Sigma) was added to a final concentration of 5% (v/v). The samples were vortexed for 1 min, maintained on ice at 4°C overnight, the samples were incubated at 37°C for 2 h, and then centrifuged at $3000 \times g$ at room temperature for 10 min to separate the aqueous (TxS-A) and detergent phases (TxS-D). Both phases were removed carefully, dialyzed against distilled water, and lyophilized. The Triton X-114 insoluble pellet was resuspended in 1 ml of 1% sarkosyl, incubated at room temperature for 15 min, and the samples centrifuged at $5000 \times g$ for 10 min at room temperature. The soluble supernatant was removed, and the insoluble pellet resuspended in 1 ml of distilled water, constituting the sarkosyl-soluble (TxI-SS) and sarkosyl-insoluble (TxI-SI) fractions, respectively. All fractions were analyzed on a 4–12% bis-tris NuPAGE gel (Invitrogen) and visualized by the SilverSnap (Pierce) silver stain kit.

OMV Extraction

OMV were purified from *F. tularensis* strains by one of two procedures. The method described for isolation of OMV and outer membrane tubules (OMT) from *F. novicida* (McCaig et al., 2013) was slightly modified. Briefly, bacterial cultures were grown in 1 L of CDMB for ~5 h with appropriate antibiotic to exponential phase, the bacteria removed by successive, differential low-speed centrifugation ($5,000 \times g$, followed by $7500 \times g$, for 30 min each), and the supernatant passed through a $0.45 \mu\text{m}$ syringe filter (Nalgene, Rochester, NY). The filtered supernatant was concentrated from 1 L to about 50 ml using an Amicon tangential flow filtration unit with a 100-kDa molecular mass cutoff membrane (Millipore, Darmstadt, Germany). The concentrated cell-free medium was then ultracentrifuged at $100,000 \times g$ for 1 h at 4°C. The OMV/T pellet was resuspended in 10 mM HEPES (pH 7.5) containing 0.05% sodium azide, and ultracentrifuged again. The pelleted OMV/T was resuspended in 1–2 ml of HEPES buffer with sodium azide and stored at -20°C until use.

The second OMV method (referred to as OMV_A) used more closely mimics the CLC extraction procedure, and was modified from a previously published method for *Brucella* (Gamazo et al., 1989; Avila-Calderón et al., 2012). Overnight cultures of *F. tularensis* strains from CDMB were grown at 32°C on 5 CDMA plates with appropriate antibiotic. Bacteria were scraped off the agar plates and suspended in 100 ml sterile phosphate buffered saline (PBS), pH 7.3. The bacterial cells were removed by centrifugation at $10,000 \times g$ for 30 min. The supernatant was passed through a $0.45 \mu\text{m}$ filter (Millipore) and sodium azide was added to 0.05%, final concentration. The supernatant was ultracentrifuged at $100,000 \times g$ for 2 h at 4°C. The OMV pellet was washed twice with PBS and the OMV suspended in 1 ml of sterile PBS. The OMV_A were aliquoted and stored at -20°C . Total protein concentrations of OMV from each method were determined using the BCA protein kit (Pierce), as per manufacturer's instructions.

CLC Compositional Analysis

Urea-extracted CLC was concentrated using a 100-kDa Centriprep filter unit (Millipore), and the sample separated into soluble and insoluble fractions (material that precipitates following concentration), as described above. Trypsin digests of the fractions were analyzed by nano-liquid chromatography-mass spectrometry (nLC-MS/MS using a “CapLC” (capillary chromatography system) (Waters) coupled to a “QTOF Ultima” hybrid quadrupole time-of-flight mass spectrometer (Waters) as described (Fulton et al., 2015). Peptide extracts were injected into a $75\text{-}\mu\text{m}$ internal diameter \times 150-mm PepMap C₁₈ nanocolumn (Dionex/LC packings), and resolved by gradient elution (5–75% acetonitrile, 0.12% formic acid in 30 min, 350 nL/min). MS/MS spectra were acquired on doubly, triply, and quadruply charged ions. Peak lists were automatically generated by ProteinLynx (Waters) with the following parameters: smoothing—four channels, two smoothes, Savitzky Golay mode; centroid—minimum peak width at half height of four channels, centroid top 80%. nLC-MS/MS spectra of the tryptic peptides were searched against the NCBI nr (NCBI nr 20050724; 2693904 sequences) and *F. tularensis* LVS genome sequence using MASCOT 2.0.1 (Matrix Science, UK) to identify protein homologs. The following parameters were used for mass spectral identification: peptide tolerance of 1.5 Da, MS/MS tolerance of 0.8 Da, possible one missed cleavage site, variable modifications including carbamidomethylation of cysteine residues, oxidation of methionine, formation of pyroglutamate at *N*-terminal glycine, and *N*-terminal acetylation. Peptide identifications were accepted if they met all of the following criteria: MASCOT peptide score > 25, mass accuracy < 100 ppm. In addition, all MS/MS spectra were manually assessed for data quality and high confidence identification, requiring a clear series of high mass *y* ions and correct charge state assignment for all fragments. However, proteins that were heavily glycosylated could not be identified using this method.

Peptide composition of in-gel proteolytic digests were performed using trypsin (Promega, Madison, WI, USA) at a ratio of 30:1 (protein/enzyme, w/w) in 50 mM ammonium bicarbonate at 37°C overnight. The resulting protein digests were analyzed by nLC-MS/MS nano-liquid chromatography as described above. In addition, ion pairing normal-phase liquid chromatography (IP-NPLC) was used for enrichment and identification of putative glycopeptides from the urea-extracted CLC of WbtI_{G191V_P10}, as described previously (Thomas et al., 2011).

Glycose composition of type A CLC was determined by combined GC/MS of the per-*O*-trimethylsilyl (TMS) derivatives of the monosaccharide methyl glycosides produced from the sample by acidic methanolysis, as described (Merkle and Poppe, 1994). Amino acid analysis of the urea-extracted CLC was performed by the University of California at Davis Proteomics Institute (Ozols, 1990; Kataoka et al., 2001).

Transmission Electron Microscopy

Francisella tularensis strains were grown on CDMA (with appropriate antibiotic) for 5 days at 32°C. The cells were gently scraped into 0.1 M sodium cacodylate buffer (pH 7.5) containing 3% glutaraldehyde and turned end-over-end for 2 h.

Type A strains were left in the fixative at 4°C for up to 5 days. Periodically, cell death was verified by streaking 50 µl aliquots of fixed cells onto CDMA and incubating for 5 days. If no growth occurred after this time period the cells were removed from the BSL-3 facility. Samples were bound to formvar-coated slot grids, stained with 0.5% uranyl acetate for 10 s, and viewed with a JEOL 100 CX-II transmission electron microscope (Ward and Inzana, 1994).

Generation of Hyperimmune Rabbit Serum

Antiserum to WbtI_{G191V}_P10 CLC was raised in a New Zealand white rabbit by subcutaneous immunization of 100 µg phenol-extracted purified CLC mixed 1:1 in Freund's complete adjuvant, injected into 6 sites. Two weeks later, the immunization was repeated with 100 µg phenol-extracted purified CLC in Freund's incomplete adjuvant. Two weeks after this injection, the rabbit was immunized intravenously with 500 µg CLC at weekly intervals until hyperimmune serum (ELISA titer > 1:6,400) was obtained.

CLC-Protein Conjugation and Mouse Challenge

CLC was purified from LVS O-antigen mutant WbtI_{G191V}_P10, which was enhanced for CLC production as previously described (Bandara et al., 2011). The purified CLC was conjugated to keyhole limpet hemocyanin (KLH) or purified *Salmonella* flagellin protein through an adipic acid dihydrazide (ADH) spacer as described (Schneerson et al., 1980). Briefly, the immunogenic protein carrier was conjugated to ADH at pH 4.7 with 1-ethyl-3-(3-dimethylaminopropyl)carbodiimide (EDAC). Reactive groups on the glycosyl moiety of the CLC were generated with cyanogen bromide at pH 10.5, and conjugated to either KLH or flagellin through ADH at pH 8.5. The CLC-conjugate was eluted through a Sepharose S-300 size exclusion column and collected in the void volume. Fractions were tested for protein (absorbance at 280 nm), pooled, dialyzed against distilled water, and lyophilized. After lyophilization, if some insolubility was observed the samples were sonicated to regain clarity. To confirm conjugation was successful, CLC conjugates were analyzed by SDS-PAGE on 4–12% bis-tris gels with unconjugated CLC and the protein carrier as a control.

The CLC's protective efficacy against LVS challenge was assessed in groups of 6 BALB/C mice immunized intradermally (ID) with CLC-KLH or CLC-flagellin protein conjugates twice 6 weeks apart. The first and second immunizations were administered with Freund's Complete and Incomplete adjuvants, respectively. Mice were challenged with 5 × LD₅₀ of LVS intranasally (IN) (5000 CFU) or ID with 2 × 10⁷ CFU. Blood samples were collected from mice prior to immunization, post-vaccination (at 6 weeks), and 3 days post-challenge. Serum samples were cryo-preserved at -80°C. Serum cytokine levels were determined in triplicate using the Bio-Plex Pro™ Mouse Cytokine Th1/Th2 Assay (Bio-Rad, Hercules, CA) following the manufacturer's instructions.

To determine the protective efficacy of type A CLC to type A lethal challenge, groups of 4–8 mice were immunized subcutaneously (SC) with either crude CLC, a concentrated,

semi-purified HMS CLC extract (both from SCHU S4 using 1 M urea), or water only. Mice were immunized with 50 µg of CLC ID twice 6 weeks apart or 3 months apart, with the first and second immunizations containing Freund's complete and Freund's incomplete adjuvant, respectively, or monophosphoryl lipid A (MPLA). Mice were IN-challenged with 100 or 150 CFU of *F. tularensis* SCHU S4 grown in supplemented BHI broth, washed in PBS, and adjusted to 10⁹ CFU/ml, determined spectrophotometrically and confirmed by viable plate count.

To assess if mutagenesis of the glycosylation locus attenuated type A strains as it does LVS and *F. novicida*, 6 BALB/c mice were each challenged IN with 100 CFU of SCHU S4 or SCHU S4Δ0798-99. Challenge doses were confirmed by viable plate count. Clinical symptoms of animals were recorded and any mice that became moribund were humanely euthanized with excess CO₂.

Statistics

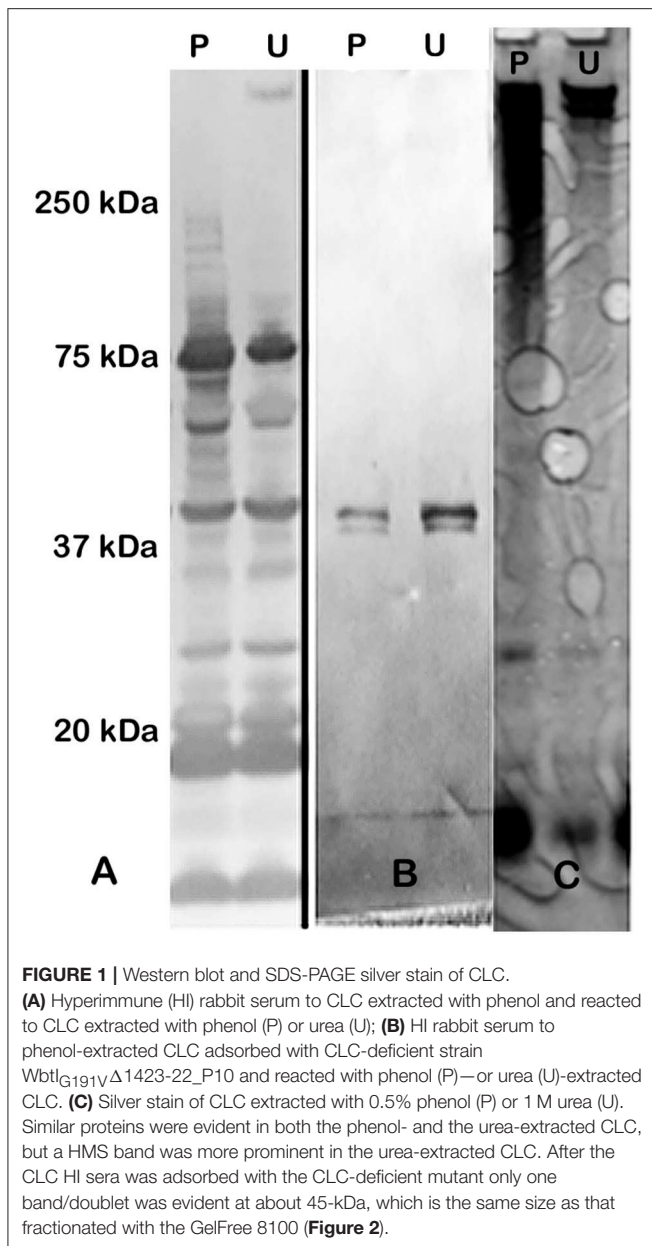
Statistical analyses were performed using Microsoft Excel software (Redmond, WA) and GraphPad InStat software (La Jolla, CA). Protection data were analyzed by Fisher's Exact Test with Yates continuity correction. Differences in cytokine responses were measured by Tukey-Kramer multiple comparison test. Other variables were determined using students *t*-test and expressed as the mean ± standard deviation. Results with a *p* < 0.05 were considered statistically significant.

RESULTS

Comparison of Urea- and Phenol-Extracted CLC

Extraction of the CLC with 1 M urea greatly increased its solubility compared to extraction with 0.5% phenol (data not shown). However, when the urea was removed by dialysis with distilled water, or the material was concentrated through a 100-kDa filter > 2-fold, the material aggregated and became insoluble. The CLC extracted by urea and phenol were similar based on electrophoretic profile (Figure 1C) and by Western blotting with hyperimmune rabbit serum to CLC extracted with phenol (Figures 1A,B). Hyperimmune serum to CLC extracted with urea resulted in similar Western blot results (not shown). When immune serum was adsorbed with mutant WbtI_{G191V}Δ1423-22_P10, most of the proteins were eliminated, except for a doublet at about 45-kDa (Figure 1B). The high molecular size band/smear at about 250-kDa was present in CLC extracted with phenol (P) or urea (U), but was more of a diffuse band in the phenol extract, possibly due to some degradation of proteins (Figure 1C). The band/smear at about 250-kDa was not present in the Western blot, likely because the HMS material did not transfer out of the gel as readily as lower molecular size material. Overall, electrophoretic, and immunological analyses indicated the preparations extracted with urea or phenol were very similar. Therefore, most of the extractions of CLC from *F. tularensis* were performed using 1 M urea.

To attempt to further resolve the specific bands/components of the HMS material at about 250-kDa, the GelFree 8100 fractionation system, which separates analytes based on



electrophoretic mobility, was used. **Figure 2** shows the urea-extracted CLC of fractions F1-F12 following SDS-PAGE. Interestingly, there were no bands or smear above 150-kDa after fractionation. The larger protein bands last appeared faintly in fraction 9; a smaller 45-kDa band was clearly present in fractions 5–8 and 11–12. This 45-kDa band was also the only band evident on a Western blot of the CLC using immune serum adsorbed with the CLC-deficient mutant (**Figure 1B**). Unfortunately, protein identification using mass spectrometry failed to identify this 45-kDa protein, likely due to glycosylation, which can suppress the MS signal from peptide fragment ions. Therefore, the HMS appeared to be an aggregate of (glyco)proteins, rather than a single protein or polysaccharide.

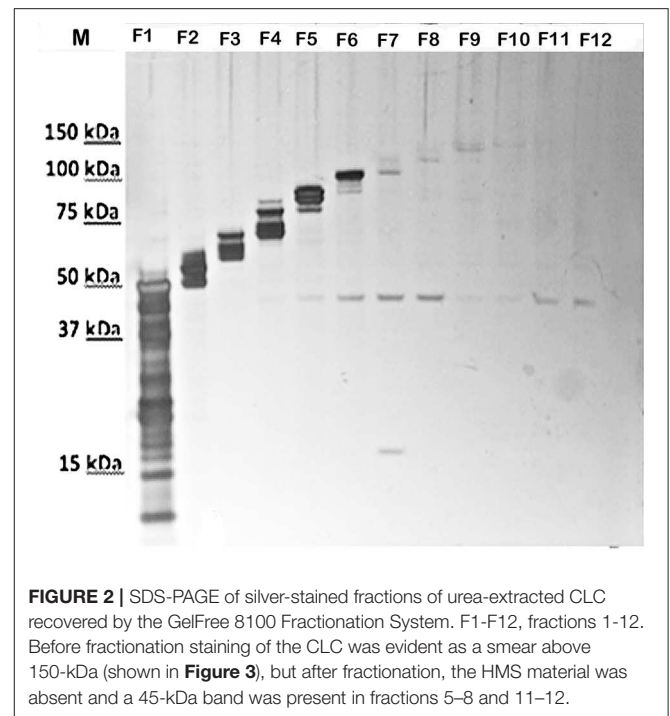


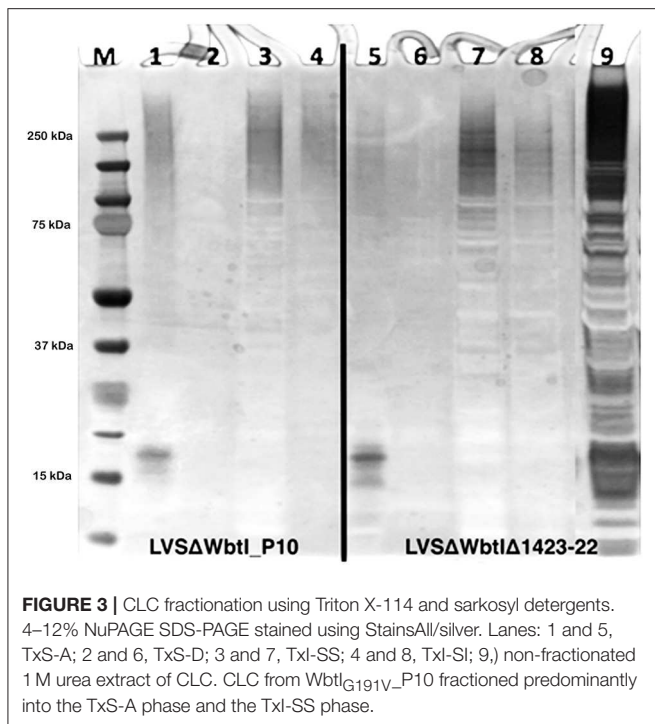
TABLE 2 | Protein concentrations of Triton X-114 and sarkosyl fractions.

<i>F. tularensis</i> strain	Protein (μg/ml)
<i>Wbtl_{G191V}_P10</i>	
TxS-A	352
TxS-D	364
TxI-SS	302
TxI-SI	20
<i>Wbtl_{G191V}Δ1423-22_P10</i>	
TxS-A	426
TxS-D	392
TxI-SS	775
TxI-SI	330

TxS, Triton X-114 soluble; TxI, Triton X-114 insoluble; A, aqueous; D, detergent; SS, sarkosyl soluble; SI, sarkosyl insoluble.

Detergent Fractionation

To further enhance the solubility of the CLC and clarify its composition, the CLC extracts were subjected to differential detergent stabilization using Triton X-114 alone or in combination with sarkosyl. Similar amounts of soluble protein were recovered in the Triton X-114 aqueous (TxS-A) and detergent (TxS-D) fractions of CLC from both the LVS O-antigen mutant and the double LVS O-antigen/CLC mutant (**Table 2**). O-antigen mutants were used to avoid interference of the O-antigen glycoses with carbohydrate components on glycoproteins of the CLC, particularly for analysis by SDS-PAGE and StainsAll/silver stain, which stains carbohydrate components (see below). However, most of the HMS diffuse material partitioned into the TxS-A phase. The Triton X-114



insoluble (TxI) material (recovered following Triton X-114 extraction and centrifugation) from CLC of the O-antigen mutant WbtIG191V_P10 was far more soluble (~15:1) when subsequently extracted with 1% sarkosyl (TxI-SS) than the Triton X-114 insoluble material from the CLC of the O-antigen/CLC double glycosylation mutant WbtIG191VΔ1423-22_P10 (~2:1). When these fractions were analyzed by SDS-PAGE using StainsAll/Silver, substantial amounts of (glyco)protein in the Triton X-114-soluble aqueous phases (Figure 3, lanes 1 and 5), and soluble detergent phases (Figure 3, lanes 2 and 6) were not evident in the CLC preparations of WbtIG191V_P10 or WbtIG191VΔ1423-22_P10, except protein(s) at about 18-kDa from the TxS-A fractions. The increased amount of proteinaceous material solubilized by sarkosyl and visualized with StainsAll/Silver (Figure 3, lanes 3 and 7) was substantial (StainsAll negatively stains proteins, which appear as ghost bands on the gel), and much less protein remained in the sarkosyl-insoluble fraction (pellet recovered following sarkosyl extraction and centrifugation) (Figure 3, lanes 4 and 8; lane 9 contains unfractionated CLC). Overall, a greater amount of protein was present in the CLC of WbtIG191VΔ1423-22_P10 compared to the O-antigen mutant. Although the glycosylation mutant made much less CLC than WbtIG191V_P10, when compared 1:1 by weight, the CLC extracted from the CLC glycosylation mutant contained more protein than the parent that fractionated differently. This increased proportion of protein in the CLC glycosylation mutant is likely due to less carbohydrate in the CLC and therefore proportionately more protein.

Impact of Growth Medium on CLC Expression

CLC is normally extracted from bacteria that have been grown for an extended period of time on CDMA. To determine if CLC

was enhanced/upregulated under any other growth conditions, WbtIG191V_P10 was grown in broth and on agar of CDM, BHI, and MH. The CLC and HMS band/smear was highly expressed upon growth of bacteria on CDMA and BHIA, but not MHA (gel electrophoretic data not shown), supporting prior analysis of *F. tularensis* surface antigens following growth on these media (Zarrella et al., 2011; Holland et al., 2017). When *F. tularensis* was grown for 10 days in CDMB or BHIB, CLC was not detected in the broth medium. However, when WbtIG191V_P10 was grown for 10 days in MHB, material similar to the HMS CLC band/smear appeared to be released into the broth supernatant following centrifugation of the cells (Supplementary Figure 1). When the bacterial cells grown in MHB for 10-days were extracted for CLC using urea, only faint evidence of a band in the region of the HMS band appeared with silver staining. Therefore, the production and/or localization of CLC can be influenced by the growth medium, with both CDM and BHI favoring production and cellular retention of CLC.

Composition of the CLC

Analysis of the urea-extracted CLC identified a large percentage of acidic and hydrophobic amino acids (Supplementary Table 2), which is indicative of proteins that will self-aggregate and be highly insoluble in aqueous solutions. Mass spectrometry analysis of in-gel digests did not identify any proteins, and manual inspection of the MS/MS spectra showed no evidence of spectra containing characteristic peptide y and b ions. However, the nLC-MS/MS spectra of in-gel tryptic digests of both 200-kDa and 170-kDa bands showed a 420-Da repeating unit (Figures 4A,B). The spectra showed the chains to be variable in length. MS/MS of a doubly charged ion from the 200-kDa MS spectrum also showed fragment ions separated by 420 Da, indicating a chain of seven units of 420 Da. The speculative addition and loss of a 17-Da ammonia residue was also observed in the MS and MS/MS spectra (Figures 4B,C). Target MS/MS of an ion at m/z 421, showed fragment ions at m/z 210, 192, 178, 146, and 123. A loss of 17 Da, likely corresponding to ammonia was observed (Figure 4D). These data suggest that the high molecular weight bands are comprised of chains potentially glycan in nature, with a subunit of 420-Da. There was also evidence of a 420-Da unit in the band larger than 250-kDa, but the longer chains were not observed.

Further analysis of the urea-extracted CLC that was concentrated through a 100-kDa Centriprep filter unit was performed. Following concentration, some CLC material fell out of solution and was recovered by centrifugation at 3000 rpm as the insoluble fraction. The carbohydrate content of the insoluble and soluble fractions of the CLC were similar, yielding just over 10% carbohydrate/mg of CLC (soluble, 112 μg carb/mg CLC; insoluble, 138 μg carb/mg CLC). The predominant sugars identified were glucose, galactose, and mannose, as previously reported (Bandara et al., 2011). However, many samples also contained hydroxylated fatty acids and 3-deox-D-manno-2-octulosonic acid (KDO), indicating the presence of outer membrane LPS (data not shown).

Based on mass spectrometry analysis a total of 68 proteins were identified in the LVS urea-extracted CLC, which were

TABLE 3 | Proteins identified in the soluble fraction of CLC from LVS.

Identifier	Proteins previously reported, novel, or among 20 most common (T20):	Description	Protein score	Mass (Da)	Peptide_exp
Soluble					
FTL_1191	T20, P,C	Chaperone protein dnaK (heat shock protein family 70 protein)	222	69,140	0.00046
FTL_0009	E, S	Outer membrane protein	122	19,465	8.40E-05
FTL_1474	N	Transcriptional elongation factor	73	17,692	1.50E-07
FTL_0225	S	Protein chain elongation factor EF-Ts	68	30,940	6.70E-07
FTL_1592	N	Acetyl-CoA carboxylase, biotin carboxyl carrier protein subunit	60	16,394	3.40E-06
FTL_1907	N	Cell division protein	52	39,720	2.10E-05
FTL_1461	P, C	Purine nucleoside phosphorylase	50	26,848	2.50E-05
FTL_0113	S	Intracellular growth locus, subunit c	47	22,119	6.60E-05
FTL_0014	N	Single-strand binding protein	43	17,512	0.00014
FTL_1494	P, E, S	hypothetical protein	41	18,147	0.00033
FTL_1714	T20, P, S, C	Chaperone protein, groEL (Yaron S, <i>E. coli</i> 2000)	39	57,367	0.00026
FTL_0227	N	Ribosome recycling factor	38	20,540	0.00043

T20, Top 20 proteins found in *F. novicida* OMV (Pierson et al., 2011); P, Proteins previously associated with pathogenesis (Pechous et al., 2008); E, Proteins found in exponential phase OMV/T (McCaig et al., 2013); S, Proteins found in early stationary phase OMV/T (McCaig et al., 2013); C, Proteins found in culture filtrate (Konecna et al., 2010); N, Novel to this work.

5 other prominent OMV proteins (FTL_1146, FTL_1743, and FTL_1592, FTL_1442, FTL_1772) (Pierson et al., 2011). Overall, of the 12 proteins identified in the CLC soluble fraction, 8 were also present in OMV (FTL_1474, FTL_1907, FTL_0014, and FTL_0227), and of the 56 proteins identified in the CLC insoluble fraction, 38 were also present in OMV (Table 3). Nine proteins identified in the CLC and in OMV/T (noted in Tables 3, 4) have previously been associated with pathogenesis (Pechous et al., 2008). The soluble portion of the CLC, which contains the HMS smear (data not shown), was also digested and analyzed by nLC-MS/MS. No proteins were identified. However, manual inspection of the data showed an MS/MS spectrum dominated by a 1157-Da glycan-related ion. This moiety likely corresponded to the previously reported hexasaccharide modification of proteins in *F. tularensis* (Figure 5) (Thomas et al., 2011). The doubly charged form of this oxonium ion was also observed at m/z 579, from which carbohydrate related fragment ions were observed as neutral losses of monosaccharides in the sequence 203-223-203-162-162-203 or 203-162-162-203-223-203 (total glycan mass is 1156 Da). These masses plausibly represent monosaccharides such as HexNAc (203) and hexose (162). The loss of 223 does not correspond to a known monosaccharide and is indicated as X in Figure 5. A doubly charged ion at m/z 911 likely corresponds to the unmodified form of the peptide, giving a predicted peptide mass of 1,823, corresponding to a total glycopeptide mass of 2,977, less the 1,156 Da hexasaccharide moiety. The intensity of the carbohydrate ions obscured peptide related γ and b type fragment ions, making sequencing of the peptide challenging. A short peptide sequence was determined from putative type γ ions in the high m/z region of the spectrum, corresponding to the amino acid sequence (Q/K)(I/L)VSE, which was not sufficient to identify the complete peptide.

Comparison of OMV/T With CLC

Because the CLC appeared to share many proteins with those previously identified in OMV, further comparison of OMV/T to CLC was carried out. There were distinct differences in the shape and type of OMV/T observed when OMV/T were extracted from cells grown in broth or on agar. When OMV/T were extracted from either mutants WbtI_{G191V}_P10 or WbtI_{G191V} Δ 1423-22_P10 grown in broth medium, the vesicles were predominately circular in appearance (Figures 6A–D, respectively), including LVS_P10 and LVS Δ 1423-22_P10 (not shown), although some tubes were present, particularly from WbtI_{G191V} Δ 1423-22_P10. When the OMV/T_A were extracted from bacteria grown on solid agar, the particles from LVS_P10 had an approximately even distribution of circular vesicles and tubes (Figures 7A,B), while the OMV/T_A from LVS Δ 1423-22_P10 (CLC glycosylation-deficient mutant) were predominantly tubular in shape (Figures 7C,D). When both O-antigen deficient mutants WbtI_{G191V}_P10 (Figures 7E,F) and its CLC glycosylation-deficient double mutant WbtI_{G191V} Δ 1423-22_P10 (Figures 7G,H) were grown on solid agar, only circular OMV_A, but not tubes, were seen. Therefore, when the bacteria were grown in broth the vesicles were predominately circular, regardless of whether the CLC was glycosylated or O-antigen was present. However, growth of the bacteria on agar promoted OMT_A formation by LVS_P10 (Figures 7A,B), but the CLC glycosylation mutant of the parent formed even more tube-shaped vesicles (Figures 7C,D). Mutants grown on agar that lacked O-antigen produced predominately circular vesicles (Figures 7E,F), but if the mutant lacked both O-antigen and CLC glycosylation there was overall less OMV/T_A produced (Figures 7G,H). Therefore, the presence of O-antigen and/or CLC glycosylation also influenced the shape and amount of OMV/T_A produced.

TABLE 4 | Proteins identified in the insoluble fraction of CLC from LVS.

Identifier	Proteins previously reported, novel, or among 20 most common (T20):	Description	Protein_score	Mass (Da)	Peptide_expect
Insoluble					
FTL_1751	E, S	Elongation factor Tu (EF-Tu)	969	43,363	2.00E-05
FTL_1714	T20, P, C	Chaperone protein, groEL	802	57,367	2.90E-06
FTL_1191	P, C	Chaperone protein dnaK (heat shock protein family 70 protein)	394	69,140	1.10E-07
FTL_1907	E, S	Cell division protein	381	39,720	3.10E-08
FTL_0113	N, P	Intracellular growth locus, subunit C	368	22,119	1.30E-05
FTL_0234	E, S	Elongation factor G (EF-G)	250	77,681	2.00E-05
FTL_0112	P, S	Intracellular growth locus, subunit B	226	57,881	2.50E-13
FTL_1795	E, S	ATP synthase beta chain	224	49,834	3.40E-07
FTL_0891	N	Trigger factor (TF) protein (peptidyl-prolyl cis/trans isomerase)	190	49540	1.70E-10
FTL_0094	P, E, S	ClpB protein	178	95,987	1.00E-07
FTL_0225	N	Protein chain elongation factor EF-Ts	177	30,940	1.40E-06
FTL_1146	T20, C	Glyceraldehyde-3-phosphate dehydrogenase	161	35,391	0.0003
FTL_0267	P, S	Chaperone Hsp90, heat shock protein HtpG	151	72,326	1.00E-07
FTL_1791	N, C	Superoxide dismutase	148	21,926	9.30E-07
FTL_1912	E, S	30S ribosomal protein S1	145	61,631	0.00017
FTL_1461	N, C	Purine nucleoside phosphorylase	132	26,848	0.0007
FTL_0436	N	Isoleucyl-tRNA synthetase	127	106,904	6.00E-13
FTL_0572	E, S	Hypothetical protein	113	51,945	1.10E-11
FTL_0260	S	30S ribosomal protein S4	107	23,222	8.10E-11
FTL_0597	N	NAD dependent epimerase	105	36,427	1.80E-07
FTL_0895	N, C	Histone-like protein HU form B	105	9,468	1.20E-10
FTL_1190	N	Chaperone protein grpE (heat shock protein family 70 cofactor)	102	22,022	2.50E-06
FTL_0166	S	Universal stress protein	102	30,202	2.10E-06
FTL_1746	S	50S ribosomal protein L10	101	18,720	1.90E-10
FTL_0949	N	Ribose-phosphate pyrophosphokinase	97	34,887	2.70E-06
FTL_0987	S	Lactate dehydrogenase	94	34,055	5.90E-07
FTL_0588	N	Isocitrate dehydrogenase	93	82,332	7.70E-05
FTL_0834	S	Rhodanese-like family protein	88	27,847	4.90E-09
FTL_1553	P, S	Succinyl-CoA synthetase beta chain	87	41,516	1.30E-06
FTL_1527	S	Enolase (2-phosphoglycerate dehydratase)	85	49,480	4.30E-09
FTL_1701	P	GlpX protein	83	34,820	1.90E-08
FTL_0923	S	Glutaredoxin 2	83	25,135	1.30E-08
FTL_1224	N	Thioredoxin 1	78	12,194	6.60E-08
FTL_1743	T20,P,S,E	DNA-directed RNA polymerase, β subunit	77	157,289	6.20E-08
FTL_1591	S	Acetyl-CoA carboxylase, biotin carboxylase subunit	76	50,019	7.50E-08
FTL_0097	N	Hypothetical protein	76	13,785	6.10E-05
FTL_1780	N, C	Triosephosphate isomerase	76	27,638	5.80E-08
FTL_0232	S	30S ribosomal protein S12	69	13,806	9.70E-07
FTL_1350	N	Glycyl-tRNA synthetase beta subunit	66	77,973	4.80E-07
FTL_1140	N	Malonyl coA-acyl carrier protein transacylase	62	33,480	2.30E-06
FTL_0233	S	30S ribosomal protein S7	61	17,796	2.60E-06
FTL_1138	N	acyl carrier protein	61	10,653	2.30E-06
FTL_1240	S	Phospho-2-dehydro-3-deoxyheptonate aldolase	60	40,853	1.80E-06

(Continued)

TABLE 4 | Continued

Identifier	Proteins previously reported, novel, or among 20 most common (T20):	Description	Protein_score	Mass (Da)	Peptide_expect
FTL_1747	S	50S ribosomal protein L1	57	24,626	4.70E-06
FTL_1275	N	Dethiobiotin synthetase	55	24,487	9.70E-06
FTL_1592	T20	Acetyl-CoA carboxylase, biotin carboxyl carrier protein subunit	53	16,394	1.60E-05
FTL_1334	N	L-serine dehydratase 1	52	49,977	2.70E-05
FTL_0387	N	Aspartate transaminase	52	44,355	2.60E-05
FTL_1442	T20, S	Enoyl-[acyl-carrier-protein] reductase (NADH)	49	27,757	4.10E-05
FTL_0916	E, S	Ketol-acid reductoisomerase	46	37,855	7.30E-05
FTL_1797	N	ATP synthase alpha chain	46	55,502	5.20E-05
FTL_0311	S	Dihydrolipoamide dehydrogenase	44	50,495	9.90E-05
FTL_1772	T20, S	Aconitate hydratase	44	102,639	0.00028
FTL_1784	E	2-oxoglutarate dehydrogenase E1 component	39	105,613	0.00029
FTL_0739	N	Glucose inhibited division protein A	36	69,721	0.00053
FTL_1022	N	Coproporphyrinogen III oxidase	36	35,854	0.00053

T20, Top 20 proteins found in *F. novicida* OMV (Pierson et al., 2011); P, Proteins previously associated with pathogenesis (Pechous et al., 2008); E, Proteins found in exponential phase OMV/T (McCaig et al., 2013); S, Proteins found in early stationary phase OMV/T (McCaig et al., 2013); C, Proteins found in culture filtrate (Cervenka et al., 2010). N = Novel to this work.

There was a significant size difference ($p < 0.0055$) of both the OMV_A and the OMT_A from LVS_P10 and LVSΔ1423-22_P10 compared to WbtI_{G191V}_P10 and WbtI_{G191V}Δ1423-22_P10 following growth of all strains on CDMA (Figure 7). The average size of the OMV_A extracted from LVS_P10 (Figures 7A,B) ranged from 20 to 200 nm in diameter, while the average OMV_A extracted from WbtI_{G191V} was 10–40 nm in diameter (Figures 7E,F). The average size of the OMT_A extracted from plate-grown LVS_P10 was much larger than the vesicular form, with an average length of 500 nm, which was equivalent to the length of OMT occasionally seen in the WbtI_{G191V} strain. Therefore, the presence of O-antigen and growth on agar also promoted formation of larger OMV/T_A.

Interestingly, protein concentrations of purified OMV/T increased in the CLC-deficient mutants in both strains when the bacteria were grown in broth, but when the bacteria were grown on agar (as done for CLC-extraction), the protein content decreased in the WbtI_{G191V}Δ1423-22_P10 mutant compared to WbtI_{G191V} (Table 2).

When WbtI_{G191V}_P10 was examined by negative stain TEM the typical electron dense material was present surrounding the bacterial cell (Figure 8A), which appeared similar to low power TEM of OMV_A (Figure 7). However, following higher magnification of the urea-extracted CLC, individual circular vesicles were observed (Figure 8B) that were similar in ultrastructural appearance to OMV.

Protective Efficacy of CLC

The CLC was conjugated to either KLH or flagellin because the material was initially believed to be predominately polysaccharide. Conjugation of CLC to either protein was confirmed by SDS-PAGE, in which the conjugated CLC

appeared as a band/smear above 200-kDa (Figure 9B). The CLC-conjugate provided some protection against lethal LVS challenge of BALB/c mice. However, protection of mice challenged by the IN route was less effective than by the ID route. Mice immunized with the flagellin-CLC conjugate, followed by IN challenge, were the least protected (33% of mice survived) (Figure 9A). Protection was improved in mice immunized with CLC conjugated to KLH (66%) after IN challenge (one-sided $p = 0.03$). Only mice challenged by the ID route were completely protected (100%) against mortality when immunized with either KLH—or flagellin-conjugates (one-sided $p = 0.001$). Results of the mice immunized with KLH-CLC are superimposed with results of mice immunized with flagellin-CLC (Figure 9A). However, the LVS challenge dose was severe at $5 \times \text{LD}_{50}$, which was ~ 5000 CFU for IN and $\sim 2 \times 10^7$ CFU for ID challenge.

Sera were collected from immunized BALB/c mice prior to immunization, post-immunization, and post-challenge for cytokine analysis. There was no significant difference in the response to cytokines IL-2, IL-4, IL-5, GM-CSF, or TNF- α by BALB/c mice immunized by either route with CLC-protein conjugates after challenge with LVS compared to mice immunized with PBS or pre-immunization (data not shown except for TNF- α). However, IL-12 levels were significantly increased in both KLH-CLC and flagellin-CLC immunized mice, compared to mice immunized with PBS and prior to immunization (Figures 9C,D) ($p < 0.001$). Mice that made a significantly greater response to IL-10, IL-12, or IFN- γ after challenge ($p < 0.001$) were better protected than control mice in which that response did not occur. Of interest, the IL-10, IL-12, and IFN- γ response of mice immunized with flagellin-CLC was not significantly increased following IN challenge, and these mice were not significantly protected (Figures 9A,E).

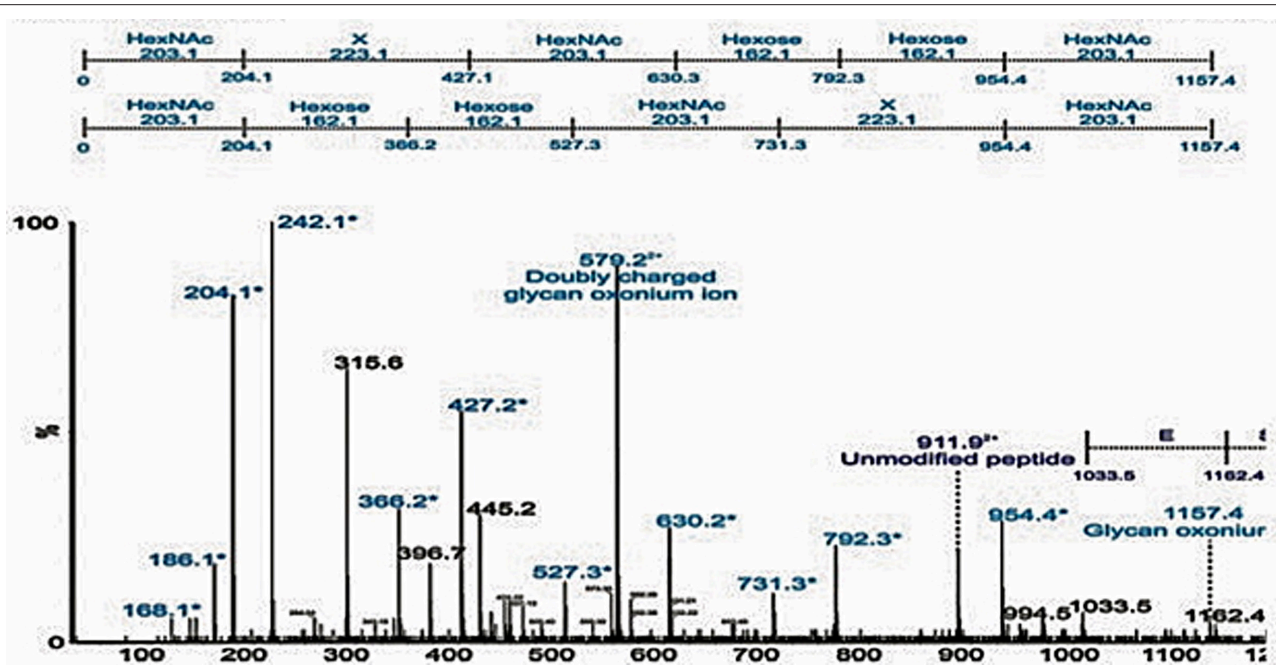


FIGURE 5 | Detection of glycopeptides in the soluble capsule extract. nLC-MS/MS spectrum of a triply protonated glycopeptide at m/z 993.7, enriched from soluble fraction using ion-pairing normal phase liquid chromatography (IP-NPLC). Relative ion abundance is shown on the y axis, and m/z is shown on the x axis. The spectrum is dominated in the low- m/z region by a glycan related ions, indicated in light blue and with an asterisk. In particular, a glycan-related oxonium ion was visible at m/z 1157, corresponding to a previously reported hexasaccharide modification of proteins in *F. tularensis*.

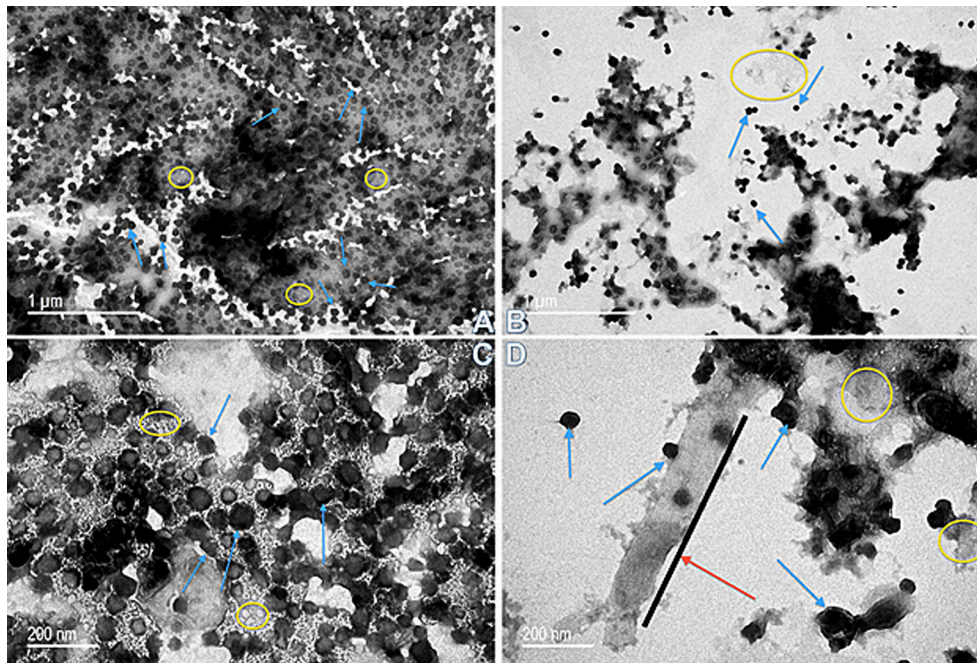


FIGURE 6 | Transmission electron microscopy of OMV/T purified from *F. tularensis* strains grown in broth. (A) OMV/T from Wbtl_{G191V}_P10 (50 k magnification); (B) Wbtl_{G191V}Δ1423-22_P10 (50 k magnification); (C) Wbtl_{G191V}_P10 (120 k magnification); (D) Wbtl_{G191V}Δ1423-22_P10 (120 k magnification). Spherical OMV were found in both the O-antigen mutant (Wbtl_{G191V}_P10) and, to a lesser extent, the CLC glycoase-deficient double mutant (Wbtl_{G191V}Δ1423-22_P10). At the higher magnification formation of OMT were visible by Wbtl_{G191V}Δ1423-22_P10 in addition to OMV, which was not commonly seen in the O-antigen mutant. Red arrows/black lines, OMT; blue arrows, OMV; yellow circles, non-specified material between OMV/T.

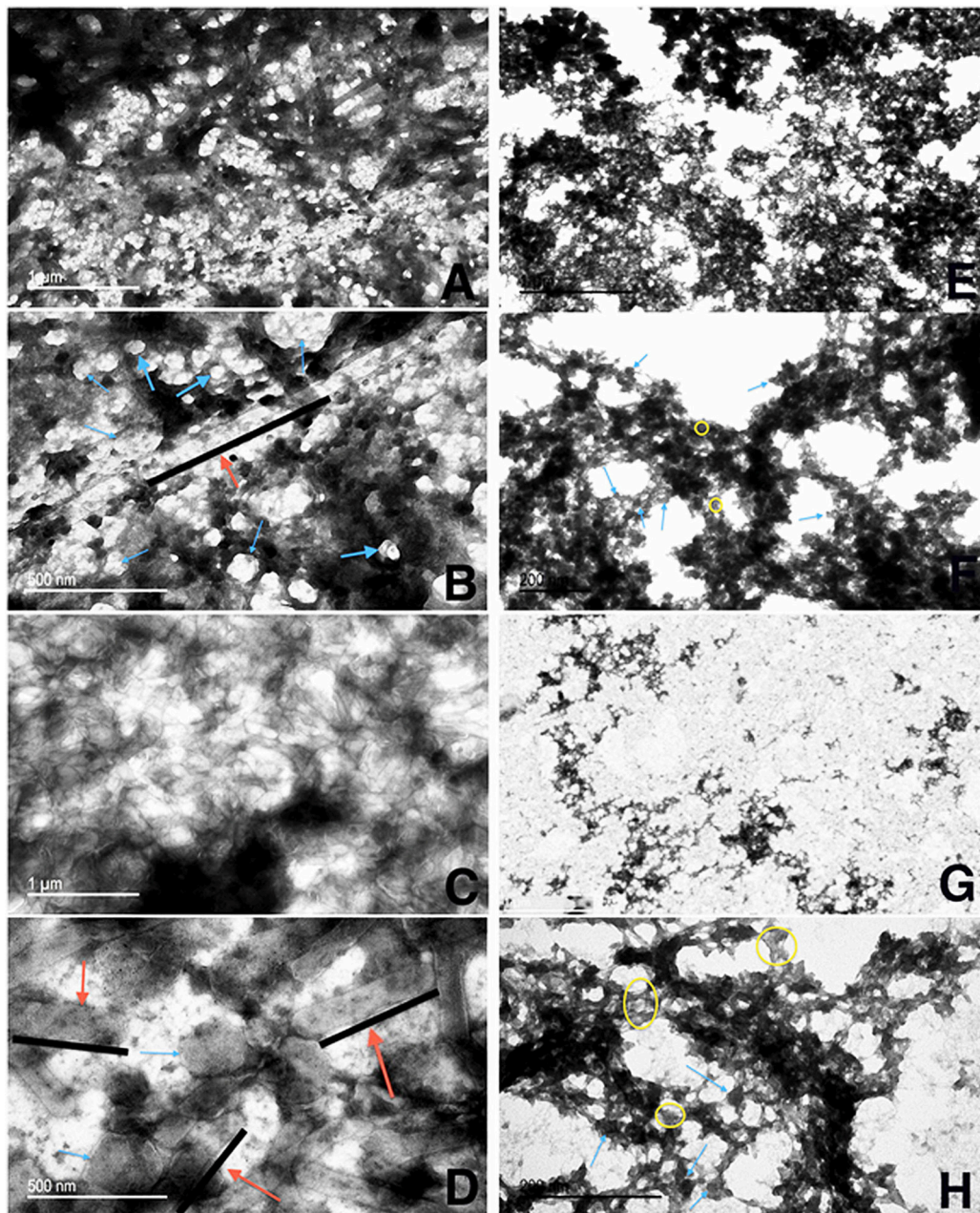


FIGURE 7 | Transmission electron microscopy of OMV/T_A purified from *F. tularensis* strains grown on agar. OMV/T_A were isolated from LVS_P10, LVSΔ1423-22_P10, Wbtl_{G191V}_P10, or Wbtl_{G191V}Δ1423-22_P10 grown on CDM agar following a modified protocol (Gamazo et al., 1989; Avila-Calderón et al., 2012). **(A,B)** LVS_P10 (50 k magnification and 120 k magnification, respectively); **(C,D)** LVSΔ1423-22_P10 (50 k magnification and 120 k magnification, respectively); **(E,F)** Wbtl_{G191V}_P10 (50 k magnification and 120 k magnification); **(G,H)** Wbtl_{G191V}Δ1423-22_P10 (50 k magnification and 120 k magnification, respectively). Red arrows, OMT_A (along black lines); blue arrows, OMV_A; yellow circles, non-specified material between the OMV/T_A.

Mice immunized with non-conjugated CLC in Freund's or MPLA adjuvants (as described in Methods) and challenged IN with 100 or 150 CFU of SCHU S4 were not significantly protected (**Table 5**). There was a time delay to morbidity and mortality by 4-6 days in a few mice immunized 3 months apart compared to control mice, but no significant difference in survival.

The Type A Capsule-Like Complex

Colonies of *F. tularensis* type A strains SCHU S4 and clinical isolate TI0902 were more mucoid and iridescent when subcultured in CDMB and grown at 32 or 37°C on CDMA than when these strains were not subcultured. These results were similar to those obtained when LVS (Bandara et al., 2011) and *F. novicida* (Freudenberger Catanzaro et al., 2017) were similarly

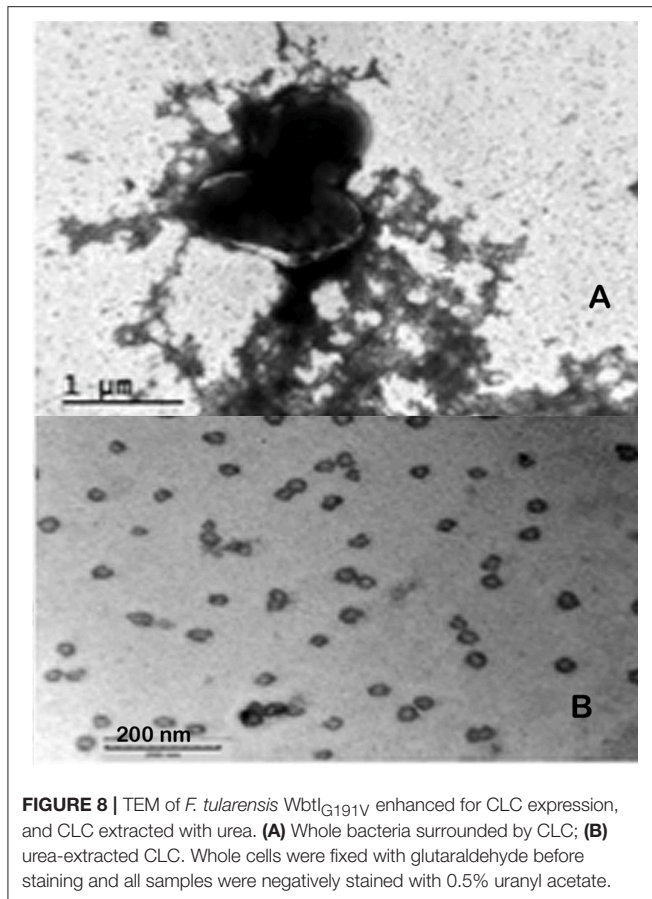


FIGURE 8 | TEM of *F. tularensis* WbtI_{G191V} enhanced for CLC expression, and CLC extracted with urea. **(A)** Whole bacteria surrounded by CLC; **(B)** urea-extracted CLC. Whole cells were fixed with glutaraldehyde before staining and all samples were negatively stained with 0.5% uranyl acetate.

subcultured in CDMB and CDMA to enhance CLC expression. However, initial efforts to visualize the CLC on the surface of type A strains using negative stain TEM techniques were less successful than with LVS or *F. novicida*. We concluded this was due to the extended period of time the bacteria needed to remain in fixative and at 4°C to verify that no viable cells remained in the culture and were safe to remove from the BSL-3 laboratory. With slight modifications we were able to visualize the darker staining electron dense material surrounding both SCHU S4_P10 (not shown) and TI0902_P10 cells (**Figure 10B**) that was greatly diminished in the parent that was not subcultured in CDMB and CDMA (**Figure 10A**). The CLC from the type A strains appeared very similar to that observed around LVS (**Figure 8A**). Following electrophoresis and StainsAll/silver stain of the CLC a HMS smear, in addition to some lower molecular size bands, were prominent in phenol-extracted CLC from strains SCHU S4 and TI0902 subcultured in CDMB and CDMA (**Figure 11B**). The urea-extracted type A CLC presented a less diffuse HMS band/smear by SDS-PAGE, similar to LVS CLC, and also included the additional lower molecular size bands. In addition, the type A CLC antigens were immunologically similar to the LVS CLC (phenol and urea extractions; **Figure 1A**) and reacted with hyper-immune rabbit serum to LVS CLC (**Figure 11A**). Qualitatively, the electrophoretic profile of the CLC extracts were similar whether the cells were grown on CDMA at 32 or 37°C. However,

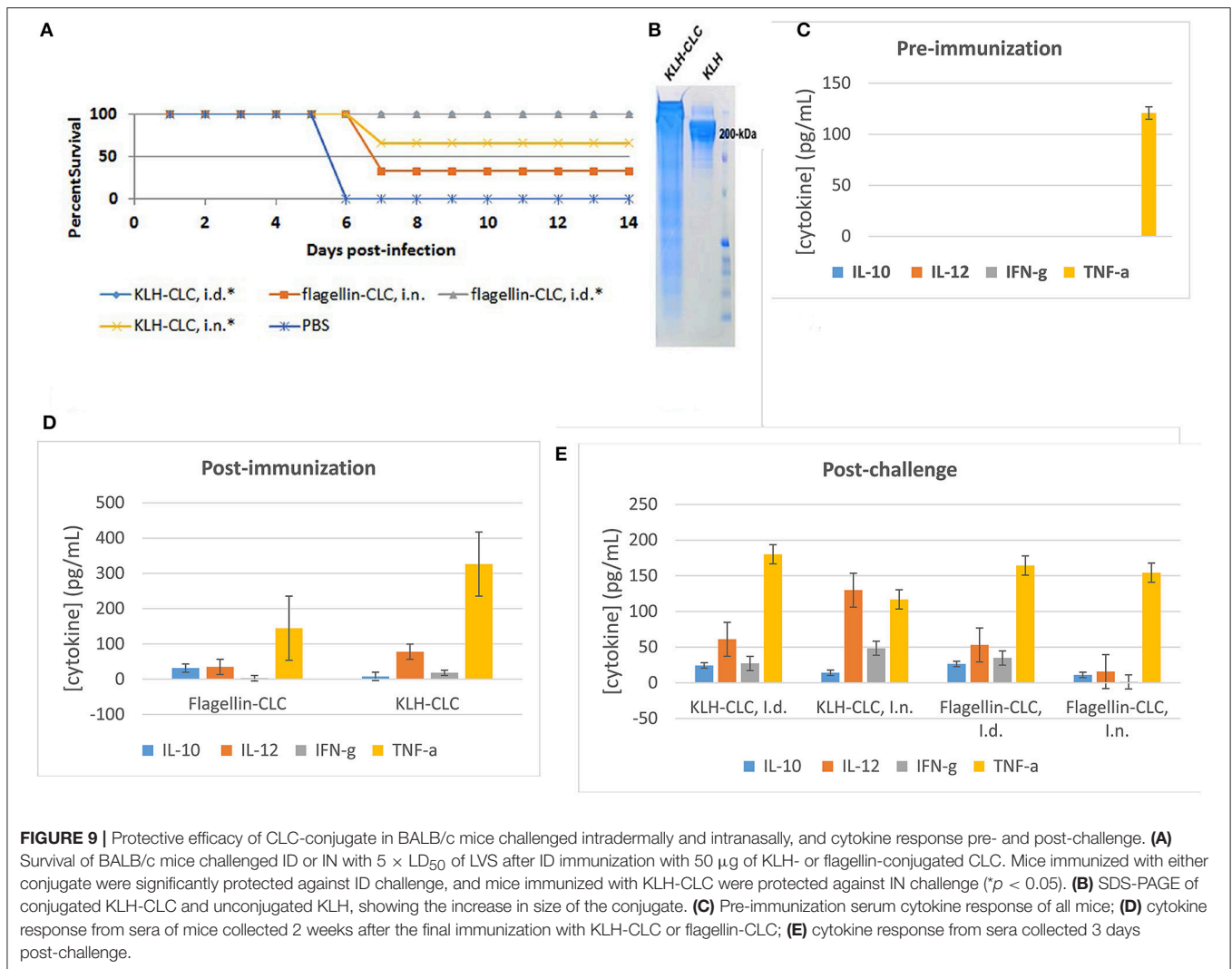
quantitatively there appeared to be more proteins, particularly the larger molecular size proteins, in the CLC extracted from cells grown at 32°C. Carbohydrate analysis of purified CLC from *F. tularensis* SCHU S4 yielded similar results to the LVS CLC: there was about 5–10% carbohydrate, which consisted of glucose, galactose, and mannose (data not shown).

Mutagenesis of FTT_0798-99 resulted in a significant ($p < 0.05$) loss of carbohydrate on SCHU S4Δ0798-99 (16.39 mg carbohydrate/g bacterial weight compared to 28.57 mg carbohydrate/g bacterial weight for SCHU S4). However, all mice inoculated IN with 100 CFU of SCHU S4 or SCHU S4Δ0798-99 died or needed to be euthanized in <6 days (data not shown). Furthermore, mice challenged with the mutant did not live longer than mice challenged with the parent. Therefore, inactivation of the CLC glycosylation locus had no significant effect on the virulence of SCHU S4, as mutagenesis of the corresponding genes FTL_1423 and FTL_1422 did in LVS (Bandara et al., 2011).

DISCUSSION

The CLC of *F. tularensis* remains a novel, elusive antigen, shown to be necessary for virulence in LVS and *F. novicida* (Bandara et al., 2011; Freudenberger Catanzaro et al., 2017). However, isolation and analysis of the CLC has been challenging due to self-aggregation and insolubility of the CLC during purification. By changing the chaotropic extraction buffer to 1M urea a marked increase in solubility and ease of manipulation was obtained, but confirmation that extraction of the CLC with 1M urea resulted in the same antigen extracted with 0.5% phenol (Bandara et al., 2011) was necessary. SDS-PAGE electrophoretic profiles of the CLC extracted by phenol or urea and stained with StainsAll/Silver showed that these antigens were similar, though the banding pattern of the HMS was more diffuse following phenol compared to urea extraction. The more diffuse banding was likely the result of protein denaturation by the phenol. Western blot electrophoretic profiles using immune sera generated to WbtI_{G191V}_P10 CLC extracted with either phenol or urea and types A and B CLC antigens extracted by either reagent were very similar. However, the larger molecular size bands apparently did not transfer efficiently out of the gel. Nonetheless, the CLC antigens from types A and type B strains were similar, regardless of the extraction method.

The individual components of the HMS material have been difficult to resolve. If the HMS CLC is an aggregate of glycoproteins or a mixture of (glyco)proteins and polysaccharide, individual components should be resolved using a size exclusion system based on electrophoretic mobility. The GelFree 8100 cartridge is capable of fractionating components up to 500-kDa. However, the largest CLC band visualized by silver stain was just under 150-kDa after fractionation, and no bands or diffuse HMS material was observed with StainsAll/Silver. Thus, the HMS CLC observed was likely the result of aggregates of CLC (glyco)-proteins, which were separated into individual components during GelFree fractionation. The 45-kDa band that appeared in the highest molecular size GelFree fractions (>90-kDa) was also the only component reactive after hyper-immune



serum to CLC after adsorption with CLC-deficient mutant cells. Therefore, the 45-kDa protein could be involved in the aggregation of the CLC. Furthermore, the 45-kDa protein has been recognized as an immuno-reactive glycoprotein in mouse sera following immunization with OMP's (Huntley et al., 2008). Although identification of this band was unsuccessful following concentration of the fractions and mass spectrometry (likely due to glycosylation) this protein was similar in size to outer membrane protein FopA, which is also glycosylated, highly immunogenic, and potentially protective (Hickey et al., 2011).

To further increase the solubility and characterize the CLC, extraction with Triton X-114 was tested, which was previously used to purify the *F. tularensis* O-antigen capsular polysaccharide (Apicella et al., 2010). However, Triton-X114-insoluble material could be further extracted into soluble components with sarkosyl. The total CLC protein solubilized with Triton X-114 fractionated relatively equally between the TxS-A phase and TxS-D phase. However, the HMS material from the O-antigen mutant partitioned primarily into the TxS-A phase, as determined by SDS-PAGE. These results suggested that the CLC

consisted of both hydrophilic and hydrophobic components, such as glycoproteins (that may partition into the hydrophilic TxS-A phase), and integral membrane proteins, OMP, LPS, and lipoproteins (that may partition into the TxS-D phase), as is well-documented (Bordier, 1981; Tandon et al., 1989). Partitioning of the HMS into TxS-A is also consistent with a larger amount of hydrophilic carbohydrate in this material. Most of the CLC extracted from glucose-deficient mutant WbtI_{G191V}Δ1423-22_P10 was not solubilized in Triton X-114. However, the TxI-SS fraction of the double mutant did demonstrate a diffuse, darker staining HMS material by SDS-PAGE and silver staining, indicating the mutant CLC contained different proteins or glucose-deficient proteins than the parent CLC. We have previously reported that WbtI_{G191V}Δ1423-22_P10 (Bandara et al., 2011), and an *F. novicida* mutant lacking genes from the same glycosylation locus (Freudenberger Catanzaro et al., 2017), are deficient in, but continue to produce, a lesser amount of carbohydrate-deficient CLC. The difference in protein content between the O-antigen deficient parent and the glucose-deficient CLC mutant was evident in the ratio of

TABLE 5 | Protective efficacy of *F. tularensis* type A CLC against type A SCHU S4 challenge of mice.

Number of mice	Immunogen	Challenge dose	Time to euthanasia post-challenge (PC)
4	Water ^a	100 CFU	4/4 at 4 days PC
8	Crude CLC in FA ^{a,b}	100 CFU	4/4 at 4 days PC
8	HMS CLC in FA ^{a,c}	100 CFU	4/4 at 4 days PC
5	HMS CLC in MPLA ^{a,d}	100 CFU	4/4 at 4 days PC
5	HMS CLC in FA ^{e,b}	150 CFU	3/5 at 1 day PC; 2/5 at 5 days PC
5	HMS CLC in MPLA ^{e,d}	150 CFU	4/5 at 4 days PC; 1/5 at 7 days PC

^aMice were immunized subcutaneously with 50 µg of CLC twice 6 weeks apart.

^bFA, Freund's Adjuvant, first immunization was with Complete Adjuvant and the second immunization was with Incomplete Adjuvant. Crude CLC was derived from WbtI_{G191V_P10} cells that had been extracted with 1 M urea and the bacterial cells removed by centrifugation.

^cHMS CLC, semi-purified CLC including the high molecular size surface antigen was concentrated.

^dMPLA, Monophosphoryl lipid A adjuvant.

^eMice were immunized twice 3 months apart.

TxI-SS:TxI-SI fractions. The CLC from WbtI_{G191V_P10} had a protein ratio of 15:1 (TxI-SS:TxI-SI) vs. 2:1 for CLC from the double, glucose-deficient mutant. In support of our previous report (Freudenberger Catanzaro et al., 2017), mutagenesis of the glycosylation locus alone does not appear to affect protein content, but does affect association with the cell surface, which does affect recovery of the CLC.

We have previously reported that the CLC could be extracted from *F. tularensis* cells subcultured in CDMB and then grown for several days on CDMA at 32°C, but could not be recovered from the broth medium of shaken cultures (Bandara et al., 2011). We now confirm those results, and that the CLC can also be recovered from *F. tularensis* cells grown on BHIA, and at 37°C, but not from MHA. However, *F. tularensis* WbtI_{G191V_P10} shed some HMS material, similar to what was recovered by CLC extraction, when the bacteria were grown in MHB for 10 days. One possibility is that the HMS material shed during growth in MHB is part of the CLC, but remains attached to the cell when grown on CDMA. The MH broth-shed HMS material was also similar to the HMS carbohydrate previously described (Zarella et al., 2011). This HMS carbohydrate is “missing” during bacterial growth in MHB, but is present when the bacteria are grown in BHI, which is proposed to mimic the bacterial environment during host infection. Nonetheless, the growth media CDM and BHI influenced production and retention of the CLC on the cell surface.

A large number of *Francisella* surface proteins are known to be glycosylated, including pili, DsbA, FTH_0069, FopA, Tul4, LemA, and others (Balonova et al., 2010). Many of the CLC proteins were also glycosylated, as evidenced by staining of electrophoretically separated glycoproteins with StainsAll and by chemical analysis. Further evidence of glycosylation was supported by the presence of a 420-Da repeating unit of the HMS material, which is most likely a repeating glycan unit. An amino acid analysis of the CLC indicated the proteins

consisted predominately of acidic or hydrophobic amino acids, which would promote self-aggregation and aqueous insolubility of the CLC. Many of the 56 proteins in the CLC extracted from WbtI_{G191V_P10} were surface proteins and proteins involved in virulence (including some FPI proteins). Sixty-percent of these proteins have also been identified in the OMV of *F. novicida* (McCaig et al., 2013). Proteins identified previously in *Francisella* OMV and OMV/T have numbered in the hundreds (Pierson et al., 2011; McCaig et al., 2013). However, the CLC extract analyzed in this study consisted of substantially fewer proteins, which may be due to the extraction methods used during the purification process. In addition to similarities in protein composition, GC-MS analysis confirmed that while the predominant sugars in the CLC were glucose, galactose, and mannose, LPS components (KDO and lipid A fatty acids) were also in many of the samples analyzed, supporting the presence of outer membrane components. There was also TEM ultrastructural similarity between CLC particles isolated with urea and OMV from *F. novicida* and *F. philomiragia* (Pierson et al., 2011).

The shape and size of OMV/T isolated from *F. tularensis* was also dependent on whether the bacteria were grown in broth or on agar (larger tubes), and whether the LPS O-antigen was present and the CLC glycosylated. O-antigen mutants generally made smaller vesicles, and the CLC glucose-deficient mutants were predominately tubular in shape. However, from bacteria with both O-antigen and CLC carbohydrate absent, much fewer OMV/T were observed. Therefore, glycosylation, which may promote a more hydrophilic surface, may promote more of the circular vesicle shape and more OMV in general.

An effective vaccine for *F. tularensis* is proposed to require both cell-mediated and humoral immunity (Elkins et al., 2007; Eyles et al., 2008; Kirimaneswara et al., 2008; Reed et al., 2014). The *F. tularensis* OMP and OMV/T have been shown to induce a pro-inflammatory response by the host (Huntley et al., 2008; McCaig et al., 2013), which also occurs following immunization with the CLC. Immunization of mice with the CLC produced an increase in pro-inflammatory cytokines, particularly IL-12 and IFN-γ. In the BALB/c mouse model, CLC conjugated to an immunogenic protein was protective against lethal LVS challenge. One hundred percent survival was obtained using either KLH or flagellin as the conjugative protein when mice were challenged ID with LVS. Significant protection against *F. novicida* IN challenge has also been established using OMV, but the protection was incomplete and did not lead to 100% survival of OMV-vaccinated mice (Pierson et al., 2011). However, a vaccine for tularemia needs to protect against the aerosol route of infection by the more virulent type A strains. BALB/c mice immunized by the ID route with type A CLC and Freund's Complete adjuvant were not protected against IN challenge with a high lethal dose of *F. tularensis* SCHU S4. The challenge dose of SCHU S4 given to the mice (500 CFU) in the present study was ~10 times higher than the challenge dose given by Huntley et al. who reported a 50% survival rate following immunization of mice with a mixture of OMPs (Huntley et al., 2008). Differences in the preparation of OMPs compared to CLC and differences in challenge dose could account for the differences in protection

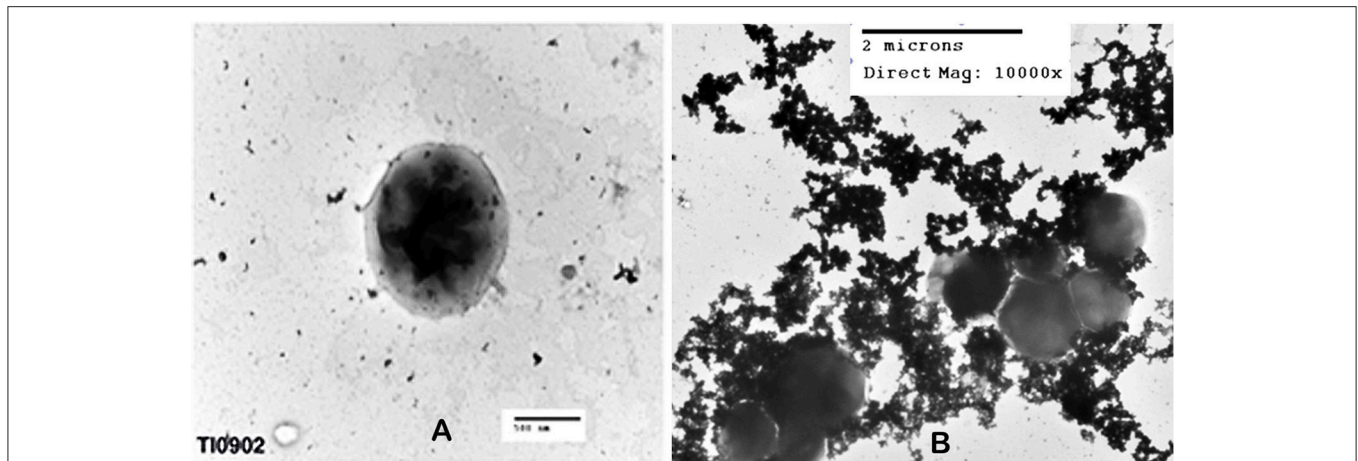


FIGURE 10 | TEM of *F. tularensis* type A clinical isolate strain TI0902. The bacteria were fixed in glutaraldehyde buffer overnight and stained with 0.5% uranyl acetate. **(A)** Strain TI0902 following growth in BHI broth with rapid shaking. **(B)** Strain TI0902 subcultured daily for 10 days in CDM broth followed by growth at 32°C for several days on CDM agar, and demonstrating the CLC. Similar CLC material was observed surrounding CDM subcultured type A strain SCHU S4 (not shown). A representative image of the CLC-enhanced O-antigen mutant of strain LVS is shown in **Figure 8**.

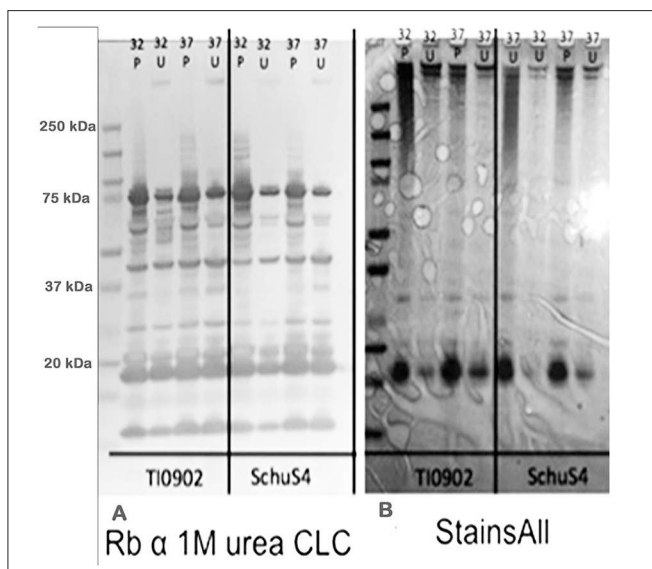


FIGURE 11 | Western blot and electrophoretic profiles of CLC extracted from type A strains TI0902 and SCHU S4 by phenol or urea at 32 or 37°C. **(A)** Western blot of rabbit serum to urea-extracted LVS CLC with CLC extracted from type A strains TI0902 and SCHU S4. **(B)** StainsAll stain of CLC extracts from strains TI0902 or SCHU S4. P, CLC extracted with phenol; U, CLC extracted with urea. The type A strains were subcultured daily in CDMB for 10 consecutive days and then grown on CDMA at 32°C for an additional 5 days.

between studies. Immunization of mice with CLC derived from type A strain SCHU S4 did not protect mice against high dose IN challenge with SCHU S4. Therefore, CLC alone would not be adequate for a type A tularemia vaccine, but could have potential as a component of a subunit vaccine, or may protect against a lower challenge dose of virulent type A *F. tularensis*.

Deletion of the LVS glycosylation genes FTL_1423 and FTL_1422 significantly decreased the CLC material ($p = 0.01$)

and attenuated the strain in mice (Bandara et al., 2011). Thomas et al. reported that deletion of the FTL_1423 homolog FTT_0798 resulted in the loss of an O-linked 1156-Da glycan moiety on type A *F. tularensis* DsbA, but virulence was not affected (Thomas et al., 2011). Our work supported this observation in that deletion of FTT_0798 and FTT_0799 also did not adequately attenuate type A strain SCHU S4, at least not against high dose respiratory challenge, although there was a similar loss of cell carbohydrate content.

CONCLUSION

We present evidence that the CLC appears similar to OMV/T in appearance and composition, and therefore over-expression of OMV/T in *F. tularensis* type A and B strains may contribute to the presence of CLC. This evidence is based on: (i) the CLC appears similar to OMV/T by TEM, and both CLC and OMV/T are differentially expressed depending on O-antigen and CLC (glycosyl transferase) deficiencies, and (ii) ~60% of the proteins identified in the CLC matched previously identified OMV/T proteins in *F. novicida*, and (iii) the CLC contains some components that are consistent with outer membrane content. Alternatively, it is also possible that CLC preparations are contaminated with OMV/T, or that OMV/T preparations also contain CLC (e.g., the non-specific material highlighted by yellow circles in **Figures 6, 7**). Contaminating proteins or other extracellular material have been noted to be present in OMV preparations from Gram-negative bacteria derived by ultracentrifugation (Bauman and Kuehn, 2006; Chutkan et al., 2013). Whether OMV/T are integral components of the *F. tularensis* CLC, or the CLC is a contaminant of OMV/T preparations warrants further investigation. A glucose-deficient CLC type A mutant was not attenuated in mice and the CLC was not protective against high-dose type A IN challenge of mice. However, differential expression of CLC, OMV,

and OMT appears to be connected, and more insight into their interrelationship could help elucidate novel virulence mechanisms of *F. tularensis*.

ETHICS STATEMENT

This study was carried out in accordance with the recommendations of Virginia Tech's Animal Welfare Assurance policy, as described in A-3208-01 (expr. 7-31-2021) and USDA-APHIS-AC Registration Certificate # 52-R-0012 (expr. 10-01-2018) by the Virginia Tech Institutional Animal Care and Use Committee. The protocol was approved by the Virginia Tech Institutional Animal Care and Use Committee.

AUTHOR CONTRIBUTIONS

ST and KF performed the amino acid sequencing and glycoprotein identification. Mutants used were constructed by AB and NM. All other procedures were performed by AC unless otherwise noted in text. Experimental design was conceived by AC and TI. AC and TI wrote and edited the majority of the manuscript. AB, NM, KF, and ST contributed to writing sections of the manuscript.

REFERENCES

- Apicella, M. A., Post, D. M., Fowler, A. C., Jones, B. D., Rasmussen, J. A., Hunt, J. R., et al. (2010). Identification, characterization and immunogenicity of an O-antigen capsular polysaccharide of *Francisella tularensis*. *PLoS ONE* 5:e11060. doi: 10.1371/journal.pone.0011060
- Avila-Calderón, E. D., López-Merino, A., Jain, N., Peralta, H., López-Villegas, E. O., Sriranganathan, N., et al. (2012). Characterization of outer membrane vesicles from *Brucella melitensis* and protection induced in mice. *Clin. Dev. Immunol.* 2012:352493. doi: 10.1155/2012/352493
- Balanova, L., Hernychova, L., Mann, B. F., Link, M., Bilkova, Z., Novotny, M. V., et al. (2010). Multimethodological approach to identification of glycoproteins from the proteome of *Francisella tularensis*, an intracellular microorganism. *J. Proteome Res.* 9, 1995–2005. doi: 10.1021/pr9011602
- Bandara, A. B., Champion, A. E., Wang, X., Berg, G., Apicella, M. A., McLendon, M., et al. (2011). Isolation and mutagenesis of a capsule-like complex (CLC) from *Francisella tularensis*, and contribution of the CLC to *F. tularensis* virulence in mice. *PLoS ONE* 6:e19003. doi: 10.1371/journal.pone.0019003
- Bauman, S. J., and Kuehn, M. J. (2006). Purification of outer membrane vesicles from *Pseudomonas aeruginosa* and their activation of an IL-8 response. *Microbes Infect.* 8, 2400–2408. doi: 10.1016/j.micinf.2006.05.001
- Bordier, C. (1981). Phase separation of integral membrane proteins in Triton X-114 solution. *J. Biol. Chem.* 256, 1604–1607.
- Brooks, G. F., and Buchanan, T. M. (1970). Tularemia in the United States: epidemiologic aspects in the 1960s and follow-up of the outbreak of tularemia in Vermont. *J. Infect. Dis.* 121, 357–359. doi: 10.1093/infdis/121.3.357
- Cervenka, R., Zelinková, H., Konečná, M., and Komárek, J. (2010). Electrochemical modification of a graphite platform for a solid sampling electrothermal atomic absorption spectrometry of mercury. *Anal. Sci.* 26, 989–993. doi: 10.2116/analsci.26.989
- Chen, W., Shen, H., Webb, A., KuoLee, R., and Conlan, J. W. (2003). Tularemia in BALB/c and C57BL/6 mice vaccinated with *Francisella tularensis* LVS and challenged intradermally, or by aerosol with virulent isolates of the pathogen: protection varies depending on pathogen virulence, route of exposure, and

ACKNOWLEDGMENTS

We would like to thank Kathy Lowe for her technical expertise and guidance in electron microscopy, TRACCS staff for their excellent animal care at the Virginia-Maryland College of Veterinary Medicine, Cheryl Ryder and Kelly Freudenberger-Catanzaro for technical assistance, and Dr. Parastoo Azadi and colleagues at the University of Georgia Complex Carbohydrate Research Center for glycoside analysis. This work was supported, in part, by grant U54-AI57168 from the National Institute of Allergy and Infectious Diseases/National Institutes of Health to the mid-Atlantic Regional Center for Excellence, the Virginia-Maryland College of Veterinary Medicine, the Tyler J. and Frances F. Young endowment, and the Department of Energy-funded (DF-FG02-93ER-20097) Center for Plant and Microbial Complex Carbohydrates.

SUPPLEMENTARY MATERIAL

The Supplementary Material for this article can be found online at: <https://www.frontiersin.org/articles/10.3389/fcimb.2018.00182/full#supplementary-material>

- host genetic background. *Vaccine* 21, 3690–3700. doi: 10.1016/S0264-410X(03)00386-4
- Cherwonogrodzky, J. W., Knodel, M. H., and Spence, M. R. (1994). Increased encapsulation and virulence of *Francisella tularensis* live vaccine strain (LVS) by subculturing on synthetic medium. *Vaccine* 12, 773–775. doi: 10.1016/0264-410X(94)90284-4
- Chutkan, H., Macdonald, L., Manning, A., and Kuehn, M. J. (2013). Quantitative and qualitative preparations of bacterial outer membrane vesicles. *Methods Mol. Biol.* 966, 259–272. doi: 10.1007/978-1-62703-245-2_16
- Dennis, D. T., Inglesby, T. V., Henderson, D. A., Bartlett, J. G., Ascher, M. S., Eitzen, E., et al. (2001). Tularemia as a biological weapon: medical and public health management. *JAMA* 285, 2763–2773. doi: 10.1001/jama.285.21.2763
- Elkins, K. L., Cowley, S. C., and Bosio, C. M. (2007). Innate and adaptive immunity to *Francisella*. *Ann. NY. Acad. Sci.* 1105, 284–324. doi: 10.1196/annals.1409.014
- Eyles, J. E., Hartley, M. G., Laws, T. R., Oyston, P. C., Griffin, K. F., and Titball, R. W. (2008). Protection afforded against aerosol challenge by systemic immunisation with inactivated *Francisella tularensis* live vaccine strain (LVS). *Microb. Pathog.* 44, 164–168. doi: 10.1016/j.micpath.2007.08.009
- Freudenberger Catanzaro, K. C., Champion, A. E., Mohapatra, N., Cecere, T., and Inzana, T. J. (2017). Glycosylation of a capsule-like complex (CLC) by *Francisella novicida* is required for virulence and partial protective immunity in mice. *Front. Microbiol.* 8:935. doi: 10.3389/fmicb.2017.00935
- Fulton, K. M., Mendoza-Barberá, E., Twine, S. M., Tomás, J. M., and Merino, S. (2015). Polar glycosylated and lateral non-glycosylated flagella from *Aeromonas hydrophila* strain AH-1 (serotype O11). *Int. J. Mol. Sci.* 16, 28255–28269. doi: 10.3390/ijms161226097
- Gamazo, C., Winter, A. J., Moriyón, I., Riezu-Boj, J. I., Blasco, J. M., and Diaz, R. (1989). Comparative analyses of proteins extracted by hot saline or released spontaneously into outer membrane blebs from field strains of *Brucella ovis* and *Brucella melitensis*. *Infect. Immun.* 57, 1419–1426.
- Golovliov, I., Baranov, V., Krocova, Z., Kovarova, H., and Sjöstedt, A. (2003). An attenuated strain of the facultative intracellular bacterium *Francisella tularensis* can escape the phagosome of monocytic cells. *Infect. Immun.* 71, 5940–5950. doi: 10.1128/IAI.71.10.5940-5950.2003

- Hartley, M. G., Green, M., Choules, G., Rogers, D., Rees, D. G., Newstead, S., et al. (2004). Protection afforded by heat shock protein 60 from *Francisella tularensis* is due to copurified lipopolysaccharide. *Infect. Immun.* 72, 4109–4113. doi: 10.1128/IAI.72.7.4109-4113.2004
- Hickey, A. J., Hazlett, K. R., Kirimanjeshwara, G. S., and Metzger, D. W. (2011). Identification of *Francisella tularensis* outer membrane protein A (FopA) as a protective antigen for tularemia. *Vaccine* 29, 6941–6947. doi: 10.1016/j.vaccine.2011.07.075
- Holland, K. M., Rosa, S. J., Kristjansdottir, K., Wolfgeher, D., Franz, B. J., Zarrella, T. M., et al. (2017). Differential growth of *Francisella tularensis*, which alters expression of virulence factors, dominant antigens, and surface-carbohydrate synthases, governs the apparent virulence of Ft SchuS4 to immunized animals. *Front. Microbiol.* 8:1158. doi: 10.3389/fmicb.2017.01158
- Huntley, J. F., Conley, P. G., Rasko, D. A., Hagman, K. E., Apicella, M. A., and Norgard, M. V. (2008). Native outer membrane proteins protect mice against pulmonary challenge with virulent type A *Francisella tularensis*. *Infect. Immun.* 76, 3664–3671. doi: 10.1128/IAI.00374-08
- Inzana, T. J., Glindemann, G. E., Snider, G., Gardner, S., Crofton, L., Byrne, B., et al. (2004). Characterization of a wildtype strain of *Francisella tularensis* isolated from a cat. *J. Vet. Diagn. Invest.* 16, 374–381. doi: 10.1177/104063870401600502
- Jones, B. D., Faron, M., Rasmussen, J. A., and Fletcher, J. R. (2014). Uncovering the components of the *Francisella tularensis* virulence stealth strategy. *Front. Cell. Infect. Microbiol.* 4:32. doi: 10.3389/fcimb.2014.00032
- Kantardjiev, T., Ivanov, I., Velinov, T., Padeshki, P., Popov, B., Nenova, R., et al. (2006). Tularemia outbreak, Bulgaria, 1997–2005. *Emerg. Infect. Dis.* 12, 678–680. doi: 10.3201/eid1204.050709
- Kataoka, H., Matsumura, S., Yamamoto, S., and Makita, M. (2001). “Capillary gas chromatographic analysis of protein and nonprotein amino acids in biological samples,” in *Methods in Molecular Biology, Amino Acid Analysis Protocols*, eds C. Cooper, N. Packer, and K. Williams (Totowa, NJ: Humana Press), 101–122.
- Keim, P., Johansson, A., and Wagner, D. M. (2007). Molecular epidemiology, evolution, and ecology of *Francisella*. *Ann. N. Y. Acad. Sci.* 1105, 30–66. doi: 10.1196/annals.1409.011
- Kirimanjeshwara, G. S., Olmos, S., Bakshi, C. S., and Metzger, D. W. (2008). Humoral and cell-mediated immunity to the intracellular pathogen *Francisella tularensis*. *Immunol. Rev.* 225, 244–255. doi: 10.1111/j.1600-065X.2008.00689.x
- Konecna, K., Hernychova, L., Reichelova, M., Lenco, J., Klimentova, J., Stulik, J., et al. (2010). Comparative proteomic profiling of culture filtrate proteins of less and highly virulent *Francisella tularensis* strains. *Proteomics* 10, 4501–4511. doi: 10.1002/pmic.201000248
- Larsson, P., Oyston, P. C., Chain, P., Chu, M. C., Duffield, M., Fuxelius, H. H., et al. (2005). The complete genome sequence of *Francisella tularensis*, the causative agent of tularemia. *Nat. Genet.* 37, 153–159. doi: 10.1038/ng1499
- Li, J., Ryder, C., Mandal, M., Ahmed, F., Azadi, P., Snyder, D. S., et al. (2007). Attenuation and protective efficacy of an O-antigen-deficient mutant of *Francisella tularensis* LVS. *Microbiology* 153, 3141–3153. doi: 10.1099/mic.0.2007/006460-0
- Lindemann, S. R., Peng, K., Long, M. E., Hunt, J. R., Apicella, M. A., Monack, D. M., et al. (2011). *Francisella tularensis* Schu S4 O-antigen and capsule biosynthesis gene mutants induce early cell death in human macrophages. *Infect. Immun.* 79, 581–594. doi: 10.1128/IAI.00863-10
- McCaig, W. D., Koller, A., and Thanassi, D. G. (2013). Production of outer membrane vesicles and outer membrane tubes by *Francisella novicida*. *J. Bacteriol.* 195, 1120–1132. doi: 10.1128/JB.02007-12
- McCrum, F. R. (1961). Aerosol infection of man with *Pasteurella tularensis*. *Bacteriol. Rev.* 25, 262–267.
- McRae, S., Pagliari, F. A., Mohapatra, N. P., Gener, A., Mahmoud, A. S., Gunn, J. S., et al. (2010). Inhibition of AcpA phosphatase activity with ascorbate attenuates *Francisella tularensis* intramacrophage survival. *J. Biol. Chem.* 285, 5171–5177. doi: 10.1074/jbc.M109.039511
- Meibom, K. L., Barel, M., and Charbit, A. (2009). Loops and networks in control of *Francisella tularensis* virulence. *Future Microbiol.* 4, 713–729. doi: 10.2217/fmb.09.37
- Merkle, R. K., and Poppe, I. (1994). Carbohydrate composition analysis of glycoconjugates by gas-liquid chromatography/mass spectrometry. *Meth. Enzymol.* 230, 1–15. doi: 10.1016/0076-6879(94)30003-8
- Modise, T., Ryder, C., Mane, S. P., Bandara, A. B., Jensen, R. V., and Inzana, T. J. (2012). Genomic comparison between a virulent type A1 strain of *Francisella tularensis* and its attenuated O-antigen mutant. *J. Bacteriol.* 194, 2775–2776. doi: 10.1128/JB.00152-12
- Mohapatra, N. P., Soni, S., Rajaram, M. V., Strandberg, K. L., and Gunn, J. S. (2013). Type A *Francisella tularensis* acid phosphatases contribute to pathogenesis. *PLoS ONE* 8:e56834. doi: 10.1371/journal.pone.0056834
- Nano, F. E., Zhang, N., Cowley, S. C., Klose, K. E., Cheung, K. K., Roberts, M. J., et al. (2004). A *Francisella tularensis* pathogenicity island required for intramacrophage growth. *J. Bacteriol.* 186, 6430–6436. doi: 10.1128/JB.186.19.6430-6436.2004
- Olsufjev, A. (1966). “Tularemia,” in *Human Diseases With Natural Foci*, ed Y. N. Pavlovsky (Moscow: Foreign Languages Publishing House), 219–281.
- Oyston, P. C. (2008). *Francisella tularensis*: unravelling the secrets of an intracellular pathogen. *J. Med. Microbiol.* 57, 921–930. doi: 10.1099/jmm.0.2008/000653-0
- Ozanic, M., Marecic, V., Lindgren, M., Sjöstedt, A., and Santic, M. (2016). Phenotypic characterization of the *Francisella tularensis* ΔdpC and ΔiglG mutants. *Microbes Infect.* 18, 768–776. doi: 10.1016/j.micinf.2016.07.006
- Ozols, J. (1990). “Amino acid analysis,” in *Guide to Protein Purification, Methods Enzymol.*, ed M. P. Deutscher (San Diego, CA: Academic Press), 587–601.
- Pechou, R. D., McCarthy, T. R., Mohapatra, N. P., Soni, S., Penoske, R. M., Salzman, N. H., et al. (2008). A *Francisella tularensis* Schu S4 purine auxotroph is highly attenuated in mice but offers limited protection against homologous intranasal challenge. *PLoS ONE* 3:e2487. doi: 10.1371/journal.pone.0002487
- Pierson, T., Matrakas, D., Taylor, Y. U., Manyam, G., Morozov, V. N., Zhou, W., et al. (2011). Proteomic characterization and functional analysis of outer membrane vesicles of *Francisella novicida* suggests possible role in virulence and use as a vaccine. *J. Proteome Res.* 10, 954–967. doi: 10.1021/pr1009756
- Qin, A., Scott, D. W., Thompson, J. A., and Mann, B. J. (2009). Identification of an essential *Francisella tularensis* subsp. tularensis virulence factor. *Infect. Immun.* 77, 152–161. doi: 10.1128/IAI.01113-08
- Raynaud, C., Meibom, K. L., Lety, M. A., Dubail, I., Candela, T., Frapy, E., et al. (2007). Role of the wbt locus of *Francisella tularensis* in lipopolysaccharide O-antigen biogenesis and pathogenicity. *Infect. Immun.* 75, 536–541. doi: 10.1128/IAI.01429-06
- Reed, D. S., Smith, L. P., Cole, K. S., Santiago, A. E., Mann, B. J., and Barry, E. M. (2014). Live attenuated mutants of *Francisella tularensis* protect rabbits against aerosol challenge with a virulent type A strain. *Infect. Immun.* 82, 2098–2105. doi: 10.1128/IAI.01498-14
- Saslaw, S., Eigelsbach, H. T., Prior, J. A., Wilson, H. E., and Carhart, S. (1961). Tularemia vaccine study. II. Respiratory challenge. *Arch. Intern. Med.* 107, 702–714. doi: 10.1001/archinte.1961.03620050068007
- Schneerson, R., Barrera, O., Sutton, A., and Robbins, J. B. (1980). Preparation, characterization, and immunogenicity of *Haemophilus influenzae* type b polysaccharide-protein conjugates. *J. Exp. Med.* 152, 361–376. doi: 10.1084/jem.152.2.361
- Scott, T. A., and Melvin, E. H. (1953). Determination of dextran with anthrone. *Anal. Chem.* 25, 1656–1661. doi: 10.1021/ac60083a023
- Sebastian, S., Dillon, S. T., Lynch, J. G., Blalock, L. T., Balon, E., Lee, K. T., et al. (2007). A defined O-antigen polysaccharide mutant of *Francisella tularensis* live vaccine strain has attenuated virulence while retaining its protective capacity. *Infect. Immun.* 75, 2591–2602. doi: 10.1128/IAI.01789-06
- Sjöstedt, A. (2007). Tularemia: history, epidemiology, pathogen physiology, and clinical manifestations. *Ann. N. Y. Acad. Sci.* 1105, 1–29. doi: 10.1196/annals.1409.009
- Sunagar, R., Kumar, S., Franz, B. J., and Gosselin, E. J. (2016). Tularemia vaccine development: paralysis or progress? *Vaccine (Auckl)* 6, 9–23. doi: 10.2147/VDT.S85545
- Tandon, N. N., Lipsky, R. H., Burgess, W. H., and Jamieson, G. A. (1989). Isolation and characterization of platelet glycoprotein IV (CD36). *J. Biol. Chem.* 264, 7570–7575.
- Thomas, R. M., Titball, R. W., Oyston, P. C., Griffin, K., Waters, E., Hitchen, P. G., et al. (2007). The immunologically distinct O antigens from *Francisella tularensis* subspecies tularensis and *Francisella novicida* are both virulence determinants and protective antigens. *Infect. Immun.* 75, 371–378. doi: 10.1128/IAI.01241-06

- Thomas, R. M., Twine, S. M., Fulton, K. M., Tessier, L., Kilmury, S. L., Ding, W., et al. (2011). Glycosylation of DsbA in *Francisella tularensis* subsp. *tularensis*. *J. Bacteriol.* 193, 5498–5509. doi: 10.1128/JB.00438-11
- Ward, C. K., and Inzana, T. J. (1994). Resistance of *Actinobacillus pleuropneumoniae* to bactericidal antibody and complement is mediated by capsular polysaccharide and blocking antibody specific for lipopolysaccharide. *J. Immunol.* 153, 2110–2121.
- Zarella, T. M., Singh, A., Bitsaktsis, C., Rahman, T., Sahay, B., Feustel, P. J., et al. (2011). Host-adaptation of *Francisella tularensis* alters the bacterium's surface-carbohydrates to hinder effectors of innate and adaptive immunity. *PLoS ONE* 6:e22335. doi: 10.1371/journal.pone.0022335

Conflict of Interest Statement: The authors declare that the research was conducted in the absence of any commercial or financial relationships that could be construed as a potential conflict of interest.

Copyright © 2018 Champion, Bandara, Mohapatra, Fulton, Twine and Inzana. This is an open-access article distributed under the terms of the Creative Commons Attribution License (CC BY). The use, distribution or reproduction in other forums is permitted, provided the original author(s) and the copyright owner are credited and that the original publication in this journal is cited, in accordance with accepted academic practice. No use, distribution or reproduction is permitted which does not comply with these terms.



Molecular Survey of Tularemia and Plague in Small Mammals From Iran

Ehsan Mostafavi^{1,2*}, Ahmad Ghasemi^{1,2,3}, Mahdi Rohani^{1,4}, Leila Molaeipoor^{2,5,6},
Saber Esmaeili^{1,2,3}, Zeinolabedin Mohammadi^{7,8}, Ahmad Mahmoudi^{1,2,7,8},
Mansour Aliabadian^{7,8} and Anders Johansson⁹

¹ National Reference Laboratory for Plague, Tularemia and Q Fever, Research Centre for Emerging and Reemerging Infectious Diseases, Pasteur Institute of Iran, Kabudar Ahang, Iran, ² Department of Epidemiology and Biostatistics, Research Centre for Emerging and Reemerging Infectious Diseases, Pasteur Institute of Iran, Tehran, Iran, ³ Department of Bacteriology, Faculty of Medical Sciences, Tarbiat Modares University, Tehran, Iran, ⁴ Department of Microbiology, Pasteur Institute of Iran, Tehran, Iran, ⁵ Department of Epidemiology, School of Public Health, Iran University of Medical Sciences, Tehran, Iran, ⁶ Student Research Committee, Faculty of Public Health Branch, Iran University of Medical Sciences, Tehran, Iran, ⁷ Rodentology Research Department, Applied Animal Institute, Ferdowsi University of Mashhad, Mashhad, Iran, ⁸ Department of Biology, Faculty of Science, Ferdowsi University of Mashhad, Mashhad, Iran, ⁹ Department of Clinical Microbiology and the Laboratory for Molecular Infection Medicine Sweden, Umeå University, Umeå, Sweden

Introduction: Plague and tularemia are zoonoses and their causative bacteria are circulating in certain regions of Iran. This study was conducted to investigate potential disease reservoirs amongst small wildlife species in different regions of Iran.

Methods: Rodents, insectivores and hares from 17 different provinces of the country were collected in 2014 and 2015. Samples were taken from the spleens of the animals and Real-time PCR was applied to detect nucleic acid sequences that are specific to *Francisella tularensis* and *Yersinia pestis*, respectively.

Results: Among 140 collected rodents, 25 distinct species were identified out of which five were the most common: *Microtus paradoxus* (21% out of 140 rodents), *Apodemus witherbyi* (12%), *Microtus irani* (11%), *Mus musculus* (11%) and *Microtus socialis* (10%). Seventeen insectivores were collected and identified as *Crocidura suaveolens* (82%) and *C. leucodon* (18%). Fifty-one hares were collected and identified as *Lepus europaeus* (57%), *Lepus tolai* (14%) and *Lepus* sp. (29%). Three out of 140 explored rodents (1.91%) were positive for *F. tularensis*, an *A. witherbyi*, a *Mus musculus domesticus*, and a *Chionomys nivalis* collected from Golestan, Khuzestan and Razavi Khorasan provinces, respectively. Two hares (3.92%) were *F. tularensis*-positive, a *L. europaeus* from Khuzestan and a *Lepus* sp. from the Sistan and Baluchistan province. None of the tested animals were positive for *Y. pestis*.

Conclusion: This is the first report of direct detection of *F. tularensis* in mammals of Iran and the first-time observation of the agent in a snow vole, *C. nivalis* worldwide. The results indicate that tularemia is more widespread in Iran than previously reported including the Northeast and Southwestern parts of the country. Future studies should address genetic characterization of *F. tularensis* positive DNA samples from Iran to achieve molecular subtyping and rule out assay cross-reactivity with near neighbor *Francisella* species.

Keywords: tularemia, plague, hares, rodentia, insectivora

OPEN ACCESS

Edited by:

Daniel E. Voth,
University of Arkansas for Medical
Sciences, United States

Reviewed by:

Andrey P. Anisimov,
State Research Center for Applied
Microbiology and Biotechnology,
Russia
Roger Derek Pechous,
University of Arkansas for Medical
Sciences, United States

*Correspondence:

Ehsan Mostafavi
mostafaviehsan@gmail.com

Received: 06 February 2018

Accepted: 07 June 2018

Published: 10 July 2018

Citation:

Mostafavi E, Ghasemi A, Rohani M,
Molaeipoor L, Esmaeili S,
Mohammadi Z, Mahmoudi A,
Aliabadian M and Johansson A (2018)
Molecular Survey of Tularemia and
Plague in Small Mammals From Iran.
Front. Cell. Infect. Microbiol. 8:215.
doi: 10.3389/fcimb.2018.00215

INTRODUCTION

Emerging and reemerging infectious diseases stand amongst the most challenging problems for public health entities around the world and more than half of them are zoonotic (Parhizgari et al., 2017). Changes in social, economic, environmental, and ecological factors may precipitate the conditions for the reemergence of these infectious diseases (Gupta et al., 2012). Plague and tularemia are two zoonotic diseases that are reported from Iran (Karimi et al., 1981; Esamaeili et al., 2013; Zargar et al., 2015).

Plague is a lethal zoonotic disease that historically has caused pandemics around the world. The causative agent of this disease is the bacterium *Yersinia pestis*. Plague is still endemic in certain regions of Africa, Asia, and North and South America (Dubynskiy and Yeszhanov, 2016). Since 1990, most of human plague infections are reported from African countries (Williamson, 2016). Wild rodents and fleas on their bodies are regarded as the main reservoirs of *Y. pestis* in nature (Bitam et al., 2010); although other wild animals such as mammalian carnivores and insectivores can also play a role as the reservoir of the infection (Poland and Dennis, 1999). Infection of rodents lead to severe damages in liver and spleen, and demise in a period less than 3 days (Bevins et al., 2012). Rabbits and hares can also be infected with *Y. pestis* and may like rodents transmit the infection to humans by direct contact or indirectly via infected flea bites (Fratini et al., 2017). From 1943 to 1965, nine plague outbreaks were reported amongst humans in the western areas of Iran. In these outbreaks, rodents and hares were regarded as the main reservoirs (Shahraki et al., 2016). The last report of plague among rodents in Iran was in 1978 in the Eastern Azerbaijan province, northwest of Iran (Karimi, 1980). The studies on plague in wildlife in Iran were discontinued for a while but were restarted in 2011 and 2012 (Mostafavi and Keypour, 2017) when antibodies against *Y. pestis* were found in rodents and dogs of northwest Iran (Esamaeili et al., 2013). Over recent years, several plague outbreaks have been reported from Iran's neighboring countries such as Afghanistan, Saudi Arabia and Jordan (Saeed et al., 2005; Leslie et al., 2011).

Tularemia is caused by the bacterium *Francisella tularensis* and a vast range of rodents, hares, insectivores, ticks, flies and mosquitoes have been implicated as potential disease reservoirs (Goethert and Telford, 2009; Ulu-Kilic et al., 2013; Zargar et al., 2015). The disease is typically rapidly progressing in small mammals resulting in necrosis distributed in multiple organs including the spleen and death usually follows within a few days, alternatively, a chronic disease type with granulomas in the liver have been described (Maurin and Gyuranecz, 2016). There is incomplete knowledge of the worldwide tularemia burden among humans but generally, it is assumed to be a disease of the Northern hemisphere only. Between 2000 and 2012, 250 to 2500 human cases were reported from countries of Europe and from Turkey (Hestvik et al., 2015; Sanyaolu et al., 2016). Human mortality is generally low but disease and its symptoms including fever and fatigue may be long-lasting (Erdem et al., 2014). Outbreaks in proximity to rivers in Russia, Europe, and in Turkey points toward an important role of water in the survival

of the bacterium and that aquatic rodents may serve as disease reservoirs (Sjöstedt, 2007; Kaysser et al., 2008; Clark et al., 2012). Turkey, one of Iran's neighboring countries, is accounted as an endemic region for this disease (Sahin et al., 2007). Humans can be infected via direct contact with infected animals or via bites of infected arthropods, intake of contaminated water or food, or via inhalation of *F. tularensis*-contaminated aerosols. There are several different clinical forms of disease in humans depending on the infectious route of the bacterium, all of which includes swelling of lymph nodes and may progress to septic disease (Barker and Klose, 2007). The first report of possible tularemia in Iran goes back to 1973 when antibodies against *F. tularensis* were found in domestic livestock and one hedgehog in the northwest and east of Iran, respectively (Arata et al., 1973). The first and thus far only report of a human case of tularemia was from the Marivan district, Kurdistan province of west Iran, in 1980 (Karimi et al., 1981). Studies that are more recent have shown a relatively high prevalence of *F. tularensis*-specific antibodies in the blood of humans living in the west, southeast and southwest parts of Iran. The results of these studies suggest that tularemia may be underdiagnosed in Iran and that enhanced disease surveillance would be valuable (Esmaeili et al., 2014a,b; Khoshdel et al., 2014; Zargar et al., 2015). In 2013, *F. tularensis*-specific antibodies were found in rodents in the southeast and west of Iran indicating that small mammals may be involved in disease transmission (Pourhossein et al., 2015; Mostafavi et al., 2017).

This study was conducted to evaluate the infection of small mammals including rodents, insectivores and hares with *Y. pestis* and *F. tularensis* in order to gain better information regarding the status of these agents in the wildlife of Iran.

MATERIALS AND METHODS

In this cross-sectional study, small mammals were captured alive in different provinces (central, northern, southern, eastern and western) of Iran in 2014 and 2015. The captured animals were sprayed with a pesticide in order to destruct the ectoparasites on their bodies; they were then dispatched to predetermined stations and euthanized. The captured small mammals were identified according to standard identification keys (Corbet, 1978; Kryštufek et al., 2005). Splenic samples were collected for molecular studies and preserved in microtubes containing 70% alcohol before being sent to the diagnostic laboratory.

DNA extraction from tissue samples was completed using the QIAamp DNA Mini Kit. In order to trace and identify *F. tularensis* and *Y. pestis* in tissue samples, the extracted DNA was subjected to pathogen-specific Real-time PCR assays using a Rotor-Gene 6600 (Corbett Life Science). The gene targets for *Y. pestis* were the chromosomal *yihN* gene and the plasmid genes *cafI* and *pla* (Table 1). The same genes cloned into the plasmid pUC57 were used as positive control (provided by the Pasteur Institute of Iran). For *Francisella* spp. we used the *ISFtu2* gene for a first screening step and the *fopA* gene for confirmation of the presence of *F. tularensis* as a second step. The DNA of *F. tularensis* subsp *holarctica* NCTC 10857 was used as a positive

control. The DNA amplification was done in a volume of 25 μ l for 40 cycles after an initial denaturation at 95°C for 10 min. The cycling for *Y. pestis* was 95°C for 15 s, 58°C for 30 s, and 72°C for 30 s whereas for *F. tularensis* it was 95°C for 15 s, 58°C for 60 s, and 72°C for 60 s. As an internal control, the β -actin gene (Qiagen company) was used (Emanuel et al., 2003; Versage et al., 2003; Stewart et al., 2008; Bushon et al., 2010).

All procedures performed in this study involving capturing and euthanizing of the animals were in accordance with international ethical standards. The institutional animal and human ethical committee of the Pasteur institute of Iran approved the project. Gloves, mask, face shield and gown were worn by personnel handling animals in the field and by laboratory personnel handling animal specimens. Personnel specifically trained in handling pathogenic agents performed the laboratory work. Procedures involving potentially infectious material were performed within a class II plus biological safety cabinet.

RESULTS

Altogether, 208 specimens from 140 rodents, 17 insectivores and 51 hares were collected from 17 different provinces (Figure 1, Table 2). The rodents were from 11 provinces including Northern Khorasan, Razavi Khorasan, Golestan, Fars, Zanjan, Chaharmahal and Bakhtiari, Semnan, Sistan and Baluchistan, Khuzestan, Kerman and Kermanshah. Of the 25 studied rodent species, *Microtus paradoxus*, *Apodemus witherbyi*, *Microtus irani*, *Mus musculus*, and *Microtus socialis* were most common with a frequency of 30 (21.4%), 17 (12.1%), 16 (11.4%), 15 (10.7%), and 14 (10.0%), respectively. The insectivores were identified as 14 (82.4%) *Crocidura suaveolens* and 3 (17.6%) *Crocidura leucodon*. *C. suaveolens* was collected from different parts of the country (Golestan, North Khorasan, Zanjan, Chaharmahal and Bakhtiari, while *C. leucodon* was collected from a restricted area in northern Iran (Semnan and North Khorasan). The captured hares were 29 (56.9%) *Lepus europaeus*, 7 (13.7%) *Lepus tolai* and 29 (29.4%) other *Lepus* sp. *L. europaeus* was collected in Zanjan, Khuzestan, Ardebil, Eastern Azerbaijan, Western Azerbaijan and Qom whereas the *Lepus* sp. were from Sistan and Baluchistan, Southern Khorasan, Kerman and Hormozgan. *L. tolai* was collected from the Golestan province (Table 2).

Out of all wild-caught animals, three rodents and two hares were positive for *F. tularensis*. The rodents were one each of *Apodemus uralensis* (Toskestan, Golestan province), *Mus musculus domesticus* (Izeh, Khuzestan), and *Chionomys nivalis* (Zoshk village, Mashhad, Razavi Khorasan province). The hares were a *L. europaeus* from Khuzestan and a *Lepus* sp. from the Sistan and Baluchistan province. There was no detection of *Y. pestis* in any of the animals (Table 2).

DISCUSSION

This study is the first report of direct detection of *F. tularensis* in rodents and hares in Iran and to the best of our knowledge, the first report of infection in the rodent species *C. nivalis* worldwide.

Our study also expands the known geographic distribution of *F. tularensis* in Iran. In contrast, *Y. pestis* was not detected in any of the wild-caught animals examined.

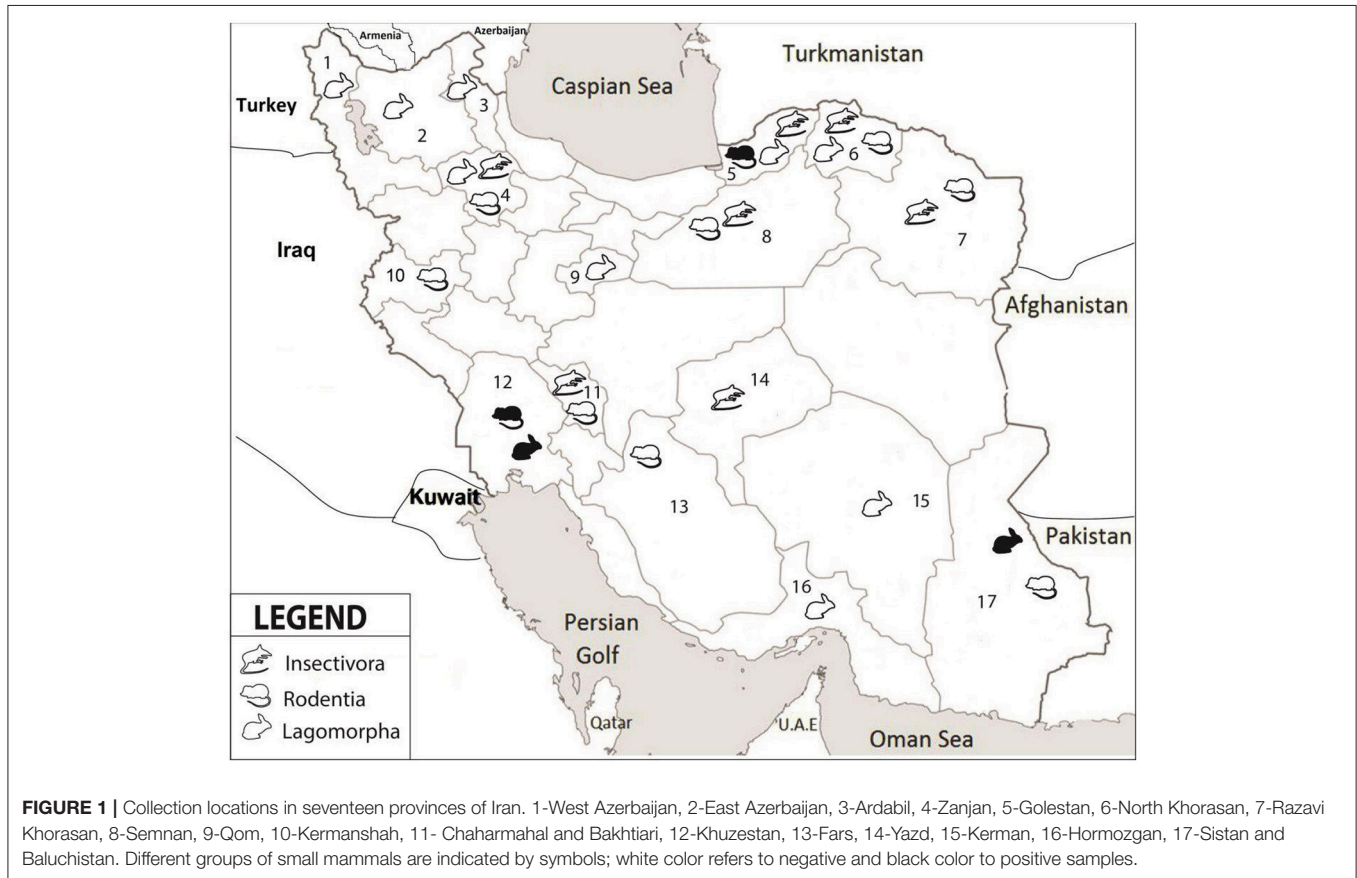
The *F. tularensis* positive samples from animals in Northeast and Southwestern parts of Iran suggests that tularemia is widely distributed in Iran. An early study performed 1969 to 1970 using sampling with serology of >4,600 small mammals and 200 cattle and sheep showed that tularemia existed in the northwest and at one location at the very east of the country (Arata et al., 1973). Over the years, additional serology findings have verified that tularemia exists also in other parts of Iran. Recent studies of rodents in the southeast and west of Iran showed the presence of antibodies against *F. tularensis* (Pourhossein et al., 2015; Mostafavi et al., 2017). In another study of humans in 2014 in the Sistan and Baluchistan province southeast of Iran, the seroprevalence of tularemia among butchers and workers of slaughterhouses was estimated to be 6.5% (Esmaeili et al., 2014b). In addition, a study on humans with risk factors for acquiring tularemia reported a 14.4% prevalence of antibodies against tularemia in Kurdistan, west Iran (Esmaeili et al., 2014a). Finally, a study of rural children in the Chaharmahal and Bakhtiari province, southwest of Iran, showed that the prevalence of antibodies to *F. tularensis* was 6% (Khoshdel et al., 2014).

Given our findings of *F. tularensis* in rodents and hares in several areas of the country including in the Northeast and the Southwest and several previous studies with findings of *F. tularensis* antibodies in humans and animals, it is noticeable that there have been no human cases or tularemia reported in Iran since 1980 (Karimi et al., 1981). Tularemia in other countries, however, is often a diagnostic challenge to the practicing doctor, especially in areas where it seldom appears (Eliasson et al., 2005). Because the clinical diagnosis is based on awareness of the disease, giving rise to a clinical suspicion, and that it may resemble other diseases, we think that tularemia may be underdiagnosed in Iran. Recent publications from Turkey illustrate that the diagnosis may easily be overlooked because it often mimics other conditions of fever such as tuberculosis and other diseases that may cause enlarged lymph nodes (Karabay et al., 2013; Erdem et al., 2014; Yildirim et al., 2014). A presence of tularemia among humans in Iran's neighboring countries such as Azerbaijan (Clark et al., 2012), Armenia (Melikjanyan et al., 1996), and Turkey (Helvaci et al., 2000; Sahin et al., 2007; Balci et al., 2014) suggests that tularemia may be underdiagnosed in Iran.

In the present study, positive samples of *F. tularensis*-infection were observed in three rodents (*A. uralensis*, *M. musculus domesticus*, and *C. nivalis*) and two hares (*L. europaeus* and *Lepus* sp.) in the north, southeastern and southwestern Iran. The House mouse and the pygmy field mouse (*A. uralensis*) have previously been reported as a source of *F. tularensis* (Sakiyev et al., 2013; Unal et al., 2014). However, the natural infection of the European snow vole (*C. nivalis*) with *F. tularensis* was to the best of our knowledge not reported. More than 200 species of mammals have been identified as reservoirs of tularemia and many of them are rodents. Aquatic rodents are thought to play a crucial role in disease maintenance and the connection between this bacterium and natural

TABLE 1 | Primers and probes used for detection of *F. tularensis* and *Y. pestis*.

Agent	Gene target	Primer and probe	Sequence (5' to 3')	Amplicon size (bp)	Reference
<i>F. tularensis</i>	ISFtu2 (chromosome)	ISFtu2F	TTGGTAGATCAGTTGGTAGGATAACC	97	Versage et al., 2003
		ISFtu2R	TGAGTTTTATCCTCTGACAACAATATTC		
	Probe	FAM-AAAATCCATGCTATGACTGATGCTTTAGGTAATCCA-TAMRA			
<i>fopA</i> (chromosome)	fopA-F	AACAATGGCACCTAGTAATATTTCTGG	87	Bushon et al., 2010	
	fopA-R	CCACCAAAGAACCATGTTAAACC			
	Probe	FAM-TGGCAGAGCGGGTACTAACATGATTGGT-5-TAMRA			
<i>Y. pestis</i>	<i>yihN</i> (chromosome)	Chrom F	CGTTTACCTTCACCAAACCTGAAC	128	Stewart et al., 2008
		Chrom R	GGTTGCTGGGAACCAAAGAAGA		
	Probe	Texas Red-TAAGTACATCAATCACACCGGACCCGCTT-BHQ-2			
	<i>caf1</i> (plasmid)	pMT1 F	CCGTTATCGCCATTGCATTATTGG	194	
		pMT1 R	GCCAAGAGTAAGCGTACCAACAAG		
	Probe	FAM-AAGCACCACCTGCAACGGCAACTCTT-BHQ-1			
	<i>pla</i> (plasmid)	pPCP1 F	ATTGGACTTGCAGGCCAGTATC	144	
		pPCP1 R	ATAACGTGAGCCGGATGTCTTC		
		Probe	FAM-AAATTCAGCGACTGGGTTCCGGGCACA-BHQ-1		



waters (Christova and Gladnishka, 2005; Keim et al., 2007). The significance of rodents in the transmission of this disease is also strengthened by the observation that several tularemia outbreaks in humans were following outbreaks among rodents (Mörner, 1992; Johansson et al., 2014; Rodríguez-Pastor et al.,

2017). Those rodents which have been described to play a role in the transmission of tularemia throughout the world were mostly from the genera *Microtus* (vole), *Arvicola* (water vole), *Apodemus* (field mice), and *Myodes* (Red Vole) (Kaysser et al., 2008; Gyuranecz et al., 2010). The observation of *F. tularensis*

TABLE 2 | Sampling locations of wild-caught rodents, insectivores, and hares.

Animal group	Province (no. of collected animals)	Sampling site	Species (no.)
Rodents and insectivores	Golestan (30)	Gorgan, Toskestan, Aliabad-e Katul	<i>Apodemus uralensis</i> *(5), <i>Microtus paradoxus</i> (10), <i>Mus musculus</i> (9), <i>Crocidura suaveolens</i> (4), <i>Rattus rattus</i> (1), <i>Apodemus witherbyi</i> (1)
	North Khorasan (32)	Bojnord (Darkesh, Dasht, Gachranlo)	<i>M. paradoxus</i> (19), <i>M. musculus</i> (4), <i>C. suaveolens</i> (1), <i>A. witherbyi</i> (3), <i>Meriones persicus</i> (1), <i>Crocidura leucodon</i> (2)
	Razavi Khorasan (21)	Mashhad, Moghan, Dargaz	<i>Microtus transcaspicus</i> (3), <i>Chionomys nivalis</i> *(4), <i>A. witherbyi</i> (9), <i>M. musculus</i> (1), <i>Blanfordimys afghanus</i> (1), <i>M. persicus</i> (1), <i>C. suaveolens</i> (1), <i>M. paradoxus</i> (1)
	Zanjan (16)	Soltanieh, Mahneshan, Anguran	<i>C. suaveolens</i> (7), <i>Microtus mystacinus</i> (1), <i>Microtus qazvinensis</i> (5), <i>Mus macedonicus</i> (3)
	Semnan (9)	Shahmirzad, Jashlobar	<i>M. mystacinus</i> (5), <i>A. witherbyi</i> (3), <i>C. leucodon</i> (1)
	Chaharmahal and Bakhtiari (15)	Lordegan, Shahrekord	<i>Microtus socialis</i> (14), <i>C. suaveolens</i> (1)
	Kermanshah (1)	Songhor	<i>M. qazvinensis</i> (1)
	Fars (17)	Shiraz, Mamasani	<i>Microtus irani</i> (16), <i>A. witherbyi</i> (1)
	Kerman (6)	Kerman	<i>Microtus kermanensis</i> (5), <i>M. musculus</i> (1)
	Khuzestan (7)	Izeh	<i>Calomyscus bailwardi</i> (3), <i>M. musculus domesticus</i> * (3), <i>M. persicus</i> (1)
Sistan and Baluchistan (3)	Iran Shahr	<i>Jaculus branfordi</i> (3)	
Hares	East Azerbaijan (2)	Shabestar, Mianeh	<i>Lepus europaeus</i> (2)
	West Azerbaijan (1)	Urmia	<i>L. europaeus</i> (1)
	Ardabil (5)	Parsabad Moghan, Bilesovar, Meshkinshahr, Khalkhal	<i>L. europaeus</i> (5)
	South Khorasan (4)	Khusf, Shosf	<i>L. europaeus</i> (4)
	Golestan (7)	Gorgan, Incheh Borun, Gonbad, Kordkuy	<i>Lepus tolai</i> (7)
	Zanjan (8)	Sohrein, Tarom, Zarinabad, Mahneshan, Khodabandeh, Dandi	<i>L. europaeus</i> (8)
	Kerman (4)	Anbarabad, Kahnuj	<i>Lepus</i> sp. (4)
	Khuzestan (8)	Shushtar, Ramhormoz	<i>L. europaeus</i> * (8)
	Hormozgan (2)	Sardasht, Rudan	<i>Lepus</i> sp. (2)
	Sistan and Baluchistan (9)	Mirjaveh, Maskutan, Bazman	<i>Lepus</i> sp.* (9)
	Qom (1)	Kahak	<i>L. europaeus</i>

**F. tularensis* was detected.

in hares is also in accordance with previous knowledge of that *Lepus* (hares) are important hosts, contributing significantly to the maintenance of the natural cycle of the agent and carrying a potential to produce infection in humans (Hopla and Hopla, 1994). Our findings of *F. tularensis* in a *L. europaeus* from Khuzestan and a *Lepus* sp. from the Sistan and Baluchistan province can be put into the context that infected rabbits and hares were reported in the tularemia epidemics in 1983, 1990–1992, 2005, and 2007 in Germany (Runge et al., 2011; Stalb et al., 2017). Another example is that in 1988, one case of tularemia was reported in a hare from the genus *Lepus* in Sudan (Mörner et al., 1988).

Two main bacterial subtypes may cause tularemia, *F. tularensis* subsp. *tularensis* (type A) and *F. tularensis* subsp. *holarctica* (type B) which are traditionally connected with different disease ecologies. Type A is extensively seen in the USA and is said to be mainly connected with a terrestrial cycle of

the disease (rabbits and hares are mammal hosts; arthropods including ticks serve as vectors). Type B bacteria are related with an aquatic cycle and have mostly been found in outbreaks associated with rivers, lakes, ponds and brooks (semi-aquatic rodents are mammal hosts and mosquitoes or flies serve as vectors) (Hopla, 1974; Hopla and Hopla, 1994; Helvacı et al., 2000; Ulu et al., 2011; Maurin and Gyuranecz, 2016). Because *F. tularensis* subsp. *holarctica* with connections to water has been repeatedly detected in the neighboring country Turkey (Helvacı et al., 2000; Sahin et al., 2007; Balci et al., 2014), it is probable that *F. tularensis* identified in this study would be of this subtype. In Turkey, multiple phylogenetic groups of *F. tularensis* subsp. *holarctica* have been found indicating that much genetic diversity of this subspecies exists in proximity to Iran (Özsürekcı et al., 2015). The presence of *F. tularensis* subsp. *holarctica* would also fit with the observation that the European brown hare (*L. europaeus*) typically serves as host for *F. tularensis* subsp.

holarctica as verified in studies in countries such as Germany (Runge et al., 2011; Stalb et al., 2017) and Sweden (Mörner et al., 1988). Another possibility is that the *F. tularensis* subsp. *mediasiatica* exists in Iran, as this subspecies has been found in Kazakhstan, Turkmenistan, Uzbekistan and in the Altai region of Russia (Champion et al., 2009). The current knowledge, however, suggests that subsp. *mediasiatica* is rare in these geographical areas, which are located relatively distant to Iran (Timofeev et al., 2017).

The last reported human case of plague in Iran goes back to 1965 in the Kurdistan region, west of Iran; despite identification of active foci of plague in the wildlife of western and northwestern parts of the country there have been no human cases ever since. In our study, there was no positive case of *Y. pestis* amongst the studied rodents and hares although several of the captured rodents such as *M. persicus*, *M. musculus*, and *Rattus rattus* were previously identified as potential reservoirs of plague (Meyer et al., 1965; Saunders and Giles, 1977; Karimi, 1980). The role of hares in the transmission of plague has also been proposed (Hopkins and Gresbrink, 1982).

In natural foci of plague in Iran, four species of the genus *Meriones* have been shown to play a crucial role in the transmission of this disease (Shahraki et al., 2016). Recent studies performed in 2011 and 2012 identified antibodies against *Y. pestis* in rodents (1%) and in dogs (3.5%) of the Kurdistan-Hamadan border (Esamaeili et al., 2013); this would imply an ongoing infection cycle in these regions. We suspect that the number of animals studied originating in the west of Iran, the area previously described to be a focus of plague, may have been too small to identify positive samples. In light of the resurgence of plague after long time periods in other countries, e.g., after 50 years in Algeria in 2008, the health system of Iran must continue the surveillance of this disease.

A limitation of our study is that bacterial culture was not performed; this was not feasible with a study design including participation of multiple provinces and demands of in-time dispatch of samples to multiple laboratories. Another limitation is that we have not subtyped the *F. tularensis*. With the current results at hand, we suggest that future studies of tularemia in Iran should include comprehensive sampling from habitats and regions where positive samples were identified in this study and differentiation of the *F. tularensis* subtype. Although we used a PCR assay targeting the *fopA* gene that according to the literature should be specific to *F. tularensis* and the closely related pathogen *F. novicida*, there is a possibility that other *Francisella* species may have cross-reacted with the primers and probes used. The *Francisella* genus contains much diversity that was only recently

discovered (Emanuel et al., 2003; Challacombe et al., 2017). A recent study from the Iberian Peninsula of Europe, e.g., found a *F. hispaniensis*-like DNA sequence in the wood mouse *Apodemus sylvaticus* (de Carvalho et al., 2016).

CONCLUSION

This study reports the first molecular detection of *F. tularensis* amongst rodents and hares in Iran and the first reported detection in the snow vole, *C. nivalis*, worldwide. Future studies should include additional characterization of the infectious agent. The present study and several previously conducted studies, indicate that tularemia is an endemic infectious disease of Iran. The current knowledge could be used to motivate information and educational activities among physicians and healthcare workers to increase disease awareness and diagnostic skills.

AUTHOR CONTRIBUTIONS

EM had role in design of the study, receiving the funds, managing the study and writing and finalizing the draft of the manuscript. AG, SE, and MR had the role in laboratory testing, writing and finalizing the draft of the manuscript. AM, ZM, and MA had role in sampling, writing and finalizing the draft of the manuscript. LM and AJ had role in analysis of the data, writing and finalizing the draft of the manuscript.

ACKNOWLEDGMENTS

The authors would like to sincerely thank Pasteur Institute of Iran and the center for communicable disease control of Ministry of Health (Grant No. 810), Ferdowsi University of Mashhad (Project No. 32482), and National Institute for Medical Research Development (Grant No. 957145) for their financial support. We would also like to express our gratitude to the Rodentology department of research at Ferdowsi University of Mashhad for conducting a part of the sampling. We would like to remark Professor Jamshid Darvish, who had a great role in design and performance of this study. He established the field of Rodentology in Iran, he was the head of the Institute of Applied Zoology at Ferdowsi University of Mashhad, Iran and recently passed away on November 15, 2017. The sampling of this study was conducted in parallel with running two PhD projects (AM and ZM) at the Ferdowsi University of Mashhad.

REFERENCES

- Arata, A., Chamsa, M., Farhang-Azad, A., Mešcerjakova, I., Neronov, V., and Saidi, S. (1973). First detection of tularaemia in domestic and wild mammals in Iran. *Bull. World Health Organ.* 49, 597–603.
- Balci, E., Borlu, A., and Kilic, A. U., Demiraslan, H., Oksuzkaya, A., and Doganay, M. (2014). Tularemia outbreaks in Kayseri, Turkey: an evaluation of the effect of climate change and climate variability on tularemia outbreaks. *J. Infect. Public Health.* 7, 125–132. doi: 10.1016/j.jiph.2013.09.002
- Barker, J. R., and Klose, K. E. (2007). Molecular and genetic basis of pathogenesis in *Francisella tularensis*. *Ann. N. Y. Acad. Sci.* 1105, 138–159. doi: 10.1196/annals.1409.010
- Bevins, S. N., Baroch, J. A., Nolte, D. L., Zhang, M., and He, H. (2012). *Yersinia pestis*: examining wildlife plague surveillance in China and the USA. *Integr. Zool.* 7, 99–109. doi: 10.1111/j.1749-4877.2011.00277.x
- Bitam, I., Dittmar, K., Parola, P., and Whiting, M. F., and Raoult, D. (2010). Fleas and flea-borne diseases. *Int. J. Infect. Dis.* 14, e667–e676. doi: 10.1016/j.ijid.2009.11.011

- Bushon, R. N., Kephart, C. M., Koltun, G. F., Francy, D. S., Schaefer, F. W., and Alan Lindquist, H. D. (2010). Statistical assessment of DNA extraction reagent lot variability in real-time quantitative PCR. *Lett. Appl. Microbiol.* 50, 276–282. doi: 10.1111/j.1472-765X.2009.02788.x
- Challacombe, J. F., Petersen, J. M., Hodges, D., Pillai, S., and Kuske, C. R. (2017). Whole-genome relationships among *Francisella* bacteria of diverse origins define new species and provide specific regions for detection. *Appl. Environ. Microbiol.* 83:e02589-16. doi: 10.1128/AEM.02589-16
- Champion, M. D., Zeng, Q., Nix, E. B., Nano, F. E., Keim, P., Kodira, C. D., et al. (2009). Comparative genomic characterization of *Francisella tularensis* strains belonging to low and high virulence subspecies. *PLoS Pathog.* 5:e1000459. doi: 10.1371/journal.ppat.1000459
- Christova, I., and Gladnisha, T. (2005). Prevalence of infection with *Francisella tularensis*, *Borrelia burgdorferi* sensu lato and *Anaplasma phagocytophilum* in rodents from an endemic focus of tularemia in Bulgaria. *Ann. Agric. Environ. Med.* 12, 149–152.
- Clark, D. V., Ismailov, A., Seyidova, E., Hajiyeva, A., Bakhishova, S., Hajiyev, H., et al. (2012). Seroprevalence of tularemia in rural Azerbaijan. *Vector-Borne and Zoonotic Dis.* 12, 558–563. doi: 10.1089/vbz.2010.0081
- Corbet, G. B. (1978). *Mammals of the Palaearctic Region*. London, UK; Ithaca, NY: British Museum (Natural History); Cornell University Press.
- de Carvalho, I., Toledo, A., Carvalho, C., Barandika, J., Respicio-Kingry, L., Garcia-Amil, C., et al. (2016). *Francisella* species in ticks and animals, Iberian Peninsula. *Ticks Tick Borne Dis.* 7, 159–165. doi: 10.1016/j.ttbdis.2015.10.009
- Dubynskiy, V. M., and Yeszhanov, A. B. (2016). Ecology of *Yersinia pestis* and the Epidemiology of Plague. *Adv. Exp. Med. Biol.* 918, 101–170. doi: 10.978-94-024-0890-4_5
- Eliasson, H., Sjöstedt, A., and Bäck, E. (2005). Clinical use of a diagnostic PCR for *Francisella tularensis* in patients with suspected ulceroglandular tularaemia. *Scand. J. Infect. Dis.* 37, 833–837. doi: 10.1080/00365540500400951
- Emanuel, P. A., Bell, R., Dang, J. L., McClanahan, R., David, J. C., Burgess, R. J., et al. (2003). Detection of *Francisella tularensis* within infected mouse tissues by using a hand-held PCR thermocycler. *J. Clin. Microbiol.* 41, 689–693. doi: 10.1128/JCM.41.2.689-693.2003
- Erdem, H., Ozturk-Engin, D., Yesilyurt, M., Karabay, O., Elaldi, N., Celebi, G., et al. (2014). Evaluation of tularaemia courses: a multicentre study from Turkey. *Clin. Microbiol. Infect.* 20, O1042–O1051. doi: 10.1111/1469-0691.12741
- Esmaeili, S., Azadmanesh, K., and Naddaf, S. R., Rajerison, M., Carniel, E., and Mostafavi, E. (2013). Serologic survey of plague in animals, Western Iran. *Emerg. Infect. Dis.* 19, 1549–1551. doi: 10.3201/eid1909.121829
- Esmaili, S., Esfandiari, B., Maurin, M., Gouya, M. M., Shirzadi, M. R., Amiri, F. B., et al. (2014a). Serological survey of tularemia among butchers and slaughterhouse workers in Iran. *Trans. R. Soc. Trop. Med. Hyg.* 108, 516–518. doi: 10.1093/trstmh/tru094
- Esmaili, S., Gooya, M. M., Shirzadi, M. R., Esfandiari, B., Amiri, F. B., Behzadi, M. Y., et al. (2014b). Seroprevalence survey of tularemia among different groups in western Iran. *Int. J. Infect. Dis.* 18, 27–31. doi: 10.1016/j.ijid.2013.08.013
- Fratini, F., Verin, R., Ebani, V. V., Ambrogi, C., Bertelloni, F., Turchi, B., et al. (2017). Experimental infection with *Yersinia pseudotuberculosis* in European brown hare (*Lepus europaeus*, Pallas). *Asian Pac. J. Trop. Med.* 10, 285–291. doi: 10.1016/j.apjtm.2017.03.008
- Goethert, H. K., and Telford, III S. R. (2009). Nonrandom distribution of vector ticks (*Dermacentor variabilis*) infected by *Francisella tularensis*. *PLoS Pathog.* 5:e1000319. doi: 10.1371/journal.ppat.1000319
- Gupta, S. K., Gupta, P., Sharama, P., Shrivastava, A. K., and Soni, S. K. (2012). Emerging and re-emerging infectious diseases, future challenges and strategy. *J. Clin. Diagn. Res.* 6, 1095–1100.
- Gyuranecz, M., Dénes, B., Dán, Á., Rigó, K., Földvári, G., Szeredi, L., et al. (2010). Susceptibility of the common hamster (*Cricetus cricetus*) to *Francisella tularensis* and its effect on the epizootiology of tularemia in an area where both are endemic. *J. Wildl. Dis.* 46, 1316–1320. doi: 10.7589/0090-3558-46.4.1316
- Helvacı, S., Gedikoglu, S., Akalin, H., and Oral, H. (2000). Tularemia in Bursa, Turkey: 205 cases in ten years. *Eur. J. Epidemiol.* 16, 271–276. doi: 10.1023/A:1007610724801
- Hestvik, G., Warns-Petit, E., Smith, L. A., Fox, N. J., Uhlhorn, H., Artois, M., et al. (2015). The status of tularemia in Europe in a one-health context: a review. *Epidemiol. Infect.* 143, 2137–2160. doi: 10.1017/S0950268814002398
- Hopkins, D. D., and Gresbrink, R. A. (1982). Surveillance of sylvatic plague in Oregon by serotesting carnivores. *Am. J. Public Health* 72, 1295–1297. doi: 10.2105/AJPH.72.11.1295
- Hopla, C. (1974). Ecology of tularemia. *Adv. Vet. Sci. Comp. Med.* 18, 25–53.
- Hopla, C. E., and Hopla, A. K. (1994). “Tularemia,” in *Handbook of Zoonoses*, eds G. W. B. Steele and J. H. Steele (Boca Raton, FL: CRC Press Inc.), 113–126.
- Johansson, A., Lärkeryd, A., Widerström, M., Mörtberg, S., Myrtännäs, K., Öhrman, C., et al. (2014). An outbreak of respiratory tularemia caused by diverse clones of *Francisella tularensis*. *Clin. Infect. Dis.* 59, 1546–1553. doi: 10.1093/cid/ciu621
- Karabay, O., Kilic, S., Gurcan, S., Pelitli, T., Karadenizli, A., Bozkurt, H., et al. (2013). Cervical lymphadenitis: tuberculosis or tularaemia? *Clin. Microbiol. Infect.* 19, E113–E117. doi: 10.1111/1469-0691.12097
- Karimi, P. (1980). [Discovery of a new focus of zoonotic plague in the eastern Azarbaijan region of Iran]. *Bull. Soc. Pathol. Exot. Filiales* 73, 28–35.
- Karimi, Y., Salarkia, F., and Ghasemi, M. (1981). Tularemia: first human case in Iran. *J. Med. Coun. Iran* 8, 134–141.
- Kaysser, P., Seibold, E., Mätz-Rensing, K., Pfeffer, M., Essbauer, S., and Spletstoeser, W. D. (2008). Re-emergence of tularemia in Germany: Presence of *Francisella tularensis* in different rodent species in endemic areas. *BMC Infect. Dis.* 8:157. doi: 10.1186/1471-2334-8-157
- Keim, P., Johansson, A., and Wagner, D. M. (2007). Molecular epidemiology, evolution, and ecology of *Francisella*. *Ann. N. Y. Acad. Sci.* 1105, 30–66. doi: 10.1196/annals.1409.011
- Khoshdel, A., Saedi Dezaki, E., Ganji, F., Habibian, R., Imani, R., Taheri, E., et al. (2014). First seroprevalence survey of children with tularemia infection in Chaharmahal va Bakhtiari province, Iran. *Iranian J. Pathol.* 9, 23–27.
- Kryštufek, B., Vohralík, V., and Janžeković F. (2005). *Mammals of Turkey and Cyprus: Rodentia I: Scuriidae, Dipodidae, Gliridae, Arvicolinae*. Koper: Zgodovinsko društvo za južno Primorsko.
- Leslie, T., Whitehouse, C., Yingst, S., Baldwin, C., Kakar, F., Mofleh, J., et al. (2011). Outbreak of gastroenteritis caused by *Yersinia pestis* in Afghanistan. *Epidemiol. Infect.* 139, 728–735. doi: 10.1017/S0950268810001792
- Maurin, M., and Gyuranecz, M. (2016). Tularaemia: clinical aspects in Europe. *Lancet Infect. Dis.* 16, 113–124. doi: 10.1016/S1473-3099(15)00355-2
- Melikjanyan, S., Vanyan, A., Avetisyan, A., Avetisyan, A., and Bakunts, N. (1996). GIS analysis of tularemia outbreaks in Armenia, 1996–2013. *Online J. Public Health Inform.* 6:e45. doi: 10.5210/ojphi.v6i1.5108
- Meyer, K., McNeill, D., and Wheeler, C. (1965). Results of a preliminary serological survey of small mammal populations for plague on the island of Hawaii. *Bull. World Health Organ.* 33, 809–815.
- Mörner, T. (1992). The ecology of tularaemia. *Rev. Sci. Tech.* 11, 1123–1130. doi: 10.20506/rst.11.4.657
- Mörner, T., Sandström, G., Mattsson, R., and Nilsson, P.-O. (1988). Infections with *Francisella tularensis* biovar palaearctica in hares (*Lepus timidus*, *Lepus europaeus*) from Sweden. *J. Wildl. Dis.* 24, 422–433. doi: 10.7589/0090-3558-24.3.422
- Mostafavi, E., and Keypour, M. (2017). History of Plague Research Center of Pasteur Institute of Iran (1952–2016). *J. Res. His Med.* 6, 139–158.
- Mostafavi, E., Shahraki, A. H., Japoni-Nejad, A., Esmaeili, S., Darvish, J., Sedaghat, M. M., et al. (2017). A field study of plague and tularemia in rodents, Western Iran. *Vector Borne Zoonotic Dis.* 17, 247–253. doi: 10.1089/vbz.2016.2053
- Özsürekli, Y., Birdsell, D. N., Çelik, M., Karadag-Öncel, E., Johansson, A., Forsman, M., et al. (2015). Diverse *Francisella tularensis* Strains and Oropharyngeal Tularemia, Turkey. *Emerg. Infect. Dis.* 21, 173–175. doi: 10.3201/eid2101.141087
- Parhizgari, N., Gouya, M. M., and Mostafavi, E. (2017). Emerging and re-emerging infectious diseases in Iran. *Iranian J. Microbiol.* 9, 122–142.
- Poland, J. D., and Dennis, D. T. (1999). “Plague manual: epidemiology, distribution, surveillance and control,” in *Treatment Plague* (Geneva: World Health Organization), 55–62.
- Pourhossein, B., Esmaeili, S., Gyuranecz, M., and Mostafavi, E. (2015). Tularemia and plague survey in rodents in an earthquake zone in southeastern Iran. *Epidemiol. Health* 37:e2015050. doi: 10.4178/epih/e2015050
- Rodriguez-Pastor, R., Escudero, R., Vidal, D., Mougeot, F., Arroyo, B., Lambin, X., et al. (2017). Density-dependent prevalence of *Francisella tularensis*

- in fluctuating vole populations, northwestern Spain. *Emerg. Infect. Dis.* 23, 1377–1379. doi: 10.3201/eid2308.161194
- Runge, M., von Keyserlingk, M., Braune, S., Voigt, U., Grauer, A., Pohlmeier, K., et al. (2011). Prevalence of *Francisella tularensis* in brown hare (*Lepus europaeus*) populations in Lower Saxony, Germany. *Eur. J. Wildl. Res.* 57, 1085–1089. doi: 10.1007/s10344-011-0522-1
- Saeed, A. A., Al-Hamdan, N. A., and Fontaine, R. E. (2005). Plague from eating raw camel liver. *Emerg. Infect. Dis.* 11, 1456–1457. doi: 10.3201/eid1109.050081
- Sahin, M., Atabay, H. I., Bicakci, Z., Unver, A., and Otlu, S. (2007). Outbreaks of tularemia in Turkey. *Kobe J. Med. Sci.* 53, 37–42.
- Sakiyev, K., Ospanova, S., and Abdrakhmanova, K. (2013). Current state and consistent pattern of distribution of a tularemia in the territory of the pavlodar region (North Kazakhstan). *Sci. J. Pavlodar State Pedagogical Institute*. 1, 35–41.
- Sanyaolu, A., Okorie, C., Mehraban, N., Ayodele, O., and Tshitenge, S. (2016). Epidemiology of Zoonotic Diseases in the United States: a comprehensive review. *J. Infect. Dis. Epidemiol.* 2:021. doi: 10.23937/2474-3658/1510021
- Saunders, G., and Giles, J. (1977). A relationship between plagues of the house mouse, *Mus musculus* (Rodentia: Muridae) and prolonged periods of dry weather in south-eastern Australia. *Wildl. Res.* 4, 241–247. doi: 10.1071/WR9770241
- Shahraki, A. H., Carniel, E., and Mostafavi, E. (2016). Plague in Iran: its history and current status. *Epidemiol. Health.* 38:e2016033. doi: 10.4178/epih.e2016033
- Sjöstedt, A. (2007). Tularemia: history, epidemiology, pathogen physiology, and clinical manifestations. *Ann. N. Y. Acad. Sci.* 1105, 1–29. doi: 10.1196/annals.1409.009
- Stalb, S., Polley, B., Danner, K.-J., Reule, M., Tomaso, H., Hackbare, A., et al. (2017). Detection of tularemia in European brown hares (*Lepus europaeus*) and humans reveals endemic and seasonal occurrence in Baden-Wuerttemberg, Germany. *Berliner und Münchener Tierärztliche Wochenschrift.* 130, 293–239. doi: 10.2376/0005-9366-16079
- Stewart, A., Satterfield, B., Cohen, M., O'Neill, K., and Robison, R. (2008). A quadruplex real-time PCR assay for the detection of *Yersinia pestis* and its plasmids. *J. Med. Microbiol.* 57, 324–331. doi: 10.1099/jmm.0.47485-0
- Timofeev, V., Bakhteeva, I., Titareva, G., Kopylov, P., Christiany, D., Mokrievich, A., et al. (2017). Russian isolates enlarge the known geographic diversity of *Francisella tularensis* subsp. *mediasiatica*. *PLoS ONE* 12:e0183714. doi: 10.1371/journal.pone.0183714
- Ulu, K. A., Kiliç, S., Sencan, I., Çiçek, S. G., Gürbüz, Y., Tütüncü, E., et al. (2011). [A water-borne tularemia outbreak caused by *Francisella tularensis* subspecies *holarctica* in Central Anatolia region]. *Mikrobiyoloji Bulteni* 45, 234–247.
- Ulu-Kilic, A., Gulen, G., Sezen, F., Kilic, S., and Sencan, I. (2013). Tularemia in central Anatolia. *Infection* 41, 391–399. doi: 10.1007/s15010-012-0355-1
- Unal Yilmaz, G., Gurcan, S., Ozkan, B., and Karadenizli, A. (2014). Investigation of the presence of *Francisella tularensis* by culture, serology and molecular methods in mice of Thrace Region, Turkey. *Mikrobiyoloji Bulteni* 48, 213–222. doi: 10.5578/mb.7028
- Versage, J. L., Severin, D. D., Chu, M. C., and Petersen, J. M. (2003). Development of a multitarget real-time TaqMan PCR assay for enhanced detection of *Francisella tularensis* in complex specimens. *J. Clin. Microbiol.* 41, 5492–5499. doi: 10.1128/JCM.41.12.5492-5499.2003
- Williamson, E. (2016). *Pathogenesis of Yersinia pestis in Humans. Human Emerging and Re-emerging Infections: Viral and Parasitic Infections*. New Jersey: John Wiley & Sons, Inc.
- Yildirim, S., Turhan, V., Karadenizli, A., Önem, Y., Karagöz, E., Eroglu, C., et al. (2014). Tuberculosis or tularemia? A molecular study in cervical lymphadenitis. *Int. J. Infect. Dis.* 18, 47–51. doi: 10.1016/j.ijid.2013.09.004
- Zargar, A., Maurin, M., and Mostafavi, E. (2015). Tularemia, a re-emerging infectious disease in Iran and neighboring countries. *Epidemiol. Health* 37:e2015011. doi: 10.4178/epih/e2015011

Conflict of Interest Statement: The authors declare that the research was conducted in the absence of any commercial or financial relationships that could be construed as a potential conflict of interest.

The reviewer RP and handling Editor declared their shared affiliation.

Copyright © 2018 Mostafavi, Ghasemi, Rohani, Molaeipoor, Esmaeili, Mohammadi, Mahmoudi, Aliabadian and Johansson. This is an open-access article distributed under the terms of the Creative Commons Attribution License (CC BY). The use, distribution or reproduction in other forums is permitted, provided the original author(s) and the copyright owner(s) are credited and that the original publication in this journal is cited, in accordance with accepted academic practice. No use, distribution or reproduction is permitted which does not comply with these terms.



Phylogenetic Lineages of *Francisella tularensis* in Animals

Paola Pilo*

Vetsuisse Faculty, Institute of Veterinary Bacteriology, Department of Infectious Diseases and Pathobiology, University of Bern, Bern, Switzerland

Tularemia is a zoonotic disease caused by the facultative intracellular bacterium *Francisella tularensis*. This microorganism can infect a plethora of animal species and its ecology is particularly complex. Much research was performed to understand its biology but many questions are still open, especially concerning the life cycle of this bacterium in the environment related to physical and biological parameters. Numerous animals are major hosts of *F. tularensis* but precise reservoir species are not yet well defined. Moreover, the exact range of species susceptible to tularemia is not clear and is complicated by the differences in virulence and ecology observed among the subspecies of *F. tularensis*. Indeed, different life cycles in nature, including the animal species concerned, were previously described for *F. tularensis* subsp. *tularensis* and *F. tularensis* subsp. *holarctica*. Recently, molecular techniques showing adequate discrimination between strains were developed, leading to the possibility to investigate links between phylogenetic lineages and infection in animals. New perspectives in research are now possible thanks to the information available and the simplicity of the molecular procedures. Current studies are unfolding the evolution of *F. tularensis* and these developments will lead to the elucidation of geographical and ecological differences observed by veterinarians, microbiologists and conservation biologists. However, systematic, coordinated collection of data and extensive sampling are important to efficiently assemble the findings of future research.

Keywords: tularemia, animals, phylogenetic lineages, host specificity, ecology

OPEN ACCESS

Edited by:

Marina Santic,
University of Rijeka, Croatia

Reviewed by:

Anders Johansson,
Umeå University, Sweden
Paul Edward Carlson,
Food and Drug Administration,
United States
John S. Gunn,
The Ohio State University,
United States

***Correspondence:**

Paola Pilo
paola.pilo@vetsuisse.unibe.ch

Received: 30 October 2017

Accepted: 11 July 2018

Published: 31 July 2018

Citation:

Pilo P (2018) Phylogenetic Lineages of *Francisella tularensis* in Animals. *Front. Cell. Infect. Microbiol.* 8:258. doi: 10.3389/fcimb.2018.00258

INTRODUCTION

Tularemia is a zoonotic disease known since the beginning of the last century. The disease was first described by McCoy in rodents in 1911 (McCoy, 1911) and the causative microorganism, *Francisella tularensis*, was later isolated from squirrels (McCoy and Chapin, 1912). The first bacteriologically confirmed human case description followed in 1914 (Wherry and Lamb, 1914). *F. tularensis* was subsequently isolated from hundreds of animal species (Mörner, 1992; WHO., 2007) and several arthropod vectors were identified (reviewed in Petersen et al., 2009). Because of the broad spectrum of potential vectors and hosts and the complex biology of the causative microorganism, the detailed understanding of the ecology of this bacterium is still unclear and many questions are still open regarding tularemia in animals, including which ones are incidental or reservoir species.

Tularemia occurs in parts of North America and Eurasia and seems to be restricted to the Northern Hemisphere. However, human and animal cases were recently described in Australia (Jackson et al., 2012; Eden et al., 2017). Over time, the geographic distribution and phenotypic

characteristics including the virulence of *F. tularensis* strains appeared to be linked to the taxonomy of this bacterium and the species was divided into three clinically relevant subspecies: *tularensis* (type A), *holarctica* (type B), and *mediasiatica* (Olsufjev and Meshcheryakova, 1982; Eliasson et al., 2006). Briefly, the subspecies *tularensis* seemed to be confined to North America, showing high virulence to humans and animals. It is phenotypically characterized by its capacity to ferment glycerol and citrulline. Strains belonging to the subspecies *holarctica* were isolated from North America and Eurasia, displayed moderate virulence to humans and animals and were unable to ferment glycerol and citrulline. Interestingly, phenotypic variability was observed among these strains supporting a supplementary subdivision (Olsufjev and Meshcheryakova, 1982). The biotype “EryR” is erythromycin resistant, the biotype “EryS” is erythromycin sensitive and the biotype “japonica” is able to ferment glycerol. Subsequently, the subspecies *mediasiatica* was isolated from Central Asia and the strains exhibited moderate virulence but fermented glycerol and citrulline (Sjöstedt, 2015).

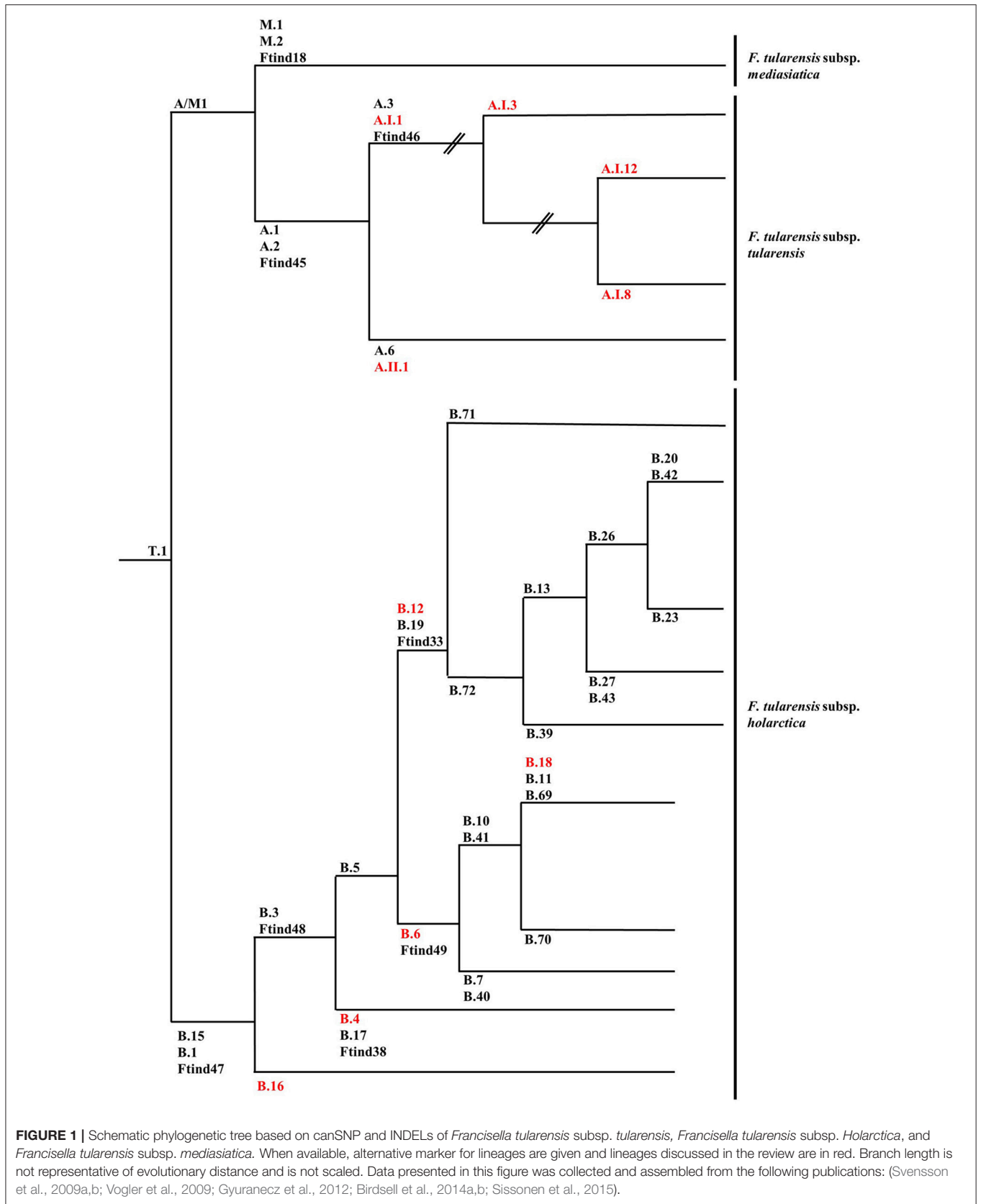
One of the first aspects considered by scientists to investigate the biology of *F. tularensis* was the variability in the degree of virulence of strains in experimental animal infections. Researchers rapidly described a severe and a mild form of tularemia among animals (Davis et al., 1934; Bell et al., 1955; Olsufjev and Meshcheryakova, 1982). Indeed, laboratory animals were used to isolate strains and to assess their degree of virulence (Davis et al., 1934; Philip and Davis, 1935). The quantitative measurement of virulence was mainly based on the amount of bacteria needed to kill the host and the number of days of survival after subcutaneous infection with a small number of bacteria. Later, Bell et al. (1955) standardized the protocols in mice, guinea pigs and rabbits. Furthermore, they confirmed a decreased sensitivity of rabbits compared to mice and guinea pigs to the strain 425F4G (*F. tularensis* subsp. *holarctica*). This observation and the phenotypic differences described above led to the confirmation of the taxonomic differentiation between *F. tularensis* subsp. *tularensis* and *F. tularensis* subsp. *holarctica* (Olsufjev and Meshcheryakova, 1982).

Although tularemia is described as potentially affecting hundreds of vertebrate species in natural settings, infections in lagomorphs and rodents are principally reported (Mörner, 1992). Moreover, isolated cases or outbreaks in captive primates, domestic cats and sheep are also documented. In animals, the clinical course of the disease appears to be dependent upon the susceptibility and sensitivity of the species (see section Tularemia in Animals of this review) (WHO., 2007). However, little information about clinical manifestations in naturally infected animals or the complete range of species affected is available.

The recent rapid development of sequencing methods allowed progress in the subdivision and typing of this microorganism. This is of major importance in the goal to dissect differences observed in ecology and epidemiology of *F. tularensis*. For these reasons, this review focuses principally on recent literature available on animal species naturally infected with this bacterium, excluding invertebrates, and highlights the data on genetic lineages associated with animal species.

GENETIC TYPING OF STRAINS OF *F. TULARENSIS*

The first attempts to type strains of *F. tularensis* using molecular approaches were hampered by the genetic homogeneity of the *F. tularensis* genome. Repetitive extragenic palindromic element PCR (REP-PCR), enterobacterial repetitive intergenic consensus sequence PCR (ERIC-PCR), random amplified polymorphic DNA (RAPD), pulsed-field gel electrophoresis (PFGE), and restriction fragment length polymorphism (RFLP) assays were assessed but gave little discrimination among strains or were troubled by reproducibility issues between laboratories (de la Puente-Redondo et al., 2000; Johansson et al., 2000; García Del Blanco et al., 2002; Thomas et al., 2003). The more recent development of a method based on the amplification of variable-number tandem repeats (VNTRs), which are fast evolving markers, allowed an adequate differentiation of strains and simplified comparisons between laboratories (Farlow et al., 2001; Johansson et al., 2001, 2004). The analysis of comprehensive collections of strains by multiple-loci VNTR analysis (MLVA) enabled the confirmation of the subdivision of *F. tularensis* subsp. *tularensis* in two major clades (A.I and A.II), while *F. tularensis* subsp. *holarctica* was separated into five clades (B.I, B.II, B.III, B.IV, and B.V) (Johansson et al., 2004). *F. tularensis* subsp. *mediasiatica* was recently divided into three clades: M.I, M.II, and M.III (Timofeev et al., 2017). However, bias inherent to the evolution of VNTRs does not permit solid phylogenetic studies since these markers are prone to homoplasy resulting from convergent evolution. To circumvent this drawback, assays based on canonical single nucleotide polymorphism (canSNP) and on canonical insertions/deletions (INDELs) were established (Figure 1) (Larsson et al., 2007; Vogler et al., 2009). As an example, the five clades initially described for *F. tularensis* subsp. *holarctica* were reduced to four clades (B.12 [B.I], B.4 [B.II], B.6 [B.IV] and B.16 [B.V]) because of inconsistent classification using MLVA (Figures 1, 2) (Svensson et al., 2009b; Karlsson et al., 2013). The development of these molecular tools for the typing of *F. tularensis* allowed not only better discrimination of strains and the possibility to perform population genetics and epidemiological studies but also to design rational panels of PCRs based on hierarchical schemes (Svensson et al., 2009b). These canSNP and INDEL systems were further applied to study worldwide collections of strains and new markers specific to distinct branches of the phylogenetic tree were identified. These improvements performed in the typing techniques of *F. tularensis* led to identify precise links between lineages and macrogeographical origin of strains, and to confirm the geographical overlapping of distinct subspecies and lineages. A large number of research groups investigated the distribution of the genetic diversity of strains in their respective countries. These studies led to the discovery of a very precise and vast amount of sublineages derived from basal lineages. As a consequence, the cladistic nomenclature was particularly detailed in the recent years (Chanturia et al., 2011; Hansen et al., 2011; Vogler et al., 2011; Gyuranecz et al., 2012; Karlsson et al., 2013; Müller et al., 2013; Origgi et al., 2014; Wang et al., 2014; Karadenizli et al., 2015; Kilic et al., 2015; Sissonen et al., 2015;



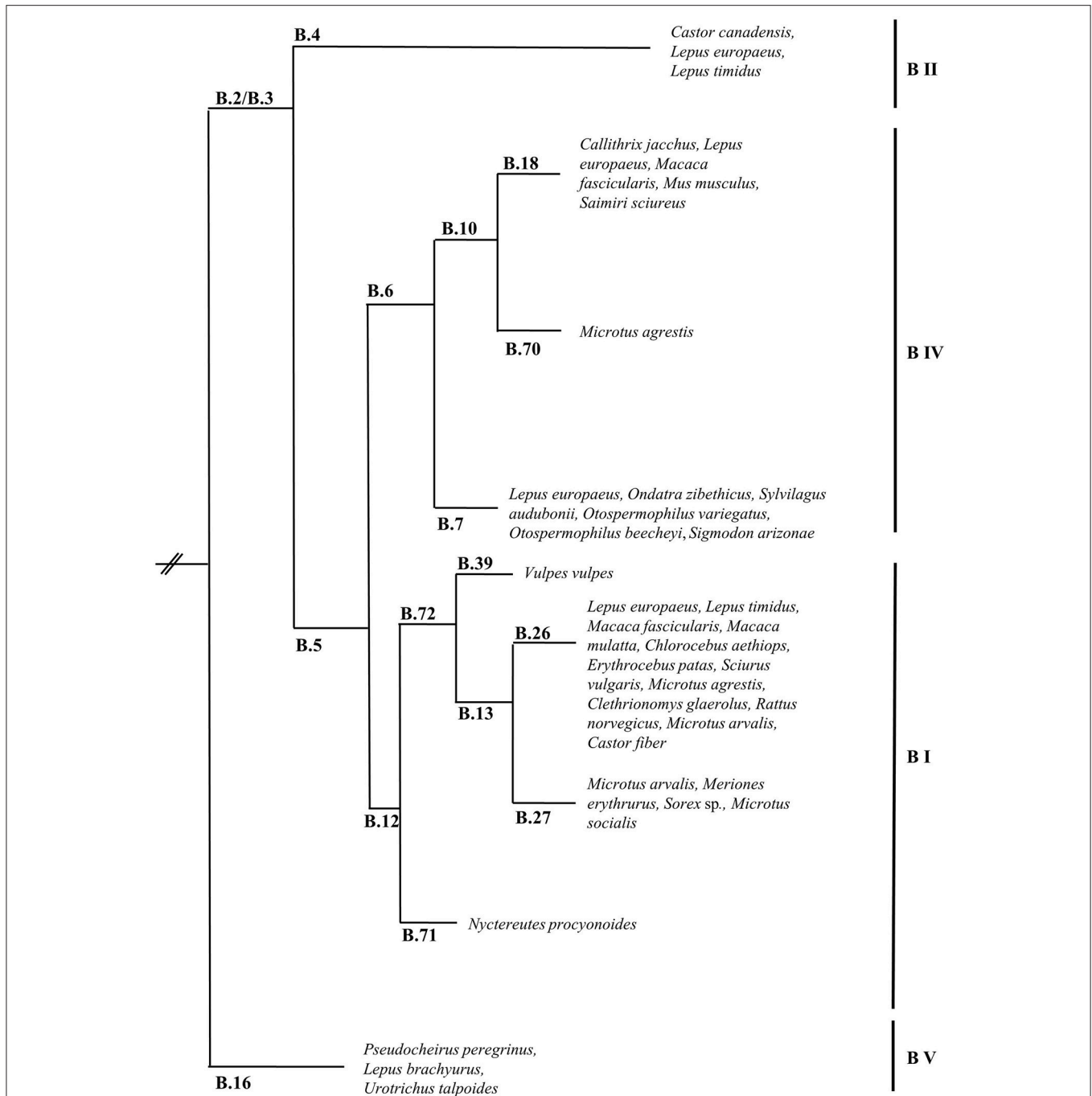


FIGURE 2 | Schematic phylogenetic tree based on canSNP and INDELS of *Francisella tularensis* subsp. *holarctica* showing the major lineages and confirmed lineages of strains isolated from animal species (only of species specifically named in the literature). Branch length is not representative of evolutionary distance and is not scaled. Data presented in this figure was collected and assembled from the following publications: (Farlow et al., 2001; Abril et al., 2007; Fujita et al., 2008; Svensson et al., 2009b; Vogler et al., 2009; Chanturia et al., 2011; Gyuranecz et al., 2012; Müller et al., 2013; Origgi et al., 2014; Elashvili et al., 2015; Sissonen et al., 2015; Dwibedi et al., 2016; Myrtennas et al., 2016; Schulze et al., 2016; Eden et al., 2017).

Dwibedi et al., 2016; Myrtennas et al., 2016; Schulze et al., 2016).

The early population studies carried out using PFGE, MLVA, and canSNPs in North America uncovered novel information and new hypotheses concerning the biology and potential life

cycle of *F. tularensis*. Firstly, strains of *F. tularensis* subsp. *tularensis* presented a higher genetic diversity than strains of *F. tularensis* subsp. *holarctica* suggesting a recent emergence of the subspecies *holarctica* (Johansson et al., 2004). Furthermore, particular lineages seemed to be associated with variation in

virulence and potential animal host and vector specificity (Farlow et al., 2005; Staples et al., 2006; Kugeler et al., 2009). Molecular epidemiological investigations, using *PmeI* PFGE, of strains isolated in the USA showed differences in case fatality rates of tularemia in humans depending on lineages of *F. tularensis* subsp. *tularensis*; with A.Ia: 4%; A.Ib: 24%; A.II: 0% and *F. tularensis* subsp. *holarctica* lineage B: 7% (Staples et al., 2006; Kugeler et al., 2009). This finding was later tested and experimentally confirmed in C57BL/6 mice (Molins et al., 2010). However, the clustering observed by PFGE typing is not completely compatible with the canSNP typing. Indeed, all A.Ia strains belong to the sublineage A.I.12 (successively tested by the canSNP method) but strains previously assigned to cluster A.Ib are disseminated in all the new identified sublineages: A.I.3, A.I.8, and A.I.12 (Figure 1). Concerning the potential virulence and ecological niches inhabited by the lineages of *F. tularensis* subsp. *holarctica*, less information is available. Specificities might be subtler for this subspecies than for *F. tularensis* subsp. *tularensis* due to the relative recent emergence of this subspecies resulting in low genetic heterogeneity. For *F. tularensis* subsp. *mediasiatica* there is very little data available on potential ecological niche differences among genetic lineages.

Links between *F. tularensis* lineages, virulence and niches are particularly interesting as several distinct life cycles related to ecological parameters have been described but the molecular mechanisms underlying these differences are still unknown. A well-defined differentiation and characterization of the lineages is central in order to expand knowledge in this field.

ECOLOGY OF *F. TULARENSIS*

Since the first description of tularemia and ensuing isolation of *F. tularensis*, several researchers investigated the host range, vectors and spread of this microorganism. Early on, it became clear that the epidemiology of tularemia is strictly connected to biological and physical features and an incredible diversity of ecological cycles of *F. tularensis* were designated. However, despite the large amount of research published on the ecology of *F. tularensis*, little is known about its life cycle in nature and the specific role of biological and physical parameters.

In North America, two major cycles were generally characterized: a terrestrial or sylvatic cycle and an aquatic cycle (Mörner, 1992). The terrestrial cycle mainly involves lagomorphs and more specifically *Sylvilagus* sp. and ticks, while the aquatic cycle comprises semi-aquatic rodents like the American beaver *Castor canadensis* and the muskrat *Ondatra zibethicus* (Mörner, 1992). It was later discovered that *F. tularensis* subsp. *tularensis* was involved in the sylvatic cycle and *F. tularensis* subsp. *holarctica* was isolated from animal species of the aquatic cycle.

In Eurasia, most of the studies were performed in former USSR and Scandinavia. In former USSR, ticks, rodent species like the water vole *Arvicola terrestris*, the common vole *Microtus arvalis*, the hamster *Cricetus* sp., the house mouse *Mus musculus* and lagomorphs, *Lepus* sp., are mainly affected by *F. tularensis* subsp. *holarctica* (Hopla, 1974). In Scandinavia, mosquitos,

the mountain hares *Lepus timidus*, the European brown hare *L. europaeus*, the lemming *Lemmus lemmus* and the field vole *M. agrestis* are most frequently described as possibly contributing to the biological cycle of this bacterium (Hopla, 1974; Morner et al., 1988b; Rossow et al., 2014; Hestvik et al., 2017). In Eastern and Western Europe, *F. tularensis* subsp. *holarctica* is more often isolated or identified from ticks, the European brown hare *L. europaeus* and the common vole *M. arvalis* (de la Puente-Redondo et al., 2000; Kaysser et al., 2008; Gyuranecz et al., 2010; Decors et al., 2011; Origgi et al., 2014; Rodriguez-Pastor et al., 2017). In Japan, ticks and the Japanese hare *L. brachyurus* are confirmed hosts of *F. tularensis* subsp. *holarctica* (Fujita et al., 2008; Park et al., 2009). The host range of *F. tularensis* subsp. *mediasiatica*, isolated in Central Asia, is virtually unknown because of the very limited number of strains that have been isolated so far.

Beyond the animal species regularly identified as infected with *F. tularensis*, the microorganism has also been isolated from hundreds of other species (Hopla, 1974). However, the defined role of each one of these species in the ecology of *F. tularensis* is not distinctly defined and might be different and / or restricted to specific geographical areas. Particularly, some confusion about incidental and reservoir hosts should be clarified. Indeed, all incidental hosts are not required for the perpetuation (long term maintenance) of an infectious agent and some incidental animal hosts might only represent a “bridge” for *F. tularensis* between wildlife and humans (Telford and Goethert, 2010).

TULAREMIA IN ANIMALS

Tularemia in animals is extremely complex because of the numerous species described as being susceptible to this disease. Additionally, there might be differences between observations made in natural versus experimental infections, and importantly regarding the epidemiologic relevance of the experimental results in the environment. Despite the countless experiments performed and published describing the development of tularemia in animals, the route of transmission, the organs affected, the progress of lesions and inflammatory host responses as well as the range of animal species acting as reservoir between epizootics need to be clarified with regard to the various *F. tularensis* lineages.

Historically, animal species affected by *F. tularensis* were classified in three groups according to their susceptibility (to infection) and sensitivity (severity of clinical manifestation) (Hopla, 1974; WHO., 2007; Mörner and Addison, 2008): class 1 «acute disease after inoculation of 1–10 bacteria with rapid multiplication in blood and tissues»; class 2 «death after inoculation of 10⁸-10⁹ bacteria; survival may occur at lower doses and then provide immunity» and class 3 «genera resistant to *F. tularensis*» (Hopla, 1974; WHO., 2007). Since this classification is primarily based on the bacterial dose necessary to cause death and the ability to spread *via* the blood and lymphatic streams, it mainly results from observations made after experimental infection. Nevertheless, the natural occurrence, progress of infection, and development of efficient immunity

in specific species might also be parameters to consider to enable animal species to be grouped to understand their role in the maintenance and perpetuation of *F. tularensis* in the environment. In future investigations, species highly susceptible and sensitive to *F. tularensis* infection might be considered as incidental hosts, while animal species moderately susceptible or resistant may be considered in terms of their role in the long term maintenance and spread of this bacterium.

Countless rodent species belonging to the Families of *Cricetidae* and *Muridae* are highly susceptible and sensitive to *F. tularensis*. They develop acute tularemia and succumb quickly after infection (Larson, 1945; Ditchfield et al., 1960; Mörner, 1992; Origgi et al., 2015). Several lagomorphs are similarly affected by this disease (Burroughs et al., 1945; Morner et al., 1988b; Park et al., 2009). It is worth mentioning that variabilities in sensitivity to *F. tularensis* among susceptible species are known. For example, the common rabbit (*Oryctolagus cuniculus*) was used to differentiate *F. tularensis* subsp. *tularensis* and *F. tularensis* subsp. *holarctica* and it is generally considered as susceptible but less sensitive to *F. tularensis* subsp. *holarctica* (Sjöstedt, 2015). Although *O. cuniculus* was found to be naturally infected with *F. tularensis* subsp. *holarctica*, more details about the health status of the rabbits and pathological lesions are required (Runge et al., 2011; Lopes de Carvalho et al., 2016). Moreover, the sensitivity of animal species was suggested to be influenced by rodenticides or pesticides released in the environment but this aspect needs confirmation (Vidal et al., 2009; Bandouchova et al., 2011). Sporadic cases or outbreaks in rodents and lagomorphs are frequently reported and these species are without doubt involved in a part of the life cycle of *F. tularensis* in the environment. However, not all species may be incidental hosts and the susceptibility and sensitivity of the different species should be carefully described. The situation in beavers is noteworthy and deserves more attention in the future. Beavers in North America (*Castor canadensis*) are known to be part of the enzootic cycle of *F. tularensis* (Scott, 1940; Jellison et al., 1942) and strains isolated from this animal species belong to *F. tularensis* subsp. *holarctica* (Mörner, 1992; Kugeler et al., 2009). However, only a few strains of *F. tularensis* subsp. *holarctica* were isolated from beavers in Europe (Sissonen et al., 2015; Schulze et al., 2016). *C. fiber* is the native species of beaver in Eurasia and this finding presents questions on the susceptibility of *C. fiber* to *F. tularensis*. *C. canadensis* was intentionally introduced in Eurasia in 1937, more specifically in Finland and populations still exist in an area spanning Finland and Russia (Parker et al., 2012). Interestingly, the two beaver isolates characterized by Sissonen and colleagues are from Finland and were isolated from *Castor* sp. meaning the exact species was not identified. However, the authors stated that those beavers were found in areas where only *C. canadensis* is known to live (Sissonen et al., 2015). Recently, *F. tularensis* subsp. *holarctica* was isolated from the carcass of an Eurasian beaver, *C. fiber*, found in the Berlin/Brandenburg region in Germany (Schulze et al., 2016). *C. fiber* was previously shown to raise antibodies against *F. tularensis* but isolation of the microorganism was not reported (Morner et al., 1988a). Investigations aiming to assess the susceptibility and sensitivity of *C. fiber* to *F. tularensis* should

be supported and more precisely, studies evaluating their cause of death, in association with serological studies.

Some other wildlife species of the Order *Soricomorpha* (previously named *Insectivora*) like *Talpa* sp. and the Order *Eulipotyphla* like *Sorex* sp. were also described as being naturally infected with *F. tularensis* (Kohls and Steinhau, 1943; Elashvili et al., 2015). Moreover, some non-human primate species are also considered as very susceptible species and reports of cases due to *F. tularensis* subsp. *tularensis* and *F. tularensis* subsp. *holarctica* in zoos were published (Posthaus et al., 1998; Hoelzle et al., 2004; Abril et al., 2007; Gyuranecz et al., 2009; Ketz-Riley et al., 2009). Occasional infections in birds were reported, mainly from North America but also from Sweden. Birds are generally considered as resistant to *F. tularensis* infection and as having no relevant role as hosts in the epidemiology of this bacterium (reviewed in Mörner, 2008).

Over the last decade, the quantity of studies detecting *F. tularensis* in wildlife animals and in the environment has risen extraordinarily. The increased awareness and number of animals tested, led to isolation of *F. tularensis* from species previously described as not being particularly susceptible to this bacterium e.g., species belonging to the Order Carnivora, like the red fox, *Vulpes vulpes*, or the stone marten, *Martes foina* (Origgi et al., 2013; Schulze et al., 2016). The relevance of these species in the cycle of *F. tularensis* and their epidemiological significance are still to be investigated but might represent single occurrences.

Production and companion animals, other than rodents and lagomorphs, are a particular concern because of their proximity to human beings. Tularemia in the domestic cat (*Felis catus*) is reported in North America. It seems to be mainly associated with *F. tularensis* subsp. *tularensis* but *F. tularensis* subsp. *holarctica* was also isolated from a few feline cases (Baldwin et al., 1991; Woods et al., 1998; Farlow et al., 2001; DeBey et al., 2002; Staples et al., 2006). Feline tularemia has not been reported outside North America. It is important to investigate if cases have been missed in other countries or if feline tularemia is principally due to *F. tularensis* subsp. *tularensis*, which is only circulating in North America, or is a consequence of other still unknown parameters. Dogs (*Canis familiaris*) appear to be more resistant to *F. tularensis* and until recently, most of the sporadic cases of tularemia were reported from North America (Meinkoth et al., 2004). However, a report of tularemia in a dog in Norway was published in 2014. The dog developed clinical manifestations after hunting a mountain hare (*L. timidus*). The case was investigated by serology and a 32-fold increase in titer in 2 weeks was noticed by the authors. However, the case could not be bacteriologically confirmed but *F. tularensis* subsp. *holarctica* was isolated from the bone marrow of the captured mountain hare (Nordstoga et al., 2014). Tularemia outbreaks in sheep (*Ovis aries*) were reported in North America and were associated with *F. tularensis* subsp. *tularensis* (O'Toole et al., 2008). More studies are needed regarding animals used for production as well as companion animals, with particularly emphasis on host specificity of the different subspecies of *F. tularensis*. This is necessary to confirm or refute which animal species can be naturally infected and can act as incidental or reservoir hosts. This information is crucial to understand the maintenance and

perpetuation of *F. tularensis* but also to evaluate the real risk for transmission to humans.

LINEAGES OF *F. TULARENSIS* AND ANIMAL SPECIES

The recent advent of new technologies and improvements in typing systems for *F. tularensis*, led to new perspectives, resulting in better understanding of the epidemiological situation of tularemia in animals. As mentioned above, many studies were performed in the last decade to characterize the population genetics of *F. tularensis* strain collections and some of these included animal strains. Moreover, few case reports comprise the typing of the isolated *F. tularensis*.

F. tularensis subsp. *tularensis* is divided into two clades A.I and A.II (Figure 1) (Farlow et al., 2005; Staples et al., 2006; Kugeler et al., 2009). Clade A.I predominates in Eastern North America, but occurs thorough North America, while A.II prevails in Western North America. In the study published by Kugeler et al. 184 animal strains were characterized and the authors observed a non-random distribution of the subspecies of *F. tularensis* in animals. In the case of lagomorph species there was an association with specific lineages (the classification used by Kugeler et al. is based on PFGE and not on canSNPs). Briefly, the strains from lagomorphs (cottontail rabbits and jackrabbits) were principally type A (90%, $n = 52$; total $N = 58$) and 40% of the 52 strains were A.I. Unfortunately, the lagomorph species was only described in 31 cases but still revealed remarkable information. All eight A.I strains were isolated from the eastern cottontail (*S. floridanus*) and the 23 strains isolated from the desert cottontail (*S. audubonii*) were A.II (Kugeler et al., 2009). Strains isolated from hares in Quebec, Canada, were all A.I but the hare species was not defined (Antonation et al., 2015). Six strains isolated from hares in Alaska were also A.I (Hansen et al., 2011). Kugeler and colleagues analyzed 44 feline strains and 41 belonged to the subspecies *tularensis*, with 80% percent of these strains being A.I (Kugeler et al., 2009). Interestingly, another study found that all but one feline isolate tested (total $N = 27$) were A.I (Larson et al., 2014).

Regarding *F. tularensis* subsp. *holarctica*, four clades are described: B.16 (*F. tularensis* subsp. *holarctica* biotype japonica), B.4, B.6, and B.12 (Figures 1, 2) (Svensson et al., 2009b; Karlsson et al., 2013). B.16 is found in Japan and Australia, B.4 is present in Eurasia and North America, B.6 is circulating in North America and Europe and B.12 in Eurasia and North America. Recently, an additional clade of *F. tularensis* subsp. *holarctica* from Tibet, China, was described by Lu et al. (2016). Although strains of *F. tularensis* subsp. *holarctica* are circulating in North America, Eurasia and Australia, a more in depth focus on the lineages of this subspecies was recently described in Eurasia. Unlike *F. tularensis* subsp. *tularensis*, differences in virulence among the lineages of *F. tularensis* subsp. *holarctica* are less clear. So far, a well-defined predilection of specific lineages of *F. tularensis* subsp. *holarctica* for particular host species was not identified (Figure 2). However, some recent observations deserve to be investigated in more detail. *F. tularensis* subsp. *holarctica* was

isolated from *L. europaeus* in many countries (Morner et al., 1988b; Gyuranecz et al., 2010; Decors et al., 2011; Müller et al., 2013; Rijks et al., 2013; Nordstoga et al., 2014; Origgi and Pilo, 2016; Hestvik et al., 2017). In Sweden, the first animal tularemia case was diagnosed in 1931 in the mountain hare (Hestvik et al., 2017). Mörner and colleagues also investigated the presence of *F. tularensis* in *L. europaeus* and *L. timidus* from Sweden but they could not detect it in *L. europaeus* (Morner et al., 1988b). The first case in the European brown hare in Sweden was only identified in 2002 (Hestvik et al., 2017). The reason for this late discovery is still unknown and merits further studies. In 2010, Gyuranecz and colleagues published a study describing the pathological lesions due to *F. tularensis* subsp. *holarctica* lineage B.13 in *L. europaeus*. The common finding of this study is a polyserotitis with the pericardium, the lung and the kidney as the main affected organs (Gyuranecz et al., 2010). However, Origgi and Pilo found that the most affected organs in *L. europaeus* infected with *F. tularensis* subsp. *holarctica* lineage B.FTNF002-00 [B.6, subgroup B18, this subgroup is specific to Western Europe (Dwibedi et al., 2016)] were the spleen and the liver (Origgi and Pilo, 2016). It has to be mentioned that the hares investigated by Gyuranecz and colleagues were hunted, while the hares investigated by Origgi and Pilo were terminally-ill. The group of Gyuranecz subsequently performed an experimental infection in Fischer 344 rats with strains belonging to both lineages (Kreizinger et al., 2017). They did not observe variance in pathological lesions due to the strains but found differences in weight loss values, recovery time, and mortality. In the study published by Hestvik and colleagues, the pathology resulting from natural infection with *F. tularensis* subsp. *holarctica* in the mountain hare and in the European brown hare was characterized. They found similar pathological lesions in both hare species. The lineages of the 23 strains of *F. tularensis* subsp. *holarctica* were characterized and seven found to belong to B.6 (subgroup B.7), while 16 were B.12 (basal sublineage B.26, subgroups B.23, B.39, and B.20) and originated from 21 *L. europaeus* and two *L. timidus*. No differences were observed in the pathological lesions due to both lineages (Hestvik et al., 2017). Sissonen and colleagues reported that among the strains analyzed in their study, one strain isolated from *L. timidus* was B.4 and one strain isolated from *L. europaeus* was B.6 sublineage B.7. Additionally, 50 strains were B.12 (24 from *L. timidus* and 26 from *L. europaeus*) (Sissonen et al., 2015).

In Japan, the lineage B.16 (*F. tularensis* subsp. *holarctica* biotype japonica) is often isolated from the Japanese hare, *L. brachyurus*. However, a recent report from Turkey identified a strain of *F. tularensis* subsp. *holarctica* B.16 based solely on phenotypic characteristics (Kilic et al., 2013). Moreover, the distribution of this lineage might be more extended than previously thought since *F. tularensis* subsp. *holarctica* biotype japonica was recently isolated in Australia from ringtail possums (*Pseudocheirus peregrinus*) (Eden et al., 2017). Finally, Wang and colleagues published a study including isolates of *F. tularensis* from the Tibetan region identified by canSNP analysis as belonging to the lineage B.16 (Wang et al., 2014). Lu and colleagues subsequently investigated isolates from the same region and some were also identified as B.16. However, these isolates do not ferment glycerol, which is a distinguishing

phenotype of *F. tularensis* subsp. *holarctica* biotype japonica. Analysis of region of differences (RD) and MLVA further showed an intermediate position of the Tibetan isolates between those belonging to lineage B.16 and those of the other lineages B.4, B.6, and B.12. The authors therefore proposed to add a major lineage to the subspecies *holarctica* (Lu et al., 2016).

A recent article published by Timofeev and colleagues analyzed 25 strains of *F. tularensis* subsp. *mediasiatica* and compared them to four strains previously analyzed by MLVA. Among those strains, seven were isolated from animals other than arthropods. One strain of M.II was isolated from a Siberian red vole and the six other strains belonged to M.I and were recovered from hares and gerbils (Timofeev et al., 2017).

These findings highlight the necessity to expand and intensify sampling, particularly in Asia and Oceania, to better understand the geographical and animal distribution of the lineages *F. tularensis* subsp. *holarctica* and *F. tularensis* subsp. *mediasiatica*.

CONCLUSION

Tularemia in animals is a vast topic and despite the large amount of research performed on *F. tularensis* in animals, many questions are still open. It is clear that rodent and lagomorph species are affected by this microorganism in all countries where *F. tularensis* is present. However, it is still unclear whether these animal species are important for long term maintenance of *F. tularensis* in the environment. In fact, details on which species are incidental or reservoir hosts are still to be defined with more precision. In this respect, serological methods are important and give useful information but for a full interpretation of the results, complementary investigations should be performed. Positive serological results inform about the infection of an animal with *F. tularensis* but does not necessarily imply the development of clinical manifestations or determine the potential shedding of *F. tularensis*. It would therefore be important when possible to couple serological studies with field observations and / or extra sampling to clarify these aspects in the future. Furthermore, the route of infection, the progress of the infection within different hosts, the host immune response of specific animal species and the role of ecological factors also merits more attention. Another noteworthy parameter to consider is that animal species belonging to other Orders than Rodentia and Lagomorpha are most of the time ignored in studies and during routine diagnostics. Additionally, the complexity of the ecology of *F. tularensis* means short studies may only reflect a partial picture of the situation and sustained and coordinated efforts will be required to unravel particularly striking observations. For example, epizootics or sporadic cases “appear” and “disappear,” sometimes without implementation of specific measures to control the disease (Dobay et al., 2015). This simple observation can raise a multitude of questions: Does the source of infection exist for a limited time? Do animal populations develop immunity? Are there major individual

variations in terms of susceptibility and sensitivity? Are biological and / or physical parameters involved? If yes, how and to which degree? This shows how little information is available and gives a modest insight into the questions that need to be answered.

The recently developed rapid sequencing technologies open novel perspectives for rational design of studies and are a great opportunity to better understand the ecology and epidemiology of *F. tularensis* in distinct geographical areas. Phylogenetic data of *F. tularensis* in animals is becoming available but is still fragmented and needs to be confirmed. The molecular tools available today are rapid and safe. Moreover, they allow a low or high resolution of typing and even enable the possibility to mix both depending on the questions to answer. For routine diagnostic laboratories, the most important analysis should lead to the confirmation of presence or absence of *F. tularensis*. These laboratories usually do not attempt to cultivate *F. tularensis* because of safety concerns and a very high resolution of typing is not always necessary. However, if a case is interesting enough for publication, authors might consider including both the animal species and the lineage of *F. tularensis*. A technical aspect deserving more development and extensive validation is the application of PCR for typing directly from clinical specimens. The establishment of protocols for typing without the requirement of previous cultivation of *F. tularensis* would be a useful development for diagnostic laboratories.

In summary, a large body of information is available about tularemia in animals, in particular concerning the animal species that are mostly affected. However, the numerous animal host species and number of subspecies of *F. tularensis* complicates the understanding of the biology in specific environments. More precision is needed in the definitions used to describe studies and the integration of several disciplines is crucial to overcome the complexity of *F. tularensis*. The development of methods to discriminate strains can add data to better understand variations in the ecology of this bacterium and research is currently being performed in this field. Additionally, extensive sampling including full documentation would be very informative about the evolution and genetic diversity of *F. tularensis* in animals. Hence, detailed field, clinical, pathological and laboratory information is crucial to subsequently test experimentally functional hypotheses on the spread and life style of *F. tularensis*.

AUTHOR CONTRIBUTIONS

The author confirms being the sole contributor of this work and approved it for publication.

ACKNOWLEDGMENTS

Work related to *Francisella tularensis* is supported by the Swiss Federal Office for the Environment (contract number 15.0023.KP / O234-1291).

REFERENCES

- Abril, C., Nimmervoll, H., Pilo, P., Brodard, I., Korczak, B., Seiler, M., et al. (2007). Rapid diagnosis and quantification of *Francisella tularensis* in organs of naturally infected common squirrel monkeys (*Saimiri Sciureus*). *Vet. Microbiol.* 127, 203–208. doi: 10.1016/j.vetmic.2007.08.006
- Antonation, K. S., Bekal, S., Cote, G., Dallaire, A., and Corbett, C. R. (2015). Multiple-locus variable-number tandem-repeat analysis of *Francisella tularensis* from Quebec, Canada. *Lett. Appl. Microbiol.* 60, 328–333. doi: 10.1111/lam.12371
- Baldwin, C. J., Panciera, R. J., Morton, R. J., Cowell, A. K., and Waurzyniak, B. J. (1991). Acute tularemia in three domestic cats. *J. Am. Vet. Med. Assoc.* 199, 1602–1605.
- Bandouchova, H., Pohanka, M., Kral, J., Ondracek, K., Osickova, J., Damkova, V., et al. (2011). Effects of sublethal exposure of European brown hares to paroxon on the course of tularemia. *Neuro. Endocrinol. Lett.* 32(Suppl. 1), 77–83.
- Bell, J. F., Owen, C. R., and Larson, C. L. (1955). Virulence of *Bacterium tularensis*. I. A study of the virulence of *Bacterium tularensis* in mice, guinea pigs, and rabbits. *J. Infect. Dis.* 97, 162–166. doi: 10.1093/infdis/97.2.162
- Birdsell, D. N., Johansson, A., Ohrman, C., Kaufman, E., Molins, C., Pearson, T., et al. (2014a). *Francisella tularensis* subsp. Tularensis group A.I, United States. *Emerg. Infect. Dis.* 20, 861–865. doi: 10.3201/eid2005.131559
- Birdsell, D. N., Vogler, A. J., Buchhagen, J., Clare, A., Kaufman, E., Naumann, A., et al. (2014b). TaqMan real-time PCR assays for single-nucleotide polymorphisms which identify *Francisella tularensis* and its subspecies and subpopulations. *PLoS ONE* 9:e107964. doi: 10.1371/journal.pone.0107964
- Burroughs, A. L., Holdenried, R., Longanecker, D. S., and Meyer, K. F. (1945). A field study of latent tularemia in rodents with a list of all known naturally infected vertebrates. *J. Infect. Dis.* 76, 115–119. doi: 10.1093/infdis/76.2.115
- Chanturia, G., Birdsell, D. N., Kekelidze, M., Zhgenti, E., Babuadze, G., Tsertsvadze, N., et al. (2011). Phylogeography of *Francisella tularensis* subspecies holarctica from the country of Georgia. *BMC Microbiol.* 11:139. doi: 10.1186/1471-2180-11-139
- Davis, G. E., Philip, C. B., and Parker, R. R. (1934). The isolation from the rocky mountain wood tick (*Dermacentor andersoni*) of strains of B. Tularensis of low virulence for guinea pigs and domestic rabbits. *Am. J. Epidemiol.* 19, 449–456. doi: 10.1093/oxfordjournals.aje.a118003
- DeBey, B. M., Andrews, G. A., Chard-Bergstrom, C., and Cox, L. (2002). Immunohistochemical demonstration of *Francisella tularensis* in lesions of cats with tularemia. *J. Vet. Diagn. Invest.* 14, 162–164. doi: 10.1177/104063870201400213
- Decors, A., Lesage, C., Jourdain, E., Giraud, P., Houbbron, P., Vanhem, P., et al. (2011). Outbreak of tularaemia in brown hares (*Lepus europaeus*) in France, January to March 2011. *Euro Surveill.* 16:19913.
- de la Puente-Redondo, V. A., del Blanco, N. G., Gutierrez-Martin, C. B., Garcia-Pena, F. J., and Rodriguez Ferri, E. F. (2000). Comparison of different PCR approaches for typing of *Francisella tularensis* strains. *J. Clin. Microbiol.* 38, 1016–1022.
- Ditchfield, J., Meads, E. B., and Julian, R. J. (1960). Tularemia of Muskrats in Eastern Ontario. *Canad. J. Pub. Health.* 51, 474–478.
- Dobay, A., Pilo, P., Lindholm, A. K., Origi, F., Bagheri, H. C., and Konig, B. (2015). Dynamics of a tularemia outbreak in a closely monitored free-roaming population of wild house mice. *PLoS ONE* 10:e0141103. doi: 10.1371/journal.pone.0141103
- Dwivedi, C., Birdsell, D., Larkeryd, A., Myrtennas, K., Ohrman, C., Nilsson, E., et al. (2016). Long-range dispersal moved *Francisella tularensis* into Western Europe from the East. *Microb. Genom.* 2:e000100. doi: 10.1099/mgen.0.000100
- Eden, J. S., Rose, K., Ng, J., Shi, M., Wang, Q., Sintchenko, V., et al. (2017). *Francisella tularensis* ssp. Holarctica in Ringtail Possums, Australia. *Emerg. Infect. Dis.* 23, 1198–1201. doi: 10.3201/eid2307.161863
- Elashvili, E., Kracalik, I., Burjanadze, I., Datukishvili, S., Chanturia, G., Tsertsvadze, N., et al. (2015). Environmental monitoring and surveillance of rodents and vectors for *Francisella tularensis* following outbreaks of human tularemia in Georgia. *Vector Borne Zoonotic Dis.* 15, 633–636. doi: 10.1089/vbz.2015.1781
- Eliasson, H., Broman, T., Forsman, M., and Back, E. (2006). Tularemia: current epidemiology and disease management. *Infect. Dis. Clin. North Am.* 20, 289–311. doi: 10.1016/j.idc.2006.03.002
- Farlow, J., Smith, K. L., Wong, J., Abrams, M., Lytle, M., and Keim, P. (2001). *Francisella tularensis* strain typing using multiple-locus, variable-number tandem repeat analysis. *J. Clin. Microbiol.* 39, 3186–3192. doi: 10.1128/JCM.39.9.3186-3192.2001
- Farlow, J., Wagner, D. M., Dukerich, M., Stanley, M., Chu, M., Kubota, K., et al. (2005). *Francisella tularensis* in the United States. *Emerg. Infect. Dis.* 11, 1835–1841. doi: 10.3201/eid1112.050728
- Fujita, O., Uda, A., Hotta, A., Okutani, A., Inoue, S., Tanabayashi, K., et al. (2008). Genetic diversity of *Francisella tularensis* subspecies holarctica strains isolated in Japan. *Microbiol. Immunol.* 52, 270–276. doi: 10.1111/j.1348-0421.2008.00036.x
- García Del Blanco, N., Dobson, M. E., Vela, A. I., De La Puente, V., Gutiérrez, C. B., Hadfield, T. L., et al. (2002). Genotyping of *Francisella tularensis* strains by pulsed-field gel electrophoresis, amplified fragment length polymorphism fingerprinting, and 16S rRNA gene sequencing. *J. Clin. Microbiol.* 40, 2964–2972. doi: 10.1128/JCM.40.8.2964-2972.2002
- Gyuranecz, M., Birdsell, D. N., Spletstoesser, W., Seibold, E., Beckstrom-Sternberg, S. M., Makrai, L., et al. (2012). Phylogeography of *Francisella tularensis* subsp. Holarctica, Europe. *Emerg. Infect. Dis.* 18, 290–293. doi: 10.3201/eid1802.111305
- Gyuranecz, M., Fodor, L., Makrai, L., Szoke, I., Janosi, K., Krisztalovics, K., et al. (2009). Generalized tularemia in a vervet monkey (*Chlorocebus aethiops*) and a patas monkey (*Erythrocebus patas*) in a zoo. *J. Vet. Diagn. Invest.* 21, 384–387. doi: 10.1177/104063870902100316
- Gyuranecz, M., Szeredi, L., Makrai, L., Fodor, L., Meszaros, A. R., Szepe, B., et al. (2010). Tularemia of European brown hare (*Lepus europaeus*): a pathological, histopathological, and immunohistochemical study. *Vet. Pathol.* 47, 958–963. doi: 10.1177/0300985810369902
- Hansen, C. M., Vogler, A. J., Keim, P., Wagner, D. M., and Hueffer, K. (2011). Tularemia in Alaska, 1938–2010. *Acta Vet. Scand.* 53:61. doi: 10.1186/1751-0147-53-61
- Hestvik, G., Uhlhorn, H., Sodersten, F., Akerstrom, S., Karlsson, E., Westergren, E., et al. (2017). Tularaemia in European Brown Hares (*Lepus europaeus*) and Mountain Hares (*Lepus timidus*) characterized by Histopathology and Immunohistochemistry: organ lesions and suggestions of routes of infection and shedding. *J. Comp. Pathol.* 157, 103–114. doi: 10.1016/j.jcpa.2017.06.003
- Hoelzle, L. E., Corboz, L., Ossent, P., and Wittenbrink, M. M. (2004). Tularaemia in a captive golden-headed lion tamarin (*Leontopithecus chrysomelas*) in Switzerland. *Vet. Rec.* 155, 60–61. doi: 10.1136/vr.155.2.60
- Hopla, C. E. (1974). The ecology of tularemia. *Adv. Vet. Sci. Comp. Med.* 18, 25–53.
- Jackson, J., McGregor, A., Cooley, L., Ng, J., Brown, M., Ong, C. W., et al. (2012). *Francisella tularensis* subspecies holarctica, Tasmania, Australia, 2011. *Emerg. Infect. Dis.* 18, 1484–1486. doi: 10.3201/eid1809.111856
- Jellison, W. L., Kohls, G. M., Butler, W. J., and Weaver, J. A. (1942). Epizootic tularemia in the beaver, *Castor canadensis*, and the contamination of stream water with *Pasteurella tularensis*. *Am. J. Epidemiol.* 36, 168–182. doi: 10.1093/oxfordjournals.aje.a118815
- Johansson, A., Farlow, J., Larsson, P., Dukerich, M., Chambers, E., Byström, M., et al. (2004). Worldwide genetic relationships among *Francisella tularensis* isolates determined by multiple-locus variable-number tandem repeat analysis. *J. Bacteriol.* 186, 5808–5818. doi: 10.1128/JB.186.17.5808-5818.2004
- Johansson, A., Goransson, I., Larsson, P., and Sjøstedt, A. (2001). Extensive allelic variation among *Francisella tularensis* strains in a short-sequence tandem repeat region. *J. Clin. Microbiol.* 39, 3140–3146. doi: 10.1128/JCM.39.9.3140-3146.2001
- Johansson, A., Ibrahim, A., Goransson, I., Eriksson, U., Gurycova, D., Clarridge, J. E. III, et al. (2000). Evaluation of PCR-based methods for discrimination of *Francisella* species and subspecies and development of a specific PCR that distinguishes the two major subspecies of *Francisella tularensis*. *J. Clin. Microbiol.* 38, 4180–4185.
- Karadenizli, A., Forsman, M., Simsek, H., Taner, M., Ohrman, C., Myrtennas, K., et al. (2015). Genomic analyses of *Francisella tularensis* strains confirm disease transmission from drinking water sources, Turkey, 2008, 2009 and 2012. *Euro Surveill.* 20:21136. doi: 10.2807/1560-7917.ES2015.20.21.21136
- Karlsson, E., Svensson, K., Lindgren, P., Byström, M., Sjödin, A., Forsman, M., et al. (2013). The phylogeographic pattern of *Francisella tularensis* in Sweden indicates a Scandinavian origin of Eurosiberian tularaemia. *Environ. Microbiol.* 15, 634–645. doi: 10.1111/1462-2920.12052

- Kayser, P., Seibold, E., Matz-Rensing, K., Pfeffer, M., Essbauer, S., and Spletstoesser, W. D. (2008). Re-emergence of tularemia in Germany: presence of *Francisella tularensis* in different rodent species in endemic areas. *BMC Infect. Dis.* 8:157. doi: 10.1186/1471-2334-8-157
- Ketz-Riley, C. J., Kennedy, G. A., Carpenter, J. W., Zeidner, N. S., and Petersen, J. M. (2009). Tularemia type A in captive Bornean orangutans (*Pongo pygmaeus pygmaeus*). *J. Zoo Wildl. Med.* 40, 257–262. doi: 10.1638/2007-0170.1
- Kilic, S., Birdsell, D. N., Karagoz, A., Celebi, B., Bakaloglu, Z., Arikan, M., et al. (2015). Water as source of *Francisella tularensis* infection in humans, Turkey. *Emerg. Infect. Dis.* 21, 2213–2216. doi: 10.3201/eid2112.150634
- Kilic, S., Celebi, B., Acar, B., and Atas, M. (2013). *In vitro* susceptibility of isolates of *Francisella tularensis* from Turkey. *Scand. J. Infect. Dis.* 45, 337–341. doi: 10.3109/00365548.2012.751125
- Kohls, G. M., and Steinhilber, E. A. (1943). Tularemia: spontaneous occurrence in shrews. *Public Health Rep.* 58, 842–842. doi: 10.2307/4584475
- Kreuzinger, Z., Erdelyi, K., Felde, O., Fabbri, M., Sulyok, K. M., Magyar, T., et al. (2017). Comparison of virulence of *Francisella tularensis* ssp. holarctica genotypes B.12 and B.FTNF002-00. *BMC Vet. Res.* 13:46. doi: 10.1186/s12917-017-0968-9
- Kugeler, K. J., Mead, P. S., Janusz, A. M., Staples, J. E., Kubota, K. A., Chalcraft, L. G., et al. (2009). Molecular epidemiology of *Francisella tularensis* in the United States. *Clin. Infect. Dis.* 48, 863–870. doi: 10.1086/597261
- Larson, C. L. (1945). The susceptibility of the golden hamster (*Cricetus auratus*) to Tularemia. *Public Health Rep.* 60, 839–841. doi: 10.2307/4585319
- Larson, M. A., Fey, P. D., Hinrichs, S. H., and Iwen, P. C. (2014). *Francisella tularensis* bacteria associated with feline tularemia in the United States. *Emerg. Infect. Dis.* 20, 2068–2071. doi: 10.3201/eid2012.131101
- Larsson, P., Svensson, K., Karlsson, L., Guala, D., Granberg, M., Forsman, M., et al. (2007). Canonical insertion-deletion markers for rapid DNA typing of *Francisella tularensis*. *Emerg. Infect. Dis.* 13, 1725–1732. doi: 10.3201/eid1311.070603
- Lopes de Carvalho, I., Toledo, A., Carvalho, C. L., Barandika, J. F., Respcio-Kingry, L. B., Garcia-Amil, C., et al. (2016). *Francisella* species in ticks and animals, Iberian Peninsula. *Ticks Tick Borne Dis.* 7, 159–165. doi: 10.1016/j.ttbdis.2015.10.009
- Lu, Y., Yu, Y., Feng, L., Li, Y., He, J., Zhu, H., et al. (2016). Phylogeography of *Francisella tularensis* from Tibet, China: evidence for an asian origin and radiation of holarctica-type tularemia. *Ticks Tick Borne Dis.* 7, 865–868. doi: 10.1016/j.ttbdis.2016.04.001
- McCoy, G. W. (1911). A plague-like disease of rodents. *Public Health Bull.* 43, 53–71.
- McCoy, G. W., and Chapin, C. W. (1912). Further observations on a plague-like disease of rodents with a preliminary note on the causative agent, *Bacterium tularense*. *J. Infect. Dis.* 10, 61–72. doi: 10.1093/infdis/10.1.61
- Meinkoth, K. R., Morton, R. J., and Meinkoth, J. H. (2004). Naturally occurring tularemia in a dog. *J. Am. Vet. Med. Assoc.* 225, 545–547. doi: 10.2460/javma.2004.225.545
- Molins, C. R., Delorey, M. J., Yockey, B. M., Young, J. W., Sheldon, S. W., Reese, S. M., et al. (2010). Virulence differences among *Francisella tularensis* subsp. *Tularensis* clades in mice. *PLoS ONE* 5:e10205. doi: 10.1371/journal.pone.0010205
- Mörner, T. (1992). The ecology of tularemia. *Rev. Off. Int. Epizoot.* 11, 1123–1130. doi: 10.20506/rst.11.4.657
- Mörner, T. (2008). “Tularemia,” in *Infectious Diseases of Wild Birds*, eds N. J. Thomas, D. Bruce Hunter, and C. T. Atkinson (Ames, IA: Blackwell Publishing Professional), 352–359. doi: 10.1002/9780470344668.ch19
- Mörner, T., and Addison, E. (2008). “Tularemia,” in *Infectious Diseases of Wild Mammals*, eds E. S. Williams and I. K. Barker (Ames, IA: Iowa State University Press), 303–312. doi: 10.1002/9780470344880.ch18
- Morner, T., Sandstrom, G., and Mattsson, R. (1988a). Comparison of serum and lung extracts for surveys of wild animals for antibodies to *Francisella tularensis* biovar palaeartica. *J. Wildl. Dis.* 24, 10–14. doi: 10.7589/0090-3558-24.1.10
- Morner, T., Sandstrom, G., Mattsson, R., and Nilsson, P. O. (1988b). Infections with *Francisella tularensis* biovar palaeartica in hares (*Lepus timidus*, *Lepus europaeus*) from Sweden. *J. Wildl. Dis.* 24, 422–433. doi: 10.7589/0090-3558-24.3.422
- Müller, W., Hotzel, H., Otto, P., Karger, A., Bettin, B., Bocklisch, H., et al. (2013). German *Francisella tularensis* isolates from European brown hares (*Lepus europaeus*) reveal genetic and phenotypic diversity. *BMC Microbiol.* 13:61. doi: 10.1186/1471-2180-13-61
- Myrtennas, K., Marinov, K., Johansson, A., Niemcewicz, M., Karlsson, E., Bystrom, M., et al. (2016). Introduction and persistence of tularemia in Bulgaria. *Infect. Ecol. Epidemiol.* 6:32838. doi: 10.3402/iee.v6.32838
- Nordstoga, A., Handeland, K., Johansen, T. B., Iversen, L., Gavier-Widen, D., Mattsson, R., et al. (2014). Tularemia in Norwegian dogs. *Vet. Microbiol.* 173, 318–322. doi: 10.1016/j.vetmic.2014.06.031
- Olsufjev, N. G., and Meshcheryakova, I. S. (1982). Intraspecific taxonomy of tularemia agent *Francisella tularensis* McCoy et Chapin. *J. Hyg. Epidemiol. Microbiol. Immunol.* 26, 291–299.
- Oraggi, F. C., Frey, J., and Pilo, P. (2014). Characterisation of a new group of *Francisella tularensis* subsp. *Holarctica* in Switzerland with altered antimicrobial susceptibilities, 1996 to 2013. *Euro Surveill.* 19:20858. doi: 10.2807/1560-7917.ES2014.19.29.20858
- Oraggi, F. C., König, B., Lindholm, A. K., Mayor, D., and Pilo, P. (2015). Tularemia among free-ranging mice without infection of exposed humans, Switzerland, 2012. *Emerg. Infect. Dis.* 21, 133–135. doi: 10.3201/eid2101.140906
- Oraggi, F. C., and Pilo, P. (2016). *Francisella tularensis* clades B.FTN002-00 and B.13 are associated with distinct pathology in the European Brown hare (*Lepus europaeus*). *Vet. Pathol.* 53, 1220–1232. doi: 10.1177/0300985816629718
- Oraggi, F. C., Wu, N., and Pilo, P. (2013). *Francisella tularensis* infection in a stone marten (*Martes foina*) without classic pathological lesions consistent with tularemia. *J. Vet. Diagn. Invest.* 25, 519–521. doi: 10.1177/1040638713489124
- O’Toole, D., Williams, E. S., Woods, L. W., Mills, K., Boerger-Fields, A., Montgomery, D. L., et al. (2008). Tularemia in range sheep: an overlooked syndrome? *J. Vet. Diagn. Invest.* 20, 508–513. doi: 10.1177/104063870802000417
- Park, C. H., Nakanishi, A., Hatai, H., Kojima, D., Oyama, T., Sato, H., et al. (2009). Pathological and microbiological studies of Japanese Hare (*Lepus brachyurus angustidens*) naturally infected with *Francisella tularensis* subsp. *holarctica*. *J. Vet. Med. Sci.* 71, 1629–1635. doi: 10.1292/jvms.001629
- Parker, H., Nummi, P., Hartmann, G., and Rosell, F. (2012). Invasive North American beaver *Castor canadensis* in Eurasia: a review of potential consequences and a strategy for eradication. *Wildlife Biol.* 18, 354–365. doi: 10.2981/12-007
- Petersen, J. M., Mead, P. S., and Schriefer, M. E. (2009). *Francisella tularensis*: an arthropod-borne pathogen. *Vet. Res.* 40:7. doi: 10.1051/vetres:2008045
- Philip, C. B., and Davis, G. E. (1935). Tularemia: observations on a strain of low initial virulence from rabbit ticks. *Public Health Rep.* 50, 909–911. doi: 10.2307/4581587
- Posthaus, H., Welle, M., Mörner, T., Nicolet, J., and Kuhnert, P. (1998). Tularemia in a common marmoset (*Callithrix jacchus*) diagnosed by 16S rRNA sequencing. *Vet. Microbiol.* 61, 145–150. doi: 10.1016/S0378-1135(98)00180-1
- Rijks, J. M., Kik, M., Koene, M. G., Engelsma, M. Y., van Tulden, P., Montizaan, M. G., et al. (2013). Tularemia in a brown hare (*Lepus europaeus*) in 2013: first case in the Netherlands in 60 years. *Euro Surveill.* 18:20655. doi: 10.2807/1560-7917.ES2013.18.49.20655
- Rodriguez-Pastor, R., Escudero, R., Vidal, D., Mougeot, F., Arroyo, B., Lambin, X., et al. (2017). Density-dependent prevalence of *Francisella tularensis* in fluctuating vole populations, Northwestern Spain. *Emerg. Infect. Dis.* 23, 1377–1379. doi: 10.3201/eid2308.161194
- Rossow, H., Sissonen, S., Koskela, K. A., Kinnunen, P. M., Hemmilä, H., Niemimaa, J., et al. (2014). Detection of *Francisella tularensis* in voles in Finland. *Vector Borne Zoonotic Dis.* 14, 193–198. doi: 10.1089/vbz.2012.1255
- Runge, M., von Keyserlingk, M., Braune, S., Voigt, U., Grauer, A., Pohlmeier, K., et al. (2011). Prevalence of *Francisella tularensis* in brown hare (*Lepus europaeus*) populations in Lower Saxony, Germany. *Eur. J. Wildl. Res.* 57, 1085–1089. doi: 10.1007/s10344-011-0522-1
- Schulze, C., Heuner, K., Myrtennas, K., Karlsson, E., Jacob, D., Kutzer, P., et al. (2016). High and novel genetic diversity of *Francisella tularensis* in Germany and indication of environmental persistence. *Epidemiol. Infect.* 144, 3025–3036. doi: 10.1017/S0950268816001175
- Scott, J. W. (1940). Natural occurrence of tularemia in Beaver and its transmission to man. *Science* 91, 263–264. doi: 10.1126/science.91.2359.263
- Sissonen, S., Rossow, H., Karlsson, E., Hemmila, H., Henttonen, H., Isomursu, M., et al. (2015). Phylogeography of *Francisella tularensis*

- subspecies holarctica in Finland, 1993–2011. *Infect. Dis.* 47, 701–706. doi: 10.3109/23744235.2015.1049657
- Sjöstedt, A. B. (2015). “Francisella,” in *Bergey’s Manual of Systematics of Archaea and Bacteria*, ed W. B. Whitman (Hoboken, NJ: John Wiley and Sons Ltd), 1–18. doi: 10.1002/9781118960608
- Staples, J. E., Kubota, K. A., Chalcraft, L. G., Mead, P. S., and Petersen, J. M. (2006). Epidemiologic and molecular analysis of human tularemia, United States, 1964–2004. *Emerg. Infect. Dis.* 12, 1113–1118. doi: 10.3201/eid1207.051504
- Svensson, K., Bäck, E., Eliasson, H., Berglund, L., Larsson, P., Granberg, M., et al. (2009a). Landscape epidemiology of tularemia outbreaks in Sweden. *Emerg. Infect. Dis.* 15, 1937–1947. doi: 10.3201/eid1512.090487
- Svensson, K., Granberg, M., Karlsson, L., Neubauerova, V., Forsman, M., and Johansson, A. (2009b). A real-time PCR array for hierarchical identification of *Francisella* isolates. *PLoS ONE* 4:e8360. doi: 10.1371/journal.pone.0008360
- Telford, S. R. 3rd, and Goethert, H. K. (2010). Toward an understanding of the perpetuation of the agent of tularemia. *Front. Microbiol.* 1:150. doi: 10.3389/fmicb.2010.00150
- Thomas, R., Johansson, A., Neeson, B., Isherwood, K., Sjöstedt, A., Ellis, J., et al. (2003). Discrimination of human pathogenic subspecies of *Francisella tularensis* by using restriction fragment length polymorphism. *J. Clin. Microbiol.* 41, 50–57. doi: 10.1128/JCM.41.1.50-57.2003
- Timofeev, V., Bakhteeva, I., Titareva, G., Kopylov, P., Christiany, D., Mokrievich, A., et al. (2017). Russian isolates enlarge the known geographic diversity of *Francisella tularensis* subsp. *mediasiatica*. *PLoS ONE* 12:e0183714. doi: 10.1371/journal.pone.0183714
- Vidal, D., Alzaga, V., Luque-Larena, J. J., Mateo, R., Arroyo, L., and Vinuela, J. (2009). Possible interaction between a rodenticide treatment and a pathogen in common vole (*Microtus arvalis*) during a population peak. *Sci. Total Environ.* 408, 267–271. doi: 10.1016/j.scitotenv.2009.10.001
- Vogler, A. J., Birdsell, D. N., Lee, J., Vaissaire, J., Doujet, C. L., Lapalus, M., et al. (2011). Phylogeography of *Francisella tularensis* ssp. *holarctica* in France. *Lett. Appl. Microbiol.* 52, 177–180. doi: 10.1111/j.1472-765X.2010.02977.x
- Vogler, A. J., Birdsell, D., Price, L. B., Bowers, J. R., Beckstrom-Sternberg, S. M., Auerbach, R. K., et al. (2009). Phylogeography of *Francisella tularensis*: global expansion of a highly fit clone. *J. Bacteriol.* 191, 2474–2484. doi: 10.1128/JB.01786-08
- Wang, Y., Peng, Y., Hai, R., Xia, L., Li, H., Zhang, Z., et al. (2014). Diversity of *Francisella tularensis* subsp. *holarctica* lineages, China. *Emerg. Infect. Dis.* 20, 1191–1194. doi: 10.3201/eid2007.130931
- Wherry, W. B., and Lamb, B. H. (1914). Infection of man with *Bacterium tularensis*. *J. Infect. Dis.* 15, 331–340. doi: 10.1093/infdis/15.2.331
- WHO. (2007). *WHO Guidelines of Tularemia*. Geneva: World Health Organization WHO.
- Woods, J. P., Crystal, M. A., Morton, R. J., and Panciera, R. J. (1998). Tularemia in two cats. *J. Am. Vet. Med. Assoc.* 212, 81–83.

Conflict of Interest Statement: The author declares that the research was conducted in the absence of any commercial or financial relationships that could be construed as a potential conflict of interest.

Copyright © 2018 Pilo. This is an open-access article distributed under the terms of the Creative Commons Attribution License (CC BY). The use, distribution or reproduction in other forums is permitted, provided the original author(s) and the copyright owner(s) are credited and that the original publication in this journal is cited, in accordance with accepted academic practice. No use, distribution or reproduction is permitted which does not comply with these terms.



Cross Sectional Study and Risk Factors Analysis of *Francisella tularensis* in Soil Samples in Punjab Province of Pakistan

OPEN ACCESS

Edited by:

Marina Šantić,
University of Rijeka, Croatia

Reviewed by:

Ronald Mark Wooten,
University of Toledo, United States
Kuldeep Dhama,
Indian Veterinary Research Institute
(IVRI), India

Umer Naveed Chaudhry,
Roslin Institute, University
of Edinburgh, United Kingdom

*Correspondence:

Masood Rabbani
mrabbani@uvas.edu.pk

Specialty section:

This article was submitted to
Bacteria and Host,
a section of the journal
Frontiers in Cellular and Infection
Microbiology

Received: 20 August 2018

Accepted: 12 March 2019

Published: 05 April 2019

Citation:

Muhammad J, Rabbani M,
Shabbir MZ, Muhammad K, Ghori MT,
Chaudhry HR, UI Hassnain Z, Jamil T,
Abbas T, Chaudhry MH,
Haisem-ur-Rasool M, Ali MA, Nisar M,
Kirimanjeswara GS and Jayarao BM
(2019) Cross Sectional Study and Risk
Factors Analysis of *Francisella
tularensis* in Soil Samples in Punjab
Province of Pakistan.
Front. Cell. Infect. Microbiol. 9:89.
doi: 10.3389/fcimb.2019.00089

Javed Muhammad^{1,2}, Masood Rabbani^{1*}, Muhammad Zubair Shabbir¹,
Khushi Muhammad¹, Muhammad Taslim Ghori³, Haroon Rashid Chaudhry³,
Zia UI Hassnain¹, Tariq Jamil¹, Tariq Abbas⁴, Muhammad Hamid Chaudhry⁵,
Muhammad Haisem-ur-Rasool¹, Muhammad Asad Ali¹, Muhammad Nisar⁴,
Girish S. Kirimanjeswara⁶ and Bhushan M. Jayarao⁶

¹ University of Veterinary and Animal Sciences, Lahore, Pakistan, ² University of Swabi, Swabi, Pakistan, ³ The Islamia University, Bahawalpur, Pakistan, ⁴ Department of Epidemiology and Public Health, Cholistan University of Veterinary and Animal Sciences, Bahawalpur, Pakistan, ⁵ GIS Centre, University of the Punjab, Lahore, Pakistan, ⁶ The Pennsylvania State University, University Park, PA, United States

Tularemia is an endemic zoonotic disease in many parts of the world including Asia. A cross-sectional study was conducted to determine genome-based prevalence of *Francisella tularensis* (*Ft*) in soil, assess an association between its occurrence in soil and likely predictors i.e., macro and micro-nutrients and several categorical variables, and determine seroconversion in small and large ruminants. The study included a total of 2,280 soil samples representing 456 villages in eight districts of the Punjab Province of Pakistan followed by an analysis of serum antibodies in 707 ruminants. The genome of *Ft* was detected in 3.25% ($n = 74$, 95% CI: 2.60–4.06) of soil samples. Soluble salts (OR: 1.276, 95% CI: 1.043–1.562, $p = 0.015$), Ni (OR: 2.910, 95% CI: 0.795–10.644, $p = 0.106$), Mn (OR: 0.733, 95% CI: 0.565–0.951, $p = 0.019$), Zn (OR: 4.922, 95% CI: 0.929–26.064, $p = 0.061$) and nutrients clustered together as PC-1 (OR: 4.76, 95% CI: 2.37–9.54, $p = 0.000$) and PC-3 (OR: 0.357, 95% CI: 0.640, $p = 0.001$) were found to have a positive association for the presence of *Ft* in soil. The odds of occurrence of *Ft* DNA in soil were higher at locations close to a water source, including canals, streams or drains, [$\chi^2 = 6.7$, OR = 1.19, 95% CI: 1.05–3.09, $p = 0.004$] as well as places where animals were present [$\chi^2 = 4.09$, OR = 2.06, 95% CI: 1.05–4.05, $p = 0.02$]. The seroconversion was detected in 6.22% ($n = 44$, 95% CI: 4.67–8.25) of domestic animals. An occurrence of *Ft* over a wide geographical region indicates its expansion to enzootic range, and demonstrates the need for further investigation among potential disease reservoirs and at-risk populations, such as farmers and veterinarians.

Keywords: *Francisella tularensis*, soil, domestic animals, Punjab province, Pakistan

INTRODUCTION

Tularemia is caused by the bacterium *Francisella tularensis* (*Ft*), a category A classified select agent by the Center for Disease Control and Prevention (<https://www.selectagents.gov/SelectAgentsandToxinsList.html>). *Francisella tularensis* (*Ft*) is a pleomorphic Gram-negative intracellular bacterium (Schulert and Allen, 2006) that has zoonotic implications across many parts of the globe (Oyston, 2008; Vogler et al., 2009). Four subspecies, namely, *tularensis*, *mediasiatica*, *holarctica*, and *novicida*, have been identified (Sjösted, 2005; Champion et al., 2009; Penn, 2015). The presence of *Ft* subspecies *holarctica* has been reported in Europe and Asia, whereas *Ft* subspecies *tularensis* has been reported in North America (Garaizar et al., 2006). Among the Asian countries, most of the outbreaks and cases have been reported in Turkey (607 cases in 2012), China (31 cases in 1986), and Iran (36 cases in 2013) (Esmaili et al., 2014; Gürçan, 2014). The organism has a broad and complex host distribution that includes vertebrates, invertebrates, and environmental matrices such as soil, aerosols, and water (Kuske et al., 2006; Silvestri et al., 2016). Humans can acquire infection through inhalation, an arthropod bite, ingestion of contaminated food, or water, as well as through contact with infected tissues or fluid from animals (Oyston, 2008; Ulu-Kilic and Doganay, 2014; Silvestri et al., 2016). Individuals living in rural areas or those in close proximity to animals/disease reservoirs, especially farmers and veterinarians, are considered the most at-risk population for tularemia (Lévesque et al., 1995; Ulu-Kilic and Doganay, 2014). Though glandular, oculo-glandular, ulcero-glandular, typhoidal, and pneumonic symptoms are common in affected humans, the clinical signs and severity of disease depend on the entry route and infectivity dose (<10 CFU) (Helvacı et al., 2000; Bossi et al., 2004; Pechous et al., 2009). Just as in humans, clinical signs in animals are varied. Cats are more susceptible than dogs and remain mostly in non-clinical form however in some cases, symptoms may include fever, lymphadenopathy, anorexia, oral ulceration, hepatosplenomegaly, and dehydration (Gliatto et al., 1994; Woods et al., 1998).

Different subspecies of *Ft* have been reported worldwide with varying geographic distribution and disease potential. Occurrence of tularemia caused by the most virulent type (*F. tularensis*: biovar A) has been reported only from North America, while cases caused by the less virulent type (*F. holarctica*: biovar B) have been observed in Europe, North America, and Asia (Garaizar et al., 2006; Oyston, 2008; Esmaili et al., 2014; Ulu-Kilic and Doganay, 2014). However, there is a paucity of data on the enzootic range of *Ft* in Pakistan. Since *Ft* has the potential to survive and persist in the environment for a longer period of time (Sjöstedt, 2007), we undertook a study to determine the prevalence of *Ft* in soil from eight districts of Punjab province of Pakistan followed by an evaluation of seroconversion in small and large ruminants. Besides several soil characteristics that included macro- and micronutrients, the study also examined likely risk factors that could be associated with its occurrence in soil, and therefore can contribute toward human and animal exposures. It is anticipated that the findings will be valuable to local, as well as global public health agencies for

evaluating potential disease burden, identifying reservoirs, and developing strategies to prevent and control tularemia in animal and human populations.

MATERIALS AND METHODS

Study and Sampling Design

A cross-sectional study was conducted in Punjab province (31.1704°N and 72.7097°E) from 2011 to 2015. The province has nine administrative divisions, 36 districts and approximate 4,883 villages. It dominates agriculture, and has the largest human and livestock populations in the country. Punjab province contains five rivers (“punj” means five and “ab” means water) which together provide one of the country’s largest irrigation systems for agricultural cultivation. Besides rivers and canals, ground-water (tube-well) as well as natural rain (barani) are being used to irrigate some of the areas in the province. Though mechanical (automatic) plowing is widespread across many districts in the province, animal-based plowing (manual) is also employed at some places in the province. We used three-stage sampling design. Since an incidence rate of *Ft* in Pakistan is not known, we selected districts representing the main livestock production areas of the province where there exists an increased annual incidence of human and animal disease (Directorates of Human and Animal Health, Punjab Province).

Assuming 50% prevalence, 95% CI and 5% margin of error, the required number of villages was 357, however, we included 456 villages representing 10% of each of the study district to increase the validity of the results using WinEpi software (<http://www.winepi.net/uk/sample/indice.htm>). From each village, we conveniently selected five sites for soil sampling; four were from livestock barns where human and animals were living in close proximity, while one represented an agricultural land only. The geographical coordinates were noted using Garmin (Dakota, U.S.A). After removing 3–5 inches of top-surface soil at each site, a total of 2,280 sample (~250–300 gram each) were collected from 456 villages representing districts Sheikhpura ($n = 295$), Gujranwala ($n = 360$), Faisalabad ($n = 370$), Sargodha ($n = 370$), Sahiwal ($n = 255$), D.G. Khan ($n = 215$), Chakwal ($n = 190$), and Attock ($n = 225$). A brief history of each study site along with information about different categorical variables or risk factors such as distance from animal market, main road and water source, animal’s density in a village, number of households in a village, number of domestic animals in a village, cover ground (vegetation) was recorded (Table 1).

Genome Extraction and PCR Based Identification

Genomic DNA was extracted from 0.25 gram of each soil sample (PowerSoil® DNA Isolation Kit, MoBio, USA) as per manufacturer’s instruction, and was subjected to real time PCR (CFX 96, BioRad, USA) using a highly sensitive and specific assay (Christensen et al., 2006) with minor modifications. The quantification of DNA was performed using the NanoDrop 1000 spectrophotometer (Thermo scientific, USA). The used real time PCR (RT-PCR) primers (Forward:

TABLE 1 | Eigenvalues and percentage of inertia explained by each principal component.

Component	Initial eigenvalues			Extraction sums of squared loadings		
	Total	% of Variance	Cumulative %	Total	% of Variance	Cumulative %
1	2.143	30.619	30.619	2.143	30.619	30.619
2	1.914	27.339	57.957	1.914	27.339	57.957
3	1.351	19.299	77.256	1.351	19.299	77.256
4	0.895	12.783	90.039			
5	0.348	4.978	95.017			
6	0.285	4.076	99.093			
7	0.064	0.907	100.000			

5'-CAGCATAACAATAAACCCACAAGG-3' and Reverse: 5'-TCAGCATACTTAGTAATTGGGAAGC-3') and probe [5' (FAM)-TTACAAATGGCAGGCTCCAGAAGGTT-3' (TAMRA)], which targeted the *tul4* gene (Lipoprotein/outer-membrane protein, 103 bp). A 25 μ L reaction was comprised of a final concentration of 1X PCR buffer, 5 mM of MgCl₂, 0.25 mM of dNTPs, 0.25 mg/mL of bovine serum albumin, 0.6 μ M of each of forward and reverse primer, 0.025 μ M of probe and 0.5 U of Taq-polymerase along with soil-extracted genomic DNA (10–30 ng). Thermal cycling conditions included one cycle of 95°C for 5 min followed by 45 cycles of each of denaturation at 94°C for 5 s and annealing at 60°C for 20 s, and then one cycle of cooling at 40°C for 1 min. The assay was optimized and validated using the control (*tul4* gene PCR products) and the proficiency testing samples that were kindly provided by the Pennsylvania State University, USA. The necessary assay controls such as dsDNA PCR product (positive control) and dDiethyl-pyrocyanate water (negative control) were used each time. To rule out any potential contamination in processing and/or false-positivity, each sample that exhibited a positive result was gel-electrophoresed (**Supplementary Material**), and the process described above was repeated thrice beginning from the genome extraction.

Serum Analysis

Blood samples (~5 mL) were collected conveniently from *Ft*-positive site representing goat ($n = 200$), sheep ($n = 175$), cattle ($n = 179$), and buffalo ($n = 153$) representing district Chakwal, Gujranwala, Faisalabad, Attock, Sahiwal, Sargodha, and Dera Ghazi Khan in Punjab Province, Pakistan. The separated sera were stored at -80°C until further use. Sera (1 μ L) were analyzed for anti-*Ft*-enzyme linked immunosorbent assay (ELISA) antibodies using an SERION ELISA classic *Ft* kit (Virion/Serion, Germany) according to the manufacturer's instructions. A specific secondary alkaline phosphatase antibody (ThermoFisher, USA) was used for goat (F(ab')₂-rabbit anti-goat IgG H+L), sheep (F(ab')₂-donkey anti-sheep IgG H+L), cattle (goat anti-bovine IgG (H+L)), and buffalo (goat anti-bovine IgG H+L). Optical density of sera were read within 60 min at 405 nm against substrate blank and 655 for reference and field samples as per manufacturer's recommendations. Only valid samples with OD value of substrate blank <0.25 and variation between OD values of standard serums not higher than 20% were

considered for further analysis. The positive and negative serum samples were analyzed using Microsoft[®] Excel-based software tool SERION activity with reference to lower cut off value 0.42 and upper cut off value 1.43 provided by manufacturer. Samples below the lower cut off value were considered as negative while samples above the upper cut off value were measured as positive.

Soil Chemistry Analysis and Risk Factors

Soil samples (~500 g) were analyzed, using previously optimized protocols for pH (Committee et al., 1978), moisture (McLean, 1982), texture (Robert and Frederick, 1995), total soluble salts (Magistad et al., 1945), phosphorus (Brown, 1998), copper, chromium, calcium, nickel, manganese, iron, cobalt, lead, cadmium, sodium, magnesium, and potassium (Soltanpour and Schwab, 1977), nitrogen (Fierer et al., 2001), and organic matter (Nelson and Sommers, 1982).

Statistical Analysis

The RT-PCR results along with numerical (soil characteristics) and categorical variables (potential risk factors) were compiled into a Microsoft Excel spreadsheet. In an earlier study (Muhammad et al., 2017), we described association between physio-chemical characteristics of soil and the presence/absence of *Ft* DNA in soil samples. In this study, we further explored these data and other potential variables to quantify factors associated with detection of bacterial DNA in soil. The data on physio-chemical characteristics of soil were not normally distributed (Shapiro-Wilk test, $p \leq 0.05$); therefore, Mann-Whitney *U*-test was applied to assess the effect of those numeric variables on soil positivity. In **Figure 2** the variables with $p \geq 0.2$ were included in further analyses. The correlation matrix plot revealed collinearity among the selected variables, and correlated variables ($r \geq 0.3$) were subjected to principal component analysis (PCA) (Abdi and Williams, 2010; Pourhoseingholi et al., 2012). PCA reduces dimensionality in the data and transforms the variables into a new set of uncorrelated variables called principal components. The Bartlett test of sphericity was significant ($p < 0.05$) and The Kaiser–Meyer–Olkin (KMO) measure of sampling adequacy was 0.582 ($p < 0.05$), indicating appropriateness of dataset for PCA. The first three principal components had an eigenvalue >1 and were used as covariates in binary logistic regression. A Chi Square test was used to evaluate association between the occurrence of *Ft* DNA in soil and categorical variables. A Fisher

Exact test was used as alternative to Chi square test where any of its assumption was violated. The regression model included the presence/absence of *Ft* DNA in soil samples as a dependent variable. The independent variables in the model were moisture, P, Ni, Mn, Na, Zn, PC1, PC2, and PC3. The model also included categorical variables with $p \geq 0.2$. A backward likelihood ratio method was used to select covariates in the regression. A $p \leq 0.05$ was considered significant in the outcome of regression analysis (Nandi et al., 2016). The data were analyzed in R using “FactoMineR,” “factoextra,” and “corrplot” packages (Table 3).

RESULTS

The Prevalence of *Ft* in the Soil of the Studied Districts

Because of differences in the density of the villages in each district, the number of villages and samples varied accordingly from 38 in Chakwal ($n = 190$), to 74 in both Sargodha and Faisalabad ($n = 370$ each). *Ft* DNA was detected in 74 of 2,280 samples (3.24%, 95% CI: 2.60–4.06). There were some villages where *Ft* DNA was detected at more than one location. These included, one each from Attock (Gharibwal) and Faisalabad districts (482-GB). Compared to the other districts, an increased incidence rate of *Ft* was observed in Faisalabad ($n = 15$), Gujranwala ($n = 17$), and Attock ($n = 10$). The prevalence was highest in district Chakwal [(13.1%, (5.26%, 95% CI: 2.88–9.41) followed by Gujranwala (4.72%, 95% CI: 2.97–7.43), Attock (4.44%, 95% CI: 2.43–7.98), Faisalabad (4.05%, 95% CI: 2.47–6.58), Dera Ghazi Khan (3.72%, 95% CI: 1.90–7.17), Sargodha (3.24%, 95% CI: 1.86–5.58), and Sahiwal (0.78%, 95% CI: 0.21–2.81). None of the soil sample originating from district Sheikhupura were positive for *Ft* DNA (Figure 1). Interestingly, a total of 20 samples (4.3%, 95% CI: 2.86–6.68) representing agriculture land with no apparent human interaction were also found to be positive where there was no apparent animal and human interaction.

Relationship Between Soil Chemistry and Categorical Variables to Occurrence of *Ft* in Soil

In the earlier study, we described association between physio-chemical characteristics of soil and presence/absence of *Ft* DNA in soil samples using a simple *t*-test and chi-square (Muhammad et al., 2017). In this study, we further explored these data and other potential variables to quantify factors associated with detection of bacterial DNA in soil. Table 1 shows eigenvalues, percentage variance and cumulative percentage of variance of principal components. The first three principals had eigenvalues > 1 and cumulatively explained 77.26% of total variance (inertia) in the dataset. Varying between + 1 and –1, the values (≥ 0.4) of the loadings represent the correlation between each variable and a principal component (Table 2). As the absolute value of the loading increases, the importance of the variable to the principal component becomes greater. Component 1 (PC1) explained 30.619% variance. It loaded positively on clay, Cd, Pb and negatively on slit, organic matter, and N. Component 2 (PC2) explained 27.339 % variance. It loaded positively on organic matter and N and negatively on silt. Component 3 (PC3) explained 19.299% variance and loaded positively on silt, Cd, Pb and negatively on clay. The variable *Ft* was significantly linked to PC1 and PC3 ($p \leq 0.05$. For PC1, variable *Ft* explained 26% variance in the coordinates whereas correlation coefficient was 5% for PC3. The PC1 and PC3 have partitioned data into *Ft* positive and negative sites. Figure 3 displays quality of representation (squared cosine, \cos^2) of variables and individuals (sampling sites) along the first two principal components. The angles between variables show degree of correlation, and their lengths represent importance for the respective components. Clay, Cd, and Pb were evidenced to be more important for PC1. Organic matter and N were contributed greatly in PC2. Clay and slit were negatively correlated with each other. The sampling points in the periphery had better representation (\cos^2 values closer to 1).

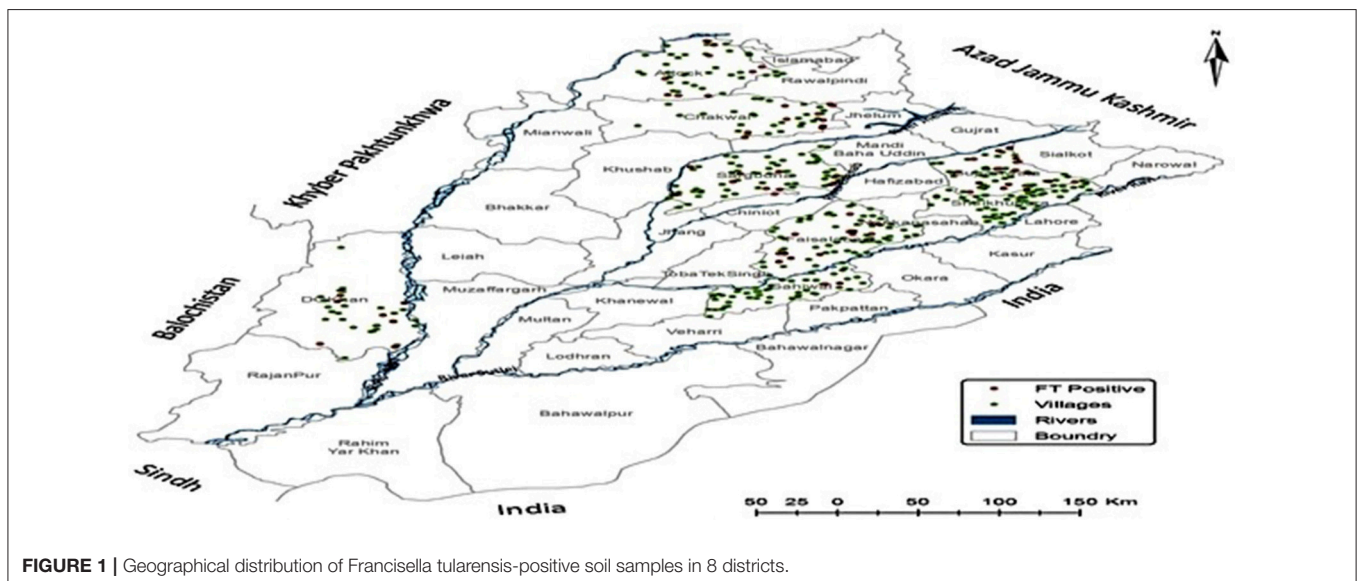


FIGURE 1 | Geographical distribution of *Francisella tularensis*-positive soil samples in 8 districts.

The logistic regression analysis had AIC value (143.64), Nagelkerke R Square (0.547) and -2 Log likelihood (124.352). The accuracy of the model was 81.4. The Hosmer & Lemeshow test of the goodness of fit suggested fitness of the model at $p = 0.792$ (>0.05). Variables significantly associated with positivity of soil samples were soluble salts (OR: 1.276, 95% CI: 1.043–1.562), Ni (OR: 2.910, 95%CI: 0.795–10.644), Mn (OR:0.733, 95% CI:0.565-0.951), Zn (OR: 4.922, 95% CI:0.929–26.064), and those clustered together as PC1 (OR: 4.760, 95% CI:2.373–9.548) and PC3 (OR:0.357, 95%CI:0.199–0.640), distance from animal market (OR: 0.57, 95% CI:0.30–1.07), distance from water source (OR:1.19, 95%CI: 1.19–3.09), Animal density (OR:1.56, 95%CI: 0.97–2.43), number of households in a village (OR:0.38, 95% CI: 0.20–0.71) and domestic animals in a village (OR:2.069, 95% CI: 1.05–4.05). A unit increase in PC1 means an increase in the risk of soil positivity whereas PC3 had protective effect. Moisture, P, Na, and PC2 were non-significant and therefore removed from the regression equation through

stepwise methods of covariate selection. The experimentation with regression revealed that varimax rotation and dropping some of the correlated variables did not improve the model (AIC, Nagelkerke R Square and -2 Log likelihood values not shown).

Seroconversion in Domestic Animals to *Ft* in the Studied Districts

The seroconversion was found in 6.22% of small and large ruminants ($n = 44$, 95% CI: 4.67–8.25) Spatial distribution of seropositivity in animals has been illustrated in **Figure 4** where a village has been red highlighted corresponding to seroconversion in any of the study animals. A significant difference ($p < 0.05$) was found in the prevalence of serum anti-*Ft*-ELISA antibodies among cattle (11.17%, 95% CI: 7.35–16.62), and buffalo (8.49%, 95% CI: 5.04–14.0), sheep (5.7%, 95%CI: 3.13–10.19), and goat (0.5%, 95% CI: 0.00–2.78). The exposure rate was much more in large ruminants (9.94%, 95% CI: 7.17–13.63) than small ruminants (2.93%, 95 CI: 1.64–5.17). Likewise, a significant difference was observed for gender ($\chi^2 = 15.35$, $p = 0.000$) where seropositivity was much more in female animals (16.3%) than male animals (6.2%) while a non-significant difference was observed in age groups of small [<2 years (4%) v/s 2–4 years (2%) v/s >4 years (14.2%), $\chi^2 = 3.81$, $p = 0.14$] and large ruminants [<3 years (10.8%) v/s 3–6 years (7.9%) v/s >6 years (33%), $\chi^2 = 1.85$ $p = 0.39$].

TABLE 2 | Factor-loading matrix for the phyto-chemical attributes of soil sampled identified by principal component analysis.

	Component		
	1	2	3
Silt	-0.524	-0.467	0.572
Clay	0.593		-0.567
Organic Matter	-0.515	0.820	
Cd	0.693		0.523
Cr			0.623
Pb	0.646		
N	-0.533	0.809	

DISCUSSION

The molecular diagnostic assay (RT-PCR) had a high sensitivity and specificity with a detection limit as low as <100 genome copies, and therefore allows simultaneous examination of numerous samples with rapid turnaround time (Christensen

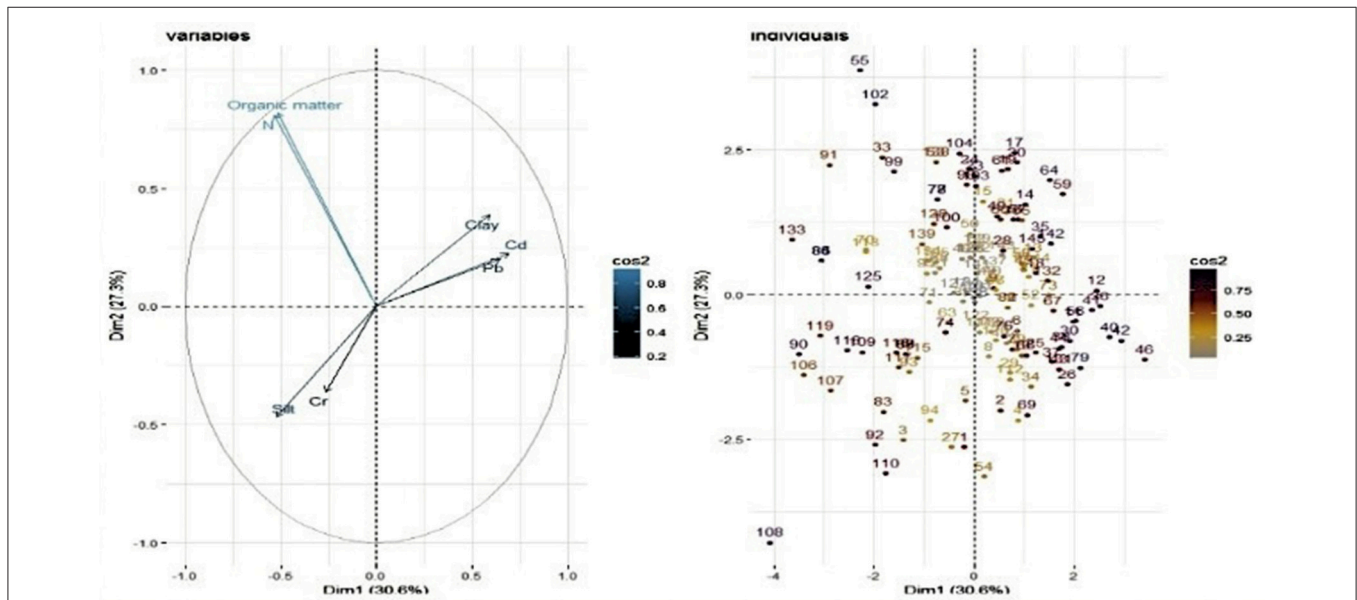


FIGURE 2 | Biplot showing representation of sampling points (called individuals) and physiochemical attributes (variables) in multivariate principal component space.

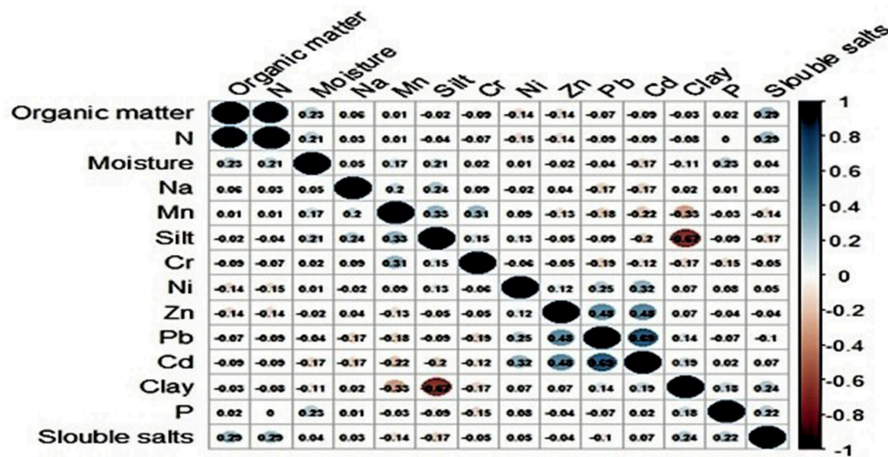


FIGURE 3 | Representation (squared cosine, \cos^2) of variables and individuals (sampling sites) along first two principal components.

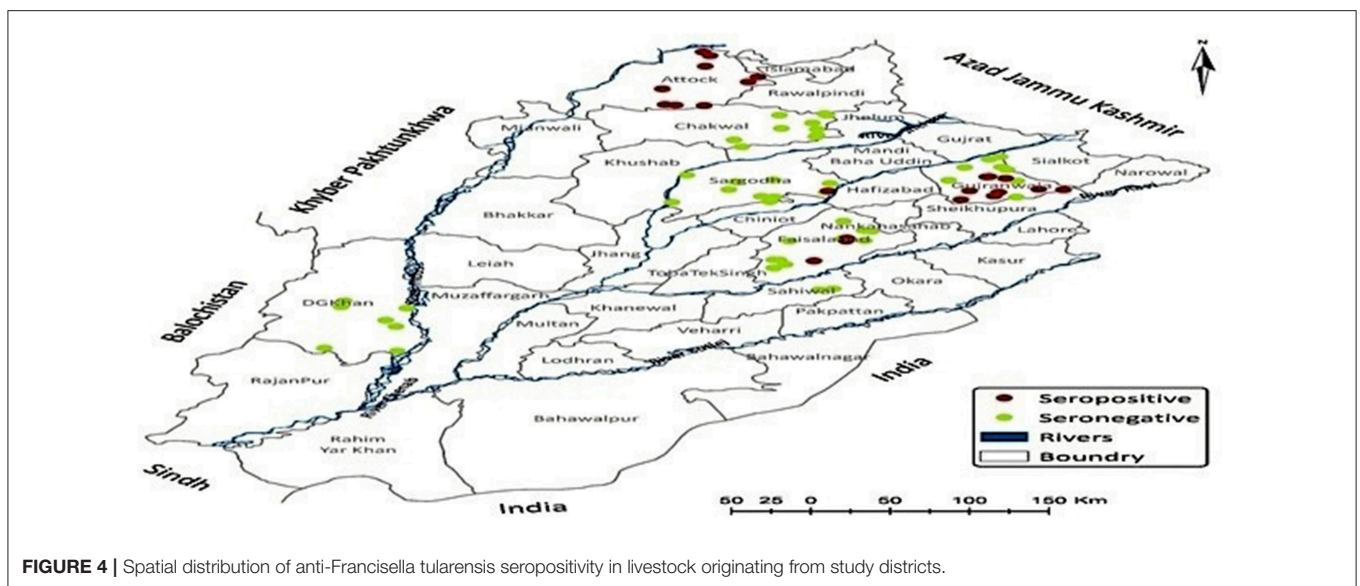


FIGURE 4 | Spatial distribution of anti-*Francisella tularensis* seropositivity in livestock originating from study districts.

et al., 2006). Such assays are typically used for surveillance of extremely dangerous pathogens (EDPs) in the natural environment, particularly in settings such as Pakistan that lack a highly contained laboratory, trained personnel, culturing facilities, and repositories for isolating archives. With regards to detection of antibodies, the biological marker (lipopolysaccharide or LPS) employed for the detection of seroconversion does not produce any cross-reaction with any component of currently known bacteria (Schmitt et al., 2005; Jenzora et al., 2008), and hence is a suitable macromolecule for the detection of antibodies while monitoring a large number of samples originating from domestic animals and humans (Sharma et al., 2013).

Despite evidence of *Ft* in soil, there have been no reported tularemia outbreaks or cases in Punjab province to-date. There are a number of potential reasons for why this may be the case.

Firstly, clinical cases may remain undiagnosed or misdiagnosed due to lack of laboratory based diagnostic capabilities throughout the country, as well as due to the fact that the clinical manifestations of tularemia can be fairly general. Moreover, strains isolated from the northern hemisphere are much more virulent than those isolated from Europe and Asia (Sjöstedt, 2007; Oyston, 2008). Lastly, the lack of reported cases could be due to climate and micro- and macro-nutrient characteristics of the soil supporting the persistence of *Ft* in the environment without any concomitant infection or outbreak (Dennis et al., 2001; Oyston, 2008; Alkhuder et al., 2010). Though it requires further evaluation of potential disease reservoirs (primarily rodents), and isolation and subsequent genomic characterization of prevailing strains, the more frequent occurrence of *Ft* in soil at sites close to water sources may be indicative of the prevalence of a less virulent strain (Ulu-Kilic and Doganay,

TABLE 3 | Outcome of logistic regression analysis showing association between presences of DNA of *Francisella tularensis* soil samples and its potential risk factors.

	B	S.E.	Wald	df	Sig.	Exp(B)	95% C.I. for EXP(B)	
							Lower	Upper
Soluble salts	0.244	0.103	5.606	1	0.018	1.276	1.043	1.562
Ni	1.068	0.662	2.606	1	0.106	2.910	0.795	10.644
Mn	-0.310	0.133	5.483	1	0.019	0.733	0.565	0.951
Zn	1.594	0.850	3.511	1	0.061	4.922	0.929	26.064
PC1	1.560	0.355	19.294	1	0.000	4.760	2.373	9.548
PC3	-1.030	0.298	11.934	1	0.001	0.357	0.199	0.640
Distance from animal market	0.534	0.975	9.318	1	0.05	0.57	0.30	1.07
Water source (canal/stream/drain)	-2.051	2.762	13.956	1	0.004	1.19	1.19	3.09
Animal density in a village	0.927	0.175	8.59	1	0.07	1.56	0.97	2.43
Number of households in a village	-1.823	0.690	3.489	1	0.002	0.38	0.20	0.71
Domestic animal	0.121	0.378	7.321	1	0.02	2.069	1.05	4.05
Ground cover (vegetation)	-0.781	0.782	6.812	1	0.08	1.49	0.88	2.51
Constant	-3.647	1.381	6.978	1	0.008	0.026		

2014). Previous studies have shown that *Ft* can survive in water, soil, mud, animal waste, and frozen meat for an extended period of time (Eliasson et al., 2006; Sjöstedt, 2007). An area in close proximity to water may have a higher probability for the presence of *Ft*, however the presence of mammalian host may be required for manifestation of disease (Desvars et al., 2015). Although an increased persistence of *Ft* has been observed in environments lacking humidity (Wilkinson, 1966; Dennis et al., 2001), the organism cannot remain viable under desiccation conditions (Faith et al., 2012). A significant association between the occurrence of *Ft* in soil and the presence of animals at the same site may correspond to the presence of disease reservoirs at locations in Punjab province where *Ft* was identified, such as the rodents that are found frequently at livestock barns and surrounding areas. It has been observed that an increase in the human population can decrease the number of rodents in the fields and corresponding areas (Sutherst, 2004); in contrast, an increase in the animal population can lead to an increase in the rodent population and consequently an increase in the risk of *Ft* (Gürçan, 2014). Most of the positive samples were collected in irrigated and cropland areas (Chakwal, Gujranwala, and Faisalabad), that are interconnected with each other. In fact, compared to areas with forests and water, a previous study showed that *Ft* was primarily observed in croplands where rodents were found to be a common vector for *Ft* infections (Hightower et al., 2014).

Our findings show that it is difficult to define the relationship between the characteristics of the studied analytes and the persistence of *Ft* in soil. However, this study provides insight between *Ft* and its relationship with soil texture and metals requiring that further investigations are conducted in order to ascertain more definitive outcomes. Metals including iron, zinc, copper, and manganese play a key role in biochemical reactions and are present in most of the organism as constituents of different biological molecules (Hood and Skaar, 2012). Copper, magnesium, manganese, zinc, nickel, cadmium and sodium were

observed to have a role in persistence of *Ft* in soil, although further investigation of these elements is needed. Indeed, some studies emphasized that survival and persistence of different organisms in soil is influenced by the soil texture (Nicholson et al., 2005). For instance, *Burkholderia pseudomallei* and *Ft* has the potential to survive for 30 months and 14 weeks, respectively, in clay soil (Thomas and Forbes-Faulkner, 1981; Cieslik et al., 2018). Generally, soil with an increase in clay support enhanced growth of organisms as compared to soil with increased concentration of sand (Locatelli et al., 2013). A potential association between *Ft* DNA and Magnesium could be correlated with its role while maintaining negative charge in LPS of outer membrane and therefore stability of organism in unfavorable conditions (Leadbetter and Poindexter, 2013; Wu et al., 2016). Similar to *Ft*, intracellular bacteria including *Salmonella enterica*, *Listeria monocytogenes*, *Brucella abortus*, and *Yersinia pestis* require zinc for intracellular survival and replication (Desrosiers et al., 2010; Corbett et al., 2012; Ma et al., 2015). Cadmium is normally toxic to bacteria however it has several mechanisms to develop resistance including (1) enzymes which make cell wall impermeable, (2) mechanism of efflux, (3) binding of metal ions, and (4) enzymes which convert toxic metals to non-toxic (Ron et al., 1992; Abbas et al., 2017). The persistence of *Ft* in cadmium high concentration soil presents a potential mechanism of resistance that need to be explored in future studies.

A large proportion of ruminants (goat, sheep, cattle, and buffalo) were found to be seropositive for anti-*Ft* antibodies. All the seropositive animals were clinically healthy and were devoid of symptoms suggestive of *Ft* infection. This is not surprising, because both active and passive forms of *Ft* have previously been evidenced in humans, rodents, and wild animals, (Wobeser et al., 2009) and therefore a varying rate (4–19%) of asymptomatic tularemia could be expected (Kiliç, 2010). Indeed, the clinical form of the infection depends on the route of entry of the pathogen into the body and the immune status of the host

(Gürcan, 2014). The percent prevalence of anti-*Ft* antibodies was significantly higher in large ruminants (cattle and buffalo) than small ruminants (sheep and goat). Interestingly, previous studies have shown that cattle and sheep are comparatively resistant to *Ft* and remain asymptomatic (Mörner et al., 1988; Pfahler-Jung, 1989; Winn and Koneman, 2006). Some animals are very sensitive to tularemia, and succumb to infection soon after development of specific antibodies, whereas cattle, pigs, and sheep are more resistant, despite even having a significantly high antibody titer (Hopla, 1974; Valdes and Valdes, 2018). Animals may not show clinical signs even after years of infection, possibly owing to the presence of post-exposure cellular and humoral immunity (Bevanger et al., 1994; Ericsson et al., 1994; Magnarelli et al., 2007). A recent study revealed that both small and large ruminants, independent of their genders, are frequently exposed to soil contaminated with *Ft* supporting the findings by previous studies showing that cattle maintain some degree of *Ft* resistance (Dienst Jr, 1963; Scheel et al., 1992; Jacobs, 2002). Similarly, another study showed that both male and female mice are susceptible to *Ft* where male mice develop severe clinical signs and high mortality as compared to female (Sunagar et al., 2016). These observations may be due to differences in immune response development in male and female mice. An example of this was shown during *Streptococcus pneumoniae* infections, where immune system inefficiency was noted to be higher in female mice as compared to male mice (Wiemken et al., 2014).

In conclusion, this study provides a preliminary confirmation of the presence of *Ft* in the Punjab Province of Pakistan and its potential association with several soil characteristics (macro- and micro-nutrients) at a higher statistical resolution. Future studies involving unexplored geographical areas of the country, disease reservoirs including rodents, and evaluation of the at-risk human population (the farmers and veterinarians), are needed.

ETHICS STATEMENT

Blood samples were collected from cattle, buffalo, sheep, and goat following the guidelines of International Animal Care and Use Committee (IACUC) with prior consent of the farm's owner. All samples were analyzed after approval from the Ethical

Research Board at the University of Veterinary and Animal Sciences, Lahore, Pakistan vide approval No: DR/236 dated 16th May, 2013.

AUTHOR CONTRIBUTIONS

BMJ, MZS, MR and KM: conceived and designed the study; JM, MZS, MH, ZUH, HRC, MTG, TJ, and MAA: sample collection and laboratory procedure across the study districts; JM, MZS, MN, TA and MHC: data analysis; JM, MZS, GSK and BMJ: manuscript write-up and necessary editing. All authors read and approved the manuscript.

FUNDING

The study was financially supported by the Defense Threat Reduction Agency, Basic Research Award number HDTRA1-10-1-0080 to The Pennsylvania State University, USA (Prime Awardees) and University of Veterinary and Animal Sciences, Lahore Pakistan (Subcontract Awardees).

ACKNOWLEDGMENTS

We thank Livestock and Dairy Development Department, the local veterinarians, the farmers and the laboratory technicians (Muhammad Naeem Akhtar, Imran Shafiq, Muhammad Arshad, Muhammad Asif, and Babar Nawab) for their assistance in soil sample collection procedures across the study districts and subsequent processing at University Diagnostic Laboratory and Quality Operations Laboratory of University of Veterinary and Animal Sciences, Lahore. We thank Alexandra Jamison (Fogarty International Center, National Institute of Health, USA) and Tyler David Pearson Goralski (Department of Biochemistry and Molecular Biology, The Pennsylvania State University, USA) for necessary text correction and editing.

SUPPLEMENTARY MATERIAL

The Supplementary Material for this article can be found online at: <https://www.frontiersin.org/articles/10.3389/fcimb.2019.00089/full#supplementary-material>

REFERENCES

- Abbas, S., Rafatullah, M., Hossain, K., Ismail, N., Tajarudin, H., and Khalil, H. A. (2017). A review on mechanism and future perspectives of cadmium-resistant bacteria. *Int. J. Environ. Sci. Technol.* 15, 243–262. doi: 10.1007/s13762-017-1400-5
- Abdi, H., and Williams, L. J. (2010). Principal component analysis. *Wiley Interdisciplin. Rev. Comput. Stat.* 2, 433–459. doi: 10.1002/wics.101
- Alkhuder, K., Meibom, K. L., Dubail, I., Dupuis, M., and Charbit, A. (2010). Identification of *trkH*, encoding a potassium uptake protein required for *Francisella tularensis* systemic dissemination in mice. *PLoS ONE* 5:e8966. doi: 10.1371/journal.pone.0008966
- Bevanger, L., Maeland, J. A., and Kvan, A. (1994). Comparative analysis of antibodies to *Francisella tularensis* antigens during the acute phase of tularemia and eight years later. *Clin. Diagn. Lab. Immunol.* 1, 238–240.
- Bossi, P., Tegnell, A., Baka, A., Van Loock, F., Hendriks, J., Werner, A., et al. (2004). Bichat guidelines for the clinical management of tularaemia and bioterrorism-related tularaemia. *Euro Surveill.* 9, E9–E10. doi: 10.2807/esm.09.12.00503-en
- Brown, J. R. (1998). *Recommended Chemical Soil Test Procedures for the North Central Region*. Columbia, WA: Missouri Agricultural Experiment Station, University of Missouri.
- Champion, M. D., Zeng, Q., Nix, E. B., Nano, F. E., Keim, P., Kodira, C. D., et al. (2009). Comparative genomic characterization of *Francisella tularensis* strains belonging to low and high virulence subspecies. *PLoS Pathog.* 5:e1000459. doi: 10.1371/journal.ppat.1000459
- Christensen, D. R., Hartman, L. J., Loveless, B. M., Frye, M. S., Shipley, M. A., Bridge, D. L., et al. (2006). Detection of biological threat agents by real-time PCR: comparison of assay performance on the RAPID, the LightCycler, and the Smart Cycler platforms. *Clin. Chem.* 52, 141–145. doi: 10.1373/clinchem.2005.052522

- Cieslik, P., Knap, J., and Bielawska-Drozd, A. (2018). *Francisella tularensis*—review. *Postępy Mikrobiologii* 57, 58–67.
- Committee, CSS., Science, CSS., and McKeague, J. (1978). *Manual on Soil Sampling and Methods of Analysis*. Pinawa, MB: Canadian Society of Soil Science.
- Corbett, D., Wang, J., Schuler, S., Lopez-Castejon, G., Glenn, S., Brough, D., et al. (2012). Two zinc uptake systems contribute to the full virulence of *Listeria monocytogenes* during growth *in vitro* and *in vivo*. *Infect. Immun.* 80, 14–21. doi: 10.1128/IAI.05904-11
- Dennis, D. T., Inglesby, T. V., Henderson, D. A., Bartlett, J. G., Ascher, M. S., Eitzen, E., et al. (2001). Tularemia as a biological weapon: medical and public health management. *JAMA* 285, 2763–2773. doi: 10.1001/jama.285.21.2763
- Desrosiers, D. C., Bearden, S. W., Mier, I., Abney, J., Paulley, J. T., Fetherston, J. D., et al. (2010). Znu is the predominant zinc importer in *Yersinia pestis* during *in vitro* growth but is not essential for virulence. *Infect. Immun.* 78, 5163–5177. doi: 10.1128/IAI.00732-10
- Desvars, A., Furberg, M., Hjertqvist, M., Vidman, L., Sjöstedt, A., Rydén, P., et al. (2015). Epidemiology and ecology of tularemia in Sweden, 1984–2012. *Emerg. Infect. Dis.* 21:32. doi: 10.3201/eid2101.140916
- Dienst Jr, F. (1963). Tularemia: a perusal of three hundred thirty-nine cases. *J. Louisiana State Med. Soc.* 115:114.
- Eliasson, H., Broman, T., Forsman, M., and Bäck, E. (2006). Tularemia: current epidemiology and disease management. *Infect. Dis. Clin. North Am.* 20, 289–311. doi: 10.1016/j.idc.2006.03.002
- Ericsson, M., Sandström, G., Sjöstedt, A., and Tärnvik, A. (1994). Persistence of cell-mediated immunity and decline of humoral immunity to the intracellular bacterium *Francisella tularensis* 25 years after natural infection. *J. Infect. Dis.* 170, 110–114. doi: 10.1093/infdis/170.1.110
- Esmaili, S., Gooya, M. M., Shirzadi, M. R., Esfandiari, B., Amiri, F. B., Behzadi, M. Y., et al. (2014). Seroepidemiological survey of tularemia among different groups in western Iran. *Int. J. Infect. Dis.* 18, 27–31. doi: 10.1016/j.ijid.2013.08.013
- Faith, S., Smith, L. K., Swatland, A., and Reed, D. S. (2012). Growth conditions and environmental factors impact aerosolization but not virulence of *Francisella tularensis* infection in mice. *Front. Cell. Infect. Microbiol.* 2:126. doi: 10.3389/fcimb.2012.00126
- Fierer, N., Schimel, J. P., Cates, R. G., and Zou, J. (2001). Influence of balsam poplar tannin fractions on carbon and nitrogen dynamics in Alaskan taiga floodplain soils. *Soil Biol. Biochem.* 33, 1827–1839. doi: 10.1016/S0038-0717(01)00111-0
- Garaizar, J., Rementeria, A., and Porwollik, S. (2006). DNA microarray technology: a new tool for the epidemiological typing of bacterial pathogens? *FEMS Immunol. Med. Microbiol.* 47, 178–189. doi: 10.1111/j.1574-695X.2006.00081.x
- Gliatto, J. M., Rae, J. F., McDonough, P. L., and Dasbach, J. J. (1994). Feline tularemia on Nantucket island, Massachusetts. *J. Vet. Diagn. Invest.* 6, 102–105. doi: 10.1177/104063879400600120
- Gürçan, S. (2014). Epidemiology of tularemia. *Balkan Med. J.* 31:3. doi: 10.5152/balkanmedj.2014.13117
- Helvacı, S., Gedikoglu, S., Akalin, H., and Oral, H. (2000). Tularemia in Bursa, Turkey: 205 cases in ten years. *Eur. J. Epidemiol.* 16, 271–276. doi: 10.1023/A:1007610724801
- Hightower, J., Kracalik, I. T., Vydayko, N., Goodin, D., Glass, G., and Blackburn, J. K. (2014). Historical distribution and host-vector diversity of *Francisella tularensis*, the causative agent of tularemia, in Ukraine. *Parasites Vectors* 7:453. doi: 10.1186/s13071-014-0453-2
- Hood, M. I., and Skaar, E. P. (2012). Nutritional immunity: transition metals at the pathogen–host interface. *Nat. Rev. Microbiol.* 10:525. doi: 10.1038/nrmicro2836
- Hopla, C. E. (1974). The ecology of tularemia. *Adv. Vet. Sci. Comp. Med.* 18, 25–53.
- Jacobs, R. F. (2002). *Francisella tularensis (Tularemia). Antimicrobial Therapy and Vaccines*. New York, NY: Apple Trees Productions LLC.
- Jenzora, A., Jansen, A., Ranisch, H., Lierz, M., Wichmann, O., and Grunow, R. (2008). Seroprevalence study of *Francisella tularensis* among hunters in Germany. *FEMS Immunol. Med. Microbiol.* 53, 183–189. doi: 10.1111/j.1574-695X.2008.00408.x
- Kiliç, S. (2010). A general overview of *Francisella tularensis* and the epidemiology of tularemia in Turkey. *Flora* 15, 37–58.
- Kuske, C. R., Barns, S. M., Grow, C. C., Merrill, L., and Dunbar, J. (2006). Environmental survey for four pathogenic bacteria and closely related species using phylogenetic and functional genes. *J. Forens. Sci.* 51, 548–558. doi: 10.1111/j.1556-4029.2006.00131.x
- Leadbetter, E. R., and Poindexter, J. S. (2013). *Bacteria in Nature: Volume 3: Structure, Physiology, and Genetic Adaptability*. Belrin; Heidelberg: Springer Science & Business Media.
- Lévesque, B., De Serres, G., Higgins, R., D'Halewyn, M.-A., Artsob, H., Grondin, J., et al. (1995). Seroepidemiologic study of three zoonoses (leptospirosis, Q fever, and tularemia) among trappers in Québec, Canada. *Clin. Diag. Lab. Immunol.* 2, 496–498.
- Locatelli, A., Spor, A., Jolivet, C., Piveteau, P., and Hartmann, A. (2013). Biotic and abiotic soil properties influence survival of *Listeria monocytogenes* in soil. *PLoS ONE* 8:e75969. doi: 10.1371/journal.pone.0075969
- Ma, L., Terwilliger, A., and Maresso, A. W. (2015). Iron and zinc exploitation during bacterial pathogenesis. *Metallomics* 7, 1541–1554. doi: 10.1039/C5MT00170F
- Magistad, O., Reitemeier, R., and Wilcox, L. (1945). Determination of soluble salts in soils. *Soil Sci.* 59, 65–76. doi: 10.1097/00010694-194501000-00010
- Magnarelli, L., Levy, S., and Koski, R. (2007). Detection of antibodies to *Francisella tularensis* in cats. *Res. Vet. Sci.* 82, 22–26. doi: 10.1016/j.rvsc.2006.06.003
- McLean, E. (1982). “Soil pH and Lime requirement,” in *Methods of Soil Analysis. Part 2. Chemical and Microbiological Properties (Methodssoilan2)*, ed A. L. Page (Madison, WI: American Society of Agronomy, Soil Science Society of America), 199–224.
- Mörner, T., Sandström, G., and Mattsson, R. (1988). Comparison of serum and lung extracts for surveys of wild animals for antibodies to *Francisella tularensis* biovar palaeartica. *J. Wildl. Dis.* 24, 10–14.
- Muhammad, J., Rabbani, M., Muhammad, K., Wasim, M., Ahmad, A., Sheikh, A., et al. (2017). Physicochemical factors affecting persistence of *Francisella tularensis* in soil. *J. Anim. Plant Sci.* 27, 1047–1050.
- Nandi, A., Mandal, A., Wilson, M., and Smith, D. (2016). Flood hazard mapping in Jamaica using principal component analysis and logistic regression. *Environ. Earth Sci.* 75:465. doi: 10.1007/s12665-016-5323-0
- Nelson, D., and Sommers, L. E. (1982). “Total carbon, organic carbon, and organic matter,” in *Methods of Soil Analysis. Part 2. Chemical and Microbiological Properties (methodssoilan2)* (Madison, WI: American Society of Agronomy, Soil Science Society of America), 539–579.
- Nicholson, F. A., Groves, S. J., and Chambers, B. J. (2005). Pathogen survival during livestock manure storage and following land application. *Bioresour. Technol.* 96, 135–143. doi: 10.1016/j.biortech.2004.02.030
- Oyston, P. C. (2008). *Francisella tularensis*: unravelling the secrets of an intracellular pathogen. *J. Med. Microbiol.* 57, 921–930. doi: 10.1099/jmm.0.2008/000653-0
- Pechous, R. D., McCarthy, T. R., and Zahrt, T. C. (2009). Working toward the future: insights into *Francisella tularensis* pathogenesis and vaccine development. *Microbiol. Mol. Biol. Rev.* 73, 684–711. doi: 10.1128/MMBR.00028-09
- Penn, R. L. (2015). “*Francisella tularensis* (tularemia),” in *Mandell, Douglas, and Bennett's Principles and Practice of Infectious Diseases, 8th Edn*, eds J. E. Bennett and M. J. Blaser (Philadelphia, PA: Elsevier), 2590–2602.
- Pfahler-Jung, K. (1989). *Die globale Verbreitung der Tularämie*. Berlin: Kommission bei Duncker & Humblot.
- Pourhoseingholi, M. A., Mehrabi, Y., Alavi-Majd, H., and Yavari, P. (2012). Using latent variables in logistic regression to reduce multicollinearity, A case-control example: breast cancer risk factors. *Italian J. Publ. Health* 5, 65–71. doi: 10.2427/5857
- Robert, G., and Frederick, R. (1995). *Introductory Soil Science Laboratory Manual*. New York, NY: Oxford University Press.
- Ron, E. Z., Minz, D., Finkelstein, N., and Rosenberg, E. (1992). “Interactions of bacteria with cadmium,” in *Microorganisms to Combat Pollution*, ed E. Rosenberg (Dordrecht: Springer), 37–46. doi: 10.1007/978-94-011-1672-5_4
- Scheel, O., Sandvik, T., Hoel, T., and Aasen, S. (1992). [Tularemia in Norway. A clinical and epidemiological review]. *Tidsskr. Nor. Laegeforen.* 112, 635–637.
- Schmitt, P., Spletstoesser, W., Porsch-Özcürümez, M., Finke, E.-J., and Grunow, R. (2005). A novel screening ELISA and a confirmatory Western blot useful for diagnosis and epidemiological studies of tularemia. *Epidemiol. Infect.* 133, 759–766. doi: 10.1017/S0950268805003742
- Schulter, G. S., and Allen, L. A. H. (2006). Differential infection of mononuclear phagocytes by *Francisella tularensis*: role of the macrophage mannose receptor. *J. Leukocyte Biol.* 80, 563–571. doi: 10.1189/jlb.0306219

- Sharma, N., Hotta, A., Yamamoto, Y., Fujita, O., Uda, A., Morikawa, S., et al. (2013). Detection of *Francisella tularensis*-specific antibodies in patients with tularemia by a novel competitive enzyme-linked immunosorbent assay. *Clin. Vacc. Immunol.* 20, 9–16. doi: 10.1128/CVI.00516-12
- Silvestri, E. E., Perkins, S. D., Rice, E. W., Stone, H., and Schaefer, F. W. (2016). Review of processing and analytical methods for *Francisella tularensis* in soil and water. *Ann. Microbiol.* 66, 77–89. doi: 10.1007/s13213-015-1144-8
- Sjösted, A. (2005). Genus I. *Francisella* Dorofe'ev 1947, 176AL, in *Bergey's Manual of Systematic Bacteriology, The Proteobacteria, Vol. 2*, ed G. George (New York, NY: Springer), 200–210.
- Sjösted, A. (2007). Tularemia: history, epidemiology, pathogen physiology, and clinical manifestations. *Ann. NY. Acad. Sci.* 1105, 1–29. doi: 10.1196/annals.1409.009
- Soltanpour, P. A., and Schwab, A. P. (1977). A new soil test for simultaneous extraction of macro-and micro-nutrients in alkaline soils 1. *Commun. Soil Sci. Plant Anal.* 8, 195–207. doi: 10.1080/00103627709366714
- Sunagar, R., Kumar, S., Franz, B. J., and Gosselin, E. J. (2016). Vaccination evokes gender-dependent protection against tularemia infection in C57BL/6Tac mice. *Vaccine* 34, 3396–3404. doi: 10.1016/j.vaccine.2016.04.054
- Sutherst, R. W. (2004). Global change and human vulnerability to vector-borne diseases. *Clin. Microbiol. Rev.* 17, 136–173. doi: 10.1128/CMR.17.1.136-173.2004
- Thomas, A., and Forbes-Faulkner, J. (1981). Persistence of *Pseudomonas Pseudomallei* soil. *Austr. Veter. J.* 57, 535–536. doi: 10.1111/j.1751-0813.1981.tb05804.x
- Ulu-Kilic, A., and Doganay, M. (2014). An overview: tularemia and travel medicine. *Travel Med. Infect. Dis.* 12, 609–616. doi: 10.1016/j.tmaid.2014.10.007
- Valdes, J. J., and Valdes, E. R. (2018). Biological agents: threat and response. *Handb. Sec. Sci.* 1–31. doi: 10.1007/978-3-319-51761-2_16-1
- Vogler, A. J., Birdsell, D., Price, L. B., Bowers, J. R., Beckstrom-Sternberg, S. M., Auerbach, R. K., et al. (2009). Phylogeography of *Francisella tularensis*: global expansion of a highly fit clone. *J. Bacteriol.* 191, 2474–2484. doi: 10.1128/JB.01786-08
- Wiemken, T. L., Carrico, R. M., Klein, S. L., Jonsson, C. B., Peyrani, P., Kelley, R. R., et al. (2014). The effectiveness of the polysaccharide pneumococcal vaccine for the prevention of hospitalizations due to *Streptococcus pneumoniae* community-acquired pneumonia in the elderly differs between the sexes: results from the community-acquired pneumonia organization (capo) international cohort study. *Vaccine*. 32, 2198–2203. doi: 10.1016/j.vaccine.2014.02.048
- Wilkinson, T. (1966). Survival of bacteria on metal surfaces. *Appl. Microbiol.* 14, 303–307.
- Winn, W. C., and Koneman, E. W. (2006). *Koneman's Color Atlas and Textbook of Diagnostic Microbiology*. Philadelphia, PA: Lippincott Williams & Wilkins.
- Wobeser, G., Campbell, G. D., Dallaire, A., and McBurney, S. (2009). Tularemia, plague, yersiniosis, and Tyzzer's disease in wild rodents and lagomorphs in Canada: a review. *Can. Vet. J.* 50:1251.
- Woods, J., Crystal, M., Morton, R., and Panciera, R. (1998). Tularemia in two cats. *J. Am. Vet. Med. Assoc.* 212, 81–83.
- Wu, X., Ren, G., Gunning, III, W. T., Weaver, D. A., Kalinoski, A. L., Khuder, S. A., et al. (2016). FmvB: a *Francisella tularensis* magnesium-responsive outer membrane protein that plays a role in virulence. *PLoS ONE* 11:e0160977. doi: 10.1371/journal.pone.0160977

Conflict of Interest Statement: The authors declare that the research was conducted in the absence of any commercial or financial relationships that could be construed as a potential conflict of interest.

Copyright © 2019 Muhammad, Rabbani, Shabbir, Muhammad, Ghori, Chaudhry, Ul Hassnain, Jamil, Abbas, Chaudhry, Haisem-ur-Rasool, Ali, Nisar, Kirimanjeswara and Jayarao. This is an open-access article distributed under the terms of the Creative Commons Attribution License (CC BY). The use, distribution or reproduction in other forums is permitted, provided the original author(s) and the copyright owner(s) are credited and that the original publication in this journal is cited, in accordance with accepted academic practice. No use, distribution or reproduction is permitted which does not comply with these terms.

Advantages of publishing in Frontiers



OPEN ACCESS

Articles are free to read for greatest visibility and readership



FAST PUBLICATION

Around 90 days from submission to decision



HIGH QUALITY PEER-REVIEW

Rigorous, collaborative, and constructive peer-review



TRANSPARENT PEER-REVIEW

Editors and reviewers acknowledged by name on published articles

Frontiers

Avenue du Tribunal-Fédéral 34
1005 Lausanne | Switzerland

Visit us: www.frontiersin.org

Contact us: info@frontiersin.org | +41 21 510 17 00



REPRODUCIBILITY OF RESEARCH

Support open data and methods to enhance research reproducibility



DIGITAL PUBLISHING

Articles designed for optimal readership across devices



FOLLOW US

[@frontiersin](https://twitter.com/frontiersin)



IMPACT METRICS

Advanced article metrics track visibility across digital media



EXTENSIVE PROMOTION

Marketing and promotion of impactful research



LOOP RESEARCH NETWORK

Our network increases your article's readership